



AGRICULTURAL RESEARCH INSTITUTE

**PUSA**







# Transactions of the Faraday Society

---

FOUNDED 1903

---

TO PROMOTE THE STUDY OF ELECTROCHEMISTRY, ELECTROMETALLURGY,  
PHYSICAL CHEMISTRY, METALLOGRAPHY, AND KINDRED SUBJECTS

---

VOL. XLI, 1945

---

GURNEY AND JACKSON  
LONDON: 98 GREAT RUSSELL STREET  
EDINBURGH: TWEEDDALE COURT

PRINTED IN GREAT BRITAIN AT  
THE UNIVERSITY PRESS  
ABERDEEN

# STUDIES IN THE MOLECULAR FORCES INVOLVED IN SURFACE FORMATION.

## II. THE SURFACE FREE ENERGIES OF SIMPLE LIQUID MIXTURES.

BY J. W. BELTON AND M. G. EVANS.

*Received 10th February, 1944.*

We propose in this paper to calculate by a statistical method the surface free energies of binary liquid systems which form perfect solutions. We shall then show that this treatment is consistent with the Gibbs thermodynamic discussion of surfaces of discontinuity; and finally we shall extend the treatment to certain special cases of solutions which are not perfect.

A perfect solution may be defined <sup>1</sup> as one in which :

(a) the molecular species (1) and (2) pack in the same way, so that a molecule of, say, species (1) has the same number of nearest neighbour contacts as a molecule of species (2),

(b) the molecular volumes  $V_1$  and  $V_2$  are such that in any mixture the two species pack in the same way as in the pure liquids; the volume  $V$  of any mixture of  $n_1$  molecules of (1) and  $n_2$  molecules of (2) is

$$V = n_1 V_1 + n_2 V_2,$$

(c) the free volumes,  $v_1$  and  $v_2$  are such that the approximation

$$n_1 v_1 + n_2 v_2 = (n_1 + n_2) \frac{1}{(v_1 n_1 v_2 n_2) n_1 + n_2}$$

is applicable,

(d) the total potential energy,  $W$ , of the system can be regarded as the sum of the contributions of nearest neighbours, and there is no change in the potential energy when a molecule of species (1) surrounded by molecules of its own kind, exchanges position with a molecule of species (2) surrounded by molecules of species (2). This implies that there is no heat of mixing, or that  $\epsilon_{12} = \frac{1}{2}(\epsilon_{11} + \epsilon_{22})$  where  $\epsilon_{11}$ ,  $\epsilon_{22}$ ,  $\epsilon_{12}$  are the potential energies of a 1—1, a 2—2 and a 1—2 contact respectively.

The free energy of such a solution is given by

$$F = n_1 \chi_1 + n_2 \chi_2 - n_1 kT \ln \phi_1 J_1 - n_2 kT \ln \phi_2 J_2 + n_1 kT \ln x_1 + n_2 kT \ln x_2 \quad (1)$$

where  $\chi_1$  and  $\chi_2$  are the potential energies,  $\phi_1$  and  $\phi_2$ ,  $J_1$  and  $J_2$  are respectively the translational and rotational contributions to the partition functions of species (1) and (2), and  $x_1$  and  $x_2$  are their mole fractions.

In general the composition of the surface will be different from that in the bulk. Let us assume that this discontinuity is restricted to the surface layer of molecules which contains  $n_{1s}$  molecules of species (1) and  $n_{2s}$  molecules of species (2) with corresponding mole fractions  $x_{1s}$  and  $x_{2s}$ . With respect to the potential energy, however, the discontinuity also includes the second layer, so that in calculating the free energy change involved in surface formation, both layers must be taken into account. Any other layer parallel to the surface will be part of the homogeneous bulk phase.

We may calculate the free energy of surface formation in two stages :

(a) the formation of a layer at the surface of  $n_1$  molecules of species (1) and  $n_2$  molecules of species (2), *i.e.* of a layer of same composition as the bulk and (b) the formation on this layer of a surface layer of  $n_{1s}$  and  $n_{2s}$  molecules of the two species. The free energy of surface formation is the

<sup>1</sup> Fowler and Guggenheim, *Statistical Thermodynamics*, p. 353.

sum of the terms involved in these two processes. The free energy of  $n_1$  molecules of species (1) and  $n_2$  molecules of species (2) in the bulk is given by equation (1). The free energy of these molecules at the surface is

$n_1\chi'_1 + n_2\chi'_2 - n_1kT \ln \phi'_1 J'_1 - n_2kT \ln \phi'_2 J'_2 + n_1kT \ln x_1 + n_2kT \ln x_2$  where the primed terms refer to this layer in the surface; the mole fractions are the same as those in the bulk. The free energy change in forming this layer is then

$$n_1(\chi'_1 - \chi_1) + n_2(\chi'_2 - \chi_2) - n_1kT \ln \frac{\phi'_1 J'_1}{\phi_1 J_1} - n_2kT \ln \frac{\phi'_2 J'_2}{\phi_2 J_2} \quad (2)$$

The free energy of  $n_{1s}$  and  $n_{2s}$  molecules of species (1) and (2) in the bulk is  $n_{1s}\chi_1 + n_{2s}\chi_2 - n_{1s}kT \ln \phi_1 J_1 - n_{2s}kT \ln \phi_2 J_2 + n_{1s}kT \ln x_1 + n_{2s}kT \ln x_2$  where the subscript  $s$  refers to the surface layer. The free energy change involved in the formation of this layer is

$$n_{1s}(\chi_{1s} - \chi_1) + n_{2s}(\chi_{2s} - \chi_2) - n_{1s}kT \ln \frac{\phi_{1s} J_{1s}}{\phi_1 J_1} - n_{2s}kT \ln \frac{\phi_{2s} J_{2s}}{\phi_2 J_2} + n_{1s}kT \ln \frac{x_{1s}}{x_1} + n_{2s}kT \ln \frac{x_{2s}}{x_2} + n_1kT \ln \frac{\phi'_1 J'_1}{\phi_1 J_1} + n_2kT \ln \frac{\phi'_2 J'_2}{\phi_2 J_2} \quad (3)$$

in which we assume that the  $\phi$  and  $J$  terms for the second layer are the same as in the bulk of the solution, and that  $n_1 + n_2 = n_{1s} + n_{2s}$ . The total free energy of surface formation is the sum of expressions (2) and (3).

### The Evaluation of the Potential Energy Terms.

The potential energy of a perfect solution, as we have stated above, can be expressed as the sum of the contributions between nearest neighbours. Let  $Z_B$  be the number of nearest neighbours in the bulk of the solution, where  $Z_B$  is independent of the composition. The total potential energy of  $n_1$  molecules of species (1) and  $n_2$  molecules of species (2) is given by

$$W = (n_1 + n_2) \frac{1}{2} Z_B [x_1^2 \epsilon_{11} + x_2^2 \epsilon_{22} + 2x_1 x_2 \epsilon_{12}] \\ = (n_1 + n_2) \frac{1}{2} Z_B [x_1 \epsilon_{11} + x_2 \epsilon_{22} + 2x_1 x_2 (\epsilon_{12} - \frac{1}{2}(\epsilon_{11} + \epsilon_{22}))]$$

For a perfect solution which fulfils condition (d), page 1, this reduces to

$$W = (n_1 + n_2) \frac{1}{2} Z_B (x_1 \epsilon_{11} + x_2 \epsilon_{22}) \\ = n_1 \chi_1 + n_2 \chi_2 \quad (4)$$

where

$$\chi_1 = \frac{1}{2} Z_B \epsilon_{11} \quad \text{and} \quad \chi_2 = \frac{1}{2} Z_B \epsilon_{22}$$

Let  $Z_s$  be the number of contacts with neighbours in the surface layer in the plane of the surface, and let  $Z'$  be the total number of contacts for a molecule in the surface. We shall assume that the packing is uniform and that  $Z'$  is also the number of contacts of a molecule within the second layer plus those with the layer below it. The number of nearest neighbour contacts for a molecule in the bulk is then

$$Z_B = Z_s + 2(Z' - Z_s)$$

from which

$$Z_s - Z' = Z' - Z_B$$

The change in potential energy in forming a surface of  $n_1$  and  $n_2$  molecules of the same composition as the bulk (cf. equation (2)) is

$$(\frac{1}{2} Z' n_1 \epsilon_{11} - \frac{1}{2} Z_B n_1 \epsilon_{11}) + (\frac{1}{2} Z' n_2 \epsilon_{22} - \frac{1}{2} Z_B n_2 \epsilon_{22})$$

or

$$\frac{1}{2} (Z' - Z_B) (n_1 \epsilon_{11} + n_2 \epsilon_{22}) \quad (5)$$

The potential energy of  $n_{1s}$  and  $n_{2s}$  molecules in the bulk is

$$\frac{1}{2} Z_B n_{1s} \epsilon_{11} + \frac{1}{2} Z_B n_{2s} \epsilon_{22} \quad (6)$$

Their potential energy when formed into a layer on the surface is

$$(n_{1s} + n_{2s}) \frac{1}{2} Z_s [x_{1s}^2 \epsilon_{11} + x_{2s}^2 \epsilon_{22} + 2x_{1s}x_{2s} \frac{1}{2}(\epsilon_{11} + \epsilon_{22})] + (n_{1s} + n_{2s})(Z' - Z_s)[x_{1s}x_{1s}\epsilon_{11} + x_{2s}x_{2s}\epsilon_{22} + (x_{1s}x_{2s} + x_{2s}x_{1s})\frac{1}{2}(\epsilon_{11} + \epsilon_{22})] \quad (7)$$

which reduces to

$$\frac{1}{2} Z' (n_{1s}\epsilon_{11} + n_{2s}\epsilon_{22}) + \frac{1}{2} (Z' - Z_s) \left[ \frac{n_{1s} + n_{2s}}{n_1 + n_2} n_{1s}\epsilon_{11} + \frac{n_{1s} + n_{2s}}{n_1 + n_2} n_{2s}\epsilon_{22} \right] \quad (8)$$

The change in potential energy in forming this layer is then

$$\frac{1}{2} (Z' - Z_B)(n_{1s}\epsilon_{11} + n_{2s}\epsilon_{22}) + \frac{1}{2} (Z' - Z_s)\alpha(n_{1s}\epsilon_{11} + n_{2s}\epsilon_{22}) \quad (9)$$

where  $\alpha = n_{1s} + n_{2s}/n_1 + n_2$ . We shall now make the simplifying assumption that the two species have the same molecular dimensions, so that  $n_1 + n_2 = n_{1s} + n_{2s}$  or  $\alpha = 1$ . The potential energy change involved in surface formation is the sum of expressions (5) and (9) which is

$$\frac{1}{2} (Z' - Z_B)(n_{1s}\epsilon_{11} + n_{2s}\epsilon_{22}). \quad (10)$$

### The Free Energy of Surface Formation.

The free energy involved in the formation of such a surface as we have postulated is given by the sum of expressions (2) and (3) with the potential energy terms substituted, thus

$$\Delta F = \frac{1}{2} (Z' - Z_B)(n_{1s}\epsilon_{11} + n_{2s}\epsilon_{22}) - n_{1s}kT \ln \frac{\phi_{1s}J_{1s}}{\phi_1J_1} - n_{2s}kT \ln \frac{\phi_{2s}J_{2s}}{\phi_2J_2} + n_{1s}kT \ln \frac{x_{1s}}{x_1} + n_{2s}kT \ln \frac{x_{2s}}{x_2} \quad (11)$$

$$= n_{1s}\Delta F_1^0 + n_{2s}\Delta F_2^0 + n_{1s}kT \ln \frac{x_{1s}}{x_1} + n_{2s}kT \ln \frac{x_{2s}}{x_2} \quad (12)$$

where

$$\Delta F_1^0 = \frac{1}{2} (Z' - Z_B)\epsilon_{11} - kT \ln \frac{\phi_{1s}J_{1s}}{\phi_1J_1}; \quad \Delta F_2^0 = \frac{1}{2} (Z' - Z_B)\epsilon_{22} - kT \ln \frac{\phi_{2s}J_{2s}}{\phi_2J_2},$$

both of which refer to one molecule in the pure liquid of species (1) and (2) respectively; and in which we have assumed that the  $\phi_s$  and  $J_s$  terms are the same at the surface of the solution as they are at the surface of the pure solvent.

### The Conditions of Equilibrium.

There are two conditions of equilibrium which we may apply in order to find the equilibrium value of  $x_{1s}$  for a particular value of  $x_1$ .

(i) The value of  $\Delta F$  must be a minimum for variations in  $n_{1s}$  and  $n_{2s}$

$$\frac{\partial \Delta F}{\partial n_{1s}} = \Delta F_1^0 + kT \ln \frac{x_{1s}}{x_1}; \quad \frac{\partial \Delta F}{\partial n_{2s}} = \Delta F_2^0 + kT \ln \frac{x_{2s}}{x_2}$$

from which

$$\delta \Delta F = \left( \Delta F_1^0 + kT \ln \frac{x_{1s}}{x_1} \right) \delta n_{1s} + \left( \Delta F_2^0 + kT \ln \frac{x_{2s}}{x_2} \right) \delta n_{2s}. \quad (13)$$

(ii) The area of the surface  $A$  is given by

$$(n_1 + n_2)a = (n_{1s} + n_{2s})a = A \quad (14)$$

from which

$$a \delta n_{1s} + a \delta n_{2s} = 0 \quad (15)$$

where  $a$  is the area of a molecule of either species in the surface layer. Hence

$$\begin{vmatrix} \Delta F_1^0 + kT \ln \frac{x_{1s}}{x_1} & \Delta F_2^0 + kT \ln \frac{x_{2s}}{x_2} \\ a & a \end{vmatrix} = 0 \quad (16)$$

#### 4 MOLECULAR FORCES IN SURFACE FORMATION

which gives

$$\Delta F_1^0 + kT \ln \frac{x_{1s}}{x_1} = \Delta F_2^0 + kT \ln \frac{x_{2s}}{x_2} \quad (17)$$

Hence

$$\begin{aligned} \Delta F &= (n_{1s} + n_{2s})\Delta F_1^0 + (n_{1s} + n_{2s})kT \ln \frac{x_{1s}}{x_1} \\ &= (n_{1s} + n_{2s})\Delta F_2^0 + (n_{1s} + n_{2s})kT \ln \frac{x_{2s}}{x_2} \end{aligned} \quad (18)$$

Now  $\Delta F = \gamma A$  where  $\gamma$  is the surface tension; substituting  $(n_{1s} + n_{2s})a$  for  $A$  in equation (18) we obtain

$$\gamma = \frac{\Delta F_1}{a} + \frac{kT}{a} \ln \frac{x_{1s}}{x_1} = \gamma_1^0 + \frac{kT}{a} \ln \frac{x_{1s}}{x_1} \quad (19)$$

For the purpose of calculation this may be written in a more convenient form; equation (17) gives

$$\Delta F_2^0 - \Delta F_1^0 = kT \ln \frac{x_{1s}x_2}{x_1x_{2s}} \quad (20)$$

or

$$\frac{x_{1s}}{x_1} = \frac{c}{1 + (c-1)x_1} \quad (21)$$

where  $c = \exp(\Delta F_2^0 - \Delta F_1^0)/kT = \exp(a(\gamma_2^0 - \gamma_1^0)/kT)$ .

Equation (19) then becomes

$$\gamma = \gamma_1^0 + \frac{kT}{a} \ln \frac{c}{1 + (c-1)x_1} \quad (22)$$

#### Treatment based on Gibbs Thermodynamic Equations.

We shall now discuss the above treatment in relation to the thermodynamic treatment of surfaces of discontinuity of Gibbs.<sup>2</sup> We may draw two geometrical surfaces, one, AA', in the vapour phase, the other, BB', in the homogeneous liquid so that  $\nu$  layers of molecules are included in the surface phase. The dividing surface, S, may be placed just above the surface layer. The fundamental equations of Gibbs for a surface of discontinuity is

$$dE^s = TdS^s + \gamma dA + \mu_1 dn_1^s + \mu_2 dn_2^s + \dots \quad (23)$$

or

$$dF^s = \gamma dA + \mu_1 dn_1^s + \mu_2 dn_2^s + \dots \quad (24)$$

from which we obtain

$$\gamma A = F^s - n_1^s \mu_1 - n_2^s \mu_2 \quad (25)$$

and

$$-A d\gamma = n_1^s d\mu_1 + n_2^s d\mu_2 + \dots \quad (26)$$

The superscript <sup>s</sup> denotes that these terms are excesses to be associated with the dividing surface S, and are the differences between that term for the region between BB' and S when the surface layer has a composition different from that of the bulk (Fig. 1(a)) and the term for the same region on the assumption that the phases are completely homogeneous up to the dividing surface S (Fig. 1(b)).

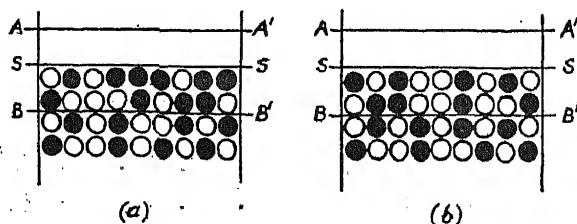


FIG. 1.

<sup>2</sup> Gibbs, *Scientific Papers*, Vol. I, p. 219.

The surface tension of the solution may be obtained from equation (25). We shall again assume that the liquid is close-packed and that the sizes of the two molecular species are identical. We then have

$$\begin{aligned}
 F^s = & \frac{1}{2}Z'(n_{1s}\epsilon_{11} + n_{2s}\epsilon_{22}) - n_{1s}kT \ln \phi_{1s}J_{1s} - n_{2s}kT \ln \phi_{2s}J_{2s} \\
 & + n_{1s}kT \ln x_{1s} + n_{2s}kT \ln x_{2s} \\
 & + (\nu - 1)[\frac{1}{2}Z_B(n_{1\epsilon_{11}} + n_{2\epsilon_{22}}) - n_1kT \ln \phi_1J_1 - n_2kT \ln \phi_2J_2 \\
 & + n_1kT \ln x_1 + n_2kT \ln x_2] \\
 & - \nu[\frac{1}{2}Z_B(n_{1\epsilon_{11}} + n_{2\epsilon_{22}}) - n_1kT \ln \phi_1J_1 - n_2kT \ln \phi_2J_2 \\
 & + n_1kT \ln x_1 + n_2kT \ln x_2] \quad (27)
 \end{aligned}$$

The value of  $F^s$  is independent of the position of the geometrical surface  $BB'$  so long as it is drawn in the homogeneous region. The potentials in the bulk phase are given by

$$\mu_1 = \frac{\partial F_B}{\partial n_1} = \frac{1}{2}Z_B \epsilon_{11} - kT \ln \phi_1J_1 + kT \ln x_1 \quad (28)$$

$$\mu_2 = \frac{\partial F_B}{\partial n_2} = \frac{1}{2}Z_B \epsilon_{22} - kT \ln \phi_2J_2 + kT \ln x_2 \quad (29)$$

The surface excesses of molecules of species (1) and (2) are

$$n_1^s = n_{1s} - n_1 \quad (30)$$

$$n_2^s = n_{2s} - n_2 \quad (31)$$

These values of  $F^s$ ,  $\mu_1$ ,  $\mu_2$ ,  $n_1^s$  and  $n_2^s$  may be substituted in equation (25), when we obtain

$$\begin{aligned}
 \gamma A = & \frac{1}{2}(Z' - Z_B)(n_{1s}\epsilon_{11} + n_{2s}\epsilon_{22}) - n_{1s}kT \ln \frac{\phi_{1s}J_{1s}}{\phi_1J_1} \\
 & - n_{2s}kT \ln \frac{\phi_{2s}J_{2s}}{\phi_2J_2} - n_{1s}kT \ln \frac{x_{1s}}{x_1} - n_{2s}kT \ln \frac{x_{2s}}{x_2} \quad (32)
 \end{aligned}$$

which is identical with equation (11). Further, we may define the potential of species (1) and (2) in the surface layer in a manner analogous to their definitions in the bulk; thus

$$\mu_1^\sigma = \frac{\partial F^\sigma}{\partial n_1^\sigma} = \gamma a + \mu_1 \quad (33)$$

$$\mu_2^\sigma = \frac{\partial F^\sigma}{\partial n_2^\sigma} = \gamma a + \mu_2 \quad (34)$$

in which the superscript  $\sigma$  refers to the surface phase.\* In order to obtain  $\mu_1^\sigma$  and  $\mu_2^\sigma$ , the free energy of the surface phase must be differentiated with respect to the total number of molecules of species (1) and of species (2) in it. Their values must be independent of the position of the geometrical surface  $BB'$ ; if this plane is drawn to include another layer of molecules, the free energy of this layer must be added to  $F^\sigma$  and the differentiation carried out with respect to  $n_1$  and to  $n_2$  more molecules of species (1) and (2). If we denote the various layers by 1, 2 etc., then

$$\mu_1^\sigma = \frac{\partial F_{1+2}^\sigma}{\partial (n_{1s} + n_1)} = \frac{\partial F_{1+2+3}^\sigma}{\partial (n_{1s} + 2n_1)} = \text{etc.}$$

We may therefore write

$$\mu_1^\sigma = \frac{1}{2}Z' \epsilon_{11} - kT \ln \phi_{1s}J_{1s} + kT \ln x_{1s} \quad (35)$$

$$\mu_2^\sigma = \frac{1}{2}Z' \epsilon_{22} - kT \ln \phi_{2s}J_{2s} + kT \ln x_{2s} \quad (36)$$

\*  $F^\sigma$  here is the free energy involved in the formation of the surface layer on a surface of the same composition as the bulk; that is the potential energy is that between molecules in the surface layer plus the energy of interaction between this layer and the layer below it.



Hence

$$\begin{aligned}\gamma a &= \frac{1}{2}(Z' - Z_B)\epsilon_{11} - kT \ln \frac{\phi_{1S} J_{1S}}{\phi_{1I} J_1} + kT \ln \frac{x_{1S}}{x_1} \quad (37) \\ &= \frac{1}{2}(Z' - Z_B)\epsilon_{22} - kT \ln \frac{\phi_{2S} J_{2S}}{\phi_{2I} J_2} + kT \ln \frac{x_{2S}}{x_2}\end{aligned}$$

from which

$$\gamma = \gamma_1^0 + \frac{kT}{a} \frac{x_{1S}}{x_1} = \gamma_2^0 + \frac{kT}{a} \frac{x_{2S}}{x_2} \quad (38)$$

### The Gibbs Adsorption Equation.

We must now show that these results are consistent with equation (26), which is the Gibbs adsorption equation. From equations (26), (28) and (29) we obtain

$$\begin{aligned}\frac{d\gamma}{dx_1} &= -\frac{(n_1^S - n_1)kT}{A} \frac{1}{x_1} + \frac{(n_2^S - n_2)kT}{A} \frac{1}{x_2} \\ &= \frac{kT}{a} \left[ \frac{x_{1S}}{x_1} - \frac{x_{2S}}{x_2} \right] \\ &= \frac{kT}{a} \left[ \frac{c - 1}{1 - (c - 1)x_1} \right] \quad (39)\end{aligned}$$

which is the value obtained by differentiation of equation (37) with respect to  $x_1$ . If we adopt the usual convention and put  $n_1^S = 0$  then

$$-d\gamma = \Gamma_{2(1)} d\mu_2 = \Gamma_{2(1)} kT d \ln x_2 \quad (40)$$

where  $\Gamma_{2(1)}$  is the value of  $n_2^S/A$  on this convention. The physical significance of  $\Gamma_{2(1)}$  is given by equations (39) and (40) from which

$$\Gamma_{2(1)} = \frac{1}{A} [n_{2S} - n_{1S} n_2/n_1] \quad (41)$$

This result may, of course, be obtained directly from equation (26). The value of  $\Gamma_{1(2)}$ , i.e. on the convention that  $\Gamma_2 = 0$  may be obtained in a similar manner. It may be noted that on the assumptions we have made about the nature of the surface phase, it is not possible to draw the dividing surface  $S$  in such a way that the value of  $n_1^S$  is zero unless that of  $n_2^S$  is also zero. The number of molecules per unit area in the surface layer may be calculated from equations (41) and (14); thus

$$\frac{n_{1S}}{A} = [1 - \Gamma_{2(1)} a] \frac{x_1}{a} \quad (42)$$

$$\frac{n_{2S}}{A} = [1 - \Gamma_{1(2)} a] \frac{x_2}{a} \quad (43)$$

We have calculated the values of  $n_{1S}$  and  $n_{2S}$  (given in molecules per sq. cm.  $\times 10^{-14}$ ) for a number of mixtures from these relations and we have tabulated them in Table II.

The application of the Gibbs method of treatment to systems in which the discontinuity is restricted to a single layer of molecules has been developed by Butler,<sup>3</sup> who showed by purely thermodynamic methods that the surface tension of a solution is given by equation (38), which, when the solution is not perfect, may be written

$$\gamma = \gamma_1^0 + \frac{kT}{a} \ln \frac{x_{1S} f_{1S}}{x_1 f_1} \quad (44)$$

where  $f$  denotes the appropriate activity coefficient.

The special case in which  $n_1^S$  and  $n_2^S$  are zero is of interest, that is when the composition of the surface layer is identical with that of the bulk ( $x_{1S} = x_1$ ;  $x_{2S} = x_2$ ). The surface tension of a mixture of any composition is then equal to those of the pure components, and further this can occur only when the surface tensions of the components are the same.

<sup>3</sup> Butler, *Proc. Roy. Soc. A*, 1932, 135, 348.

### Extension to the Case of Unequal Molecular Areas.

In the foregoing treatment we have assumed that the molecular areas of the two species are the same. This restriction is, however, not included in the attributes of a perfect solution given on page 1, and it has been shown<sup>1</sup> that conditions (a) and (d) may hold simultaneously even if the ratio of the molecular diameters is as great as 1.26; thus a variation of the ratio of the molecular areas between 1 and 1.59 is possible. The case treated here is that of a perfect solution in which the molar volumes of the components are not the same. As the volume of such a solution is given by  $x_1 V_1 + x_2 V_2$ , so the area of a layer is given by  $x_1 a_1 + x_2 a_2$  in the bulk and  $x_{1s} a_{1s} + x_{2s} a_{2s}$  in the surface. The contribution of the mixing terms to the free energy will be that of a perfect solution. It must be remembered that we are concerned with unit areas (*cf.* equation (46)) not molar areas.

The total potential energy change involved in surface formation is given by the sum of equations (5) and (9) as before

$$\frac{1}{2}(Z' - Z_B)(n_{1s}\epsilon_{11} + n_{2s}\epsilon_{22}) + \frac{1}{2}(Z' - Z_B)(n_{1\epsilon_{11}} + n_{2\epsilon_{22}})(1 - \alpha) \quad (45)$$

but  $\alpha$  is not now equal to unity. Let us denote the effective areas of molecules of the two species in the surface layer by  $a_{1s}$  and  $a_{2s}$  respectively; these will be different from those in the bulk,  $a_1$  and  $a_2$ , and will be regarded as independent of  $x_{1s}$  and  $x_{2s}$ . We shall also have

$$n_1 a_1 + n_2 a_2 = n_{1s} a_{1s} + n_{2s} a_{2s} \quad (46)$$

We cannot now replace the  $\phi'J'$  terms in the second layer by the bulk terms  $\phi J$  when the surface layer is added. We shall assume that the fraction of the  $\phi'J'$  terms which may be so replaced is the fraction of the surface covered, and that for the fraction of the surface which remains uncovered these terms may be replaced by  $\phi_s J_s$  terms. The fraction of the molecular species (1) or of species (2) in the second layer that will be covered is

$$(n_{1s}x_1 + n_{2s}x_2 + n_{1s}x_2 + n_{2s}x_1)/(n_1 + n_2)$$

i.e.  $\alpha$ , while the fraction remaining uncovered will be  $(1 - \alpha)$ . In the process of surface formation the fraction covered will suffer no change in their  $\phi J$  terms, while for those uncovered the terms will change from  $\phi J$  to  $\phi_s J_s$ . The free energy change involved in surface formation is then

$$\begin{aligned} \Delta F = & \frac{1}{2}(Z' - Z_B)(n_{1s}\epsilon_{11} + n_{2s}\epsilon_{22}) + \frac{1}{2}(Z' - Z_B)(n_{1\epsilon_{11}} + n_{2\epsilon_{22}})(1 - \alpha) \\ & - n_{1s}kT \ln \frac{\phi_{1s}J_{1s}}{\phi_1J_1} - n_{2s}kT \ln \frac{\phi_{2s}J_{2s}}{\phi_2J_2} - n_1(1 - \alpha)kT \ln \frac{\phi_{1s}J_{1s}}{\phi_1J_1} \\ & - n_2(1 - \alpha)kT \ln \frac{\phi_{2s}J_{2s}}{\phi_2J_2} + n_{1s}kT \ln \frac{x_{1s}}{x_1} + n_{2s}kT \ln \frac{x_{2s}}{x_2} \quad (47) \end{aligned}$$

The conditions of equilibrium are now :

$$\begin{aligned} \text{(i)} \quad \frac{\partial \Delta F}{\partial n_{1s}} = & \Delta F_1^0 + kT \ln \frac{x_{1s}}{x_1} - \frac{1}{2}(Z' - Z_B)\epsilon_{11}x_1 - \frac{1}{2}(Z' - Z_B)\epsilon_{22}x_2 \\ & + x_1kT \ln \frac{\phi_{1s}J_{1s}}{\phi_1J_1} + x_2kT \ln \frac{\phi_{2s}J_{2s}}{\phi_2J_2}, \\ \frac{\partial \Delta F}{\partial n_{2s}} = & \Delta F_2^0 + kT \ln \frac{x_{2s}}{x_2} - \frac{1}{2}(Z' - Z_B)\epsilon_{11}x_1 - \frac{1}{2}(Z' - Z_B)\epsilon_{22}x_2 \\ & + x_1kT \ln \frac{\phi_{1s}J_{1s}}{\phi_1J_1} + x_2kT \ln \frac{\phi_{2s}J_{2s}}{\phi_2J_2}, \end{aligned}$$

from which

$$\begin{aligned} \delta \Delta F = & \left( \Delta F_1^0 + kT \ln \frac{x_{1s}}{x_1} - x_1 \Delta F_1^0 - x_2 \Delta F_2^0 \right) \delta n_{1s} \\ & + \left( \Delta F_2^0 + kT \ln \frac{x_{2s}}{x_2} - x_1 \Delta F_1^0 - x_2 \Delta F_2^0 \right) \delta n_{2s} = 0 \quad (48) \end{aligned}$$

$$\text{(ii)} \quad a_{1s} \delta n_{1s} + a_{2s} \delta n_{2s} = 0 \quad (49)$$

Combining these two we obtain

$$\Delta F_2^0 + kT \ln \frac{x_{2s}}{x_2} = \left( \Delta F_1^0 + kT \ln \frac{x_{1s}}{x_1} - x_1 \Delta F_1^0 - x_2 \Delta F_2^0 \right) \frac{a_{2s}}{a_1} + x_1 \Delta F_1^0 + x_2 \Delta F_2^0,$$

and substituting this value in equation (47)

$$\Delta F = \frac{A}{a_{1s}} \Delta F_1^0 + \frac{A}{a_{1s}} kT \ln \frac{x_{1s}}{x_1} + (x_1 \Delta F_1^0 + x_2 \Delta F_2^0) \left[ \frac{(n_1 + n_2)a_1 - (n_{1s}a_{1s} + n_{2s}a_{2s})}{a_{1s}} - 1 \right] \quad (50)$$

Thus

$$\begin{aligned} \gamma &= \frac{\Delta F}{A} = \frac{\Delta F_1^0}{a_{1s}} + \frac{kT}{a_{1s}} \ln \frac{x_{1s}}{x_1} + (x_1 \Delta F_1^0 + x_2 \Delta F_2^0) \left[ \frac{n_1 + n_2}{n_{1s}a_{1s} + n_{2s}a_{2s}} - \frac{1}{a_{1s}} \right] \\ &= \gamma_1^0 + \frac{kT}{a_{1s}} \ln \frac{x_{1s}}{x_1} + \frac{a_1 - a_{1s}}{a_{1s}} \left( \gamma_1^0 + \frac{kT}{a_1} \ln \frac{x_{1s}}{x_1} \right) \\ &\quad + (x_1 \gamma_1^0 + x_2 \gamma_2^0) \left[ \frac{n_1 + n_2}{n_1 a_1 + n_2 a_2} - 1 \right] \frac{a_1}{a_{1s}} \\ &= \gamma_1^0 + \frac{kT}{a_{1s}} \ln \frac{x_{1s}}{x_1} + \beta \quad \quad \quad (51) \end{aligned}$$

The sign of  $\beta$  will depend on the relative values of  $a_1$ ,  $a_{1s}$  and  $a_2$ . It must be emphasised that equation (51) applies to an ideal solution, and pointed out that the term  $\beta$  is absent from equation (44) derived thermodynamically by Butler. This term cannot, of course, be written as an activity coefficient, either  $f_{1s}$  or  $f_1$ , both of which in this case must be equal to unity. We shall discuss this equation further when we consider experimental data.

### Application to Experimental Data.

Equation (22) gives the surface tension of an ideal liquid mixture in terms of the surface tensions of the pure components and the composition. It may be noted that when  $\gamma_1^0 = \gamma_2^0$ ,  $c = 1$ , and the curve is then a horizontal line; when  $\gamma_1^0 \simeq \gamma_2^0$  the curve is approximately a straight line joining the surface tension values of the pure components, and equation (22) reduces to the simple mixture law,

$$\gamma = \gamma_1^0 x_1 + \gamma_2^0 x_2.$$

As equation (22) applies to ideal solutions, and as the components of these are usually closely related substances, the surface tensions of which are not far apart, we should expect the simple mixture law to apply in such cases. An examination of the available data shows that equation (22) gives good agreement with the experimental values when the mixtures are ideal, but that discrepancies are found when there is a departure from ideal behaviour.

We have collected these data in Table I, which we have divided into two parts. The table gives the mean area per molecule in  $\text{\AA}^2$  calculated, from density data, the surface tensions of the pure components in dynes/cm. the value of  $c$ , and in the last two columns the observed and calculated values of  $\gamma$  corresponding to a bulk mole fraction of 0.5. The agreement between the observed and calculated values is good for those mixtures in Part I of the table; methyl alcohol-ethyl alcohol at  $50^\circ$ , however, shows a discrepancy. The data of Kremann and Meingast are not so suitable for our purpose as those of the other authors. Their measurements were made with a view to finding the effect of temperature on the surface tension, and the  $\gamma - x$  curves plotted from their values are in many cases not smooth; the observed value given in these cases is the mean of the values for two mixtures for which the experimental error may be comparatively large.

TABLE I.

Mixture.	$T$ ( $^{\circ}\text{K}.$ ).	$a$ ( $\text{\AA}^2$ ).	$\Delta\gamma$ dyne/cm.	$c$ .	$\gamma_1^0$ dyne/cm.	$\gamma_2^0$ dyne/cm.	$\gamma_{\text{obs.}}$ dyne/cm.	$\gamma_{\text{calc.}}$ dyne/cm.
<b>Part I.</b>								
1 Benzene- <i>m</i> -Xylene <sup>4</sup> .	291.2	37.7	0.00	1.00	28.40	28.40	28.40	28.40
2 Methyl alcohol-Ethyl alcohol <sup>5</sup>	273	22.35	0.553	1.034	23.643	23.090	23.40	23.37
3 " "	303	22.84	0.303	1.016	21.058	20.756	20.91	20.91
4 " "	323	23.07	0.246	1.013	19.446	19.200	19.24	19.34
5 $\text{H}_2\text{O}-\text{D}_2\text{O}$ <sup>8</sup>	298	11.2	1.15	1.03	72.06	70.91	71.48	71.48
6 <i>m</i> -Xylene- <i>o</i> -xylene <sup>7</sup>	293	41.3	1.27	1.14	28.90	30.17	29.20	29.52
7 <i>m</i> -Xylene- <i>p</i> -xylene <sup>7</sup>	293	41.7	0.53	1.059	28.90	28.37	28.50	28.63
8 <i>o</i> -Xylene- <i>p</i> -xylene <sup>7</sup>	293	41.5	1.80	1.204	30.17	28.37	—	29.22
9 Chlorobenzene-bromobenzene <sup>7</sup>	293	37.0	3.49	1.380	33.11	36.60	34.65	34.72
<b>Part II.</b>								
10 Benzene-Toluene <sup>4</sup>	291.2	44.8	0.34	1.039	28.40	28.05	28.15	28.22
11 Benzene-chloroform <sup>4</sup>	291.2	32.45	1.58	1.141	28.40	26.82	27.30	27.60
12 Benzene-carbon tetrachloride <sup>6</sup>	323	44.0	2.00	1.218	22.98	24.98	23.73	23.92
13 Benzene-ethyl alcohol <sup>4</sup>	298	28.2	6.118	1.52	27.263	21.145	23.65	23.90
14 Benzene-ethylene dichloride <sup>4</sup>	287	26.0	3.22	1.234	29.65	32.87	30.50	31.15
15 Chloroform-acetone <sup>4</sup>	291.2	30.0	3.58	1.31	23.75	27.33	25.64	25.46
16 Chloroform-ether <sup>4</sup>	291.2	30.0	9.83	2.10	27.33	17.50	20.82	21.74
17 Acetone-Carbon disulphide <sup>4</sup>	287	26.0	8.80	1.79	33.19	24.39	25.40	28.1

The data of Part II of the table do not show such good agreement between the observed and calculated values. These discrepancies may arise from several causes: the mixtures may not be ideal in their behaviour, they may not pack in the way we have postulated, the areas of the molecules in the surface may not be identical, nor may they be the same as those calculated from the density of the bulk, there may be a heat of mixing term, and finally the discontinuity between the phases may not be restricted to a single layer of molecules at the surface. All these effects may be simultaneously operative in producing a divergence from equation (22). The unreliability of the experimental data in some cases makes it difficult to decide how closely a mixture approximates to an ideal system. Table III, which is taken largely from Hildebrand,<sup>9</sup> gives some data for these mixtures which show their deviations from ideal laws

<sup>4</sup> Whatmough, *Z. physik. Chem.*, 1902, **39**, 129.

<sup>5</sup> Morgan and Scarlett, *J. Amer. Chem. Soc.*, 1917, **39**, 2275.

<sup>6</sup> Belton, *Trans. Faraday Soc.*, 1935, **31**, 1642.

<sup>7</sup> Kremann and Meingast, *Sitz. b. Akad. Wiss. Wien*, 1914, **123**, 821.

<sup>8</sup> Jones and Ray, *J. Chem. Physics*, 1937, **5**, 505.

<sup>9</sup> Hildebrand, *Solubility of Non-Electrolytes*, p. 60.

at temperatures not far removed from those of the surface tension data ; it gives the difference between the observed and calculated surface tensions ( $\Delta\gamma$ ), the deviation per cent. from Raoult's law (R. Law %), the change in volume per cent. on mixing ( $\Delta V$  %), and the heat effect per mole on mixing ( $\Delta H$ ). The signs of these differences are such that the curves calculated from equation (22) are in all these cases closer to the straight line joining the surface tensions of the pure components. It is of interest to note that in all the examples quoted, the observed surface tension lies below that calculated ; this is so for mixtures 16 and 17 in which the deviations from Raoult's law and the heat of mixing are comparatively large values of opposite sign. This is, however, not universally

TABLE II.

Mixture.	1.		2.		3.		4.		5.		6.	
$x_1$ .	$n_{1s}$ .	$n_{2s}$ .	$n_{1s}$ .	$n_{2s}$ .	$n_{1s}$ .	$n_{2s}$ .	$n_{1s}$ .	$n_{2s}$ .	$n_{1s}$ .	$n_{2s}$ .	$n_{1s}$ .	$n_{2s}$ .
0	0	2.65	0	4.47	0	4.38	0	4.34	0	8.93	0	2.42
0.1	0.26	2.38	0.45	4.03	0.44	3.94	0.44	3.90	1.03	7.90	0.27	2.15
0.3	0.80	1.86	1.37	3.10	1.33	3.05	1.32	3.02	2.73	6.20	0.80	1.42
0.5	1.33	1.33	2.27	2.20	2.21	2.77	2.19	2.45	4.43	4.40	1.28	1.14
0.7	1.86	0.80	3.16	1.31	3.08	1.30	3.05	1.29	6.31	2.62	1.76	0.66
0.9	2.38	0.26	4.04	0.43	3.45	0.43	3.91	0.43	8.06	0.87	2.21	0.21
1.0	2.68	0	4.47	0	4.38	0	4.34	0	8.93	0	2.42	0

Mixture.	7.		8.		9.		10.		11.		12.	
$x_1$ .	$n_{1s}$ .	$n_{2s}$ .	$n_{1s}$ .	$n_{2s}$ .	$n_{1s}$ .	$n_{2s}$ .	$n_{1s}$ .	$n_{2s}$ .	$n_{1s}$ .	$n_{2s}$ .	$n_{1s}$ .	$n_{2s}$ .
0	0	2.40	0	2.41	0	2.70	0	2.23	0	3.08	0	2.29
0.1	0.25	2.15	0.28	2.13	0.36	2.34	0.23	2.00	0.33	2.75	0.27	2.00
0.3	0.75	1.45	0.42	1.59	1.09	1.70	0.69	1.54	1.01	2.07	0.78	1.49
0.5	1.23	1.17	1.32	1.09	1.56	1.14	1.14	1.04	1.49	1.49	1.26	1.01
0.7	1.71	0.64	1.78	0.63	2.06	0.64	1.38	0.65	2.24	0.84	1.68	0.59
0.9	2.17	0.23	2.21	0.20	2.50	0.20	2.01	0.22	2.81	0.27	2.08	0.10
1.0	2.40	—	2.41	0	2.70	0	2.23	0	3.08	0	2.27	0

true ; mixtures of methyl alcohol and ethyl iodide and of acetic acid and pyridine, which show minima in their vapour pressure composition curves, show surface tensions greater than those calculated from the simple mixture law. The case of acetone-chloroform is interesting in that although it shows wide deviations from Raoult's law (a minimum in the vapour pressure composition curve) the surface tensions of mixtures follow the simple mixture law and are greater than those calculated from equation (22). The system ethylene dibromide-propylene dibromide follows Raoult's law, but the surface tension curve is again below the straight line by about 0.5 dyne/cm. at a mole fraction 0.5.\*

\* Yajnik, Shurma and Bharadwaj (*J. Ind. Chem. Soc.* III, 63, 1926) have given data in support of the view that when Raoult's law is obeyed the surface tension curve is a straight line, when the deviation from Raoult's law is positive that of the surface tension is negative and vice versa. Their data are recorded in terms of volume per cent. and do not in all cases give smooth curves. Although ethylene dibromide-propylene dibromide and benzene-ethylene chloride mixtures both obey Raoult's law, the surface tension-mole fraction curve is well below the straight line of the simple mixture law in both cases.

TABLE III.

Mixture.	$\Delta\gamma$ .	$c$ .	R. Law %.	$\Delta V\%$ .	$\Delta H$ .
Benzene—Toluene . . . .	0.07	1.342	+9	+0.16	- 19
Chloroform . . . . .	0.30	1.418	-0.6	—	+ 97
Carbon tetrachloride . . .	0.19	—	+3.5	0.06	- 18
Ethyl alcohol . . . . .	0.35	1.52	+60	-0.01	-350
Ethylene dichloride . . .	0.65	1.23	0	+0.34	- 10
Chloroform—Acetone . . .	-0.1	1.25	-26	-0.23	+459
Ether . . . . .	0.88	1.86	-71	-1.5	+650
Acetone—Carbon disulphide .	3.2	1.79	+35	+1.6	- 9

Deviations from equation (22) caused by a difference in the area of the molecules of the two species are given by equation (51). We may calculate the value of the term  $\beta$  for the special case in which the areas in the surface and the bulk are the same ( $a_1 = a_{1s}$ ,  $a_2 = a_{2s}$ ) and for a bulk mole fraction  $x_1 = x_2 = 0.5$ ; then

$$\beta = \frac{1}{2}(\gamma_1^0 + \gamma_2^0) \frac{a_1 - a_2}{a_1 + a_2} . . . . . (52)$$

We may note that in this case  $(n_{1s} - n_1)a_1 = (n_2 - n_{2s})a_2$  but

$$(n_{1s} + n_{2s}) \neq n_1 + n_2.$$

When  $a_1 = a_2$  then  $\beta = 0$ . Thus in the mixture heavy water-water,  $\gamma_1^0 = \gamma_{D_2O} = 70.91$ ,  $\gamma_2^0 = 72.06$  dynes/cm.,  $a_1 = 11.2A^2$ ,  $a_2 = 11.55A^2$  and  $\beta = -1.1$  dyne/cm. In the mixture methyl alcohol-ethyl alcohol at  $0^\circ C$ ,  $\gamma_1^0 = 23.090$ ,  $\gamma_2^0 = 23.643$  dynes/cm.,  $a_1 = 11.52A^2$ ,  $a_2 = 89.7A^2$ , from which  $\beta = 2.9$  dyne/cm.

The value of  $x_{1s}$ , however, will be different from those calculated from equation (20). The value corresponding to equation (51) is given by (48) and (49)

$$\left(\frac{x_{1s}}{x_1}\right)^{a_2} \left(\frac{x_2}{x_{2s}}\right)^{a_1} = \exp. \frac{x_1 a_1 (\Delta F_2^0 - \Delta F_1^0) + x_2 a_2 (\Delta F_2^0 - \Delta F_1^0)}{kT} \quad (53)$$

For  $x_1 = x_2 = 0.5$ , we have

$$\frac{(2x_{2s})^{a_2}}{[2(1 - x_{1s})]^{a_1}} = \exp. \frac{(a_1 + a_2)(\gamma_2^0 a_2 - \gamma_1^0 a_1)}{2kT} . . . . . (54)$$

The value so calculated for the heavy water-water mixture is  $x_{1s} = 0.515$  which gives

$$\gamma = 70.91 + 0.74 - 1.1 = 70.55 \text{ dynes/cm.}$$

For the methyl alcohol-ethyl alcohol mixture  $x_{1s} = 0.19$  which gives

$$\gamma = 23.090 - 3.3 + 2.9 = 22.89 \text{ dynes/cm.}$$

The agreement with the observed value is poor compared with that given by equation (22). We must conclude therefore that either (a) the effective areas  $a_1$  and  $a_2$  in the surface are identical even though those calculated from the molar volumes of the pure components are different,\* or (b) the areas in the surface are different from those in the bulk, in which case we have no means of calculating  $x_{1s}$ ,  $x_{2s}$ ,  $a_{1s}$  and  $a_{2s}$  independently.

\* In the tabulated values we have used the mean area of the two components calculated in this way. It would now appear that a better method would have been to calculate the mean area from the molar volume of the mixture; values so calculated, however, are very little different from those used.

## Summary.

The free energy of surface formation and the surface tensions of ideal binary mixtures have been calculated by a statistical method. The treatment is discussed in relation to the thermodynamic theory of surfaces of discontinuity of Gibbs, and is extended to include regular solutions. Good agreement with the available experimental data is found for ideal mixtures; the deviations of non-ideal mixtures are discussed.

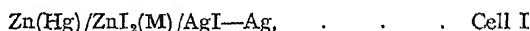
*Physical Chemistry Department,  
The University, Leeds 2.*

# A THERMODYNAMIC STUDY OF BIVALENT METAL HALIDES IN AQUEOUS SOLUTION. PART XI. THE OSMOTIC AND ACTIVITY COEFFICIENTS OF ZINC IODIDE AT 25°.

By R. H. STOKES.\*

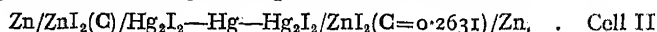
*Received 17th April, 1944.*

The thermodynamic properties of zinc iodide solutions have only recently been the subject of precise measurement. In 1938 Bates<sup>1</sup> made extensive measurements of the e.m.f. of the cell:



at concentrations between 0.005 and 0.8 molal (M) and over the temperature range 5°-40°. From these measurements he derived the standard potential of the Zn electrode, the activity coefficient and the relative partial molal heat content and specific heat of zinc iodide.

In 1943 Egan and Partington<sup>2</sup> reported measurements of the cell:



E.m.f.s were determined at 25° and 35° over the concentration range 0.002 to 0.26 molar (C). Similar measurements by Baxter<sup>3</sup> were quoted by Egan and Partington; these were at 25° and covered the concentration range 0.005 to 0.25 molar. A double cell of this type does not enable a determination of the standard electrode potential to be made but, by suitable computation, it does give values of the activity coefficient.

If the experimental measurements of Bates, Egan and Partington, and Baxter are consistent, the e.m.f.s of Cells I and II, containing the same molality of  $\text{ZnI}_2$ , should differ by an amount independent of the molality, the difference depending only on the standard potential of Cell I, the potential of the right hand half cell of II and the  $\text{Ag}-\text{AgI}$  and  $\text{Hg}-\text{Hg}_2\text{I}_2$  potentials. The same is true of the quantity  $(E + 3k \log M)$  where  $k = 2.303RT/2F$ .

By converting molar (C) to molal (M) concentration units and comparing the three values of  $(E + 3k \log M)$  it may be shown that the three sets of data are consistent up to a concentration of 0.05 M. Above this concentration, although the measurements of Baxter and of Egan and Partington on the same type of cell are in agreement, there is a large discrepancy with the determinations of Bates, amounting to almost 50 mv. at 0.25 M. Corresponding to this difference in e.m.f. the data of

\* Communicated by Dr. R. A. Robinson.

<sup>1</sup> Bates, *J. Amer. Chem. Soc.*, 1938, 60, 2983.

<sup>2</sup> Egan and Partington, *J. Chem. Soc.*, 1943, 157.

<sup>3</sup> Thesis, London University, 1939.

Egan and Partington give the extremely high activity coefficient at 0.25 M. of approximately 2.0 in contrast to a value of the order of 0.56 obtained by Bates. Since the normal experimental error in cells of this type should not be more than 0.1 or 0.2 mv. the discrepancy is serious, and an independent check of the data by another method is clearly desirable. We have now completed a series of isopiestic vapour pressure measurements on  $\text{ZnI}_2$  at 25° over the concentration range 0.1 to 2.5 M.

**Experimental.**— $\text{ZnI}_2$  was prepared by reaction between A.R. zinc and A.R. iodine under distilled water in a stream of  $\text{H}_2$ , the mixture being raised to the boiling point in order to complete the reaction. An excess of Zn remained and the solution precipitated basic salt on cooling. This was redissolved by the addition of a small amount of pure HI solution freshly decolourised by Zn, and the solution was allowed to stand over metallic Zn in an atmosphere of  $\text{H}_2$  for some days. It was then boiled again and no precipitate was observed on cooling. This stock solution was analysed gravimetrically for Zn as  $\text{ZnNH}_4\text{PO}_4$  and for I as  $\text{AgI}$ , the results indicating a stoichiometric ratio of Zn : I = 1.002 : 2.000. The solution was stored under  $\text{H}_2$  in a saturator flask from which it was driven out by  $\text{H}_2$  pressure as required. It remained clear and colourless throughout, and a further set of analyses towards the end of the work showed that there had been no change in composition.

Weighed portions of this stock solution were equilibrated with KCl in the usual apparatus.<sup>4</sup> The  $\text{ZnI}_2$  solutions were contained in Pt crucibles

TABLE I.—ISOPIESTIC MOLALITIES AT 25°.

$M\text{ZnI}_2$	$M\text{KCl}$
0.1052	0.1540
0.1244	0.1836
0.1458	0.2173
0.3055	0.4877
0.3660	0.6002
0.4968	0.8616
0.5181	0.9066
0.7138	1.346
0.8570	1.674
0.9435	1.881
1.124	2.289
1.228	2.517
1.343	2.770
1.520	3.122
1.709	3.477
1.833	3.704
2.050	4.077
2.099	4.151
2.513	4.810

TABLE II.—VAPOUR PRESSURES OF ZINC IODIDE SOLUTIONS AT 25° (IN MM. HG.).

Isopiestic.		Bates (e.m.f.).		Egan and Partington (e.m.f.).	
$M$ .	$p_0 - p$ .	$M$ .	$(p_0 - p)$ .	$M$ .	$(p_0 - p)$ .
0.1052	0.120	0.07441	0.085	0.0486	0.0557
0.1244	0.143	0.1224	0.142	0.0691	0.100
0.1458	0.169	0.1771	0.209	0.0827	0.125
0.3055	0.373	0.3289	0.402	0.1009	0.164
0.3660	0.457	0.4176	0.535	0.1229	0.210
0.4968	0.653	0.8008	1.169	0.1350	0.233
0.5181	0.687			0.1694	0.311
0.7138	1.019			0.1964	0.369
0.8570	1.268			0.2243	0.435
				0.2669	0.535

or in square Pt dishes, and the KCl in Ag dishes. A few points were run using the hydrogen-vacuum technique used for ferrous chloride and described in Part VIII of this series.<sup>5</sup> It was found, however, that no

<sup>4</sup> Robinson and Sinclair, *J. Amer. Chem. Soc.*, 1934, 56, 1830.

<sup>5</sup> Stokes and Robinson, *Trans. Faraday Soc.*, 1941, 37, 419.



detectable oxidation occurred if the dishes containing the  $\text{ZnI}_2$  solutions were weighed quickly and placed in the desiccator, which was then evacuated and "rinsed" with  $\text{H}_2$  several times in succession before the final evacuation. As this simpler method eliminated the tedious and less accurate analysis of each equilibrium solution, it was adopted for the remainder of the work.

In Table I are recorded the molalities of the isopiestic pairs of solutions, the KCl molality being the second of each pair. Agreement between duplicate dishes was of the order of 0.1 %. Molalities of  $\text{ZnI}_2$  were based on the iodide analyses.

### Discussion.

**Vapour Pressure of Zinc Iodide Solutions.**—Whilst the calculation of activity coefficients is complicated by the question of the value to be

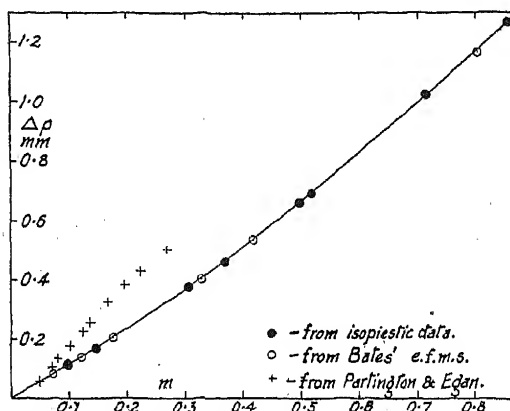


Fig. 1. Vapour pressure lowerings of zinc iodide solutions at 25°

assigned to the most dilute solution accessible to the isopiestic technique, and hence depends upon the accuracy of the e.m.f. measurements below this concentration, as well as upon the correctness of the extrapolation for the standard potential, the osmotic coefficients and vapour pressures are not open to this objection. Consequently it was decided to use the vapour pressures in the comparison of the isopiestic and e.m.f. results. Table II gives the vapour pressure lowerings of  $\text{ZnI}_2$  solutions calculated from the isopiestic data in Table I together with the osmotic coefficients of KCl given by Robinson and Harned.<sup>6</sup> Table II also gives the vapour pressure lowerings calculated from Bates' results. This calculation was made as follows. From the fundamental relations:

$$\bar{G}_2 = \bar{G}_2^0 - nF(E - E_0)$$

$$N_1 d\bar{G}_1 = -N_2 d\bar{G}_2$$

$$d\bar{G}_1 = RT \ln p/p_0$$

it follows that for a 1-2 salt at 25°

$$\log p/p_0 = 0.6091 \int_0^M M dE. \quad (1)$$

This integral may be evaluated with great ease by taking advantage of the fact that the graph of  $E$  versus  $\log M$  is almost a straight line. Substitution of  $z = (E + a \log M)$  gives:

$$\log p/p_0 = 0.6091 \int_0^M M dx - (0.6091/2.303)aM.$$

For this integration a value of  $a = 0.08325$  was found convenient. By

<sup>6</sup> Robinson and Harned, *Chem. Rev.*, 1941, 28, 439.

a suitable choice of the value of  $a$ ,  $\int M dx$  can be kept small enough for accurate graphical evaluation.

The last two columns of Table II contain values of the vapour pressures calculated in a similar way from the 25° results of Egan and Partington.

It must be emphasised that this method of calculating the vapour pressures from the e.m.f. results is the most direct possible, involving only the actual experimental data and the laws of thermodynamics. No appeal is made to any theory of strong electrolytes and no extrapolations are involved. The plots of these vapour pressure lowerings, shown in Fig. 1, reveal excellent agreement between the data of Bates and the present work, whilst the results calculated from the measurements of Egan and Partington are so markedly different as to suggest that at the higher concentrations their values are affected by some systematic error.

#### Osmotic Coefficients.—

These were calculated from the isopiestic data of Table I and the standard values for KCl. They are given in Table III.

#### Activity Coefficients.—

Since the isopiestic vapour pressure results have provided good evidence for the reliability of the e.m.f. data of Bates, his activity coefficient at 0.1224 M. may be taken as a reference value. It would be as well, however, to first consider the extrapolation of his data to yield the standard potential of the  $ZnI_2$  cell since this value is needed in the calculation of the activity coefficient.

TABLE III.—OSMOTIC AND ACTIVITY COEFFICIENTS OF ZINC IODIDE AT 25°.

$m.$	$\phi.$	$\gamma.$
0.1	0.893	0.581
0.125	0.901	0.572
0.15	0.907	0.565
0.2	0.921	0.559
0.3	0.957	0.566
0.4	0.997	0.585
0.5	1.039	0.612
0.6	1.084	0.648
0.7	1.126	0.686
0.8	1.164	0.727
0.9	1.199	0.769
1.0	1.227	0.809
1.2	1.267	0.880
1.4	1.288	0.938
1.6	1.295	0.982
1.8	1.294	1.017
2.0	1.289	1.043
2.2	1.282	1.065
2.5	1.269	1.089

Egan and Partington used a plot of  $(E + 3k \log C)$  against  $\sqrt{C}$ . This, however, is only reliable if there is a linear dependence of  $\log \gamma$  on  $\sqrt{C}$ . The La Mer, Gronwall and Greiff equation, which they also employed, is more satisfactory, but in the case of the large ions of  $ZnI_2$  it gives results which are experimentally indistinguishable from those of the simple Debye-Hückel form :

$$-\log f = \frac{0.5091 z_1 z_2 \sqrt{\mu}}{1 + 0.3286a \sqrt{\mu}} \quad (2)$$

where  $\mu$  is expressed in terms of molarities.

Thus if we put  $a = 6.33$  Å. we can reproduce by equation (2) the activity coefficients calculated by Egan and Partington from the La Mer, Gronwall and Greiff equation with a diameter of 6.1 Å. (column 9 of their Table IX). It is therefore clear that in this case at least there is nothing to be gained by the use of the more cumbersome La Mer form.

Equation (2), with an added term linear in  $\mu$ , has been shown to be capable of describing the activity coefficients of the alkali halides up to 1 M., and it may therefore be anticipated that it will also be satisfactory for 1:2 halides up to the same ionic strength, and therefore satisfactory for the extrapolation of the standard potential. This was the method

used by Bates. However, in view of the slight changes in the universal constants of equation (2), necessitated by Birge's <sup>7</sup> recent revision of these constants, we have recalculated the data of Bates using the extrapolation function :

$$E'_0 = E + k \log 4 + 3k \log M - 3k \left\{ \frac{1.0182 \sqrt{\mu}}{1 + 0.3286a \sqrt{\mu}} + \log (1 + 0.054M) \right\}.$$

We find that the value  $a = 6.0$  A. gives a satisfactorily linear extrapolation to  $E_0 = 0.61040$  volt which is only 0.1 mv. lower than Bates' value. The stoichiometric activity coefficients derived from this value of  $E_0$  and Bates' unsmoothed 25° e.m.f.s above 0.1 M. are given in Table IV, along with those calculated by the Debye-Hückel equation :

TABLE IV.—COMPARISON OF ACTIVITY COEFFICIENTS OF ZINC IODIDE AT 25°.

<i>M.</i>	Bates e.m.f.	Equation (3).	Isopiestic Data.
0.1224	0.572	0.571	(0.572)
0.1771	0.564	0.563	0.561
0.3289	0.568	0.573	0.570
0.4176	0.594	0.591	0.589
0.8008	0.736	—	0.727

$$-\log \gamma = \frac{1.018 \sqrt{\mu}}{1 + 1.972 \sqrt{\mu}} - 0.1105 \mu + \log (1 + 0.054M). \quad (3)$$

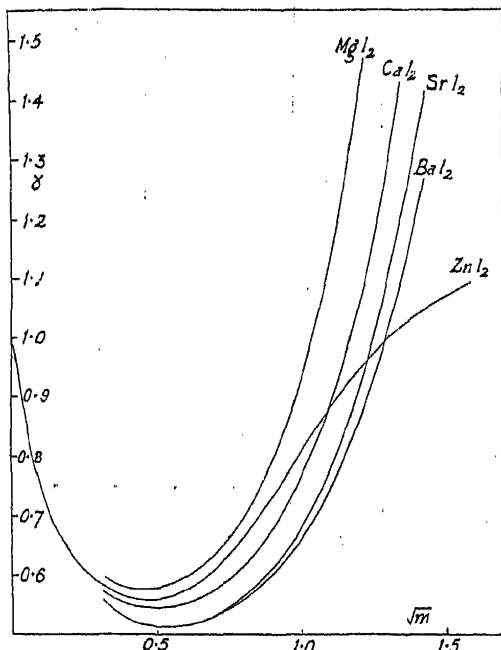


FIG. 2—Activity coefficients of Bivalent Metal Iodides at 25°

those for several other bivalent metal iodides. The curve follows the normal

Using the value of  $\gamma = 0.572$  at  $0.1224M$ , derived from e.m.f. data, as a reference value, activity coefficients have been computed from isopiestic data by the equation of Randall and White.<sup>8</sup> These are given at round molalities in Table III. Table IV gives  $\gamma$  values interpolated from the results of Table III at molalities corresponding to those quoted by Bates. The agreement with the results of Bates is satisfactory except at  $0.8008$  M. where the e.m.f. result may be affected by the solubility of  $AgI$  in the electrolyte. The agreement with the theoretical equation (3) is also satisfactory.

In Fig. 2 the activity coefficient curve for  $ZnI_2$  is compared with

<sup>7</sup> Birge, *Rev. Mod. Physics*, 1941, 13, 233.

<sup>8</sup> *J. Amer. Chem. Soc.*, 1926, 48, 2514.

pattern up to about 1 M., after which it begins to fall off and crosses the other curves. In this respect zinc iodide resembles zinc bromide and chloride, though the effect is least marked in the iodide. Experiments shortly to be published show that this effect is due to the formation of complex ions or to incomplete dissociation. In this connection it must be remarked that neither of these phenomena would explain abnormally high values, as was claimed by Egan and Partington, for these effects lower the activity coefficient as is exemplified in the case of the cadmium halides.<sup>9</sup>

A point of great interest in connection with the osmotic coefficients is that up to 0.5 M. the values for zinc iodide are almost coincident with those for magnesium iodide.<sup>10</sup> This is to be ascribed to the fact the cationic radii are nearly equal, the values for the unhydrated ions, derived from crystallographic data,<sup>11</sup> being 0.65 Å. for  $Mg^{++}$  and 0.74 Å. for  $Zn^{++}$ . Both ions may therefore be expected to hydrate to the same extent so that the observed similarity of the osmotic coefficients gives strong support for the view that the effective ion diameter is the chief factor governing the behaviour of these salts. That the resemblance is not found with the bromides and chlorides is explicable on the grounds that in zinc bromide and chloride complex or intermediate ion formation sets in at lower concentrations. In the absence of these disturbing effects, the chloride and bromide should show effective ion diameters between 5 and 6 Å., so that extrapolations using smaller diameters than this must be regarded with some uncertainty.

#### Summary.

Isopiestic vapour pressure measurements have been made on  $ZnI_2$  solutions at 25°. The values obtained for the vapour pressures and activity coefficients are consistent with the e.m.f. measurements of Bates but differ considerably from those of Egan and Partington. Up to an ionic strength of unity the activity coefficients are given within experimental error by the extended Debye-Hückel equation. There is evidence that complex ion formation begins to play a significant part in solutions more concentrated than 1 M.

Auckland University College,  
New Zealand.

<sup>9</sup> Robinson and Harned, *Chem. Rev.*, 1941, 28, 446.

<sup>10</sup> Robinson and Stokes, *Trans. Faraday Soc.*, 1940, 36, 733.

<sup>11</sup> Pauling, *Nature of the Chemical Bond*, Chap. X. Cornell University Press, Ithaca, New York, 1939.

---

## THE EFFECT OF SOLVENT TYPE ON THE VISCOSITY OF VERY DILUTE SOLUTIONS OF LONG CHAIN POLYMERS.

BY ELIZABETH M. FRITH.

Received 18th May, 1944.

### 1. Introduction.

The limiting intrinsic viscosity  $[\eta]^*$  of polymer solutions at zero concentration is known to depend on the solvent used. In general, solutions in "good" solvents (which we take to be those which interact with

\*  $[\eta]$  is the limiting value at infinite dilution of the ratio  $\eta_{sp}/c$  where  $\eta_{sp}$  is the specific viscosity of the solution. Throughout this paper  $\eta_{sp}/c$  is retained for all finite concentrations and  $[\eta]$  refers to this ratio at zero concentration only.

the polymer chain) give higher  $[\eta]$  values than solutions of polymers in "bad" solvents or solvent-precipitant mixtures where there is some sort of polymer solvent repulsion. A qualitative explanation of this effect has been given by Mark,<sup>1</sup> Huggins<sup>2</sup> and others: if the interaction energy  $w_{PS}$  between a polymer link P and a solvent molecule S is positive, when the energy scale is so defined that the corresponding energies  $w_{PP}$  and  $w_{SS}$  are zero, then P—P links will be preferred in solution to P—S contacts and the statistically kinked molecule will coil up more on itself. The most probable distance between the ends of the polymer molecule will therefore be decreased and the viscosity will be low. Conversely, if  $w_{PS}$  is less than zero, there is direct P—S interaction and the polymer molecule will tend to uncurl, forming in the extreme case a solvated hulk. Thus the average value of the distance between the molecular ends will be greater, and the viscosity of the solution higher than the corresponding values in an energetically indifferent solvent.

The exact connection between viscosity, molecular weight and the distance between chain ends is still obscure. Huggins<sup>2</sup> and Kuhn<sup>4</sup> have, however, shown that for perfectly flexible randomly kinked chains, the intrinsic viscosity  $[\eta]$  at zero concentration is proportional to the number of links in the chain. Further, if  $L_0$  is the distance between the chain ends,  $\overline{L_0^2}$  the mean square distance, statistical theory shows that  $\overline{L_0^2}$  is directly proportional to  $p$  the number of chain links, so that the intrinsic viscosity  $[\eta]$  is directly proportional to  $\overline{L_0^2}$ . Following Kuhn

$$\eta_{sp}/c \approx \frac{3\pi}{64} \frac{N}{1000} \cdot b \cdot \overline{L_0^2} \quad (1)$$

where  $c$  is the concentration of polymer in monomeric units per litre;  $b$  is the "effective hydrodynamic length of a link" and is equal to  $(\lambda \cos \frac{1}{2}\beta)$  where  $\beta$  is the valency angle and  $\lambda$  the actual monomeric spacing along the chain.  $N$  is Avogadro's number.

In the following sections we give a semi-quantitative interpretation of Mark's theory by considering, to a very crude approximation, the effect of a finite interaction energy on  $\overline{L_0^2}$ . To do this, in effect we have to calculate molecular distributions when certain orientations of the molecule are preferentially weighted. Using standard statistical results we are able to obtain a relationship between  $\eta_{sp}/c$  and  $w_{PS}$  in solutions of low, but still finite, concentrations. The exact extrapolation to zero concentration has not yet proved tractable, but we shall see how an effect will persist.

It follows from this method of approach that we consider only completely flexible polymers, of which rubber is the most typical. We necessarily exclude all completely crystalline polymers which will only go into solution when there are strong attractive forces between the polymer and the solvent. We consider only small deviations from random mixing due to small polymer solvent interactions. Gee and Treloar<sup>5</sup> have shown experimentally, for the system rubber-benzene, that the solubility is almost entirely due to a large increase of entropy. We consider only solutions of this type and calculate the effect of small heats of mixing as a corrective factor. Ultimately the approximation we use is equivalent to a solution with the randomness of mixing slightly altered by a small energy of interaction.

## 2. General Viscosity-Concentration Relationships.

The intrinsic viscosity ratio  $\eta_{sp}/c$  is not constant, but increases with the polymer concentration. Over the concentration range considered

<sup>1</sup> Alfrey Bartovics and Mark *J.A.C.S.*, 1942, 64, 1557.

<sup>2</sup> Huggins, *J. Applied Physics*, 1943, 14, 246.

<sup>3</sup> Huggins, *J. Physic. Chem.*, 1943, 43, 439.

<sup>4</sup> Kuhn and Kuhn, *Helv. Chim. Acta*, 1943, 26, 1394.

<sup>5</sup> Gee and Treloar, *Trans. Faraday Soc.*, 1942, 38, 147.

here (0.0-0.2 %) the increase is almost linear and we may write

$$\eta_{sp}/c = A + Bc \quad (2)$$

where  $A$  and  $B$  are constants. In a general way  $B$  represents the increasing resistance to flow imposed by the increase of the number of polymer-polymer contacts between separate chains. This is borne out by the fact that the slope of the  $\eta_{sp}/c - c$  curve is steeper for a high molecular weight polymer than for one of the same type but lower molecular weight. Huggins<sup>6</sup> has given a formula of the type

$$\eta_{sp}/c = [\eta] + k[\eta]^2c$$

where  $k$  is approximately unity, showing the greater sensitivity of the slope rather than the intercept of the viscosity/concentration-concentration curve towards molecular weight variations. This same sensitivity persists when we consider interactions between solvent and polymer as we shall see below. Various other attempts have been made to calculate curves of this type from hydrodynamic reasoning, but we do not need to consider them further here. We note, however, that any tendency towards solvation caused by a negative interaction  $w_{ps}$  will promote intramolecular contacts between separate chains as the polymer chains uncurl, thus increasing the slope of the  $\eta_{sp}/c - c$  curve above its value in an indifferent solvent. Curling up of the polymer chains in a bad solvent reduces these contacts and flattens the curve. We shall see below that very small differences in  $w_{ps}$  will appreciably alter the  $\eta_{sp}/c - c$  slope in this way. The limiting value  $[\eta]$  is only affected when the chains undergo a much more drastic action of coiling up on themselves. Thus we should expect different solvents to show relatively greater effects on the slopes rather than on the intercepts of the  $\eta_{sp}/c - c$  curves. This is in agreement with the published experimental work of Mark on polystyrene.<sup>1,7</sup>

In the next sections we use Kuhn's formula (1) for the limiting  $[\eta]$  value and calculate the first approximate effect of a finite  $w_{ps}$ . In these calculations we introduce a concentration term and obtain finally an equation of the type (2) where  $B$  is now a function of  $w_{ps}$ . We need to consider first in some detail the current statistical theories of high polymers in solution.

### 3. Polymer-Solvent Equilibrium.

The formulæ used in this section were originally obtained by Rushbrooke<sup>8</sup> and have recently been considerably extended to the particular case of high polymers by Guggenheim.<sup>9</sup> If we consider a system of  $N_p$  polymer molecules each of  $p$  links and  $N_s$  solvent molecules the average number  $\bar{X}$  of P-S contact pairs is given in the form of a quasichemical equilibrium.

$$(qN_p - \bar{X})(N_s - \bar{X}) = \bar{X}^2 \cdot e^{2w/zkT} \quad (3)$$

where  $z$  is the co-ordination number of the quasilattice on which the liquid structure is built;  $2w/z$  is the interaction energy between P, a polymer link, and S a solvent molecule so that the total change in heat content on mixing  $\Delta H = \bar{X} \cdot w$ ;  $q$  is a modified chain length such that  $zq$  is the number of nearest neighbour sites along the polymer chain. In deriving this formula it is necessary to assume that the polymeric chain,

<sup>6</sup> Huggins, *J.A.C.S.*, 1942, 64, 2716.

<sup>7</sup> Bartovics and Mark, *J.A.C.S.*, 1943, 65, 1901.

<sup>8</sup> Rushbrooke, *Proc. Soc. Roy.*, A, 1938, 166, 296.

<sup>9</sup> Guggenheim, *Proc. Roy. Soc.*, in press.

while kinked, is never coiled right back on itself \* so that  $p$  and  $q$  are simply related by the expression :

$$xq = xp - 2(p - 1).$$

An important limitation is imposed on the use of statistical formulae of this type by this definition. So far no valid calculations have been made which take into account molecular coiling and the usefulness of this type of approach is consequently restricted. The physical significance of equation (3) is at once apparent when we realise that  $(qN_p - \bar{X})$  is proportional to the equilibrium number of polymer-polymer contact pairs, and  $(N_s - \bar{X})$  to the number of solvent-solvent contacts. Thus equation (3) asserts that a "quasi-chemical equilibrium" exists between types PP, SS and PS of pairs in solution. We can now solve the quasi-chemical equilibrium equation for  $\bar{X}$ . Let  $\bar{X}_0$  be the value of  $\bar{X}$  in a solution formed by random mixing of the components with zero heat effect and let  $x$  be the modified volume fraction  $qN_p/(qN_p + N_s)$  of polymer in solution.

Then

$$\bar{X}_0^2 = \frac{1}{4}(\beta + 1)^2 \bar{X}^2$$

where

$$\beta^2 = 1 + 4x(1 - x)(e^{2w/zkT} - 1).$$

For our case when  $x$  and  $w/kT$  are, by hypothesis, small, this reduces to

$$\bar{X}^2 = \left[ 1 - 2x(1 - x) \cdot \frac{2w}{zkT} \right] \bar{X}_0^2. \quad (4)$$

From these equations we see at once that if  $w$  is negative,  $\bar{X} > \bar{X}_0$  so that attractions between polymer and solvent will promote an increased number of polymer solvent contacts. This increase in  $\bar{X}$  is due, in the main, to changes in P—P contacts between different chains. At the same time the molecular chains will be slightly straightened out, and there will be a corresponding increase in  $\bar{X}$  not given by the quasi-chemical equilibrium formula. The extent of each effect will depend obviously on  $w/zkT$ , and their relative importance will depend on the concentration of the solution : changes in  $\bar{X}$  due to molecular kinking will persist down to infinitely dilute solutions while the value of  $\bar{X}$  given in equation (4) tends to a value independent of  $w$  as  $x$  tends to zero. This point has been further discussed by Orr.<sup>10</sup> Use of equation (4) thus automatically excludes considerations of infinitely dilute solutions in this connection (see Section 4).

In the next section we consider more explicitly the effect of solvent on molecular length and the consequent differences in the viscosity relationships to be expected between solutions of polymer in different solvents.

#### 4. One-Dimensional Molecule.

We consider first, for simplicity, a hypothetical one-dimensional molecule whose links bend forward and backward on themselves in a straight line. We allow this molecule to be superimposed on a lattice framework of co-ordination number  $z$ : for the moment we allow this lattice to be two-dimensional. Then if the chain is surrounded by solvent, the number of polymer solvent contacts  $z\bar{X}$  is directly proportional to  $L$ , the actual length between the ends of the chain. To see this we may consider a simplified case of a chain of  $p$  links, outstretched length  $p\lambda$  bent back on itself in one dimension so that its total length is  $L$ . This is

\* The term "coiling back" represents a somewhat extreme view. More correctly we have to assume that contacts between two different elements of one chain are few compared with contacts between two separate chain molecules.

<sup>10</sup> Orr, *Trans. Faraday Soc.*, 1944, 40, 320.

shown diagrammatically simplified in Fig. 1. The total amount of chain which runs backwards is  $\frac{1}{2}(p\lambda - L)$ . If we allow the co-ordination number  $z$  to be 4 we can count up the actual number of free sites (polymer solvent contacts) along the various parts of the chain. Thus

$$\begin{aligned} z\bar{X} &= (z\bar{X}_{AB} + z\bar{X}_{BF}) + (z\bar{X}_{BC} + z\bar{X}_{DE}) + z\bar{X}_{CD} \\ &= \left[ \frac{p\lambda}{\lambda} - \frac{3\lambda}{2}(p\lambda - L) \right] \cdot 2 + \left[ \frac{1}{\lambda}(p\lambda - L) \right] \cdot 1 + 0 \\ &= 2L/\lambda. \end{aligned}$$

We assume the solution is dilute so that all contacts along the chain are polymer-solvent ones and that contacts between different polymer chains can, to a first approximation, be ignored. This result is quite general and holds for any lattice where nearest neighbours of a given site are not nearest neighbours of each other. This fundamental restriction of lattice type is inherent also in the derivation of the quasi-chemical equilibrium formula and limits in effect our choice of  $z$  to its value  $z = 4$  for a square lattice. In considering polymer solutions we are concerned with an average  $z$  value and one which is not necessarily integral. However, recent calculations by Orr<sup>10</sup> have shown that a low co-ordination number in the range  $z = 4.5$  is necessary to fit the experimental results for rubber, so that this type of error is not likely to be very serious.

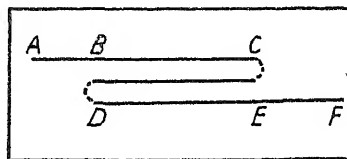


FIG. 1.—Hypothetical one-dimensional molecule used as model.

In the final analysis we do not need  $L$  the actual length of the molecule, but  $\bar{L}^2$  the mean square length. We have to take  $\bar{L}^2$  as directly proportional to  $\bar{X}^2$ , but the exact value of the polymer solvent contact number is not immediately clear. In solutions of extremely low concentration  $\bar{X}$  is given, as in this section, by a direct count of contacts along separate chains, but when the polymer chains are no longer independent of each other,  $\bar{X}$  is more correctly given by the quasi-chemical equilibrium formula. The critical concentration at which the polymer chains cease to move independently is very low: rough calculations show it to be about 0.01 %<sup>10a</sup>. For solutions of small but finite concentrations we have to modify this crude approach and as a first approximation take  $\bar{L}^2$  directly proportional to the value of  $\bar{X}^2$  given by the quasi-chemical equilibrium equation, realising again that the effect of coiling back of the molecules is enhanced by the increasing effect of intramolecular contacts between separate chains as the concentration increases. We can write then

$$\bar{L}^2 = [1 - 2\kappa(1 - \kappa)(e^{2w/2kT} - 1)]\bar{L}_0^2 \quad (5)$$

where first order terms in  $w/zkT$  only are considered and where  $\bar{L}_0^2$  is the mean square length of the molecule in an indifferent solvent (or no solvent at all). This formula for  $\bar{L}^2$  can then be used in conjunction with the Kuhn or Huggins equation to write down a formula for comparative viscosities of different polymer solutions in terms of parameters  $\kappa$  and  $w$ . Before considering this equation we may see, however, how a similar equation for  $\bar{L}^2$  can be derived from more formal considerations.

### 5. Statistical Determination of $\bar{L}^2$ .

We consider a one-dimensional molecule as before. The problem of determining the mean square length  $\bar{L}_0^2$  of the chain itself is the well-

<sup>10a</sup> Campbell and Johnson, *Trans. Faraday Soc.*, 1944, 40, 233.



known statistical theorem of the random walk. The  $p$  chain links are all of length  $\lambda$  and there is an equal probability that a given link will contribute a length  $\lambda$  in the forward or the backward direction. Interaction with a solvent will alter the probability of polymer-polymer links along the chain in the way we have been considering so that there is no longer necessarily an equal probability of the chain links running forward or backward with equal effect. In particular we may consider a group of chain links of length  $A$  forming a statistical chain element in the solution, and suppose that all forward orientations of this element contribute a  $A$  and all negative or backward orientations  $-bA$  to the total length  $L$ . In an indifferent solvent  $a = b = 1$  and the "steps" of the walk are equal. In any other solvent the ratio  $a/b$  is to be regarded as some measure of the polymer-solvent interaction and we have to determine the molecular distribution for a random walk with unequal steps in the forward and backward directions.

We can now calculate the distribution of the elementary groups. The procedure is standard and follows the statistical treatment given originally by Fowler.<sup>11</sup> We consider a chain of  $p$  elements, and suppose that  $p_A$  elements are orientated in a forward direction where they each contribute  $aA$  towards the length  $L$  and  $p_B$  in a backward direction with a contribution each of  $-bA$ .<sup>\*</sup> The terms "forward" and "backward" are to some extent arbitrary and are to be referred to the original direction of the first "step" considered here as "forward". Then all possible distribution of the original  $p$  elements are possible subject to the conditions,

$$\begin{aligned} p_A + p_B &= p, \\ p_A \cdot aA - p_B \cdot bA &= L. \end{aligned}$$

We require the distribution function  $\phi(L)$  where  $\phi(L)dL$  is the frequency with which the molecular chain has a total length between  $L$  and  $L + dL$ . The total number of complexions,  $\phi(L)$ , of the assembly for a total chain length  $L$ , is simply  $\sum_{A, B} \frac{p!}{p_A! p_B!}$  summed for all  $p_A$  and  $p_B$  which obey the above conditions. This number is then the coefficient of  $x^L$  in the expansion of the generating function  $(x^{aA} + x^{-bA})^p$ . This coefficient is most simply given by the contour integral below and we write

$$\phi(L) = \frac{1}{2\pi i} \int_{\gamma} \frac{(x^{aA} + x^{-bA})^p dx}{x^{L+1}}.$$

This integral can be evaluated by the method of steepest descents since we can assume that  $p$  and  $L$  are both large in a fixed ratio. The whole contribution to the integral comes effectively from the col  $x = \theta$  where the factor  $\frac{(x^{aA} + x^{-bA})^p}{x^L}$  has a unique minimum value. This col condition can be written

$$\frac{\partial}{\partial \log x} \cdot \log \left[ \frac{(x^{aA} + x^{-bA})^p}{x^L} \right]_{x=\theta} = 0 \quad \text{or} \quad x \frac{\partial}{\partial x} \cdot \log \left[ \frac{(x^{aA} + x^{-bA})^p}{x^L} \right]_{x=\theta} = 0.$$

Writing now  $x^{aA} = e^{aA \log x}$  we have

$$L = pA \cdot \frac{a\theta^{aA} - b\theta^{-bA}}{\theta^{aA} + \theta^{-bA}} = pA \cdot \frac{ae^{aA \log \theta} - be^{-bA \log \theta}}{e^{aA \log \theta} + e^{-bA \log \theta}}.$$

<sup>11</sup> Fowler, *Statistical Thermodynamics* (Cambridge, 1939), pp. 30-37.

<sup>\*</sup> This method of weighting the lengths of the elementary groups of chain links has been used in preference to the orthodox method of weighting the numbers of groups with a given length in order to simplify the mathematical treatment.

If  $L \ll pA$  it is justifiable to expand the exponentials in this formula and consider only the first two terms in each series. This means physically that the long chains are not fully stretched. Results obtained from experiments on the stretching of rubber suggest that this assumption is quite justified under ordinary conditions.

The condition for the col then becomes finally

$$A \log \theta = \frac{2L/pA - (a - b)}{a^2 + b^2 - L/pA(a - b)}.$$

We can now obtain the distribution  $\phi(L)$  in a simple form since  $\frac{\partial}{\partial L} \log \phi(L) = -\log x$  where  $x$  is now the single point  $x = \theta$ . If  $a - b$  is small (which we regard as equivalent to a small heat of mixing  $w$ ), then the final distribution is given by

$$\begin{aligned} \frac{\partial}{\partial L} \log \phi(L) &= \frac{-2L}{pA^2(a^2 + b^2)} \\ \phi(L) &= \text{Const. } e^{-L^2/\{pA^2(a^2 + b^2)\}} \end{aligned} \quad (5)$$

This distribution reverts to the well-known expression

$$\phi(L_0) = \text{Const. } e^{-L_0^2/2p\lambda^2} \quad (6)$$

for the special case of no preferred orientations and an ordinary chain link as the statistical element. Corresponding to these two distributions we can at once write down the mean square lengths  $\overline{L^2}$  and  $\overline{L_0^2}$ . Thus

$$\overline{L^2} = pA^2(a^2 + b^2) \quad (7)$$

$$\overline{L_0^2} = 2p\lambda^2. \quad (8)$$

If we now tentatively identify our elementary group of links with the single link of length  $\lambda$  and write for convenience  $b = 1$ ,  $a = 1 + a'$  where  $a'$  is small, we obtain from equations (7) and (8) a relationship which is formally similar to that obtained from the quasi-chemical equilibrium method

$$\overline{L^2} = \overline{L_0^2}(1 + a').$$

To this approximation, then, both methods of approach are similar so that using Kuhn's equation (1) we may write

$$\begin{aligned} \frac{\eta_{sp}}{c} &= \text{Const. } \overline{L^2} = \text{Const. } \overline{L_0^2} (1 + a') \\ &= \text{Const. } 2p\lambda^2 [1 - 2\chi(1 - \chi)(e^{2w/2kT} - 1)] \\ &= \left(\frac{\eta_{sp}}{c}\right)_0 - \text{Const. } \frac{\chi(1 - \chi)w}{kT} \end{aligned} \quad (9)$$

since  $w/kT$  is small, where  $(\eta_{sp}/c)_0$  is the value of the intrinsic viscosity in a solution for which  $w = 0$ . This equation will be discussed later.

## 6. Three-Dimensional Molecules.

The three-dimensional problem is less tractable as we cannot in this case easily count the configurational P—S arrangements. The formal identity obtained in the one-dimensional case between the two methods of estimating  $\overline{L^2}$  suggests, however, a three-dimensional similarity. It is possible to calculate the distribution of molecular lengths  $\phi(L)dL$  along any specified  $z$  direction by methods exactly analogous to those of the last section. We have to consider again a group of chain links forming a statistical element of length  $A$  and suppose that solvent interaction makes certain orientations of this element contribute  $aA$  and other  $bA$  to the length of the element, the two sets of contributions being in opposite

senses. When we allow for the distribution of these elements about the specified direction  $z$ , and carry out the calculations as before, we obtain

$$\phi(L) = \text{Const. } e^{-3\pi^2/(pA^2(a^2+b^2))}.$$

For the case of zero interaction the flights of the problems are random and of equal length ( $a = b = 1$ ) and we may identify  $A$  with the link length  $\lambda$ . Then

$$\phi(L_0) = \text{Const. } e^{-3\pi^2/2p\lambda^2}.$$

The mean square lengths  $\overline{L^2}$  and  $\overline{L_0^2}$  of these two distributions are then given by

$$\begin{aligned}\overline{L^2} &= \frac{1}{3}\{pA^2(a^2 + b^2)\} \\ \overline{L_0^2} &= \frac{2}{3}p\lambda^2.\end{aligned}$$

We should now need to know how the elementary statistical element in solution,  $A$ , is related to the ordinary chain link. In general we may write  $A = \beta\lambda$  where  $\beta$  is a small number greater than unity,  $\beta$  will depend to some extent on the solvent but the exact relationship cannot be predicted. In general  $\beta$  will be finally absorbed in undetermined constants and for the moment we write  $\beta = 1$ . Then, as before, writing  $b = 1$  and  $a = 1 + a'$  where  $a'$  is small, we have

$$\overline{L^2} = \overline{L_0^2}(1 + a') \quad (10)$$

which is identical with the formula obtained in the one-dimensional case.

Since the formulæ for  $\overline{L^2}$  obtained by formal statistical reasoning are the same then in one and three dimensions, we might also expect that the one-dimensional formula (5) connecting  $\overline{L^2}$  with  $\overline{L_0^2}$  in terms of the interaction energy  $w$  might also have its three-dimensional analogue. We can see approximately that this will happen as, provided that there is no extensive back coiling, a three-dimensional chain can be analysed in components of the type shown in Fig. 1, and to this order of accuracy the square  $(z\overline{X})^2$  of the total number of P-S contacts will be directly proportional to the mean square length  $\overline{L^2}$ . Then approximating as before, and using the Fowler Rushbrooke relationship for a small heat of mixing  $w$  and a low concentration of polymer  $x$ , we may write

$$\overline{L^2} \simeq \left[1 - \text{Const.} \frac{x(1-x)w}{kT}\right] \frac{2}{3}p\lambda^2. \quad (11)$$

which is formally similar to the statistical result (10) and of the required form in  $w$ . We may write then finally for the viscosity of a polymer solution

$$\begin{aligned}\frac{\eta_{sp}}{c} &= \text{Const.} \frac{2}{3}p\lambda^2[1 - 2x(1-x)(c^2w/2kT - 1)] \\ &= \left(\frac{\eta_{sp}}{c}\right)_0 - \text{Const.} \frac{x \cdot w}{kT}\end{aligned} \quad (12)$$

since  $x$ , the polymer concentration and  $w/kT$ , the heat term, are both assumed small. The application of this equation will be discussed in the next section. We may note here, however, that since the statistical element in the solution is not necessarily the chain link, but is itself a function of the solvent, the term  $\left(\frac{\eta_{sp}}{c}\right)_0$  is itself solvent dependent. This limiting variation of the  $\eta_{sp}/c$  ratio at zero concentration is well known experimentally and the  $\beta$  factor is probably in part responsible. Variations in  $\beta$ , however, are likely to be small in comparison with coiling effects which we have up till now neglected, and the persistence of a

solvent effect down to zero concentration is more easily explicable on this basis.

### 7. Discussion.

The exact application of equation (12) to experimental data is not yet quite feasible, but we may note briefly how a first check-up may be made. Though not in any familiar units,  $\alpha$  is a measure of the polymer concentration  $c$ , so we may write equation (12) in the form in which viscosity results are usually presented,

$$\frac{\eta_{sp}}{c} = [\eta]_{w=0} + \frac{Bwc}{kT} + B'c \quad (12a)$$

where the  $B'$  factor is introduced to account for other types of variation with concentration and where  $B$  is constant. The theory thus indicates a solvent dependence of the slope but not of the intercept of the  $\eta_{sp}/c - c$  curve. To the approximation used in dealing with the quasi-chemical equilibrium formula, the mixing is random and the heat term involved is given by  $\Delta H = \bar{X}w$  where  $\bar{X}$  is simply  $qN_p N_s / (qN_p + N_s)$ .<sup>\*</sup> This is easily verified by expanding the exponential term in the expression obtained for  $\bar{X}$  in equation (3). In the absence of any experimental values for  $w$ , we use Hildebrand's<sup>12</sup> theory for this type of regular solution and write  $w$  proportional to the square of the difference of the square roots of the cohesive energy densities of the liquids concerned. These quantities can be determined with fair accuracy since the cohesive energy density  $E/V$  is simply equal to  $(L - RT)/V$  where  $L$  is the measured latent heat and  $V$  the molecular volume. Thus we may write, considering only solvent variations,

$$\frac{\eta_{sp}}{c} = \left( \frac{\eta_{sp}}{c} \right)_{w=0} - \frac{\text{Const.}}{RT} \left[ \sqrt{\frac{E_s}{V_s}} - \sqrt{\frac{E_p}{V_p}} \right]^2 \cdot c \quad (13)$$

Hildebrand's derivation assumes implicitly that  $w$ , or the heat of mixing, is essentially positive. The use of equations of this type is at once limited since it is known that for many mixing processes  $w$  is negative: we may mention explicitly the systems nitrocellulose-acetone<sup>13</sup> and cellulose acetate-tetrachlorethane<sup>14</sup> where heat is evolved on mixing. However, equation (13) shows (for these restricted systems) how the slope of the  $\eta_{sp}/c - c$  curve should vary with the  $E/V$  value of the solvent used and suggests a direct correlation with other data. Gee<sup>15</sup> has shown how the equilibrium swelling  $Q$  of a high polymer can be directly related to the cohesive energy density of the swelling agent, so that if  $Q$  is measured as a volume fraction of liquid imbibed

$$f(Q) = \beta V_s \left[ \sqrt{\frac{E_s}{V_s}} - \sqrt{\frac{E_p}{V_p}} \right]^2$$

where  $f(Q) = T\Delta S_s/x_p^2$  is a function of the partial molar entropy  $\Delta S_s$  of swelling and of the volume fraction  $x_p$  of the rubber in the swollen phase. If we compare this equation with equation (13) we see that the slope of the  $\eta_{sp}/c - c$  curve of dilute solutions of a polymer should be intimately connected with the equilibrium swelling under different conditions in the

\* The theory developed above assumes that small departures from a random configuration of the polymer chains is responsible for differences in  $\eta_{sp}/c$ . Orr<sup>10</sup> has however shown that the effect of a small finite heat term on the mixing entropy is small so that  $\bar{X}$  has approximately the same value as in the random case and  $\Delta H$  can be first estimated using this approximate value.

<sup>12</sup> Hildebrand, *Solubility* (Reinhold, 1936), p. 72.

<sup>13</sup> Schulz, *Z. physik. Chem.*, 1942, 52, 253.

<sup>14</sup> Haggard and Van der Wyk, *Helv. Chim. Acta.*, 1940, 23, 484.

<sup>15</sup> Gee, *Trans. Faraday Soc.*, 1942, 38, 418.

same liquid. It is possible to test this prediction directly only in the case of a polymer of the rubber class since, in general, a polymer will either dissolve or become swollen in a liquid. However, in the case of rubber, vulcanised specimens can be made to swell and remain completely insoluble, while unvulcanised rubbers can be used for solutions. There is certain evidence that vulcanisation does not completely destroy all the specific properties of a rubber, and assuming that we can extrapolate results, comparison is justified. A direct correlation between  $Q$  and the slope of the viscosity curve has in this way been obtained. Details and extended applications of this theory to the case of mixed solvents and plasticiser interactions will be published later. Although the use of Hildebrand's approximation indicates a relationship between  $Q$  and heats of mixing only for systems where  $w$  is positive, more general considerations show such a relationship will exist for all values of  $w$  and we may infer that the connection is quite general.

We would not, of course, expect to give accurate predictions of the slope of the  $\eta_{sp}/c - c$  curve as we have neglected all factors other than solvent-solute interactions. However, the above analysis does provide a semi-quantitative explanation of the experimental facts and to this extent is perhaps useful.

We may note a further point in connection with equation (12). We can see at once that the effect of solvent will be damped down by increasing temperature. The quasi-chemical equilibrium theory assumes that  $w$  is temperature independent, so that increasing the temperature of a solution in a good solvent will decrease the corrective term in  $w$  and hence lower the viscosity. In a bad solvent increase of temperature will raise the viscosity towards its mean value. These effects have been noted by Mark<sup>1</sup> for polystyrene solutions. In toluene (which we may consider a good solvent in this sense) the viscosity at 80° C. was lower than its value at 20°, while in toluene mixed with methyl alcohol—which acts as a precipitant—the same polystyrene showed a higher viscosity at 80° than at 20°. The effect can, of course, be predicted qualitatively since an increase of temperature will, by increasing molecular motions, tend to restore the random molecular configuration, and hence the unbiased viscosity.

The extrapolation to zero concentration remains to be explained as equation (12) shows no solvent effect on the  $[\eta]$  intercept. Experiments, however, show that  $[\eta]$  for solutions in a good solvent is appreciably higher than the same ratio in a bad solvent. We have to interpret this mainly by considering a more extensive back coiling of the polymer chain caused by large interaction between two regions of polymer links in the same chain. No account of this effect has yet been given in mathematical form, and we can only say now that if the effect persists, variations in the limiting viscosity ratio will be possible. Since, however, this back coiling is altogether more drastic than the effects we have been considering, we would expect the effect of solvent to be less marked in the limiting viscosity case than on the slope of the curve. This is quite in agreement with the experimental data and is a good example of the degree to which current mathematical theories can be directly applied to experiment.

### Summary.

A semi-quantitative discussion is given of the viscosity relationships of polymers in various solvents. Quasi-thermodynamic reasoning, based on modern statistical theories, show how the slope of the ordinary viscosity concentration ( $\eta_{sp}/c - c$ ) curve is related to the interaction energy between solvent and polymer, and it is shown how small differences in interaction energy appreciably alter the slope. These differences are traced back to slight kinking of the long molecular chains in agreement with the

qualitative views of Mark. Retention of a solvent effect on  $[\eta]$  at zero concentration is demonstrated but not proved; it is inferred that more extensive coiling of the chains is necessary than the slight kinking which affects the slope.

I wish to express my thanks to Professor E. K. Rideal for many stimulating discussions during the course of this work and to Dr. E. A. Guggenheim for much helpful criticism. I should also like to record my gratitude to the late Professor Sir R. H. Fowler for his encouragement and advice during the development of this paper.

*Department of Colloid Science,  
The University, Cambridge.*

---

## THE INFRA-RED SPECTRA OF FURAN AND THIOPHEN.

BY H. W. THOMPSON AND R. B. TEMPLE.

*Received, 25th May, 1944.*

Furan and thiophen are structurally related and fairly simple molecules the spectra of which, if considered together, may be expected to lead to values for the molecular vibration frequencies. The spectroscopic data also bear upon the question of whether these molecules are planar, or alternatively have a buckled ring. The Raman spectrum of furan has been measured by Bonino<sup>1</sup> and by Reitz,<sup>2</sup> and the infra-red spectrum by Bonino and by Pickett.<sup>3</sup> Raman data for thiophen were also obtained by Bonino and by Reitz, and the infra-red spectrum was measured by Coblenz,<sup>4</sup> by Barnes and Brattain,<sup>5</sup> and by Barnes, Liddel and Williams.<sup>6</sup>

We have recently measured the infra-red spectra of these substances using markedly higher resolving power than that previously employed, and although it does not seem possible to allocate unambiguously all the molecular vibration frequencies, the results show clearly that some of the earlier data were interpreted incorrectly, and the rotational contour now observed with some of the bands provides an additional basis for the vibrational assignments.

### Experimental.

The furan was a sample kindly given to us by Dr. Plant of the Dyson Perrins Laboratory. It had been prepared from furoic acid,<sup>7</sup> dried over anhydrous sodium sulphate and fractionated. The final product boiled at 31.5° C./760 mm. A commercial sample of "pure" thiophen was re-purified by mercuration as described by Dimroth,<sup>8</sup> dried over sodium sulphate, and fractionated. It boiled at 83.3-83.5° C./761 mm.

Two spectrometers were used. One was an automatically recording instrument with 30° rock salt prism in Littrow mounting. This spectrometer which was used for the region 7-14 $\mu$ , had high resolving power; the effective slit widths are shown on the diagrams below. For the regions 3-7 $\mu$  and 14-20 $\mu$  a Hilger D 88 spectrometer fitted with a highly sensitive

<sup>1</sup> *Z. physikal. Chem.*, B, 1934, 35, 327.

<sup>2</sup> *J. Chem. Physics*, 1942, 10, 669.

<sup>3</sup> *Publ. Carneg. Inst. Wash.*, 1905, No. 35.

<sup>4</sup> *J. Chem. Physics*, 1935, 3, 446.

<sup>5</sup> *Ind. Eng. Chem. Anal. Edn.*, 1943, 15, 659.

<sup>7</sup> *Org. Synth.*, 1, 269.

<sup>2</sup> *Ibid.*, 1938, 38, 375.

<sup>8</sup> *Ber.*, 1899, 32, 758.

Schwarz vacuum thermocouple, and with fluorite and sylvine prisms,

TABLE I.—FURAN.

Infra-red (Vapour).	Raman (Liquid).
588 } 605 } 626 }	601 dp
—	724 p
724 } 744 } 764 }	—
837	839 dp
863 } 872 } 882 }	871 dp
985 } 994 } 1006 }	986 p
—	1034 dp
1057 } 1067 } 1077 }	1061 p
—	1137 p
1166 } 1175 } 1185 } 1190 }	1171 dp
1260 } 1270 } 1282 }	1270 dp
1340 ?	
1374 } 1381 } 1395 }	1380 p
1458 ? 1486 1558 ? 1579 1596	1483 p

Other infra-red bands at :

1718	2445
1908	2620
1995	2680
2040	2755
2105	2900
2200	2960
2260	3185
2365	

Other Raman displacements :

3089 p
3121 p
3154 p

was used. Readings were usually taken at intervals of  $0.01\mu$ . Vapours were measured in absorption cells 20 cm. and 7 cm. in length having end plates of rock salt or sylvine; liquids were examined in thin cells made by separating a pair of polished rock salt plates by a washer of the desired thickness.

### Results.

The absorption curves for furan vapour are shown in Fig. 1. Table I gives the positions of the bands in wave numbers, together with the most recent Raman data. The infra-red data agree substantially with those given by Pickett. It will be noticed that with few exceptions the infra-red bands belong to one or other of two types. In one case, for example at 605 and 744, the contour consists of a sharp central peak with a fairly strong maximum on each side of it, the spacing between the outer pair of maxima being 38-40  $\text{cm}^{-1}$ . In the other type of band there are three similar absorption maxima, but the central peak is rather less marked and the spacing between the outer pair of maxima is about 20  $\text{cm}^{-1}$ .

The absorption curves for thiophen are shown in Fig. 2, and the positions of the bands are given in Table II. The spectrum of a thin layer of liquid was measured over the entire range. Between 500-1500  $\text{cm}^{-1}$  the vapour also was used in order to bring out rotational contour of the fundamental absorption bands. Here, too, as with furan, the bands show characteristic differences in rotational contour. Thus there is a band at 710 with three sub-maxima, the spacing between the outer pair being about 28  $\text{cm}^{-1}$ , and several similar bands with three sub-maxima but spacing about 20  $\text{cm}^{-1}$ , and a third type of band with two sub-maxima about 13  $\text{cm}^{-1}$  apart.

### Discussion.

We may first regard furan and thiophen as planar. They will then have  $C_{2v}$  symmetry, with a twofold axis of rotation  $zz$  (Fig. 3) and two planes of symmetry,  $\sigma_y$  and  $\sigma_x$ . There will be 21 normal modes which can

be divided into classes according to their symmetry properties as given in Table III.

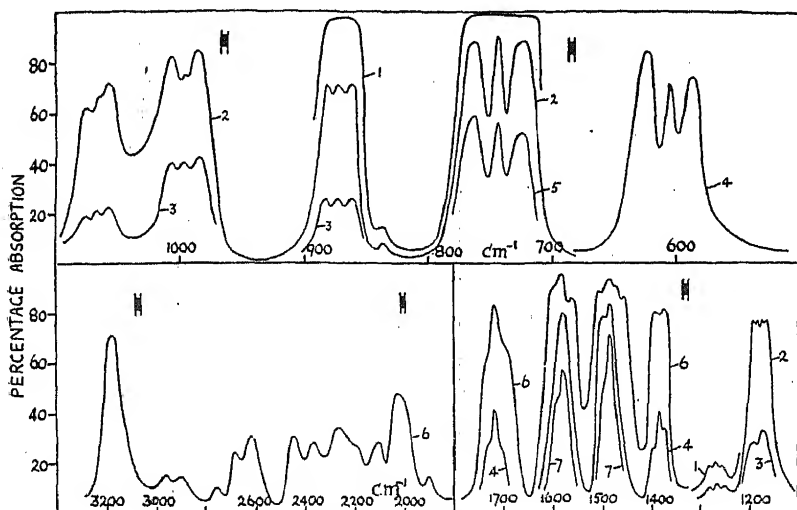


FIG. 1.—Furan.

- |                         |                          |
|-------------------------|--------------------------|
| (1) 7 cm. path, 360 mm. | (5) 20 cm. path, 5 mm.   |
| (2) 7 cm. path, 100 mm. | (6) 20 cm. path, 300 mm. |
| (3) 7 cm. path, 20 mm.  | (7) 20 cm. path, 25 mm.  |
| (4) 20 cm. path, 60 mm. |                          |

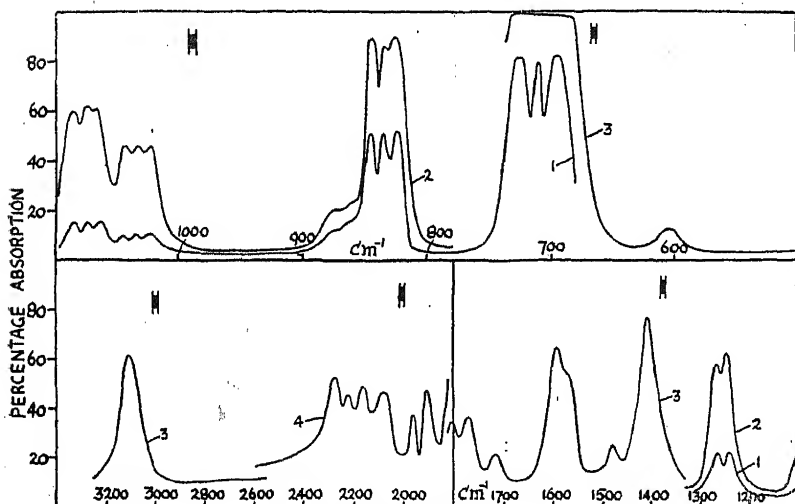


FIG. 2.—Thiophen.

- |                         |                                |
|-------------------------|--------------------------------|
| (1) 7 cm. path, 80 mm.  | (3) <i>c.</i> 0.08 mm. liquid. |
| (2) 20 cm. path, 50 mm. | (4) <i>c.</i> 0.2 mm. liquid.  |

The molecular dimensions of furan have been determined by Pauling and Schomaker,<sup>9</sup> with the following results:  $r_{OH} = 1.09$  A.,  $r_{CO} = 1.41$  A.,  $r_{OO} = 1.46$  A.,  $r_{O:C} = 1.35$  A.,  $\angle C\hat{O}C = 107^\circ$ ,  $\angle C=\hat{C}-C = 107^\circ$ . Using these

<sup>9</sup> *J. Am. C.S.*, 1939, 61, 1769.



values, the three principal moments of inertia  $A$ ,  $B$  and  $C$  will have values close to 90, 90 and  $180 \times 10^{-40}$  g. cm.<sup>2</sup>. The two lower moments are about the axes  $zz$  and  $xx$ . The molecule will thus behave roughly like a symmetrical rotator, having two equal moments of inertia, and as

TABLE II.—THIOPHEN.

Infra-red.		Raman (Liquid.)
Vapour.	Liquid.	
		? 375 dp 453 dp 565 dp 604 p 686 dp
605	605	—
696 } 710 } 724 }	710	—
826 } 836 } 846 }	836	748 dp 832 p
865 } 878 }	872	866 dp
	909	898 dp
1025 } 1035 } 1046 }	1035	1032 p
1067 } 1077 } 1088 }	1077	1079 p
1245 } 1260 }	1252	—
—	1290	—
—	—	1358 p
1405	1405	1404 p

Other infra-red bands at :

1479	1960
1565	2090
1590	2168
1715	2230
1770	2280
1805	3110
1905	

Other Raman displacements :

2996 p
3078 p
3108 p

We can therefore confidently fix all eight of the  $A_1$  class of vibrations as follows : 724, 994, 1067, 1137, 1381, 1486, with two values around 3000. That 994, 1137 and 1486 are associated with  $A_1$  fundamentals is also supported by measurements on the ultraviolet absorption spectrum

regards their rotational contour the infra-red bands will be of two types. In Badger and Zumwalt's notation,<sup>10</sup> the  $A$  and  $B$  type bands will have three sub-maxima, the outer spacing being about  $20 \text{ cm.}^{-1}$ , and the central peak rather weak. The  $C$  type bands, in which the change of electric moment occurs parallel to the axis  $yy$ , will have a stronger central peak with two side maxima about  $36 \text{ cm.}^{-1}$  apart. In the case of furan the  $A_1$  and  $B_1$  classes of vibration will be expected to give the former type of contour, and the  $B_2$  class will give the latter.

We can now attempt to allocate magnitudes to the normal frequencies of furan. As regards the eight vibrations of class  $A_1$ , two—the C—H stretching modes—will have values close to  $3000 \text{ cm.}^{-1}$ , and the remaining six will have values below about  $1600 \text{ cm.}^{-1}$ . There are just six polarised Raman lines of this magnitude, namely, 724, 986, 1061, 1137, 1380 and 1483. Bands corresponding to 724 and 1137 have not been observed in the infra-red spectrum, but the remaining four are seen at 994, 1067, 1381, and 1486. All these bands have the contour and spacing of sub-maxima expected for this class of vibration.

<sup>10</sup> *J. Chem. Physics*, 1938, 6, 711.

by Pickett,<sup>11</sup> where frequencies of 848, 1068, 1395 are found in the excited state. Only totally symmetrical vibrations should be excited here, and the values will be rather lower than those of the same vibrations in the ground state.

All the remaining Raman lines are depolarised and all three other classes of vibration are active. On this basis alone, therefore, magnitudes cannot be assigned to the different classes. We may, however, expect one  $B_1$  type ring vibration to be largely determined by a stretching of the carbon-carbon double bonds. The infra-red band at 1579 is probably connected with this mode. The contours of the infra-red bands are also helpful. Thus, the band at 872 and probably that at 1270 have three sub-maxima with outer spacing about 20  $\text{cm}^{-1}$ . Since all the  $A_1$  class vibrations have been assigned and the  $A_2$  fundamentals cannot appear, these frequencies must be connected with vibrations in the  $B_1$  class. Miss Pickett assigned the band at 1270 (given by her as 1264) to a totally symmetrical  $A_1$  oscillation, but commented on the questionability of this. Her argument seems to have been based largely upon a comparison of the normal frequencies of furan with those of pyrrole. This will be discussed below.

The infra-red bands at 605 and 744 have the three-branch contour but with a stronger central peak and wider spacings of about 38 and 40  $\text{cm}^{-1}$ . These are unquestionably  $B_2$  class fundamentals, which would give exactly this type of contour. In this connection, Miss Pickett's interpretation must be in error, due to inadequate resolving power and

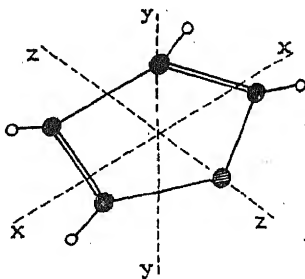


FIG. 3.

TABLE III

Class.	Symmetry with respect to			Moment Change Parallel to	Permitted in		Number of Modes.	Form.
	$C_2^z$	$\sigma_x$	$\sigma_y$		Infra-red.	Raman.		
$A_1$	s	s	s	zz	yes	yes (p)	8	4 ring deformation 2 C—H bending 2 C—H stretching
$A_2$	s	as	as	—	no	yes (dp)	3	1 ring deformation 2 C—H bending
$B_1$	as	as	s	xx	yes	yes (dp)	7	3 ring deformation 2 C—H bending 2 C—H stretching
$B_2$	as	s	as	yy	yes	yes (dp)	3	1 ring deformation 2 C—H bending

failure to resolve the central peak at 744, since she attributed the two side-maxima at 724 and 764 to separate vibrations of classes  $A_1$  and  $B_2$ . In this way the band was also wrongly correlated with the Raman interval 724. In the same way Miss Pickett does not seem to have obtained the central peak of the band at 605 corresponding to the Raman frequency 601, which made the interpretation of the side branches of this band uncertain.

<sup>11</sup> *J. Chem. Physics*, 1940, 8, 293.

There now remain undetermined three frequencies of the  $A_1'$  class, two of the  $B_1$  class and one of  $B_2$ . Three Raman intervals 839, 1034, and 1171 have not been allocated. There is a weak infra-red band at 837 corresponding to the first of these, and the infra-red band at 1180 may be connected with the last, although the peculiar contour of this band suggests that it may be double. No infra-red absorption has been detected at 1034  $\text{cm}^{-1}$ . It is therefore possible that the values 837, 1034 and 1180 are fundamentals, but allocation of any of them to a specific mode can only be speculative. It might, however, be argued that since 1034 does not appear in the infra-red, it is an  $A_1$  fundamental, and the single peak at 837 may imply a strong central branch of a  $B_2$  vibration band, while the band at 1180 has a contour more like that of a  $B_1$  vibration than anything else.

The polarised Raman interval 3154 is probably the harmonic of the fundamental at 1579. In this case there will be a pair of C—H stretching modes with value about 3090 and another pair of about 3120.

It might have been hoped to apply the selection rules operating for overtones and combinations in the infra-red spectrum, in allocating the fundamentals to the symmetry classes where the other methods, used above, fail. Thus  $(A_1 + A_2)$  and  $(B_1 + B_2)$  combinations are not allowed, whereas  $(A_1 + B_1)$ ,  $(A_1 + B_2)$ ,  $(A_2 + B_1)$ , and all first harmonics, are permitted. Unfortunately there are already so many fundamentals of widely differing frequency that it is possible within the existing selection rules to interpret satisfactorily all the observed bands in terms of the fundamentals already assumed. It may be noted, however, that two bands at 2680 and 2900 are perhaps best explained as combinations by assuming that the weak band at 1340 is due to a fundamental and not to the combination  $(605 + 744)$ .

We can attempt to determine the normal vibration frequencies of thiophen in the same way. If it is assumed to have  $C_{2v}$  symmetry, the selection rules and number and types of modes will again be that shown in Table III. According to Pauling and Schomaker,<sup>9</sup> the dimensions are  $r_{\text{CH}} = 1.74 \text{ \AA}$ ,  $r_{\text{OH}} = 1.09 \text{ \AA}$ ,  $r_{\text{OO}} = 1.44 \text{ \AA}$ ,  $r_{\text{C:O}} = 1.35 \text{ \AA}$ , and  $\hat{\text{CSC}} = 91^\circ$ ,  $\text{C}=\hat{\text{C}}-\text{S} = 112^\circ$ ,  $\text{C}-\hat{\text{C}}=\text{C} = 113^\circ$ . The principal moments of inertia will then be about 105, 160 and  $265 \times 10^{-40}$ , and the molecule will be an asymmetrical rotator with  $S = -0.08$  and  $\rho = 0.9$  in Badger and Zimmwalt's notation. The  $A$  type bands, from  $A_1$  class vibrations, in which the change of electric moment is parallel to the least axis  $zz$ , may then be expected to have three sub-maxima, the outer pair being about 19  $\text{cm}^{-1}$  apart; the  $B$  type bands from class  $B_1$  vibrations will have a double maximum with spacing about 12  $\text{cm}^{-1}$ , and the  $C$  type bands from class  $B_2$  vibrations will have a strong central peak flanked by a pair of sub-maxima about 28  $\text{cm}^{-1}$  apart.

There are just six polarised Raman frequencies less than 1600  $\text{cm}^{-1}$ , namely 604, 832, 1032, 1077, 1358, 1404. Together with the two C—H stretching vibration frequencies (about 3080 and 3110), these can be allocated at once to class  $A_1$ . The Raman interval 604 is very weak in the infra-red and in this respect is like the corresponding ring deformation of furan at 724, which was not observed in the infra-red at all. Four of the five remaining frequencies are found in the infra-red at 836, 1035, 1077 and 1405, the first three of these showing the  $A$  type contour, although the observed separation of outer sub-maxima is rather greater than that calculated above. The  $A_1$  vibration frequencies can thus be taken as 605, 836, 1035, 1077, 1358 and 1405.

All the other Raman lines will be depolarised, and since all classes of vibration are active in the Raman effect, the observed values cannot be allocated on this basis alone. We should, however, expect a frequency of the  $B_1$  class controlled by a vibration of the carbon-carbon double bonds to be about 1580. The infra-red band at 1590 is assigned to this mode.

The contour of the infra-red bands of the vapour is again useful. Thus, the band at  $710\text{ cm}^{-1}$  has a  $C$  type contour with outer sub-maxima about  $28\text{ cm}^{-1}$  apart, and it is therefore allocated to the  $B_2$  class. Also the bands at  $872$  and  $1252$  each have a double maximum with spacings about  $13\text{ cm}^{-1}$  and  $15\text{ cm}^{-1}$  respectively. Although these separations are rather greater than that calculated above for the  $B$  type bands, there can be little doubt that they are in fact such bands, and belong to vibrations in the  $B_1$  group. This leaves unallocated three vibrations in the  $A_2$  class, and two in each of the classes  $B_1$  and  $B_2$ . Raman intervals which have not so far been assigned are  $375$ ?,  $453$ ,  $565$ ,  $686$ ,  $748$ ,  $898$ , and the infra-red bands below  $1400$  are  $909$  and about  $1290$ . It seems likely that the doubtful Raman interval  $375$  may arise from the combination ( $832-453$ ); also the weak infra-red band at about  $909$  is probably the harmonic of  $453$ , and the still weaker infra-red band at about  $1290$  can be explained by the combinations ( $453 + 832$ ) or ( $686 + 604$ ). This leaves  $453$ ,  $565$ ,  $686$ , and  $748$  for plausible fundamentals, but there is no means of allocating any of them to specific types of vibration. As in the case of furan, a consideration of the overtones and combination bands is not helpful since satisfactory interpretation of most of the bands can be obtained with the established frequencies in more than one way. If the infra-red measurements could be extended out to  $25\mu$  so as to cover the region of the frequency  $453\text{ cm}^{-1}$ , the nature of this vibration might be ascertained.

The small differences found between the calculated and observed spacings of sub-maxima in some of the bands may arise either from small errors in calculating the spacings by extrapolation from Badger and Zumwalt's curves, or because the molecular dimensions assumed are slightly incorrect.

Lord and Miller<sup>12</sup> have recently measured the infra-red and Raman spectra of pyrrole and some deuterated pyrroles, and have assigned values to the normal vibration frequencies. There should be a close similarity between the frequencies of pyrrole and furan, and some correspondence of these with certain of the frequencies of thiophen. In Table IV the three sets of results are shown together.

As regards the frequencies in the  $A_1$ —totally symmetrical—class, there is a marked correspondence between the three molecules. The considerations outlined above do not in themselves allow us to decide which magnitude is associated with each particular mode within the class, but since the frequencies of pyrrole have been assigned using other considerations, we can arrange those of furan and thiophen as shown, remembering that the ring frequencies may change most in passing along the series. The correlation with the other classes of vibration are too incomplete yet to be considered in detail.

If furan and thiophen were non-planar, the selection rules for the Raman and infra-red spectra would differ from those given above for  $C_{2v}$  symmetry. Some authors have attempted to infer which type of symmetry exists from the number of frequencies which appear in the different types of spectrum, and from the number of polarised Raman frequencies. These considerations do not seem to us very significant, since not only may the selection rules break down with liquids owing to molecular distortions, but also the fact that a given vibration is permitted to appear in the Raman effect or in the infra-red absorption spectrum is not necessarily an indication that it will have sufficient intensity to be actually observed. A more satisfactory argument might be to correlate the observed rotational contour of the bands with the values of the moments of inertia, which will differ according to whether the molecule is planar or has a buckled structure. Unfortunately, the changes in the moments of inertia for slight buckling of the ring are not very marked, and the spacings between the maxima in the infra-red bands cannot be determined with very high precision.

<sup>12</sup> *J. Chem. Physics*, 1942, 10, 328.

TABLE IV

Class.	Type.	Pyrrole.	Furan.	Thiophen.
$A_1$	Ring	711	724	604
	C—H deformation	1076	1067	1032
	Ring	1144	994	832
	C—H deformation	1237	1137	1077
	Ring	1384	1381	1358
	Ring	1467	1486	1404
	C—H stretching	3100	(3090)	(3080)
	C—H stretching	3133	(3120)	(3110)
	N—H stretching	3400	absent	absent
$A_2$	Ring	(510)		
	C—H deformation	711	?, ?, ?	?, ?, ?
	C—H deformation	868		
$B_1$	Ring	647		
	C—H deformation	1015	872, 1270,	872, 1252,
	C—H deformation	1046	?, ?	?, ?
	Ring	1418		
	Ring	1530	1579	1590
	C—H stretching	3111	(3090)	(3080)
	C—H stretching	(3133)	(3120)	(3110)
	N—H deformation	(1146)	absent	absent
$B_2$	N—H deformation	565	absent	absent
	C—H deformation	768		
	Ring	838	605, 744,	710, ?, ?
	C—H deformation	(1046)	837	
	Probable fundamentals unallocated		1034	686, 748,
				453, 565

It may, however, be noticed that the calculated and observed spacings for the planar model with the dimensions assumed above do not quite agree in some cases, but here again the calculated spacings may be slightly in error for the reasons given above. On the whole, the results seem to be in satisfactory agreement with planar structures of  $C_{2v}$  symmetry.

### Summary.

The infra-red spectra of furan and thiophen have been measured and compared with the Raman spectra. Selection rules, band contours, and other considerations have been used in attempting to assign values to the molecular vibration frequencies. Attention has been drawn to some misinterpretations of earlier data with furan. These two molecules appear to have a planar structure in the symmetry class  $C_{2v}$ .

We are grateful to the Government Grant Committee of the Royal Society and to the Chemical Society for grants in aid of apparatus.

*The Physical Chemistry Laboratory,  
Oxford.*

# THE ABSORPTION SPECTRA OF THE CHLORO ETHYLENES IN THE VACUUM ULTRA-VIOLET.

By A. D. WALSH.

Received 26th September, 1944.

The spectra of ethylene and several of its alkyl derivatives have been studied by Price and Tutte.<sup>1</sup> The spectra of the chloro ethylenes are important because of the light they shed on the effects of halogen substitution adjacent to a double bond. While these molecules give uninteresting continua in the near ultra-violet, their spectra in the vacuum ultra-violet are full of interesting structure. These spectra have been photographed on a Lyman continuum as background with a normal incidence vacuum spectrograph designed by Dr. W. C. Price and built in the Laboratory of Physical Chemistry, Cambridge. The grating was of glass, ruled with 15,000 lines to the inch and the dispersion was linear and about 16.8 Å/mm., the exact value depending upon the precise experimental arrangement. The photographic plates consisted of Ilford Q emulsion coated on microscope cover glass so as to bend easily into the Rowland circle.

## The Spectrum of Vinyl Chloride.

Crude vinyl chloride, an I.C.I. product, was available. This contained ethylene and was therefore purified by liquefaction, followed by pumping off the vinyl chloride from the crude liquid at the temperature of dry ice. The resulting gas was free from ethylene as shown by the spectrum obtained.

The spectrum (Plate 1) begins with a strong, diffuse, region of absorption, its maximum being about 1850 Å. A few faint, diffuse, bands are visible on the long wavelength side. Accurate measurement of these bands is impossible, but the order of magnitude of their separations is shown in Table I.

TABLE I.—THE FREQUENCIES OF THE VINYL CHLORIDE BANDS BETWEEN 1800 AND 1600 Å.

cm.<sup>-1</sup>

57330

1380

58710

1300

60010

1440

61450

TABLE II.—THE FREQUENCIES OF THE 1585 Å. PROGRESSION IN VINYL CHLORIDE.

cm.<sup>-1</sup>

63048

64420 (Predissociated) 1372

65807 1387

67145 1338

68545 1400

69920 1375

TABLE III.—THE FREQUENCIES OF THE VINYL CHLORIDE 1471 Å. PROGRESSION.

cm.<sup>-1</sup>.

67979

1199

69178

1242

70420

The frequency involved is almost certainly the C=C valence vibration reduced by the excitation from its value of 1608 cm.<sup>-1</sup> in the ground

<sup>1</sup> Price and Tutte, *Proc. Roy. Soc., A*, 1940, 174, 207.

state.<sup>2</sup> The analogous region of absorption in ethylene has a similar frequency of 1370 cm.<sup>-1</sup> (1623 cm.<sup>-1</sup> in the ground state).

At 1585 Å. a new vibrational system starts and extends to 1430 Å. The strong bands of this system are shown in Table II. The frequency involved is ~1375 cm.<sup>-1</sup>.

At 1462 Å. an especially strong band occurs. A band similar in position and intensity occurs in the spectra of chloroprene and phenyl chloride. It is thought to be due to the non-bonding electrons of the chlorine atom and to be analogous to the "D" bands of the alkyl chlorides.<sup>3,4</sup>

Another vibrational progression starts at 1471 Å., overlapping with the 1585 Å. system. The strong bands of this system are given in Table III. The frequency involved is ~1200 cm.<sup>-1</sup>; it presumably represents the symmetrical C=C valence vibration further reduced by the increasing excitation.

About 1350 Å. bands begin that are fairly obviously Rydberg in character: that is, they crowd together and decrease in intensity towards shorter wavelengths, eventually fusing into a continuum of absorption around 1240 Å. It was found possible to pick out two well-developed Rydberg series denoted by the formulae

$$\nu_0^n = 80645 - \frac{R}{(n + 0.95)^2} \quad (1)$$

$$\nu_0^n = 80700 - \frac{R}{(n + 0.15)^2} \quad (2)$$

The two series have approximately the same limit,  $9.95 \pm 0.01V$ . The reality of this ionisation potential is strongly supported by the appearance

TABLE IV.—THE OBSERVED AND CALCULATED FREQUENCIES OF THE RYDBERG BANDS OF VINYL CHLORIDE.

<i>n</i> .	$\nu_{\text{obs.}}$ cm. <sup>-1</sup>	$\nu_{\text{calc.}}$ cm. <sup>-1</sup>
Series 1		
2	67979	68035
3	73649	73612
4	76176	76166
5	77541	77545
6	78367	78374
7	78909	78909
8	79298	79275
9	79551	79536
10	79737	79730
Series 2		
2	c. 55000	55960
3	69606	69641
4	74357	74328
5	76567	76562
6	77797	77799
7	78558	78553
8	79034	79047

of the bands converging to it and by the continuous absorption starting at this point. An enlarged photograph of the region of the limit is given in Plate 1. Table IV shows the accuracy with which the equations (1) and (2) respectively reproduce the observed frequencies.

The short vibrational progressions associated with the early Rydberg bands suggest that a weakly-bonding electron is being excited. As in the case of ethylene, it is probable that the ionisation limit found corresponds to the removal of a  $\pi$  electron from the double bond.

There are indications of a third Rydberg series beginning with the 1585 Å. band and proceeding to approximately the same limit as series (1) and (2). The Rydberg denominator is  $(n + 0.35)^2$ .

The  $n = 2$  member of series (2) falls in the region around 1850 Å. The general appearance of this region, however, strongly

suggests that the  $N \rightarrow V$  transition of the  $\pi$  electrons of the double bond

<sup>2</sup> Hibben, *The Raman Effect*, Reinhold, 1939.

<sup>3</sup> Price, *J. Chem. Physics*, 1936, 4, 539.

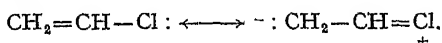
<sup>4</sup> Price, *ibid.*, 1936, 4, 547.

also occurs here. (For the explanation of the symbolism  $N \rightarrow V$  see Mulliken.<sup>5</sup>) The 1850 Å. region is thus to be interpreted as mixed Rydberg— $N \rightarrow V$  in type, just as is the first region of absorption in ethylene. This means that the first Rydberg transition should be more antibonding than the second, which is indeed found to be the case in ethylene. In vinyl chloride, however, the diffuseness of the vibrational bands in the 1850 Å. region makes it impossible to say whether the frequency there is greater or less than that found in the second electron level.

In ethylene (see ref. 1), the first Rydberg transition (1745 Å.) overlaps the  $N \rightarrow V$  transition on the long wavelength side of the latter: it causes the absorption region to have a sharp long wavelength onset, comparatively independent of pressure. The two transitions can be readily distinguished, the  $N \rightarrow V$   $\nu_{\max}$  occurring at 1630 Å. In all the chloroethylenes and also in the alkyl ethylenes, the shape of the first absorption region is that of a fairly smooth hump and it is much more difficult to distinguish between the  $N \rightarrow V$  and first Rydberg transitions. This is due to the facts that in the substituted ethylenes (a) the size of the molecule is greater and (b) the ionization potential is lower (so that the first Rydberg band falls at longer wavelengths). Though in the ethylene molecule, as Mulliken<sup>6</sup> has pointed out, the electron in the first excited state would spend most of its time outside the hydrogen atoms, in the substituted ethylenes this is no longer true and the first Rydberg orbital, lying within the nuclear framework, is greatly perturbed by the intravalence shell  $N \rightarrow V$  transition. Similarly, acetaldehyde is like ethylene in that absorption begins sharply at long wavelengths (1650 Å.), but in acetyl chloride and chloral the onset is gradual.<sup>7</sup>

All the strong bands of the vinyl chloride spectrum are thus accounted for.

The ionization limit and the electronic levels as a whole are shifted to long wavelengths relative to ethylene. The high electronegativity of the chlorine atom would lead one to expect the opposite on a simple inductive effect. The explanation is doubtless that resonance is occurring between the  $\pi$  electrons of the double bond and the non-bonding  $p\pi$  lone pair of the chlorine:



Support for this is found in the fact that the band identified as due to the non-bonding chlorine electrons lies at slightly shorter wavelengths (1462 Å.) than in ethyl chloride, indicating a higher ionisation potential and a positive charge on the chlorine atom.

Similar effects occur in the other chloro ethylenes. The resonance is in accord with the results of electron diffraction: Brockway, Beach and Pauling<sup>8,9</sup> find in all the chloro ethylenes reduced C—Cl distances (corresponding to resonance to  $\text{C}=\text{Cl}^+$ ), relative to the C—Cl distance in ethyl chloride.

First regions of absorption similar to the 1850 Å. region of vinyl chloride occur in the spectra of all the chloro ethylenes and are all to be interpreted as  $N \rightarrow V$  in type, with perhaps some Rydberg character. As the number of chlorine atoms is increased, the increasing conjugation of the  $\pi$  electrons of the C=C bond with the  $p\pi$  chlorine electrons pushes the transition more and more to long wavelengths.

<sup>5</sup> Mulliken, *J. Chem. Physics*, 1939, 7, 20.

<sup>6</sup> Mulliken, *Revs. Mod. Physics*, 1942, 14, 265.

<sup>7</sup> Walsh, *Results to be published*.

<sup>8</sup> Brockway, Beach and Pauling, *J. Am. Chem. Soc.*, 1935, 57, 2693.

<sup>9</sup> Pauling, *Nature of the Chemical Bond*, Cornell, 1940, p. 215.



### The Spectrum of *cis* Dichloroethylene.

The *cis* dichloroethylene used was a B.D.H. product of boiling point 58-60° C.

As in all the other chloroethylenes, the spectrum (Plate 2) begins with a strong, diffuse, region of absorption. The maximum is at about 1900 Å. There is no measurable structure in this region. A system of strong bands occurs in the region 1700-1600 Å. The frequencies and frequency differences of the main bands are shown in Table V. The 1420 cm.<sup>-1</sup> difference must be the symmetrical C=C valence frequency, reduced by the excitation from its value of 1587 cm.<sup>-1</sup> in the ground state.<sup>10, 11</sup> The 810 cm.<sup>-1</sup> difference is probably the symmetrical C—Cl valence vibration (873 cm.<sup>-1</sup> in the ground state).

A rich vibrational system with many sharp bands extends from 1535 to about 1430 Å. Its structure is difficult to unravel without introducing many arbitrary frequency differences. A few fragmentary progressions from it are shown in Table VI.

TABLE VI.—PROGRESSIONS IN THE 1535-1430 Å. REGION OF *cis* DICHLOROETHYLENE.

cm. <sup>-1</sup>		cm. <sup>-1</sup>
65860		66671
	1426	203
67286		66874
	1393	213
68679		67087

In both these latter systems the symmetrical C = C valence vibration (~ 1410 cm.<sup>-1</sup>) appears and also a frequency ~ 250 cm.<sup>-1</sup>. The latter, by analogy with ethylene, may represent a twisting of the CHCl groups about the C=C bond.

At 1427 and 1347 Å. strong bands occur which may be due to slight *trans* impurity, since bands in these positions are the strongest bands of the *trans* spectrum. Continuous absorption sets in about 1300 Å., rather earlier than in the case of *trans* dichloroethylene.

The spectra of the *cis* and *trans* dichloroethylene have been previously studied by Mahncke and Noyes.<sup>12</sup> They found two Rydberg series in the *cis* form:

$$\nu_n = 77703 - \frac{R}{(n - 0.045)^2} \quad (3)$$

$$\nu_n = 78103 - \frac{R}{(n - 0.01)^2} \quad (4)$$

<sup>10</sup> Paulsen, *Z. physik. Chem., B*, 1935, 28, 132.

<sup>11</sup> Trumpy, *Z. Physik*, 1934, 90, 133.

<sup>12</sup> Mahncke and Noyes, *J. Chem. Physics*, 1935, 3, 536.

TABLE V.—FREQUENCIES OF THE BANDS OF *cis* DICHLOROETHYLENE IN THE 1700-1600 Å. REGION.

cm. <sup>-1</sup>	
59749	805 } 1423
60554	
61172	
	810 } 1418
61982	
62590	

A third vibrational system appears to have its origin at 1414 Å. The main bands of this system and their differences are shown in Table VII.

TABLE VII.—FREQUENCIES OF THE BANDS OF THE 1414 Å. SYSTEM OF *cis* DICHLOROETHYLENE.

cm. <sup>-1</sup>	
70723	256 } 1416
70981	
71241	
72141	270 } 1406
72411	
72655	
73547	

The ionisation potentials to which (3) and (4) lead differ by 0.05 volt. Only four members were observed for each series: great reliance cannot therefore be placed upon their limits. The probable greater contrast of our plates has enabled us to observe these series rather better than could Mahncke and Noyes. Our revised formulæ are

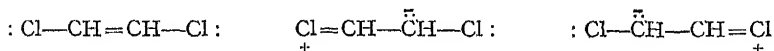
$$\nu_0^n = 77850 - \frac{R}{(n + 0.93)^2} \quad . \quad . \quad . \quad (5)$$

$$\nu_0^n = 77937 - \frac{R}{(n + 0.05)^2} \quad . \quad . \quad . \quad (6)$$

Series (5) starts with the same two bands as series (3) and series (6) with the same two bands as series (4). Table VIII shows the accuracy with which equations (5) and (6) respectively reproduce the observed frequencies.

Five members were observed for series (5) and four members for series (6). The 1900 Å. region may in part represent the first member of series (6) ( $\nu_{\max.} = 52630 \text{ cm.}^{-1}$ ,  $\nu_{\text{calc.}} = 53053 \text{ cm.}^{-1}$ ). The limits of the two series are the same within the accuracy of the extrapolation and correspond to  $9.61 \pm 0.02 \text{ v.}$  Support for this value is found in the facts that both series proceed to approximately the same limit, that the limit coincides with the onset of continuous absorption and that Mahncke and Noyes found an electron impact value of  $9.7 \pm 0.3 \text{ v.}$  The Rydberg series are presumably due to the excitation of a  $\pi$  electron from the C=C bond.

At about 1467 Å. a very strong doublet occurs which is probably analogous to the "D" bands found in the alkyl chlorides and due to the non-bonding  $p\pi$  chlorine electrons. The components lie at 1464 and 1469 Å. They are thus shifted slightly to long wavelengths relative to vinyl chloride, indicating a smaller positive charge on each chlorine atom in *cis* dichloroethylene than on the single chlorine atom in vinyl chloride. The resonance forms for the dichloroethylene, similar to those already written for vinyl chloride, are



Each chlorine atom thus bears a positive charge in only one out of three resonance forms, whereas in vinyl chloride the single chlorine atom bears a positive charge in one out of two resonance forms. This is doubtless why the chlorine atom in vinyl chloride bears a greater positive charge in the resonance hybrid than do the chlorine atoms in dichloroethylene.

The C=C bond is subject to twice as great an inductive effect by the chlorine atoms in dichloroethylene as in vinyl chloride. In spite of this, the first maximum occurs at 1900 Å. as against 1850 Å. in vinyl chloride and the ionisation potential of the  $\pi$  electrons of the C=C bond at 9.16 as against 9.95 v., showing the predominance of the mesomeric effect over the inductive effect.

TABLE VIII.—THE OBSERVED AND CALCULATED FREQUENCIES OF THE RYDBERG BANDS OF *cis* DICHLOROETHYLENE.

<i>n</i> .	$\nu_{\text{obs.}}$ cm. <sup>-1</sup> .	$\nu_{\text{calc.}}$ cm. <sup>-1</sup> .
Series (5)		
2	65182	65068
3	70725	70747
4	73331	73334
5	74749	74730
6	75575	75565
Series (6)		
3	65840	66140
4	71220	71247
5	73652	73634
6	74941	74939

### The Spectrum of *trans* Dichloroethylene.

The *trans* dichloroethylene used was a B.D.H. product of boiling point 47-48° C.

The spectrum as a whole is noticeably more diffuse than that of the *cis* molecule. It begins with a diffuse region of absorption, of maximum about 1950 Å. On the short wavelength side of this, between 1800 and 1550 Å., a few diffuse bands can be observed. At 1530 Å. a strong vibrational progression starts. Many frequencies seem to be appearing here, but Table IX shows the main regularities. The bands are very sharp.

The frequency of about 1435 cm.<sup>-1</sup> is undoubtedly the symmetrical C = C valence frequency reduced by the excitation from its value of 1577 cm.<sup>-1</sup> in the ground state. The 730 cm.<sup>-1</sup> frequency is probably the symmetrical C—Cl valence vibration (847 cm.<sup>-1</sup> in the ground state<sup>10, 11</sup>). The 180 cm.<sup>-1</sup> frequency possibly represents the symmetrical lowest Raman frequency (349 cm.<sup>-1</sup>).

At 1427 Å. occurs the strongest band of the whole spectrum. Thenceforward, bands occur, crowding together and decreasing in intensity towards shorter wavelengths in the familiar manner of Rydberg bands. They fuse into a continuum about 1240 Å. It was found possible to arrange many of the bands into a Rydberg series represented by

$$\nu_0^n = 80285 - \frac{R}{(n + 0.28)^2} \quad (7)$$

The accuracy of this representation is shown in Table X. The limit

TABLE X.—OBSERVED AND CALCULATED FREQUENCIES OF THE RYDBERG BANDS OF *trans* DICHLOROETHYLENE.

<i>n</i> .	$\nu_{\text{obs.}}$ cm. <sup>-1</sup>	$\nu_{\text{calc.}}$ cm. <sup>-1</sup>
3	70081	70086
4	74268	74292
5	76350	76349
6	77505	77503
7	78220	78214
8	78738	78684

TABLE IX.—FREQUENCIES OF THE 1530 Å. BANDS OF *trans* DICHLOROETHYLENE.

cm. <sup>-1</sup>			
65419			
65789	370	732	
66151			1444
66335	184		
66863			
67222	359	727	
67590			1429
67770	180		
68292			
68655	363	764	
69056			
69223	167		

the *trans* than in the *cis* form. Only when the upper orbital of the first transition contains the same atomic framework in two molecules can comparative predictions of their ionisation potentials be made from their first regions of absorption.

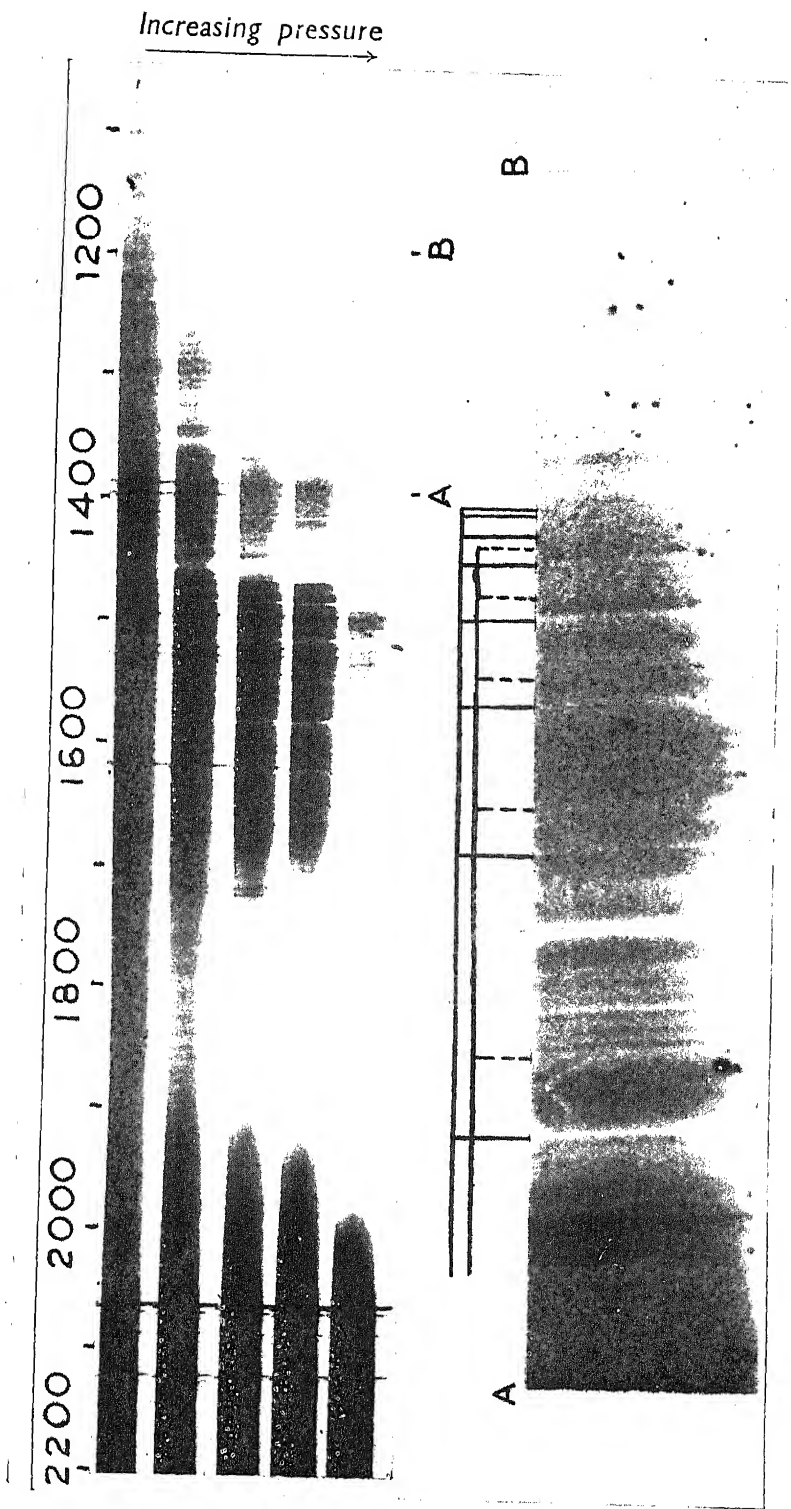
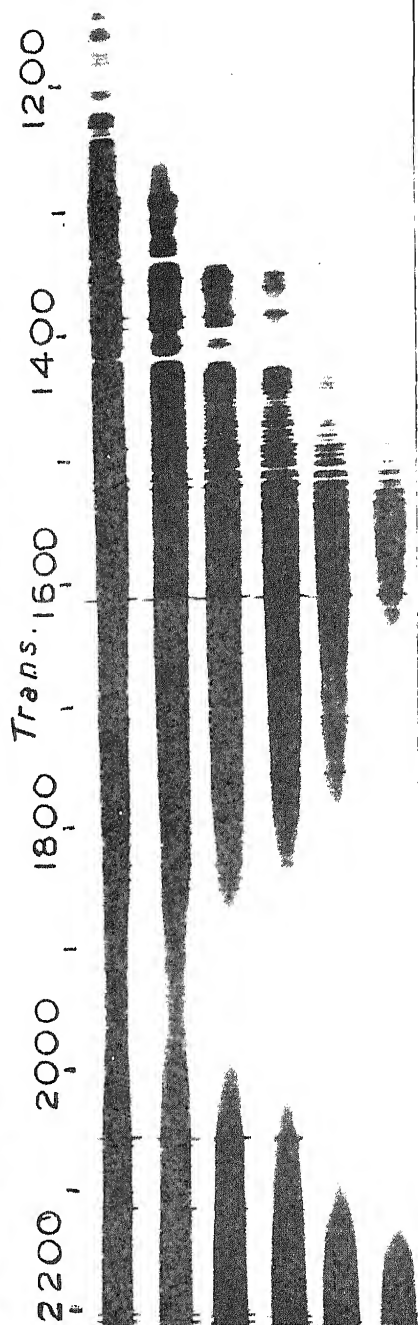
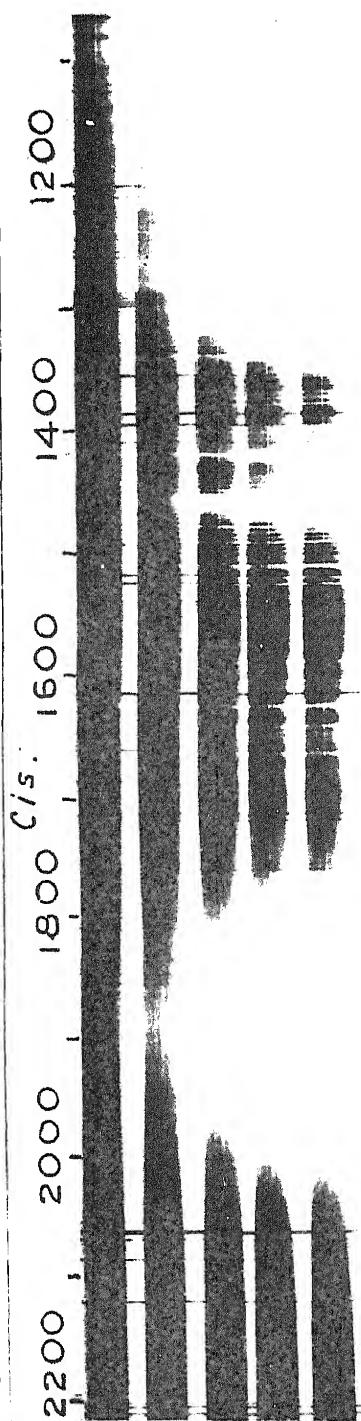


PLATE 1.—The Spectrum of Vinyl Chloride.

Increasing pressure →



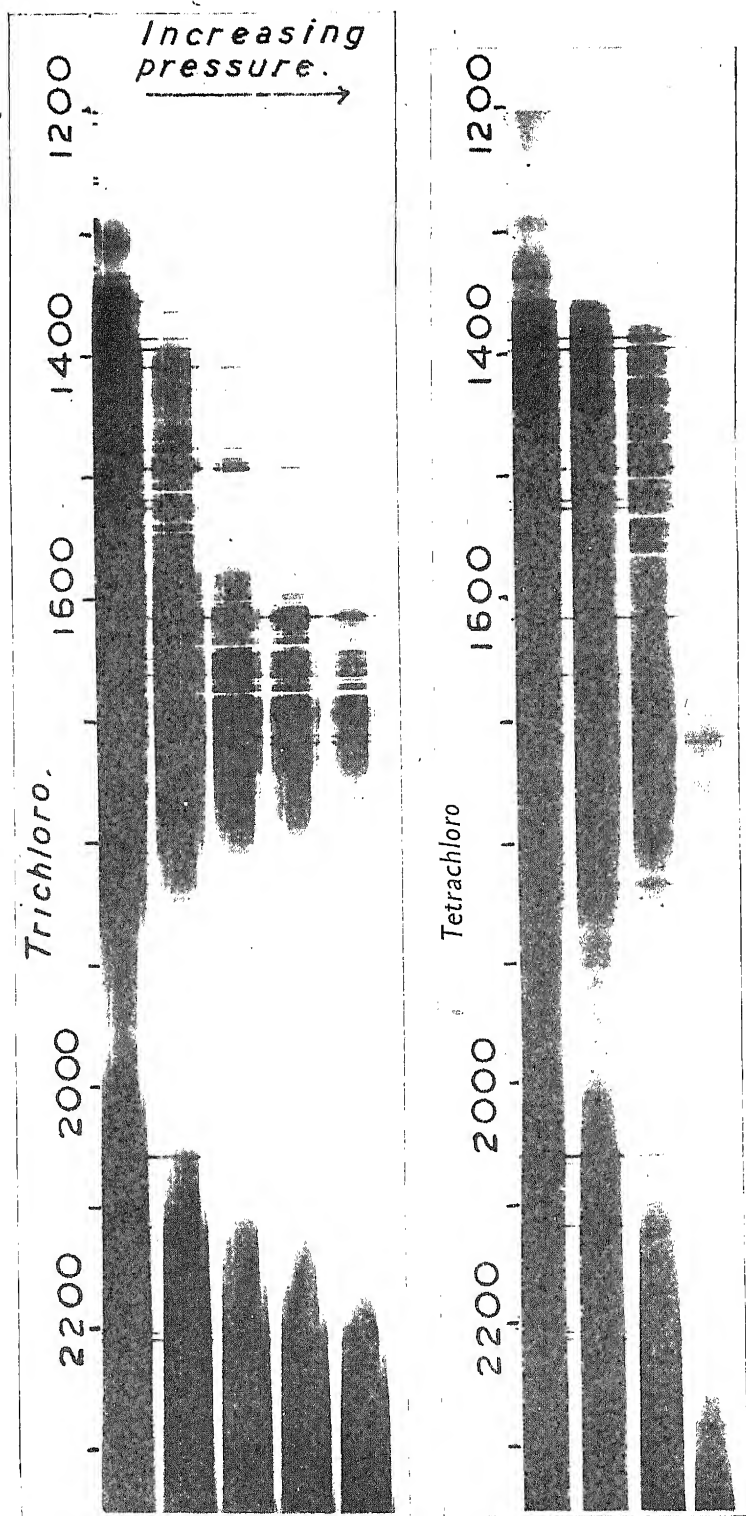


PLATE 3.—The Spectra of Trichloro and Tetrachloroethylene.



Since the resonance hybrid has something of the character of a diene, it may be that the *trans* dichloroethylene has a higher ionisation potential than the *cis* for the same reasons (*e.g.* repulsion of the double bond electrons in the *cis* form) that cause *trans* dienes to have higher first ionisation potentials than *cis* dienes.<sup>13, 14</sup> On the other hand, the first strong, diffuse, absorption in these dichloroethylenes is interpreted as  $N \rightarrow V$ . Such absorption is pushed further and further to long wavelengths the greater the resonance. The chlorine atoms bear positive charges in the resonance hybrids. Hence, in the *cis* form, their repulsion results in molecular strain (such as slight twisting from the planar condition) which in turn reduces the resonance (for resonance, the axis of symmetry of the  $2p\pi$  electrons must be parallel with the axis of symmetry of the double bond  $\pi$  electrons) and so relieves the strain. The resonance is thus less in *cis* than in *trans* dichloroethylene and the  $N \rightarrow V$  transition is at longer wavelengths in *trans* than in *cis*, as observed. The position is rather like that in unsymmetrical methyl styrene<sup>7</sup> where the repulsion of the methyl and phenyl groups causes a slight twisting about the Ph—C bond, with a consequent reduction in conjugation energy between the  $\pi$  electrons of the benzene ring and of the C=C bond, resulting in certain regions of the spectrum being shifted to short wavelengths relative to styrene, in strong contrast to the usual effect of methyl substitution. Other examples of steric hindrance reducing conjugation are to be found in the reviews by Lewis and Calvin<sup>15</sup> and by Mulliken and Rieke.<sup>16</sup>

The "D" bands due to the non-bonding  $p\pi$  chlorine electrons do not appear strongly in *trans* dichloroethylene. They are probably present in the neighbourhood of 1467 Å. but it is difficult to be sure of their exact identity. One expects them to lie slightly on the short wavelength side of the corresponding bands in *cis* dichloroethylene, as a consequence of the greater resonance in the *trans* form.

As mentioned in the discussion of the *cis* spectrum, the spectra of the dichloroethylenes have been previously reported by Mahncke and Noyes.<sup>12</sup> In several respects, the interpretation of the spectra given here is in disagreement with that given by Mahncke and Noyes. The discrepancy in the case of the *cis* ionisation potential has already been noted. For the first ionisation potential of the *trans* form, Mahncke and Noyes were unable to find any Rydberg series, but gave an electron bombardment value of 11.3 v. It is improbable, however, that the separation of the *cis* and *trans* ionisation potentials would be as much as 1.7 v.; corresponding regions in the spectra are shifted by very much smaller energy amounts than that. 11.3 v. is probably the approximate value of a higher ionisation potential of *trans* dichloroethylene. Judging from the position of the "D" bands in *cis* dichloroethylene, the ionisation potential of the  $p\pi$  chlorine electrons is  $\sim 10.9$  v. The ionisation potential of the  $p\pi$  chlorine electrons in *trans* dichloroethylene is probably not far different (a little higher). It may therefore be that the value 11.3 v. represents the ionisation potential of the non-bonding chlorine electrons, since electron impact values are usually a few tenths of a volt higher than spectroscopic ionisation potential values.

### The Spectrum of Trichloroethylene.

Commercial trichloroethylene was purified by fractional distillation, that boiling at 88° C. being used.

The spectrum (Plate 3) begins with a strong, diffuse, region of absorption of maximum about 1960 Å. No structure is visible in this region, except possibly a few very faint bands on the short wavelength side.

<sup>13</sup> Price and Walsh, *Proc. Roy. Soc., A*, 1940, 174, 220.

<sup>14</sup> *Ibid.*, 1941, 179, 201.

<sup>15</sup> Lewis and Calvin, *Chem. Rev.*, 1939, 25, 302.

<sup>16</sup> Mulliken and Rieke, *Rep. on Prog. in Physics*, 1941, 8, 231.





Since the resonance hybrid has something of the character of a diene, it may be that the *trans* dichloroethylene has a higher ionisation potential than the *cis* for the same reasons (*e.g.* repulsion of the double bond electrons in the *cis* form) that cause *trans* dienes to have higher first ionisation potentials than *cis* dienes.<sup>13, 14</sup> On the other hand, the first strong, diffuse, absorption in these dichloroethylenes is interpreted as  $N \rightarrow \bar{V}$ . Such absorption is pushed further and further to long wavelengths the greater the resonance. The chlorine atoms bear positive charges in the resonance hybrids. Hence, in the *cis* form, their repulsion results in molecular strain (such as slight twisting from the planar condition) which in turn reduces the resonance (for resonance, the axis of symmetry of the  $2p\pi$  electrons must be parallel with the axis of symmetry of the double bond  $\pi$  electrons) and so relieves the strain. The resonance is thus less in *cis* than in *trans* dichloroethylene and the  $N \rightarrow \bar{V}$  transition is at longer wavelengths in *trans* than in *cis*, as observed. The position is rather like that in unsymmetrical methyl styrene<sup>7</sup> where the repulsion of the methyl and phenyl groups causes a slight twisting about the Ph—C bond, with a consequent reduction in conjugation energy between the  $\pi$  electrons of the benzene ring and of the C=C bond, resulting in certain regions of the spectrum being shifted to short wavelengths relative to styrene, in strong contrast to the usual effect of methyl substitution. Other examples of steric hindrance reducing conjugation are to be found in the reviews by Lewis and Calvin<sup>15</sup> and by Mulliken and Rieke.<sup>16</sup>

The "D" bands due to the non-bonding  $p\pi$  chlorine electrons do not appear strongly in *trans* dichloroethylene. They are probably present in the neighbourhood of 1467 Å. but it is difficult to be sure of their exact identity. One expects them to lie slightly on the short wavelength side of the corresponding bands in *cis* dichloroethylene, as a consequence of the greater resonance in the *trans* form.

As mentioned in the discussion of the *cis* spectrum, the spectra of the dichloroethylenes have been previously reported by Mahncke and Noyes.<sup>12</sup> In several respects, the interpretation of the spectra given here is in disagreement with that given by Mahncke and Noyes. The discrepancy in the case of the *cis* ionisation potential has already been noted. For the first ionisation potential of the *trans* form, Mahncke and Noyes were unable to find any Rydberg series, but gave an electron bombardment value of 11.3 v. It is improbable, however, that the separation of the *cis* and *trans* ionisation potentials would be as much as 1.7 v.; corresponding regions in the spectra are shifted by very much smaller energy amounts than that. 11.3 v. is probably the approximate value of a higher ionisation potential of *trans* dichloroethylene. Judging from the position of the "D" bands in *cis* dichloroethylene, the ionisation potential of the  $p\pi$  chlorine electrons is  $\sim 10.9$  v. The ionisation potential of the  $p\pi$  chlorine electrons in *trans* dichloroethylene is probably not far different (a little higher). It may therefore be that the value 11.3 v. represents the ionisation potential of the non-bonding chlorine electrons, since electron impact values are usually a few tenths of a volt higher than spectroscopic ionisation potential values.

### The Spectrum of Trichloroethylene.

Commercial trichloroethylene was purified by fractional distillation, that boiling at 88°C. being used.

The spectrum (Plate 3) begins with a strong, diffuse, region of absorption of maximum about 1960 Å. No structure is visible in this region, except possibly a few very faint bands on the short wavelength side.

<sup>13</sup> Price and Walsh, *Proc. Roy. Soc., A*, 1940, 174, 220.

<sup>14</sup> *Ibid.*, 1941, 179, 201.

<sup>15</sup> Lewis and Calvin, *Chem. Rev.*, 1939, 25, 302.

<sup>16</sup> Mulliken and Rieke, *Rep. on Prog. in Physics*, 1941, 8, 231.

At 1686 Å. a strong band occurs which is evidently the origin of a vibrational progression extending to 1550 Å. The frequencies of the main bands of this system and their assignments are shown in Table XI.

The vibrational structure of the weaker bands of the region is complicated and it may be that more than one electronic level occurs in the absorption. The 1400  $\text{cm}^{-1}$  frequency must be the symmetrical  $\text{C}=\text{C}$  valence vibration, reduced by the excitation from its value of 1585  $\text{cm}^{-1}$  in the ground state.<sup>17</sup> The 660  $\text{cm}^{-1}$  frequency is probably the  $\text{C}-\text{Cl}$  symmetrical valence vibration (775  $\text{cm}^{-1}$  in the ground state) also reduced by the excitation.

At 1585 Å. the continuum weakens considerably and at 1553 Å. a strong band initiates another vibrational progression. The frequencies and assignments of the main bands in this region are shown in Table XII. A  $\text{C}=\text{C}$  valence vibration occurs with practically the same value as in the first system. The 426  $\text{cm}^{-1}$  vibration is probably a  $\text{C}-\text{Cl}$   $\delta$  frequency.

Below 1400 Å. only diffuse absorption occurs. It is noticeable that,

TABLE XII.—FREQUENCIES AND ASSIGNMENTS OF THE 1553 Å. BANDS OF TRICHLOROETHYLENE.

$\nu_{\text{obs.}}$ $\text{cm}^{-1}$	Assignment.	$\nu_{\text{calc.}}$ $\text{cm}^{-1}$
64373	00	
64799	$\omega_1$	64799
65778	$\omega_2$	65773
66194	$\omega_2 + \omega_1$	66199
67163	$2\omega_2$	67173
67602	$2\omega_2 + \omega_1$	67599
68555	$3\omega_2$	68573

$$\omega_1 = 426 \pm 10 \text{ cm}^{-1} \quad \omega_2 = 1400 \pm 10 \text{ cm}^{-1}.$$

If the 1686 Å. and 1553 Å. bands are consecutive members of a Rydberg series, an ionisation potential of  $\sim 71,000 \text{ cm}^{-1}$  (8.8 v.) is indicated. Other bands can be found to fit such a series, giving the possible formula

$$\nu_n = 70,890 - \frac{R}{(n + 0.10)^2} \quad (8)$$

Table XIII shows the agreement between observed and calculated frequencies. The series is presumably due to the excitation of a  $\pi$  electron

<sup>17</sup> Dadiou and Kohlrausch, *Physik. Z.*, 1929, 138, 635.

TABLE XI.—FREQUENCIES AND ASSIGNMENTS OF THE TRICHLOROETHYLENE 1686 Å. BANDS.

$\nu_{\text{obs.}}$ $\text{cm}^{-1}$	Assignment.	$\nu_{\text{calc.}}$ $\text{cm}^{-1}$
59295	0000	
59582	$\omega_1$	59575
59697	$\omega_1 + \omega_2$	59695
59961	$\omega_4$	59955
60705	$\omega_3$	60695
60985	$\omega_3 + \omega_1$	60975
61104	$\omega_3 + \omega_1 + \omega_2$	61095
61362	$\omega_3 + \omega_4$	61355
62091	$2\omega_3$	62095
62362	$2\omega_3 + \omega_1$	62375
62483	$2\omega_3 + \omega_1 + \omega_2$	62495
62784	$2\omega_3 + \omega_4$	62755

$$\omega_1 = 280 \pm 10 \text{ cm}^{-1}, \quad \omega_2 = 120 \pm 10 \text{ cm}^{-1}, \\ \omega_3 = 1400 \pm 15 \text{ cm}^{-1}, \quad \omega_4 = 660 \pm 20 \text{ cm}^{-1}.$$

relative to the first region of absorption, this is stronger than in vinyl chloride or in the dichloroethylenes. In tetrachloroethylene it is stronger still. Hence it is mainly due to the electrons in the  $\text{C}-\text{Cl}$  bonds or to the chlorine non-bonding electrons and similar to the absorption found with carbon tetrachloride.

from the C=C bond. The 1960 Å. region may represent the first member of the series, although as already stated the first region of absorption of all the chloroethylenes is also to be interpreted as of  $N \rightarrow V$  character.

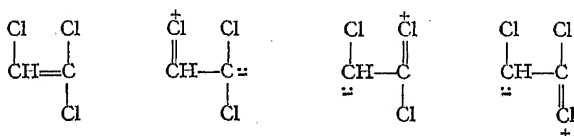
TABLE XIII.—OBSERVED AND CALCULATED FREQUENCIES OF THE RYDBERG BANDS OF SERIES (8).

$n$ .	$\nu_{\text{obs.}}$ cm. <sup>-1</sup>	$\nu_{\text{calc.}}$ cm. <sup>-1</sup>
3	59295	59471
4	64373	64362
5	66677	66671
6	67944	67941
7	68678	68713
8	69233	69217

The limit corresponds to 8.75 v. The ionisation potential cannot, however, be regarded as definitely established until confirmed by an electron impact determination.

The shift of the first maximum of absorption to long wavelengths relative to the dichloroethylenes and the plausible ionisation potential of 8.75 v.

indicate that the mesomeric effect due to the three chlorine atoms puts more negative charge into the region of the C=C bond than the inductive effect takes away. The mesomeric forms are



When two chlorine atoms are situated on opposite sides of the C=C bond, the spectrum of the non-bonding chlorine electrons seems to be suppressed. Thus, whereas the chlorine "D" bands are prominent in chloroprene, monochloro benzene, *o*-dichloro benzene, vinyl chloride and *cis* dichloroethylene, they are weak (if present at all) in *trans* dichloroethylene. Similarly they do not appear strongly in trichloro and tetrachloroethylene. A theoretical explanation of this phenomenon would seem desirable. Possibly the bands become diffuse as in the spectrum of carbon tetrachloride.

### The Spectrum of Tetrachloroethylene.

The tetrachloroethylene used was a pure product obtained from Messrs. Harrington. It had a boiling point of 120° C.

The ultraviolet absorption spectrum begins with a strong, diffuse region of absorption, of maximum around 1970 Å. With increasing pressure this absorption spreads rapidly both to long and to short wave-lengths: in this respect it is to be

TABLE XIV.—FREQUENCIES AND FREQUENCY DIFFERENCES IN THE 1900 Å. SYSTEM OF TETRACHLOROETHYLENE.

cm. <sup>-1</sup>	
Obscured.	
50801	c. 450
51275	471
51742	
52186	444
52641	455
53127	
53522	395
54020	498
54457	
55766	1309
57113	1347
58493	1380
59799	1306

## 44 ABSORPTION SPECTRA OF THE CHLORO ETHYLENES

contrasted with the first region of absorption in ethylene. On the short wavelength side of the maximum a clearly marked progression of bands can be seen. The origin of this progression is probably obscured by emission lines. The system extends to 1700 Å.: the frequencies of the bands and their differences are shown in Table XIV. The bands are too diffuse for very accurate measurement.

The main frequency differences are thus

$$1350 \pm 30 \text{ cm.}^{-1}$$

and  $450 \pm 30 \text{ cm.}^{-1}$ . Of these, the first is evidently the totally symmetrical C=C valence vibration reduced by the excitation from its value of  $1569 \text{ cm.}^{-1}$  in the ground state.<sup>17</sup> The second is perhaps the C=C  $\delta$  frequency of  $509 \text{ cm.}^{-1}$  in the ground state.

In ethylene there is a strong vibrational progression in the first (mixed Rydberg:  $N \rightarrow V$ ) region of absorption. There are traces of vibrational progressions in the first absorption regions of all the chloroethylenes, but only in tetrachloroethylene is the progression really well marked.

Around 1600 Å. a second diffuse region of absorption occurs, weaker

TABLE XVI.—FREQUENCIES AND ASSIGNMENTS OF THE BANDS OF THE 1427 Å. PROGRESSION IN TETRACHLOROETHYLENE.

$\nu_{\text{obs.}}$ cm. <sup>-1</sup>	Assignment.	$\nu_{\text{calc.}}$ cm. <sup>-1</sup>
70097	000	
70343	$\omega_1$	70342
70598	$\omega_2$	70557
70838	$\omega_2 + \omega_1$	70802
71040	$2\omega_2$	71007
71436	$\omega_3$	71430
71898	$\omega_3 + \omega_2$	71890
72303	$\omega_3 + 2\omega_2$	72350
72754	$2\omega_3$	72763
73194	$2\omega_3 + \omega_2$	73214

$$\omega_1 = 245 \pm 30 \text{ cm.}^{-1}, \quad \omega_2 = 460 \pm 30 \text{ cm.}^{-1}, \\ \omega_3 = 1333 \pm 10 \text{ cm.}^{-1}.$$

latter frequencies being slightly increased by the excitation. 1569, 445 and  $236 \text{ cm.}^{-1}$  are the frequencies of the totally symmetrical vibrations in the ground state, intense in the Raman effect.

TABLE XV.—FREQUENCIES AND ASSIGNMENTS OF THE TETRACHLOROETHYLENE BANDS IN THE 1573 Å. SYSTEM.

$\nu_{\text{obs.}}$ cm. <sup>-1</sup>	Assignment.	$\nu_{\text{calc.}}$ cm. <sup>-1</sup>
63557	000	
63817	$\omega_1$	63817
64030	$\omega_2$	64037
64907	$\omega_3$	64900
65167	$\omega_3 + \omega_1$	65160
65394	$\omega_3 + \omega_2$	65387
65812	$\omega_3 + 2\omega_2$	65862
66240	$2\omega_3$	66240
66725	$2\omega_3 + \omega_2$	66720
67213	$2\omega_3 + 2\omega_2$	67195
67581	$3\omega_3$	67580
67786	$3\omega_3 + \omega_1$	67840
68082	$3\omega_3 + \omega_2$	68060
68529	$3\omega_3 + 2\omega_2$	68540
68915	$4\omega_3$	68923
69350	$4\omega_3 + \omega_2$	69403

$$\omega_1 = 260 \pm 20 \text{ cm.}^{-1}, \quad \omega_2 = 480 \pm 10 \text{ cm.}^{-1}, \\ \omega_3 = 1343 \pm 5 \text{ cm.}^{-1}.$$

than the first and of maximum about 1615 Å. On the short wavelength side of this, at 1573 Å., a vibrational progression commences, the bands of which are sharp and strong. The frequencies of the bands and their assignments are shown in Table XV. Three main vibrations are present: that of  $1343 \text{ cm.}^{-1}$  is the C=C valence vibration in the excited state, that of  $480 \text{ cm.}^{-1}$  is perhaps a C=C deformation frequency of value  $445 \text{ cm.}^{-1}$  in the ground state and that of  $260 \text{ cm.}^{-1}$  is perhaps the Raman frequency of  $236 \text{ cm.}^{-1}$ , both these

At 1427 Å. a third vibrational progression starts. The frequencies and assignments of the bands in this progression are shown in Table XVI. The frequency differences involved are very similar to those in the second region.

A fourth, weaker, progression overlaps the third, with its origin at 1381 Å. At 1360 Å., however, the continuum weakens considerably and thenceforward only diffuse absorption occurs.

Except for the 1970 Å. region, the bands of tetrachloroethylene lie at shorter wavelengths than those of trichloroethylene. This indicates a higher ionisation potential for the  $\pi$  electrons of the C=C bond. If the 1573 Å. and 1427 Å. bands are consecutive members of a Rydberg series leading to this ionisation potential, a value of  $\sim 77000 \text{ cm.}^{-1}$  (9.5 v.) is indicated. The exact amount of charge present in the C=C bond depends upon the resultant of the mesomeric and inductive effects. A higher ionisation potential than for trichloroethylene must mean either that the addition of a fourth chlorine atom causes a greater inductive than extra mesomeric effect or that symmetry factors cause the difference.

There seem to be no bands in the spectrum that can correspond to the "D" bands found in the spectra of the alkyl chlorides and due to the non-bonding  $p\pi$  chlorine electrons.

### Summary.

The spectra of vinyl chloride, *cis* and *trans* dichloroethylene, trichloroethylene and tetrachloroethylene have been photographed in the vacuum ultraviolet. Well-developed Rydberg series have been found for the first ionisation potentials of the first three of these molecules. The limits are 9.95 v. (vinyl chloride); 9.61 v. (*cis* dichloroethylene); and 9.91 v. (*trans* dichloroethylene). A possible Rydberg series with a limit at 8.8 v. is indicated for trichloroethylene. These ionisation potentials are all due to the excitation of one of the  $\pi$  electrons of the double bond. The spectra as a whole show the importance of the conjugation of the  $p\pi$  non-bonding lone pair electrons on the chlorine atoms with the  $\pi$  electrons of the C=C bond.

This work was carried out in 1940, war-time conditions having delayed its publication. The author desires to thank Dr. W. C. Price for his constant encouragement and help.

*The Laboratory of Physical Chemistry,  
Cambridge.*

---

## AN APPARATUS TO MEASURE CONTACT ANGLES.

BY J. W. L. BEAMENT.

*Received 12th October, 1944.*

The apparatus described is being used to investigate variations with temperature in the hydrophilic properties of lipid extracts of the insect cuticle and changes in the surface of the cuticle after moulting, by measurement of the angle of contact of water droplets.

**For Lipoid Extracts.**—The lipid film is laid down from a chloroform solution as a uniform layer on a glass coverslip and supported in the surface of a beaker of water by cork slips. Hot and cold water are mixed in the large conical flask, rates of flow being adjusted so that either a constant temperature is obtained or a steady rate of increase in temperature. A constant pressure of outflow from the sidearm is ensured by the lead (attached to a filter pump) at the water surface, and the outflowing water passes into the beaker and also through the fine glass jet (Y) into the centre of the droplet on the waxed coverslip. Water is removed from the droplet by the second jet (X) which just touches the top of it, and is attached to

the filter pump. In this way the surface of the drop is always being removed and the water kept clean. The positions of the jets are variable by the two worm screws supporting them so that any constant size of droplet can be used, or by raising the suction jet an advancing boundary is obtained; by lowering it, a receding boundary.

When water has been flowing regularly for some minutes the temperatures of the drop and of the surface of the bath on which the coverslip

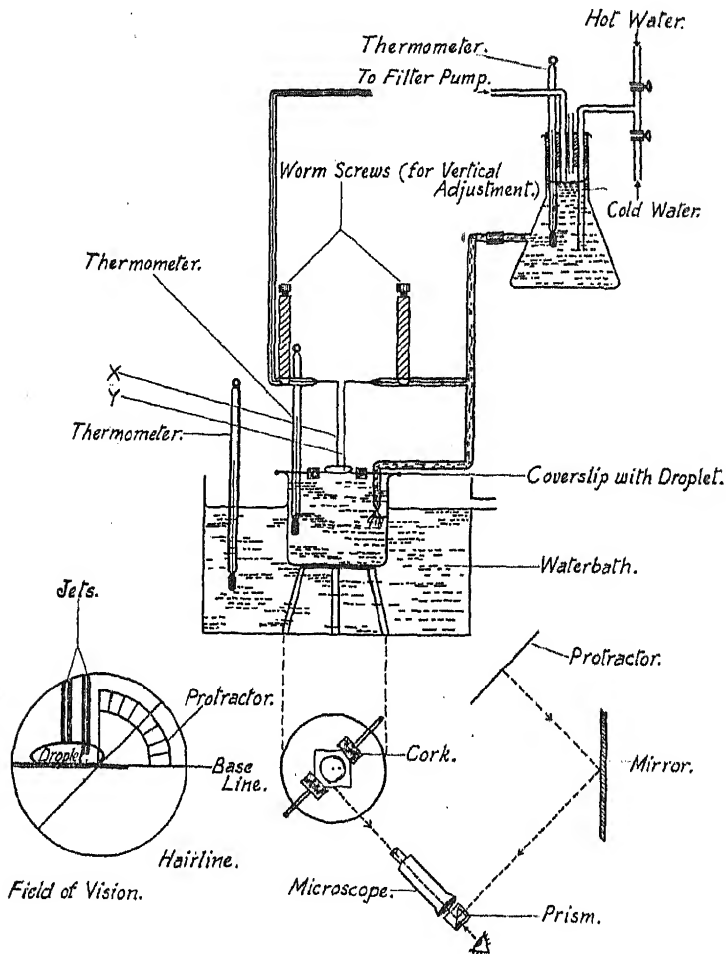


FIG. 1.

rests are approximately the same and can be determined thermometrically. At high temperatures it is necessary to keep the water bath heated.

**For the Insect Cuticle Surface.**—The insect is harnessed on a slip of celluloid attached to a multiple joint so that it can be placed at any required angle to the observer. The jets are placed over it as above the coverslip. By this means the variation in hydrophil properties with time (and not temperature) are obtained.

**Measurement of the Angle of Contact.**—The droplet is observed in the plane of the coverslip through a low-power compound microscope having a rotatable hairline placed diametrically in the focal plane of the eyepiece.

A transmitting and reflecting prism is placed in front of the eyepiece so that the image of a protractor reflected in a mirror at  $45^\circ$  to the system is brought into superposition with the image of the droplet and the hairline. The positions of the components are adjusted so that in the field of view, the base line of the protractor is in line with the edge of the coverslip, or insect surface, with the protractor centre at the edge of the drop and at the optical centre of the microscope. Having obtained unity of plane by elimination of ellipses in the various images, rotation of the hairline gives perfect alignment with the graduations of the protractor. Direct readings of the contact angle can thus be obtained and rapid changes followed, keeping the hairline tangential to the image of the edge of the droplet.

This optical system has been used to measure the contact angle by the method of tilting an immersed surface until the liquid meniscus is plane, and for other angular and linear variables.

An account of results obtained with this apparatus will appear later.<sup>1</sup>

*Agricultural Research Council Unit of Insect Physiology ;  
London School of Hygiene and Tropical Medicine.*

<sup>1</sup> Beament (1945), *J. exp. Biol.* (in the press).

---

## REVIEWS OF BOOKS.

**Natural and Synthetic Fibers.** A Looseleaf Literature and Patent Digest. Edited by MILTON HARRIS and H. MARK. First Year, 1944 ; issued monthly. (New York: Interscience Publishers, Inc.) Subscription price per year, \$60. Binder, \$3.

Having already invested \$63 in this publication, I can hardly find fault with it without confessing to a blunder on my own part. I have no wish to find fault with it though, suppressed or otherwise, except that it is a lot of money. I like it very much.

Inspired by the fact that the textile industry is now passing over from a state of traditional empiricism to one of scientific reasonableness and is therefore, like every other branch of science, generating an increasing flow of papers of many kinds, the Editors and Publishers are aiming at a highly systematic Literature and Patent Service devoted to the physical and chemical structure of fibres and all the properties and processing of fibres and fabrics that ultimately rest on such structure. (This claim must not be taken too literally, since the solid part of all living things is mostly of a fibrous nature.) There is nothing new in the idea of abstracts of fibre papers, of course—the Textile Institute, for example, has long issued them—but this particular Service is distinguished by two main features : (1) the abstracts are so comprehensive that they contain most of the facts and data of the original papers and reproduce besides the important graphs, photographs, and other diagrams ; and (2) they are in loose-leaf form and are arranged according to a filing system based in the first place on chemical composition, and then on numerous aspects concerned with manufacturing processes, structure, properties and reactions, and analytical methods and testing. This sounds complicated, but the introductory classification and instructions are clear, and when these have been read it is easy enough to insert the loose leaves in their appropriate places as they arrive, and it is gratifying afterwards to be able to find one's way about so quickly among a literature that is undoubtedly growing formidable.



About fifty journals will be surveyed (together with American, British and German patent sources), and the Publishers estimate that they will supply approximately 1000 pages in the first twelve issues.

W. T. A.

**Colorimetric Determination of Traces of Metals.** By E. B. SANDELL.  
(Vol. III of Chemical Analysis, a series of monographs on analytical chemistry and its applications.) (New York: Interscience Publishers, Inc., 1944. Price \$7.00.)

With the increasing use in industry of pure, or nearly pure, metals and alloys of carefully specified composition, the need for methods of accurate analysis both in the teaching laboratory and in industry becomes more and more important. In order to meet this need there has been in recent years a tendency to introduce physical and physico-chemical methods, and also to develop new, or modify old, chemical methods so that very small traces of certain elements may be *determined* within narrow tolerances. Among these the colorimetric method has been extended towards lower and lower limits, and a considerable number of new determinations appears in the literature every year.

In collecting together in one volume the most interesting examples of this method, Professor Sandell has earned the gratitude of all analysts who have occasion to resort to microchemical methods. Selection has, of course, been necessary, but since it has been made with a view to providing representative methods for a large number of metals rather than giving an exhaustive treatment of a few best methods, the result is an exceedingly useful handbook in which one or two methods for almost every metal may be found.

The volume is arranged in two parts. The general part discusses micromethods in general in an effort to portray the proper position of the colorimetric method in relation to gravimetric and spectroscopic analysis, paying special attention to sources of error and limitations which must be borne in mind in assessing the limits of experimental error. This part includes a useful chapter on general colorimetric reagents. The second and larger part deals with the metals in alphabetical order, a system which facilitates reference. In every case, one or more methods are discussed after a short note on separations; the procedures are then given in detail, followed by instructions for the application of the method to particular cases. Adequate references to the original literature are given in almost every case.

The book is produced according to the high standard we have come to expect from Interscience Publishers.

E. R. R.

# THE EFFECT OF TEMPERATURE ON THE DENSITY OF POLYTHENE.

BY E. HUNTER AND W. G. OAKES.

*Received 16th May, 1944.*

The polymerisation of ethylene in suitable high pressure conditions gives very long chain hydrocarbons,<sup>1</sup> now known as polythenes, which are solid at ordinary temperatures and show a crystal structure.<sup>2</sup> The cell dimensions and atomic positions have been established by C. W. Bunn,<sup>3</sup> who has also observed that the crystallinity is incomplete at ordinary temperatures, for the X-ray photographs show a band due to the presence of amorphous material.<sup>4</sup> The intensity of this band increases and that of the crystal structure lines decreases with rising temperature until finally, at some temperature in the neighbourhood of 120-125° C., no trace of crystallinity remains. The idea that very long molecules may exist partly in the crystalline and partly in the amorphous condition has been employed by Mark,<sup>5</sup> Fuller, Baker and Pape,<sup>6</sup> and Bunn,<sup>7</sup> to account for the physical behaviour of those long chain polymers which show crystallinity. This theory, applied to polythenes, suggests that because of its great length the average molecule may pass through, and tie together, several crystals. In the crystals there will be orderly arrangement, between them regions of disorder crossed by paraffin chains. The amorphous and crystalline regions cannot be regarded as mechanically separable phases, since it is an essential point of the theory that the same molecule may at the same time be over part of its length in the crystalline condition and over the remainder in the amorphous. With rising temperature, increased thermal motion will cause a growth of the amorphous regions at the expense of the crystalline regions until a temperature is reached at which the material is entirely amorphous and indistinguishable from a viscous liquid composed of long molecules. A polythene at ordinary temperatures can thus be expected to have a density intermediate between that of a wholly crystalline high molecular weight paraffin and that of the supercooled liquid, and measurements of its density over a wide range of temperature should give some indication of the relative proportions of the crystalline and amorphous regions and how they change with temperature. In the course of work done to assist in the technical applications of polythenes it has been possible to measure the density over the full temperature range in which marked changes in crystallinity might be expected.

**Experimental Measurements at Room Temperature.**—A flotation method, accurate to 0.001 gm./c.c. was used for measurement of density at room temperature. Small pieces of polythene are put into a beaker with 100 c.c. of an ethyl alcohol-water mixture (52 %  $C_2H_5OH$  by weight,  $d_{20} = 0.910$  g./c.c.) in a thermostat at 20° C. (or 25° C.) and, while stirring gently, distilled water at the same temperature is run in from a burette until the test pieces remain suspended, neither sinking nor floating. The density of the final solution is measured in a standard pyknometer. For

<sup>1</sup> British Patent 471590.

<sup>2</sup> U.S. Patent 2153553.

<sup>3</sup> Bunn, *Trans. Faraday Soc.*, 1939, 35, 482.

<sup>4</sup> Bunn, forthcoming publication.

<sup>5</sup> Mark, *J. Physic. Chem.*, 1940, 44, 764.

<sup>6</sup> Fuller, Baker and Pape, *J. Amer. Chem. Soc.*, 1940, 62, 3275.

<sup>7</sup> Bunn, *Proc. Roy. Soc., A.*, 1942, 180, 82.

routine measurements a graph showing the density of the final solution as a function of the volume of water added may be constructed, and the densities of the polythene samples simply read off from this graph. It is necessary to thermostat the solution to avoid convection currents which would otherwise make the estimation of the final point difficult, and if great sensitivity is required, to allow time for the dissipation of heat of dilution of the alcohol solution.

Soon after systematic measurements of the densities of polythenes were begun it was found that the density of a particular specimen was to a certain extent dependent on its previous thermal history. A specimen of thin polythene film which had been "shock-cooled," i.e. cooled quickly from the molten state by plunging it into cold water, was found to have a density lower than that of a similar specimen of the same sample which had been cooled slowly from the molten state. The effect of rate of cooling on the density is illustrated by Table I.

TABLE I.

<i>Rate of cooling</i>	<i>Density (20° C.)</i>
(a) 120°-100° C. in 120 min.	0.926 g./c.c.
(b) 120°-100° C. in 3 min.	0.922 g./c.c.
(c) 120°-100° C. in 2 secs. (approx.)	0.918 g./c.c.

Changes in the rate of cooling below 100° C. were found to have no measureable effect on the density, but it was observed that on annealing a specimen of "shock-cooled" polythene film at 100° C., its density (at 20° C.) was raised but was still below that of the "slow-cooled" specimen of the same sample. For example the density of specimen (c) in Table I after annealing at 100° C. for 1 hour was 0.920 (20° C.).

It will be seen later that these changes in density are associated with changes in the degree of crystallinity.

**Measurements between 0° and 170° C.**—The changes in density of a number of samples of polythene in the range 0° to 170° C. were measured using standard pyrex dilatometers of the weight thermometer type, with mercury as the filling liquid. Specimens were in the form of moulded cylinders weighing about 20 grams. During their preparation special care was taken to eliminate all gas bubbles and cavities; this was ensured by casting each cylinder in a boiling tube, kept between 150° and 200° C. under hard vacuum for several hours until all bubbles had dispersed, before cooling slowly under vacuum. The top of the cylinder containing the cavity caused by thermal contraction during cooling was cut away, to leave a completely bubble-free specimen to be sealed into the dilatometer. To eliminate air bubbles in the dilatometer itself, the apparatus was connected to an oil diffusion pump and filled with mercury while under hard vacuum. The final filling was completed with the bulb, containing the polythene specimen, at 0° C. The temperature was raised in suitable steps to 170° C. and the mercury expelled weighed at each step. Between about 60° C. and the melting point it was found that at least 24 hours at constant temperature was necessary before the volume became constant. Below 60° C. and above the melting point equilibrium was established in a few hours. Some measurements were made just below the melting point after cooling down from the molten state. In these cases it was observed that supercooling could occur and that a much longer period was necessary for equilibrium to be established and the point obtained during heating up repeated.

The absolute density values were based on the values at 20° C. or 25° C. measured by the flotation method. To calculate the density at other temperatures the standard dilatometer method was used, corrections being applied for expansion of the mercury, for expansion of the dilatometer bulb, and for exposed capillary.

**Measurements between 20° C. and -180° C.**—Linear thermal expansion coefficients were measured in the range 20° C. to -180° C. in an apparatus similar to that recommended by the A.S.T.M. for plastic materials.<sup>8</sup> The changes in length of annealed extrusion-moulded rods, 10 cm. long, 1 cm. diam., were measured on a dial gauge reading to 0.0001 cm., at 10° intervals down to -100° C. A small thermostat employing liquid air cooling and controlled to  $\pm 0.2^\circ$  C. was used down to -100° C. and a final point at -180° C. was obtained in liquid air. It was found that after 30 mins. at each temperature further changes in length were negligible. Density values, based on an independent determination at 20° C., were calculated from the coefficients of linear expansion using the theoretical relation  $\alpha = (1 + \beta)^3 - 1$  [where  $\alpha$  = coeff. of cubical expansion  $\beta$  = coeff. of linear expansion.]

The experimental results are given in Table II as specific volumes (c.c./g.) at the temperature of measurement, in the order in which the measurements were made.

### Discussion.

The tabulated results show that the manner of density variation is much the same for all the specimens examined. In Fig. 1, curves 1 and 2, which show the results for specimens V and VI, are typical of polythenes of normal average molecular weight. Curve 3 shows the results for the lowest average molecular weight specimen examined, No. 1. In general, on heating from room temperature a range in which the volume changes are not remarkable merges into one through which larger and larger rates of change appear, giving the curves a pronounced concavity upwards. This rapid rise in volume terminates abruptly at a temperature above which volume increases linearly and more slowly with rising temperature. The temperature of this abrupt change is presumably that at which solid first appears on cooling; within a few degrees it is the same as that at which the liquid changes from transparency to translucency on cooling and above which no birefringence can be seen under the polarising microscope,<sup>4</sup> and for polythenes of medium molecular weight is close to the "softening point" shown by the ball and ring test.<sup>9</sup> In the sub-normal temperature range there are signs of a transition occurring at about -40° C. in the particular specimen examined.

Although a tendency may be noted for increased molecular weight to raise the temperature at which the last crystals vanish on heating and to decrease the specific volume of solid (particularly at higher temperatures),

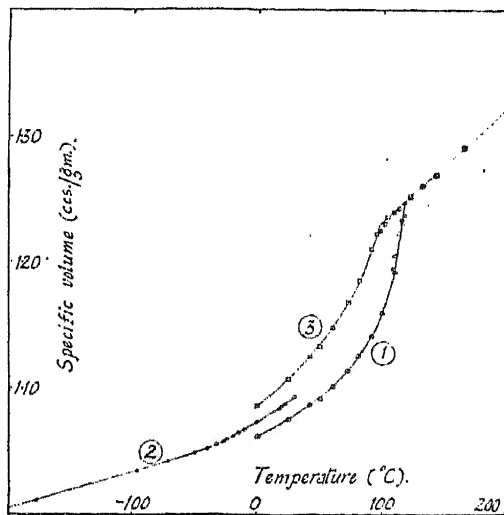


FIG. 1.

<sup>8</sup> A.S.T.M., D.696-42.T.

<sup>9</sup> A.S.T.M., E.28-42.T. disc 0.8 mm. thick.

TABLE II.

Specimen I. [ $\eta$ ] = 0.29		Specimen II. [ $\eta$ ] = 0.48.		Specimen III. [ $\eta$ ] = 0.51		Specimen IV. [ $\eta$ ] = 0.64	
$t(^{\circ}\text{C.})$	$v(\text{c.c.})/\text{g.}$	$t(^{\circ}\text{C.})$	$v(\text{c.c.})/\text{g.}$	$t(^{\circ}\text{C.})$	$v(\text{c.c.})/\text{g.}$	$t(^{\circ}\text{C.})$	$v(\text{c.c.})/\text{g.}$
0.0	1.086	0.0	1.073	0.0	1.069	0.0	1.070
25.0	1.108	25.0	1.088	20.0	1.081	25.0	1.085
42.0	1.126	35.0	1.096	31.7	1.089	35.0	1.092
50.0	1.133	49.8	1.107	46.6	1.101	46.0	1.100
60.0	1.149	60.2	1.115	62.0	1.116	53.9	1.106
72.4	1.169	69.7	1.120	74.1	1.129	60.2	1.111
81.2	1.186	81.4	1.136	95.2	1.168	69.7	1.121
91.2	1.212	90.0	1.149	100.6	1.178	81.4	1.135
100.5	1.232	98.3	1.168	106.8	1.203	90.0	1.148
109.4	1.242	101.9	1.175	112.3	1.234	98.3	1.165
122.7	1.254	104.3	1.182	115.0	1.252	101.9	1.172
132.8	1.262	106.6	1.191	117.6	1.257	104.3	1.178
142.4	1.272	109.2	1.203	125.4	1.264	106.6	1.186
164.3	1.292	111.3	1.218	137.0	1.274	109.2	1.196
113.3	1.245	113.0	1.240	150.0	1.286	111.3	1.208
94.6	1.225	115.8	1.241	169.5	1.304	113.0	1.236
97.3	1.227	119.2	1.253	23.2	1.083	115.8	1.244
104.1	1.238	125.4	1.258	81.8	1.141	119.2	1.259
		140.2	1.271	86.2	1.149	125.4	1.264
				90.2	1.155	140.2	1.278
				94.5	1.163		
				101.6	1.181		

Specimen V. [ $\eta$ ] = 0.74.		Specimen VI. [ $\eta$ ] = 0.81.		Specimen VII. Polythene.		Specimen VIII. 87.5 % Polythene 12.5 % Polyiso-butylene.
$t(^{\circ}\text{C.})$	$v(\text{c.c.})/\text{g.}$	$t(^{\circ}\text{C.})$	$v(\text{c.c.})/\text{g.}$	$t(^{\circ}\text{C.})$	$v(\text{c.c.})/\text{g.}$	$v(\text{c.c.})/\text{g.}$
0.0	1.061	30.0	1.0943	0.0	1.070	1.071
25.0	1.076	22.6	1.0882	25.0	1.085	1.086
42.0	1.087	20.0	1.0858	38.2	1.093	1.095
50.7	1.092	18.0	1.0844	50.6	1.104	1.104
61.0	1.102	10.0	1.0787	60.8	1.112	1.114
72.4	1.115	0.0	1.0725	73.0	1.125	1.125
81.2	1.126	— 10.1	1.0667	83.3	1.138	1.136
91.2	1.142	— 15.0	1.0641	90.0	1.147	1.145
100.5	1.161	— 19.5	1.0616	100.0	1.166	1.164
109.4	1.195	— 25.0	1.0591	108.0	1.185	1.183
122.7	1.254	— 27.2	1.0577	115.6	1.250	1.239
132.8	1.263	— 32.5	1.0555	121.2	1.255	1.244
142.4	1.272	— 39.5	1.0519	137.8	1.269	1.258
164.3	1.292	— 50.0	1.0485			
113.3	1.223	— 71.0	1.0417			
115.8	1.232	— 96.0	1.0342			
117.2	1.249	— 178.0	1.0105			
108.0	1.196					
110.2	1.206					
112.7	1.225					
115.3	1.235					
117.2	1.239					

Intrinsic viscosity  $[\eta] = \left( \frac{1}{c} \log \eta_{\text{rel.}} \right)_{c \rightarrow 0}$  where  $c$  = concentration in g./100 ml.

$$\eta_{\text{rel.}} = \frac{\text{time of flow (solution)}}{\text{time of flow (solvent)}}$$

measured in an Ostwald No. 1 Viscometer (B.S.S. 188-1937) in tetralin at 75° C.

detailed comparison of the behaviour of the specimens shows that average molecular weight alone does not fix specific volume; specimens can be found which have slightly lower specific volumes at a particular temperature than others of rather higher average molecular weight. These finer differences arise from variations in the breadth of distribution of molecular weights in the specimens.

From curves 1 and 2 of Fig. 1 expansion coefficients have been calculated and plotted in Fig. 2. The volumes and their rates of change between 50° C. and 120° C. are evidently consistent with the polythene structure having amorphous regions which grow rapidly with increasing temperature in this range. The ability to retrace the curve on repeated slow heating and cooling with only minor hysteresis effects is interesting by contrast with rubber and polystyrene. Wood, Bekkedahl and Peters<sup>10</sup> heated "stark" rubber (with a melting point above room temperature) and found a type of expansion resembling that now observed for polythene, but on cooling the material remained amorphous and the original rapid change in dimensions observed between 35° C. and 40° C. was not reversed. In polystyrene, where crystallinity does not arise, cooling at a finite rate leads to a linear fall in volume with temperature until the neighbourhood of 80° C. is reached. At lower temperatures the fall in volume is also linear

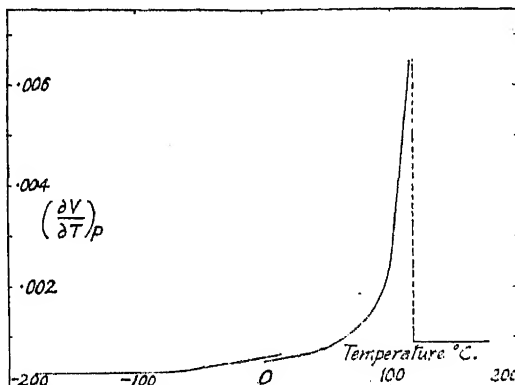


FIG. 2.

but at a lower rate.<sup>11</sup> Alfrey, Goldfinger and Mark<sup>12</sup> have observed that behaviour in the upper temperature range is reversible but that while the coefficient of expansion in the lower range is constant the specific volume depends on the rate at which the specimen has been cooled. They explain the transition as a change from conditions in which, because of the high temperature, diffusion of the long molecules is sufficiently rapid for the liquid to follow its equilibrium structure on cooling to conditions in which, because of the lower temperature, diffusion is extremely slow and the liquid is unable to attain its equilibrium structure through being "frozen" in a less compact arrangement. In this "frozen" condition expansion will be similar in mechanism and magnitude to that of a crystal lattice. The transition from one expansion coefficient to another will occur in a temperature range where relaxation time is comparable to the experimental time-scale. When polythene is cooled there may thus be two different factors affecting the final volume. The specific volume of the amorphous material after rapid cooling may be higher than the equilibrium value of a supercooled liquid because of "freezing", and the weight ratio of crystalline to amorphous material may depend on rate of cooling. No direct evidence on the first point is yielded by the measurements now reported. The relatively minor difference in density between shock-cooled and slow-cooled polythene, and the fact that these densities are closer to that of the

<sup>10</sup> Wood, Bekkedahl, Peters, *J. Res. Nat. Bur. Stand.*, 1939, **23**, 571.

<sup>11</sup> Patnode and Scheiber, *J. Amer. Chem. Soc.*, 1939, **61**, 3449.

<sup>12</sup> Alfrey, Goldfinger and Mark, *J. App. Physics*, 1943, **14**, 700.

crystal than that of the supercooled liquid, suggest that while crystallisation may be modified it cannot be seriously hindered by rapid cooling.

Rough estimates of the proportion of crystalline material present in polythene at different temperatures have been made in the following way. The observed specific volume of a sample is assumed to be related to the proportions and specific volumes of the crystalline and amorphous material by the expression,

$$V_{\text{Obs.}} = x \cdot V_{\text{Cryst.}} + (1 - x) V_{\text{Amorph.}}$$

where  $x$  is the weight fraction of  $-\text{CH}_2-$  groups in the crystalline form. A linear extrapolation of the volume-temperature line downwards from the  $170^{\circ}$ - $120^{\circ}$  C. range is assumed to give the specific volumes of the amorphous regions in the solid at temperatures up to  $115^{\circ}$  C. The specific volume of the polythene crystal is 1.00 at room temperature<sup>(3, 4)</sup>; its volume expansion coefficient is assumed to be approximately  $6 \times 10^{-4}$  c.c. per c.c. per  $^{\circ}\text{C.}$ , a value reported by van Hook and Silver<sup>13</sup> for  $\text{C}_{16}$  to  $\text{C}_{21}$  paraffins at temperatures  $10^{\circ}$  C. below their melting points, in agreement with measurements of Müller.<sup>14</sup>

From these data and the volume-temperature curve 1 of Fig. 1 the percentages of crystalline material at various temperatures have been calculated and are shown to the nearest 5 % in Table III.

TABLE III.

Temperature.	0	20	40	50	60	70	80	90	95	100	105	110	115
Wt. % of Crystalline Material	55	55	55	55	55	55	50	45	45	40	35	25	10

These figures suggest that about half of the final proportion of crystalline material appears on cooling less than ten degrees below the temperature of the first signs of crystallinity, and that below  $60$ - $70^{\circ}$  C. the relative proportions of the two types of structure cease changing with temperature. The calculated values for the fraction of crystallinity are probably too low, especially at the lower temperatures. The material in the amorphous regions has not the same freedom to diffuse as the molecules of a wholly liquid medium, since it consists of chains whose ends are enclosed in crystals. At a sufficiently low temperature the limited possibilities of volume readjustment in the amorphous regions will be suspended by the "freezing" effect discussed by Alfrey, Goldfinger and Mark. Thus at all temperatures the specific volume of material in the amorphous regions is likely to be higher than that obtained by extrapolation of the liquid line.

The density-temperature relationships of the polythene specimens which have been examined can be explained in the following way. In the true liquid condition (above  $120^{\circ}$  C.) relaxation times are too short to prevent the attainment of equilibrium. Below a temperature in the neighbourhood of  $120^{\circ}$  C. (the precise value depending on the composition of the specimen) crystalline material appears in proportions determined by the temperature. At temperatures down to  $60$ - $70^{\circ}$  C., readjustment of the crystalline-amorphous ratio after a temperature change is apparently fairly rapid, but when  $60^{\circ}$  C. is reached further variation of the ratio with falling temperature does not occur. Below  $60^{\circ}$  C. the material in the amorphous regions adjusts itself to temperature changes by segmental movement. On cooling to a sub-normal temperature a point is reached (at  $-40^{\circ}$  for the specimen examined) where there are signs of a transition. This may be interpreted

<sup>13</sup> van Hook and Silver, *J. Chem. Physics*, 1942, 10, 686.

<sup>14</sup> Müller, *Proc. Roy. Soc., A*, 138, 1932, 514.

as the temperature at which the amorphous material becomes "frozen" and below which expansions or contractions have the magnitude to be expected from a structure in which diffusion processes are negligible.

Alfrey, Goldfinger and Mark point out that changes in mechanical behaviour can be expected on passing into the "frozen" state. There may possibly be a relation between the temperature at which brittleness develops in a polythene (as judged by the usual flexure tests) and the lower transition temperature, for the material of specimen VI, with a transition temperature in curve 2 (Fig. 1) of  $-45^{\circ}\text{C}$ . survives flexing at  $-25^{\circ}\text{C}$ . but fails at  $-45^{\circ}\text{C}$ . It will be necessary to examine the thermal expansions of a wider series of polythenes to determine this matter, for brittleness temperature depends on molecular weight; polythenes of higher molecular weight which can be flexed below  $-100^{\circ}\text{C}$ . have been made and it is intended to examine the density-temperature relationships of these materials. It is not clear how the lower brittleness temperature of long chain material is to be explained simply in terms of the freezing of movement in the amorphous regions which are likely to contain only segments of molecules and thus to have properties relatively independent of specimen molecular weight.

Although the physical behaviour of long chain molecules in flow processes can largely be explained on the assumption that the flow steps do not involve the motion of the whole chain but merely of parts of it, average chain length has some part in determining the density-temperature characteristics of polythene. It is seen from Fig. 1 that the amount of crystalline material present at temperatures in the region of  $100^{\circ}\text{C}$ . depends on average molecular weight. From the fact that polythene can be partially fractionated from saturated solutions it can be concluded that a tendency exists for the crystals, at any temperature, to contain the longer molecules of the complex rather than the shorter ones, *i.e.* for the longer chains to be less soluble, in any medium, than the shorter ones. The general nature of the volume-temperature relationships in polythenes can indeed be deduced as phenomena to be expected in a multi-component system in which the components have melting points dependent on molecular weight and which are capable of forming mixed crystals in equilibrium with liquid over a wide temperature range. In such a system the first crystallisation temperature will be lower the greater the proportion of lower melting point components; the first crystals will be richer in higher molecular weight components than the whole complex; the ratio of crystalline to liquid (amorphous) material will vary with temperature between the limits of the liquidus and solidus surfaces and, because of the slow rate of transfer of matter between crystalline and amorphous phases, the composition of the two phases may depend on rate of cooling. Differences in density and in mechanical properties between shock-cooled and slow-cooled specimens are to be expected, and the process of annealing a shock-cooled polythene at  $100^{\circ}\text{C}$ . has a similarity to that of annealing an alloy at a temperature slightly below the melting point. This analogy with a formal phase-rule system, however, must be used cautiously, for it is incomplete, since although the amorphous and crystalline regions in polythene can be expected to have different thermodynamic properties they cannot be treated as mechanically separable phases.

Table II includes measurements on a polythene (VII) and a polythene-polyisobutylene mixture (VIII) containing  $87\frac{1}{2}\%$  by weight of the material of specimen VII. In the solid state the specific volumes of the two materials are practically identical at each temperature; above  $115^{\circ}$  in the liquid the mixture has a lower specific volume than the polythene, but the same expansion coefficient. By a similar method to that used above, with the assumption that no polyisobutylene is present in the crystalline regions, it can be shown that the ratio of amorphous polythene to crystalline polythene is the same in the mixture as in unblended polythene. The close similarity



Throughout the operation the temperature of the outer bath was adjusted to be equal to that of the oil in the calorimeter, thus maintaining adiabatic conditions. The temperature rise of the calorimeter contents due to various measured inputs of electrical energy was measured, time being allowed for the calorimeter temperature to reach a steady state between the successive periods of heating. In this way the total heat contents at various temperatures, referred to the heat contents at 20° C. as zero, were measured both with and without the polythene sample, the difference giving the total heat of the polythene alone.

(b) **Heat of Solution.**—The solubility of polythene in hydrocarbon solvents is very low at room temperatures, but becomes appreciable at higher temperatures. The heat of solution was thus measured at 80° C. In order to increase the rate of solution the polythene was made into powder by precipitation from hot benzene solution by the addition of excess acetone.

In the first method the apparatus was similar to that described above. The lid of the enclosing vessel carried thermocouples, heater and stirrer, and a glass funnel through which solvent and polythene powder were introduced. The assembly was placed in the thermostat at the required temperature, and a weighed amount of xylene, previously heated, was added. The temperatures of the xylene and the outer bath were then adjusted until both were steady at the required temperature. Polythene powder, which had been allowed to reach the same temperature in a weighed container fitting into a silver tube in the outer bath, was then added rapidly to the solvent through the glass funnel. The temperatures of the solvent and the solid before mixing, and of the solution after mixing, were read at minute intervals. After mixing, and while solution was taking place, the temperature of the outer bath was reduced to follow the change in temperature of the solution until the latter was steady.

The specific heat of the solution was measured over the appropriate temperature range by observing the temperature rise corresponding to a known input of electrical energy to the calorimeter. From the decrease in temperature of the solution the heat absorbed on dissolving the polythene was calculated.

The second method was devised in an attempt to reduce the time required for a heat of solution determination, at the expense of accuracy, in order that it might be used as a routine test for the determination of the degree of crystallinity of polythene samples. A Dewar vessel, suspended in a thermostat at the appropriate temperature, served as the calorimeter, and polythene powder was added to the xylene as before. Temperature readings were taken at intervals before and after the mixing, and the decrease in temperature due to mixing was calculated by an extrapolation from a temperature-time plot. Heat capacities of calorimeter and solution were measured as before.

### Experimental Results.

(a) **Heat Content (Enthalpy).**—Fig. 1 shows the values for the heat content of a sample of polythene at temperatures up to 165° C. referred to the heat content at 20° C. as zero. After the first determination, the sample was cooled down and the experiment was repeated, but the results were not coincident with the first series. This may be due to experimental error, which, because of the low heat capacity of the polythene compared with that of the calorimeter, may not be less than  $\pm 5\%$ . A possible contributory cause is, however, lack of attainment of true thermodynamic equilibrium between the crystalline and amorphous regions in polythene. This lack of complete reversibility of the crystalline-amorphous change has been shown by measurement of the heat capacity over the range 95–105° C., cooling and repeating the measurement. In the second case a lower value for the specific heat over that range was obtained, indicating that more crystalline material was dispersed on heating than was

re-formed during the subsequent cooling process. The time-dependent nature of crystallization processes in polymers is well known. The actual experimental error in the second determination is believed to be less than in the first, and greater time was allowed for equilibrium to be attained.

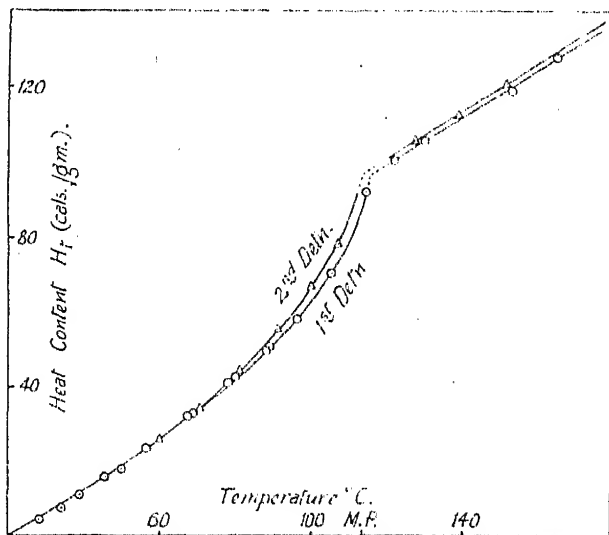


FIG. 1.—Heat content of 1 gr. of polythene.

The break in the curve at about  $115^{\circ}\text{C.}$  corresponds to similar breaks in the specific volume-temperature curves and to the melting of the polythene to a transparent liquid.

(b) Specific Heat.

—The slope of the enthalpy-temperature curve (Fig. 1) at any temperature gives the specific heat. Fig. 2 shows a plot of specific heat as a function of temperature for the polythene sample examined. It is of interest to compare these values with those obtained for pure paraffins of chain length about 12 to 20. In the case of liquid paraffins, data on specific heat on the range  $115\text{--}170^{\circ}$  is rare, but the work of Huffman, Parks and Barmore<sup>5</sup> suggests that, as the chain length increases the value of  $C_p$  at  $0^{\circ}\text{C.}$  is approaching a value of about 0.51. The temperature coefficient

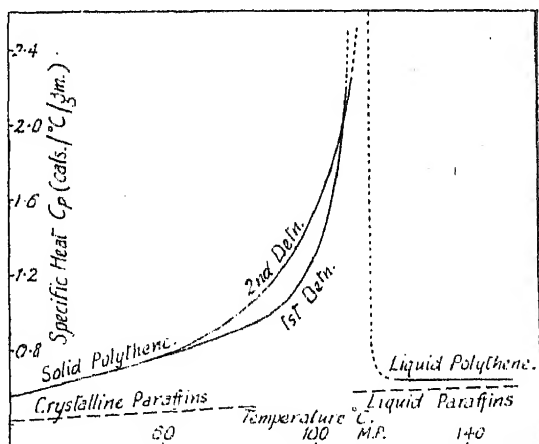


FIG. 2.—Specific heat of polythene.

<sup>5</sup> Huffman, Parks and Barmore, *J.A.C.S.*, 1931, **53**, 876.

of  $C_p$  for a liquid paraffin is about 0.0008 cal. per degree per g., and hence at a temperature  $t$ , we may write  $C_p = 0.51 + 0.0008 t$ . This corresponds to the line drawn in Fig. 2; at temperatures just above the melting point the specific heat of liquid polythene appears to be somewhat higher than the results on short chain paraffins would suggest, but at higher temperatures agreement is better. This point will be discussed later.

The specific heat of pure solid paraffins may be represented approximately<sup>6</sup> by the equation  $C_p = 0.40 + 0.0012 t$  (where  $t$  = temperature in °C.). The line representing this equation is shown in Fig. 2. It is seen that even at 20° the specific heat of the solid polythene (0.55) is greater than that of pure paraffins, and that the value increases at an increasing rate as the temperature approaches the melting point, indicating an increasing rate of disordering of the solid structure, culminating in the disappearance of crystallinity at the temperature (115° for this sample) normally referred to as the "melting point".

(c) **Heat of Fusion.**—Ubbelohde<sup>6</sup> has pointed out the difficulty of assigning a value of heat of fusion to a paraffin which shows an order disorder transition over a temperature range instead of a sharply defined

TABLE I.—HEAT OF FUSION OF SOLID POLYTHENE.

Temp. °C.	$H_{t, l}$ cal./g.	$H_{t, s}$ cal./g.	$H_{t, l} - H_{t, s}$ cal./g.
20	43.4	0	43.4
40	54.2	11.6	42.6
60	65.1	25.6	39.5
80	76.5	43.1	33.4
90	82.2	53.5	28.7
100	88.1	66.4	21.7
110	94.1	84.5	9.6
115	97.0	97.0	0.0

the change in this term follow the change in degree of crystallinity of the polythene.

This calculation is clearly sensitive to the extrapolation of the enthalpy of the liquid polythene, and hence to the value of the specific heat chosen. If we use the expression  $C_p = 0.51 + 0.0008 t$ , which is approximately valid for liquid paraffins, the enthalpy  $H_{t, l}$  of one gram of liquid polythene at any temperature  $t$  °C. is given by

$$H_{t, l} = 97 - \int_t^{115} (0.51 + 0.0008 t) dt,$$

(the enthalpy at 115° being 97 cal., referred to the value for solid polythene at 20° as zero—see Fig. 1). Table I shows values of the difference between  $H_{t, l}$  and the enthalpy of the solid  $H_{t, s}$  at a series of temperatures, based on the second determination (Fig. 1).

In view of the assumptions made above regarding the heat content attributed to liquid polythene below the melting point, these values are not to be regarded as absolute, but indicate the general trend of the decrease in crystallinity of the solid as temperature increases.

(d) **Heat of Solution.**—Some values for the heats of solution of polythene powders in xylene, to give 5 % solutions by weight, are shown in Table II.

If  $(H_{l, t} - H_{s, t})$  is the difference in heat content between liquid and solid polythene, and  $\Delta H_m$  is the heat of mixing of liquid polythene with the solvent, the heat of solution  $\Delta H_{sol}$  is given by

$$\Delta H_{sol} = H_{l, t} - H_{s, t} + \Delta H_m$$

<sup>6</sup> Ubbelohde, *Trans. Faraday Soc.*, 1938, **34**, 282, 292.

The heat of mixing of liquid polythene with xylene has not been measured, but by analogy with the heat of mixing of heptane and of medicinal paraffin with xylene it is probably of the order of  $-5$  calories per gram. The heat of solution of polythene should therefore be about 5 calories more negative than the heat of fusion at the same temperature. That this is very approximately so is shown by a comparison of the figures for sample 3 in Table II with those in Table I, which refer to a similar polythene.

TABLE II.—HEATS OF SOLUTION OF POLYTHENE IN XYLENE.

Sample Number.	Molecular Weight.*	Temperature,	Heat of Soln. cal./g.	Method.
1	11,800	78.08	-33.35	1
		78.95	-33.53	
		79.59	-33.09	
2	10,000	81.0	-33.2	2
3	15,600	80.5	-36.8	2
		90.5	-27.1	
		95.0	-25.0	

\* Calculated from the intrinsic viscosity  $[\eta]$  in tetralin at 75°C. using the formula  $M.W. = 20,000 [\eta]$ . Molecular weights calculated in this way may not even bear a linear relation to true weight average molecular weights.

(e) **Degree of Crystallinity.**—As the chain length increases the heat of fusion of linear paraffins at 25°C. approaches a value of about 56.5 calories per gram.<sup>7</sup> This figure refers to the crystal form stable at low temperatures, which corresponds in structure to the crystalline regions in polythene. If an entirely crystalline polythene could be made, the difference in heat content between the crystals and the liquid would thus be about 56.5 calories per gram at 25°C. If therefore we assume that the

heat content of the amorphous regions of polythene is equal to that which liquid polythene would have if it could be cooled to the same temperature, the degree of crystallinity of the polythene is given by

Fraction in crystalline state

$$= \frac{H_{l,t} - H_{s,t}}{56.5}$$

$$\text{or} = \frac{\Delta H_{sol} - \Delta H_m}{56.5}$$

The change, with temperature, of the degree of crystallinity of the sample of Table I is shown in Fig. 3. Here again the values must not be regarded as absolute,

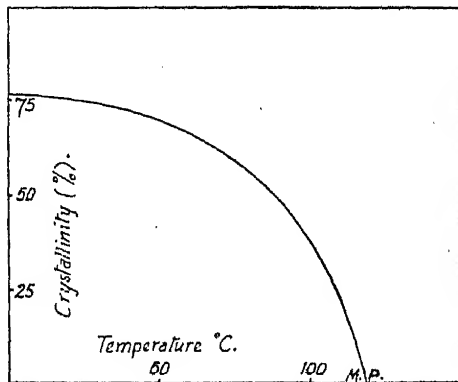


FIG. 3.—Change of crystallinity with temperature.

owing to the assumption made about the heat content of the amorphous regions, and because no account has been taken of the change with temperature in the heat of fusion of entirely crystalline paraffins.

### Order-Disorder Transitions in Polythene.

Ubbelohde<sup>6</sup> has shown that the melting of pure paraffins such as octadecane is to be regarded as an order-disorder transition extending ten degrees or more either side of the temperature normally regarded as the

<sup>7</sup> Parks and Huffmann, *Ind. Eng. Chem.*, 1931, 23, 1138.

melting point. This phenomenon shows itself in abnormally high specific heats in the region of the melting point. Increase in heat capacity below the melting point has been attributed<sup>6</sup> to changes within the crystal lattice, while high specific heats above the melting point are regarded as confirmation of the theory that hydrocarbon molecules are to some extent associated in parallel groups even above the melting point, extra heat being required to cause a more random structure. Both of these effects are probably present in polythene. It has already been noted that the specific heat of liquid polythene just above the melting point is unexpectedly high, and electron diffraction work on polythene<sup>8</sup> has shown the maintenance of some degree of orientation or alignment of molecules above the melting point.

Although some change in the crystal lattice may play some part in causing the rise in specific heat of polythene in the temperature range 20-115° C. it is probable that the main effect is the decrease in proportion of the crystalline material, rather than a change in the properties of the crystallites themselves. As the temperature is raised the crystallites disperse; they may perhaps be regarded as dissolving in the surrounding amorphous regions. It is most improbable that the crystallites would all be of the same size, and the smallest will probably disappear first. Melting of the individual crystallites may be preceded by some change in the lattice such as rotation of the molecules.

On cooling from the melt, the reverse changes occur, but as noted above, there may be a hysteresis effect. The liquid consists of a mixture of curled chains of length up to at least 2000 carbon atoms for the samples examined in the course of this work. Although the general arrangement is random there will be regions in which two or more chains are approximately parallel for portions of their length. On cooling, a state is reached when the van der Waals' forces between the chains outweigh the thermal agitation, and crystallization over portions of the chains can occur. The shortest chains and any molecules or portions of long molecules which do not fit readily into the normal paraffin crystal structure, and which therefore pass from one crystallite to another (tie molecules) or project from the crystallites, form the amorphous regions. As the temperature decreases greater lengths of the chains take their places in crystalline regions and the amorphous content decreases. The ease of movement to equilibrium positions will decrease as temperature decreases, and a state akin to that of a glass will be reached in which the structure is apparently stable and almost independent of temperature, but is not in true thermodynamic equilibrium. If cooling occurs rapidly the molecules have even less chance of attaining equilibrium positions, and the well known phenomenon of shock cooling or quenching, leading to a more amorphous product is observed.

Although shock cooling polythene from the melting point leads to a solid form containing a higher proportion of amorphous material, it has not yet been possible to make, by shock cooling or any other means, a sample of polythene in a completely amorphous state at room temperature, as has been reported in the case of "Saran". Polythene clearly crystallizes very readily; this may be connected with the simplicity of the hydrocarbon chain. The size of the repeating unit ( $-\text{CH}_2-$ ) is so small that the chance of adjacent molecules being in a favourable position for crystallization is high. In the case of polyvinylidene chloride, nylon or rubber, it is not sufficient that the chains should be parallel. Before crystallization can occur the molecules must adjust their positions so that the chlorine atoms, amide groups or methyl groups are in the appropriate positions. This may involve movements of relatively large portions of chains past one another.

In the calculation of degree of crystallinity from the heat capacity results, it has been assumed that the heat content of the amorphous regions

<sup>8</sup> Charlesby, *Trans. Faraday Soc.*, 1942, 38, 320.

is equal to that of the supercooled liquid. This will only be true if the portions of the molecules in the amorphous regions can take up unstrained equilibrium conditions at all temperatures. Since the amorphous regions are made up partly of molecules extending from one crystallite to another it is difficult to see how these can take up entirely unstrained positions. As more and more of the units of the chains move into crystal structures on reducing the temperature, the strain on the remainder will increase, and the heat content of the amorphous regions may be greater than that of an unstrained liquid. The values for the degree of crystallinity in Fig. 3 would in this case be somewhat low.

The change with temperature in the degree of crystallinity shown by the heat capacity results is similar to that shown by specific volume-temperature curves (2), but the absolute values of crystallinity are appreciably higher (75 % compared with 55 % for a polythene of molecular weight about 16000).<sup>\*</sup> These estimates are both based on extrapolated figures, one for the heat capacity and the other for the density of the amorphous regions of the polythene at temperatures below the melting point. If instead of using published data for the specific heat of long chain liquid paraffins we use a linear extrapolation of the observed heat content of liquid polythene, we obtain a somewhat lower value (65 %) for the degree of crystallinity at 20° C. We consider, however, that since the rather high value for the specific heat of polythene just above its melting point, like that of other linear paraffins,<sup>6</sup> may be due to some form of order, or structure, the use of published data on the specific heat of liquid paraffins well removed from their melting points is more satisfactory. A further source of uncertainty is the degree of strain of the tie molecules in the amorphous regions, which as noted above, must effect the heat content.

Although the gradual nature of the transition from crystalline to amorphous regions in a polymer leads to a certain vagueness in the meaning of any figure for the degree of crystallinity, one probable cause of the discrepancy between the values obtained from density and heat content data on similar polythenes has already been suggested. It is pointed out in the previous paper<sup>2</sup> that values of crystallinity calculated from volume-temperature relationships by using an extrapolation of the liquid line are likely to be too low, since amorphous material in the solid is not free to adopt as low a specific volume as the free liquid. If we calculate the density of the amorphous regions in a typical polythene of overall density 0.925, assuming a crystal content of 75 % (based on heat capacity data), and using a figure of 1.00 for the density of the crystalline regions,<sup>9</sup> we obtain a value of about 0.76, less than the density of liquid polythene at the melting point. Such a low density of the amorphous regions, if confirmed, would be of importance in connection with the absorption of liquids by polythene and diffusion through polythene.

### Summary.

The heat capacity of a sample of polythene over the range 20-165° C., and the heats of solution of samples in xylene at 78-95° C. have been measured. The specific heat of solid polythene at 20° C. is about 0.55, and is greater than the specific heat of entirely crystalline short chain paraffins. As the temperature is raised the specific heat increases, reaching a value of about 1.0 at 90° C. and 2.0 at 110° C. These results indicate a disordering of the structure of the solid beginning below 50° C. and becoming increasingly marked as the temperature is raised, culminating in

<sup>\*</sup> The third method of estimating degree of crystallinity (3), based on estimation of X-ray intensities, gives values of about 70-75 % for similar polythenes, but as with the other methods, too much reliance must not be placed on the absolute values.

<sup>9</sup> Bunn, *Proc. Roy. Soc. A.*, 1942, 180, 80.

a relatively sharp change to a liquid structure at about 115° C. The changes are similar to those shown by density measurements and are believed to be due to a decrease in the proportion of the long molecules which pass through crystallites.

The difference between the heat capacity of solid polythene and the extrapolated heat capacity of liquid polythene at the same temperature (the heat of fusion), is 43.4 calories per gram at 20° C., decreasing to 28.7 at 90° C. and 9.6 at 110° C. Values for the heat of solution in xylene are similar to the heat of fusion at the same temperature. A comparison with the heat of fusion of entirely crystalline paraffins indicates that at room temperature the polythene sample whose heat capacity was measured was approximately 75 % crystalline.

Lack of complete reversibility of heat capacity measurement shows that thermodynamic equilibrium between crystalline and amorphous regions is not attained instantaneously.

The authors wish to acknowledge the assistance of Mr. J. L. Matthews and Mr. C. G. Scott.

*Imperial Chemical Industries Research Dept.,  
Alkali Division, Northwich.*

---

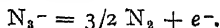
## THE KINETICS OF THE ELECTRODEPOSITION OF THE AZIDE ION

By H. P. STOUT.

*Received 10th July, 1944.*

The kinetics of the electrodeposition of hydrogen and oxygen from aqueous solution have been studied exhaustively, and a number of theories as to the precise nature of the reaction have been put forward. These reactions are peculiar in that in each case the products are constituents of the solvent, and in addition complications arise owing to the fact that hydrogen and hydroxyl ions are hydrated in aqueous solution. The electrodeposition of a substance which is not a constituent of the solvent, and the ions of which are not hydrated in solution, might, therefore, be expected to follow a different course from the deposition of hydrogen and oxygen. According to the theory of ionic solution put forward by Bernal and Fowler,<sup>1</sup> univalent ions of radius greater than 1.6 Å. are to be regarded as unhydrated in aqueous solution, in the sense that they do not carry along a co-ordinated shell of water molecules. The azide ion comes in this category, and although it has been shown that the electrodeposition of the ion is an irreversible process,<sup>2, 3</sup> no detailed investigation of the kinetics of the reaction appear to have been made. The following series of experiments were therefore carried out in an attempt to elucidate further the nature of the deposition process.

**Nature of the Electrode Reaction.**—On electrolysis of an aqueous solution of sodium azide using a platinum anode, nitrogen is evolved in amount corresponding to the reaction <sup>4</sup>



At an aluminium electrode, however, only two-thirds of the theoretical amount of nitrogen is evolved, the remaining one-third appearing in the

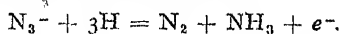
<sup>1</sup> Bernal and Fowler, *J. Chem. Physics*, 1933, 1, 515.

<sup>2</sup> Blokker, *Rec. Trav. Chim.*, 1937, 56, 52.

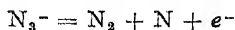
<sup>3</sup> Reisenfeld and Muller, *Z. Elektrochem.*, 1935, 41, 87.

<sup>4</sup> Briner and Winkler, *J. Chemie Physique*, 1922, 20, 214.

form of ammonia. This is presumably due to the reduction of the azide ion by nascent hydrogen formed by solution of the anode in the electrolyte, which gives a slightly alkaline reaction, thus

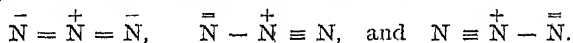


In the presence of platinum black, sodium azide is hydrolysed to ammonia and nitrogen, the rate of hydrolysis being greatly increased if the platinum surface is saturated with hydrogen.<sup>5</sup> Both these reactions are catalysed by the metal surface, and as only one atom of nitrogen is liberated as ammonia, it seems likely that one nitrogen atom in the ion behaves differently from the other two, and that the ion decomposes thus

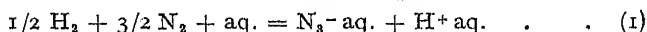


the nitrogen atom being adsorbed on the metal surface. Hydrogen on the surface would then react with the adsorbed atom to form ammonia. The rate of reaction would, of course, be controlled by the rate of removal of adsorbed nitrogen atoms. This is in accord with the fact that hydrogen catalyses the exchange reaction between the two isotopic nitrogens,  $\text{N}_2^{14}$  and  $\text{N}_2^{15}$ , on an iron surface, ammonia, or at least an imido bond, being formed as an intermediate product.<sup>6</sup>

**Structure of the Azide Ion.**—The structure of the azide ion is not known with certainty, but the evidence from infra-red and Raman spectra of the ion in solution points to a linear and symmetrical arrangement of the atoms, with an internuclear distance <sup>7</sup> of 1.12 Å. This is in good agreement with the internuclear distance of 1.15 Å. calculated on the basis of equal resonance between the three structures <sup>8</sup>



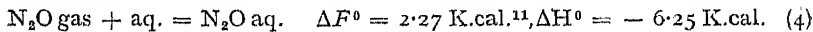
**Free Energy of Formation of  $\text{N}_3^-$  aq.**—The free energy of formation of the azide ion in solution is the free energy change in the reaction



A search of the literature has failed to reveal sufficient data for the exact calculation of  $\Delta F^\circ$ , but an approximate value may be estimated from the free energy changes in the following reactions :—



The heat of formation of hydrazoic acid gas is 71.9 K.cal.<sup>9</sup> and of aqueous hydrazoic acid 54.6 K.cal.,<sup>10</sup> which gives  $\Delta H^\circ$  for reaction (3) as -17.3 K.cal. The corresponding entropy change  $\Delta S^\circ$  may be estimated roughly by comparison with the  $\Delta S^\circ$  for the solution of nitrous oxide



The  $\Delta S^\circ$  of this reaction is therefore -28.3 cal. per degree. As nitrous oxide has a linear structure corresponding <sup>8, 12</sup> to resonance between  $\bar{\text{N}} = \overset{+}{\text{N}} = \text{O}$  and  $\text{N} \equiv \overset{+}{\text{N}} - \text{O}$ , and as hydrazoic acid gas contains the linear group -NNN corresponding to resonance <sup>8</sup> between  $-\text{N} = \overset{+}{\text{N}} = \text{N}$  and  $-\text{N} - \overset{+}{\text{N}} \equiv \text{N}$ , the entropy change on solution would be expected to

<sup>5</sup> See Audrieth, *Chem. Rev.*, 1934, **15**, 169.

<sup>6</sup> Joris and Taylor, *J. Chem. Physics*, 1939, **7**, 893.

<sup>7</sup> Sutherland and Penney, *Proc. Roy. Soc., A*, 1936, **156**, 678.

<sup>8</sup> Pauling, "The Nature of the Chemical Bond," 1940, p. 199.

<sup>9</sup> Eyster and Gillette, *J. Chem. Physics*, 1940, **8**, 369.

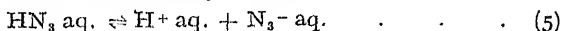
<sup>10</sup> Bichowsky and Rossini, "Thermochemistry of Chemical Substances," 1936.

<sup>11</sup> *Int. Crit. Tables*, 1930, **7**, 241.

<sup>12</sup> Bailey and Cassie, *Physical Rev.*, 1932, **39**, 534.



be of the same order in each case, and so the entropy of solution of  $\text{HN}_3$  gas may be taken as about  $-30$  cal. per degree. The free energy change on solution of  $\text{HN}_3$  gas will therefore be about  $-8.4$  K.cal. for gas at one atmosphere pressure and unit activity of acid.



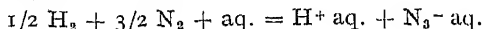
The dissociation constant<sup>13</sup> of hydrazoic acid is  $2.8 \times 10^{-5}$ , and so the free energy change for reaction (5) is  $6.2$  K.cal. The free energy change in reaction (1) is equal to the sum of the free energy changes in reactions (2), (3) and (5) and is therefore  $76.3$  K.cal. and this is the free energy of formation of the azide ion. It will be noted that the error introduced in estimating the entropy of solution of  $\text{HN}_3$  is not of great importance as the contribution of reaction (3) amounts to only  $11\%$  of the whole. It will also be seen that the free energy of formation of  $\text{HN}_3$  aq. is  $70.1$  K.cal. which is rather greater than the value of  $65.3$  K.cal. given by Latimer,<sup>14</sup> but as the latter is based on an entropy of  $48$  cal. per degree for  $\text{HN}_3$  estimated by comparison with a value of  $50$  cal. per degree for  $\text{HNO}_2$ , it is probably less accurate than the former estimate.

**The Reversible Potential of the  $\text{N}_3^- - \text{N}_2$  Electrode.**—The reversible potential of the normal azide-nitrogen system measured against a normal hydrogen electrode is the E.M.F. of the cell



for unit activity of both ions and at one atmosphere pressure. As the free energy change in the reaction is  $76.3$  K.cal., the E.M.F. of the cell is  $3.3$  volts, hydrogen being positive, and so the reversible potential of the normal azide-nitrogen electrode is  $-3.3$  volts against the normal hydrogen electrode.

**Entropy of  $\text{N}_3^-$  Ion.**—For the reaction



$\Delta H^\circ$  is  $58.4$  K.cal.,<sup>10</sup>  $\Delta F^\circ$  is  $76.3$  K.cal., and so  $\Delta S^\circ = -60$  cal. per degree. Taking absolute entropy<sup>15</sup> of  $\text{H}_2$  as  $29.7$ , of  $\text{N}_2$  as  $45.9$ , and of  $1/2 \text{H}^+$  as  $-4.6$ , all in cal. per degree, it follows that the absolute entropy of  $\text{N}_3^-$  aq. must be approximately  $28$  cal. per degree.

**Entropy of  $\text{N}_3^-$  (gas).**—It is interesting to compare this value for the entropy of the azide ion in solution with the entropy calculated for a hypothetical gaseous ion  $\text{N}_3^-$ . Taking the ion as linear and symmetrical with the  $\text{N}-\text{N}$  distance  $1.15$  Å, the moment of inertia is  $4.56 \times 10^{-40}$  g. cm.<sup>2</sup>, and the rotational entropy given by

$$\frac{S_{\text{rot}}}{Nk} = \ln \frac{4\pi^2 I k T}{h^2} + 1$$

becomes  $S_{\text{rot}} = 12.2$  cal. per degree per g. mol. at  $298^\circ \text{K}$ . The translational entropy is given by

$$\frac{S_{\text{trans}}}{Nk} = \ln \frac{(2\pi M k T)^{3/2}}{h^3} \cdot \frac{kT}{P} + \frac{5}{2}$$

and so  $S_{\text{trans}} = 32.6$  cal. per degree per g. mol. at  $298^\circ \text{K}$ . The frequencies of vibration of the gaseous ion are unknown, but taking them equal to those in solution,<sup>7</sup> namely,  $\nu_1 = 1350$ ,  $\nu_2 \sim 630$ , and  $\nu_3 \sim 2080$ , the entropy of vibration given by

$$\frac{S_{\text{vib}}}{Nk} = \sum \left[ \frac{h\nu}{kT} \left( \frac{e^{-h\nu/kT}}{1 - e^{-h\nu/kT}} \right) - \ln(1 - e^{-h\nu/kT}) \right]$$

becomes  $S_{\text{vib}} = 0.32$  cal. per degree per g. mol. at  $298^\circ \text{K}$ .

<sup>13</sup> Quintin, *Compt. rend.*, 1940, 210, 625.

<sup>14</sup> Latimer, "Oxidation States of the Elements," 1940, p. 83.

<sup>15</sup> Eastman, *Chem. Rev.*, 1936, 18, 257.

<sup>16</sup> Latimer, *ibid.*, 1936, 18, 349.

The total entropy of the gaseous ion is thus 45.1 cal. per degree per g. mol., and comparing this with the value of 28 cal. per degree per g. mol. for the aqueous ion, it appears that the hypothetical entropy of solution of the  $N_3^-$  ion is about -17 cal. per degree per g. mol.

### Experimental.

The electrolytic cell used is shown diagrammatically in Fig. 1. It was made of soda glass and consisted of an anode compartment A, and a cathode compartment C, separated by an ungreased tap  $T_2$ . When closed, the latter effectively prevented diffusion of hydrogen from cathode to anode without seriously obstructing the current flow. A capillary tube B, carrying an ungreased tap  $T_1$ , was sealed through the wall of the anode compartment and the end drawn out to a fine tip. The other end dipped into a beaker containing a saturated solution of potassium chloride, and this was connected by a salt bridge to a saturated calomel half cell. The anode, a piece of platinum, palladium, or iridium foil, was welded to a wire of the same metal, which in turn was welded to a length of platinum wire. This was sealed into a glass tube, D, which fitted into a ground glass joint, J, at the top of the anode compartment, the length of wire being such that the foil was about 1 mm. from the tip of the capillary tube. The cathode compartment was open to the atmosphere and had a length of platinum wire sealed into it as the electrode. To fill the cell, electrolyte was blown in from a flask through the tube, E, by nitrogen under pressure from a cylinder, all the taps except  $T_4$  being open. After filling the anode and cathode compartments and the capillary tube B, which required about 15 c.c. of solution, all taps were closed and the nitrogen supply connected directly to the tube E. On opening  $T_3$ , the solution could be stirred by blowing through it a stream of gas, and by opening  $T_3$  and  $T_4$  a stream of nitrogen could be passed through the gas space in the anode compartment. The electrodes were prepared by cleaning in strong nitric acid, followed by heating to a high temperature. Before use the cell was cleaned with chromic acid and washed with distilled water.

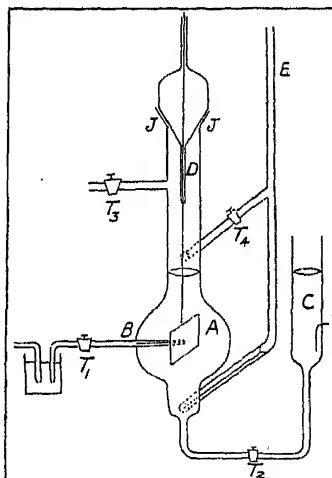


FIG. 1.—The electrolytic cell.

Solutions of sodium and ammonium azides were used as electrolytes. Commercial sodium azide was purified by dissolving in distilled water and precipitating with alcohol, the precipitate being dried and finally recrystallised from distilled water. Ammonium azide was prepared from barium azide solution by double decomposition with excess of ammonium sulphate. After filtering off the precipitated barium sulphate, the filtrate was treated with alcohol, when ammonium azide was precipitated. The precipitate was then dried in a desiccator under reduced pressure.

The water used in making up the solutions was distilled twice, the final product having a conductivity of between  $10^{-6}$  and  $10^{-7}$  reciprocal ohms per c.c. Before use the solutions were saturated with nitrogen, purified from oxygen by passing over heated copper.

The electrical circuit was similar to that used by Bowden and Rideal.<sup>17</sup> Potentials were measured on a Cambridge potentiometer used in conjunction with a Compton electrometer as a null instrument. The current,

<sup>17</sup> Bowden and Rideal, *Proc. Roy. Soc., A*, 1928, 120, 59.

supplied by a high tension battery and controlled by a series of grid leak resistances, was determined from the potential drop across a standard resistance in series with the cell.

**pH of Azide Solutions.**—Owing to the catalytic decomposition of an azide solution by platinised platinum, a reversible hydrogen electrode cannot be used for measuring the pH of such a solution, and a glass electrode filled with Normal hydrochloric acid saturated with quinhydrone was used in its stead. Calibration was carried out against a hydrogen electrode in a series of buffer solutions. In this way the pH of *N/10* sodium azide was found to be 9.4, and of *N/10* ammonium azide 7.2, both of which are of the order expected in view of the fact that hydrazoic acid is a weak acid with a dissociation constant of  $2.8 \times 10^{-5}$ .

## Results.

Electrolysis of sodium azide solutions at—

(a) **Platinum anodes.**—*N/10* solutions of sodium azide were electrolysed at room temperature over a range of current densities, and the potential of the platinum anode measured against a saturated calomel cell. The relation between potential and the logarithm of the current density was found to be linear over the range from  $10^{-7}$  to  $10^{-1}$  amp. per apparent sq. cm., and as the potentials were unaffected by stirring the solution with nitrogen gas, it appears that the electrode reaction is irreversible and exhibits the characteristics of "activation overpotential."<sup>18</sup> In Fig. 2 is shown a typical  $V$ -log  $i$  curve, the slope,  $b$ , being 58 millivolts corresponding to a value of 0.98 for the factor  $\alpha \left( = \frac{2.3RT}{bF} \right)$ . Actually the

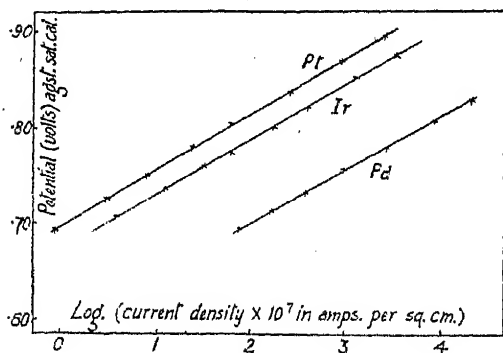


FIG. 2.

slope was found to vary between 57 and 60 millivolts according to the particular electrode used, and so  $\alpha$  may be slightly greater than 1.0. The  $V$ -log  $i$  curves were extremely reproducible, the difference between consecutive runs on the same anode rarely being greater than two or three millivolts. Consecutive runs on different anodes showed variations up to about 15 millivolts at the same current density. At currents below

$10^{-7}$  amp. per sq. cm. the potential fell steeply to more negative values, probably owing to the presence of oxidisable impurities in the solution.

(b) **Palladium and Iridium Anodes.**—A palladium electrode substituted for the platinum electrode gave a similar  $V$ -log  $i$  curve, but in this case the slope was 54 mv. corresponding to  $\alpha = 1.1$ . At a given potential, however, the current density was about 100 times greater than on platinum. With an iridium electrode, the slope of the  $V$ -log  $i$  curve was 60 mv., equivalent to a value of  $\alpha$  rather less than 1.0. The current density, however, was then only 2 or 3 times as great as on platinum.  $V$ -log  $i$  curves for these metals are shown in Fig. 2.

**Effect of Varying pH.**—The electrolysis of solutions of sodium azide in aqueous hydrazoic acid has been investigated by Reisenfeld and Muller,<sup>3</sup> who found no change in the rate of deposition at constant potential over

<sup>18</sup> Bowden and Agar, *Ann. Rep. Chem. Soc.*, 1938, 35, 90,

the  $pH$  range of 2 to 6. In order to extend this range to the alkaline side of neutrality, a series of solutions of various  $pH$  values was made up from mixtures of sodium azide and sodium hydroxide, and  $V$ -log  $i$  curves determined in the usual way. These curves were then compared with the  $V$ -log  $i$  curves obtained for solutions of sodium hydroxide only, of similar  $pH$ , the  $pH$  value in each case being measured with the glass electrode. Between  $pH$  13.7 and 10.4 the two sets of  $V$ -log  $i$  curves, for the same platinum electrode, were identical and analysis of the evolved gases showed these to be oxygen in each case.

The  $V$ -log  $i$  curve for sodium hydroxide of  $pH$  9.4, however, was found to lie above the corresponding curve for  $N/10$  sodium azide solution which also has a  $pH$  of 9.4, i.e. the current at a given potential is greater for the latter solution than the former. In the case of the azide solution the gas evolved is, of course, nitrogen and not oxygen. Ammonium azide solution

of strength  $N/10$  with a  $pH$  of 7.2, gave a  $V$ -log  $i$  curve practically identical with that for  $N/10$  sodium azide. In Fig. 3 is given a series of  $V$ -log  $i$  curves covering the  $pH$  range 9.4 to 13.7, all the curves being obtained with the same platinum anode.

It appears from the foregoing that, at a given potential, the rate of deposition of the azide ion from solutions tenth normal with respect to this ion, is independent of  $pH$  between 7.2 and 9.4 and this, taken in conjunction with Reisenfeld and Muller's work,

indicates that the rate of deposition is independent of  $pH$  over the range 2 to 9.4. For  $pH$  greater than about 10, in solutions tenth normal with respect to the azide ion, the rate of deposition of oxygen is greater than that of the azide ion at the same electrode potential, and consequently oxygen and not nitrogen is evolved at the anode.

#### Effect of Varying Azide Ion Concentration.

A series of  $V$ -log  $i$  curves for sodium azide solutions of strength  $N$ ,

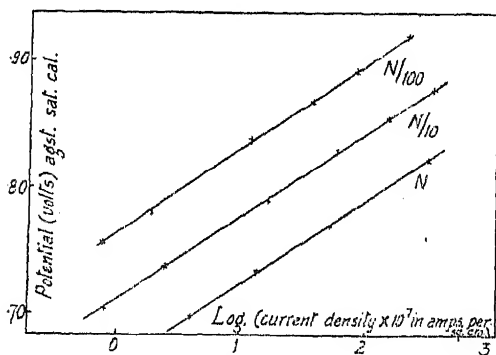


FIG. 4.

$N/10$ , and  $N/100$ , was obtained using the same platinum anode in each case. Typical curves are shown in Fig. 4, from which it will be seen that at a given potential a tenfold increase in azide ion concentration causes a tenfold increase, approximately, in the rate of deposition.

**Effect of Temperature on  $\alpha$ .**—A series of  $V$ -log  $i$  curves was determined at two different temperatures in order to observe the effect of this variable on azide deposition. The cell was placed in an air thermostat maintained at either 25° C. or 47° C. the actual temperature of the electrode

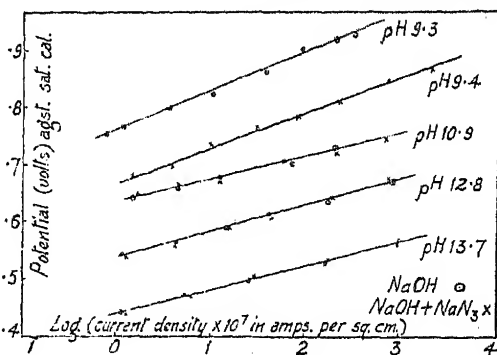


FIG. 3.

being measured by means of a copper-constantan thermocouple. One junction was enclosed in the thin-walled tube carrying the electrode, the tube being filled with toluene to ensure good thermal contact. The cold junction was in ice, and the temperature was obtained from readings of a millivoltmeter in series with the thermocouple. It was found that raising the temperature decreased the electrode potential, the current being held constant, but the slope of the  $V$ - $\log i$  curve appeared to be unchanged. Two representative curves for 25° C. and 47° C. are shown in Fig. 5. Alternate heating and cooling had no appreciable effect on the reproducibility of the curves.

The fact that the slope is the same at both temperatures indicates that  $\alpha$  increases with temperature, for otherwise the slope would be expected to increase ( $b = \frac{2.3 RT}{\alpha F}$ ). As the change in  $\alpha$  is only of the order of a few per cent. for a 20° C. rise in temperature, it is necessary to test whether

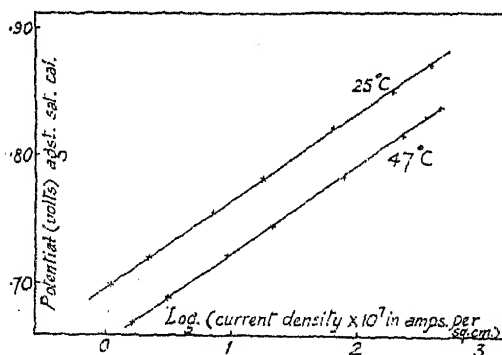


FIG. 5.

it is really significant in the statistical sense, or whether it may be ascribed to experimental error. This may be done by calculating the regression coefficients for the lines of regression of  $\frac{2.3 RT}{F} \log i$  on electrode potential at the two temperatures, and then applying Fisher's "t" test for the significance of the difference of the two coefficients.<sup>19</sup> The regression coefficients are equal to the value

of  $\alpha$  at each temperature, and putting

$$\frac{2.3 RT}{F} \log i = \theta, \text{ gives}$$

$$\alpha_T = \frac{\Sigma(V - \bar{V})(\theta - \bar{\theta})}{\Sigma(V - \bar{V})^2}$$

where  $\bar{\theta}$  and  $\bar{V}$  are the mean values of  $\theta$  and  $V$ .

The variance,  $S_T^2$ , of the regression coefficient is estimated from the equation

$$S_T^2 \cdot n \Sigma(V - \bar{V})^2 = \Sigma(\theta_T - \bar{\theta}_T)^2 - \alpha_T^2 \Sigma(V - \bar{V})^2$$

where  $(n + 2)$  is the number of pairs of observations, and the variance of the difference between the regression coefficients at the two temperatures is then given by

$$S_{T_1, T_2}^2 = \frac{n_1 S_{T_1}^2 \Sigma(V_1 - \bar{V}_1)^2 + n_2 S_{T_2}^2 \Sigma(V_2 - \bar{V}_2)^2}{n_1 + n_2} \times \left[ \frac{1}{\Sigma(V_1 - \bar{V}_1)^2} + \frac{1}{\Sigma(V_2 - \bar{V}_2)^2} \right]$$

The required value of "t" may then be calculated from

$$t = \frac{\alpha_{T_1} - \alpha_{T_2}}{\sqrt{S_{T_1, T_2}^2}}$$

<sup>19</sup> Fisher, "Statistical Methods for Research Workers," 7th edn., p. 146.

and the probability of this being exceeded purely by chance for two sets of observations differing only through sampling errors may be obtained from tables.<sup>20</sup> The number of degrees of freedom with which the tables are to be entered is simply  $(n_1 + n_2)$ . In Table I are given the details of the calculation of the regression coefficients for temperatures of 25° C. and 47° C. and for two different platinum electrodes. For the first electrode with 34 degrees of freedom the value of " $t$ " is 6.13, and for the second electrode with 62 degrees of freedom,  $t = 3.12$ . Referring to the tables of " $t$ ", the 1 % level of significance for 34 degrees of freedom is found to be about 2.75, and for 62 degrees of freedom about 2.6. The actual values of " $t$ " obtained thus represent a higher significance level than 1 %, and consequently the increase in  $\alpha$  with temperature must be regarded as a definite "effect." Taking the mean change in  $\alpha$  for both electrodes, it appears that a rise in temperature from 25° C. to 47° C. produces an increase in  $\alpha$  of about 8 %, giving an estimate for  $d\alpha/dT$  over this range of  $4 \times 10^{-3}$  degrees<sup>-1</sup>.

TABLE I.—VARIATION OF REGRESSION COEFFICIENT OF  $2.3 \cdot \frac{RT}{F} \cdot \log i$  ON POTENTIAL WITH TEMPERATURE.

Temp. °C.	Electrode 1.		Electrode 2.	
	47	25	47	25
Mean pot. agst. cal. $\bar{V}$ mv.	773.3	808.7	753.7	795.2
Mean $\frac{2.3RT}{F} \log i = \theta_T$	1.681	1.694	1.658	1.688
$\Sigma(V - \bar{V})^2$	$35.67 \times 10^{-3}$	$34.26 \times 10^{-3}$	$66.83 \times 10^{-3}$	$90.90 \times 10^{-3}$
$\Sigma(\theta_T - \bar{\theta}_T)^2$	$37.34 \times 10^{-3}$	$28.98 \times 10^{-3}$	$74.94 \times 10^{-3}$	$92.32 \times 10^{-3}$
$\Sigma(V - \bar{V})(\theta_T - \bar{\theta}_T)$	$36.48 \times 10^{-3}$	$31.48 \times 10^{-3}$	$70.69 \times 10^{-3}$	$91.37 \times 10^{-3}$
Regression coeff. $\alpha_T = \frac{\Sigma(V - \bar{V})(\theta_T - \bar{\theta}_T)}{\Sigma(V - \bar{V})^2}$	1.023	0.919	1.058	1.005
No. of pairs of observations	18	18	24	40
$n[\Sigma(V - \bar{V})^2] \cdot S_T^2$	$0.10 \times 10^{-3}$	$0.06 \times 10^{-3}$	$0.16 \times 10^{-3}$	$0.53 \times 10^{-3}$
$S_{T_1, T_2}^2$	$0.270 \times 10^{-3}$		$0.289 \times 10^{-3}$	
$t = \frac{\alpha_{T_1} - \alpha_{T_2}}{\sqrt{S_{T_1, T_2}^2}}$	6.13		3.12	
No. of degrees of freedom	34		62	
Value of $t$ for $P=1\%$	2.75		2.6 approx.	

**The Energy of Activation.**—The discharge of an azide ion is a process which must occur in several stages, each stage probably requiring a certain energy of activation. The reaction rate as measured by the current density will, however, be controlled by the slowest stage, and the energy of activation of the reaction as a whole will be that corresponding to this

<sup>20</sup> Fisher, "Statistical Methods," p. 177.

slowest stage. If at temperature  $T^\circ$  K. and potential  $V$  volts, the energy of activation is  $H_v$  cal. per g. mol., then assuming a Maxwellian distribution of energy amongst the reactants it follows that the current density  $i_{T,v}$ , is given by<sup>18</sup>

$$i_{T,v} = k \cdot e^{-H_v/RT}$$

where  $k$  is a constant for the particular reaction concerned.

Assuming the energy of activation is a function of the electrode potential and that increasing the potential by  $\Delta V$  volts decreases the energy of activation by  $\alpha_T \Delta V \cdot F$ , where  $\alpha_T$  is a constant at constant temperature,, then

$$i_T = k \cdot e^{(-H_v + \alpha_T \Delta V \cdot F)/RT}$$

and therefore

$$\left[ \frac{\partial(\ln i)}{\partial V} \right]_T = \frac{\alpha_T F}{RT}$$

The energy of activation is given by

$$\left[ \frac{\partial(\ln i)}{\partial T} \right]_V = \frac{H_v}{RT^2}$$

and the temperature coefficient of potential by the quantity  $\left( \frac{dV}{dT} \right)_i$  and as

$$\frac{d(\ln i)}{dT} = \left[ \frac{\partial(\ln i)}{\partial T} \right]_V + \left[ \frac{\partial(\ln i)}{\partial V} \right]_T \cdot \left( \frac{dV}{dT} \right)_i$$

at constant  $i$ ,

$$0 = \left[ \frac{\partial(\ln i)}{\partial T} \right]_V + \left[ \frac{\partial(\ln i)}{\partial V} \right]_T \cdot \left( \frac{dV}{dT} \right)_i$$

$$i.e. \quad H_v = -\alpha_T F T \left( \frac{dV}{dT} \right)_i$$

Thus the calculation of the energy of activation requires a knowledge of the value of  $\alpha_T$  and the temperature coefficient of potential at constant current.

**Temperature Coefficient of Potential.**—The temperature coefficient of potential at constant current was determined from the change in

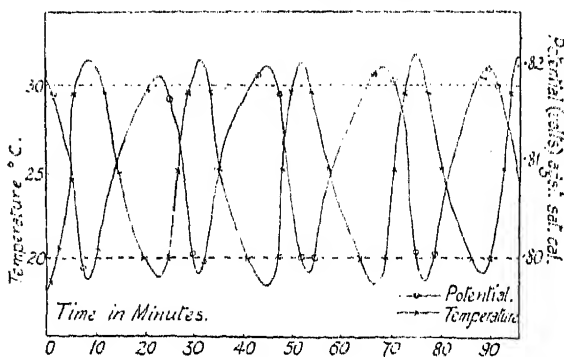


FIG. 6.

potential of the electrode on alternate heating and cooling of the cell. Heating was carried out in an air thermostat, and cooling effected by placing a jacket of ice round the cell. Temperatures were measured by means of the thermocouple previously described. The cell was heated rapidly over a range of 15°C., then cooled to room temperature and reheated, the whole process being repeated several times until the potential at a given temperature became approximately constant. The potentials and temperatures were read at two-minute intervals, and plotted on temperature *vs.* time and potential *vs.* time graphs as shown in Fig. 6. The peak potentials cor-

responded to the temperature of the cell. The cell was heated rapidly over a range of 15°C., then cooled to room temperature and reheated, the whole process being repeated several times until the potential at a given temperature became approximately constant. The potentials and temperatures were read at two-minute intervals, and plotted on temperature *vs.* time and potential *vs.* time graphs as shown in Fig. 6. The peak potentials cor-

respond to the peak temperatures, and comparison of the times at which these were attained shows that there was no appreciable lag between the actual electrode temperatures and the thermocouple temperatures. From the graphs the potentials at 20° C. and 30° C. were read off for each heating and cooling, and the mean potential change for this temperature interval calculated, from which the temperature coefficient of potential was obtained. The value of the latter is, of course, dependent on the current density at which the measurements are carried out, and in Table II are given the values of  $dV/dT$  for three different platinum electrodes in  $N/10$  azide solution, together with an estimate of the variance.

TABLE II.—TEMPERATURE COEFFICIENT OF POTENTIAL FOR PLATINUM ELECTRODES IN  $N/10$  SODIUM AZIDE SOLUTION.

Electrode	Current density amps./sq. cm.	Degrees of freedom.	Mean value of $dV/dT$ , mv. per °C.	Sum of squares of deviations from the mean.
1	$2.5 \times 10^{-5}$	12	-176	1644
2	$2.0 \times 10^{-5}$	7	-199	110
3	$2.0 \times 10^{-5}$	10	-184	356

Mean value of  $dV/dT = -185$  mv. per °C.

Mean variance from 29 degrees of freedom = 73 (mv. per °C.)<sup>2</sup>.

The mean value of  $\alpha$  for these electrodes was found to be 0.95, and so taking the mean temperature as 25° C., and the mean  $dV/dT$  as -185 mv. per degree, the energy of activation is 12.0 K.cal. per g. mol. at a potential of 0.81 volt against saturated calomel.

**The Steric Factor.**—The steric factor for the reaction may be evaluated by substituting in the equation

$$\frac{i}{F} = pn\sqrt{\frac{RT}{2\pi M}} e^{-H_v/RT}$$

where  $F$  is the Faraday,  $n$  the number of g. ions per c.c.,  $M$  the ionic wt., and  $p$  the steric factor. The mean value of  $p$  calculated in this way for the three electrodes of Table II is 0.14, referring to platinum in  $N/10$  solution at a potential of 0.81 volt against saturated calomel. This is of the same order as for hydrogen deposition at a cathode, where  $p$  varies from about 1 on some platinum electrodes down to  $10^{-5}$  on mercury.

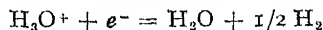
### Discussion.

The salient points emerging from the foregoing are that the anodic deposition of the azide ion is a reaction showing the characteristics of activation overpotential, giving a linear  $V$ -log  $i$  curve with  $\alpha$  approximately equal to unity. The reaction occurs at measurable rates only at the extremely high overpotential of ca. 4 volts, the reversible potential in  $N$  solution being -3.3 volts against saturated calomel. Increase in temperature causes a small but significant increase in  $\alpha$ , and the rate of reaction varies with different electrode metals and with varying concentrations of azide ion.

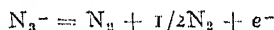
The kinetics of the reaction are similar in some respects to those for the cathodic deposition of hydrogen, for the latter also gives a linear  $V$ -log  $i$  curve and the rate of reaction varies with different electrode metals and with varying concentration of hydrogen ion. In other respects the two reactions are rather different, for  $\alpha$  in the case of hydrogen deposition ranges between about 0.25 and 2.0 according to the particular electrode and solution used, and there seems no evidence to show that it varies with temperature. Moreover hydrogen deposition on platinum takes place at an appreciable rate at the reversible potential.



The overall reaction for hydrogen deposition is

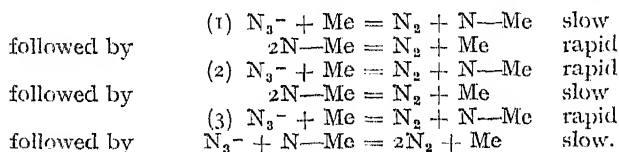


but this will take place in stages, the slowest of which will determine the rate of reaction. Similarly, for the deposition of the azide ion the overall reaction may be regarded as



considering the ion to be unhydrated, although this will again occur in stages, the slowest being rate determining.

Many theories have been advanced to describe the slow process in the deposition of hydrogen, but these fall broadly into two classes postulating (a) the neutralisation of the ion or (b) the formation of the  $\text{H}-\text{H}$  bond, as the rate determining step.<sup>18, 21</sup> The stage (b) may take place either by the direct desorption of two adsorbed atoms, or by the combination of an adsorbed atom with a hydrogen ion in solution. Analogously, three possible mechanisms for the azide reaction may be postulated:—



Process (1) has the neutralisation of the ion as the rate determining step, with the desorption of N atoms taking place relatively rapidly. (2) and (3) both postulate the neutralisation of the ion as occurring rapidly, the slow process being the desorption of atoms, which will take place by the faster of the two alternative methods available. In all these processes, however, the neutralisation of the ion is considered to result in the formation of a nitrogen molecule and an adsorbed nitrogen atom, instead of three adsorbed nitrogen atoms, in accordance with the evidence given previously indicating that one nitrogen atom behaves differently from the other two.

Considering first the neutralisation of the ion as the slow process, it appears that in general  $\alpha$  will be determined by the ratio of the slopes of two Morse curves, and as Adam<sup>22</sup> has pointed out cannot exceed unity. This process cannot, therefore, be rate determining in the azide case, but must be regarded as occurring rapidly compared with the desorption of atoms.

Although the neutralisation of the ion may occur rapidly, it is likely to be a rather irreversible process, and the reverse reaction at best will only take place at a very slow rate. Consequently, it is probable that the concentration of nitrogen atoms on the electrode surface will approach the saturation value, and under these conditions the simple desorption mechanism (2) would be expected to give a very small value of  $\alpha$ , much less than unity. To account for  $\alpha = 1$  on this hypothesis would require a surface only partially saturated with nitrogen atoms, the extreme case of a very sparsely covered surface corresponding to  $\alpha = 2$ . If the surface is only partially saturated, however, then presumably the formation of ions from adsorbed atoms must proceed at a rate comparable with the neutralisation of ions, and this would seem rather unlikely.

The alternative mechanism for desorption, involving combination of an adsorbed atom with an ion, also leads to difficulties over the value of  $\alpha$ . The current will be given by

$$i = k[\text{N}_3^-][\text{N}-\text{Me}]e^{\alpha F/RT}$$

and if the surface is approaching saturation,  $[\text{N}-\text{Me}]$  will be approxi

<sup>21</sup> Wirtz, *Z. Elektrochem.*, 1938, 44, 303.

<sup>22</sup> Adam, "The Physics and Chemistry of Surfaces," 2nd edn., chap. 8.

mately constant. The value of  $\alpha$  will presumably depend on the relative slopes of the Morse curves for the approach of an  $N_3^-$  ion to the electrode, and for the separation of two nitrogen molecules from the electrode, and just as in the case of the ion neutralisation reaction would be expected to be less than unity. Should the surface be only partially saturated, then the  $[N-Me]$  would be expected to increase with potential, and

$$i = k[N_3^-]e^{VF/RT} e^{\alpha_1 VF/RT}$$

where the first exponential gives the change in concentration of adsorbed atoms, and the second the change in activation energy. The observed value of  $\alpha$  is then  $(1 + \alpha_1)$  and should be greater than unity.<sup>23</sup> There seems no reason why  $\alpha_1$  should be extremely small, however, as would have to be the case. It appears, therefore, that neither the neutralisation nor the desorption mechanisms lead satisfactorily to the experimentally observed value of  $\alpha$ .

The temperature variation of  $\alpha$  is also difficult to account for although a possible explanation may lie in a change in the mobility of the adsorbed layer. Roberts<sup>24</sup> has shown that the heat of adsorption for a mobile layer is less than for an immobile layer, and thus if the mobility of the adsorbed layer of nitrogen atoms increases appreciably with temperature, the heat of adsorption would be expected to decrease. In this event, the slope of the appropriate Morse curve, might be changed, and this would lead to a change in the value of  $\alpha$ . This situation could, of course, arise in any of the above processes, as they all involve the adsorption of atoms.

It is apparent from the foregoing that the experimental results for the deposition of  $N_3^-$  present difficulties in explanation, and no satisfactory theory seems possible at present. Further work would be desirable, particularly as regards the adsorption of nitrogen on platinum and other metals with which it does not readily form nitrides.

The work described was carried out in the Laboratory of Physical Chemistry, Cambridge, and my thanks are due to Professor Norrish for the facilities afforded me. I am also indebted to Dr. J. N. Agar and Dr. F. P. Bowden for much helpful advice and criticism.

Acknowledgement is due, also, to the Department of Scientific and Industrial Research for an Assistantship, and to the Chemical Society for grants for apparatus.

### Summary.

The anodic deposition of the azide ion from aqueous solution at platinum, palladium, and iridium, electrodes is an irreversible process giving a linear  $V$ -log  $i$  curve with  $\alpha$  approximately equal to 1. The reaction is  $N_3^- = 3/2 N_2 + e^-$ , and the reversible potential for unit activity of  $N_3^-$  is estimated to be  $-3.3$  volts against a normal hydrogen electrode. Deposition occurs at measurable rates only at the high overpotential of ca. 4 volts. Increase in temperature causes a small but significant increase in  $\alpha$ , and the energy of activation is about 12 K.cal. per g. mol. at a potential of 0.81 volt against saturated calomel. The rate of reaction at a given potential varies with electrode metal, and with concentration of solution, but is independent of  $pH$  up to 9.4. At higher  $pH$ 's oxygen is preferentially evolved.

The reaction is paralleled to some extent by the cathodic deposition of hydrogen, but no theory of the types advanced in the latter case seems capable of accounting for the azide deposition satisfactorily.

<sup>23</sup> Frumkin, *Acta Physicochim. U.R.S.S.*, 1937, 7, 475.

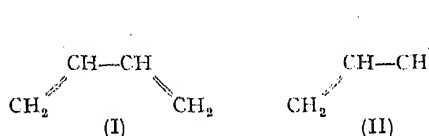
<sup>24</sup> Miller and Roberts, *Proc. Camb. Phil. Soc.*, 1941, 37, 82.

# THE IONIZATION POTENTIALS OF BUTADIENE.

By T. M. SUGDEN AND A. D. WALSH.

Received 10th November, 1944.

As a consequence of the interaction of its four  $\pi$  electrons, butadiene is expected to exist in two forms which may be designated *s-cis* (I) and *s-trans* (II) (Mulliken <sup>1, 2</sup>).



Because of the different symmetry of these molecules, the selection rules for electronic transitions differ. In particular, the intra-valence-shell transition

$N \rightarrow V_2$  is forbidden for *s-trans* but allowed for *s-cis*. In consequence, for *s-trans*  $N \rightarrow V_1$  should be strong and  $N \rightarrow V_2$  weak; while for *s-cis* the reverse should hold (Mulliken <sup>1</sup>).

Since the far ultra-violet absorption spectrum, described by Price and Walsh,<sup>3</sup> shows strong absorption for  $N \rightarrow V_1$  (around 2100 Å.), butadiene may be taken to be largely *s-trans* at room temperature. However, the absorption in the neighbourhood of 1700-1750 Å., identified as  $N \rightarrow V_2$ , though weaker than that at 2100 Å., is yet sufficiently strong to make it appear that an appreciable proportion of the butadiene molecules are in the *s-cis* form at room temperature. Mulliken<sup>1</sup> estimates 20 %.

More recently, Rasmussen, Tunncliffe and Brattain<sup>4</sup> have found that the 2200-2400 Å. absorption is strongly temperature-dependent. The optical density increases with temperature. This suggests an equilibrium at room temperature between *s-cis* and *s-trans* molecules and that the proportion of the latter increases with temperature. As a consequence of coincidences between the observed Raman frequencies at -80° C. and the infra-red frequencies at room temperature, they conclude that at low temperatures butadiene is entirely *s-cis*, but predominantly *s-trans* at room temperature.

Price and Walsh<sup>3</sup> found two prominent Rydberg series both leading to the same limit, 9.02v. This is presumably the ionization potential of *s-trans* butadiene. Other, weaker, bands were present, but on the basis of the spectroscopic observations alone it was not possible to say whether these afforded any indication of an ionization potential for the *s-cis* form. The ionization potentials of butadiene have since been further studied by one of us (T.M.S.), using the electron impact method of Mackay.<sup>5</sup> The results obtained by the electron impact method are much less accurate than those determined by spectroscopic Rydberg series, but they have the great advantage of indicating clearly the *existence* of an ionization potential: used in conjunction with spectroscopic methods they form a very powerful tool. The experimental details of the electron impact investigations will be published elsewhere: here we wish to refer only to the results for butadiene.

The curve of ion current/accelerating potential, shown in the accompanying figure, exhibits a very peculiar anomaly which has hitherto not been observed for any other substance. Positive ions begin to appear

<sup>1</sup> Mulliken, *J. Chem. Physics*, 1939, **7**, 121.

<sup>2</sup> Mulliken, *Rev. Mod. Physics*, 1942, **14**, 265.

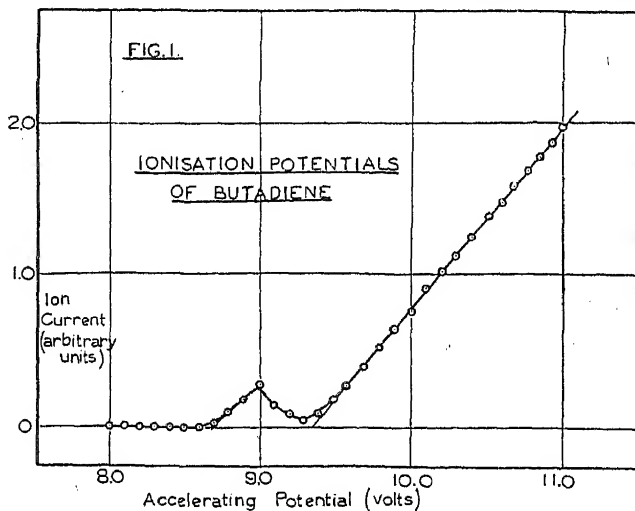
<sup>3</sup> Price and Walsh, *Proc. Roy. Soc.*, 1940, **174**, 220.

<sup>4</sup> Rasmussen, Tunncliffe and Brattain, *J. Chem. Physics*, 1943, **9**, 432.

<sup>5</sup> Mackay, *Phil. Mag.*, 1923, **46**, 828.

and give an increasing current with rising applied potential at a point corresponding to an ionization potential of 8.7 v. obtained by linear extrapolation. At rather higher values of the potential difference the ion current falls off and shows a minimum before rising again at a value somewhat above 9 v.

The curve suggests the existence of two butadiene ionization potentials in the range 8.5 to 9.5 v. The upper ( $\sim 9.3$  v.) doubtless corresponds to



the value found by Price and Walsh: electron impact values are often a few tenths of a volt higher than spectroscopic values. The lower ionization potential of  $\sim 8.7$  v. might plausibly be ascribed to *s-cis* butadiene: its discovery prompted a re-examination of the weak bands of the butadiene electronic spectrum.

It is possible to arrange certain of these weaker bands into the following Rydberg series

$$\nu_0^n = 70606 - \frac{n}{(m + 0.90)^2} \quad (1)$$

The series is plausible since there is very good agreement between the observed and calculated frequencies (Table I), as many as six members being observed, and since the intensity decreases regularly in the passage to higher members. The limit corresponds to 8.71 v. Taken alone, the spectroscopic evidence would probably justify acceptance of this Rydberg series; in conjunction with the electron bombardment results, we believe it provides strong support for the existence of an ionization potential of the above value. If so, 8.71 v. must be the first ionization potential of *s-cis* butadiene.

TABLE I.—TABLE SHOWING THE OBSERVED AND CALCULATED FREQUENCIES OF THE BANDS OF SERIES (1).

<i>n</i> .	$\nu_{\text{obs.}}$ cm. <sup>-1</sup> .	$\nu_{\text{calc.}}$ cm. <sup>-1</sup> .
3	63372	63391
4	Obscured by 1515 doublet	66036
5	67451	67454
6	68299	68301
7	68850	68848
8	69216	69221
9	69500	69486

The  $n = 3$  member of series (1) appears as a doublet. The  $n = 2$  member of the series should fall in the 1700-1750 Å. region: that is, it is plausible to identify the  $N \rightarrow V_2$  transition as the first member of the series ( $\nu_{\text{max.}} = 57800$ ,  $\nu_{\text{calc.}} = 57558 \text{ cm.}^{-1}$ ). This rather supports the assignment of the series to *s-cis* butadiene, since the  $N \rightarrow V_2$  absorption is known to be due to the *s-cis* form and since it is a general rule that an  $N \rightarrow V$  transition of an electron may also be classified as the first member of a Rydberg series for that electron. Examples are to be found in the spectra of the chloroethylenes (Walsh <sup>6</sup>), of aldehydes (Walsh <sup>7</sup>), of hexatriene (Price and Walsh <sup>8</sup>) and in the various derivatives of acetylene (Price and Walsh <sup>9</sup>). Similarly it is probable that the 2100 Å. region of butadiene may be classified not only as the  $N \rightarrow V_1$  transition but also as the first member of one of the Rydberg series found for *s-trans* butadiene.

There remains the difficulty of the minimum in the curve of ion current/accelerating potential. Such a minimum has not previously been observed in electron impact work with a large number of substances. If the vapour consisted of an equilibrium mixture of *s-cis* and *s-trans* isomers a continually increasing current would be expected, though a break would occur at about 9.1 v., corresponding with the appearance of *s-trans* positive ions. It appears that between the two ionization potentials either *s-cis* positive ions are being removed or are not being formed in the expected number.

We are inclined tentatively to explain the minimum as due to the second of these causes. The four  $\pi$  electrons of butadiene occupy in pairs orbitals  $\chi_1$  and  $\chi_2$ . The ionization potentials here discussed refer to the positive ion  $\chi_1^+\chi_2$ . Before the ion current curve begins to fall off, presumably only a  $\chi_2$  electron is excited on collision with a bombarding electron. Suppose, however, an energy level of the  $\chi_1$  electrons lies between the *s-cis* and *s-trans*  $\chi_2$  ionization potentials. Then when this energy value is reached, some of the collisions of the *s-cis* molecules with electrons lead not to excitation and ionization of  $\chi_2$  electrons, but to excitation of  $\chi_1$  electrons. It is true that excitation of a  $\chi_1$  electron may still lead to  $\chi_2$  removal, as a result of a process of auto-ionization; but it also facilitates conversion of *s-cis* to *s-trans* molecules. The net result is therefore that some collisions which previously resulted in  $\chi_2$  ionization now result instead in the formation of *s-trans* molecules. The excited *s-trans* molecules will not form ions because the minimum *s-trans* ionization potential is higher than the energy corresponding to the falling part of the curve. The current therefore falls off. The *cis*  $V_2$  state might possibly be available as a suitable energy level for this explanation to hold.

### Discussion.

It may be significant that the difference (0.31 v.) of the ionization potentials found for *s-cis* and *s-trans* butadiene is just the amount by which the ionization potential of *cis* dichloroethylene (9.61 v.) is less than that of *trans* dichloroethylene (9.91 v.). The dichloroethylenes, of course, possess resonance structures giving the hybrid something of a conjugated diene form.

The results of Rasmussen *et al.*<sup>4</sup> indicate an appreciable difference in stability between *s-cis* and *s-trans* butadiene. The present work shows that the ground states of the least strongly bound  $\pi$  electrons in the two forms differ by as much as 0.3 v.

It might be expected in consequence that the  $N \rightarrow V_1$  transition of the *s-cis* form might appear at a much longer wavelength than that of

<sup>6</sup> Walsh, *Results in course of publication.*

<sup>7</sup> Walsh, *Results in course of publication.*

<sup>8</sup> Price and Walsh, *Results in course of publication.*

<sup>9</sup> Price and Walsh, *Results in course of publication.*

the *s-trans* form. This is not necessarily so, however, for in the case of the dichloroethylenes the *trans* ionization potential is 0.3 v. higher than that of the *cis* and yet the *trans*  $N \rightarrow V$  transition occurs about 0.15 v. lower than that of the *cis* ( $\lambda_{\text{max.}} = 1900$  and 1950 Å. for *cis* and *trans* respectively). If *s-cis* butadiene has an  $N \rightarrow V_1$  transition falling about 50 Å. away from that of *s-trans*, the latter with its greater intensity would easily mask the former. Presumably the difference in energy of the excited states in *cis* and *trans* forms compensates for the difference in ground state.

It has always been difficult to understand the appearance of absorption in cyclopentadiene and cyclohexadiene at relatively long wavelengths compared with the open chain dienes. In order to explain it, Mulliken invoked the theory of hyperconjugation. According to this, weak conjugation could occur between unsaturation electrons and the electrons in C—H bonds. At first the effect was supposed to leave unchanged the energy of the ground state but to depress the energy of the excited  $V_1$  state. Price and Walsh<sup>10</sup> pointed out that this was quite inconsistent with the observed spectra of the cyclic dienes: all the electronic bands right up to and including the ionization potential suffered comparable shifts. The theory was later revised (Mulliken, Rieke and Brown<sup>11</sup>): hyperconjugation was no longer supposed to affect the  $V_1$  upper state, but to raise the ground state. Even in this form, there was experimental evidence not in accord with the theory (see, for example, Bateman and Koch<sup>12</sup>).

The problem arose essentially because of the comparison of the cyclic dienes with the spectra of (largely) *s-trans* butadiene. It is obviously more satisfactory to compare the absorption with that of *s-cis* butadiene. Accepting the present results, we then have a lowering of 8.71 — 8.58 v. = 0.13 v. for the ionization potential of cyclopentadiene relative to *s-cis* butadiene. This is quite within the range we should expect by a simple charge transfer effect consequent upon the addition of a  $\text{CH}_2$  group. The further lowering  $\sim 0.2$  v. in passing to cyclohexadiene may be largely explicable as due to a further charge transfer from the second  $\text{CH}_2$  group. Alternatively, it may in part be due to a widening of the angle between the double bonds and the outer single bonds, relative to cyclopentadiene. These results suggest that the changes in the ground states of the cyclic dienes relative to the *s-cis* open chain dienes do not require the invocation of any such theory as that of hyperconjugation: they are explicable simply as charge transfer and strain effects.

A considerable part of the abnormal red shift of the first absorption of cyclic dienes may be explained as due to a ground state shift consequent simply upon the *s-cis* arrangement of the conventional double bonds and not due to the nature of attached groups. Bateman and Koch<sup>12</sup> point out that the heat of hydrogenation of cyclohexadiene is much the same as that of open chain dienes. They therefore criticize any theory, such as that of charge transfer, which explains the red shift of cyclohexadiene as due to a change in the ground state. The criticism, however, is not valid. It would be valid if we were dealing with molecules containing a *single* pair of unsaturation electrons (thus Price and Tuttle<sup>13</sup> show the correlation that exists between heats of hydrogenation and  $N \rightarrow V$  frequencies for the alkyl ethylenes); but for conjugated dienes the electrons occupy *two* ground state orbitals and whereas the ionization potential refers to only one of these orbitals, the heat of hydrogenation depends upon the energies of both orbitals. In order to correlate the heats of hydrogenation of conjugated dienes with their ionization potentials, we

<sup>10</sup> Price and Walsh, *Proc. Roy. Soc.*, 1941, 179, 201.

<sup>11</sup> Mulliken, Rieke and Brown, *J. Amer. Chem. Soc.*, 1941, 63, 41.

<sup>12</sup> Bateman and Koch, *J. Chem. Soc.*, 1944, 600.

<sup>13</sup> Price and Tuttle, *Proc. Roy. Soc.*, 1940, 174, 207.

need to know the energy levels of each of the two ground state occupied orbitals.

The present results clarify somewhat the facts relating to the abnormal red shift of cyclic diene absorption. Two problems remain, however. First, why should the *cis* arrangement of the double bonds cause a red shift of the ground states of dienes? Second, what is the cause of the  $N \rightarrow V_1$  shift of cyclic dienes relative to *s-cis* butadiene?

As regards the first of these problems, Price and Walsh<sup>9</sup> have already pointed out that the lower ionization potential of *s-cis* dienes relative to *s-trans* may be due either to repulsion between the double bonds or to resonance in the *s-cis* form to structures involving interaction between electrons on the outer carbon atoms—e.g. III. The latter increase the resonance energy not only directly but also indirectly by holding the four  $\pi$  electron distributions in a more nearly planar condition. Such a question of planarity may also affect the states of the cyclic dienes, where some of the carbon atoms of the ring have trigonal valencies and some tetrahedral.

As regards the second problem, Price and Walsh<sup>10</sup> have stressed that the  $N \rightarrow V_1$  shifts of cyclic dienes relative to *s-trans* butadiene are not much more than those normally associated with ground state changes of the magnitude shown by the ionization potentials. The abnormality thus seems to lie more in the  $N \rightarrow V_1$  location for *s-cis* butadiene than for the cyclic dienes. The  $N \rightarrow V_1$  red shift seems to be shown by all molecules possessing an *s-cis* diene structure incorporated in a six-membered ring.<sup>12, 14</sup> Conversely, dienes with an *s-trans* arrangement do not seem to show this shift. We are indebted to Dr. Koch for pointing out that molecules of the type (IV) which have an *s-trans* arrangement in a cyclic structure, yet have a "normal" absorption spectrum. The abnormality of *s-cis* butadiene must be explained as due to a peculiarity of the  $V_1$  upper state, possibly consequent upon the open-chain nature of the molecule.

The authors desire gratefully to acknowledge their indebtedness to Dr. W. C. Price for his encouragement and help throughout the work that has led to the publication of this paper; and also to Dr. H. P. Koch who has given them many constructive criticisms of great value.

### Summary.

Evidence based upon the vacuum ultra-violet spectrum and electron impact determinations of ionization potentials is presented to show that butadiene exists in two forms, *s-cis* and *s-trans*, at room temperature. The *s-cis* form has a minimum ionization potential of 8.71 v. as against 9.02 v. for the *trans* isomer. This fact makes it possible to explain the low ionization potentials of cyclopentadiene and cyclohexadiene without recourse to the theory of hyperconjugation.

Physical Chemistry Laboratory,  
Cambridge.

<sup>14</sup> Booker, Evans and Gillam, *J. Chem. Soc.*, 1940, 1453.

# A THEORY OF THE CALENDER EFFECT IN RUBBER-LIKE MATERIALS.

By L. BILMES.

Received 19th September, 1944.

When raw rubber and many rubber-like materials are calendered an anisotropy is produced. This effect—the Calender effect—is well known<sup>1</sup> and is due to some sort of "freezing in" of the strains produced during calendering. The presence of these strains and the stresses to which they give rise can be shown by the anisotropy in mechanical properties and more strikingly by the effects of warming. The behaviour associated with the calender effect may be conveniently summarised under two headings.

(1) **Residual Strain.**—If a sheet of calendered material (exhibiting the calender effect) is warmed it will contract, if free to do so, in the direction of calendering and expand in the remaining two directions. This may be said to be due to the presence of residual strains in the calendered sheet. The so-called residual strain is positive (*i.e.* a tensile strain) in the direction of calendering and negative (*i.e.* a compressive strain) in the remaining two directions. The presence of these strains may also be shown by the smaller percentage elongation at break in the direction of calendering than in a direction perpendicular thereto.

(2) **Residual Stress.**—If the calendered sheet is held so that it is not free to contract in the direction of calendering, when warmed a tension will be set up in this direction and an external stress will have to be exerted to prevent the contraction of the sheet. This may be said to be due to the presence of residual stresses in the calendered sheet.

The so-called residual stresses will be in the same directions as the corresponding residual strains and their presence may also be shown by the lower tensile strength in the direction of calendering than in a direction perpendicular thereto.

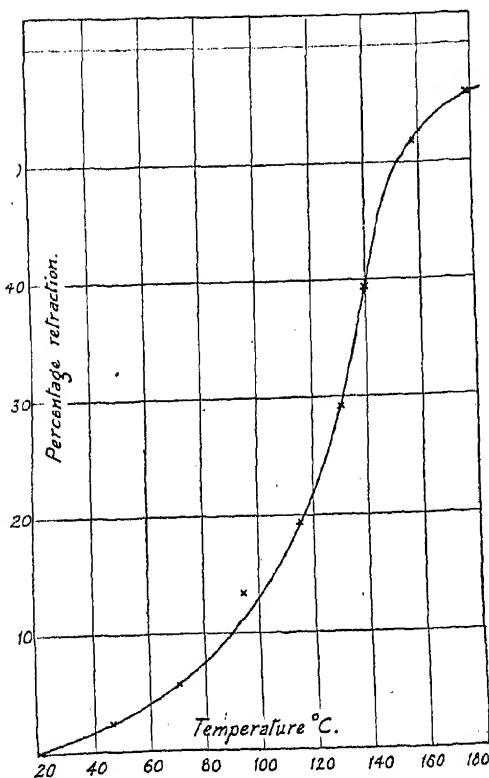


FIG. 1.

<sup>1</sup> De Visser, *Calender Effect and Shrinkage Effect of Unvulcanised Rubber*, London, 1926.



### Some Experimental Data.

Some experiments carried out with calendered P.V.C. (plasticised polyvinyl chloride) illustrate the calender effect.

(1) Strips 2.5 cm. wide, 18 cm. long and 0.1 cm. thick were cut with their length in the direction of calendering. A strip was immersed so as to hang freely in a bath of glycerine, maintained at a constant temperature, for ten minutes and then immersed in water at room temperature for 5 minutes. The percentage retraction was measured on 15 cms. of the strip. This experiment was carried out at a series of temperatures from 20° C. to 180° C. a fresh strip being used for each test and a typical curve is shown in Fig. 1.

(2) Similar strips were placed in two brass clamps 15 cm. apart (see Fig. 2). The lower clamp was fixed while the upper one was attached to a

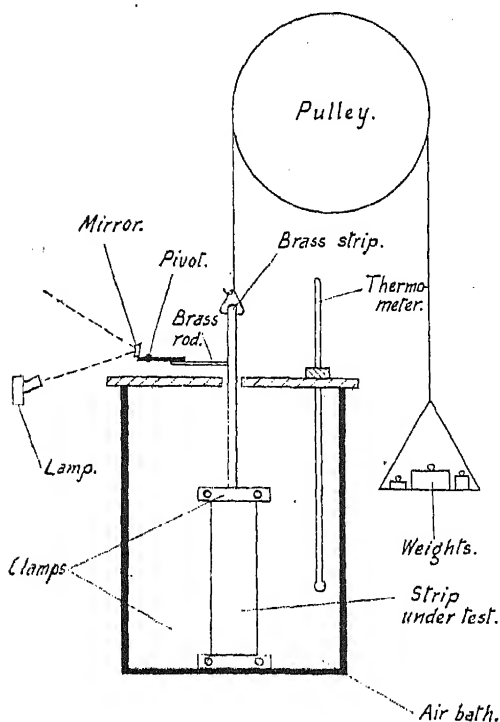


FIG. 2.

brass strip. A cord from this strip passed over a pulley wheel to a scale pan. A rod on the brass strip operated a mirror on a pivot. An extension or contraction of the strip under test was shown (magnified 200 times) by the movement of a spot of light reflected by the mirror. The strip was surrounded by an electrically heated and thermostatically controlled air bath the temperature of which—as indicated by a mercury thermometer—could be maintained constant to within about 1° C. The stress required to keep the strip at its original length was measured at a series of temperature by the weights that had to be added to the scale pan in excess of the zero load. These weights were constantly adjusted so that the spot of light remained in the same position. On raising or lowering the temperature approximately

$\frac{1}{2}$  hour was required for the bath to settle down to its new temperature and for the stress to rise or fall to an equilibrium value. (The stress was regarded as at its equilibrium value provided that it was constant to within 4 g./cm.<sup>2</sup> over a period of 10 minutes.)

The equilibrium stress was recorded at a series of increasing temperatures from 20° C. to 120° C. and thereafter at a series of decreasing temperatures. A typical curve is shown in Fig. 3. A further heating and cooling cycle gave curves coincident with CDE. No corrections were made for thermal expansions. The figure shows that the stress reaches a maximum value at 80–90° C.

The stress required to hold the strip at constant length is equal and opposite to the retractive stress in the strip, and ignoring the sign will be referred to below as the retractive stress.

### Deformation in Rubber-like Materials.

The deformation,  $D$ , produced in a rubber-like material by the action of a constant stress  $S$  can be analysed into three components.<sup>2, 3</sup>

(1) An ordinary elastic deformation,  $D_{OE}$ , proportional to  $S$  and appearing and disappearing instantaneously on the application and removal of the stress. For P.V.C.<sup>4</sup> the modulus,  $n_1 = S/D_{OE}$ , is independent of temperature and is of the order  $10^{10}$  dynes/cm<sup>2</sup>. This type of deformation corresponds to a stretching of the polymer chains.

(2) A high elastic deformation,  $D_{HE}$ , proportional to  $S$  and requiring a time for its full appearance and disappearance depending on the temperature. At a temperature of 60-100° C. when for P.V.C. the time for the full development of the deformation is relatively small the modulus,

$$n_2 = S/D_{HE}$$

is of the order of  $10^6$  dynes/cm<sup>2</sup>. This type of deformation corresponds to the uncurling of the polymer chains and the temperature dependence of the time effect is connected with the variation with temperature of the viscosity of the plasticiser.

(3) An irreversible "plastic" deformation,  $D_{VISC.}$ , proportional to  $S$  and to the time of application. The "viscosity" coefficient,  $\eta_1 = St/D_{VISC.}$ , for this type of deformation falls with temperature and, for P.V.C., is of the order  $10^4$ - $10^5$  poises at 140° C. This deformation corresponds to the sliding of the polymer chains past each other.

The behaviour of such a material can be represented by the well known model system<sup>3, 5</sup> of Fig. 4 consisting of elastic elements (springs) and viscous elements (dashpots) obeying Hooke's and Newton's laws respectively. It can easily be shown that for such a model:—

$$D = D_{OE} + D_{HE} + D_{VISC.} = \frac{S}{n_1} + \frac{S}{n_2} \left( 1 - e^{-\frac{n_2 t}{\eta_1}} \right) + \frac{St}{\eta_1} \quad (1)$$

It is clear that this model, as it stands, is not capable of providing an explanation of the experimental facts described above in connection with the

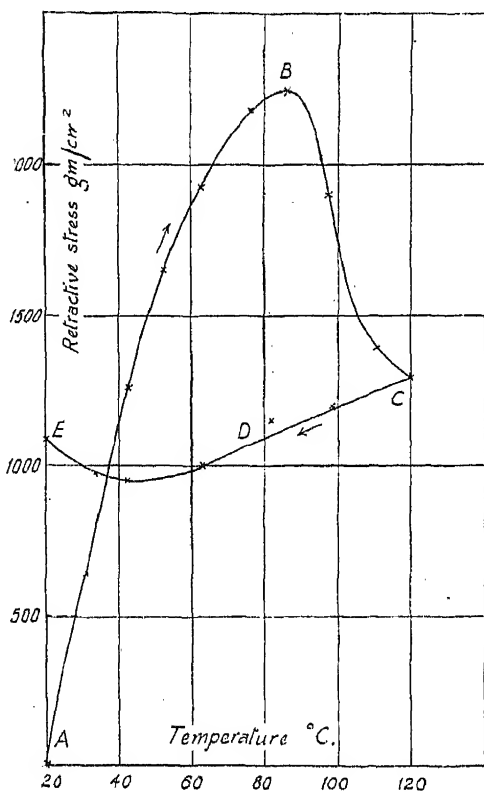


FIG. 3.

<sup>2</sup> Eley, *Trans. Faraday Soc.*, 1942, **38**, 290.

<sup>3</sup> Tuckett, *Chem. Ind.*, 1943, 430.

<sup>4</sup> Bilmes, *J.S.C.I.*, 1944, **63**, 182.

<sup>5</sup> Burgers, *First Report on Viscosity and Plasticity*, Amsterdam, 1935.

calender effect. For suppose that the model is stretched at some high temperature and then rapidly cooled in an attempt to simulate calendering conditions. After sufficient time has elapsed all the internal stresses of the model will dissipate. Owing to the presence of the viscous elements the model is not capable of retaining deformations, whereas experiments have shown that in P.V.C. sheets kept for 6 months (at  $30^{\circ}\text{C}.$ ) no measurable change in the calender effect could be detected. If, however, we are prepared to associate temperature dependent yield values,  $f_1$  and  $f_2$ , with the viscous elements,  $\eta_1$  and  $\eta_2$  it is possible to account for the experi-

mental data described above in terms of the now modified model system of Fig. 4.

### Model for the Calender Effect.

Suppose we attempt, as a preliminary, to represent the behaviour of a calendered strip by a model consisting of an elastic element in parallel with a "viscous" element possessing a yield value, see Fig. 5. Let  $n_2$  be the modulus of the spring and  $\eta_2$  and  $f_2$  the "viscosity" coefficient and yield value of the dashpot. If this model is strained to a value of strain  $x$  then the stress  $R$  required to hold it at this strain is given by:—

$$R = S - f_2$$

where  $S = n_2 x$  is the stress in the elastic element. Suppose that the model still held at the strain  $x$  is now cooled and that the yield value  $f_2$  rises with falling temperature. If the model is now released it will exhibit some recovery only if  $S$  is greater than the yield value at this temperature.

Had a temperature been chosen such that the yield value was equal to  $S$  the model on release would exhibit no recovery. The retractive stress  $R$  would then be zero, the residual stress  $S$  being exactly balanced by the yield value of the dashpot. If the temperature is now raised the stress  $R$  required to hold the model at the strain  $x$  will increase owing to the decrease of the yield value with increasing temperature. If  $R(\theta)$  represents the dependence of  $R$  upon temperature  $\theta$  and  $f_2(\theta)$  that of  $f_2$ , we can write:

$$R(\theta) = S - f_2(\theta) \quad (2)$$

Equation (2) and the model of Fig. 5 will not however provide a complete account of the  $R$ /temperature curve since it does not permit of  $R$  falling at sufficiently high temperatures. Let us now consider the effect of the second dashpot, viscosity coefficient  $\eta_1$  and yield value  $f_1$ , in series with the parallel model. We repeat the procedure described above. Supposing that  $f_1$  is very much greater than  $f_2$  we see that on warming no

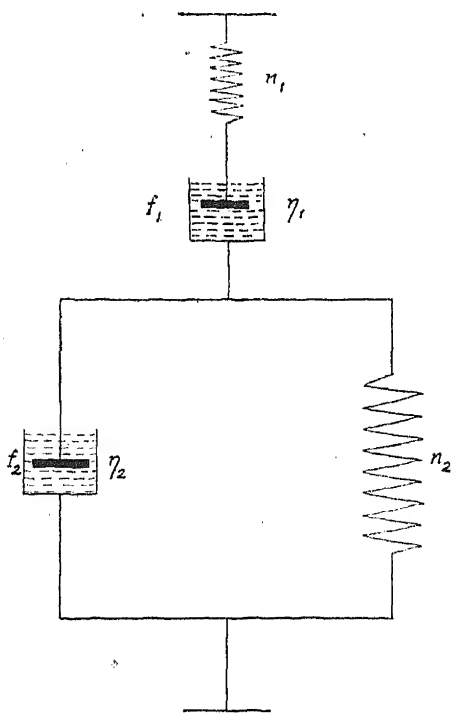


FIG. 4.

movement can take place in  $\eta_1$  until the temperature is sufficiently high for  $R$  to have increased and  $f_1$  to have decreased to make  $R$  equal to  $f_1$ . A further increase in temperature will produce an instantaneous increase in  $R$  (owing to a decrease in  $f_2$ ) whereupon flow will take place in  $\eta_1$ . As this flow continues the strain  $x$  in the spring  $n_2$  will decrease and  $R$  will decrease until it is just equal to  $f_1$ . The value of  $R$  at this and higher temperatures will be wholly dependent on the values of  $f_1$  and we can write

$$R(\theta) = f_1(\theta) \quad f_1(\theta) + f_2(\theta) \leq S,$$

$S$  being the original value of the stress in  $n_2$ .

The temperature at which  $S = f_1(\theta) + f_2(\theta)$  is the temperature at which annealing begins to take place, *i.e.* the temperature at which the residual stress  $S$  begins to be relaxed by the plastic flow that takes place in  $\eta_1$ . The residual stress  $S_1$  at some higher temperature is given by

$$S_1(\theta) - f_2(\theta) = f_1(\theta) = R(\theta)$$

and the residual strain  $x_1$  by

$$x_1(\theta) = \frac{S_1(\theta)}{n_2} = \frac{f_1(\theta) + f_2(\theta)}{n_2}.$$

On cooling  $\eta_1$  will have no effect on the  $R$ /temperature curve because the residual stress has relaxed to be equal to the sum of the yield values at the highest temperature attained and the  $R$ /temperature curve for cooling is given by

$$R(\theta) = S_1(\theta_m) - f_2(\theta)$$

where  $S_1(\theta_m)$  is the residual stress remaining at the highest temperature  $\theta_m$  attained. The complete equations for the  $R$ /temperature curve are

$$R(\theta) = 0$$

$$S \leq f_2(\theta)$$

$$R(\theta) = S - f_2(\theta)$$

$$f_1(\theta) + f_2(\theta) > S > f_2(\theta)$$

$$R(\theta) = f_1(\theta)$$

$$S \geq f_1(\theta) + f_2(\theta)$$

for rising temperatures,  
and

$$R(\theta) = S_1(\theta_m) - f_2(\theta)$$

$$S_1(\theta_m) > f_2(\theta)$$

$$R(\theta) = 0$$

$$S_1(\theta_m) < f_2(\theta)$$

for subsequent falling temperatures.

Fig. 6 shows the  $R$ /temperature curve obtained according to the above equations, assuming the shape of the yield value temperature curve. The curve of Fig. 6 bears a close resemblance to the experimental curve of Fig. 3 except that in Fig. 3 the cooling curve is not parallel to the heating up

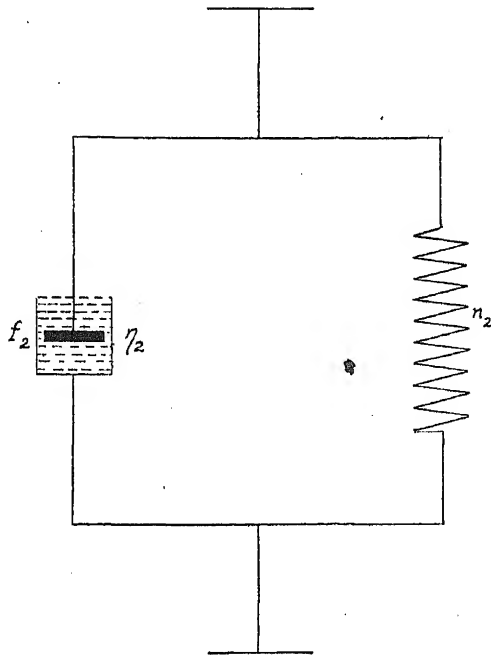


FIG. 5.

curve. This is probably due to the neglect of thermal contraction\* of both the P.V.C. and brass strip. If values for the coefficients of thermal expansion are known it should be possible by suitable design of experiment to obtain curves of the type shown in Fig. 6 if the proposed theory is correct.

It is easy to see how the presence of a yield value in  $\eta_2$  will account for the percentage retraction/temperature curve. In this case  $\eta_1$  has no effect whatsoever. The percentage retractions,  $p$ , at some temperature  $\theta$  is given by

$$\begin{aligned} p &= \frac{x - x_1(\theta)}{x} 100 \\ &= \frac{S - f_2(\theta)}{S} 100 \quad S > f_2(\theta) \\ p &= 0 \quad S < f_2(\theta) \end{aligned}$$

giving a curve similar to that shown in Fig. 2.

In terms of molecular structure the yield values  $f_1$  and  $f_2$  may have the following significance. Before chain uncurling ( $D_{im}$ ) and interchain

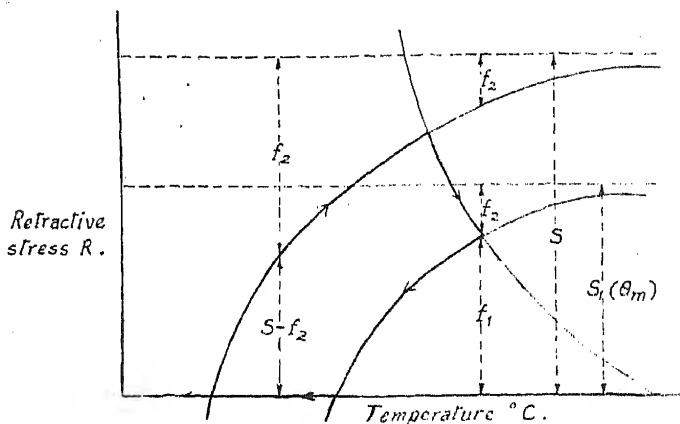


FIG. 6.

sliding ( $D_{visc.}$ ) can take place certain minimum stresses, which fall with increasing temperature, must be exceeded. This requires that equation (1) be modified to:

$$D = \frac{S}{n_1} + \frac{S - f_2}{n_2} \left( 1 - e^{-\frac{n_2}{\eta_2}} \right) + \frac{S - f_1}{\eta_1}$$

In the simple theory of the calender effect proposed here, one dimension alone—the direction of calendering—has been considered.

It is clear that the extension of the theory to three dimensions would present no novel features.

\* For over the path AB (see Fig. 3) the experimental values obtained for  $R$  will be lower than those given by the model by an amount that increases with increasing temperature. The path BC, however, is independent of thermal expansion effects,  $R$  being controlled solely by  $f_1$ , and any stresses that might now be set up by thermal expansion will be dissipated by the flow that would take place in  $\eta_1$ . On cooling two effects occur of which the path CDE is the resultant. The model requires that this path fall to zero parallel to AB, while owing to thermal contraction a continually increasing stress has to be exerted in order to keep the strip at constant length.

### Summary.

The facts relating to the calender effected are briefly stated and illustrated by experimental data obtained with calendered plasticised poly-vinyl chloride sheet. The nature of rubber-like deformation is outlined. A theory of the calender effect is proposed in terms of a mechanical model whose relation to molecular structure is indicated. The theory postulates that temperature dependent yield values be associated with the mechanisms of high elastic deformation and plastic flow.

Thanks are due to the Directors of Callender's Cable & Construction Company, Limited, in whose laboratories the experimental work was carried out, for permission to publish this paper and to E. Tunnicliff and I. K. Fisher for helpful discussions.

---

## ON THE MEASUREMENT OF THE THERMAL CONDUCTIVITY OF LIQUIDS.

By E. HUTCHINSON.

*Received 27th June, 1944.*

Data on the thermal conductivity of pure organic liquids are scarce and of the values listed in "International Critical Tables" only a few can be considered reliable. Early work in this field was done by Lees,<sup>1</sup> Goldschmidt,<sup>2</sup> Weber,<sup>3</sup> and others. More recent measurements have been made by Bridgman<sup>4</sup> and by Bates and co-workers.<sup>5</sup> The latter worker has made a very extensive study of the problem and has built a carefully designed apparatus the results from which are probably the most accurate of their kind. The method, however, has serious disadvantages in that it is based fundamentally on the Lees' disc apparatus, and in consequence very careful lagging and guard-ring corrections are needed. The apparatus is large, complicated, and measurements require considerable time as it is desirable to leave the apparatus running for several hours in order to ensure a steady state.

In this paper a very convenient method of measuring thermal conductivities is suggested: the method is based on that used by Goldschmidt<sup>2</sup> and also on one used by Melville<sup>6</sup> for measuring thermal conductivities of gases.

### Experimental.

The apparatus is shown in Fig. 1. It consists of two tungsten leads, to which are spot-welded a tungsten "coiled-coil" filament (as used in electric light bulbs) fused into a pyrex tube so that the filament lies axially down the tube. The tube, carefully selected for uniformity of bore and wall thickness, as used in these experiments was *c.* 1 cm. internal diameter and *c.* 7 cm. long. At points some 2 cm. above the junction of the filament to the upper tungsten lead two side tubes are fused on to the main tube to facilitate filling of the apparatus.

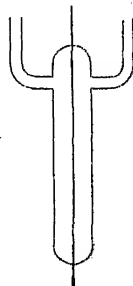


FIG. 1.

<sup>1</sup> Lees, *Phil. Trans.*, 1898, 191, 399.

<sup>2</sup> Goldschmidt, *Physik. Z.*, 1911, 12, 417.

<sup>3</sup> Weber, *Ann. Physik*, 1903, 11, 1047.

<sup>4</sup> Bridgman, *Proc. Amer. Acad. Arts and Science*, 1923, 59, 141.

<sup>5</sup> Bates, *et alii*, *Ind. Eng. Chem.*, 1933, 25, 431; 1936, 23, 494;

1941, 33, 375.

<sup>6</sup> Melville, *Trans. Faraday Soc.*, 1937, 33, 1316.

The technique of fusing the tungsten leads into the tube so that the filament is under slight tension and lies axially down the tube is readily acquired, but the alignment of the filament is facilitated by fusing glass beads on to the leads before finally sealing into the main tube.

The theory of the method is as follows. If an amount of heat  $Q$  is supplied per second by the filament a steady state is reached in which

$$Q = 2\pi l \times K \times (T - T_0) \ln \left( \frac{r_1}{r_0} \right) \quad (1)^\dagger$$

where  $K$  is the thermal conductivity of the liquid,  $l$  the length of the filament,  $r_1$  and  $r_0$ , respectively, the radius of the cylinder of liquid and the radius of the filament (c. 0.5 cm. and 0.004 cm. respectively),  $T$  and  $T_0$ , respectively, the temperatures at the surface of the filament and of the cylinder of liquid. The heat  $Q$  is generated by passing a known steady current  $I$  through the filament and measurement of the resistance of the filament gives a measure of the temperature  $T$ . The apparatus is placed in a thermostat so as to maintain a temperature  $T_0^*$  on the outer wall of the glass tube. This  $T_0^*$  is not identical with  $T_0$ , the temperature of the inner wall of the tube and outer surface of the liquid (assuming no temperature discontinuity at the liquid-glass interface: this assumption appears justified by experimental results obtained). Correction has therefore to be made for the temperature drop through the glass walls so as to obtain  $T_0$ , knowing  $T_0^*$  by actual measurement. From equation (1)

$$Q = 2\pi l \times K^* (T_0 - T_0^*) \ln \left( \frac{r_0^*}{r_1} \right)$$

where  $r_0^*$  is the external radius of the tube and  $K^*$  the thermal conductivity of the glass walls. It will be seen that since  $r_0^*$  and  $r_1$  are of the same order of magnitude then for a given heat flow  $Q$  the temperature drop through the glass ( $T_0 - T_0^*$ ) is much smaller than the temperature drop through the liquid ( $T - T_0$ ). The magnitude of the correction to be applied can be determined by direct calculation knowing the thermal conductivity of the glass or by calibration of the apparatus against carbon tetrachloride. In the present case the corrections found by the two methods agreed to within less than 1 %; in subsequent work the correction found by calibration was used as  $K_{\text{pyrex}}$  may be expected to differ slightly from sample to sample.

The theory of the apparatus implies radial flow of heat and absence of convection. Convection appears to be negligible as steady readings were obtained with the apparatus tilted even at 25° to the vertical, identical with those found with the apparatus in a vertical position. At angles greater than 25° marked irregularities and inconstancy were observed. Only small heating currents of the order 10<sup>-2</sup> amp. were used and temperature differences across the liquid column were of the order of 1° C. or less. Under these conditions end-losses as calculated by an equation due to Gregory and Archer<sup>7</sup> are less than 0.03 % so that there is no need to use the apparatus differentially as was found necessary by Goldschmidt. The apparatus does not appear sensitive to the height of liquid in the tube provided the filament is covered, and liquid was commonly poured in to about 5 mm. above the weld between filament and lead. The assumption that there is no temperature discontinuity at the glass-liquid interface has not been demonstrated, but in view of the good agreement between experimental results and the best values in the literature, together with the fact that at the glass-liquid interface the temperature gradient has fallen off to a low value, this assumption is considered valid.

There are several ways in which the various measurements necessary

<sup>†</sup> For a derivation of this equation see Roberts, *Heat and Thermodynamics* (Blackie, 1928), pp. 207, 208.

<sup>7</sup> Gregory and Archer, *Proc. Roy. Soc., A*, 1926, **111**, 95.

for a determination can be made. In the present case the resistance of the filament was measured in a standard Wheatstone Bridge circuit and the heating current evaluated by measuring the P.D. between the ends of a standard 10 ohms resistance in series with the filament. The temperature  $T_0^*$  of the thermostat in which the apparatus was placed was measured by means of a calibrated mercury-in-glass thermometer.

### Results.

The thermal conductivity of the material may be evaluated using equation (1), but a slightly different procedure was used in practice. Modifying equation (1) slightly one obtains

$$I^2R = 2\pi l \times K \times \frac{(R - R_0)}{CR_0} \ln \left( \frac{r_1}{r_0} \right) \text{ where } C \text{ is a constant}$$

$$= 2\pi l \times K^*(T_0 - T_0^*) \ln \left( \frac{r_0^*}{r_1} \right) \quad (2)$$

i.e.  $I^2R = \beta(R - R_0) = \alpha(T_0 - T_0^*) = \gamma(R_0 - R_0^*)$  where  $\alpha$ ,  $\beta$  and  $\gamma$  are constants,

where the temperature drop across the glass walls is expressed in terms of the resistance of the filament. In actual practice one does not measure  $(R - R_0)$  but  $R - R_0^*$ . Hence  $I^2R = \beta(R - R_0^*) - \beta(R_0 - R_0^*)$ . Thus if the resistance attained by the wire is plotted against heating power a graph is obtained which can be expressed by the equation

$$I^2R = (K - A) \times R \times B + C,$$

where  $A$ ,  $B$  and  $C$  are constants which can all be calculated in terms of the dimensions of the apparatus. Hence the procedure has been to plot heating power against resistance and to measure the slope of the graph from which the value of  $K$  can be derived. As explained above, the value of the constant  $A$  can be evaluated from a knowledge of the thermal conductivity of the glass, but here it was determined experimentally by calibration of the apparatus with carbon tetrachloride.

In Fig. 2 are shown typical heating power-resistance curves for three liquids, and in Table I the values obtained for the thermal conductivities compared with the most reliable data in the literature. The agreement is seen to be good.

TABLE I.—TEMP., 18° C. K. in CAL./SEC. CM. °C.  $\times 10^{-5}$ .

Compound.	$K_{\text{obsd.}}$	$K_{\text{literature.}}$
Water . . . . .	143 $\pm$ 2	140 Bates. <sup>5</sup>
Chloroform . . . . .	31.8 $\pm$ 0.5	31.0 „
Carbon tetrachloride . . . . .	38.0 $\pm$ 0.5	38.0 „
Acetone . . . . .	40.7 $\pm$ 0.5	42.5 I.C.T.
Et. alcohol . . . . .	43.6 $\pm$ 0.5	43.6 Bates. <sup>5</sup>
Et. iodide . . . . .	25.9 $\pm$ 0.5	26.0 I.C.T.
Glycerol . . . . .	67.2 $\pm$ 1.0	68.0 Bates. <sup>5</sup>

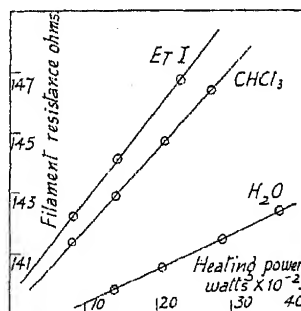


FIG. 2.

Since the electrical measurements involved can be made with great accuracy the method can be made to yield very accurate results. Further,



as the quantity of liquid required for a measurement can be made small by choice of smaller glass tubes, and as the time required for thermal equilibration is of the order of 1-2 minutes, the apparatus may possibly be used for such purposes as the study of reactions in solution, etc., in cases where ordinary analytical methods are difficult to apply.

The apparatus has been used to measure the thermal conductivity of various organic solids melted into it, but in view of the possible anisotropy of the solids and lack of precise information as to the orientation of the crystal axes in the tube, its utility in this field is somewhat limited.

### Summary.

An apparatus using a hot wire technique has been devised for the measurement of the thermal conductivity of liquids. Small quantities of liquid are required, measurements are simply and rapidly made, in contrast to other existing methods, and experiments on a few common liquids yield results agreeing to within *c.* 3 % with the most reliable data to be found in the literature.

The author wishes to acknowledge his gratitude to Professor E. K. Rideal, F.R.S., for kind advice and encouragement. Approval for publication has been granted by the Director General of Scientific Research and Development, Ministry of Supply.

*Department of Colloid Science,  
Free School Lane, Cambridge.*

## THE INTERACTION OF PLASTICISERS AND POLYMERS.

BY ELIZABETH M. FRITH.

*Received 17th October, 1944, as amended 8th December, 1944.*

The general problem of plasticiser polymer systems has two distinct aspects. The choice of a suitable plasticiser for use with a given polymer is first influenced by the degree of miscibility which is obtainable. Given sufficient miscibility (i.e. given a minimum *compatibility*), plasticisers will then be chosen for their efficiency in conferring specific properties. The efficiency of a plasticiser can simply be measured by the amount of it which is required to produce a certain degree of plasticity or softness in the plasticiser polymer mixture. This paper deals only with the problem of plasticiser compatibility; its aim is to show how compatibilities can be measured and to consider briefly the physical factors which determine good compatibility. Correlations between the chemical structure of a plasticiser and its compatibility properties are not considered. The scope is further limited to amorphous polymers on the one hand and liquid plasticisers on the other. We shall assume that the polymer and plasticiser are in thermodynamic equilibrium: the formal problem of determining the compatibility is then simply that of determining the mutual solubility relationships of a polymer and a simple liquid and requires a brief discussion of the equilibrium between a polymer and a liquid which is, in general, a solvent or swelling agent.

### Nature of the Interaction.

Since we assume that the polymer and plasticiser are in thermodynamic equilibrium, we can apply the current theories of polymer solutions. The equilibrium conditions are determined by the value  $\Delta G$  of the Gibbs' free energy change on passing from the original amorphous polymer to the swollen or dissolved state. The configurational increase in entropy corresponding to this change is large and has been calculated by Flory,<sup>1</sup> Huggins<sup>2</sup> and Guggenheim<sup>3</sup> with essentially similar results. If all the solvents or swelling agents considered have molecules roughly of the same size relative to that of the polymer chain link, the configurational increase in entropy on mixing is the same for all liquids. Thus variations in the equilibria found with different liquids must be ascribed entirely to differences in the heats of mixing. Since a direct calorimetric measurement of  $\Delta H$ , the change in heat content on mixing, is very difficult, heats of mixing are usually derived from measurements of the vapour pressure or osmotic pressure of the system over a range of temperature. Very few systems have been measured; as a general rule the heat changes are found to be small. In the rubber-benzene<sup>4</sup> system a small amount of heat is absorbed on mixing ( $\Delta H$  small and positive), rubber and toluene<sup>5</sup> mix almost without heat change; when there are attractive forces acting between the polymer and solvent heat is evolved on mixing as in the systems nitrocellulose-acetone<sup>6</sup> and cellulose acetate-tetrachlorethane.<sup>7</sup> While differences in  $\Delta H$  determine the differences in equilibrium states, the large swellings and high solubilities found in polymer systems are due mainly to the very large increase of entropy on mixing and not to big attractive forces between the polymer and liquid concerned.

If, then, the polymer mixes with the plasticiser without heat change, or if there are attractive forces acting between them, there should be complete miscibility over the whole range of composition as the heat effect is acting with the entropy effect to promote solution. But if the plasticiser is to some extent repelled by the polymer, heat is absorbed on mixing and this adverse heat effect may be large enough to produce phase separation and the limited swelling effects which are often found. A quantitative treatment of these phenomena was first given by Flory<sup>1</sup> and was worked out in detail by Guggenheim.<sup>3</sup> The condition for phase separation is, generally, that  $w/kT$  should be positive and greater than some critical value not markedly dependent on the polymer chain length;  $w$  is here a measure of the interaction energy between the plasticiser or solvent molecule and the polymer chain link. It has a value of zero if the polymer and solvent mix without heat change and is negative if there is polymer solvent attraction. Positive values of  $w$  correspond to polymer solvent repulsion. It is clear then that the formation of well-defined complexes, or stoichiometric compounds is not necessary for good compatibility. In the extreme case large attractions between the polymer and plasticiser may lead to the formation of a solvated hull in a simple chemical ratio. This appears to be the case in the system nitrocellulose-acetone where calorimetric measurements of Kargin and Papov<sup>8</sup> have suggested that a 1:1 complex is formed. In general, however, good compatibility is found when the forces between the polymer and plasticiser correspond to attraction or even slight repulsion. Comparative compatibility values should therefore be obtained from a comparative study of the heats of mixing or interaction forces between a polymer and a series of plasticisers.

<sup>1</sup> Flory, *J. Chem. Physics*, 1941, **10**, 51.

<sup>2</sup> Huggins, *J. Physic. Chem.*, 1942, **46**, 151.

<sup>3</sup> Guggenheim, *Proc. Roy. Soc., A*, 1944, **183**, 203, 213.

<sup>4</sup> Gee and Treloar, *Trans. Faraday Soc.*, 1942, **38**, 147.

<sup>5</sup> Meyer Wolff and Boissonas, *Helv. Chim. Acta*, 1940, **23**, 430.

<sup>6</sup> Schulz, *Z. physik. Chem.*, 1942, **52**, 253.

<sup>7</sup> Hagger and Van der Wyk, *Helv. Chim. Acta.*, 1940, **23**, 484.

<sup>8</sup> Kargin and Papov, *J. Physic. Chem. U.S.S.R.*, 1936, **7**, 483.

### Measurement of the Interaction.

Any type of experiment which measures directly or comparatively the interaction or attractive forces between a polymer and a series of plasticisers is thus suitable for estimating relative compatibilities. The obvious comparative method would be to measure the equilibrium swelling of a cross-linked or otherwise insoluble specimen of the polymer in a series of plasticisers: this method has the advantage of allowing controllable measurements over a range of temperature. It has been used successfully in the case of synthetic rubbers, but polymers like cellulose acetate, polyvinyl chloride or polystyrene reach equilibrium very slowly when swollen in the form of sheet or thin films and the method seems to require modification. It is obviously unsuitable when the polymer is soluble in the plasticiser. Direct measurement of the heats of mixing of polymers and plasticisers is difficult but some advance is being made using a suitable monomer as a model for the polymer link. This point is referred to later. Apart from swelling or calorimetric methods, however, it was suggested in an earlier paper<sup>9</sup> that polymer solvent interactions and possibly comparative swelling results could be obtained from a study of the usual  $\eta_{sp}/c - c$  viscosity curve obtained from measurements in dilute solution. Experiments on polymer plasticiser systems described here confirm the general prediction, although the exact form of the relationship is still admittedly not clear. The experiments are based on the following general considerations which are at least qualitatively correct.

1. The increase of the  $\eta_{sp}/c$  ratio with concentration (i.e. the initial slope of the  $\eta_{sp}/c - c$  curve) is a function of the solvent. If the solvent is attracted by the polymer chains (i.e. if  $\Delta H$  or  $w$  is negative) extended configurations of the polymer chains occur, there is increasing interaction between the chains as the concentration increases, and both the limiting ratio at zero concentrations  $[\eta]$  and the slope of the  $\eta_{sp}/c - c$  curve will be high. If there is polymer solvent repulsion coiled up polymer configurations reduce  $[\eta]$  and the slope of the curve. The theory originally suggested that the slope (but not the limiting intercept) of the  $\eta_{sp}/c - c$  curves was a linear function of  $w/kT$ .

2. Frequently the polymer is insoluble in the plasticiser or liquid in question, and in this case comparative measures of the interaction can be directly obtained from swelling measurements. It is possible also to use viscosity results provided the measurements are made in carefully chosen mixed solvents. Suppose that a polymer P is dissolved in a solvent  $S_1$  without any heat effects, so that  $w_{PS_1} = 0$ . If a second liquid or plasticiser  $S_2$  is added to the solution it is reasonable to suppose that it interacts to the same extent both with a polymer link and a single molecule of the type  $S_1$ . We can then imagine that this single interaction (which we may call  $w$ ) is responsible for any variations we may find in the viscosity curves. If then we have a dilute solution of polymer P in  $S_1$  and add varying amounts of  $S_2$  we should get a series of  $\eta_{sp}/c - c$  curves whose slopes and intercepts are functions both of the interaction  $w$  and the amount of  $S_2$  in the mixture. If, for comparative purposes, measurements are made with a fixed solvent composition, the curves should give a directly comparative measure of polymer- $S_2$  (plasticiser) interaction. In the experiments described below  $S_1$  is the solvent chosen as far as possible to comply with these conditions and  $S_2$  the added plasticiser whose relative compatibility will be related to the slopes of the  $\eta_{sp}/c - c$  curves.

### Experimental Methods and Results.

1. **Non-solvent Plasticisers.**—If the polymer is not completely soluble in the plasticiser, a direct experimental comparison can be made between viscosity results and swelling data. If the slope of the  $\eta_{sp}/c - c$  curve

<sup>9</sup> Frith, *Trans. Faraday Soc.*, 1945, **41**, 17.

for a given plasticiser content in the mixed solvent depends only on  $w$ , there should be some correlation between this slope and the equilibrium swelling of the insoluble polymer in the *pure* plasticiser. Swelling data are, however, only reliably obtained for vulcanised rubbers, and we have first tested this prediction using Gee's<sup>10</sup> published results on the swelling of lightly vulcanised synthetic rubbers. The swelling liquids used were simple aliphatic esters: while these are not plasticisers in the usual sense, they are chemically sufficiently similar to the more usual type to serve as test liquids in systems where strong dipole forces do not exist. The results are given below for the system "Neoprene"-Benzene-"Plasticiser." We assume that benzene is a suitably "indifferent" solvent for the polychloroprenes which form the basis of the Neoprene type of synthetic rubber: results given later in this paper show, however, that small deviations from this state do not invalidate the main conclusions. Gee measured the swelling of lightly vulcanised discs of Neoprene in a series of liquids and found that the results fitted a curve determined by the cohesive energy densities ( $E_s/V_s$ ) of the esters used. These results indicate then that the interaction between the ester and Neoprene is small or corresponds to a slight repulsion and we might expect, as is in practice found, that many of the pure esters will not completely dissolve unvulcanised specimens of the rubber. We have in effect then, a series containing some non-solvent plasticisers. Dilute solutions of unvulcanised specimens of Neoprene were prepared using as solvents 50 % by volume mixtures of benzene and the corresponding ester: the viscosity of each solution was measured in a standard Ostwald viscometer at 25° C. ( $\pm 0.02^\circ$  C.) relative to the appropriate solvent mixture. The increase of the viscosity ratio  $\eta_{sp}/c$  with the concentration was measured for each solution: over the range of polymer concentration 0 – 0.4 g./100 c.c., this increase was linear and the slope of the  $\eta_{sp}/c - c$  curve was readily found. Both the limiting intercept  $[\eta]$  of the  $\eta_{sp}/c$  ratio at zero concentration and the slope of the curve were dependent on the solvent used. The results are given in Table I together with Gee's figures for the equilibrium swelling  $Q$  in the pure ester and the corresponding  $E_s/V_s$  value of the ester itself.

TABLE I.—SWELLING AND VISCOSITY RELATIONSHIPS. NEOPRENE GN.

Neoprene GN-Benzene +	Intercept [ $\eta$ ].	Slope.	$Q$ .	$(E_s/V_s)^{\frac{1}{2}}$ (cal./c.c.) $^{\frac{1}{2}}$ .
Heptane . . . . .	0764	14	0.24	7.50
Isobutyl <i>n</i> butyrate . . . . .	0920	82	2.27	7.78
<i>N</i> butyl <i>n</i> butyrate . . . . .	0965	96	2.60	8.06
<i>N</i> butyl acetate . . . . .	0914	82	2.23	8.53
<i>N</i> propyl acetate . . . . .	0890	72	1.82	8.75
Ethyl acetate . . . . .	0798	50	1.14	9.08
Ethyl formate . . . . .	0718	36	0.51	9.43
Methyl acetate . . . . .	0649	22	0.49	9.58

The plots both of the limiting intercept  $[\eta]$  and the slope of the curves against the corresponding  $Q$  values are surprisingly good straight lines. Fig. 1 shows the plot of  $Q$  against the initial slopes of the viscosity curves: this plot corresponds to a more rapid increase with change of solvent than the corresponding plot for the intercept. Further evidence for this type of correlation will be presented later.

**2. Solvent Plasticisers.**—When the pure plasticiser is itself a solvent for the polymer and if the polymer cannot be vulcanised, swelling data cannot be obtained and alternative methods of correlation have to be

<sup>10</sup> Gee, *Trans. I.R.I.*, 1943, 18, 266.

devised. Purely amorphous polymers will be soluble in any plasticiser, both when there is direct attraction between the long chains and the plasticiser molecules and when there is no heat effect on mixing. This last type of solvent was called by Mark<sup>11</sup> an "indifferent" solvent and the solution is the "athermal" type discussed by Hildebrand. If the relative slopes of the viscosity curves are determined by  $w/kT$ , the viscosity slopes relating to solutions formed with evolution of heat ( $w$  negative: attraction between solvent and polymer) will be reduced by increasing temperature. Conversely the slopes found with solutions formed with

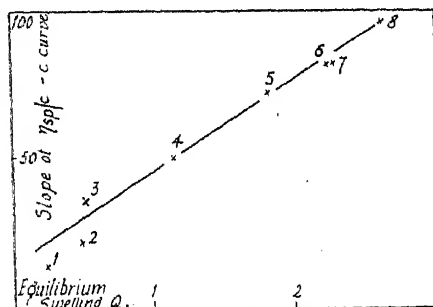


FIG. 1.—Relationship between viscosity and equilibrium swelling for Neoprene GN in a series of liquids. Viscosity measurements in 50 % by volume mixtures with benzene.

#### Liquids.

1. Heptane. 2. Methyl acetate. 3. Ethyl formate. 4. Ethyl acetate. 5. N propyl acetate. 6. N butyl acetate. 7. Isobutyl *n* butyrate. 8. N butyl *n* butyrate.

absorption of heat will be increased with temperature towards their unbiased value of a solution in an indifferent solvent. In each case the increased molecular motions at the higher temperature tend to restore the randomly kinked configuration of the polymer and hence the unbiased viscosity. Further, the viscosity relationships of an athermal solution will be unchanged by temperature.

*A priori* we should choose as a typically athermal mixture, a solution of polymer in pure monomer, provided that the monomeric molecule is not unduly polar in character. In this connection the theory has been tested by an extensive study of the system ethyl acetate-polyvinyl acetate both with and without added plasticisers. Fig. 2 shows the results of viscosity experiments on dilute solutions of polyvinyl acetate in ethyl acetate alone. The straight line is the experimental curve for solution viscosities measured at 25° C. and the dotted points the results of measurements at 50° C. There is then no effective variation of the specific viscosity with temperature and we may infer that the system ethyl acetate-polyvinyl acetate is truly athermal. The effect of the composition of the mixed solvent was then studied to amplify the arguments

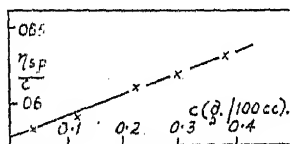


FIG. 2.—Viscosities of dilute solutions of polyvinyl acetate in ethyl acetate 25° C. and 50° C.

of case (2) of the last section. Polyvinyl acetate is soluble in dimethyl phthalate-ethyl acetate mixtures over the whole range of composition and the viscosities of the solutions in the mixed solvents are higher than those in pure ethyl acetate, indicating some degree of attraction between the polymer and the plasticiser. Fig. 3A shows the curves  $\eta_{sp}/c - c$  obtained in various solvent mixtures. The slopes of the curves, though not the limiting intercepts, are functions of the solvents and in Fig. 3B these slopes are plotted against the solvent composition. The relationship is quite linear as we might perhaps expect.

In so far then, as the solvents used are suitably "indifferent," the considerations given in the first half of this paper would seem to apply

<sup>11</sup> Alfrey, Bartovics and Mark, *J.A.C.S.*, 1942, 64, 1557.

and for comparative purposes we extrapolate some of these conclusions to other systems.

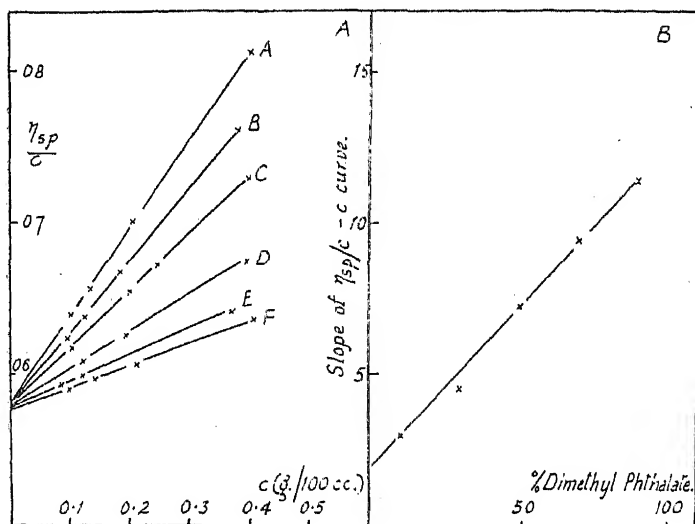


FIG. 3A.—The effect of solvent composition on the viscosity of dilute solutions of polyvinyl acetate in ethyl acetate dimethyl phthalate mixtures 25° C. A, 90 % D.M.P., 10 % E.A. B, 70 % D.M.P., 30 % E.A. C, 50 % D.M.P., 50 % E.A. D, 30 % D.M.P., 70 % E.A. E, 10 % D.M.P., 90 % E.A. F, 100 % E.A.

B. Relation between slope of  $\eta_{sp}/c - c$  curve and solvent composition.

### Comparative Measures of Compatibilities.

**1. Polyvinyl Acetate.**—Measurements have been made to test the relative compatibilities of a series of alkyl phthalates by measurements of the viscosities of dilute polymer solutions in 50 % by volume mixtures of the phthalates and ethyl acetate. A solvent composition of 50 % has

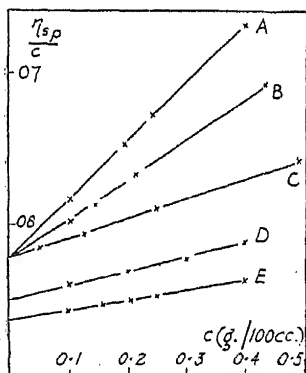


FIG. 4.—Viscosities of dilute solutions of polyvinyl acetate in 50 % mixtures of alkyl phthalates and ethyl acetate.

- A, Dimethyl phthalate 25° C.
- B, Dimethyl phthalate 50° C.
- C, Diethyl phthalate 25° C. and 50° C.
- D, Dibutyl phthalate 50° C.
- E, Dibutyl phthalate 25° C.

been chosen for convenience throughout this section: it allows relatively quick solution, even in mixtures with poor plasticisers and the comparative effects which are observed are sufficiently marked for our purpose. The results of experiments both at 25° C. and 50° C. are shown in Fig. 4.

Solutions of polyvinyl acetate in all mixtures of ethyl acetate and diethyl phthalate have viscosities at 25° C. and at 50° C. which exactly reproduce the straight line in Fig. 2; the results are shown in Fig. 4 as the line C. We may infer that diethyl phthalate, like ethyl acetate, mixes with polyvinyl acetate without heat change and that it is thus a good plasticiser. Dimethyl phthalate, as we have seen, appears to interact to some extent with this polymer and should show a superior compatibility. At 50° C. the slope of the viscosity curve for the 50 % dimethyl phthalate solution is lower than the corresponding slope at 25° C.: this confirms the conclusion we have just stated. As the temperature increases, the attractive forces between the plasticiser and polymer which cause the chains to uncoil slightly, are increasingly compensated by the thermal agitations and the relative viscosity falls as the configurational extension becomes less. The viscosities of solutions with dibutyl phthalate and dipropyl phthalate are, on the other hand, lower than those of solutions in pure ethyl acetate and the slopes of  $\eta_{sp}/c - c$  curves are increased slightly as the temperature is raised. (The curves for dipropyl phthalate mixtures are, for clarity, omitted from Fig. 4; the 25° C. curve lies between the lines D and E in the figure.) We would therefore expect these esters to be poor plasticisers for polyvinyl acetate and to have low compatibilities. The general trend of these results is in good agreement with the known plasticising action of the phthalate series.

**2. Polyvinyl Chloride.**—We have so far been concerned with relatively non-polar polymers. Polyvinyl chloride is, however, essentially polar and

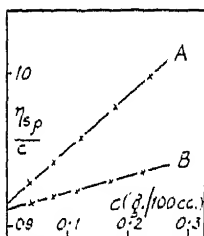


FIG. 5.—Viscosities of dilute solutions of polyvinyl chloride in cyclohexanone.

A, 25° C. B, 50° C.

will only dissolve in polar solvents. It is extremely unlikely that such solutions will be formed athermally and many of the theoretical conditions we imposed cannot now be assumed. However, experiments show that many of the effects observed with, say, the polyvinyl acetate systems, are found also with polyvinyl chloride solutions, and, although the theoretical basis is not so clear, the experimental results, for comparative purposes, are by no means invalidated. Cyclohexanone was chosen as the most suitable solvent for the polymer, and Fig. 5 shows the  $\eta_{sp}/c - c$  curves for dilute polyvinyl chloride solutions in this solvent at 25° C. and at 50° C. It is clear that increasing temperature decreases the  $\eta_{sp}/c$  values at any finite concentration, although the limiting  $[\eta]$  value at zero concentration is not affected. This decreasing value of the slope of the curves suggests that attractive forces are acting between the polymer and solvent. This means that viscosity experiments have to be made in mixed solvents which do not necessarily conform to the definition given above.

Polyvinyl chloride, however, is not soluble in the common plasticisers, and it has been possible to correlate some of the viscosity results obtained in mixed solvents with equilibrium swellings in the pure plasticisers. The viscosity results were obtained in the usual way. Fig. 6 shows the  $\eta_{sp}/c - c$  curves obtained for dilute solutions of the polymer in 50 % by volume mixtures of cyclohexanone and a series of alkyl phthalates. Generally speaking the results are in good agreement with the known compatibility properties. Dimethyl phthalate is recognised as a poor plasticiser for polyvinyl chloride, and its solutions show only a very slight increase of the  $\eta_{sp}/c$  ratio as the concentration rises. The higher members of the series show improved plasticising properties and it is further recognised that some maximum of compatibility occurs at the butyl ester. Fig. 7 shows the effect of temperature on the dimethyl phthalate and dibutyl phthalate systems. Although these systems are far from the ideal ones

studied in the last section we might expect a qualitative effect of temperature on the same lines and this is found here. The high slope of the dibutyl phthalate curve is reduced as the temperature rises: we cannot immediately say how far this effect is due to the cyclohexanone present in the mixture, but we can infer that the dibutyl phthalate either interacts directly with the polymer or has only a very small repulsive effect. The slope of the dimethyl phthalate curve is practically unchanged by temperature. Since the cyclohexanone in the solvent mixture is tending to reduce the relative viscosities at higher temperatures we must conclude that dimethyl phthalate itself is tending to repulse the polymer chains: this interaction will tend to increase the relative viscosity at higher temperatures and the net result is an apparent temperature independence of the viscosity curve. Dilute solutions of polyvinyl chloride with less than 50% of dimethyl phthalate in the solvent mixture give viscosity curves whose slopes are reduced by increasing temperature.

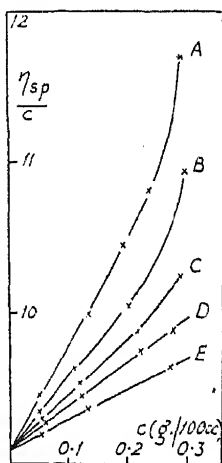


FIG. 6.—Viscosities of dilute solutions of polyvinyl chloride in 50% mixtures of cyclohexanone and alkyl phthalates, 25° C.

- A, Dibutyl phthalate.
- B, Dihexyl phthalate.
- C, Dioctyl phthalate.
- D, Diethyl phthalate.
- E, Dimethyl phthalate.

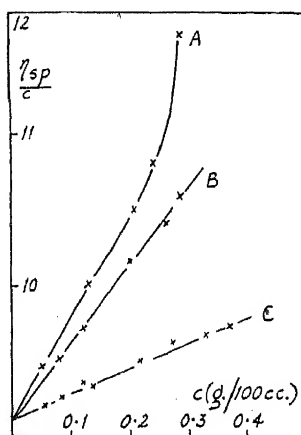


FIG. 7.—Viscosities of dilute solutions of polyvinyl chloride in 50% mixtures of cyclohexanone and alkyl phthalates.

- A, Dibutyl phthalate 25° C.
- B, Dibutyl phthalate 50° C.
- C, Dimethyl phthalate 25° C. and 50° C.

These figures were further checked by a series of rough swelling experiments. Preliminary experiments showed that polyvinyl chloride powder is swollen by plasticisers to give homogeneous gels with supernatant clear liquids. These liquids were analysed viscometrically and found to contain no polymer in agreement with Bronsted's<sup>12</sup> results for polystyrene. Weighed quantities (*c.* 0.2 g.) of the polymer were placed in small tubes and plasticiser added: the mixtures were stirred up with glass rods and left in a thermostat at 25° C. for a week. As much as possible of the supernatant liquid was sucked up by filter paper and the tube centrifuged at room temperature for ten minutes. The remaining liquid was then sucked up at 25° C. and the tube and gel weighed. While readings were mutually consistent to about 3% the accuracy is considerably reduced by temperature changes due to centrifuging at room

<sup>12</sup> Bronsted and Volquartz, *Trans. Faraday Soc.*, 1939, 35, 571.



temperature, excessive loss of excess plasticiser from the softer gels and in some cases semi-microscopic inhomogeneity. Consistent differences between the different plasticisers were, however, obtained, and in Table II we give figures for the phthalate series together with estimated values of the cohesive energy density of the plasticisers and the slopes of the curves shown in Fig. 6.

TABLE II.—VISCOSITY AND SWELLING RELATIONSHIPS POLYVINYL CHLORIDE.

Plasticiser.	$\frac{Q}{(\text{g. plast./g. PVC.})}$	Slope.	$\frac{E_s}{V_s}$ (cal./c.c.).
Dimethyl phthalate . .	5.0	48	108
Diethyl phthalate . .	5.4	74	87
Dibutyl phthalate . .	6.0	174	70
Dihexyl phthalate . .	5.7	117	60
Dioctyl phthalate . .	5.3	88	60

The equilibrium swelling appears to vary with the  $E_s/V_s$  value of the plasticiser and there is a maximum near the butyl ester, where, presumably, the  $E_s/V_s$  value of the plasticiser is most nearly equal to the corresponding  $E_p/V_p$  ratio for the polymer. We cannot at the moment, however, carry this interpretation very far, as Gee's correlation of  $Q$ , the equilibrium swelling, and the cohesive energy density of the swelling agent only applies when heat is absorbed on mixing. Without further measurement, we cannot give a more detailed interpretation of the heat changes which occur in the complicated ternary mixtures used for the viscosity experiments. Dibutyl phthalate will not dissolve polyvinyl chloride and we must suppose that steric or polar effects prevent complete miscibility. Such effects will, of course, influence the slope of the viscosity curve, but to what extent we cannot at present say. Two points are, however, clear: the comparative slopes of the viscosity curves do represent the known series of plasticiser compatibilities and the slopes are paralleled by the equilibrium swelling in the pure plasticiser.

Results for further series of plasticisers are given in Table III. In the phosphate series there is again known to be a maximum of com-

TABLE III.—VISCOSITY RELATIONSHIPS. POLYVINYL CHLORIDE SYSTEMS.

Plasticiser.	Limiting Value.	Initial Slope of Viscosity Curve.
Trimethyl phosphate . . .	0881	5
Triethyl phosphate . . .	0915	113
Tributyl phosphate . . .	0920	150
Trinonyl phosphate . . .	0900	84
Triacetin . . . . .	0805	2
Triethyl sebacate . . . .	0880	86
Tributyl sebacate . . . .	0920	176
Methyl phthalyl ethyl glycollate .	0878	88
Ethyl phthalyl ethyl glycollate .	0870	60
Butyl phthalyl butyl glycollate .	0870	72

patibility at the butyl ester and this is represented by a steep slope of the viscosity curve, and a slightly higher value of the limiting intrinsic viscosity ratio  $[\eta]$ , although this latter factor is always less affected by solvent variations than the slope of the  $\eta_{sp}/c - c$  curve. The superiority of the

butyl ester is shown again by comparison of the results for ethyl and butyl sebacates. Triacetin is given as an example of an extremely poor plasticiser and the phthalyl alkyl glycolate series to show a range of plasticisers of only medium efficiency.

**3. Cellulose Acetate.**—When we come to consider cellulose esters the highly polar nature of the common solvents makes any direct explanation of viscosity results rather difficult. As with polyvinyl chloride systems, however, truly comparative effects do obtain. Fig. 8 shows viscosity curves for a cellulose acetate dissolved in a 50 % by volume mixtures of alkyl phthalates and acetone. Dimethyl phthalate is here shown to be rather more compatible than the corresponding ethyl ester. Dibutyl phthalate-acetone mixtures in this proportion will not dissolve cellulose acetate even in these very dilute solutions. The third curve in Fig. 8 is that obtained with the same cellulose acetate in a 50 % mixture of acetone and triacetin: the crossing of the phthalate curves is somewhat unexpected, but the high slope shows that triacetin is an efficient plasticiser with good compatibility. If there is very strong dipole interaction the curves obtained may be very different in nature. Thus benzene, added to a dilute solution of cellulose acetate in cresol raises the viscosity, although it acts as a precipitant if added in sufficient quantity. Here presumably the cellulose acetate forms a compact complex with the cresol possibly with hydrogen bonds, and this complex is broken down by benzene into the original structure of extended long chains. However, when such extreme conditions are avoided, this method of approach always gives results which are in good agreement with the plasticising action of the liquids used, when this is known.

### Discussion.

The experiments described here clearly lead to the following conclusions. In all the mixed solvent experiments the comparative slopes of the viscosity curves are paralleled by the equilibrium swelling in the pure plasticiser and the slopes do represent the known series of plasticiser compatibilities. As a purely experimental method of measuring compatibilities viscosity measurements of this type seem very satisfactory. It remains to see how far the experimental results are in quantitative agreement with any theoretical predictions. The theory previously developed<sup>9</sup> to account for solvent effects basically assumed that the value of  $\eta_{sp}/c$  at zero concentration was proportional to the mean square length of the molecule, according to calculations of Huggins<sup>13</sup> and Kuhn.<sup>14</sup> Finite values of  $w$ , the interaction between polymer and solvent, alter the value of  $\bar{L}^2$  in such a way that  $\bar{L}^2 = (1 + a')\bar{L}_0^2$  where  $a'$  depends both on  $w$  and on the concentration  $c$ . In the limit of zero concentration, and of course when there are no heat effects,  $a'$  tends to zero. No further specific account was taken of the possible effects on the viscosity of

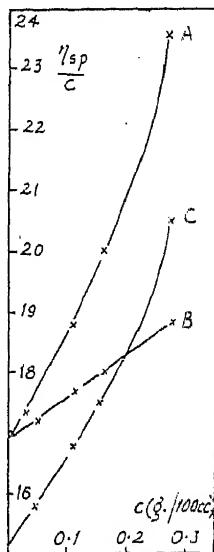


FIG. 8.—Viscosities of dilute solutions of cellulose acetate in 50 % mixtures of acetone and plasticiser, 25° C.

A, Dimethyl phthalate.  
B, Diethyl phthalate.  
C, Triacetin.

<sup>13</sup> Huggins, *J. Physic. Chem.*, 1939, **43**, 439.

<sup>14</sup> Kuhn and Kuhn, *Helv. Chim. Acta*, 1943, **26**, 1394.

increasing interaction between chains. The final equation derived for  $\eta_{sp}/c$  was written

$$\frac{\eta_{sp}}{c} = A + \left\{ B' - \frac{Bw}{kT} \right\} \cdot c$$

so that the slope of the  $\eta_{sp}/c - c$  curve should be a linear function of  $w/kT$ . In mixed solvents of the type defined and considered here,  $\eta_{sp}/c$  can be similarly calculated as a linear function of  $w/kT$  where  $w$  is the single interaction between the polymer and plasticiser  $S_2$ ;  $\eta_{sp}/c$  should also be a linear function of the volume fraction of liquid  $S_2$  in the solvent mixture. An obvious experimental check on the validity of these assumptions would be to measure directly  $\Delta H$ , the heat of mixing of the polymer and plasticiser. The direct calorimetric measurement of  $\Delta H$  is not easy and indirect measurements have to be devised which are experimentally more feasible. Gee and Treloar<sup>4</sup> showed that the heat of mixing of rubber and benzene was nearly equal to that of benzene and a simple hydrocarbon. This suggests that calorimetric measurements with systems of plasticiser and monomer should give  $\Delta H$  values closely related to the interaction between the plasticiser and the polymer link. Experiments on these lines are at present being carried out by Mr. P. Meares in this laboratory. Unpublished results on ethyl acetate-alkyl phthalate systems confirm the interpretations placed on the viscosity results shown here in Figs. 2-4. This agreement and the good correlations found with swelling data clearly show that there is a close connection between the slopes of the viscosity curves and the polymer solvent interactions. The exact form of this relationship is, however, not yet experimentally proved.

Further quantitative agreement with the theory is not obtained. The effect of solvent is essentially one of the second order. The viscosity ratio  $\eta_{sp}/c$  increases with concentration in any solvent due to increasing interference between the chains, so that the  $B'$  term in the equation for  $\eta_{sp}/c$  is large and positive and to a first approximation independent of temperature. The  $Bw/kT$  term is something like a correcting factor. Since  $1/T$  varies only slightly in the range 25°C.-50°C., the effect of temperature on the slope of the curve should be very small, and probably within the experimental error. The large variations which are obtained experimentally contradict this and the disagreement is serious. Qualitatively the predicted effect of temperature is in the right direction; as the temperature rises, the molecular movements become increasingly strong, the random configurations of the chains become more probable and the unbiased viscosity is favoured. The reasons for this failure to account exactly for the experimental results must be due to the crudeness of the underlying assumptions. In the original theory the use of Huggins' equation, assuming proportionality between  $\eta_{sp}/c$  and  $\overline{L^2}$ , is valid only in the limit of zero concentration. As the concentration increases this relationship ceases to hold exactly and the theory obviously did not take sufficient account of the increasing resistance to flow caused by increased contacts between chains. As the concentration increases then, interference between the chains accentuates and eventually overmasks the small effects originally considered. As the chains uncoil in a "good" solvent, there will of course be increased contacts between separate chains and the slope of the viscosity curve will be high. Qualitatively the suggested solvent effects will account for the experimental results, but a quantitative relationship between the polymer-solvent interaction and the slope of the viscosity curves, although demonstrated experimentally, remains theoretically unproved.

### Summary.

The general problems of plasticiser compatibility is discussed and it is suggested that a comparative measure of the compatibility can be

obtained from experiments which measure polymer plasticiser interactions ( $w$ ). Experiments are described which measure the viscosity of dilute polymer solutions in suitable mixed solvents containing the plasticiser in question. The slope of the  $\eta_{sp}/c - c$  curve is shown to be related to the equilibrium extent of swelling of the polymer in the pure plasticiser and in general the slope of the curve is a good comparative measure of the plasticiser's compatibility. The effect of temperature and composition of the mixed solvent is also discussed. The experiments are considered in the light of a previous theory of the effect of solvent on the  $\eta_{sp}/c$  ratio; the results do not support the suggested view that the slope of the  $\eta_{sp}/c - c$  curve is a simple linear function of  $w/kT$ .

My thanks are due to the Geigy Colour Company, and to Boake, Roberts & Co. Ltd. for the supply of materials. I should like to express my thanks to Professor E. K. Rideal, F.R.S., for much encouragement and advice and also to Dr. G. Gee for his help in the presentation of this paper.

*Department of Colloid Science,  
The University, Cambridge.*

---

## REVIEWS OF BOOKS.

**The Ultra-fine Structure of Coals and Cokes.** (The Proceedings of a Conference held in London, June 24th and 25th, 1943, by the British Coal Utilization Association.) H. K. Lewis and Co. Pp. 366. Price 25s.

Coal has traditionally been regarded in this country mainly as a source of heat and power, and for this reason, the amount of published fundamental research on this material has been almost negligible. It is now being recognised that coal can, in addition, provide the basis for a great new chemical industry, and this view stresses the importance of long range investigation into its properties.

The Proceedings record the success of the conference in bringing together those primarily interested in the production and use of coal, and scientists from the Universities and Technical Colleges.

It is agreed that the subjects chosen are difficult, but it is disappointing to find so little reference to the contribution which can be made by organic chemical research. Questions of the physical structure of coal are treated in some detail and there is much here to command the interest of the physicist and the physical chemist.

The papers are grouped in sections, each section being followed by a verbatim report of contributions to the discussion.

In the principal section of the Proceedings, ten papers are devoted to the structure and deformation characteristics of coal, and the authors wisely adopt methods which have been applied so successfully to the structure of polymeric materials. The topics dealt with, include the colloidal and internal structure of coal, its surface properties such as adsorption, surface area and heat of wetting, and the elastic constants of coal.

Another section deals with the application of X-ray methods to the determination of structure, identification of non-coal minerals and measurement of crystallinity.

Other sections include papers dealing with the determination of optical, magnetic and electrical properties, with the infra red spectrum of coal, and with the use of the electron microscope in coal research.

The volume contains complete author and subject indexes, and the quality of reproduction of photographs and diagrams is excellent. The Proceedings should be of the greatest use to all those interested in coal, or in the general structure of materials, and each of the twenty-two papers is worthy of study. They do, however, convey the impression that this is a collection of papers and not an integrated document. No attempt has been made to illustrate the plan underlying the work on the ultra-fine structure of coals and cokes. Perhaps this will be done in a later publication.

R. C. S.

**Determination of Particle Size in Sub-Sieve Range. Report of Discussions.** Published jointly by the British Colliery Owners Research Association. The British Coal Utilization Research Association. (London, 1944. Pp. 69. Price 7s. 6d.) Obtainable from H. K. Lewis & Co.

In these times a knowledge of the properties of fine particles finds an application in most branches of scientific work. Particle size and size distribution in the sub-sieve range is as important in mineral physics and hydrology as it is in say rubber or paint technology. What used to be regarded simply as a problem for the colloid physicist is now a day to day occurrence in many industries. Yet, although much progress has been made, the subject requires more investigation before its theoretical basis is clear.

The wide attraction and importance which the subject holds in this country is evidenced by the diversity of interests represented by research workers from Government, University and Industrial laboratories, who took part in the series of discussions of which this document is a record.

To quote Dalla Valle (the author of 'Micromeritics') "the characteristics and behaviour of small particles can be understood satisfactorily only when the methods of determining size distribution are placed on a firm basis". The present publication does much to clarify the position. It contains perhaps the clearest exposition available of the advantages and limitations of three well-known methods of size determination—the direct microscopic count, measurement of light extinction properties, and the Andreasen pipette method.

The book falls naturally into three sections, opening with an account of an informal exchange of views between a number of workers, followed by an excellent account of experimental work based upon the three selected methods, and concluding with a discussion of the findings in relation to the development of methods which can be considered adequately reproducible and accurate.

The general conclusions reached are in agreement with those of the American Society for Testing Materials (Symposium on *Particle Size Measurement*, 1941), namely that the Andreasen pipette method is accurate and rapid for particles down to  $25\mu$ , turbidity methods are most useful for rapid control determinations, while for particles in the colloid

range, or for heterogeneous powders, microscopic or centrifugal methods are necessary.

The conference was unanimous in recommending the further investigation and use of light extinction methods in cases where particles of anomalous light extinction properties are absent, and where large divergences from a mean density do not occur.

The Research Associations are to be congratulated on the success of their enterprise, and it is to be hoped that future discussions will attract even wider interests to contribute to rapid development of this field.

R. C. S.

**Systematic Inorganic Chemistry.** By DON M. YOST and HORACE RUSSELL, Jr. (New York, Prentice-Hall, Inc., 1944.) Pp. xx + 423. Price \$6.00.

The title of this book, as printed on the cover, is not fully justified by the contents; the real title of this interesting work appears only on the title page: "Systematic Inorganic Chemistry of the Fifth- and Sixth-Group Non-metallic Elements" and therefore it can be valued and judged only on considering this essential restriction. The book is a monograph of a new kind (new in the best sense of the word) on a relatively small cross-section of inorganic chemistry. The authors justify their choice with the argument that "the non-metallic elements of the fifth and sixth group of the periodic system" "and their compounds, besides being of great practical and theoretical interest in themselves, exhibit in their properties and reactions, characteristics that are common to many other substances both inorganic and organic."

We have here, therefore, the remarkable experiment of expounding chemistry as a whole by the example of a few chemical elements, in the same way as one seeks to convey the configuration of a wide expanse of country by stressing its most characteristic landmarks. In both cases one may doubt which points to choose; a "horizontal cross section" through the periodic system would perhaps be more characteristic for chemistry than the "vertical cross section" preferred by the authors, or—perhaps even better—one section as well as the other. However, once the choice is made, we have to consider how far the authors succeed in their aim "to cover a selected list of chemical topics and to include in the discussion of each enough of both the old and the new chemistry to bring out the most important features of the substances examined."

The authors have succeeded excellently in welding together old, well-known facts and new basic principles. Out of the fusion of old and new, to use the authors' words, a monograph has arisen which gives an interesting insight into chemistry and chemical research by way of consideration of the elements N, P, O, S, Se and Te.

The work under review claims to be neither a textbook nor a handbook; its contents lie between these extremes. It is not a textbook, for it presumes knowledge of essential "spectroscopic, structural, thermodynamic, chemical kinetic and nuclear properties" and that perhaps to an extent too large. There is, for instance, no explanation of the standard states (which are, after all, fixed arbitrarily) for the numerical values of the free energies of formation—the note "aq.  $a = 1$ ," p. 85, Table 22, cannot

replace such an indication. The detailed treatment of the results of nuclear physics is certainly not unjustified; a more thorough treatment of reaction kinetics (energy of activation, stationary states, chain reactions) was probably made impossible by limitations of space, though the book offers even in this branch many well thought out suggestions for "the research man or advanced student."

This monograph does not make any claim to completeness, i.e. it is not a handbook. It is restricted to critically selected references which are "either significant . . . or ones that will provide the reader with a convenient key to further information." Some modern references to the Landolt reaction, p. 329, might have been included.

The subject-matter is arranged in the following manner: each element is dealt with, furthermore the compounds of N and P with O and S, the compounds of the elements of the sixth group with H, and in varying order the halides, oxyhalides and oxyacids. A separate, most interesting chapter is given to ammonia—the excellent exposition of the solutions of alkali metals in liquid ammonia is especially noteworthy. There is also a separate chapter on the Per-compounds. The treatment of the thionic acids (thiosulphuric acid and polythionic acids) separately from the other sulphur-oxy-acids may seem unusual, though justified.

The short descriptions of technical processes are excellent in their conciseness. All figures and tables are clear and distinct. A number of tables in the appendix are useful.

A few minor discrepancies may be mentioned. The free energy of formation of  $\text{SO}_2(g)$  is given as  $-69660$  ( $25^\circ \text{C. ?}$ ) in Table 88, p. 318, and as  $-71735$  cal. ( $25^\circ \text{C.}$ ) in Table 97, p. 342 (both values are, admittedly, found in the literature). The value of the free energy of formation of  $\text{H}_2\text{O}(l)$  ( $25^\circ \text{C.}$ ) in Table 67, p. 270, is slightly different from the usual  $-56560$  cal.; at this point (*cf.* Table 97, p. 342) quotation of the source would be useful, considering its importance. The lettering of the abscissa of Fig. 68, p. 340, requires some explanation. Bodenstein's collaborator, *Z. physik. Chem.* 1922, 100, 68, is Lindner, not Linder.

The book bears the stamp of the California Institute of Technology, this well-known place of learning and research, and is dedicated to Professor William C. Bray, "able scientist, inspiring teacher"; this homage will be welcomed warmly by scientists on both sides of the Atlantic.

E. A.

# The Faraday Society.

## Minutes of the 38th Annual General Meeting

Held on Tuesday, 2nd January, 1945, at 5 p.m. at King's College, London, W.C. 2.

The President, Professor E. K. Rideal, M.B.E., D.Sc., F.R.S., was in the Chair.

1. The Minutes of the 37th Annual General Meeting, which had been printed in Volume XL on pages 91 and 92, were taken as read and confirmed. The Secretary briefly referred to the publicity which had been given, as directed at the last Annual General Meeting, to the message from two Russian colleagues.
2. The Annual Report and Statement of Accounts, together with the report of the Auditors for 1943, were presented by the Honorary Treasurer and were unanimously adopted. Before calling upon the Honorary Treasurer formally to move the adoption of the Report, the President expressed his pleasure at the continued growth of the membership despite the difficulties due to the war, and briefly referred to the activities of the Society during the year. He said that the Council were considering the possibility of giving to those members who were also members of one of the chartered chemical bodies the like privileges (as to a slightly reduced subscription and the joint payment of subscriptions) as were already accorded to members of the Institute of Physics and of the allied overseas Societies. There would shortly be a meeting between the council's representatives and representatives of the Chemical Council to discuss the possibility of the Faraday Society co-operating with the Chemical Council in their "points" scheme. The proposals they had in view would in no way affect the independent management of the affairs of the Society by its own officers, such as the holding of its General Discussions and the production of the *Transactions* in its present form, and members who desired to pay their subscriptions direct to the Society's offices would always be able to do so. The proposed co-operation would, it was felt, not only be a convenience to many present members of the Society, but would in all probability induce increasing numbers of physical chemists, not only in this country but more particularly in the Dominions and overseas, to join the Society.



106 MINUTES OF 38TH ANNUAL GENERAL MEETING

3. The Officers and Ordinary Members of Council were elected as follows :—

*President.*

PROF. E. K. RIDEAL, M.B.E., D.Sc., F.R.S.

*Vice-Presidents who have held the Office of President.*

SIR ROBERT ROBERTSON, K.B.E., D.Sc., F.R.S.

PROF. F. G. DONNAN, C.B.E., Ph.D., F.R.S.

PROF. C. H. DESCH, D.Sc., F.R.S.

PROF. N. V. SIDGWICK, Sc.D., D.Sc., F.R.S.

PROF. M. W. TRAVERS, D.Sc., F.R.S.

*Vice-Presidents.*

PROF. J. E. COATES, O.B.E., D.Sc.

PROF. W. C. M. LEWIS, D.Sc., M.A.,

PROF. A. FINDLAY, PRES. R.I.C., D.Sc.

F.R.S.

PROV. W. E. GARNER, D.Sc., F.R.S.

PROF. S. SUGDEN, D.Sc., F.R.S.

R. LESSING, Ph.D.

*Honorary Treasurer.*

R. E. SLADE, D.Sc.

*Chairman of the Publications Committee.*

PROF. A. J. ALLMAND, D.Sc., F.R.S.

*Ordinary Members of the Council.*

T. BEACALL, O.B.E.

PROF. M. POLANYI, F.R.S.

C. R. BURY, B.A.

H. W. THOMPSON, M.A., B.Sc., D.Phil.

A. CARESS, B.A., Ph.D.

O. J. WALKER, Ph.D.

PROF. M. G. EVANS, D.Sc.

O. H. WANSBOROUGH-JONES, M.A.,

R. W. LUNT, Ph.D.

Ph.D.

PROF. H. W. MELVILLE, Ph.D., F.R.S.

4. The thanks of the Society were accorded with acclamation to the retiring Officers and Members of Council for their services.

This concluded the business of the meeting.

# THE NUMBER OF ARRANGEMENTS ON A LATTICE OF MOLECULES EACH OCCUPYING SEVERAL SITES.

BY E. A. GUGGENHEIM.

(Department of Chemical Technology, Imperial College, London.)

Received 31st July, 1944.

1. **Introduction.**—The number of distinguishable ways of arranging  $N$  molecules each occupying two sites (dimers) on a lattice of  $N_s > 2N$  sites was determined by Chang<sup>1</sup> using a modification of Bethe's method of constructing a grand partition function for a sample site and its immediate neighbours. The same method was applied by Miller<sup>2</sup> to determine the number of distinguishable ways of arranging  $N$  molecules, each occupying three sites (trimers) on a lattice of  $N_s > 3N$  sites. By extrapolation Miller correctly guessed the formula for  $N$  molecules each occupying  $r$  sites ( $r$ -mers), but did not attempt any proof.

In a recent paper<sup>3</sup> I have by an entirely different method derived a general formula for the number of distinguishable arrangements of a mixture of any number of types of molecules each with its own geometric properties. This treatment obviates any need for extending Chang's technique to polymers with  $r > 3$  or to mixtures of two or more types of molecules. There would nevertheless be some satisfaction in confirming that my method and Chang's do in fact lead to the same formulæ in more complicated cases. It is accordingly the object of this paper to apply a simplified modification of Chang's technique to two more complicated assemblies and to verify that the results are in agreement with the general formula obtained by my alternative method. The two examples chosen are (a) the arrangement of  $N_T$  trimers and  $N_D$  dimers on  $N_s > 3N_T + 2N_D$  sites, and (b) the arrangement of  $N$  tetramers on  $N_s > 4N$  sites.

2. **Notation.**—Let  $N_i$  denote the number of molecules of type  $i$  each occupying  $r_i$  sites,  $N_s$  the total number of sites, and  $N_0$  the number of empty sites, so that

$$N_s = N_0 + \sum_i r_i N_i. \quad (2.1)$$

Let  $\theta$  denote the fraction of sites occupied by molecules of type  $i$ , so that

$$\theta_i N_s = r_i N_i. \quad (2.2)$$

$$(1 - \sum_i \theta_i) N_s = N_0. \quad (2.3)$$

Let  $z$  denote the number of neighbours of any given site. Then the number of sites which are neighbours of a molecule of type  $i$  is not  $r_i z$  (except in the trivial case  $r_i = 1$ ) but say  $q_i z$ , where  $q_i < r_i$  because some of the sites adjoining a site occupied by an element of an  $i$  molecule are occupied by the next element of the same molecule. In the present paper I shall, for the sake of simplicity, consider only rigid straight chain molecules. For these the relation between  $q_i$  and  $r_i$  is

$$z(r_i - q_i) = 2(r_i - 1). \quad (2.4)$$

<sup>1</sup> Chang, *Proc. Roy. Soc. A*, 1939, **169**, 512; *Proc. Camb. Phil. Soc.*, 1939, **35**, 265.

<sup>2</sup> Miller, *Proc. Camb. Phil. Soc.*, 1942, **38**, 109; 1943, **39**, 54.

<sup>3</sup> Guggenheim, *Proc. Roy. Soc. A*, 1944, **183**, 203.

Let  $\sigma_i$  denote the symmetry number equal to 2 or 1 according as the molecules of type  $i$  have or have not a centre of symmetry. Let  $f_i$  denote the partition function of a molecule of type  $i$  attached to a specified set of  $r_i$  sites.

Let  $g(N_i, N_0)$  denote the number of distinguishable ways of arranging the mixture of  $N_i$  molecules of each type  $i$  on the  $N_s$  sites leaving  $N_0$  sites empty.

Let  $F$  denote the free energy of the assembly and  $\mu_i$  Gibbs' partial potential for the molecules of type  $i$ , so that (at negligible pressures)

$$F = \sum_i N_i \mu_i, \quad (2.5)$$

$$\partial F / \partial N_i = \mu_i. \quad (2.6)$$

Finally, let  $\lambda_i$  denote the absolute activity of the species  $i$  defined by

$$\mu_i = kT \log \lambda_i, \quad (2.7)$$

where  $k$  is Boltzmann's constant and  $T$  is the absolute temperature.

**3. General Configurational Formulæ.**—My previous paper<sup>3</sup> was concerned with liquid mixtures and accordingly  $N_0$  was tacitly assumed to be zero. The formula there obtained for  $g(N_i, 0)$  for rigid straight molecules is

$$\log g(N_i, 0) = \frac{1}{2}z \log (\sum_i q_i N_i)! - \sum_i \log N_i! - (\frac{1}{2}z - 1) \log (\sum_i r_i N_i)! + \sum_i N_i \log (z/\sigma_i). \quad (3.1)$$

This formula is immediately extended to the case  $N_0 \neq 0$  in the form

$$\log g(N_i, N_0) = \frac{1}{2}z \log (N_0 + \sum_i q_i N_i)! - \log N_0! - \sum_i \log N_i! - (\frac{1}{2}z - 1) \log (N_0 + \sum_i r_i N_i)! + \sum_i N_i \log (z/\sigma_i). \quad (3.2)$$

If the independent variables are changed from  $N_i, N_0$  to  $N_i, N_s$ , by using (2.1) one obtains

$$\log g(N_i, N_s) = \frac{1}{2}z \log (N_s - \sum_i [r_i - q_i] N_i)! - \log (N_s - \sum_i r_i N_i)! - \sum_i \log N_i! - (\frac{1}{2}z - 1) \log N_s! + \sum_i N_i \log (z/\sigma_i). \quad (3.3)$$

In the assemblies considered by Chang and those to be considered in the present paper  $N_s$  is a constant characteristic of the assembly; for this reason (3.3) is more useful and relevant than (3.2) in which  $N_0$  is implicitly dependent on the  $N_i$ 's.

**4. Thermodynamic Functions.**— $g(N_i, N_s)$  is closely related to the thermodynamic properties of an assembly consisting of  $N_s$  sites over which are distributed  $N_i$  molecules of each type  $i$  when there is no mutual interaction energy between any two molecules. This type of assembly is a model suited to certain problems of adsorption of a perfect gas on a solid surface. Chang concerned himself both with assemblies of this type and also with assemblies with non-zero energy of interaction between pairs of molecules. It is important to emphasise that zero energy of interaction is an essential condition of the following treatment.

The free energy  $F$  of such an assembly is (at zero or negligible pressure) related to  $g(N_i, N_s)$  and the partition functions  $f_i$  by

$$F = -kT \log g(N_i, N_s) - kT \sum_i N_i \log f_i. \quad (4.1)$$

Substituting from (3.3) into (4.1) and differentiating with respect to  $N_i$ , keeping  $N_s$  constant, one obtains for  $\mu_i$

$$\mu_i/kT = \frac{1}{2}z(r_i - q_i) \log (N_s - \sum_i [r_i - q_i] N_i) - r_i \log (N_s - \sum_i r_i N_i) + \log (N_i \sigma_i / f_i z), \quad (4.2)$$

or using (2.4)

$$\mu_i/kT = (r_i - 1) \log (N_s - \frac{2}{z} \sum_i [r_i - 1] N_i) - r_i \log (N_s - \sum_i r_i N_i) + \log (N_i \sigma_i / f_i z). \quad (4.3)$$

The corresponding formula for the absolute activity  $\lambda_i$  is according to (2.7)

$$\lambda_i = \frac{\sigma_i N_i (N_s - 2 \Sigma_i [r_i - 1] N_i / z) r_i^{-1}}{z f_i (N_s - \Sigma_i r_i N_i) r_i}, \quad (4.4)$$

or from (2.2)

$$\lambda_i = \frac{\sigma_i \theta_i \left( 1 - \frac{2}{z} \frac{\Sigma_i r_i - 1}{r_i} \theta_i \right) r_i^{-1}}{z r_i f_i (1 - \Sigma_i \theta_i) r_i}, \quad (4.5)$$

Whereas formulæ (3.3) and (4.5) are derivable from each other by purely thermodynamic reasoning, it is (4.5) which is obtained the more directly by Chang's method. The two special cases of (4.5) which will be derived by Chang's method are the following.

(a) For a mixture of trimers  $T$  and dimers  $D$

$$\frac{\lambda_T f_T}{\sigma_T} = \frac{\theta_T \left( 1 - \frac{4\theta_T}{3z} - \frac{\theta_D}{z} \right)^2}{3z(1 - \theta_T - \theta_D)^3}, \quad (4.6)$$

$$\frac{\lambda_D f_D}{\sigma_D} = \frac{\theta_D \left( 1 - \frac{4\theta_T}{3z} - \frac{\theta_D}{z} \right)}{2z(1 - \theta_T - \theta_D)^2}; \quad (4.7)$$

(b) For tetramers

$$\frac{\lambda_f}{\sigma} = \frac{\theta \left( 1 - \frac{3\theta}{2z} \right)^3}{4z(1 - \theta)^4}. \quad (4.8)$$

**5. Number of Sample Sites.**—In obtaining a formula for  $\lambda_D f_D$  for dimers, from which he derived the corresponding formula for  $g(N, N_s)$ , Chang used two central sites and all their  $2(z - 1)$  other nearest neighbours. Miller, on the other hand, showed that for the particular end in view it would have been sufficient to use one central site and its  $z$  nearest neighbours. He also used this set of sites to determine  $\lambda_T f_T$  for trimers. Miller expressed the view that the extension of the method to more complicated assemblies would be "extraordinarily complicated". Actually the number of sites used by Miller is still unnecessarily great. The minimum requirement of the set of sites is that there shall be room on it for at least one molecule of any of the types considered. Thus for dimers it is sufficient to consider only 2 sites, for rigid trimers only 3, for rigid tetramers 4. It is this reduction in the number of sites considered, which has enabled me without undue labour to progress further than Chang or Miller. I would again emphasise that this simplification in procedure is restricted to assemblies with zero energy of interaction between the molecules.

**6. Parameters in Grand Partition Function.**—The grand partition function for the selected sample set of sites consists of a sum of terms, one term for each distinguishable manner of occupation of the set of sites. Each of these terms is a product of factors corresponding to the several molecules or parts of molecules occupying any of the sites. Each molecule of type  $i$  completely located on the sample set of sites contributes a factor  $\lambda_i f_i$ . Each empty site contributes the factor unity. On the other hand, the factor contributed by molecules of type  $i$  partly located on the sample set of sites is not  $\lambda_i f_i$  nor any fractional power of  $\lambda_i f_i$ ; such a factor is represented formally by a symbol such as  $\xi_i$  or  $\zeta_i$  or  $\epsilon_i$ . The relation between these extra parameters and the  $\lambda_i f_i$ 's has then to be determined by equations expressing the condition that each site of the sample set is equivalent to any other site. I shall refer to such equations as equivalence conditions.

As the present discussion is restricted to assemblies of molecules with

zero energy of interaction, the parameters of the form  $e^{-w/kT}$  usually denoted by  $\eta$ , reduce to unity and are therefore not required.

**7. An Assembly of Trimers and Dimers.**—For the treatment of a mixture of  $N_T$  rigid straight trimers and  $N_D$  dimers on  $N_S$  sites I use a sample set of 3 sites, namely a central site  $a$  and its two neighbours  $b$  and  $b'$ . For the sake of brevity I assume that both types of molecule have centres of symmetry. There is no difficulty in amending the argument to deal with unsymmetrical molecules. The number of distinguishable orientations of each molecule becomes doubled with the final result that  $\frac{1}{2}f$  has to be replaced by  $f$  in accordance with formulæ (4.5) to (4.8). The distinguishable methods of occupation and the corresponding terms in the grand partition function are collected in Table I.

The first column merely gives a number by which to refer to each type of configuration. The second column specifies the configuration or type of configuration.

TABLE I.—RIGID STRAIGHT TRIMERS  $T$  AND DIMERS  $D$  ON A CENTRAL SITE  $a$  AND 2 NEIGHBOUR SITES  $b$  AND  $b'$ .

Reference Number.	Configuration $b \quad a \quad b'$	Term in Grand Partition Function.
1	$T-T-T$	$\lambda_T f_T$
2	$T-T \quad U$	$\xi_T(1 + \epsilon_T + \epsilon_D)$
2'	$U \quad T-T$	$\xi_T(1 + \epsilon_T + \epsilon_D)$
3	$U \quad T \quad U$	$3(\frac{1}{2}z - 1)\xi_T(1 + \epsilon_T + \epsilon_D)^2$
4	$D-D \quad U$	$\lambda_D f_D(1 + \epsilon_T + \epsilon_D)$
4'	$U \quad D-D$	$\lambda_D f_D(1 + \epsilon_T + \epsilon_D)$
5	$U \quad D \quad U$	$2(\frac{1}{2}z - 1)\xi_D(1 + \epsilon_T + \epsilon_D)^2$
6	$U \quad 0 \quad U$	$(1 + \epsilon_T + \epsilon_D)^2$

is labelled  $U$ . In this case the relevant contribution to the grand partition function is a sum of terms corresponding to the alternative methods of occupation of the site or sites labelled  $U$ .

The third column contains the terms of the grand partition function corresponding to the configurations given in the second column. These entries will be discussed in order of simplicity. In configuration 1 a single trimer occupies all three sites and so contributes the term  $\lambda_T f_T$ . In configurations 4 and 4', which are mirror images of each other, a dimer occupies two of the sites and so contributes a factor  $\lambda_D f_D$ ; the factor contributed by the remaining site is 1 if it is empty and is by definition  $\epsilon_T$  or  $\epsilon_D$ , according as it is occupied by a trimer or a dimer. In configuration 6 the central site being unoccupied contributes unity, and each of the neighbour sites contributes factors 1 or  $\epsilon_T$  or  $\epsilon_D$ , according to its manner of occupation. It is important to observe that the use of the same factors  $\epsilon_T$ ,  $\epsilon_D$  in configurations 4 and 6 (also in 2, 3 and 5) is dependent on the essential condition of zero energy of interaction leading to complete randomness in the arrangement of the molecules.

In configurations 2 and 2', which are mirror images of each other, the central site and one of its neighbours are occupied by two elements of the same trimer. The factor contributed by these two sites is defined as  $\xi_T$ . The factor contributed by the remaining neighbour site is 1 or  $\epsilon_T$  or  $\epsilon_D$ , just as in configurations 4 and 6.

The central site  $a$  is labelled  $T$  if occupied by a trimer, by  $D$  if occupied by a dimer, and by 0 if empty. When the central site and either neighbour site are occupied by the same molecule, the neighbour site is labelled in the same manner as the central site and a hyphen is inserted. When either neighbour site is not occupied by the same molecule as the central site, its manner of occupation is left unspecified and it

In configuration 3 the central site is occupied by one element of a trimer which does not occupy either of the neighbour sites. There are 3 elements of this trimer, any one of which may occupy the central site, and there are  $\frac{1}{2}z - 1$  alternative orientations other than that already dealt with under configurations 1, 2 and 2'. Each of these alternative  $3(\frac{1}{2}z - 1)$  configurations has an equal weight, and so contributes the same factor to the grand partition function; this factor is denoted by  $\zeta_T$ . The two neighbour sites each contribute as usual a factor which may be 1 or  $\epsilon_T$  or  $\epsilon_D$ . Configuration 5 is similar to 3 except that the central site, instead of being occupied by a trimer, is occupied by a dimer which can have  $2(\frac{1}{2}z - 1)$  alternative configurations other than those already included in 4 and 4'. Each of these configurations contributes the same factor, which is denoted by  $\zeta_D$ . The two neighbour sites make their usual contributions of 1 or  $\epsilon_T$  or  $\epsilon_D$ .

The next step is to write down the equivalence conditions which will be required to eliminate the parameters  $\xi_T$ ,  $\zeta_T$ ,  $\zeta_D$ ,  $\epsilon_T$  and  $\epsilon_D$ . It is clear that configurations 1, 2, 2' and each one of the  $3(\frac{1}{2}z - 1)$  configurations included in 3 are equivalent.

It follows that

$$\lambda_T f_T = \xi_T(1 + \epsilon_T + \epsilon_D) = \zeta_T(1 + \epsilon_T + \epsilon_D)^2. \quad (7.1)$$

Similarly from the equivalence of configurations 4 or 4' and each one of the  $2(\frac{1}{2}z - 1)$  configurations included in 5 it follows that

$$\lambda_D f_D = \zeta_D(1 + \epsilon_T + \epsilon_D). \quad (7.2)$$

Comparison of the terms corresponding to site *a* empty, site *b* occupied by a trimer with those corresponding to *a* occupied by a trimer, *b* empty leads to the equivalence condition

$$\epsilon_T(1 + \epsilon_T + \epsilon_D) = \xi_T + 3(\frac{1}{2}z - 1)\zeta_T(1 + \epsilon_T + \epsilon_D), \quad (7.3')$$

which by the use of (7.1) reduces to

$$\epsilon_T = \frac{1}{2}(3z - 4)\zeta_T. \quad (7.3)$$

Similarly comparison of the terms corresponding to site *a* empty, site *b* occupied by a dimer with those corresponding to site *a* occupied by a dimer, site *b* empty leads to the equivalence condition

$$\epsilon_D(1 + \epsilon_T + \epsilon_D) = \lambda_D f_D + 2(\frac{1}{2}z - 1)\zeta_D(1 + \epsilon_T + \epsilon_D), \quad (7.4')$$

which by the use of (7.2) reduces to

$$\epsilon_D = (z - 1)\zeta_D. \quad (7.4)$$

Finally the ratios  $\theta_T : \theta_D : (1 - \theta_T - \theta_D)$  are equal to the ratios of the terms corresponding to the central site *a* being occupied by a trimer or occupied by a dimer or being empty respectively. Collecting together these three kinds of terms and using (7.1) and (7.2), one obtains

$$\theta_T : \theta_D : (1 - \theta_T - \theta_D) = \frac{3}{2}z\zeta_T : z\zeta_D : 1. \quad (7.5)$$

This completes the set of relations required. It only remains to eliminate  $\xi_T$ ,  $\zeta_T$ ,  $\zeta_D$ ,  $\epsilon_T$ ,  $\epsilon_D$ , so as to obtain relations between  $\lambda_T f_T$ ,  $\lambda_D f_D$  and  $\theta_T$ ,  $\theta_D$ .

Solving (7.5) for  $\zeta_T$  and  $\zeta_D$ , one obtains

$$\zeta_T = \frac{2\theta_T}{3z(1 - \theta_T - \theta_D)}, \quad (7.6)$$

$$\zeta_D = \frac{\theta_D}{z(1 - \theta_T - \theta_D)}. \quad (7.7)$$

From (7.3) and (7.6) it follows that

$$\epsilon_T = \left(1 - \frac{4}{3z}\right) \frac{\theta_T}{1 - \theta_T - \theta_D} \quad (7.8)$$

and from (7.4) and (7.7)

$$\epsilon_D = \left(1 - \frac{1}{z}\right) \frac{\theta_D}{1 - \theta_T - \theta_D} \quad (7.9)$$

whence

$$1 + \epsilon_T + \epsilon_D = \frac{1 - \frac{4\theta_T}{3z} - \frac{\theta_D}{z}}{1 - \theta_T - \theta_D} \quad (7.10)$$

Now substituting from (7.6) and (7.10) into (7.1) one obtains

$$\lambda_T f_T = \frac{2\theta_T \left(1 - \frac{4\theta_T}{3z} - \frac{\theta_D}{z}\right)^2}{3z(1 - \theta_T - \theta_D)^3} \quad (7.11)$$

Similarly substituting from (7.7) and (7.10) into (7.2) one finds

$$\lambda_D f_D = \frac{\theta_D \left(1 - \frac{4\theta_T}{3z} - \frac{\theta_D}{z}\right)}{z(1 - \theta_T - \theta_D)^2} \quad (7.12)$$

It will be observed that (7.11) and (7.12) are identical with (4.6) and (4.7) respectively when one puts  $\sigma_T = \sigma_D = 2$ . It is thus confirmed that Chang's method applied to an assembly of trimers and dimers leads to

TABLE II.—RIGID STRAIGHT TETRAMERS ON 4 SITES OF WHICH  $a, a'$  ARE CENTRAL and  $b, b'$  THEIR RESPECTIVE NEIGHBOURS.

Reference Number.	Configuration. $b \ a \ a' \ b'$	Term in Grand Partition Function.
1	$T-T-T-T$	$\lambda f$
2	$T-T \ T-T$	$\xi_2$
3	$T-T-T \ U$	$\xi_3(1 + \epsilon)$
3'	$U \ T-T-T$	$\xi_3(1 + \epsilon)$
4	$T-T \ T \ U$	$4(\frac{1}{2}z - 1)\xi_4(1 + \epsilon)$
4'	$U \ T \ T-T$	$4(\frac{1}{2}z - 1)\xi_4(1 + \epsilon)$
5	$T-T \ 0 \ U$	$\xi_5(1 + \epsilon)$
5'	$U \ 0 \ T-T$	$\xi_5(1 + \epsilon)$
6	$U \ T \ T \ U$	$16(\frac{1}{2}z - 1)^2\xi_6(1 + \epsilon)^2$
7	$U \ T \ 0 \ U$	$4(\frac{1}{2}z - 1)\xi_7(1 + \epsilon)^2$
7'	$U \ 0 \ T \ U$	$4(\frac{1}{2}z - 1)\xi_7(1 + \epsilon)^2$
8	$U \ 0 \ 0 \ U$	$(1 + \epsilon)^2$

## 8. An Assembly of

**Tetramers.**—For the treatment of  $N$  rigid straight tetramers on  $N$  sites, I use a sample set of 4 sites, namely two central sites  $a, a'$  and their respective neighbours  $b, b'$ . For the sake of brevity I again assume that the molecules have a centre of symmetry. The distinguishable methods of occupation and the corresponding terms in the grand partition function are collected in Table II.

As the construction of Table II is in many respects similar to that of Table I, I shall describe it as briefly as possible. In the second column each central site  $a$  or  $a'$  is labelled  $T$  if occupied by a tetramer, and by 0 if empty. Sites occu-

pied by the same tetramer are connected by a hyphen. When the two central sites  $a$  and  $a'$  are occupied by different tetramers, both are

labelled  $T$  but they are not connected by a hyphen. When either neighbour site  $b$  or  $b'$  is not occupied by the same molecule as the corresponding central site  $a$  or  $a'$ , its manner of occupation is left unspecified and it is labelled  $U$ .

The third column gives the terms in the grand partition function corresponding to the configurations shown in the second column. Configuration 1 is the only one in which a complete molecule is located on the set of sites, and it contributes the term  $\lambda f$ . Each neighbour site  $b$  or  $b'$ , when not occupied by the same molecule as the corresponding central site  $a$  or  $a'$ , contributes a factor 1 if empty and a factor denoted by  $\epsilon$  when occupied. The use of the same factor  $\epsilon$  throughout is a consequence of the essential assumption of zero energy of interaction. It follows that configuration 8, in which the two central sites  $a, a'$  are empty, contributes the factor  $(1 + \epsilon)^2$ .

Of the remaining configurations certain pairs denoted by the same number primed and unprimed are mirror images of each other, and so contribute identical terms. The factor  $4(\frac{1}{2}z - 1)$ , which occurs in several places and occurs squared in configuration 6, is the product of the number of distinct elements in a tetramer, namely 4, and the number of distinct orientations other than that along the line  $baa'b'$ , namely  $(\frac{1}{2}z - 1)$ . The remaining factors denoted by  $\xi_2, \dots, \xi_7$  are parameters defined by the table.

One now has to write down the equivalence conditions required to eliminate  $\xi_2, \dots, \xi_7$  and  $\epsilon$ . Comparison of configurations 1, 3, 5, 7 leads to the equivalence conditions

$$\lambda f = \xi_3(1 + \epsilon) = \xi_5(1 + \epsilon)^2 = \xi_7(1 + \epsilon)^3 \quad (8.1)$$

and comparison of 2, 4, 6 to

$$\xi_2 = \xi_4(1 + \epsilon) = \xi_6(1 + \epsilon)^2 \quad (8.2)$$

A relation between  $\xi_5$  and  $\xi_7$  can be obtained as follows. Consider only those configurations in which no two of the sites  $b, a, a', b'$  are occupied by the same molecule. These configurations are 6, 7, 7' and 8. In such configurations it is clear that the manner of occupation of the pair of sites  $a, b$  is independent of that of the pair of sites  $a', b'$ . From this it follows immediately that  $\xi_5 : \xi_7$  is equal to  $\xi_7 : 1$ , whence

$$\xi_5 = \xi_7^2 \quad (8.3)$$

Another equivalence condition is obtained as follows. Form the sum of the terms corresponding to the configurations, 5 and 7, in which  $a$  is occupied and  $a'$  is empty and take the ratio of this sum to the term corresponding to the configuration 8 in which  $a$  is empty and  $a'$  is empty. This ratio must be equal to the ratio of the sum of terms corresponding to  $a$  occupied,  $b$  empty to the sum of terms corresponding to  $a$  and  $b$  empty. But the latter ratio is  $\epsilon$ . Hence

$$\frac{\xi_5(1 + \epsilon) + 4(\frac{1}{2}z - 1)\xi_7(1 + \epsilon)^2}{(1 + \epsilon)^2} = \epsilon, \quad (8.4')$$

which by use of (8.1) reduces to

$$\epsilon = (2z - 3)\xi_7 \quad (8.4)$$

Finally one forms the sum of all terms corresponding to configurations 1, 2, 3, 3', 4, 4', 5, 6, 7 with  $a$  occupied and the sum of the remaining configurations 5', 7', 8 with  $a$  empty. One then equates the ratio of these sums to  $\theta/(1 - \theta)$ . One thus obtains a rather long formula, which, however, by use of (8.1) - (8.4) reduces to

$$\frac{\theta}{1 - \theta} = \frac{2z\epsilon}{2z - 3} \quad (8.5)$$



whence

$$\epsilon = \frac{(2z-3)\theta}{2z(1-\theta)}, \quad (8.6)$$

$$1 + \epsilon = \frac{2z-3\theta}{2z(1-\theta)}. \quad (8.7)$$

Finally from (8.1), (8.4), (8.6) and (8.7) one obtains

$$\lambda f = \frac{\epsilon(1+\epsilon)^3}{2z-3} = \frac{\theta(2z-3\theta)^3}{(2z)^4(1-\theta)^4}. \quad (8.8)$$

This can be rewritten as

$$\frac{\lambda f}{2} = \frac{\theta \left(1 - \frac{3\theta}{2z}\right)^3}{4z(1-\theta)^4}, \quad (8.9)$$

which is identical with (4.8) when one sets  $\sigma = 2$ . Thus for an assembly of tetramers Chang's method again leads to complete agreement with that of my previous paper.

**9. An Assembly of Dimers.**—It has already been mentioned that an assembly of dimers only was treated by Chang using 2 central sites with their  $2(z-1)$  neighbours and later by Miller using a single central site with its  $z$  neighbours. I shall now show briefly that for the treatment of such an assembly it is sufficient to consider two sites, a central one  $a$  and a neighbour  $b$ .

When a dimer occupies both sites the term in the grand partition function is  $\lambda f$ . When the central site  $a$  is occupied by a dimer, which does not also occupy the site  $b$ , the contribution to the grand partition function is written as  $(z-1)\xi(1+\epsilon)$ . When the central site  $a$  is empty the contribution to the grand partition function is  $(1+\epsilon)$ .

The equivalence conditions are

$$\lambda f = \xi(1+\epsilon), \quad (9.1)$$

$$(z-1)\xi = \epsilon, \quad (9.2)$$

$$\frac{\theta}{1-\theta} = \frac{\lambda f + (z-1)\xi(1+\epsilon)}{1+\epsilon} = \frac{z\epsilon}{z-1}. \quad (9.3)$$

By elimination of  $\xi$  and  $\epsilon$  from (9.1), (9.2), and (9.3) one obtains

$$\lambda f = \frac{\epsilon(1+\epsilon)}{z-1} = \frac{\theta(1-\theta/z)}{z(1-\theta)^2}, \quad (9.4)$$

in agreement with Chang, Miller and formula (4.7), when one writes  $\theta_T = 0$ ,  $\theta_D = \theta$ .

**10. The Parameters  $\epsilon_i$ .**—In paragraphs 7 to 9 I have used, with appropriate simplifications, the kind of argument previously used by Chang and Miller. I have deliberately avoided introducing the considerations used in my own treatment of these problems. I shall now show how such considerations lead more directly to the evaluation of the parameters  $\epsilon_i$ .

The fraction of sites occupied by molecules of type  $i$  or the frequency of occupation of a given site by molecules of type  $i$  is of course

$$\frac{r_i N_i}{N_0 + \sum_j r_j N_j}. \quad (10.1)$$

When, however, a pair of neighbouring sites are considered, and the manner of occupation of the one is given, while it is specified that the two sites are *not occupied by the same molecule*, then the frequency of occupation of the second site is given not by (10.1), but by

$$\frac{q_i N_i}{N_0 + \sum_j q_j N_j}. \quad (10.2)$$

But by the definition of the  $\epsilon_i$ 's this fraction is equal to

$$\frac{\epsilon_i}{1 + \sum_j \epsilon_j} \quad (10.3)$$

It follows that

$$\epsilon_i = \frac{q_i N_i}{N_0} = \frac{q_i \theta_i / r_i}{1 - \sum_j \theta_j} \quad (10.4)$$

According to the definition (2.4) of  $q_i$ , this can be rewritten as

$$\epsilon_i = \left(1 - \frac{2[r_i - 1]}{zr_i}\right) \frac{\theta_i}{1 - \sum_j \theta_j} \quad (10.5)$$

Formulae (7.8), (7.9) and (8.6) are all special cases of (10.5).

### Summary.

The statistical treatment by Chang of molecules each occupying two sites (dimers) and by Miller of molecules each occupying three sites (trimers) has been simplified and extended to a mixture of dimers and trimers and to molecules each occupying four sites (tetramers). The resulting formulae are in agreement with those obtained in a previous paper by a more powerful method. An essential condition of this treatment is zero energy of interaction between molecules.

I am greatly indebted to the late Sir Ralph Fowler, F.R.S., for his encouragement and interest in this work.

## THE ABSORPTION SPECTRA OF SOME MONONITRONAPHTHYLAMINES, WITH OBSERVATIONS ON THEIR STRUCTURES.

By H. H. HODGSON AND D. E. HATHWAY.

*Received 6th October, 1944.*

The mononitronaphthylamines, all of which are known except 7-nitro-2-naphthylamine, can be broadly classified into pure yellow and orange-red compounds. The yellow class contains only three members, all of which are homonuclear, viz. the 2-nitro-1-, 3-nitro-1-, and 4-nitro-1-naphthylamines, whereas the orange-red class includes not only all the homonuclear members which have the amino-group in 2-position, viz., 1-nitro-, 3-nitro-, and 4-nitro-2-naphthylamines, but also all the heteronuclear compounds. Such a clear cut distinction would seem to indicate a difference in structure. Since resonance into no fewer than 13 ionic structures is possible (7 for the  $\alpha$ - and 6 for the  $\beta$ -substituted compounds),<sup>1</sup> it appeared of interest to examine the absorption spectra of selected mononitronaphthylamines to ascertain how far resonance takes place in particular individuals. Many conclusions derived by Hodgson and Turner,<sup>2</sup> in a speculative discussion based on Pauling's theory of resonance, now receive experimental confirmation.

Previous physical data on the nitronaphthylamines include the measurement of dipole moments,<sup>3, 4</sup> though no absorption spectra have as yet

<sup>1</sup> Pauling, *Nature of the Chemical Bond*, Cornell University Press, 1940, p. 152.

<sup>2</sup> Hodgson and Turner, *J. Soc. Dyers and Col.*, 1943, 59, 219.

<sup>3</sup> Vassiliev and Sirkin, *J. Physic. Chem. Russ.*, 1938, 12, 153.

<sup>4</sup> Vassiliev and Sirkin, *Acta Physicochim* (U.R.S.S.), 1938, 9, 203.

been recorded. Since it is the polarisability of the molecule and not the dipole moment that is of immediate importance to the problem of colour,<sup>5</sup> this mode of investigation has now been pursued.

**Experimental.**—An Adam Hilger, Medium Quartz Spectrophotometer was used. The spark-gap, of capacity 0.005 F, gave a 22,000 voltwave-peak. The cell was 1 cm. in length. All measurements were taken in absolute alcohol.

**Results.**—Table I shows the positions of the band-heads, which were found from large-scale drawings.

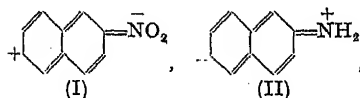
TABLE I.

	$\lambda_{\max.}$	$\log_{10}\epsilon_{\max.}$	$\lambda_{\max.}$	$\log_{10}\epsilon_{\max.}$	$\lambda_{\max.}$	$\log_{10}\epsilon_{\max.}$
<b>Monosubstituted Naphthalenes</b> (see Fig. 1).						
$\alpha$ -naphthylamine	245m $\mu$	4.36			325m $\mu$	3.71
$\beta$ -naphthylamine	240	4.76	282.5m $\mu$	3.79	346	3.23
$\alpha$ -nitro-naphthalene	243	4.02			342	3.59
$\beta$ -nitro-naphthalene	259	4.40	307	3.92	352	3.44
<b>Mononitronaphthylamines</b> (see Figs. 2 and 3).						
<b>Homonuclear.</b>						
1-nitro-2-naphthylamine	228m $\mu$	4.63	324m $\mu$	3.61	420m $\mu$	3.73
4-nitro-2-naphthylamine	231	4.63			350/450	3.36
						(ca. 410m $\mu$ )
2-nitro-1-naphthylamine	280	4.27			447	3.94
3-nitro-1-naphthylamine	274	4.12			431	3.40
4-nitro-1-naphthylamine	269	3.94			443	4.18
<b>Heteronuclear.</b>						
5-nitro-1-naphthylamine	276	3.95	346	3.28	430/440	3.28
8-nitro-1-naphthylamine	276	4.20	350	3.37	426/434	3.39

Lauer<sup>6</sup> reports naphthalene, in absolute alcohol, as showing 4 bands between  $\lambda$  289/269m $\mu$  ( $\log_{10} \epsilon_{\max.}$  4.9/4.4) and 10 bands between  $\lambda$  338/293m $\mu$  ( $\log_{10} \epsilon_{\max.}$  0.50/3.70), using an instrument of greater resolving power.

### Discussion.

The spectra of  $\alpha$ -nitronaphthalene and  $\alpha$ -naphthylamine are very similar with two bands each at almost identical wavelengths; the spectra of  $\beta$ -nitronaphthalene and  $\beta$ -naphthylamine, however, have three bands, the two extreme ones being of nearly the same wavelength as those of the  $\alpha$ -isomerides, with a third band between them. From this fact it would appear that: (1) within  $\lambda$  2000-5000 Å, the nucleus and not the substituent



groups is the absorbing unit; (2) the  $\alpha$ - or  $\beta$ - positions of the nitro- and amino- groups in the naphthalene nucleus are of primary importance, with regard to absorption, and that the acid or basic characters of the nitro- and amino-groups as auxochromes<sup>5, 7</sup> play a secondary rôle; (3) auxochromes in the  $\beta$ -position give rise to an additional resonance form which contributes the third band to the spectrum. It is well established that

<sup>5</sup> Lewis and Calvin, "The Colour of Organic Substances," *Chemical Reviews*, 1939, **25**, 282.

<sup>6</sup> Berichte, 1936, **69**, 987.

<sup>7</sup> Wizinger, *Organische Farbstoffe*, Ferd. Dummlers Verlag, Berlin und Bonn, 1933.

electronic effects are readily transmitted between the 2- and 6-positions,<sup>8, 9, 2</sup> and it seems a reasonable assumption that an extra resonance form is set up, viz. (I, II) in addition to the resonance forms common to both  $\alpha$ - and  $\beta$ -compounds, viz. (III, IV). When both groups are present there may or may not be new resonating states in the molecule, according as to whether their positions favour fresh electronic paths.<sup>5</sup> In the case of the yellow nitronaphthylamines, viz. the 2-nitro-, 3-nitro- and 4-nitro-1-naphthylamines, there is a much larger absorption in the ultraviolet than with

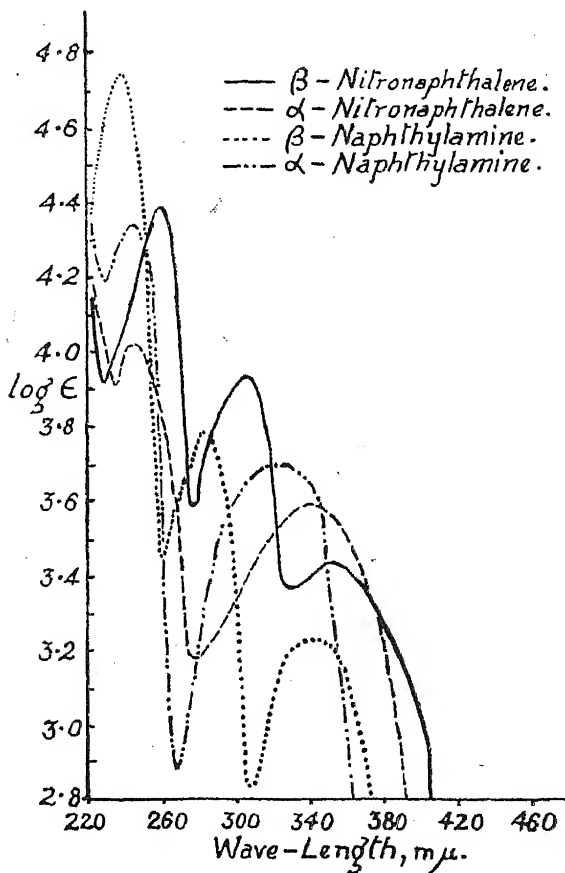
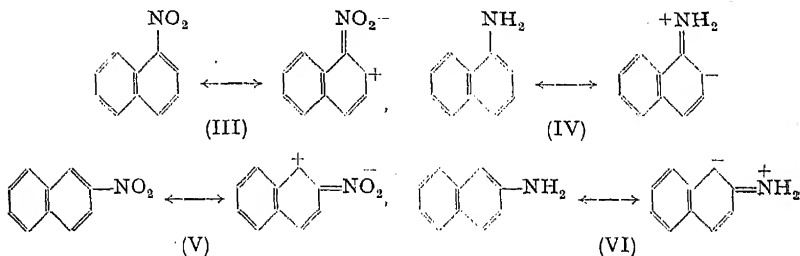


FIG. 1.

<sup>8</sup> Robinson and Thompson, *J. Chem. Soc.*, 1932, 2015.<sup>9</sup> Bell, *ibid.*, 1932, 2732.

the red isomers, which implies that there is considerable additional strain in their molecules. Resonance is assumed to operate entirely homonuclearly in a molecule of Erlenmeyer structure, with a permanent central double-bond which acts as a restraint. The ionic resonance structures are possibly (VII) to (IX).

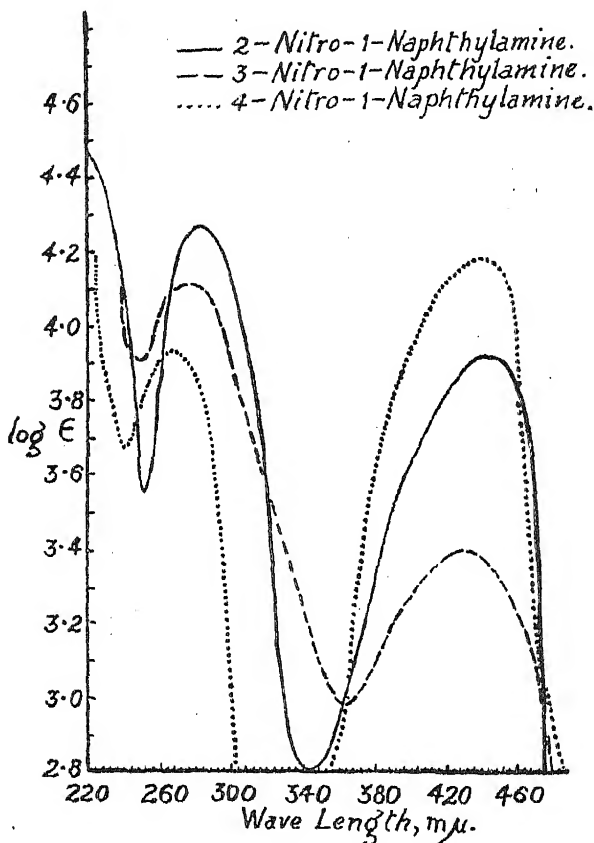
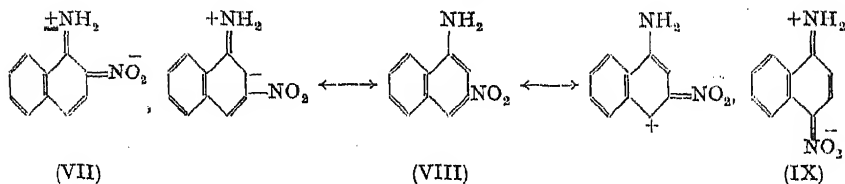


FIG. 2.



The subtractive effect of the separate possible resonances in 3-nitro-1-naphthylamine prevents the 3-nitro-group from resonating into the 7-position, hence the non-appearance of the middle band of  $\beta$ -nitronaphthalene. The negative inductive effect (-I) of the second nucleus in homonuclear derivatives<sup>10, 11</sup> can be expected to strengthen the polarisation of the  $\alpha$ -amino-group and so prevent the 2-nitro-group from resonating into the

<sup>10</sup> Hodgson and Elliott, *J. Soc. Dyers and Col.*, 1938, 54, 264.

<sup>11</sup> Hodgson and Elliott, *J. Chem. Soc.*, 1935, 1850.

6-position. The parallel between the spectrum of 4-nitro-aniline and 4-nitro-1-naphthylamine is of interest. Lewis and Calvin<sup>5</sup> point out that 4-nitroaniline has a dipole moment considerably greater than the sum of the moments of nitrobenzene and aniline, which they regard as an illustration of the principle that a displacement from the "ideal" molecule renders further displacement easier. Such a displacement is exemplified by the absorption spectrum which exhibits two strong bands of almost equal intensity due to an abnormal increase in the mobility of the electrons through the additive effect of the two auxochromes. In the spectrum of

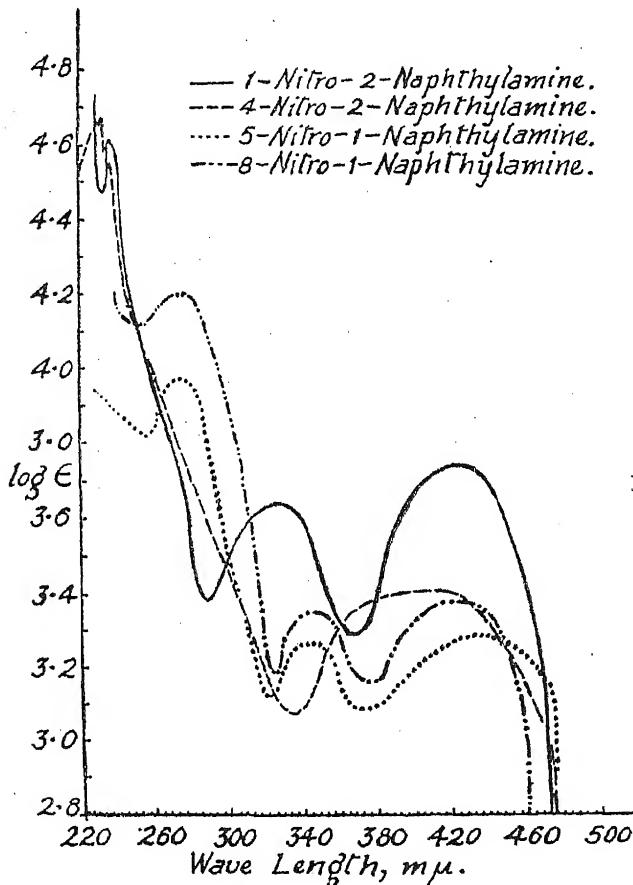
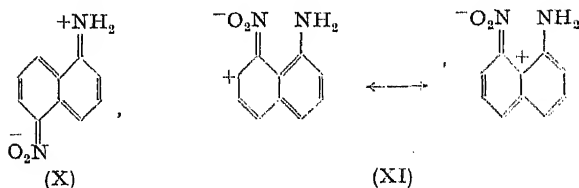
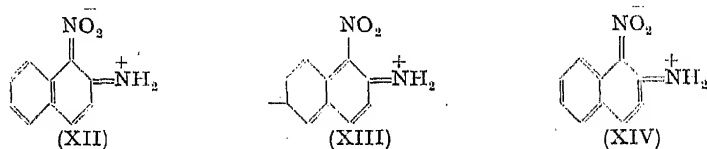


FIG. 3.

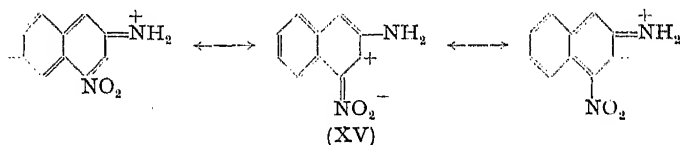
4-nitro-1-naphthylamine, as compared with the spectrum of the other nitronaphthylamines measured, the same persistence of two strong bands occurs. These bands are so similar to those of 4-nitroaniline as to support the conclusion already drawn from the yellow colour that the oscillations are mainly homonuclear: *i.e.* that the central double-bond exists. In the two cases of heteronuclear nitronaphthylamines examined, 5-nitro- and 8-nitro-1-naphthylamines, the former can resonate into a quinonoid and the latter into ionic resonance structures (as in the case of azobenzene and *m*-nitroaniline), in which the resonance effects are additive. In these cases the colour is red, and facile resonance is again shown by the presence of three bands.



The remaining red compounds examined, *viz.* 1-nitro-2- and 4-nitro-2-naphthylamines, both exhibit absorption in the same regions as the heteronuclear nitronaphthylamines: the exceedingly broad band for 4-nitro-2-naphthylamine extending over the region occupied by the second and third bands of the latter compounds. In the case of 1-nitro-2-naphthylamine the presence of the third band shows ease of resonance into the 6-position (facilitated possibly by the negative inductive effect of the second nucleus) which will now reduce the polarisation of the 1-nitro-group in the resonance form (XII) and facilitate the possible form (XIII), which would then tend to resonate into the form (XIV), with a single central bond in harmony with



the structures for the heteronuclear isomers. In 4-nitro-2-naphthylamine one can therefore expect facile resonance into the forms (XV)



which, unlike the resonating structures of 3-nitro-1-naphthylamine have additive instead of subtractive effects, and possess a central single bond, with consequential ease of polarisation. It is noteworthy that in the cases of 1-nitro-2- and 4-nitro-2-naphthylamines the short wavelength absorption band is shifted further into the ultraviolet than that of other compounds now examined.

Previous workers <sup>12, 13</sup> have recorded the absorption spectra of  $\alpha$ - and  $\beta$ -naphthaquinones, and their work is comparable with our own, since both teams of workers used absolute alcohol as a solvent. Incidentally, in the naphthalene series, spectra in absolute alcohol are more consistent with vapour spectra than are spectra taken in any other solvent.

#### $\alpha$ -Naphthaquinone

$\lambda_{\text{max.}}$	$\log_{10} \epsilon_{\text{max.}}$
256m $\mu$	4.13
334	3.44

#### $\beta$ -Naphthaquinone

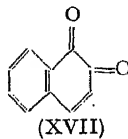
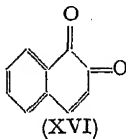
$\lambda_{\text{max.}}$	$\log_{10} \epsilon_{\text{max.}}$
250m $\mu$	4.35
340	3.40
405	3.40

Red  $\beta$ -naphthaquinone possesses 3 bands which occupy similar positions to our bands for the red mononitronaphthylamines, whereas  $\alpha$ -naphthaquinone with 2 bands in the ultraviolet has a spectrum nearly identical with  $\alpha$ -naphthylamine. These results are in agreement with the plausible

<sup>12</sup> Macbeth, Price and Winzor, *J. Chem. Soc.*, 1935, 327.

<sup>13</sup> Goldschmidt and Graef, *Berichte*, 1928, 61, 1862.

speculation by Hodgson and Turner<sup>2</sup> for a single bond formula, (XVI), instead of the accepted Erlenmeyer formula (XVII) for  $\beta$ -naphthaquinone. The proposed structure now falls into line with those for the other red compounds, and indicates greater mobility of electronic oscillation, since long conjugate systems may now be established. The old formula with its permanent central double bond restricts oscillation within a single nucleus, whereas in the central single bond structure the whole of the naphthalene system is available for oscillation. Our interpretation of the data for the  $\alpha$ - and  $\beta$ -naphthaquinones affords substantiating evidence for our theory of the colour of the mononitronaphthylamines.



### Summary.

A study of the absorption spectra of  $\alpha$ - and  $\beta$ -amino- and nitro-naphthalenes and of certain selected mononitronaphthylamines has enabled the following tentative conclusions to be made for the structure of these molecules :

1. Yellow mononitronaphthylamines exhibit two absorption bands within the region  $\lambda$  2310-4500A whereas their red isomers have a third band within  $\lambda$  3380-3500A.
2. The above two extreme bands are characteristic of  $\alpha$ - and  $\beta$ -nitro- and amino-naphthalenes but the middle band is characteristic of the  $\beta$ -compounds only.
3. In the mononitronaphthylamines all the bands are shifted towards the longer wavelengths and so indicate relief of electronic strain in the molecule.
4. All three bands are characteristic of heteronuclear nitro-naphthylamines and of those homonuclear isomers in which the amino-group is in the  $\beta$ -position. These compounds are all red and it is assumed that their structures possess a single central bond, in contrast to the more strained yellow forms which are assumed to owe their strain to the presence of a central double bond.

The red colour of  $\beta$ -naphthaquinone is at once explicable if its formula be written with a central single bond : this substance exhibits three bands within the region  $\lambda$  2310-4500A.

The authors wish to express their gratitude to Professor E. L. Hirst, F.R.S., for providing facilities for one of us (D.E.H.) to take all the spectra in his laboratories and for his interest in the work ; also to Dr. J. K. N. Jones and Mr. M. E. Foss, both of the staff of the Department of Organic Chemistry, Bristol University, who helped in reading the plates. Our thanks are due to Imperial Chemical Industries (Dyestuffs Division) for a scholarship (to D.E.H.) and for materials used in preparing the nitro-naphthylamines.

*Department of Colour Chemistry,  
Technical College, Huddersfield.*



# A CALCULATION OF THE LATENT HEAT OF VAPORISATION BASED ON A REVISED EQUATION OF STATE.

By D. B. MACLEOD.

Received 28th November, 1944.

In a recent paper<sup>1</sup> the author examined the consequences that followed from assuming the volume of the molecules, as represented by  $b$  in Van der Waals' equation, to be a function of  $p + a/v^2$ , the total pressure. Writing  $P$  for  $p + a/v^2$ , the quantity  $b$  was expressed as  $b_0(1 - BP + CP^2)$ , that is, it was assumed to be compressible in much the same way as an ordinary solid. Van der Waals' equation then became  $P[v - b_0(1 - BP + CP^2)] = RT$ . The revised equation was shown to cover both the liquid and vapour phases of a fluid satisfactorily and to give a reasonable explanation for the departure of  $RT_c/P_cV_c$ , in actual fluids, from the theoretical value of 2.66.

It led to the conclusion, however, that in passing from the vaporous condition to the liquid condition, the molecules of typical organic molecules underwent a contraction in volume of from 30 to 40 per cent. If this is so, then a considerable amount of work has been done on the molecules themselves during condensation and this has to be supplied again, during the process of evaporation, in the form of latent heat of vaporisation. The molecule, itself, can be regarded as a condensed form of matter in much the same sense as a liquid or a solid. It is held together by attractive forces, balanced when in equilibrium by static repulsive forces as well as by disruptive forces due to the kinetic energy of its constituents. Its potential energy is less in a contracted form than in an expanded form.

## Latent Heat of Vaporisation.

An attempt to calculate the latent heat of vaporisation, based on Van der Waals' equation of state, was made by Bakker. It is discussed by Lewis in Vol. II of his well-known volumes on Physical Chemistry. Bakker equated  $\lambda$ , the latent heat of vaporisation, to  $\int_{v_1}^{v_2} \frac{a}{v^2} dv + p(v_2 - v_1)$ , where  $v_2$  is the specific volume of the vapour and  $v_1$ , the specific volume of the liquid. The first term represents  $\lambda_i$ , the internal latent heat, or the work done against the cohesion of the molecules, and the second term  $\lambda_e$ , the external work. The values of  $\lambda$ , calculated from this equation, were very considerably lower than the values calculated from the Clausius-Clapeyron equation. Quoting from Lewis, the latent heats of vaporisation, for  $\text{CCl}_4$  and  $\text{C}_6\text{H}_6$  at their boiling points, from Bakker's equation are 5.18 and 5.05 K.cal. per g. molecule respectively, whereas the true values should be 7.13 and 7.29. This want of agreement can only mean that Van der Waals' equation is not the true equation of state for these substances. A similar discrepancy occurs with a wide variety of other substances.

In the present paper an extra term is introduced to allow for the work done on the molecules, namely  $\int_{b_1}^{b_2} P db$ . The equation is then written

$$\lambda = \int_{v_1}^{v_2} \frac{a}{v^2} dv + p(v_2 - v_1) + \int_{b_1}^{b_2} P db.$$

<sup>1</sup> *Trans. Faraday Soc.*, 1944, 40, 439.

The second term,  $p(v_2 - v_1)$ , is the same as in Bakker's equation and requires no further explanation. It is necessary, however, to draw attention to the fact that the value of  $a$ , calculated from the revised equation of state is, invariably, higher than that calculated from the simple Van der Waals' equation. For example, the values of  $a$  quoted by Lewis for  $\text{CCl}_4$  and  $\text{C}_6\text{H}_6$  are 19.20 and 18.36 respectively, whereas the values obtained, by the author, for the same substances<sup>1</sup> are, in the same units, 22.16 and 20.73. This makes the quantity from the first term of the equation greater than that given by Bakker's equation, but it still leaves a discrepancy of the order of 1000 cal. per g. molecule in the neighbourhood of the boiling point.

Because of the complex nature of the term  $\int_{b_1}^{b_2} P db$ , it is not possible to integrate it directly. In the earlier paper<sup>1</sup> the values of  $b$  for each corresponding value of  $P$ , were obtained. They are set out in columns 4 and 5 of the following table.  $b$  can be obtained from the constants supplied or from the relation

$$v - b = RT/P.$$

By plotting a  $P, b$  curve, the work represented by

$$\int_{b_1}^b P db$$

can be obtained by counting squares or by the use of a planimeter. It can then be converted into heat units.

In this paper, the latent heats of vaporisation for the three substances,  $\text{CCl}_4$ ,  $\text{C}_6\text{H}_6$  and  $\text{C}_5\text{H}_{12}$ , are calculated. The constants required were published earlier.<sup>1</sup> The latent

heats are given from the neighbourhood of the boiling points to the critical temperatures. The results are set out in Table I and shown graphically in the accompanying diagram. The experimental quantities—the pressure and the molecular volumes—are obtained from the International Critical Tables. The latent heats are shown in four separate

columns,  $\lambda_1$ ,  $\lambda_0$  and  $\lambda_m$ , the last named being the term  $\int_{b_1}^b P db$ . They are expressed in K.cal. per g. molecule.  $\lambda_1$  is the sum of these three quantities.  $\lambda_0$  is the corresponding quantity calculated from the equation

$$\lambda_0 = T \frac{dp}{dT} (v_2 - v_1).$$

A comparison of the last two columns shows a satisfactory agreement. There remains, however, a systematic discrepancy of a few per cent. For each of the three substances  $\lambda_1$  commences by being less than  $\lambda_0$ , reaches the same value about midway between the boiling point and the

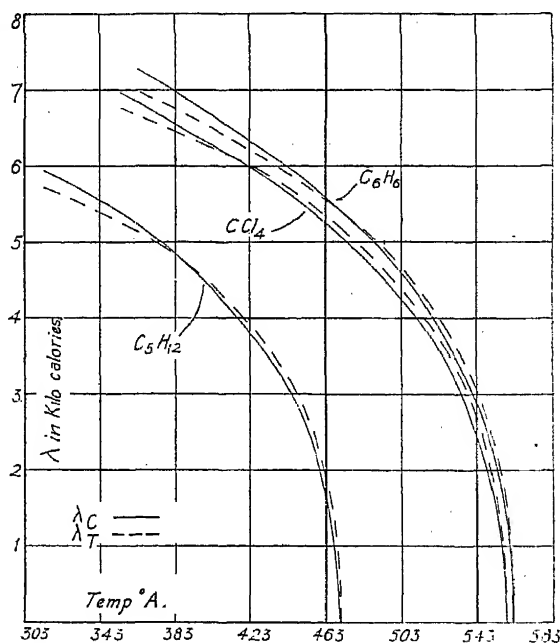


TABLE I.

$T$ (°C.).	$P$ (in Bars).	M.V.		$P$ (in Bars).	$h$ .	$\lambda_1$ .	$\lambda_e$ .	$\lambda_m$ .	$\lambda_t$ .	$\lambda_0$ .
		Liq.	Vap.							

**Carbon Tetrachloride.**  $a = 2.216 \times 10^7$   $b_0 = 151.4$ .

353	1.118	104.3	25240	2038	89.8	5.06	0.67	1.06	6.79	7.00
363	1.483	105.8	19250	1981	90.5	4.98	0.68	1.03	6.69	6.86
373	1.944	107.4	14950	1924	91.2	4.90	0.69	1.00	6.59	6.72
383	2.509	109.3	11750	1859	92.0	4.80	0.70	0.97	6.47	6.62
393	3.189	110.8	9290	1809	92.6	4.72	0.70	0.94	6.36	6.43
403	4.002	112.6	7550	1752	93.4	4.63	0.71	0.92	6.26	6.37
413	4.969	114.5	6160	1695	94.1	4.54	0.72	0.88	6.14	6.19
423	6.077	116.5	5065	1636	94.9	4.44	0.72	0.85	6.01	6.04
433	7.383	118.6	4220	1582	95.7	4.34	0.72	0.81	5.87	5.90
443	8.860	121.0	3524	1522	96.6	4.23	0.72	0.78	5.73	5.69
453	10.54	123.5	2933	1463	97.6	4.11	0.71	0.74	5.56	5.42
463	12.42	126.5	2464	1401	98.8	3.97	0.70	0.71	5.38	5.25
473	14.60	129.5	2075	1335	100.0	3.84	0.68	0.68	5.20	5.06
483	17.02	133.1	1752	1268	101.2	3.68	0.66	0.63	4.97	4.81
493	19.75	136.6	1481	1208	102.4	3.52	0.63	0.58	4.73	4.54
503	22.75	141.8	1250	1125	104.4	3.31	0.60	0.52	4.43	4.26
513	26.15	147.5	1052	1044	106.4	3.09	0.57	0.49	4.15	3.96
523	29.90	154.3	878.0	960.6	108.8	2.83	0.52	0.44	3.79	3.57
533	34.05	163.7	717.6	860.7	111.9	2.50	0.45	0.35	3.30	3.10
543	38.19	187.7	568.2	667.8	119.6	1.89	0.35	0.23	2.47	2.41
558.16	45.60		276.1						0	0

**Benzene.**  $a = 2.073 \times 10^7$   $b_0 = 135.6$ .

363	1.344	97.00	21660	2206	83.1	5.08	0.69	1.09	6.87	7.30
373	1.781	98.40	16597	2143	83.8	5.00	0.70	1.05	6.75	7.18
383	2.321	99.9	12980	2079	84.5	4.92	0.72	1.01	6.65	7.02
393	2.974	101.4	10130	2018	85.2	4.84	0.72	0.97	6.53	6.78
403	3.761	103.1	8124	1956	85.9	4.75	0.72	0.93	6.40	6.64
413	4.694	104.9	6610	1891	86.6	4.64	0.73	0.90	6.27	6.48
423	5.782	106.7	5416	1821	87.3	4.55	0.73	0.86	6.14	6.37
433	7.07	108.6	4509	1766	88.1	4.45	0.74	0.83	6.02	6.22
443	8.52	110.8	3733	1702	89.0	4.34	0.74	0.80	5.88	5.92
453	10.17	113.0	3133	1639	89.9	4.23	0.73	0.77	5.73	5.79
463	12.06	115.4	2618	1570	90.7	4.10	0.72	0.74	5.56	5.61
473	14.20	118.1	2197	1500	91.7	3.97	0.71	0.71	5.39	5.35
483	16.61	121.3	1853	1426	92.9	3.82	0.69	0.68	5.19	5.17
493	19.37	124.7	1554	1352	94.2	3.65	0.66	0.56	4.87	4.90
503	22.43	128.6	1315	1276	95.6	3.47	0.63	0.52	4.62	4.59
513	25.81	133.3	1092	1192	97.2	3.26	0.59	0.48	4.33	4.23
523	29.62	139.1	912.2	1110	99.7	3.02	0.55	0.44	4.01	3.82
533	33.82	146.4	751.5	1001	101.8	2.72	0.49	0.39	3.60	3.40
543	38.49	156.5	606.0	884.8	105.1	2.35	0.41	0.32	3.08	2.90
561.5	48.56		256.2						0	0

**Pentane.**  $a = 2.114 \times 10^7$   $b = 169.6$ .

313	1.18	118.8	21170	1498	101.3	4.23	0.59	0.92	5.74	5.94
323	1.59	120.8	16000	1450	102.2	4.15	0.61	0.88	5.64	5.88
333	2.14	123.1	12020	1397	103.2	4.06	0.61	0.84	5.51	5.77
343	2.83	125.4	9115	1348	104.1	3.98	0.61	0.80	5.39	5.56
353	3.65	128.0	7128	1294	105.2	3.88	0.61	0.77	5.26	5.43
363	4.67	130.8	5531	1240	106.3	3.77	0.61	0.73	5.11	5.26
373	5.88	133.9	4417	1184	107.5	3.66	0.60	0.70	4.96	5.06
383	7.32	137.3	3564	1128	108.9	3.54	0.60	0.66	4.80	4.89
393	8.99	141.2	2880	1070	110.5	3.40	0.59	0.62	4.61	4.64
403	10.93	145.2	2332	1014	111.9	3.26	0.57	0.58	4.51	4.41
413	13.20	150.4	1865	952	114.1	3.09	0.54	0.54	4.17	4.08
423	15.76	156.4	1512	880	116.2	2.90	0.51	0.48	3.89	3.80
433	18.74	163.8	1218	807	118.9	2.70	0.47	0.44	3.61	3.47
443	22.09	173.0	979.6	729	122.1	2.40	0.42	0.36	3.18	3.03
453	25.83	186.2	770.0	636	126.6	2.06	0.36	0.30	2.72	2.51
470.2	33.50		309.9						0	0

critical temperature, and then becomes slightly higher than  $\lambda_c$ . Some part of this discrepancy may be due to the, admittedly, approximate method of calculating the molecular constants. In the original paper <sup>1</sup>  $b_c$  was taken to be equal to  $v_c/2$  but it was emphasised that this could only be regarded as approximately true for a large class of substances. A better agreement could be obtained by a process of trial and error in the neighbourhood of the approximate value. For a relatively incompressible molecule like hydrogen a value  $b_c = 0.36 v_c$  was found most satisfactory.

The author is inclined to think, however, that the systematic nature of the discrepancy indicates a possible variation of  $a$  with the volume of the molecule. A slight increase in  $a$  with the contraction of the molecule would certainly give a better agreement. It is not proposed, however, to speculate on such a relation at this stage. To a first approximation, the agreement is very satisfactory and gives considerable support to the idea of a compressible molecule. It is highly significant, if these conclusions are accepted, that about fifteen per cent. of the latent heat of vaporisation of a liquid at its boiling point, represents work done on the molecules themselves.

In Table II the corresponding figures for hydrogen, in the neighbourhood of the boiling point, are set out.

TABLE II.—HYDROGEN

$T$ (° A.).	$P$ (in Bars).	M.V.		$P$ (in Bars).	$\lambda_t$ .	$\lambda_c$ .	$\lambda_m$ .	$\lambda_t$ .	$\lambda_c$ .
		Liq.	Vap.						
19.86	0.91	28.03	1890	286.0	189	40	4	233	216
20.40									
23.21	2.27	29.73	757.5	255.8	173	40	3	216	

$$a = 2.240 \times 10^6, \quad b = 23.49(1 - 0.03186 P)$$

The latent heat is represented in cal. per g. molecule. The value quoted for  $\lambda_c$  is that given in the International Critical Tables for the boiling point 20.40° A. The Landolt Bornstein Tables quote two values for the same temperature, namely 220 and 230. Laby gives a value of 246. The values calculated by the author are, therefore, within the probable range of uncertainty of the experimental determinations of the vapour pressures and molecular volumes. It is noticeable that the contribution of the molecular portion to the total, is only about 2 % in the case of hydrogen. The smaller value could be anticipated from the low compressibility and small molecular volume of hydrogen.

Table III sets out the constants calculated for argon. This substance was not included in the original paper. The figures showing the application of the revised equation of state to argon are, therefore, given together with the constants obtained. In the last column,  $\lambda_c$ , of the latent heat table, the first value is that given by the International Critical Tables for the latent heat at the boiling point 87.34° A. The subsequent values in this column have been calculated from the Clausius Clapeyron equation, from the data available in the International Critical Tables. If the author's general treatment has a sound physical basis, it is necessary to regard argon, in spite of it being a monatomic gas, as more compressible than hydrogen. The departure of  $RT_c/p_c v_c$  for argon, from the theoretical value of 2.56, is certainly much greater than in the case of hydrogen, being 3.5 in the former case and 3.0 for hydrogen. This, from the author's point of view, would indicate a greater compressibility. Apart from this, argon can be treated in a manner similar to other fluids with very satisfactory results.

The ratio of  $b_c/v_c$  is intermediate between that of hydrogen and the typical organic substances.

TABLE III.—ARGON

$T$ (° A.).	$P$ (in Bars).	M.V.		$p + \frac{a}{b^2}$		$\frac{RT}{v - b'}$	
		Liq.	Vap.	Liq.	Vap.	Liq.	Vap.
89.87	1.5	29.03	4980	1641	1.53	1680	1.53
97.63	2.9	30.10	2735	1526	3.10	1526	3.03
111.79	7.6	32.58	1072	1308	8.80	1297	9.02
122.26	13.7	35.03	587.9	1139	17.7	1138	18.5
137.51	28.8	40.96	249.3	851.8	51.0	857.9	53.5
147.85	43.0	51.66	135.1	560.0	118.6	560	121.8
150.58	48.0	75.15		292.4		291.0	

$a = 13.8 \times 10^5$ ,  $b_c = 0.427v_c$ ,  $b_0 = 34.78$ .  $B = 0.03147$ ,  $C = 0.07825$ .

$T$ (° A.).	$\lambda_l$	$\lambda_c$	$\lambda_m$	$\lambda_t$	$\lambda_c$
87.34					1500
89.87	1131	178	150	1459	
97.63	1085	188	142	1415	
111.79	978	185	122	1285	1270
122.26	885	181	100	1166	1186
137.51	672	139	65	876	865
147.85	393	86	32	512	490

### Summary.

1. The latent heats of vaporisation, from the boiling points to the critical temperatures, have been calculated for several typical substances. The basis of the calculation is the author's recently published equation of state.

2. In that equation of state, evidence was adduced that molecules contract considerably in passing from the vaporous to the liquid condition. Allowance has been made, in this paper, for the work required to overcome this contraction.

3. The calculated values accord very closely with those obtained from the Clausius Clapeyron equation.

*Physics Department,  
Canterbury University College,  
Christchurch, New Zealand.  
4th October, 1944.*

# THE MELTING OF POLYTHENE.

By R. B. RICHARDS.

Received 17th November, 1944.

Formulae representing the increase in melting-point  $T_F$  as chain length  $Z$  increases in the normal paraffin series have been given by Garner, van Bibber and King.<sup>1</sup>

$$T_F = \frac{0.6085Z - 1.75}{0.001491Z + 0.00404} \quad (1)$$

and by Meyer and van der Wyk<sup>2</sup>

$$\frac{1}{T_F} = 2.395 \times 10^{-3} + \frac{17.1 \times 10^{-3}}{Z} \quad (2)$$

According to equations (1) or (2) a normal paraffin of chain length  $Z = 1000$  would have a melting-point of  $134^\circ$  C. or  $141^\circ$  C. respectively. Pure paraffins melt quite sharply, although a second crystal phase may be formed some degrees below the melting-point, and density<sup>3</sup> and heat capacity<sup>4</sup> measurements have shown that in such paraffins as octadecane melting may best be regarded as an order-disorder transition extending a few degrees either side of the temperature usually regarded as the melting-point.

The melting behaviour of polythene differs from the behaviour of pure paraffins in two ways. Firstly, the order-disorder transition extends over a wider temperature range, as shown by density<sup>5</sup>, heat capacity<sup>6</sup> and X-ray and optical<sup>7</sup> measurements, and the solid appears not to be entirely crystalline even at room temperature. Secondly, the melting-point, at which all trace of crystal structure has disappeared, is appreciably lower than the values given by equations (1) or (2) for pure  $n$ -paraffins of comparable chain length. The usual value for a polythene of chain length  $Z$  about 1000 is  $105$ – $115^\circ$  C. and the highest value observed so far is  $126^\circ$  C.\*

When the melting-points of a wide range of polythenes are considered, it is at once apparent that average chain length is not the sole factor controlling the melting-point. Samples with the same molecular weight can vary as much as  $15^\circ$  in melting-point. This variation in  $T_F$  at a constant average value of  $Z$  seems to be most pronounced at lower chain lengths. The low value of the melting-point of polythene is believed to be fundamentally due to the imperfection of crystallisation of polythene, and the presence of amorphous regions formed by portions of long chains passing from one crystallite to another, or protruding from crystallites, and also by any molecules which will not fit into the crystal structure. The variations may arise from the effects of changes in :

<sup>1</sup> Garner, van Bibber and King, *J. Chem. Soc.*, 1931, 1533.

<sup>2</sup> Meyer and van der Wyk, *Helv. Chim. Acta*, 1937, 20, 1313.

<sup>3</sup> van Hook and Silver, *J. Chem. Physics*, 1942, 10, 686.

<sup>4</sup> Ubbelohde, *Trans. Faraday Soc.*, 1938, 34, 282.

<sup>5</sup> Hunter and Oakes, *Trans. Faraday Soc.*, 1945, 41, 49.

<sup>6</sup> Raine, Richards and Ryder, *Trans. Faraday Soc.*, 1945, 41, 56.

<sup>7</sup> Bunn and Alcock, *Trans. Faraday Soc.* (in press).

\* Long chain paraffinic hydrocarbons of M.P.  $132$ – $134^\circ$  C. have been made by the Fischer-Tropsch synthesis<sup>8</sup> from CO and H<sub>2</sub>.

<sup>8</sup> Pichler and Buffleb, *Brennstoff-Chem.*, 1940, 21, 257.

- (a) the degree of chain branching, and
- (b) the molecular weight distribution,

on the perfection of crystallisation.

Frith and Tuckett<sup>9</sup> have discussed the melting of crystalline polymers, and have shown that the free energy of a system of crystallites and amorphous regions is a non-linear function of the proportion of amorphous material, and that there is a certain proportion of amorphous material corresponding to a minimum free energy, and hence to thermodynamic equilibrium at any temperature below the melting-point  $T_F$ . These authors have, however, only considered a polymer composed entirely of identical very long unbranched chains. Normal polythene, however, apart from being composed of molecules which may be somewhat branched,<sup>10, 11</sup> contains species with a wide range of molecular weights, and in particular, contains an appreciable portion of material of molecular weight below about 1500. Such material can be extracted by cold solvent, and is a liquid or grease at ordinary temperatures. The properties of polythene have been found to be sensitive to molecular weight distribution, and especially to the proportion of this low molecular weight material. In this paper the effect of low molecular weight hydrocarbons on the change of crystallinity with temperature and the melting-point will be considered. The problem will be treated by an extension of the statistical thermodynamics of Frith and Tuckett,<sup>9</sup> and the theoretical results will be compared with observed data on polythene.

### Theoretical.

#### The Melting of a Polythene containing Short Chain Material.—

The melting-point and the change of crystallinity with temperature are studied by setting up an equation for the free energy  $G$  of 1 g. of polythene in terms of the weight proportions in the amorphous ( $\theta$ ) and crystalline ( $1 - \theta$ ) regions. This procedure is discussed more fully by Frith and Tuckett.<sup>9</sup> The effect of short chain material, which is assumed to lie entirely in the amorphous regions, is calculated by making use of an expression due to Flory<sup>12</sup> for the entropy of mixing of a polymer and a "short chain" solvent. The value of  $\theta$  which corresponds to a minimum value of  $G$  and hence to equilibrium is calculated for any temperature.

**The Entropy of the Solid.**—Consider 1 g. of material consisting of  $sg$ . of a linear hydrocarbon of comparatively low molecular weight  $M$ , and  $(1 - s)$  g. of polythene of molecular weight so high that the chains all pass through a number of crystallites. Crystallisation is considered as starting from points of entanglement or from adjacent parallel portions of the long chains. As temperature decreases, crystallites grow round these nuclei, greater and greater lengths of the long chains taking their place in a crystal structure. Let  $n$  be the average number of carbon atoms, along the polythene chain, between the points on the chain at which crystallisation starts. If all of the low molecular weight hydrocarbon is in the amorphous region, the weight of the high molecular weight component in the amorphous region is  $(\theta - s)$  g. The average length  $Z_a$  of polythene chain in an amorphous region, that is passing from one crystallite to another, is :

$$n(\theta - s)/(1 - s).$$

The number of such free portions of polythene chain in the amorphous regions, which is also equal to the number of lengths of  $n$  methylene groups in the whole, is given by :

$$N' = \frac{N(1 - s)}{14n}$$

where  $N$  is Avogadro's number.

<sup>9</sup> Frith and Tuckett, *Trans. Faraday Soc.*, 1944, 40, 251.

<sup>10</sup> Fox and Martin, *Proc. Roy. Soc. A*, 1938, 167, 257.

<sup>11</sup> Thompson. *Unpublished*.

<sup>12</sup> Flory, *J. Chem. Physics*, 1942, 10, 51.

The number of low molecular weight molecules is given by :

$$n' = \frac{Ns}{M}$$

In order to calculate the entropy of the amorphous regions, we need to know how many lattice sites are occupied by each free polythene chain. The statistical segment may be the methylene group or some larger unit, of  $\xi$  methylene groups. The average number of segments per free polythene chain portion in the amorphous regions is given by :

$$x = \frac{n}{\xi} \cdot \frac{(\theta - s)}{(1 - s)}$$

We are now in a position to calculate the entropy  $S$  of the amorphous regions, making use of Flory's equation<sup>12</sup> for the entropy of mixing of  $n'$  pure solvent and  $N'$  perfectly arranged polymer molecules,

$$\Delta S_{\text{mixing}} = -k \left[ n' \ln \frac{n'}{n' + xN'} + N' \ln \frac{N'}{n' + xN'} \right] + k(x - 1)N' \ln \frac{\gamma - 1}{e} - kN' \ln 2 \quad (3)$$

(where  $\gamma$  is the co-ordination number of the lattice).

The original entropy  $S_0$  of the low molecular weight material and the perfectly ordered polymer will be given by :

$$S_0 = sS_a + (\theta - s)S_B$$

and the entropy of the crystalline regions will be given by :

$$S_K = (1 - \theta)S_B$$

where  $S_A$ ,  $S_B$  are the entropies per gram of perfectly ordered low molecular weight material and polythene respectively.

In addition, the expression for the entropy of the amorphous regions will contain a term  $\Delta S_P$  involving the changes in rotational, vibrational and translational degrees of freedom of the polythene on passing from the crystalline to the amorphous state. (The entropy of mixing  $\Delta S_{\text{mixing}}$  only takes account of the entropy increase due to the increase in configurational disorder, and this, as Flory points out, is only a part of the entropy of fusion of a polymer.) The extra entropy term will be a function of the free chain length  $Z_a$ , and by analogy with Huggins' <sup>13</sup> equation for the entropy of gaseous linear paraffins will probably be of the type :

$$\Delta S_P = \frac{1}{14Z_a} \cdot (a + bZ_a + c \ln Z_a) \text{ cal./g.}$$

The overall entropy  $S$  per gram is therefore given by :

$$*S = (1 - \theta)S_B + sS_a + (\theta - s)S_B + \Delta S_{\text{mixing}} + \Delta S_P$$

or :

$$\begin{aligned} S = & (1 - s)S_B + sS_a \\ & - k \left[ \frac{sN}{M} \ln \left( \frac{\frac{sN}{M}}{\frac{sN}{M} + \frac{N(\theta - s)}{14\xi}} \right) + \frac{N(1 - s)}{14n} \ln \left( \frac{\frac{N(1 - s)}{14n}}{\frac{sN}{M} + \frac{N(\theta - s)}{14\xi}} \right) \right] \\ & + k \left( \frac{n}{\xi} \cdot \frac{\theta - s}{1 - s} - 1 \right) \frac{N(1 - s)}{14n} \ln \frac{\gamma - 1}{e} - \frac{KN}{14n} (1 - s) \ln 2 \\ & + \frac{1 - s}{14n} \left( a + bn \cdot \frac{\theta - s}{1 - s} + c \ln \frac{n(\theta - s)}{1 - s} \right) \quad (4) \end{aligned}$$

<sup>13</sup> Huggins, *J. Physic. Chem.*, 1939, **43**, 1083.



When  $s = 0$ , we have an expression for the entropy of polythene alone.

$$S_{s=0} = S_B + \frac{KN}{14n} \ln n\theta - \frac{KN}{14n} \ln \xi + \frac{KN}{14n} \left( \frac{n\theta}{\xi} - 1 \right) \ln \frac{\gamma - 1}{e} - \frac{KN \ln 2}{14n} + \frac{1}{14n} (a + bn\theta + c \ln n\theta) \quad (5)$$

or :

$$S_{s=0} = \frac{1}{14n} [A + Bn\theta + (R + c) \ln n\theta] \quad (6)$$

Frith and Tuckett deduce a similar expression, but the parameter of  $\ln n\theta$ , which, as will be seen later, governs the sharpness of the melting-point of the polymer, is  $R$  in place of  $R + c$ ; this is because they have only taken account of the configurational entropy. For a hydrocarbon gas, in which freedom of rotation, vibration and translation is at a maximum the value of  $R + c$  is 8.0.<sup>13</sup> The value for amorphous polythene, in which the movement of chain is restricted, is likely to be between 8 and  $R$ .

**The Minimum Free Energy Conditions.**—If the heat of fusion per gram of the polythene crystallites is  $L_F$  (assumed independent of temperature) and the heat content of one gram of crystallites at  $T_0$  is  $H_0$  and the specific heat of the crystallites is  $C_p$ , the heat content at a temperature  $T$  of one gram of polythene containing a fraction of amorphous material is given by :

$$H = H_0 + \theta L_F + (T - T_0)C_p.$$

This assumes that there is no heat of mixing of amorphous polythene with the added low molecule weight paraffin. The free energy per gram at  $T$  is thus

$$G = H_0 + \theta L_F + (T - T_0)C_p - TS.$$

For equilibrium at any temperature, the degree of crystallinity shall be such that  $G$  has a minimum value, *i.e.*, that :

$$\frac{dG}{d\theta} = 0.$$

At a temperature  $T$  therefore :

$$L_F - T \frac{dS}{d\theta} = 0, \quad \text{or} \quad \frac{L_F}{T} = \frac{dS}{d\theta} \quad (7)$$

Differentiating the entropy expression, we have :

$$\frac{dS}{d\theta} = kN \left( \frac{s}{M} + \frac{1-s}{14n} \right) \frac{1}{\theta - s \left( 1 - \frac{14\xi}{M} \right)} + \frac{KN}{14\xi} \ln \frac{\gamma - 1}{e} + \frac{b}{14} + \frac{(1-s)c}{14n} \cdot \frac{1}{\theta - s} = \frac{L_F}{T}.$$

Hence :

$$\frac{14L_F}{RT} = \frac{14 \left( \frac{s}{M} + \frac{1-s}{14n} \right)}{\theta - s \left( 1 - \frac{14\xi}{M} \right)} + \frac{(1-s)c}{Rn} \cdot \frac{1}{\theta - s} + \frac{1}{\xi} \ln \frac{\gamma - 1}{e} + \frac{b}{R} \quad (8)$$

This equation gives the variation in degree of crystallinity, at a temperature  $T$ , with the proportion  $s$  and molecular weight  $M$  of added low molecular weight material. If the parameters in the expression (4) for entropy (such as  $n$ ,  $\xi$ ,  $a$ ,  $b$  and  $c$ ) do not change with temperature, equation (8) also gives the variation of crystallinity with temperature. When  $s = 0$  equation (8) reduces to :

$$\frac{14nL_F}{T(R+c)} = \frac{1}{\theta} + \frac{nR}{\xi(R+c)} \ln \frac{\gamma - 1}{e} + \frac{bn}{R+c} \quad (9)$$

which is, of course, similar to the expression obtained by Frith and Tuckett, except for the presence of the parameters  $\zeta$ ,  $c$  and  $b$ .

**Assumptions and Approximations.**—Before proceeding to a discussion of the quantitative implications of equation (8), and to a comparison with experimental data on polythene, it may be worth while reviewing critically the assumptions made in its derivation.

(1) It is assumed that crystallites grow from nuclei spaced at an average distance of  $n$  carbon atoms along the hydrocarbon chain, greater lengths of the chains taking their places in an ordered crystal structure as temperature decreases. It is further assumed that such nuclei have a "statistical permanency," and that once a crystallite has begun to grow it does not break up, and that no new nuclei are formed at lower temperatures. This is implicit in the assumption that  $n$  does not change with temperature. It is doubtful whether this gives an adequate picture of the melting mechanism, which will be discussed in a later section. However, the fundamental feature of the above theoretical treatment is the relation of the average length of free polythene chain, and hence  $\theta$ , to the entropy of the polythene, and this, apart from the method of averaging, is not affected by the mechanism of crystallite growth.

(2) An average length  $Z_a$  of the polymer chain in the amorphous region has been related to  $\theta$ , the weight fraction of amorphous material. In practice, a distribution of crystallite size and in  $Z$  is to be expected. The equation used for the entropy of mixing and total entropy were deduced for polymers of one chain length only, and ought to be modified for a distribution of size of  $Z$ .

(3) It is assumed that all of the added low molecular weight material remains in the amorphous phase. In the case of materials such as heptane, this is probably not far from the truth. The formation of crystallites from molten polythene is somewhat akin to the crystallisation of a paraffin such as  $C_{60}H_{122}$  from a liquid paraffin, and in such cases little mixed crystal formation is found.

(4) It is assumed that each molecule of the added material, whatever its molecular weight, is statistically equivalent to one polythene segment. Another parameter  $\beta$ , the number of short chain molecules equivalent to one polythene segment, could be introduced, and this could be made a function of  $M$ . Similarly, the added material might be regarded as being composed of  $\chi_b$  segments, of length  $\zeta_b$ , methylene groups, with consequent modifications of the entropy equations.

(5) The constants in the equations relating the entropy of the amorphous regions to the free length  $Z_a$  of the polythene chain, are assumed to be independent of  $\theta$ . As pointed out by Frith and Tuckett, this is only likely to be valid when the amorphous content is high and steric effects due to the rigidity of the crystalline regions are small, *e.g.*, when  $\theta > 0.5$ .

(6) The calculation of the heat content  $H$  assumes a zero heat of mixing of amorphous polythene and the added hydrocarbon.

(7) No account is taken of the change of  $L_p$  with temperature. This is quite small. A more serious approximation may be to relate the entropy only to chain length, and to regard it as independent of temperature.

(8) This treatment is only valid for a two phase (crystalline and amorphous) system. This is found only over a limited temperature range; below a certain temperature a third phase may separate out. This new phase may be liquid, as in polythene-heptane or polythene-cetene mixtures, or crystalline, as in the case of polythene-paraffin wax mixtures. The full phase relations between polythene and solvents are to be discussed in a forthcoming paper.

In view of the somewhat formidable array of assumptions listed above, it may seem presumptuous to attempt any quantitative comparison between the theoretical treatment and experimental data. Nevertheless, in the succeeding sections, the manner in which the crystallinity and melting-point of polythene-hydrocarbon mixtures vary with the

molecular weight  $M$  and weight fraction  $s$  of the added hydrocarbon, as indicated by equation (8), will be considered, and these theoretical results will be compared with the behaviour observed in practice.

### Comparison with Experimental Data.

**Change of Crystallinity with Temperature.**—In the absence of low molecular weight material, equation (9) indicates a linear relation between  $1/\theta$  and  $1/T$ . The slope of this line, that is, the sharpness of the melting, is governed by the values of  $L_p$ ,  $n$  and  $c$ . A high heat of fusion  $L_p$  should thus lead not only to a high melting-point, but also to sharp melting. A high value of  $n$  will also lead to a sharp melting-point. The value of  $n$ , the average distance between points from which crystallites grow, seems likely to be governed, partly at least, by molecular flexibility. Flexible molecules are likely to form suitable intermolecular contacts at points closer to each other along the chain than will rigid molecules. The structure of the chain will also affect the value of  $n$ , and we may expect  $n$  to be smaller for polythene, in which almost any region where portions of chain are approximately parallel can act as a crystal nucleus, than for rubber in which suitable ordering of methyl groups and double bonds is necessary. (Frith and Tuckett use values of  $n = 700$  for rubber and  $n = 200$  for polythene.)

The change of the degree of crystallinity with temperature has been followed quantitatively by measurements of density<sup>8</sup> and heat capacity.<sup>6</sup>

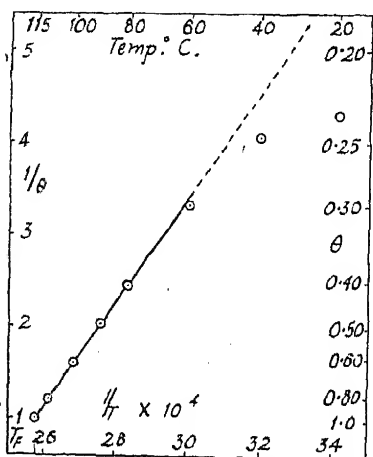


FIG. 1.—Change of Crystallinity with temperature.

also be due to the breakdown of the validity of the assumption (5) in the above list, that the parameters in equations (4), (8) and (9) are independent of  $\theta$ .

The value of the slope  $d\left(\frac{1}{\theta}\right)/d\left(\frac{1}{T}\right)$  in Fig. 1 is 5500. The value, according to equation (9), is  $14nL_p/(R+c)$ . Taking  $L_p$  as 56.5 cal./g.<sup>6</sup>, we have :

$$d\left(\frac{1}{\theta}\right)/d\left(\frac{1}{T}\right) = \frac{791n}{R+c}.$$

Table shows values of  $d\left(\frac{1}{\theta}\right)/d\left(\frac{1}{T}\right)$  for various values of  $n$  and  $R+c$ .

Frith and Tuckett showed that the changes in density with temperature followed generally the course predicted by their version of equation (9), (with  $R$  in place of  $R+c$ ), but that the observed melting was less sharp than their equation demanded. The heat capacity changes indicate a similar variation in crystallinity, and Fig. 1 shows a plot of  $1/\theta$  against  $1/T$  for a polythene of molecular weight about 15,000. Over the temperature range 115°–70° the curve is linear, as predicted by equation (9), but at lower temperatures the polythene is more amorphous than the linear relation would indicate. This is no doubt partly due to lack of attainment of thermodynamic equilibrium between crystalline and amorphous regions, which is a common feature of crystalline polymers, but may

A value of  $n = 50$  means that the average crystallite in normal polythene contains lengths of about 40 chain C atoms. This is believed to be reasonably consistent with the sharpness of the X-ray patterns. The observed slope of 5500 would then correspond to a value of  $R + c$  of about 7. It should be emphasised that the value of 5500 refers to a normal polythene containing an appreciable quantity of low molecular weight material which, as will be shown later, reduces the value of  $d\left(\frac{1}{\theta}\right)/d\left(\frac{1}{T}\right)$ . The value for a polythene consisting only of very long chains is likely to be higher than 5500, and a value of 8000 has been obtained from density measurements on a higher molecular weight polythene containing less low molecular weight material.

**The Melting-point.**—The value of  $T_F$  at which all crystalline material has disappeared, is given by putting  $\theta = 1$  in equation

$$\frac{14L_F}{RT_F} = \frac{14\left(\frac{s}{M} + \frac{1-s}{14n}\right)}{1-s\left(1 - \frac{14\zeta}{M}\right)} + \frac{1}{\zeta} \ln \frac{\gamma-1}{e} + \frac{b}{R} + \frac{c}{Rn} \quad (10)$$

and when  $s = 0$ ,

$$\frac{14L_F}{RT_F} = \frac{1}{n} + \frac{1}{\zeta} \ln \frac{\gamma-1}{e} + \frac{b}{R} + \frac{c}{Rn} \quad (11)$$

The melting-point of a high molecular weight polythene entirely free of short chains is not, of course, known. The highest value observed is  $126^\circ \text{C.}$ ; we will put  $T_F = 400^\circ \text{A}$  when  $s = 0$ . Then, using values of  $56^\circ$  for  $L_F$ , 50 for  $n$  and 2 for  $c$ , we have:

$$\frac{1}{\zeta} \ln \frac{\gamma-1}{e} + \frac{b}{R} = 0.9583.$$

We can now examine the effect of additions of material of low molecular weight  $M$  on the melting-point, using equation (10). The effect of various additions of hydrocarbons of molecular weight 100, 200, 400 and 1000 is shown in Fig. 2. As  $s$  increases or  $M$  decreases, the melting-point is reduced. The values of  $T_F$  in Fig. 2 were obtained with  $\zeta = 1$ ; higher values of  $\zeta$  lead to slightly higher melting-points.

We may compare these calculated melting-point depressions with those observed when low molecular weight hydrocarbons are added to polythene. Fig. 3 shows the melting-point of mixtures of a polythene (M.W. 14,000) with heptane (M.W. 100), cetene-2 (M.W. 224), paraffin wax (M.W.

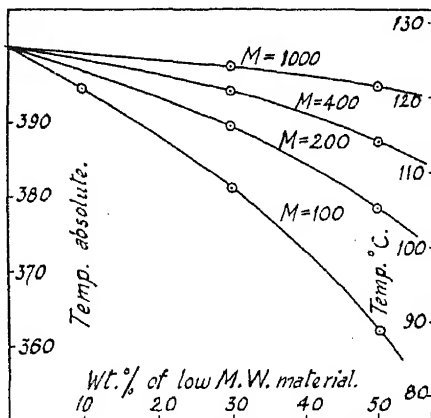


FIG. 2.—Calculated melting-point depression.

350), and a polythene of M.W. 650. The melting-point is depressed most by the lower molecular weight materials, and the actual values of the depression are similar to those calculated from equation (10) and shown in Fig. 2. No doubt more precise quantitative agreement could be obtained by adjusting values of  $\zeta$ ,  $n$  and  $c$ , but in view of the assumptions made in the derivation of equation (10), it does not seem justifiable to attempt to take a quantitative correlation too far at this stage.

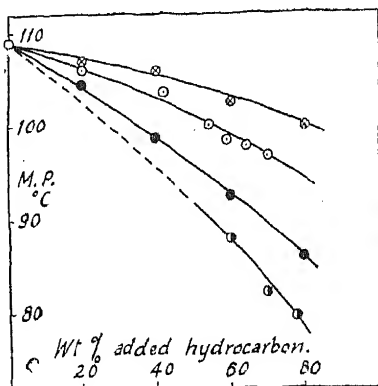


FIG. 3.—Observed melting-point depression.

- Heptane, M.W. 100.
- Paraffin wax, M.W. 350.
- Cetene-2, M.W. 224.
- Degraded polythene, M.W. 650.

**Effect of Low M.W. Material on Crystallinity below the Melting-point.**—It can be seen from equation (8), that the addition of low molecular weight material to polythene leads not only to a reduction in melting-point, but also to a more amorphous material below the melting-point and to a more gradual melting. As an example, Fig. 4 shows the effect of 10 % and 20 % of a hydrocarbon of molecular weight 200 on the crystallinity of a polythene of melting-point 127° C., at temperatures down to 20°, as indicated by equation (8).

For comparison, Fig. 5 shows the observed change in crystallinity of a polythene and the same polythene mixed with 10 % of vaseline. The degree of crystallinity was followed by linear coefficient of expansion, and hence density, measurements, using the method of calculation described by Hunter and Oakes.<sup>5</sup> As previously pointed out,<sup>5, 6</sup> this method may lead to values of  $\theta$  which are too high. A similar series of  $\theta - T$  curves is shown by the polythenes of varying average molecular weight whose density changes are reported by Hunter and Oakes. Apart from the change in average molecular weight these samples differed in the proportion of low molecular weight material which could be extracted by cold solvents.

**Melting-point and Crystallinity at Ordinary Temperatures.**—According to equation (8), as  $S$  increases and  $M$  decreases, the melting-

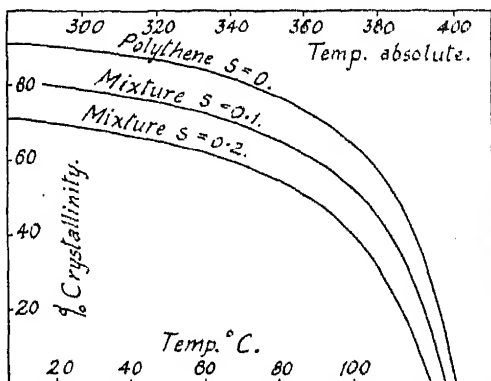


FIG. 4.—Calculated effect of low M.W. material on crystallinity.

point  $T_F$  and the degree of crystallinity at any temperature below  $T_F$  both decrease. We may thus expect to find that polythenes with low melting-points have low degrees of crystallinity, and hence low densities, at room temperature. This is shown in Fig. 6, a plot of melting-point against density for a number of polythenes made under different polymerisation conditions, samples made by thermal degradation of polythene, and mixtures. The densities recorded in Fig. 6 were measured after annealing at a high temperature, usually  $100^\circ\text{C}$ ., for one hour, but are not to be regarded as corresponding to equilibrium degrees of crystallinity. All of the samples whose densities and melting-points were recorded in Fig. 6 had molecular weights above 5000.

#### Chain Branching, Crystallinity and Melting-point.

It was noted earlier that changes in the degree of molecular chain branching might partly account for the variations in the melting behaviour of polythene samples. Although it has been shown that changes in the proportion of short chain material leads to parallel changes in melting-point and crystallinity at ordinary temperatures, all of the variations in Fig. 6 for example, may not be due to variations in this factor, but may also be due to changes in the degree of chain branching. It would, in fact, be very

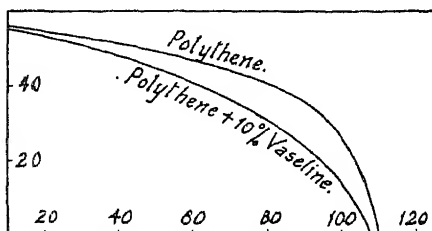


FIG. 5.—Observed effect of vaseline on crystallinity of polythene.

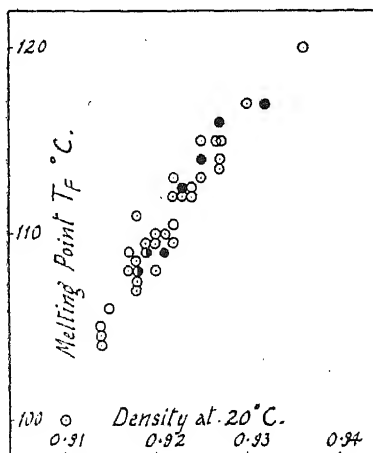


FIG. 6.—Relation between melting-point and crystallinity (density) at  $20^\circ\text{C}$ .

- Polythenes (different polymn. conditions).
- Thermal degradation products of polythene.
- ⊙ Polythene—paraffin mixtures.

difficult to interpret all of this variation in terms of changes in molecular weight distribution alone. Fig. 3 shows that a depression in melting-point of  $10^\circ\text{C}$ . is caused by about 40 % of cetene, of molecular weight 224, or 60 % of paraffin wax, of molecular weight 350. Such quantities of very low molecular weight material are certainly not present in normal polythene samples, although there may be such a variation in melting-point at a constant molecular weight. The amount of material which can be extracted from a normal polythene of molecular weight about 15,000 by leaching with cold benzene (or which remains in solution when a solution of polythene in benzene is cooled to room temperature) is usually in the

range 0.5 to 5.0 %, and has an average molecular weight of the order of 1000. Extraction of this material, or addition of similar quantities of it to polythene only varies the melting-point by one or two degrees, and there seems to be no doubt that variations in chain branching largely contribute to the differences in melting-point and crystallinity of polythene. It is worth noting here that it is very difficult to distinguish between the effects of a broadening molecular distribution and an increase in chain branching, because there is evidence<sup>10</sup> that in a given sample of polythene the lower molecular weight species have more frequent side groups. The fact that the cold-soluble fraction of polythene, although it has a molecular weight of the order of 1000, is a largely amorphous grease, indicates that it is probably far from being a straight chain paraffin.

The effect of chain branching on solid structure is normally considered in terms of the inability of a short side group (or, in the case of a long side

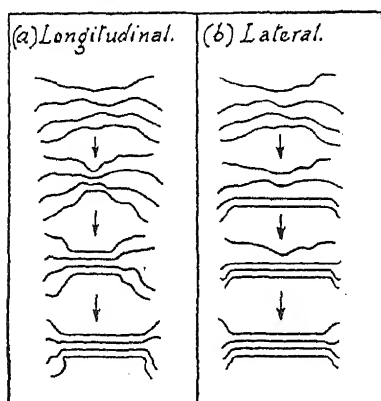


FIG. 7.—Extreme types of crystallite growth mechanisms.

group of the fork), to fit into the normal crystal structure, but the effect may also be considered as being due to the alteration of the balance between the entropy and heat content factors which governs melting phenomena. The addition of low molecular weight material decreases the melting-point and crystallinity because it increases the entropy of the amorphous regions. Chain branching may have the same effect. A side methyl group may increase the ease of rotation about the adjacent C—C bonds. This will lead to a greater number of possible configurations in the amorphous state, and, by changing the values of  $n$ ,  $\zeta$ ,  $b$  and  $c$  in equations, would decrease  $T_g$  and  $\theta$  at any value of  $T$ .

Apart from the effect on the flexibility of the chains, it seems possible that the configurational entropy of the amorphous regions may be increased merely because a segment bearing a side group differs from the normal segment of unbranched chains, thus leading to a greater number of statistically distinguishable configurations.

**The Melting Mechanism.**—It is noted above that the model on which the theoretical treatment of the melting of polythene is based assumes growth of crystallites from a number of nuclei, increasing lengths of molecules taking their place in ordered regions as temperature is decreased. This may be called longitudinal crystal growth (Fig. 7 (a)). Bunn and Alcock<sup>7</sup> have, however, pointed out that the X-ray and optical behaviour of polythene in the region 20–120° C. indicates that crystallite growth, like crystal growth in short chain paraffins, probably takes place predominantly by a side to side accretion of approximately parallel portions of chains—lateral crystal growth (Fig. 7(b)). Furthermore, it seems probable that all of the crystal nuclei are not formed at the same temperature, new ones being formed as  $T$  decreases. Conversely, as the temperature is raised, the smallest crystallites, containing the shortest lengths of polythene chain, are likely to disappear first, the largest persisting, with no appreciable diminution in size, until the higher temperatures.

A somewhat analogous behaviour would be found on heating a suspension in a liquid paraffin of a mixture of crystals of solid paraffins of varying chain length, e.g.  $C_{16}H_{34}$  to  $C_{80}H_{162}$ . The lower molecular weight crystals

might be completely dissolved before the higher had been appreciably affected, because of the great sensitivity of solubility to chain length. This analogy might be carried a little further, in order to show that the gradual melting of polythene is partly due to the distribution of crystallite size. For example, if one assumes (a) a distribution of crystallite size about an average, and (b) an increase with chain length in the temperature  $T_p$  at which each crystallite melts or dissolves in the amorphous regions similar to the change of melting-point of crystalline paraffins with chain length, it is easy to see that the overall crystallinity must change in a manner qualitatively similar to that observed in practice. But the distribution of crystallite size must not be regarded as the fundamental cause of a wide melting range in a crystalline polymer. The theoretical treatments given by Frith and Tuckett<sup>9</sup> and in this paper are valid for a system in which all crystallites have the same size at any given temperature, and, returning once again to the analogy of a suspension of a crystalline paraffin in a liquid hydrocarbon, even when only one species of paraffin is present, the percentage of crystalline matter in the system as a whole will vary continuously with temperature.

### Summary.

The melting-points of polythene samples are normally 20-30° below the value expected for a pure linear paraffin of comparable chain length, the melting process extends over a much wider temperature range and the solid is not entirely crystalline even at room temperature. Samples with the same average molecular weight, as indicated by intrinsic viscosities, can vary as much as 15° in melting-point. These variations may be due to changes in molecular weight distribution and in the degree of chain branching.

By an extension of the statistical thermodynamic treatment of Frith and Tuckett, an equation is derived for the variation, with temperature, of the degree of crystallinity of a long chain linear paraffin containing various proportions of short chain paraffinic liquids which are concentrated in the amorphous regions of the solid. From this equation a further equation is derived for the change of melting-point with the proportion and molecular weights of the added liquid. The theoretical results are found to be in fair agreement with observed data for the depression of melting-point by paraffins of various molecular weights. The theoretical results suggest that there should be a connection between the crystallinity, and hence density, of the solid at ordinary temperatures and the melting-point of the sample; this is shown to be in accord with observed data.

The presence of side groups will have an effect similar to that of short molecules, and by increasing the entropy of the amorphous regions will lead to a more amorphous polymer. Part of the variability in melting-point and crystallinity in polythene is no doubt due to variation in the degree of chain branching.

The author wishes to acknowledge the assistance of Miss E. D. Carter.

*Imperial Chemical Industries Research Dept.,  
Alkali Division, Northwich.*



# THE TEMPERATURE DEPENDENCE OF IONIC DISSOCIATIONS.

BY H. O. JENKINS.

Received 22nd May, 1944.

Several equations have been suggested to account for the variation of the ionisation constants of weak electrolytes with temperature. For example, the equation,<sup>1</sup>

$$\log K = A/T + \frac{B \log T}{T} + \frac{C \log^2 T}{T} + D \quad (1)$$

has been found to be satisfactory for formic, acetic, propionic, and butyric acids in water over a range of 50° C. and provisionally for formic acid in 70 % dioxane-water mixtures, where  $A$ ,  $B$ ,  $C$  and  $D$  are constants for an acid in the particular solvent in which dissociation takes place. It was considered important to extend the range of the equation, and especially to discover whether (a) it always applied to dissociations in media of dielectric constants widely different from that of water, (b) it held for the dissociation of substances which are not fatty acids and which may have ionisation constants of a different order of magnitude. Now the form of the equation chosen to express the temperature variation of ionisation constant influences to some extent the calculated values of the various thermodynamic constants such as  $\Delta H^\circ$ ,  $\Delta S^\circ$  and  $\Delta C_p$ . Thus the opportunity has been taken of computing some thermodynamic constants, pertaining to the equilibria studied, using the new equation as basis, comparing the values obtained with those calculated from other suggested equations, and of considering their variation with changing dielectric constant of medium. The Table gives the results in compact form.

## Discussion.

The values of  $\Delta G^\circ_{298.1}$ ,  $\Delta S^\circ_{298.1}$  and  $\Delta H^\circ_{298.1}$  are mostly in agreement with those obtained using other equations as bases. For example, for acetic acid in 20 % dioxane-water,  $\Delta H^\circ_{298.1} = -102$  cal., and  $\Delta S^\circ_{298.1} = -24.6$  cal./deg., whereas Everett and Wynne-Jones<sup>8</sup> give  $\Delta H^\circ_{298.1} = -70$  cal., and  $\Delta S^\circ_{298.1} = -24.4$  cal./deg., using the equation

$$\log K = A/T + \frac{\Delta C_p}{R} \log T + B$$

with the assumption that  $\Delta C_p$  is invariant with respect to temperature. For formic acid in 20 % dioxane-water, Harned and Done,<sup>3</sup> using the equation

$$\log K = -A/T + B - CT,$$

calculate  $\Delta H^\circ_{298.1} = -354$  cal. and  $\Delta S^\circ_{298.1} = -26.9$  cal./deg. These compare satisfactorily with the new values now quoted. Owen,<sup>7</sup> using

<sup>1</sup> Jenkins, *Trans. Faraday Soc.*, 1944, 40, 19.

<sup>2</sup> Harned and Kazarijian, *J. Am. Chem. Soc.*, 1936, 58, 1912.

<sup>3</sup> Harned and Done, *ibid.*, 1941, 63, 2579.

<sup>4</sup> Wright, *ibid.*, 1934, 56, 314.

<sup>6</sup> Harned and Hamer, *ibid.*, 1933, 55, 2194.

<sup>7</sup> Owen, *ibid.*, 1934, 56, 1695.

<sup>8</sup> Everett and Wynne-Jones, *Trans. Faraday Soc.*, 1939, 35, 1380.

Acid.	A	B	C	D	$\Delta G^{\circ}_{298.1}$	$\Delta H^{\circ}_{298.1}$	$\Delta S^{\circ}_{298.1}$	$\Delta C_p^{\circ}_{298.1}$	$\Delta C_p^{\circ}_{298.1}$
1. Acetic in water	-477.500	-4607.951	2492.551	-16.0988	6484	-120	-22.1	-39.1	-37.1
2. Acetic in 20 % dioxane-water	-82031.42	71558.95	-16090.03	-6.3805	7222	-102	-24.6	-51.8	-39.3
3. Acetic in 45 % dioxane-water	-60194.68	50551.47	-10784.02	-2.4969	8599	-392	-30.2	-53.6	-43.6
4. Acetic in 70 % dioxane-water	-124366.02	110171.4	-25232.55	12.6752	11293	-615	-39.9	-66.4	-48.1
5. Formic in water	-13179.30	6612.350	-75.4314	-12.8765	5114	-50.7	-17.3	-45.9	-42.0
6. Formic in 20 % dioxane-water	-14932.00	8094.64	-377.260	-13.5304	5599	-380	-20.4	-47.9	-43.7
7. Formic in 45 % dioxane-water	-58801.32	48868.87	-10231.20	-3.3416	6942	-1102	-27.0	-57.5	-47.4
8. Formic in 70 % dioxane-water	-65198.80	55230.10	-11865.39	-3.0420	9566	-1510	-37.2	-56.1	-45.4
9. Chloroacetic	23933.3	-26992.0	7896.06	-21.2725	3901	-1107	-16.8	-33.6	-34.8
10. Glycine, First acid dissociation	-101333.0	90696.4	-21121.3	18.554	3202	1043	-7.25	—	-30.0
11. Glycine, Basic dissociation	17366.0	-19880.1	5687.34	-14.269	5752	2710	-10.2	-21.0	-22.2
12. Water	-18966.68	9081.341	-630.1332	-12.8087	10084	13463	-18.9	-47.7	-43.4
13. Meta-boric	-140600.0	125782.0	-29371.00	21.5980	12593	3191	-31.5	-59.5	-39.6

the equation for metaboric acid,  $\Delta H^{\circ}$

$$= 3.68 \times 10^{-4} RT^2(76.7 - t)$$

finds that

$$\Delta H^{\circ}_{298.1} = -3360 \text{ cal.},$$

which can be compared with -3191 cal. For water, Harned and Hamer,<sup>6</sup> using an equation of the form,

$$\log K =$$

$$-a/T - b \log T - cT + D$$

find  $\Delta H^{\circ}_{298.1} = 13490 \text{ cal.}$ , whereas the value now found is 13463 cal. These agreements are unlikely to be fortuitous, only prevailing at 25°C. One other example may however be mentioned, the temperature now being 273.1° K. For water  $\Delta H^{\circ}_{273.1}$  Harned and Hamer find a value of 14513 cal. while the value given by the new equation can be calculated to be 14599 cal.

However the values calculated for  $\Delta C_p$  vary considerably and show very little agreement with those

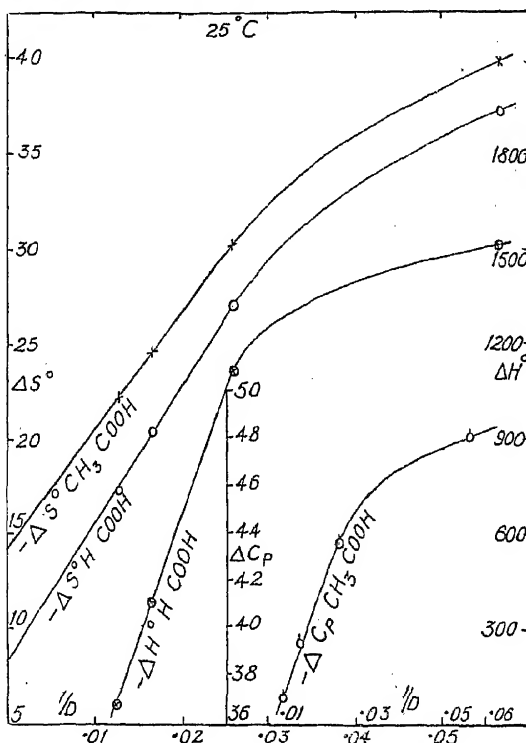


FIG. 1.

found using the other equations. Occasionally we find what appears at first sight to be reasonable agreement. Thus Harned and Hamer give for water  $\Delta C_p^{298.1}$  as  $-42.5$  cal./deg. whereas our value is  $-43.4$  cal./deg. This harmony, wherever it exists, is soon destroyed when we examine the effect of temperature on  $\Delta C_p$ . For water at  $0^\circ\text{C}$ . Harned and Hamer give  $\Delta C_p^{273.1} = -40.1$ , and at  $50^\circ\text{C}$ .  $\Delta C_p^{323.1} = -45.1$  or  $(\Delta C_p^{323.1} - \Delta C_p^{273.1}) = -5.0$  cal./deg. The corresponding quantity calculated using equation (1) as basis is

$$(\Delta C_p^{323.1} - \Delta C_p^{273.1}) = (-39.7 + 47.7) = +8.0 \text{ cal./deg.}$$

Again for formic acid in 20 % dioxane-water

$$(\Delta C_p^{323.1} - \Delta C_p^{273.1}) = -47.1 + 39.8 = -7.3 \text{ cal./deg.}$$

according to Harned and Done, whereas the corresponding quantity using equation (1) is  $+8.4$  cal./deg. Everett and Wynne-Jones<sup>8</sup> assume an invariant  $\Delta C_p$  with respect to temperature and no agreement can in general be expected. However these authors, starting from the Born equation, deduce that  $\Delta C_p$  should be given by

$$\Delta C_p = -\frac{Z^2 e^2 B(B-1)}{2\nu} \frac{1}{DT} \quad (2)$$

Inserting values of  $D$  and  $T$  for water, it can be shown that there is a 6 % increase in the absolute magnitude of  $\Delta C_p$  over a range of  $50^\circ\text{C}$ . In the figure will be found  $\Delta S^\circ_{298.1}$  and  $\Delta C_p^{298.1}$  for acetic acid, and  $\Delta S^\circ_{298.1}$  and  $\Delta H^\circ_{298.1}$  for formic acid plotted against the reciprocal of the dielectric constant of the medium for water-dioxane mixtures. In each case the linear relation only holds in dilute water solution and breaks down in solutions of low dielectric constant. A closer inspection of the graph published by Everett and Wynne-Jones ( $\Delta S^\circ_{298.1}$  against  $1/D$  for acetic acid) reveals that their line is really a curve. Their argument, however, that only part of the entropy is electrostatic is re-inforced and the non-electrostatic parts can easily be obtained from the graphs for acetic and formic acids. The similarity of the curves for  $\Delta S^\circ$ ,  $\Delta C_p$  and  $\Delta H^\circ$  is striking and may prove useful in the theoretical elucidation of the problem of  $\Delta C_p$  which no doubt is a composite quantity.

### Summary.

The experimental data for the electrolytic dissociation of many weak acids in water and dioxane-water mixtures have been subjected to a theoretical analysis, using the equation

$$\log K = A/T + B \log T/T + C \log^2 T/T + D.$$

This equation has been found to be satisfactory. Agreement with other equations has been found for  $\Delta H^\circ$ ,  $\Delta G^\circ$  and  $\Delta S^\circ$ , but not for  $\Delta C_p$ . A similar type of curve is given when  $\Delta S^\circ$ ,  $\Delta H^\circ$  and  $\Delta C_p$  is plotted against the reciprocal of the dielectric constant of the medium.

*St. Martin's Vicarage,  
Bradley, Bilston, Staffs.*

# KINETIC ENERGY, POTENTIAL ENERGY AND FORCE IN MOLECULE FORMATION.

BY C. A. COULSON AND R. P. BELL.

*Received, 31st July, 1944.*

## Kinetic Energy, Potential Energy and the Virial Theorem in Quantum Theory.

In any conservative dynamical system where magnetic interactions can be neglected it is possible to assign a quantitative meaning not only to the total energy  $E$ , but also to the kinetic energy  $T$  and the potential energy  $V$ . This is equally true in classical mechanics and in quantum theory, but in both cases the total energy  $E$  has a status different from that occupied by  $T$  and  $V$ . Thus in classical mechanics  $E$  is a constant of the motion, while both  $T$  and  $V$  will in general vary with the time. In enclosed systems (*e.g.* atoms, molecules, or particles in containers) this variation will be a periodic one, and values can be given to the time averages of  $T$  and  $V$ . The position is similar in quantum theory, which in general predicts only "average" or "expectation" values of any dynamical variable  $G$ , usually denoted by  $\bar{G}$ . However there is this difference, that the quantum-mechanical value is not a time average but a probability average. In the case of the total energy we find that  $(\bar{E})^n = \bar{E}^n$  for any value of  $n$ : hence  $E$  has a definite value, and the bar can be omitted. Such quantities are described as constants of the motion. The same is not true for  $T$  and  $V$ , which are not constants of the motion, and only average values of these quantities can be predicted theoretically or observed in practice. In any system composed of charged particles and represented by a wave-function  $\psi$  the usual rules of the quantum theory give

$$\bar{V} = \int \psi^* \left\{ \sum_{i,j} \frac{e_i e_j}{r_{ij}} \right\} \psi dv, \quad \bar{T} = -\frac{\hbar^2}{8\pi^2} \int \psi^* \left\{ \sum_i \frac{1}{m_i} \nabla_i^2 \right\} \psi dv \quad (1)$$

with the usual notation.

It is not possible to devise any type of experiment which will measure directly the average internal kinetic or potential energy of an atom or molecule. These quantities are, however, accessible in principle, since if we determine completely the distribution of charge and momentum in a molecular system (*e.g.* by investigations of electron diffraction or the Compton effect) the values of  $\bar{T}$  and  $\bar{V}$  can be calculated. Thus<sup>1</sup> the complete velocity distribution for electrons in H, He and H<sub>2</sub> has been calculated theoretically and observed experimentally by means of the shape or profile of the modified Compton line. However, for any equilibrium system involving only Coulomb forces, if  $E$  is known there is no point in making such observations, since the values of  $E$ ,  $\bar{T}$  and  $\bar{V}$  are related very simply by the *virial theorem*

$$E = -\bar{T} = \frac{1}{2}\bar{V} \quad (2)$$

which is equally valid in classical mechanics and in quantum theory.

**Application to Diatomic Molecules.**—In an atom the only internal kinetic energy belongs to the electrons, while in a molecule both the

<sup>1</sup> Hicks, *Physic. Rev.*, 1937, **52**, 436.

electrons and the nuclei will have internal kinetic energy. However, owing to the much greater mass of the latter, the theoretical problem can be divided into two parts.

(a) An idealised system is considered in which the nuclei have no kinetic energy, and are held fixed at an arbitrary distance  $R$  apart. By solving the wave equation for the electrons a number of electronic energy levels are obtained, of which only the lowest will be considered here. The value of the energy, and also the shape of the electron distribution, will depend on the value chosen for the distance  $R$ , and we shall write the energy of the lowest level as  $E(R)$ .  $E(R)$  is a total energy, and involves the kinetic energy of the electrons and the potential Coulombic energies of the electrons and nuclei.

(b) A second artificial system is considered in which the nuclei move subject to a potential energy given by  $V'(R) = E(R)$ , and the electrons are not explicitly considered. Solution of the wave equation for this system gives the rotational and vibrational levels for nuclear motion in the lowest electronic level.

This procedure is of course only an approximate substitute for an exact solution of the complete wave equation, but it can be shown<sup>2</sup> that it represents a very good approximation provided that the nuclei are not too close together. It is clear that the virial theorem in the simple form (2) cannot be applied directly to either of the stages (a) or (b) above. In (a) it is necessary to imagine the application of an external force  $dE/dR$  to each nucleus in order to hold them a distance  $R$  apart, and the potential energy of the system is thus not wholly Coulombic. The same applies to the artificial potential energy  $V'(R) = E(R)$  in (b).

However, in the fixed-nucleus problem (a) for a diatomic molecule a more general form of the virial theorem can be used with profit, as has been shown by Slater.<sup>3</sup> This is derived from the general relation

$$2\bar{T} = - \sum_i (\bar{x}_i F_{x_i} + \bar{y}_i F_{y_i} + \bar{z}_i F_{z_i}) \quad . \quad . \quad . \quad (3)$$

where  $x_i$ ,  $F_{x_i}$ , etc., are the co-ordinates and the components of force acting on the nuclei and electrons. The forces on the right hand side of (3) are composed partly of the Coulomb forces between the nuclei and electrons, and partly of the impressed forces  $\pm dE/dR$  on each nucleus. The former contribute as before  $-\bar{V}$  to the virial, and the latter give two terms which combine together in the form  $-RdE/dR$ . Hence (3) can be written

$$2\bar{T} = -\bar{V} - RdE/dR \quad . \quad . \quad . \quad (4)$$

or alternatively, since  $E = \bar{T} + \bar{V}$ ,

$$\bar{T} = -E - RdE/dR = -d/dR(RE)$$

$$\bar{V} = 2E + RdE/dR = \frac{1}{R} d/dR(R^2E) \quad . \quad . \quad . \quad (5)$$

If  $dE/dR = 0$  (*i.e.* at the equilibrium internuclear distance  $R = R_0$ ) these equations reduce to (2), since for this value of  $R$  the system is held in equilibrium by Coulomb forces alone. At other internuclear distances equation (5) makes it possible to calculate  $\bar{T}$  and  $\bar{V}$  from spectroscopic data, since these yield a curve for the dependence of  $E$  upon  $R$ . This equation has been obtained for a diatomic molecule in which there is only one internuclear distance, but it is easily extended by the addition of more terms to the case of a polyatomic molecule.

Some confusion has arisen about the use of the terms "potential energy" and "force" in molecule formation. Thus the plot of  $E(R)$

<sup>2</sup> Born and Oppenheimer, *Ann. Physik.*, 1927, 84, 427.

<sup>3</sup> Slater, *J. Chem. Physics*, 1933, 1, 687.

against  $R$  is often referred to as a "potential-energy curve." It does in fact represent the potential energy of the external force which must be applied to bring the nuclei from infinity to the distance  $R$ , and it plays the part of a potential energy in calculating the quantum levels for nuclear vibration, as in (b) of page 142. On the other hand, in the actual molecule the only true potential-energy terms are those of Coulombic interaction, and a considerable part of the change of  $E(R)$  with  $R$  is due to changes in the kinetic energy of the electrons. The difference in interpretation clearly arises from the fact that by separating the effects (a) and (b) earlier we are in each case dealing with an artificial system involving an external constraint which is foreign to the actual interactions in the molecule itself. A simple mechanical parallel is obtained by considering the arrangement in Fig. 1. The rotating mass  $M$  is attached to an elastic string which passes through a ring at  $O$  and is held in place by an external force  $F$ . If now the distance  $OM$  is shortened by a slight increase in  $F$ , the work done by  $F$  (potential energy) is balanced partly by a change in the potential energy of the stretched string and partly by a change in the kinetic energy of rotation of  $M$ .

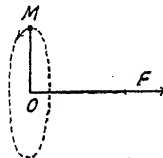


FIG. 1.

Apart from questions of nomenclature, it is important to realise that when the nuclei of a molecule are displaced, the orbits of the electrons are altered, so that there is a change not only in the Coulombic potential energy of the electrons and nuclei, but also in the kinetic energy of the electrons. Failure to realise this has led to misconceptions about the nature and magnitude of the forces acting on the nuclei in a molecule. Thus both Hellmann<sup>4</sup> and Feynman<sup>5</sup> have concluded that "the force on any nucleus (considered fixed) is just the classical electrostatic attraction exerted on the nucleus in question by the other nuclei and by the electron charge distribution for all the electrons." This erroneous conclusion is formally justified by the equations †

$$\bar{F} = -\frac{\partial E}{\partial R} = -\int \psi^* \frac{\partial H}{\partial R} \psi dv = -\int \psi^* \frac{\partial V}{\partial R} \psi dv \quad (6)$$

Since  $H = T + V$ , there is an obvious error in these equations due to the omission of the term  $\partial T / \partial R$ . This corresponds to the part of the force depending on variations in kinetic energy. It is true that the operator

$T \left( = -\frac{\hbar^2}{8\pi^2 m} \nabla^2 \right)$  formally involves only the electronic co-ordinates, so

that it might be concluded that  $\partial \bar{T} / \partial R = \int \psi^* \frac{\partial T}{\partial R} \psi dv = 0$ . However, the

quantity which we really want is  $\frac{\partial}{\partial R} \int \psi^* T \psi dv$ , and it is easily seen that this is not zero. For example, in the simple case of one electron in the field of two nuclei,  $\psi$  is most naturally written in terms of  $r_A$  and  $r_B$ , the distances of the electron from the two nuclei. In order to carry out the evaluation of  $\bar{T}$  we must express both  $\nabla^2$  and  $\psi$  in terms of the same variables, and in doing so  $R$  will appear explicitly in either  $\nabla^2$  or  $\psi$ : hence the value of  $\frac{\partial}{\partial R} \int \psi^* T \psi dv$  will not in general be zero. It is thus not permissible to take the operator  $\partial / \partial R$  inside the integral sign: i.e. we cannot write  $\frac{\partial}{\partial R} \int \psi^* T \psi dv = \int \psi^* \frac{\partial T}{\partial R} \psi dv$ , at least if we retain the ordinary significance for  $\partial T / \partial R$ . Similarly, we may not (as both Hellmann and

<sup>4</sup> Hellmann, "Einführung in die Quantenchemie," Leipzig, 1937, p. 285.

<sup>5</sup> Feynman, *Physic. Rev.*, 1939, 56, 340.

† Feynman,<sup>5</sup> p. 341, equation (3).

Feynman do) write  $\frac{\partial \bar{V}}{\partial R} = \int \psi^* \frac{\partial V}{\partial R} \psi dv$ ; for  $V$  is a function of  $r_A$ ,  $r_B$  and  $R$ , and we cannot assign any meaning to a change of  $V$  in which  $R$  varies but  $r_A$  and  $r_B$  are kept constant.

### Approximate Wave-functions and the Virial Theorem.

It is never possible to obtain exact wave-function for molecular problems (other than  $H_2^+$ ), and there is usually some choice between different forms of approximate function, each having adjustable parameters. The usual test for estimating the quality of an approximate function is to compare the observed and calculated values of the total energy  $E$ . For a given type of wave-function the adjustable parameters should be chosen so that the value of  $E$  is a minimum with respect to the variations of any of them. In the neighbourhood of this minimum the value of  $E$  is insensitive to relatively large changes in the wave-function. As pointed out by Slater,<sup>3</sup> an independent and more sensitive test is provided by comparing the calculated values of  $\bar{T}$  and  $\bar{V}$  (equation (1)) with those derived from spectroscopic data (equation (5)). It is sometimes stated<sup>6</sup> that the only ultimate criterion for the validity of variation wave-functions lies in comparison with observed values of  $E$ . This is of course not the case. In addition to the comparison of  $\bar{T}$  and  $\bar{V}$  values, there are a number of other criteria quite independent of experimental data, of which the most straightforward is to test how far the wave-function satisfies the wave-equation for different values of the co-ordinates.<sup>7</sup>

The values of  $\bar{T}$  and  $\bar{V}$  obtained from approximate wave-functions by means of equation (1) will not in general satisfy the virial relations (2) or (5). Thus Hirschfelder and Kincaid<sup>8</sup> have shown that the Heitler-London perturbation wave-functions for  $H_2$  and  $H_2^+$  give values of  $\bar{T}$  and  $\bar{V}$  for  $R = R_0$  which conflict wildly with (2). However, this limitation to the application of the virial relations has not always been realised. Thus Frenkel<sup>9</sup> in treating  $H_2^+$  by the Heitler-London method first derives expressions for  $\bar{T}$  and  $\bar{V}$ , and states that the corresponding expression for  $E$  can be obtained either from  $E = \bar{T} + \bar{V}$ , or from equation (5). Actually, of course, different expressions are obtained in the two cases, only the former method yielding the correct result.<sup>†</sup>

The extent to which an approximate wave-function satisfies the virial relations can be used as an index of its quality, independent of experiment. Thus, suppose we consider any physically reasonable wave-function involving a single parameter  $\lambda$ . The virial relation will be satisfied for a particular value  $\lambda_i$ , and from this point of view  $\lambda_i$  can be regarded as the "best" value of the parameter. Another value,  $\lambda_m$ , can be obtained by the usual variational procedure of minimising  $E$ , but in general  $\lambda_i$  and  $\lambda_m$  will be different. However, there is one type of variational parameter for which  $\lambda_i$  and  $\lambda_m$  are identical. This is the scale-factor (or screening constant)  $s$ , which occurs in the wave-function as a factor multiplying all distances between particles. Fock<sup>10</sup> has proved that if the scale-

<sup>6</sup> E.g. Dushman in "Physical Chemistry" (Taylor and Glasstone, 1942), Vol. 1, p. 338.

<sup>7</sup> See e.g. Coolidge and James, *J. Chem. Physics*, 1933, 1, 825; *Physic. Rev.*, 1937, 51, 860; Bartlett, Gibbons and Dunn, *ibid.*, 1935, 47, 679.

<sup>8</sup> Hirschfelder and Kincaid, *Physic. Rev.*, 1937, 52, 658.

<sup>9</sup> Frenkel, "Wave Mechanics—Elementary Theory" (2nd edition, Oxford, 1936, p. 289).

<sup>†</sup> In Frenkel's treatment each of the integrals  $L$ ,  $M$  and  $I$  occurring on the expressions for  $\bar{T}$  and  $\bar{V}$  has been incorrectly evaluated, and a further error has been made in writing down the final formula for  $\bar{T} + \bar{V} = E$  (p. 292). However, not even these incorrect formulæ are consistent with equation (5).

<sup>10</sup> Fock, *Z. Physik*, 1930, 63, 855.

factor in an atomic wave-function is adjusted so as to give the minimum value of  $E$ , then the virial relation  $\bar{T} = -\frac{1}{2}\bar{V} = -E$  is automatically satisfied. Hirschfelder and Kincaid<sup>8</sup> have shown that the same result applies to a molecule with equilibrium internuclear distances. We shall now show that this result can be extended to any arbitrary internuclear distances provided that we use the more general virial relation (5).

$E$ ,  $\bar{T}$  and  $\bar{V}$  can be written as functions of the internuclear distance  $R$  and the scale-factor  $s$ . From dimensional considerations we have

$$\begin{aligned}\bar{T}(s, R) &= s^2 \bar{T}(1, sR), & \bar{V}(s, R) &= s \bar{V}(1, sR) \\ E(s, R) &= s^2 \bar{T}(1, sR) + s \bar{V}(1, sR)\end{aligned}\quad (7)$$

For every value of  $R$  there will be a value  $s = s'(R)$  which will make  $E$  a minimum;  $s'(R)$  is therefore defined by the equation

$$\left[ \left\{ \frac{\partial E(s, R)}{\partial s} \right\} \right]_{R=s'(R)} = 0 \quad (8)$$

and hence from (7)

$$\left[ 2s \bar{T}(1, sR) + \bar{V}(1, sR) + s^2 R \frac{d\bar{T}(1, sR)}{d(sR)} + sR \frac{d\bar{V}(1, sR)}{d(sR)} \right]_{s=s'(R)} = 0 \quad (9)$$

Multiplying by  $s$  and using (7) this becomes

$$\left[ 2E(s, R) - \bar{V}(s, R) + R \left\{ \frac{\partial E(s, R)}{\partial R} \right\} \right]_{s=s'(R)} = 0 \quad (10)$$

The differential coefficient in (10) implies that  $E(s, R)$  is first differentiated with respect to  $R$ , after which  $s$  is put equal to  $s'(R)$ . However, the order of these processes can be inverted, since we have

$$\frac{dE(s'(R), R)}{dR} = \frac{ds'(R)}{dR} \left[ \left\{ \frac{\partial E(s, R)}{\partial s} \right\} \right]_{s=s'(R)} + \left[ \left\{ \frac{\partial E(s, R)}{\partial R} \right\} \right]_{s=s'(R)} \quad (11)$$

and the first term on the right is zero from (8). Equation (10) then becomes

$$2E(s'(R), R) - \bar{V}(s'(R), R) + R \frac{dE(s'(R), R)}{dR} = 0 \quad (12)$$

*i.e.*, the virial relations (5) are satisfied provided that  $s$  is given the proper functional dependence upon  $R$  required by the condition of minimum energy.

Either (8) or (12) can be used for determining the best value of the scale-factor for a given value of  $R$ , but for non-equilibrium values of  $R$  equation (8) will be the more convenient. However, at the equilibrium distance  $R_0$  (supposed known) the replacement of (8) by

$$\bar{T}(s_0, R_0) = \frac{1}{2} \bar{V}(s_0, R_0) = 0 \quad (13)$$

will often save some algebraic working. Moreover, if  $s'(R)$  has been determined from (8) for a range of values of  $R$ , then equation (13) is a more sensitive test for determining the value of  $R_0$  than is the condition  $dE/dR = 0$ .

As already mentioned, if  $\lambda$  is a parameter other than a scale factor, the best values  $\lambda_a$ ,  $\lambda_v$ , obtained respectively from the variation and virial conditions will not be identical. Since  $\lambda_a$  gives the best value of  $E$  obtainable with the given type of function, the value  $E_i$  corresponding to  $\lambda$ , will be a less accurate value than  $E_a$ , though it seems likely that in many cases the difference between  $E_i$  and  $E_a$  will not be great. However, it should be pointed out that if a trial wave-function contains more than one adjustable parameter, then the virial condition provides only one relation between the parameters, while the condition of minimum energy provides as many equations as there are parameters, thus enabling the



values of all of them to be determined. In most molecular problems, therefore, the usefulness of the virial condition will be restricted to the improvement of a wave-function already arrived at by a variational process.

### Application to the Molecules $H_2^+$ and $H_2$ .

The various approximate wave-functions which have been suggested for these two molecules are frequently made a basis for the treatment of other molecules, and for general ideas on the nature of the chemical bond. It is therefore of interest to consider the true values for the kinetic and potential energies of these two molecules, and to compare them with the predictions of different types of approximate wave-function.

(a) **Exact Values of  $E$ ,  $\bar{V}$  and  $\bar{T}$ .**—In the case of  $H_2^+$  the most accurate estimate of the true values is obtainable from the exact theoretical treatment of Hylleraas.<sup>11</sup> It has been shown<sup>12</sup> that the energy levels predicted by this treatment are in complete accord with the rather scanty spectroscopic data. For the  $H_2$ -molecule the energy curve has been derived

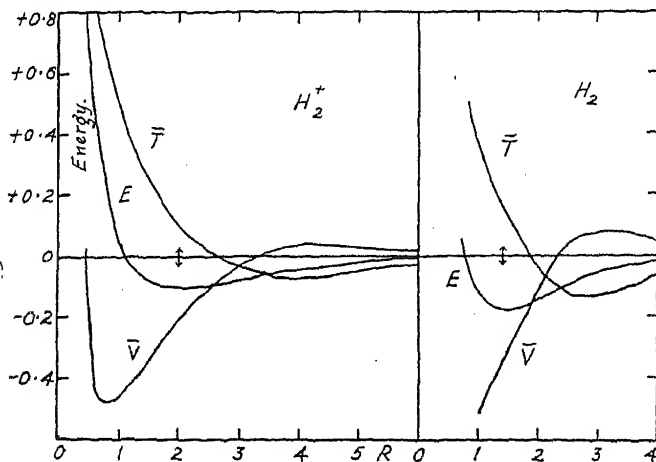


FIG. 2.

from the observed spectrum by Rydberg.<sup>13</sup> For both molecules we have calculated  $\bar{T}$  and  $\bar{V}$  from  $E(R)$  by using the virial relation (12),  $dE/dR$  being obtained by taking differences and interpolating. In both cases a small extrapolation has been made for large values of  $R$ , assuming a curve of the Morse type,

Figure 2 shows the curves thus obtained, expressed in atomic units of distance (0.528 Å.) and energy (27.08 e.v.). The curves have been displaced vertically so as to make  $E$ ,  $\bar{T}$  and  $\bar{V}$  each zero for infinite inter-nuclear separation. (If a common energy zero were taken for  $E$ ,  $\bar{V}$  and  $\bar{T}$ , then the curves would be considerably separated for large values of  $R$ ; e.g. for  $H_2^+$  the asymptotic values when  $R$  tends to infinity are  $E = -0.500$ ,  $\bar{T} = +0.500$ ,  $\bar{V} = -1.000$ , all measured relative to infinite separation of the individual electrons and nuclei. However, the method of plotting adopted here is more convenient when considering the process of bond formation.) The curves for  $\bar{T}$  and  $\bar{V}$  are not known as accurately as  $E$ , but there can be no doubt about their general shape. Somewhat similar curves have been previously deduced by Slater<sup>3</sup> by assuming that  $E$  is

<sup>11</sup> Hylleraas, *Z. Physik*, 1931, 71, 750.

<sup>12</sup> Sandeman, *Proc. Roy. Soc., Edinburgh*, 1935, 55, 72; Richardson, *Proc. Roy. Soc. A*, 1935, 152, 503; Beutler and Jünger, *Z. Physik*, 1936, 101, 304.

<sup>13</sup> Rydberg, *Z. Physik*, 1932, 73, 382.

of the form  $-A/r^n + B/r^m$ , though his curves differ from ours in several respects.

Figure 2 illustrates several points which are likely to apply to bond formation in general. As the two atoms approach, the first effect is an increase in  $\bar{V}$ , more than counterbalanced by a decrease in  $\bar{T}$ . With decrease in  $R$ ,  $\bar{V}$  passes through a maximum, followed soon afterwards by a minimum in  $\bar{T}$ . In the neighbourhood of the equilibrium point (marked by an arrow in Fig. 2) the binding energy is due to a decrease in  $\bar{V}$ , a part of which is counterbalanced by an increase in  $\bar{T}$ . When  $R$  becomes considerably less than  $R_0$ , the increase of  $\bar{T}$  predominates over the decrease in  $\bar{V}$ , leading to repulsion, and finally at very small inter-nuclear distances  $\bar{V}$  also increases. The last effect is shown in the curve for  $H_2^+$ , but not in that for  $H_2$ . This is because the spectroscopic data give no information about the course of the energy curve when the total energy exceeds the dissociation energy of the molecule. In the case of  $H_2^+$ , the theoretical treatment shows the rise in  $\bar{V}$  to be due to repulsion between the nuclei, and there is thus no doubt that it will occur in all molecules for sufficiently small values of  $R$ . It is interesting to note that the curves for  $H_2^+$  are throughout similar to those for  $H_2$ , i.e. there are no essential differences in behaviour between the one-electron and the two-electron bond.

Slater<sup>3</sup> has shown how this rather complex behaviour of  $E$ ,  $\bar{V}$  and  $\bar{T}$  can be plausibly interpreted in terms of electron distribution and the uncertainty principle. Here we shall only point out that any picture of the chemical bond in terms of potential energy alone is not even qualitatively correct, and may be quite misleading. Similarly, any separation of the total energy into energy of attraction and energy of repulsion is illusory, and conclusions based on such a separation must be open to question.<sup>14</sup>

(b) **Approximate Wave-functions for  $H_2^+$  and  $H_2$ .**—The simplest types of approximate wave-function for these molecules are those built up from hydrogen-like atomic wave-functions. If the exponents of these atomic functions are left unaltered, the corresponding molecular functions are described as "perturbation wave-functions," while if an adjustable scale-factor is inserted in the atomic functions the term "variation wave-function" is used. In the case of the  $H_2$  molecule the atomic functions can be combined in two ways, corresponding to the electron-pair and molecular orbital methods of calculation. Unless otherwise stated, our calculations refer to the electron-pair method. The wave-functions and the energy-curves derived from them have been discussed in detail in a previous paper.<sup>15</sup>

Figures 3 and 4 (full curves) show the values of  $\bar{T}$  and  $\bar{V}$  obtained by applying equation (1) to these approximate wave-functions. The true values (cf. Fig. 2) are shown by the broken curves. It will be seen that the variation method predicts curves which are of the right general form, and which lie quite close to the true values. This is to be expected, since the variation method gives reasonable values for the total energy, and we have already seen that the introduction of a scale factor automatically satisfies the virial relation, thus ensuring a reasonable apportionment between kinetic and potential energy. On the other hand the perturbation method gives curves which bear no resemblance to the true state of affairs, except for very large values of  $R$ . In the neighbourhood of  $R = R_0$  the perturbation method does not even predict the correct signs for  $\bar{T}$  and  $\bar{V}$  (relative to  $R = \infty$ ). We must therefore conclude that the perturbation

<sup>14</sup> See e.g. Evans and Warhurst, *Trans. Faraday Soc.*, 1939, **35**, 593.

<sup>15</sup> Coulson, *Trans. Faraday Soc.*, 1937, **33**, 1479.

method gives a very misleading picture of the changes which take place in the distribution and momenta of the electrons when two atoms combine to form a molecule. Although it gives a reasonable curve for the total energy, this results from the cancellation of large errors in both  $\bar{T}$  and  $\bar{V}$ .

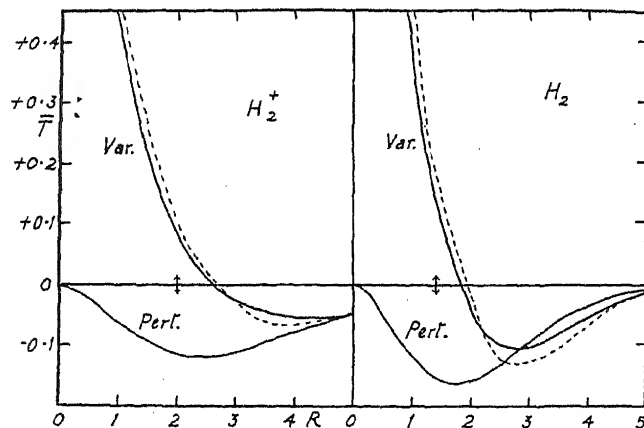


FIG. 3.

The extent of the errors involved can be seen from Table I, which compares the values of  $dE/dR$  and  $-(\bar{T} + E)/R$  derived from the perturbation functions: for a correct wave-function or for a wave-function which includes a scale-factor, these two quantities are equal (*cf.* equation (5)). Agreement is again bad except for large values of  $R$ .

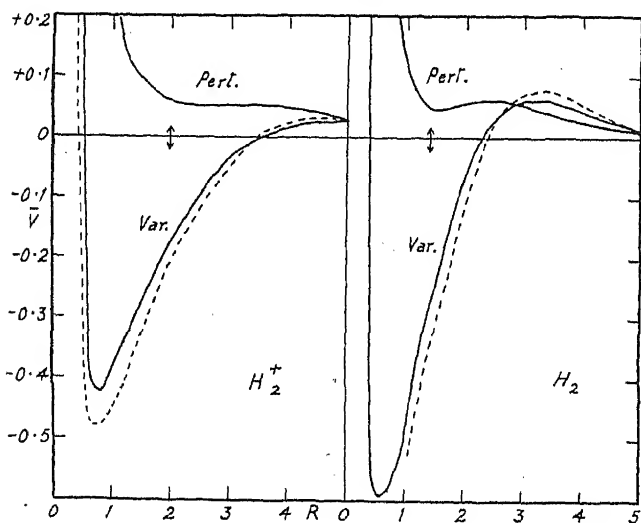


FIG. 4.

We have also carried out a few calculations with molecular orbital wave-functions for  $H_2$ , both with and without the introduction of a scale-factor. For moderate values of  $R$  the results differ only slightly from those of the corresponding electron-pair calculations, being a little less accurate. For large values of  $R$  where it is known that the approximations involved in molecular orbital wave-functions is invalid, the results are, of course, greatly in error.

TABLE I.—PERTURBATION WAVE-FUNCTIONS

$H_2^+$			$H_2$		
$R$	$dE/dR$	$-(\bar{T} + E)/R$	$R$	$dE/dR$	$-(\bar{T} + E)/R$
0.5	-3.751	-2.109	0.5	-3.7	-1.44
1.0	-0.732	-0.146	1.0	-0.55	+0.118
1.5	-0.209	+0.061	1.5	-0.049	+0.181
2.0	-0.054	+0.084	2.0	+0.058	+0.131
2.5	-0.001	+0.073	2.5	+0.066	+0.080
3.0	+0.019	+0.057	3.0	+0.048	+0.045
4.0	+0.022	+0.030	4.0	+0.016	+0.012
5.0	+0.014	+0.014	5.0	+0.004	+0.003

It should be emphasised that the satisfactory behaviour of the variation wave-functions is only obtained if the scale-factor is allowed to vary with  $R$ . The use of a

fixed scale factor would give satisfactory agreement for a particular value of  $R$ , but the variation of  $\bar{T}$  and  $\bar{V}$  with  $R$  would be misrepresented, as in the perturbation treatment. Fig. 5 shows the variation of  $E$ ,  $\bar{V}$  and  $\bar{T}$  with the scale-factor  $s$  for a fixed value of  $R$  near

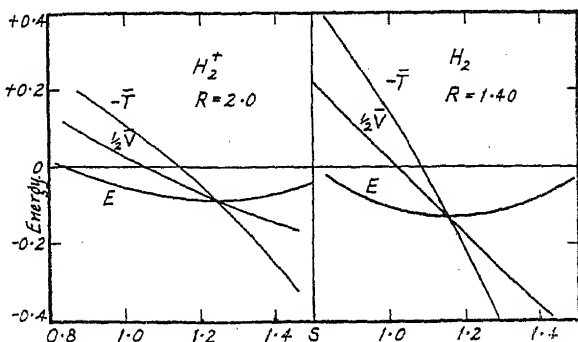


FIG. 5.

the equilibrium point. It will be seen that  $\bar{T}$  and  $\bar{V}$  are much more sensitive to small variations in  $s$  than is  $E$ .

### Summary.

1. The virial theorem is used to distinguish between the potential and kinetic energies associated with a molecular bond.

2. The relation between these two energies and the force on a nucleus is investigated, and certain inaccuracies in the literature are corrected.

3. It is shown that the virial theorem is automatically satisfied for all internuclear distances provided that a scale-factor, which varies with the internuclear distance, is included in the approximate wave-function. Unless the virial theorem is satisfied, the potential and kinetic energies are usually much more inaccurate than the total energy of the wave-function would lead one to suppose. The use of such improper wave-functions may easily lead to quite false conclusions.

4. These points are illustrated by detailed calculations for  $H_2^+$  and  $H_2$ , both in their ground state. It is possible here to compare the calculated values with those deduced from the observed spectrum.

University College, Dundee.  
Balliol College, Oxford.

# STATISTICAL THERMODYNAMICS OF THE SURFACE OF A REGULAR SOLUTION.

BY E. A. GUGGENHEIM.

Received 12th October, 1944.

## 1. Introduction.

Two recent papers, one by Schuchowitzky,<sup>1</sup> the other by Belton and Evans,<sup>2</sup> deal with the dependence of the surface tension of a binary mixture on its composition. In both these papers the essential assumption is that the difference in composition of the surface from the bulk is confined to a unimolecular layer.

Whereas both the papers mentioned above are concerned mainly, though not entirely, with binary *perfect* solutions, the present paper gives a detailed treatment by statistical mechanics of the surface of a binary *regular* solution. The technique used is the construction of the grand partition function as described by Fowler.<sup>3</sup>

## 2. Bulk Phase of Regular Solution.

It is convenient to begin by summarising briefly the assumed properties of a regular solution and quoting the relevant formulæ which will be required later. Only binary solutions will be considered, the two kinds of molecules being denoted by A and B respectively. A set of sufficient assumptions for a mixture of A and B molecules to be a regular solution has been stated by Fowler and Guggenheim.<sup>4</sup> The two most important of these assumptions are that every molecule whether A or B has the same number  $z$  of nearest neighbours and that the total intermolecular potential energy may be regarded as the sum of contributions from pairs of closest neighbours. A mixing energy  $w$  is defined such that if one starts with two pure liquids and interchanges an interior A molecule with an interior B molecule the total increase of potential energy is  $zw$ . Alternatively  $w/z$  may be defined as the excess potential energy of an AB pair of neighbours over the mean of the energies of an AA and a BB pair.

With this model of a regular solution the thermodynamic properties can be determined with various degrees of accuracy. The zeroth order approximation, which completely neglects deviations from complete randomness due to non-zero  $w$ , and called by Fowler and Guggenheim<sup>5</sup> the "crude treatment" will be used here. Let the molecular fractions of A and B in the mixture be  $x_A$  and  $x_B$ , so that  $x_A + x_B = 1$ . The partial potentials  $\mu_A$ ,  $\mu_B$  of Gibbs for the molecules A, B in the solution are then related to their values  $\mu_A^0$ ,  $\mu_B^0$  in the pure liquids by<sup>6</sup>

$$\mu_A = \mu_A^0 + kT \log x_A + x_B^2 w, \quad (2.1)$$

$$\mu_B = \mu_B^0 + kT \log x_B + x_A^2 w. \quad (2.2)$$

<sup>1</sup> Schuchowitzky, *Acta Physicochimica U.R.S.S.*, 1944, 19, 176.

<sup>2</sup> I was not aware of Schuchowitzky's paper until the present paper had already been submitted for publication. References to Schuchowitzky's paper have been inserted subsequently.

<sup>3</sup> Belton and Evans, *Trans. Faraday Soc.*, 1945, 41, 1.

<sup>4</sup> Fowler, *Proc. Camb. Phil. Soc.*, 1938, 34, 382.

<sup>5</sup> Fowler and Guggenheim, *Statistical Thermodynamics*, Cambridge University Press (1939), henceforth referred to as F. and G., § 814.

<sup>6</sup> F. and G., § 818.

Instead of the partial potentials  $\mu$  it will be convenient to make frequent use of the absolute activities <sup>6</sup>  $\lambda$  defined by

$$\mu = kT \log \lambda. \quad (2.3)$$

Corresponding to (2.1), (2.2) one has

$$\log \lambda_A = \log x_A \lambda_A^0 + x_B^2 w / kT, \quad (2.4)$$

$$\log \lambda_B = \log x_B \lambda_B^0 + x_A^2 w / kT, \quad (2.5)$$

where the superscript <sup>0</sup> refers to the value in the pure liquids.

### 3. Model for Surface.

I assume firstly that the molecules in the surface are packed in the same manner as in the bulk making the same contributions per pair of neighbours to the potential energy, and secondly that the difference in composition from that of the bulk is confined to a single layer of molecules at the surface. Consider now any molecule in the surface layer. Let the number of its neighbours in this layer be  $lz$  and the number of its neighbours in the next layer be  $mz$ , its total number of neighbours thus being  $(l + m)z$ . It is clear that the corresponding total number of neighbours of an interior molecule will be  $(l + 2m)z$ , but by definition this number is  $z$ . Consequently

$$l + 2m = 1. \quad (3.1)$$

In a simple cubic lattice  $z = 6$ ,  $l = 2/3$  and  $m = 1/6$ , while in a close packed lattice  $z = 12$ ,  $l = 1/2$  and  $m = 1/4$ .

### 4. Thermodynamic Functions of Pure Liquids.

Consider now a quantity of the pure liquid A containing  $N_A$  interior molecules and  $N'_A$  surface molecules. Molecular partition functions  $f_A$  and  $f'_A$  can be defined such that the total (Helmholtz) free energy  $F$  of the system has the form

$$F = -N_A kT \log f_A - N'_A kT \log f'_A. \quad (4.1)$$

The molecular partition function  $f_A$  will contain the factor  $\exp(\chi_A/kT)$ , while  $f'_A$  will contain the factor  $\exp([l + m]\chi_A/kT)$ , where  $\chi_A$  denotes the molecular energy of evaporation at the absolute zero. There may also be differences between  $f_A$  and  $f'_A$  in the factors for some of the rotational or vibrational degrees of freedom.

At ordinarily low pressures, when one may ignore the difference between the (Helmholtz) free energy  $F$  and the Gibbs' function  $G$ , the molecular (Helmholtz) free energy  $\mu_A$  in the bulk phase is effectively equal to the molecular partial potential  $\mu_A$  and consequently

$$\lambda_A^0 f_A = 1. \quad (4.2)$$

If the surface tension of the pure liquid A is  $\gamma_A$  and the surface area is  $A$ , then

$$\begin{aligned} \gamma_A A &= F - (N_A + N'_A) \mu_A \\ &= F - (N_A + N'_A) kT \log \lambda_A^0 \\ &= -N'_A kT \log \lambda_A^0 f'_A \\ &= N'_A kT \log (f_A / f'_A), \end{aligned} \quad (4.3)$$

or, if  $a$  denotes the area per molecule in the surface layer,

$$\gamma_A a = -kT \log \lambda_A^0 f'_A = kT \log (f_A / f'_A). \quad (4.4)$$

An analogous set of relations holds for the pure liquid B.

<sup>6</sup> F. and G., § 602.

Any one of formulæ (4.1), (4.3) or (4.4) may be regarded as defining the partition function  $f'_A$  of a molecule A in the surface of the pure liquid. My object in devoting so much space to the definition and properties of  $f'_A$  is to make it quite clear that when one comes to construct a partition function for a surface layer of a mixture, if a factor  $\exp(-w/zkT)$  is used for each AB contact, then the contributions of AA and BB contacts are correctly taken care of by using one  $f'_A$  factor for each A molecule in the surface layer and one  $f'_B$  factor for each B molecule in the surface layer.

### 5. Surface Layer of Mixture.

Consider a mixture of A and B, of molecular fractions  $x_A$  and  $x_B$  respectively, having the form of a cylinder or prism of cross-section  $\frac{1}{2}A$ . Imagine this to be sliced in two normal to its axis of symmetry, thus creating two new free surfaces each of area  $\frac{1}{2}A$ , the total area of the newly created surface thus being  $A$ . Let the number of molecules in a layer of area  $A$  be denoted by  $N'$ . Now imagine the whole of the new surface area  $A$  to be covered over with a fresh layer of  $N'$  molecules of which  $N'_A = x'_A N'$  are of type A and  $N'_B = x'_B N'$  of type B, so that  $x'_A + x'_B = 1$ .

Whenever I refer to a thermodynamic function of the surface layer, I shall mean the *excess of the function for the final system after covering with the new layer over that for the initial system before slicing in half*. I shall also denote by  $W$  the product of  $w/z$  and the excess number of AB contacts in the final system over the number in the initial system.

### 6. G.P.F. of Surface Layer.

The ordinary partition function of the surface layer as defined in the previous section is

$$\frac{N'!}{(x'_A N')! (x'_B N')!} (f'_A)^{x'_A N'} (f'_B)^{x'_B N'} e^{-W/kT} \quad (6.1)$$

I recall that  $f'_A, f'_B$  were defined in § 4 and  $W$  in § 5 in such a manner that all contributions to the intermolecular energy from AA and BB contacts as well as AB contacts are correctly included in (6.1).

The corresponding grand partition function  $\mathcal{E}$  is given by

$$\mathcal{E} = \sum_{x'_A, x'_B} \frac{N'!}{(x'_A N')! (x'_B N')!} (\lambda_A f'_A)^{x'_A N'} (\lambda_B f'_B)^{x'_B N'} e^{-W/kT} \quad (6.2)$$

where the summation extends over all values of  $x'_A$  and  $x'_B$  subject to

$$x'_A + x'_B = 1 \quad (6.3)$$

Using an approximation equivalent to Stirling's theorem, since  $N'$  is very large, one can with sufficient accuracy replace (6.2) by

$$\mathcal{E} = \sum_{x'_A, x'_B} \left( \frac{\lambda_A f'_A}{x'_A} \right)^{x'_A N'} \left( \frac{\lambda_B f'_B}{x'_B} \right)^{x'_B N'} e^{-W/kT} \quad (6.4)$$

where the summation is subject to (6.3).

It is now necessary to express  $W$  as the correct multiple of  $w/z$ . Using the zeroth ("crude") approximation mentioned in § 2, one assumes complete randomness in the surface layer as in the bulk. In the slicing process described in § 5 the number of AB contacts destroyed, assuming complete randomness, would be  $\frac{1}{2}mzN'(x_A x_B + x_B x_A)$ ; thus the number *created* would be

$$- \frac{1}{2}mzN'(x_A x_B + x_B x_A) \quad (6.5)$$

In covering the newly formed surface with a new layer of  $N'$  molecules, again assuming complete randomness, the number of AB contacts created within the new layer is

$$lzN'x'_A x'_B \quad (6.6)$$

and the number created between the new layer and the underlying layer is

$$mzN'(x'_A x_B + x'_B x_A). \quad (6.7)$$

Adding (6.5), (6.6) and (6.7) one thus obtains for the net increase in the number of AB contacts

$$zN'\{lx'_A x'_B + m(x'_A x_B + x'_B x_A - x_A x_B)\}. \quad (6.8)$$

Multiplying this by  $w/z$  one obtains for  $W$

$$W = N'w\{lx'_A x'_B + m(x'_A x_B + x'_B x_A - x_A x_B)\}. \quad (6.9)$$

In view of (6.3) and the analogous relation between  $x_A$  and  $x_B$ , one can replace (6.9) by the equivalent

$$W = N'wx'_A(lx_B'^2 + mx_B^2) + N'wx'_B(lx_A'^2 + mx_A^2). \quad (6.10)$$

The reason for preferring the form (6.10) to (6.9) will appear later.

Substituting from (6.10) into (6.4), one obtains finally for the grand partition function

$$\begin{aligned} \mathcal{E} = \sum_{x'_A, x'_B} [\lambda_A f'_A \exp \{- (lx_B'^2 + mx_B^2)w/kT\}/x'_A]^{x'_A N'} \\ \times [\lambda_B f'_B \exp \{- (lx_A'^2 + mx_A^2)w/kT\}/x'_B]^{x'_B N'}, \end{aligned} \quad (6.11)$$

where the summation is over all  $x'_A, x'_B$  subject to (6.3).

## 7. Maximisation.

As usual one may with sufficient accuracy replace  $\mathcal{E}$  by its maximum term  $\mathcal{E}^*$ . Differentiating  $\mathcal{E}$  with respect to  $x'_A$  and  $x'_B$ , subject to  $dx'_A + dx'_B = 0$ , and equating to zero one obtains

$$\begin{aligned} \mathcal{E}^* &= [\lambda_A f'_A \exp \{- (lx_B'^2 + mx_B^2)w/kT\}/x'_A]^{x'_A N'} \\ &= (\lambda_B f'_B \exp \{- (lx_A'^2 + mx_A^2)w/kT\}/x'_B)^{x'_B N'}. \end{aligned} \quad (7.1)$$

In other words the condition of maximisation is that the two factors within the square brackets [ ] in (6.11) should be equal to each other.

Taking logarithms and multiplying by  $-kT$  one obtains from (7.1)

$$\begin{aligned} -kT \log \mathcal{E}^* &= N'kT \log \frac{x'_A}{\lambda_A f'_A} + N'w(lx_B'^2 + mx_B^2) \\ &= N'kT \log \frac{x'_B}{\lambda_B f'_B} + N'w(lx_A'^2 + mx_A^2). \end{aligned} \quad (7.2)$$

## 8. Surface Tension.

At negligible pressures there is an extremely simple relation between the grand partition function of the surface layer and the surface tension  $\gamma$ , namely

$$\gamma A = -kT \log \mathcal{E} \simeq -kT \log \mathcal{E}^*. \quad (8.1)$$

Using (7.2) and introducing the area per molecule  $a = A/N'$  one obtains

$$\begin{aligned} \gamma a &= kT \log \frac{x'_A}{\lambda_A f'_A} + w(lx_B'^2 + mx_B^2) \\ &= kT \log \frac{x'_B}{\lambda_B f'_B} + w(lx_A'^2 + mx_A^2). \end{aligned} \quad (8.2)$$



Substituting for  $\lambda_A$ ,  $\lambda_B$  from (2.4), (2.5) into (8.2), using (4.2) and (3.1), one obtains

$$\begin{aligned}\gamma a &= kT \log \frac{x'_A f_A}{x_A f'_A} + w l (x_B'^2 - x_B^2) - w m x_B^2 \\ &= kT \log \frac{x'_B f_B}{x_B f'_B} + w l (x_A'^2 - x_A^2) - w m x_A^2. \quad (8.3)\end{aligned}$$

By comparison of (8.3) with formula (4.4) for the surface tension  $\gamma_A$  of the pure liquid A and the analogous formula for  $\gamma_B$ , one finds

$$\begin{aligned}\gamma &= \gamma_A + \frac{kT}{a} \log \frac{x'_A}{x_A} + \frac{w}{a} l (x_B'^2 - x_B^2) - \frac{w}{a} m x_B^2 \\ &= \gamma_B + \frac{kT}{a} \log \frac{x'_B}{x_B} + \frac{w}{a} l (x_A'^2 - x_A^2) - \frac{w}{a} m x_A^2. \quad (8.4)\end{aligned}$$

Equations (8.4) together with (6.3) form a set of 3 simultaneous equations determining  $x'_A$ ,  $x'_B$  and  $\gamma$  in terms of  $x_A$ ,  $x_B$ ,  $\gamma_A$  and  $\gamma_B$ .

### 9. Surface Tension of Perfect Solution.

In the special case when the mixing energy  $w$  is zero the regular solution becomes a perfect solution and formula (8.3) simplifies to

$$e^{-\gamma a/kT} = \frac{x_A f'_A}{x'_A f_A} = \frac{x_B f'_B}{x'_B f_B} = x_A \frac{f'_A}{f_A} + x_B \frac{f'_B}{f_B}. \quad (9.1)$$

By using (4.4) this can be transcribed as

$$e^{-\gamma a/kT} = x_A e^{-\gamma_A a/kT} + x_B e^{-\gamma_B a/kT}, \quad (9.2)$$

which is perhaps the most instructive form for the dependence of  $\gamma$  on composition in a perfect solution. It is surprising that neither Schuchowitzky nor Belton and Evans give this form of the mixing law for the surface tensions of perfect solutions, but only less symmetrical forms equivalent to it.

In an equimolecular mixture  $x_A = x_B = \frac{1}{2}$  and (9.2) can be transformed to

$$\gamma = \bar{\gamma} - \frac{kT}{a} \log \cosh (\Delta a/2kT) \quad (x_A = x_B = \frac{1}{2}), \quad (9.3)$$

where

$$\bar{\gamma} = \frac{1}{2}(\gamma_A + \gamma_B), \quad \Delta = \gamma_B - \gamma_A. \quad (9.4)$$

Since for liquids forming perfect solutions with each other  $\Delta/\bar{\gamma}$  is unlikely to exceed 0.1, one may usually with sufficient accuracy replace (9.3) by

$$\gamma = \bar{\gamma} - \frac{\Delta a}{8kT} \quad (x_A = x_B = \frac{1}{2}), \quad (9.5)$$

obtained by replacing  $\log \cosh (\Delta a/2kT)$  by the first term of its expansion as a power series.

### 10. Other Thermodynamic Functions.

Following Gibbs one defines the various thermodynamic functions of a surface as the excess for the actual system over an idealised system in which composition and densities (of matter, energy and entropy) are imagined to remain homogeneous right up to a hypothetical geometrical surface parallel to the interface. When this hypothetical geometrical surface is shifted normal to the interface, the values of the thermodynamic functions associated with the surface become altered, but the important relations between these functions remain invariant.<sup>8</sup> Among these rela-

<sup>8</sup> Cf. Guggenheim and Adam, *Proc. Roy. Soc., A*, 1933, 139, 218.

tions are the following, valid at constant temperature and at negligible pressure.

$$dF^S = \gamma dA + \mu_A dN_A^S + \mu_B dN_B^S \\ = \gamma dA + kT \log \lambda_A dN_A^S + kT \log \lambda_B dN_B^S, \quad (10.1)$$

$$F^S = \gamma A + \mu_A N_A^S + \mu_B N_B^S \\ = \gamma A + N_A^S kT \log \lambda_A + N_B^S kT \log \lambda_B \\ = N_A^S F_A^S + N_B^S F_B^S, \quad (10.2)$$

$$F_A^S = \gamma a + \mu_A = \gamma a + kT \log \lambda_A, \quad (10.3)$$

$$F_B^S = \gamma a + \mu_B = \gamma a + kT \log \lambda_B, \quad (10.4)$$

$$-d\gamma = \frac{N_A^S}{A} d\mu_A + \frac{N_B^S}{A} d\mu_B = \frac{N_A^S}{A} kT d \log \lambda_A + \frac{N_B^S}{A} kT d \log \lambda_B. \quad (10.5)$$

The superscript S has been attached to functions associated with the surface to distinguish from those associated with the bulk phase. It has not been attached to  $\gamma$  and  $A$  since these quantities cannot be associated with a bulk phase; nor to  $\mu$  and  $\lambda$  since these have the same value in the surface as in the bulk phase. In particular  $F^S$  denotes the free energy of the surface and  $F_A^S, F_B^S$  the corresponding partial molecular free energies in the surface. Since the pressure is assumed negligible the Gibbs function  $G$  is indistinguishable from the (Helmholtz) free energy  $F$ . In formulæ (10.3), (10.4) I have used the same symbol  $a$  for the partial molecular area of either A or B because in the present model they are assumed equal; it would generally be more correct to write  $a_A$  in (10.3) and  $a_B$  in (10.4).

To correlate the formulæ of the previous sections with those associated with Gibbs' geometrical surface, it is most convenient to place this immediately to the inner side of the outermost unimolecular layer. This leads to

$$N_A^S = N'_A = \kappa'_A N', \quad N_B^S = N'_B = \kappa'_B N'. \quad (10.6)$$

One can then deduce from (8.2), (10.3) and (10.4)

$$F_A^S = kT \log \frac{\kappa'_A}{f'_A} + w(l\kappa_B'^2 + m\kappa_B'^2), \quad (10.7)$$

$$F_B^S = kT \log \frac{\kappa'_B}{f'_B} + w(l\kappa_A'^2 + m\kappa_A'^2). \quad (10.8)$$

$$\frac{F^S}{N'} = \kappa'_A kT \log \frac{\kappa'_A}{f'_A} + \kappa'_B kT \log \frac{\kappa'_B}{f'_B} \\ + w(l\kappa'_A \kappa'_B + m\kappa'_A \kappa_B'^2 + m\kappa'_B \kappa_A'^2). \quad (10.9)$$

If Gibbs' geometrical is placed elsewhere, the relations between  $N_A^S, N_B^S$  on the one hand and  $N'_A, N'_B$  on the other become altered and all the thermodynamic functions become correspondingly modified, but  $\gamma$  remains invariant.

## 11. Comparison with Experiment.

The theoretical formulæ for perfect solutions have already been compared with experiment by Schuchowitzky<sup>1</sup> and by Belton and Evans;<sup>2</sup> the agreement is reasonably good. Unfortunately I do not know of any pair of liquids forming a regular solution for which accurate experimental data are available for both the surface tensions and the heat of mixing, which determines  $w$ . I therefore postpone any attempt to compare my more general formulæ with experiment.

**Summary.**

The grand partition function is constructed for a binary regular solution on the assumption that the difference in composition of the surface from the bulk is confined to a unimolecular layer. From this the dependence of the surface tension on the composition is deduced.

*Imperial College,  
London.*

## A SIMPLE SINGLE-WIRE SURFACE PRESSURE BALANCE.

BY KENNETH G. A. PANKHURST.

*Received 28th December, 1944.*

In the course of some work on monolayers just before the war, a single-wire surface pressure balance was designed and used for high and low surface pressure measurements.

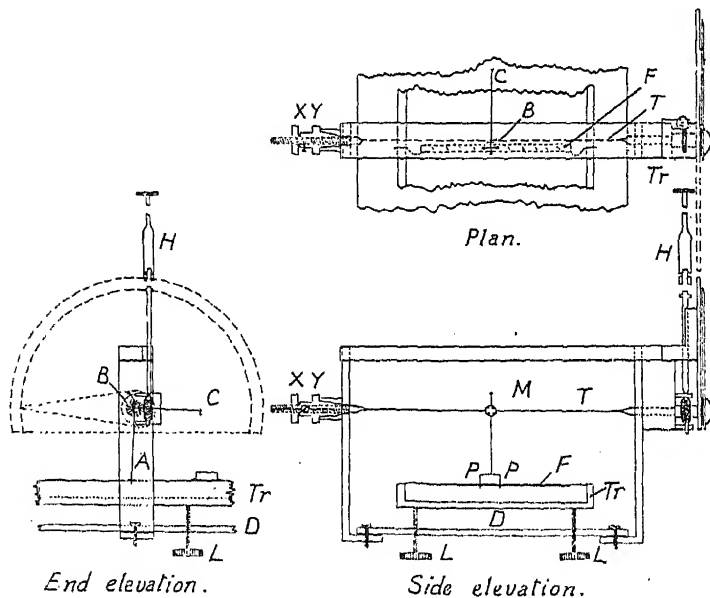


FIG. 1.

Although several single-wire instruments have been used by various workers, this particular design was capable of a sensitivity of *ca.* 0.01 dyne/cm., which is believed to be much greater than that hitherto achieved by such instruments and compared favourably with Adam and Jessop's sensitive two-wire design.<sup>1</sup> A few details of its construction have already been given,<sup>2</sup> but some further information may be of use to those wishing to construct a simple yet sensitive surface pressure balance.

Fig. 1 is a detailed diagram of the instrument which has a phosphor-

<sup>1</sup> Adam, *The Physics and Chemistry of Surfaces*, Oxford, 1938, 2nd ed., pp. 29 ff.

<sup>2</sup> Pankhurst, *Proc. Roy. Soc., A*, 1942, **179**, 393.

bronze torsion wire, T, *ca.* 20 cm. long and situated some 5 cm. above the surface of the liquid. The mirror, M, indicating the position of the float, is mounted at the centre of this wire. Some sensitivity is lost through the mirror being further from the surface than when mounted on a lower wire, but this is offset by an increase in length of torsion wire of about 50 per cent. A paraffin-coated mica float, F, separates the clean from the film-covered surface, the ends being joined to the sides of the trough by silk threads *lightly* vaselined or paraffined, as used by Guastalla,<sup>3</sup> making a film-tight seal. A light framework, ABC, soldered on to the torsion wire carries a holder for the mirror at B, and has two prongs, P, which are a *slightly* loose fit in two holes in the float. The wire can be tensioned and its torsional zero adjusted by two concentric cones, X and Y, at one end; the torsion applied to balance the surface pressure on the float being measured by a torsion head, operated through a worm gear by a vertical detachable insulated handle, H. Calibration was effected in the usual way by hanging a weight from C. The torsion wire which governs the sensitivity of the instrument is readily replaced with a soldering iron. For normal use a wire 0.20 mm. diameter was used, giving a sensitivity of *ca.* 0.20 dyne/cm./degree twist. For low pressure work this was replaced by one 0.11 mm. diameter, thereby increasing the sensitivity to about 0.019 dyne/cm./degree.

The machine was screwed on to a base plate, D, *ca.* 65 cm. long and 20 cm. wide, which was supported on three levelling screws (not shown in Fig. 1). The trough, Tr, is also supported on three levelling screws, L, which operate through the base plate. Air currents must be carefully avoided, especially for low pressure work. Adequate protection was given by the large Faraday cage necessary for the electrical shielding of the apparatus when surface potentials are measured and in which the apparatus is normally used.

The *modus operandi* was essentially that described by Adam.<sup>1</sup> The size of trough need not be rigidly standardised, although a long narrow type is desirable (*ca.* 60 cm.  $\times$  14 cm.  $\times$  1.5 cm. internal dimensions). The whole apparatus was made of brass which was nickel plated, with the exception of the trough which was of fused silica to enable surface potentials to be measured concurrently. The nickel plating, however, is a non-essential refinement.

My thanks are due to Professor N. K. Adam, F.R.S., for his interest and useful suggestions, and to Mr. G. W. Alliss who constructed the instrument.

*The Department of Chemistry,  
Chelsea Polytechnic, London, S.W.3.*

<sup>3</sup> Guastalla, C.R. *Acad. Sci.*, Paris, 1929, 189, 241.

---

## THE ABSORPTION SPECTRUM OF METHYLGLYOXAL.

BY SHO-CHOW WOO AND SZE-TSENG CHANG.

(Communicated by JOSEPH NEEDHAM, F.R.S.)

Received 22nd January, 1945.

### Introduction.

It is well known that organic compounds containing one C=O group, or more such groups not in conjugated positions, all show a characteristic absorption maximum in the near ultraviolet, *e.g.* aldehydes, ketones and acids give maxima at  $\lambda$ 2900, 2700 and 2100  $\mu$ . respectively; while some

of the compounds containing one  $\text{—}\overset{\text{O}}{\parallel}\text{C—}\overset{\text{O}}{\parallel}\text{C—}$  group, *e.g.* glyoxal and diacetyl,<sup>1</sup> show an additional absorption maximum at 4000-4500 Å. The origin and electronic transitions of these absorption maxima have been recently explained by McMurry and Mullikan; and McMurry.<sup>2</sup> But most of the latter class of compounds so far investigated spectroscopically have been dialdehydes and diketones. Methylglyoxal is perhaps the only  $\alpha$ -ketonic aldehyde whose ultra-violet absorption spectrum has ever been studied.<sup>3</sup> But unfortunately, even here, the investigation is not sufficiently thorough. For example, it has been investigated only in aqueous solution and no maximum found at 4000-4500 Å. Besides, the results obtained by different authors do not agree very well, which might be due to impure material used for investigation and inaccurate methods of quantitative determination.

It was thought that the absence of the longer wave-length maximum as given by previous investigators might probably be due to complications involved in the aqueous solution. From a review of the literature, especially by Harries, Meisenheimer, Fischer, Riley and their collaborators,<sup>4</sup> it can be seen that the chemical study of methylglyoxal is complicated by (1) its great affinity for water, mono- and semi-hydrates having been found and the last  $\frac{1}{4}$  H<sub>2</sub>O being removable only with difficulty; (2) its great ease of polymerisation, polymers, (CH<sub>3</sub>COCHO)<sub>n</sub> with *n* = 2, 3, 4 and  $\infty$  having been reported; (3) its polymerisation being catalysed by traces of water; and (4) its tendency to enolise. All these complications would certainly affect the characteristics of the spectrum, as seen from the cases of aldehydes,<sup>5</sup> pyruvic acid<sup>6</sup> and other tautomeric compounds.<sup>7</sup> It was the purpose of the present work to detect the existence of the predicted absorption maximum at 4000-4500 Å., to measure the molecular extinction coefficients in non-aqueous solutions of the anhydrous monomer and to study the effects of water, alcohol, etc., on the characteristics of the spectrum and hence the structure of the molecule.

### Experimental.

**Materials.**—The methylglyoxal used in this investigation was prepared by the method of Riley, Morley and Friend,<sup>4</sup> the higher boiling point portion after further purification by vacuum distillation being used for the preparation of solutions.\* But the non-aqueous solutions so prepared also did not show the required longer wave-length maximum. This was probably due to the fact that the compound existed in these solutions as hydrates. Following Meisenheimer, we prepared the partially dehydrated solutions in acetone and ether by drying them for days with

<sup>1</sup> Luethy, *Z. physikal. Chem.*, A, 1923, 107, 285.

<sup>2</sup> McMurry and Mullikan, *Proc. Nat. Acad. Sci.*, 1940, 26, 312; McMurry, *J. Chem. Physics*, 1941, 9, 231; 1941, 9, 241.

<sup>3</sup> Neuberg and Schou, *Biochem. Z.*, 1927, 191, 466; Fischler, Hauss and Tauler, *ibid.*, 1930, 227, 156; Marchlowski, Pizlo and Urbanczyk, *ibid.*, 1933, 264, 437.

<sup>4</sup> (a) Meisenheimer, *Ber.*, 1912, 45, 2635; (b) Fischler and Taube, *ibid.*, 1924, 57, 1502; 1926, 59, 851; (c) Riley, Morley and Friend, *J. Chem. Soc.*, 1932, 1875; (d) Moulds and Riley, *ibid.*, 1938, 621. For other references see <sup>4(a)</sup>.

<sup>5</sup> (a) Luethy, *Compt. rend.*, 1923, 176, 1547; (b) Schou, *ibid.*, 1926, 182, 965; 1927, 184, 1452; (c) Wolf and Herold, *Z. physikal. Chem.*, B, 1929, 5, 124; B, 1931, 12, 165.

<sup>6</sup> Henri and Fromageot, *Bull. Soc. Chim.*, 1925, 37, 845; Fromageot and Perraud, *Biochem. Z.*, 1930, 223, 213; Fromageot, Pelletier and Ehrenstein, *Bull. Soc. Chim.*, 1932, 51, 1283.

<sup>7</sup> See, *e.g.*, Lowry, Mouren and MacConkey, *J. Chem. Soc.*, 1928, 3167.

\* The authors want to express their sincere thanks to Drs. S. T. Yang and C. H. Kao of the Department of Chemistry, South Western Associated University, for their kindness in giving them the selenium required in the preparation.

strongly ignited calcium chloride and after filtration distilling off the solution. The solutions so obtained did show a weak absorption in the required wave-length region. For the measurement of the molecular extinction coefficients it is, however, necessary to have the anhydrous monomeric compound which, as pointed out by Moulds and Riley, can be obtained only with difficulty. The method of Meisenheimer, and of Fischer and Taube, of distilling the partially dehydrated compound *in vacuo*, passing its vapour over calcium chloride and condensing it at liquid-air temperature could not be used here on account of the lack of equipment and, moreover, the loss by this distillation may be considerable. Thus we had to be content with the preparation of its anhydrous solutions, which was accomplished as follows.

Riley, Morley and Friend found that methylglyoxal forms an azeotropic mixture with acetone, and we have also found that it is volatile with ether and chloroform. Hence instead of passing its vapour alone over  $\text{CaCl}_2$ , which is essential for complete dehydration, we may use ether, acetone or chloroform as the carrier of its vapour, so that the boiling-point and viscosity of the liquid may be greatly decreased. This greatly facilitated the operation and minimised the loss. The special apparatus used for this purpose is shown in Fig. 1. The solution of methylglyoxal in acetone, ether or chloroform was delivered into the flask through A. Upon heating, the mixed vapour passed through tube B where it was dehydrated by the freshly ignited calcium chloride. The condensed mixture returned to the flask through C. After one or two hours' reflux, the mixture was distilled by replacing C and B respectively with a cork and a tube like B containing anhydrous  $\text{CaCl}_2$ . As shown by their spectrum, the solutions so obtained must have reached their anhydrous state.

The solvents, acetone, ether and chloroform, used were respectively of Merck (*pro analysi*), Squibb (for anesthesia), and Mallinckrodt (for anesthesia) grades. They were further purified by the usual method of dehydration and redistillation. They were prepared just before use.

#### Quantitative Determination of Methylglyoxal.—

For the quantitative determination of methylglyoxal we have tried several methods, but only Friedemann's method<sup>8</sup> gave consistent results. The method of Fischler and Boettner,<sup>9</sup> though sometimes self-consistent, gave lower results. Since both of these methods were considered quantitative by these authors only because they gave self-consistent results for certain samples of methylglyoxal solution, the concentrations of which, however, were not definitely determined by some other reliable methods, their validity had still to be examined. By comparing the determined quantities with weighed amounts of pure phenylglyoxal mono-hydrate, we have proved the quantitateness of Friedemann's method to within 1% of error. The only drawback we found in this method was that when  $\text{H}_2\text{O}_2$  was used the methylglyoxal solution acquired a yellow colour which made the end point somewhat inaccurate. From a systematic study we also proved the incompleteness of the Fischler-Boettner method, and from this have worked out a new method which agrees very well with that of Friedemann.

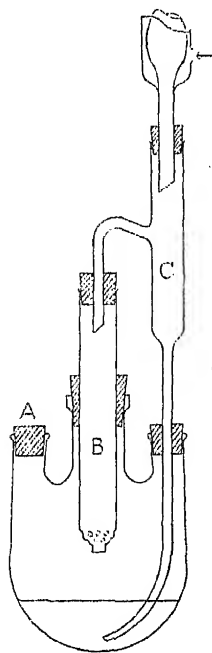


FIG. 1.

<sup>8</sup> Friedemann, *J. Biol. Chem.*, 1927, **73**, 331.

<sup>9</sup> Fischler and Boettner, *Z. analyt. Chem.*, 1928, **74**, 28.

**Measurement of Extinction Coefficients.**—The extinction coefficients were determined with a Hilger Spekker photometer and a medium quartz spectrograph, using a tungsten steel spark as the light source. Since it was found that the extinction coefficients at the longer wave-length maximum decreased with time, the spectrograms must be obtained as soon as possible after the preparation of the solutions. For chloroform solutions it was sometimes found necessary to reflux the solution immediately before the measurement.

The effect of water on the spectrum was determined by measuring the change of extinction coefficients of the longer wave-length maximum at intervals from 3 minutes to 2 hours after the addition of a definite quantity of water to the acetone solution, until it was found that they practically remained constant within these intervals.

The effect of alcohol has also been studied in the same manner as that of water. It was found that the extinction coefficients decreased continuously and hence no steady value could be obtained.

In order to study whether the decrease of extinction coefficients was due to absorption of atmospheric moisture, photochemical change or polymerisation, or all three, an acetone solution of the anhydrous compound was preserved in a dark place in a small flask with its glass stopper sealed with wax and after nine months its extinction coefficients were measured again.

### Results and Discussion.

The results of the extinction coefficient measurements are represented in the curves of Fig. 2 where those for pure acetone (curve 1) and diacetyl in hexane (curve 2) are also reproduced for comparison.

It will be seen that the spectra of all the methylglyoxal solutions show the same ketone characteristic absorption maximum at  $\lambda 2700\text{--}2800\text{ \AA.}$  with only slight modifications, while that of its aqueous solution (curve 6)

does not show the  $\begin{array}{c} \text{O} \quad \text{O} \\ \parallel \quad \parallel \\ \text{—C—C—} \end{array}$  characteristic maximum at  $\lambda 4000\text{--}4500\text{ \AA.}$  at all. That the absence of this maximum is chiefly due to the hydration of the methylglyoxal molecule is definitely shown by the fact that the maximum appeared as soon as the acetone (curve 3') and ether (curve 4') solutions were partially dehydrated, and also that as shown by Moulds and Riley, methylglyoxal is monomeric in aqueous solution. Moreover, the hydration must have taken place at the aldehyde group, since it has been shown by different investigators<sup>6</sup> that the intensity of the  $\text{=C=O}$  maximum is decreased considerably by water for aldehydes but not for ketones. Among the most prominent cases are formaldehyde in water, and chloral-hydrate, where this maximum disappears completely; and glyoxal in water where both this and the longer wave-length one vanish entirely. With two hours of refluxing in our specially designed apparatus we have brought the molecular extinction coefficient of the acetone and ether solutions of methylglyoxal to a value of  $\log \epsilon = 1.14$  at  $\lambda 425$  and  $440\text{ m}\mu$  respectively. Since the values for glyoxal and diacetyl in hexane are respectively  $\log \epsilon = 0.55$  at  $\lambda 464\text{ m}\mu$ ,  $0.45$  at  $\lambda 450\text{ m}\mu$ ,  $0.38$  at  $\lambda 431\text{ m}\mu$  and  $\log \epsilon = 1.31$  at  $\lambda 450\text{ m}\mu$ ,  $1.28$  at  $\lambda 442\text{ m}\mu$ ,  $1.29$  at  $\lambda 423\text{ m}\mu$ , it is reasonable to suppose that the value for methylglyoxal given above actually represents the molecular extinction coefficient of the anhydrous compound.

When a small quantity of water was added to the acetone solution of methylglyoxal, the extinction coefficients of the  $\lambda 4300\text{ \AA.}$  maximum increased somewhat. But since acetone itself also gives the latter maximum, a maximum also somewhat affected by the addition of water,<sup>10</sup> and since our solution was so dilute in methylglyoxal ( $0.0891\text{ M.}$ ), it was not possible to calculate the effect on methylglyoxal alone. After the

<sup>10</sup> Ley and Arends, *Z. physikal. Chem., B*, 1931, 12, 132.

addition of water, the extinction coefficients reached their steady values almost instantaneously. Assuming the  $\lambda_{4300 \text{ \AA}}$  maximum as solely due

to the  $\begin{array}{c} \text{O} \quad \text{O} \\ \parallel \quad \parallel \\ -\text{C}-\text{C}- \end{array}$  group, which is probably the case, we can calculate the effective concentrations of molecules containing this group from the

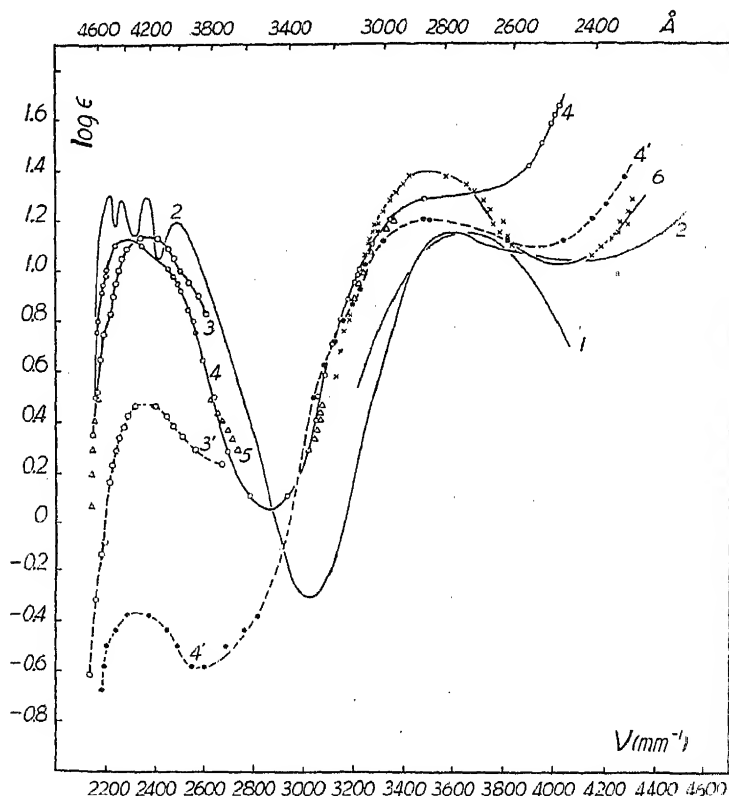


FIG. 2.

1.	—	$\text{CH}_3\text{COCH}_3$	Pure.
2.	—	$\text{CH}_3\text{COCOCH}_3$	In hexane.
3.	○—○	$\text{CH}_3\text{COCHO}$	In acetone (0.0891 m.).
3'.	○—○	$\text{CH}_3\text{COCHO}$	In acetone, partially dehydrated (0.2053 m.).
4.	○—○	$\text{CH}_3\text{COCHO}$	In ether (0.3148 m.).
4'.	●—●	$\text{CH}_3\text{COCHO}$	In ether, partially dehydrated (0.7631 m.?, detd. as semicarbazone).
5.	△—△	$\text{CH}_3\text{COCHO}$	In chloroform, ordinarily dried and de- polymerised (0.1025 m.).
6.	X—X	$\text{CH}_3\text{COCHO}$	In water (0.0635 m.).

extinction coefficients. Thus, according to Lambert-Beer's law, we have the molecular coefficient  $\epsilon$  at a certain wave-length  $\lambda$  given by

$$\begin{aligned} \epsilon_\lambda &= 1/cl (\log I_0/I)_\lambda = 1/cK_\lambda \\ &= 1/c'l' (\log I_0/I')_\lambda = 1/c'K'_\lambda, \end{aligned}$$



where  $c$ ,  $l$ ,  $K_\lambda$  and  $c'$ ,  $l'$ ,  $K'_\lambda$  are the concentrations, absorption lengths and extinction coefficients of the original and diluted solutions respectively. Hence by measurement of the extinction coefficients  $K'_\lambda$  for the diluted solution we calculate its effective concentration  $c'$  from the molecular extinction coefficients  $\epsilon$  which have been determined from the known original concentration  $c$  and extinction coefficients  $K_\lambda$ . The concentrations so obtained without correction for dilution are plotted in Fig. 3,

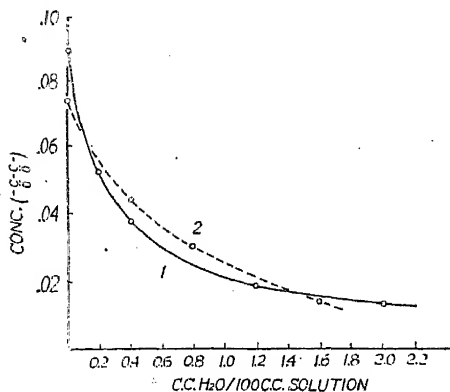


FIG. 3.

will be discovered. Besides, the catalysis of polymerisation and depolymerisation respectively by traces or large amounts of water may make the system even more complicated. It is obvious that a determination of the concentration of only one of the molecular species in it is not sufficient to elucidate the complicated mechanism of such a system.

This can also be seen from the fact that the  $\text{—}\overset{\text{O}}{\parallel}\text{C—}\overset{\text{O}}{\parallel}\text{C—}$  concentration determined for the same solution after being allowed to stand in an ordinary reagent bottle for one day dropped apparently from 0.0891 to 0.0737  $m\mu$ , not following the same curve (see curve 3) as the original.

Wolf and Herold<sup>(6)</sup> have investigated the effect of water and alcohol on the spectra of saturated aldehydes. They found that the extinction coefficients at the  $\lambda_{2900}$  A. maximum decreased immediately to a constant value after the aldehyde is mixed with water but only gradually after it was mixed with alcohol, an equilibrium value being established after one day. From the rate of the decrease of free aldehyde concentration they could determine the rate of formation of semiacetal and acetal. Our results on the effect of water and alcohol on methylglyoxal showed the

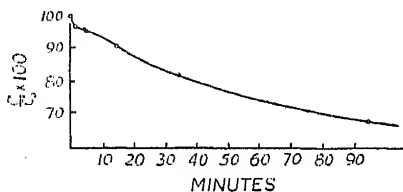


FIG. 4.

same characteristics. The variation of the  $\text{—}\overset{\text{O}}{\parallel}\text{C—}\overset{\text{O}}{\parallel}\text{C—}$  concentration (corrected for dilution) with time after the addition of 0.4 c.c.  $\text{C}_2\text{H}_5\text{OH}$  to 100 c.c. of 0.0890  $m\mu$  methylglyoxal solution is given in Fig. 4. It will be seen that this curve has the same form as those obtained by Wolf and Herold for saturated aldehydes and shows between 3-10 minutes an inflection which according to Wolf and Herold signifies the change of rate of concentration decrease by the formation of acetal from semiacetal.

After nine months' preservation in a wax-sealed flask in a dark place,

the concentration of  $\begin{array}{c} \text{O} \quad \text{O} \\ \parallel \quad \parallel \\ -\text{C}-\text{C}- \end{array}$  decreased from 0.0891 m. to 0.0293 m.

This indicates that the decrease of the  $\begin{array}{c} \text{O} \quad \text{O} \\ \parallel \quad \parallel \\ -\text{C}-\text{C}- \end{array}$  concentration must be partly due to polymerisation.

### Summary.

(1) The existence of the  $\lambda_{4300}$  A. absorption maximum due to the conjugated carbonyl groups has been proved for anhydrous methylglyoxal in non-aqueous solvents.

(2) A new method for the preparation of anhydrous methylglyoxal in non-aqueous solvents has been described.

(3) The molecular extinction coefficient of the  $\lambda_{4300}$  A. maximum for anhydrous methylglyoxal has been found to be:  $\text{CH}_3\text{COCHO}$  in acetone,  $\log \epsilon = 1.14$  at  $\lambda_{425}$  m $\mu$ , and in ether  $\log \epsilon = 1.14$  at  $\lambda_{440}$  m $\mu$ .

(4) The decrease of the  $\begin{array}{c} \text{O} \quad \text{O} \\ \parallel \quad \parallel \\ -\text{C}-\text{C}- \end{array}$  concentration with the addition of water to the acetone solution of methylglyoxal is regarded primarily as due to the hydration of the aldehyde group.

(5) The decrease of the  $\begin{array}{c} \text{O} \quad \text{O} \\ \parallel \quad \parallel \\ -\text{C}-\text{C}- \end{array}$  concentration with the addition of alcohol to the acetone solution of methylglyoxal is regarded as due to the formation of semi-acetal and acetal.

*The Institute of Chemistry, Academia Sinica,  
Kunming, China.*

## THE ADAPTATION OF *BACT. LACTIS AEROGENES* TO VARYING CONCENTRATIONS OF AN ANTIBACTERIAL DRUG (PROFLAVINE).

BY D. S. DAVIES, C. N. HINSELWOOD AND J. M. PRYCE.

*Received 18th November, 1944.*

In a previous paper<sup>1</sup> we described qualitative and quantitative observations on the adaptation of *Bact. lactis aerogenes* to resist the antibacterial action of three basic dyes, proflavine, methylene blue and crystal violet, each used at a single concentration. The effects described were explained in terms of the hypothesis that the dye interferes with the operation, but not the synthesis, of a certain member of a series of enzymes responsible for the utilisation of the foodstuffs in cell growth. The growth of other enzymes, dependent on substances in consequent short supply, is retarded and this hinders the growth of the cell as a whole. The rate of synthesis of the inhibited enzyme is, however, not affected, with the result that this enzyme expands in relation to the rest of the cell. This expansion serves to compensate for its decreased activity in the presence of the drug, so that the total output per cell of the essential products returns to the normal level.

One consequence of this assumption is that the precise degree of adjustment of the enzyme balance, *i.e.* the degree of adaptation, should depend upon the extent to which the enzyme has been inhibited. This,

<sup>1</sup> Davies, Hinshelwood and Pryce, *Trans. Faraday Soc.*, 1944, 40, 397.

in turn, should be determined by the drug concentration at which training has been carried out, so that the modified cells should possess an immunity quantitatively related to the training concentration. What follows is a theoretical and experimental analysis of this problem.

**General considerations.**—In the previous paper (Part IV) we considered an adaptive system consisting of two enzymes: the first produces an active intermediate, which is partly used by the second and partly lost into the medium or otherwise, and attains in the region between the two enzymes a concentration  $c$ . The rate of synthesis of the second enzyme,  $R$ , is related to  $c$  by an expression having the form of a Langmuir adsorption isotherm.  $R = kc/(1 + bc)$ . The curve relating  $c$  and  $R$  is referred to as the  $c$ - $R$  curve and resembles Fig. 1. In the present work we are concerned with the adaptation of the bacteria to grow without lag in the presence of proflavine. The lag has been supposed to end when a critical

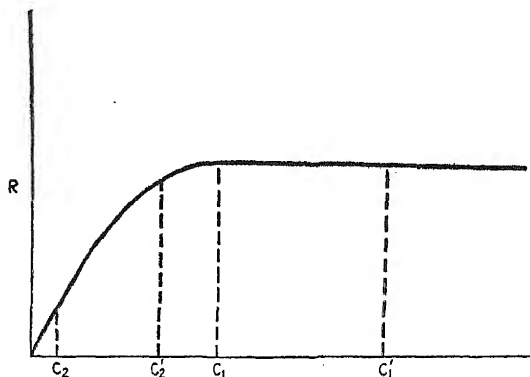


FIG. 1.—Relation between rate of action of enzyme and concentration of intermediate.

concentration of some metabolite is built up. This must not be confused with the intermediate of concentration  $c$  above, but is itself, directly or indirectly, a product of enzyme 2. The synthesis of enzyme 2 and the rate of formation of its products will be linked together: we therefore make the working hypothesis that the minimum lag (with respect to age),<sup>2</sup>  $L$ , of the cells is inversely proportional to  $R$ . Thus  $L = (A/k)(bc + 1)/c$ . In the absence of drug, when the cells are at the age of minimum lag,  $c = c'_1$ , which is constant for a given strain of cells and depends upon the balance of enzymes 1 and 2. In the presence of the drug  $c'_1$  is assumed to be reduced to a value  $c$  since the operation of enzyme 1 is impeded. The minimum lag,  $L_0$ , in absence of drug is then given by

$$L_0 = (A/k)(bc'_1 + 1)/c'_1$$

and the increase in presence of drug by

$$L - L_0 = (A/k)\{1/c - 1/c'_1\} \quad (1)$$

This can be used in conjunction with an equation for the variation of  $c$  with the drug concentration,  $m$ , to express the relation of  $L$  and  $m$  for various values of  $c'_1$ , the latter, which is constant for a given strain, characterising the degree of training.

In the simplest case  $c$  will be reduced in proportion to the drug concentration, so that  $c = c'_1 - fm$ , where  $f$  is a constant for a given drug. Substituting for  $c$  in 1 we have then

$$L - L_0 = \frac{A}{k(c'_1 - fm)} - \frac{A}{kc'_1}$$

whence

$$1/(L - L_0) = \frac{k}{A} \left\{ \frac{c'^2_1}{fm} - c'_1 \right\} \quad (2)$$

<sup>2</sup> Lodge and Hinshelwood, *J. Chem. Soc.*, 1943, 213.

### Proflavine Adaptation and Lag.

With the object of applying these equations, various series of experiments were carried out. *Bact. lactis aerogenes* was subcultured in presence of a particular concentration,  $P$ , of proflavine until it had become completely trained, *i.e.* until further subcultures caused no further increase in the drug resistance: 6 to 10 subcultures were deemed sufficient for this purpose. For the higher values of  $P$  the initial subculture was made with cells already trained at an intermediate concentration. The trained culture was tested by transferring 0.1 c.c. portions, at the end of the logarithmic phase, into a series of media containing a range of proflavine concentrations. Cells of the age chosen grew with a minimum lag, the value of which was measured for each of the proflavine test concentrations ( $m$ ). This minimal lag,  $L$ , was plotted against the test concentration. The whole series of tests was then repeated for cells trained at a higher value of the concentration  $P$ .

Figure 2 illustrates the results obtained for values of  $P$  from 0 to 164 mg./l. (this concentration unit is equivalent to parts per million). It is

seen that for each trained strain there is a certain range of tolerance to the drug, but that for test concentrations greater than a certain limit the lag rises rapidly towards infinite values. Special conditions apply to the results for very high values of  $P$ , which will be considered separately. For the present we shall deal only with the range up to about 400 mg./l.

TABLE I.

$m_{1000}$	$m_{1000} - 40$	$P$
30	-10	0
50	10	10
62	22	22
84	42	43
114	74	84
137	97	112
242	202	164
490	450	430

In Fig. 2 the spacing along the  $m$ -axis between adjacent curves is approximately equivalent to the difference in the corresponding values of the training concentration,  $P$ . This is shown by Table I which gives the values of  $m_{1000}$ , the value of the test concentration for which the minimum lag reaches 1000 minutes (in the standard test at 40.0°). The agreement between the last two columns indicates a very close correlation between the proflavine concentration and the degree of adaptation which it evokes.

We may now test the applicability of equation (2). Since, for a given strain, only  $L$  and  $m$  are variables, plotting  $1/(L - L_0)$  against  $1/m$  should give a straight line of slope  $kc'_1^2/Af$  and intercept  $-kc'_1/A$ . From these values we can find relative values of  $c'_1$  for each strain, since  $c'_1 = f \times \text{slope}/(-\text{intercept})$ . For most values of  $P$  straight lines are obtained over a wide enough range to allow the calculation of  $c'_1$ . The results are given in Table II, in which comparison of the first and last columns reveals a close relation between  $c'_1$  and  $P$ . This is expressed approximately by the equation

$$c'_1 = f(P + 54).$$

Since  $f$  is constant,  $c'_1$  is a measure of the degree of adaptation. Its value is in fact determined mainly by the horizontal spacing of the curves in Fig. 2 and small variations in their shape will not much affect it.

On the basis of equation (2) and the experimental results we obtain the equation

$$1/(L - L_0) = 1.0 \times 10^{-4}\{(P + 54)^2/m - (P + 54)\} \quad (3)$$

which gives the lag  $L$  of organisms trained at a proflavine concentration  $P$  when tested in a proflavine concentration  $m$ .  $L_0$  is the value of  $L$  when  $m = 0$  and in all our experiments had a value of about 70 minutes.

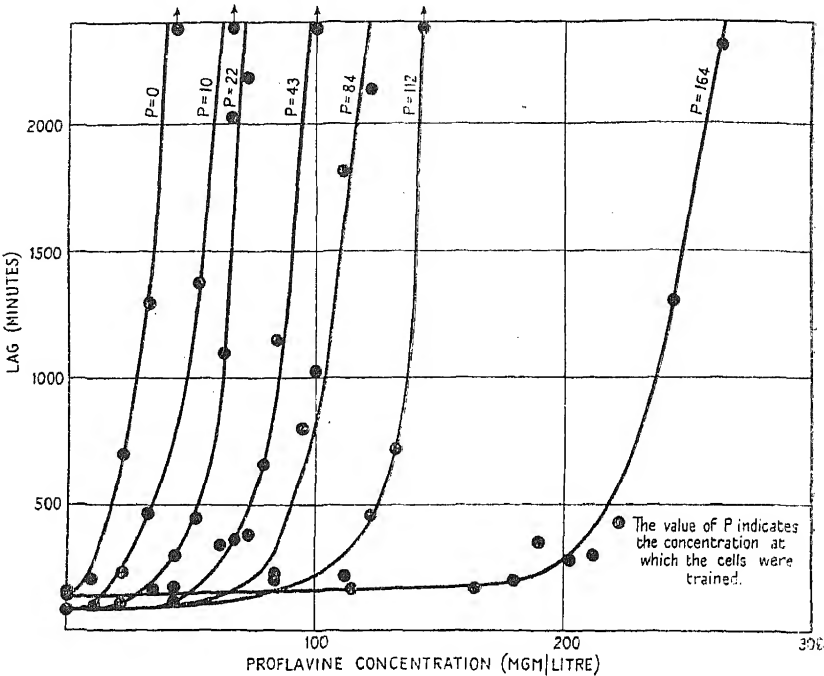


FIG. 2.—Relation between lag (minimal) and proflavine concentration for various trained strains of cells.

Calculations of  $L$  from this equation gives curves almost coinciding with those obtained experimentally (cf. Fig. (3)). Equation (3) predicts that the lag increases asymptotically to infinity when the test concentration exceeds

TABLE II.

$P(\text{mg./l.})$	$c'_1/f$	$(c'_1 - 54f)/f$
0	54	0
10	65	11
22	77	23
43	99	45
84	123	69
112	152	98
164	265	211
430	570	516

the training concentration by 54 mg./l. This corresponds well with observation. In detail, however, certain deviations from equation (2) are observed. In the plots of  $1/(L - L_0)$  against  $1/m$  the values of  $c'_1$ , obtained as above, should be proportional to the actual slopes,  $kc'_1^2/4f$ . This is found to hold when  $c'_1$  does not exceed 150f, beyond which point there is considerable deviation.

The intercepts should be proportional to  $c'_1$ . For lower values of  $c'_1$  there is good agreement but deviations occur for values greater than 150f. We will now consider the significance of the relation

$$c'_1 = f(P + 54). \quad (4)$$

Let us consider a hypothetical curve showing the relation between  $c$ , the concentration of the active metabolite and  $R$  the rate of working of the enzyme (Fig. 1).

Suppose the steady value of  $c$  for normal cells in the absence of the drug is  $c_1$ . We have assumed that in the presence of an amount  $m$  of proflavine  $c$  is reduced to  $c_2$  where  $c_2 = c_1 - fm$ . If training occurs  $c_2$  increases to some value  $c'_2$ . If the trained cells are now transferred to a medium free from drug, they will be able to produce the intermediate more freely than before and  $c$  will increase from  $c'_2$  to  $c'_1$ . If  $P$  is the training concentration,  $c'_1$  will therefore be related to  $c'_2$  by the relation

$$c'_1 = c'_2 + fP$$

and if  $c'_2$  is constant for all degrees of training,  $c'_1$  is a simple function of  $P$ .

Now, experiment has shown that  $c'_1 = 54f + Pf$ , which shows that  $c'_2$  has the value  $54f$  and is in fact constant for all values of  $P$ . This confirms the view that when proflavine reduces  $c$  below the flat part of

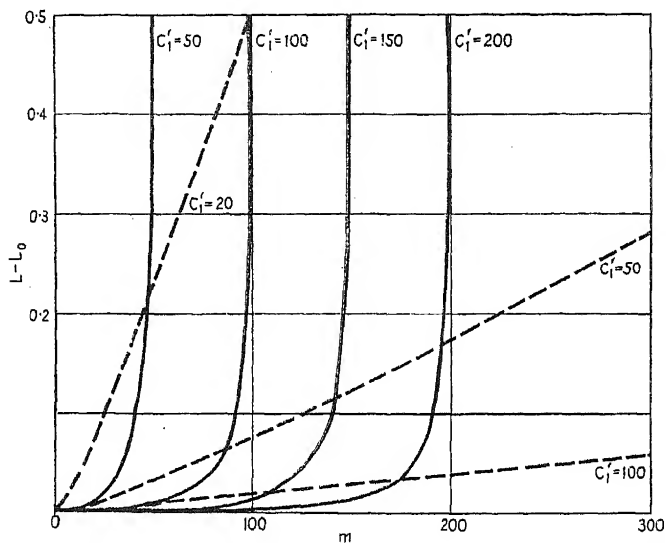


FIG. 3.—Forms of lag-concentration curve for  $K = \infty$  and for  $K = 2.5$ , for different trained strains. Continuous curves:  $K = \infty$ , broken lines:  $K = 2.5$ .

the  $c$ - $R$  curve, the resulting training always restores  $c$  to the same constant value. The fact that the family of experimental curves governed by (4) includes that for the untrained cells ( $P = 0$ ) indicates that  $c'_2 = c_1$ . When no training has occurred  $c'_1$  coincides with  $c_1$ : hence

$$c_1 = c'_1 = 54f + 0 = c'_2.$$

Thus it appears that the level to which  $c$  is restored each time by adaptation is the normal level. That  $c_1$  represents a point only just on the flat part of the curve is indicated by the small degree of tolerance of the cells to the drug when  $P = 0$ . The above arguments require that the maximum amount of proflavine which the cells will tolerate without considerable inhibition should be approximately equal to the training concentration as is actually found.

### Quantitative Differences in the Action of Drugs.

In the above treatment it was assumed that  $c = c'_1 - fm$ , i.e. that the drug causes something like a quantitative titration of an active product. We are not yet in a position to say what the precise mechanism of the inhibition is, but we must take into account the possibility that it is governed by a reversible process. This could be schematised, for example, as follows:—

drug + active product = inactive product + displaced groups.

The effect of the drug would be expressible in terms of an equilibrium constant,  $K = x^2/(a-x)(M-x)$ , where  $a$  and  $M$  are the initial amounts of active product and drug and  $x$  the amount inactivated.  $c$  would decrease as  $x$  increased, and as an approximation we might identify  $c$  with  $(a-x)$ , also writing  $M = fm$ , where  $f$  is a constant for conversion of units. Then

$$(a-x) = a - \frac{a+M - [a^2 - 2aM(1-2/K) + M^2]^{\frac{1}{2}}}{2(1-1/K)}$$

$$\text{Whence } c = c'_1 - \frac{c'_1 + fm - [c'^2_1 - 2c'_1 fm(1-2/K) + f^2 M^2]^{\frac{1}{2}}}{2(1-1/K)}.$$

This may be combined with (1), using arbitrary values for the constants, to discover the type of relation between the minimum lag and the drug concentration indicated by the theory for different values of  $K$ .

Figure 3 shows the families of curves obtained for varying values of  $c'_1$  at two standard values of  $K$ , namely infinity and 2.5: the constants  $f$  and  $A/k$  having been set equal to unity. It will be seen that for very large values of  $K$ ,  $(L-L_0)$  rapidly approaches infinity as  $m$  increases, and that the calculated family of curves closely resembles that found experimentally in the case of proflavine. In the theoretical treatment of these experiments given above the assumption that  $K$  was large was in fact tacitly made. For smaller values of  $K$ , over comparable ranges of  $L$  values, the family of curves has a very different appearance. It will be of interest to investigate the lag-concentration relations for other drugs in the light of this comparison. Preliminary results with methylene blue show some resemblance to the dotted curves in the figure, but it cannot be said whether the parallel is exact.

Since the actions of drugs, which fall short of an effectively complete titration of the active intermediate are unlikely to be describable by a scheme as simple as that given above, it will be preferable to approach the matter empirically, writing  $c = c'_1 - \phi(m)$ ,  $\phi$  being a function to be determined by comparison with experiment. As we have seen, with proflavine  $\phi(m) = fm$ , where  $f$  is constant, describes the results very well. Other drugs are under investigation.

In conclusion it may be remarked that, apart from any assumptions, the essential results of this paper are directly related to experiment in the following ways: the almost quantitative titrating action of the proflavine follows from the steep rise of the lag towards infinity at definite values of the drug concentration: the principle that training restores some function almost precisely to its normal and original level follows from the spacing of the family of lag-concentration curves at intervals corresponding to the training concentrations.

### Summary.

Previous work indicated that when bacteria become adapted to resist the action of drugs an adjustment of enzyme balance occurs, and that there should be a quantitative relation between the degree of adjustment and the concentration of the drug which provokes the "training". Theor-

etical equations are given connecting the lag (minimal with respect to age) of a given strain of cells, tested at various drug concentrations, with the steady concentration established in the cell of an essential metabolite whose synthesis the drug impairs. In this way the effect of training at various drug concentrations can be predicted.

Experimental curves have been determined showing the relation between lag and proflavine concentration for strains of *Bact. lactis aerogenes* trained respectively to a series of increasing concentrations of the drug. These curves form a family, the spacing of which is directly related to the concentration at which training occurred. They are adequately described by the equations. One conclusion from the results is that the concentration,  $c$ , of the intermediate metabolite is at first reduced by an amount directly proportional to the proflavine concentration, and that subsequent adaptation restores  $c$  to precisely its normal level. The simple behaviour holds over a considerable range of drug concentrations (0-200 mg./l.) but appears to break down at very high concentrations (to which, although with more difficulty, the cells are still adaptable).

*Physical Chemistry Laboratory,  
Oxford University.*

## REVIEWS OF BOOKS.

**Bibliography of Solid Adsorbents.** By V. R. DERTZ. (United States Cane Sugar Refiners and Bone Char Manufacturers, and the National Bureau of Standards. Washington D.C., 1944. Pp. xxxi + 877.)

As its title indicates this is not a text-book or review article but, to quote from the title-page, "An annotative bibliographical survey of the scientific literature on bone char, activated carbons, and other technical solid adsorbents for the years 1900 to 1942 inclusive." Accordingly no attempt is made to assess any work referred to, nor to indicate any probable trends for future research, fundamental or industrial. Nevertheless it is an interesting and significant publication, jointly sponsored by government and industry, being the beginning of a broad programme of fundamental research on sugar refining problems in general.

Following a brief historical review of the development of commercial adsorbents, principally in relation to the sugar refining industry, the bibliography of 6002 references is set out over some 800 pages, each individual reference following closely the pattern set by Chemical Abstracts. The seven main chapters, each subdivided into a number of sub-sections, are as follows:—

- I. Adsorption of Gases and Vapours on Solid Adsorbents.
- II. Adsorption from Solutions on Solid Adsorbents.
- III. Thermal Effects in Adsorption Processes.
- IV. Theories of Adsorption.
- V. Refining of Sugars and Other Applications of Adsorbents.
- VI. General Information on Adsorbents and Special Methods of Investigation.
- VII. Preparation of Carbon Adsorbents.

Of these Chapter VI is of particularly general interest as it illustrates the diverse impact of solid adsorbents not only upon industry, agriculture



and the arts, but upon many aspects of research problems in organic and physical chemistry, in biochemistry, and in medicine.

In addition to the main and sub-sections there are very full author and subject indexes, and it is felt that this compilation is one type of summary of scientific literature for which there will be an increasing need as the bounds of science are further extended.

Although no attempt has been made to check the degree of completeness of the references, neither the reviewer nor any of his colleagues has noted any omissions. In fact the field seems to have been covered extremely comprehensively, a tribute to the author in view of its magnitude and diversity.

A. E. A.

**Catalogue of Lewis's Medical Scientific and Technical Lending Library**  
(London, H. K. Lewis & Co. Ltd. Pp. viii and 922. Price To  
Subscribers: 12s. 6d. net. To non-subscribers: 25s. net.)

This well-known book has been brought up-to-date to the end of 1943. The previous complete edition was issued in 1937 and it says much for its popularity that a new edition should be required so soon instead of as heretofore after an interval of ten years, bridged by supplements.

This is a specially interesting production as in only three years' time the library will celebrate its centenary. The volume is worth possessing whether the reader is a subscriber to the library or not, as it provides a convenient and very full catalogue of current scientific and technical literature. Its completeness can only be judged by a painstaking check with the contents of the reader's actual (or desired) library. The reviewer can say, however, that every book in his own library seems to be catalogued.

The alphabetical author index occupies 714 post 8vo pages, the classified subject index 207, the remaining space being devoted to an alphabetical list of the subject headings. The volume is excellently printed and bound and the only error detected is that Eve's "Rutherford" is in the subject but not in the author index.

# THE APPLICATION OF INFRA-RED SPECTRA TO CHEMICAL PROBLEMS

## A GENERAL DISCUSSION.

A GENERAL DISCUSSION held by the Faraday Society on 2nd January, 1945, in the Large Lecture Theatre at King's College, University of London, from 10 a.m. to 5 p.m. (By kind permission of the Principal and Delegacy of the College.)

Over 250 members and visitors were present and the Chair was taken throughout by the President (Professor E. K. Rideal). The papers which had been circulated in Advance Proof before the meeting and the Discussion thereon appear in the following pages.

## INTRODUCTION.

BY THE PRESIDENT.

The purpose of our meeting here to-day is to discuss some recent advances in infra-red spectroscopy. We have to deplore the death, after a short illness, of Sir John Fox, the Government Chemist. We had hoped that he, always an enthusiastic worker in this field, would have opened this discussion. Not only do we miss him here to-day, but our Society has suffered a great loss in his death. He was one of our most active and kindly members, willingly taking on burdens which the Society from time to time loaded him with.

It is one of the difficulties inherent in war time that the Secrecy Act intervenes with different degrees of rigour in the various nations. Here in this country much work in the field of infra-red spectroscopy has still to be withheld from publication. Our trans-Atlantic cousins are more fortunate in this respect. We have to thank Drs. Sutherland and Thompson for the trouble they have gone to and the great care they have exercised in separating the secret from the non-secret, permitting here and there a peep behind the scenes.

The successful complete analysis of the vibration rotation spectra of even simple triatomic molecules still proves to be a formidable undertaking. Its extension to higher polyatomic molecules, an important field of enquiry, may however be facilitated by the great technological advances which have been made in recent years, both in resolving power and in mechanisation and speed of recording. The next important development in infra-red analysis consists in the correct assignment of the fundamental frequencies to the specific intra-molecular atomic vibrations. This has been accomplished for a large number of triatomic and several polyatomic molecules. Information derived in this way has proved of service in the evaluation of specific heat and entropy data required for the computation of chemical equilibria for obtaining the axes of symmetry, moments of inertia and bond lengths. The replacement of hydrogen by deuterium in molecules containing hydrogen results in specific vibrations moving to lower frequencies, thus serving to check and confirm the assignments, evaluate more distances and check force fields. Again, these assignments in simple molecules permit us to develop the idea of vibrations localised inside particular groups and thus we can utilise the infra-red analysis for

the identification of particular groups in more complex organic molecules. Since the infra-red vibrational frequencies involve a change in dipole moment in the molecule or group, when we are considering a particular vibration in a compound, slight alterations in the magnitude of the vibrational quantum indicate that the constraints in the intra-molecular oscillations, *i.e.* the force constants, are affected by the proximity of other groups (*e.g.* dipole interaction) or by the mode and position of attachment of the group to the rest of the molecule. Closer analyses of these shifts are required since definite information on the force fields round groups are clearly of the greatest importance in Organic Chemistry.

The possibility of assignment of individual interatomic vibrations and frequencies within a particular group is proving of the greatest importance in the examination of the natural and synthetic polymers. It is well known that the evaluation of the ratio between 1 : 2 and 1 : 4 addition in the synthetic asymmetric vinyl class of polymers presents great experimental difficulties. Exact evaluation of this ratio under different conditions of polymerisation would take us another very definite step forward in the elucidation of the kinetics of the formation of this class of polymers. It is an interesting speculation whether the "link" or kinetic unit of which the macromolecular chains are formed (as postulated from data on viscosity and colligative properties) is revealed in the infra-red spectrum.

Another general field of investigation by means of infra-red analysis which merits detailed attention is the hydrogen bond. Thermochemical and colligative data, *e.g.* the freezing-point depressions have permitted us to get rough approximations to the free energy and heat changes involved in several hydrogen bondings. Even more accurate analysis of the equilibria between bonded and non-bonded species over a wide range in temperature is now possible; the importance of such is not restricted to the simple groups OH, NH and SH, but hydrogen bonding may play an important part in both the structure of the proteins and the remarkably large changes in entropy associated with the phenomenon of inactivation or denaturation.

Finally, one might mention the advances in radar which permit us to examine the infra-red spectrum in the region of a few centimetres. It is hoped that this interesting region may be examined in the near future.

## GENERAL INTRODUCTION.

BY PROFESSOR C. K. INGOLD.

It is probable that infra-red spectroscopy has entered upon a new period of rapid progress as a direct result of certain technical improvements about which we are to hear to-day. That, I imagine, is the main reason why the Council of the Faraday Society, with its usual quick perception of the directions which scientific progress is pursuing, decided to hold this meeting.

As everyone knows, long-wave spectroscopy has contributed very largely to our knowledge of the structures of polyatomic molecules: for instance, the precise geometry of the water molecule has been determined in this way, and could have been determined in no other way. Vibrational spectra are the only source of our knowledge, incomplete as this still is, of the inter-atomic forces which hold molecules together and govern the relative motions of their atoms.

Apart from these direct results, vibrational spectroscopy has a series of applications which may be broadly called "analytical". But they include something more than the (practically important) detection and estimation in mixtures of substances whose spectra are known because they can be determined by the use of pure compounds. It is possible to detect special groups or types of combination, for example, the associated

hydroxyl group—the so-called hydrogen bond—as was illustrated in some of the work of the late Sir John Fox. Again, a valuable method is provided by vibrational spectroscopy for the study of ionisation, as of nitric and perchloric acid in the recent work of Redlich; furthermore, evidence has been provided of the presence in quantity in certain solutions of ions which chemists have, on the whole, been slow to recognise, for example, the nitrosyl ion,  $\text{NO}^+$ . For the detection and estimation of isotopic isomers, as is necessary in the study of many reactions involving deuterium, vibrational spectroscopy provides the only means at our disposal.

Hitherto, Raman spectroscopy has contributed more than has absorption spectrometry in the infra-red to our knowledge of molecular vibration frequencies. The difference is, of course, mainly due to the greater technical facility of Raman work. With the new technical developments that Dr. Sutherland and Dr. Thompson have described it seems likely that the balance of facility may now lie in the other direction.

With regard to the application of infra-red spectrometry, the programme includes, as you will have noticed, a representative selection of studies, some dealing with simple molecules, such as ozone, one with a macromolecular crystal, the diamond, and several with the difficult problems presented by non-crystalline, usually inhomogeneous, macromolecules, both natural and artificial.

The consideration of all this interesting material, on technique and on application, is our main work to-day. I speak for all present when I express our gratitude to the schools of spectroscopy at Cambridge and at Oxford for the excellent co-operative effort which has made this meeting possible.

# DEVELOPMENTS IN THE TECHNIQUE OF INFRA-RED SPECTROSCOPY.

By G. B. B. M. SUTHERLAND AND H. W. THOMPSON.

*Received 28th November, 1944.*

## Spectrometers.

In the period immediately following the last war, very marked developments took place in the technique of infra-red spectroscopy. In 1919 Imes and Randall<sup>1</sup> resolved for the first time the rotational fine structure of the fundamental absorption bands of all the hydrogen halides. This was accomplished by using an "echelette" grating of the type invented by Wood<sup>2</sup> which concentrates the diffracted radiation largely into one order of the spectrum. Furthermore, this rotational fine structure could be interpreted on the basis of the then developing quantum theory to yield a value for the moment of inertia of the molecule and hence for the hydrogen-halide internuclear distance. Two new tools were thus available in the infra-red: (1) "echelette" gratings, which increased the resolving power by a factor of the order of 10, revealing rotational fine structure hitherto practically unobservable; (2) quantum theory, which enabled one to interpret this rotational fine structure in terms of energy levels. These levels could in turn be expressed as functions of the moments of inertia of the molecule leading ultimately to the determination of internuclear distances. The result was a concentration of effort in the experimental field on achieving the highest resolving power and by 1939 the infra-red could be covered from the visible to beyond  $150\mu$  with a resolving power sufficient to separate comfortably lines differing in frequency by about  $0.5\text{ cm}^{-1}$ . The extent of this advance can be gauged when we recall that the separation of the HI lines first resolved in 1919 was  $12.5\text{ cm}^{-1}$ . It should be added that this advance in technique was not entirely due to the use of echelette gratings; improved thermocouples and optical systems were developed, especially by Pfund,<sup>3</sup> while the extension of the new technique to the extremely difficult long wave region beyond  $30\mu$  is largely due to Randall<sup>4</sup> and his co-workers.

Since the natural width of a spectral line in the infra-red (except at low temperatures) is probably of the order of a few tenths of a wave number ( $\text{cm}^{-1}$ ) it is clear that the practical limit of resolving power for rotational fine structure is now being approached. Moreover, the number of molecules which have moments of inertia sufficiently small and a degree of symmetry sufficiently great, to possess a rotational fine structure with separations greater than  $0.5\text{ cm}^{-1}$  is very limited. By 1939 the majority of these had been investigated and it was becoming clear that the field of research opened by high resolving power after the last war was getting somewhat limited in scope. If infra-red spectroscopy was to continue to be a useful tool in the investigation of molecular structure, some means would have to be found of tackling the larger molecules. This meant at least a temporary return to the older empirical method of Coblenz<sup>5</sup> in

<sup>1</sup> Imes, *Astrophysic. J.*, 1919, **50**, 251. Randall and Imes, *Physic. Rev.*, 1920, **15**, 152.

<sup>2</sup> Wood, *Phil. Mag.*, 1910, **20**, 770.

<sup>3</sup> Pfund, *J. Opt. Soc. Amer.*, 1927, **14**, 337, and *Rev. Sci. Instr.*, 1937, **8**, 417.

<sup>4</sup> Randall, *Rev. Mod. Physics*, 1938, **10**, 72.

<sup>5</sup> Coblenz, *Investigation Infra-Red Spectra*, Publications of Carnegie Inst. of Washington, 1905 and 1906.

which the spectra of large numbers of molecules of similar structure are correlated. One is thus able to pick out frequencies characteristic of certain groupings and eventually to identify these groupings in complex molecules of unknown structure. In other words, *high resolving power becomes temporarily of much less importance than speed of recording*. The spectra of 20 compounds of a related structural character, taken with moderate resolving power, are much more valuable than the spectra of one or two of them taken with the highest resolving power over the same region of the spectrum.

Accordingly much attention is now being given to the rapid recording of infra-red spectra and it is this particular aspect of infra-red technique which will be discussed most fully in what follows. Quite apart from the use of infra-red spectra to advance knowledge of molecular structure, it has a rapidly growing field of application as a straight analytical tool. *The infra-red spectrum of a chemical compound is probably the most characteristic physical property of that compound*. It is in general far superior to properties such as refractive index or boiling point as a means of identifying a compound, particularly when it occurs in a mixture with two or three others. Although refractions, for instance, may be more accurate at present on the quantitative side, preliminary *qualitative* identification by infra-red spectra is essential. If, therefore, the technique of infra-red spectroscopy can be improved so that a spectrum can be obtained in a time comparable with that required for a measurement of refraction or boiling point the chemist will have a new analytical tool of great power.

In what follows we shall not specifically consider grating spectrometers although of course many of the accelerating devices can equally well be employed to speed up the recording of grating spectra over the range of each grating. The echelette effect limits the range of each grating so much that the automatic recording of an infra-red spectrum from 2 to  $15\mu$  with gratings, will always remain a difficult problem. Again, grating work is seldom worth while unless one has the compound in the gaseous state, since the true width of the majority of infra-red bands of liquids and solids below  $30\mu$  is usually well within the resolving power of the appropriate prism. It might be added, however, that Wood <sup>6</sup> has continued to improve his technique for echelette gratings with 7200 lines to the inch (suitable for the  $3\mu$  region of the spectrum) so much that over 90 % of the incident energy can now be concentrated into one spectral order.

### Prism Materials.

Rock salt still remains the most useful dispersive material in the infra-red out to  $15\mu$ . Only in the region between  $2.5$  and  $6\mu$  is one likely to find it seriously defective in resolving power. For this region lithium fluoride has recently been introduced <sup>7</sup> with excellent results, although it is inferior in resolving power to quartz in the region in which the latter is used (visible to  $3.5\mu$ ). The absorption band of quartz at  $2.9\mu$  is a great nuisance, especially in quantitative work. Between  $3.5$  and  $6\mu$  lithium fluoride has twice the dispersive power of fluorite but beyond that point the transmission of lithium fluoride falls rapidly to zero, whereas fluorite can be used out to  $9\mu$ . In view of the fact that artificial crystals of lithium fluoride sufficiently large for prisms are now being made commercially in the U.S.A. <sup>8</sup> while fluorite and quartz are becoming increasingly difficult to obtain, this material is likely to become the most useful supplement to rock salt for the short wave end of the infra-red.

Beyond  $15\mu$  sylvine (to  $21\mu$ ) and potassium bromide (to  $30\mu$ ) still remain the only suitable materials. It is worth noting that large artificial crystals of the latter are also being made commercially in the U.S.A. <sup>8</sup>

<sup>6</sup> R. W. Wood, *Private Communication*.

<sup>7</sup> Wright, *Rev. Sci. Instr.*, 1944, **15**, 22.

<sup>8</sup> The Harshaw Chemical Co., Cleveland, Ohio, U.S.A.

### Optical Systems.

There are no particular advances to report in this field. The Littrow arrangement is usually favoured in that it effectively doubles the base of the prism and so gives the maximum resolving power.<sup>9</sup> It is desirable to bring the beam of radiation to a focus on the specimen under examination before concentrating it on the entrance slit of the spectrometer since this minimises (1) the area of specimen required, (2) the size of the windows when a long absorption cell has to be used for gases and (3) the losses due to scattering in the case of solid films.

No infra-red spectrometer gives a pure spectrum and the exact causes of this have still to be fully examined. This impurity is not usually important in prism spectrometers at wavelengths below  $5\mu$  but at longer wavelengths there is always an appreciable amount of short-wave radiation mixed with the long wave which is being determined. The former may arise from multiple reflections, from heating of the slits, from scattering or other causes and in practice is impossible to eliminate. The effects of this spurious radiation can be nullified, however, by using a shutter, to admit the infra-red radiation to the system, consisting of a material transparent to the short wave radiation but opaque to the long wave. Thus the short wave radiation falls on the thermocouple all the time and so produces no deflection when the shutter is "opened". Suitable materials for such shutters are:—

Glass or quartz—opaque beyond  $5\mu$   
Fluorite—opaque beyond  $10\mu$   
Rock salt—opaque beyond  $17\mu$

When the highest accuracy is required it may be necessary to compensate for the small amount of short wave radiation reflected by the shutter by introducing a shutter transparent to the long wave radiation (*e.g.* of KBr) when the opaque shutter is removed.<sup>12b</sup> Since most of the spurious radiation is usually of very short wavelength (presumably arising from the maximum energy of the Nernst filament near  $2\mu$ ) its effects can also be diminished by differential scattering. For this purpose films of MgO on rock salt<sup>10</sup> have been tried with varying success.

### Calibration.

The accurate determination of wavelengths in the infra-red is still a matter for investigation. In rapid prism work, although the highest accuracy is not essential, it has been difficult to determine frequencies to better than  $\pm 10 \text{ cm.}^{-1}$  without great trouble because of the lack of secondary standards. These are now becoming available. The frequencies of some 150 lines between 5 and  $15\mu$  in the spectra of gaseous ammonia, carbon dioxide and water have been determined by Oetjen, Kao and Randall<sup>11</sup> using (1) a rock salt prism spectrometer of high resolving power and (2) a grating spectrometer with slit widths adjusted to give the same resolving power as the prism spectrometer. In this way highly accurate standard wavelengths can be obtained for the calibration of prism spectrometers giving frequencies to  $\pm 2 \text{ cm.}^{-1}$  or better. The lines in the atmospheric water vapour spectrum between 5 and  $8\mu$  and the  $\text{CO}_2$  bands near  $14\mu$  give particularly useful calibration check points many of which are superimposed on every run in which atmospheric absorptions have not been eliminated.

<sup>9</sup> For a description of the optical system of a typical modern prism spectrometer see "Infra-Red Spectroscopy," by Barnes and others. Reinhold, 1944.

<sup>10</sup> Pfund, *J. Opt. Soc. Amer.*, 1934, 24, 143.

<sup>11</sup> Oetjen, Kao and Randall, *Rev. Sci. Inst.*, 1942, 13, 515.

### Detection and Recording.

It is here that the main improvements in technique have been made. Automatic recording has virtually displaced the old manual plotting of a spectrum point by point. In principle this merely involves continuous photographic recording of the galvanometer deflection on a rotating drum, the motion of which is related to the rotation of the prism in traversing the spectrum; in practice it means that the thermocouple must be fast in response as well as sensitive and the whole system sufficiently free from drift and unsteadiness (arising from thermal electrical or mechanical disturbances in the neighbourhood) to enable one to utilise the full optical resolving power of the spectrometer. Automatic recording is not by any means new but until recently considerable sacrifice in resolving power was necessary in order to achieve stability, since wide slits had to be used to maintain the signal to noise ratio at a workable value.

The principal advance here has come from the introduction of the new Hilger-Schwarz permanently evacuated thermocouple which has a response time considerably less than one second, coupled with very good

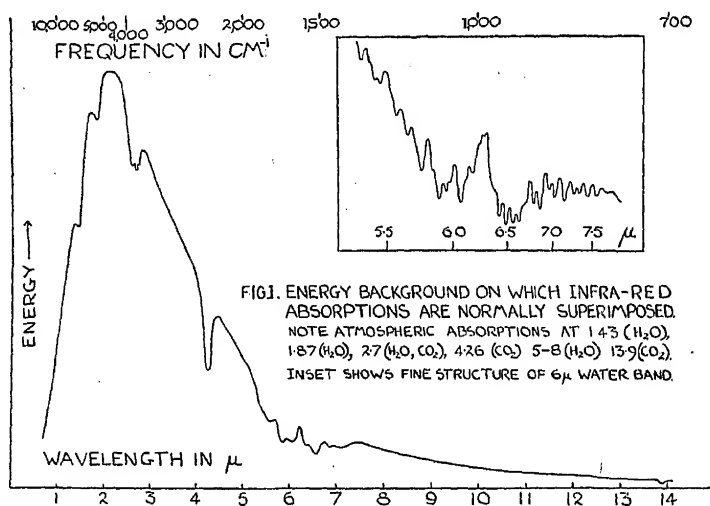


FIG. 1. ENERGY BACKGROUND ON WHICH INFRA-RED ABSORPTIONS ARE NORMALLY SUPERIMPOSED. NOTE ATMOSPHERIC ABSORPTIONS AT 1.43 ( $\text{H}_2\text{O}$ ), 1.87 ( $\text{H}_2\text{O}$ ), 2.7 ( $\text{H}_2\text{O}$ ,  $\text{CO}_2$ ), 4.26 ( $\text{CO}_2$ ) 5-8 ( $\text{H}_2\text{O}$ ) 13.9 ( $\text{CO}_2$ ). INSET SHOWS FINE STRUCTURE OF 6.3  $\mu$  WATER BAND.

sensitivity. The output from this is fed to a moving coil galvanometer of 2 sec. period and of moderate sensitivity but with a strained suspension to reduce susceptibility to mechanical disturbances. The deflections of this galvanometer are made to actuate some form of photoelectric relay<sup>12</sup> which in turn feeds the secondary galvanometer. Formerly it was customary to use a very sensitive and therefore long period galvanometer as primary or even alone without amplification. There is a considerable gain in speed and stability by using a fast, relatively insensitive primary and amplifying its deflections.

The record obtained from such a single beam instrument is, of course, not a true absorption spectrum; it is merely a spectral record of the energy transmitted by the substance under examination. Since the radiation emitted by the source has approximately a "black-body" distribution with wavelength and is partially absorbed by atmospheric water vapour and carbon dioxide, the absorption bands in which we are interested are superimposed on a highly variable background such as that illustrated in Fig. 1. This means that much time has to be spent

<sup>12</sup> (a) Moss, *J. Sci. Instr.*, 1935, 12, 141. (b) Conn, Lee and Sutherland, *Proc. Roy. Soc., A*, 1940, 176, 484.



in converting the modified energy curve into a true spectrum by calculating percentage absorption at a very large number of key points along the record. Although the labour involved in this can be reduced by devices such as those described later in the paper by Willis and Philpotts, the time involved is very considerable. In addition there is always some doubt whether the incident energy background against which these absorption percentages are calculated is really accurately known, since it is not recorded simultaneously with the absorption curve. In regions of intense atmospheric absorption around  $2.8$ ,  $4.2$  and  $5.75\mu$  this last difficulty becomes extremely serious. To overcome these drawbacks double beam spectrometers are making their appearance which give a direct record of percentage absorption. These automatically compensate for any variations in the incident energy, whether due to Planck distribution law, atmospheric absorption or variations in heater current to the source.

### Double Beam Spectrometers.

The first spectrometer of this type was designed by Hardy<sup>13</sup> the basic principles of whose method can best be followed by reference to Fig. 2. Two equal beams of radiation from the source N (Nernst filament) are

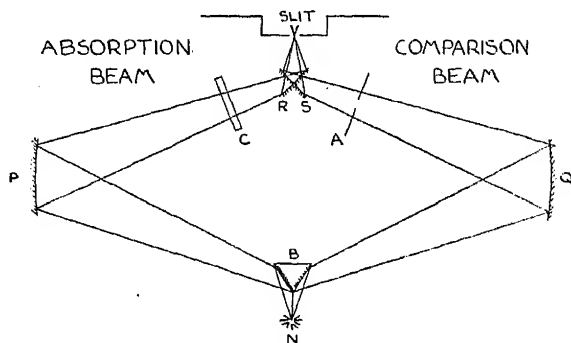


FIG 2 EXTERNAL ARRANGEMENT OF DOUBLE BEAM SPECTROMETER

N=SOURCE. B=REFLECTING PRISM. P,Q=CONCAVE MIRRORS.  
A=APERTURE. C=ABSORPTION CELL. R,S=PLANE MIRRORS.

selected by the mirrors P, Q, which direct the rays respectively on to the two plane mirrors, R, S. These are set vertically one above the other and approximately at right angles. The result is that the beam NPR illuminates the top half of the entrance slit of the spectrometer, while NQS illuminates the lower half. The two beams go through the spectrometer in the normal way and are finally brought to focus on two identical matched thermocouples set vertically one above the other. When the two beams are properly balanced there will be no deflection when the two thermocouples are connected in opposition at any point in the spectrum. Suppose now an absorbing compound is put into the NPR beam while a variable aperture A (e.g. iris diaphragm) is introduced into the NQS beam. Mechanical arrangements are made so that as the spectrum is traversed, the aperture A can be closed and opened to match the absorption due to the specimen C in the other beam and the position of the aperture recorded against prism angle, or wavelength. This gives a true percentage absorption spectrum provided the aperture has been properly calibrated. The disadvantages of this spectrometer are (1) that it is not fully automatic since an observer is required to operate the aperture control and keep the beams balanced, (2) that the speed of recording is determined by the

<sup>13</sup> Hardy and Ryer, *Physic. Rev.*, 1939, 55, 1112.

speed of the mechanical operation of the shutter. Although the former can be overcome by photo-mechanical devices,<sup>14</sup> the latter is inherent in the method.

An alternative type of double beam instrument has been developed at the Laboratories of the Standard Oil Co. of New Jersey.<sup>15</sup> In this instrument no variable aperture is used but the ratio of the outputs from the separate thermocouples of the two beams is continuously recorded as the spectrum is traversed. The thermocouple voltages are amplified to an order of few millivolts. These are then fed to a recording potentiometer, the amplified thermocouple output on the comparison beam taking the place of the e.m.f. on the slide wire while the amplified thermocouple output on the absorption beam takes the place of the "unknown voltage." The essentials of the amplifier used have been given by Matheson, McAlister and Sweeney<sup>16</sup> while a further discussion of this amplifier has been given by Lawson.<sup>17</sup>

Spectrometers of this type are now being tried out at Oxford and Cambridge. The amplifiers were built by Pye Radio; the recording potentiometers were supplied by the Cambridge Instrument Co., while all the rest of the spectrometer was made by Adam Hilger Ltd. Until the spectrometers have been in actual operation discussion of the detailed difficulties encountered is bound to be incomplete and unsatisfactory. It may be stated, however, that the amplifier and potentiometer have been successfully operated on a single beam instrument using a fixed voltage on the slide wire in place of the voltage from a comparison beam. The record is obtained as a pen and ink tracing, an advance over the usual photographic method in that the spectrum is visible as it is being traced.

### Future Developments.

If infra-red spectroscopy is to fulfil its present promise as a tool for chemical and structural analysis the speed of recording must be still further increased and the apparatus made less susceptible to outside disturbances. It now takes approximately half an hour to record a spectrum from  $2\mu$  to  $15\mu$  and a special room is required free from thermal, mechanical and electrical disturbances. If the present thermocouple could be replaced by an A.C. bolometer of equal sensitivity and the spectrometer shutter were opened and closed at a fixed frequency it should be possible to eliminate most of the troubles arising from the above disturbances, since no galvanometer would be required, and by careful tuning, the receiver would respond only to impulses coming with the period of the shutter. If in addition, the speed of the bolometer could be increased to give a response time of the order of  $1/50$  sec. the possibility arises of recording the impulses on a cathode ray screen and so obtaining an instantaneous picture of an infra-red spectrum. Considerable progress has already been made in this direction in the United States.<sup>18</sup>

<sup>14</sup> E.g. such as one described by Pompeo and Penther, *Rev. Sci. Instr.*, 1942, 13, 218.

<sup>15</sup> Private communication.

<sup>16</sup> McAlister, Matheson and Sweeney, *Rev. Sci. Instr.*, 1941, 12, 314.

<sup>17</sup> Lawson, *Electronic Engineering*, 1944, 17, 114.

<sup>18</sup> Baker and Robb, *Rev. Sci. Instr.*, 1943, 14, 356, 359, 362.

## SOURCES OF RADIATION AND ABSORPTION CELLS.

BY H. W. THOMPSON AND D. H. WHIFFEN.

*Received 28th November, 1944.*

The absorption cells normally used for infra-red work have windows of rock salt or other alkali halides, which require to be polished. Although the surfaces need not be as true as those used at shorter wavelengths in the ultraviolet, it may be necessary in making a thin cell for use with liquids to polish surfaces to a flatness of  $10^{-4}$  mm. The deterioration of the surfaces due to atmospheric or contaminant moisture also makes it necessary to re-polish frequently. We have found the following procedure useful. Plates about  $1\frac{1}{2}$  in. square and  $\frac{1}{8}$  in. to  $\frac{1}{4}$  in. thick are first obtained by cleaving a clear block of natural crystal, or by cutting a block of synthetic material with a fine saw or wet wire. If necessary the plates are first trimmed, and then ground roughly flat with coarse emery powder, using a little water as lubricant. All granules of the coarse emery are then removed by washing with alcohol, and the plates ground with fine emery, again using a little water as lubricant. After washing with alcohol the plate has a smooth opaque surface, and can then be finally polished on a pitch pad made as follows.<sup>1</sup> A molten blend containing 90 % Swedish pitch with 10 % beeswax is poured into a shallow can, about 8 in. square and  $\frac{3}{4}$  in. deep, so that the liquid mixture just fills the can. It is allowed to cool and when just above softening temperature a wire mesh (about 25/in.) is pressed upon the surface so as to produce crossed furrows. After allowing to solidify further, the mesh is removed, and the indented flat surface finally allowed to harden. The surface is then painted with a liberal coating of a sludge of rouge and water, or water-alcohol, and the flat plates are polished upon this by hand until the rouge and water have been rubbed clear. If the preliminary grinding with fine emery has been efficient, perfectly clear flats can be obtained within a few minutes. Once a plate has been polished in this way, slight fogging by atmospheric moisture can easily be removed by a quick polish on a chamois leather pad moistened with rouge and alcohol.

Two sources of infra-red radiation remain pre-eminent for the region  $1-25\mu$ . The Nernst filament is perhaps most convenient in manipulation, and if run from the A.C. mains through a variac transformer, it can be made to operate without additional stabilizers such as barettor lamps. Its defect is a tendency to burn out at the platinum leads before the material of the filament itself has lost its value. Ebers and Nielsen<sup>2</sup> have described a method for overcoming this. Another method of mounting is to platinize the ends of a straight filament by successively immersing in platinum chloride solution and heating in a flame, and then support the filament between a pair of metal cups. If the platinizing is satisfactory, a good electrical contact can be obtained with adequate stability, but the method is not always successful. A laboratory method for making Nernst glowers has been described by Griffiths.<sup>3</sup>

The other common source is an electrically heated rod of carborundum material, available commercially as Globar in several sizes. The rod is usually mounted between aluminium cup electrodes held together with

<sup>1</sup> Glazebrook, *Dictionary of Applied Physics*, Vol. IV, p. 326.

<sup>2</sup> Ebers and Nielsen, *Rev. Sci. Instr.*, 1940, 11, 429.

<sup>3</sup> Griffiths, *Phil. Mag.*, 1925, 59, 263.

springs, and is best surrounded by a water cooling jacket, since otherwise it leads to undesirable changes in room temperature. At wavelengths beyond about  $15\mu$  the Globar emitter is somewhat superior to the Nernst filament as regards intensity of radiation. Its higher power consumption is a disadvantage. Smith<sup>4</sup> has described another source of radiation consisting of an electrically heated carbon rod *in vacuo*, and stated to be better than the Globar at wavelengths beyond  $10\mu$ .

Absorption cells for gases are usually made by cementing flat windows to the ends of cylindrical glass tubes of any desired length. For liquids, cells are made by separating a pair of flats with a washer of thin metal foil or other suitable material, leaving small gaps for filling along the upper edge. When volatile liquids, solutions in carbon disulphide or ill-smelling liquids are being measured, it is desirable to seal off the cell after filling. This can be done by means of amalgam seals,<sup>5</sup> or by inserting narrow metal lead-in tubes to the cell through holes drilled into one rock salt flat; the lead-in tubes can then be closed by corks or rubber caps. Various types of cell have been described by Randall,<sup>6</sup> Barr,<sup>7</sup> Nielsen,<sup>8</sup> Smith,<sup>9</sup> and Smith and Miller.<sup>1</sup>

<sup>4</sup> Smith, *Rev. Sci. Instr.*, 1942, 13, 63.

<sup>5</sup> Gildart and Wright, *Rev. Sci. Instr.*, 1941, 12, 204.

<sup>6</sup> Randall, *ibid.*, 1939, 10, 195.

<sup>7</sup> Barr, *ibid.*, 1941, 12, 396.

<sup>8</sup> *Ind. Eng. Chem. Anal. Ed.*, 1943, 15, 609.

<sup>9</sup> Smith, *Rev. Sci. Instr.*, 1942, 13, 65.

<sup>10</sup> Smith and Miller, *J. Opt. Soc. Amer.*, 1944, 34, 130.

---

## MEASUREMENT OF CELL THICKNESS.

By G. B. B. M. SUTHERLAND AND H. A. WILLIS.

*Received 28th November, 1944.*

The accurate measurement of the thickness of the absorption cell used for liquids in the infra-red is now a matter of considerable importance in quantitative work. Unless thicknesses of cells used can be measured easily and accurately exact extinction coefficients cannot be obtained and each worker will require samples of pure materials to calibrate his cells for quantitative work. Smith and Miller<sup>1</sup> have recently used the interference method (normally employed in the visible region of the spectrum with half silvered plates<sup>2</sup>) to obtain the thickness of the air film between the two plates of the absorption cell. This method has the following drawbacks: (1) the interference bands are obtained as a weak pattern superimposed on the steep slope of main energy curve (Fig. 1*a*), (2) the number of fringes obtained decreases very rapidly as the cells become thinner so that the accuracy diminishes when cells go below  $10\mu$  in thickness, (3) it is slow in that an actual spectral run has to be made and measured up to get the required result.

The first disadvantage may be removed in a double beam spectrometer where the main energy background of the cell beam can be "balanced out" by the energy of the comparison beam to give an interference pattern on a "flat" instead of a "sloping" background (Fig. 1*b*). The junctions of the thermocouples of the separate beams are connected in series in opposition and the beams balanced. The cell is then introduced and the beams re-balanced by reducing the aperture of the comparison beam to allow for the loss of energy in the cell. This last operation requires some

<sup>1</sup> Smith and Miller, *J. Opt. Soc. Amer.*, 1944, 34, 130.

<sup>2</sup> Cf. for examples Searle, *Exptl. Optics*, p. 343. Cambridge Univ. Press, 1925.

skill as the interference fringes are present and the balance must be made mid-way between two extremes. When this is accomplished an interference pattern similar to that shown in Fig. 1b is obtained. Such a pattern can be measured with a very high degree of accuracy. The precision is illustrated in Fig. 1c where the fringe number ( $n$ ) is plotted against the

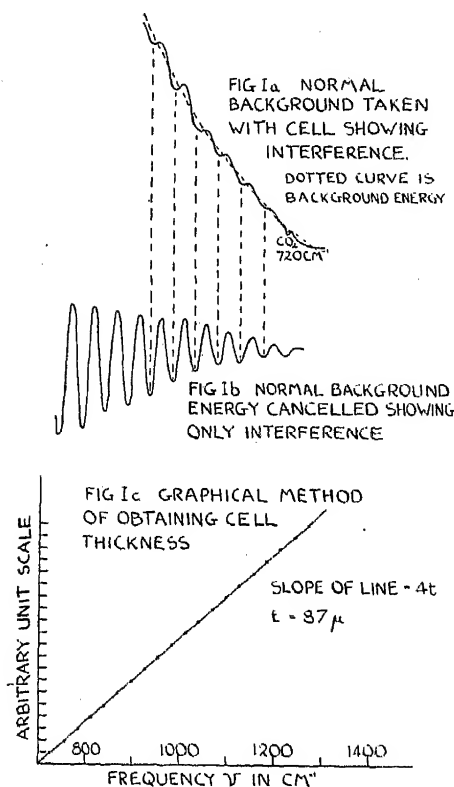
frequency ( $\nu$ ) of successive extremes giving an excellent straight line. Since

$$2t = n \frac{\lambda}{2}$$

where  $\lambda$  is the wavelength of any extreme value of the energy (i.e. complete reinforcement or complete cancellation),  $t$  is the thickness of the air film and  $n$  any integer

$$\therefore n = \frac{4t}{\lambda} = 4t\nu.$$

Recently we have been investigating an alternative method of measuring cell thickness by interference fringes in the visible region of the spectrum. The principle of this method<sup>3</sup> is to set the cell at  $45^\circ$  to the beam of white light and pick up the light reflected from the two faces bounding the air film. Interference then occurs between two rays of comparable intensity and the bands are fairly easily picked up in the visible region of any suitable spectrometer. The most convenient means of making this



method rapid and accurate have still to be worked out in detail but the disadvantages enumerated above in the transmission method in the infra-red have certainly been overcome. Thus when cells less than 0.005 mm. in thickness are used there will still be an appreciable number of bands in the visible region of the spectrum while the spacing in the infra-red will have become so wide that accurate measurement of the maxima and minima on the varying background is very difficult. The reflection method can of course be used in the infra-red for cells of moderate thickness but the cell would not be in its normal position, and some arrangement would have to be made (as in the use of the visible spectrum) to ensure that the same portion of the cell was measured as that used in the absorption run, if the thickness of the cell is found to be non-uniform.

<sup>3</sup> The suggestion to use a reflection technique was made by Dr. G. F. C. Searle, F.R.S., to whom we should like to express our gratitude for his interest in this problem.

# AN ABSORPTION CELL FOR MOLTEN SOLIDS AND HEATED LIQUIDS.

BY R. E. RICHARDS AND H. W. THOMPSON.

*Received 28th November, 1944.*

It has recently become necessary to construct an absorption cell which can be used for liquids above room temperature. This is important not only for studying the change of spectrum with state of aggregation—solid or liquid—but also for measuring the absorption of molten solids which are either effectively insoluble in all solvents, or for which the only known solvents are unsuitable spectroscopically. A cell of this type which has been used successfully between 20–200° C. is shown diagrammatically in Fig. 1. The cell holders A and B are made of  $\frac{1}{2}$  in. plywood. Glued to the holder A is the heater H, which is constructed as follows. About 2 metres of nichrome wire (30 ohms per metre) are wound on a core made by cutting a 1 in. square from an asbestos card 2 in. square. This heating element is insulated on both sides by asbestos board frames cut to a size slightly larger than that of the heater core. The whole is cemented together with a little water glass, which is baked to a hard solid. The heater leads are connected to the terminals T, and the heater fed from the 100 volt mains through a suitable rheostat.

Two thermocouples are made by silver-soldering iron and constantan wires together. These are connected in series and the twin couple is calibrated by immersing the pair of hot junctions in baths at known temperatures, using a millivoltmeter. This combination has a linear relation between E.M.F. and temperature over a wide range and certainly up to 200° C. One of the couples is embedded in the cell side of the heater and held in place by an annular frame made of thick asbestos paper P. The other couple is similarly embedded in the asbestos board frame F, which is glued to the frame B. The thermocouple leads are taken out through the small holes GG in the cell holders. The cold junctions are kept at room temperature at a junction box.

The cell plates PP, which can be of rock salt, sylvine or potassium bromide according to the region being studied, are sandwiched between the heater and the asbestos frame F. The thickness of the absorbing layer is controlled by the thickness of the washer W used between the plates. For very thin films, no washer is necessary, provided that the plates are polished to a slightly convex surface.

For a cell made from plates of equal thickness, the temperature shown by the millivoltmeter when connected to the two thermocouples wired in

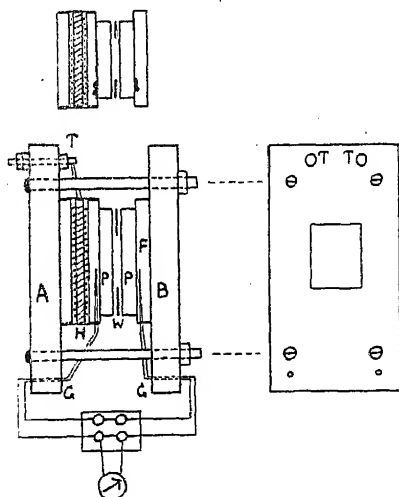


FIG. 1

series is that of the middle of the cell. This can be verified by the determination of melting points using the hot cell. With the plates normally used this temperature can be recorded to within a few ° C. Measurements have been made at 200° C., but in order to avoid cracking the cell plates, sudden changes of temperature must be avoided and the plates must not be touched with cold or moist surfaces when hot.

For operating the cell, a small amount of the solid is first melted on to the plates, which are then pressed together hot and placed in the mount. It is important that the cell should be used with the heater on the side away from the spectrometer slit in order to avoid detection of radiation emitted by the heater. Solid films can be conveniently formed by allowing the liquid to cool while sandwiched between the plates, and this seems to produce solid films with less scattering than those prepared in other ways.

---

## SOLVENTS FOR USE IN THE INFRA-RED.

By P. TORKINGTON AND H. W. THOMPSON.

*Received 28th November, 1944.*

In order to measure the infra-red absorption spectra of solids or highly absorbing liquids it is often desirable, and sometimes essential, to use solutions in organic solvents. Although some attempts have been made to use it in special cases, water is unsatisfactory as a solvent not only because of its extensive infra-red absorption, but also since it would attack the plates of alkali halide which normally form the absorption cell. Unless there are special interactions between solute and solvent, the spectra of the two substances are additive, and to obtain that of the solute, allowance must simply be made for absorption by the solvent. While in theory this can be done if the spectrum of the appropriate thickness of solvent is known, it is not very practicable in most cases where quantitative accuracy in the optical densities is required in those regions where both solute and solvent absorb. The aim should be to use high concentrations of solute and thin layers of solution, so that the bands of the former should be as far as possible brought out against those of the thin layer of solvent. Even in the most favourable cases however, weak bands of the solute may be masked by stronger bands of solvent, and complete absorption by the latter in some spectral regions may make it impossible to detect absorption bands of the solute at all. The difficulties are accentuated if the nature of the problem involved makes it desirable to use dilute solutions, since in this case there will be thicker layers of solvent.

It is therefore desirable to measure the absorption spectrum of the solute in a solvent which has no appreciable absorption over the range of spectrum studied, and since all solvents have absorption at some wavelengths it follows that in order to map out the complete spectrum of the solute several solvents may have to be used, the choice of which will depend upon the solubility of the solute in each of them and upon their particular regions of transmission.

Work of this kind made it desirable to have a reference table of the spectra of common solvents, from which polar and non-polar solvents could be chosen to cover any spectral range. In Fig. 1 the spectra are shown between 3-20 $\mu$  of some solvents which are normally available in quantity, and which can be satisfactorily purified by distillation or other simple means. Other substances have been used with advantage in special problems, but these have been omitted since they are less generally available. Similarly, commercial xylene has been omitted, not only because of the complexity of its spectrum but also since its composition is variable.

Also, whilst tetrachloroethylene ( $C_2Cl_4$ ) seems to be a very convenient solvent for several regions, it has not been included since different commercial samples have been found to contain impurities which are not easily removed. Other substances such as normal hexane or ethyl alcohol have been omitted in favour of substances of the same class which have a simpler spectrum.

The spectra of many of the compounds given have been described previously in scattered publications, notably those of Coblenz,<sup>1</sup> and Barnes, Liddel and Williams.<sup>2</sup> The spectra given by Coblenz were

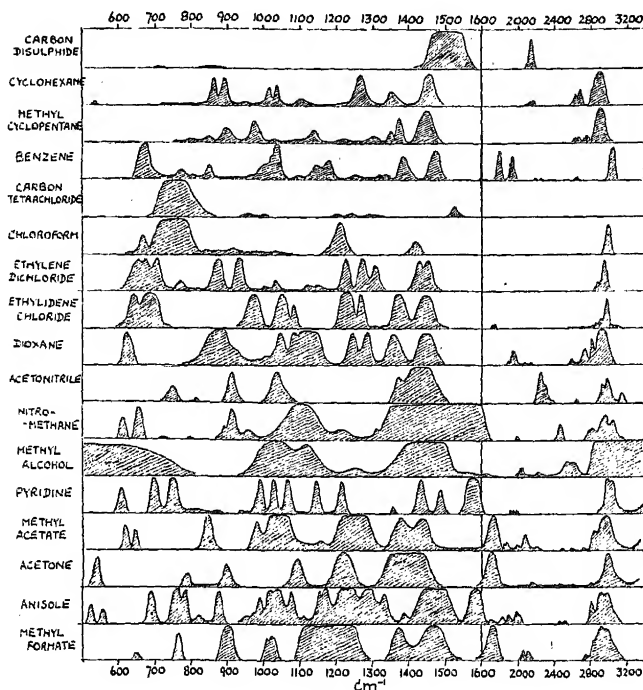


FIG. 1.

obtained using rather lower resolving power than is now generally available, and in some cases impurities seem to have been present. Those given by Barnes relate only to the range  $5\text{--}10\mu$ . The data of Fig. 1 were obtained with an absorption cell about  $0.1\text{ mm.}$  in thickness, and using a good spectrometer of the type described above, and they cover the range  $3\text{--}20\mu$ . This cell thickness has been found convenient for much quantitative analytical work. When much thicker cells are used the bands broaden considerably, and in the region  $1600\text{--}3000\text{ cm.}^{-1}$  ( $6\text{--}3\mu$ ) feebler bands not shown in the Figure may become appreciable. It should also be noted that all the data given in the Figure were obtained using a rock salt prism; using a quartz prism for the region of  $3000\text{ cm.}^{-1}$  some of the bands given split into several components.

The most useful solvents for different regions are listed in Table I.

<sup>1</sup> Coblenz, *Carng. Inst. Wash. Public.*, No. 35, 1905.

<sup>2</sup> *Ind. Eng. Chem. Anal. Ed.*, 1943, 15, 659.



TABLE I.

Spectral Range.		Good Solvents.	Less Satisfactory, but Possible Solvents.
cm. <sup>-1</sup> .	$\mu$ .		
500-600	20-16.7	Carbon disulphide, cyclohexane, benzene, carbon tetrachloride, chloroform, dioxane, methyl formate	Several.
600-700	16.7-14.3	Carbon disulphide, cyclohexane, acetone, carbon tetrachloride, acetonitrile	Methyl formate, anisole, pyridine, dioxane.
700-800	14.3-12.5	Carbon disulphide, cyclohexane, dioxane, nitromethane, methyl acetate	Ethylidene chloride, acetone.
800-900	12.5-11.1	Ethylidene chloride, acetonitrile	Carbon disulphide, nitromethane, methyl alcohol, pyridine, methyl formate, acetone.
900-1000	11.1-10.0	Carbon disulphide	Cyclohexane, carbon tetrachloride, chloroform, methanol, acetonitrile, methyl formate, methyl acetate, acetone.
1000-1100	10.0-9.1	Carbon disulphide, carbon tetrachloride, chloroform	Methyl cyclopentane, acetone, methyl formate.
1100-1200	9.1-8.3	Carbon disulphide, carbon tetrachloride, ethylidene chloride, acetonitrile	Cyclohexane, chloroform, acetone.
1200-1300	8.3-7.7	Carbon disulphide, acetonitrile	Methyl cyclopentane, carbon tetrachloride, chloroform, pyridine.
1300-1400	7.7-7.1	Carbon disulphide, carbon tetrachloride, chloroform, pyridine	Ethylene dichloride.
1400-1500	7.1-6.6	Carbon tetrachloride	Chloroform.
1500-1600	6.6-6.2	Cyclohexane, methyl cyclopentane, benzene, chloroform, dioxane, acetonitrile, methyl acetate, acetone	Methanol, methyl formate.
1600-2000	6.2-5.0	Carbon disulphide, cyclohexane, carbon tetrachloride, chloroform, acetonitrile	Nitromethane, methanol, pyridine.
2000-2400	5.0-4.1	Cyclohexane, methyl cyclopentane, benzene, carbon tetrachloride, chloroform, nitromethane, ethylidene chloride, pyridine	Acetone, anisole, methanol
2400-2800	4.1-3.6	Carbon disulphide, benzene, carbon tetrachloride, chloroform, ethylene dichloride, acetonitrile, pyridine, methyl formate	Acetone, anisole.
2800-3200	3.6-3.1	Carbon disulphide, carbon tetrachloride	Benzene, chloroform.

# TWO TIME-SAVING DEVICES IN THE CONVERSION OF ENERGY RECORDS INTO PERCENTAGE ABSORPTION CURVES.

BY H. A. WILLIS AND A. R. PHILPOTTS.

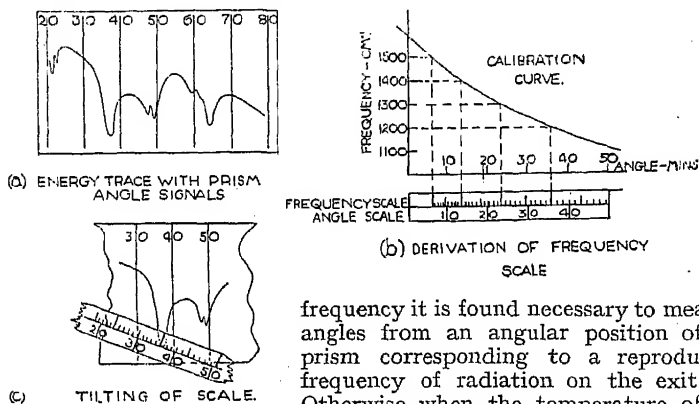
*Received 28th November, 1944.*

Any of the older types of hand operated spectrometers can very rapidly be made automatic by arranging to drive the prism at a constant angular rate and using an independent recording camera for the galvanometer deflections. The two devices described were constructed so that frequency and percentage absorption might be read off directly from the records obtained with such a converted spectrometer.

## (1) A Frequency Calibrator for Spectrometers with Prisms Rotated at Constant Speed.

In order to relate the recorded bands to the prism position, signals are made at equal increments of prism angle on the record. The calibrator gives the frequency of any band by reference to these signals (see Fig. 1a). Having determined the relation between prism angle and

FIGURE I FREQUENCY SCALE



frequency it is found necessary to measure angles from an angular position of the prism corresponding to a reproducible frequency of radiation on the exit slit. Otherwise when the temperature of the prism changes, the resulting change in deviation will cause a shift of the calibration curve along any "absolute" angle scale. In practice the "absolute" position of a particular absorption band was found to vary but the angular separation of two particular bands remained constant. Very small rotations of the prism relative to its divided circle (such as may arise in interchanging prisms) give the same effect. The reproducible frequency chosen as the "zero" of our scale was the point of maximum transmission in the  $6.2\mu$  water vapour band since this is found in the atmospheric absorption which is superimposed on single beam records.

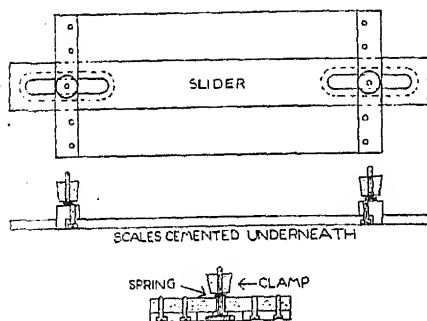
The calibrator consists of an angle scale equal to that on the record with the corresponding frequency scale (Fig. 1b) alongside. These are mounted on a transparency and arranged so that they can slide past each other. If every record contains the  $6.2\mu$  water band the correct relative

position of the scales can be adjusted for each one and the frequencies read off directly when the angle scale of the calibrator is laid over the angle scale signals on the record.

Since the prism and recording paper have separate drives and motors which can have mechanical imperfections, it may be found that the distance along the paper is not linear with prism angle. The error caused by this effect can be reduced by assuming linearity between adjacent signals only. The calibrator can then be made with the distance between angle graduations slightly larger than the largest distance between signals observed. The instrument is used tilted so that the distance representing an increment of angle on the scale fits between the signals bounding the

corresponding increment on the record. The frequency can be read off on the projected scale (Fig. 1c).

FIGURE II CONSTRUCTION OF CALIBRATOR



The stock of the slide rule was made of two 1-in. strips of Perspex bolted to metal cross-pieces with a third strip sliding between, both edges of the slider being utilised. The slider was provided with two screw clamps to prevent slipping after the "zero" has been set. The construction is shown in Fig. II. To obtain accurate scales large drawings were made, photographed and printed on

to film at the correct enlargement. The film scales were cemented underneath the slide rule.

This type of instrument has also been found useful with a spectrometer having an approximate wavelength drum, the calibration and signals being made with reference to drum readings.

## (2) A Direct Reading Percentage Absorption Scale for Energy Records.

The single beam recording spectrometer gives a trace showing the amount of energy transmitted by the absorbing medium. On this are drawn the zero line connecting points of zero transmission at each end of the range and the curve showing the "background" of energy available when there is no absorption. At any frequency a line is drawn at right angles to the direction of travel of the paper. If this cuts the zero line at Z, the energy trace at E and the background curve at B, the problem is to measure the ratio  $BE/BZ$  directly (see Fig. IIIa).

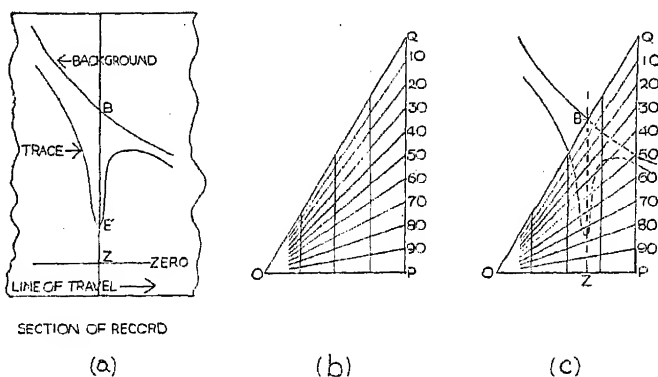
The network shown in Fig. IIIb is used. It is obvious that any line parallel to PQ with its ends in OP and OQ is cut into ten equal parts by the obliques. The diagram mounted on a transparency is moved along the record until with ZB parallel to PQ, Z lies on OP and B on OQ. The percentage absorption can now be read off using the obliques as the 10 % values (Fig. IIIc).

When the background is steep the maximum absorption of a band comes at an appreciable distance from the point where the energy curve is nearest the zero line. By moving the scale along the record the absorption maximum can be quickly found; the true frequency of the band corresponds to the position of this point.

Two methods of construction have been used. The network was drawn, photographed and printed out on a half-plate. This was bound to a clear half-plate to protect the emulsion. By using a reduction in size a more

accurate diagram is obtained. A large instrument was made by scribing the lines on a sheet of Perspex and filling them with black paint.

FIGURE III PERCENTAGE ABSORPTION SCALE



We wish to acknowledge valuable assistance from Messrs. E. E. Webb and R. E. Stonebridge in the construction of these instruments.

*The Physical Chemistry Laboratories,  
Oxford and Cambridge.*

#### GENERAL DISCUSSION.

Dr. W. C. Price (*Billingham*) said: I should like to add two additional methods of measuring cell thickness and a short description of a wedge cell which enables a continuous range of thicknesses to be used.

If a thin cover glass is placed in front of half of the objective of the telescope of a prism spectrometer so as to divide the field along a line parallel to the prism edge, then when the spectrometer is illuminated with white light it can be observed that a number of regularly spaced dark bands cross the continuous spectrum. The bands are known as Talbot's bands, and are only produced if the glass has been introduced from the red side. The number of bands between any two wavelengths is given by  $(\mu_1 - 1/n_1 - \mu_2 - 1/n_2)t$ . If a rock salt cell is half filled with benzene and suitably placed in front of the objective of the spectrometer so that the film of benzene takes the place of the cover glass then dark bands are similarly obtained. If  $n$  is the number of dark bands occurring between the  $C$  and  $F$  hydrogen lines, then the thickness of the cell in microns is  $n/0.301$ . The spectrometer has, of course, to be turned so that the prism edge is horizontal in order to obtain the bands with benzene.

The following method can be used for cells, the faces of which are not in the best optical condition. The cell is placed in series with a variable thickness quartz cell in front of the slit of a quartz spectrograph illuminated with a steady source of ultra-violet light preferably a hydrogen lamp. First the rock salt cell is filled with a 10% solution of benzene in a U.V. transparent solvent such as hexane or ethanol and the solvent is placed in the  $Q$  cell. A set of five or ten exposures is then taken. The R.S. cell is then filled with solvent and the  $Q$  cell with a 1% benzene solution and a set of exposures taken in between the first set, the thickness of the  $Q$  cell now being varied until the absorption obtained matches the first set. The thickness of the R.S. cell is one-tenth the matching thickness of the  $Q$  cell. A similar method can be used with infra-red

instead of ultra-violet absorption, but to obtain accurate results it is essential that both cells should be kept in the beam and that there should be no association between solute and solvent.

We have used wedge cells made from plates of quartz or rock salt as variable thickness cells. These are placed directly in front of the slit and moved transversely across the beam. The small prism effect introduced does not produce a measurable displacement of a band, and so does not upset the calibration. The two plates are in contact at one end and are separated at the other by a spacing foil. The thickness scale is linear across the cell and can be easily standardised by an accurately known feeler gauge. Only small quantities of liquid are required and the cells are easily cleaned.

The President enquired how great an error would be introduced in these methods of cell measurement if the end plates were not parallel or again if either or both plates had plane surfaces but were not of uniform thickness. In some measurements Mr. Kemball had been carrying out on the surface tension of mercury by the method of the sessile drop it had been found that very large errors were introduced when a wedge shaped but smooth plate was used.

Dr. Sutherland (*Cambridge*) said: The interference method depends on the *inside* surfaces of the cell being plane and parallel where the light beam traverses them. Lack of parallelism of the inner faces would cause the bands to disappear but lack of parallelism of the outer faces to the inner faces or to one another is of no consequence.

Professor C. K. Ingold (*London*) recalled that an attempt to develop infra-red technique on somewhat different lines had been initiated by Czerny and Mollet and interrupted by the war. Dr. Pol Mollet had been working on the subject at University College in 1939. In this method, the infra-red spectrum is received on a special screen, on which it can be photographed. The method thus brings the advantages of the photographic method into the infra-red region of fundamental vibration frequencies. The special screen consists of a sheet of celluloid, a few tenths of a micron thick, with a similarly thin coating, on the one side, of lamp black, and, on the other, of paraffin oil, deposited by condensation from the vapour. Each infra-red image of the slit produces a change of thickness of the oil film by partial local evaporation, and, when the screen is simultaneously illuminated by white light, the whole infra-red spectrum stands out as a coloured interference pattern, which can be photographed. So far, the method has been developed to cover the spectrum out to about  $10\mu$ , and within this range good photographs, sharp and rich in detail, have been obtained.

Dr. Sutherland (*Cambridge*) said: I should like to add that the double beam spectrometer at Cambridge has now been in operation and satisfactory records have been obtained in which atmospheric absorptions have been completely eliminated. The measurement of percentage absorption, however, is not yet entirely satisfactory.

In this connection I wish to acknowledge the contributions made by Mr. P. B. Fellgett in overcoming many of the practical difficulties encountered in getting a new piece of apparatus to function in the designed manner.

It should also be added that Messrs. Adam Hilger are now in a position to supply the complete spectrometer.

Dr. Thompson (*Oxford*) said: The technique which Professor Ingold has mentioned was, I believe, developed by Czerny, and is very interesting. Further work on these lines might be valuable, but I am inclined to think that the development of bolometers for detector systems may be more profitable. Another useful line of work may be the development of infra-red filters.

Dr. A. E. Martin (*London*) said that in his experience a very simple method for determining cell thickness was to weigh the cell empty and

then again filled with liquid, deducing the thickness from the weight of liquid, the density and area of liquid film being known. Usually the cell was constructed of two fluorite plates, 1 inch diameter and 0.1 inch thick, spaced with a suitable washer of metal foil extending to the full diameter of the plates. Such a cell, weighing less than 10 g., would, of course, be held in a brass mount when used in the spectrometer. This method is useful for films of thickness 0.001 to 0.1 mm. ( $\sim 0.3$  to 30 mg.) or so.<sup>1</sup> Layers rather thicker than 0.1 mm. are more conveniently measured with the help of a micrometer.

Mr. F. I. G. Rawlins (*London*) (*communicated*): As perhaps something of a veteran in the infra-red, I should like to offer a few brief comments of a general character. The historic figure of  $12.5 \text{ cm.}^{-1}$  for the separation of the HI lines had been reduced to  $3.35 \text{ cm.}^{-1}$  (average) at Cambridge in 1928 for NO. We used a species of tandem system—prism plus reflection grating—and the slow rate of progress in mapping a (gas) spectrum entirely by hand-setting was past belief as judged by the standards before the present meeting. Nevertheless, we achieved what in those days was our purpose, namely the establishment of a reasonable molecular model for the substance in question. Fundamentally infra-red work was more strictly physical than now, the recent developments towards chemical analysis resting essentially upon prior knowledge of the appropriate dynamics. Obviously, these modern analytical applications are exceedingly valuable, and illustrate the trend of any branch of natural science to become in some degree a tool once the ferocity of its embryo technique has been sufficiently tamed. Of the infra-red this is especially true. Associated with this progress in methods of recording has gone the elimination of the erratic readings of intensity so baffling in early days.

During those early years, in the laboratory at Marburg-Lahn, where so much pioneer work was done, the voice of Professor Schaefer could often be heard saying "*Lesen Sie schnell*"; and so we did, to the best of our ability. But all too seldom were our intensities reasonably reproducible, due to the manifold disturbances mentioned by present contributors. A year or so later, however, there was real improvement, due to thermopile construction and shielding. As for the present time of about half an hour to plot a spectrum from  $2\mu$  to  $15\mu$ , one can only speak of the progress implied as almost fabulous. Concerning instrumentation, the good points of the Littrow principle were appreciated fairly early, and I set up a modified form of it in 1925-26, combined with concentration of the beam upon a minute crystal area. Recording was with a radiomicrometer from which the polished cone had been removed. The sharpness of response of the whole system was remarkable. Schaefer had not long before been experimenting with polarized infra-red radiation using selenium mirrors in his efforts to disentangle crystal frequencies by reflection. Unfortunately, somewhat large errors occurred, due to the rather primitive angular setting device employed. Enhanced success with crystal technique rendered it needless at the time to study reflection spectra further.

Dr. Sutherland (*Cambridge*) said: In reply to Dr. Martin, we have also used the method of weighing when the highest accuracy was not required. It is, however, slow compared to the interference method now proposed, and gives an average value for the thickness, whereas the interference method employing a small aperture can be used to study in detail that part of the cell through which the radiation is passing. Defects are apt to occur in a cell after it has been used for some time and an optical method of examination has distinct advantages.

I should like to assure Mr. Rawlins that infra-red spectrometers can still at times be very erratic, yes, even baffling, in spite of all the recent improvements. At least there was no cyclotron to contend with in Cambridge in the old days.

<sup>1</sup> See Fox and Martin, *Proc. Roy. Soc. A*, 1940, 174, 238.

## A THERMOCOUPLE-BOLOMETER DETECTOR.

By G. K. T. CONN.

Received 13th November, 1944.

The sensitivity of the radiation detector used in the spectrometer limits the practical resolution obtainable in the infra-red region of the spectrum. Any means of improving and controlling the sensitivity of the detector has an immediate and direct bearing on the accuracy and ease with which measurements may be made. The two principal instruments available are the bolometer and the thermocouple, of which the latter has hitherto been most commonly used. Both instruments in their present form are extremely inefficient, for example, the best radiation thermocouples have an efficiency of about  $10^{-8}$  %. The purpose of the present paper is not to discuss the general problem of radiation detection, which receives attention elsewhere, but to show how the sensitivity of thermocouples may be controlled and appreciably improved by adapting the principle of the bolometer. Experimental results are given, providing orders of magnitude which will be convenient in applying the technique to thermocouples already in use.

The bolometer uses the change in resistance of a metal strip which follows from the rise in temperature on irradiation. If a thermocouple be placed in one arm of a balanced Wheatstone bridge, irradiation leads not only to a thermoelectric e.m.f. but to a change in the resistance of the thermoelectric wires. The resultant galvanometer deflection is due to two effects which may be briefly designated thermoelectric and bolometric respectively. The temperature of the junction prior to irradiation is controlled by the current flowing in two ways. Due to the Seebeck-Peltier effect at the junction, there may be a rise above or a fall below room temperature. This follows since the power consumed at the junction changes sign when the supply current is reversed. The joule heating of the thermoelectric wires and at the junction itself leads to a rise in temperature. Changes in temperature of the junction due to irradiation may thus increase or decrease the thermoelectric e.m.f. according to the direction of the current. Whatever the direction of the current, irradiation leads to an increase in the effective bolometer resistance. The bolometric contribution to the subsequent deflection of the bridge galvanometer can be varied by varying the supply current. The effects are much enhanced by working *in vacuo* and are easily demonstrated by observing the change in resistance of a thermo-junction at low currents when the supply current is reversed.

In the arrangement described above, variation of sensitivity is obtained by varying the supply current. Because of the joule heating effect of the current, the resistance will alter accordingly. It is not only convenient to work with a galvanometer through which no current passes prior to irradiation, but if the galvanometer deflection is to be amplified by photoelectric means such a condition is essential. This can readily be achieved by suitably altering the balance arm of the Wheatstone bridge. As illustration, Fig. 1 shows the manner in which galvanometer deflection varied with supply current to the bridge for a platinum wire *in vacuo*.

(This wire was of  $6.5\mu$  diameter and 4.5 cm. long.) The various curves were obtained for the different values of the balancing resistance given. The remaining bridge resistances were each  $100\Omega$ . By varying this balancing resistance the galvanometer can be set at zero for any value of the supply current. A smooth control of this resistance is readily obtained by putting a high variable resistance in parallel with it. The maximum current through the galvanometer may obviously be considerable and it is advisable first to find the approximate value of the resistance with an insensitive instrument.

Experiments have been made with a number of commonly used thermojunctions such as Iron/Constantan, Chromel/Alumel, Chromel/Constantan, Hutchins' Alloys, and junctions of which one element is Bismuth and the second an alloy of Bi (95 %) — Sn (5 %). As is to be expected, the relative importance of the effects considered depends on the component wires. Constantan, for example, has a low temperature coefficient of resistance which is reflected in the sensitivity obtained. Thinner wires, which have a higher resistance, show a greater bolometric effect than those of a heavier gauge. The rise in temperature of the junction due to the current may affect the construction of a thermocouple intended to be used at room temperature. For instance, the receiver is often attached to the junction by black wax which softens about  $50^\circ\text{C}$ ., or by a low melting point solder such as Wood's metal, which melts at about  $60^\circ\text{C}$ . Such factors must be borne in mind if the suggested arrangement is applied to junctions already in operation and are illustrated by the experiments. The aim has not been to obtain the highest sensitivity possible, but to consider what improvements are practicable with existing detectors.

The thermocouples were mounted in a glass envelope and illuminated by an electric lamp bulb placed at a suitable distance. All measurements were made at a pressure of  $10^{-4}$  mm. Hg. or better. The distance of the lamp was adjusted until a convenient deflection of 5 to 10 cm. was obtained on the Moll recording galvanometer with no current flowing. The deflection was then determined for various values of the supply current. Positive values of the current are those for which the thermoelectric and bolometric effects are additive. Each deflection was verified for at least two values of the balancing resistance and thus two positions of the galvanometer zero, of which one was the position of balance. The changes in the balancing resistance were a small fraction of the total.

The deflection due to irradiation for a given current through the thermocouple was divided by the deflection obtained with zero supply current. This ratio,  $G$  is shown in Fig. II plotted against the current,  $i$ , flowing through the junction. Thus the benefit in any particular case is clearly given as a function of supply current.

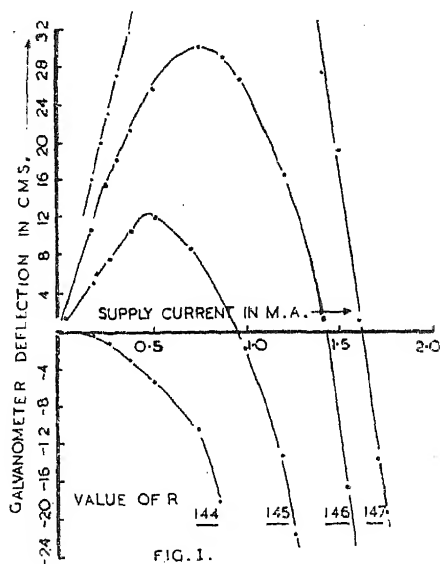
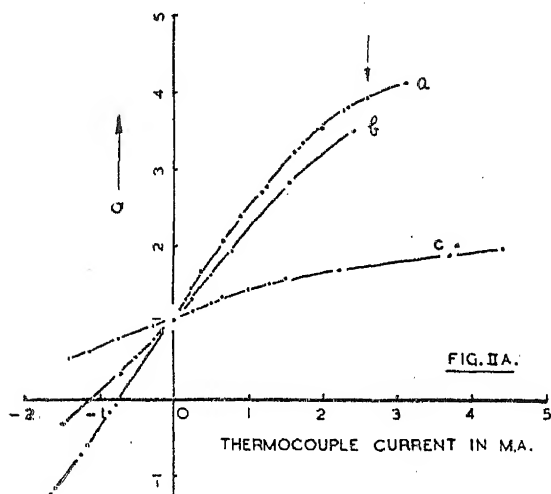


FIG. 1.



In Fig. IIa are presented the results obtained with three different junctions. The curve labelled (a) was obtained with wires of Chromel and Alumel about  $15\mu$  in diameter. The receiver, of platinum foil about  $1.3\mu$  thick coated with camphor black, was attached by black wax. The resistance was 94 ohms. At the point marked by the arrow the receiver moved slightly due to softening of the wax; this was indicated by a drop



in the deflection for zero current. Thus, between room temperature and the softening point of the wax, improvement by a factor of four\* is obtained. Reversal of the current leads to zero deflection where the two effects cancel at  $-0.65$  M.A. Curve (b) was obtained with a similar junction of resistance  $75\Omega$ . The lower resistance is reflected in the lower bolometric effect. Curve (c) was obtained with a junction of Chromel and Constantan and illustrates

the effect of having one wire of low temperature co-efficient of resistance. The Chromel wire was about the same length as in (a) but the Constantan wire available, of 48 S.W.G., was very much longer so that the resistances of the two were approximately matched. The resistance of the whole junction was  $108\Omega$  and offers appropriate comparison with (a). The slope is clearly very much lower.

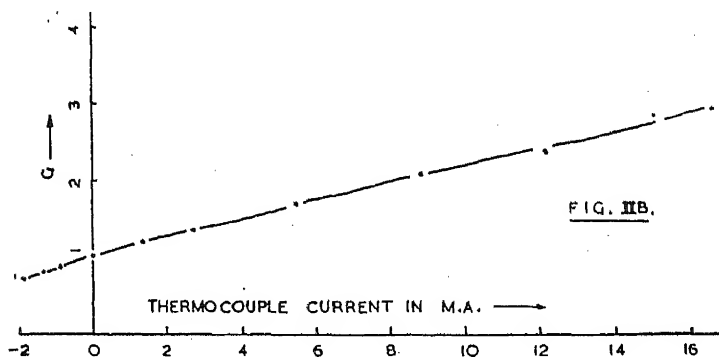


Fig. IIb shows a curve obtained with a junction made of Hutchins' alloys, which are commonly used in radiation detection. One metal was composed of Bi 97 % — Sb 3 %, while the other was of Bi 95 % — Sn 5 % ;

\*It may be mentioned that a factor of seven has been obtained by working at higher temperatures.

all proportions are by weight. These were drawn down by the Taylor process in soda glass which was then etched off with hydrofluoric acid. The wires, about 5 mm. long were soldered by radiation with a tiny piece of Wood's metal and had a resistance of about  $13.8\Omega$ . The receiver, of gold foil about  $0.5\mu$  thick, was coated with evaporated zinc black and attached to the junction by the Wood's metal solder. It will be seen that a factor  $G$  of about 4 was obtained. Readings were discontinued because this thermocouple was constructed for another purpose and the risk of burning it out had to be avoided. When junctions containing bismuth or bismuth alloys are used, unsteadiness of the galvanometer follows if the output be pushed to extreme. In these, there is not only the well known change of electrical resistance in a magnetic field but there is also a change in the thermoelectric power on application of a magnetic field.<sup>1</sup>

The improvement of sensitivity obtained by combining the principle of the bolometer is clearly appreciable and is readily achieved. Moreover, since unsteadiness of the thermocouple system often proves troublesome it is clear that by the same means the system may on occasion be desensitised with consequent increase in stability. In the case of the Chromel/Alumel junction (a) an improvement in the sensitivity by a factor of 4 is reported. Of this output three parts are clearly due to a bolometric effect and one part to thermoelectric. The indication, significant of advantages inherent in bolometer systems, is confirmed by work on bolometers which is presented elsewhere.

In conclusion, there are several points to which attention should be drawn. In certain cases the full gain indicated above may not be realised. If a second junction be used to compensate for variations in room temperature, it may be incorporated in the bridge circuit as the balancing resistance. If the remaining resistances which shunt the galvanometer be large, there is no reduction in the observed galvanometer deflection due to incorporation of the thermocouple in the bridge circuit. If no compensator be used, however, the output e.m.f. is in series with the balancing resistance and is consequently reduced. Thus if the thermocouple alone be used with the galvanometer, then the deflection for a given e.m.f. is proportional to  $1/(R + R_g)$ , where  $R$  and  $R_g$  are the resistances of the thermocouple and the galvanometer respectively. Incorporated in a balanced Wheatstone bridge, the same thermocouple e.m.f. produces a deflection proportional to  $1/(2R + R_g)$ , due to the presence of the balancing resistance. If  $R = R_g$ , that is the galvanometer matches the thermocouple, incorporation in the bridge thus reduces the deflection by a factor  $2/3$ . This must be redressed before a positive gain is achieved.

The steadiness of the galvanometer depends on constancy in the bridge circuit. If the highest sensitivities be in mind and the galvanometer is to be used with an amplifier, fixed resistances must be used. In such cases, extreme steadiness in output of the battery is essential and reference may be made to the papers of White<sup>2</sup> and Potter<sup>3</sup> in this connection. Where a galvanometer of current sensitivity of the order of  $10^{-7}$  mm. at a metre per ampere is used, a post-office box of the stud variety is permissible. Plug boxes often give rise to irregularity due to variable contact resistances. Variation in the current must, of course, be obtained by resistance box, not rheostat.

### Summary.

The sensitivity of thermocouple detectors may be enhanced and controlled by using the fact that the electrical resistance of the thermocouple wires changes with temperature. This application of the principle of the

<sup>1</sup> Borelius and Lindh, *Ann. Physik*, 1916, 51, 607; 1917, 53, 97. Grüneisen and Gielessen, *ibid.*, 1936, 26, 449.

<sup>2</sup> White, *Physic. Rev.*, 1906, 23, 447.

<sup>3</sup> Potter, *J. Sci. Inst.*, 1934, 11, 95.

bolometer is obtained by incorporating the thermo-junction in a Wheatstone bridge circuit. Control is obtained by varying the relative importance of the two effects, and appreciable improvement, by factors varying from two to four, in the sensitivity of thermocouples already in use can be expected. Experimental results for certain commonly used junctions are presented and precautions to be observed are briefly considered.

*Department of Physics,  
The University, Sheffield.*

#### GENERAL DISCUSSION.

Dr. M. M. Davies (*Leeds*) said: In the combined thermocouple-bolometer described by Dr. Conn, the element is operated at temperatures up to  $50^{\circ}$ . Part of the zero instability with thermocouple detectors often comes from atmospheric temperature fluctuations, *e.g.* in the form of draughts—disturbances which may even be noticeable with matched vacuum elements. It might thus be anticipated that working with an element having a considerable temperature difference from its surroundings would, *with a given detecting system*, greatly increase zero fluctuations from this source. Does Dr. Conn's experience confirm this anticipation, and does his experience suggest that the sensitivity increases in greater proportion than the zero instability?

Dr. Sutherland (*Cambridge*) said: In regard to Dr. Davies' question about the sensitivity of bolometers to draughts, I would emphasise the final paragraph in the paper by Dr. Thompson and myself, where it is pointed out that the use of A.C. should largely eliminate the effects of such disturbances.

With reference to the use of bolometers in infra-red spectroscopy, it seems likely that the advantages these devices offer over thermocouples in the way of increased speed for a given sensitivity will be even more important in the near future than the very interesting increases in absolute sensitivity reported by Dr. Conn.

Dr. Conn (*Sheffield*) said: In the past infra-red analysis, though of wide application, has been limited because of a notoriously laborious technique. Development of sensitive detectors with a fast time of response will do much to extend its practical utility. In certain cases, however, detectors of specific design for a particular class of problem are desirable. For example, application to reaction kinetics has not been mentioned in the previous papers but yields direct and significant results.<sup>1</sup> In such applications quantitative estimates of the proportions of the reacting components are of vital importance. Hence, a means of measuring the absolute intensity of absorption in the reaction vessel itself (or in a vessel directly connected to it) is required for reliable measurements. Such a method, using an adaptation of the Pirani gauge is being developed.

There are two points to be made in answering Dr. Davies. If a thermocouple detector be used with a matched compensating thermocouple, zero instability due to thermal, mechanical or electrical disturbance can be reduced to very small proportions by careful design and construction. There are, of course, factors peculiar to bolometers, but in all cases a practical limit is set by Brownian disturbance of the recording galvanometer. This limit is proportional to the absolute temperature. Since the system described is used at a slightly higher temperature, the Brownian limit is higher. The effect is, however, small: for example, taking room temperature at  $20^{\circ}$  C. and an operating temperature of  $50^{\circ}$  C., the Brownian limit is raised by a factor of 323/293. In the measurements discussed in the paper, no elaborate means of ensuring thermal stability have been

<sup>1</sup> Benedict, Morekawa, Barnes and Taylor, *J. Chem. Physics*, 1937, 5, 1; Conn and Twigg, *Proc. Roy. Soc. A*, 1939, 171, 70.

adopted, and no compensator was used. Moreover, it should be pointed out that the radiation was not focussed on the receiver. The susceptibility to temperature change is thus tested somewhat drastically. My experience is that if the temperature rise is kept within the limits mentioned, the accuracy is not impaired. Vindication is obtained by examining the spread of the points plotted. I should add, however, that I have had to take the precaution of lagging carefully when working with similar systems at considerably higher temperatures.

## THE USE OF INFRA-RED ABSORPTION IN ANALYSIS.

### A. INTRODUCTION.

BY H. W. THOMPSON AND G. B. B. M. SUTHERLAND.

*Received 12th December, 1944.*

A number of papers have recently been published, mainly from American laboratories, in which the application of infra-red spectroscopy to problems of qualitative and quantitative analysis has been described.<sup>1</sup> Similar work has been in progress for some years in this country, and attention may now be drawn to its growing importance for analytical purposes in both routine and research laboratories of organic and physical chemistry.<sup>2</sup> In other papers we have discussed some of the ways in which the method can be applied to problems of internal molecular structure and diagnosis, and we shall here outline briefly its application to the qualitative and quantitative analysis of molecules in general.

When a molecule absorbs electromagnetic radiation of wavelength  $1-25\mu$ , the energy is used to excite molecular vibrations. A non-linear molecule of  $n$  atoms has in general  $(3n - 6)$  fundamental or "normal" modes of vibration, each having a definite frequency, and such frequencies may be absorbed by the molecule from a beam in which a continuous range of frequencies is present. The characteristic modes of these normal vibrations for a given molecule differ from each other, and are associated with different changes in the molecular electric moment, upon which the infra-red absorption depends. It therefore always happens that the vibrations are excited with different intensities, and some may be so feebly absorbed as not to be observed at all. Also, when a molecule contains several identical groups, *e.g.*  $\text{CH}_3$ , some of the vibration frequencies group closely around definite values, and may for practical purposes coincide. These factors lead to a simplification with larger molecules of what might otherwise imply a spectrum of unmanageable complexity.

Now the magnitudes of the characteristic molecular frequencies are determined by the masses of the atomic nuclei and the forces which hold them together. Certain linkages, *e.g.*  $\text{C}-\text{H}$ ,  $\text{O}-\text{H}$ ,  $\text{N}-\text{H}$ , retain their individuality in different compounds, and give rise to frequencies which are only slightly affected by the rest of the molecule; others, *e.g.*  $\text{C}=\text{C}$ ,  $\text{C}=\text{O}$ , give a fairly constant frequency in different compounds, but their exact values are rather more influenced by their environment in the molecule, and by varying electronic influences. In principle, however, no two molecules other than a pair of optical isomers can have an exactly similar array of frequencies, and although two closely related molecules

<sup>1</sup> Wright, *Ind. Eng. Chem. Anal. Ed.*, 1941, 13, 1. Barnes and others, *ibid.*, 1943, 15, 83, 659. Brattain and Beek, *J. Appl. Physics*, 1942, 13, 699.

<sup>2</sup> H. W. Thompson, *Tilden Lecture, J.C.S.*, 1944, 183.

may have several absorption bands at identical wavelengths, we may expect to find some spectral region in which differences can be found. In this sense the infra-red spectrum is a fingerprint of the molecule, and with structural isomers of relatively simple molecules, as well as with highly complex organic structures, this spectrum may well be the most characteristic physical property of the compound.

Analysis usually involves two stages. It is first necessary to know qualitatively what compounds are present, or at any rate to be sure that no unknown component has absorption bands which interfere with or mask the key absorption bands of the component under consideration. If independent methods give this information, the infra-red spectrum can be used to show that no other unsuspected substances are present. The spectra of each of the pure compounds must be known, and all the observed absorption bands must be accounted for by reference to these. Any bands which cannot be correlated in this way will imply the presence of an unsuspected component. It should be emphasised here that failure to detect a small amount of a particular component in the infra-red spectrum is not always proof of its absence, since in complex mixtures it may happen that the only strong bands of some particular compound are masked by overlapping bands of others. The sensitivity of the method depends on several factors, and can only be assessed by reference to each individual case. Thus whereas it may be possible in some cases to detect 0.01 % of a component, there are others in which 5 % of a compound might be missed in a complex mixture. Quantitative measurements described below may in some cases suggest an unallocated small residuum, but this will depend upon the accuracy with which all the major components can be determined.

Obviously the tendency for feeble bands to become submerged in stronger absorption regions will be minimised by using the best possible resolving power. Much would be gained in this direction by using grating spectrometers, especially for gas analysis, but for practical purposes and in general for all liquids and solids a good prism spectrometer is nearly always preferable and instruments of this kind are now available giving sufficiently high resolving power for most problems.

When the components of a mixture are known, quantitative analysis can be attempted by methods based upon the theoretical absorption laws or upon empirical calibration. The key wavelengths to be used for each component will be selected on the basis of (a) intrinsic intensity of the bands, (b) freedom from overlap with bands of other components. In complex cases it is often essential to compromise between these two factors. It may sometimes be preferable to use a relatively feeble absorption band for the determination of a particular component rather than a more intense one which is partly overlaid by a band of some other substance, since by a correct choice of cell thickness or concentration the percentage absorption can be brought into a region of convenient measurement.

According to Beer's law, the intensities of radiation of a given wavelength before ( $I_0$ ) and after ( $I$ ) passing through a sample are related as follows:—

$$I = I_0 e^{-EcL}, \text{ or } E = 1/cL \log I_0/I = 1/cL \cdot d$$

in which  $c$  is the molar concentration,  $L$  the path length,  $E$  the molecular extinction coefficient, and  $d$  the optical density. The incomplete resolving power of infra-red spectrometers, as well as the spread of vibration bands resulting from factors such as change of rotational energy which may occur simultaneously with the vibrational transition, imply that an integrated form of the above equation over the whole band should be used. This raises the question whether the percentage absorption  $A$  at a band peak should in fact be related to  $I_0$  and  $I$  by the equation  $I_0/I = 100/(100 - A)$ , or whether areas under band envelopes should be taken as a more correct

measure of the absorbed energy. Test measurements have shown that in many cases at least, the percentage absorption at the band peaks can be safely used, unless (i) there is some effect such as intermolecular association causing excessive and unsymmetrical broadening, or (ii) the absorption band shows a rotational structure which varies abnormally with pressure or concentration. In the latter event, which may well occur in the analysis of vapours of low molecular weight, it is clear that care must be taken to select a suitably low resolving power by choice of slit widths.

If with a mixture the optical densities are additive, we have, at a wavelength  $\lambda$ ,

$$d^\lambda = \sum d_i^\lambda = \sum c_i L E_i^\lambda.$$

In order to determine the concentrations of each of  $n$  components it will be necessary to determine the optical densities of the mixture of  $n$  wavelengths, each being a key for one component;  $n$  linear equations will then be obtained of the form,

$$d^\lambda = L(c_1 E_1^\lambda + c_2 E_2^\lambda + \dots + c_n E_n^\lambda).$$

If the extinction coefficients  $E_i$  are known for each of the pure components at each of the  $n$  wavelengths, it will then be possible in theory to solve the group of linear homogeneous equations for the unknown concentrations. This method is standard, and has been used in ultra-violet work for some time. The accuracy obtainable, however, will vary from one example to another for several reasons. For example, the maximum of the key band of compound A may lie on the steep side of an absorption band of compound B. In such a case the coefficient  $E_B$  is changing rapidly with wavelength, and an accurate value cannot easily be obtained, for small errors in the wavelength setting or a change in resolving power may affect it seriously. Again, with multi-component systems, care is needed in solving the group of linear equations if errors are to be avoided. When more than three or four components are present, complete self-consistency of the equations is rarely found, but quick approximation methods can be used to obtain the most satisfactory solutions for the concentrations. Nielsen and Smith<sup>3</sup> have discussed the circumstances which are most favourable for high sensitivity and accuracy. As regards the former it is necessary that the component in question shall have one band of high extinction coefficient at a wavelength where all the other components have either negligible or very small absorption. Highest accuracy will be obtained in determining the concentration<sup>4</sup> if the percentage absorption at the peak is about 63 %, but the concentrations leading to this may be such as to cause greater overlapping, and so it may be better to work at rather lower optical densities. Usually about 50 % absorption at the peaks is a good working value.

In computational methods of this kind, it is also necessary to make allowance for the absorption by the cell, and also by the solvent, if this is not zero. Thus, loss of energy by reflexion at the faces of the absorption cell will mean that the linear plots of  $d_i$  against  $c_i$  for the pure components do not pass through the origin, and the positive intercept on the axis of optical density will give a measure of the "cell constant". Nielsen and Smith<sup>3</sup> have set out the relevant mathematical formulation in detail.

When Beer's law does not apply to the pure components, or if correspondingly the optical densities in a mixture are not additive, empirical calibration can be set up for the analysis by reference to mixtures of known composition examined under fixed experimental conditions, and by means of matching, or from graphical calibrations the analysis can often be carried out rapidly with satisfactory accuracy. Barnes, Liddel and Williams<sup>4</sup> and Wright<sup>5</sup> have described several examples of this kind.

<sup>3</sup> Nielsen and Smith, *Ind. Eng. Chem.*, 1943, **15**, 609.

<sup>4</sup> Barnes, Liddel and Williams, *Ind. Eng. Chem. Anal. Ed.*, 1943, **15**, 659.

<sup>5</sup> Wright, *Ind. Eng. Chem. Anal. Ed.*, 1941, **13**, 1.

Apart from the difficulty of measuring optical densities in the infra-red with high precision, other problems at present are the accurate measurement of cell thickness, and the choice of suitable solvents in the examination of solid substances. These have been discussed elsewhere.<sup>6</sup> If the same absorption cell can be used without deterioration throughout a series of measurements, it will not be necessary to know its thickness; alternatively, the thickness of a new cell can be measured with reference to a master cell by using the absorption of some standard substance.

One of the great merits of infra-red analysis is its speed. For most purposes it has marked advantages over analogous methods using an ultra-violet spectrophotometer. The ultra-violet bands of complex molecules are usually broad maxima which overlap badly in a mixture; by contrast infra-red bands are sharp and well-defined. The infra-red spectra must always be more characteristic than the ultra-violet spectra since the former depend on the whole nuclear framework of the molecule, whereas the latter depend essentially on electronic excitation which is usually highly localised in one part of the molecule. Moreover, decomposition of the substance seldom occurs when it is irradiated with infra-red radiation. At the same time, infra-red and ultra-violet analysis should be used to supplement each other where appropriate, and this is particularly valuable when one or two of the components present have strong ultra-violet absorption and the remainder have not, so that the former can be picked out more easily.

Apart from the analysis of mixtures in general, one of the most valuable uses of the infra-red absorption is for the detection of impurities in substances, when these cannot be detected by other methods. If only two components are present, the submersion of feeble bands due to the impurity by the stronger bands of the major component is not likely to occur so much as when many components are present; and while no general statement can be made, it is usually possible to detect 1 %, and often much less, of an impurity if the cell thickness and concentration are chosen correctly. Another obvious application is the use of infra-red absorption for following the rates of reactions, such as polymerisations, for which other continuous methods are inconvenient. The direct control of industrial production by continuously following the concentrations of key intermediates or products is also possible. For this purpose it is sometimes possible to use infra-red filters and thereby avoid the prism dispersive system, and these, coupled with bolometers and suitable amplifiers offer much promise for future work, and for automatic control.

Some typical examples of analyses which have been worked out during recent years are given below. These have been chosen from a large number to indicate the different types of system to which the method is applicable.

*The Physical Chemistry Laboratories,  
Oxford and Cambridge.*

<sup>6</sup> See other papers in this discussion.

---

## B. EXAMPLES OF ANALYSES.

By D. H. WHIFFEN, P. TORKINGTON AND H. W. THOMPSON.

(1) **Cresols and Xylenols.**—The analysis of cresols and xylenols is an industrial problem of considerable importance, and no very satisfactory quick chemical method is at present available. We have recently developed a method for the analysis of cresylic acid by which the percentage of each isomer can be determined from a single measurement requiring about fifteen minutes. The details of this work are being published

elsewhere,<sup>7</sup> but it will be outlined here as an example of a straightforward infra-red analysis capable of high accuracy.

Between  $3\text{--}20\mu$  there are several marked differences between the spectra of the isomeric cresols which could be used for identification and analysis.

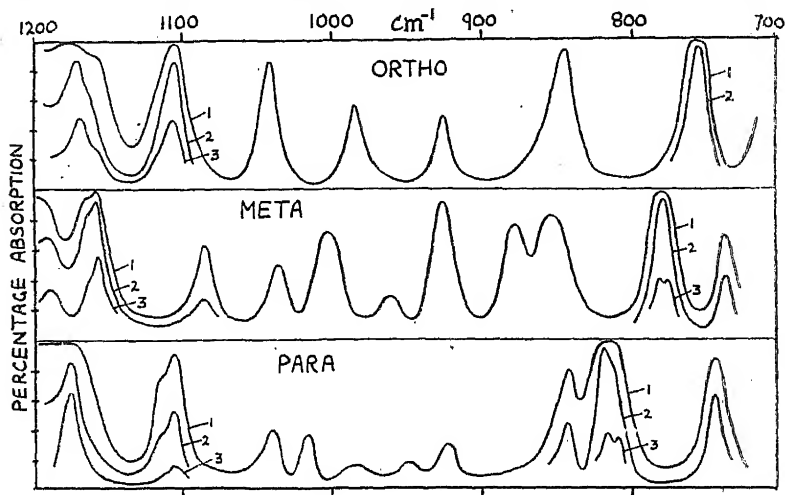


FIG. 1a.—Cresols in Carbon Disulphide (1) 20 %, (2) 5 %, (3) 1 %.

Figure 1a shows the spectra between  $8\text{--}14\mu$  ( $1200\text{--}700\text{ cm}^{-1}$ ) measured with solutions in carbon disulphide. Each isomer has a very intense band in the region  $700\text{--}850\text{ cm}^{-1}$  which is connected with a wagging motion of the C—H bonds perpendicular to the plane of the aromatic nucleus. These bands lie at about  $752$ ,  $776$  and  $815\text{ cm}^{-1}$  for the ortho, meta and para derivatives, and are so much more intense than most of the other bands in the spectrum that if the concentrations are reduced so as to bring down the percentage absorption at the peaks to conveniently measurable values, other bands are scarcely appreciable. They are therefore well suited to analysis, particularly also since there is hardly any overlapping between the bands of the separate isomers. In the actual analyses, cyclohexane was used as solvent, since it has no absorption in this region, and is less troublesome than carbon disulphide. The optical density of the key bands was determined for each isomer

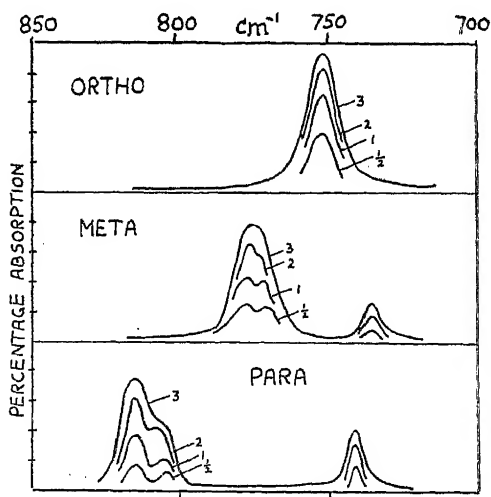


FIG. 1b.—Cresols in Cyclohexane. Figures on curves denote % concentration.

<sup>7</sup> Whiffen and Thompson, *J.C.S. in the press; Chemistry and Industry*, Sept. 23, 1944.



using 0.5-5 % solutions in a rock-salt cell about 0.1 mm. thick (Fig. 1b). From these measurements, the optical density was plotted against concentration (moles per litre) for each isomer, and approximate linearity showed that Beer's law is roughly applicable at these dilutions. The molecular extinction coefficients could be obtained by dividing the slope of these lines by the cell thickness; the latter was not accurately determined, but since the same cell was used throughout the calibration measurements and those with unknown mixtures, absolute values for the extinction coefficients are not required. The optical densities at the three key wavelengths were then similarly determined using solutions of the unknown mixtures containing a known weight per litre. Since the bands do not appreciably overlap, the weights of each isomer can be read off the curves directly, and should total the weight taken, and give the percentage composition. The method was tested against synthetic mixtures of known composition, typical results being as follows:

	<i>g. per c.c.</i>				<i>percentage</i>		
	<i>ortho</i>	<i>meta</i>	<i>para</i>	<i>total</i>	<i>ortho</i>	<i>meta</i>	<i>para</i>
Mixture 1—							
taken . . .	0.31	1.61	1.41	3.33	9.3	48.4	42.3
found . . .	0.30	1.60	1.45	3.35	8.9	47.8	43.3
Mixture 2—							
taken . . .	0.60	1.61	1.27	3.48	17.2	46.2	36.6
found . . .	0.60	1.65	1.30	3.55	16.9	46.4	36.7

Similar agreement was obtained with other samples made up independently in another laboratory. One of these contained only about 90 % cresols, with 10 % of miscellaneous impurities, and the infra-red determination not only gave a total of approximately 90 % cresols but also suggested the nature of some of the impurities. Subsequent work and discussions have shown that this method for the analysis of cresylic acid may well be adopted for purposes of standardisation in the near future.

The analysis of xylenols can be carried out in a similar way. The spectra of these substances in carbon disulphide solution have been given elsewhere.<sup>7</sup> They are more complex than those of the cresols but characteristic bands exist. It would be difficult to analyse a mixture of all six xylenols with high accuracy, but with comparatively easy preliminary fractionation, satisfactory determinations can be made. Thus, the following scheme can be followed:—

		<i>Key bands (cm.<sup>-1</sup>).</i>
Fraction A.	2.6 dimethyl phenol with cresols	1090, 904.
Fraction B.	2.4 dimethyl phenol	770, 804, 873.
	2.5 dimethyl phenol	800, 850, 993.
	? 2.3 dimethyl phenol	1066
Fraction C.	3.4 dimethyl phenol	730, 807, 855, 1116, 1295.
	3.5 dimethyl phenol	830.

There may, of course, be some slight overlap between these cuts, but this is not serious. Also, small amounts of the ethyl phenols can be detected and estimated if present. In these cases, it is impossible to give a general statement about the accuracy obtainable, which will vary with the particular mixture involved, but the method is far superior and quicker than any other method at present in use.

(2) **Anilines, Methyl Anilines and Toluidines.**—It was required to detect and estimate small amounts of dimethyl aniline and of toluidines in a mixture containing predominantly aniline and methyl aniline. The spectra of thin layers (about 0.05 mm. or less) of aniline, N-methyl aniline, NN-dimethyl aniline, and of the corresponding toluidines are shown in Fig. 2. As regards the first three of these, NN-dimethyl aniline has a band at 943 cm.<sup>-1</sup> which lies clear of bands of the others, and can be

used for its estimation if more than about 0.5 % is present. Between 1200-1400  $\text{cm}^{-1}$  there are differences between the spectra, and if good resolving power is used, preferably with the better dispersion of a fluorite prism, key bands for the aniline and methyl aniline lie at 1278 and 1323  $\text{cm}^{-1}$ . There is, however, a strong band of N-methyl aniline at 1268 which interferes with the determination of aniline by 1278, and the aniline is best determined by difference. The para toluidines have a strong band

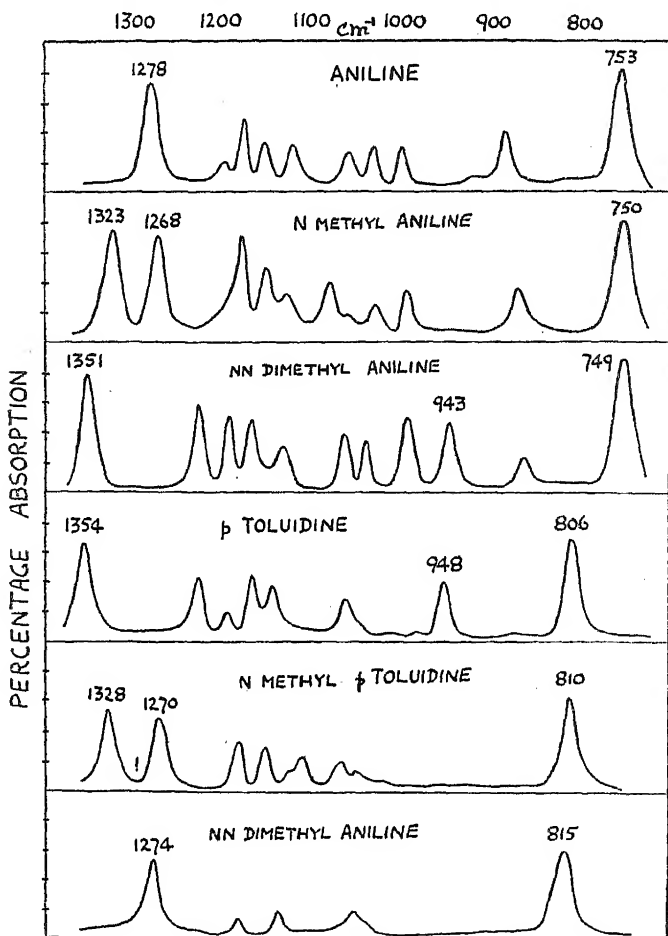


FIG. 2.

The bottom curve is erroneously labelled; it should be NN Dimethyl *p* Toluidine.

in the region of 810  $\text{cm}^{-1}$  (the analogue of the para cresol band at 815  $\text{cm}^{-1}$ ); and NN-dimethyl para toluidine has a band at 948 which lies close to that of NN-dimethyl aniline. The toluidine band at 810 is so intense that if a suitable cell thickness is chosen, 1 % or less can be detected. If it is present, correction may have to be applied in determining the NN-dimethyl aniline from the band at 943  $\text{cm}^{-1}$ . In the examples studied, no toluidines were found, so that a direct calibration could be set up for the band at 943 showing percentage of NN-dimethyl aniline against percentage absorption or optical density, using the same absorption cell

throughout. With concentrations of NN-dimethyl aniline up to 20 %, it could be determined to about  $\pm 3$  % of the amount present, *i.e.*  $20 \pm 0.6$  per cent., though better figures should be obtainable. The corresponding meta toluidines have a band at  $774 \text{ cm}^{-1}$  by which they could be differentiated. Ortho toluidines have a strong band at about  $750 \text{ cm}^{-1}$  overlying the strong band of the anilines, but by means of other bands in the spectra the ortho derivatives could be estimated if present in more than traces.

(3) **Dimethyl Butadienes.**—It was necessary to estimate the composition of mixtures of 1,1 dimethyl 1,3 butadiene and 1,3 dimethyl 1,3 butadiene. Bands in the region  $6-14\mu$  provide an easy means for doing this,<sup>2</sup> and since the key bands are both sharp and intense, less than 1 % of either component can be detected in the other. The spectra of thin layers (about 0.05 mm.) are shown in Fig. 3. Key bands are as follows:—

1,1 dimethyl 1,3 butadiene 1218, 1061, 995  $\text{cm}^{-1}$ .  
1,3 dimethyl 1,3 butadiene 1019, 935, 815  $\text{cm}^{-1}$ .

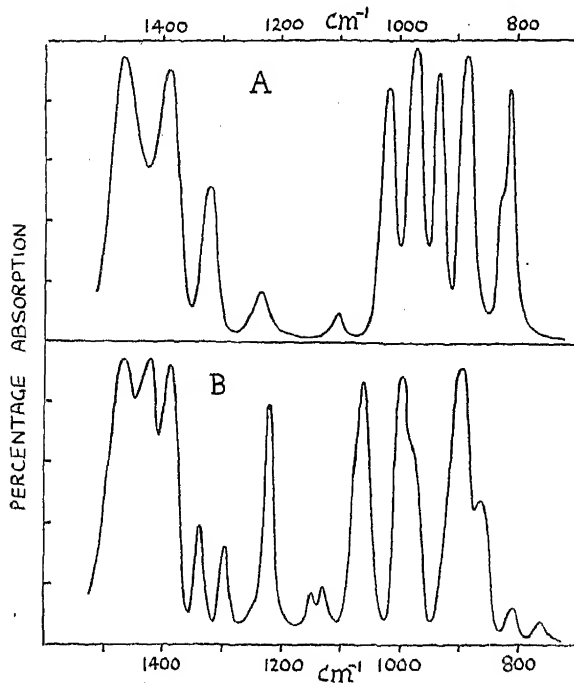
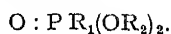


FIG. 3.—A. 1,3 dimethyl 1,3 butadiene.  
B. 1,1 dimethyl 1,3 butadiene.

The analysis can be carried out either from the usual calibration curves, or by matching with the spectra of known mixtures.

(4) **Alkyl and Aryl Phosphites and Phosphonates.**—Another type of mixture was that of alkyl or aryl phosphites and phosphonates



It was required to know whether there are key bands for each class of compound, without regard to the particular alkyl radicals. The spectra were measured using 1-5 % solutions in chloroform,

and cell thickness about 0.1 mm. of each of the following:—

di <i>para</i> tolyl methane phosphonate	$\text{CH}_3 . \text{P} : \text{O} (\text{O-}i\text{para tolyl})_2$
di <i>ortho</i> tolyl butane phosphonate	$\text{C}_4\text{H}_9 . \text{P} : \text{O} (\text{O-}i\text{ortho tolyl})_2$
di <i>ortho</i> tolyl butyl phosphite	$(\text{C}_4\text{H}_9-\text{O})\text{P} (\text{O-}i\text{ortho tolyl})_2$
tri <i>ortho</i> tolyl phosphite	$\text{P}(\text{O-}i\text{ortho tolyl})_3.$

Although differing in other parts of the spectrum, the two phosphites were found to have a strong band at  $870 \text{ cm}^{-1}$ , and the phosphonates a similar band at  $940 \text{ cm}^{-1}$ . These were used to detect qualitatively small amounts of each class of compound in the other class. Accurate quantitative estimations were not made, but it should be possible to

determine upwards of 10 % of either compound in the other with an accuracy of not less than about  $\pm 5$  % on the amount present (*i.e.* 10 %  $\pm 0.5$ ), and to detect upwards of about 2 %. Greater accuracy and sensitivity might be possible using carefully calibrated solutions in carbon disulphide, and in any case the determination can be made in a few minutes. The nature of the alkyl or aryl radicals is also revealed by other bands in the spectra.

(5) **Impurities in 2.4 Dichloro-benzoic Acid.**—Samples of 2.4 dichloro-benzoic acid found to be unsatisfactory for a synthetic process were suspected to contain a small amount of impurity not identifiable by ordinary methods. The impurity seemed likely to be either 4 chloro-benzoic acid or 2.4.5 trichloro-benzoic acid. Since the chloro-benzoic acids are readily soluble only in liquids which themselves have many absorption bands, the spectra of the solid compounds were first surveyed. For this purpose a thin layer of each of the three pure compounds and of the unsatisfactory 2.4 dichloro-benzoic acid was deposited on a rock-salt flat by evaporation of a solution in chloroform. Each compound has a number of sharp absorption bands between 700 and 1400  $\text{cm}^{-1}$ . The impure

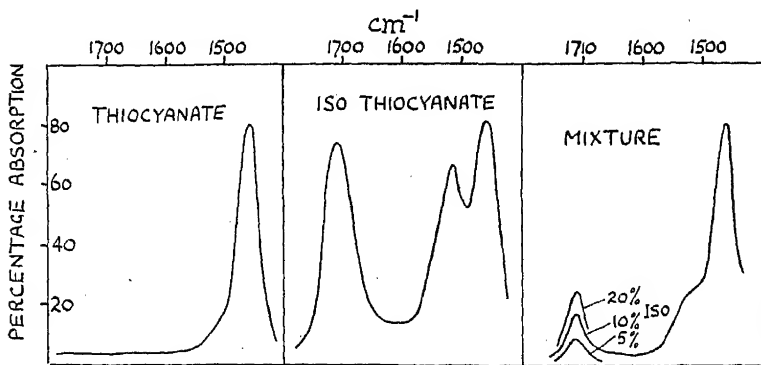


Fig. 4.—Dodecyl Thiocyanate and Isothiocyanate.

product showed a weak band at 1080  $\text{cm}^{-1}$ , not present in the spectra of either the pure 2.4 dichloro-benzoic acid or 4 chloro-benzoic acid, but present as an intense band in the spectrum of 2.4.5 trichloro-benzoic acid, thus indicating the impurity. In this region 2.4 dichloro-benzoic acid has bands at 1117 and 1056  $\text{cm}^{-1}$ , and 4 chloro-benzoic acid has bands at 1117 and 1018  $\text{cm}^{-1}$ .

For quantitative estimations, 1 % solutions of the pure components were made in carbon tetrachloride, and mixtures of these made so as to contain 80/20, 90/10, and 95/5 % of 2.4 dichloro-benzoic acid with the trichloro derivative. The spectrum of the solution of the impure product was compared with those of the known mixtures, and the percentage of the trichloro-benzoic acid determined by interpolation. A cell about 0.2 mm. thick was used for these determinations. It is possible to detect and estimate upwards of a few per cent. of the impurity in this way, and, if necessary, the method could be improved so that less could be detected.

(6) **Alkyl Thiocyanates and Isothiocyanates.**—Mixtures of thiocyanates and isothiocyanates provide another simple case for infra-red analysis. The spectra of the dodecyl salts over the range 1400–1800  $\text{cm}^{-1}$  are shown in Fig. 4. The thiocyanate has a strong band at 1460, due to a vibration of  $\text{CH}_2$  groups, whilst the isothiocyanate has in addition two bands at 1710 and 1515  $\text{cm}^{-1}$ . The band at 1710 can be used to determine the iso compound in a mixture, and curves are shown for various percentages.

(7) **A Mixture of Four Stereoisomers.**—A spectacular example of outstanding interest and significance was recently provided by the analysis of a crude solid product containing four stereoisomers. The details of this analysis will be published at some future date, but at present only the following notes may be given. Other methods for analysing the mixture involved laborious methods of fractional crystallisation, and chemical methods were not available. The isomers differed widely in their solubility in different organic solvents. It was first necessary to find the positions of key bands for each component. A survey had therefore to be made of their individual spectra in a series of solvents chosen so that (i) the solubilities were sufficient, (ii) the spectral range could be entirely covered without interference of the absorption bands of solvent. These conditions necessitated the trial of several solvents for each particular isomer. It was eventually found possible to find a key band for each isomer by using two solvents, methyl acetate and ethylidene chloride, each solution giving a determination of two of the components. In this way it was possible to analyse for all four isomers by making two spectral measurements, in a total time of about 1 hour. Moreover, since each isomer was determined absolutely, the total weight taken could be compared with the total weight determined, and an estimate made of the residual impurities in the crude. The value of this kind of analysis with such a system of stereoisomers is obviously great.

(8) **Impurities in Solvents and Analytical Reagents.**—We have had to use many solvents in work of this kind, and since fairly large quantities have at times to be used, it is important to have some check on the purity of commercial products. In some cases the most careful fractionation and other purification failed to give a suitably pure solvent, and the infra-red spectrum was found to be an invaluable aid in checking this. For example, samples of ethylidene chloride and tetrachloro-ethylene have been found often to contain small amounts of disturbing impurities, probably other chlorinated paraffins, which could never have been detected by other methods. It has become clear that the infra-red spectrum is an excellent criterion of purity of such chemicals.

(9) **Substances of Biological Importance and Pharmaceuticals.**—Many compounds of this class have been studied during recent years. With a complex mixture of highly complicated molecules, the spectra are always difficult to disentangle, and accurate analysis for any one of the components may be difficult. On the other hand the method is extremely valuable for detecting small amounts of impurity in a supposedly pure compound, and it is here that the spectra are of greatest value. Also, if the identity of two compounds is in doubt, the spectrum may be the only satisfactory method of establishing this. Much progress has been made already not only with many compounds of pharmaceutical interest, but also in the experimental technique of preparing films of these substances suitable for measurement.

*The Physical Chemistry Laboratory,  
Oxford.*

#### GENERAL DISCUSSION.

Dr. Sutherland (Cambridge) said: Before opening the discussion on this paper, I should like to say how regrettable it is that we cannot have with us to-day Professor Jean Lecomte, who was doing such remarkable work in the application of infra-red spectroscopy to analytical problems in the years immediately preceding the war.

When this paper was planned, it was intended that there should be a third section containing some examples of analyses by infra-red spectroscopy done in Cambridge. Unfortunately, it was not possible to get this section prepared in time, so I shall mention now a few examples of analyses which would have been incorporated in the proposed Section "C".

The detection of small quantities of ethyl alcohol in acetaldehyde has been investigated by Mr. Philpotts. Down to  $\frac{1}{2}$  % of alcohol can be detected using the alcohol band at  $1052\text{ cm}^{-1}$ . The hydroxyl band was not used, as acetaldehyde has a band at  $2.9\text{ }\mu$ , but it is probable that under higher resolving power use of the monomeric alcohol band at  $2.75\text{ }\mu$  would enable us to put the limit of detection very much lower. In the course of this work bands were found which did not belong to either of the components of the mixture. It is possible that these are due to the formation of a hemi-acetal.

In the terpene field, it has been found by Mr. Ramsay that  $\alpha$  pinene can be detected by a characteristic band at  $787\text{ cm}^{-1}$  in a complex mixture of camphene, dipentene, terpinolene and cyclofenchene, when the amount present is as low as 2 %. In the conversion of iso-borneol to camphor, the remaining iso-borneol can readily be detected and estimated from the hydroxyl band near  $2.9\text{ }\mu$ . Here there is practically no lower limit to the amount detectable since there is no interference from the camphor in this region of the spectrum.

A particularly interesting new application of infra-red analysis has been in the differentiation of amino-acids. In certain nutritional problems it is important to be able to detect and estimate iso-leucine in leucine. The spectra of these compounds, as well as of their formyl and acetyl derivatives, have been obtained by Mr. Darmon. The spectrum of the iso form is in all cases different from that of the other form. The quantitative side is still under investigation and the present position is that the iso-leucine/leucine ratio can be determined with an accuracy of about 5 %, provided there is at least 10 % iso-leucine in the mixture.

With reference to the Oxford examples, the applicability of the method to the cresols has been confirmed by Mr. Philpotts. In the case of the xylenols, however, we have found that in practice ethyl phenols which occur with the xylenols mask some of the key bands mentioned by Dr. Thompson, and further work is now being done by Mr. Willis, which we hope will make it possible to analyse mixtures rich in the ethyl phenols.

We hope to publish full details of these various analyses in the near future.

Dr. R. J. W. Le Fèvre (London) said: Previous speakers have, quite appropriately, stressed the *differences* between the infra-red spectra of isomeric compounds. For the organic chemist there is at least one type of enquiry, namely, the recognition of geometrical isomerism, for which information regarding the degree of *similarity* to be expected will be of interest. From what has been said concerning the origin of these spectra and the way in which certain linkage frequencies appear somewhat independent of the molecule in which they occur, it seems possible that two molecules which are structurally identical, but spatially different might have infra-red spectra at least as alike as are the visible and ultra-violet spectra for such compounds. Have sufficient *cis-trans* isomers been examined to say whether this is so? I hope the answer is yes, because the indications to-day are that organic chemists may shortly have available an analytical method surpassing the older spectroscopy, not only in experimental convenience and speed, but also in ease of interpretation in terms of the details of molecular structure. In particular, I am thinking of geometrical isomerism in compounds having doubly linked nitrogen atoms ( $A-N=N-B$ ), the existence of which, postulated by Hantzsch, has recently been disputed by Hodgson.<sup>1</sup> For example, Hodgson argues that the *syn*- and *anti*-aryldiazocyanides are not *cis* and *trans* isomeric forms of  $R-N=N-CN$ , but are related as *iso*- and *normal*-nitriles, both *trans*:

$R-N=N-\overset{+}{N}\rightleftharpoons C$  and  $R-N=N-C\equiv N$ , respectively. With such molecules, *certain* of whose link moments will be so different and in which,

<sup>1</sup> J.C.S., 1944, 395.

therefore, *all* link moments will be in considerably different electrical environments, surely the infra red "fingerprints" would also greatly differ.

Incidentally, I suppose no infra-red spectra of *n*- and *iso*-nitriles have yet been recorded.

**Dr. Thompson:** In reply to Dr. Lefèvre, although information about the spectra of *cis* and *trans*-isomers is accumulating, and in many cases well-marked differences have been found, I do not think that we are yet in a position to predict on theoretical grounds how the spectra should differ, except perhaps in some very simple cases. The mathematical treatment of complex molecules as vibrating systems is not at present very satisfactory, mainly because too little is known about the force fields in such molecules.

With regard to the relative merits of ultra-violet and infra-red analysis, I agree of course that the application of the former must not be minimised. In some cases it is preferable to the latter, and in others a simultaneous use of both ultra-violet and infra-red absorption is useful.

I agree with Dr. Sutherland that the presence of ethyl phenols in xylene mixtures complicates the problem, and in these cases preliminary fractionation is essential, but the new method is considerably in advance of any other yet devised.

**Mr. Philpotts (Cambridge)** said: I should like to make a point about the magnitude of the errors in an analysis such as the cresylic acid problem described by Dr. Thompson. It may be shown from Beer's Law that the percentage error  $E$  in estimating a concentration  $c$  is connected with the error  $\delta A$  in measuring the percentage absorption  $A$  by the expression—

$$E = \frac{100\delta c}{c} = f(A) \times \delta A.$$

When  $A$  has the optimum value of 63 the function  $f(A) = e$ , the base of natural logarithms. So that an error of 1 in the percentage absorption leads to roughly 3 % error in the estimate of concentration even in the most favourable case. The consistency of the results quoted for the cresols, therefore, implies an accuracy of 1 or better in measuring  $A$ . We have found in practice that we cannot obtain this accuracy with a single determination of the absorption, but only by averaging several readings for the unknown solutions and for the standards.

**Mr. R. R. Gordon (Middlesex)** said: In the earlier part of Dr. Thompson's paper he made the statement that Beer's Law is generally followed in the infra-red region of the spectrum and he outlined a method of analysis based on molecular extinction coefficients and the solution of systems of simultaneous equations. This is a method which we have found to be applicable with success to the ultra-violet region, but in very few cases have we found a linear relationship to hold between optical density and concentration in the infra-red region. Without exception all the materials we have examined have been hydrocarbons and the same non-linearity applies to gas as well as liquid phase examination. It is certainly true to say that inter-molecular association may cause a departure from Beer's Law, but that this is not the only factor involved in such departures is evident from our work in which molecular association may be dismissed. The degree of curvature is dependent on the shape of the absorption band being greatest for narrow bands, and is due to the effect of the slit width. In other words, it is an instrumental effect.

The degree of curvature may be reduced by correcting the optical densities for scattered radiation, but it is not removed even by this means. It is to be regretted that Dr. Thompson did not deal with this question of scattered radiation as we feel that it is of importance in quantitative analysis.

The examples of analyses quoted by Dr. Thompson were clearly chosen for purposes of demonstration, but I think a note of caution should be

sounded here, since the problem of precision quantitative analysis is by no means so simple as in the examples quoted.

**Dr. Thompson** (*communicated*): I would just add a rejoinder to Dr. Gordon's remarks. I am not very clear what he means by an instrumental effect giving rise to deviations from Beer's law. It is, of course, well understood that the measured breadth of infra-red absorption bands depends on the resolving power of the instrument, which depends among other things upon the slit widths used. But we have now reached a stage in technique when, for liquids or solutions at least, a further reduction in slit widths may have no further advantage and may in fact be undesirable on other grounds. Of course, too, it is well known that failure to eliminate false radiation due to scattering is bound to lead to inaccurate values for the measured optical densities. Methods for dealing with this scattered radiation have already been discussed in the paper on technique by Dr. Sutherland and myself. It may be that errors arising from causes such as these have led to some of the apparent deviations from Beer's law which Dr. Gordon has encountered. Alternatively, this may have arisen from the use of too concentrated solutions. As we have already stated, it is usually preferable to work with dilute solutions and to adjust the path length of solution so as to obtain a convenient percentage absorption.

Dr. Gordon suggests that the analyses which we have given were selected preferentially; in fact, they were chosen so as to illustrate different kinds of chemical problem, and the sensitivity and accuracy which can be expected in such cases, as well as the limitations, are clearly stated. There is now abundant experimental evidence and experience to illustrate the usefulness of infra-red analysis, and the more sceptical and pessimistic views expressed by Dr. Gordon are, in my opinion, unjustified.

---

## THE ASSIGNMENT OF THE VIBRATIONAL FREQUENCIES, AND THE FORCE FIELD OF THE OZONE MOLECULE.

By Miss D. M. SIMPSON.

*Received 16th November, 1944.*

It is perhaps presumptuous to attempt to add to the already extensive literature on ozone. The structure of this molecule has provided a tantalising subject for investigation and conjecture, and the published papers are remarkable for the apparent incompatibility of their conclusions. My own interest in this substance was aroused during an investigation of its far ultra-violet absorption spectrum.<sup>1</sup> Calculations on the force constants of the molecule were made at that time, but the results were too incomplete to warrant publication. Since then, several further papers on ozone have appeared,<sup>2, 3</sup> and it therefore seemed of value to summarise the available evidence on the size and shape of the molecule, to consider briefly its possible electronic configurations, and then to use this information to rediscuss the assignment of the observed vibrational frequencies and to employ these frequencies to calculate the force constants of the molecule.

That the probable shape of the ozone molecule is an isosceles triangle has been appreciated for some time. The absence of any strong Raman

<sup>1</sup> Price and Simpson, *Trans. Faraday Soc.*, 1941, **37**, 106.

<sup>2</sup> Mulliken, *Rev. Mod. Physics*, 1942, **14**, 204.

<sup>3</sup> Shand and Spurr, *J.A.C.S.*, 1943, **65**, 179.



line,<sup>4, 18</sup> and the number and fine structure of the infra-red bands,<sup>5, 6</sup> preclude a linear or an equilateral form. There has, however, been a considerable diversity of opinion about the size of the apical angle; some authors considering it to be acute, 40° or 60°, and others that it was of the order of 120°, so that the structure is similar to that of sulphur dioxide. The electron diffraction data<sup>3</sup> show unambiguously that the angle is obtuse,  $127 \pm 3^\circ$ , with O—O distances of 1.26 and  $2.24 \pm 0.2$  Å.; the experimental scattering curves could not be matched by those calculated with an apical angle of about 40°. Additional evidence for this wide-angled structure may possibly be deduced from work on the X-ray diffraction of liquid oxygen. Sharrah and Gingrich<sup>7</sup> found indications of several different O—O distances. They consider that a small quantity of ozone, with bond lengths of 1.25–1.30 Å. and 2.24 Å. may have been present in the oxygen, whose interatomic distance was 1.25–1.30 Å.

The three moments of inertia  $M_A$ ,  $M_B$ ,  $M_C$ , of the ozone molecule calculated from Shand and Spurr's data are 67.56, 5.60 and  $73.16 \times 10^{-40}$  g. cm.<sup>2</sup>. These are respectively parallel and perpendicular to the symmetry axis in the plane of the molecule, and perpendicular to the plane of the molecule. The ratio  $\rho = M_B/M_A = 0.083$  is less than one, so that the  $\nu_1$ ,  $\nu_2$  totally symmetrical vibrations, in which the change in electric moment is parallel to  $M_A$ , should show a doublet structure in their infra-red absorption bands, and the vibration  $\nu_3$ , in which it is parallel to  $M_B$ , should give a  $Q$  branch. All vibrations, and all combinations and overtones are permitted in both the Raman and the infra-red spectrum. For the general case:

$$\nu = n_1\nu_1 + n_2\nu_2 + n_3\nu_3 \quad n_1 n_2 n_3 \text{ integral}$$

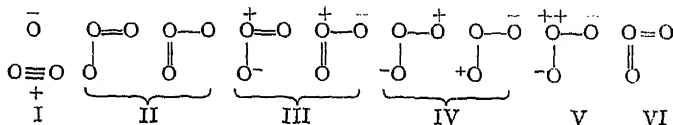
the change in electric moment is parallel to  $M_A$  for  $n_3$  even, and parallel to  $M_B$  for  $n_3$  odd.

The ozone molecule with  $\rho = 0.083$  belongs to the class of nearly linear asymmetric top molecules discussed by Nielsen.<sup>8</sup> His diagrams show that the  $\nu_1$ ,  $\nu_2$  bands should have no  $Q$  branches, and  $\nu_3$  a well-defined  $Q$  branch, in agreement with the above conclusions. Since ozone is so nearly a symmetrical top molecule a rough estimation of the  $PR$  separation of the "parallel" band  $\nu_3$  may be obtained using the formula of Gerhard and Dennison:<sup>9</sup>

$$\Delta\nu = \frac{S(\beta)}{\pi} \sqrt{\frac{kT}{A}}; \log_{10} S(\beta) = \frac{0.721}{(\beta + 4)^{1.13}} \quad \beta = I/\rho \quad A = M_A \text{ or } M_C.$$

The value obtained for ozone is 27 cm.<sup>-1</sup>: and the doublet separations of the "perpendicular" bands  $\nu_1$ ,  $\nu_2$  would not be very different.

The ozone molecule possesses eighteen "molecular" electrons, that is, electrons derived from the outer atomic shells. Possible electronic configurations, consistent with its isosceles triangular form are:—



The ionic structure I,<sup>2</sup> must of necessity be associated with a small apical angle, and would, as Shand and Spurr point out, possess the abnormal

<sup>4</sup> Sutherland and Gerhard, *Nature*, 1932, 130, 241.

<sup>5</sup> Gerhard, *Physic. Rev.*, 1932, 42, 622.

<sup>6</sup> Hettner, Pohlman and Schumacher, *Z. Physik*, 1934, 91, 372; *Z. Electrochem.*, 1935, 41, 524.

<sup>7</sup> Sharrah and Gingrich, *J. Chem. Physics*, 1942, 10, 504.

<sup>8</sup> Nielsen, *Physic. Rev.*, 1931, 38, 1432.

<sup>9</sup> Gerhard and Dennison, *Physic. Rev.*, 1933, 43, 197.

physical properties and large dipole of a highly polar substance, which are not shown by ozone. Similar objections may be given to the structure V. The resonating forms II<sup>10</sup> are unlikely, because they would be probably paramagnetic, whereas ozone at most is only weakly so.<sup>11, 12</sup>

The resonating structures III, IV,<sup>1, 3, 13</sup> which should be wide-angled, appear to be the most probable. The dipole moment calculated for III (IV does not contribute) is  $1.62 \times 10^{-18}$  esu.<sup>3</sup> The observed value is, however, only  $0.49 \times 10^{-18}$  esu.<sup>13</sup> It is difficult to attribute such a discrepancy either to the approximate method of calculation, or to the fact that the ozone measurements were made in liquid oxygen solution. Samuel<sup>10</sup> has therefore suggested the structure VI, with a small dipole arising between the di- and tetravalent oxygen atoms. As oxygen has no *2d* orbitals comparable to the *3d* sulphur orbitals occupied in the analogous structure for sulphur dioxide,<sup>14</sup> the extra electrons on the central oxygen atom are "promoted," in which state they will be bonding. This promotion produces a decrease in the bond energy of the second double bond compared with the first one, so that the heat of formation, 6.15 ev., is much smaller than that calculated for two oxygen-oxygen double bonds  $2 \times 5.09$  ev.

For any of the structures III, IV or VI the force constant of the oxygen-oxygen linkage, of length 1.26 Å., would be expected to lie somewhere between its value for a single bond, and that for the oxygen molecule. In hydrogen peroxide, with a frequency of 875 cm.<sup>-1</sup>,<sup>15</sup> and an O—O distance of 1.46 Å.,<sup>17</sup> the calculated value of the force constant is about  $3.7 \times 10^5$  dynes/cm.; for the oxygen molecule, with a frequency of 1550 cm.<sup>-1</sup> and an interatomic distance of 1.204 Å., it is  $11.3 \times 10^5$  dynes/cm.<sup>21</sup>

Only one investigation of the Raman spectrum of ozone has been described.<sup>4, 18</sup> No strong lines were obtained, merely a doubtful weak doublet at 1280 cm.<sup>-1</sup>. All frequencies  $\Delta\nu > 1750$  cm.<sup>-1</sup> would have been reabsorbed by ozone under the conditions of the experiment.

The infra-red observations available are those of Gerhard<sup>5</sup> who used a grating to study two of the stronger bands, and of Hettner, Pohlman and Schumacher<sup>6</sup> who investigated the region  $0.5\text{--}27\mu$  with a prism spectrometer. In addition, the ozone absorption in the region  $9\text{--}10\mu$  has been mapped by Adel<sup>19, 20</sup> as part of a study of the atmospheric absorption of solar radiation. In this work the other interesting regions of absorption of ozone are overlaid by the stronger bands of water and carbon dioxide. The vibrational frequencies found are given in Table I, together with the more possible frequency assignments.

The fourth and fifth columns give the observed intensities and contours, and the last column gives the contours predicted for the assignment which is considered later in this present discussion.

The most detailed information available is that of Adel on the 1043 cm.<sup>-1</sup> band. Records taken using a prism<sup>19</sup> show its doublet structure distinctly, and this is confirmed in the more detailed grating results.<sup>20</sup> The line spacing of the *P* branch is fairly regular, but that of the *R* branch is distorted, as it is overlaid by the rotational structure of the 1064 cm.<sup>-1</sup> band of carbon dioxide. The centre at 1043 cm.<sup>-1</sup> is clearly visible, and there is no sign of a *Q* branch. Gerhard<sup>5</sup> has interpreted his own results in this region by suggesting that the absorption which shows irregular spacing

<sup>10</sup> Samuel, *J. Chem. Physics*, 1944, **12**, 180.

<sup>11</sup> Wulf, *Proc. Nat. Acad. Sci.*, 1927, **13**, 744.

<sup>12</sup> Lainé, *Ann. Physique*, 1935 (XI), **3**, 461.

<sup>13</sup> Lewis and Smyth, *J.A.C.S.*, 1939, **61**, 3063.

<sup>14</sup> Kimball, *J.C.P.*, 1940, **8**, 188.

<sup>15</sup> Pauling, *J.A.C.S.*, 1932, **54**, 3570.

<sup>16</sup> Penney and Sutherland, *Trans. Faraday Soc.*, 1934, **30**, 898.

<sup>17</sup> Schomaker and Stevenson, *J.A.C.S.*, 1941, **63**, 37.

<sup>18</sup> Sutherland, *Proc. Roy. Soc. A.*, 1933, **141**, 515.

<sup>19</sup> Adel, *Astro. J.*, 1939, **89**, 320.

<sup>20</sup> Adel, *ibid.*, 1941, **94**, 451.

of the lines is complex, arising from two frequencies one at 1033 cm.<sup>-1</sup> with a doublet contour and the other at 1055 cm.<sup>-1</sup> with a *Q* branch. However, the more detailed curves of Adel would appear to rule out this possibility, and indeed Gerhard's absorption may well be interpreted as a doublet band with a centre at 1045 cm.<sup>-1</sup>.

The 710 cm.<sup>-1</sup> is clearly shown to have a doublet structure from the results of Hettner, Pohlman and Schumacher,<sup>21</sup> the dispersion in this region of the spectrum being sufficient to show up the contour with a well-defined centre at the above frequency. The 2105 cm.<sup>-1</sup> band, as seen in Gerhard's curve,<sup>6</sup> shows a definite but rather wide *Q* branch, and irregular line spacing of the *PR* branches.

TABLE I.

Observed Values.					Assignment.				
(6)	(5)	(19) (20)	I.	C.	(6) (2)	(21)	(22)	Present Work	
3050 cm. <sup>-1</sup>	2108 cm. <sup>-1</sup>		W	?	$\nu_1 + \nu_2$	$3\nu_1$	—	$\nu_2 + \nu_3$ ; $3\nu_2$	$Q, D$
2800 cm. <sup>-1</sup>			W	?	$\nu_1 + \nu_3$	$2\nu_1 + \nu_2$	—	$\nu_1 + \nu_2$	$D$
2105 cm. <sup>-1</sup>			S	$Q$	$\nu_1$	$2\nu_1$ ; $3\nu_2$	$\nu_3$	$\nu_2$	$Q$
1740 cm. <sup>-1</sup>			W	?	$\nu_2 + \nu_3$	$\nu_3$	—	$\nu_1$	$B$
1037 cm. <sup>-1</sup>	1055 cm. <sup>-1</sup>	1043 cm. <sup>-1</sup>	VS	D	$\nu_2$	$\nu_1$	$\nu_1$	$\nu_2$	D
725 cm. <sup>-1</sup>	1033 cm. <sup>-1</sup>		S	D	$\nu_3$	$\nu_2$	$\nu_3$	$\nu_1 - \nu_2$	D
710 centre									
695 cm. <sup>-1</sup>									

The *PR* doublet separation of the 1043 cm.<sup>-1</sup> band, read off from Adel's recordings, is about 25 cm.<sup>-1</sup> <sup>20, 22</sup>; that derived from Gerhard's curve for 2105 cm.<sup>-1</sup> is about 30 cm.<sup>-1</sup>, and the Hettner, Pohlman, Schumacher data gives 30 cm.<sup>-1</sup> for the 710 cm.<sup>-1</sup> frequency. These seem to be in reasonable agreement with the results calculated above, as it is rather difficult to be sure of the exact positions of maximum intensity on a curve showing line structure.

There is little doubt that the 1043 cm.<sup>-1</sup> frequency is to be attributed to a totally symmetrical vibration  $\nu_1$  or  $\nu_2$ , for as Dr. Wulf<sup>2</sup> has pointed out a frequency of about this size, associated with the ground state, is found to have the same combining properties as the vibrationless ground state in the ultra-violet absorption spectrum.<sup>23</sup> It is interesting to notice that the lower 710 cm.<sup>-1</sup> frequency, which from its infra-red contour must have the same symmetry as the 1043 cm.<sup>-1</sup> vibration, does not appear to figure in the ultra-violet absorption. This suggests that it may not be a fundamental.

The three frequencies of a triangular molecule with atoms *mMm* and an apical angle  $2\alpha$  are given by:—

$$m(\lambda_1 + \lambda_2) = f(1 + (2m/M) \cos^2 \alpha) + (d' + 2d)(1 + (2m/M) \sin^2 \alpha) + 2f' \quad (1)$$

$$\frac{M\lambda_1\lambda_2}{(M + 2m)} = \frac{2f' \cdot f}{m^2} \cos^2 \alpha + \frac{2f'}{m} \left( \frac{2d}{m} + \frac{d'}{m} \right) \sin^2 \alpha + \frac{f}{m} \left( \frac{2d}{m} + \frac{d'}{m} \right) \quad (2)$$

$$\lambda_3 = (f/m + (4d'/m) \cos^2 \alpha)(1 + (2m/M) \sin^2 \alpha) \quad (3)$$

where  $\lambda_1 = 4\pi^2\nu_1^2$ ,  $\lambda_2 = 4\pi^2\nu_2^2$ ,  $\lambda_3 = 4\pi^2\nu_3^2$

$f, f'$  are the force constants of the *mM*, *mm* bonds;  $d, d'$  are the deformation force constants of the apical and basal angles respectively, defined so that the change in potential energy for an alteration  $\delta\theta$  of total angle is  $V = \frac{1}{2}ds^2(\delta\theta)^2$ , where  $s$  is the relevant bond length. The deformation

<sup>21</sup> Penney and Sutherland, *Proc. Roy. Soc. A.*, 1936, 156, 654, 678.

<sup>22</sup> Adel, Slipher and Fouts, *Physic. Rev.*, 1936, 49, 288.

<sup>23</sup> Jakowlewa and Kondratjew, *Physik. Z., Sowjet.*, 1936, 9, 106.

constants in the published literature are not all equivalent; the convention given above is that of K. W. F. Kohlrausch.<sup>24</sup>

The equations for a valency force field are obtained if  $f'$ ,  $d'$  are zero, and those for a central force field if  $d$ ,  $d'$  are put equal to nought. In each case there are three equations to determine three unknowns, two force constants and the apical angle. These sets of equations may be used in the following ways. (i) When the apical angle is already known from other data and the force constants are calculated from two of the equations, then the third may be used as a test for the self-consistency of the force field. (ii) Alternately if two only of the frequencies are known, an estimate of the third may be obtained. (iii) If the two force constants are eliminated from the three equations, then as was shown by Bailey and Cassie,<sup>25</sup> the following results are obtained:—

Valency Force Field—

$$\frac{\lambda_1 \lambda_2}{\lambda_3} \frac{x^3}{1 + 2m/M} - \sum_1^3 \lambda_i x + 2\lambda_3 \left(1 + \frac{m}{M}\right) = 0 \quad (4) \quad x = 1 + (2m/M) \sin^2 \alpha.$$

Central Force Field—

$$\begin{aligned} & \left[ \frac{4}{1 + 2m/M} \cdot \frac{m^2}{M^2} \cdot \frac{\lambda_1 \lambda_2}{\lambda_3} + \sum_1^3 \frac{2m}{M} \lambda_i \right] \sin^4 \alpha \\ & + \left[ \frac{4}{1 + 2m/M} \cdot \frac{m}{M} \cdot \frac{\lambda_1 \lambda_2}{\lambda_3} + \left[ \sum_1^3 \left(1 - \frac{2m}{M}\right) \lambda_i \right] - 2 \left[ 1 + \frac{m}{M} \right] \lambda_3 \right] \sin^2 \alpha \\ & + \left[ \frac{1}{1 + 2m/M} \frac{\lambda_1 \lambda_2}{\lambda_3} - \sum_1^3 \lambda_i + 2 \left(1 + \frac{m}{M}\right) \lambda_3 \right] = 0 \quad (5) \end{aligned}$$

If all three frequencies are known, these equations may be used to calculate the apical angle directly. The calculated angle may be compared with results obtained experimentally; this gives an alternative method of checking the self-consistency of the force field employed. (iv) A further very useful method of using the equations (4) and (5) has now been investigated. It is possible to rewrite equation (4) in the form:—

$$\lambda_1 = \frac{\lambda_3 \left[ \lambda_2 x - \lambda_3 \left[ 2 + \frac{2m}{M} - x \right] \right]}{x \left[ \frac{\lambda_2 x^2}{1 + 2m/M} - \lambda_3 \right]} \quad (6)$$

For given values of  $x$ ,  $\lambda_2$ , the  $\lambda_1/\lambda_3$  graph has the general shape shown in Fig. 1. The diagram shows that there are limits A, B between which  $\lambda_3$  cannot lie if  $\lambda_1$  is to be positive, and limits C, D between which  $\lambda_1$  does not exist. These can be readily derived from equation (6) and are given by the expressions:—

$$\begin{aligned} (\lambda_3)_B &= \frac{\lambda_2 x}{(2 + 2m/M - x)} & (\lambda_3)_A &= \frac{\lambda_2 x^2}{(1 + 2m/M)} \\ (\lambda_1)_D, (\lambda_1)_C &= \frac{\lambda_2 [P \pm Q] [x - 1] (x - (1 + 2m/M)) \mp Q}{(1 + 2m/M) (\mp Q)} \end{aligned} \quad (7)$$

where  $P = x[2 + 2m/M - x]$ ,

$$Q = \sqrt{x[2 + 2m/M - x][1 - x][x - (1 + 2m/M)]}.$$

Hence the graphs obtained by plotting  $(\lambda_3)_A$ ,  $(\lambda_3)_B$ ,  $(\lambda_1)_D$ ,  $(\lambda_1)_C$  against  $\lambda_2$  for a given value of  $x$ , are all straight lines passing through the origin. Moreover it can be shown that the slopes of all these lines are positive

<sup>24</sup> K. W. F. Kohlrausch, *Der Smekal-Raman Effekt, Ergänzungsband*, Julius Springer, 1938, p. 65.

<sup>25</sup> Bailey and Cassie, *Proc. Roy. Soc. A.*, 1932, **137**, 622.

for  $1 < \kappa < 1 + 2m/M$ , that is, for  $0 < \sin^2 \alpha < 1$ , so that the corresponding values of  $(\nu_3)_A$ ,  $(\nu_3)_B$ ,  $(\nu_1)_D$ ,  $(\nu_1)_C$  are all real. The equation (5) for the central force field gives analogous, but rather more complicated expressions in terms of  $\sin^2 \alpha$ . The expressions (7) are rather insensitive

to alteration of the angle but those derived for the central force field are very sensitive to its variation. If therefore the apical angle of a bent triatomic molecule is known, it is possible to construct the straight line graphs, and from these to read off at once whether a suggested assignment is acceptable.

Of the six frequencies observed in the infra-red spectrum of ozone  $3050 \text{ cm.}^{-1}$  and  $2800 \text{ cm.}^{-1}$  are too high to be fundamentals, so that there are twelve ways of choosing  $\nu_1 \nu_2 \nu_3$  from the four remaining bands  $2105 \text{ cm.}^{-1}$ ,  $1740 \text{ cm.}^{-1}$ ,  $1043 \text{ cm.}^{-1}$ ,  $710 \text{ cm.}^{-1}$ . The above analysis (iv) was

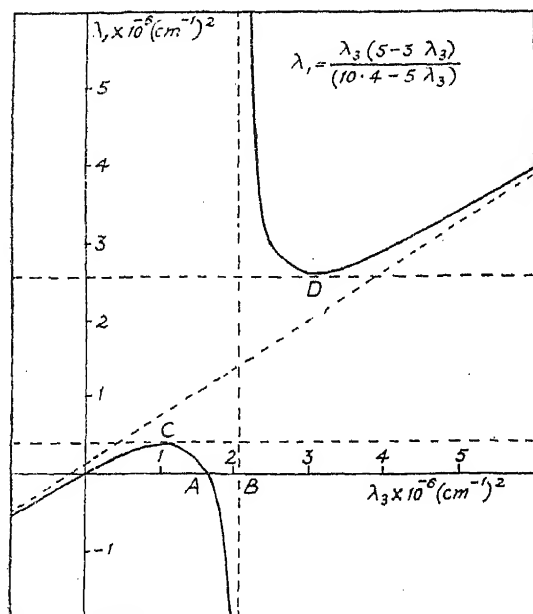


FIG. 1.

carried out for ozone with  $m = M$ ,  $2\alpha = 127^\circ$ . It was found that six combinations were theoretically possible using a valency force field, and one only for a central force field. The assignments:—

$\nu_1$ $1740 \text{ cm.}^{-1}$	$\nu_2$ $710 \text{ cm.}^{-1}$	$\nu_3$ $2105 \text{ cm.}^{-1}$	Valency Force Field
$2105 \text{ cm.}^{-1}$	$710 \text{ cm.}^{-1}$	$1740 \text{ cm.}^{-1}$	Valency and Central Force Fields

are unacceptable because they do not make  $1043 \text{ cm.}^{-1}$  a totally symmetrical fundamental. The combinations:—

$\nu_1$ $1740 \text{ cm.}^{-1}$	$\nu_2$ $1043 \text{ cm.}^{-1}$	$\nu_3$ $710 \text{ cm.}^{-1}$	Valency Force Field.
$2105 \text{ cm.}^{-1}$	$1043 \text{ cm.}^{-1}$	$710 \text{ cm.}^{-1}$	" " "
$2105 \text{ cm.}^{-1}$	$1043 \text{ cm.}^{-1}$	$1740 \text{ cm.}^{-1}$	" " "

can be eliminated, because the contour relationships are incorrect. This leaves only the assignment:

$$\nu_1 \ 1740 \text{ cm.}^{-1} \quad \nu_2 \ 1043 \text{ cm.}^{-1} \quad \nu_3 \ 2105 \text{ cm.}^{-1}$$

to be discussed, using a valency force field.

This new assignment with the corresponding interpretations of the other infra-red absorption bands is shown in Table I, together with the more plausible previous combinations. Hettner, Pohlman and Schumacher<sup>6</sup> who discussed several possible assignments using both valency and central force fields, concluded that the best results were given with the frequencies indicated, using a central force field, with force constants of  $f = 20.8 \times 10^5 \text{ dynes/cm.}$  and  $f' = 3.86 \times 10^5 \text{ dynes/cm.}$  and an apical angle of  $39^\circ$ . Penney and Sutherland<sup>21</sup> gave an extensive discussion of the applicability of the central and valency force fields to tri-

atomic molecules. Using a valency force field and the assignment shown, they calculated the force constants of the ozone molecule to be  $f = 11.5 \times 10^5$  dynes/cm., and  $k_\alpha = 2.34 \times 10^{-11}$  dyne-cm./radian  $\equiv 2d/s^2$ , for O—O = 1.29 Å., and  $2\alpha = 120^\circ$ . Adel, Slipher and Fouts<sup>22</sup> remark that they were unable to obtain any real values of the valency or central force constants from their choice of frequencies. Mulliken<sup>2</sup> gave a critical discussion of the Hettner-Pohlman-Schumacher assignment, using the electronic configuration I for the molecule, but did not calculate any force constants.

Table II summarises the results of calculations now made for each of the above frequency assignments, using a valency force field and an angle  $2\alpha = 127^\circ$ . The values of  $f$  and  $d$  in units of  $10^5$  dynes/cm. were derived from equations (3), (2), (1) respectively. The left-hand side of equation (1) is shown in column 8, and the right-hand side, calculated from the  $f$  and  $d$  values of equations (3) and (2), in column 9; both are in units of  $10^5$  dynes/cm. Column 10 gives the percentage deviation between these two last results, calculated on the mean value. Column 11 gives the apical angle, calculated direct from equation (4). Column 12 shows the value of the O—O distance in Å. derived from the relevant value of  $f$  using Badger's relationship<sup>26</sup> and the last column gives the calculated average value of the specific heat  $C_p$  for the range 300–476° K.

TABLE II.

Refer- ence.	$\nu_1$ cm. <sup>-1</sup>	$\nu_2$ cm. <sup>-1</sup>	$\nu_3$ cm. <sup>-1</sup>	$f(3)$	$d(2)$	$d(1)$	L.H.S. (1)	R.H.S. (1)		Apical Angle	O—O (in Å.)	$C_p$ Av. cal.
Present work	1740	1043	2105	15.98	3.023	3.12	38.591	38.009	- 1.3 %	125°	1.17	8.86
(2), (6)	2105	1043	710	1.82	38.90	11.26	61.13	204.98	+ 110 %	33°	1.69	9.80
(21)	1043	710	1740	10.91	0.735	— ve	14.93	19.09	+ 25 %	164°	1.23	9.89
(22)	1043	710	2105	15.98	0.503	— ve	14.93	24.95	+ 50 %	Unreal	1.17	9.80
1	2	3	4	5	6	7	8	9	10	11	12	13

The observed value for the specific heat  $C_p$  in the range 300–476° K. is  $10.94 \pm 0.30$  cal.<sup>27</sup> Lewis and von Elbe<sup>27</sup> quote 10.39 cal. as the result calculated by Kassel using the (incorrect) frequencies 528, 1033, and 1355 cm.<sup>-1</sup> of Gerhard.<sup>5</sup> They attribute the lack of agreement to the presence of a low lying electronic state. Since any possible combination of the observed frequencies cannot give a result greater than 9.89 cal. for this range, the actual discrepancy must be considerably larger. As there is no independent information about this possible electronic state, it follows that the specific heat data cannot furnish a method for discriminating between the above assignments.

The Hettner-Pohlman-Schumacher-Mulliken assignment, although it gives the relative intensity relationships correctly, is unlikely because it gives incorrect contours for the bands. Further it suggests a molecule with a small apical angle, using either the valency or the central force fields. The self-consistency using the known value of the apical angle and a valency force field is non-existent, and the sizes of the force constants and the O—O distance are absurd. The force constants obtained using a central force field are also rather unlikely. Some of these objections have already been discussed by Penney and Sutherland.<sup>21</sup>

The Penney-Sutherland assignment gives the correct contours, and a sensible value for the force constant  $f$  and the O—O distance, although the size of  $d$  is rather small. However, the calculated apical angle is too large, and the self-consistency of the valency force field equations for the observed angle is poor. The force constants  $f$  and  $d$  only have real values when calculated from equations (3) and (2). Moreover, as these authors

<sup>26</sup> Badger, *J.C.P.*, 1934, 2, 128.<sup>27</sup> Lewis and Elbe, *J.C.P.*, 1934, 2, 294.

themselves point out, the intensity relationships are a little odd, for  $\nu_3$  is much less strong than  $\nu_1$ , and the combination band at  $2105 \text{ cm.}^{-1}$  is too intense.

The Adel assignment<sup>22</sup> predicts the contours correctly, but it is inadequate because it gives unreal values for the direct calculation of the apical angle, and for the force constants  $f$ ,  $d$  from equations (1) and (2); the self-consistency of the valency force field equations using the observed value of the angle is bad. Further the size of  $f$  seems a little large, and that of the O—O distance somewhat small.

In favour of the present assignment it may be said that it gives a calculated value of the apical angle which is in good agreement with the experimental result, and that it predicts the contours of the bands correctly as far as they can be checked. The force constants derived from the valency force field equations with the observed apical angle are all real, the two values of  $d$  differing by only 0.5 %, and the self-consistency of about 1 % is excellent. Since  $\nu_1$  at  $1740 \text{ cm.}^{-1}$  is very near the limit of self absorption of the Raman investigations, then it may not have shown up under the experimental conditions. Moreover if  $710 \text{ cm.}^{-1}$  is attributed to a combination frequency, then it is unlikely that it would be found associated with the ground state in the ultra-violet absorption, and its rather surprising absence is thus explained. Against this interpretation it should be noted that both the force constants seem high so that the O—O distance is too low, although admittedly use of the Badger formula is a somewhat approximate method of obtaining interatomic bond lengths in polyatomic molecules. It is, however, difficult to suggest any electronic formula for the molecule which could simultaneously explain both the experimental O—O distance, and such high values of the force constants. Further, the  $\nu_1$  frequency, although correctly less intense than  $\nu_3$ , seems very weak compared with the combination band  $\nu_1 - \nu_2$ . It is also difficult to understand how a difference band can be so strong, although the absorption corresponding to the initial level  $\nu_2$  appears very intense in both the laboratory and atmospheric investigations.

The main objection to both the Penney-Sutherland and the Adel assignments, is that it is impossible to obtain real values of the force constants from the chosen sets of frequencies using a valency force field. It might be argued that if a more general force field were used, this difficulty would not arise. The most general force field for a bent triatomic symmetrical molecule requires four force constants. Since ozone has only three vibrational frequencies, only three of these constants can be calculated. The wide-angled structure of ozone suggests that it would be sensible to choose  $f$ ,  $f'$  and  $d$ , since the deformation constant  $d'$  of the basal angles will probably be small. The values of  $f$ ,  $f'$  and  $d$  can be obtained from equations (1), (2), (3) direct, if  $d'$  is zero, but the arithmetic is more straightforward if the equivalent equations of Rosenthal<sup>28</sup> are used. Calculations were made for the Penney-Sutherland, Adel and present assignments; that of Hettner-Pohlman-Schumacher-Mulliken being considered too unlikely to merit further investigation. The two former still gave unreal values for the force constants. For the present interpretation, the following results were obtained:

$$f = 15.97; f' = 0.5315 \text{ or } 5.183; d = 3.381 \text{ or } 1.591.$$

The first set is similar to that derived from the valency force field with a small force constant  $f'$  between the basal atoms. It would seem to be the more plausible, as in the other set the deformation constant  $d$  seems small in comparison to  $f'$ . No check on the values of these force constants is available, but they are quoted here to show that the superiority of the

<sup>28</sup> J. E. Rosenthal, *Physic. Rev.*, 1934, 45, 426.

present assignment persists, even when a field more general than the valency force field is employed.

The final justification of this or any other assignment will not be possible until more detailed measurements are made on the structure of the infra-red bands, and on the Raman spectrum. In the meantime it is felt that the present interpretation provides a more consistent treatment of the vibrational frequencies and of the force constants of the ozone molecule than has yet been advanced.

I should like to express my gratitude to Dr. Sutherland for all the interest that he has taken in this work, and to thank him for the very helpful discussions I have had with him.

### Summary.

Using the experimental evidence now available on the size and shape of the ozone molecule, a new assignment of the vibrational frequencies has been made, and force constants have been calculated from this, using valency and three constant force fields. The present results are compared critically with those obtained with the previously suggested interpretations of the frequencies.

*The Laboratory of Physical Chemistry,  
Cambridge.*

---

## THE C—C VALENCY VIBRATIONS OF ORGANIC MOLECULES.

BY LOTTE KELLNER.

*Received 11th December, 1944.*

It is well known that the infra-red and Raman spectra of organic molecules can be divided up into the valency and deformation oscillations of the constituent groups of the molecule. The valency and deformation vibrations appertaining to a certain linkage are well separated from each other since the angle forces amount to, at the most, 25 % of the valency forces. On the other hand, the valency vibrations of two different bonds will not overlap and therefore not interact with each other if the masses of the linked atoms are appreciably different as in the case of the C—C and C—H linkages for instance. Bartholomé and Teller<sup>1</sup> (1932) have shown that the valency vibrations of the C—C single bond vibrations lie between 809 and 1143 cm.<sup>-1</sup>. But within this region, we may expect a certain overlapping with C—H bending vibrations due to the angular forces in the CH<sub>3</sub> and CH<sub>2</sub> groups of the molecule. In other words, not all the frequencies observed between 809 and 1143 cm.<sup>-1</sup> are necessarily C—C valency vibrations. In the following, an attempt has been made to calculate the C—C valency vibrations of hydrocarbons and compare them with the observed spectra.

### 1. Valency Vibrations of an Open Chain.

The oscillations of an open chain of  $n$  mass points of equal mass  $m$  will be considered. Adjacent linkages form the angle  $\theta$  with each other. The aliphatic hydrocarbons can be assumed to consist of equal masses since the mass of the CH<sub>3</sub> groups at the ends of the chain is very little

<sup>1</sup> Bartholomé and Teller, *Z. physik. Chem. B.*, 1932, 19, 366.



different from the mass of the  $\text{CH}_2$  groups which make up the chain. All the mass points lie in one plane. The angle forces are neglected. A harmonic potential is assumed to act between the mass points,  $V$ , so that

$$V = \frac{1}{2}f \sum_{r=1}^{n-1} l_r^2 \text{ where } f \text{ is the force constant and the } l_r \text{ are the displacements}$$

of the bonds from their equilibrium positions. The following calculation follows Bartholomé and Teller (1932) with a slight alteration in the numbering of the  $l_r$ . If  $\nu$  denotes the frequency of the oscillations, they are obtained as the solutions of the simultaneous equations:

$$\begin{aligned} 4\pi^2\nu^2ml_1 &= f\{2l_1 + \cos\theta l_2\} \\ 4\pi^2\nu^2ml_2 &= f\{2l_2 + \cos\theta(l_1 + l_3)\} \\ 4\pi^2\nu^2ml_r &= f\{2l_r + \cos\theta(l_{r-1} + l_{r+1})\} \\ r &= 2, 3, \dots, n-2. \end{aligned} \quad (1)$$

The three equations have identical form, if  $l_0 = 0$  and  $l_n = 0$ .  $l_r$  is assumed to be  $\sin r\alpha$ . Equations (1) have then the solutions:

$$4\pi^2\nu^2m = 2f(1 + \cos\theta \cos\alpha).$$

$\alpha$  is determined from the condition  $l_n = 0$ , i.e.  $\sin n\alpha = 0$ . Therefore,  $\alpha = \frac{\pi k}{n}$ , where  $0 < k < n$ . This condition furnishes the  $n-1$  solutions of equations (1):

$$4\pi^2\nu^2m = 2f\left(1 + \cos\theta \cos\frac{\pi k}{n}\right) \quad (2)$$

Equation (2) has been used to calculate the valency vibrations of hydrocarbons; the results are tabulated in Table I and compared with the observed frequencies. It follows from (2) that two chains of  $n'$  and  $n''$  mass points have a number of valency frequencies in common if  $n'$  and

$n''$  have common multiples. In the calculations the factor  $\frac{1}{2\pi}\sqrt{\frac{2f}{m}}$  has been assumed to be  $990 \text{ cm}^{-1}$ , the C—C valency vibration of ethane. The letters "Ra" and "i.r." in Table I refer to the Raman and infra-red spectra respectively. The data for the Raman spectra have been taken from Landolt-Börnstein,<sup>2</sup> *Physikalisch-Chemische Tabellen*. The infra-red spectra of propane have been investigated by Bartholomé<sup>3</sup> (1933) while those of butane, hexane, octane and dodecane have been observed by W. W. Coblentz<sup>4</sup> (1905). All the frequencies observed in the region 809 to  $1143 \text{ cm}^{-1}$  are given in the table. The agreement between calculated and observed frequencies is amazingly good. Though the angle forces in the molecule as well the differences in the mass of the  $\text{CH}_3$  and  $\text{CH}_2$  groups have been neglected, the difference between observed and calculated values does not exceed 4% and is on the average nearer 1%. All the observed bands can be assigned to definite valency vibrations. On the other hand, the calculated bands between 1102 and 1125 have not been observed in a single instance.

## 2. Valency Vibrations of a Closed Chain.

In the case of hydrocarbons of a cyclic structure (cyclopropane, etc.), the ring is composed of  $\text{CH}_2$  groups linked together by single C—C valencies. The system of equations from which  $\nu$  is determined, reads now:

$$4\pi^2\nu^2l_r = f\{2l_r + \cos\theta(l_{r-1} + l_{r+1})\} \quad (3)$$

<sup>2</sup>Landolt-Börnstein, *Physikalisch-Chemische Tabellen*, 3. Ergänzungsband, p. 952.

<sup>3</sup>Bartholomé, *Z. physik. Chem.*, B, 1933, 23, 152.

<sup>4</sup>Coblentz, *Infra-red Investigations*, 1905.



$r = 1, 2, \dots n$ . Each mass point has two neighbours, and  $n$  mass points are linked together by  $n$  valencies. If again  $l_r = \sin r\alpha$ , and  $l_1 = l_{n+1}$ , the solution of (3) is:

$$4\pi^2\nu^2m = 2f\left(1 + \cos\theta \cos \frac{2\pi k}{n}\right), 0 < k \leq n. \quad (4)$$

The C—C linkages form now regular polygons with  $n$  sides, and  $\theta$  is determined by  $\theta = \pi/n(n-2)$ . The case of cyclohexane is an exception: the molecule is puckered, possessing a tetrahedral valency angle. In Table II, the frequencies calculated from (4) are compared with the observed bands. The agreement between calculated and observed vibrations is less good than in the case of the open chains (between 5 and 10 %). It is to be expected that the interaction between valency and angle forces should be greater since it is known from chemical evidence that the bonds in cyclic aliphatic compounds are under strain.

TABLE II.—C—C VALENCY VIBRATIONS OF RING-SHAPED ALIPHATIC HYDROCARBONS.

Compound.	Frequencies in cm. <sup>-1</sup> .							
C <sub>3</sub> H <sub>6</sub>	calc.	857		857				
	obs. Ra	866		866				
C <sub>5</sub> H <sub>10</sub>	calc.	825			942	942	1147	
	obs. Ra	887			1031	1031	1200	
C <sub>6</sub> H <sub>12</sub>	calc.	808	904	904	1072	1072	1162	
	obs. Ra	805	—	—	1050	1050	1160	
	i.r.	795	915	915	1050	1050	—	
C <sub>7</sub> H <sub>14</sub>	calc.	608	776	776	1058	1058	1237	1237
	obs. Ra	—	729	729	1005	1005	1165	1282
C <sub>8</sub> H <sub>16</sub>	calc.	537	700	700	990	990	1215	1296
	obs. Ra	—	760	760	988	988	1177	1299

### 3. Isomers.

The isomeric forms of the aliphatic hydrocarbons possess side chains which may branch off at different points of the main chain. General formulæ, from which the valency vibrations can be calculated, have been derived for the possible isomeric structures.

(A) **One Side Chain at one End of the Main Chain.**—The whole chain is assumed to consist of  $n$  mass points. The first two links (called here  $l_1'$  and  $l_1''$ ) branch both off from the next link  $l_1$ . We have the  $n-1$  equations:

$$\begin{aligned} 4\pi^2\nu^2ml_1' &= f\{2l_1' + \cos\theta(l_1'' + l_1)\} \\ 4\pi^2\nu^2ml_1'' &= f\{2l_1'' + \cos\theta(l_1' + l_1)\} \\ 4\pi^2\nu^2ml_1 &= f\{2l_1 + \cos\theta(l_1' + l_1'' + l_2)\} \\ 4\pi^2\nu^2ml_r &= f\{2l_r + \cos\theta(l_{r-1} + l_{r+1})\} \end{aligned}$$

$$r = 2, 3, \dots n-3. \quad l_{n-2} = 0.$$

A subtraction of the first two equations leads to the solution

$$4\pi^2\nu^2m = 2f(1 - \frac{1}{2}\cos\theta)$$

<sup>5</sup> Lambert and Lecomte, *Ann. Physique*, 1938, 10, 503.

which fulfils all  $n - 1$  equations if  $l_1 = l_2 = \dots = l_{n-3} = 0$ . This vibration is antisymmetric to the plane which contains  $l_1, \dots, l_{n-3}$ . If the first two equations are added and the following notation is adopted:  $l_1' + l_1'' = l_0, l_0 + l_1 = l_{-1}$ , all equations have the form:

$$4\pi^2\nu^2ml_r = f\{2l_r + \cos \theta(l_{r-1} + l_{r+1})\}$$

which can be simultaneously satisfied if  $l_r = \sin(r\alpha + \beta)$ . Then:

$$4\pi^2\nu^2m = 2f(1 + \cos \theta \cos \alpha),$$

where  $\alpha$  is determined by the equation  $2 \sin \alpha = \tan(n-2)\alpha$ . This expression furnishes  $n - 3$  solutions. The last solution is obtained from  $l_r = \sinh(r\alpha + \beta)$ . Then  $4\pi^2\nu^2m = 2f(1 + \cos \theta \cosh \alpha)$ , and  $\alpha$  is determined by  $2 \sinh \alpha = \tanh(n-2)\alpha$ . The vibrations of these isomers lie no longer between the same limits as those of the normal compounds. In Table III the vibrations calculated from the formulæ are compared with the observed frequencies.

TABLE III.—C—C VIBRATIONS OF ISOMERIC COMPOUNDS

Compound.	Frequencies in cm. <sup>-1</sup> .					
C . C . C	calc.	809		1070	1070	
C	obs. Ra	794	964	1098	1098	
C . C . C . C	calc.	792	964		1105	1105
C	obs. Ra	802	902	956	1019	1142
C . C . C . C . C	calc.	797	905	1034	1070	1120
C	obs. Ra	808	890	950	1043	1150

(B) **One Side Chain at each End of the Main Chain.**—The valency vibrations are calculated in a way analogous to section (A). The computation leads to the following solutions:

$$4\pi^2\nu^2m = 2f(1 + \cos \theta \cos \alpha),$$

where

$$\tan(n-4)\alpha = \frac{4 \sin \alpha}{1 - 4 \sin^2 \alpha}$$

$$4\pi^2\nu^2m = 2f(1 + \cos \theta \cosh \alpha),$$

where

$$\tanh(n-4)\alpha = \frac{4 \sinh \alpha}{1 + 4 \sinh^2 \alpha}$$

$$4\pi^2\nu^2m = 2f(1 - \frac{1}{2} \cos \theta).$$

This last equation occurs twice. The degeneracy occurring here is spurious, it is caused by neglecting the angle forces. Case (B) is illustrated by an octane isomer:

C . C . C . C . C . C	calc.	773	809	950	1070	1070	1070	1138
C                    C	obs. Ra	778	839	962	1048	1048	1048	1150

(C) **Three Side Chains Branching off from First Link of the Chain.**—The equations determining the vibrations are:

$$4\pi^2\nu^2m = 2f(1 + \cos \theta \cos \alpha),$$

where  $\alpha$  is determined by

$$\tan(n-3)\alpha = \frac{3 \sin \alpha}{2 + \cos \alpha}$$

$$4\pi^2\nu^2m = 2f(1 + \cos \theta \cosh \alpha),$$

where  $\alpha$  is determined by

$$\tanh (n-3) \alpha = \frac{3 \sinh \alpha}{2 + \cosh \alpha},$$

$$4 \pi^2 \nu^2 m = 2f(1 - \frac{1}{2} \cos \theta).$$

The last solution occurs three times. The formulæ give the following

frequencies for the hexane isomer  $\begin{array}{c} \text{C} \\ \cdot \\ \text{C} \cdot \text{C} \cdot \text{C} \cdot \text{C} \cdot \text{C} \\ \cdot \\ \text{C} \end{array}$ :

$\begin{array}{c} \text{C} \\ \cdot \\ \text{C} \cdot \text{C} \cdot \text{C} \cdot \text{C} \cdot \text{C} \\ \cdot \\ \text{C} \end{array}$	calc.	690			954	1070	1070	1070
	obs. Ra	725	760	874	932	947	1057	1057 1143

**(D) One Side Chain Branches off from every Link of the Main Chain.—**

If it is assumed that the main chain contains  $n-1$  linkages, the whole molecule will consist of  $2n-1$  linkages or  $2n$  mass points. The following formulæ are obtained for the vibrations:

$$4 \pi^2 \nu^2 m = 2f\{1 + \frac{1}{2} \cos \theta \cos \alpha \pm \frac{1}{2} \cos \theta \sqrt{\cos^2 \alpha + 2 \cos \alpha + 2}\}$$

where  $\alpha = \frac{\pi k}{n}$ ,  $0 < k < n$  ( $2n-2$  solutions),

and  $4 \pi^2 \nu^2 m = 2f$ .

The vibrations lie between the limits

$$\frac{1}{2\pi} \sqrt{\frac{2f}{m} \{1 + \frac{1}{2} \cos \theta + \frac{1}{2} \cos \theta \sqrt{5}\}}$$

and  $\frac{1}{2\pi} \sqrt{\frac{2f}{m} (1 - \cos \theta)}$ .

For  $\cos \theta = -\frac{1}{3}$  and  $\frac{1}{2\pi} \sqrt{\frac{2f}{m}} = 990$ , the frequencies extend from 672 to 1143  $\text{cm}^{-1}$ . The solutions have been applied to the following two cases:

$\text{C} \cdot \text{C} \cdot \text{C} \cdot \text{C} \cdot \text{C}$	calc.	777	937	990	1092	1117
$\begin{array}{c} \cdot \\ \text{C} \end{array}$	obs. Ra	747	810 875 950	1014	1034	1158
$\text{C} \cdot \text{C} \cdot \text{C} \cdot \text{C} \cdot \text{C} \cdot \text{C}$	calc.	736	866	962	990	1090 1102
$\begin{array}{c} \cdot \\ \text{C} \cdot \text{C} \end{array}$	obs. Ra	733	754 801 840 897	955	984	1034 1054 1123

**(E) Two Side Chains Branch off from every Link of the Main Chain.—**

If the main chain, again, consists of  $n-1$  linkages, the whole molecule will contain  $3n-1$  linkages or  $3n$  mass points. The vibrations are obtained from the formulæ:

$$4 \pi^2 \nu^2 m = 2f\{1 + \frac{1}{2} \cos \theta (2 \cos \alpha + 1 \pm \sqrt{17 + 12 \cos \alpha + 4 \cos^2 \alpha})\}$$

with  $\alpha = \frac{\pi k}{n}$ ,  $0 < k < n$ .

$$4 \pi^2 \nu^2 m = 2f(1 - \frac{1}{2} \cos \theta).$$

The last solution occurs  $(n+1)$  times. This case is illustrated by the example:

$\begin{array}{c} \text{C} \cdot \text{C} \\ \cdot \\ \text{C} \cdot \text{C} \end{array}$	calc.	749	905	1070	1070	1111
$\begin{array}{c} \cdot \\ \text{C} \cdot \text{C} \end{array}$	obs. Ra	737	771 850	945	1053	1053 1150

The largest possible frequency is the same as in the case of the normal compounds ( $1143 \text{ cm.}^{-1}$ ); but the smallest possible frequency shifts to

$$\frac{1}{2\pi} \sqrt{\frac{2f}{m} \{1 + \frac{1}{4} \cos \theta (3 + \sqrt{33})\}},$$

*i.e.*  $514 \text{ cm.}^{-1}$  so that the range of valency vibrations overlaps the region of the deformation frequencies. Consequently, the agreement between calculated and observed frequencies is no longer so good as in the case of the normal compounds. Furthermore, the spectra of the isomeric compounds show, in the region under survey, a greater number of bands than can be ascribed to valency vibrations. We have, here, therefore, a certain superposition of the range of bending oscillations over that of the valency vibrations. This did not occur in the spectra of the normal chains; every band observed could be assigned to a valency vibration. The tables show that the agreement between calculated and observed vibrations improves with the length of the chain as is to be expected. In the case of very long chains, the bands will merge into one another so that the appearance of the spectrum becomes more and more that of a continuous band stretching from the upper to the lower limit computed above. As has been shown, the extension of the continuous band will vary with the structure of the substance under analysis.

### Summary.

The C—C valency vibrations of aliphatic hydrocarbons have been theoretically calculated. General formulæ are developed for the valency vibrations of normal chains of  $\text{CH}_2$  groups, isomers and cyclic molecules.

The C—C valency frequencies of a number of hydrocarbons of varying structure have been computed by means of these formulæ and are compared with the observed spectra. From the agreement between calculated and observed values it can be concluded that the interaction between bending and stretching vibrations is only a second order effect. It is, therefore, possible to identify the C—C valency vibrations of any hydrocarbon by applying the formulæ given in the paper to the compound under consideration.

*Imperial College of Science and Technology,  
London.*

## THE FORCE CONSTANTS OF SOME CH, NH AND RELATED BONDS.

By J. W. LINNETT.

*Received 4th December, 1944.*

It has been realised for some time that the presence of a given grouping of atoms in a molecule results in that molecule possessing vibration frequencies characteristic of the atomic grouping. Thus all molecules containing the C—H group have at least one vibration frequency of  $3000 \pm 300 \text{ cm.}^{-1}$ . The magnitude of the observed frequency, which corresponds to the C—H valency vibration, depends mainly on the masses of the carbon and hydrogen atoms and on the force constant of the C—H bond. The approximate magnitude is given by  $4\pi^2\nu^2\mu = k$ , where  $\nu$  is the frequency,  $\mu$  is the reduced mass of the link, and  $k$  is the force constant. This approximation is quite good if there is no other atomic grouping in the molecule having a characteristic frequency about the same as that

being considered. If such a grouping is present, then the two motions resonate with one another, the frequencies change, and neither resulting frequency is characteristic of either particular grouping alone.

In many organic molecules there is no atomic grouping, other than C—H, which possesses a frequency at all close to  $3000\text{ cm}^{-1}$ , so the above equation gives the observed magnitude quite well when the C—H group is like that in chloroform. With a  $\text{CH}_2$  group, however, there are two C—H groups, both of which will tend to give vibration frequencies of the same magnitude, and these will interact. In this case therefore the valency vibrations of the whole  $\text{CH}_2$  group must be considered. This gives one symmetrical and one antisymmetrical valency vibration. Similarly  $\text{CH}_3$  must be considered as a group, rather than each CH separately, giving a symmetrical and a doubly degenerate vibration. The case of  $\text{CH}_4$  may be considered separately. It seems probable that the interaction between the vibrations of two similar groups in different parts of the molecule is slight. For instance, the interaction between the two methyl groups in dimethylacetylene,<sup>1</sup> and even in ethane,<sup>2</sup> does not have a large effect on the CH vibration frequencies and can be ignored even in a fairly exact treatment.

Therefore, providing we restrict ourselves to molecules having no other grouping with a characteristic frequency near  $3000\text{ cm}^{-1}$ , we may calculate the force constants of the C—H bonds in the molecule by using the frequencies observed in the infra-red and Raman spectra which are characteristic of the CH,  $\text{CH}_2$  or  $\text{CH}_3$  grouping, together with the simple formula appropriate for the grouping.

The alternative approach to the problem leads to a similar result. In this one constructs the complete equations for all the vibration frequencies of the molecule in terms of all the force constants, and then factorises off from the equation the expression for the highest frequency. This can be done simply to quite a close approximation when the frequencies involved are much greater than any others that the molecule possesses, as has been shown by Crawford and Edsall.<sup>3</sup> The resulting formulæ are the same whichever approach is used.

In the present paper the first method has been used for calculating the force constants of C—H and N—H bonds in a variety of molecules. A few O—H, S—H and similar bonds have also been considered. Comparison of the force constants is a more satisfactory way of comparing a number of C—H or N—H bonds than is a simple comparison of the observed frequencies, since the latter depend on the atomic grouping (e.g. whether CH,  $\text{CH}_2$  or  $\text{CH}_3$ ) as well as on the strength of the bond. A similar comparison of C—H force constants has been made by Fox and Martin for hydrocarbons.<sup>4</sup> They compared the constants in the saturated  $\text{CH}_3$ ,  $\text{CH}_2$  and CH groups, the ethylenic  $\text{CH}_2$ , the acetylenic CH, and the benzenoid CH groups. Their findings, in most respects, confirm the conclusions of the present examination though they did not interpret their results in the manner here described, but only noted the considerable change in C—H force constant resulting from structural changes.

### Formulæ.

The formulæ used are :—

- |                           |                                  |   |
|---------------------------|----------------------------------|---|
| (1) MH group :            |                                  | $\lambda = k(R_1 + R_2).$                             |
| (2) $\text{MH}_2$ group : | Symmetrical                      | $\lambda = k(R_1 + 2R_2 \cdot \cos^2 \theta)$         |
|                           | Antisymmetrical                  | $\lambda = k(R_1 + 2R_2 \cdot \sin^2 \theta).$        |
|                           | where $2\theta$ = the HMH angle. |   |
| (3) $\text{MH}_3$ group : | Symmetrical                      | $\lambda = k(R_1 + 3R_2 \cdot \cos^2 \phi)$           |
|                           | Degenerate                       | $\lambda = k(R_1 + \frac{3}{2}R_2 \cdot \sin^2 \phi)$ |

<sup>1</sup> Linnett, *Trans. Faraday Soc.*, 1941, **37**, 469. Crawford and Brinkley, *J. Chem. Physics*, 1941, **9**, 69.

<sup>2</sup> Linnett, *ibid.*, 1940, **8**, 91.

<sup>3</sup> Crawford and Edsall, *J. Chem. Physics*, 1939, **7**, 223.

<sup>4</sup> Fox and Martin, *Proc. Roy. Soc., A*, 1940, **175**, 208.

where  $\phi$  is the angle between the MH bonds and the symmetry axis of the  $\text{MH}_3$  group.

$$(4) \text{ MH}_4 \text{ group: } \begin{array}{ll} \text{Symmetrical} & \lambda = k \cdot R_1 \\ \text{Degenerate} & \lambda = k(R_1 + \frac{1}{3}R_2). \end{array}$$

assuming a tetrahedral arrangement.

In the above formulæ  $\lambda = 4\pi^2\nu^2$  where  $\nu$  is the vibration frequency, and  $R_1$  and  $R_2$  are the reciprocals of the masses of the H and M atoms respectively.

In the rest of the paper the force constants will be given in units of  $10^5$  dynes per cm. That is a force constant of  $5 \times 10^5$  dynes per cm. will be referred to as a force constant of 5 units.

Figures for the vibration frequencies have been taken from the original papers of a variety of workers on infra-red and Raman spectra; and also from books such as those of Spenser, Hibben and Kohlrausch. References are given in special cases.

## Results.

### C—H Bond.

**Some Substituted Methanes.**—The force constants of a number of C—H bonds in methane and some of its derivatives are shown in Tables

TABLE I.—THE C—H FORCE CONSTANT IN METHANE AND SOME OF ITS DERIVATIVES

X	H	F	Cl	Br	I	$\text{C}_6\text{H}_5$	COOH	$\text{COO}^-$
$\text{CH}_3\text{X}$	4.97	4.71	4.90	4.95	5.00	4.90	4.97	4.97
$\text{CH}_2\text{X}_2$	4.97	4.89	4.95	4.96	4.94	4.73	4.92	4.88
$\text{CHX}_3$	4.97	—	4.96	4.97	—	—	—	—

TABLE II.—THE C—H FORCE CONSTANT IN SOME METHYL COMPOUNDS

X	CH <sub>3</sub>	NH <sub>2</sub>	OH	OCH <sub>3</sub>	SH	SCH <sub>3</sub>	COCl	COBr	CONH <sub>2</sub>	
CH <sub>3</sub> X	4.81	4.69	4.71	4.95	4.94	4.90	4.90	4.88	4.94	
X	COCH <sub>3</sub>	CHO	CO	COOH	O.CO.H	CN	NC	SCN	NO <sub>2</sub>	ZnCH <sub>3</sub>
CH <sub>3</sub> X	4.85	4.98	4.94	5.02	5.00	5.01	4.94	5.06	4.78	

TABLE III.—THE C—H FORCE CONSTANTS IN SOME OTHER ALIPHATIC COMPOUNDS

X	Cl	Br	CN	OH	$\text{NH}_2$	$\text{C}_6\text{H}_5$	Cl	Cl
Y	$\text{CH}_2\text{Cl}$	$\text{CH}_2\text{Br}$	$\text{CH}_2\text{CN}$	$\text{CH}_2\text{OH}$	$\text{CH}_2\text{NH}_2$	$\text{CH}_2\text{C}_6\text{H}_5$	COCl	$\text{C}_6\text{H}_5$
$\text{CH}_2\text{XY}$	4.84	4.88	4.86	4.62	4.53	4.80	4.86	4.92
X	Cl	Br	CN	OH	$\text{NH}_2$	$\text{C}_6\text{H}_5$	Cl	Cl
Y	$\text{CHCl}_2$	$\text{CHBr}_2$	$\text{CHCN}$	$\text{CHOH}$	$\text{CH}_2\text{NH}_2$	$\text{CH}_2\text{C}_6\text{H}_5$	COCl	$\text{C}_6\text{H}_5$
$\text{CHX}_2\text{Y}$	4.85	4.86	4.86	4.86	4.86	4.86	4.86	4.86

I, II and III. The force constant given for the C—H bond in methane is the mean of ten figures obtained from  $\text{CH}_4$  and its four deuterated derivatives. The mean deviation from 4.97 is 0.07 units, which suggests that the figure is fairly reliable. The normal force constant of the C—H bond in methane and its derivatives will therefore be taken to be 4.97 units. Further reference to Tables I and II shows that in many cases the force constant of the C—H bond does not deviate appreciably from the normal value. This can be seen particularly well for the chlorine,



bromine and iodine derivatives of methane (*cf.* Fox and Martin<sup>4</sup>). In these cases, therefore, the C—H bond seems to be the same as in methane. There are, however, several cases where the force constant does deviate from the normal value.

In methyl fluoride the C—H force constant is 4.71, which is low compared with 4.97 beyond the limits of error. It is probable that this is to be associated with a high contribution of the ionic term in the C—F link, which results in the methyl group having a positive charge. It will be seen later that the N—H bond in the ammonium ion has a much smaller force constant than that in ammonia. Therefore, from this, the positive charge on the methyl group would be expected to lead to a reduction of the C—H force constant. That a considerable contribution of the ionic term, much greater than in the other alkyl halides, is to be expected in methyl fluoride can be seen from Pauling's electronegativity tables.<sup>5</sup> In methylene fluoride, the force constant is very nearly normal. This may arise because the second fluorine atom reduces the positive charge on the carbon atom by the contribution of structures such as  $\overset{+}{\text{F}}=\text{CH F}$ , the positive charge resulting from the ionisation of one fluorine atom being transferred from the carbon to the second fluorine atom.<sup>6</sup>

In methylamine and methyl alcohol also, the C—H force constant is markedly lower than the normal. It is difficult to believe that this effect is due to a positive charge on the carbon atom, since the electronegativity difference between carbon and nitrogen (0.5) is much less than between carbon and fluorine (1.5), being the same as that between carbon and chlorine (0.5). Continuing the series  $\text{CH}_3\text{NH}_2$ ,  $\text{CH}_3\text{OH}$  to ethane,  $\text{CH}_3 \cdot \text{CH}_3$ , it will be seen that in this molecule also the C—H force constant is below the normal value (*cf.* Fox and Martin<sup>4</sup>), though less so than in methyl alcohol or methylamine. It seems possible that the reduction may be due to the contribution of structures such as  $\overset{+}{\text{H}}\text{CH}_2=\text{CH}_2\text{H}$  in ethane, such contributing structures having been suggested by Gorin, Walter and Eyring to account for restricted rotation in ethane.<sup>7</sup> Analogous structures in methyl alcohol and methylamine may be the reason for the low value of the C—H force constant in these cases. It will be shown later that the N—H force constant is less in methylamine than in ammonia as would be anticipated if this explanation is the correct one. In molecules such as ethylene dichloride and dibromide (Table III) the C—H force constant is also lower than in methane, but not as low as in ethane. In these molecules there are fewer possibilities of resonance with double bond structures since there are fewer hydrogen atoms to use. On the other hand, in ethylene glycol and ethylene diamine the reduction in the C—H force constant is even greater than in methyl alcohol or methylamine. According to the above explanation, this is because there are now more resonance possibilities since each methylene group is between another methylene and a hydroxyl, or amino, group with both of which the above type of resonance is possible. The C—H force constants in methane and ethane parallel the C—H bond energies determined by Stevenson to be 101 and 96 K.cal. per g. mol. respectively.<sup>8</sup> For the force constants there is a 3 % reduction on passing from methane to ethane and for the bond energies a 5 % reduction.

Fox and Martin gave the force constants of the  $\text{CH}_3$ ,  $\text{CH}_2$ , and CH groups in saturated hydrocarbons as 4.75, 4.56 and 4.56 units compared with 5.04 units in methane. This shows a steady reduction in the series which would be expected from the present explanation. Each  $\text{CH}_2$  is between two other carbon atoms and so can assume double bond structures

<sup>5</sup> Pauling, *Nature of the Chemical Bond*, Section II, 11a.

<sup>6</sup> Brockway, *J. Physic. Chem.*, 1937, 41, 185.

<sup>7</sup> Gorin, Walter and Eyring, *J.A.C.S.*, 1939, 61, 1876.

<sup>8</sup> Stevenson, *J. Chem. Physics*, 1942, 10, 291.

with the carbon atoms on each side, which means that the C—H bond should be weakened still further compared with ethane in which there is only one C—C bond to assume a partial double bond character. In confirmation of this Fox and Martin give the C—H force constant in the methyl group in higher hydrocarbons as 4.75, which is approximately the same as in ethane. Fox and Martin state that the value for the CH group is of doubtful reliability.

In only one case does the C—H force constant seem to be definitely higher than in methane and that is in nitromethane, and then by only 0.09 units. In zinc dimethyl the force constant of the C—H bond seems to be definitely low.

**The Ethylenic C—H Bond.**—In Table IV are shown the C—H bond force constants of some ethylenic derivatives. Omitting, for the moment, those containing chlorine it will be seen that the force constant is close

TABLE IV.—THE C—H FORCE CONSTANTS IN SOME DERIVATIVES OF ETHYLENE

X Y	H H	Cl H	Cl Cl	H Cl	H Br	H I
X. CH=CX.Y	5.08	5.17	5.18	5.16	5.11	5.09

to 5.1 units (Fox and Martin give 5.05). This is definitely higher than the normal methane C—H force constant. On the electron pair bond theory the carbon valencies in methane are produced equivalent by  $sp^3$  hybridisation.<sup>9</sup> In ethylene, however, there are formed three equivalent bonds by  $sp^2$  hybridisation.<sup>10</sup> The C—H linkages are each formed by one of these. It seems therefore that the force constant of 5.1 units is the normal value of the C—H bond when  $sp^2$  hybridisation is involved.

In the three chlorine substituted ethylenes the C—H force constant is rather higher (5.17). If this is real, it is presumably to be associated with the resonance that occurs in these chlorethylenes, since it occurs in all the chlorine derivatives but in no others.<sup>11</sup>

In acetylacetone there is a Raman frequency of 3070  $cm^{-1}$ . If this is interpreted as arising from the enol form, and, in this, from the central CH group, the force constant is calculated to be 5.13 units. This value is consistent with that for an ethylenic C—H bond which this would be in the enol form of acetylacetone.

**Benzenoid C—H Bond.**—In Table V are given the force constants of the C—H bond in benzene and a variety of its derivatives, as calculated

TABLE V.—THE C—H FORCE CONSTANT IN SOME DERIVATIVES OF BENZENE

X	H	CH <sub>3</sub>	CH <sub>2</sub> Cl	CH <sub>2</sub> CN	CH <sub>2</sub> OH	CH <sub>2</sub> NH <sub>2</sub>	CH <sub>2</sub> NO <sub>2</sub>
C <sub>6</sub> H <sub>5</sub> X	5.10	5.08	5.08	5.09	5.07	5.08	5.10
X	Cl	Br	I	CN	OH	SH	NH <sub>2</sub>
C <sub>6</sub> H <sub>5</sub> X	5.12	5.12	5.08	5.12	5.10	5.10	5.06
X	NHC <sub>6</sub> H <sub>5</sub>	C≡CH	NO <sub>2</sub>	CHO	COCH <sub>3</sub>	COOCH <sub>3</sub>	COCl
C <sub>6</sub> H <sub>5</sub> X	5.12	5.10	5.07	5.09	5.12	5.14	5.13

from the symmetric vibration frequency. It will be seen that, in all cases, the C—H force constant is within 0.04 units of 5.1 (Fox and Martin give 5.12). Now in benzene, as in ethylene, three equivalent carbon bonds are formed by  $sp^2$  hybridisation,<sup>12</sup> so that we should expect the C—H

<sup>9</sup> Pauling *J.A.C.S.*, 1931, 53, 1367.

<sup>10</sup> Penney, *Proc. Phys. Soc.*, 1934, 46, 333.

<sup>11</sup> Brockway, Beach and Pauling, *J.A.C.S.*, 1935, 57, 2693. Thompson and Linnett, *J.C.S.*, 1937, 1393.

<sup>12</sup> Bowen, *Ann. Rep.*, 1943, 12.

force constant in benzene to be the same as in ethylene. This is found to be so, both having the value of 5.1 units.

**Acetylenic C—H Bond.**—This can be found from acetylene, alkyl-acetylenes and phenyl acetylene where the values are 6.05, 5.97 and 5.92 units respectively (Fox and Martin give 5.92). In acetylene two equivalent bonds are formed by  $sp$  hybridisation and the C—H bond is formed by one of these. So 6.0 units seems to be the force constant characteristic of  $sp$  hybridisation. We therefore obtain the series:  $sp^3$ , 4.97;  $sp^2$ , 5.1;  $sp$ , 6.0. As the proportion of the  $s$ -orbital in the bond forming orbital increases the force constant of the bond increases. This is surprising as the  $sp^3$  bond is supposed to be the strongest, and the strength to decrease as the proportion of  $s$ -orbital in the bond orbital increases. However, there is no doubt that there is the increase in the force constant in the above series.

**Aldehydic C—H Bond.**—The force constants of some aldehydic C—H bonds are listed in Table VI. It will be seen that the constant is much

TABLE VI.—THE C—H FORCE CONSTANT IN SOME ALDEHYDES

R	H	CH <sub>3</sub>	CCl <sub>3</sub>	C <sub>6</sub> H <sub>5</sub>	OH	OCH <sub>3</sub>	NH <sub>2</sub>
R. CHO	4.43	4.37	4.48	4.67	4.75	4.40	4.53

smaller than that in methane, being approximately 4.4 or 4.45 if formic acid and benzaldehyde are excluded. The carbonyl bond has quite a large dipole moment as a result of resonance with the structure  $=\overset{+}{C}-\overset{-}{O}$  which is said by Pauling to contribute equally with the normal electronic arrangement represented by  $=C=O$ .<sup>13</sup> This would lead to a large positive charge being located on the carbon atom and, by analogy with methyl fluoride, this would result in a decrease in the C—H force constant. The reason why the C—H force constant in formic acid and in benzaldehyde is greater than in formaldehyde and acetaldehyde may be because in these cases the positive charge on the carbon atom is somewhat reduced in formic acid by transfer to the oxygen of the hydroxyl (*cf.* CH<sub>3</sub>F<sub>3</sub>), and partly neutralised in benzaldehyde by polarisation of the benzene nucleus.<sup>14</sup> The force constant in formamide is increased slightly relative to that in formaldehyde, so in this case it appears that the nitrogen takes some of the positive charge by a small contribution of the structure

H.  $\overset{+}{C} \begin{array}{l} \nearrow O \\ \searrow NH_2 \end{array}$ , though the effect is less than in the acid.

The force constant of the C—H bond in CH<sub>3</sub>.CH=N.OH, acetaldoxime, is 4.42 units, which shows the same reduction as that in the aldehydes.

**C—H Bond Lengths.**—By the application of one of the various relations between bond lengths and force constants it should be possible to calculate the C—H bond lengths in the compounds that have been considered. The Douglas Clark relation ( $h \cdot r_e^6 = \text{a constant}$ ) is found to be satisfactory.<sup>15</sup> For the following three cases which may be taken as standard, we have: (a) ground state of the CH diatomic molecule:  $h = 4.35$ ,  $r_e = 1.120 \text{ \AA}$ ,  $h \cdot r_e^6 = 8.58$ ; (b) CH<sub>4</sub>:  $h = 4.97$ ,  $r_e = 1.093$ ,  $h \cdot r_e^6 = 8.47$ ; (c) C<sub>2</sub>H<sub>2</sub>:  $h = 6.0$ ,  $r_e = 1.057$ ,  $h \cdot r_e^6 = 8.37$ . Taking the Douglas Clark constant to be 8.47 we should calculate for (a) from  $h = 4.35$ ,  $r_e = 1.118$ ; and for case (c) from  $h = 6.0$ ,  $r_e = 1.059 \text{ \AA}$ . Both

<sup>13</sup> Lowry, *J.C.S.*, 1923, 822. Pauling, *Nature of the Chemical Bond*, Section II, 12a.

<sup>14</sup> Pauling, *loc. cit.*<sup>13</sup>, Section VI, 25d.

<sup>15</sup> Douglas Clark, *Phil. Mag.*, 1934, 18, 459.

are within 0.2 % so we may expect this method to give quite a good value for the bond length. Moreover cases (a) and (c) are at the extremes of bond length to be obtained for the C—H link. Table VII gives a few bond lengths calculated on the basis of the above formula. It will be seen that the C—H bond length can vary over a range of about 5 %, or 0.055 Å.

**Summary for C—H Bonds.**—It seems that there are three main factors which affect C—H bond force constants:

(1) The type of carbon bond orbital used in the linkage, whether  $sp^3$ ,  $sp^2$  or  $sp$ ; (2) the extent to which there is a positive charge located on the carbon atom, the constant being smaller the greater the positive charge; (3) the extent to which double bond forms involving ionic structures contribute as in ethane, methyl alcohol and methylamine.

### N—H Bond.

**Ammonia and Aliphatic Amines.**—The force constant of the N—H bond in ammonia is 6.49 units, this being the mean of three figures which have a mean deviation of 0.05 units. In methylamine the constant is 6.30, and in dimethylamine 6.15 units. This shows the same reduction of the force constant of the N—H bond as was observed for the C—H bond in ethane, methylamine and methyl alcohol. It is worth noting that in methylamine there is a simultaneous reduction of both the CH and the N—H force constants, and not an increase of one accompanying a decrease of the other. This simultaneous reduction in both force constants is explained if it arises from contributions of structures such as  $^+HCH_2=NH$  and  $HCH_2=NH^+$ . This will also explain why in dimethylamine the N—H force constant is smaller than in methylamine. Benzylamine also gives a smaller N—H force constant (6.19) than ammonia.

**Ammonium Ion.**—Using the frequencies given by Ananthakrishnan<sup>16</sup> for the ammonium ion the N—H force constant is found to be 5.36 units which is much less than in ammonia. It is difficult to obtain figures for the N—H force constant in methylammonium ions because the C—H and N—H frequencies are so close that it is impossible to separate them (see Introduction). However,  $CH_3 \cdot ND_3^+$  gives the N—D force constant to be 5.4, and in  $ND_3^+ \cdot ND_3^+$  it is 5.24 units.<sup>17</sup> So a value of approximately 5.35 units may be regarded as satisfactory for the N—H force constant in an ammonium type ion. This shows the large reduction in the N—H force constant resulting from the location of a positive charge on the group. A similar effect accounted for the low values for the C—H force constants in methyl fluoride and in aldehydes. It must be remembered that in ammonia the nitrogen atom uses predominantly  $p$ -orbitals for bond formation whereas in the ammonium ion there is  $sp^3$  hybridisation of the nitrogen orbitals. However, though this might lead

TABLE VII.—SOME C—H BOND LENGTHS CALCULATED FROM THE FORCE CONSTANTS.

Molecule.	Force Constant.	C—H Bond Length.
Methane . . . . .	4.97	1.093 Å.
Ethylene . . . . .	5.1	1.088
Benzene . . . . .	5.1	1.088
Acetylene . . . . .	6.0	1.059
Formaldehyde . . . . .	4.43	1.114
CH <sub>3</sub> F . . . . .	4.71	1.103
CH <sub>3</sub> Cl . . . . .	4.90	1.095
CH <sub>3</sub> Br . . . . .	4.95	1.094
CH <sub>3</sub> I . . . . .	5.00	1.092

<sup>16</sup> Ananthakrishnan, *Proc. Ind. Acad. Sci., A*, 1937, 5, 85.

<sup>17</sup> Edsall and Scheinberg, *J. Chem. Physics*, 1940, 8, 520.

to a slight reduction in the N—H force constant it does not seem probable that this can account for the whole of the large reduction from 6.49 to 5.36 if we consider the figures for the effect of  $sp^3$ ,  $sp^2$  and  $sp$  hybridisation on the C—H constants. For the C—H bonds the effect of changing hybridisation on the force constant seemed to be decreasing as one approached a more wholly  $p$ -bond orbital. However, the large reduction on passing from ammonia to the ammonium ion may be a combination of the charge and hybridisation effects.

**Other Amines.**—The N.H force constant in aniline is 6.35, and in diphenylamine 6.21 units, which shows a steady decrease from 6.49 in ammonia on attaching the phenyl group to the nitrogen atom. It is probable that this arises from resonance contributions to the structure, such

as in aniline  $\text{C}_6\text{H}_5=\overset{+}{\text{N}}\text{H}_2$ , which increase the positive charge on the nitrogen and so reduce the N—H force constant.<sup>18</sup>

In the ion  $\text{NH}_3^+ \cdot \text{NH}_2$  the force constant of the N—H bond in the amino group is 5.83 units, which shows a very great reduction compared with ammonia indicating that the positive charge on the  $\text{NH}_3^+$  group is shared, to a considerable extent, with the  $\text{NH}_2$  group.

In the guanidinium ion,  $\text{C}(\text{NH}_2)_3^+$ , the N—H force constant is 6.00 units. This ion is probably a resonance hybrid of three structures of the

type:  $(\text{NH}_2)_2\text{C}=\overset{+}{\text{N}}\text{H}_2$ , which means that the positive charge is largely shared between the three nitrogen atoms.<sup>19</sup> This would explain why the N—H force constant is low compared with that in ammonia, though rather closer to that in ammonia than to that in the ammonium ion.

**Amides and Urea.**—The N—H force constant in formamide is 6.31, in acetamide 6.41, in diacetamide 6.11, and in succinimide 6.12 units. This shows a reduction compared with ammonia and probably arises from

the contribution of structures such as  $\text{--}\overset{\text{O}}{\parallel}\text{C}-\overset{+}{\text{N}}\text{H}_2$ , though the small re-

duction in formamide and acetamide indicates that the contribution of these structures is only slight, as was concluded from the C—H force constant in formamide. The positive charge on the nitrogen atom is increased in diacetamide and succinimide by the action of two adjacent carbonyl groups.

In urea (N—H force constant, 6.43) the effect of the carbonyl is divided between two amino groups and the positive charge on each amino group seems to be very slight because the N—H force constant is only slightly less than in ammonia. The contribution of the ionic structures to resonance in urea would therefore seem, from the above evidence, to be slight though the evidence of bond lengths is that it is considerable.<sup>20</sup>

The N—H force constant in several imino-ethers of the general formula  $\text{R}_1 \cdot \text{C}(=\text{NH}) \cdot \text{OR}$  is 6.12 units, which shows a reduction below that of ammonia.

**N—H Bond Lengths.**—The Douglas Clark relation  $k \cdot r_e^6 = \text{a constant}$  does not seem to be satisfactory for the N—H linkages, and  $k \cdot r_e^{7.6} = \text{a constant}$  has been used. Three test cases give: (1) one state of the NH diatomic molecule:  $k = 2.84$ ,  $r_e = 1.123 \text{ \AA.}$ , constant = 6.85; (2) a second state of the NH diatomic molecule:  $k = 5.16$ ,  $r_e = 1.041$ , constant = 7.00; (3) Ammonia:  $k = 6.49$ ,  $r_e = 1.01 \text{ \AA.}$ , constant = 7.00. These three cases cover a very wide range, and considering this the constancy is very good. Since the range with which we are concerned is that covered by (2) and (3) the constant will be taken to be 7.00. This gives for several of the N—H bond lengths: ammonium ion, 1.036  $\text{\AA.}$ ; acetamide 1.012; urea, 1.011; aniline, 1.013; guanidinium ion, 1.020  $\text{\AA.}$

<sup>18</sup> Pauling, *loc. cit.* <sup>13</sup>, Section VI, 27.

<sup>19</sup> Pauling, *loc. cit.* <sup>13</sup>, Section VI, 25e.

<sup>20</sup> Wyckoff and Corey, *Z. Krist.*, 1934, 89, 462.

The accuracy does not warrant the fourth significant figure, but this has been included to show the kind of change in bond length to be expected from certain structural changes. The changes in bond length are not as great with the N—H bond as with the C—H bond.

**Summary for N—H Bonds.**—There is a large reduction in force constant on passing from ammonia to the ammonium ion, and in other cases the presence of a positive charge on the nitrogen leads to a reduction of the N—H force constant (*cf.* guanidinium). A carbonyl group adjacent to the N—H group appears to confer a small positive charge on the nitrogen by resonance with ionic structures. A benzene ring behaves similarly. A methyl group attached to the N—H group reduces the force constant probably because of resonance with ionic double-bond structures.

### Other M—H Bonds.

**Some O—H Bonds.**—Using the figures of Dennison<sup>21</sup> we find the O—H force constant in water to be 8.3 units. That in methyl alcohol (using O—H and O—D) is 7.65 units. Here there is the reduction in the O—H constant as compared with that in water, as there was in the N—H constant in methylamine as compared with that in ammonia. The C—H force constant also is less in methyl alcohol than in methane. The explanation is presumably similar to that suggested for methylamine.

The fundamental OH absorption band in the infra-red spectrum of phenol has been studied by Fox and Martin.<sup>22</sup> The band is at 3612 cm.<sup>-1</sup>, which gives the force constant of the O—H bond in phenol to be 7.26 units. The O—H force constant in phenol is then lower than that in water, which suggests that there is a positive charge on the oxygen atom

from such contributing structures as  $\bar{C}_6H_5-\overset{+}{O}H$  (*cf.* aniline). This is consistent with the chemical behaviour of phenol and with its dipole moment.

**Some S—H Bonds.**—The S—H force constant in hydrogen sulphide is 4.0; in methyl mercaptan, 3.8; and in thiophenol, 3.8 units. It will be seen that the S—H constant is lower in  $CH_3SH$  than in  $H_2S$  (*cf.* the O—H and N—H bonds). However, in  $CH_3SH$  the C—H constant is normal within the limits of error (Table II). Also the S—H force constant is lower in thiophenol than in  $H_2S$ , as the O—H constant was lower in phenol than in water. The percentage lowering for the S—H bond on attaching the phenyl group (5 %) is not as great as the percentage lowering for the O—H bond (*ca.* 10 %), as would be expected, since the structure  $\bar{C}_6H_5=\overset{+}{S}H$  is probably less important than the corresponding structure in phenol.

**The P—H Bond.**—The P—H bond in phosphine has a force constant of 3.10 units.

**The F—H and Cl—H Bonds.**—The force constants of the F—H and Cl—H bonds are respectively 9.62 and 5.13 units. It will be seen that these fall into the series F—H, O—H, N—H, C—H (9.62, 8.35, 6.49 and 4.97 units); and Cl—H, S—H, P—H (5.13, 4.02 and 3.10 units). In all three cases available the ratios of the corresponding force constants in the first and second series are within 3 % of 2.00. There is no indication of any marked change in bond type on passing from  $NH_3$  to  $CH_4$  as might have been expected since HF,  $H_2O$  and  $NH_3$  involve the heavy atom using *p*-orbitals, whereas in  $CH_4$  there is  $sp^3$  hybridisation. This suggests that in the series HF to  $CH_4$  there is a steady increase in hybridisation of the *s*-orbital with the *p*-orbitals in passing from HF to  $CH_4$ , there being complete  $sp^3$  hybridisation in  $CH_4$ . As against this the bond lengths in the series are: F—H, 0.917; O—H, 0.958; N—H, 1.01; and C—H,

<sup>21</sup> Dennison, *Rev. Mod. Physics*, 1940, 12, 175.

<sup>22</sup> Fox and Martin, *Proc. Roy. Soc., A*, 1937, 162, 419.

1.093 Å. Here there is a much bigger change between  $\text{NH}_3$  and  $\text{CH}_4$  (0.083) than between either HF and  $\text{H}_2\text{O}$  (0.04) or  $\text{H}_2\text{O}$  and  $\text{NH}_3$  (0.05).

**The B—H Bond.**—Using the frequencies 2523 and 2625  $\text{cm}^{-1}$  for a  $\text{BH}_2$  grouping<sup>23</sup> one finds that the B—H force constant to be 3.6 units. It is interesting that this constant continues the series F—H, O—H, N—H, C—H. The mean change for each step in this series is 1.55 units, and from the C—H to the B—H bond is 1.4 units.

### Summary.

The force constant for a number of C—H, N—H and similar bonds have been calculated. It has been found possible to give a normal value for a given bond force constant and in most cases to account, in a consistent manner, for deviations from the normal value.

*Inorganic Chemistry Laboratory,  
University Museum,  
Oxford.*

### GENERAL DISCUSSION \*

Dr. M. M. Davies (Leeds) said: I should like to ask Dr. Simpson whether she has attempted to use the rotational fine structure observed by Adel in the  $9.5\mu$  band to confirm the moments of inertia deduced from the electron diffraction results? This would provide an important experimental check for the  $127^\circ$  value of the apical angle and for the electron-diffraction structure as a whole, whose validity I feel is assumed to some considerable extent in Dr. Simpson's conclusions.

In Table II Dr. Simpson uses various criteria to compare the assignments which have been suggested: *i.e.* the equality between columns 6 and 7: between 8 and 9: and the agreement in column 11 with the electron diffraction value of the apical angle. But these are not independent criteria. Thus would it not be correct to say of the Penney-Sutherland assignment *either* that it is inconsistent to the extent of 25 %, *or* that it predicts an apical angle of  $164^\circ$ ? Apart from the electron-diffraction data, can the latter value be excluded?

Further, if one accepts Dr. Simpson's assignments, which certainly seem to give the best interpretation possible at present, there remains to be explained the abnormally large value of  $f = 15.98 \times 10^6$  dynes/cm., which is of the order normally observed for triple bonds and is much larger than the force constant in  $\text{O}_2$  itself (11.3). It is difficult to see how a conventional interpretation of the electronic structure VI could account for the observed dipole moment. Any *ad hoc* assumption about the moment between the tetravalent and divalent oxygen atoms seems merely to correspond to an indirect assumption of the contribution of such forms as III to the molecular structure. In such ionic structures as III would not the bonding force between the charged oxygens be raised above the double-bond value? Thus, a reasonable combination of the structures III and VI might well account both for the observed dipole moment and the large force constant.

Miss D. M. Simpson (Cambridge), in reply to Dr. Davies, said: The band at  $1043 \text{ cm}^{-1}$  as observed by Adel shows a very marked convergence of the rotational lines of the R branch while those of the P branch are spread out. It would be useless to attempt to analyse the fine structure unless both branches were free from interfering absorption. Even so this would not be easy, since the ozone molecule is an asymmetrical top. The most that I have been able to do is to show that the observed PR doublet

<sup>23</sup> Longuet-Higgins and Bell, *J.C.S.*, 1943, 250.

\* On the three preceding papers.

separation is in reasonable agreement with that calculated using moments of inertia derived from the electron diffraction data.

The three frequencies of a triatomic molecule may be used to calculate uniquely two force constants and the apical angle. The most acceptable assignment is that which provides sensible values for the force constants, and an apical angle in reasonable agreement with the experimental figure. The self-consistency of the force constants or of the right and left hand sides of equation (1), using the observed value of the angle, gives an alternative method of assessing the adequacy of an assignment.

Dr. Davies seems somewhat unhappy about the electron diffraction data. The published curves appear fairly convincing to a non-expert, and personally I feel that the proposed structure is not seriously at fault. Certainly it is justifiable to assume that the apical angle is greater than  $60^\circ$ , which means that  $\nu_1\nu_2$  should have a doublet contour, and  $\nu_3$  a Q branch. Only four of the possible twelve assignments give the correct contour relationships, those of Adel, Penney and Sutherland, the present interpretation and

$$\nu_1 = 1740 \text{ cm.}^{-1}, \quad \nu_2 = 710 \text{ cm.}^{-1}, \quad \nu_3 = 2105 \text{ cm.}^{-1}.$$

The latter gives a calculated value of  $116^\circ$  for the apical angle, but appears somewhat improbable, as it makes the very strong band at  $1043 \text{ cm.}^{-1}$  a combination frequency. If the electron diffraction data are considered unreliable, the information available at present is insufficient to decide which of these assignments is correct. Such information would be supplied by determinations of (i) the contour of the  $1740 \text{ cm.}^{-1}$  band and (ii) the variation with temperature of the intensities of the  $1043 \text{ cm.}^{-1}$  and  $710 \text{ cm.}^{-1}$  bands.

I do not feel that I can accept Dr. Davies' explanation of the abnormally large force constant of the O—O linkage. A force constant of this magnitude would be associated with a bond length of about  $1.17 \text{ \AA.}$ , and I find it difficult to believe that the electron diffraction value ( $1.26 \text{ \AA.}$ ) is in error to such an extent.

Dr. W. C. Price (*Billingham*) said: Miss Simpson's proposed frequency assignment for ozone implies that the two basal oxygen atoms are joined to apical oxygen by bonds of almost triple bond strength. This cannot be reconciled with any plausible electronic structure for the molecule. The only reasonable electronic structure for the above type of binding is the resonating single double bond structure occurring in sulphur dioxide and approximated to most closely by the force constants derived for the Penney-Sutherland frequency assignment. However, there is no such similarity between the electronic spectra of ozone and sulphur dioxide as is invariably found between other groups of molecules with related structure. As the acute angle structure seems also to have been eliminated we are left only with unsymmetrical linear or obtuse angle forms in which two atoms are joined by a triple bond and the third is attached by a weak bond of a type not encountered in the normal states of stable molecules. The analysis presented in the present paper certainly brings out the necessity of a re-examination of the electron diffraction and infra-red results on the ozone molecule.

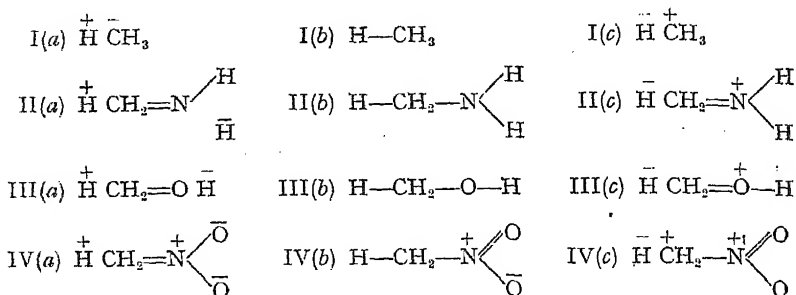
Mr. H. C. Longuet Higgins (*Oxford*) (*communicated*): Dr. Linnett has offered an explanation why some methane derivatives have C-H force constants smaller than methane, but has not accounted for the isolated case of nitromethane, whose C—H force constant is definitely larger than that of methane.

Three main types of resonance structure are possible in methane derivatives: type (a) in which the H atom bears a + charge, type (b) in which the C—H link is purely covalent, and type (c) in which the H atom bears a - charge.

Type (a) would be expected to be most important in nitromethane, whose pseudoacidic properties independently suggest a contribution from



IV(a), whereas IV(c) is excluded by Pauling's Adjacent Charge Rule. Type (c), on the other hand, would be expected to make most contribution in methylamine and methyl alcohol, where the (c) structures certainly have lower energies than the (a); this is supported by the small N—H and O—H force constants in these molecules. Methane will occupy an intermediate position.



So there are two possible interpretations of the facts: either we may suppose that (a) type structures *increase* the C—H force constant, as they contribute most to nitromethane, less to methane and hardly at all to methylamine; or that (c) type structures *decrease* the force constant, as they contribute least to nitromethane, more to methane and most to methylamine. Either of these interpretations is sufficient alone, but they are not mutually exclusive. Both interpretations may be expressed by saying that the C—H force constant increases with increasing electropositivity of the H relative to the C.

Hence one may put forward the following generalisation: "*The M—H force constant for a given element M (=C, N, O, S) and bond type, increases with increasing electropositivity of the H relative to the M in a series of molecules, and decreases with increasing electropositivity of the M relative to the H.*" This generalisation includes those established by Dr. Linnett for the

loosening one observes on passing from M—H to  $\overset{+}{\text{M}}-\text{H}$ .

Hitherto we have made no assumption about the direction of the C—H dipole, but if we suppose H to be electropositive to C as indicated by Pauling's electronegativity scale, then the mutual reduction of the opposed

$\text{CH}_3$  dipoles in ethane (due to the high energy of the state  $\overset{+}{\text{H}} \overset{-}{\text{C}} \text{H}_3-\overset{-}{\text{C}} \text{H}_3 \overset{+}{\text{H}}$ ) will lead to a decrease in electropositivity of the H relative to the C which explains the observed lowering of force constant in ethane.

Dr. M. M. Davies (Leeds) said: It may be worth emphasising that, as Dr. Linnett is probably well aware, the force constants in Tables I to VI can, at best, be regarded as accurate to the first decimal place. Besides the approximations involved in the simplified theory of the vibrations, it is frequently difficult to locate the origin of complex infra-red bands without high dispersion, whilst in Raman spectra a number of frequencies often occur in a narrow region and their exact assignment is uncertain. Thus even in the case of methane, where these practical difficulties are overcome, there remains a mean deviation of 0.07 units in the C—H force constant. One reason for this spread in the values is certainly that the anharmonicity factors have been ignored.

In the interpretation of the results, reference to the possibility of resonance with some appropriate electronic distribution is not always convincing. Such a solution is so generally available that, unless supported by independent evidence, it savours of a *deus ex machina*. An instance where it is probably justified is in accounting for the unusually high value of the acetylenic C—H force constant. The chemistry of these compounds

and the formation of their metallic derivatives indicates that the form  $\equiv\overset{+}{\text{C}}:\overset{+}{\text{H}}$  probably has an important part in their structure: the ionic bond would be expected to raise the restoring force in the C—H link above its normal covalent value.

For many other cases (not included amongst Dr. Linnett's molecules) differences of the order found cannot plausibly be explained by any electronic changes in the bond concerned. In a large number of hydroxylic compounds intramolecular interactions, which are independent of concentration and are equally pronounced in the gaseous state as in solution, give rise to changes in the O—H force constant. These differences are found between the isomeric forms of the same molecule: *ortho*-chlorophenol and benzoin might be mentioned as typical examples. In such cases, where the O—H force constant may change by 0.25 units or more, the changes are due to an interaction of a predominantly electrostatic (*i.e.* dipole) nature between the oscillator concerned (O—H) and an adjacent group in the same molecule. Such simple dipole effects might well account for some of the present results—*e.g.* the influence of a carbonyl group on an adjacent N—H bond.

Dr. J. W. Linnett (*Oxford*) said: I agree with Mr. Longuet-Higgins that the force constant of an M—H bond seems to depend on the charge distribution within the bond. Though the C—H bond in methane is the obvious standard to take, it probably does not have an even charge distribution and zero bond moment; and therefore other charge distributions must be related to this as standard. Mr. Longuet-Higgins' explanation of the high C—H force constant in nitromethane as being due to the carbon atom being more electronegative than that in methane seems to me to be a likely one. The modified explanation of the CH, NH and OH force constants in methylamine and methyl alcohol seems very possible. The interpretation of the ethane case is interesting, though it must be remembered that double-bonded formulæ involving hyper-conjugation have been suggested for this molecule from other evidence.

It is also true that the large positive charge on the hydrogen atom in acetylene, as indicated by the formation of acetylides, may be a contributing factor to the high force constant in acetylene in addition to the change in hybridisation. This point was raised by Dr. Davies.

With reference to Dr. Davies' remark on the accuracy of the values of the force constants, no conclusions have been drawn in the present paper from changes in force constant of less than 0.1 of a unit. I agree with Dr. Davies' that force constants can probably be affected by the steric effect of neighbouring groups. I think I have probably avoided in the present series cases where such an effect might interfere (*e.g.* *ortho*-substituted derivatives of benzene).

Dr. G. K. T. Conn (*Sheffield*) (*communicated*): The specific values of the force constants obtained by interpreting the dynamics of a molecule in terms of a particular potential field, particularly a drastically simplified field such as that used by both Dr. Kellner and Dr. Linnett, must always be treated with reserve. The influence of factors such as anharmonicity and Coriolis coupling is obvious, but the values obtained are always to some extent a function of the field used. Dr. Baber and I have been engaged recently in some calculations on formaldehyde and deuterio-formaldehyde which illustrate this. The most general harmonic function controlling the five planar frequencies of the  $\text{YZX}_3$  molecule contains nine force constants. We have obtained two sets of values: (a) for  $\text{H}_2\text{CO}$  and  $\text{D}_2\text{CO}$  using the observed frequencies, (b) using frequencies corrected for anharmonicity. The effect of this correction on the two important constants controlling stretching of the C=O and C—H bond is shown in Table I.

The difference between the values is appreciable being of the order of 8 %. Use of the Valence force field emphasises this. Since there are

only four constants, separate values may be obtained for  $\text{H}_2\text{CO}$  and  $\text{D}_2\text{CO}$ . Moreover the C—H constant can be calculated both for the parallel group

TABLE I.

	(d).	(b).
C=O	$12.7 \times 10^5$	$11.5 \times 10^5$ dynes/cm.
C—H	$3.7 \times 10^5$	$4.0 \times 10^5$ dynes/cm.

of three frequencies and the perpendicular group of two. The results, using the observed frequency values, are shown in Table II.

Miss Simpson and Dr. Sutherland (Cambridge) and Dr. Thompson (Oxford) (communicated): We have for some time been engaged in

TABLE II.

	$\text{H}_2\text{CO}$		$\text{D}_2\text{CO}$	
	Parallel.	Perpendicular.	Parallel.	Perpendicular.
C=O	$13.2 \times 10^5$	—	Imaginary	—
C—H	$4.0 \times 10^5$	4.3	Imaginary	4.7

the correlation and calculation of the frequencies of hydrocarbon molecules, and our results are not in agreement with those of Dr. Kellner. We would point out first that more experimental data have been published<sup>1-7</sup> than have

apparently been employed by Dr. Kellner, and the agreements between calculated and observed values are not so striking when these data are included. More important, however, is the fact that we have available much unpublished data on hydrocarbons, which make the disagreements still more marked. We have established correlations between the structure and the spectra of hydrocarbons and the characteristic frequencies of certain groupings are not reproduced by Dr. Kellner's treatment. On the other hand, application of the usual valency force field, which does not ignore angle deformation forces, as Dr. Kellner has done, gives good agreement with the experimental figures in many cases. We hope to publish at least some of these results in the near future.

<sup>1</sup> J. W. Linnett, *J.C.P.*, 1938, 6, 692.

<sup>2</sup> G. B. Bonino and R. Manzoni Ansidea, *Proc. Ind. Acad. Sci. A*, 1938, 8, 405.

<sup>3</sup> E. J. Rosenbaum, A. von Grosse and H. F. Jacobsen, *J.A.C.S.*, 1939, 61, 689.

<sup>4</sup> E. J. Rosenbaum, *J.C.P.*, 1941, 9, 295.

<sup>5</sup> E. J. Rosenbaum and H. F. Jacobsen, *J.A.C.S.*, 1941, 63, 2841.

<sup>6</sup> R. S. Rasmussen, *J.C.P.*, 1943, 11, 249.

<sup>7</sup> T. P. Wilson, *J.C.P.*, 1943, 11, 369.

## THE INFRA-RED SPECTRA OF FLUORINATED HYDROCARBONS. I.

By P. TORKINGTON AND H. W. THOMPSON.

Received, 22nd November, 1944.

The anomalous properties of fluorine as a member of the halogens are well known. A problem of current interest is the nature of carbon-fluorine links. Many partially or fully fluorinated hydrocarbons have been prepared in recent years, and it is remarkable to find that replacement of hydrogen by fluorine often leads to a large lowering of the boiling point. No satisfactory explanation of this at present exists. It has also been found that whilst compounds with a single fluorine atom attached to

carbon can be hydrolysed without great difficulty, the introduction of a second fluorine atom on the same carbon atom leads to far greater stability and resistance to hydrolysis.

The infra-red spectra of fluorinated hydrocarbons may provide another source of information about these compounds, either by giving values for the molecular vibration frequencies from which some idea can be obtained about the force constants of bonds; or by indicating with the simpler molecules the most satisfactory values for moments of inertia and bond lengths.

We have measured the infra-red absorption of a number of partially and fully fluorinated paraffins, olefines, naphthenes and aromatic hydrocarbons, as well as those of some related compounds containing long carbon chains, such as polyvinyl fluoride. This paper deals with fluorinated ethylenes and related compounds. Raman spectra of many fluorinated and mixed halogenated hydrocarbons have been recorded, and some have been correlated by Glockler.<sup>1</sup>

### Experimental Method.

The compounds examined were supplied by I.C.I. (General Chemicals) Ltd., and had been prepared as follows.

**Vinyl Fluoride.**—Ethylene dibromide was converted by treatment with alcoholic potash into vinyl bromide, from which 1.2.2 tribromo ethane was obtained by addition of bromine. Treatment with a mixture of antimony fluoride and antimony pentachloride led to 1.2 dibromo 2 fluoro ethane, which was then treated with zinc in alcohol. The product was distilled through a low temperature still, with B.Pt. — 70° C.

**Vinylidene Fluoride.**—Methyl chloroform was fluorinated by treatment with anhydrous hydrogen fluoride under pressure, forming 1 chloro 1.1 difluoro ethane, which was purified by distillation. Pyrolysis in a platinum tube at 750° C. gave vinylidene fluoride. Hydrogen chloride was removed by scrubbing through water, and after drying with calcium chloride, the product was distilled through a Podbielniak, with B.Pt. — 86° C.

**1.1 Fluorochloroethylene.**—1 fluoro 1.1 dichloro ethane was prepared by fluorination of methyl chloroform with hydrogen fluoride. This was pyrolysed at 750° C. and the product distilled through a Podbielniak, with B.Pt. — 25° to — 26° C.

**Tetrafluoroethylene.**—Chloroform was converted into chlorodifluoromethane by means of antimony pentachloride and antimony trifluoride, and the product was pyrolysed. The tetrafluoroethylene obtained was then distilled through a Podbielniak column, with B.Pt. — 78° C.

**1.1 Dichloro 2.2 difluoro Ethylene.**—This was obtained by removal of hydrogen chloride from 1.1 difluoro 1.2.2 trichloro ethane. B. Pt. 19° C.

The spectra were measured between 3-20 $\mu$ , using a Littrow spectrometer of high resolving power<sup>2</sup> for the region 6-14 $\mu$ , and an improved Hilger D 88 instrument with quartz (3.35 $\mu$ ), fluorite (3.7 $\mu$ ) or sylvine (14-20 $\mu$ ) prism. The absorption cell was 20 cm. in length and several pressures of vapour were used so as to bring out the features of particular absorption bands. The pressures used are shown on the diagrams as mm. mercury on each curve.

### Results and Discussion.

The spectral absorption curves are shown in Figs. 1-5. Raman data for 1.1 dichloro 2.2 difluoro ethylene have been given by Hatcher and Yost.<sup>3</sup>

<sup>1</sup> Glockler and Leader, *J. Chem. Physics*, 1940, 8, 699.

<sup>2</sup> Whiffen and Thompson, *J.C.S. (in press)*.

<sup>3</sup> *J. Chem. Physics*, 1937, 5, 992.

Unfortunately the Raman spectra of the fluorinated ethylenes could not yet be measured since they are gaseous at normal temperatures. Without these additional data, assignment of magnitudes to the fundamental vibrational modes is difficult, and we can be guided only by

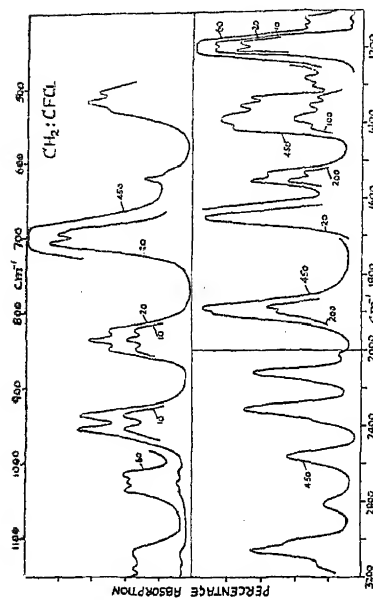


FIG. 3.—1,1 Fluoro Chloroethylene.

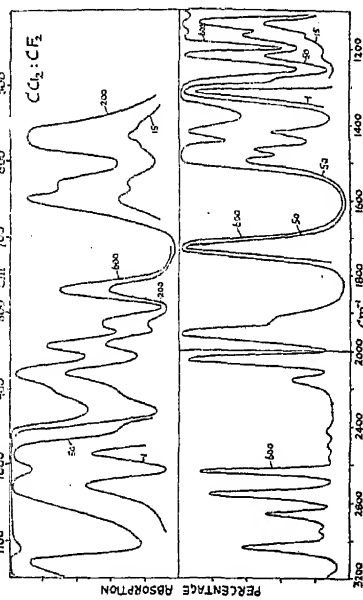


FIG. 4.—1,1 Dichloro 2,2 Difluoroethylene.

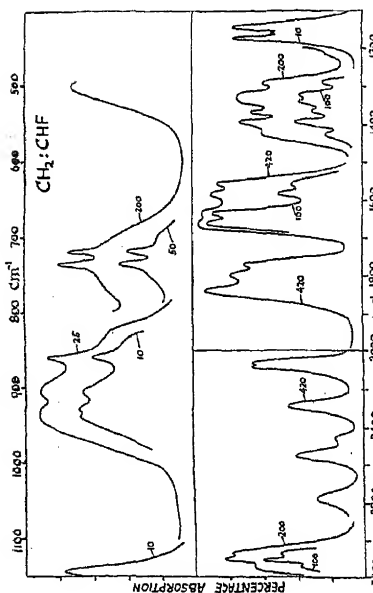


FIG. 1.—Vinyl Fluoride.

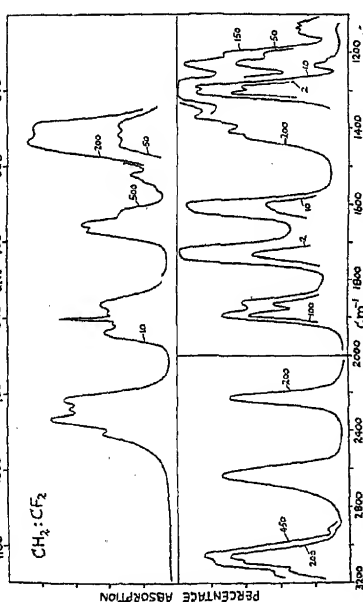


FIG. 2.—Vinylidene Fluoride.

(i) the correlation of band contours with plausible molecular dimensions, (ii) the intensities of bands, (iii) the application of selection rules where some symmetry exists, (iv) parallelism with related molecules, for example between vinyl fluoride and the other vinyl halides.

The bond lengths in some of these compounds have been determined by electron diffraction. Brockway<sup>4</sup> found that whereas the C—F link has a length close to 1.41 Å. in methyl fluoride and fluorochloromethanes containing only one fluorine atom, this bond shortens to 1.36 Å. if two or more fluorine atoms are attached to the central carbon atom. He also suggested that in these compounds the angle  $\text{Cl}-\hat{\text{C}}-\text{Cl}$  is rather greater than  $\text{F}-\hat{\text{C}}-\text{F}$ . Now on passing from chlorinated paraffins to the simple chlorinated olefines, the C—Cl bond appears to shorten by about 5 %. Thus in methyl chloride it is 1.76 Å., but in vinyl chloride and vinylidene chloride it is 1.69 Å.

If we assume that there is a similar effect on passing from the saturated to unsaturated fluorinated hydrocarbons, the C—F bond length in vinyl fluoride will be taken as about 1.36 Å. Assuming then for vinyl fluoride  $r_{\text{CH}} = 1.08$  Å.,  $r_{\text{CC}} = 1.34$  Å.,  $r_{\text{CF}} = 1.36$  Å., with  $\text{HCH} = 120^\circ$  and  $\text{H}-\hat{\text{C}}-\text{F} = 112^\circ$ ,  $\text{C}-\hat{\text{C}}-\text{F} = 124^\circ$ , the moments of inertia will be approximately 13, 80 and  $93 \times 10^{-40}$  g. cm.<sup>2</sup>. The molecule will therefore approximate to a symmetrical rotator, with least axis of inertia inclined at about  $30^\circ$  to the C=C bond. In Badger and Zumwalt's nomenclature,<sup>5</sup>  $\rho = 5.4$  and

$$S = -0.95,$$

and using that of Gerhard and Dennison<sup>6</sup>  $\beta = 5.6$ . The "parallel" type bands will have three sub-maxima, the outer pair about 27 cm.<sup>-1</sup> apart, with the central peak fairly weak. The "perpendicular" bands will have a strong central

peak flanked by shoulders. Some of the bands will be hybrid if the change of electric moment has components parallel to more than one of the principal axes of inertia. There are twelve normal modes, the general forms of which have been described elsewhere for the analogous case of vinyl chloride.<sup>7</sup> The contour of several of the absorption bands (Fig. 1) is striking. Thus, those at 715, 732 and 860 cm.<sup>-1</sup> are clearly perpendicular in type, and that at 1153 cm.<sup>-1</sup> has a parallel type contour. The band with sub-maxima at 910-926-937 appears to be a hybrid. It seems unlikely that any of these bands or that at about 500 cm.<sup>-1</sup> could be explained by any combination or difference. Six frequencies are thus fixed, to which will be added the three C—H stretching modes, two C—H deformations and the C=C stretching mode. The C—H stretching frequencies can be taken as  $\nu_{\text{CH}_2}^{\text{a}} = 3080$ ,  $\nu_{\text{CH}}^{\text{b}} = 3110$ , and  $\nu_{\text{CH}_2}^{\text{b}} = 3135$ ; that due to the stretching of the C=C bond as 1650 cm.<sup>-1</sup>, where there is a strong infra-red band with roughly parallel type contour and which is not interpretable as a combination. The other

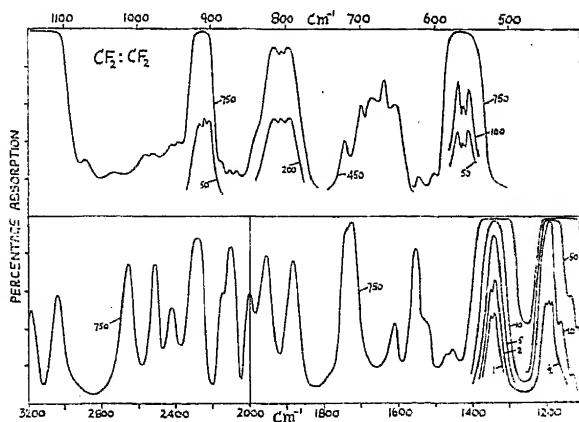


FIG. 5.—Tetrafluoroethylene.

<sup>4</sup> *J. Physics. Chem.*, 1937, 41, 747.

<sup>5</sup> *J. Chem. Physics*, 1938, 6, 711.

<sup>6</sup> *Physics. Rev.*, 1933, 43, 197.

<sup>7</sup> Thompson and Torkington, *Proc. Roy. Soc.*, in press; *J.C.S.*, 1944, 303.

<sup>8</sup> Kohlrausch, "The Raman Effect."

TABLE I.—VINYL FLUORIDE.

cm. <sup>-1</sup>	interpretation.	cm. <sup>-1</sup>	interpretation.
500	fundamental	1634	1650 } fundamental
715	fundamental	1664	
732	fundamental	1773	
860	fundamental	1800	
924	fundamental	1842	2 × 924
1140	1153 } fundamental	2066	2074 } 1153 + 924
1166		2083	
1220	500 + 715	2294	2 × 1153
1290	1306 } fundamental	2463	1153 + 1306
1323		2558	1393 + 1153
1340	1352 } (860 + 500)		1650 + 924
1363		2793	2 × 1393
	1393 } fundamental		1650 + 1153
	1425 } 2 × 715	3080	fundamental
		3110	fundamental
1560	1572 } 715 + 860	3135	fundamental
1585			

amount. Although in principle possible, it is unlikely that any overtone or combination could give rise to such intense absorption as that shown by the strong band at 1730 cm.<sup>-1</sup> with vinylidene fluoride. The only other possible value for this frequency would be 1600, another strong infra-red band. This is improbable; not only is 1600 adequately explained as the harmonic of 801, but also, none of the bands at higher frequencies can be explained as combinations involving 1600. Moreover, the value 1730 for the C=C stretching frequency falls into line with other results given below.

The assignment of the remaining frequencies of vinylidene fluoride is less obvious, but the most likely possibility is that the two C—F stretching frequencies lie at 921 and 1295 cm.<sup>-1</sup>. Both are very strongly absorbed, the latter being the most intense band found. 921 would be the symmetrical and 1295 the antisymmetrical mode. This assignment implies that the symmetrical CF<sub>2</sub> stretching mode has a band with the three branch contour, which would involve a change of electric moment parallel to the least axis, and this would have to lie along the C=C bond. If we assume for the molecular dimensions  $r_{\text{CO}} = 1.34$  Å.,  $r_{\text{CH}} = 1.08$  Å.,

$r_{\text{CF}} = 1.36$  Å., and  $\text{F}-\hat{\text{C}}-\text{F} = 116^\circ$ , the moments of inertia are 77, 89 and  $166 \times 10^{-40}$  g. cm.<sup>2</sup>, with the least axis at right angles to the double bond. Interchange of the least and middle axes could not be achieved by shortening the C=C bond, but only by a shortening of the C—F bonds, or diminution of the  $\text{F}-\hat{\text{C}}-\text{F}$  angle, or both. Since a large decrease in the angle is improbable, some shortening of the link must occur. It would be satisfactory if the  $\text{F}-\hat{\text{C}}-\text{F}$  angle were reduced to  $112^\circ$  and the C—F bonds shortened to about 1.30 Å.

The positions of the bands are given in Table II, with possible interpretations. From the contour found, we might associate 680 with a planar rocking mode, and 557 with the symmetrical deformation of the CF<sub>2</sub> group, but without the Raman data it is impossible to be more definite.

The spectrum of 1 fluoro 1 chloroethylene is shown in Fig. 3. Here most of the bands will be hybrids and the contours are not very helpful, but several facts emerge. Thus the band at 835 has a well-defined C type contour, and can be associated with the out-of-plane bending of the CH<sub>2</sub> group. This value falls into line with the data on related molecules as follows:

CH <sub>2</sub> : C Cl <sub>2</sub>	872
CH <sub>2</sub> : C ClF	835
CH <sub>2</sub> : CF <sub>2</sub>	801



Here again, therefore, introduction of fluorine leads to a drop in the bending frequency of the other end of the molecule. The very intense band at  $1189\text{ cm.}^{-1}$  is attributed to the C—F stretching mode, corresponding to

TABLE II.—VINYLIDENE FLUORIDE.

cm. <sup>-1</sup>	interpretation.	cm. <sup>-1</sup>	interpretation.
544	559 ? fundamental (A)	1203	1295 fundamental (B)
559		1230	
569		1285	
612		1305	
662	(C)	1370	
677	680 ? fundamental (B)	1403	
685		1420	
780		1600	2 × 801
795	801 fundamental (C)	1730	fundamental
801		1862	945 + 921
808		1894	2 × 945
820		2227	1295 + 921
910	1295 + 945		
921	1730 + 921		
935	fundamental 921 (A)	2632	
954	? fundamental 945 (B)	2920	
1122	1133 fundamental (A)	3055	fundamental
1133		3085	
1143		3140	fundamental

$1153$  in vinyl fluoride. The hybrid band at  $693$  may be due to the C—Cl stretching vibration, corresponding to  $724$  in vinyl chloride. The C=C

TABLE III.—FLUORO-CHLORO-ETHYLENE.

cm. <sup>-1</sup>	cm. <sup>-1</sup>	cm. <sup>-1</sup>	
501	1119	1645	stretching frequency occurs at $1645\text{ cm.}^{-1}$ , corresponding to $1650$ in vinyl fluoride and $1610$ in vinyl chloride. This again confirms that introduction of fluorine for hydrogen causes an increase in the C=C stretching frequency, but the effect is not so big with a single fluorine atom attached to carbon as it is with two. The band at $516\text{ cm.}^{-1}$ may be connected with the deformation of the C—F bond, and that at $945$ ( $937$ - $953$ ) with a planar $\text{CH}_2$ rocking mode found at $925$ with vinyl fluoride
516	1140	1883	
530	1180	1898	
621	1198 } 1189	2020	
693	1280	2120	
707	1297	2310	
823	1328	2565	
835	1347	2825	
850	1383	3015	
937	1405	3055	
953	1529	3140	
1015	1548		
1025			
1037			

and  $1030$  in vinyl chloride. The symmetrical and antisymmetrical stretching frequencies of the  $\text{CH}_2$  group are probably  $3055$  and  $3140\text{ cm.}^{-1}$ . Further assignments are at present impossible, but the positions of the bands are given in Table III.

The spectrum of 1, 1 difluoro 2, 2 dichloro ethylene is shown in Fig. 4. Hatcher and Yost<sup>3</sup> found the following Raman displacements:  $255$  (6),  $435$  (7),  $454$  (1),  $562$  (6),  $622$  (4),  $648$  (2),  $883$  ( $\frac{1}{2}$ ),  $1027$  (2),  $1123$  (1),  $1735$  (6),

1976 ( $\frac{1}{2}$ ). The twelve vibrations of this molecule fall into four groups; eleven vibrations are permitted in the infra-red as fundamentals, and five should be polarised in the Raman spectrum. The five polarised Raman frequencies will be associated with the symmetrical stretching of  $\text{CF}_2$  and  $\text{CCl}_2$  groups, the symmetrical deformations of these groups, and the stretching of the carbon-carbon double bond. There are five strong Raman lines at 255, 435, 562, 622 and 1735. These cannot, however, be the five polarised fundamentals, since we shall take 1735 as the  $\text{C}=\text{C}$  stretching mode, and the  $\text{C}-\text{F}$  stretching frequency must exceed 622. Mere intensity is therefore not a guide to polarisation in the Raman effect. 255 can be confidently assigned to the symmetrical deformation of the  $\text{CCl}_2$  group, which has a value 295 in vinylidene chloride. As regards the strong Raman interval 1725, corresponding to the strong infra-red band at 1730  $\text{cm}^{-1}$ , this must be assigned to the  $\text{C}=\text{C}$  stretching frequency. Apart from the correspondence between the two spectra here, there is no other infra-red band between 1500-1900  $\text{cm}^{-1}$  which could be assigned to this vibration. We find again therefore, as with vinylidene fluoride, that when two fluorine atoms are attached to the double bond, its stretching frequency is markedly increased. Other coincidences between Raman and infra-red data are 562/570, 622/630, 648/650, 883/881, 1027/1028, 1123/1130. The most satisfactory interpretation is to allocate 622 to the symmetrical  $\text{CCl}_2$  stretching mode, 435 to the symmetrical  $\text{CF}_2$  deformation, both being strong in the Raman effect. The outstandingly intense infra-red bands lie at 1315, 990 and 1028  $\text{cm}^{-1}$ . Of these 1028 and 1315 are assigned to the symmetrical and antisymmetrical stretching modes of the  $\text{CF}_2$  group.

It will be noticed that the former is comparatively weak in the Raman spectrum, and this seems to be true for  $\text{C}-\text{F}$  bonds in other monofluoro derivatives. In vinylidene fluoride the two  $\text{CF}_2$  group stretching frequencies were taken as 921, 1295. The infra-red band at 570, corresponding to the strong Raman displacement of 562, appears to have a marked central Q branch, which may indicate that it is an out-of-plane bending motion of the  $\text{CF}_2$  group. The infra-red band at 881 may be due to the

TABLE IV.

1.1. DICHLORO 2.2 DIFLUORO ETHYLENE.

Cm. <sup>-1</sup> .		Interpretation.
Raman.	Infra-red.	
255		fundamental
435		fundamental
454		fundamental
562	570	fundamental
622	630	fundamental
648	650	fundamental
	770	1028-255
	814	
	841	
883	880	fundamental
	906	(2 × 454), (650 + 255)
	950	
	990	570 + 435
1027	1028	fundamental
1123	1130	(2 × 570), (880 + 255)
	1170	
	1220	570 + 650
	1285	(630 + 650), (1028 + 255)
	1315	fundamental
	1423	
	1470	1730 - 255.
	1500	883 + 620
1735	1730	fundamental
	1920	1028 + 880
	1955	{ 1315 + 680
1976		{ 1730 + 255
	2050	2 × 1028
	2160	1730 + 435
	2430	
	2490	
	2570	
	2640	2 × 1315
	2760	1760 + 1028
	2860	
	2950	
	3040	1730 + 1315

antisymmetrical  $\text{CCl}_2$  stretching mode, which lies at 794 with vinylidene chloride.

On this basis most of the combinations and overtones can be interpreted as in Table IV. The two missing fundamentals are the twisting mode and a planar rocking mode, and values cannot be determined for these. If

TABLE V.—TETRAFLUOROETHYLENE.

$\text{cm.}^{-1}$	type of contour.	$\text{cm.}^{-1}$	type of contour.
552	559 A	1070	1186 fundamental A
559		1125	
567		1157	
600	? C	1179	1340 fundamental B
620	? C	1186	
655	666 C	1195	
666		1335	1340 fundamental B
676		1344	
697	? C	1459	
720	? C	1521	1550
799	807 A	1550	
807		1607	
815		1724	1880
868	876 A	1880	
876		1952	
886		2000	2100
903	910 A	2100	
910		2140	
918		2280	2420
949	952 B	2420	
956		2510	
981	985 B	2655	3040
990		3040	
1035		3185	

they were taken as 300 and 400 respectively, other combinations could be explained, but there are insufficient data to justify this.

The spectrum of tetrafluoroethylene is particularly interesting, not only in connection with C—F links, but also because of the difficulty of analysing the corresponding data with ethylene and tetra-deuteroethylene. Unfortunately only five of the twelve fundamentals are permitted to appear in the infra-red spectrum, and no first overtones are allowed, so that in the absence of Raman data there is little hope of fixing many of the fundamentals at present. It may, however, be possible from the values of a few of these to use

a normal co-ordinate treatment from which rough values of the others can be inferred. The spectral curves are shown in Fig. 5 and the bands are listed in Table V. The fundamentals fall into groups like those of ethylene. In the infra-red the following will be allowed:

- $B_{2u}$  C—F stretching  
 $\text{CF}_2$  deformation  
 Change of electric moment parallel to C=C bond
- $B_{2u}$  C—F stretching  
 $\text{CF}_2$  rocking  
 Change of electric moment perpendicular to C=C bond
- $B_{1u}$   $\text{CF}_2$  bending  
 Change of electric moment perpendicular to plane of molecule.

Assuming for the molecular dimensions  $r_{\text{CH}} = 1.06 \text{ \AA.}$ ,  $r_{\text{CC}} = 1.34 \text{ \AA.}$ ,

$r_{\text{CF}} = 1.30 \text{ \AA.}$ ,  $\text{F}-\hat{\text{C}}-\text{F} = 112^\circ$ , the moments of inertia are about 146, 259 and  $405 \times 10^{-40}$ , and the molecule is an asymmetrical rotator with least axis along the double bond and major axis perpendicular to the molecular plane. In Badger and Zumwalt's terminology, the  $B_{2u}$  vibrations will have *A* contour, the  $B_{2u}$  will have *B* contour and the  $B_{1u}$  band *C* contour. The *A* contour will be three sub-maxima with outer spacing about 16  $\text{cm.}^{-1}$ , the *B* contour a pair of maxima 9-10  $\text{cm.}^{-1}$  apart, and the *C* bands will have a central peak with side branches 18-20  $\text{cm.}^{-1}$  apart.

The bands observed can be seen to fall very well into the three classes expected, and the spacings of the sub-maxima agree roughly with those calculated. The assignment of fundamentals is not, however, clear

The C—F stretching modes will have the highest frequencies, and should not exceed say  $1400\text{ cm}^{-1}$ . There are at least five *A* type bands below this value, three *B* bands and several *C* bands. The allowed fundamental bands will include two *A* bands, two *B* and one *C* band. Perhaps the best guide is that the bands at  $1186$  and  $1340\text{ cm}^{-1}$  are extremely intense and far stronger than any other bands in the spectrum. Although intensity alone is no certain indication of a fundamental, it seems certain that  $1186$ , an *A* band, is the  $B_{3u}$  C—F stretching frequency; and  $1340$ , a *B* band, the  $B_{2u}$  C—F stretching fundamental. No other fundamental can be definitely fixed, although  $559$  may be the  $B_{3u}$   $\text{CF}_2$  deformational mode. The C=C stretching mode will be inactive either as fundamental or overtone, and the band at  $1724$  must arise from a combination. On the other hand several of the bands above  $1800\text{ cm}^{-1}$  can be explained as combinations with a frequency of about  $1730$  rather than with a lower magnitude. Before any further progress can be made it will be necessary to have Raman data from which some of the low frequencies can be obtained.

In spite of the incomplete assignments, several points emerge from the comparison of these compounds. Most striking is the increase of the C=C stretching frequency when two fluorine atoms are attached to the carbon atom. Thus:

$\text{CH}_2 : \text{CH}_2$	1626	$\text{CH}_2 : \text{CF}_2$	1730
$\text{CH}_2 : \text{CHCl}$	1610	$\text{CCl}_2 : \text{CF}_2$	1730
$\text{CH}_2 : \text{CHF}$	1650	$\text{CF}_2 : \text{CF}_2$	? 1730
$\text{CH}_2 : \text{CFCl}$	1645		
$\text{CH}_2 : \text{CCl}_2$	1620		

The decrease in the out-of-plane bending frequency of the  $\text{CH}_2$  group when fluorine is attached to an adjacent carbon atom may also be relevant in this connection, for this must arise from some effect transmitted through the double bond. It is also interesting that the rotational contour of some of the bands is better explained if there is some shortening of the C—F links.

The other striking feature is that bands connected with C—F stretching vibrations are very strong in the infra-red. As pointed out above, these vibrations do not seem to be so strongly excited in the Raman effect as the symmetry and selection rules might lead us to expect. More significant is the result that with compounds containing the  $\text{CF}_2$  group the pair of C—F stretching frequencies are at least several times more intense in the infra-red than the C—F band of compounds containing the CF link. The intensity of these infra-red bands is connected with the rate of change of electric moment during the vibration. It would therefore appear that compression or extension of C—F bonds leads to an unusually large change of electric moment, particularly with compounds containing the  $\text{CF}_2$  group. Similar results have been found with other fluorinated hydrocarbons to be discussed later.

### Summary.

The infra-red spectra of vinyl fluoride, vinylidene fluoride, 1 chloro 1 fluoro ethylene, 1, 1 dichloro 2, 2 difluoro ethylene, and tetrafluoro ethylene have been measured. The band contours have been correlated with the molecular structure, and attempts have been made to assign magnitudes to the normal vibration frequencies. Peculiarities have been noticed in these spectra, particularly with compounds containing the  $\text{CF}_2$  group, which seem to be connected with changes in electronic structure consequent upon the introduction of fluorine atoms.

Our thanks are due to I.C.I. (General Chemicals) Ltd. for the fluorinated hydrocarbons, and to the Government Grant Committee of the Royal Society for a grant in aid of apparatus.

*The Physical Chemistry Laboratory,  
Oxford.*

## GENERAL DISCUSSION.

Dr. W. G. Price (*Billingham*) said: I should like to put forward a suggestion that a considerable reduction in the resonance effect between the halogen and the ethylenic bond accompanied by an increase in the oppositely directed inductive effect is the cause of the differences which are found between the fluorine and the other halogen substituted ethylenes. The extent of the resonance effect depends on the smallness of the difference between the energies of the states  $H_2C=CH\ddot{X}$  and  $H_2\ddot{C}-CH=\ddot{X}^+$ . The variation in this difference from halogen to halogen depends largely on the difference between the ionisation potentials of the lone pair halogen

electrons and the double bond orbital of  $C=\ddot{X}^+$ . Now the ionisation potentials of the lone pair electrons are roughly 9, 10 and 11 volts for I, Br and Cl respectively.<sup>1</sup> For fluorine no accurate data are available but it is doubtful if it is less than 16 volts. The ionisation potential associated with a carbon-halogen double bond probably only suffers half this increase because of sharing with the carbon atom. Thus it probably requires considerably more energy to lift the fluorine lone pair into the carbon-halogen double bond than is required for the other halogens. The consequent reduction in resonance effect accompanied by an increase in inductive effect due to the greater electronegativity of fluorine results in a smaller electron density in the neighbourhood of the far carbon atom with corresponding lowering of CH valence and deformation frequencies as indicated in the article by J. W. Linnett (This symposium).

Dr. Thompson said: I think that the interpretations suggested by Dr. Price for some of the peculiarities found with the fluorinated ethylenes are essentially sound. As regards the intensity of the bands, it is important to remember that this is determined not so much by the actual molecular electric moment as by the rate at which this moment changes.

I may draw attention to one interesting correlation of the data on fluoroethylenes with the force constants calculated by Dr. Linnett in the earlier paper. He found a diminution in the force constants of C—H bonds when fluorine is attached to carbon. This falls into line with the decrease found in some of the frequencies of bending of C—H bonds in the fluoroethylenes.

<sup>1</sup> R. S. Mulliken, *J. Chem. Physics*, 1935 onwards.

## THE INFRA-RED SPECTRA OF COMPOUNDS OF HIGH MOLECULAR WEIGHT.

By H. W. THOMPSON AND P. TORKINGTON.

*Received 22nd November, 1944.*

Many methods are at present being used to explore the reasons for the differences in physical behaviour of various types of polymers, plastics, rubbers and other compounds of high molecular weight. The peculiar rheological and electrical properties of many of these substances must be connected with the internal molecular structure and with the way in which the molecules can pack together in the solid and liquid states. Valuable information has already been obtained using the diffraction of X-rays, and some chemical methods have also given useful indications of the nature of the polymerisation processes. The determination of

molecular weights and chain lengths of fibre-like polymers has also led to important correlations. No method, however, has provided all the information which might enable us to formulate rules correlating properties with structure.

It is clear that any method will have advantages which can examine the sample without the use of chemical reagents, and from this standpoint spectroscopy should be useful. The infra-red absorption spectra of substances of this type consist essentially of bands which correspond to the absorption of characteristic vibration frequencies of the whole molecule, or of particular units within it. Since, theoretically, no two molecules having a different nuclear skeleton have the same set of vibrational frequencies, we may expect small differences between the spectra of closely related molecules, and a careful analysis of the vibrational spectra may reveal the occurrence of special groups, or the arrangement of the nuclear skeleton within these molecules. For this analysis reference data from the spectra of simple related molecules may first be required. Apart from giving such fundamental structural information, however, the infra-red spectra can be used empirically for many practical purposes. Small differences in the properties of samples of the same polymer can sometimes be correlated empirically with small differences in their spectra. The effect of different plasticizing or vulcanizing agents, leading for instance to cross-linking, can also be explored by spectral changes. On the fundamental side too, it is valuable from the standpoint of molecular dynamics to assemble data on long chain polymeric substances as a basis for the calculation of the vibration frequencies of these molecules as systems of weighted chains. If the molecular dynamics could be understood more completely, it might prove a useful adjunct to the consideration of thermodynamic properties.

We have recently surveyed the infra-red spectra of many compounds of high molecular weight belonging to different classes, partly to develop the experimental methods for examining these substances, but also to discover the type of information which can be obtained, and the most profitable lines for a more systematic attack. Papers describing some of the work are at present in the press,<sup>1</sup> and other detailed accounts will shortly be published. This article summarises typical measurements and results on a variety of compounds and is intended to illustrate the broad principles of this spectroscopic approach.<sup>2</sup>

Most compounds of this type are usually examined in the solid state. Some can be obtained as thin films by rolling or cutting; these are measured as such. In order to bring out all the features of the spectrum several thicknesses of a given substance are desirable. The optimum thickness for different types of substance varies considerably. With essentially non-polar materials it may vary from 0.1 mm. to several mm., but with other substances it may be necessary to have films thinner than 0.005 mm. Coherent films of many substances can be conveniently made by the evaporation of solutions from the surface of water or mercury, or from a heated glass plate, although in some cases it is difficult to remove the solvent completely. With other compounds it may be more satisfactory, and it is sometimes essential, to evaporate solutions on a hot rock salt or bromide plate, leaving an irregular solid layer; this method is suitable for the study of very thin layers of incoherent materials. Liquids are measured in a cell of the conventional type, and molten solids using a cell of the kind described in a previous paper.<sup>3</sup> Some solid powders

<sup>1</sup> Parts I and II, *Proc. Roy. Soc. in the press*; see also J.C.S., 1944.

<sup>2</sup> See also Sears, *J. Appl. Physics*, 1941, 12, 35. Stair and Coblenz, *J. Res. Nat. Bur. Stand.*, 1935, 15, 295. Williams, *Physics*, 1936, 7, 399. Wells, *J. Appl. Physics*, 1940, 11, 137. Barnes, Liddel and Williams, *Ind. Eng. Chem. Anal. Ed.*, 1943 15, 83.

<sup>3</sup> R. E. Richards (*preceding paper*).

have been studied by spreading them between rock salt plates moistened with carbon tetrachloride or a high boiling paraffin.

One important group of compounds is the class of hydrocarbon-type polymers, parts of the spectra of some of which are shown in Fig. 1. For some time it was thought that the polymerisation of ethylene to form "polythene" gave a product having an uninterrupted straight chain of methylene groups. The infra-red bands of polythene in the region of  $3\mu$ , where frequencies corresponding to the stretching vibrations of C—H linkages are absorbed, led Fox and Martin<sup>4</sup> to suggest that some methyl groups must be present. Polythene has relatively few absorption bands

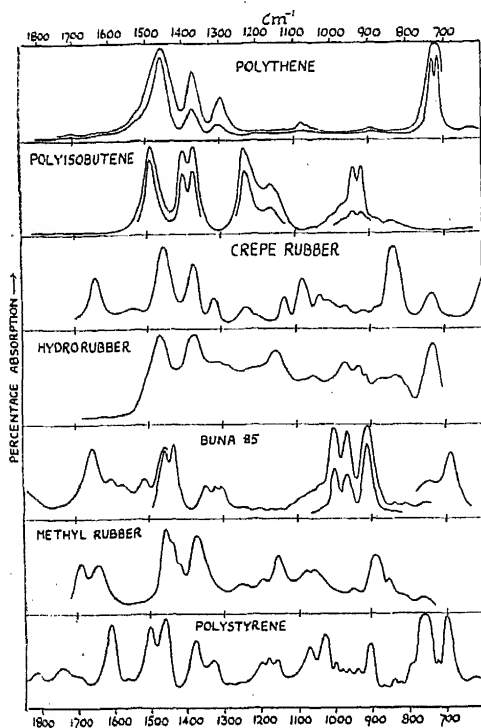


FIG. 1.

between  $3\text{--}20\mu$ . Reference to the spectra of paraffinic hydrocarbons enables us to identify most of the vibrations. Thus the band at  $1460\text{ cm}^{-1}$  is connected with deformational motions of the methylene ( $\text{CH}_2$ ) groups, and that at  $725\text{ cm}^{-1}$  with a vibration of the long carbon-carbon chain. The band at  $1375\text{ cm}^{-1}$  lies at the position characteristic of the symmetrical deformation of a methyl group, and this provides independent confirmation of Fox and Martin's earlier conclusion. By careful measurement of the optical densities and calibration of this methyl group band in branched chain paraffins, an estimate of the content of methyl groups can be made, and is found to be roughly one methyl group per fifty methylene groups. The feebler bands in the spectrum of polythene are less easily explained. One interesting feature how-

ever is the weak absorption at about  $1720\text{ cm}^{-1}$ , indicating  $>\text{CO}$  groups. These could arise if oxygen were taken up during the catalytic polymerisation; their presence at intervals along the carbon-carbon chain may markedly affect the electrical properties of the substance. On the other hand it is possible using ether or xylene to extract from polythene samples of lower molecular weight which may be rich in the ketonic material, and there is obviously scope for further work on this.

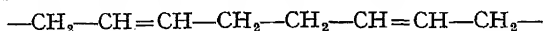
Polyisobutene also has a simple spectrum. The band at about  $1485\text{ cm}^{-1}$  is connected with the deformational vibration of methylene groups, but it lies at a rather higher frequency than is usually found with paraffins ( $1460\text{ cm}^{-1}$ ). The symmetrical deformation of the methyl groups appears to be double ( $1370\text{--}1400\text{ cm}^{-1}$ ) and there is no obvious explanation for this, although it seems to occur with many paraffins having a pair of methyl radicals attached to the same carbon atom. The bands of polyisobutene near  $1200\text{ cm}^{-1}$  and  $950\text{ cm}^{-1}$  are almost certainly

<sup>4</sup> *Proc. Roy. Soc., A*, 1940, **175**, 208.

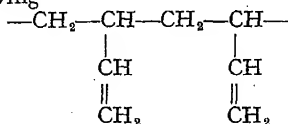
due to vibrations of the distorted carbon tetrahedron  $\begin{array}{c} \text{C} \\ | \\ -\text{C}-\text{C}-\text{C}- \\ | \\ \text{C} \end{array}$  present

in the chain, and whilst exact calculations cannot yet be made, comparison with values for the vibration frequencies of such systems of C—C links suggests that there may be a slight weakening of the bonds in polyisobutene. The packing of methyl groups is known to be difficult in this case, and might well lead to strain and weakening of the carbon-carbon bonds.

The spectrum of a sample of Buna 85 made by the sodium-catalysed polymerisation of 1,3 butadiene is also shown in Fig. 1. This polymerisation can proceed by either 1,4 addition giving



or by 1,2 addition, giving



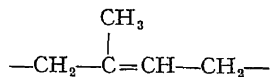
or by a combination of these processes. There are important structural differences in the two types of condensate. Thus, the former contains a recurring skeleton of the type  $\text{R}_1\text{CH}=\text{CH} \cdot \text{R}_2$  and the latter of the type  $\text{R} \cdot \text{CH}=\text{CH}_2$ . From measurements on the infra-red spectra of some simple olefines<sup>1</sup> we recently found a rule for differentiating between compounds of the type

- (i).  $\text{R} \cdot \text{CH}=\text{CH}_2$ ;                      (ii)  $\text{R}_1\text{CH}=\text{CH} \text{R}_2$ ;                      (iii)  $\text{R}_1\text{R}_2\text{C}=\text{CH}_2$

in which R is an alkyl radical. Compounds of class (i) have two intense bands at about 909 and 990  $\text{cm}^{-1}$ , those of class (ii) have a strong band at about 965  $\text{cm}^{-1}$  and those of class (iii); a similar band at about 890  $\text{cm}^{-1}$ . Compounds of the type  $\text{R}_1\text{R}_2\text{C}=\text{CHR}_3$  were found to have a band at about 840  $\text{cm}^{-1}$ , though few compounds of this type have been examined. These characteristic frequencies are associated with deformational modes of C—H bonds attached to the C=C bond. The correlations were used originally in connection with the spectra of cracked polythenes, where the appearance of compounds of the isobutylene class (iii) provide further evidence for the occurrence of side chain alkyl groups. Since this work was done, Rasmussen and Brattain have reached similar conclusions from measurements on a much larger series of olefinic hydrocarbons.<sup>2</sup>

The spectrum of Buna 85 shows intense bands at 909, 965 and 990  $\text{cm}^{-1}$  indicating that both 1,2 and 1,4 addition has occurred, and estimates can be made of the relative extent of each type. There is also the characteristic vibration frequency of the C=C bond at about 1650  $\text{cm}^{-1}$ . The pair of bands at 1435 and 1460  $\text{cm}^{-1}$  is probably connected with two slightly differing  $\text{CH}_2$  deformations, such as might occur from the types  $-\text{CH}_2-$  and  $=\text{CH}_2$ . The pendent vinyl groups revealed by bands at 909, 990  $\text{cm}^{-1}$  may be expected to disappear if subsequent treatment leads to the formation of cross linkages.

Crepe rubber, which consists essentially of a recurring skeleton



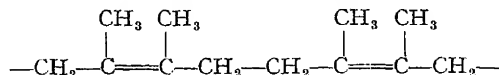
shows the infra-red bands to be expected. Thus, there is that due to the C=C oscillation at 1645  $\text{cm}^{-1}$ , the  $\text{CH}_2$  deformational mode at 1460  $\text{cm}^{-1}$

<sup>2</sup> (Private communication.)

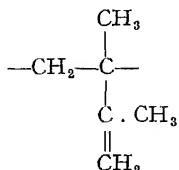


and the  $\text{CH}_2$  deformation at  $1375 \text{ cm.}^{-1}$ . The band at  $840 \text{ cm.}^{-1}$  corresponds to a tri-alkyl olefine as explained above. Crepe rubber also has a band near  $600 \text{ cm.}^{-1}$ , and this spectral region is of interest with treated or vulcanized rubbers. In hydro-rubber the  $\text{C}=\text{C}$  oscillation has disappeared, and the band at  $735 \text{ cm.}^{-1}$  is similar to those found with some simple paraffins with a methyl group attached along the chain.

Two samples of methyl rubber have been examined, made respectively by the slow polymerisation of 2,3 dimethyl butadiene in sunlight and by sodium. The curve of Fig. 1 relates to the former, although no definite difference could be established between the two products. Here again, polymerisation could proceed by 1,4 addition, giving

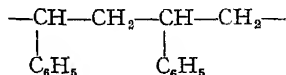


or by 1,2 addition giving

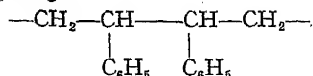


or by a combination of both. The infra-red spectrum suggests the occurrence of both types of condensation. Thus the band at  $890 \text{ cm.}^{-1}$  indicates that the isobutylene structure resulting from 1,2 addition, and as with Buna 85 the composite nature of the absorption at  $1440\text{--}1460$  suggests that two kinds of  $\text{CH}_2$  deformation occur, presumably from the  $\text{—CH}_2\text{—}$  and  $=\text{CH}_2$  groups. There is no characteristic band of the tetra-alkyl olefine type  $\text{R}_1\text{R}_2\text{C}=\text{CR}_3\text{R}_4$ , but the pair of bands at  $1645$ ,  $1690 \text{ cm.}^{-1}$  would agree with the presence of two types of  $\text{C}=\text{C}$  link. Compounds of the type  $\text{R}_1\text{R}_2\text{C}=\text{CH}_2$  would have absorption at about  $1645 \text{ cm.}^{-1}$ , and although no infra-red data are available for comparison, the Raman frequencies of alkyl olefines<sup>6</sup> suggest that with tri- or tetra-alkyl derivatives the  $\text{C}=\text{C}$  bond frequency lies higher at  $1680\text{--}1690 \text{ cm.}^{-1}$ . The methyl group deformation again appears intense at  $1375 \text{ cm.}^{-1}$ .

Many of the bands in the spectrum of polystyrene are common to simple aromatic hydrocarbons with one alkyl side chain. The intense absorption at about  $760 \text{ cm.}^{-1}$  is similar to that found with isopropyl benzene. Substantially, the spectrum would agree with a simple head to tail condensation giving



Insufficient data are yet available to decide whether some head to head condensation occurs, giving



Polystyrene has a band at  $1380 \text{ cm.}^{-1}$ , however, which might indicate the presence of methyl groups, formed by inclusion in the chain of the

grouping  $\begin{array}{c} \text{CH}_3 \\ | \\ \text{—C—} \\ | \\ \text{C}_6\text{H}_5 \end{array}$ . This cannot, however, be regarded as proved, since

<sup>6</sup> Hibben, "The Raman Effect."

the band in question may be due to a combination or overtone frequency.

In Fig. 2 the spectra of several monomers related to the above polymers are shown. The important practical result is that the spectrum of a polymer always shows marked differences from that of its monomer, and this often provides an easy means for following the rate of a polymerisation process, or for the determination of small amounts of residual monomer in the polymer.

Another immediate problem is whether the lengthening of a long chain polymeric system produces changes in the spectrum, from which an estimate of the chain length can be made. This does not seem very promising. Samples of polyisobutene having mean molecular weights between 1000 and 100,000 showed no significant change in the spectrum. Indeed the spectra of lower normal paraffins suggest that when there are more than about ten carbon atoms in the chain the spectral differences are very slight. Some differences found in the spectra of polythenes with molecular weights 1000-13,000 appear to have arisen from the presence of varying amounts of substances other than the polythene chain itself. Fig. 2 includes the spectra of samples of squalene (I) and dihydromyrcene (II) which seemed interesting in this connection as being closely analogous to a 6-unit and 2-unit rubber, respectively.

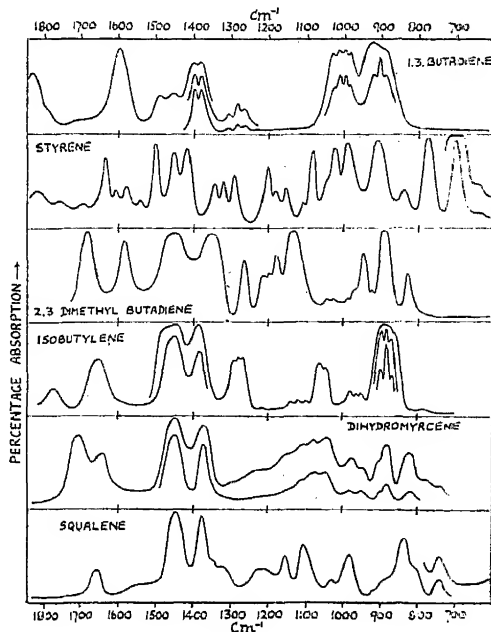
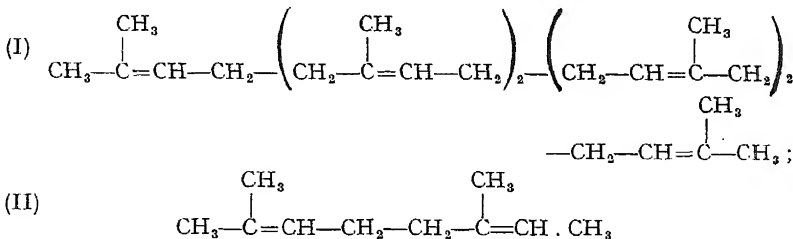


FIG. 2.



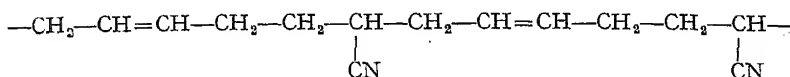
There are some marked similarities between the spectrum of squalene and that of crepe rubber, but several important differences. The band with squalene at  $982\text{ cm}^{-1}$  is not easily explained and until the purity of the squalene can be established a more detailed consideration is unjustified; it may be noted, however, that some trimethyl ethylenes<sup>7</sup> have a band

<sup>7</sup> G. P. Harris, *unpublished data*; see also Barnes, Liddel and Williams, *Ind. Eng. Chem. Anal. Ed.* 1943, **15**, 659.

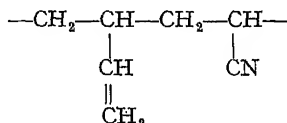
at about  $980\text{ cm.}^{-1}$ , and this may therefore arise from the end groups in squalene.

There is no doubt that the sample of dihydromyrcene examined had become oxidised, as revealed by the band at about  $1720\text{ cm.}^{-1}$ , and the broad background absorption in the region of  $1100\text{ cm.}^{-1}$ . This latter region of absorption has been found with oxidised polythenes and oxidised rubbers and will be considered later in connection with the spectra of esters, ketones, aldehydes and other oxygenated compounds.

The method described above for determining the proportions of 1.2 or 1.4 addition in the polymerisation of butadiene or alkyl butadienes can be applied to other processes to determine the mechanism of interpolymerisation. Thus, when butadiene is condensed with acrylonitrile, straight chains might be formed of the type

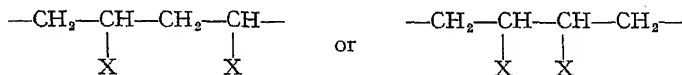


which will have the intense band at  $965\text{ cm.}^{-1}$ , or pendant vinyl groups may remain, as in the structure



giving rise to the bands at  $909, 990\text{ cm.}^{-1}$ . In a previous paper<sup>8</sup> we have described a sample of Perbunan in which the bulk of the condensation had proceeded by 1.4 addition, but in other samples of butadiene-acrylonitrile interpolymer variations seem to occur. Exactly similar considerations can be applied to Buna S, the interpolymer between butadiene and styrene. If the factors which cause any particular type of addition to be preferred can be ascertained in this way, an important advance will be made in our understanding of the polymerisation reactions. No general rules about this are so far apparent. Samples of butadiene polymerised under different conditions and with very different chain lengths appear to show a roughly constant ratio of 1.2 to 1.4 addition. On the other hand this ratio varies appreciably among the different chemical interpolymers. The chemical nature of the polymerising components should have some effect on this ratio, and it seems unlikely that it can be determined by purely statistical considerations.

Another immediate problem is the determination of head to head or head to tail addition in the polymerisation of vinyl compounds. Thus, the compound  $\text{CH}_2=\text{CH}-\text{X}$  may lead to



It seemed possible that a comparison of the spectra of the polymers with those of other compounds such as  $\text{X} \cdot \text{CH}_2\text{CH}_2\text{CH}_2\text{X}$  or  $\text{XCH}_2\text{CH}_2\text{X}$  would throw light on this. Fig. 3a shows the spectra of polyvinyl acetate, polymethyl acrylate and polymethyl methacrylate with those of the corresponding monomers. The absorption of these polymers is far more intense than that of the non-polar hydrocarbon-type substances, and the spectra are more complex. In analysing the spectra a first step was to decide which bands are primarily concerned with oscillations within the side chain radicals, and which involve motions of the weighted carbon chain. In polyvinyl acetate we should expect the side chains to be

<sup>8</sup> J.C.S., 1944, 597.

$\text{—O—C—CH}_3$ , and in the acrylates  $\text{—C—OCH}_3$ . We have therefore

measured the spectra of a large number of esters and ketones of which the most important in this connection are those containing one of the following structures :

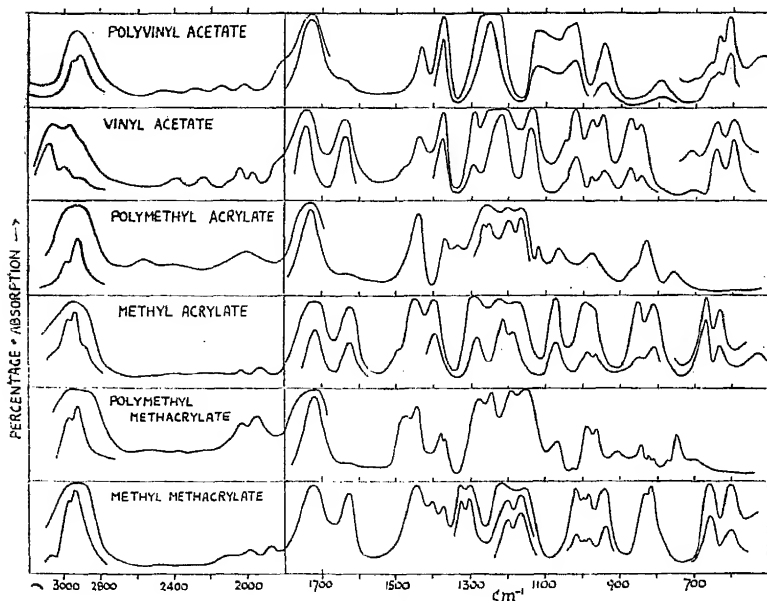
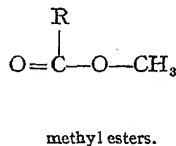
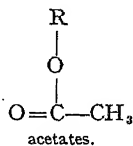
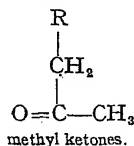
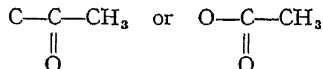


FIG. 3a.

Detailed results will be given elsewhere, but several features are relevant here. Thus, methyl ketones with the exception of acetone have an intense band at  $595\text{ cm}^{-1}$ , whereas other ketones have no analogous band. Acetates have an intense pair of bands at about  $610, 635\text{ cm}^{-1}$  not found with formates or esters of higher fatty acids. These low frequencies are presumably connected with motions of the



skeleton. Formates have an extremely intense absorption at about  $1200\text{ cm}^{-1}$ , which is paralleled in the acetates by a band at  $1245\text{ cm}^{-1}$ , and these vibrations are probably controlled by a motion within the skeleton  $\text{O}=\text{C—O—C}$ . There is a similar strong band with many alkyl ethers<sup>9</sup> at  $1120\text{--}1140\text{ cm}^{-1}$ , and with some aryl alkyl ethers and anhydrides at about  $1240\text{ cm}^{-1}$ , so that this region of absorption may be

<sup>9</sup> Unpublished data ; see also Barnes, Liddel and Williams.<sup>1</sup>

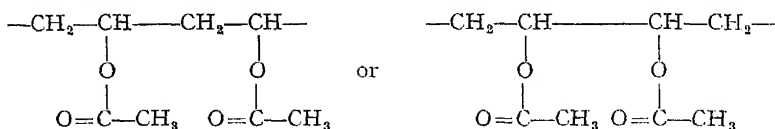
associated mainly with the  $\text{—C—O—C—}$  part of the skeleton, modified in some cases by the contiguous carbonyl group.

Polyvinyl acetate has bands at 610, 635  $\text{cm.}^{-1}$  associated with the acetate side chains; in agreement with the above, polymethyl acrylate and methylacrylate show no such bands in this region. All these polymers show intense absorption in the region of 1150-1250  $\text{cm.}^{-1}$ , since all have the modified ether linkage. This region of absorption is more complex with the acrylates than with polyvinyl acetate, and it is worth noting here that the same result is found with methyl esters of higher fatty acids, which would be expected on the basis of structure to be more closely analogous to the acrylate polymers with the structure  $\text{R—C—OCH}_3$ .

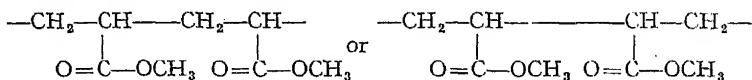


All the polymers show the characteristic carbonyl group absorption at 1720-1730  $\text{cm.}^{-1}$ , and the deformational vibration of methyl groups at about 1375  $\text{cm.}^{-1}$ . In polyvinyl acetate this latter band seems relatively more intense than with the acrylates; in the former case the methyl group is attached to carbon and contiguous to the carbonyl group, and in the latter it is attached to oxygen. In polymethyl methacrylate the band due to the methyl group deformation seems to split, with components at 1370 and 1380  $\text{cm.}^{-1}$ ; this polymer contains two kinds of methyl group, whereas the other two polymers contain only one. The bands at about 1445  $\text{cm.}^{-1}$  are connected with  $\text{CH}_2$  group deformations, and that at 1480 with polymethyl methacrylate may also arise from another unsymmetrical  $\text{CH}_3$  group deformation which is absent with the other two polymers. There are some interesting differences with these polymers in the frequencies of the  $\text{C—H}$  stretching vibration bands between 2900-3000  $\text{cm.}^{-1}$ . All the polymers show a feeble band at about 1630  $\text{cm.}^{-1}$ ; whether this is due to the presence of residual monomer, or to some unexpected type of condensation, is not clear.

Condensation of vinyl acetate may lead to skeleton units of the type



and condensation of methyl acrylate to



For reference, the spectra of compounds such as diacetyl glycol, diacetyl trimethylene glycol, isopropyl acetate, methyl isobutyrate and methyl succinate, are required. A number of these compounds have been examined, but the data are still not complete enough to provide unambiguous conclusions. On the other hand there is a marked parallelism between the spectra of polyvinyl acetate and isopropyl acetate (Fig. 3b), and a far greater similarity between those of polymethyl acrylate and methyl isobutyrate than between that of polymethyl acrylate and any other relevant esters which have been measured. This may imply that the predominant type of condensation is head to tail.

Similar comparisons have been made between the spectra of polyvinyl and polyvinylidene chloride and those of simple chlorinated paraffins; and some structural correlations have been deduced. Here too, however, more reference data are required. A related problem arises with the halothenes made by chlorination of polythene. Continued chlorination leads to well-marked changes in the spectrum (Fig. 4). Thus, as the percentage of chlorine increases, the band at 722  $\text{cm.}^{-1}$  connected with the long

carbon-carbon chain vibration diminishes in intensity, and when about 50 % of chlorine by weight is present this band has entirely disappeared. This band is known to appear with chains of four or more carbon atoms. Taken together these facts give some suggestions about the distribution of chlorine atoms along the chain, but allowance must be made for the simultaneous chlorination of the methyl groups. The band at 1375 connected with the methyl groups also weakens as the chlorination proceeds, and that at 1460  $\text{cm}^{-1}$  associated with a  $\text{CH}_2$  group deformation also weakens slowly. As with simple chlorinated paraffins this methylene group deformation is lowered if a chlorine atom is attached to a neighbouring carbon atom, and in the halothenes bands appear at 1440  $\text{cm}^{-1}$  and lower frequencies in addition to that at 1460  $\text{cm}^{-1}$ . The latter disappears when the percentage of chlorine is such that there are effectively no undisturbed methylene groups. From correlations with the spectra of simple chlorinated paraffins it may be possible to get more exact ideas about the distribution of chlorine atoms along the carbon chain. It is interesting to notice that the vibrational spectra of polyvinyl chloride and polyvinylidene chloride are different from those of halothenes with the same percentage of chlorine by weight.

The infra-red spectra of Neoprenes—polychloroprenes—also reveal differences in samples made under different conditions of polymerisation, and although the structural differences have not yet been fully elucidated, it is useful from the theoretical side to compare the course of the polymerisation of chloroprene with that of butadiene, isoprene or similar substances.

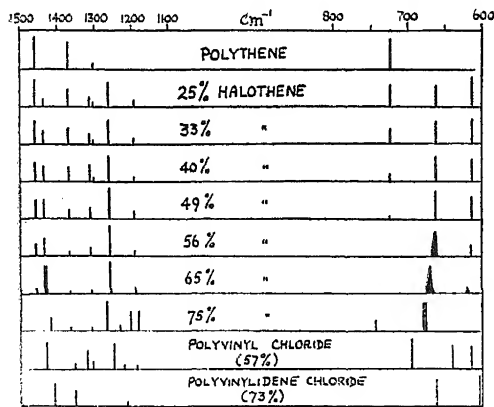


FIG. 4.

method for the estimation of the proportions of the components which are combined in the product. With Buna S, the butadiene-styrene interpolmer, phenyl groups can be estimated from their absorption at 760  $\text{cm}^{-1}$ , and with the butadiene-acrylonitrile polymers such as Perbunan, Hycar, or Butaprene, the cyanide group can be estimated from the band at about 2250  $\text{cm}^{-1}$ . At present the main experimental difficulty in this work is the preparation of films of known thickness, and it may be necessary in practice to use an internal standard for control of this, such as the absorption of some characteristic unit such as

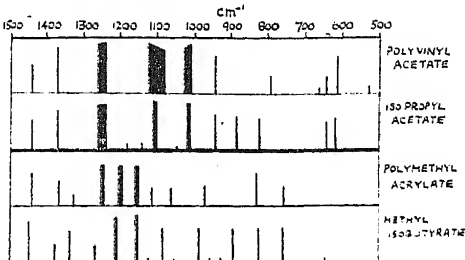


FIG. 3b.

a methylene group. If in some interpolymerisation process, each component independently polymerises, the separate polymers can often be

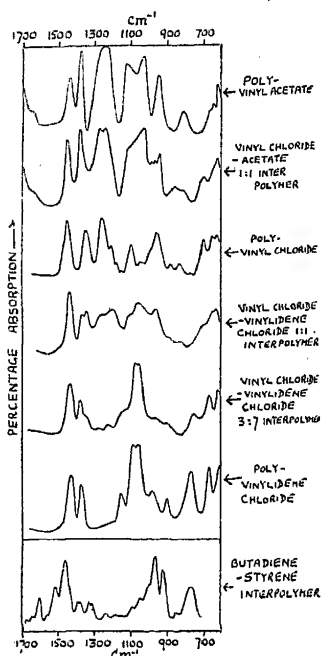


FIG. 5.

detected in the final mixture by means of their characteristic absorption bands. When varying amounts of propylene are allowed to polymerise with ethylene in the formation of a polythene, the take-up of propylene can be followed by the absorption of the bands due to methyl groups, as well as by changes in the spectrum of the product. The spectra of some typical interpolymers are shown in Fig. 5.

The spectra of other compounds of high molecular weight are shown in Fig. 6. There are two important differences between that given here for polyvinyl alcohol and the curve given by Barnes, Liddel and Williams.<sup>10</sup> These workers found two fairly strong bands at 1240 and 1740  $\text{cm}^{-1}$ , which must have been due to acetate groups remaining in a product made by the hydrolysis of polyvinyl acetate. The band at 1740  $\text{cm}^{-1}$  due to carbonyl groups is not detectable in our curve, but the feeble band at about 1240  $\text{cm}^{-1}$  may imply a small amount of polyvinyl acetate impurity. As explained above, this is the most intense band in the spectra of acetates. Although polyvinyl alcohol has relatively few absorption bands, correlation with the molecular structure is

difficult. Comparisons have been made with the spectra of ethylene glycol, isopropyl alcohol, trimethylene glycol, butane 1,4 diol and similar

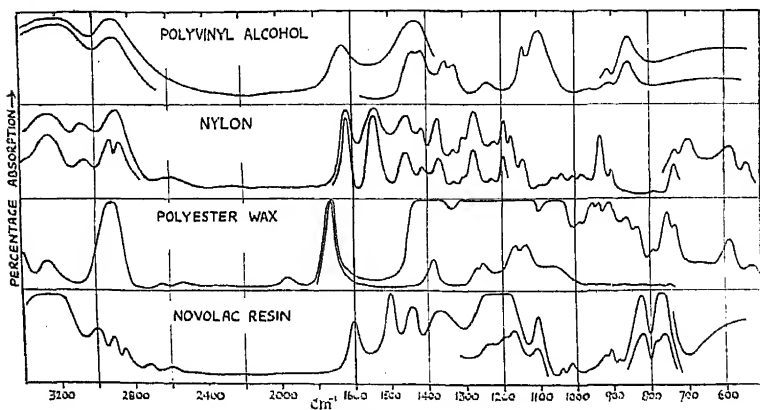
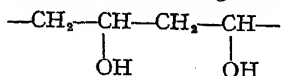


FIG. 6.

substances. The results are not very convincing, though there is some similarity with isopropyl alcohol, which might imply the structure

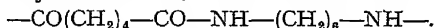


<sup>10</sup> Barnes, Liddel and Williams <sup>1</sup>.

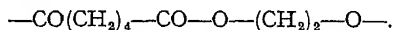
On the other hand, the similarity with trimethyl glycol is not so obvious. The band at about  $1100\text{ cm.}^{-1}$  with polyvinyl alcohol is certainly connected with the hydroxyl group, and that at about  $1430\text{ cm.}^{-1}$  with a deformation of C—H bonds. The broad region of absorption from about  $700\text{ cm.}^{-1}$  to lower frequencies has been found with other oxygenated hydrocarbons and some oxidised hydrocarbon polymers; its exact significance is unknown, but methyl alcohol has a broad absorption band in this region. Other features suggest that a small amount of residual water was present in the sample of polyvinyl alcohol, which was a film made by evaporation of an aqueous solution from a heated glass plate. Thus the band at about  $1650\text{ cm.}^{-1}$  might be due to adsorbed liquid water; if it were connected with a C=C bond formed by loss of water during the heating in preparing the film, we should expect to find another strong band due to the olefinic part of the skeleton formed, probably at  $965\text{ cm.}^{-1}$ , and none is observed. The broad band between  $3000\text{--}3400\text{ cm.}^{-1}$  seems to imply some O—H interaction such as hydrogen bonding, though here, too, the true spectrum may be masked by residual water.

Nylon 66 has also been measured, not only because of its intrinsic importance, but also in relation to other work on the infra-red absorption of amides, amino acids and proteins. The most striking feature of the spectrum is the displacement of the carbonyl group band from its usual position at  $1720\text{--}1740\text{ cm.}^{-1}$  to about  $1630\text{ cm.}^{-1}$ . This occurs with amides in general,<sup>11</sup> and must arise from some form of interaction between the carbonyl and NH groups. Several interpretations have been discussed. In the case of nylon hydrogen bonding of the type  $\text{—C=O—H—N—}$  may be formed by interaction between units in different chains or within the same chain. Pauling has suggested that in the case of amides, resonance may occur between ionic structures localised in the  $\text{—CO—NH—}$  part of the skeleton. Much of the absorption by nylon between  $1200\text{--}1700\text{ cm.}^{-1}$  must be due to vibrations of the  $\text{—C—CO—NH—C—}$  part of the structure. The broad bands in the region of  $3100\text{--}3300\text{ cm.}^{-1}$  also suggest that the N—H bonds are subject to interactions or electronic influences which lead to abnormal stretching vibration frequencies. If the bands in the region of  $3\mu$  and  $6\mu$  are examined in greater detail it may be possible to get more information about this molecule.

A comparison of the spectra of poly-esters and poly-ester-amides with that of Nylon is also interesting. With Nylon, a condensate from adipic ester and hexamethylene diamine, there is the fundamental unit

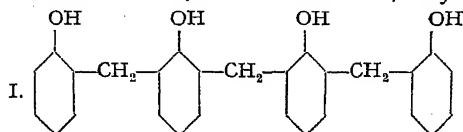


In the poly-esters, such as that formed from adipic ester and ethylene glycol, there is the unit



In this case the carbonyl frequency is found at its normal position, and there is the customary intense ester band at  $1100\text{--}1200\text{ cm.}^{-1}$ . Here, too, the bands in the region of  $3000\text{--}3400\text{ cm.}^{-1}$  connected with C—H stretching vibrations, and possibly with end groups, are informative. Similar points emerge from the spectra of poly-ester-amides, where both the normal carbonyl group frequency and that diminished by an adjacent NH group arise.

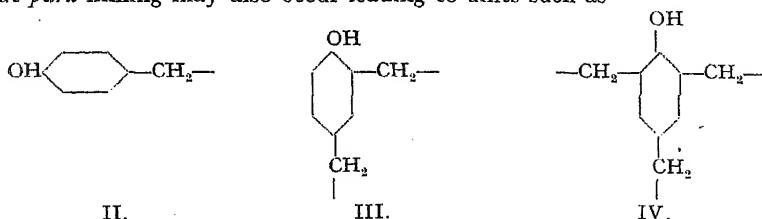
Another type of compound which lends itself to infra-red examination is that formed by the condensation of a phenol or cresol with formaldehyde. Fig. 6 shows the spectrum of a Novolac resin made from phenol and formaldehyde. In this condensation several possible structures can be formed. A simple union of the molecules, with loss of water, may lead to the chain



<sup>11</sup> Hibben, "The Raman Effect"; see also ref. <sup>10</sup>.

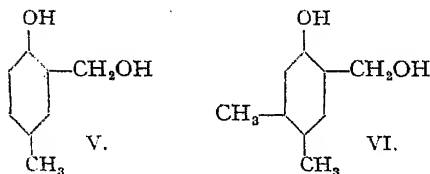


but *para* linking may also occur leading to units such as



It seemed possible that if reference data were available from the spectra of substances such as cresols, xlenols, hydroxy and dihydroxy diphenyl methanes, and monoalcohols of the cresols, some structural correlations might be obtained, and this has already been confirmed. Thus, benzene has a very strong absorption band at  $671\text{ cm}^{-1}$  which has been assigned<sup>12</sup> to a vibrational mode involving the motion of the 6-carbon ring as a rigid unit through the plane of the six hydrogen atoms. When a single substituent is attached to benzene, such as OH,  $\text{NH}_2$ ,  $\text{NHCH}_3$ ,  $\text{N}(\text{C}_2\text{H}_5)_2$ , Cl,  $\text{OCH}_3$ , or an alkyl radical, the "benzenoid" frequency shifts to  $740\text{--}760\text{ cm}^{-1}$ . If two such substituents are present the exact value of this frequency depends not so much upon their chemical nature as upon their relative position—*ortho*, *meta* or *para*. With *ortho* compounds it is at about  $740\text{--}750\text{ cm}^{-1}$ , with *meta* at  $770\text{--}790\text{ cm}^{-1}$ , and with *para* at  $810\text{--}830\text{ cm}^{-1}$ . The data with xlenols<sup>13</sup> suggested that in trisubstituted benzenes the corresponding vibration still persists, and that its frequency may be determined primarily by the arrangement of the substituents in the 1.2.3, 1.2.4 or 1.3.5 positions. Comparison with the spectra of other trisubstituted benzenes show that a useful fairly general rule can be set up, that 1.2.3 compounds have an intense band at about  $760\text{--}770\text{ cm}^{-1}$ , 1.2.4 compounds at  $800\text{--}815\text{ cm}^{-1}$ , and 1.3.5 compounds at  $825\text{--}835\text{ cm}^{-1}$ . Although there are some limitations to this rule, the data already suggest some regularities among the radicals which do not conform.

Applying these arguments to the spectrum of the Novolac resin shown in Fig. 6, the two bands at about  $760$  and  $820\text{ cm}^{-1}$  are particularly important. If the resin had contained a simple chain shown above as I, the bands in this part of the spectrum should correspond to those of *ortho* cresol and 1.2.6 xlenol. The "benzenoid" frequency of the former was at about  $752\text{ cm}^{-1}$ , and of the latter at about  $762\text{ cm}^{-1}$ . Either of these skeleton units could therefore account for the Novolac band at  $760\text{ cm}^{-1}$ , but some other nuclear structural arrangement must give rise to the band at  $820\text{ cm}^{-1}$ . A satisfactory interpretation would be to assume that the resin contains some *para* substituted nuclei, which could either be II or III.



since benzene derivatives with 1.2.3.5 substitution have an intense "benzenoid" band at about  $850\text{ cm}^{-1}$ , of which the resin shows no sign. Similarly, the 1.2.4.5 skeleton can be excluded, since 2 hydroxy 4.5 dimethyl benzyl alcohol (VI.) has the intense "benzenoid" band at  $855$ , 5 ethyl pseudocumene at  $870$  and durene at  $865\text{ cm}^{-1}$ .

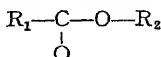
<sup>12</sup> Ingold and others, *J.C.S.*, 1936, 971.

<sup>13</sup> Whiffen and Thompson, *J.C.S.* (in the press).

Thin solid films of 2 hydroxy 5 methyl benzyl alcohol (V) have a strong band at about  $815\text{ cm}^{-1}$ , and the *para* hydroxy diphenyl methanes (2.4' or 4.4') have bands at about  $820\text{ cm}^{-1}$ . Groupings of the type IV are probably absent from the resin,

The strong band with the Novolac at  $1200\text{ cm}^{-1}$  is connected with vibrations involving the hydroxyl groups, and other bands can be related to characteristic oscillations of the aromatic nucleus. The broad hydroxylic absorption at about  $3300\text{ cm}^{-1}$  is also informative, but these details are left for detailed consideration elsewhere.

Fig. 7 shows the spectra of three typical cellulose materials. Cellulose acetate and acetobutyrate have the carbonyl group absorption at  $1740\text{ cm}^{-1}$ , which is absent in the cellulose ether. The latter has a very intense band at about  $1100\text{ cm}^{-1}$ , which was connected above with the ether linkage  $\text{—C—O—C—}$ . Both acetate and acetobutyrate have similar intense absorption between  $1000\text{—}1250\text{ cm}^{-1}$  connected with the



part of the structure. The small differences in this region between the two esters is noteworthy. Cellulose acetate has the strong methyl band at  $1375\text{ cm}^{-1}$ , but when butyrate radicals are introduced other C—H deformation frequencies appear at about  $1415$  and  $1460\text{ cm}^{-1}$ . The variations in position and intensity of some of the bands in the region  $2800\text{—}3600\text{ cm}^{-1}$  with the different celluloses are very important, since these are connected with C—H and O—H stretching vibrations and from them we may determine residual hydroxyl groups and the extent of hydrogen bonding.

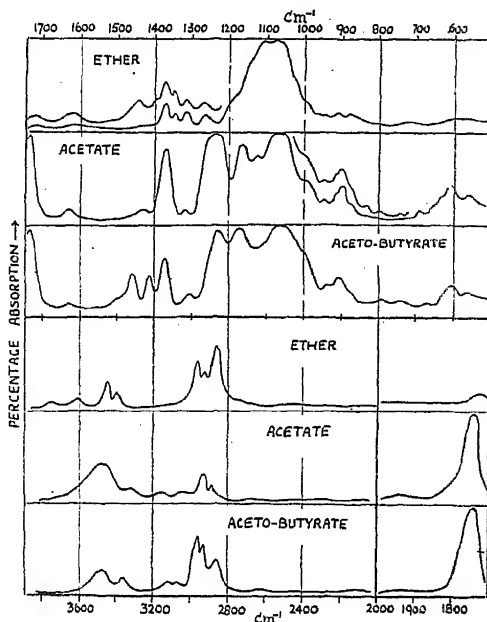


FIG. 7.

Some general considerations affecting infra-red measurements with large molecules must now be mentioned. For example, some of the correlations which have hitherto been made between vibrational spectrum and structure have been arrived at by comparing the spectra of substances in different states of aggregation. Measurements now show that such comparisons must be made cautiously, for the spectrum of a substance may change very strikingly when it changes its physical state. Displacement of vibration bands on passing from vapour to liquid have long been known, particularly in comparing Raman data for liquids with infra-red data on the corresponding vapours; and it is well known that band contours with vapours may be entirely absent with the liquids. The marked changes, both in wavelength and intensity, of vibration bands on passing from liquid to solid which have recently been observed with compounds of very different chemical nature are surprising. In the same way the spectrum of a pure liquid has been found to differ from that of a dilute solution in ways which must arise from causes other than intermolecular association or hydrogen bond formation. There are possible theoretical reasons for these changes in both the frequencies and intensities. For example, in the case of a long chain molecule in the solid state, not only

may the potential energy function in the solid lattice become altered upon melting, leading to shifts in frequencies, but also the internal molecular shape may change and lead to changes in the selection rules or factors which determine the relative intensities of bands.

Such changes in spectrum with solid and liquid have been found with compounds like the cresols and xylenols, but also with long chain paraffins. Usually the bands are sharper and more numerous with the solid. The pair of sharp peaks with polythene at about  $722\text{ cm.}^{-1}$  becomes a single broad band with liquid polythene waxes, as it is with the lower straight chain paraffins. These changes may have significant implications. For instance, the two feeble bands of polythene at  $1080$  and  $890\text{ cm.}^{-1}$  appear to vary in relative intensity in samples of polythene for which X-ray work has shown different ratios of crystalline and amorphous material. If melting leads to the twisting and interweaving of long chains such differences in the relative intensity of bands may arise.

Another promising line of attack is the use of polarised infra-red radiation for the study of oriented long chain polymers such as polythene, nylon, and protein materials. The spectra of the sample with the oriented chains successively parallel or perpendicular to the plane of polarisation of the incident radiation, might be expected to show differences from which information could be obtained about the disposition and orientation of polar groups along the chain. Some measurements on this effect have already given promising results.

Again, with rubbery materials, it has been suggested that differences in physical behaviour may be related to the proportions of sol and gel in the material. It is therefore interesting to compare the spectra of the sol and gel. Unfortunately the experimental difficulties in preparing films of gels suitable for examination are often great.

A more fundamental question is the mathematical treatment of the vibration frequencies of long chains or weighted ring systems. Although some approaches have been made, little progress has so far been achieved. Before any detailed treatment is possible more reference data are required, and the present survey may indicate some ways in which these may be used.

We wish to acknowledge the invaluable help which we have received from many firms who supplied samples for examination, particularly I.C.I. (Alkali) Ltd., I.C.I. (Dyestuffs) Ltd., I.C.I. (Plastics) Ltd., Messrs. Courtaulds and Messrs. Bakelite Ltd. Our thanks are also due to the Chemical Research Laboratory, Teddington, for certain pure chemicals, and to Dr. E. H. Farmer for squalene and dihydromyrcene. Many of the correlations obtained from paraffinic, aromatic and certain olefinic hydrocarbons have been derived from a joint programme of work with Dr. G. B. M. Sutherland and others.

We are also grateful to the Government Grant Committee of the Royal Society for a grant in aid of apparatus.

*The Physical Chemistry Laboratory,  
Oxford.*

## SOME INFRA-RED STUDIES ON THE VULCANISATION OF RUBBER.

BY N. SHEPPARD AND G. B. B. M. SUTHERLAND.

*Received 16th November, 1944.*

The two most effective ways of altering the physical and mechanical properties of natural rubber are vulcanisation\* and the addition of carbon black. There is, however, little understanding of the structural changes brought about by these processes, in spite of extensive research by chemical and physical methods. For instance, in vulcanisation it is not yet decided how the sulphur atoms are incorporated in the rubber polymer, what proportion are in bridges formed between the isoprene chains, whether such bridges are formed by  $\text{—C—S—S—C—}$  or  $\text{—C—S—C—}$  links, whether one double bond is broken for each sulphur atom incorporated and so on. An ancillary problem is the effect of certain "accelerators" on the speed of vulcanisation about which even less is known. Again in the case of reinforcement of rubber by materials such as carbon black there is controversy on the structural relationship of the carbon black and the rubber. Until such structural problems have been solved on the molecular scale there is little hope of controlling the macroscopic properties of rubber compounds in a truly scientific manner. This paper gives a preliminary account of the application of infra-red spectroscopy to some of these problems.

The spectra of the following types of materials have been obtained with a prism spectrometer of good resolving power between 2 and  $18\mu$ :—

- (a) natural rubber,
- (b) natural rubber + sulphur } before
- "      "      + sulphur + accelerators } " curing,"
- (c) Same as (b) after "curing" for various periods,
- (d) natural rubber + carbon black + sulphur + accelerators (uncured and cured).

The results are described in sections corresponding to this classification. The rubber and rubber compounds were generally examined in the form of thin films (approximately  $1/20$  mm. thick) which were evaporated from benzene solution on clean glass or water surfaces. In a few cases the films were cut from bulk material using a microtome.

**The Spectrum of Natural Rubber.**—The infra-red absorption spectrum of natural rubber has been investigated by several authors<sup>1-5</sup> who have covered the range from 1 to  $14\mu$ . In the present work the spectrum has been examined between 2 and  $18\mu$ , with improved resolving power. Fig. 1 shows a percentage absorption curve for a thickness of rubber of 0.05 mm. and is in good agreement with the earliest spectrum recorded,

\* The words vulcanisation and curing are used synonymously throughout this paper.

<sup>1</sup> Stair and Coblenz, *J. Research Nat. Bur. Standards* 1935, **15**, 295.

<sup>2</sup> Williams, *Physics*, 1936, **7**, 399.

<sup>3</sup> Williams, *J. Chem. Physics*, 1936, **4**, 460.

<sup>4</sup> Williams and Taschek, *J. App. Physics*, 1937, **8**, 496.

<sup>5</sup> Sears, *J. App. Physics*, 1941, **12**, 35.

<sup>6</sup> Barnes, Liddell and Williams, *Ind. Eng. Chem. (Anal.)*, 1943, **15**, 83.

<sup>7</sup> Barnes, Liddell and Williams, *ibid.*, 1943, **15**, 659.

<sup>8</sup> Williams and Dale, *J. App. Physics*, 1944, **15**, 585.

*viz.* that due to Stair and Coblentz. Increased resolving power has enabled us to establish some of their weaker bands more definitely; we have also detected a new weak band at  $4.98\mu$ .

Agreement with the results of some of the other authors cited above is less satisfactory, but, when due allowance has been made for possible errors in wavelength determination, the remaining differences can all be accounted for by oxidation which gives rise to intense new bands at approximately  $3.0$ ,  $5.8$  and  $9.75\mu$ . These additional absorptions have been found by Stair and Coblentz in the spectrum of heavily oxidised rubber, and have been confirmed by other work in this laboratory.<sup>9</sup>

In addition to the band at  $4.98\mu$  the present work has revealed a new wide absorption band in the rubber spectrum extending from  $16.6$  to  $17.7\mu$ .

**Spectra of Uncured Natural Rubber Mixes containing Sulphur and Various Accelerating Agents.**—Rubber may be vulcanised by heating

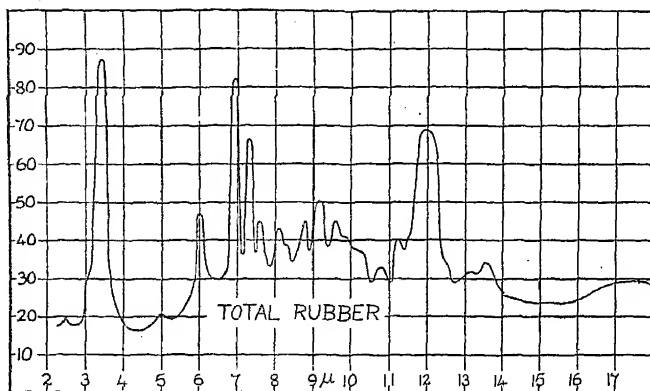


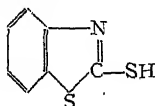
FIG. 1.—The infra-red spectrum of natural rubber containing small amounts of proteins, fatty acids, etc.

(curing) with sulphur alone, but the time required is greatly reduced and the properties of the vulcanised material improved by the addition of small quantities of various materials.<sup>10</sup> Accelerators may be of the basic oxide type (*e.g.* litharge and lime) or of the organic type (*e.g.* mercaptobenzothiazole \* and Santocure †). It is also found that ZnO acts as an activator for the organic accelerator. Furthermore, stearic acid is known to enhance the activity of ZnO, when the latter is acting as an accelerator activator. The compositions of the first series of mixes investigated are shown in Table I, being chosen to cover the most important cases just enumerated. The spectra of the first and last of these mixes are shown in Fig. 2.

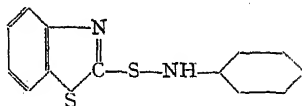
<sup>9</sup> Harding and Sutherland, *to be published shortly*.

<sup>10</sup> Cf. *Chemistry and Technology of Rubber*, by Davies and Blake. *Monograph of Amer. Chem. Soc.*, 1937, Reinhold.

\* Structural formula



† The structural formula of Santocure is



Comparison of these spectra with those of pure natural rubber (Fig. 1) and of mixes A2 and A3 (not reproduced) revealed the following facts:

- (a) The presence of sulphur in unvulcanised rubber causes no new bands in the rubber spectrum;
- (b) The presence of Santocure causes a new band to appear at  $13.3\mu$ .
- (c) The presence of stearic acid with sulphur and associated accelerators causes a new band to appear at  $6.52\mu$ .

TABLE I.

(Mixes are conventionally described as x parts by weight of added material per 100 parts of natural rubber.)

Mix Number.	Rubber.	Sulphur.	Zinc Oxide.	Stearic Acid.	Santocure.
A1	100	10	—	—	—
A2	100	10	5	2	—
A3	100	3	5	—	1
A4	100	3	5	2	1

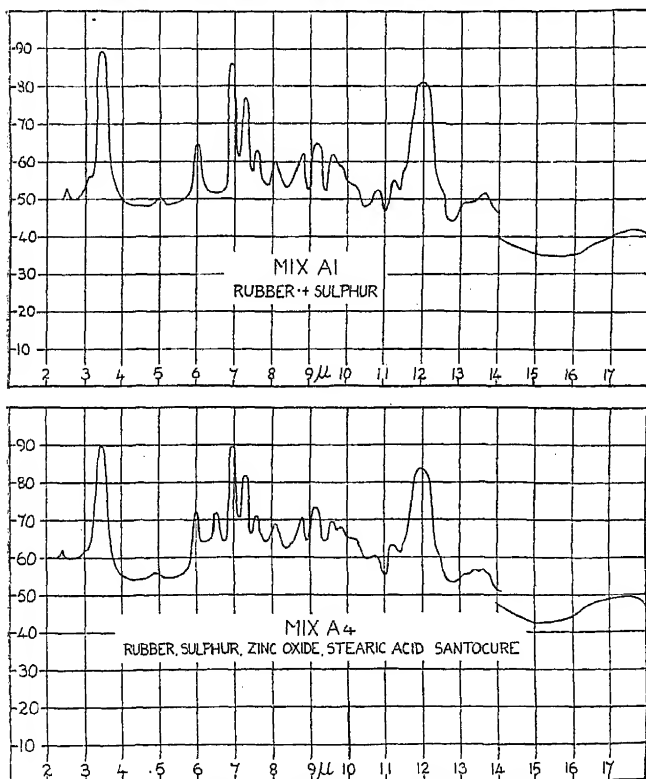


FIG. 2.—The infra-red spectra (a) of a "straight" sulphur mix containing 10 parts of sulphur, (b) of an accelerated mix containing 3 parts sulphur, 2 parts stearic acid, 5 parts zinc oxide, and 1 part Santocure.

In FIG. 2b the band at  $13.4\mu$  should have been drawn at  $13.3\mu$ .

The first two results are what one would normally expect from the spectra of the mixtures since sulphur has no bands sufficiently strong to appear

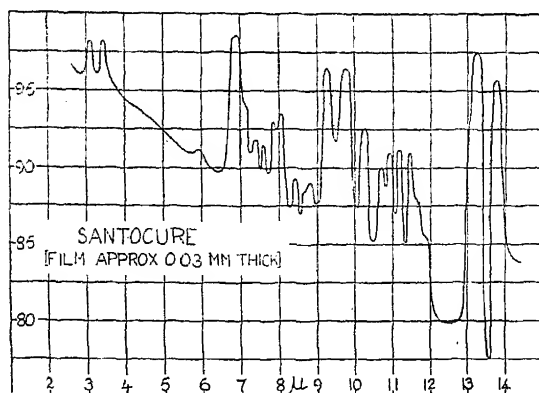


FIG. 3.—The infra-red spectrum of a solid film of the organic accelerator, Santocure.

at this concentration,<sup>11</sup> and in the spectrum of Santocure (Fig. 3) the strongest band is at  $13.3\mu$ . The third result is of considerable interest since stearic acid (Fig. 4a) has no band in this region. In order to try and settle the origin of this new band the series of mixes given in Table II was made up and examined. The results are shown in column 7 of the table, which lists the intensity of the  $6.52\mu$ . band relative to any of the moderately intense rubber bands as a standard. They are also illustrated in Fig. 5.

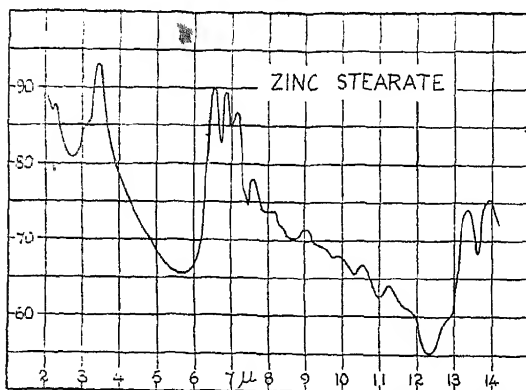
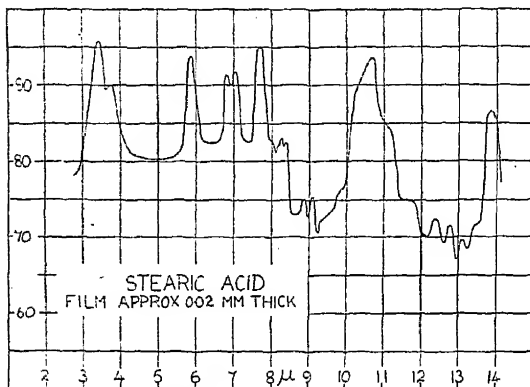


FIG. 4.—The infra-red spectra of solid films of (a) Stearic acid (b) Zinc stearate.

The following conclusions may be drawn:—

(a) The  $6.52\mu$  band is due to some interaction between stearic acid and "rubber" since the presence of added materials is not necessary for its appearance (Mixes B4 and B5).

(b) Since the intensity of the  $6.52\mu$  band is enhanced only by the presence of ZnO (Mix C3),

<sup>11</sup> Taylor and Rideal, *Proc. Roy. Soc. A*, 1927, 115, 589.

either the interaction between "rubber" and stearic acid is one which is increased by ZnO, or ZnO plus stearic acid (which presumably form zinc stearate) give a band in the same position. Mix B2 shows that zinc oxide alone does not give rise to the band.

The possibility of the band being due to zinc stearate was next tested by doing the spectrum of this substance. A very intense band was found in the same position ( $6.52\ \mu$ ) (Fig. 4*b*); this is in fact the most intense band in the spectrum of zinc stearate apart from bands which are characteristic of the CH vibrations and so overlap intense rubber bands. There are therefore strong reasons for associating the  $6.52\ \mu$  band with the presence of stearate ions but this will be more fully discussed later.

#### Spectra of Vulcanised Rubber Mixes.

—We shall report here only the work on Mixes A1 and A4 after curing. These are representative of the two extremes in vulcanising technique, the former being a "straight" mixture of rubber and sulphur, the latter containing, in addition to sulphur, an accelerator (Santocure) and accelerator activators (zinc oxide and stearic acid). The spectra are shown in Figs. 6*a* and 6*b*.

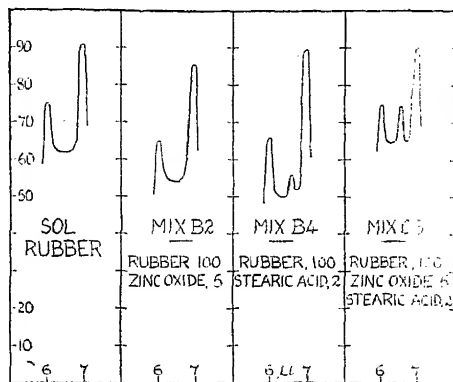


FIG. 5.—Spectra to illustrate the connection of the  $6.52\ \mu$  band with the presence of stearic acid.

TABLE II.

Mix Number.	Rubber.	Sulphur.	Zinc Oxide.	Stearic Acid.	Santocure.	Strength of $6.52\ \mu$ Band.
B1	100	3	—	—	—	—
B2	100	—	5	—	—	—
B3	100	—	—	—	I	—
B4	100	—	—	2	—	Weak
B5	100	—	—	5	—	Medium
C1	100	—	—	2	I	Weak
C2	100	3	—	2	I	Weak
C3	100	—	5	2	—	Strong

Comparison of the spectra of these vulcanised rubbers with the spectra of corresponding uncured mixes (Figs. 2*a* and 2*b*) reveals new bands in the vulcanised rubbers at  $10.4\ \mu$  and  $17.0\ \mu$ . The latter is very weak but seems to be above experimental error in the case of cured Mix A1 (Fig. 6*a*). The  $10.4\ \mu$  band has been reported previously by Sears.<sup>5</sup> In addition to the new bands it is important to notice that the  $6.52\ \mu$  band arising from the presence of stearic acid in Mix A4 has disappeared on curing as also has the Santocure band at  $13.3\ \mu$ .

It is interesting to note that the  $6\ \mu$  band of natural rubber shows no alteration in intensity other than a possible slight increase. The



absolute intensity of this band is hard to determine as it occurs in a region of intense atmospheric absorption due to water vapour but in these mixes and for these times of curing it certainly does not decrease in intensity. There are in fact no appreciable diminutions in any of the bands of rubber on light vulcanisation.

**Spectra of Rubbers containing Carbon Black.**—We report here the results on a mix of the A4 type, (1) containing 5 parts of carbon, before curing; (2) containing 26 parts of carbon, after curing. The spectra are shown in Figs. 7 and 8. Considering first the spectrum of the rubber mix containing 5 parts of carbon (Fig. 7) we see that nowhere is the absorption less than 75 %, and that this background of continuous absorption

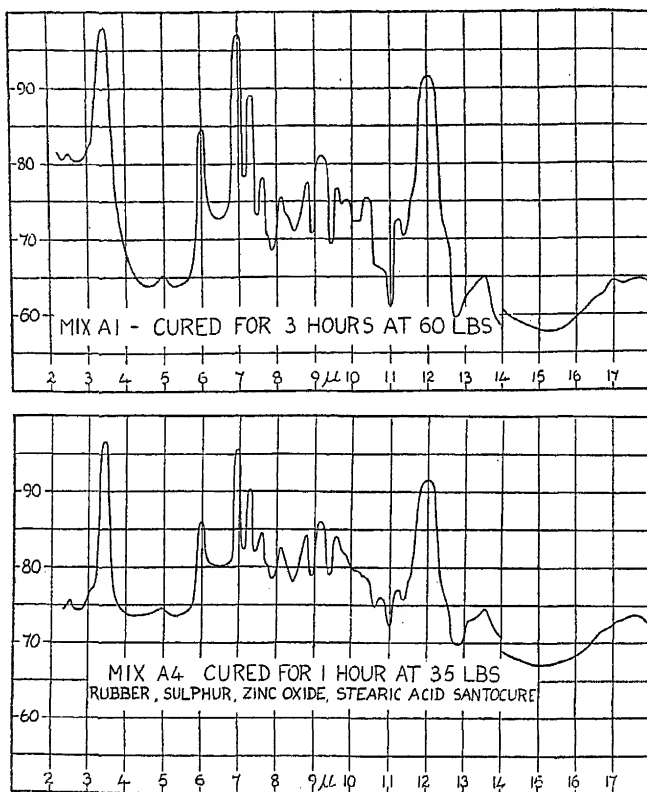


FIG. 6.—The infra-red spectra of cured films of (a) Mix A1 cured for 3 hours at 60 lbs./sq. in steam pressure ( $145^{\circ}\text{C.}$ ) and (b) Mix A4 cured for 1 hour at 35 lbs./sq. in steam pressure ( $127^{\circ}\text{C.}$ ).

increases rapidly on passing to shorter wavelengths. This is an effect which is always present when finely powdered materials are studied in the infra-red region of the spectrum and is due to scattering of the incident radiation by the particles present—in this case by the carbon particles. Such "Rayleigh" scattering is well known to increase in passing to shorter wavelengths. A comparison of the bands superimposed on the scattering background in Fig. 7 with the spectrum of the carbon free Mix A4 shows nothing new. The comparison of intensities is less certain because the scattering effect militates against accurate measurements, but there would seem to be no changes which are not within experimental error.

Although an addition of approximately 5 % carbon might be expected to show at least the first signs of any new or changed frequencies, it was thought advisable to check the work with a rubber containing at least twenty parts of carbon, especially as such heavy loadings are used in practical rubber compounding. It was found, however, that such a rubber

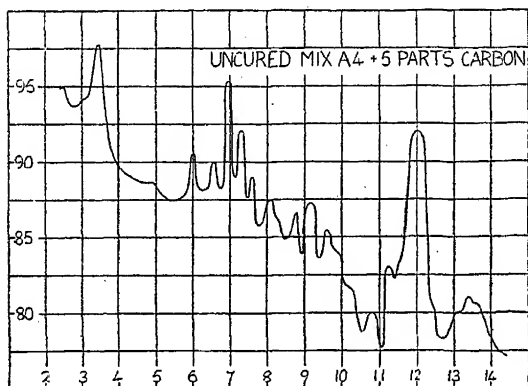


FIG. 7.—The infra-red spectrum of an uncured accelerated mix (A4) with 5 parts of carbon.

gave virtually no transmission in the usual thicknesses we had employed (presumably due to the increased scattering by the carbon black). It was therefore necessary to develop a microtome technique of cutting extremely thin films of vulcanised rubber.

The spectrum of such a film is shown in Fig. 8. It is obvious that the effective thickness of rubber in the path of the radiation is now much too

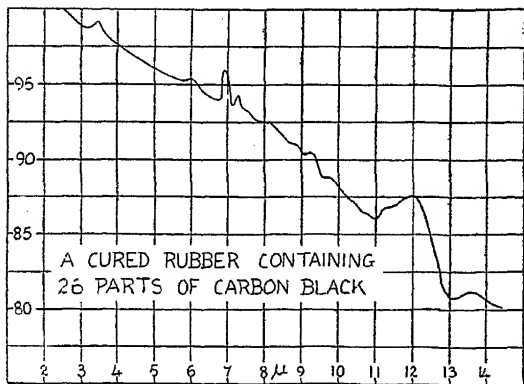


FIG. 8.—An "absorption" curve for a very thin microtome cut film of a cured rubber containing 26 parts of carbon, showing weak rubber absorption bands superimposed on a general scattering background.

small. Nevertheless the characteristic rubber spectrum can just be distinguished above the scattering background. Although intensities cannot be measured with any degree of accuracy it would not appear that carbon affects the gross structure of the infra-red spectrum of rubber (vulcanised or unvulcanised) to any appreciable extent.

### Discussion.

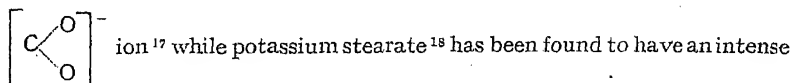
At present the infra-red spectrum of rubber, like that of any polymer, can only be partially interpreted. Following the general rules for such spectra<sup>12</sup> we have the following assignments :—

<sup>12</sup> Cf. *Infra-Red Spectroscopy*, by Barnes, Gore, Liddel and Williams. Reinhold (1944).

Class	Wavelength in $\mu$ .	Detailed Interpretation
Hydrogen Frequencies	3.4	$\nu_{OH}$ valency
	6.9	$\delta_{CH}$ deformation ( $CH_2$ and $CH_3$ groups)
	7.3	$\delta_{OH}$ deformation ( $CH_3$ group)
Double Bond Frequencies	6.0	$\nu_{C=C}$ valency

None of the other bands in rubber can yet be assigned with any degree of certainty although it is probable that the weak band at  $2.5 \mu$  is a combination band arising from the transitions to levels of the type  $\nu_{OH} + \delta_{OH}$ . The weak band near  $3.0 \mu$  was at first assigned to  $\nu_{OH}$ , the hydroxyl presumably arising from slight oxidation. More recent work indicates that this band is separate from the oxidation band at  $3.0 \mu$  and its wavelength is  $3.1 \mu$ . It now seems more probable that it is either a weak combination band or a CH fundamental frequency. If the latter is true it would indicate the existence of a CH group in rubber in which the CH distance is about  $1.06 \text{ \AA}$ , *i.e.* virtually the same as that found in  $C_2H_2$  ( $1.057 \text{ \AA}$ )<sup>13</sup> and HCN ( $1.06 \text{ \AA}$ ),<sup>14</sup> and considerably less than that found in methane ( $1.093 \text{ \AA}$ )<sup>15</sup> and ethylene ( $1.085 \text{ \AA}$ ).<sup>16</sup> This may be the CH distance of the "lone" hydrogen on the ethylene bond. Thus although the part of the infra-red spectrum which arises from the skeletal vibrations of the isoprene chains (*i.e.* from  $7.5$  to  $18 \mu$ ) cannot yet be interpreted we have in the short wave region "tracer" bands which should make it possible to follow changes which vulcanisation may cause in C—H and C=C bonds.

**The Stearic Acid Band at  $6.52 \mu$ .**—This is the only band appearing in the spectrum of rubber mixes before curing which is not due to the separate components of the mixture. Since it coincides with an intense band in zinc stearate and is intensified when zinc oxide accompanies the stearic acid, the natural deduction is that this band is due to the stearate ion. The stearate ion would be expected to have a frequency very close to this value arising from the unsymmetrical valency vibration of the



band at  $6.45 \mu$ . However, if we accept this interpretation it is difficult to explain how the stearic acid comes to be ionised in rubber before the addition of zinc oxide. Furthermore natural rubber generally contains 1.2 % of carboxylic acids and therefore the addition of zinc oxide to rubber

might be expected to produce  $\left[ \text{X}-\begin{array}{c} \text{O} \\ \diagup \text{C} \diagdown \\ \text{O} \end{array} \right]^-$  ions which should give the

$6.52 \mu$  band. The fact that zinc oxide in rubber does not give rise to the band can of course be accounted for if we suppose that more than

2 % of  $\left[ \text{X}-\begin{array}{c} \text{O} \\ \diagup \text{C} \diagdown \\ \text{O} \end{array} \right]^-$  ions are necessary to make the band detectable.

Further quantitative work is required to resolve these difficulties. Meanwhile there is definite spectroscopic evidence that zinc stearate is formed

<sup>13</sup> (a) Herzberg, Patat and Spinks, *Z. Physik*, 1934, **92**, 87. (b) Herzberg, Patat and Verleger, *Z. Physik*, 1936, **102**, 1.

<sup>14</sup> Herzberg and Spinks, *Proc. Roy. Soc. A.*, 1934, **147**, 434.

<sup>15</sup> Ginsburg and Barker, *J. Chem. Physics*, 1935, **3**, 668.

<sup>16</sup> Thompson, *Trans. Faraday Soc.*, 1939, **35**, 697.

<sup>17</sup> Cf. the same frequency at  $6.48 \mu$  in the acetate ion, Davies and Sutherland, *J. Chem. Physics*, 1938, **6**, 755.

<sup>18</sup> The spectrum of potassium stearate has recently been obtained by Ramsay in Professor Rideal's laboratory in another connection.

when zinc oxide and stearic acid are added to rubber before vulcanisation, and that this zinc stearate is destroyed as vulcanisation proceeds.

It should perhaps be added that we also have evidence that when stearic acid is added to rubber some of it remains unaltered since it can be detected by means of its characteristic carbonyl band near  $5.8\mu$ .

**Changes in the Spectrum produced by Vulcanisation.**—Before discussing the new bands at  $10.4$  and  $17\mu$  it is useful to consider what changes in the spectrum might have been expected, according as the sulphur is incorporated in different ways. Spectroscopically the new bond easiest to detect would be the S—H bond which would give a band very close to  $3.9\mu$ . No trace of such a band has been found so we may rule out the formation of mercaptans in vulcanisation. If —C—S—C— linkages are formed a rough calculation shows that the associated new bands will lie beyond  $13\mu$ ; if —C—S—S—C— linkages are formed the S—S bond should be distinguishable from the C—S bond but it will be expected to give a band beyond  $20\mu$ . If C=S bonds are formed one may expect the corresponding valency vibration to become active in the region between  $6.5$  and  $15\mu$ . Until much more work has been done on the spectra of sulphur-hydrocarbon compounds of known structure it will not be possible to say whether any carbon-sulphur bonds detected occur in a chain or in a ring structure. Finally we may look for changes in the original rubber spectrum. Thus if sulphur is incorporated at the expense of C=C double bonds we may expect a diminution in the intensity of the  $6\mu$  band, while any alteration in the ratio of  $\text{CH}_2$  to  $\text{CH}_3$  groups will be reflected in a corresponding alteration in the relative intensity of the  $6.9$  and  $7.3\mu$  bands associated with these groups.

With these considerations in mind the simplest interpretation of the new bands at  $10.4$  and  $17\mu$  is that the former is due to C=S bonds while the latter is due to C—S bonds. Unfortunately the simplest interpretation is not necessarily the correct one, but it does seem probable that the  $17\mu$  band arises from C—S bonds. In dimethyl sulphide Thompson<sup>19</sup> has assigned the two C—S valency vibrations to frequencies at  $691$  and  $742\text{ cm}^{-1}$ . When the methyl groups are replaced by carbon chains these frequencies might be expected to be altered sufficiently for one of them to move to  $17\mu$ . No infra-red data exist on organic sulphides for the region beyond  $16\mu$  but the Raman spectrum of diallyl sulphide<sup>20</sup> shows a frequency corresponding to an infra-red absorption at  $16.9\mu$ . We are hoping to examine shortly the spectra of a number of organic sulphides and so confirm this assignment. Since C=S bonds are unlikely on chemical grounds, the next simplest spectroscopic interpretation of the  $10.4\mu$  band is that it derives from a combination of the —C—S—C— deformation frequency with one of the C—S valency frequencies of the same group. It might, however, be purely a frequency of the carbon part of the molecular framework which has become "active" through the alteration of symmetry caused by the introduction of a sulphur atom into the framework. Here again further fundamental work on simpler molecules of known structure is required.

Probably the most interesting spectroscopic result so far derived is the negative one that the intensity of the C=C band at  $6\mu$  is not altered by vulcanisation with 10 parts of sulphur unless perhaps to be somewhat intensified. A number of other vulcanised rubbers have been examined in the course of this work including one containing 33 parts of sulphur. Even this compound after curing for six hours at  $145^\circ\text{C}$ . showed only a small decrease in the intensity of the  $6\mu$  band. This does not prove conclusively that the ethylenic linkages are virtually unaffected by vulcanisation. The intensity of the  $6\mu$  band is a function of the asymmetry of the groups attached to the carbon atoms at either end of the bond.

<sup>19</sup> Thompson, *Trans. Faraday Soc.*, 1941, **37**, 38.

<sup>20</sup> Venkateswaran, *Ind. Journ. Physics*, 1931, **6**, 51.

If this asymmetry is increased on some double bonds by part of the sulphur while the rest of the sulphur is compounded by the complete rupture of other double bonds, the intensity of the  $6\mu$  band may either increase or decrease according to the relative effects of these two processes. There is in fact some evidence that the  $6\mu$  band increases in intensity at first and subsequently (after long curing with 10 % or more sulphur) decreases. In any case it does seem certain that an appreciable degree of unsaturation remains even with 33 % sulphur and a considerable degree of vulcanisation.

**Effect of Carbon Black on Rubber Spectrum.**—It has already been remarked that no new bands are produced by the addition of carbon black and the only appreciable changes in intensity are those caused by the scattering effect of the carbon particles which makes the bands appear progressively stronger as we move to shorter wavelengths. A few measurements have been made to see whether Rayleigh's law is obeyed in these phenomena. The results indicate that whereas Rayleigh's law would give

$$\log I/I_0 = -K/\lambda^4$$

(where  $\lambda$  is the wavelength of the radiation,  $I$  is the intensity of the transmitted radiation, and  $I_0$  is the intensity of the incident radiation) the intensities in our curves obey a law where the index of  $\lambda$  is approximately unity. The carbon particles in these experiments had a mean diameter of  $0.03\mu$ . One might have expected Rayleigh's law to hold if no aggregation took place since the wavelengths were at least 100 times the size of the particle. If, however, aggregation took place and the particle size became of the same order as the wavelength then anomalous scattering will result. Pfund<sup>21</sup> has investigated phenomena of this type experimentally and shown that when the particle size becomes of the same order as the wavelength a sharp change in the intensity of the scattered radiation is to be expected. Further work is required on the fundamentals of this subject before accurate quantitative deductions can be made, but we can state that the intensity of the scattered radiation in the infra-red indicates that the carbon black in these rubbers aggregates from an initial size to  $0.03\mu$  to a particle of the order of  $1\mu$  in diameter. Fuller details of these experiments will be published in due course.

### Summary.

Infra-red absorption spectra have been determined between 2 and  $18\mu$  for the following materials (a) natural rubber, (b) natural rubber + sulphur and/or various accelerating agents, before and after vulcanisation, (c) natural rubber mixes containing carbon black, before and after vulcanisation. The accelerating agents studied were zinc oxide, Santocure and stearic acid. New bands have been detected in natural rubber at  $3.1$ ,  $4.98$  and  $16.6$ – $17.7\mu$ . Evidence has been found for the existence of stearate ions in rubber mixes to which zinc oxide and stearic acid have been added. The addition of stearic acid alone to natural rubber also gives rise to a band in the position associated with the stearate ion ( $6.52\mu$ ). The explanation of this phenomenon is not clear. Vulcanised rubber shows two bands at  $10.4\mu$  and  $17\mu$  not present in uncured rubber. The latter is probably associated with C—S bonds. Vulcanisation produces very little effect on the C=C frequency of rubber at  $6\mu$  so that appreciable unsaturation would appear to exist in highly vulcanised rubber. Carbon black produces no marked alteration in the spectrum of rubber (vulcanised or unvulcanised) other than effects due to scattering. The variation of this scattering with wavelength indicates that the size of the carbon aggregate in rubber is of the order of  $1\mu$ .

This work is part of a programme of fundamental research on the infra-red spectra of rubber and rubber compounds made possible by

<sup>21</sup> Pfund, *J. Opt. Soc. Amer.*, 1933, 23, 375; *ibid.*, 1934, 24, 143.

assistance from the Dunlop Rubber Co. Ltd. The cured films examined were all prepared in the Dunlop Research Laboratories by Mr. L. F. H. Bovey whose help has been indispensable. We wish also to record our thanks to Mr. E. F. Powell and Mr. D. Bulgin of the same department for the benefit of many stimulating discussions.

*The Laboratory of Physical Chemistry,  
Cambridge.*

#### GENERAL DISCUSSION.\*

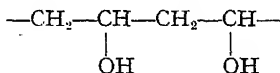
Dr. Sutherland (Cambridge) said: We have carried out a considerable amount of work on polymers in Cambridge along the same general lines as those described by Dr. Thompson and Mr. Torkington, and, broadly speaking, our results and conclusions are in agreement with theirs. It was originally planned that our results should also be presented at this meeting, but pressure of other work has made this impossible. It may stimulate discussion if I indicate a few points on which we differ.

First with regard to the rule for classifying compounds with an ethylenic linkage (which is an extension of an earlier rule given by Lambert and Lecomte<sup>1</sup>) certain diallyl compounds recently investigated by Mr. Willis appear to break this rule, *e.g.* diallyl succinate, which has the 990  $\text{cm}^{-1}$  band but not the 909  $\text{cm}^{-1}$  band. Again, in the course of work on rubber, several compounds have been examined in which the  $\text{R}_1\text{R}_2\text{C}=\text{CHR}_3$  structure was known to exist, but no strong band was found at 840  $\text{cm}^{-1}$ , *e.g.* trimethyl ethylene. I feel, therefore, that further work is required to define the exact limitations of this rule before it can be applied with complete confidence.

With reference to the possible existence of  $\text{CH}_3$  groups in polystyrene being indicated by the band at 1380  $\text{cm}^{-1}$ , I would draw attention to a note by Wright<sup>2</sup> on the short wave region of this spectrum, which proved (using the characteristic bands for  $\text{CH}_3$  first established by Fox and Martin<sup>3</sup>) that there cannot be more than one  $\text{CH}_3$  group per 100 units in the polystyrene chain.

With reference to the spectra of natural rubber and related compounds, a considerable amount of work has been done here by Mr. Harding under the auspices of the British Rubber Producers' Research Association. Interesting differences have been found between the spectra of natural rubber, guttapercha (the  $\alpha$  and  $\beta$  forms of which give different spectra) and synthetic polyisoprene. With regard to the rubber and guttapercha, these differences are presumably due to *cis/trans* isomerism, and a study is now in progress of simpler analogues of these isomers.

As regards the spectrum of polyvinyl alcohol, I would point out that Lecomte<sup>4</sup> has given empirical rules, which are fairly reliable in differentiating between a primary, secondary and tertiary alcohol. The characteristic band of a secondary alcohol, according to Lecomte, is at 1100  $\text{cm}^{-1}$ , which would indicate for polyvinyl alcohol the structure—



Recent work in Cambridge on alcohols gives general confirmation to Lecomte's rules.

In the case of nylon which we have also investigated, I should like to point out that the infra-red spectrum gives bands at 3.0  $\text{m}\mu$  and 6.0  $\text{m}\mu$

\* On the two preceding papers.

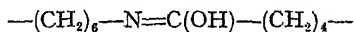
<sup>1</sup> Lambert and Lecomte, *C.R.*, 1938, 206, 1007.

<sup>2</sup> Wright, *Rev. Sci. Instr.* 1944, 15, 22.

<sup>3</sup> Fox and Martin, *Proc. Roy. Soc. A*, 1940, 175, 208.

<sup>4</sup> Lecomte, *C.R.*, 1925, 180, 825; *Le Spectre Infrarouge*, Paris, 1928.

which might indicate respectively the presence of OH and C=N bonds, so that it is not possible at this stage to exclude groupings of the type



in nylon.

**Mr. D. A. Ramsay** (*Cambridge*) said: The spectra of several polystyrenes have been investigated in the region 2.0-15.0  $\text{m}\mu$ , of which the rheological properties differed. No significant differences were detected in this region of the spectrum, hence the differences in the rheological properties must be related to structural differences, which do not appreciably influence the infra-red spectrum, *e.g.* variations in chain length rather than chain branching.

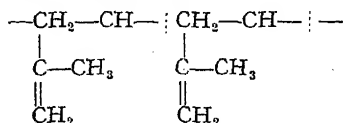
A further sample of polystyrene, which from its abnormal swelling properties and anomalous viscosity measurements was believed to be cross-linked, again displayed no differences in this region of the spectrum. Hence it was concluded that the amount of cross-linking was small. Further work, however, is still required to enable us to determine the minimum amount of cross-linking detectable in polystyrene by the infra-red method.

Samples of polystyrene polymerised under various conditions have been examined but in general the differences observed were very small. A sample of polystyrene polymerised in the presence of 2 % benzoyl peroxide catalyst, however, exhibited two new frequencies of appreciable intensity at 1276  $\text{cm}^{-1}$  and 1105  $\text{cm}^{-1}$  which are not due to benzoyl peroxide. Whether these are due to alterations in the polystyrene chain or to the presence of C—O—C linkages is not yet settled.

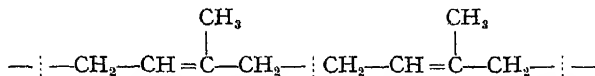
**Mr. Harding** (*Cambridge*) said: I should like to draw attention to a particularly interesting result we have obtained from infra-red studies of rubber and of synthetic polyisoprene.

In the infra-red spectrum between 1300  $\text{cm}^{-1}$  and 700  $\text{cm}^{-1}$ , the strongest absorption band of rubber is at 840  $\text{cm}^{-1}$ , whereas synthetic polyisoprene has its strongest band at 890  $\text{cm}^{-1}$ . A band at the latter position, as Dr. Thompson and others have pointed out, is probably char-

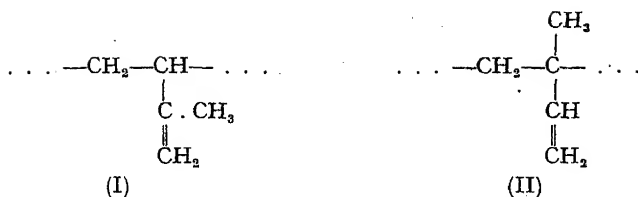
acteristic of the  $\begin{matrix} \text{R}_1 \\ \text{R}_2 \end{matrix} \text{C}=\text{CH}_2$  grouping. This suggests that the polymerisation of isoprene takes place chiefly by 1 : 2 addition, giving the structure—



A weak band in synthetic polyisoprene at 840  $\text{cm}^{-1}$  indicates that there may be some 1.4 addition in the polymerisation, giving the normal rubber structure—

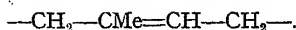


**Dr. Thompson** (*communicated*): I am most interested in Mr. Harding's comments on polyisoprene, but cannot agree with his implied generalisation that isoprene always polymerises predominantly by 1 : 2 addition. We also have measured the spectra of some films of synthetic polyisoprene, and have found that some samples may actually predominate in the 1.4 addition, as suggested by the very strong band at 840  $\text{cm}^{-1}$ . Also, using the key bands which have already been mentioned for the other types of olefinic linkage, the spectra suggest that, in some polyisoprene samples at least, the 1 : 2 addition can occur in either of two ways, leading to structures of the type (I) and (II), in which the pendent groups are different. (I) is in the substituted isobutylene class, and (II) in the vinyl class.



It is clear from all these results that particular conditions may favour the different methods of condensation, and we have here a good method for analysing them.

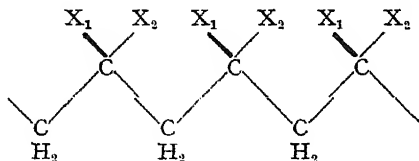
**Dr. H. P. Koch** (*Welwyn*) said: Mr. Harding has observed marked dissimilarities in the spectra of rubber and gutta-percha, and some of these differences must be connected with the geometrical isomerism of the two polymers about the double bond of the repeating unit



In order to establish such a correlation we hope to have pure samples of the *cis*- and *trans*-isomers of dihydromyrcene available for infra-red investigation shortly. Some progress would then be possible in the interpretation of those parts of the spectra associated with the internal molecular shape of the polymeric chains. It may be pointed out in this connection that the analogous pair of isomeric alcohols, geraniol and nerol, failed to reveal significant differences in their Raman spectra.<sup>5</sup>

The difficulty of finding independent standards for checking or calibrating infra-red absorption intensities of interpolymer spectra could be partly overcome by supplementation with data from ultra-violet spectroscopy which is a powerful analytical tool whenever conjugated or aromatic centres are present in the molecule. Many polymers can be made to give clear solutions in ultra-violet transparent solvents such as *cyclo*-hexane for this purpose. Thus, the proportion of styrene combined in Buna S can be estimated by measuring the absorption band at 260 mμ, and it has been shown previously<sup>6</sup> how the mode of combination of Novolac resins with rubber could be determined by ultra-violet analysis.

**Dr. Alwyn G. Evans** (*Manchester*) said: The use of the infra-red technique to determine whether monomer molecules link up on polymerisation by the head to tail method or by the head to head method is interesting, especially for monomers of the 1 : 1 disubstituted ethylene type. For such monomers, e.g.  $\text{CH}_2 = \text{CX}_1\text{X}_2$ , the head to tail polymerisation leading to the structure



gives rise to the possibility of steric hindrance between the substituent groups X on one carbon atom and those on the next carbon but one. When the substituent groups X are  $\text{CH}_3$ , that is, when the monomer is isobutene, it is found that this steric interference between the methyl groups is quite large. A model of the polyisobutene molecule of the head to tail type can only be built up by successive rotation of the isobutene units with respect to each other so that the methyl group of one isobutene unit fits in between the two methyl groups of the next isobutene unit.

<sup>5</sup> Dupont, Desreux and Dulou, *Bull. Soc. Chim.*, 1937, 4, 2016.

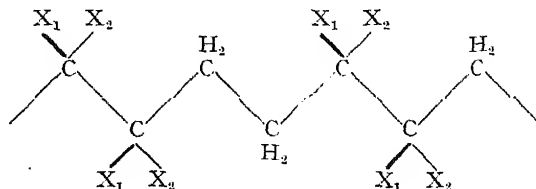
<sup>6</sup> Cunneen, Farmer and Koch, *J.C.S.*, 1943, 472.



The structure so obtained is quite rigid, although the model carbon atoms used have a smaller van der Waals radius than the normal.<sup>1</sup> It is to this steric interference that the low heat of polymerisation of isobutene has been attributed.<sup>7, 8</sup>

From the infra-red examination of polyisobutene, Thompson and Torkington conclude that there may be a slight weakening of the carbon-carbon bonds, and this they attribute to the steric hindrance in the molecule.

The head to head, tail to tail, polymerisation would lead to the structure :



in which there is no possibility of steric interference between the substituent groups X. A model of the polyisobutene molecule of this structure shows the absence of steric hindrance. Rotation about the carbon-carbon bonds can occur in contrast to the rigid structure obtained for the head to tail model.

On polymerisation the isobutene molecules join up with each other by the head to tail method to give a polymer in which there is strong steric hindrance, and a consequent reduction of carbon-carbon bond strength. The fact that the alternative head to head, tail to tail method of polymerisation, which would give an unstrained polymer molecule, does not occur, is of importance from the point of view of the mechanism of polymerisation. By increasing the size of the groups X, the head to tail structure will become more and more sterically unfavourable compared with the head to head, tail to tail structure. It would be interesting to see whether such an increase in the size of the groups X were accompanied by an increasing proportion of head to head addition, or whether, as in di-isobutene, where  $X_1$  is  $\text{CH}_3$  and  $X_2$  is  $\text{CH}_2\text{C}(\text{CH}_3)_2$ , polymerisation is stopped altogether, and dimerisation occurs?

Dr. A. Wassermann (London) said : I should like to draw attention to the importance of spectroscopic measurements for entropy calculations, which in turn are of interest in connection with the mechanism of certain low or high molecular polymerisations. As an example I refer to the reactions of butadiene. The first step in the high molecular polymerisation leads to species of the formula  $\text{C}_8\text{H}_{12}$ . One such species can be represented by the straight chain di-radical (A) referred to in Dr. Thompson's and Torkington's paper. The formation of a bond between the first and sixth carbon atoms leads to 4-vinylcyclohexane (B) which, at about  $600^\circ \text{ abs.}$ , is the product of the homogeneous gaseous dimerisation of butadiene. It is of interest to find out whether (A) is an intermediate in the formation of (B) or whether the primary steps in the high molecular polymerisation and in the dimerisation are fundamentally different. In order to decide this question attempts have been made<sup>7</sup> to estimate the entropy change,  $\Delta S$ , of the two processes 2 butadiene = (A) and 2 butadiene = (B). The quantity  $\Delta S$  can be regarded as being the sum of three terms

$$\Delta S = \Delta S_{\text{rig.}} + \Delta S_{\text{vib.}(\alpha)} + \Delta S_{\text{vib.}(\beta)},$$

where  $\Delta S_{\text{rig.}}$  comprises the contributions of the various species supposed to be rigid,  $\Delta S_{\text{vib.}(\alpha)}$  relates to relatively stiff vibrations of frequencies higher than  $1000 \text{ cm.}^{-1}$  and  $\Delta S_{\text{vib.}(\beta)}$  relates to the lower vibrations, or to

<sup>7</sup> A. G. Evans and Polanyi, *Nature*, 1943, **152**, 738.

<sup>8</sup> Flory, *J.A.C.S.*, 1943, **65**, 372.

torsional oscillations in the range 200 to 1000  $\text{cm}^{-1}$  and to free or restricted internal rotations. The calculations \* lead to the following result

$$\left. \begin{aligned} \Delta S/R &= -6 \pm 3 \text{ for species A} \\ \Delta S/R &= -12 \pm 5 \text{ for species B} \end{aligned} \right\} (T = 600^\circ).$$

Both these figures are compatible with the experimental entropy change as deduced from kinetic measurements; it follows, therefore, that this method of approach cannot be used to find out whether the formation of (B) is a side reaction of the low molecular link of a polymersation chain. The large inaccuracies are mainly due to the present incomplete knowledge of  $\Delta S_{vib.(\beta)}$  but entropy calculations of the type here considered will doubtlessly lead to useful results if we know more about the vibrations and torsional oscillations down to 150  $\text{cm}^{-1}$ . It is improbable that in benzene and in simple aromatic compounds, such low frequencies occur,<sup>10</sup> but it is nevertheless possible that in other cyclic compounds some of the frequencies are very low.<sup>11</sup> The necessary information can probably be obtained by a combined investigation of the infra-red and Raman spectra, by a determination of the band spacings in fluorescence and phosphorescence spectra and by measurements of the specific heats.

**Mr. L. W. Marrison** (*Widnes*) (*communicated*): It would be interesting to know if the authors of this paper have been able to correlate the absorptions at 3.0, 5.8 and 9.75  $\mu$ , observed in the spectrum of oxidised rubber, with any particular type of oxygen-containing structure. The possible analogy with the ketonic absorption at 1720  $\text{cm}^{-1}$  observed by Thompson and Torkington in polythene seems to be very suggestive.

**Dr. Sutherland** (*Cambridge*) (*communicated*): The absorptions at 3.0 and 5.8  $\mu$  occurring in oxidised rubber are due respectively to OH and C=O valency vibrations. These bands have been studied further by Mr. Harding and myself to see whether quantitative estimations of the OH and C=O bonds in oxidised rubber can be made by this means. Although rough estimates can be made fairly readily, accurate determinations (especially of the OH) present certain problems which have not yet been satisfactorily solved. The exact interpretation of the band at 9.75  $\mu$  (which is much less well defined, since there are in fact several new overlapping bands due to oxidation in the region beyond 7.5  $\mu$ ) is not yet clear but it is almost certainly to be associated with C—O bonds.

**Dr. Thompson** said: With regard to some of the points made by Dr. Sutherland, I agree that the rules for differentiating classes of olefines must be used carefully with other than hydrocarbon molecules. Mr. Torkington has also found, for example, that in the allyl halides, as also with the vinyl halides,<sup>12</sup> the frequencies of the bending oscillations of the C—H bonds shift according to the halogen atom which is attached, but rules are gradually being built up from which such shifts may be anticipated.

We, too, have found with samples of nylon, other points of the kind mentioned by Dr. Sutherland but not given in detail in our paper.

I was particularly interested in the work described by Sheppard and Sutherland on vulcanisation, since Mr. Torkington and I have made some similar measurements in which the vulcanisation by sulphur chloride was studied. The spectra of samples of crepe rubber which have been subjected to sulphur chloride vapour for varying times show marked differences, as shown in the diagram.

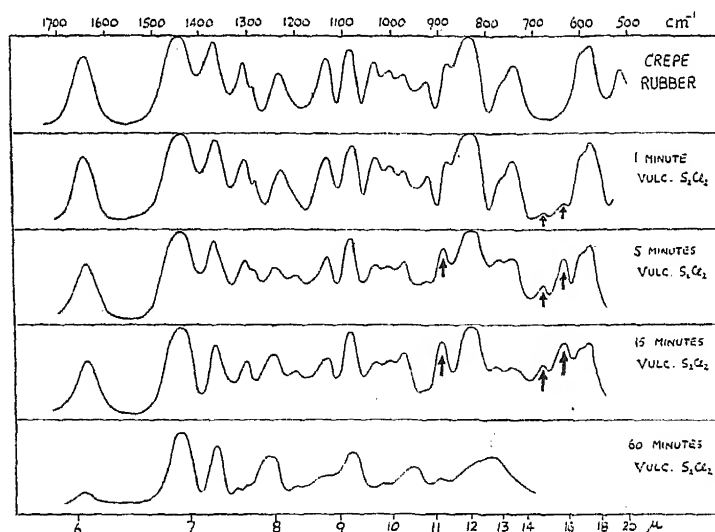
\* Kistiakowsky and Ransom, *J. Chem. Physics*, 1939, 7, 725; Wassermann, *J. Chem. Soc.*, 1942, 612.

<sup>10</sup> Compare, for instance, Lord, Ahlberg and Andrews, *J. Chem. Physics*, 1937, 5, 649.

<sup>11</sup> Wassermann, *Proc. Roy. Soc. A*, 1941, 178, 370.

<sup>12</sup> *J.C.S.* (1944), 303.

As vulcanisation proceeds new bands appear, notably at 635, 680 and 895  $\text{cm}^{-1}$ , although there are other changes in the spectrum too. We should naturally try to correlate these new bands with the formation of C—S or S—S linkages, and to this end Mr. Trotter has been measuring the spectra of some alkyl disulphides, including the dimethyl, diethyl, dipropyl and dibenzyl derivatives, between 3-20  $\mu$ . These alkyl disulphides have bands in the range 500-700  $\text{cm}^{-1}$ , but no very certain correlation can yet be made with the bands in the vulcanised rubber.



It is interesting also to note that when vulcanisation by sulphur chloride occurs, there is no marked change, in the early stages at least, in the absorption near 1600  $\text{cm}^{-1}$  associated with the carbon-carbon double bonds, which agrees with the result found by Sheppard and Sutherland.

As regards the peculiar band at about 6.5  $\mu$  associated by Sheppard and Sutherland with the stearate ion, we have also found that many sodium or potassium salts of fatty acids such as acetic, propionic, butyric, benzoic and oleic acid, have a band in the region 1530-1570  $\text{cm}^{-1}$  (6.4-6.5  $\mu$ ) which agrees with their conclusion. The way in which the frequency associated with the carbonyl group varies in different compounds has been studied exhaustively by Mr. Trotter, and appears to lead to some very useful structural correlations which will be given later elsewhere.

The points raised by Dr. Evans about polyisobutylene and polyvinylidene chloride are interesting. I agree with him that what is required is a systematic study of how the various modes of condensation of olefinic compounds are related to the chemical and physical nature of the other radicals present such as halogen, cyano or alkyl groups. We hope shortly to undertake a planned investigation of this kind.

With regard to the other questions raised, the changes brought about in the oxidation of polythene can be very well explored by infra-red absorption, and have given interesting results.

Mr. Sheppard (Cambridge) said, in introducing his paper with Dr. Sutherland: We should like to add the following points:—

(1) The classification of C—H bond strengths by Dr. Linnett (earlier paper in this discussion) makes it unlikely that the "lone" hydrogen atom attached to the double bond in rubber could give rise to a  $\nu$  C—H absorption band at as low a wavelength as 3.1  $\mu$ , and hence it would seem

more likely that this is a weak combination frequency. An alternative explanation is that rubber contains a small number of  $C\equiv C$  triple bonds, and that it is hydrogen atoms attached to these which give rise to the absorption band at  $3.1\ \mu$ . In agreement with this the band at approximately  $5.0\ \mu$  could be interpreted as the valency vibration of such triple bonds. We are now also of the opinion that the possibility of this band being due to the hydroxyl absorption cannot be excluded.

(2) Further work has been carried out on accelerated mixes of the type A<sub>4</sub> containing larger amounts of sulphur and accelerator with the object of detecting any new bands other than those found in cured mix A<sub>1</sub>, *i.e.* of detecting any bands which can be directly related to changes in the nature of the product brought about by the use of accelerators. No such bands have been discovered, and it would seem that the use of this type of organic accelerator (mercapto benzo thiazole type) gives rise to the same final changes in the rubber molecule as does straight sulphur vulcanisation. Another result in support of this view is that the intensity of the  $10.4\ \mu$  band in a wide series of vulcanisates is clearly related to the amount of sulphur incorporated. Similar quantitative work is now in progress on the  $17.0\ \mu$  band, and on the extension of these spectra to  $30\ \mu$ .

(3) In many cases, especially when "ultra-accelerators" are used, good properties of the vulcanisate can be obtained with the incorporation of much smaller amounts of sulphur than we have discussed. This suggests the possibility that some of the changes which we have observed in the spectrum on vulcanisation may not be directly related to the important physical properties by which we characterise a vulcanised rubber, but are to be correlated with secondary physical effects. Work is now in progress on mixes in which the optimum vulcanisation properties are obtained with the minimum amounts of vulcanising agents.

Mr. J. Harvey (London) (*communicated*): It is interesting to note, from the work described in the paper of Thompson and Torkington, the introduction of a new weapon in the attack on the structure of natural and synthetic polymers, and from the evidence presented it is clear that we may expect in the near future to know very much more than we know at present of the chemical configuration of these materials.

Three points may be raised for further comment. Firstly, in connection with the degree of polymerisation of these materials, it is stated that no significant differences have been noted in the spectra of samples of polyisobutylene of different molecular weight. It is to be expected that, for polymers such as polyvinyl chloride or polystyrene, a band or bands due to end-groups should be observable, the intensity of which would give some measure of the degree of polymerisation. Moreover, the assignment of bands to end-groups might lead to an advancement of knowledge of these groups about which little information is available in many cases at the present time. Polyisobutylene, it is felt, is not a good example, for if the chain termination is a methyl group, as is possible, the effect suggested will probably not be observable.

Secondly, the section dealing with head to head or head to tail configurations is noted; it will be interesting in due course to know how far the results of the present investigations bear out the configurations put forward by Marvel and his co-workers<sup>13</sup> on the results of a chemical examination.

Finally, it is to be hoped that workers in this field will soon have an opportunity of including in their studies an examination of the so-called mixtures of polymers and plasticisers. The suggestion has been put forward<sup>14</sup> that in some cases, notably with polymers derived from monomers of the type  $CH_2=CHR$ , the interaction which takes place may include the formation of bonds of a weak chemical nature. Hydrogen bonds are

<sup>13</sup> E.g. Marvel and Riddle, *J.A.C.S.*, 1940, **61**, 2666.

<sup>14</sup> Harvey, *Distribution of Electricity*, 17, 318.

envisaged between the active groups (carboxyl groups in the case of esters such as phthalates) of the plasticiser molecule and the carbon atoms, to which the substituents are attached, in the polymer chain.

It is thought that a comparison of the absorption spectra of the separate components with those of mixtures of polymer and plasticiser may give confirmation to this hypothesis. In this study, an examination of the C—H stretching vibrations at about  $3\ \mu$  may be of use, and it is perhaps unfortunate that in only four of the spectra of vinyl-type polymers recorded, does the scale extend down to this wavelength.

**Dr. Thompson** (*communicated*): Many of the subjects referred to by Mr. Harvey have already been tackled, and work on these lines is developing rapidly. It is not possible to discuss here the results so far achieved, but these will be given in later papers.

**Dr. L. Kellner** (*London*) (*communicated*): Thompson and Torkington raise the question whether an estimate of the length of the chain can be formed from the spectra produced by compounds of varying chain length. At the present stage of theoretical treatment, there does not seem much hope that this question can be solved. I have shown in my contribution, "The C—C valency vibrations of organic molecules", that the C—C—valency vibrations of a normal chain lie between 809 and  $1143\text{ cm}^{-1}$  whatever the length of the chain. The number of frequencies within these limits increases with the number of links. The bands, therefore, crowd closer and closer together, but it is practically impossible to resolve the bands in the case of molecules of high molecular weight. On the other hand, it may not be impossible to estimate the length of a chain from the intensity of the complex band between 809 and  $1143\text{ cm}^{-1}$ . For that purpose, it would be necessary to make an experimental investigation of the influence of the number of linkages on the intensity of the corresponding bands and to calculate the total absorption between 809 and  $1143\text{ cm}^{-1}$  for every molecule under investigation. In the case of compounds containing side chains involving C—C, C—N and C—O bonds, the side chains form an integral part of the whole molecule where the vibrations are concerned. The spectrum corresponds then to that of an isomer of the normal chain with the side chains occurring at regular intervals. The case of C=O, C—H, C—Cl, etc., groups in the side chains is, of course, different since their oscillations are practically independent of the C—C frequencies of the main chain.

**Dr. Sutherland** (*Cambridge*) (*communicated*): There are two points which Mr. Sheppard and I should like to make with reference to the absorption spectra given by Mr. Torkington and Dr. Thompson for rubber vulcanised by sulphur chloride. Among the changes in the spectra which were not specifically listed by them we note that a band near  $10.4\ \mu$  gradually increases in intensity during vulcanisation. This is where we found the most marked change in the spectrum with straight sulphur vulcanisation and suggests that these two methods produce some common structural change in rubber. The second point is that since vulcanisation by sulphur chloride involves the chemical incorporation of chlorine as well as sulphur into the rubber, it is to be expected that some of the new bands may involve Cl linkages which are not essentially related to vulcanisation.

**Mr. Torkington and Dr. Thompson** (*communicated*): We agree with Mrs. Kellner that the changes in the spectrum of a long chain paraffin as the number of carbon atoms increases are very small, and give little hope of a direct determination of the chain length from the magnitudes of special types of chain frequency. We also agree with her that the mathematical treatment of such systems as vibrating groups of atoms is not yet far advanced, nor as precise as one might wish. We do not agree, however, with the approximations in the model which she would suggest for some of the molecules in attempting to compute the vibration frequencies, since it is not possible to separate the carbon-carbon oscillations

from other vibrations to the extent which she suggests. As already stated in this discussion, with Miss Simpson and Dr. Sutherland, a more exact treatment is possible for hydrocarbon molecules, and Mrs. Kellner's speculations about the strengthening of a band in the region of  $1000\text{ cm.}^{-1}$  in the case of long chain paraffins are not confirmed by the facts.

The determination of chain-lengths by other, less direct, methods, in which, for example, the estimation of end groups may be important, is being carefully explored.

---

## THE INFRA-RED ABSORPTION SPECTRA OF COALS AND COAL EXTRACTS.

BY C. G. CANNON AND G. B. B. M. SUTHERLAND

*Received 11th December, 1944.*

Although much research has been done on the structure of coals, the spectroscopic approach to this problem (at least in the infra-red) appears to have been entirely neglected. This is not surprising, as the technical difficulties encountered in obtaining the infra-red spectrum of coal are very considerable. An account of a preliminary investigation made in this laboratory has already been published:<sup>1</sup> this work showed that a discrete spectrum existed, provided the sections could be made sufficiently thin. Further investigations have confirmed that coal has a discrete spectrum with many recognisable and identifiable absorption bands. Partly because of the great difficulty in obtaining the spectrum of coal, and partly for their intrinsic interest, various extracts and products have also been examined, *viz.* pyridine extracts, pitch extracts, "shock-heater" distillates and humic acids.

### Experimental.

In general, spectra have been recorded between  $1\mu$  and  $14.5\mu$  using a rock-salt prism spectrometer of high resolving power. In order to get a reasonable transmission of radiation without opening the spectrometer slits so widely that resolving power is unduly sacrificed, the thickness of the coal should be of the order of  $0.01\text{ mm.}$  and the area of the specimen approximately  $20 \times 5\text{ mm.}$  It has so far proved impossible to obtain such films without having them prepared on a mount transparent to infra-red, *e.g.* a rock-salt or fluorite plate. The former is ideal in having no absorption between the visible and  $15\mu$  but is awkward as it precludes the use of water as a grinding lubricant and is difficult to handle even with rubber gloves; the latter will stand up to water but only transmits from the visible to about  $10\mu$ . As a mountant we have used halothene<sup>2</sup> (a halogenated polythene) which has good adhesive properties and has very low absorption over large portions of the infra-red. Canada balsam was found to be useless as a mountant, because of its heavy and complex absorption spectrum.

Solutions and liquid specimens of extracts were examined in a rock-salt cell about  $85\mu$  thick, or evaporated from the solvent to give a thin film on rock salt, or (in the case of strongly absorbing materials) squeezed between two rock-salt plates to give a capillary layer probably only a few  $\mu$  thick. Aqueous solutions have not yet been attempted as this would restrict us to the fluorite region below  $10\mu$ , and even here the absorption

<sup>1</sup> Sutherland, Fellgett and Willis, *The Ultra-fine Structure of Coals and Cokes*, B.C.U.R.A., 1943.

<sup>2</sup> We are indebted to I.C.I. (Paints) Ltd., for the halothene used in these experiments.

of the water is so strong that considerable limitations would be placed on the spectra obtainable.

A film of pyridine extract was prepared on a rock-salt plate by deposition from a pyridine solution, the solvent being removed in a vacuum dessicator. No satisfactory spectrum of the absorption of the film was obtained, although several thicknesses were tried, because the scattering of the particulate film masked all but the strongest bands.

An attempt was made to examine a finely powdered coal suspended in Nujol—a technique often very successful with solids which cannot be dissolved in suitable solvents or prepared as thin films—but the results were very disappointing. The scattering was so great, even in Nujol, that no satisfactory spectrum could be obtained.

For the preparation of thin sections it has been found that while wet grinding, followed by polishing, was the most rapid and efficacious method of getting the thickness down, the surface of such a section on drying in a vacuum desiccator became criss-crossed with fine cracks. This was, presumably, due to non-uniform shrinkage on desorption of water. Dry grinding avoided this effect, but considerably lengthened the process.

A slice of coal about 25 mm. square and between 3 and 6 mm. thick was cut from a lump, care being taken to select a region containing wide bands of vitrain (the most homogeneous of the macro-petrological constituents) and with the minimum of visible cracks or cleavage planes. One face of this rough slice was ground on successively finer grades of emery paper stretched over plate glass, the surface being rotated through 90° with each change of paper to eliminate scratches. The final polish was obtained on "selvyt" cloth (stretched over plate glass) which had been uniformly dusted with dry Goddard's Plate Powder.

After removing as much adsorbed water as possible by leaving in a vacuum dessicator for 1 day, the slice was immersed in a 20 % solution of halothene in xylene, over which the pressure was reduced with a water pump in order to fill any cracks with halothene. This process strengthened the coal and eliminated any air which would otherwise appear as bubbles when the slice was mounted on the fluorite plate. The solvent was evaporated off under a vacuum and the slice was mounted on the plate with a concentrated solution of halothene in xylene, the slice, plate and mountant being previously warmed. The coal slice was pressed on very tightly in order to give the minimum thickness of halothene, and placed in a vacuum dessicator for about 24 hours to remove the solvent. The mounted slice was then ground down on emery paper as before until it was about 0.1 mm. thick. The final polishing was carried out with great care and continued until the section looked reddish brown by transmitted light. A rough measurement of the thickness of the section was made with an accurate micrometer. The sections were kept in a dessicator to avoid adsorption of water.

The pyridine extracts were prepared by refluxing the powdered coal (-72 British Standard Sieve) with dried and redistilled pyridine for 5 hours, filtering, and concentrating by distilling off about 90 % of the pyridine. Approximately 10 % by weight of the coal was extracted by this process, and the concentrated solution used to obtain the spectrum contained 30 % by weight of the extracted "coal material."

Humic acids are prepared from coals by mild oxidation (of the finely powdered samples) with reagents such as hydrogen peroxide, alkaline potassium permanganate, etc. In this case 20 % hydrogen peroxide was used, and the humic acids formed were extracted by adding 10 % sodium hydroxide solution, filtering, and precipitating the acids with hydrochloric acid. The precipitate was filtered off, washed and dried. A 30 % solution (by weight) in pyridine was used to obtain the infra-red absorption spectrum.

The "shock-heater" films were prepared at the British Coal Utilisation Research Association Laboratories. The powdered coal was contained

in a copper boat and was "shock-heated" by passing large transient currents through filaments suspended above the coal. A high vacuum was maintained and the products were deposited on a rock-salt plate placed between the coal sample and a condensation trap cooled by solid  $\text{CO}_2$ . This film was continuous, transparent and dark reddish brown by transmitted light.

The pitch distillate extracts were supplied by Dr. A. S. C. Lawrence, who had prepared them in the following manner. The fraction boiling between  $296^\circ$  and  $326^\circ$  C. of a Metrocoalite Low Temperature Tar was extracted with petrol ether. The resinous residue (about  $\frac{2}{3}$ ) was vacuum distilled and the first fraction was a sticky oil (sample D). When this was treated with 25 % KOH, about one-third was dissolved. The recovered saponified material was distilled under atmospheric pressure and boiled between  $340^\circ$  and  $365^\circ$  forming a very viscous liquid (sample B).

### General Description of Spectra.

A representative selection has been made of the spectra so far obtained and these are reproduced in Figs. 1-5. The details of the specimens and of the conditions under which the absorptions were measured are given in Table I below. Although some work has been done on the spectra of

TABLE I.—DETAILS OF SPECIMENS AND CORRELATION WITH DIAGRAMS OF SPECTRA.

Specimen.	Absorption Conditions.	Region of Spectrum.	Figure No.
Thin section of Warwickshire Bright Coal (Ryder seam) vitrain bands	Section c. $10\mu$ thick mounted on fluorite plate with halothene	$1-10\mu$	1
Pyridine extract of Warwickshire bright coal (Ryder seam)	30 % coal material in concentrated extract. Capillary layer between rock-salt plates	$1-15\mu$	2
Humic acids prepared from Warwickshire bright coal (Ryder seam)	30 % solution in pyridine. Capillary layer between rock-salt plates	$1-15\mu$	3
"Shock-heater" vacuum distillate from Warwickshire bright coal (Ryder seam)	Thin film deposited on rock-salt plate	$1-15\mu$	4
Resinous fractions vacuum distilled from coal tar in the pitch range	Melted to give capillary layer between rock-salt plates	$1-15\mu$	5

coals of varying rank and their extracts, this work is not yet complete and we confine ourselves here to one low rank coal (Warwickshire bright coal from the Ryder seam) giving the spectrum of (1), a thin section (Fig. 1); (2) the pyridine extract (Fig. 2); (3) the humic acids (Fig. 3); and (4) a "shock-heater" distillate (Fig. 4). In Fig 5 we have reproduced the spectra again on a smaller scale to enable comparisons to be made more readily and we have added here the spectra of two pitch distillates supplied by Dr. Lawrence. In Fig. 1 the spectrum of a thin film of halothene is shown in miniature along the foot of the diagram, as halothene was the mountant used for this section. The thickness of the coal plus halothene film was about  $20\mu$  and the halothene was roughly estimated as  $10\mu$ . There are accordingly certain portions of the spectrum (above halothene bands) which are uncertain as regards intensity and these have been indicated with a broken line. Again in Figs. 2 and 3 the pyridine spectrum is shown in miniature



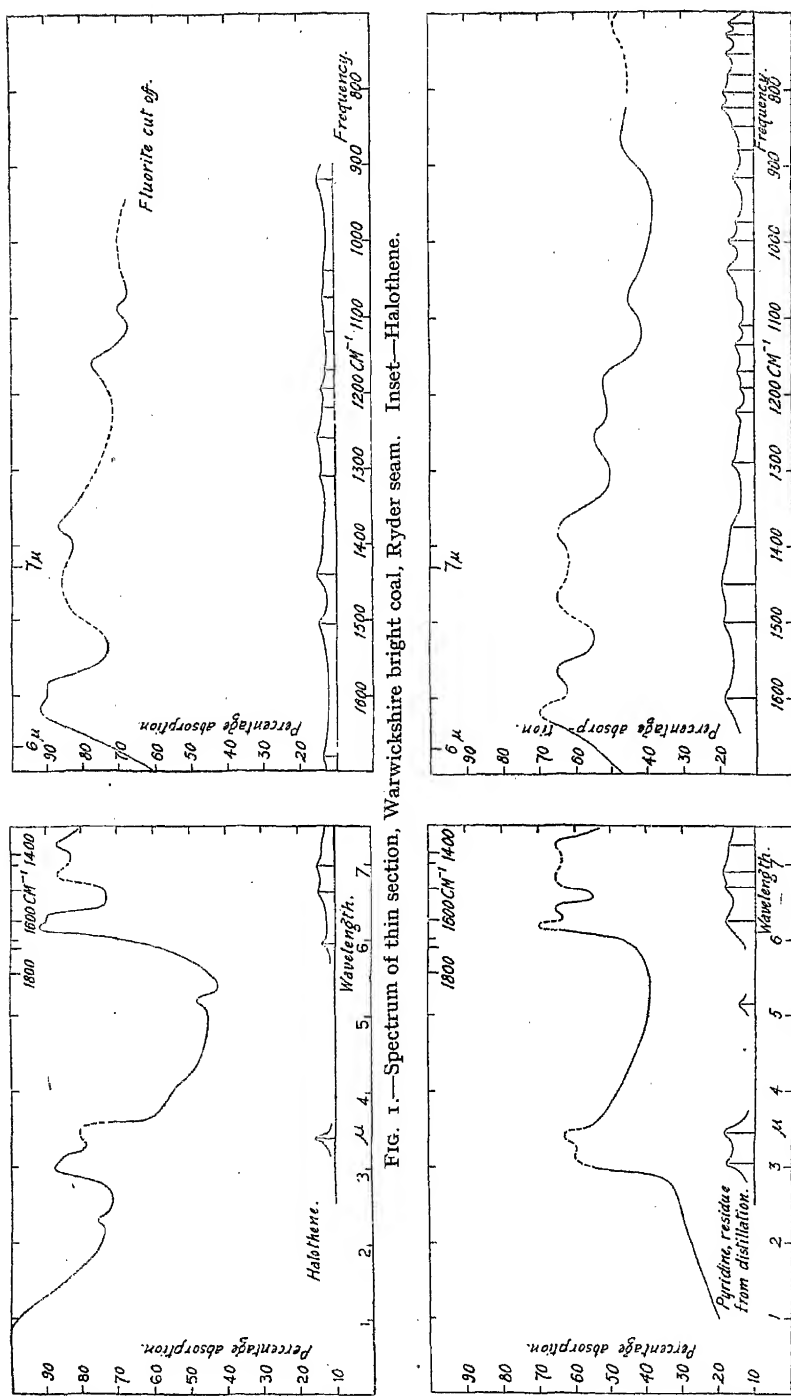


FIG. 1.—Spectrum of thin section, Warwickshire bright coal, Ryder seam. Inset—Halotheane.

FIG. 2.—Spectrum of pyridine extract, Warwickshire bright coal, Ryder seam. Inset—Residue from pyridine distillation.

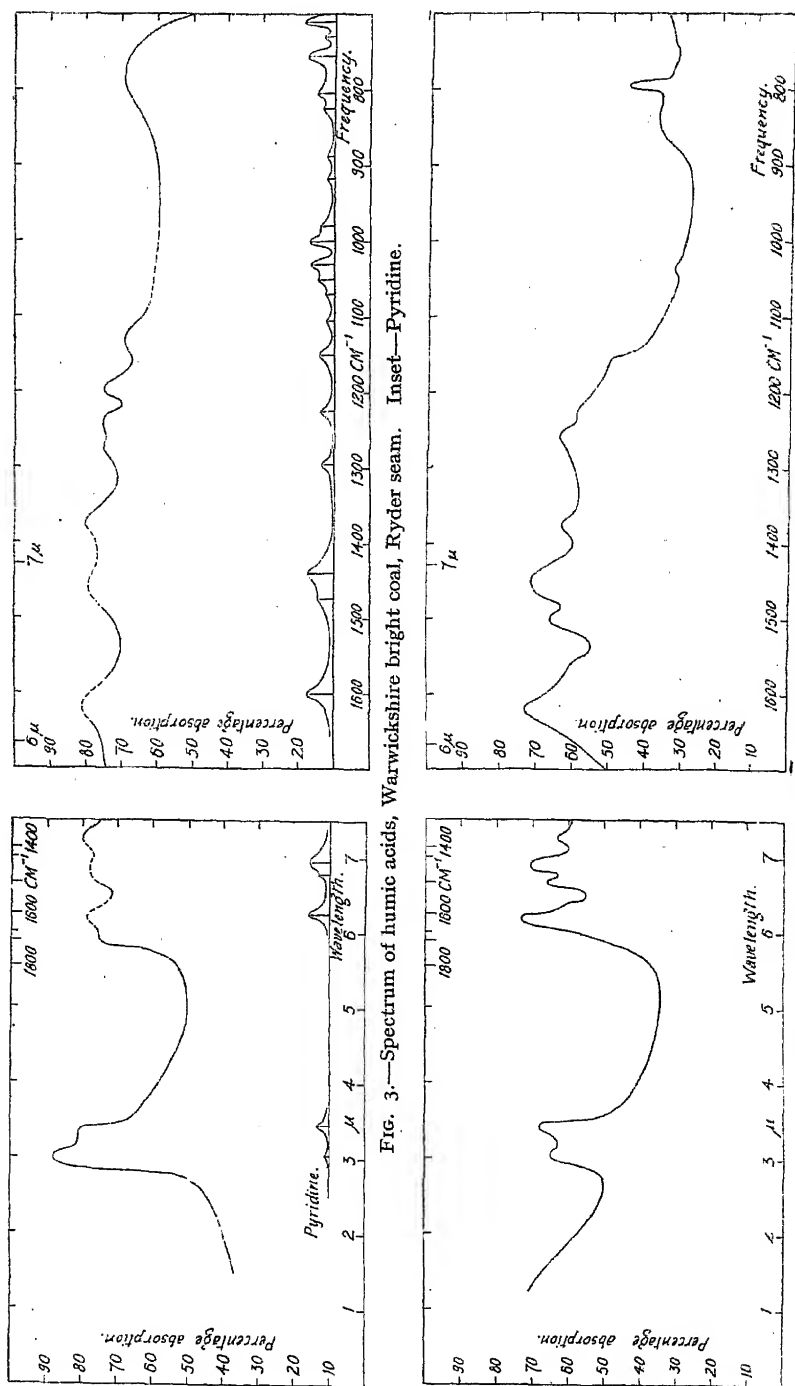


FIG. 3.—Spectrum of humic acids, Warwicksire bright coal, Ryder seam. Inset—Pyridine.

FIG. 4.—“Shock heater” film, Warwicksire bright coal, Ryder seam.

and the less certain portions of these spectra are similarly indicated. The accurate "subtraction" of the halothene and pyridine spectra is a matter of some difficulty, particularly as in the case of the spectrum in Fig. 2

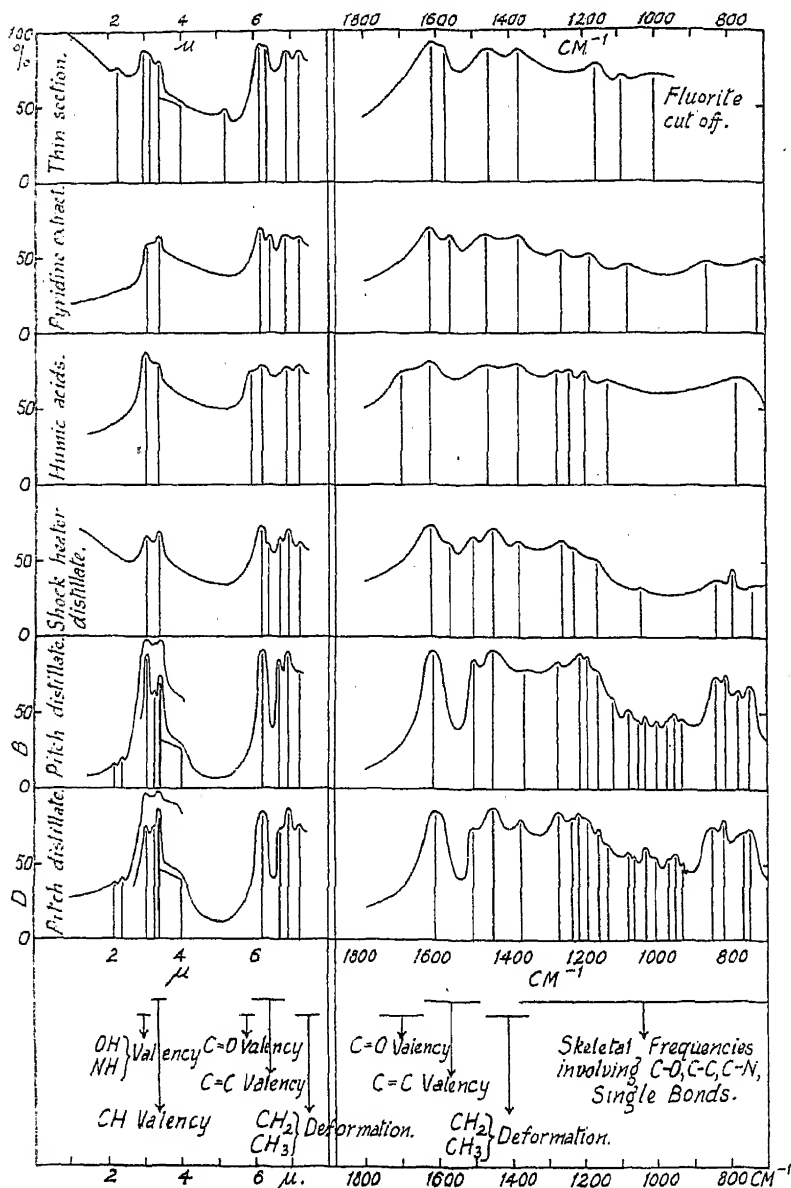


FIG. 5.—Summary of spectra (Figs. 1 to 4) and pitch distillates.

it is not the spectrum of pure pyridine which is involved but that of pyridine in which impurities have been concentrated by distillation to the same degree as in concentrating the coal extract. The pyridine used obviously contains a little impurity from the presence of the band (OH ?) at  $3\mu$ , and ( $\alpha$ -picoline ?) at  $1375\text{ cm}^{-1}$ .

The spectra have been set out partly on a linear wave-length scale (1 to  $7.5\mu$ ) and partly on a linear wave-number scale (1700 to 700  $\text{cm.}^{-1}$ , i.e. 5.7 to  $14.3\mu$ ). From a theoretical standpoint a linear wave-number scale should be used throughout, but the resolving power so far employed in the 1 to  $7.5\mu$  region hardly justifies its use at this stage since it might give a misleading impression of the accuracy in frequency determination.

### Interpretation.

The general interpretation of these spectra is straightforward but the detailed interpretation is most difficult. Following the usual lines<sup>3</sup> for complex molecules, it is easy to make certain rough assignments, viz.:

Class.	Position.	Assignment.
Hydrogenic valency vibrations . . .	$\left\{ \begin{array}{l} 3.0-3.05\mu \\ 3.2-3.5\mu \end{array} \right.$	OH... and NH... CH
Double and triple bond vibrations . . .	$\left\{ \begin{array}{l} 5.9\mu \\ 6.2\mu \\ 6.7\mu \end{array} \right.$	C=O in COOH —C=C—C=C— in aromatic ring
Hydrogenic deformation vibrations . . .	$\left\{ \begin{array}{l} 6.9\mu \\ 7.25\mu \end{array} \right.$	CH <sub>2</sub> and CH <sub>3</sub> groups CH <sub>3</sub> group

These have been indicated on Fig. 5. In the region beyond  $7.3\mu$  we are generally dealing with skeletal frequencies which cannot be assigned to particular bonds.

We shall now consider the separate regions of absorption in detail starting from the short wavelength end of the spectrum. It will be noticed that the spectra of the coal section and of the "shock-heater" distillate differ from all the others in showing a sharp rise in absorption in going from 3 to  $1\mu$ . This is almost certainly a scattering effect indicating that material must be present in both cases in the form of small particles (*cf.* the effect of carbon black on the absorption spectrum of rubber<sup>4</sup>). Further work should give an estimate of the particle size.

**The OH Valency Vibration.**—It will be noticed that the absorption band of highest frequency (of appreciable intensity) in all the spectra occurs very close to  $3\mu$  (3300  $\text{cm.}^{-1}$ ). When OH and NH bonds are present in the unassociated state, one normally observes bands near  $2.75$  and  $2.85\mu$  respectively. When association takes place the frequencies are lowered, the bands become broader and shift to  $3.0-3.3\mu$ . The band at  $3\mu$  is accordingly assigned to hydroxyl absorption with the hydrogen of the hydroxyl bonded to some other atom. There may also be some absorption due to NH bonds similarly associated (or even unassociated—*cf.* ethyleneimine<sup>5</sup> band at  $3.01\mu$ ) superimposed on the hydroxyl absorption, although the analysis<sup>6</sup> of the coal shows that this is likely to be small. It is interesting that the intensity of this OH absorption varies with respect

<sup>3</sup> *Cf.* Barnes, Gore, Liddel and Williams, *Infra-Red Spectroscopy*. Reinhold,

1944.

<sup>4</sup> Sheppard and Sutherland, accompanying paper in this discussion on Rubber.

<sup>5</sup> Thompson and Harris, *J. Chem. Soc.*, 1944, 301.

<sup>6</sup> Analysis of Warwickshire bright coal, Ryder seam (supplied by Analytical Laboratory of B.C.U.R.A.).

Volatile matter (dry ash free) . . . . .	38 per cent.
Carbon (dry mineral free, Parr's basis) . . . . .	81 "
Hydrogen " " " " . . . . .	5.0 "
Oxygen " " " " . . . . .	12.3 "
Nitrogen " " " " . . . . .	1.7 "
Approx. atomic ratios referred to oxygen = 1 . . . . .	C <sub>8.8</sub> H <sub>0.6</sub> ON <sub>0.18</sub>

to the neighbouring CH absorption at  $3.4\mu$  in the different specimens. Thus the OH/CH ratio would appear to be greater in this coal than in its pyridine extract. The humic acids show strong OH absorption in addition to COOH. The "shock-heater" distillate still shows considerable OH absorption as do the pitch distillates. It is therefore unlikely that much of this OH absorption is due to adsorbed water, although some of the difference between coal and its pyridine extract may possibly arise from this cause. Further work is required with higher resolving power to separate out any overlapping bands here before definite conclusions can be drawn.

**The CH Valency Vibrations.**—The band associated with this vibration lies adjacent to and on the long wave side of the OH frequency. It will be noticed that in the case of the pitches there appear to be two CH bands, the weaker lying at  $3.25\text{--}3.3\mu$ , the stronger at approximately  $3.4\mu$ . The coal section also shows a shoulder (at approximately  $3.2\mu$ ) on the side of the OH band, and the coal section, the pyridine extract and the humic acids all show strong absorption at  $3.4\mu$ . It may well be that the weaker absorption at  $3.2\mu$  is present in the two latter but is lost in the general high level of absorption of the two pyridine solutions. The normal position for the CH band in a saturated hydrocarbon is  $3.4\mu$ . However, in unsaturated hydrocarbons (including aromatics) some of the CH frequencies, arising from CH bonds adjacent to an unsaturated bond, occur at a shorter wavelength (*c.*  $3.25\mu$ ). The appearance of the bands around  $3.25\mu$  in the pitches and coal section is therefore an indication of some degree of unsaturation (including aromatisation). Higher resolving power is again required in order to get the full information available from this portion of the spectrum. Thus it may be possible to estimate the degree of aromatisation from an intensive study of this region.

**The C=O Frequency.**—The only spectrum showing a C=O frequency is that of the humic acid extract. The band here is at  $5.9\mu$  ( $1695\text{ cm.}^{-1}$ ), the normal position for this band in carboxylic acids.<sup>3</sup> The possibility of absorption due to C=O bonds occurring beyond  $6\mu$  and so overlapping C=C absorptions, cannot be ignored, but the absence of any strong absorption band between  $5.6$  and  $5.7\mu$  ( $1750\text{ cm.}^{-1}$ ) can be taken as a fairly definite proof that C=O in the ester form and acid anhydride form is absent from all the materials examined.

**The C=C Frequencies.**—Although it is well known that any molecule with a C=C bond has a frequency near  $1650\text{ cm.}^{-1}$  ( $6.05\mu$ ), the variation of this frequency with the environment of the bond is still a subject for investigation both on the experimental and theoretical side. From the observational side the established facts are that in simple unsaturated aliphatic hydrocarbons the frequency is remarkably constant around the value of  $1650\text{ cm.}^{-1}$ , but when conjugation occurs the frequency is lowered to about  $1600\text{ cm.}^{-1}$  ( $6.25\mu$ ). In hydrocarbons containing one benzene ring there is (with the exception of some of the simple para disubstituted benzenes) always an absorption band at this same wavelength ( $6.25\mu$ ). This is assigned to a mode of vibration of the aromatic ring, which is principally controlled by the C—C force constants. Whether the frequency persists in molecules containing several benzene rings fused together is not yet known. It might be expected to be modified to lower values as the number of condensed rings increases, and this point is now being investigated. For the present, it is reasonable to assign the band at  $1620\text{ cm.}^{-1}$  ( $6.2\mu$ ), which appears in the spectrum of coal and its extracts to the presence of simple aromatic material. It will be noticed, however, that in the spectra of the thin section, the pyridine extract and "shock-heater" distillate, there is a band at  $1575\text{ cm.}^{-1}$  ( $6.35\mu$ ). This band may either be due to some characteristic substitution or linking of the aromatic rings (*e.g.* it has been found by us in several diphenyl compounds), or it may indicate a more highly condensed aromatic component in the coal structure for which the frequency at  $1600\text{ cm.}^{-1}$  ( $6.25\mu$ )

characteristic of simpler aromatics has been lowered in the manner just indicated.

The new frequency we come to in this region is the one at  $1500\text{ cm.}^{-1}$  present in the two pitch distillates and in the "shock-heater" distillate. This is again a frequency characteristic of all the simple aromatics. It is in general much more intense than the  $1600\text{ cm.}^{-1}$  frequency and the reversal of the intensity here probably means that there is something contributing to the absorption at  $1600\text{ cm.}^{-1}$  as well as the aromatic ring (e.g. conjugated double bonds in chains or rings outside the aromatic ring). The fact that the  $1500\text{ cm.}^{-1}$  frequency has not been observed in the other spectra reproduced here should not be taken to mean that it is absent. The general level of absorption is so high in these other spectra that a weaker band might easily be masked in the thicknesses we have employed. Moreover pyridine has absorption in this region which makes the detection of this band difficult in cases where it is used as a solvent.

**CH Deformation Frequencies.**—In saturated hydrocarbons these occur close to  $1460\text{ cm.}^{-1}$  ( $6.85\mu$ ) for  $\text{CH}_2$  and  $\text{CH}_3$  groups and to  $1380\text{ cm.}^{-1}$  ( $7.25\mu$ ) for  $\text{CH}_3$  groups. When the hydrogens are attached directly to carbon atoms on a double (or conjugated double) bond, the deformation frequencies are not so constant in position and may occur with as low a frequency as  $890\text{ cm.}^{-1}$ . The correlation rules for the latter are not yet entirely clear and so we shall not consider them here. The fact that *all* the materials show strong bands very close to  $1450\text{ cm.}^{-1}$  and  $1380\text{ cm.}^{-1}$  is strong evidence for the presence of a considerable proportion of methylene and methyl groups in their component molecules. It may be significant that pitch distillate D shows the methyl group frequency more intense than pitch distillate B, but it would be premature to draw conclusions at this stage, since bands can occasionally occur at  $1375\text{ cm.}^{-1}$  which are quite unconnected with methyl groups.

**Region of Skeletal Frequencies.**—No assignments can be attempted here which would be of any value. It is interesting to note, however, that in this region the spectrum of the coal section differs from that of the pyridine extract and also from that of the "shock-heater" distillate. The spectrum of the last, while markedly different from the two former, is not dissimilar in general character to the spectra of the pitch distillates. It might seem reasonable to conclude that while the pyridine extract of coal differs spectroscopically from the parent coal, it does resemble the coal more than a distillate obtained by shock heating, but it must be remembered that in this particular case the amount of the coal extracted by the pyridine was only 10 %. Further work is required to test whether the spectra of pyridine extracts, which contain higher percentages of the coal (obtained by prolonged pressure extraction) are the same as those obtained by gentler treatment. It is important to notice that all the coal extracts and distillates (including humic acid) contain strong bands between  $1200$  and  $1250\text{ cm.}^{-1}$ , which are either not present or are much weaker in coal.<sup>7</sup> It is also probably very significant that the further one purifies the extract (e.g. pitch distillates) the greater is the number of separate absorption bands which become discernible in this region, indicating that in the parent coal and in the extracts obtained by less drastic methods, there are probably several constituents, the bands of which are smeared out into a continuum.

### General Remarks and Conclusions.

In addition to the work reported here, it may be mentioned that some thin sections of coals of higher rank have been examined and all show spectra similar to the one in Fig. 1. Although definite differences are discernible, further work is required on several more specimens to ensure

<sup>7</sup> Such bands are common to many aromatic ethers.

that these differences can be correlated with the rank of the coal. It should also be remembered that coal is by no means homogeneous, and we have, in fact, found differences between one part of a section and another. Thus progress in the spectroscopy of coal will be slow until the preparation of the sections is made easier. Another difficulty in connection with the spectra of thin sections of coal is the possibility that in grinding and polishing, the local high temperatures developed may cause some alteration in the coal material and the spectra we have obtained are really those of coal plus a thin surface film of "melted" coal. On the other hand, in the pyridine extracts of coals of various ranks, most of these difficulties are avoided. It is worth noting that the spectra of pyridine extracts of coals of varying rank were more similar than the spectra of the parent coals, indicating that similar materials are extracted by pyridine from all coals.

The general conclusion from this work is that infra-red analysis can profitably be applied to coal and its extracts. As the technique improves and as more data become available on the spectra of pure compounds, it should be possible to estimate the proportions of various groups present in coal, such as OH, C=O, CH (attached to saturated and unsaturated carbon atoms) and even degree of aromatisation. Ultimately one may hope that the basic structural unit will be identified and at least valuable information will be obtained concerning the chemical groupings present in such a unit. If there is no predominating unit in the coal structure, chemical and physical methods now being pursued will presumably enable some separation of the various units to be made and infra-red analysis will be of great value in following this separation and finally identifying the separate units.

### Summary.

Infra-red absorption spectra have been obtained with a rock-salt prism spectrometer between  $1\mu$  and  $14\mu$  for a low rank coal—

- (a) in very thin section,
- (b) in pyridine extract,
- (c) in a "shock-heater" film.

Spectra have also been obtained of humic acids from the same coal and of pitch distillates. The spectrum of this coal differs from that of its pyridine extract and its "shock-heater" distillate. The following chemical groups can be identified in these spectra, viz., OH (with hydrogen bonded), CH (aliphatic and aromatic), C=O (in humic acids) and the  $\text{—C=C—C=C—}$  in aromatic rings. Further work under higher resolving power should enable one to estimate some of these groups in coal and its extracts.

This work represents part of a programme of research on the spectra of coals carried out for the British Coal Utilisation Research Association in the laboratory of Physical Chemistry, Cambridge, by kind permission of Professor R. G. W. Norrish, F.R.S.; thanks are due to the Programmes Advisory Committee of B.C.U.R.A. for permission to publish.

The authors are also indebted to R. H. Smith (B.C.U.R.A.) for the preparation of the humic acids and the "shock-heater" film, to W. J. Edwards (B.C.U.R.A.) for advice on the preparation of thin sections, and to Dr. A. S. C. Lawrence for the pitch distillate extracts.

*Laboratory of Physical Chemistry,  
Cambridge.*

# SOME NEW PECULIARITIES IN THE INFRA-RED SPECTRUM OF DIAMOND.

BY G. B. B. M. SUTHERLAND AND H. A. WILLIS.

*Received 20th November, 1944.*

The discovery in 1934 by Robertson, Fox and Martin<sup>1</sup> of two types of diamond differing in infra-red absorption and several other physical properties, stimulated much research in this field but there is still no satisfactory explanation of the difference between the two types. Since no work has been done on the infra-red spectrum of diamond since that of Robertson, Fox and Martin,<sup>2</sup> it was considered worth while to investigate a number of new diamonds made available by Dr. R. Winstanley Lunt in connection with parallel research which he is carrying out on the mechanical properties of diamond. Although only six diamonds have so far been examined several new features have been revealed to which we should like to draw attention.

## Experimental.

Of the six diamonds examined three were Type I (V.M. 91, Ia and Ib), and three Type II (BP4, BP7 and D22) as judged by their transmission in the ultra-violet. The infra-red spectrum of each of these has been investigated with a rock salt prism instrument of high resolving power between 1 and 14  $\mu$ . The results for the type I diamonds are shown in Fig. 1. Considerable care was taken to get the intensities accurately since all these diamonds had flat parallel (octahedral) faces and it was felt that one of the few aspects not considered by Robertson, Fox and Martin<sup>1</sup> was the absolute intensities of the infra-red bands. It will be observed that the spectra of the three diamonds have the following qualitative features in common :—

- (1) Strong bands at 4.0, 4.6 and 5.0  $\mu$ .  
Strong bands at 7.78 and 8.3  $\mu$ .
- (2) Medium bands at 2.8 and 3.15  $\mu$ .  
Medium bands at 9.05  $\mu$ .

All these features, with the exception of the 9.05  $\mu$  band, were reported as common to type I diamonds by Robertson, Fox and Martin.<sup>1</sup> The bands at 7.78 and 8.3  $\mu$  are the particular ones which are absent in type II diamonds. It might be expected that the intensities of these bands, which are the distinguishing characteristic of all type I diamonds, would be proportional to the thicknesses of the specimens, but this is clearly not the case. Although in the thickest diamond VM91, (2.15 mm.) these bands are most intense, in Ia (thickness 1.205 mm.) and Ib (thickness 1.165 mm.) the intensities are anomalous in that the thinner diamond shows the greater absorption. The same is true of the 9.05  $\mu$  band and generally for wavelengths beyond 9  $\mu$ . On the other hand, for bands at wavelengths below 6  $\mu$  the intensities of the bands common to the three diamonds are related to the thicknesses of the respective diamonds in the normal way.

In addition to these quantitative differences there are several interesting qualitative differences in the spectra of these three diamonds of type I.

<sup>1</sup> R. Robertson, J. J. Fox and A. E. Martin, *Phil. Trans.*, 1934, 232, 465.

<sup>2</sup> *Ibid.*, *Proc. Roy. Soc. A*, 1936, 157A, 579.



For instance, VM91 and Ib each show a small band at  $7.27\ \mu$  which was also reported by Robertson, Fox and Martin,<sup>1</sup> whereas in Ia this band is absent but another band appears at  $7.08\ \mu$ . Again VM91 and Ib each have a weak band at  $9.9\ \mu$  (also noted by Robertson, Fox and Martin) which, however, is absent in Ia. There are other obvious differences between the three spectra in Fig. 1, but as these are of a minor character and are closer to the limit of experimental error we shall not particularise them here.

The spectra of the three type II diamonds examined are not reproduced, as the transmission of all three was never more than 1 or 2 % throughout the whole range of the spectrum with a complete blackout between  $4.5$  and  $5\ \mu$ . Whether this is a real continuous absorption or merely an

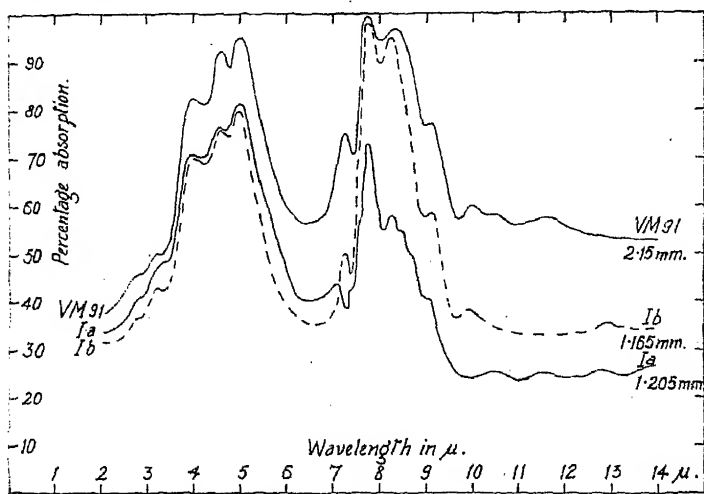


FIG. 1.—The Infra-red Absorption Spectra of Type I Diamonds of Various Thicknesses—VM 91 (2.15 mm.), Ia (1.205 mm.) and Ib (1.165 mm.)—between 1 and  $14\ \mu$ .

intense scattering effect is still to be determined. These diamonds were admittedly all very "rough" in comparison with the three of type I which had perfectly parallel faces and no imperfections in the regions used for transmission; nevertheless, it seems unlikely that scattering can entirely account for this failure to transmit over so wide a range. One of these diamonds had previously been examined by Robertson, Fox and Martin (D22, in their notation). They did not remark on this peculiarity and the only type II diamond of which they illustrate the spectrum (D2, thickness 2.09 mm.) shows about 60 % transmission in the region from 7 to  $14\ \mu$ .<sup>\*</sup> We might add that our three type II diamonds were all examined in the ultra-violet and showed the usual transmission down to  $2250\ \text{\AA}$ . although an exposure time roughly ten times that required for VM91 was needed to get comparable intensities in the regions of the spectrum where both types are free from absorption bands.

### Discussion.

Although much attention has been given to the Raman spectrum of diamond and in particular to the explanation of the strong Raman line

<sup>\*</sup> Note added in Proof.—Sir Robert Robertson has since kindly informed us that D22 gave a transmission of about 55 % in this region but that very careful positioning was required. We have not yet had an opportunity of re-checking our results.

at  $1332\text{ cm.}^{-1}$ , little consideration has been given to the detailed explanation of the infra-red spectrum since the original discussion by Robertson, Fox and Martin.<sup>1</sup> These authors suggested that the infra-red and Raman frequencies below  $7\text{ }\mu$  might be interpreted in terms of four fundamentals, viz. :—

$$\begin{aligned}\nu_1 &= 1332\text{ cm.}^{-1} \text{ (Raman)} \\ \nu_2 &= 2095\text{ cm.}^{-1} \\ \nu_3 &= 2481\text{ cm.}^{-1} \\ \nu_4 &= 84\text{ cm.}^{-1}.\end{aligned}$$

Since that time theoretical and experimental evidence has accumulated to show that the possibility of any molecule (or molecular lattice) built up from C—C single bonds having fundamental frequencies higher than  $1500\text{ cm.}^{-1}$  is extremely small. The valency vibration of the C—C bond in ethane is close to  $1000\text{ cm.}^{-1}$  and any system of identical coupled oscillators, all having such a frequency in the uncoupled state, may be expected to show a spread on either side of (at the most) a few hundred  $\text{cm.}^{-1}$ . Naturally, on the low frequency side there will also be new frequencies arising from the deformation motions of the carbon atoms in which the inter-nuclear distances are not so much affected, but in no circumstances can fundamental frequencies as high as  $2000\text{ cm.}^{-1}$  be produced.

The first step in the explanation of the vibration spectrum of diamond was the suggestion by Nath<sup>3</sup> that the Raman frequency at  $1332\text{ cm.}^{-1}$  could be interpreted as the relative vibration of the two cubic face centred lattices whose superposition gives the diamond lattice. He thus accounted for the appearance of this frequency in the Raman spectrum and its absence in the infra-red. He did not explain however, the rich infra-red spectrum nor the anomaly of type I and type II diamonds. More recently, a completely new theory of the diamond lattice has been proposed by Raman,<sup>4</sup> Bhagavantam<sup>5</sup> and Chelam<sup>6</sup> based on eight fundamental frequencies for the diamond lattice. In order to obtain agreement with observations on ultra-violet absorption,<sup>7</sup> fluorescence,<sup>8</sup> Raman spectra<sup>9</sup> and specific heat<sup>10</sup> the following values have been assigned to these eight fundamentals:

$$565, 784, 1013, 1088, 1149, 1248, 1284, 1332\text{ cm.}^{-1}$$

Without going into the details of this theory, we would point out that such an assignment leaves unexplained the prominent infra-red absorption bands at  $9.05$ ,  $8.30$  and  $7.27\text{ }\mu$ , i.e.,  $1105$ ,  $1208$  and  $1376\text{ cm.}^{-1}$ .

With reference to the differences observed between type I and type II diamonds, Raman<sup>11</sup> has recently suggested that there are four types of diamond, two having lattices with tetrahedral symmetry, the other two having lattices with octahedral symmetry. According to Raman<sup>11</sup> the characteristic frequency observed in the Raman spectrum at  $1332\text{ cm.}^{-1}$  in all diamonds will be forbidden in the infra-red of diamonds with octahedral symmetry but allowed in those with tetrahedral symmetry. Raman states that this frequency is observed in the infra-red spectra of the majority of diamonds thus associating his "tetrahedral" diamonds with the type I diamonds and his "octahedral" diamonds with type II diamonds. We would emphasise that the Raman frequency at  $1332\text{ cm.}^{-1}$  does not coincide with any strong absorption frequency in the infra-red. The maximum of the infra-red absorption in this region ( $7.78\text{ }\mu$ ) occurs at a frequency of  $1285\text{ cm.}^{-1}$  and not, as stated by Raman,<sup>11</sup> "between  $1350$  and

<sup>3</sup> N. S. N. Nath, *Proc. Ind. Acad. Sci.*, 1934, 1, 333.

<sup>4</sup> C. V. Raman, *ibid.*, 1943, 18, 237.

<sup>5</sup> S. Bhagavantam, *ibid.*, 1943, 18, 251.

<sup>6</sup> E. V. Chelam, *ibid.*, 1943, 18, 257, 327 and 334.

<sup>7</sup> K. S. Bai, *ibid.*, 1944, 19, 253.

<sup>8</sup> R. S. Krishnan, *ibid.*, 1944, 19, 216.

<sup>10</sup> B. Dayal, *ibid.*, 1944, 19, 224.

<sup>9</sup> A. Mari, *ibid.*, 1944, 19, 232.

<sup>11</sup> C. V. Raman, *ibid.*, 1944, 19, 139.

$1300 \text{ cm.}^{-1}$  ( $7.40$  and  $7.69 \mu$ ). On the other hand, weak Raman frequencies have been reported<sup>12</sup> at  $1288$  and  $1382 \text{ cm.}^{-1}$  which coincide with the infra-red frequencies of  $1285$  and  $1376 \text{ cm.}^{-1}$  within the limits of experimental error.

The differences which we have observed between the infra-red spectra of various type I diamonds might have been expected from the fact, that type I diamonds differ considerably in the ultra-violet.<sup>1, 7</sup> However, on examining these three diamonds in the ultra-violet it was found that Ia and VM91 were similar (in having bands at  $3160 \text{ \AA}$ .,  $3085 \text{ \AA}$ . and  $3064 \text{ \AA}$ ) while Ib was different (having no such bands). Thus differences in the ultra-violet do not correspond with those in the infra-red. The recent work of Rendall<sup>13</sup> has shown that a single diamond may not be uniform in its ultra-violet transmission. The same phenomenon may be anticipated in the infra-red, although it will not be possible to demonstrate it so beautifully. This aspect is now being studied. In the meantime, we would point out that the anomalies in the intensities of absorption bands common to Ia and Ib in the infra-red could be explained on these grounds if Ia had portions of type II in its structure or if there are two classes of type I having different intensity relationships in the anomalous bands.

In an interesting and valuable survey of the facts concerning the various physical characteristics of type I and type II diamonds, Lonsdale<sup>14</sup> has pointed out that X-ray work shows type I diamonds to be generally more "perfect" in structure than type II to which must be attributed a "mosaic" structure. This does not explain the difference in the infra-red spectra of the two types near  $8 \mu$  (as Dr. Lonsdale herself points out), but it might explain greater scattering by type II diamonds, which appears to be a property of the three type II diamonds examined by us. We do not propose to offer any new explanation at this stage either of the general interpretation of the vibration spectrum of diamond or of the general division into two types on spectroscopic grounds. From the new results which we report here on a few diamonds it is clear that much more experimental work is required in the infra-red to establish all the facts before embarking on fresh theories. Our purpose in this paper was to call attention to some new facts and to stress the serious discrepancies which exist at present between theory and experiment in the infra-red spectra of diamonds.

### Summary.

The infra-red absorption spectra of six diamonds have been investigated between  $1$  and  $14 \mu$  using a rock salt prism spectrometer of high resolving power. Three of the diamonds were of Type I and three of Type II. In all three type I diamonds a new absorption band has been detected at  $9.05 \mu$ , while one diamond has a new band at  $7.08 \mu$  not hitherto reported by other observers. This same diamond lacks a band at  $7.27 \mu$  common to the other two diamonds. The relative intensities of the  $8 \mu$  group of bands are anomalous in two of the type I diamonds, being more intense in the thinner specimen. Some of the discrepancies existing between the current theories of diamond structure and the infra-red absorption data are discussed.

Laboratory of Physical Chemistry,  
Cambridge.

<sup>12</sup> S. Bhagavantam, *Ind. J. Physics*, 1930 5(2), 573.

<sup>13</sup> C. R. Rendall, *Proc. Ind. Acad. Sci.*, 1944, 19, 293.

<sup>14</sup> K. Lonsdale, *Nature*, 1944, 153, 669.

## GENERAL DISCUSSION.

Sir Robert Robertson (*London*) said that on reviewing his records of the infra-red spectrum of the band about  $8\ \mu$ , he confirmed that on some diamonds of the ordinary kind (Type 1) there was a small fringe, as found by the authors, at  $9.05\ \mu$ . The wavelength difference between this and the nearest tip of the band was slightly greater,  $103\ \text{cm.}^{-1}$ , than that between the two tips,  $81\ \text{cm.}^{-1}$ , and than between the fringe on the other side of the band and the nearest tip,  $83\ \text{cm.}^{-1}$ .

He thought it would be interesting to follow up the differences in intensity of the absorption bands, but recommended duplication of the readings with different settings, the importance of which is brought out in the footnote.\*

He agreed with the authors that Raman was not justified in identifying the Raman frequently with one in the infra-red. When his work was being done such a coincidence was searched for, but his colleagues and he had rejected the identity of position, as is brought out in their main paper (reference 1).

If this is so, Raman's use of the Placzek selection rules, in his endeavour to assign different symmetries to the two types of diamond, cannot be upheld.

---

## BOND TORSION IN THE VIBRATIONS OF THE BENZENE MOLECULE.

By R. P. BELL

*Received 22nd January, 1945.*

Of the 20 fundamental vibration frequencies of the benzene molecule, 11 are active in either the Raman or the infra-red spectrum, and can be identified with certainty. Nearly all the remainder can be plausibly identified with weak lines appearing in the spectrum of liquid benzene (in violation of the selection rules), using the information obtained from the spectra of deuterated benzenes. The most recent and complete assignment is that of Pitzer and Scott.<sup>1</sup> The simplest normal co-ordinate treatment which has been carried out is that of Wilson,<sup>2</sup> using a valency-force potential function containing six constants. Wilson's numbering of the frequencies has been followed by most subsequent authors, and will be used here. His equations have been compared with the numerical data for benzene by Lord and Andrews.<sup>3</sup> For the 14 planar vibrations there are no discrepancies greater than 10%, which is as good as could be expected for a potential function without cross terms. On the other hand, the agreement is much worse for the six out-of-plane vibrations. The equations involve two force constants, one ( $h$ ) corresponding to valency bending about a single carbon atom, and the other ( $k$ ) to twisting of the benzenoid bond between two carbon atoms. Lord and Andrews used the observed values  $\nu_{10} = 849\ \text{cm.}^{-1}$ ,  $\nu_{16} = 400\ \text{cm.}^{-1}$  to obtain the two force constants, which were then used to calculate the remaining out-of-plane frequencies. The first three columns of Table I show the comparison with Pitzer and Scott's assignment.

The large discrepancies found have been attributed by some authors <sup>4</sup>

<sup>1</sup> Pitzer and Scott, *J. Amer. Chem. Soc.*, 1943, **65**, 814.

<sup>2</sup> Wilson, *Physic. Rev.*, 1934, **45**, 706.

<sup>3</sup> Lord and Andrews, *J. Physic. Chem.*, 1937, **41**, 149.

<sup>4</sup> Crawford and Edsall, *J. Chem. Physics*, 1939, **7**, 223.

to large interactions between different parts of the benzene ring. The discrepancy between  $\nu_{10}$  and  $\nu_{11}$  is particularly striking, since in Wilson's treatment both frequencies involve only the one force constant  $h$ . There is also a serious difficulty connected with the value given by Lord and Andrews for the torsional force constant  $\kappa$ . Expressed in dyne cm./radian this has the value  $4.9 \times 10^{-12}$ , while the corresponding value for ethylene, derived from the twisting frequency  $825 \text{ cm.}^{-1}$ ,<sup>5</sup> is  $1.7 \times 10^{-12}$ . It seems

TABLE I  
OBSERVED AND CALCULATED FREQUENCIES IN  $\text{CM.}^{-1}$ .

Frequency.	Observed.	Calc. (Wilson).	Error.	Calc. (Bell.).	Error.
$B_{2g} \begin{cases} \nu_4 & . & . \\ \nu_5 & . & . \end{cases}$	685 1016	538 1520	-21% +50%	610 1120	-11% +10%
$E_{1g} \nu_{10} . .$	849	(849)	—	(849)	—
$A_{2u} \nu_{11} . .$	671	783	+17%	(671)	—
$E_{2u} \begin{cases} \nu_{16} & . & . \\ \nu_{17} & . & . \end{cases}$	400 985	(400) 1160	— +18%	370 1060	-7% +8%

very unlikely that the resistance to twisting should be three times as great in the benzenoid C—C as it is in ethylene, since the benzenoid link has only partial double-bond character.

All these difficulties can be removed by taking a more reasonable physical picture of the torsional potential energy. Considering torsion of the bond  $C_2-C_3$  in Fig. 1(a), Wilson's treatment takes into account only the relative twist of the two bonds  $C_3-C_1$  and  $C_3-C_4$ . However, there is no physical justification for neglecting the relative twist of the

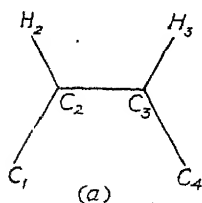


FIG. 1(a).

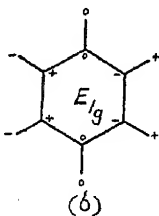


FIG. 1(b).

bonds  $C_3-H_2$  and  $C_3-H_3$ , especially since the hydrogen atoms will usually move through greater distances than the carbon atoms. If we are to use only one torsional force constant, the best measure of the net torsion about a given C—C link is  $\phi_C + \phi_H$  where  $\phi_C$  and  $\phi_H$  are respectively the relative angular

twists of the C—C and C—H bonds attached to the given link, signs being taken into account. The potential energy of the out-of-plane vibrations can then be written as

$$(1) \quad 2V = \Sigma h d^2 \mu^2 + \Sigma k' (\phi_C + \phi_H)^2$$

where  $\mu$  is the angle between a C—H link and the plane of the three adjacent carbon atoms, and  $d$  is the length of the C—H link. The equations for the frequencies are then as follows, where

$\lambda = 4\pi^2\nu^2$ ,  $a$  = radius of carbon ring,  $\beta = a/d$ ,  $Q = 4k'/3a^2$ ,  $M$  = mass of carbon atom,  $m$  = mass of hydrogen atom.

$$\begin{aligned} (2) \quad B_{2g}(\nu_4, 5) \quad & Mm\lambda^2 - \lambda[h\{M + m(\beta + 4)^2/\beta^2\} + 4Q\{M\beta^2 + m(\beta - 2)^2\}] \\ & + 144hQ = 0 \\ (3) \quad E_{1g}(\nu_{10}) \quad & Mm\lambda = (h + \beta^2Q)\{M + m(\beta + 1)^2/\beta^2\} \\ (4) \quad A_{2u}(\nu_{11}) \quad & Mm\lambda = h(M + m) \\ (5) \quad E_{2u}(\nu_{16}, 17) \quad & Mm\lambda^2 - \lambda[h\{M + m(\beta + 3)^2/\beta^2\} + 3Q\{M\beta^2 + m(\beta - 1)^2\}] \\ & + 48hQ = 0 \end{aligned}$$

<sup>5</sup> Gallaway and Barker, *J. Chem. Physics*, 1941, 10, 118.

With the exception of  $A_{2u}$ , these equations differ from those of Wilson, and in particular  $E_{1g}(\nu_{10})$  now involves the torsional constant  $Q$ . This point can be seen qualitatively from Fig. 1(b), which represents the simplest form of this degenerate vibration. There is no torsion in the carbon skeleton, which rotates as a whole without deformation, but there is a relative twist of the C—H links about four of the C—C bonds.

The force constant  $h$  is obtainable directly from (4) by putting  $\nu_{11} = 671$ , and the torsional constant can then be obtained by assuming one other frequency. We have taken  $\nu_{10} = 849$  in preference to  $\nu_{10} = 400$ , since the latter appears only in violation of the selection rules, and its assignment is less certain. This gives  $h = 2.44 \times 10^4$  dynes/cm.,  $h' = 7.7 \times 10^{-12}$  dyne cm./radian. The remaining frequencies can then be calculated from equations (2) and (5), giving the values in the last two columns of Table I. The agreement with experiment is much better than for Wilson's equations, being about as good as for the planar vibrations. It becomes even better if we re-assign some of the weak infra-red bands of liquid benzene to give  $\nu_4 = 610$ ,  $\nu_5 = 1170$ , which seems about as probable as the assignment given by Pitzer and Scott. In any case, the serious discrepancy between  $\nu_{10}$  and  $\nu_{11}$  has disappeared, and the value of the force constant for bond torsion is now physically reasonable, being about half that for ethylene. Better agreement can of course be obtained by introducing cross terms into the potential function,<sup>6</sup> but a less accurate treatment involving fewer constants may be useful for many purposes, *e.g.* for predicting the vibration frequencies and thermodynamic properties of substituted benzenes.

Equations analogous to Wilson's have been applied<sup>4</sup> to triboron triamine ( $B_3N_3H_6$ ) and there are large discrepancies for the out-of-plane vibrations closely resembling those found for benzene. It seems probable that also these discrepancies could be reduced if the torsion due to movement of the hydrogen atoms were taken into account.

*Balliol College, Oxford.*

<sup>6</sup> See, *e.g.* Bernard, Manneback and Verleysen, *Ann. Soc. Sci. Bruxelles*, 1939, 59, 376.

## Contents

	PAGE
Introduction. By the President . . . . .	171
General Introduction. By Professor C. K. Ingold . . . . .	172
Developments in the Technique of Infra-Red Spectroscopy. By G. B. B. M. Sutherland and H. W. Thompson . . . . .	174
Sources of Radiation and Absorption Cells. By H. W. Thompson and D. H. Whiffen . . . . .	180
Measurement of Cell Thickness. By G. B. B. M. Sutherland and H. A. Willis . . . . .	182
An Absorption Cell for Molten Solids and Heated Liquids. By R. E. Richards and H. W. Thompson . . . . .	183
Solvents for Use in the Infra-Red. By P. Torkington and H. W. Thompson . . . . .	184
Two Time-saving Devices in the Conversion of Energy Records into Percentage Absorption Curves. By H. A. Willis and A. R. Philpotts . . . . .	187
<i>General Discussion.</i> —Dr. W. C. Price, The President, Dr. Sutherland, Professor C. K. Ingold, Dr. Thompson, Dr. A. E. Martin, Mr. F. I. G. Rawlins . . . . .	189
The Application of Infra-Red Spectra to Chemical Problems—	
A Thermocouple-Bolometer Detector. By G. K. T. Conn . . . . .	192
<i>General Discussion.</i> —Dr. M. M. Davies, Dr. Sutherland, Dr. Conn . . . . .	196
The Use of Infra-red Absorption in Analysis—	
A. Introduction. By H. W. Thompson and G. B. B. M. Sutherland . . . . .	197
B. Examples of Analyses. By D. H. Whiffen, P. Torkington and H. W. Thompson . . . . .	200
<i>General Discussion.</i> —Dr. Sutherland, Dr. R. J. W. Le Fèvre, Dr. Thompson, Mr. Philpotts, Mr. R. R. Gordon . . . . .	206
The Assignment of the Vibrational Frequencies, and the Force Field of the Ozone Molecule. By Miss D. M. Simpson . . . . .	209
The C—C Valency Vibrations of Organic Molecules. By Lotte Kellner . . . . .	217
The Force Constants of some CH, NH and Related Bonds. By J. W. Linnett . . . . .	223
<i>General Discussion.</i> —Dr. M. M. Davies, Miss D. M. Simpson, Dr. W. C. Price, Mr. H. C. Longuet Higgins, Dr. J. W. Linnett, Dr. G. K. T. Conn, Dr. Sutherland, Dr. Thompson . . . . .	232

# CONTENTS

297

	PAGE
The Infra-Red Spectra of Fluorinated Hydrocarbons. I. By P. Torkington and H. W. Thompson . . . . .	236
General Discussion.—Dr. W. C. Price, Dr. Thompson . . . . .	246
The Infra-Red Spectra of Compounds of High Molecular Weight. By H. W. Thompson and P. Torkington . . . . .	246
Some Infra-Red Studies on the Vulcanisation of Rubber. By N. Sheppard and G. B. B. M. Sutherland . . . . .	261
General Discussion.—Dr. Sutherland, Mr. D. A. Ramsay, Mr. Harding, Dr. Thompson, Dr. H. P. Koch, Dr. Alwyn G. Evans, Dr. A. Wassermann, Mr. L. W. Marrison, Mr. Sheppard, Mr. J. Harvey, Dr. L. Kellner, Mr. Torkington . . . . .	271
The Infra-Red Absorption Spectra of Coals and Coal Extracts. By C. G. Cannon and G. B. B. M. Sutherland . . . . .	279
Some New Peculiarities in the Infra-Red Spectrum of Diamond. By G. B. B. M. Sutherland and H. A. Willis . . . . .	289
General Discussion.—Sir Robert Robertson . . . . .	293
Bond Torsion in the Vibrations of the Benzene Molecule. By R. P. Bell . . . . .	293
Author Index . . . . .	297

## AUTHOR INDEX \*

Bell, R. P., 293.	Price, W. C., 189, 233, 246.
Cannon, C. G., 279.	Ramsay, D. A., 272.
Conn, G. K. T., 192, 196, 235.	Rawlins, F. I. G., 191.
Davies, M. M., 196, 232.	Richards, R. E., 183.
Evans, A. G., 273.	Rideal, E. K., 171, 190.
Gordon, R. R., 208.	Simpson, D. M., 209, 232.
Harding, A. J., 272.	Sheppard, N., 261, 276.
Harvey, J., 277.	Robertson, R., 293.
Ingold, C. K., 172, 190.	Sutherland, G. B. B. M., 174, 181, 190,
Kellner, L., 217, 278.	196, 197, 206, 236, 261, 271, 279, 289.
Koch, H. P., 273.	Thompson, H. W., 174, 180, 183, 184,
Le Fèvre, R. J. W., 207.	190, 197, 200, 209, 236, 236, 246, 272.
Linnett, J. W., 223, 235.	Torkington, P., 184, 200, 236, 246, 278.
Longuet Higgins, H. C., 233.	Wassermann, A., 274.
Marrison, L. W., 275.	Whiffen, D. H., 180, 206.
Martin, A. E., 190.	Willis, H. A., 181, 187, 289.
Philpotts, A. R., 187, 208.	

\* Page numbers in Clarendon type indicate a paper contributed in Advance Proof for Discussion.



# RATES OF PYROLYSIS AND BOND ENERGIES OF SUBSTITUTED ORGANIC IODIDES.

## PART II.

BY E. T. BUTLER, ERNA MANDEL AND M. POLANYI.

Received 7th June, 1944.

We continue here<sup>1</sup> our account of the pyrolysis of organic iodides at low pressures and brief times of reaction. Under these conditions it is claimed that the rates are substantially determined by the primary decomposition  $RI = R + I$  and thus characterise the bond energy  $C-I$  in various compounds  $RI$ .

This paper contains data concerning the pyrolysis of (1) cyclohexyl-iodide, (2)  $\beta$ -phenylethyl-iodide, (3) *isopropyl*iodide, (4) *t*-butyl-iodide, (5) dichloriodomethane, (6) dibromiodomethane, (7)  $\beta$ -chloroethyl-iodide and (8) iodoform. For the first two of these the bond energy could be determined with considerable certainty, since the value of the activation energy was the same whether calculated as

$$Q = \frac{-RT^2 d \ln k_1}{dT} \quad (1)$$

or as

$$Q^* = 2.3 RT(13 - \log k_1) \quad (2)^*$$

where  $k_1$  is the mono-molecular rate constant (see below). For the compounds (3) to (7)  $Q$  is smaller than  $Q^*$  and the latter, which is taken to represent the bond-energy, is hence less certain. For iodoform only a rough estimate could be made.

### Experimental.

All results are expressed, as in Part I, as first-order constants  $k_1$  and  $k_{HD}$ , which must not prejudice the question of the actual kinetic mechanism involved.

The only experimental variation as compared with Part I consisted in an extended analysis of the pyrolytic products of *iso*-propyl-iodide.

For this purpose the apparatus of Fig. 1 was attached at G in Fig. 1 of our previous communication.<sup>1</sup>

An attempt was first made to separate from the reaction products any *s*-tetramethyl-ethane which might have been formed by the dimerisation of *isopropyl* radicals. The reaction products were first washed with alkali and thiosulphate, dried with  $P_2O_5$ ,

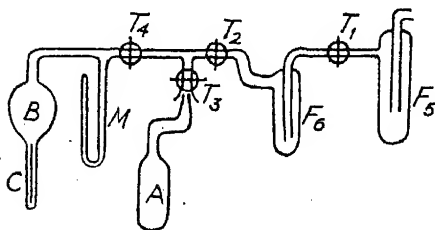


FIG. 1.

and subjected to microdistillation by the method of Benedetti-Pichler<sup>2</sup> as modified by Blumenthal.<sup>3</sup> The boiling points of the various fractions

<sup>1</sup> Butler and Polanyi, *Trans. Faraday Soc.*, 1943, 39, 19.

\* In accordance with our procedure in Part I we employ the value  $10^{13}$  for  $A$  in the equation  $k_1 = A e^{-Q^*/RT}$ .

<sup>2</sup> G etter, Niederl and Benedetti-Pichler, *Microchemie*, 1932, 11, 173.

<sup>3</sup> Blumenthal, Ph.D. Thesis, Manchester University, 1940. Submitted by Blumenthal and Herbert or publication to the *Trans. Far. Soc.*

were measured by Emich's micro-method.<sup>4</sup> In this way it was found that the distillate consisted entirely of unchanged *isopropyl* iodide, there being no *di-isopropyl* although it was estimated that 2 % could have been detected.

Analysis of the gaseous products was carried out in the following way. The hydrogen iodide was absorbed in caustic soda solution (placed in trap  $F_5$  before the beginning of the run, outgassed, and cooled in liquid air during the run). The gaseous hydrocarbons were then distilled off from the rest of the contents of  $F_5$  by warming this trap to  $-78^\circ$ , cooling  $F_5$  in liquid air and opening  $T_1$ . Complete separation was effected by alternately heating and cooling  $F_5$ ,  $T_1$  being closed while  $F_5$  was at room temperature and opened when  $F_5$  was at  $-78^\circ$ .

The hydrocarbons collected in  $F_5$  were then distilled into the bulb A containing a standard solution of bromine in aqueous KBr. Absorption of the olefines was effected by closing  $T_3$  and allowing A to warm up to room temperature with vigorous shaking. The residual bromine was titrated against standard thiosulphate. The olefine dibromide formed during the absorption was identified as propylene dibromide from its boiling point.

The remaining saturated hydrocarbons were distilled into the narrow capillary C attached to the calibrated bulb B, A being at  $-78^\circ$  and C at liquid air temperature during this process. Then  $T_4$  was closed and C allowed to warm to  $-78^\circ$  and the pressure measured in M. No increase in pressure occurred on allowing C to warm to room temperature. The saturated gas was identified as propane by measuring the vapour pressure at  $-97^\circ$  and  $-119^\circ$ .

### Discussion.

The data for the pyrolysis of cyclohexyl iodide, presented in Table I, show that this compound, like the aliphatic iodides discussed in Part I,

TABLE I.—PYROLYSIS OF CYCLOHEXYL IODIDE

Exp.	Temp. (°C.).	Total Pressure (mm.).	Iodide Pressure (mm. $\times 10^{-2}$ ).	Contact Time (sec.).	$k_I$ (sec. $^{-1} \times 10^{-2}$ ).	$k_{HI}$ (sec. $^{-1} \times 10^{-2}$ ).
50	445	4.76	2.09	1.29	0.779	—
40	445	5.35	2.55	1.11	0.632	35.9
39	445	5.06	2.85	0.622	1.25	60.8
41	445	5.79	2.73	0.565	1.04	57.8
49	445	4.79	2.86	0.053	0.944	46.2
51	429	4.81	2.68	1.32	0.462	34.7
46	429	4.50	2.74	0.714	0.480	28.8
48*	429	4.95	2.57	0.646	0.275	29.6
47	400	6.08	4.95	1.19	0.070	4.39
45	400	4.81	2.81	0.694	0.106	8.26
43	400	5.16	2.74	0.672	0.085	6.53

\* Carrier-gas : nitric oxide.

gives both free iodine and hydrogen iodide on decomposition. In fact, hydrogen iodide is in this case the predominant product, the amount formed being from 40 to 80 times that of free iodine. This prevented the investigation of the pyrolysis over a very wide range of conditions since it was essential to limit the extent of decomposition to small percentages.

<sup>4</sup> Emich, *Monatsh. Chem.*, 1917, 38, 219.

The results show that the monomolecular constants  $k_1$  at any one temperature are of the same order of reproducibility as those for *n*-propyl and *n*-butyl iodides (Part I). The variations at constant temperature are not very systematic, apart from a tendency towards lower values at the highest contact times at 445°. Replacement of nitrogen by nitric oxide as carrier-gas (Exp. 48) resulted in a rather lower value of  $k_1$ . The variations in  $k_{HI}$  are rather more considerable than those in  $k_1$  but again show no definite trend.

When  $\log k_1$  is plotted against  $1/T$  for the results in Table I (using values of  $k_1$  at a fixed contact time of approximately 0.6 sec.) and the

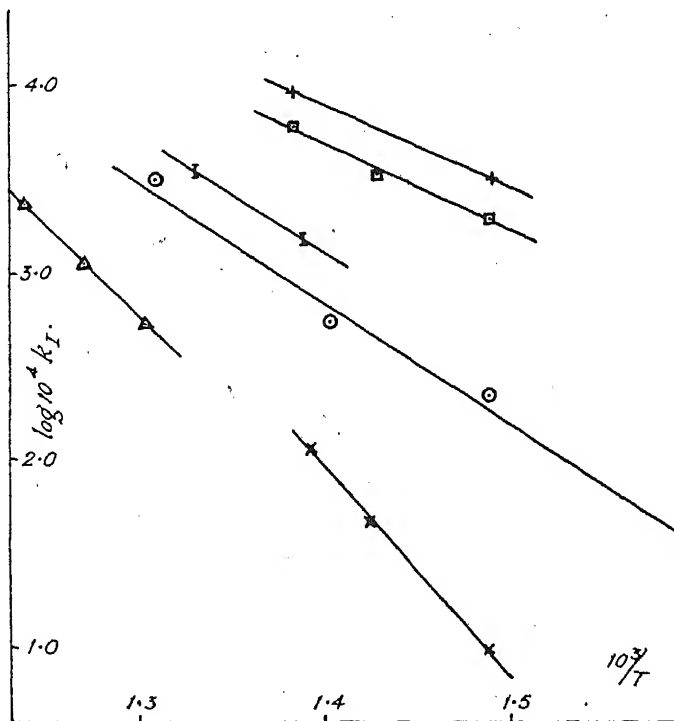


Fig. 2—Variation of rates of pyrolysis with temperature (at contact time  $\sim 0.6$  sec.).

○ Isopropyl iodide.    △ Phenylethyl iodide.    + Dibromiodomethane.  
 × Cyclohexyl.    □ Dichloriodomethane.    I Chloroethyl iodide.

best straight line drawn through the points (Fig. 2), the activation energy  $Q$  is calculated at 49.5 k.cal./mole from the slope. By the alternative method of deriving the activation energy from the equation  $k = 10^{13} e^{-\frac{Q^*}{RT}}$ , we obtain a value of 49.2 k.cal. (using  $k_1$  at the lowest temperature, 400°, and contact time 0.6 sec.).

The agreement of these two values for the activation energy proves in our opinion the assumption that the process measured is really the monomolecular disruption of the C—I bond. The fact that the reproducibility of the  $k_1$  values is not very good may again be explained by the assumption that the process  $2I = I_2$  occurs with less than 100 % yield on account of the recombination  $R + I = RI$ . In view of the coincidence between  $Q$  and  $Q^*$  the recombination cannot be extensive and it was therefore neglected in our evaluation (comp. Part I, p. 26).

Comparing the rate of pyrolysis of cyclohexyl iodide with that of isopropyl iodide at 400° given below we find the ratio of  $k_1$  for isopropyl : cyclohexyl to be 20 : 1.

Our observations for  $\beta$ -phenyl ethyl iodide (Table II) offer a similar picture to that of cyclohexyl iodide. Owing to the low volatility of this iodide no extensive variations in the reaction conditions could be undertaken. Under constant conditions the reproducibility is fairly good (compare Exps. 29 and 30 at 516°, and 28, 35 and 36 at 494°) and the variation with contact time is not very pronounced. Replacement of nitrogen by hydrogen as carrier-gas (Exps. 33 and 34) causes only a slight increase in  $k_1$  but a larger increase in  $k_{HI}$ . Comparing these results with those for *n*-propyl iodide (Part I) we find the rates  $k_1$  at 494° to be almost equal.

TABLE II.—PYROLYSIS OF  $\beta$ -PHENYLETHYL IODIDE

Exp.	Temp. (°C.).	Total Pressure (mm.).	Iodide Pressure (mm. $\times 10^{-3}$ ).	Contact Time (sec.).	$k_1$ (sec. <sup>-1</sup> $\times 10^{-2}$ ).	$k_{HI}$ (sec. <sup>-1</sup> $\times 10^{-2}$ ).
31	535	8.63	5.10	0.502	23.6	43.7
38	516	5.38	5.80	1.05	9.82	15.3
32	516	6.82	7.34	0.867	18.1	36.9
37	516	4.58	5.30	0.833	9.95	22.9
29	516	5.36	4.54	0.572	11.7	15.5
30	516	5.45	4.94	0.534	12.7	15.9
34*	516	5.09	6.72	0.479	14.9	42.2
33*	516	5.49	5.22	0.251	14.0	67.4
28	494	5.16	3.67	0.610	4.36	—
36	494	4.69	4.31	0.606	5.36	—
35	494	4.99	6.95	0.538	6.78	10.2

\* Carrier-gas: hydrogen.

In the case of phenyl ethyl iodide we again observe good agreement between the activation energies  $Q$  and  $Q^*$ ; the former (calculated from the slope of the  $\log k_1 / \frac{1}{T}$  curve is 49.5 k.cal. while the latter (from  $k_1$  taken as before at the lowest temperature and shortest time, namely at 494° and 0.6 sec.) is 50 k.cal.

Isopropyl iodide (Table III) was investigated more thoroughly than the other iodides discussed in this paper. The reason for this was that the reproducibility of the results seemed to be poorer than it was in the case of the alkyl iodides studied in Part I. Certain experiments (Nos. 6, 16, 8, 1, 7—mostly early ones) at 440° gave values of  $k_1$  about twice as high as those generally observed and have been excluded from the discussion of the effect of the variables on  $k_1$  and  $k_{HI}$ . General reproducibility—apart from the excluded experiments—is illustrated in Table III by comparison of the pairs of experiments 13 and 9, 17 and 19, 23 and 21, and is fairly good although inferior to that obtained with ethyl iodide in Part I. Influence of iodide pressure, seen by comparing Exps. 13, 9 with 17, 19 is slight, a sevenfold increase in the pressure causing a 30 % drop in  $k_1$  and a 10 % drop in  $k_{HI}$ . A three-fold increase in the total pressure (Exps. 10, 15) caused only a 30 % fall in  $k_1$ . Variation of contact time disclosed no definite trend in the values of  $k_1$  or  $k_{HI}$ .

The homogeneity of the decomposition was tested in this case by packing the reaction vessel with glass-wool, the surface area being thereby increased about tenfold (Exps. 24 and 25). This produced an increase

in  $k_1$  of only about 30 % and an even smaller rise in  $k_{HI}$  and shows that the reaction is predominantly homogeneous. The effect of replacing nitrogen as carrier-gas by deuterium and hydrogen respectively is shown in experiments 26 and 27. The result in both cases is a slight reduction in  $k_1$  which contrasts with the opposite behaviour of ethyl iodide in Part I.

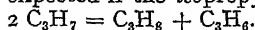
TABLE III.—PYROLYSIS OF *Isopropyl* Iodide

Exp.	Temp. (°C.).	Total Pressure (mm.).	Iodide Pressure (mm. $\times 10^{-2}$ ).	Content Time (sec.).	$k_I$ (sec. $^{-1} \times 10^{-2}$ ).	$k_{HI}$ (sec. $^{-1} \times 10^{-2}$ ).
18	492	5.23	24.2	0.571	30.7	—
6	440	6.20	52.5	2.06	11.2	—
16	440	5.96	79.0	1.86	12.5	—
8	440	11.39	24.4	0.688	11.5	—
1	440	5.74	23.6	0.675	8.71	—
7	440	4.77	29.2	0.058	12.0	—
3	400	6.19	64.3	1.60	2.00	—
2	400	5.01	27.4	0.758	2.18	—
4	400	5.29	27.0	0.055	2.1	—
12	400	6.42	4.65	2.08	1.30	2.85
14	400	4.90	3.34	0.712	1.58	2.50
11	400	5.53	3.49	0.652	1.69	2.28
5	354	7.01	19.9	0.572	0.30	—
Varying iodide pressure—						
13	440	4.79	3.46	0.689	7.10	17.5
9	440	5.00	3.58	0.655	6.60	—
17	440	5.42	23.6	0.616	4.60	—
19	440	5.50	24.6	0.597	5.04	15.2
Varying total pressure—						
15	440	6.35	10.5	1.88	3.62	—
10	440	1.98	8.11	1.45	5.88	—
Varying contact time						
22	440	6.49	25.7	1.51	8.19	18.1
17	440	5.42	23.6	0.616	4.60	—
19	440	5.50	24.6	0.597	5.04	15.2
28	440	6.19	17.6	0.580	5.75	—
23	440	6.29	25.1	0.562	5.28	12.9
21	440	6.26	25.5	0.562	5.43	15.4
20	440	6.58	22.7	0.522	5.58	7.8
Packing with glass-wool—						
24	440	5.99	26.7	0.572	7.12	19.8
25	440	6.44	25.7	1.50	8.86	18.9
Carrier-gas: D <sub>2</sub> —						
26	440	6.01	27.0	0.672	3.13	16.7
H <sub>2</sub> —						
27	440	6.45	18.0	0.436	4.78	20.1

At the lower temperature of 400° we note a thirtyfold variation of contact time in Exps. 3, 2 and 4 which leaves unaffected the value of  $k_I$ .

In Exps. 20-28 the hydrocarbon products of the decomposition were isolated and measured. They were found to consist entirely of propane and propylene, there being no trace of the *sym*-tetramethylethane which

might be expected if the direct combination of two *isopropyl* radicals occurred. The data in Table IX show that, when allowance is made for the propylene formed along with hydrogen iodide, the ratio  $I : C_3H_8 : C_3H_6$  is within the limits of experimental error 2 : 1 : 1 which is what would be expected if the *isopropyl* radicals are removed by disproportionation :



For *isopropyl* iodide the activation energy  $Q$  derived from the slope of the  $\log k_1/\frac{1}{T}$  curve (using values of  $k_1$  at contact time 0.6 sec. and com-

parable values of the other variables) is 29.2 k.cal. (see Fig. 2), which is much lower than the value  $Q^* = 46.1$  k.cal. calculated from  $k_1$  at 400°.

As in Part I (for allyl and benzyl iodide) and also in the cases of dichloroiodomethane, dibromiodomethane and  $\beta$ -chloroethyl iodide mentioned below, we here encounter the fact that when  $Q$  differs from  $Q^*$  the former is always the smaller. In our conception of the reaction this suggests that an appreciable reduction in the yield of free iodine occurs and that this effect increases at higher temperatures. Accordingly we assume that the best value for the activation energy is obtained by calculating  $Q^*$  from data observed at the lowest temperatures. This conclusion is confirmed here—as it has been in other cases mentioned in Part I—by the remarkable stability of  $k_1$  with respect to variations of contact time at the lower observational temperatures.

In Table IV we give a few results for the pyrolysis of *t*-butyl iodide. This gave an even larger proportion of HI to free iodine than cyclohexyl

TABLE IV.—PYROLYSIS OF *T*-BUTYL-IODIDE.

Exp.	Temp. (°C.).	Total Pressure (mm.).	Iodide Pressure (mm. $\times 10^{-2}$ ).	Contact Time (sec.).	$k_I$ (sec. $^{-1} \times 10^{-2}$ ).	$k_{HI}$ (sec. $^{-1} \times 10^{-2}$ ).
158	400	6.81	4.24	0.264	1.58	61.0
159	401	6.76	4.15	0.0233	4.90	366.0
154	341	7.12	4.58	0.282	0.128	—
157	345	7.21	5.68	0.261	—	40.7

iodide and was not extensively investigated. From the value of  $k_1$  at 400° we roughly estimate  $Q^*$  at 45.1 k.cal.

The rates of pyrolysis ( $k_1$ ) of ethyl, *isopropyl* and *t*-butyl iodides at 400° C. are roughly in the ratio 1 : 40 : 80.

The effect of negative substitution in the  $\alpha$ -position on the rate of pyrolysis is illustrated in Tables V and VI for the cases of dichloriodomethane and dibromiodomethane respectively. On account of the low vapour pressures of these compounds large variations in the iodide pressure could not be made. Results for the former compound show fairly good reproducibility. There is no hydrogen iodide formed and no iodine monochloride could be detected in the reaction products. At 450°  $k_1$  shows no significant variations either with contact time or iodide pressure. The results at 400° are less accurate on account of the smaller amount of free iodine formed and the reproducibility is not so good. Dibromiodomethane gave less reproducible results; there is no marked variation of  $k_1$  with iodide pressure but a reduction occurs at the highest contact times, both at 450° and 398°. Comparison of the rates of pyrolysis  $k_1$  at 450°, ethyl iodine : dichloriodomethane : dibromiodomethane = 1 : 100 : 160, shows that negative substitution in this position causes a large increase in rate.

The activation energies  $Q$  for dichloriodomethane and dibromiodomethane derived from the temperature coefficient (Fig. 2) are 19 and 20

k.cal. respectively, both of which are much lower than the corresponding values of  $Q^*$  calculated from  $k_1$  at  $400^\circ$  which are 42.4 and 41.4 respectively. This behaviour has been discussed above in the similar case of isopropyl iodide.

TABLE V.—PYROLYSIS OF DICHLOROIODOMETHANE.

Exp.	Temp. (°C.).	Total Pressure (mm.).	Iodide Pressure (mm. $\times 10^{-1}$ ).	Contact Time (sec.).	$k$ (sec. $^{-1} \times 10^{-2}$ ).
67	450	4.51	4.40	1.32	48.6
63	450	5.74	0.808	1.25	47.0
62	450	4.89	1.77	0.808	56.6
66	450	4.15	0.700	0.793	58.0
65	450	4.56	1.00	0.717	59.7
58	450	4.57	1.04	0.677	61.8
64	428	4.39	1.09	0.779	29.8
61	428	5.11	1.10	0.662	32.9
59	428	5.63	0.714	0.602	34.0
55	400	3.57	1.03	1.69	13.9
53	400	4.54	0.952	0.707	17.6
50	400	5.89	0.798	0.633	16.1
54	400	5.72	0.687	0.618	22.5
55	400	5.12	1.61	0.055	24.0

TABLE VI.—PYROLYSIS OF DIBROMOIODOMETHANE.

Exp.	Temp. (°C.).	Total Pressure (mm.).	Iodide Pressure (mm. $\times 10^{-2}$ ).	Contact Time (sec.).	$k_I$ (sec. $^{-1} \times 10^{-2}$ ).
68	450	3.93	10.9	1.38	61.6
73	450	4.96	1.68	1.27	54.9
72	450	4.84	1.44	0.680	80.8
69	450	5.49	3.38	0.593	98.6
71	450	5.45	3.59	0.052	104
74	398	4.16	1.56	1.50	10.5
75	398	4.18	1.40	0.820	26.9
7	398	5.58	3.91	0.630	32.9

TABLE VII.—PYROLYSIS OF  $\beta$ -CHLOROETHYL IODIDE

Exp.	Temp. (°C.).	Total Pressure (mm.).	Iodide Pressure (mm. $\times 10^{-1}$ ).	Contact Time (sec.).	$k_I$ (sec. $^{-1} \times 10^{-2}$ ).	$k_{HI}$ (sec. $^{-1} \times 10^{-2}$ ).
83	478	6.15	1.35	0.612	33.8	32.0
87	448	5.13	2.39	1.18	15.5	5.82
85	448	7.25	2.59	1.01	15.6	5.80
84	448	6.19	1.71	0.647	13.3	4.69
86	448	6.18	1.04	0.048	11.5	3.46

Negative substitution in the  $\beta$ -position is illustrated by the results for  $\beta$ -chloroethyl iodide (Table VII). The rate constants  $k_I$  and  $k_{HI}$  at  $448^\circ$  are quite reproducible and show no definite variation with contact time.

The value of  $k_I$  at  $448^\circ$  is about 30 times that of ethyl iodide.  $Q$  has the value 30 k.cal., while  $Q^*$  at  $448^\circ$  is 45.9 k.cal. The difference between these is less than it is in the case of the  $\alpha$ -substituted iodides, and may indicate a smaller reduction in yield of iodine by the recombination reaction.

A few results for iodoform are appended in Table VIII. These were irreproducible, and the fact that much carbon was deposited in the reaction

TABLE VIII.—PYROLYSIS OF IODOFORM.

Exp.	Temp. ( $^\circ\text{C}$ .)	Total Pressure (mm.)	Iodide Pressure (mm. $\times 10^{-1}$ .)	Contact Time (sec.)	$k_I$ (sec. $^{-1} \times 10^{-2}$ .)
78	303	6.49	2.84	0.710	13.9
82	296.5	7.20	8.80	1.23	0.354
79	296.5	5.07	5.20	0.853	4.83
80	296.5	7.21	5.31	0.765	1.92
81	291	5.85	3.40	0.777	0.83

TABLE IX.—PRODUCTS OF PYROLYSIS OF ISOPROPYL IODIDE.

Exp.	$\frac{I}{RI}$	$\frac{HI}{RI}$	$\frac{C_3H_8}{RI}$	$\frac{C_3H_6}{RI}$	$\frac{C_3H_6-HI^*}{RI}$
	mole %				
20	3.26	5.85	(0.70)	8.09	(2.24)
21	3.22	8.27	1.32	9.00	(0.73)
22	12.56	25.0	5.95	29.2	4.2
23	3.30	7.79	1.54	9.18	1.39
24	4.30	11.3	2.06	13.6	2.3
25	13.10	26.0	7.05	35.4	9.4
26	2.12	10.75	1.46	12.6	1.8
27	2.42	9.81	1.56	10.9	1.1

\* This is the amount of propylene formed by disproportionation.

TABLE X

Iodide.	$Q^*$ k.cal.	$k(430) \times 10^{-5}$ .	$T(1\%/\text{sec.})$ .
Ethyl . . . .	52.2	50	489
isoPropyl . . . .	46.1	4,000	398
tert-Butyl . . . .	45.1	9,000	385
Cyclohexyl . . . .	49.2	470	443
$\beta$ -phenylethyl . . . .	50.0	270	456
Dichloromethyl . . . .	42.4	32,000	343
Dibromomethyl . . . .	41.4	70,000	329
Di-iodomethyl . . . .	(37)	(3,000,000)	(266)
$\beta$ -Chloroethyl . . . .	45.9	2,500	395

vessel during the pyrolysis suggests that more than one iodine atom is removed per iodoform molecule. The results at the lowest temperature ( $303^\circ$ ) suggest that  $Q^*$  is about 37 k.cal.

### Discussion of Bond Energies.

In Table X we have reproduced the results for ethyl iodide from the previous paper. According to the foregoing discussion only the values for cyclohexyl and  $\beta$ -phenyl ethyl iodide can be claimed as correct, while



the others may be somewhat larger than the true values on account of an appreciable reduction of the decomposition due to recombination.

Apart from this recombination we may mention the possibility that part of the hydrogeniodide formed results from a secondary reaction of iodine atoms with the free radicals. However, in the cases in which  $Q$  and  $Q^*$  agree, there is no room for such an assumption. Nor can this assumption generally explain that  $Q$  is sometimes smaller than  $Q^*$  since this happens in cases ( $\alpha$ -halogenomethyl iodides as well as allyl and benzyl iodide in Part I) where no  $H-I$  is formed. It does not seem profitable therefore to pursue this possibility here any further.

Of the observed reductions of the  $C-I$  bond energies listed in the table, the case of *iso*-propyl and *t*-butyl have already been discussed in Part I by reference to hyper-conjugation. We note that the  $C-I$  bond strength in phenylethyl iodide is about the same as that of *n*-propyl iodide, which appears fairly reasonable from the point of view of hyper-conjugation. On the other hand the case of cyclohexyliodide seems curious since one would expect the bond to be very noticeably weaker than in *n*-propyl iodide, in view of the joining together of two chains—both longer even than the propyl chain—at the  $\alpha$ -carbon.

The observed weakening effect of negative substitution on the bond strength deserves special emphasis. No indication of this had been present in the literature, apart from the analogous cases of acetyl and acetyl iodide described in Part I. The resonance picture given there for the effect of oxygen may be applied as well to the case of halogen.

The effect of negative substituents in an organic halide on the reactivity of the halogen atom with Na-vapour has been discussed theoretically by Evans and Polanyi.<sup>5</sup> There should always be present an increase in the rate of reaction beyond that which could be caused by bond weakening. There is no sufficient ground to apply this theory to the cases of dihalogenation investigated in the present paper; but the situation presented by dihalogenation has been successfully discussed from a similar point of view in a recent paper by A. G. Evans and H. Walker.<sup>6</sup>

*The University,  
Manchester.*

<sup>5</sup> *Nature*, 1941, 148, 436.

<sup>6</sup> A. G. Evans and H. Walker, *Trans. Faraday Soc.*, 1944, 40, 384.

## THE SOLUBILITY OF HYDROGEN IN ZIRCONIUM AND ZIRCONIUM-OXYGEN SOLID SOLUTIONS.

BY (MRS.) M. N. A. HALL, S. L. H. MARTIN AND A. L. G. REES.

*Received 6th November, 1944.*

No satisfactory and complete data on the solubility of hydrogen in zirconium are available, although the large capacity of this metal for hydrogen has been established for some time.<sup>1</sup> This capacity for dissolving large quantities of hydrogen is a common feature of a number of metals, including Pd, V, Th, Ti, Ta and the rare earth metals. Of these hydrogen-enriched metals\* the palladium-hydrogen system alone has

<sup>1</sup> Winkler, *Ber.*, 1890, 23, 2041.

\* Sieverts and Gotta<sup>2</sup> termed these "half-metallic" hydrides (i.e. hydrides retaining some physical metallic appearances and properties), intermediate between the "salt-like" hydrides of Na, Ca, etc. (which are well-characterised compounds) and the purely "metallic" hydrides of Fe, Co, Ni, Pt, etc. (which retain most fully the properties of the metals). Ubbelohde (*Proc. Roy. Soc., A*,

been studied in any detail.<sup>2</sup> For zirconium, Sieverts and Roell<sup>3</sup> have determined isobars at 760 mm. pressure and the isotherms for 800° and 1100° C. on a powder containing 91 % zirconium metal, but they could obtain neither consistency nor reproducibility. The maximum solubility attained corresponded to a composition of  $\text{ZrH}_{1.75}$ . Later, however, Sieverts, Gotta and Halberstadt<sup>4</sup> obtained compositions  $\text{ZrH}_{1.92-1.95}$  with samples of ductile metal. This system is also of interest from another point of view; recent experiments on the paramagnetic susceptibility have shown that the 4d band of zirconium becomes filled at compositions approximating to  $\text{ZrH}_2$ .<sup>5</sup>

In the present paper an account of an investigation into the solubility of hydrogen in zirconium is given. Furthermore, as it was found in the course of our experiments that oxygen had a profound effect on the characteristics of hydrogen sorption, a systematic study of the effect was made. In this respect de Boer and Fast<sup>6</sup> have shown that oxygen forms true solid solutions with zirconium up to 40 atom % at least.

### Experimental.

Preliminary experiments showed the behaviour of zirconium towards hydrogen to follow that described in the literature, surface contamination, particularly with oxygen and nitrogen, retarding, or even completely inhibiting, the sorption of hydrogen at the lower temperatures. It was found also that the presence of oxygen dissolved in the zirconium produced radical changes in the sorption.

The system was studied isothermally over the pressure range 1-760 mm., at temperatures between room temperature and 1050° C. and for oxygen contents from 0.50 atom %. Isotherms were determined with increasing pressures by the addition of measured amounts of hydrogen to the reaction vessel.

The principle of the method of measurement was essentially that used by earlier workers<sup>7</sup> in cases involving large solubilities, but the apparatus was somewhat modified. It was constructed of soft glass, the vacuum taps and ground joints being lubricated with previously degassed Apiezon "N" grease which has an exceedingly low vapour pressure at room temperature. The clear silica reaction vessel was connected to the apparatus by a silica-to-glass ground joint carefully screened from radiant heat and some 9 ins. from the furnace which had a long uniform temperature zone. To maintain constant volume and prevent the introduction of mercury vapour or dissolved gases from the mercury, a glass Bourdon gauge<sup>8</sup> was used as a null instrument for measuring gas pressures, the external balancing pressures being read on a wide-bore mercury manometer. Pressure measurements could be made to  $\pm 0.3$  mm. Large glass bulbs attached to the system served as hydrogen storage vessels. The apparatus could be evacuated to  $10^{-6}$  mm. Hg with a mercury diffusion pump backed by a rotary oil pump, an intervening liquid air trap preventing the entry of mercury vapour into the apparatus. The glass parts were as far as possible degassed by frequent torching while pumping. External

1937, 159, 195) on the other hand has considered them as alloys of the metal with metallic hydrogen. For the present purposes we will, however, refer to the "zirconium-hydrogen system" and consider the term "solution" in its broadest sense including the formation of true solid solutions, distinct phases and/or compounds. (See also Smithells 1937, *Gases and Metals*, p. 139.)

<sup>2</sup> Sieverts and Gotta, *Z. anorg. Chem.*, 1928, 172, 1.

<sup>3</sup> Sieverts and Roell, *ibid.*, 1926, 153, 289.

<sup>4</sup> Sieverts, Gotta and Halberstadt, *ibid.*, 1930, 187, 155.

<sup>5</sup> Fitzwilliam, Kaufmann and Squire, *J. Chem. Physics*, 1941, 9, 678.

<sup>6</sup> de Boer and Fast, *Rec. trav. chim.*, 1940, 59, 161.

<sup>7</sup> Sieverts, *Z. Metallk.*, 1929, 21, 37.

<sup>8</sup> Farkas and Melville, *Experimental Methods in Gas Reactions*, London, 1939, p. 85.

furnace temperatures were measured to  $\pm 3^\circ \text{C}$ . with a calibrated Pt/Pt-Rh thermocouple situated immediately against the reaction vessel.

Relevant volumes were calibrated manometrically by expansion from a known volume. The correction factors necessary for calculating hydrogen unabsorbed at equilibrium from observed pressures were determined for the relevant temperature and pressure ranges using hydrogen in the absence of zirconium, since the temperature gradient between the reaction vessel and the remainder of the system made unreliable their consideration as two component volumes at distinct temperatures. The external temperatures as read were calibrated against those registered by a similar thermocouple placed inside the tube in air, to correct for differences due to heat conduction along the silica tube.

### Materials.

(i) **Hydrogen.**—Cylinder hydrogen was purified by passing at the rate of  $\sim 30 \text{ cm}^3/\text{minute}$  through a layer of palladised asbestos at  $\sim 140^\circ \text{C}$ ., a liquid air trap, and a layer of zirconium powder at  $1000^\circ \text{C}$ . to ensure removal of last traces of oxygen and nitrogen.

(ii) **Oxygen.**—Spectrally pure oxygen (British Oxygen Co.) was used throughout.

TABLE I.  
ANALYTICAL DATA FOR ZIRCONIUM SAMPLES.

	A.	B.	C.	D.
Zirconium + Hafnium (as Zirconium) . . . .	99.0	97.8	92.8	85.2
Other metals (Fe, Mg, Ti, Al) . . . . .	0.10	0.31	3.0	1.53
Oxygen . . . . .	0.4	1.0	3.2	11.7
Hydrogen . . . . .	< 0.05	< 0.05	0.5	0.4
Carbon . . . . .	< 0.05	0.36	0.30	0.30
Water . . . . .	—	—	0.0	0.9
Total . . . . .	99.5	99.47	99.8	100.0

(iii) **Zirconium.**—The samples available were: (A) compact ductile metal, (B) wire of  $120\mu$  diameter (both thoroughly polished and degreased before use), (C) and (D) powders from two different sources. Both (A) and (B) had been obtained by deposition of the metal from  $\text{ZrI}_4$  in the vapour phase, (C) by the high temperature reduction of  $\text{K}_2\text{ZrF}_6$  with metallic Na, and (D) by the reduction of  $\text{ZrO}_2$  with Na and Mg.<sup>9</sup> On a basis of spectrographic analyses, the four samples were completely analysed chemically, except for Hf which was present in all. A Hf content of 0.5 atom % ( $\sim 1\%$  Hf) previously given for Zr from the same source<sup>6</sup> has been accepted for our purposes. As Hf also absorbs large quantities of hydrogen, the use of a value for Zr + Hf expressed as Zr does not materially affect our results. From the analytical data given in Table I,\* sample (A) is seen to be the purest, the most significant difference being in the oxygen contents of the four samples.

<sup>9</sup> de Boer, *Ind. Eng. Chem.*, 1927, 19, 1256.

\* The determination of Hf as Zr would tend to give total analyses here 0.5 % less than 100 % (1 % Hf  $\approx$  0.51 % Zr by weight). The relative impurity of (C) and (D) might on the other hand bias their totals to 100 %. Our main results are, however, based on the purer samples (A) and (B), the O and C in which were probably introduced during the rolling and drawing processes through the surface.

### Procedure.

Zirconium samples (0.5-1.0 g.) were contained in narrow porcelain boats and placed in the reaction vessel well within the uniform temperature zone of the furnace. To prevent surface contamination of the sample through its gettering action on the system, the reaction vessel was first evacuated to  $\sim 10^{-5}$  mm. Hg at room temperature, twice flushed with hydrogen, and heated to  $1050^{\circ}$  C. in a small pressure of hydrogen. The sample was then degassed at this temperature for 15-30 minutes, shut off from the pumps and cooled to the required temperature. In between isotherms the samples were always heated to  $1050^{\circ}$  before being opened to the pumps.

For experiments on the effect of oxygen, sample (B) was used, as sufficient of (A) was not available and preliminary experiments had shown that it was difficult to secure complete homogeneous distribution of the oxygen in the powder sample (C), which was moreover relatively impure. A new sample was used for each set of isotherms at a particular oxygen content. The sample was degassed in the usual manner, kept at  $900^{\circ}$  C., and over a period of 2 to 4 hours allowed to absorb completely successive small portions of oxygen admitted from a known amount. Finally, to ensure homogeneity, it was heated for 8-11 hours at  $950^{\circ}$ , when the residual oxygen pressure was  $< 10^{-4}$  mm. X-ray analysis of samples containing up to 36 atoms % oxygen proved the oxygen to be in true solid solution, in agreement with the observations of de Boer and Fast.<sup>6</sup> A check analysis of the oxygen content in one case gave 15.3 % compared with 15.0 % calculated from the volume added.

For hydrogen sorption, the criterion used for the establishment of equilibrium (which was relatively rapid, never requiring more than 30 mins. for any point), was that the pressure change over ten minutes should not be greater than 0.3 mm.

### Accuracy and Probable Errors.

An accuracy of 1 % is indicated from the pressure and volume measurements, but other possible sources of error are :—

- (i) Non-homogeneity of sample.
- (ii) Analytical errors.
- (iii) Incomplete degassing of samples. Since isotherms at  $\sim 1000^{\circ}$  C. indicate an equilibrium pressure of  $\sim 1$  mm. for the absorption of  $\sim 1$  cm.<sup>3</sup>/g. Zr, this appears an unlikely source.
- (iv) Introduction of traces of impurity (oxygen and nitrogen) during vacuum treatment or from hydrogen. At the slightest indication of contamination the experiments were stopped and a new sample taken.
- (v) Absorption of hydrogen by components of the apparatus or its diffusion through the silica at high temperature. Blank tests up to  $1000^{\circ}$  C. showed these effects to be negligible. At the highest temperatures the amount of hydrogen remaining in the gas phase equalled that originally added to within  $\pm 1$  cm.<sup>3</sup> in a total volume of some 700 cm.<sup>3</sup>. These tests served also to check the volume and pressure calibrations.
- (vi) An uncertainty of about  $\pm 5^{\circ}$  C. in the furnace temperatures at the higher temperatures.

The extent of the reproducibility is perhaps best indicated by those absorption isotherms in the figures which were repeated two or more times. In Fig. 1 the two  $750^{\circ}$  C. isotherms were obtained with the same sample after an interval of 16 days during which some 12 other isotherms had been determined. Duplicate sets of points are shown for the isotherms at  $750^{\circ}$  C. (four sets for three different samples)  $850^{\circ}$  and  $950^{\circ}$  in Fig. 2, at  $850^{\circ}$  (different samples) in Fig. 3, at  $565^{\circ}$ ,  $750^{\circ}$  and  $850^{\circ}$  in Fig. 6,  $750^{\circ}$  C. in Fig. 8, and  $850^{\circ}$  C. in Fig. 9.

## Results.

The isotherms are represented graphically in Figs. 1 to 3 and 5 to 9, whilst the isobars for samples (A), (B) and (C) at 760 mm. pressure are given in Fig. 4, and those for all samples at 500 mm. pressure in Fig. 10. The solubilities are expressed throughout as  $\text{cm}^3$  hydrogen at N.T.P./g.  $\text{Zr} + \text{Hf}$  (determined as Zr) actually present in the sample. Even with

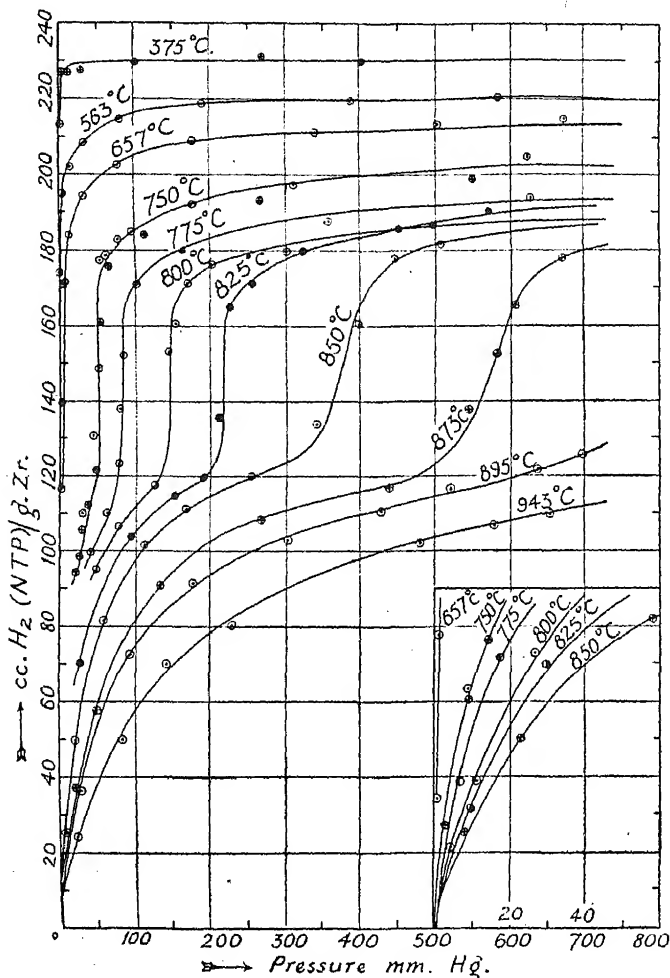


FIG. 1.—Isotherms for compact Zr sample A; 0.023 atom Oxygen per atom Zr. Whole series on same sample of 0.04093 gm., with duplicate sets of points for 750° C.

*Inset.*—Initial portions of isotherms on expanded pressure scale.

the powder samples, the isotherms below 350° C. were invariably slower to reach equilibrium saturation than those above this temperature. However, a satisfactory value for the saturation solubility at room temperature could be obtained by allowing the zirconium to cool slowly (over a period of 12-15 hours) in a high pressure of hydrogen. The results for sample (A) are given in Table II.

A saturation value of  $240 \text{ cm.}^3/\text{g. Zr}$  was thus indicated for  $20^\circ \text{C.}$ , corresponding to  $\text{ZrH}_{1.95}$ . For sample (B), values of  $234\text{--}238 \text{ cm.}^3/\text{g.}$  at pressures from  $550\text{--}650 \text{ mm.}$  were obtained, indicating a mean value of  $236 \text{ cm.}^3/\text{g.}$  at  $20^\circ \text{C.}$

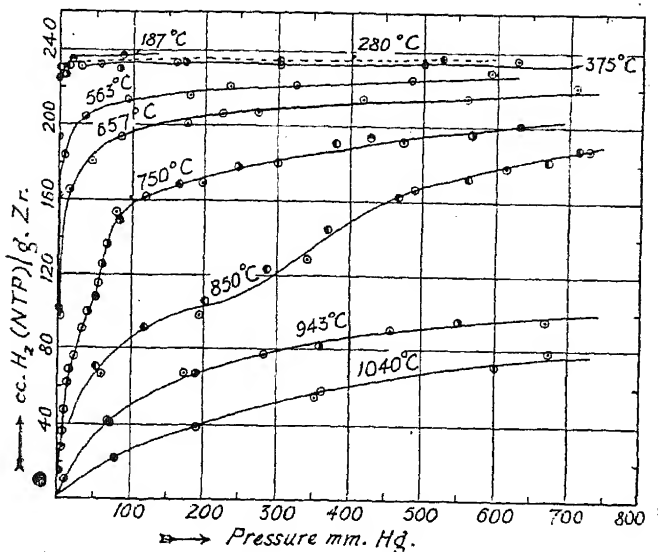


FIG. 2.—Isotherms for ductile Zr wire sample B;  $0.058$  atom oxygen per atom Zr.

$750^\circ \text{C.}$  :  $\circ, \bullet$  1st isotherms on  $0.5 \text{ gm.}$   
 $\bullet$  2nd isotherm on  $0.25 \text{ gm.}$   
 $\bullet$  2nd " on  $0.5 \text{ gm.}$

$850^\circ$  and  $943^\circ \text{C.}$  : Duplicate sets on separate  $0.5 \text{ gm.}$  samples.

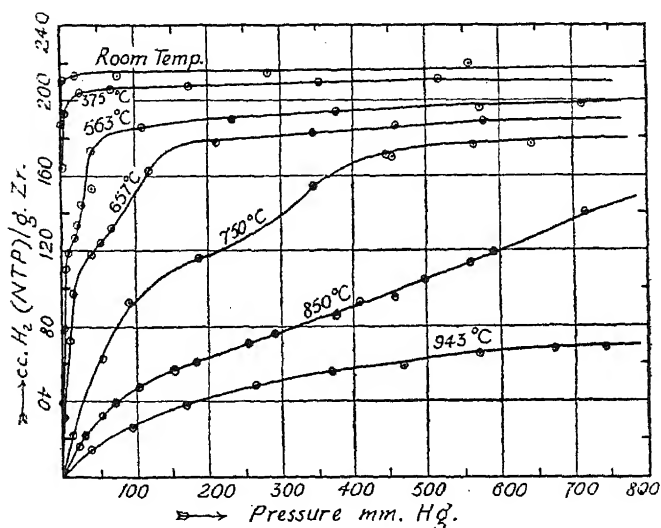


FIG. 3.—Isotherms for Zr powder sample C;  $0.196$  atom oxygen per atom Zr. Each isotherm on separate  $1 \text{ gm.}$  sample.

Desorption experiments on samples (B) and (D) demonstrated the existence of hysteresis, illustrated in Figs. 6 and 9. This phenomenon was not fully investigated but did occur consistently at all temperatures with sample (D).

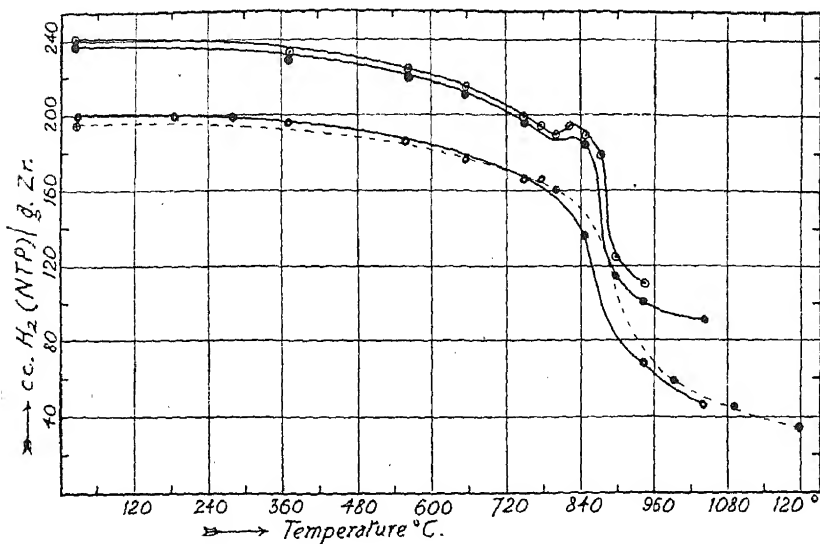


FIG. 4.—Isobars at 760 mm. Hg pressure for different samples.

- Sample A—0.023 atom oxygen per atom Zr.
- " B—0.058 " " "
- ⊙ " C—0.196 " " "
- ⊗ Results of Sieverts and Roell<sup>3</sup>.

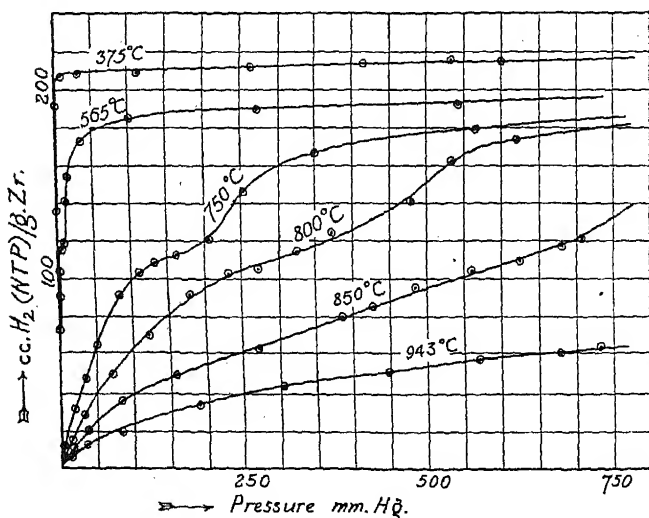


FIG. 5.—Isotherms for Zr wire Sample B + 2.44 % O<sub>2</sub>; 0.190 atom oxygen per atom Zr. All on same preparation.

## General Remarks and Discussion.

With all samples, there was a noticeable diffusion of the Zr metal into the porcelain boats; this was particularly marked with the powders. Nevertheless, the amount of Zr rendered unavailable for sorption by this means was certainly less than 1 part in 1000. With the powder samples, it was also noticed that a black deposit formed in the cooler parts of the silica tube; this consisted essentially of Fe, the main metallic impurity.

TABLE II.—SATURATION SOLUBILITY OF HYDROGEN IN DUCTILE ZIRCONIUM (SAMPLE (A)) AT 20° C.

Temperature from which Cooling took place (°C.).	Equilibrium Pressure of Hydrogen (mm. of Hg).	Volume of Hydrogen Dissolved (cm. <sup>3</sup> at N.T.P. per g. Zr).
400	552.5	238.8
700	74.0	238.0
825	558.0	242.3

In all cases the isotherms in the region 750–950° C. were very sensitive to the experimental conditions. The "kink" in the isotherm was noticeable as the point at which a slow sorption started, whereas for the initial points equilibrium was always rapidly attained. It must be stressed that reproducibility of isotherms in this region was only obtained by rigorous adherence to the precautions against contamination outlined earlier in this paper. Contamination by O and N is undoubtedly responsible for the marked "ageing" phenomena observed by Sieverts and Roell.<sup>3</sup>

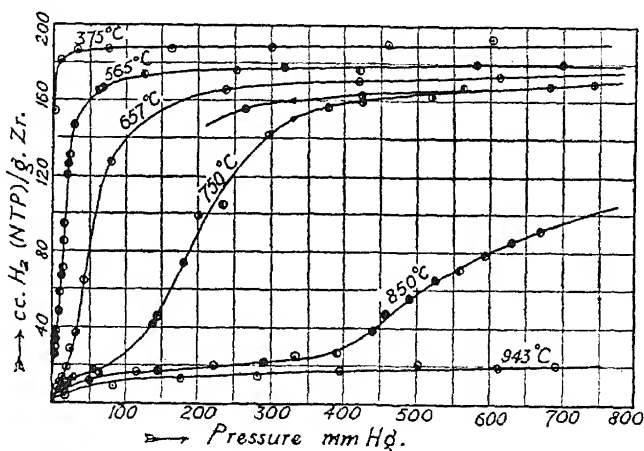


FIG. 6.—Isotherms for Zr wire Sample B + 5.0 % O<sub>2</sub>; 0.362 atom oxygen per atom Zr. 565° C. points on different preparations. 750° C. : → absorption, ← desorption curves.

Surface contamination is probably responsible for the disagreement amongst earlier workers as to the temperature at which zirconium begins to take up hydrogen. Fitzwilliam, Kaufmann and Squire<sup>5</sup> and Hukagawa and Nambo<sup>10</sup> state that sorption only takes place above 500° C., whereas de Boer and Fast<sup>11</sup> maintain that sorption is relatively rapid even at 300–400° C. Our results are in agreement with the latter work, as we have found appreciable sorption to take place even at room temperature. The explanation of this discrepancy is that oxygen does not diffuse rapidly into the metal lattice from the surface below 500° C. and the former authors

<sup>10</sup> Hukagawa and Nambo, *Electrotech. J. (Japan)*, 1941, 5, 27.

<sup>11</sup> de Boer and Fast, *Rec. trav. chim.*, 1936, 55, 350.



had not taken the precaution of heating their samples to a high temperature to "clean" the surface, ordinarily covered by a thin oxide film. Degassed powders containing oxygen in solid solution were found to be more liable to spontaneous ignition on exposure to air at room temperature than were samples containing little oxygen.

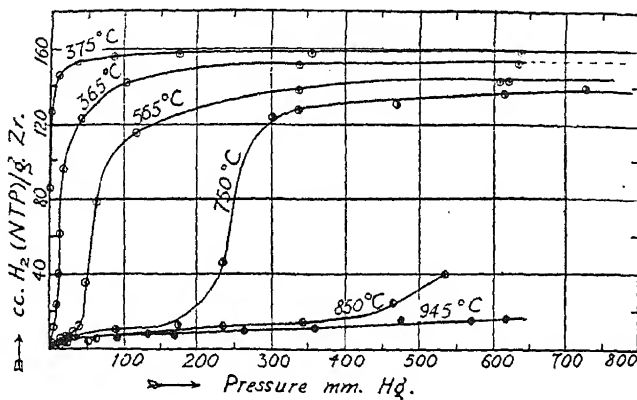


FIG. 7.—Isotherms for Zr wire Sample B + 10.1 %  $O_2$ ; 0.650 atom oxygen per atom Zr. All on same preparation.

The general shape of the isotherms and the presence of a hysteresis effect indicate a strong resemblance to the Pd—H system, where the existence, below a critical temperature, of a two-phase region, in which the composition is independent of pressure, has been ascribed by Lacher<sup>12</sup>

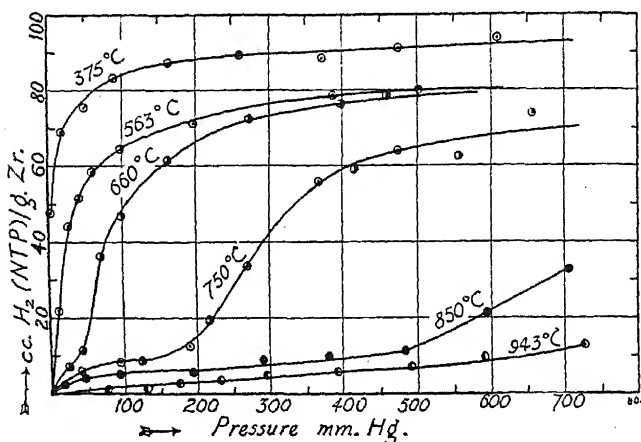


FIG. 8.—Isotherms for Zr wire Sample B + 16.4 %  $O_2$ ; 1.015 atom oxygen per atom Zr. All, including duplicate of 750° C., on same preparation.

to the interaction of dissolved H atoms. Observations on the systems, Ti-, Ce- and La-H, point to a similar behaviour.<sup>13, 14</sup> A single solution process demands the two-phase region to be disposed symmetrically in

<sup>12</sup> Lacher, *Proc. Roy. Soc. A.*, 1937, 161, 525.

<sup>13</sup> Kirschfeld and Sieverts, *Z. physik. Chem.*, 1929, 145, 227.

<sup>14</sup> Sieverts and Roell, *Z. anorg. Chem.*, 1925, 146, 149.

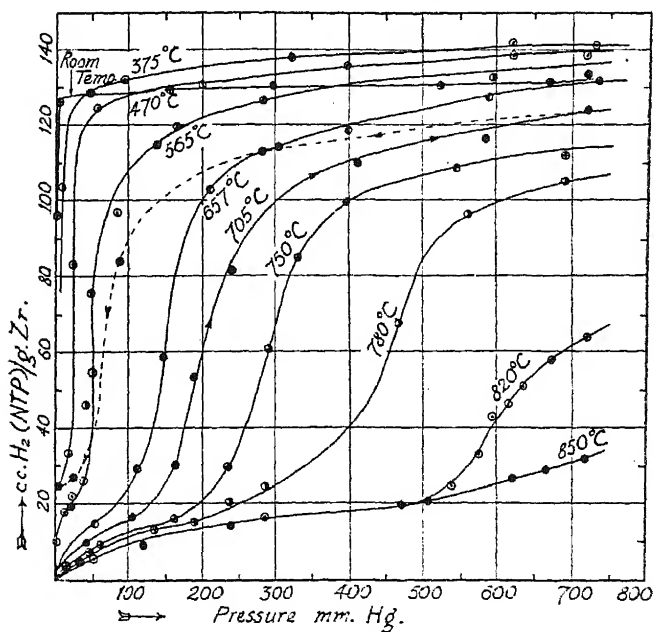


FIG. 9.—Isotherms for Zr. powder Sample D; 0.786 atom oxygen per atom Zr. Each isotherm (including duplicates) on separate 1 gm. samples.  
705° C. : → absorption, ← desorption.

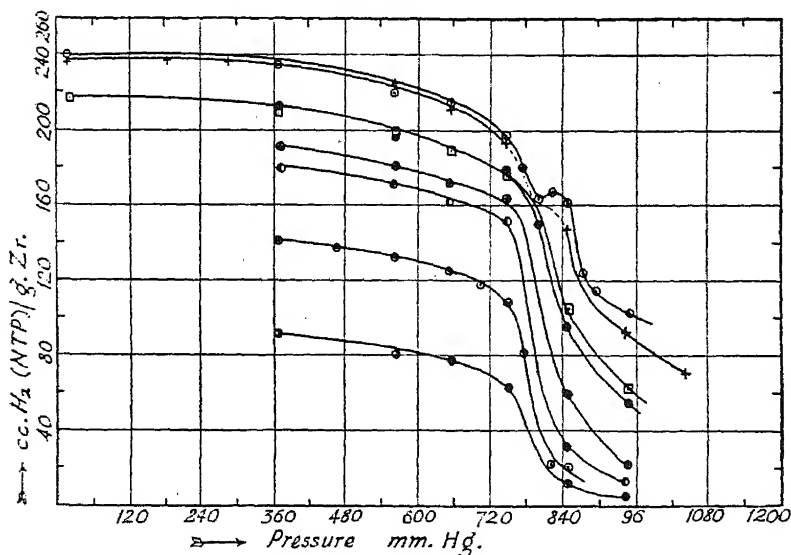


FIG. 10.—Isobars at 500 mm. Hg pressure for all samples (obtained from isotherms); figures below are atom oxygen per atom Zr.

- |                                     |                                     |
|-------------------------------------|-------------------------------------|
| ○ Sample A—0.023.                   | ⊕ B + 5 % O <sub>2</sub> —0.362.    |
| + Sample B—0.053                    | ● B + 10.1 % O <sub>2</sub> —0.650. |
| □ Powder C—0.196.                   | ⊖ Powder D—0.786.                   |
| ● B + 2.44 % O <sub>2</sub> —0.190. | ⊙ B + 16.4 % O <sub>2</sub> —1.015. |

the composition range, a requirement satisfied in the case of Pd. Inspection of the isotherms in Figs. 1 and 2, however, shows clearly that the two-phase region occurs at compositions too close to  $ZrH_2$  for this condition to be satisfied and we conclude that our isotherms represent the sum of two solution processes proceeding simultaneously, in only one of which is critical behaviour apparent. Further evidence in support of this is the marked differential effect of oxygen above and below these parts of the isotherms.

One further feature of the results in Fig. 1, to which attention should be drawn, is the intersection of the  $825^\circ$  isotherm with that of  $800^\circ C.$ , suggesting a sudden increased capacity for dissolving hydrogen above  $800^\circ C.$  This is shown as a hump in the isobars of Fig. 4, although increased oxygen content apparently suppresses the effect. Zirconium has a transition point,  $\alpha - Zr \rightleftharpoons \beta - Zr$ , from hexagonal close-packed to body-centred cubic, at  $865^\circ C.$  and de Boer and Fast<sup>11</sup> state not only that hydrogen is more soluble in the  $\beta$ -form in the low pressure region, but also that the transition point is lowered by the presence of hydrogen. Such behaviour is compatible with our observations.

From Figs. 4 and 10 it appears that with zirconium-oxygen solid solutions the volume of hydrogen sorbed at saturation is decreased by a volume equivalent to that of oxygen present. The other figures show that at any particular temperature, the volume of hydrogen sorbed before the "kink" occurs decreases at first rapidly then more slowly with increasing oxygen content, while the pressure at which the "kink" occurs increases.

These observations will be further discussed in a paper to be published at a later date, in the light of the theoretical treatment which will there be applied to the results.

### Summary.

A study of the solubility of hydrogen in zirconium and in zirconium containing oxygen in solid solution to the extent of 50 atom % has been made isothermally over a range of temperatures up to  $1000^\circ C.$  and at pressures up to 1 atmosphere, rigid precautions being taken for the elimination of surface contamination of the metal by oxide or nitride films. The isotherms exhibit critical phenomena, such as are observed in the Pd-H system, but, from the asymmetric disposition of the two-phase region and from the observed effects of oxygen on the shape of the isotherms, must involve more than one solution process. The results also reflect the existence of the known lattice transition in zirconium.

Inconsistencies prevalent in earlier work have been attributed to surface and bulk contamination of the zirconium with oxygen and nitrogen, for both of which gases it shows a remarkable affinity.

Acknowledgements are due to Mr. J. A. M. van Moll who instigated the work, to Mr. C. H. R. Gentry for his work on the chemical analysis of the zirconium samples, to Mr. F. A. Bannister, of the Natural History Museum, South Kensington, for the X-ray analysis and to the Directors of Philips Lamps Ltd., for permission to publish this paper.

*Material Research Laboratory (Philips Lamps Ltd.),  
Mitcham, Surrey.*

# THE TEXTURE OF POLYTHENE.

BY C. W. BUNN AND T. C. ALCOCK.

*Received 9th November, 1944.*

The X-ray diffraction pattern of polythene at room temperature shows (a) a number of fairly sharp reflections indicating a crystalline arrangement in the greater part of the material, and (b) a diffuse band like those given by liquids and glasses (marked A in Fig. 2)—an indication of the presence of a certain amount of amorphous (*i.e.* non-crystalline) material. The molecular structure of the crystalline part\* has been described in an earlier paper.<sup>1</sup> It consists of simple  $\text{CH}_2$  chains of great length. The purpose of the present communication is to report some evidence on the relation between crystalline and amorphous constituents, on changes which take place at temperatures up to the melting-point, and on the association of the crystalline regions in larger organised units.

**Order of Size of the Crystalline Regions.**—The X-ray reflections of the crystalline part are a little more diffuse than those given by large perfect crystals ( $> 10^{-5}$  cm.) under the same camera conditions. Reflections from different crystal planes are broadened to about the same extent. Broadening of X-ray reflections may be due to several causes—smallness of crystal size, distortions and structural imperfections, and thermal effects. The angular range of reflections on the photographs of polythene is not sufficient to make it possible to distinguish between different possible causes of broadening, by the method which has been used for metal specimens;<sup>4</sup> but it may be said that if the broadening of the reflections is due to small crystal size, the crystals in most specimens are well below 1000 Å. in diameter. Different specimens vary greatly in this respect, the apparent crystal size (using the Scherrer equation) being in some specimens 200–300 Å., while in others it is well below 100 Å. Now polythene molecules, in the specimens examined, are upwards of 1000 carbon atoms in length (in some specimens several thousands); such molecules, if fully extended as in a crystal, would be well over 1000 Å. in length; it appears, therefore, that the molecules are much longer than the crystals. This fits in with the picture now generally accepted<sup>5, 6</sup> for the structure of crystalline long-chain polymers: we imagine portions of many molecules packed side by side in precise crystalline fashion, each molecule passing through several crystalline regions. In view of the uncertainty in the interpretation of the breadth of X-ray reflections, we cannot be certain that this picture is correct in scale, but at any rate the X-ray evidence is not inconsistent with it, and moreover it gives a convincing general account of the mechanical properties—the cohesion and toughness of polythene as compared with shorter-chained hydrocarbons, and the phenomenon of cold-drawing which it exhibits in common with

\* Photographs of certain specimens show a weak extra reflection ( $d = 3.29$  Å.) which indicates the presence of a small proportion of a second crystalline phase, of different structure from the main bulk of the crystalline material. The spacing gives no clue to its identity or structure and we have so far not been able to correlate its occurrence with particular experimental conditions of polymerization or crystallization.

<sup>1</sup> Bunn, *Trans. Faraday Soc.*, 1939, **35**, 482.

<sup>2</sup> Stewart, *Physic. Rev.*, 1928, **31**, 174; **32**, 153.

<sup>3</sup> Muller, *Proc. Roy. Soc., A*, 1932, **138**, 514.

<sup>4</sup> Stokes, Pascoe and Lipson, *Nature*, 1943, **151**, 137.

<sup>5</sup> Mark, *J. Physic. Chem.*, 1940, **44**, 764.

<sup>6</sup> Bunn, *Proc. Roy. Soc., A*, 1942, **180**, 82.

other long-chain polymers; we shall return to the last-mentioned phenomenon at the end of this note.

**Structure of Amorphous Regions.**—According to the picture presented above, the amorphous regions consist of the portions of chain molecules which tie one crystalline region to the next (together with some loose ends of molecules); these portions of molecules, not being arranged in any regular manner, would give diffuse X-ray diffraction effects. The position of the diffuse band in X-ray diffraction photographs of polythene is consistent with this view. The maximum intensity occurs at an angle corresponding to a spacing (using the Bragg equation) of  $4.45\text{--}4.50$  Å. at  $18^\circ\text{C}$ . (varying a little for different specimens). This is very similar to the corresponding figure for liquid normal paraffins up to  $\text{C}_{30}$ — $4.6$  Å. according to Muller<sup>1</sup> and  $4.63$  Å. according to Stewart<sup>2</sup>—and is thus about the spacing to be expected for unbranched chains lying more or less in "contact" without regular arrangement. Although such spacings cannot be measured with any great accuracy, the small difference between the two figures may perhaps have some significance. The position of maximum intensity in the diffuse band is determined by the most frequently occurring interatomic distances, which for long paraffin molecules are (a) the distances between nearest atoms in the same molecule ( $1.5\text{--}2.5$  Å.) and (b) the distances between nearest atoms in neighbouring molecules ( $4\text{--}5$  Å.). The band corresponding to the latter is by far the stronger, on account of the smaller angle of diffraction. Now in liquid paraffins the molecules are moving about, whereas in polythene the movements of the portions of molecules constituting the amorphous regions are somewhat restricted because their ends are fixed in crystals. The distances between the nearest atoms of neighbouring molecules may thus tend to be greater in liquid paraffins than in the "frozen" amorphous regions of polythene.\*\* It should be noted that the spacing of  $4.5$  Å. does not imply that the portions of molecules in the amorphous regions are even approximately parallel: molecules lying in "contact" would be expected to be much the same distance apart at their nearest points, whatever their mutual orientation.

The amorphous regions may not consist entirely of portions of normal paraffin chains. Fox and Martin<sup>3(a)</sup> report that certain specimens of polythene give infra-red absorption bands characteristic of methyl groups; from which it appears that chain branching may sometimes occur in the polymerisation reaction. They suggest that the presence of methyl side-groups may account for certain discrepancies in the intensities of the X-ray reflections of polythene crystals—discrepancies which were explained, in the original paper on the crystal structure,<sup>1</sup> in quite a different way (partly by anisotropic thermal motions and crystal distortions and partly by the non-spherical shape of the electron cloud of the  $\text{CH}_3$  group). Actually the size of the methyl group is such that it is very unlikely that portions of chains bearing methyl side-groups could fit in the crystalline regions; these portions of the molecules would be expected to form part of the amorphous fraction. The position of the diffuse X-ray diffraction band would not be affected appreciably unless the proportion of methyl side-groups in the amorphous regions were high.

\*\* It has been shown<sup>10</sup> that the density of the amorphous part of polythene is lower than that of liquid polythene extrapolated to the same temperature. This may appear surprising since the X-ray results indicate closer "contacts" of molecules in the amorphous part; actually there is no inconsistency; molecules in the amorphous part, though closer together at their nearest points, may be on the average further apart if there are comparatively large holes in some places; this is quite a reasonable probability, since the positions of portions of molecules in the amorphous regions are restricted, their ends being "clamped" in crystals. The presence of comparatively large holes would increase small-angle X-ray scattering; this has not been investigated.

<sup>3(a)</sup> Fox and Martin, *Proc. Roy. Soc., A*, 1940, **175**, 208.

**X-Ray Diffraction Photographs at Temperatures up to 120° C.**—Changes in the structure of polythene with rising temperature have been observed by X-ray and microscopic methods. Two points of interest inspired the X-ray work. Firstly, the proportions of crystalline and amorphous material would be expected to change with rise of temperature, at any rate near what is usually called the melting-point—the temperature of disappearance of all crystalline material. Secondly, it was desired to discover whether the crystal structure changes near the melting-point. In some of the normal paraffins up to  $C_{30}$ , the symmetry of the crystal structure changes from orthorhombic to hexagonal owing to the rotation of the chain molecules about their long axes; this occurs a few degrees below the melting-point.<sup>3</sup>

X-ray powder photographs of a specimen of polythene at temperatures up to 120° C. were taken in an improvised camera—an ordinary powder camera of the Bradley and Jay type,<sup>7</sup> fitted with pancake heater coils just above and below the specimen. The polythene was in the form of a film on the surface of a piece of pure silver wire 0.25 mm. in diameter; the X-ray photographs (taken while the specimen was rotating) all showed the superimposed patterns of silver and polythene (see Fig. 2) and from the unit cell dimensions of the silver, the temperature of the specimen could be deduced. The determination of unit cell dimensions was carried out by measuring the large-angle reflections and using the extrapolation method of Bradley and Jay,<sup>7</sup> and temperatures were calculated by using Scheel's value<sup>8</sup> for the coefficient of expansion of silver between 0° and 100° C., in conjunction with our own figure (4.077%) for the lattice dimension of silver at 19° C. It appeared possible to determine the temperature of the silver to within 2° C. by this method. It is possible that the temperature of the polythene coating on the silver wire might have been a little higher than that of the silver, since the heating came from outside and polythene is a very poor conductor of heat. To reduce the temperature gradient, the silver wire was supported by a specimen holder specially made of "woodite," in place of the metal holder normally used in the camera.

Photographs of one specimen of polythene were taken at 19°, 49°, 56°, 69°, 84°, 99°, 101°, 104°, 109° and 123° C. An increase in the relative intensity of the "amorphous" band as compared with the "crystalline" reflections became obvious above 80° C. and quite marked at 101° C. At 104° C. the proportion of amorphous material appeared comparable with the proportion of crystalline material in the specimen (see Fig. 2), while at 109° C. the "crystalline" reflections were only just visible, being almost completely obscured by the intense diffuse "amorphous" band. At 123°, only the "amorphous" band was visible. Thus the process of melting occurs gradually over a considerable temperature range; although most of the change from a crystalline to an amorphous structure apparently occurs above 100° C., perceptible changes can be detected by X-ray photographs at temperatures as low as about 80° C. (The temperatures quoted apply only to the specimen of polythene used, which had a molecular weight—as measured by melt viscosity—of about 17,000. Other specimens of different molecular weight would be expected to show similar behaviour over a somewhat different temperature range.) Measurements of the density<sup>9</sup> and heat capacity<sup>10</sup> of polythene made in this laboratory are fully consistent with this picture of gradual melting, which is indeed consistent with the previously presented picture of the texture of polythene. The pull of the "tying" portions of molecules must affect the melting-points of the crystals to which they are tied, to a degree depending

<sup>7</sup> Bradley and Jay, *Proc. Physic. Soc.*, 1932, 44, 563.

<sup>8</sup> Scheel, *Z. Physik*, 1921, 5, 167.

<sup>9</sup> Hunter and Oakes, *in press*.

<sup>10</sup> Raine, Richards and Ryder, *in press*.

on the size of the crystalline regions and other local conditions; thus, on heating, portions of molecules leave the crystals and join the amorphous material at different temperatures; and some crystals melt completely before others; the result is that the proportion of amorphous, melted material increases with rise of temperature. The temperature at which melting is complete cannot be determined satisfactorily by X-ray photographs, since weak "crystalline" reflections become obscured by the intense broad "amorphous" band; microscopic methods are more satisfactory for this purpose.

We have not measured photometrically the intensity distribution in the X-ray photographs, but it is obvious by inspection that the "crystalline" reflections do not broaden appreciably with rise of temperature. Thus, melting does not occur by a gradual diminution of the size of the

crystalline regions, but by a gradual change in the proportion of comparatively large crystalline regions.

The X-ray photographs show no sign of a phase-change, such as that which occurs in some of the shorter-chained normal hydrocarbons just below their melting-points. If molecular rotation were to start, the two strongest reflections (indices 110 and 200) would move towards each other and finally coalesce to form the 100 reflection of a hexagonal crystal. This does

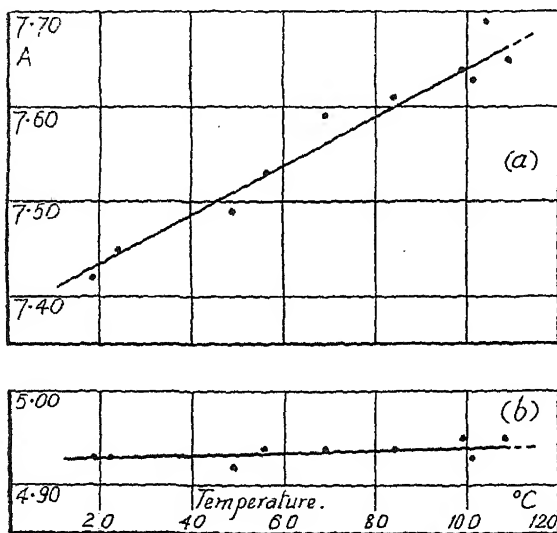


FIG. 1.—Unit cell dimensions of polythene crystals from room temperature to the melting-point.

not occur; even in the photograph taken at 109°C., when there was only a little crystalline material left, the two reflections can be seen. There appears to be only a slight change in their separation: they do move together a little—an indication presumably of increased amplitude of rotatory oscillation about their long axes.

The lattice dimensions were determined from the positions of the 200 and 020 reflections; each polythene reflection appeared as a doublet, owing to the diffraction of X-rays by a film of polythene on each side of the silver wire (the beam being absorbed by the wire itself); in most cases the centre of the doublet was taken as the "position" of the reflection, no correction for absorption being necessary. In some cases only the outer component of the doublet was clearly visible; in these circumstances the position of this component was measured, and a correction applied. Although no great accuracy was attained (the reflections being at small angles) the results were fairly consistent, and show (see Fig. 1) that the length of the *b* axis of the orthorhombic cell remains approximately constant at 4.93–4.95 Å., while that of the *a* axis increases from 7.42 Å. at 18°C. to 7.65 Å. at 100°C. (There is no similar informa-

tion on the  $c$  edge of the cell—2.534 Å. at room temperature—but this, being the repeat distance within the molecule itself, would not be expected to change.) The expansion of  $a$  (0.035 % per °C.) may be compared with the corresponding figure given by Muller for  $C_{20}H_{40}$  (0.029 % per °C. between 20° and 40° C.). Since only the  $a$  axis expands appreciably the volume coefficient of expansion should be about the same as the linear coefficient for the  $a$  axis; in view of this, compare the volume coefficient for  $C_{34}H_{70}$  (0.045 %) calculated from the density measurements of Seyer, Patterson and Keays.<sup>13</sup>

The fact that only the  $a$  axis of the cell expands on heating (increasing the axial ratio  $a:b$  towards the pseudo-hexagonal  $\sqrt{3}$  ratio) suggests that the mean plane of the zigzag carbon chain twists a little towards the  $ac$  plane of the crystal on heating; probably this means that it is chiefly the rotatory oscillations of the chain molecules about their long axes which increase their amplitude on heating; other motions, such as those associated with random distortions of the molecules from the ideal plane zigzag form, would be expected to increase both  $a$  and  $b$  axes. But the structure is still far from hexagonal even at 109° C.; complete rotation of the molecules thus does not occur. Among the shorter-chained paraffins, Muller<sup>3</sup> found that only in the range  $C_{21}$ – $C_{29}$  do the crystals become hexagonal before melting; in view of this, rotation of much longer molecules would not be expected. But in any case there are special features in a polymer structure which make it less likely: a molecule passes through more than one crystal, and is in most cases distorted in the "tying" (amorphous) regions; both these circumstances would be likely to diminish the probability of complete rotation in the crystalline regions.

The spacing corresponding to the position of maximum intensity of the diffuse band—an indication of the inter-chain distance in the amorphous material—increases slightly with rise of temperature, from 4.5 Å. at room temperature to 4.7 Å. at 109° C.

**Spherulitic Structure of Polythene.**—Examination of suitably prepared thin films of polythene in the polarizing microscope between crossed Nicols shows the existence of birefringent regions, each with a dark cross whose arms are parallel to the vibration directions of the Nicols and which therefore rotate as the Nicols are rotated (see Fig. 3). This phenomenon is typical of spherulitic aggregations of crystals: a spherulite consists of a large number of crystals radiating in all directions from a point, a particular direction of each crystal lying consistently along a radius of a sphere. Some films show surface irregularities—hillocks with fairly well-marked boundaries between them; and each hillock corresponds with a spherulite. The size of the spherulites varies greatly with the type of polythene and the manner of preparation of the film, and in shock-cooled films of certain types of polythene it may be possible to see only a faint small-scale mottled appearance. And in thicker films, more than one spherulite thick, the overlapping of different spherulites in the line of vision may also give rise to a confused mottled appearance. One of the clearest demonstrations of the spherulitic structure was provided by a specimen of polythene which came out of the polymerisation vessel as a powder; this powder proved to consist of spherulites, each showing the dark cross very clearly.

An electron microscope photograph of an extremely thin film of polythene, taken by Dr. D. G. Drummond, of the British Cotton Industry Research Association, is shown in Fig. 4. Radiating growths can be seen, with fairly definite boundaries between neighbouring units. These units can presumably be identified with the spherulites seen in the polarizing microscope, though they are much smaller owing to the method of preparation of the specimen.

<sup>13</sup> Seyer, Patterson and Keays, *J. Amer. Chem. Soc.*, 1944, 66, 179.



Use of the quartz wedge shows that the refractive index for light vibrating along the radius of the spherulite is lower than for the vibration direction perpendicular to the radius. To interpret this in terms of crystal orientation, it is necessary to know the optical properties of polythene crystals. Single crystals have never been obtained, but fibres in which the  $c$  axes of the crystals are all parallel to the fibre axes are readily obtained by cold-drawing. The refractive indices of such fibres were measured by the immersion method; the results varied a little with the degree of perfection of orientation of the crystals in the fibre, but in the most perfectly oriented specimens (as shown by X-ray diffraction photographs) the refractive indices were found to be 1.55 for light vibrating along the fibre (that is, parallel to the chain molecules) and 1.50 for the vibration direction across the fibre. The latter figure represents the average for the  $a$  and  $b$  axes of the orthorhombic crystals, since these axes are randomly disposed in all directions normal to the fibre axis. In view of the orientations of the planes of the zigzag chain molecules in the crystal<sup>1</sup>—half of them being nearly at right angles to the other half—the refractive indices for the  $a$  and  $b$  vibration directions are expected to be nearly equal. The three principal indices of a single polythene crystal are therefore:  $\alpha$  a little below 1.50,  $\beta$  a little above 1.50,  $\gamma = 1.55$ .

Returning to the spherulites, we are now able to conclude that the  $c$  axes of the crystals (the molecular axes) are perpendicular to the radii of the spherulite. Which crystal direction lies along the radius of the spherulite—whether it is the  $a$  or the  $b$  axis, or some other direction in the  $ab$  plane such as the  $[110]$  zone axis—it is impossible to say. It may seem surprising that the chain molecules do not lie along the radii but normal to them. It must be realised, however, that the radii of the spherulites are directions of crystal growth; and the situation in polythene is actually in line with the crystal morphology of the shorter-chained paraffin wax hydrocarbons, which grow as thin plates with the molecular axes normal to the plane of the plate; the crystals grow much faster in directions normal to the molecular axes than they do parallel to the molecular axes; it is evidently much easier for a molecule to add on to the edge of a sheet of molecules than to start a new layer. In the case of polythene we can scarcely imagine crystal growth (in the sense of accretion of molecules) taking place along the molecular axes; growth would occur entirely at right angles to the molecular axes: we must imagine, in the formation of a spherulite, crystals growing outwards in all directions from a point, and growing by the continual side-by-side accretion of portions of very long-chain molecules.

We may ask why spherulitic aggregations are formed, rather than individual crystalline regions unrelated in position or orientation. The answer may be something like this: a single crystal nucleus is first formed, consisting of portions of numerous molecules packed in precise fashion; the other parts of these same molecules are now to some extent constrained, and are therefore the more ready to act as centres for the growth of new nuclei—and since the molecules are flexible (by rotation round the chain-bonds) the new nuclei may take up different orientations from the first; the continuation of this process results in the growth of crystals in all directions from the original nucleus. The apparent sheaf-like character\* of the centre of a spherulite, shown in the electron microscope photograph (Fig. 4) is consistent with this idea.

If this view is correct, we should expect two things: that spherulite formation is a function of chain-length, and that other long-chain polymers should crystallize in this manner. In relation to the first point, the examination of polythene specimens and fractions of various molecular weights showed that spherulites could only be seen in specimens com-

\* It is important not to confuse the radiating growth-directions with molecular axes; the long molecules are at right angles to the growth-directions.

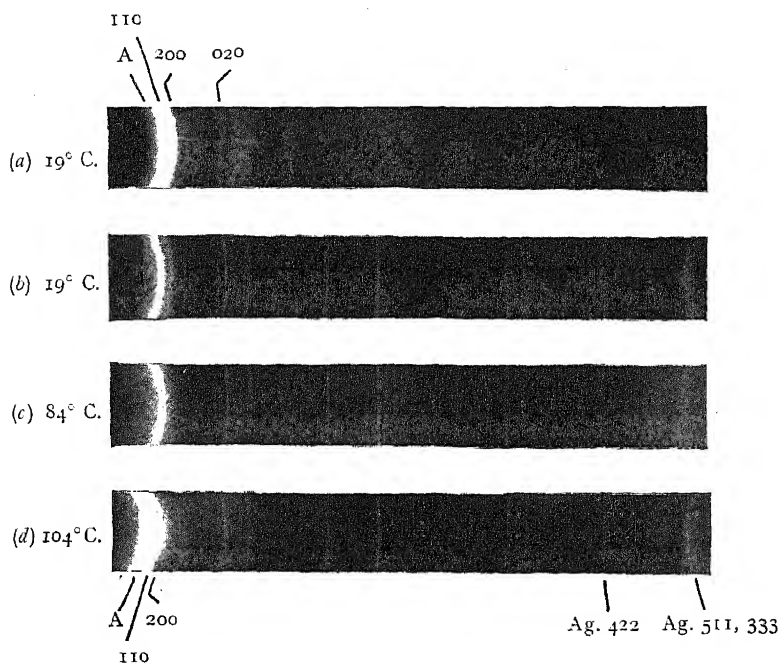


FIG. 2.—X-ray diffraction photographs.

(a) Polythene.

(b-d) Polythene on silver wire.

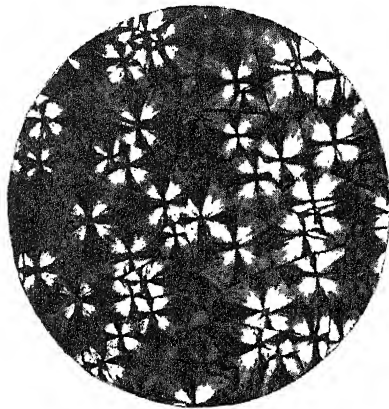


FIG. 3.—Thin film of polythene between crossed Nicols.  $\times 500$ .

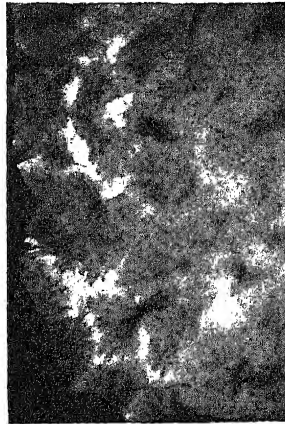


FIG. 4.—Photograph of very thin film of polythene, taken by the electron microscope.  $\times 10,000$ .

posed of molecules of average length over 300 carbon atoms. In relation to the second, both gutta-percha<sup>11</sup> and rubber,<sup>12</sup> when crystallized from solvents, are reported to form spherulites; and in the latter case the optical properties show that, as in polythene, the molecules lie at right angles to the radii of the spherulites. (Rubber molecules, like polythene molecules, have positive birefringence.)

**Microscopic Examination up to the Melting-point.**—Films of polythene were made on microscope slides by melting small pieces of the material and pressing cover glasses on to the viscous liquid. These slides were heated in a small electrically heated oven fitted with observation windows and placed on the microscope stage. The temperature was controlled by a rheostat. Observations between crossed Nicols showed that for most normal specimens of polythene (molecular weight 15,000-30,000 by melt viscosity) a diminution of birefringence—which is some indication of the amount of crystalline material—is perceptible at 100° C., but that the spherulites do not completely disappear until a temperature of 115° C. to 120° C. is reached. The actual temperature at which this occurs depends to some extent on the rate of rise of temperature; to allow time for an approach to thermal equilibrium, the temperature was raised 1° C. every half hour; in this way consistent results were obtained for any one specimen. But on slowly cooling again at the same rate, spherulites did not reappear until a temperature 3 or 4° lower was reached; and further experiments suggested that very long periods of time would be required to make the two temperatures equal. Similar hysteresis effects are found in the change of density<sup>9</sup> and heat content<sup>10</sup> with temperature. It was observed that although, on heating, there was a general diminution of the birefringence of each spherulite, sometimes certain spherulites (not always the largest) persisted after the rest had become isotropic; the longer molecules in a specimen perhaps tend to segregate, giving spherulites with higher melting-points than the rest.

Since the melting-points of different specimens vary considerably (they depend on molecular weight distribution as well as on average molecular weight—quite apart from any variations in the proportion of methyl side-groups) it is scarcely worth while to quote figures in detail. It must suffice to mention that there is a general rise of melting-point with average molecular weight up to about 20,000; and that the highest melting-point observed was 126° C.

**Mechanism of Cold-drawing.**—The phenomenon of cold-drawing (whereby an unoriented thread, on stretching, becomes drawn out to a thread in which the crystalline regions are approximately parallel to each other) appears to be exhibited by crystalline long-chain polymers generally. On stretching, part of the thread becomes thinner by a definite amount and there are very definite shoulders at the junctions of drawn and undrawn portions; on further drawing, the shoulders travel along the specimen as more and more of the undrawn material narrows to join the oriented part, the thickness of which remains constant. For polythene, the diameter is usually reduced to 40-45 % of the original, the elongation being 500-600 %. The drawn thread has some reversible elasticity, but cannot be drawn permanently thinner; any attempt to do so results in the breaking of the thread. This "necking" phenomenon seems to be typical of the highly crystalline polymers; amorphous polymers, on stretching, become thin gradually, not suddenly; and crystalline polymers near their melting-points (when the proportion of amorphous material is high) show little or no shoulder.

The question arises: "Why is there such a definite reduction in the diameter of the thread?" Since the crystals "flow" during drawing, why do they not go on flowing past each other, with continued diminution

<sup>11</sup> Kirchof, *Kautschuk*, 1929, 5, 175.

<sup>12</sup> Smith, Saylor and Wing, *Bur. Stand. J.*, 1933, 10, 479; 1934, 13, 453.

in the diameter of the thread? If we consider the phenomenon in terms of the two-phase texture described in this note, the question becomes still more acute. When an unoriented fibre is pulled, crystals are dragged out of their spherulitic associations into approximately parallel alignment; each crystal drags others after it by the tie molecules. But since each crystal is presumably tied to a number of others which are likely to pull in different directions, it will often happen that crystals break into two or more portions (not by the breaking of molecules, but by the separation of neighbouring molecules). If crystals can be broken in these circumstances, why does the breaking not continue in the drawn part with gradual thinning of the thread?

The following suggestion is offered. When crystalline regions are broken, they part along cleavage planes (probably the 110 and 100 planes in polythene).

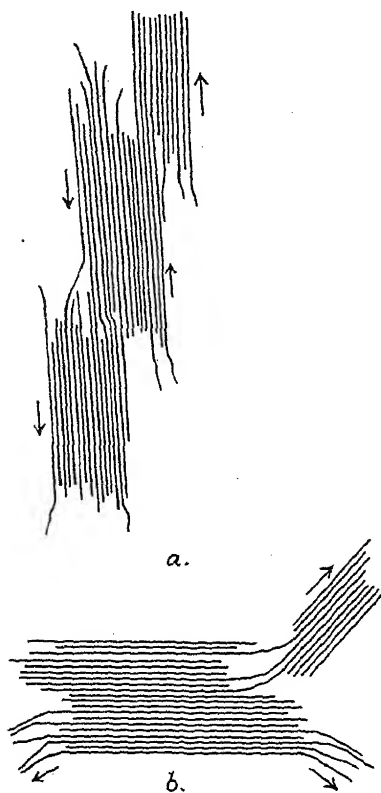


FIG. 5.—(a) Crystal rupture by shear.  
(b) Crystal rupture by tearing.

The difficulty of breaking probably depends on the direction of the stresses on a crystal. Thus, if, as in Fig. 5a, the stresses are in diametrically opposite directions along the molecular axes, the crystal parts by shearing parallel to the molecules. But if, as in Fig. 5b, the stresses are not diametrically opposite, part of the crystal may be torn off gradually, just as in stripping off a piece of adhesive tape we raise one end and strip it off progressively. The flexibility of the molecules makes this possible. In this process—rupture by tearing—side-links are broken progressively and tearing is therefore likely to be much easier than shearing, in which many potential barriers have to be surmounted simultaneously. Now in cold-drawing, on account of the random orientation of the crystals, the pull of the tie molecules will usually not be parallel to the  $c$  axes of the crystals—it will be at any angle; consequently one piece of a crystal can be separated from the rest by the comparatively easy tearing process. But as soon as it becomes parallel to the direction of drawing, any further rupture could only occur by the comparatively difficult shearing process, which would require a much

greater force than is being used; therefore the crystal in question is not subdivided further—it remains as an organised unit, and the tie molecules which still join it to unoriented material then proceed to tear off further portions of crystals which follow the leader into parallel orientation. The reduction in the diameter of a fibre in cold-drawing is thus related to the proportion of situations in which crystals can be divided by tearing rather than shearing. Quantitative treatment of this problem does not appear possible.

### Summary.

1. The interpretation of some secondary features of the X-ray diffraction patterns of polythene—the breadth of the crystal reflections, and the position of the diffuse ("amorphous") band—is considered.
2. X-ray diffraction patterns have been taken at temperatures up to the melting-point ( $\sim 120^{\circ}\text{C}$ ). Changes in the proportions of crystalline and amorphous material occur above  $80^{\circ}\text{C}$ .
3. The  $a$  edge of the orthorhombic unit cell of the crystalline part increases in length from 7.42 Å. at  $18^{\circ}\text{C}$ . to 7.65 Å. at  $100^{\circ}\text{C}$ . The  $b$  axis remains approximately constant at 4.93–4.95 Å.
4. Optical evidence indicates a spherulitic structure in polythene. The orientation of the crystals in the spherulites is deduced by reference to the optical properties of drawn fibres. On heating, the temperature at which the material becomes isotropic varies with different specimens; the highest temperature observed in any specimen was  $126^{\circ}\text{C}$ .
5. A suggestion on the mechanism of cold-drawing is offered.

*Imperial Chemical Industries Research Department,  
Alkali Division,  
Northwich, Cheshire.*

---

## SORPTION OF VAPOURS BY KERATIN AND WOOL.

By G. KING.

*Received 29th November, 1944.*

### 1. Introductory.

A previous investigation showed that owing to the very large surface-volume ratio of wool fibres, the rate of absorption of water vapour was governed almost entirely by the heat evolved and the consequent rise in temperature of the fibres during absorption. A direct study of the diffusion of water into the fibres was thus impossible, and indirect methods have had to be used to gain some insight into the diffusion process.

Two indirect methods are available. Larger molecules, such as alcohols, can be used so that the diffusion process becomes slower and therefore more likely to control the observed absorption, or the diffusion of water into horn can be studied. Horn has chemical and physical properties very similar to wool, and specimens can be chosen with a small surface-volume ratio so that diffusion into the bulk of the material is the rate controlling process. Both methods have been used in the present work to give some indication of the complex mechanism governing the diffusion of foreign molecules into keratin.

### 2. Experimental.

The experimental procedure was very similar to that used in the determination of the rate of absorption of water vapour by wool,<sup>1</sup> and need not be described in detail here.

In the case of the ethyl alcohol-wool isotherm, a period of 48 hours was allowed to elapse between readings in order to ensure that equilibrium had been reached despite the slow rate of absorption. The alcohols were, of course, kept in contact with freshly ignited quicklime during all the experiments.

<sup>1</sup> King and Cassie, *Trans. Faraday Soc.*, 1940, 36, 445.

The thin films of horn were obtained by first softening samples in boiling water and then pressing between two glass plates. The resulting slabs were dried *in situ*, and attached to a brass plate with Chatterton's compound before milling to the requisite thickness.

### 3. Absorption of Methyl and Ethyl Alcohol.

Speakman<sup>2</sup> has shown that methyl and ethyl alcohol are absorbed in large quantities by wool much as water is absorbed. An absorption isotherm was determined for ethyl alcohol to show how close the analogy is with water; it is reproduced in Fig. 1. The curve is similar though not quite so sigmoid in shape as that for water.<sup>1</sup> The weight of alcohol absorbed at saturation is 26 % as compared with 32 % for water, but it should be remembered that the moles of ethyl alcohol absorbed at

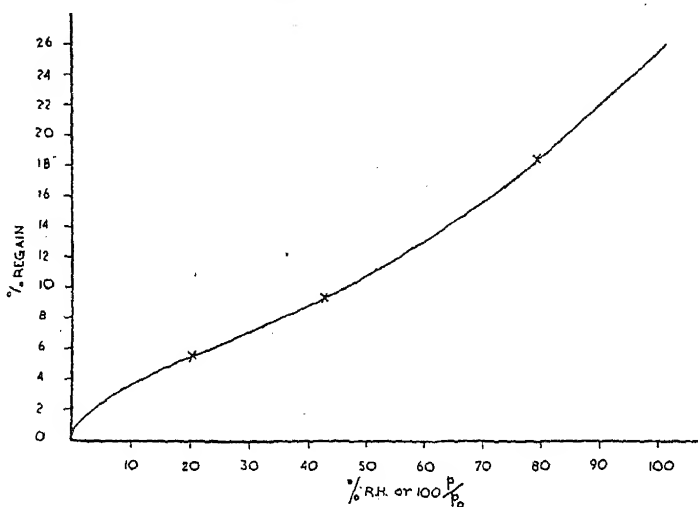


FIG. 1.

saturation by 100 gm. of wool is only one-half as compared with nearly two for water; or taking the amino acid residue weight<sup>3</sup> as 118, 0.45 moles of ethyl alcohol are absorbed at saturation vapour pressure as compared with 1.5 for water. The absorption isotherm for ethyl alcohol is therefore similar to that for water, but represents a much smaller molecular absorption.

Figs. 2 and 3 show the absorption and desorption of methyl and ethyl alcohol at different times after exposure to saturated and zero vapour pressure respectively; the absorption is from zero regain,\* and desorption is from saturation regain. It is not possible to judge from these curves alone, the degree of control due to the heat of absorption. Time-temperature data are also required, and Fig. 4 shows the increase in temperature of the wool during absorption of water, and methyl and ethyl alcohol. The increase of temperature during absorption of methyl alcohol is by no means negligible, but the flat maximum of the curve means that a slower rate of diffusion is exerting considerable control on the observed rate of absorption. Ethyl alcohol shows only a slight increase of temperature

<sup>2</sup> Speakman, *Trans. Faraday Soc.*, 1930, 26, 61.

<sup>3</sup> Astbury, *J. Chem. Soc.*, 1942, 337.

\* Regain is the weight of foreign molecules absorbed expressed as a percentage of the dry weight of wool.

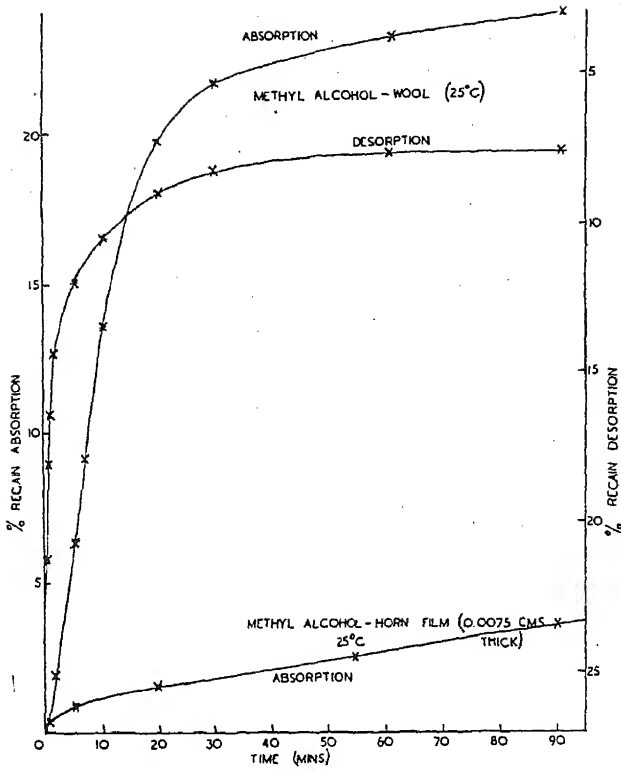


FIG. 2.

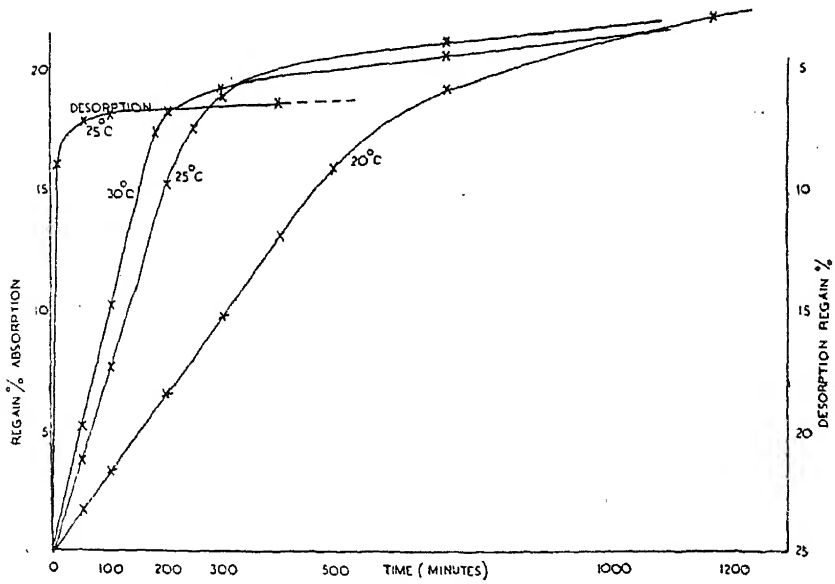


FIG. 3.



when the saturation vapour pressure is first exposed to the wool; the increase is, in fact, negligible after 5 minutes, and during this time only a very small amount of alcohol is absorbed.

The course of the absorption curve for ethyl alcohol is therefore primarily determined by the diffusion of ethyl alcohol into the fibres.

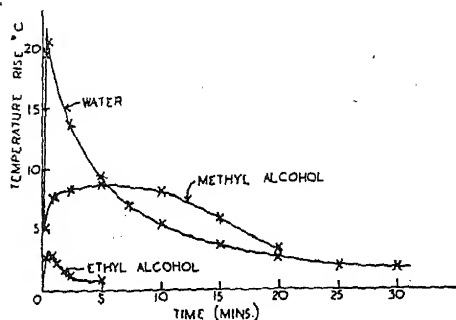


FIG. 4.

#### 4. Absorption by Horn.

Fig. 5 shows the absorption of water by horn films where diffusion into the horn is the controlling factor. The general shape of the curves is similar to that for the absorption of ethyl alcohol by wool: there is an almost linear absorption with time followed by a fairly sharp

cut off. The thicker horn films also show a parabolic increase near zero time followed by the linear increase with time. This feature is shown more strikingly by the absorption of methyl alcohol, which is reproduced in Fig. 2.

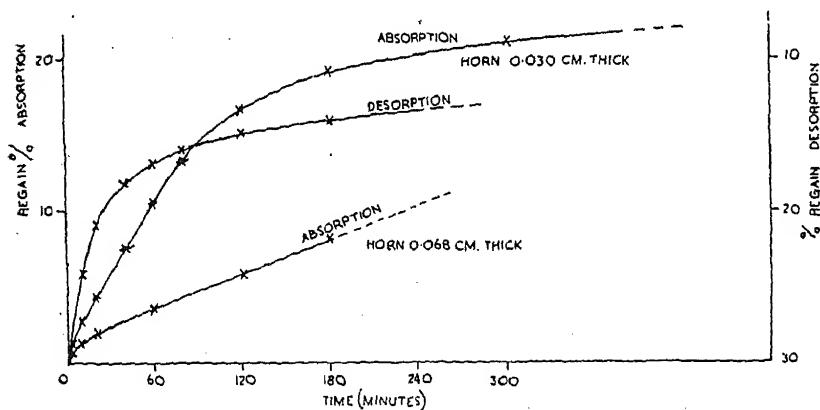


FIG. 5.

#### 5. The Diffusion Process.

The absorption curves reproduced in Figs. 2, 3 and 5, are all very different from those given by Fick's diffusion law with a constant diffusion coefficient. Daynes<sup>4</sup> explained a similar deviation from Fick's law for the diffusion of water into rubber by using equilibrium vapour pressures instead of concentrations in the diffusion equation. The deviation of the ethyl alcohol isotherm from linearity is, however, much too small to account for the deviation of the observed absorption curves from diffusion curves with a constant coefficient.

The absorption curves obtained in the present work are similar to those observed by Barrer<sup>5</sup> for the sorption of  $\text{NH}_3$  by the fibrous zeolite, natrolite. The initial portion of Barrer's curves obey the parabolic law, but they rapidly change to show an almost linear absorption with time,

<sup>4</sup> Daynes, *Trans. Faraday Soc.*, 1937, **33**, 531.

<sup>5</sup> Barrer, *Proc. Roy. Soc., A*, 1938, **167**, 392.

which he ascribes to autocatalytic absorption. The general description is that the diffusion coefficient depends on the concentration of the absorbate. It has been definitely established for other zeolites and for metal to metal inter-diffusion that the diffusion coefficient depends on the concentration of the absorbate, and Barrer<sup>6</sup> has suggested that this also holds for the diffusion of vapours through media in which sorption and swelling occur.

If the diffusion coefficient is a function of the concentration of the absorbate, Fick's law for one dimension must be written :

$$\frac{\partial c}{\partial t} = \frac{\partial}{\partial x} \left( k \frac{\partial c}{\partial x} \right) \quad (1)$$

where  $k$  is a function of  $c$ , the concentration of the absorbate,  $x$  is the distance from the origin of the co-ordinate, and  $t$  is the time. The general solution of this equation is not available at present, although Hartree<sup>7</sup> suggests that the differential analyser might be applied to the problem with some success. However, it is possible to infer from solutions for a semi-infinite solid, the course that absorption should follow for finite slabs and cylinders. Boltzmann<sup>8</sup> showed that for a semi-infinite solid, the concentration must be a function of  $x/\sqrt{t}$ , and the weight of material absorbed into a semi-infinite solid with a constant concentration at  $x = 0$  should therefore increase as  $\sqrt{t}$ . The diffusion of water and methyl alcohol into the thicker films of horn show this parabolic increase of absorption with time, as might be expected because the absorption is then not very different from diffusion into a semi-infinite slab.

The later and much more extensive stages of the absorption are, however, best inferred from solutions for the semi-infinite medium given by Hopkins<sup>9</sup> for cases where  $k$  is a simple function of  $c$ . His solution may be written :

$$c = c_1 + (c_0 - c_1)I + \mu\beta(c_0 - c_1)^2A + \mu^2(c_0 - c_1)^3[\beta^2B + \beta_1M] \quad (2)$$

where  $c = c_0$  for  $t = 0$ ,  $x > 0$

$c = c_1$  for  $t = 0$ ,  $x = 0$

$$k = k_1[I + \mu\beta(c - c_1) + \mu^2\beta_1(c - c_1)^2]; \quad I = \frac{2}{\sqrt{\pi}} \int_0^{y/\sqrt{\pi}} e^{-u^2} du.$$

$A, B, M$ , are functions of  $I$  and  $y$ , and where  $y = \frac{x}{2} \sqrt{\frac{\pi}{k_1 t}}$ ;  $\mu, \beta, \beta_1$  are constants.

When  $c_1 = 1$ ,  $c_0 = 0$ , and  $\mu = 1$ , the concentration is given by

$$c = 1 - [1 - \beta A + \beta^2 B + \beta_1 M]$$

$$k = k_1[1 + \beta(c - 1) + \beta_1(c - 1)^2].$$

If  $\beta$  is taken as 1 and  $\beta_1$  as zero,  $k$  is given by  $k_1 c$ , and if  $\beta$  is taken as 2 and  $\beta_1$  as 1, it is given by  $k_1 c^2$ . The solutions for these cases are shown in Fig. 6,  $c$  being plotted against  $y$ . The curves thus represent the variation of the concentration through the medium at any instant. It is clear from the change in shape of the curves with increase in the power of  $c$  that as the relation between  $k$  and  $c$  becomes increasingly convex towards the  $k$  axis, there is a building up of the concentration behind a slowly moving front. The building up of the front is obtained by taking the concentration distribution for the maximum value,  $k_1$ , of the diffusion coefficient and cutting away the lower portion of the curve. Alternatively, a function for  $k$  could be used which involved the minimum value  $k_0$ , when the steep front would be formed by building up the upper portion

<sup>6</sup> Barrer, *Diffusion in and through solids*, Cambridge University Press.

<sup>7</sup> Hartree, *Mem. Manchester, Lit. Phil. Soc.*, 1936, 80, 97.

<sup>8</sup> Boltzmann, *Ann. Physik.*, Lpz., 1894, 53, 959.

<sup>9</sup> Hopkins, *Physic. Soc. Proc.*, 1938, 50, 703.

# 330 SORPTION OF VAPOURS BY KERATIN AND WOOL

of the curve for  $k_0$ . Thus the lower and upper portions of the distribution are largely determined by  $k_0$  and  $k_1$  respectively, joined by an intermediate steep portion.

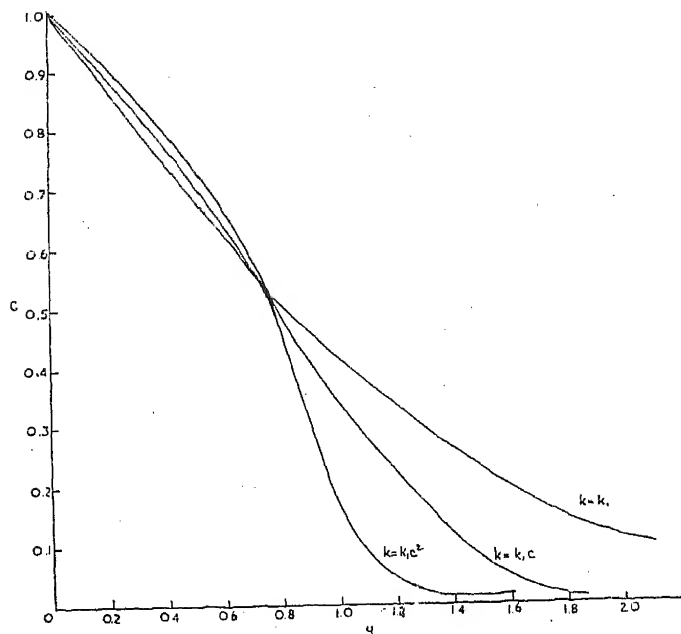


FIG. 6.

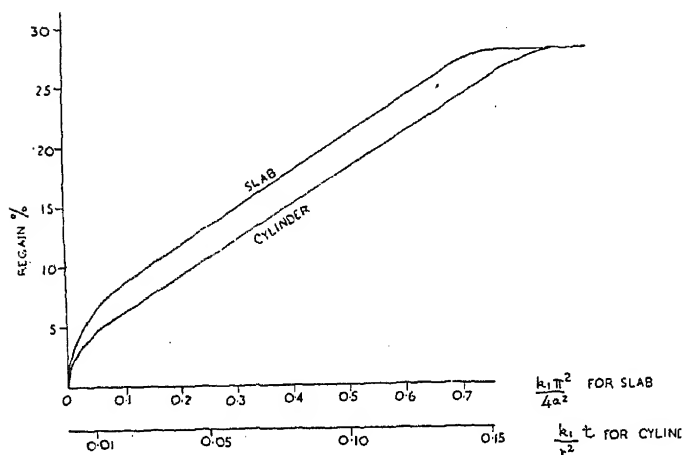


FIG. 7.

If the diffusion coefficient became infinite for values of  $c$  greater than a critical value, say  $c_2$ , the concentration would increase instantaneously from  $c_2$  to  $c_1$ . A rough first approximation to the solution for a finite slab may therefore be obtained by assuming  $k$  to be infinite for concentrations above  $c_2$  and determined by  $k_0$ , for concentrations below this

value. This method has been used to construct the curves of Fig. 7. The solutions of Fick's law for a cylinder and a finite slab were plotted to give  $c$  as a function of the distance from the centre, for different values of  $k_0 t/r^2$  for a cylinder of radius  $r$ , and of  $k_0 \pi^2 t/4a^2$  for a slab of thickness  $2a$ . The areas below the curves were then integrated to the concentration  $c_2$ , and the volume of the cylinder or slab with a concentration above this value was taken as having the saturation value.

The curves of Fig. 7 are closely similar to those, Figs. 2 and 5, obtained experimentally for diffusion into thick slabs; both the experimental and theoretical curves are initially parabolic, followed by a considerable linear increase of absorption with time, finally cutting off rather abruptly at saturation. Also in the case of the absorption of water by horn films of different thickness, Fig. 5, the slope of the linear portion of the curves varies inversely as  $a^2$  in further confirmation of the theoretical construction.

The slope of the linear region of the theoretical curve depends on the value chosen for the critical concentration  $c_2$ . It has been taken as 0.35 of the saturation concentration because many of the properties of wool change rapidly near regains corresponding to this value.

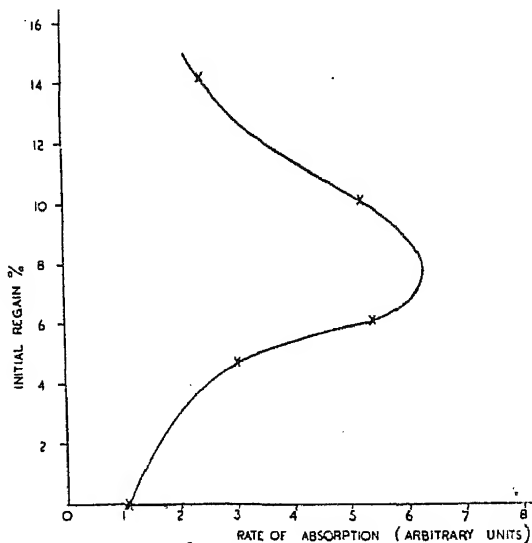


FIG. 8.

Cassie<sup>10</sup> has shown too, that water at regains below 10 to 12 % largely occupies localised sites in wool, and above this regain the water is increasingly non-localised; one would therefore expect the diffusion coefficient for water to increase rather abruptly in this region. This may be confirmed experimentally by beginning the absorption at finite initial regain values, when it is found that the rate of absorption is a function of the initial regain. Such a relation determined for the absorption of ethyl alcohol by wool is shown in Fig. 8. It is seen that a rapid increase in the absorption occurs at about 8 % regain coinciding with a value for  $c_2$  of approximately 0.35  $c_1$ .

A rough estimate of the diffusion coefficient may be made by comparing the slope of the linear region of Fig. 7 with those for the experimental curves. The data are given in Table I. The actual values cannot, of course, be much better than estimates, but they will give the order of magnitude of  $k_0$ , for the diffusion of the three molecules into keratin. The value obtained for methyl alcohol diffusing into wool fibres is surprisingly consistent with that obtained for diffusion into the horn film. The value for the fibres is less than that for the film, and this is to be expected because of the rise in temperature of the fibres, shown in Fig. 4, due to their large surface volume ratio. Similarly, the temperature effect will decrease the rate of absorption of water into the thinner horn films to give the smaller diffusion coefficient for these films.

<sup>10</sup> Cassie, *Trans. Faraday Soc.* (in the press).

It should be emphasised, however, that although the values given in Table I are consistent because they have been derived from one set of assumptions, they should only be regarded as estimates of the mean of the diffusion coefficients for the slower processes.

The temperature coefficient for ethyl alcohol is seen from Table I to be very large and corresponds to an activation energy around 30 K.cal. If this activation energy is correct, the entropy of activation must be very large to give a diffusion coefficient even so small as  $10^{-11}$ . It may be, of course, that the minimum diffusion coefficient for ethyl alcohol is considerably less than the mean value given by the present procedure.

TABLE I.  
DIFFUSION COEFFICIENTS.

System.	Fibre Diameter (cm.).	Slab Thickness (cm.).	Temperature (°C.).	Diffusion Coefficient $k_0$ (cm. <sup>2</sup> /sec.).
Water-horn . . .	—	$3.0 \times 10^{-2}$	25	$7.5 \times 10^{-9}$
Water-horn . . .	—	$6.8 \times 10^{-2}$	25	$9.0 \times 10^{-9}$
Methyl alcohol-wool	$2 \times 10^{-3}$	—	25	$1.7 \times 10^{-10}$
Methyl alcohol-horn	—	$7.6 \times 10^{-3}$	25	$2.2 \times 10^{-10}$
Ethyl alcohol-wool.	$2 \times 10^{-3}$	—	20	$3.6 \times 10^{-12}$
Ethyl alcohol-wool.	$2 \times 10^{-3}$	—	25	$7.2 \times 10^{-12}$
Ethyl alcohol-wool.	$2 \times 10^{-3}$	—	30	$11.6 \times 10^{-12}$

## 6. Desorption of Vapours.

Desorption curves are shown for ethyl alcohol in Fig. 3, and for water in Fig. 5. The initial rate of desorption is in all cases very rapid. This would be expected on the present hypotheses of diffusion in keratin, because at high regains the diffusion coefficient is large, and the rate of desorption is correspondingly large. As the regain decreases, however, the diffusion coefficient becomes small, and evolution is slow; in fact it becomes so slow that it is impossible to remove the last 6% of methyl or ethyl alcohol from wool fibres,<sup>2</sup> and Fig. 5 shows that removal of the last few per cent. of water from horn films 0.03 cm. thick would prove exceedingly difficult.

## Summary.

The absorption and desorption rates for water, methyl alcohol, and ethyl alcohol by wool and horn keratin have been investigated for those cases in which diffusion is the rate controlling process. The results confirm the conception of a diffusion coefficient which increases with concentration, and show that this leads to the building up of a steep front, which advances through the medium as the absorption proceeds. This does not affect the parabolic form of absorption for semi-infinite media but leads to an approximately linear rate in the case of finite media.

I am grateful to Mr. B. H. Wilsdon, Director of Research, for his continued interest in the work, to Dr. A. B. D. Cassie for discussion and advice, and to the Council of the Wool Industries Research Association for permission to publish the results.

Miss V. Farrow performed the computations and Mr. M. L. Wright assisted with the experimental work.

*Wool Industries Research Association,  
Torridon, Headingley, Leeds, 6.*

# THE ANODIC BEHAVIOUR OF METALS.

## PART I.—PLATINUM.

By A. HICKLING.

Received 21st December, 1944.

In the present series it is proposed to carry out a systematic study of the anodic behaviour of metals, using the cathode ray oscillograph to investigate the various electrode reactions which occur during polarisation.

A limited amount of work has been done on the variation of potential with quantity of electricity passed when a platinum electrode is forced from the hydrogen to the oxygen evolution value, with a view to ascertaining the mechanism of the electrode reactions involved.<sup>1</sup> Bowden<sup>2</sup> recorded that the change was a linear one, save for a slight break which was attributed to oxide formation, and suggested that the process corresponded to the gradual removal of a layer of hydrogen dipoles and its replacement by a layer of oxygen dipoles. Butler and co-workers,<sup>3</sup> however, have distinguished several stages: an initial slow rise of potential which is attributed to ionisation of free and adsorbed hydrogen (with an active electrode), a rapid linear rise which is ascribed to the charging of a double layer, and finally a slow linear change which is considered to correspond to the deposition of a layer of adsorbed oxygen dipoles prior to evolution of gas. Erschler and Frumkin and co-workers<sup>4</sup> have made a number of observations on the anodic polarisation of platinised and smooth platinum electrodes at very minute current densities; it is doubtful if the results obtained under these conditions, in which equilibrium is maintained throughout the very slow change, are directly comparable with those obtained in the very rapid anodic polarisation at normal current densities, but their results are in general conformity with those of Butler *et al.* Much of this previous work has been confined to acid solutions and to the measurement of quantities of electricity passed at the various stages, and the effect of relatively few variables has been ascertained. It appeared desirable, therefore, to re-investigate the polarisation under a wide range of conditions, and this has been carried out using a new experimental method.

### Experimental.

The principle of the method used for studying the polarisation process was as described previously.<sup>5</sup> The circuit has been modified in detail to make it possible to study both anodic and cathodic processes and to secure greater flexibility in working, and the improved arrangement is shown in Fig. 1 which is largely self-explanatory.

<sup>1</sup> See Butler, *Electrocapillarity*, Chap. VIII, 1940, for review.

<sup>2</sup> *Proc. Roy. Soc., A*, 1929, **125**, 446.

<sup>3</sup> Butler and Armstrong, *ibid.*, 1932, **137**, 604; Armstrong, Himsworth and Butler, *ibid.*, 1933, **143**, 89; Butler and Armstrong, *J. Chem. Soc.*, 1943, 743; Butler and Drever, *Trans. Faraday Soc.*, 1936, **32**, 427; Pearson and Butler, *ibid.*, 1938, **34**, 1163.

<sup>4</sup> Slygin and Frumkin, *Acta Physicochim. U.S.S.R.*, 1935, **3**, 791; 1936, **4**, 911; 1936, **5**, 819; Erschler and Proskurnin, *ibid.*, 1937, **6**, 195; Erschler, *ibid.*, 1937, **7**, 327; Erschler, Deborin and Frumkin, *ibid.*, 1938, **8**, 565; *Trans. Faraday Soc.*, 1939, **35**, 464. See also Ferguson and Towns, *Trans. Electrochem. Soc.*, 1943, **83**, 271, 285.

<sup>5</sup> Hickling, *Trans. Faraday Soc.*, 1940, **36**, 364.

Direct current is supplied to a condenser C (selected from a calibrated condenser block) which is in series with the electrolytic cell, a milliammeter and a pentode valve. The pentode serves to keep the charging current constant at any desired value, which latter may be changed at will by altering the bias on the screen of the pentode. Connected across the condenser-cell section of the circuit is a thyatron valve, the trip voltage of which is controlled by the grid potential. While the condenser is being charged, a steady current flows through the electrolytic cell, but when the condenser voltage reaches that required to trip the thyatron, the arrangement is short circuited and the condenser discharges, a quantity of electricity exactly equal to that originally passed flowing rapidly through the cell in the reverse direction, and the process repeats itself indefinitely. The voltage developed between the electrode being studied (in the present case the anode) and a saturated calomel reference electrode C.E. is amplified as shown and applied to the Y-plates of the cathode ray tube, while the voltage developed across the condenser is applied to the X-plates,

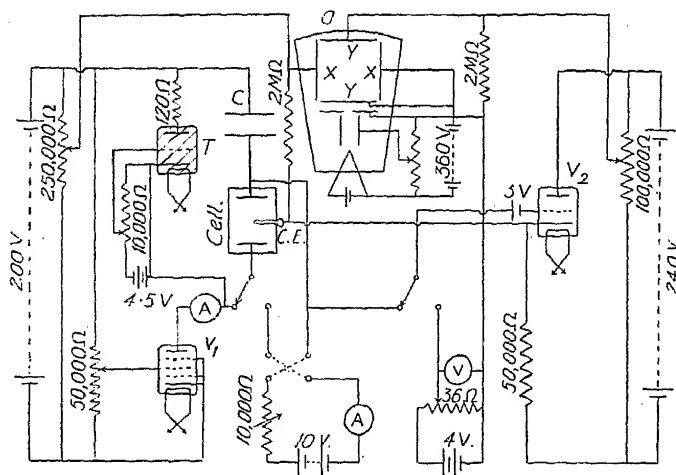


FIG. 1.—Electrical circuit.

- O. Standard Telephone and Cables gas focussed cathode ray tube, 4050 BB.  
 T. Osram thyatron, GTIC.  
 V<sub>1</sub>. Pentode Mazda, SP41.  
 V<sub>2</sub>. Triode Osram, MH4.  
 C. Condenser block, 0.02 to 6μF.

so that a stationary track representing directly the variation of potential with quantity of electricity passed is obtained on the oscillograph screen. The quantity of electricity passed in each pulse can be varied either by changing the value of C or by altering the trip voltage of the thyatron; the latter also serves as an amplitude control. By the subsidiary circuits and switching arrangements shown, the electrode can be subjected to anodic or cathodic pre-polarisation, and reference lines at known voltages can be obtained on the screen.

The electrolytic cell used is shown in Fig. 2. It consisted of a wide-mouthed jar of about 250 c.c. capacity fitted with a rubber stopper carrying anode, thermometer, gas inlet and exit tubes, and cathode and reference electrode tubes; the two latter were fitted with filter paper plugs as shown to prevent contamination of the anolyte. In general a platinum wire anode sealed into a glass tube and mounted vertically was used; it was exactly 0.1 sq. cm. in area and approximately 1 cm. in length. Prior to use it was cleaned with hot concentrated hydrochloric acid, hot concentrated nitric acid, water and heated to redness. The cathode was

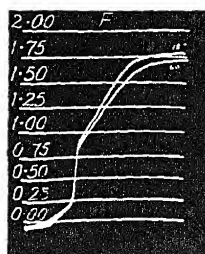
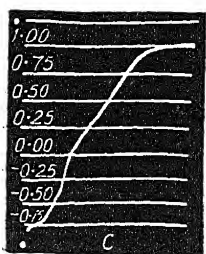
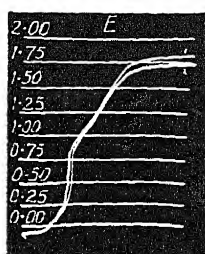
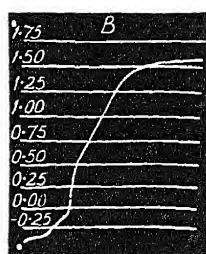
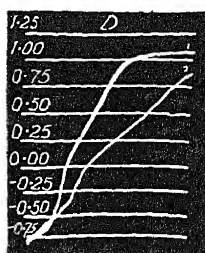
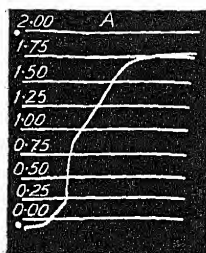


PLATE I.

[To face page 335.]



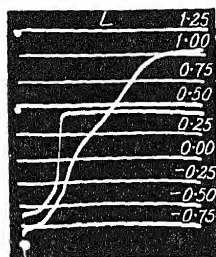
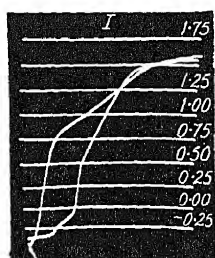
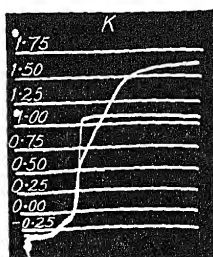
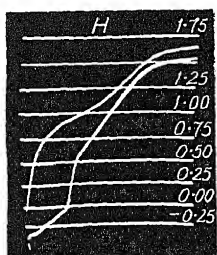
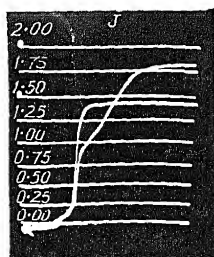
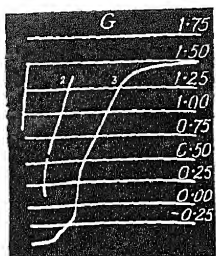


PLATE II.

a 1 cm. square of platinum foil. The electrolytic cell was mounted in a water bath and, except where otherwise stated, was maintained at 18° C.

Observations have been made mainly with three electrolytes: N-sulphuric acid, 0.2 M- $\text{KH}_2\text{PO}_4$  + 0.2 M- $\text{Na}_2\text{HPO}_4$  buffer mixture of approximately pH 6.8, and N-sodium hydroxide; these are subsequently referred to as acid, neutral, and alkaline stock solutions. Before use, the appropriate stock solution was boiled, cooled, and 200 c.c. introduced into the cell, a stream of nitrogen being passed throughout these operations. No attempt was made to remove the last traces of oxygen since it is inevitably formed in the course of anodic polarisation, and experiment showed that the phenomena studied were not appreciably affected even by the presence of large quantities of oxygen. After each experiment the solution was stirred with nitrogen to remove any accumulation of anodic products near the electrode.

The oscillograph tracks, together with suitable reference lines, were photographed using Ilford hypersensitive panchromatic plates with a 3 to 6 seconds' exposure. All potentials quoted are on the hydrogen scale.

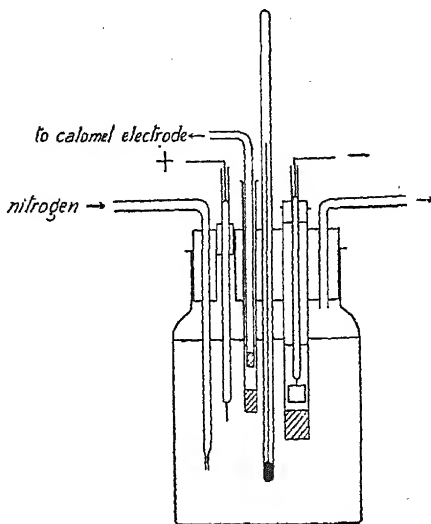


FIG. 2.—Electrolytic Cell.

## Results.

**General Factors.**—In Plate I, A, B and C are shown the characteristic oscillograms in acid, neutral and alkaline solutions severally at 18° C. and with a polarising current density (C.D.) of 0.01 amp./sq. cm., there being a 6.0  $\mu\text{F}$ . condenser in series with the cell. The spots on the extreme left of each photograph indicate the steady hydrogen and oxygen evolution potentials at the same C.D. In alkaline, but not in neutral or acid solution, the oscillogram was found to change with time, and this is shown in Plate I, D, in which track 1 was obtained immediately after switching on the pulsating current, while track 2 was obtained after 15 minutes' pulsating electrolysis. This change was accompanied by a darkening of the electrode, and it appeared to be due to an appreciable dissolution of platinum during each anodic pulse followed by its deposition in a finely divided form in the consecutive cathodic pulse, thus leading to an increase in the effective area of the electrode. Apart from this, the oscillograms were remarkably reproducible. They were unaffected by anodic and cathodic prepolarisation of the electrode (10 minutes at 0.1 amp./sq. cm.), by stirring with the gas stream, and identical tracks were obtained with different platinum electrodes provided the area in each case was the same. When the solutions were saturated with oxygen, and oxygen gas bubbled through, the sole effect was a slight shortening of the pause in the vicinity of the reversible hydrogen potential. Change of C.D. had only a slight effect on the oscillograms which is illustrated in Plate I, E; tracks 1 and 2 were obtained with C.D.s of 0.025 and 0.005 amp./sq. cm. respectively in acid stock solution at 18° C. The main parts of the oscillograms are identical, but the positive potential ultimately attained is slightly

lowered by decrease of C.D. Increase of temperature had also only a slight effect on the oscillograms. This is illustrated in Plate I, F, in which tracks at 18° and 60° C. are shown for the acid stock solution and a polarising C.D. of 0.01 amp./sq. cm.; at the higher temperature the slope of the upper portion of the oscillogram is reduced and the final positive potential slightly lowered. It has been mentioned that anodic prepolarisation had no effect on the oscillograms, and this was always so if the potential of the working electrode was taken to the hydrogen evolution value in each cathodic pulse; if, however, the quantity of electricity passed in each pulse was insufficient for this to be achieved, then anodic polarisation greatly increased the slope of the upper portion of the oscillograms and raised the positive potentials finally attained. This is illustrated in Plate II, G, by results obtained in the neutral stock solution with a polarising C.D. of 0.01 amp./sq. cm. and with three different settings of the amplitude control. In each case 5 minutes anodic prepolarisation at 0.01 amp./sq. cm. was given; the tracks were arbitrarily displaced by manipulation of the X-shift control so that they should be clearly distinguishable. Track 1, in which the quantity of electricity passed was insufficient to reduce the potential below the upper break in the normal curve, is very steep and has practically the same slope as the middle section of the usual track; track 2, in which the quantity of electricity passed was sufficient to reduce the potential slightly below the customary upper break, is appreciably less steep; track 3, in which the potential was taken to the hydrogen evolution value, is practically identical with the usual track.

The quantity of electricity passed at any stage in the anodic polarisation process studied is directly proportional to the horizontal deflection of the oscillograph, and is determined by the capacity of the series condenser and the voltage to which it is charged. By applying known deflecting voltages the oscillograph was calibrated, and 1 v. on the condenser was found to correspond to an average horizontal displacement of 1.0 mm. on the photographs. Hence the quantity of electricity passed in any stage of the polarisation, or the apparent capacity of the electrode in any section, is readily found by measurement of the recorded tracks. By using different series capacities, numerous check values were obtained. Average values from a large number of measurements are given in the Discussion.

**Influence of Catalytic Poisons.**—In Plate II, H, are shown the oscillograms for the polarisation of the platinum anode at 0.01 amp./sq. cm. in the neutral solution, and in the same solution containing 0.01 M. mercuric cyanide. In the presence of the poison, the initial slow stage in the anodic polarisation is completely eliminated, and the potential rises rapidly from the beginning. The customary upper change of direction of the track is displaced to a more positive value, and the potential then rises more slowly than usual to the oxygen evolution point. A similar behaviour was found in the presence of carbon bisulphide, and this is illustrated in Plate II, I, where the tracks are shown for an identical experiment with neutral stock solution and with the same solution saturated with carbon bisulphide. With arsenical additions ( $\text{As}_2\text{O}_3$ ,  $\text{Na}_2\text{HASO}_3$ ) the same general tendencies were apparent, but the poisoning action appeared to be comparatively slight.

**Influence of Anions.**—The effect on the oscillograms of adding various potassium salts to the stock solutions was investigated. Where the anions introduced were such that no discharge was likely, *e.g.* nitrate, fluoride, etc., no effect was apparent, but where the anions could be discharged at the anode to give products other than oxygen, the oscillograms were markedly affected. Thus in Plate II, J, are shown the oscillograms for the polarisation of the platinum anode at 0.01 amp./sq. cm. in acid stock solution, and in the same solution containing 0.1 M. potassium chloride. In Plate II, K, is shown a similar experiment with neutral stock solution,

and with the same solution containing 0.1 M.-potassium bromide. The spots on the extreme left of each photograph indicate the steady hydrogen, halogen, and oxygen evolution potentials at the same C.D. In both cases it is to be noted that the initial and middle sections of the polarisation curves are identical, but in the presence of halide the potential then rises rapidly to that of halogen liberation, and there is no sign of the usual gradual polarisation process *although this normally occurs at a potential lower than that for halogen liberation*. In Plate II, L, is shown an experiment similar to the above but with alkaline stock solution, and with the same solution containing 0.1 M.-potassium iodide. Here the initial section of each curve is much the same, although in the presence of iodide it is displaced to a rather more positive potential, but the middle sections are quite different. In the presence of iodide the potential rises rapidly, and as steeply as in acid or neutral solution, to that for iodide ion discharge, whereas in the absence of iodide the gradient is much less steep. As with acid and neutral solutions, the presence of the halide appears to eliminate entirely the upper portion of the ordinary polarisation curve, although the process to which this corresponds sets in below the iodide ion discharge potential.

### Discussion.

A platinum electrode subjected to alternate anodic and cathodic polarisation (as in the present experiments) is normally in an "active" state,<sup>6</sup> and the results obtained in the present work are in general agreement with those recorded by Butler *et al.*<sup>3</sup> for such an electrode.<sup>7</sup> Three general stages in the anodic polarisation can be detected:

- (1) An initial slow and somewhat irregular, although reproducible, rise of potential.
- (2) A rapid linear rise of potential constituting the middle section of the curves.
- (3) A slow and approximately linear change passing ultimately into oxygen evolution.

Stage (1) has been attributed<sup>3</sup> to the ionisation of free and adsorbed hydrogen, and this receives independent support in the present study from the effect of catalytic poisons and the results in solutions containing halides. This stage can be eliminated entirely in the presence of strong catalytic poisons, and it is apparently independent of the ultimate anodic products obtained on electrolysis; both these features would be expected for a stage corresponding to the ionisation of cathodically formed hydrogen. Pearson and Butler<sup>8</sup> have represented this initial section of the anodic polarisation graph as consisting of a horizontal portion of steady potential, attributed to the ionisation of free hydrogen in the solution, followed by a linear rise of potential which they consider is due to the ionisation of adsorbed hydrogen; the present oscillograms show that the actual track is more complex in detail than this simple view would imply although the general picture is confirmed. Taking the above view to be correct, measurement of the oscillograms gives the quantity of electricity required to remove the adsorbed hydrogen as approximately 420 microcoulombs

<sup>6</sup> Hammett, *J. Amer. Chem. Soc.*, 1924, 46, 7; Beans and Hammett, *ibid.*, 1925, 47, 1215; Butler and Armstrong, *J. Chem. Soc.*, 1934, 746.

<sup>7</sup> Bowden<sup>2</sup> concluded that the change of potential from the hydrogen to the oxygen evolution value was in general linear with quantity of electricity passed. This has not been found by any subsequent worker, and a careful examination of Bowden's work shows that his results were probably vitiated by the inertia of the galvanometer he used as potential indicator. In the present work, at C.D.'s, comparable with those used by Bowden, the rapid second stage in the polarisation occupies about 0.01 second. This is of the same order as the period of the galvanometer used by Bowden, which was stated to be 0.003 second, and it therefore seems likely that in his work this very rapid change would be obscured.

<sup>8</sup> *Loc. cit.*, ref. 3.

per apparent sq. cm. for acid, neutral and alkaline stock solutions; this is in reasonably close agreement with the average value of 480 microcoulombs per apparent sq. cm. obtained by the workers quoted using a different method for an active platinum electrode in dilute sulphuric acid solution.

Stage (2) has been ascribed to the charging of a double layer<sup>8</sup> and in acid and neutral solutions the present results confirm this conclusion; thus this section of the curve is not appreciably affected by catalytic poisons and the slope is substantially unchanged whether the ultimate anodic product is oxygen or halogen. Measurement of a large number of oscillograms with different capacities in series with the electrolytic cell gives average values of 200 and 300 microfarads per apparent sq. cm. for the capacity of the double layer in acid and neutral stock solutions respectively; Pearson and Butler quote a value of 280 microfarads per apparent sq. cm. for a platinum electrode in dilute sulphuric acid, which is of the same order. In alkaline stock solution it seems doubtful if the middle section of the curve can be attributed merely to the charging of a double layer; the slope is here much more gradual than in acid and neutral solutions, corresponding to an apparent capacity of about 500 microfarads per apparent sq. cm., and it is markedly changed in the presence of iodide.

The characteristics of Stage (3) in the anodic polarisation are of great interest. The onset of this stage is well defined in the present oscillograms and corresponds to potentials of +0.87, +0.50, and +0.06 v. severally for acid, neutral and alkaline stock solutions. Grube<sup>9</sup> found that the potential of platinous oxide against platinum, while not very well defined, was about +0.9 v. for the freshly prepared oxide in 2N-sulphuric acid. Assuming the ordinary equation for variation with hydrogen ion concentration, this gives values for the static oxide potential of approximately +0.88, +0.49, and +0.07 v. for the present acid, neutral and alkaline stock solutions. These are in remarkably close agreement with those corresponding to the onset of Stage (3), and it is difficult to resist the conclusion, therefore, that this represents the commencement of oxide formation at the electrode.<sup>10</sup> The quantity of electricity passed from the beginning of Stage (3) to the point at which the potential begins to approach a constant value can be estimated approximately from the oscillograms and is found to be about 1000 microcoulombs per apparent sq. cm. for all solutions; this is sufficient for the liberation of approximately  $3.1 \times 10^{15}$  atoms of oxygen. Taking the specific gravity of platinum as 21.4, the diameter of the platinum atom may be calculated to be approximately  $2.5 \times 10^{-8}$  cm., and hence there should be about  $1.6 \times 10^{18}$  atoms of metal per sq. cm. at a platinum surface. There is some uncertainty as to the ratio of the real to the apparent area at a smooth platinum surface, this having been variously estimated by different observers as between 1.5 and 3. If the commonly accepted value of 2 is taken, then it would appear that the quantity of electricity passed in Stage (3) would provide 1 atom of oxygen for each platinum atom in the electrode surface. Stage (3) would thus seem to correspond to the formation of a monatomic layer of oxygen on the platinum surface, probably in the form of platinous oxide. Butler *et al.*<sup>9</sup> have reached a similar conclusion with regard to the amount of oxygen deposited on the platinum prior to oxygen evolution, but maintain that no definite oxide is formed. The chief evidence for this point of view appears to be that in the cathodic polarisation of a platinum electrode which has previously been anodically treated, no

<sup>8</sup> *Z. Elektrochem.*, 1910, 16, 621.

<sup>10</sup> Bowden,<sup>2</sup> working with 0.2 N. sulphuric acid as electrolyte, found a break in his anodic polarisation curves at +0.87 v., and showed that platinum after superficial oxidation in various ways gave about the same potential on immersion in the oxygen saturated electrolyte. Hoar (*Proc. Roy. Soc., A*, 1933, 142, 628), from work on the oxygen electrode, also concluded that an oxide layer was formed on platinum.

depolarisation process is observed which can be distinguished from that due to reduction of oxygen in the solution near the electrode. This evidence appears to the present author to carry little weight, since it is by no means improbable that reduction of dissolved oxygen occurs through intermediate oxide formation at the electrode. The potential observations reported above would certainly seem to suggest that platinous oxide is definitely formed. During the formation of this oxide, the potential rises approximately linearly with quantity of electricity passed. This is at first sight somewhat unexpected as it might be thought that the potential would remain stationary at the static value for the oxide until the surface layer was complete. It would appear that the potential after the commencement of Stage (3) is conditioned by some very unstable species reacting rapidly to give the oxide which is being formed, since if the polarising current is interrupted the potential drops almost immediately to the static oxide value. Until extensive data are available for other metals, it appears premature to attempt to elucidate the potential mechanism further. To account for the linear rise of potential with quantity of electricity passed, it has been suggested<sup>3</sup> that oxygen dipoles are adsorbed at the electrode surface. This type of potential mechanism has frequently been advanced in recent years to account for linear changes of potential, but it should be emphasised that no direct experimental evidence of any kind is available to support it, and it must be regarded, however plausible, as a purely *ad hoc* hypothesis.

The present results raise some interesting questions as to the general mechanism of anodic processes. Whenever oxygen is the ultimate product at the anode, the oscillograms are fundamentally the same independent of the nature of the anions present. This strongly suggests that in all these cases the anodic process is essentially the same and probably corresponds to the discharge of the hydroxyl ion followed by oxygen accumulation at the electrode, this latter governing the potential exhibited. In the presence of halides, however, the anode potential rises immediately the double layer is charged to the reversible halogen potential, *even where this is higher* than that corresponding to what has been termed the oxide formation at the electrode. According to current orthodox electrochemical conceptions, this is highly paradoxical since it is normally considered that the process requiring the least potential will necessarily occur first. No simple explanation of this peculiar behaviour (about which the oscillograms J, K and L leave no doubt) is apparent, but it would seem to imply some fundamental irreversibility in the initial anodic process. It may be noted that a similar conclusion has been arrived at from electrolytic oxidation studies.<sup>11</sup>

### Summary.

1. The initial build-up of anodic polarisation at a smooth platinum anode over a wide range of conditions has been investigated by a new oscillographic method.
2. The experimental results of previous workers have been confirmed and extended, and three main stages in the polarisation have been distinguished corresponding to the ionisation of hydrogen, the charging of a double layer, and the deposition of oxygen at the electrode; it is suggested that the last process corresponds to the formation of a unimolecular layer of platinous oxide on the electrode surface.
3. Attention is drawn to a singular anomaly which occurs in the presence of halides, when the anode potential rises directly to that for halogen evolution even where this is higher than the value at which oxygen can normally begin to deposit on the anode surface.

*Department of Inorganic and Physical Chemistry,  
University of Liverpool.*

<sup>11</sup> See Glasstone and Hickling, *Chemical Reviews*, 1939, 25, 407.

# THE INTERACTION BETWEEN RUBBER AND LIQUIDS. VII. THE HEATS AND ENTROPIES OF DILUTION OF NATURAL RUBBER BY VARIOUS LIQUIDS.

BY (MISS) J. FERRY, GEOFFREY GEE and L. R. G. TRELOAR.

*Received 21st December, 1944.*

## 1. Introduction.

Considerable progress has been made in interpreting the properties of polymer solutions and gels in the light of statistical calculations of the entropy of mixing of polymers with liquids.<sup>1</sup> The basis of most of these applications has been the assumption that the Gibbs free energy of dilution  $\Delta G_0$  of such a mixture by the liquid was expressible in terms of the entropy of dilution  $\Delta S_0$ , as calculated statistically on the assumption of random mixing, and a heat of dilution  $\Delta H_0$  proportional to the square of the volume fraction  $v_2$  of the polymer. Huggins has shown that a wide variety of thermodynamic data can be represented in this way; the present paper will include a more sensitive test of the validity of the assumption.

Free energies of dilution of polymer solutions have been calculated<sup>2</sup> from data on vapour pressure, osmotic pressure, swelling pressure, and freezing point depression. Corresponding values for the heats of dilution are almost entirely lacking, and it is therefore impossible to check whether the quantity employed to relate the theoretical entropy to the experimental free energy is equal to the heat of dilution, or whether it contains also an empirical correction factor. The direct measurement of heats of dilution for polymer systems is exceedingly difficult; a new attempt to do so for mixtures of natural rubber + benzene is now in progress. Here we present estimates of the heats of mixing of natural rubber with a number of liquids, based on calorimetric measurements of the heats of mixing of low molecular liquid homologues of rubber with the same liquids, and of the entropies of mixing obtained by combining these with vapour pressure data.

## 2. Heat and Volume Changes on Mixing Dihydromyrcene and Squalene with other Liquids.

A quantity of dihydromyrcene and a much smaller amount of squalene were made available to us by Dr. E. H. Farmer, to whom our thanks are due. These substances contain respectively two and six isoprene units per molecule, and may thus be regarded as very low molecular homologues of natural rubber. The heats of mixing of dihydromyrcene with a series of liquids were measured in the calorimeter shown in Fig. 1. In order to conserve materials it was necessary to work with relatively small volumes of liquids (not more than 10 c.c. dihydromyrcene for the whole series of measurements on each liquid). The heat absorption to be measured in a typical mixing was thus of the order of 1 cal. Attempts to do this in a small vacuum jacketed calorimeter of small heat capacity were

<sup>1</sup> Huggins, *J.A.C.S.*, 1942, 64, 1712. Flory, *J. Chem. Physics*, 1942, 10, 51. Gee, *Trans. Farad. Soc.*, 1942, 38, 276, 418; 1944, 40, 463, 468. *Ann. Repts. Chem. Soc.*, 1942, 7. *Recent Advances in Colloid Science*, Vol. 2 (Interscience Publishers, in press).

<sup>2</sup> Reifs. 1 and especially Huggins, *Ann. N.Y. Acad. Sci.*, 1942, 43, 1; *Ind. Eng. Chem.*, 1943, 35, 216.

rendered inaccurate by relatively large heat losses, and the arrangement shown was finally adopted. It consisted of a thermostatted vacuum vessel almost filled with water, in which were suspended two coaxial bulbs, the tube of the inner bulb being a close fit into the outer so as to minimise loss by evaporation. The liquids A and B were in the outer and inner bulbs respectively, the lower end of the latter being sealed by a pool of mercury. Mixing of the two liquids was accomplished by raising the inner bulb out of the mercury and rotating it so that the liquid was stirred by the vanes attached to the inner bulb. Several samples of B could be added successively without removing the calorimeter from the thermostat, the inner bulb being completely emptied each time by passing a gentle stream of nitrogen through it. The water in the calorimeter was stirred by a slow stream of air presaturated with water vapour. A layer of cork, C, was found necessary in order to prevent water splashing through the exit tube. The temperature change was measured by ten copper-eureka thermocouples, T, in series, arranged at different levels, with the cold junctions in a second vacuum vessel also filled with water, and contained in the same thermostat; the connecting leads passed through a short length of lead tubing. The heater H was of *ca.* 10 ohms resistance, and permitted small measured quantities of energy to be introduced in order to determine the heat capacity. This was approximately 65 cal., so that the temperature change to be measured was of the order of a hundredth of a degree, and the thermoelectric e.m.f. a few microvolts. This was measured directly by means of a Tinsley taut suspension galvanometer, of resistance 9.5 ohms and sensitivity 180 mms. per microamp. The overall sensitivity (maximum 5 metres per degree) was determined by calibrating against Beckmann thermometers, the galvanometer deflection being very nearly proportional to the temperature difference between the hot and cold junctions.

In order to make the heat interchange with the surroundings during an experiment small compared with the quantity to be measured, it was necessary that both hot and cold junctions should be very near to the thermostat temperature.\* In order to ensure this, it was found desirable to check the cold junction temperature before and during an experiment by a Beckmann thermometer, and to leave the calorimeter in the thermostat overnight before making the first addition. Subsequent additions could be made after an interval of 1 to 2 hours. Under these conditions, the correction for heat interchange with the surroundings was small, and the temperature change on mixing was nearly that calculated from the maximum galvanometer deflection.

\* A further precaution was to make the thermocouples of sufficiently fine wire for heat loss by conduction to be negligible; 20 s.w.g. eureka and 38 s.w.g. copper were actually employed.

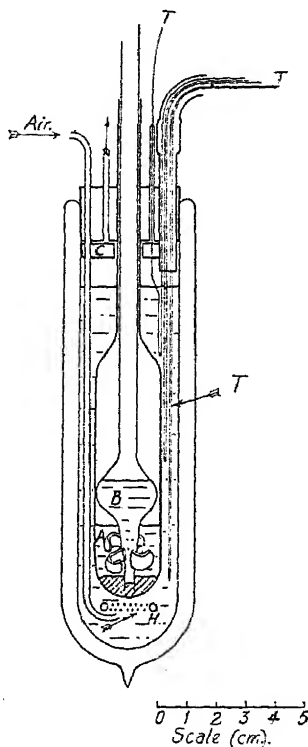


FIG. 1.—Calorimeter.



# 342 INTERACTION BETWEEN RUBBER AND LIQUIDS

A typical series of measurements of the heat of mixing of the two liquids was performed in two parts. In the first, 5 c.c. of liquid A in the outer

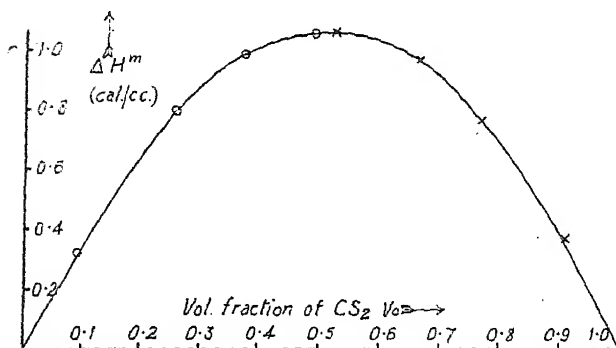
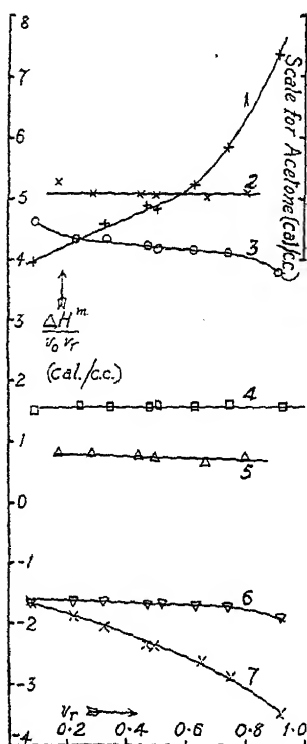


FIG. 2.—Heat of mixing of  $\text{CS}_2$  and dihydromyrcene.

bulb was diluted with four successive additions of liquid B, until the mixture contained approximately equal volumes of A and B. The procedure was then repeated, with the liquids interchanged. The heat absorptions measured were used to calculate the heat of mixing  $\Delta H^m$  of  $v_0$  c.c. of liquid A with  $(1 - v_0)$  c.c. of liquid B; results obtained in this way for  $\text{CS}_2$  + dihydromyrcene are shown in Fig. 2. In



accordance with the usage of earlier papers the volume fraction of dihydromyrcene (regarded as "rubber") is written  $v_r$ ; that of the other liquid  $v_0$ . Points in the two halves of the experiment are differently indicated, and it will be noted that all lie on a smooth, almost parabolic curve. This curve would be exactly parabolic if Hildebrand's expression<sup>3</sup> for the heat of mixing was obeyed:

$$\Delta H^m = \alpha v_0 v_r \quad (1)$$

The deviation from this form can be represented most readily by employing each experimental point to calculate a value of  $\alpha$ ; the results for a series of liquids are shown in Fig. 3. It is evident that equation (1) is obeyed with considerable accuracy by most of the liquids examined, only acetone and chloroform showing large deviations. There appears to be a real,

FIG. 3.—Heats of mixing of liquids with dihydromyrcene.

- |                    |                      |
|--------------------|----------------------|
| 1. Acetone.        | 5. Heptane.          |
| 2. Benzene.        | 6. $\text{CCl}_4$ .  |
| 3. $\text{CS}_2$ . | 7. $\text{CHCl}_3$ . |
| 4. Toluene.        |                      |

though small, deviation in the  $\text{CS}_2$  data, although the extreme points are less accurate than the remainder.

<sup>3</sup> Hildebrand, *Solubility* (Reinhold, 1936).

The constant  $\alpha$  is given, according to Hildebrand's theory by

$$\alpha = (\sqrt{e_0} - \sqrt{e_r})^2 \quad (2)$$

where  $e_0$  and  $e_r$  are the cohesive energy densities of the liquid and of dihydromyrcene;  $\alpha$  should thus always be positive, so that (2) evidently breaks down for  $\text{CHCl}_3$  and  $\text{CCl}_4$ . By comparison with other hydrocarbons we may estimate  $\sqrt{e_r}$  for dihydromyrcene as  $7.4_2$  (cal./c.c.) $^{\frac{1}{2}}$ , for squalene as  $7.7_8$  (cal./c.c.) $^{\frac{1}{2}}$  while the value for natural rubber has been previously estimated<sup>4</sup> as  $7.9_8$ . In Table I, values of  $\alpha$  calculated from (2) are com-

TABLE I.—HEAT AND VOLUME CHANGES IN DIHYDROMYRCENE MIXTURES.

Liquid.	$\sqrt{e_0}$	$\alpha$ (cal./c.c.).		$100 \frac{\Delta V^m}{v_0 v_r}$ (c.c.).
	(cal./c.c.) $^{\frac{1}{2}}$	calc.	obs.	
Benzene. . . .	9.1 <sub>8</sub>	3.1 <sub>0</sub>	5.1	1.5
Toluene . . . .	9.0 <sub>2</sub>	2.5 <sub>6</sub>	1.60	0.2
Heptane . . . .	7.5 <sub>0</sub>	0.0 <sub>1</sub>	0.7 <sub>0</sub>	-0.4
CS <sub>2</sub> . . . . .	10.0 <sub>3</sub>	6.9	4.2	1.2
CCl <sub>4</sub> . . . . .	8.5 <sub>5</sub>	1.2 <sub>8</sub>	-1.7	-0.3
Acetone . . . .	9.7 <sub>7</sub>	5.5	8 to 16	0.4
CHCl <sub>3</sub> . . . .	9.3 <sub>0</sub>	3.5	-1.6 to -3.5	0.2

pared with the experimental values, and it is evident that while there is a rough agreement as to order of magnitude for benzene, toluene, heptane, CS<sub>2</sub>, and acetone, the halogenated hydrocarbons fall completely out of line.

It has been suggested<sup>5</sup> that the general source of disagreement between calculated and experimental heats of mixing of liquids arises from the failure of the assumption involved in the derivation of equation (2) that there is no volume change on mixing. In order to test the importance of this factor in the present case the volume changes on mixing were measured in a simple modification of the apparatus described by Hildebrand and Carter.<sup>6</sup> It consisted of a U-tube of total volume ca. 7 c.c., the upper parts of the two limbs being of capillary tubing, closed at the outer ends by stoppers. The tube was filled with 3 c.c. of mercury plus 2 c.c. of each liquid under examination and thermostatted, the mercury forming a seal between the two liquids. After reading the liquid levels in the capillaries, the two liquids were mixed by allowing the mercury to flow from limb to limb and the levels again noted. The expansions observed ( $\Delta V^m$  c.c./c.c. of total liquid), are given in Table I, expressed as  $100 \Delta V^m / v_0 v_r$ , which is reproducible to  $\pm 0.2$  c.c. The energy required to compress the mixture isothermally to the volume it would have if mixing occurred without change of volume is approximately  $T\alpha_v \Delta V^m / 41.3\beta$  cal. where  $\alpha_v$ (deg. $^{-1}$ ),  $\beta$ (atm. $^{-1}$ ) are the coefficients of cubical expansion and compressibility of the mixture. For most liquids at room temperature  $T\alpha_v / 41.3\beta \approx 100$  cal./c.c., so that the last column is approximately equal, numerically, to the contribution to the heat of mixing from the work done against the intermolecular forces in the observed expansion. This contribution is by no means negligible for benzene and CS<sub>2</sub> but the lack of correlation between the last two columns shows that it does not account quantitatively for the discrepancy between the calculated and observed values of  $\alpha$ . In view of this conclusion, it was not considered worth while to investigate the constancy of the function  $\Delta V^m / v_0 v_r$ .

<sup>4</sup> Gee, *I.R.I. Trans.*, 1943, 18, 266.

<sup>5</sup> Scatchard, *Trans. Farad. Soc.*, 1937, 33, 160.

<sup>6</sup> Hildebrand and Carter, *J.A.C.S.*, 1932, 54, 3592.

### 3. Estimation of Heats of Dilution of Rubber from Calorimetric Data.

In order to obtain the heat of dilution  $\Delta H_0$ , we re-write equation (1) to give the heat absorbed  $\Delta H$ , on mixing  $N_0$  moles of liquid (molar vol.  $V_0$ ) with  $N_r$  moles of rubber (molar volume  $V_r$ ) in the form:

$$\Delta H = \frac{\alpha N_0 N_r V_0 V_r}{N_0 V_0 + N_r V_r} \quad (1')$$

and differentiate, to obtain  $\Delta H_0 \equiv \left( \frac{\partial \Delta H}{\partial N_0} \right)_{N_r} \quad (2)$

If  $\alpha$  is constant, the result is

$$\Delta H_0 / v_r^2 = \alpha V_0 \quad (3)$$

If  $\alpha$  is not constant, we may still express the experimental results in terms of  $\alpha$ , and it may then be shown that

$$\frac{\Delta H_0}{v_r^2} = V_0 \left( \alpha - v_0 \frac{\partial \alpha}{\partial v_r} \right) \quad (4)$$

Using values of  $\partial \alpha / \partial v_r$  from the smoothed curves of Fig. 3, we thus obtain  $\Delta H_0 / v_r^2$  as functions of  $v_r$  for dihydromyrcene in acetone and chloroform; for the other liquids (3) may be used with sufficient accuracy.

We have now to consider the relation between the heats of dilution of dihydromyrcene and of rubber by the same liquid. If we denote the respective "constants" of equation (1) by  $\alpha_d$ ,  $\alpha_r$ , (2) gives

$$\alpha_d = (\sqrt{e_0} - 7.42)^2; \quad \alpha_r = (\sqrt{e_0} - 7.98)^2,$$

whence

$$\alpha_d - \alpha_r = 1.12(\sqrt{e_0} - 7.70). \quad (5)$$

This equation should be true provided that the difference between the heats of dilution of dihydromyrcene and rubber can be represented completely by the difference of cohesive energy density, i.e. provided that the factors responsible for the failure of equation (2) are equally operative in both cases.

This is clearly a plausible assumption, and one would expect (5) to hold much more closely than (2). A limited test of its validity has been made by comparing the heats of mixing of benzene and heptane with dihydromyrcene and squalene. Denoting the constant of mixtures with the latter by  $\alpha_s$ , equation (5) should be replaced by

$$\alpha_d - \alpha_s = 0.72(\sqrt{e_0} - 7.60) \quad (5')$$

The experimental data for the squalene mixtures are given in Fig. 4, which shows equation (1) to be very well obeyed. Table II shows that the observed and calculated values of  $(\alpha_d - \alpha_s)$  are in excellent agreement:

TABLE II.—HEATS OF MIXING WITH SQUALENE AND DIHYDROMYRCENE.

Liquid.	$\alpha_d$ .	$\alpha_s$ .	$\alpha_d - \alpha_s$ .	
			(obs.)	(calc.)
Benzene . . .	5.1	3.9 <sub>5</sub>	1.1 <sub>8</sub>	1.1 <sub>3</sub>
Heptane . . .	0.65 to 0.8	0.8 to 0.7	$\pm 0.1_5$	0.07

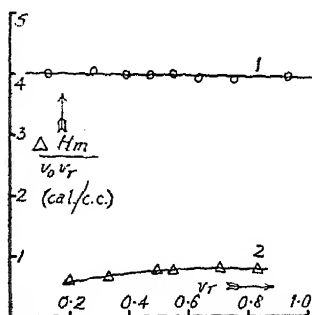


FIG. 4.—Heats of mixing of squalene with benzene (1), Heptane (2).

Values of  $\alpha_r V_0$  have therefore been computed by using the experimental values of  $\alpha_d$  and values of  $(\alpha_d - \alpha_r)$  calculated from equation (5) giving:

TABLE III.

Liquid.	$\alpha_r V_0 = \Delta H_0/v_r^2$ (cal./mole).
Benzene . . .	310
Toluene . . .	15
Heptane . . .	135
CS <sub>2</sub> . . .	95
CCl <sub>4</sub> . . .	-255

For acetone and CHCl<sub>3</sub> combination of (4) and (5) gives:

$$\Delta H_0/V_0 v_r^2 = \alpha_d - v_0 \partial \alpha_d / \partial v_r - 1.12 (\sqrt{v_0} - 7.70). \quad (6)$$

Values of  $\Delta H_0/v_r^2$  plotted in Fig. 5 were calculated from this expression. These results (Table III and Fig. 5) constitute our estimates of the heats of dilution of natural rubber by the seven liquids concerned.

One rather puzzling feature is the apparent constancy of  $\Delta H_0/v_r^2$  for most of the liquids, since the number of contacts between rubber and liquid will depend on their relative molecular surfaces, which will not be proportional to the volume fractions, except in the artificial case of infinite co-ordination number.<sup>7a</sup> It is true that this constancy has only been proved experimentally for mixtures with dihydromyrcene and squalene, but the case of benzene + squalene affords a very striking example of the disagreement between theory and experiment; according to Orr's calculations<sup>7b</sup> the value of  $\Delta H_0/v_r^2$  at  $v_r = 0$  should be only about one half of that at  $v_r = 1$ . The origin of the discrepancy remains obscure, but these experimental results, so far as they go, support the usual practice of assuming  $\Delta H_0 \propto v_r^2$  for polymer + liquid, as well as for mixtures of two liquids.

The heat of dilution obtained for benzene does not agree with our direct estimate reported earlier<sup>8</sup> according to which  $\Delta H_0/v_r^2$  varies from 160 cal./mole at  $v_r = 1$  to 60 cal./mole at  $v_r = 0$ ; we wish to defer comment on this until further work on benzene, now in progress, is completed.

#### 4. Estimation of Entropies of Dilution.

The free energy of dilution of natural rubber by each of these liquids has been calculated from the available vapour pressure data, and combined with the above thermal measurements to give an estimate of the entropy of dilution. The results are shown in Figs. 6 and 7, in which  $\Delta S_0/v_r^2$  is

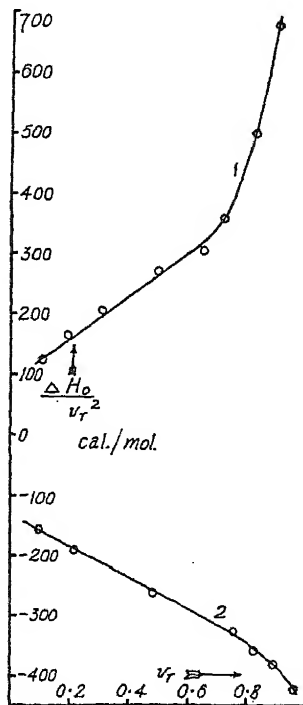


FIG. 5.—Estimated heat of dilution of natural rubber by: (1) acetone, (2) CHCl<sub>3</sub>.

<sup>7</sup> (a) Gee and Treloar, *Trans. Farad. Soc.*, 1942, 38, 147. (b) Orr, *ibid.*, 1944, 40, 320.

<sup>8</sup> Gee, *ibid.*, 1942, 38, 418; cf. 7(a).

plotted against  $v_r$ , and compared with the theoretical value obtained from Miller's equation <sup>13</sup> \*

$$\Delta S_0 = -R \left[ \ln(1 - v_r) - \frac{Z}{2} \ln \left( 1 - \frac{2v_r}{Z} \right) \right] \quad (7)$$

In Fig. 6 curves are shown for three values of the co-ordination number  $Z$ , viz. 4, 6,  $\infty$ . With  $Z = \infty$ , (7) reduces to Flory's expression <sup>14</sup>

$$\Delta S_0 = -R[\ln(1 - v_r) + v_r] \quad (8)$$

It is easily shown from (7) that

$$\left( \frac{\Delta S_0}{v_r^2} \right) = \left( \frac{\Delta S_0}{v_r^2} \right)_{Z=\infty} - \frac{R}{Z} \left( 1 + \frac{4}{3Z} \cdot v_r + \frac{2}{Z^2} \cdot v_r^2 + \dots \right) \quad (9)$$

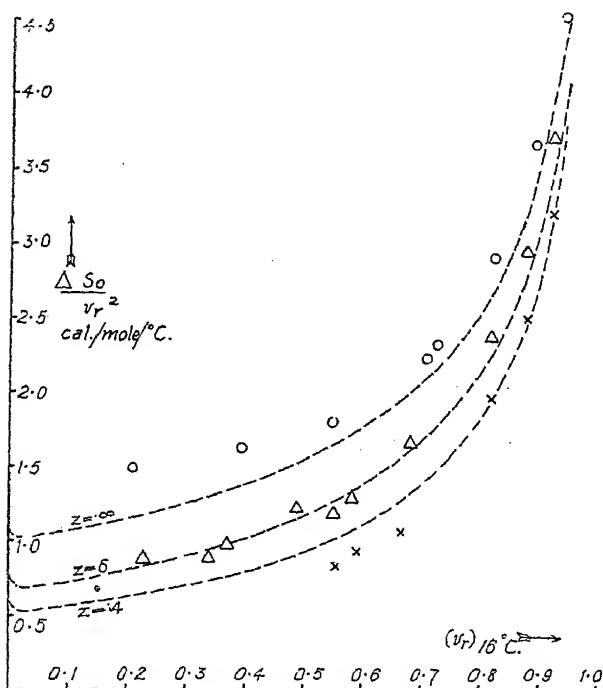


FIG. 6.—Entropy of dilution of natural rubber by hydrocarbons.  
 $\circ$  Benzene at 25° C.<sup>7a</sup>  $\Delta$  Heptane at 40° C.<sup>9</sup>  $\times$  Toluene at 25° C.<sup>10</sup>  
 Dotted curves calculated from equation (7).

so that plots of  $\Delta S_0/v_r^2 \sim v_r$  for different values of  $Z$  are nearly superposable by adding suitable constants. Huggins <sup>2</sup> has shown that a very wide range of thermodynamic data (including that used here) can be represented by an equation of the form

$$-\frac{\Delta G_0}{Tv_r^2} = \left( \frac{\Delta S_0}{v_r^2} \right)_{Z=\infty} - \frac{\mu}{RT} \quad (10)$$

<sup>9</sup> Unpublished experiments.

<sup>10</sup> Meyer and Boissonnas, *Helv. Chim. Acta*, 1940, 23, 430.

<sup>13</sup> Miller, *Proc. Camb. Phil. Soc.*, 1943, 39, 54, 131.

\* This is a simplification of the general equation, valid for polymers of high molecular weight, except in dilute solutions.

<sup>14</sup> Flory, *J. Chem. Physics*, 1941, 9, 660; 1942, 10, 51.

where  $\mu$  is a constant. Now, for those liquids for which  $\Delta H_0 = \alpha_r V_0 v_r^2$  we have also

$$-\frac{\Delta G_0}{T v_r^2} = \frac{\Delta S_0}{v_r^2} - \frac{\alpha_r V_0}{T} \quad (11)$$

Huggins' observation thus requires that for these liquids the entropy curves should be either identical or at least superposable by adding suitable constants. This is nearly true in most cases, although the present method of plotting provides a much more severe test of equation (10) than that employed by Huggins. If equation (10) holds for liquids for which  $\Delta H_0 = \alpha_r V_0 v_r^2$  it follows that  $\Delta S_0/v_r^2$  cannot be of the standard form.

It is evident from Figs. 6 and 7 that our estimated entropies of dilution, although generally of the expected form, do not agree quantitatively either among themselves or with the theoretical equation. It is unlikely that the free energies deduced from vapour pressure data can be seriously in error for  $v_r > 0.5$ , but the lower points are much less certain. Some part at least of the disagreement may arise from errors in the heats of dilution; this cannot at present be checked. Discussion of the origin of these different entropies of dilution must therefore be somewhat tentative at present.

The first point to be noted is that equation (7) was deduced on the assumption of random mixing, so that it can only be expected to apply accurately to athermal mixtures. The nearest approach to this condition is provided by toluene, heptane and  $\text{CS}_2$ , and it is satisfactory to note that these three liquids give entropy curves in fair agreement with theory, assuming low co-ordination numbers (4 to 6). There is, of course, no reason to suppose that the co-ordination number will be the same for all mixtures of rubber + liquid, or even that it will necessarily be independent of concentration in any particular mixture. The effect of finite heats

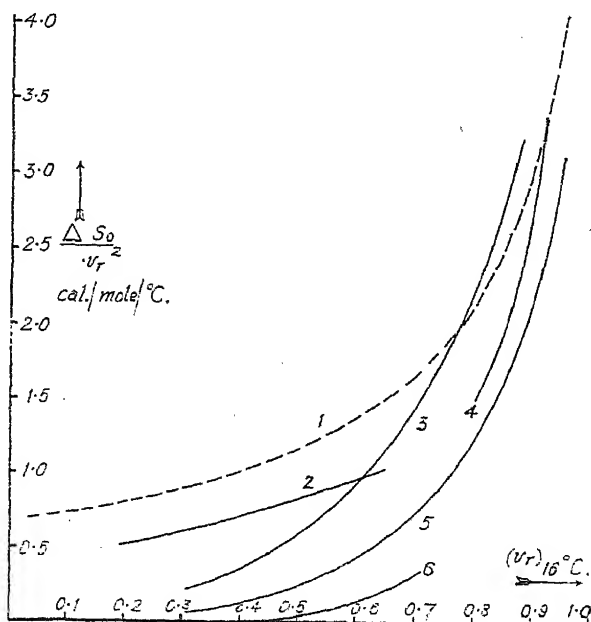


FIG. 7.—Entropy of dilution of natural rubber by polar liquids.

Curve 1. Theoretical ( $Z = 6$ ). Curve 4. Acetone at  $35^\circ \text{C}$ .<sup>12</sup>  
 2.  $\text{CS}_2$  at  $25^\circ \text{C}$ .<sup>11</sup> 5.  $\text{CHCl}_3$  at  $35^\circ \text{C}$ .<sup>12</sup>  
 3.  $\text{CCl}_4$  at  $35^\circ \text{C}$ .<sup>12</sup> 6.  $\text{CHCl}_3$  at  $25^\circ \text{C}$ .<sup>11</sup>

<sup>11</sup> Stamberger, *J.C.S.*, 1929, 2323.

<sup>12</sup> Lens, *Rec. trav. chim.*, 1932, 51, 971.

of mixing on the entropy of dilution has been estimated by Orr,<sup>7b</sup> and shown to be small for heats of mixing of the order found experimentally for most of the liquids with which we have worked, the only possible exception being acetone. The effect vanishes for  $Z = \infty$ , and for finite values of  $Z$  is positive at low  $v_r$ , negative at high. Using Orr's equation, the theoretical entropy of dilution of rubber by benzene, taking  $N_w = 310$  cal.;  $Z = 6$  is 2.08 cal./mole/°C. at  $v_r = 0.8$ , which is almost identical with the value calculated for athermal mixing. The high entropy found experimentally for benzene appears to be a specific effect, and is probably due to the fact that this liquid is known from other evidence to be rather highly ordered,<sup>15</sup> due no doubt to a tendency for the flat molecules to pack with the planes of adjacent molecules parallel. The very large expansion found on mixing with dihydromyrcene (Table I) is almost certainly connected with the breakdown of this ordered arrangement.

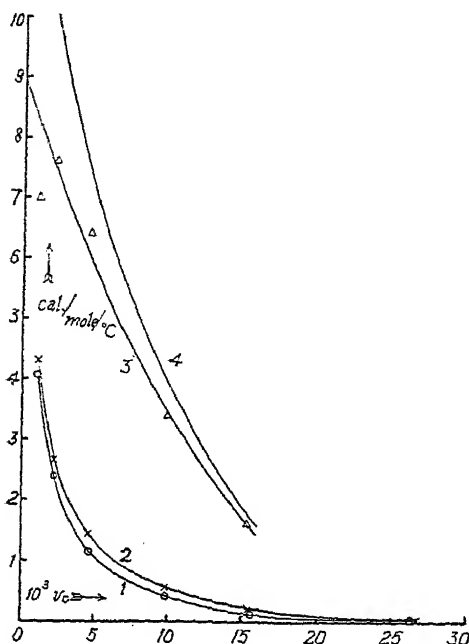


FIG. 8.—Thermodynamic functions for the system natural rubber + methyl alcohol.

- (1)  $-\frac{\Delta G_0}{Tv_r^2}$  at 25° C.
- (2)  $-\frac{\Delta G_0}{Tv_r^2}$  at 35° C.
- (3)  $\frac{\Delta H_0}{Tv_r^2}$  at 30° C. from (1) and (2).
- (4)  $\frac{\Delta S_0}{v_r^2}$  at 30° C. from (1), (2) and (3).

Acetone is an example of a liquid possessing a rather large heat of mixing with rubber, the two materials being only partially miscible. The tendency towards separation into two phases is shown by the rapid fall of both  $\Delta H_0/Tv_r^2$  and  $\Delta S_0/v_r^2$  as the acetone content is increased, indicative of increasingly non-random mixing. Although in the direction indicated by Orr's analysis, both effects are considerably greater than would be given by the theory. Taking  $N_w = 1000$  cal.,  $Z = 6$ , the calculated values at  $v_r = 0.8$  are  $\Delta H_0/v_r^2 = 680$  cal./mole;  $\Delta S_0/v_r^2 = 1.86$  cal./mole/°C. The maximum inhibition of acetone by rubber at 35° C. should be only about 8 % by volume, compared with the experimental value of ca. 20 %. It is evident therefore that neither the crude theory, as developed by Flory and Huggins, nor Orr's refinement of it, applies quantitatively to this system.

$\text{CCl}_4$  and  $\text{CHCl}_3$  present a different kind of departure from the simple theory; the entropy of mixing is again small, but for these liquids  $\Delta H_0$

<sup>15</sup> Scatchard, Wood and Mochel, *J. Physic Chem.*, 1939, 43, 119.

is negative, indicating a tendency towards complex formation between the liquid and rubber. The very small entropies of dilution at low liquid concentrations affords further evidence of order in the mixture, associated with complex formation.

### 5. Thermodynamics of the System Rubber + Methyl Alcohol.

The evidence presented above shows that, while the statistical thermodynamic theory of polymer solutions holds reasonably well for normal mixtures it is less satisfactory when the heat of mixing is large. In order to test the usefulness of the present theories in an extreme case, we have

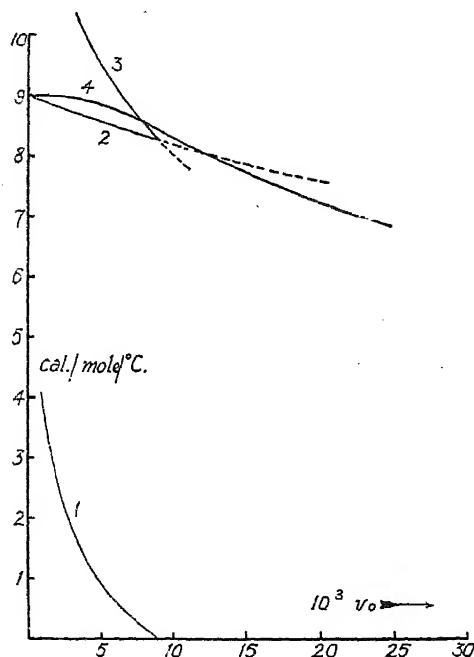


FIG. 9.—Theoretical thermodynamic functions for rubber and methyl alcohol at 30° C.

$$\begin{array}{l}
 \text{Curve 1. } -\frac{\Delta G_0}{T v_r^3} \\
 \left. \begin{array}{l} 2. \quad \frac{\Delta H_0}{T v_r^2} \\ 3. \quad \frac{\Delta S_0}{v_r^2} \end{array} \right\} \text{Theoretical for } \begin{cases} Z = 6. \\ N_w = 2.72 \text{ k. cal.} \end{cases} \\
 4. \quad \left( \frac{\Delta G_0}{T v_r^3} \right)_{\text{expt.}} + \left( \frac{\Delta S_0}{v_r^2} \right) \text{ theoretical for } \begin{cases} \Delta H_0 = 0. \\ Z = 6. \end{cases}
 \end{array}$$

studied the thermodynamic properties of mixtures of rubber + methyl alcohol. Only about 2 % of methyl alcohol is imbibed by rubber at room temperature, so that a very limited concentration range is available for study. Vapour pressures were measured at 25° C. and 35° C. by a method previously described<sup>7a</sup> and used to calculate the free energy and heat of dilution. The results are shown in Fig. 8, from which the following points may be noted:—

(i)  $\Delta H_0/v_r^2$  falls very rapidly as the alcohol content of the mixture increases. This behaviour is paralleled by the heats of solution of alcohols



in low molecular hydrocarbons,<sup>16</sup> and must be ascribed to the almost complete association of alcohols except in the most dilute solution. The very large heat of dilution as  $v_0 \rightarrow 0$  represents the energy of the hydrogen bonds, and is of the same order for methyl alcohol in rubber as for a range of alcohols in hexane and benzene.

(ii)  $\Delta S_0$  is very much less than its theoretical value, except at very small  $v_0$ , and it is evident that mixing is far from random.

(iii) These deviations are far larger than would be expected on the basis of Orr's calculation of the effect of a heat of mixing.<sup>7b</sup> The discrepancy is not surprising, since the theory does not make allowance for association, which must in this case be the dominating cause of irregularity. Fig. 9 shows the thermodynamic functions calculated from Orr's equation, assuming  $Z = 6$ , with the observed heat of dilution extrapolated to  $v_0 = 0$ . They lead to a predicted maximum imbibition of methyl alcohol at 30° C. of  $v_0 = 0.0088$ , which is the same as that calculated from the entropy of random mixing with  $\Delta H_0/v_1^2$  constant. The experimental value is some three times higher, a discrepancy very similar to that found for acetone. At the same time, curve 4 of Fig. 9 shows that Huggins' equation (10) is still quite a good approximation, the "constant"  $\mu$  varying by no more than 25 % over the available concentration range. Over most of this range, however, it is not even approximately related to the heat of dilution, and it is clear that  $\mu$  will be temperature dependent.

## 6. Conclusions.

The statistical thermodynamic theory of polymer solutions is confirmed as a valid and useful first approximation. In general, the free energy of dilution can be expressed with considerable accuracy as the difference between an "apparent heat of dilution," proportional to  $v_1^2$ , and  $T$  times the entropy of dilution calculated for random mixing. The identification of these two terms as the true heat and entropy of dilution is not generally correct, both being subject to considerable variations arising from the existence of order in the components or in the mixture. These variations, whose effects on the free energy nearly cancel, are in the direction to be expected from Orr's analysis of the effect of a finite heat of mixing, but may be considerably larger. The present theory fails most seriously in the estimation of (i) two phase equilibria, and (ii) the temperature coefficient of the free energy.

## Summary.

Calorimetric measurements of the heats of mixing of seven liquids with dihydromyrcene are used to estimate the heats of dilution of rubber by these liquids. Combining the results with free energies calculated from vapour pressure gives entropies of dilution which show significant deviations from the present statistical theory.

A thermodynamic study of rubber + methyl alcohol shows similar but larger deviations.

This work forms part of a programme of fundamental research on rubber undertaken by the Board of the British Rubber Producers' Research Association.

*British Rubber Producers' Research Association,  
48 Tewin Road, Welwyn Garden City, Herts.*

<sup>16</sup> Wolf, Pahlke and Wehage, *Z. physik. Chem.*, 1935, 28, 1.

# THE DEGRADATION OF HIGH POLYMERS.

By R. F. TUCKETT.

Received 7th December, 1944.

All current treatments of degradation have the same aim, namely, to calculate the size distribution of the resulting fragments after a given time and in terms of the average number of cuts undergone by each chain in that time. For simplicity, it is generally assumed that the polymer system is initially monodisperse though this restriction can be removed in any later development of the theory. To date, all treatments have involved two assumptions; these have been stated explicitly by Montroll and Simha<sup>1</sup> in the following form:—

"(1) The accessibility to reaction of a bond in a given chain is independent of its position in the chain and independent of the length of the parent chain.

(2) All chains in a given mixture are equally accessible to reaction."

With these assumptions, the fact that the randomly distributed cuts do not all occur at the same time is irrelevant and the resulting distribution is the same as when all the cuts are made simultaneously. On this reasonable basis, the problem becomes a purely statistical one and is soluble. In the present work, it is shown that some of the results already obtained by other methods can be derived more neatly and more generally by using the technique developed by Darwin and Fowler in their formulation of the basic theorems of statistical mechanics, namely, the method of steepest descents. Such a treatment gives the necessary average quantities directly—the results are, however, simple only for high degrees of degradation as are also those derived by other methods. The formulation of the problem makes it possible to apply the theory to poly-disperse systems immediately; moreover, the relative simplicity of the treatment suggests a method of approaching a problem which other methods have failed to solve, namely, the result when the restriction imposed by Assumption (1) is partially removed. This is perhaps a justification for advancing yet another theoretical treatment in this field where the available experimental evidence is still insufficient to decide between the theories already in existence.

As the extent of degradation can be defined in terms of either the fraction of bonds broken or the average fragment length and as a number of theoretical treatments already exist, notation has tended to become somewhat individual. Here, we take as our degradation parameter,  $l$ , the (number-) average chain length of the fragments at time  $t$ . For convenience, we give below the notations of some recent treatments.

	Kuhn <sup>2</sup>	Montroll and Simha <sup>1</sup>	Jellinek <sup>3</sup>	Present work
Initial chain length	$N + 1$	$p + 1$	$P_0$	$p$
Average number of cuts at time $t$	$s$	$r_0$	$S$	$S$
No. fragments at time $t$	$(s + 1)$	$(r_0 + 1)$	$\beta$	$b = p/l$
Degree of degradation	$\alpha = s/N$	$\alpha = r_0/p$	$\alpha = S/P_0$	—
Average fragment length	$\frac{N + 1}{s + 1}$	$\frac{p + 1}{r_0 + 1}$	$P_0/\beta$	$l$

<sup>1</sup> Montroll and Simha, *J. Chem. Physics*, 1940, 8, 721.

<sup>2</sup> Kuhn, *Ber.*, 1930, 63, 1510.

<sup>3</sup> Jellinek, *Trans. Far. Soc.*, 1944, 40, 266.

The degradation problem is mathematically similar to that of finding the partition of energy among a set of harmonic oscillators—in the subsequent development, the equations derived are compared with the analogous ones in Fowler and Guggenheim's<sup>4</sup> treatment of the latter problem.

### General Theory.

For convenience, we consider the case of  $N$  chains (each of  $p$  units). One possible initial assumption is that each chain undergoes the same number of cuts at any time  $t$ ; this would give a relatively simple "single chain" theory but it is very unlikely that the degradation process is subject to this restriction. A more general treatment considers only the total number of cuts in the system, these cuts being distributed randomly among the  $N$  chains; an advantage of the present formulation is that the general result comes out more naturally than the restricted one.

Let each chain be split on the average  $S$  times to give  $S + 1 = b$  fragments. Then, if  $l$  is the average chain length at time  $t$ , we have  $b = p/l$ . In what follows,  $l$  is used as the degradation variable for reasons which will appear later. Consider a given way of distributing the  $NS$  cuts such that there are altogether  $n_i$  fragments of length  $i$  units ( $i = 1, 2, \dots, p$  as some chains will not be degraded). Then the given set of numbers  $n_1, n_2, \dots, n_p$  (all zero or positive integers) must satisfy the relations

$$\sum_i n_i = Np/l \quad . \quad . \quad . \quad . \quad . \quad (1)$$

$$\sum_i i n_i = Np \quad . \quad . \quad . \quad . \quad . \quad (2)$$

(cf. F.G. 206, 1, 3). The size distribution of fragments corresponding to this set of numbers can be produced in  $\Omega_\sigma$  ways where

$$\Omega_\sigma = \frac{Np/l!}{n_1! n_2! \dots n_p!} \quad . \quad . \quad . \quad . \quad . \quad (3)$$

and for any distribution of  $NS$  cuts, the total number of ways (complexions),  $C$ , is given by  $\sum_\sigma \Omega_\sigma$ , the summation being taken over all possible sets of  $n_i$  subject to equations (1) and (2) above (cf. F.G. 206.5).

To define  $C$ , we define a generating function  $f(z)$  given by

$$f(z) = \omega_1 z + \omega_2 z^2 + \dots + \omega_p z^p \quad . \quad . \quad . \quad . \quad . \quad (4)$$

We shall consider two special cases.

(1)  $\omega_1 = \omega_2 = \omega_3 \dots = 1$ , corresponding to random degradation.

(2)  $\omega_2 = \omega_3 = \omega_4 \dots = 1$ ,  $\omega_1 \neq 1$ , a special case of non-random degradation.

For random splitting,  $C$  is the coefficient of  $z^{Np}$  in the expansion of  $[f(z)]^{Np/l}$  after putting all  $\omega_i = 1$ . For the moment, we retain the  $\omega_i$  for reasons which will appear shortly. Now, the coefficient  $C$  is conveniently expressed as a complex integral taken round a contour enclosing the origin  $z = 0$ . Then

$$C = \frac{1}{2\pi i} \int_{\gamma} \frac{[f(z)]^{Np/l}}{z^{Np}} \cdot \frac{dz}{z} \quad . \quad . \quad . \quad . \quad . \quad (5)$$

with  $\omega_1 = 1$ . To characterise the distribution, we have to find an expression for  $\bar{n}_i$ , the average number of  $i$ -mers in the assembly. Now, by definition,

$$\bar{n}_i = \frac{\sum_\sigma n_i \Omega_\sigma}{\sum_\sigma \Omega_\sigma} \quad . \quad . \quad . \quad . \quad . \quad (6)$$

<sup>4</sup> Fowler and Guggenheim, *Statistical Thermodynamics*, Cambridge, 1939, Chap. II, hereafter referred to as F.G.

or  $C\bar{n}_1 = \sum_{\sigma} n_1 \Omega_{\sigma}$ , the summation being subject to all sets of  $n_1$  which obey equations (1) and (2) and it can be shown that  $C\bar{n}_1$  is the coefficient of  $z^{Np}$  in the expansion of  $\omega_1 \frac{\partial}{\partial \omega_1} [f(z)]^{Np/l} \cdot (\omega_1 = 1)$ .

$$\text{Hence, } C\bar{n}_1 = \frac{1}{2\pi i} \int_{\gamma} \frac{\omega_1 \frac{\partial}{\partial \omega_1} [f(z)]^{Np/l}}{z^{Np}} \cdot \frac{dz}{z} \quad (7)$$

The integrals (5) and (7) can be evaluated in simple form by the method of steepest descents.<sup>5</sup> (This imposes a trivial restriction as the method is only valid for large  $Np/l$  and  $Np$ , a condition always fulfilled.)  $C$  is evaluated at the col  $z = \theta$  ( $0 < \theta < 1$ ) defined by:

$$\frac{\partial}{\partial \log \theta} \left[ \frac{Np}{l} \log f(\theta) - Np \log \theta \right] = 0 \quad (8)$$

$$\text{i.e. } \theta \frac{\partial}{\partial \theta} \log f(\theta) = l \quad (9)$$

For this value of  $z$  (and large  $Np/l$ ,  $Np$ ), then

$$C = \frac{[f(\theta)]^{Np/l}}{\theta^{Np}} \quad (10)$$

Now, the advantage of this method of integration is that  $\bar{n}_1$  can be evaluated directly without knowledge of  $C$  as the factors which multiply  $\frac{[f(z)]^{Np/l}}{z^{Np+1}}$  to form the integrand in (7) can be taken outside the integration sign if in them we replace  $z$  by  $\theta$ —the detailed proof of this statement is given elsewhere.<sup>5</sup> Hence, substituting in (7), we get

$$C\bar{n}_1 = \left[ \frac{Np}{l} \omega_1 \frac{\partial}{\partial \omega_1} \log f(z) \right]_{z=\theta} \frac{1}{2\pi i} \int \frac{[f(z)]^{Np/l}}{z^{Np}} \cdot \frac{dz}{z}$$

It then follows from (5) that:

$$\bar{n}_1 = \frac{Np}{l} \omega_1 \frac{\partial}{\partial \omega_1} \log f(\theta) \quad (11)$$

which on substituting for  $f(\theta)$  by using equation (4) gives

$$\bar{n}_1 = \frac{Np}{l} \frac{\omega_1 \theta^l}{f(\theta)} \quad (12)$$

In order to derive the various average molecular weights of the fragments, we require summations which are derived from the general formula for  $\bar{n}_1$  (equation 12). First  $\sum_i \bar{n}_1 = \frac{Np}{l} \frac{1}{f(\theta)} \sum_i \omega_i \theta^l = Np/l$  in agreement with (1). For  $\sum i \bar{n}_1$ , we have

$$\begin{aligned} \sum i \bar{n}_1 &= \frac{Np}{l} \frac{1}{f(\theta)} \sum i \omega_i \theta^l \\ &= \frac{Np}{l} \frac{1}{f(\theta)} \theta \frac{\partial}{\partial \theta} \sum \omega_i \theta^l \\ &= \frac{Np}{l} \frac{1}{f(\theta)} \theta \frac{\partial}{\partial \theta} f(\theta) \\ &= Np \end{aligned}$$

using equation (9), in agreement with equation (2). Similarly, we have

$$\sum \bar{n}_1 i^2 = \frac{Np}{l} \frac{1}{f(\theta)} \left[ \theta \frac{\partial}{\partial \theta} \right]^2 f(\theta) \quad (13)$$

and analogous formulæ will give  $\sum \bar{n}_1 i^a$ , ( $a = 0, 1, 2, \dots$ ).

<sup>5</sup> F.G., p. 34 *et seq.* A fuller account is given in Schrödinger, *Statistical Thermodynamics*. Dublin Institute for Advanced Studies, 1944, Chap. VI.

We now consider the special case of random degradation in which

$$\omega_1 = \omega_2 = \omega_3 \dots = 1.$$

Then

$$f(\theta) = \theta + \theta^2 + \theta^3 + \dots \theta^p \\ = \frac{\theta}{1 - \theta} (1 - \theta^p). \quad (14)$$

By definition,  $0 < \theta < 1$ , so we replace the finite sum by the sum to infinity, *i.e.*  $\frac{\theta}{1 - \theta}$  and examine later the range in which this approximation is valid, for large  $p$ ;  $\theta$  is then evaluated using equation (9).

$$\text{Then} \quad \theta \frac{\partial}{\partial \theta} \log \frac{\theta}{1 - \theta} = l \quad (15)$$

which gives  $\theta = 1 - 1/l$  or  $1 - b/p$ . Then  $\theta^p = (1 - b/p)^p$  which is very near  $e^{-b}$  for large  $p$  ( $\sim 10^2 - 10^3$ ); hence, our approximation for  $f(\theta)$  is accurate to  $< 1\%$  for  $b = 6$  and to  $< 0.1\%$  for  $b = 8$ . We continue our discussion in terms of  $b$  values  $> 8$  as this gives simple results for the average quantities. For lower  $b$ -values,  $\theta$  is best solved numerically.

Substituting for  $\theta$  in (12), we get

$$\bar{n}_1 = \frac{Np}{l} \theta^{l-1} (1 - \theta) \\ = Np \frac{1}{l^2} \left(1 - \frac{1}{l}\right)^{l-1} \quad (16)$$

and the weight-fraction of  $i$ -mers is given by

$$\frac{i\bar{n}_1}{Np} = \frac{i}{l^2} \left(1 - \frac{1}{l}\right)^{l-1} \quad (17)$$

the size distribution being completely determined by  $l$ , independent of  $N$  and  $p$ —this point has important consequences and is developed in the discussion. For  $\bar{i}$ , the number-average chain length, we get

$$\bar{i} = \frac{\sum i\bar{n}_1}{\sum \bar{n}_1} = \frac{Np}{Np/l} = l \quad (18)$$

which confirms our original definition of  $l$ . Now,  $l$  is a number average quantity obtained by any procedure which necessitates the counting of molecules, *e.g.* osmotic measurements. A weight-average quantity defined by  $\frac{\sum \bar{n}_1 \cdot i^2}{\sum \bar{n}_1 \cdot i}$  is more often required. Substituting for  $f(\theta)$  in (13)

gives  $\sum \bar{n}_1 \cdot i^2 = \frac{Np}{l} \frac{(1 + \theta)}{(1 - \theta)^2}$ . Hence  $\bar{i}^2 = \frac{1 + \theta}{(1 - \theta)^2} = l(2l - 1)$  and the weight average formula is given by:

$$\text{Weight average M.W.} = \frac{\bar{i}^2}{\bar{i}} \\ = (2l - 1). \quad (19)$$

A similar result has been given by Montroll and Simha for high degrees of degradation (*cf.* their equation 15(b) when  $\alpha(1 + p) \gg 1$ ).

From (17) we can determine the position of the maximum in  $\bar{n}_1 \cdot i$  for a given  $l$  by differentiating  $\log \bar{n}_1 \cdot i$  with respect to  $i$ . Then  $\bar{n}_1 \cdot i$  has a maximum when  $i$  is the integer nearest to  $i^*$  determined by

$$i^* = - \frac{1}{\log(1 - 1/l)} \cong l \text{ for large } l.$$

The point we wish to make is that the position of this maximum changes discontinuously with  $l$ .

### Discussion.

We first compare the results from the general theory, in which  $p/l$  is the *average* number of fragments in a chain, with those from a "single chain" theory where each chain has the same number of splits at a given time. For the same  $p/l$ , a narrower distribution might be expected in the latter case as all the chains will be split into  $p/l$  fragments whereas in the general theory, some chains will not be degraded at all.

If a single chain theory is developed on the same lines as in the previous section, we can set up equations analogous to (1) to (7) but in which  $Np$  is replaced by  $p$  throughout and the  $n_i$  refer to one chain instead of the assembly of  $N$  chains; also the upper limit of  $i$  is  $(p - p/l + 1)$  instead of  $p$ . A serious difficulty arises, however, as the integrals for  $C$  and  $C\bar{n}_1$  can only be evaluated by the method of steepest descents if  $p/l$  and  $p$  are large, *i.e.* for high degrees of degradation. Under this restriction, the final weight distributions for the two treatments are not very different; Jellinek<sup>3</sup> in his general treatment indicated that for  $p = 10^3$ ,  $p/l > 6$ , the difference for practical purposes is indistinguishable. For lower values of  $p/l$  the method is inapplicable and a single chain theory can only be developed for high degrees of degradation. The general theory is, however, valid for *all* degrees of degradation as the necessary conditions  $Np$ ,  $Np/l \gg 1$  always hold.

The general theory can be extended further to cover polydisperse systems as the weight distributions given by (17) are a function of  $l$  only. For convenience we considered initially  $N$  chains each of  $p$  links but only the product  $Np$  occurs throughout and we therefore get the same result if  $p$  is the *average* initial chain length instead of the length of every chain, provided the degree of degradation is large enough to obscure the original distribution. We can reach the same conclusion if we consider the degradation of a giant chain of  $Np$  links; this is first split randomly to create a polydisperse system of  $N$  chains of average length  $p$ ; these  $N$  chains are then highly degraded randomly. The final distribution is then seen to be independent of the position of the first  $(N - 1)$  cuts, *i.e.* independent of the initial chain distribution. Montroll<sup>6</sup> has arrived at a similar conclusion by more elaborate methods and for a slightly more restricted type of initial distributions—the argument above shows that the result is a general one. The restriction to high degrees of degradation is necessary to cover all types of initial distribution; for a fractionated polymer where the degree of polydispersity is not too large, the fragment distribution when degraded will approach that from an initially monodisperse system for a much lower degree of degradation. If degradation can be shown to be random, the conclusions above suggest a method of producing experimentally a polymer with a known distribution function—this may be of some practical use in studying the effect of polydispersity on polymer properties.

The above results are in general agreement with those developed recently in terms of a "weak link" hypothesis. The general theory corresponds to weak links distributed at random, each chain having on the average  $(p/l - 1)$  weak links; the restricted single chain theory corresponds to each chain having  $(p/l - 1)$  weak links and cannot be applied for small values of  $(p/l - 1)$ .

We also note here that, for an initially monodisperse system, the inhomogeneity function,  $U$ , defined by Schulz<sup>7</sup> comes out very simply in terms of  $l$ , as

$$U = \frac{\text{Wt. average M.W.}}{\text{No. average M.W.}} - 1 = \frac{2l - 1}{l} - 1 = 1 - \frac{1}{l},$$

*i.e.* almost constant over a large range of  $l$ .

<sup>6</sup> Montroll, *J.A.C.S.*, 1941, 63, 1215.

## Non-Random Degradation.

It has so far been assumed that all bonds in a chain are equally likely to be split. Experiments on the thermal degradation of polystyrene at high temperatures indicate that monomer production is very much greater (by a factor <sup>3</sup> of  $10^3 - 10^4$ ) than random splitting would suggest. Schulz <sup>7</sup> and Jellinek <sup>8</sup> have discussed distribution and kinetic discrepancies in terms of "weak link" theories, but these do not account for preferential monomer formation. Splitting at the ends would seem to be a much more probable process than splitting elsewhere, contrary to our initial assumptions. Simha <sup>8</sup> has considered the kinetics of degradation when it occurs only at the ends but the statistics of preferential, as distinct from exclusive, formation of monomer have not been treated previously.

The reasonable assumption is first made that the "sensitivity" of the end bonds is a property of all the fragments existing at any time and not an exclusive function of the original  $N$  chains—we are not concerned with the reason for such a sensitivity. With the same notation, a general theory is developed—its extension to polydisperse systems is as before and subject to the same restrictions. The essential problem is to find the right set of  $\omega_i$  in the generating function defined by equation (4); the necessary clue comes from the Darwin-Fowler treatment of degenerate systems as opposed to non-degenerate ones. For random splitting and a given set of  $n_i$ , the number of ways of splitting into  $p/l$  fragments is, from (3),  $\Omega_C$ . If then, we wish to weight preferentially any modes of splitting which produce monomers, we can do this by replacing  $\Omega_C$  by  $\Omega_C \omega^{n_1}$  where  $\omega$  is arbitrary numerical parameter greater than unity. (For random splitting  $\omega = 1$ );  $\omega$  may later be expressed in terms of rate constants but for the moment it is a purely artificial factor. Then the total number of complexions  $C$  is  $\sum \Omega_C \omega^{n_1}$  summed over all  $n_1$  obeying (1) and (2) just as before. Such a device will weight favourably any and every mode of splitting by which monomers are produced and only those particular modes—complexions in which  $n_1 = 0$  are not weighted. Monomer formation is thus weighted wherever it occurs which fits in with our assumption that all fragment ends at any time are "sensitive."

The above is the key move and gives just what is wanted as  $C$  is the coefficient of  $z^{Np}$  in  $[f(z)]^{Np/l}$  in which we put  $\omega_2 = \omega_3 = \dots = 1$ ,  $\omega_1 = \omega > 1$  later. As before  $C$  is expressed as a contour integral and evaluated at the col  $z = \theta$ ; equation (12) gives  $\bar{n}_1$  directly in terms of  $\theta$  which we now evaluate.

$$\begin{aligned} f(z) &= \omega z + z^2 + z^3 + \dots + z^p \\ &\approx \omega z + \frac{z^2}{1-z} (1 - z^p). \end{aligned}$$

We assume as in the random case, that  $\theta^p \ll 1$  and examine later the validity of the approximation for large  $p$  (and large  $\omega$ ). Then, from (9)

$$l = \theta \frac{\partial}{\partial \theta} \log \left( \omega \theta + \frac{\theta^2}{1-\theta} \right). \quad (20)$$

This gives, on working through and rearranging,

$$\begin{aligned} l &= \frac{(\omega - 1)\theta + \frac{\theta}{(1-\theta)^2}}{(\omega - 1)\theta + \frac{\theta}{1-\theta}} \\ &= \frac{1}{1-\theta} - \frac{(\omega - 1)\theta}{1 + (\omega - 1)(1-\theta)}. \end{aligned} \quad (21)$$

<sup>7</sup> Schulz, *Z. physik. Chem. B*, 1942, **52**, 50.

<sup>8</sup> Simha, *J. Applied Physics*, 1941, **12**, 569.

from which, putting  $(\omega - 1) = m$ , we get for  $\theta$

$$\frac{1}{1 - \theta} = \frac{1}{2}l + \frac{1}{2}\sqrt{l^2 + 4ml - 4m}. \quad (22)$$

For  $m = 0$  ( $\omega = 1$ ), this becomes  $(1 - \theta)^{-1} = \frac{1}{2}l + \frac{1}{2}\sqrt{l^2} = l$  as it should be.

The conditions under which (21) and (22) are valid for  $m \gg 1$  (a case of practical interest) need more rigorous definition than in the random case. If, on analogy with the random solution for  $\theta$ , we put  $\theta = 1 - c/p$  for  $Np/l$  total fragments, then we can identify  $1 - \theta^p$  with 1 to better than 1% if  $c > 6$ . Substituting for  $\theta$  in (22), we get finally

$$\frac{1}{c} = \frac{1}{2b} \left( 1 + \sqrt{1 + \frac{4m}{l} \left( 1 - \frac{1}{l} \right)} \right) \quad (23)$$

Table I gives  $b = p/l$  values for various  $m$  which make  $c = 6.0$  ( $p = 10^3$ )—these indicate the lowest  $p/l$  values for which

TABLE I

$\omega$ .	$m$ .	$b = p/l$ .	$l$ .
1	0	6.0	167
11	10	6.4	156
101	10 <sup>2</sup>	9.6	104
1001	10 <sup>3</sup>	40.7	24.6

$f(z) = \omega z + \frac{1-z}{z^2}$   
to  $< 1\%$ . For lower  $l$ -values,  $\theta$  may be calculated from (12).

The weight average chain length is calculated from the general formulæ for  $\Sigma \bar{n}_i i^2$  and  $\Sigma \bar{n}_i i$  and comes out as

$$\frac{1 + \theta + m(1 - \theta)^3}{l[1 + m(1 - \theta)](1 - \theta)^2} \quad (24)$$

This reduces to the previous value of  $2l - 1$  when  $\omega = 1$ . The number average value  $\bar{i}$  comes out as  $l$  always, this quantity being independent of how the cuts are placed. Finally, we get for  $\bar{n}_1$

$$\bar{n}_1 = \frac{Np}{l} \frac{\omega_1 \theta^{i-1} (1 - \theta)}{\omega - (\omega - 1)\theta} \quad (25)$$

( $\omega_1 = \omega$ ,  $\omega_2 = \omega_3 = \dots = 1$ ) and the ratio of monomers to non-monomers comes out

$$\frac{\text{Non-monomers}}{\text{Monomers}} = \beta = \omega \frac{1 - \theta}{\theta} \quad (26)$$

### Kinetic Considerations.

For random splitting, the discussion of  $Np/l$  in terms of time is fairly straightforward as current treatments assume quite reasonably that the rate of formation of breaks is proportional to the number of unbroken bonds present in the system. Hence, the  $Np/l - t$  relation can be expressed in the unimolecular form

$$\begin{aligned} \frac{d}{dt}(Np/l) &= k_1[N(p - 1) - N(p/l - 1)] \\ &= k_1[Np - Np/l]. \end{aligned} \quad (27)$$

From the boundary condition ( $t = 0$ ,  $b = 0$ ,  $l = \infty$ ), this can be integrated completely to give

$$1 - \frac{1}{l} = \theta = e^{-k_1 t} \quad (28)$$



Hence, using (17), the size distribution function can be completely specified in terms of  $k_1$  and  $t$  as

$$\frac{i\bar{n}_1}{Np} = i(1 - e^{-k_1 t})^2 e^{-(i-1)k_1 t}. \quad (29)$$

For a single chain theory, the statistics of exclusive monomer formation can be worked out according to the methods given previously, using a suitable  $f(z)$ —here, the kinetics have been discussed by Simha<sup>8</sup> and are simple as the reasonable assumption is made that the rate of monomer production is proportional to the number of reactive fragment ends. Now, for all  $i > 2$ , the "reaction"  $M_1 \rightarrow M_{i-1} + M$  does not alter the number of reactive ends and  $\bar{n}_1$  is thus very nearly linear with time, as is the total number of fragments.

The kinetics of non-random splitting have not yet been discussed—the distributions of the previous section are all in terms of a parameter,  $\omega$ . An approximate evaluation of  $\omega$  in terms of kinetic constants will now be attempted. It is supposed that two degradation processes occur simultaneously, these being:

(1) The formation of fragments by random splitting.

(2) Monomer production by splitting from sensitive fragment ends.

In such a system, we aim at calculating the ratio of monomers to polymers. For random splitting  $\bar{n}_1 = Np/l^2$  from (16) and the number of polymers is  $Np/l - \bar{n}_1 = \frac{Np}{l} \left(1 - \frac{1}{l}\right)$ . If we take over Simha's assumption, then the rate of production of extra monomers by process (2), which we denote by  $\frac{dn_1^*}{dt}$  is given by:

$$\frac{dn_1^*}{dt} = k_2 \frac{Np}{l} \left(1 - \frac{1}{l}\right). \quad (30)$$

This applies to all fragments for which  $i > 1$ ; dimers can only degrade in one position, but a single scission produces two monomers instead of one, which restores the balance. Equation (30) also assumes that process (2) does not alter the total number of polymers significantly—the exact solution has been given by Simha<sup>8</sup> but we retain the assumption so that relatively simple results can be obtained. With this restriction, then, and if  $k_1$  is the rate constant for process (1), we can substitute for  $l$  to give

$$\frac{dn_1^*}{dt} = k_2 Np (1 - e^{-k_1 t}) e^{-k_1 t}$$

from which, by direct integration,

$$n_1^* = Np \frac{k_2}{2k_1} (1 - e^{-k_1 t})^2. \quad (31)$$

Hence, the total yield of monomer is:

$$\bar{n}_1 + n_1^* = Np \left(1 + \frac{k_2}{2k_1}\right) (1 - e^{-k_1 t})^2. \quad (32)$$

The total number of fragments is given by:

$$\frac{Np}{l} + n_1^* = \frac{Np}{l} \left(1 + \frac{k_2}{2k_1}\right) = \frac{Np}{l'} \quad (33)$$

$l'$  being the number-average molecular weight. From this, we get the ratio of monomers to polymers ( $= \beta$ ) as

$$\beta = \frac{\frac{Np}{l'} \left(1 + \frac{k_2}{2k_1}\right)}{\frac{Np}{l} \left(1 - \frac{1}{l}\right)} = \frac{1 + \frac{k_2}{2k_1}}{l - 1} \quad (34)$$

Hence, equations (34), (33), (26) and (23) serve to define  $\omega$  in terms of  $k_1$ ,  $k_2$  and  $l$ .

We note here that though  $l'$  is the true number-average chain length, any actual measurement by osmotic methods using experimental, as distinct from ideal, semi-permeable membranes will probably give  $l$  rather than  $l'$ . Hence we can estimate  $k_2/k_1$  directly using (34). Also,  $\omega$  is a function of  $l$  and not a constant independent of time.

### Summary.

The random degradation of high polymers is treated as a problem in statistics which can be solved by the same technique as that for determining the partition of energy amongst a set of harmonic oscillators. The Darwin-Fowler method is used in which the various quantities required are expressed as coefficients in related power series: these are then evaluated as contour integrals by the method of steepest descents. The size distribution functions for the degraded material are then derived directly together with the various average molecular weights by the use of differential operators. On this formulation, the extension to systems which are initially polydisperse is immediate and the method is then applied to a specific case of non-random degradation in which preferential splitting at the ends of the chains occurs. The kinetics of this type of degradation, which is found experimentally, are also discussed.

It was the late Sir Ralph Fowler who first encouraged me to persevere with this line of attack on the degradation problem and I should like to record here my gratitude to him. My indebtedness to Dr. E. A. Guggenheim is also a heavy one as many stimulating criticisms and suggestions arose out of discussions with him. Finally, my thanks are due to Professor E. K. Rideal for his steady encouragement throughout.

*Dept. of Colloid Science,  
The University, Cambridge.*

## THE MODE OF ANTIBACTERIAL ACTION OF PHENOLS IN RELATION TO DRUG-FASTNESS.

BY A. H. FOGG AND R. M. LODGE.

*Received 28th December, 1944.*

During the course of a general study of the effects of sub-lethal concentrations of various antibacterials on *Bacterium lactis aerogenes*, it has become apparent that, in one respect, the compounds studied fall into two well-defined classes.

(i) In many cases, persistent cultivation of the micro-organism in the presence of a drug evokes a response which enables growth to occur more or less normally at high drug concentrations which would otherwise be lethal. The "trained" organism is then said to have acquired drug-fast characteristics. (ii) Phenols as a general class do not appear to evoke this response to anything approaching the same degree. It was thought that this implied some profound difference in the mode of action of phenols from that of those compounds towards which bacteria exhibit adaptability.

The antibacterial activities of many phenols are known to be paralleled by the way in which these compounds distribute themselves between

protein and water.<sup>1</sup> Those phenols in which the ratio,  $[\text{PHENOL}]_{\text{protein}}/[\text{PHENOL}]_{\text{water}}$ , is high have the greater antibacterial activities.

In considering any mechanism of drug action, it is necessary to take into account two factors which we may call (a) the physical process of approach of the drug to its site of action, and (b) the chemical process of action of the drug at the receptor site.<sup>2</sup> Either of these factors may be of importance under given conditions, depending upon which of them is operative in determining the intensity of action of the drug.

In what follows, the antibacterial actions of phenols in sub-lethal concentrations are compared. Also, an examination of the distribution of these phenols in the system olive oil—buffer, chosen to represent a model of the system bacterial substance—culture medium, is described.

### Methods for assessing Antibacterial Activity.

The powers of phenols as lethal agents can readily be compared by determinations of their "phenol coefficients." This is a well-established technique.<sup>3</sup> However, no method is laid down for comparison of the antibacterial activities of phenols at concentrations low enough for the test organisms to survive with restricted metabolic activity.

We therefore define a "phenol index" as the ratio of that concentration of phenol itself which produces a certain reduction in metabolic activity to that concentration of the substituted phenol needed to produce the same effect.

Since there is more than one criterion for defining the reduction in metabolic activity of the bacteria, there can be more than one phenol index. Five criteria have been selected, leading to five phenol indexes:—

Criterion.	Identifying No. of Index.
Inhibition of cell division of controlled inocula . . . . .	I
Reduction of growth rate to half its value in the absence of the phenol . . . . .	II
Increase of "early lag" <sup>4</sup> to twice its value in the absence of the phenol . . . . .	III
Increase of "late lag" <sup>4</sup> to twice its value in the absence of the phenol . . . . .	IV
Increase of "minimum lag" <sup>4</sup> to 200 minutes . . . . .	V

In Table I the phenol indexes of several substituted phenols are pre-

TABLE I.  
(Test organism : *Bact. lactis aerogenes*.)

Index No.	Phenol.	Resorcinol. <sup>5</sup>	m-cresol. <sup>5</sup>	m-nitro-phenol. <sup>6</sup>	m-chloro-phenol. <sup>6</sup>
I . . . . .	I	0.55	1.6	8.5	8.5
II . . . . .	I	0.60	1.4	7.2	9.0
III . . . . .	I	0.40	1.3	5.3	6.0
IV . . . . .	I	0.55	1.6	10.6	6.8
V . . . . .	I	0.55	1.1	8.3	—
Mean index . . . . .	I	0.5	1.4	8.0	7.6
Coefficient <sup>7</sup> . . . . .	I	0.5	2.3	7.4	7.6

<sup>1</sup> E.g., Meyer, *Archiv. exp. Path. Pharm.*, 1901, 46, 338; Reichel, *Biochem. Z.*, 1909, 22, 149; Boeseken and Waterman, *Proc. k. Akad. Wet. (Amst.)*, 1912, 14, 620.

<sup>2</sup> Ferguson, *Proc. Roy. Soc. B*, 1939, 127, 387.

<sup>3</sup> E.g., *British Standard Technique*, No. 534 (1934).

<sup>4</sup> v. Lodge and Hinshelwood, *J. Chem. Soc.*, 1943, 213, for details of lag.

sented, together with the generally accepted values for the phenol coefficients. The values of the indexes for resorcinol and *m*-cresol were derived from the data of Spray and Lodge;<sup>5</sup> the remaining indexes were determined<sup>6</sup> by methods similar to those employed before;<sup>5</sup> the phenol coefficients are those given by Suter.<sup>7</sup>

Firstly, it is apparent that there is relatively little difference between the values of the indexes for a given phenol. This implies that all the functions of the bacteria corresponding to the criteria listed above are depressed to about the same extent by a given phenol concentration. Accordingly, it suggests that phenols have a quite general depressant action on the metabolic activities of the cells.

Secondly, Table I shows that the mean value of the individual indexes is not far removed from the corresponding coefficient.

### Distribution of Phenols between Olive Oil and Buffer Solution.

Distribution of the phenols mentioned above between olive oil and aqueous buffer was investigated as follows: A known volume of a phenol solution was added to a known volume of buffer solution, and the whole then shaken with a known volume of olive oil. After standing in the thermostat overnight, some of the aqueous layer was carefully removed with a pipette and analysed colorimetrically<sup>8</sup> by comparison with the original phenol-buffer solution. The ratio of the concentration,  $c_1$ , of the phenol in the olive oil to the concentration,  $c_2$ , of the phenol in the aqueous layer (*i.e.* the distribution coefficient,  $\beta = c_1/c_2$ ) could then be calculated. This method had the advantage that it made a knowledge of the exact initial concentration of the phenol unnecessary. Each phenol was studied in at least two concentrations, and duplicates were set up for each determination. It was found that the values of  $\beta$  so obtained were constant for any given phenol, within the limits of experimental error, over the concentration range studied (50 to 200 parts per million in the buffer solution).

In order to reproduce conditions in the cultures as closely as possible, the distribution experiments were carried out at 40° C., the phosphate buffer solution held the system at the initial *pH* of the culture media (7.12), and the phenol concentrations in the aqueous layer were within the range encountered in the bacteriological work.

Table IIa records the mean values of  $\beta$  derived from not less than four determinations carried out in this way.

### Mode of Action of Phenols.

Figures for the mean index, (*c*), together with values for the *relative* distribution coefficients ( $\beta/g$ ), (*b*), are also given in Table II. From the marked parallelism, we may conclude that the various concentrations of the different phenols in the culture medium which lead to approximately the same concentration of the phenol inside the bacterial cell, lead also to a fixed intensity of antibacterial action. This strongly suggests that, once a phenol has arrived at its site of action inside the bacterium, its intensity of action, and, therefore, its mode of action, is similar to that of other phenols.

Bancroft and Richter,<sup>9</sup> using an ultra-violet microscope, have shown how the precipitation of proteins by phenol itself and by other compounds, can occur in two distinct stages, of which the first is reversible. They

<sup>5</sup> *Trans. Faraday Soc.*, 1943, 39, 424.

<sup>6</sup> Fogg, *unpublished results*.

<sup>7</sup> *Chem. Rev.*, 1941, 28, 269.

<sup>8</sup> Snell and Snell, *Colorimetric Methods of Analysis*, Vol. II (Organic and Biological), 1937, p. 357.

<sup>9</sup> *J. Physic. Chem.*, 1931, 35, 215 and 511.

TABLE II.

(Test organism : *Bact. lactis aerogenes*.)

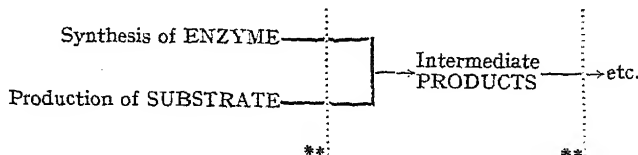
	Phenol.	Resorcinol.	<i>m</i> -cresol.	<i>m</i> -nitrophenol.	<i>m</i> -chlorophenol.	<i>m</i> -hydroxybenzoic acid.
(a) $\beta$ . . .	9.0	2.9	12.1	18.40 *	54	0.5
(b) $\beta$ , $\gamma$ . .	1.0	0.3	1.3	2.4.4 *	6	0.06
(c) Mean index (from Table I)	1.0	0.5	1.4	8.0	7.6	~0.1

find that at higher concentrations precipitation is irreversible and the cell dies. At sub-lethal concentrations precipitation is reversible and, when the visible signs of denatured protein have disappeared, normal metabolism is restored. Northrup<sup>10</sup> has also demonstrated the importance of denaturation in the deactivation of enzymes. Moreover, Cooper and her co-workers, in a long series of papers from 1912 onwards,† have shown that the antibacterial activity of a phenol is paralleled by its power of precipitating protein, which in turn varies with its protein-water distribution ratio. It is probably legitimate to state that the protein precipitating power depends upon the concentration of phenol in the protein phase and is paralleled by the protein-water distribution ratio. This suggests a hypothesis about the mode of action of phenols.

We suggest that the way in which phenols affect bacterial metabolism is possibly by the precipitation of proteins. This common effect would be consistent with the result that a given phenol concentration inside the cell leads to a given intensity of antibacterial action irrespective of the nature of the phenol. This hypothesis of a general rather than a specific action is useful in explaining certain other facts about phenols.

It is now generally accepted that intracellular enzymes involve a protein foundation with prosthetic groups attached.<sup>11</sup> If, through the action of a phenol, the protein foundation is in part precipitated, then the extent—and hence the activity—of each of those enzyme systems in the cell which depend upon protein for their foundation will be cut down to a similar extent as all the others. As a result, the rates of synthesis of the various enzymes will be reduced by the phenol in the same proportion as metabolism is slowed all through the reaction series. *E.g.*—

## ACTION OF A PHENOL.



\* Unreliable; *m*-nitrophenol could not be estimated colorimetrically by coupling with diazotised sulphanilic acid,<sup>8</sup> and reliance had to be placed on a difficult comparison of the yellow coloration developed on addition of alkali.

† *m*-hydroxybenzoic acid was found to have negligible antibacterial activity, even in saturated solution.<sup>8</sup>

<sup>10</sup> *J. Gen. Physiol.*, 1931, 14, 713; 1932, 16, 323.

† Especially Cooper, *Biochem J.*, 1912, 6, 362; 1913, 7, 175. Cooper and Woodhouse, *ibid.*, 1923, 17, 600.

<sup>11</sup> Quastel and Wooldridge, *Biochem. J.*, 1927, 21, 148 and 1224.

\*\* Retardation at these points, leading only to a reduced output of products.

Evidence for this hypothesis lies in the fact that the (lethal) coefficients, as determined by the Rideal-Walker or the Chick-Martin techniques, are in agreement with the various (sub-lethal) indexes determined by the methods given above, whether the latter are calculated on the basis of lag, growth rate or inhibitory concentration (*v.* Table I). Unless there is a general depressant effect over most cellular functions, it is difficult to imagine how all these separate indexes can be affected by a phenol to the same extent.

There are, then, strong indications that the anti-bacterial action of a given phenol is common to all phenols, and that these compounds may act by effecting a precipitation of bacterial protein which, in turn, causes a somewhat general reduction in the rate at which enzyme reactions in the cell can occur.

We know, however, that some phenols have selective action as well as their more general powers. Thus, it has already been reported that a specific concentration of *m*-cresol is able to retard the processes of cell division more than those of cell growth, the resultant phenomenon being the production of long filamentous organisms.<sup>5</sup>

### Drug-fastness.

Adaptation of bacteria to antibacterial agents is a well recognised phenomenon. For example, continued cultivation of an organism in the presence of a sulphonamide,<sup>12</sup> methylene blue, proflavine,<sup>13</sup> silver nitrate, formaldehyde, mercurochrome or acriflavine<sup>14</sup> results in a culture which is more or less immune to the action of the drug.

In sharp contradistinction to this behaviour, it appears that in the case of phenol itself and of several substituted phenols, little or no adaptation or drug-fastness is in fact apparent. Thus, it was found<sup>6</sup> that after 17 subcultures in media containing *m*-nitrophenol or *m*-chlorophenol neither the lag characteristics nor the growth rate showed any alteration on transfer back to the drug-free medium. A similar result was obtained by Spray and Lodge<sup>5</sup> with resorcinol and *m*-cresol, and by Davies, Hinshelwood and Pryce<sup>13</sup> with phenol itself. In the few cases where adaptation to phenols has been reported, it has always been on a very minor scale, and often seems to fall within the limits of experimental error. Thus, Masson<sup>15</sup> states that adaptation (to resorcinol and to salicylic acid) appears to be only temporary and transient even in the presence of the drug. Meader and Feirer<sup>14</sup> find that bacteria show only very slight response to phenol itself and to hexyl resorcinol.

Below is discussed a possible explanation of how the differing types of behaviour of bacteria towards the two classes of compounds may arise.

### Theory of Drug-fastness.\*

Since the metabolism of a bacterium must be regarded as the result of one or more series of chemical syntheses and degradations, some or all of which are made possible through the intervention of enzymes, it is necessary to assume that the reactions comprising the series are linked in some way, in order to account for the apparent "organisation" of the cellular mechanism. The simplest and most obvious method for such linking is through the formation of a product which is utilised by the next enzyme system in the series, and so on. When the series is balanced in

<sup>12</sup> Davies and Hinshelwood, *Trans. Faraday Soc.*, 1943, **39**, 431.

<sup>13</sup> Davies, Hinshelwood and Pryce, *ibid.*, 1944, **40**, 397.

<sup>14</sup> Meader and Feirer, *J. Inf. Dis.*, 1926, **39**, 237.

<sup>15</sup> *C. r. Acad. Sci.*, 1910, **150**, 189.

\* This problem is considered in detail by Davies, Hinshelwood and Pryce.<sup>13</sup>

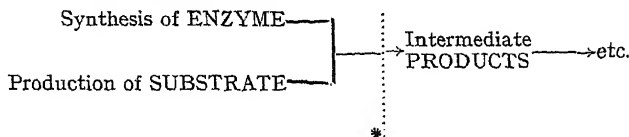
a state of dynamic equilibrium, all reactions subsequent to the slowest will be proceeding at a steady rate determined by the speed of the rate controlling stage.

The action of those drugs towards which bacteria exhibit adaptation may, perhaps, be visualised as follows. A particular enzyme reaction in the series is partially inhibited by the drug. The actual inhibition may be brought about in a number of different ways,<sup>16</sup> *viz.*, by reaction with some active prosthetic grouping in the enzyme molecule (*cf.* the antibacterial action of mercury, due to the blocking of sulphhydryl groups);<sup>17</sup> by reaction with the substrate for the enzyme process in question; or by inhibition of ancillary reactions responsible for enzyme synthesis.

If the inhibition is caused by direct interference with the enzyme itself, with the result that the enzyme is less efficient than before, the output of intermediate metabolites will be slowed, and in consequence the division rate will be reduced.

When a bacterium divides, all its enzyme systems must be duplicated for the two resultant daughter cells. When the division rate is cut down as above, the amounts of the enzymes needed to meet the duplication are reduced in the same proportion. Enzyme *action* is impaired by the drug; enzyme *synthesis*—perhaps by a completely different set of reactions—proceeds normally.

#### ACTION OF A SPECIFIC DRUG.



This means that when the growth rate, and hence the demand for enzymes, is reduced, an accumulation of enzymes results. The time needed to build up the partially inhibited enzyme to a concentration corresponding in its effect to the original (lesser) concentration of uninhibited enzyme is recognised as the time necessary for adaptation to occur.

Clearly, this type of training will be easily reversible, for the enhanced concentration of enzyme will revert to normal in the course of a few divisions when inhibition is discontinued.

The general precipitating action of phenols on many enzymes cannot give rise to the usual phenomena associated with adaptation, for the enzymes do not have the opportunity of expanding to compensate for their reduced efficiency; all enzyme reactions, including those synthesising a particular enzyme, are slowed. We do not expect that all enzyme systems are influenced to exactly the same extent by a given phenol. It is, however, likely, as we have shown above, that all enzymes are affected to a similar extent, and therefore, that drug-fast character towards phenols, if apparent, would be both slow to develop and weak.

#### Summary.

The ways in which phenols may be expected to distribute themselves between bacteria and liquid culture media have been assessed by means of a study of the distribution of these compounds between olive oil and aqueous buffer. Those phenols which have a high distribution coefficient ( $\beta$ ) are found to have a correspondingly large depressant effect on several different stages of bacterial metabolism. It is concluded that the anti-

<sup>16</sup> *E.g.*, McIlwain, *Nature*, 1944, 153, 300.

<sup>17</sup> Fildes, *Brit. J. Exp. Path.*, 1940, 21, 67.

\* Retardation at this point, leading to accumulation of both enzyme (with reduced efficiency) and substrate, as well as to a reduced output of products.

bacterial activity of the phenols studied is due mainly to their distribution relationships and to their ability to precipitate protein, and that their structure, apart from its effect on  $\beta$ , is relatively unimportant.

The apparent inability of bacteria to adapt themselves to grow normally in the presence of phenols is accounted for on this basis.

*Physical Chemistry Laboratory,  
Oxford University.*

---

## THE LAWS OF EXPANDING CIRCLES AND SPHERES IN RELATION TO THE LATERAL GROWTH OF SURFACE FILMS AND THE GRAIN-SIZE OF METALS.

BY U. R. EVANS.

*Received 8th January, 1945.*

Physical chemists and metallurgists are continually faced with problems connected with the properties of expanding circles and spheres. Such problems are met with in considering the covering of a metallic surface by films or layers of corrosion product, the formation of which starts at nuclei and spreads outwards; they are met with in calculations of the mean grain-size of cast metal, or of the grain-area of films which have solidified from the molten condition (*e.g.* during tinning or galvanizing). Methods of solution are in some cases already available, but the procedure described in this paper, based on the *Additivity of Expectation*, may be welcome on account of its simplicity. It is difficult to believe that the method has not been published before; but, if it is not new, the papers describing it are unknown to the author and to those whom he has consulted on the matter, so that a discussion of the method and the results obtained by it is felt to be justifiable.

It is proposed to consider eleven simple cases, of which the first, although of no direct interest to the physical chemist or metallurgist, will help the development of the others. Possibly most of the cases considered represent an over-simplification of what occurs in practice, but this is true of almost all problems amenable to mathematical treatment.

**I. The Expanding Circles Produced when Raindrops Fall into a Puddle.**—If raindrops fall sporadically on the surface of water, the chance that the number of circles which pass (within a certain time  $t$  from the start of the rain, which is supposed to begin suddenly, and to continue at uniform rate) over a representative point,  $P$ , is exactly  $n$ , can be expressed by Poisson's formula  $e^{-E} E^n / n!$ , where  $E$  is the "expected number," the value obtained by averaging an infinite number of counts. This is only true if the distribution of drops is truly random (it would be incorrect near trees or dripping roofs), but the formula is then an exact one. It is true that Poisson<sup>1</sup> in the classical derivation of his distribution from the Binomial Law regarded it as only approximately correct, but Fry<sup>2</sup> has obtained it from first principles without introducing any approximation.

To obtain  $E$ , it is convenient to compute the elementary contribution,  $dE$ , due to an annulus of breadth  $dr$  situated around  $P$  at radial distance  $r$ , and then to integrate for all values of  $r$  from zero to  $vt$ , where  $v$  is the radial velocity of growth from the "nuclei" (the points where the raindrops fall), which is provisionally assumed to be uniform in time and

<sup>1</sup> Poisson, *Recherches sur la Probabilité des Jugements en matière criminelle et en matière civile* (Paris: Bachelier), 1837, p. 206.

<sup>2</sup> Fry, *Probability and its Engineering Uses*, 1928, pp. 220-227 (Macmillan).



direction; clearly nuclei developing at distances exceeding  $vt$  cannot reach  $P$  within time  $t$ . Integration is permissible, because *expectation* is *additive* (often *probability* is not).

The annulus in question possesses the area  $2\pi r \cdot dr$ , and during a period equal to  $(t - r/v)$ , any point within the annulus will be capable of sending out circles which will reach  $P$  before time  $t$ . Thus

$$dE = \Omega(t - r/v) \cdot 2\pi r dr$$

where  $\Omega$  is the *two-dimensional nucleation rate*, best defined by stating that the number of nuclei formed in time-element  $dt$  and area-element  $\delta A$  is  $\Omega \delta A dt$ . Consequently

$$E = 2\pi\Omega \int_0^{vt} (tr - r^2/v) dr = \pi\Omega v^2 t^3/3 \quad (1)$$

The chance that the point  $P$  shall escape being crossed by any of the expanding circles which started after  $t = 0$  will clearly be

$$p_0 = e^{-E} = e^{-\pi\Omega v^2 t^3/3} \quad (2)$$

since both  $E^0$  and  $L_0$  are unity.

**II. The Covering of a Surface by Films Spreading out as Expanding Circles from Nuclei which Appear Sporadically in Time and Position on the still Uncovered Portion.**—The formation of superficial rust on iron exposed to the atmosphere usually starts at a limited number of points and spreads outwards. Often the nuclei represent places of settlement of corrosive dust particles—the importance of which has been demonstrated by Vernon<sup>3</sup>—but some authorities consider that they may sometimes represent sulphide inclusions in the metal. The distinction is important, since fresh dust particles may continue to settle on the unrusted portion during the period of exposure, whereas the sulphide particles will not increase in number with time. On steel, as shown by Vernon's photographs,<sup>4</sup> the rust usually spreads out in moss-like patterns, but Patterson<sup>5</sup> states that pure iron differs from steel in producing concentric rust growths. The spreading of films as expanding circles is also discussed by Canac<sup>6</sup> as a factor in the dulling of metals, whilst Sharman<sup>7</sup> describes how corrosion starting from scratch-lines on lacquered iron at first develops as expanding semi-circles, although later thread-like growth sets in. In the present section, which is concerned with the idealized case of expansion as perfect circles, it is sought to establish a relation between the area remaining uncovered ( $\alpha$ ), and the time  $t$ .

Clearly  $\alpha$  is equal to the probability  $p_0$  that a representative point shall remain uncovered. The question arises whether  $p_0$  is accurately given by equation (2). At first sight, this equation would appear inapplicable, since events are not mutually independent. Within any expanding circle, the formation of new nuclei is ruled out, which, in general, will invalidate the use of Poisson's formula to calculate the chance that  $n$  circles will cross over a given point within the time in question; indeed the situation is such that the idea of several circles passing over the representative point becomes meaningless. Nevertheless, the Poisson formula is still valid for the special case of  $n = 0$ . For any nucleation which is permitted in the "raindrop case" but is ruled out in the "film-spreading case" is such as to give rise to circles which could only reach the representative point *after* the circle within which the "disqualified" nucleus is situated. Thus the chance that the representative point shall remain uncovered by the film is exactly the same as the chance that it shall remain uncrossed by a circle from a raindrop, namely  $e^{-E}$ , where

<sup>3</sup> Vernon, *Trans. Faraday Soc.*, 1927, **23**, 159; 1935, **31**, 1686.

<sup>4</sup> Vernon, *ibid.*, 1924, **19**, 887.

<sup>5</sup> Patterson, *J. Soc. Chem. Ind.*, 1930, **49**, 203T.

<sup>6</sup> Canac, *Comptes rend.*, 1933, **196**, 51.

<sup>7</sup> Sharman, *Nature*, 1944, **153**, 621.

$E$  must be calculated in precisely the same way in the film-spreading case as in the raindrop case.

Thus the film-free area is

$$\alpha = e^{-E} = e^{-\pi\Omega v^2 t^3/3}. \quad (3)$$

Expansion shows that at very small values of  $t$ , the equation approximates to

$$\alpha = 1 - \pi\Omega v^2 t^3/3.$$

This special relation can be obtained by simple algebra—thus providing a check on the accuracy of the reasoning based on Expectation. For, when the circles are so small as to occupy a negligible fraction of the whole area, the number formed per unit area between times  $\tau$  and  $\tau + d\tau$  (where  $\tau < t$ ) will be  $\Omega d\tau$ , and, since each of these will have grown by time  $t$  to area  $\pi v^2(t - \tau)^2$ , the total area covered will be  $\pi\Omega v^2 \int_0^t (t - \tau)^2 d\tau$ ; hence  $\alpha = 1 - \pi\Omega v^2 t^3/3$ . The curves are clearly S-shaped, the gradient ( $-d\alpha/dt$ ) becoming steeper with time at small values of  $t$ , and less steep again as  $\alpha$  asymptotically approaches zero.

In the examples considered, a formula normally applicable only to conditions of mutual independence of events has been (legitimately) used in cases where events are not independent. The circumstance which justifies this procedure is simply that the particular nucleation points disqualified by the restrictions imposed are exactly those which would in any case be ineffective. It should not be assumed that the same liberties can be taken in all types of departure from mutual independence. If, owing to mutual attraction between the nuclei, they tend to form clusters, or if, owing to mutual repulsion, they tend to form a pattern, it will no longer be permissible to use the formula, even in the case of  $n = 0$ .

**III. The Covering of a Surface by Films spreading out as Expanding Circles from Predetermined Nuclei, Distributed Sporadically in Position.**—If the nuclei responsible for the expanding circles consist, not of dust particles falling on the surface during the development, but of sulphide inclusions (or even of dust particles present at  $t = 0$  which receive no subsequent additions), the relation between  $\alpha$  and  $t$  is different. Here the number of circles is indicated by a *nucleation-density*,  $\omega$ , best defined by stating that the number of nuclei present on area  $dA$  is  $\omega dA$ ; the conception of time does not arise, since all nuclei function from the commencement of exposure and no new ones subsequently come into operation. The contribution ( $dE$ ) of an annulus of radius  $r$  and breadth  $dr$  is clearly  $2\pi r dr \cdot \omega$ , so that

$$E = 2\pi\omega \int_0^{vt} r dr = \pi\omega v^2 t^2$$

and

$$\alpha = e^{-E} = e^{-\pi\omega v^2 t^2}. \quad (4)$$

—a relation obtained by Canac,<sup>6</sup> using a different method. Here again the curves are S-shaped, and the opening stage can be approximately represented by

$$\alpha = 1 - \pi\omega v^2 t^2$$

—an equation which can also be obtained by simple algebra, without using the conception of Expectation.

It will be noticed that the expression for  $\alpha$  in Cases II and III takes the form  $e^{-kt^3}$  and  $e^{-kt^2}$  respectively. The different power of  $t$  is connected with the fact that the dimensions of  $\Omega$  and  $\omega$  are not the same, being  $L^{-2}T^{-1}$  and  $L^{-2}$  respectively, and the power of  $t$  introduced *must* be such as to render the index non-dimensional.

**IV. Cases where the Growth Pattern is not a Circle.**—If the rate of expansion from each nucleus varies with direction, it is necessary to regard  $E$  as the sum of a number of elements, each corresponding to some element

of angular direction and carrying its own value of  $v^3$  in the formula. If, therefore, in equations (3) or (4),  $v$  is held to represent the R.M.S. of the velocity of outgrowth assessed over all directions, the equations remain valid, provided that no other complication is introduced.

Such a complication enters, however, if the expanding growths tend to avoid one another, which may happen if some substance necessary to growth becomes exhausted as a result of the growth; this often leads to dendritic, mossy or thread-like forms. For instance, the author,<sup>8</sup> studying the two-dimensional lead tree produced where one edge of a strip of zinc was pressed on to filter paper soaked in lead acetate solution, found that the reason why the fronds grew at their tips but not at their sides was that the area between the fronds soon became denuded of lead ions; the only manner in which the replacement of lead by zinc could proceed was for the lead tree to go out to seek its own nourishment. At this stage, lead passes into the metallic state at the tip of the fronds, zinc passes out of the metallic state at the base of the fronds, the cycle being presumably completed by passage of electrons outwards along the fronds themselves. An electrochemical process of this sort will draw ions in from a distance to the places of highest current density,\* and thus tends to make a frond maintain roughly its direction of growth, until it approaches an impoverished area, in which case it will be deflected so as to avoid such an area.

It seems possible that the moss-like rust growths seen in the photographs of Vernon and Patterson may be due to the same cause. Certainly, Sharman's thread-like corrosion patterns on lacquered steel show evidence of mutual repulsion, since, when the head of one thread chances to approach the body of another, it is deflected therefrom; this is easily understood, if it is supposed that the electrolyte needed for corrosion becomes impoverished on the flanks of each thread. Hoar<sup>9</sup> has reported cases where a certain corrosion filament on lacquered steel, in its endeavour to avoid the impoverished zone situated along the earlier part of its own track, has developed a spiral course, and finally, becoming entrapped at the centre, has ceased to grow at all.

If we consider the hypothetical case in which the threads have been effectively prevented from running into one another by the exhaustion factor, it is clear that, if the breadth of the threads and the velocity of their forward growth is constant,  $-d\alpha/dt$  will at first be practically constant. Sooner or later, however, a thread is bound to become "cornered" between the windings of other earlier threads and will then be unable to extend further. Presumably the chance of a given thread being able to continue to advance will at any moment be proportional to the effective area still uncovered, and since the rate of increase of the covered part of the surface is proportional to the number of threads still advancing, we get

$$-d\alpha/dt = k\alpha \quad \text{or} \quad \alpha = e^{-kt}. \quad (5)$$

<sup>8</sup> Evans, *Chem. Ind.*, 1925, 812; cf. King and Stuart, *J. Chem. Soc.*, 1928, 642.

\* In cases where ions are not used up in the electrodic reactions, this net movement of electrolyte into the zones where the corrosion currents are concentrated may actually cause an increase of concentration at these points. Such an effect is frequently met with in cases of intense corrosion; thus in pits in steel pipes, and at points of localized corrosion on lead cable sheaths due to stray currents, the concentration of electrolyte is locally far higher than in the main body of the water. It is perhaps unfortunate that the cases considered mathematically in most electrochemical textbooks are those in which there is a drop (not a rise) of concentration, owing to the elimination of ions in electrochemical reactions; in the electrolysis of nickel chloride between platinum electrodes, nickel ions will be removed as metallic nickel and chlorine ions as chlorine gas, so that the concentration diminishes at both poles.

<sup>9</sup> T. P. Hoar, *Unpublished observation*.

Possibly, in the case where the surface carries a certain amount of electrolyte at the outset, but receives no further amounts during the period of exposure, a marginal strip on each side of the threads may become denuded of electrolyte, and thus rendered permanently unavailable for the passage of other threads. If the fraction of the area which thus becomes incapable of being covered is  $\alpha_\infty$ , the equation should in this case become  $\alpha_t - \alpha_\infty = e^{-kt}$ . In ordinary conditions, it is likely that electrolyte will reach the surface during the outgrowth of rust, and in such cases the original equation (5) remains valid.

The expression  $\alpha = e^{-kt}$  was suggested by Vernon<sup>10</sup> in 1933 to represent the lateral spreading of rust; he assumed that it is moisture rather than electrolyte which becomes exhausted, but the basic notion is the same. The same type of equation also governs the case where the covering of a surface is uninfluenced by nuclear action, so that a point situated far from an existing film-covered area enjoys the same probability of becoming covered as a point adjacent to a film-covered area; for then, the rate of covering will be simply proportional to the uncovered fraction, so that  $-d\alpha/dt = k\alpha$  or  $\alpha = e^{-kt}$ .

**V. Growth of a New Phase spreading as Expanding Spheres starting from Nuclei which appear sporadically in Time and Position in the still Unchanged Portion.**—It is possible to apply the method developed for two-dimensional problems to three-dimensional problems, for instance the extension of a new phase from nuclei, and to calculate the connection between the unchanged fraction of the volume  $\alpha'$ , the linear velocity of outgrowth ( $v$ ) and the *three-dimensional nucleation number* ( $\Omega'$ ), which is best defined by stating that the chance of a nucleus appearing in volume  $\delta V$  and time  $\delta t$  is  $\Omega' \delta V \delta t$ .

The fraction of the volume which remains unchanged at time  $t$  is equal to the probability that a representative point will have escaped being crossed by any of the expanding spheres. This is equal to  $e^{-E}$ , where  $E$  is the expected number of spheres passing any point.

The element of expectation due to a spherical shell of radius  $r$  and thickness  $dr$  is

$$dE = 4\pi r^2 dr \cdot \Omega'(t - r/v).$$

Consequently

$$\begin{aligned} E &= 4\pi \Omega' \int_0^{vt} (r^2 t - r^3/v) dr \\ &= \pi \Omega' v^3 t^4/3. \end{aligned}$$

We can write, therefore, for the fraction of the volume still unchanged

$$\alpha' = e^{-E} = e^{-\pi \Omega' v^3 t^4/3}. \quad (6)$$

This expression has been obtained, evidently by another method, by Johnson and Mehl,<sup>11</sup> but the derivation was relegated to an Appendix which was not printed with their paper, presumably because the proof was too lengthy. It will be noted that the *fourth* power of  $t$  and the *third* power of  $v$  here appear in the index; since the dimensions of  $\Omega'$  are  $L^{-3}T^{-1}$ , the non-dimensional character of the index is still preserved.

**VI. Growth of a New Phase in a Mass spreading as Expanding Spheres starting from Predetermined Nuclei sporadically distributed in Space.**—If the nucleus-density is  $\omega'$ , best defined by stating that the chance of a nucleus occurring in volume  $dV$  is  $\omega' dV$ , then

$$\begin{aligned} dE &= 4\pi r^2 \omega' dr \\ E &= 4\pi \omega' \int_0^{vt} r^2 dr = \frac{4}{3} \pi \omega' v^3 t^3 \end{aligned}$$

so that

$$\alpha = e^{-E} = e^{-4\pi \omega' v^3 t^3/3}. \quad (7)$$

<sup>10</sup> Vernon, *Trans. Electrochem. Soc.*, 1933, 44, 36.

<sup>11</sup> Johnson and Mehl, *Amer. Inst. Min. Met. Eng. Tech. Pub.* 1089 (1939), p. 5. Copies of the Appendix are obtainable from the American Documentation Institute, 2101 Constitution Avenue, Washington, D.C.

**VII. Mean Grain-Area (Spangle-Area) obtained in the Solidification of a Thin Liquid Layer from Nuclei formed sporadically in Time and Position in the still Liquid Portion.**—When a thin layer of molten matter solidifies, the area of the grains or spangles should in general be largest where the film is thinnest, since, in the absence of complicating factors, the two-dimensional nucleation number ( $\Omega$ ) or nucleus-density ( $\omega$ ) is connected with the three-dimensional analogues ( $\Omega'$  or  $\omega'$ ) by the equations

$$\Omega = \Omega' \gamma$$

$$\omega = \omega' \gamma$$

where  $\gamma$  is the thickness. If the presence of interfaces directly affects nucleus-formation, the relation may be more complicated.\*

The grain-area should be calculable from the two-dimensional nucleation number, provided that the solidification rate is controlled by the true crystallization velocity and not by the rate of heat-removal. If predetermined nuclei are absent, the total number of grains per unit area formed throughout the solidification process will be  $\int_0^\infty \alpha \Omega dt$ , which

by (3) is equal to  $\Omega \int_0^\infty e^{-\pi \Omega v^2 t^3/3} dt$ . Writing  $x$  for  $t^3$  and  $a$  for  $\pi v^2 \Omega/3$ , the integral becomes

$$\frac{\Omega}{3} \int_0^\infty x^{-2/3} e^{-ax} dx = \frac{\Omega}{3} \cdot \frac{\Gamma(1/3)}{a^{1/3}}.$$

The mean grain-area ( $G$ ) is then the reciprocal

$$\frac{a^{1/3}}{\Omega} \cdot \frac{1}{0.893} = \frac{\sqrt[3]{\pi v^2 \Omega^{-2}/3}}{0.893}$$

so that

$$G = 1.137 \left( \frac{v}{\Omega} \right)^{2/3}. \quad (8)$$

This expression has the required dimensions,  $L^2$ .

**VIII. Mean Grain-Area (Spangle-Area) obtained on Solidification of a Liquid Layer, starting from predetermined Nuclei.**—The grain-area of coats obtained by dipping steel into molten metal is said to vary with the steel basis, which suggests that particles in the steel constitute predetermined nuclei. If predetermined nuclei alone operate, the mean number of grains per unit area is equal to the mean number of nuclei per unit area ( $\omega$ ), so that

$$G = 1/\omega. \quad (9)$$

**IX. Mean Grain-Size obtained by a Phase-Change in a Solid Mass, spreading as Expanding Spheres which start from Nuclei appearing sporadically in Time and Position in the still Unchanged Portion.**—Assuming that the phase-change is controlled by the true velocity of the crystallographic transformation, and not by the rate of heat-removal, the grain-size is related to  $v$  and  $\Omega'$  as follows:—

The number of nuclei produced in unit volume between the times  $t$  and  $t + dt$  is  $\alpha' \Omega' dt$ . Hence the total number of nuclei per unit volume formed during the complete transformation is  $\Omega' \int_0^\infty \alpha' dt$ , which by (6) is

$$\Omega' \int_0^\infty e^{-\pi \Omega' v^3 t^4/3} dt.$$

If  $a$  is written for  $\pi \Omega' v^3/3$ , and  $x$  for  $t^4$ , the integral becomes

$$\frac{\Omega'}{4} \int_0^\infty x^{-3/4} e^{-ax} dx = \frac{\Omega'}{4} \cdot \frac{\Gamma(1/4)}{a^{1/4}}.$$

\* J. N. Agar (*Priv. Comm.*, Nov. 25, 1944) suggests the equations  $\Omega = \Omega' \gamma + \Omega_2$ , and  $\omega = \omega' \gamma + \omega_2$ , where  $\Omega_2$  and  $\omega_2$  are the nucleation numbers for the interfaces.

Clearly the mean grain-size ( $G'$ ) is given by the reciprocal

$$\frac{4}{\Omega'} \cdot \frac{a^{1/4}}{\Gamma(1/4)} = \frac{\sqrt[4]{\pi \Omega'^{-3} v^3 / 3}}{0.906}$$

so that

$$G' = 1.117 \left( \frac{v}{\Omega'} \right)^{3/4} \quad (10)$$

This expression has the required dimensions,  $L^3$ .

In practice, the true state of affairs may be more complicated, since, as pointed out by Orowan,<sup>12</sup>  $v$  is abnormally low in the opening stages of growth, probably owing to the extremely high "vapour pressure" of very small crystals.

**X. Mean Grain-Size obtained by a Phase-Change in a Solid Mass, spreading as Expanding Spheres from predetermined Nuclei distributed sporadically in Position.**—The fine grain structure produced by adding iron to brass<sup>13</sup> is often thought to be due to crystallization from existing nuclei of solid iron or some compound containing it. If only predetermined nuclei are operative, the mean number of grains per unit volume is equal to the mean number of nuclei per unit volume ( $\omega'$ ), so that

$$G' = 1/\omega' \quad (11)$$

**XI. Mean Grain-Size obtained in a Solid Mass where the Rate of Solidification is controlled by the Rate of Heat-Removal.**—In solidification from the liquid state, the situation is complicated by the fact that the nucleation-rate first increases and then decreases as the temperature sinks below the freezing-point. If the rate of heat-abstraction is only just sufficient to remove the latent heat evolved, the process may become isothermal, and  $\Omega'$  may be considered constant, but the rate of solidification is now fixed by the rate of heat-removal. Often this varies in different parts of the mass and may not be constant in time, but, if we imagine a small volume where the rate of heat-removal can be regarded as constant through the solidification period, we can write

$$d\alpha'/dt = K$$

where  $K$  represents  $\frac{\text{rate of heat-removal}}{\text{density} \times \text{latent heat}}$ . Thus

$$\alpha' = K(t_0 - t)$$

where  $t_0$  is the time needed for total solidification.

The number of grains per unit volume formed in time  $dt$  is  $\alpha' \Omega' dt$ . Hence the total number per unit volume formed throughout the solidification process is

$$\Omega' \int_0^{t_0} K(t_0 - t) dt = \frac{1}{2} \Omega' K t_0^2.$$

Since  $\alpha' = 1$  when  $t = 0$ , it follows that  $t_0 = 1/K$ , so that  $\alpha'$  can be written  $1 - t/t_0$ . Since  $K t_0^2 = 1/K$ , the number of grains per unit volume is  $\Omega'/2K$ , and consequently

$$G = \frac{2K}{\Omega'} = \frac{2}{\Omega' t_0} \quad (12)$$

If the temperature sinks during the solidification process, another equation must be introduced to express the variation of  $\Omega'$  with  $t$ . But whether the temperature is constant or not, the grain-size should vary with the rate of heat-abstraction, and may thus vary in different parts of a casting. Where such a variation is not met with, it follows that either there are predetermined nuclei, or the process is not controlled by heat-removal. Orowan<sup>12</sup> points out that grain-size does not vary greatly

<sup>12</sup> E. Orowan, *Priv. Comm.*, Dec. 31, 1944.

<sup>13</sup> Johnson and Rednall, *Met. Ind. (London)*, 1921, 18, 125.

in different parts of the granular (as opposed to the acicular) zone of ingots, although the rate of heat-removal must vary. This may indicate crystallization from predetermined nuclei. Again, although crystallization of metal from the molten state is often controlled by the rate of removal of latent heat, recrystallization from a distorted solid (where probably the heat-evolution is much smaller) is thought to be dependent only on the degree of deformation and temperature, and not on the rate of removal of heat.

### Conclusions.

It is clear that much information on the mechanism of changes could be obtained by an accurate knowledge of the manner in which the unchanged fraction of a surface ( $\alpha$ ) or the unchanged fraction of the volume ( $\alpha'$ ) in any two-dimensional or three-dimensional change varies with time ( $t$ ); thus  $\alpha$  will be given by  $e^{-kt^2}$  or  $e^{-kt^3}$  according as a two-dimensional change depends on predetermined nuclei, or nuclei which keep appearing throughout the process in the continually shrinking unchanged area. Similar information should be obtainable from measurements of the mean grain-area or grain-volume obtained when the change becomes complete, and here it should be possible also to distinguish the cases where the process is controlled by chemical or crystallographic processes from those where it is controlled by the rate of removal of latent heat.

Despite much patient and careful experimental work, there is little data suitable for deciding between the various equations and hence between the corresponding mechanisms. It is hoped that the present discussion—despite its non-experimental character—may serve to direct attention to matters worthy of experimental investigation.

It may be convenient to tabulate the various expressions for the unchanged area ( $\alpha$ ), the unchanged volume ( $\alpha'$ ), the mean grain-area ( $G$ ) and the mean grain-volume ( $G'$ ) in terms of the nucleation rate ( $\Omega$  or  $\Omega'$  for two or three dimensions), the nucleation density ( $\omega$  or  $\omega'$ ), the linear velocity growth ( $v$ ) and the time ( $t$ ).

Spreading Circles from continually appearing Nuclei . . . . .	$\alpha = e^{-\pi\Omega v^2 t^3/3}$ , . . . . .	$G = 1.137 (v/\Omega)^{2/3}$
Spreading Circles from predetermined Nuclei . . . . .	$\alpha = e^{-\pi\omega v^2 t^2}$ , . . . . .	$G = 1/\omega$
Spreading Spheres from continually appearing Nuclei . . . . .	$\alpha' = e^{-\pi\Omega' v^3 t^4/3}$ , . . . . .	$G' = 1.117 (v/\Omega')^{3/4}$
Spreading Spheres from predetermined Nuclei . . . . .	$\alpha' = e^{-4\pi\omega' v^3 t^3/3}$ , . . . . .	$G' = 1/\omega'$
Spreading Spheres from continually appearing Nuclei with Growth controlled by constant rate of heat-removal . . . . .	$\alpha' = 1 - t/t_0$ , . . . . .	$G' = 2/\Omega' t_0$

where  $t_0$  represents the time of complete solidification.

### APPENDIX

#### Lateral Growth as a Complicating Factor in Film Thickening.

At least three laws for the thickening of oxide films and similar layers with time have been experimentally established. These are:—

The Rectilinear Law  $y = k_1 t$  . . . . . (13)

The Parabolic Law  $y^2 = k_2 t + k_3$  . . . . . (14)

The Logarithmic Law  $y = k_4 \log_e (k_5 t + k_6)$  . . . . . (15)

In the author's opinion, the most suitable interpretation of the Rectilinear Law is that derived at independently by Tronstad,<sup>14</sup> by Vernon<sup>15</sup>

<sup>14</sup> Tronstad, *Trans. Faraday Soc.*, 1934, 30, 1122.

<sup>15</sup> Vernon, *Met. Ind.*, 1935, 46, 239.

and by Dunn and Wilkins,<sup>16</sup> whilst the most convenient proof of the Parabolic Law is that provided by Hoar and Price;<sup>17</sup> a derivation of the Logarithmic Law has recently been published by the author,<sup>18</sup> which appears to avoid some of the difficulties of previous interpretations.

In the derivation of all these laws, it is tacitly assumed that growth begins simultaneously at all parts of the surface, and that the film at any given instant is of constant thickness everywhere. If oxidation, or any analogous change, begins at nuclei and spreads laterally, as well as downwards, more complicated equations would be necessary, and possibly some of the inconsistencies which have been met with are due to the neglect of the possibility of lateral growth.

If once it is admitted that the film is not of equal thickness everywhere, it is necessary to distinguish between those methods of measurement in which the "effect" depends on the *mean* thickness from those in which it depends on the *modal* thickness. The gravimetric and electro-metric methods will belong to the first class, and the interferometric method to the second. It should not be overlooked that there are cases where the assumption of uniform thickness has been made not merely in the interpretation of the thickness values, but even in their determination from the actual experimental measurements. For instance, Steinheil<sup>19</sup> measured the loss of transparency of thin aluminium layers during oxidation, and calculated therefrom the thickness of the oxide film, using a formula which tacitly assumed that the oxide film was uniform.

This may perhaps serve to explain the apparent discordance between his results and those of Vernon,<sup>20</sup> although possibly this might, in any case, be explained by the different experimental conditions prevailing in the two sets of experiments. According to Lustman,<sup>21</sup> Steinheil's results obey a Logarithmic Law of the form

$$y = k_7 + k_8 \log_e t \quad . \quad . \quad . \quad (16)$$

although the constants,  $k_7$ , and  $k_8$ , abruptly change their values after a certain time. Vernon's results do not seem to correspond to any similar law. Champion<sup>22</sup> has analysed Vernon's results, and states that they obey the law

$$y = k_9(1 - e^{-k_{10}t - k_{11}}) \quad . \quad . \quad . \quad (17)$$

but that here  $k_9$ ,  $k_{10}$  and  $k_{11}$  abruptly change their values after a certain time. He agrees with Lustman in making the early part of Steinheil's curves correspond to the Logarithmic Law, but suggests that the later part conforms with equation (17); he feels that there may be no inconsistency between the results of Vernon and Steinheil, since Vernon's first reading was made after 0.4 days' exposure, so that there may have been a logarithmic law operating in the earlier stages.

Equation (17) is reminiscent of those governing lateral growth, and since, in Vernon's work,  $y$  represents the *average* film thickness as obtained by weight increment, the result might perhaps be explained by assuming that the growth quickly extended inwards to some limiting thickness, perhaps—as suggested by Mott<sup>23</sup>—by the Tunnel Effect, and *then* spreads

<sup>16</sup> Dunn and Wilkins, *Review of Oxidation and Scaling of Heated Solid Metals*, 1935, p. 67 (H.M. Stationery Office).

<sup>17</sup> Hoar and Price, *Trans. Faraday Soc.*, 1938, **34**, 867.

<sup>18</sup> Evans, *Trans. Electrochem. Soc.*, 1943, **83**, 337.

<sup>19</sup> Steinheil, *Ann. Physik.* 1934, **19**, 475.

<sup>20</sup> Vernon, *Trans. Faraday Soc.*, 1927, **23**, 152.

<sup>21</sup> Lustman, *Trans. Electrochem. Soc.*, 1942, **81**, 363.

<sup>22</sup> Champion, *Priv. Comm.*, Dec. 13, 1944.

<sup>23</sup> Mott (*Trans. Faraday Soc.*, 1940, **36**, 472) has used the Tunnel Effect to develop the logarithmic law of thickening, in cases where the thickness reached does not exceed 100 Å. It appears more likely to be applicable to the oxidation of aluminium than that of zinc; for Lustman (*Trans. Electrochem. Soc.*, 1942,

[Footnote continued overleaf.]



laterally, until the whole surface was covered to the permissible thickness. However, other explanations<sup>24</sup> are available for the asymptotic character of the curves, based on the cracking of the films under internal stresses until these stresses become exhausted.

The Author would acknowledge the kindness of several friends who have read the manuscript, made helpful suggestions or contributed valuable information. They include Professor N. F. Mott, Dr. H. Jeffreys, Dr. E. Orowan, Dr. T. P. Hoar, Dr. F. S. Dainton, Dr. R. S. Thornhill, Dr. J. N. Agar, Mr. F. A. Champion, and Mr. M. Tchorabdjji.

*Corrosion Research Section,  
University Chemical Laboratory,  
Cambridge.*

### Synopsis.

Many problems, including those concerning the lateral growth of surface films, and the grain-size reached in cast metal, require a knowledge of the geometry of expanding circles or spheres. A simple method, based on the Additivity of Expectation, is described. If circles expand with velocity  $v$  from predetermined nuclei ( $\omega$  per unit area), the fraction of the surface ( $\alpha$ ) remaining uncovered in time  $t$  is  $e^{-\pi\omega v^2 t^2}$ ; if they start from nuclei which keep appearing on the uncovered fraction at nucleation rate  $\Omega$ , then  $\alpha$  is  $e^{-\pi\Omega v^2 t^3/3}$ . In three dimensions, the corresponding expressions for the unchanged volume ( $\alpha'$ ) are  $e^{-4\pi\omega'v^3 t^3/3}$  and  $e^{-\pi\Omega'v^3 t^4/3}$ . The mean grain-size reached with the two types of nucleation is  $1/\omega$  and

$1.137 \left(\frac{v}{\Omega}\right)^{2/3}$  in two dimensions, and  $1/w'$  and  $1.117 \left(\frac{v}{\Omega'}\right)^{3/4}$  in three dimensions.

All the expressions mentioned are based on the supposition that the expansion is not limited by the rate of heat-abstraction. If the change is controlled by the removal of latent heat, the temperature remaining constant, then, in three dimensions,  $\alpha$  is  $1 - t/t_0$ , and the mean grain-size attained is  $2/\Omega't_0$ , where  $t_0$  is the time needed for complete solidification.

An experimental study of the relations between  $\alpha$  (or  $\alpha'$ ) and  $t$ , or of the grain-size reached under different conditions, should provide fundamental knowledge of the mechanism of nucleation.

81, 372) has pointed out that, according to the Tunnel-Effect derivation,  $k_4$  ought to be independent of temperature, whereas the results of Vernon, Akeroyd and Strond on zinc (*J. Inst. Met.*, 1939, 65, 301) show that  $k_4$  varies with temperature. The author has been in correspondence with Professor Mott regarding the theory, developed on p. 482 of his paper, to deal with cases where the films grow to thicknesses exceeding 100 Å.; it is agreed that, seven lines from the bottom,  $(1 - a)^n$  should read  $e^{-na}$ , but the equation finally reached is not affected.

<sup>24</sup> Evans, *Trans. Electrochem. Soc.*, 1943, 83, 340.

---

## ON SOME PHYSICAL PROPERTIES OF NORMAL PARAFFINS.

BY A. MIBASHAN.

*Received 21st June, 1944 (as amended, 8th February, 1945).*

In the present paper an attempt is made to express certain physical properties of normal paraffins as functions of their "boiling point fraction," defined as the ratio  $T/T_B$  ( $T_B$  being the boiling temperature at atmospheric pressure). The relations found may serve, it appears, to extend to  $n$ -paraffins an existing theory of the liquid state.

It is known that members of homologous series display a certain regular-

ity in the variation of their physical properties. These regularities have been expressed by empirical formulæ.<sup>1, 2</sup>

The application of the theorem of corresponding states to *n*-paraffins was made by Young<sup>3</sup> who found that by plotting  $V/V_C$  vs.  $T/T_C$  for pentane, hexane, heptane and octane, the representing points fall rather close to the same curve. Data of Wilson and Bahlke<sup>4</sup> for higher *n*-paraffins fit also well into this curve. Bauer, Magat and Surdin<sup>5</sup> simplified the study of static properties of liquids by introducing a "reduced temperature," but it seems that their equation is not suited to represent the properties of *n*-paraffins.

Egloff and Kuder<sup>6, 7</sup> tried to express the molecular volume in homologous series as an additive property of the number of C atoms. Their formula, in terms of "reduced temperatures" requires, however, five arbitrary parameters.

The data used in the present paper were taken from the Landolt-Börnstein tables (for refractive indices); these data are essentially those of Dornte and Smyth.<sup>8</sup> The figures of densities at various temperatures were taken from Egloff's tables.<sup>9</sup> Boiling points and melting points were taken from the fourth edition of Doss.<sup>10</sup>

The temperature variation of different properties of *n*-paraffins is considered in the range between melting point and boiling point. The critical point was not chosen as reference point because Guldberg's rule fails for *n*-paraffins.<sup>7</sup> It was found that by expressing some physical properties as functions of  $T/T_C$ , the representing points do not fall on a single curve, but rather on a stripe, *i.e.* have appreciable dispersion. On the other hand, the same properties, when plotted against  $T/T_B$ , give fairly sharp curves. This fact seems to justify the use as variable of  $T/T_B$ , which will be called herein the "boiling point fraction" and denoted by  $\tau$ .

The properties for which the use of this variable appears to be particularly suitable are the refraction, density (molecular volume), and the expansion coefficient of the *n*-paraffins; these properties are simple functions of  $\tau$ .

### Melting Point and Boiling Point.

On the basis of experimental data Nissan and Clark<sup>11</sup> showed that for *n*-paraffins the following relation between viscosity  $\eta$  and temperature holds:

$$\eta_T = f(T_B/T) \quad (1)$$

from theoretical considerations Eyring and Kauzman<sup>12</sup> derived that for "simple" substances the viscosity at the melting point should be the same, *viz.* 0.02 poises. In other words:

$$\eta_M = k. \quad (2)$$

If *n*-paraffins satisfy both equations, we get from (1) and (2):

$$\eta_M = f(T_B/T_M) = k \quad (3)$$

which leads to

$$T_B/T_M = k'. \quad (4)$$

<sup>1</sup> Bingham and Stookey, *J.A.C.S.*, 1939, **61**, 1625.

<sup>2</sup> Wan, *J. Physic. Chem.*, 1941, **45**, 903.

<sup>3</sup> Young, *Sci. Proc. Roy. Dublin Soc.*, 1910, **12**, 374.

<sup>4</sup> Wilson and Bahlke, *Ind. Eng. Chem.*, 1934, **16**, 115.

<sup>5</sup> Bauer, Magat and Surdin, *Trans. Faraday Soc.*, 1937, **33**, 81.

<sup>6</sup> Egloff and Kuder, *J. Physic. Chem.*, 1941, **45**, 836.

<sup>7</sup> Egloff and Kuder, *Ind. Eng. Chem.*, 1942, **34**, 372.

<sup>8</sup> Dornte and Smyth, *J.A.C.S.*, 1930, **52**, 3546.

<sup>9</sup> Egloff, *Phys. Constants of Hydrocarbons*, Vol. I, 1939.

<sup>10</sup> Doss, *Phys. Constants of the Principal Hydrocarbons*, IV ed., 1943.

<sup>11</sup> Nissan and Clark, *Nature*, 1939, **143**, 722.

<sup>12</sup> Eyring and Kauzman, *J.A.C.S.*, 1940, **62**, 3113.

The experimental data confirm this conclusion. Table I gives the ratios  $T_B/T_M$ . Although the even  $n$ -paraffins have a comparatively higher melting point than the odd ones,<sup>13</sup> the difference between the average ratio  $T_B/T_M$  for odd and even C atom series is less than 3 %.

TABLE I.

No. of C. Atoms.	$T_B/T_M$ .	
	$k'$ Odd.	$k'$ Even.
6		1.915
7	2.035	
8		1.842
9	1.930	
10		1.850
11	1.895	
12		1.856
13	1.900	
14		1.890
15	1.926	
16		1.924
17	1.970	
18		1.930
Average	1.943 $\pm$ 0.092	1.886 $\pm$ 0.044

The above figures suggest that the melting points of  $n$ -paraffins are "corresponding temperatures." For odd C number paraffins the melting point represents a corresponding temperature of  $T_M/T_B = 0.515$ ; for even ones  $T_M/T_B = 0.530$ .

For isoparaffins, if  $T_B/T_M$  is calculated, wide deviations from an average value are found.\*

### The Relation between Refractive Index and Temperature.

It can be shown mathematically that there is, in fact, no difference between the theoretically founded Lorenz-Lorentz equation for specific refraction and the empirical formula of Gladstone and Dale :

TABLE II

$(n_D - 1)/\rho = S.$ (5)		No. of C. Atoms.	Temp.	$(n_D - 1)/\rho.$
For the sake of simplicity formula (5) will be used henceforth. Table II gives the calculated $S$ values for $n$ -paraffins. The deviation from the average value 0.565 is less than 0.7 %. Ward and Kurtz <sup>14</sup> give the following expression for the increments of refractive index and density : $\Delta n = 0.60\Delta\rho.$ . (6)		6	15	0.567
		6	20	0.569
		6	25	0.568
		7	20	0.567
		7	25	0.567
		8	20	0.565
		9	20	0.565
		9	25	0.565
		10	20	0.565
		10	25	0.564
		11	20	0.566
		12	20	0.563
		12	25	0.563
		13	20	0.562
		14	20	0.565
		15	20	0.570
		16	not indicated	0.564
		18	"	0.563

From equation (5), by differentiation, the more accurate value  $\Delta n = 0.565\Delta\rho$  is obtained for  $n$ -paraffins.

<sup>13</sup> Müller, *Proc. Roy. Soc., A*, 1929, 124, 317.

\* It is interesting to note that in the alkaline metals series the ratio  $T_B/T_M$  (except for Li, whose b.p. is not certain) is fairly constant and has the average value 3.10.

<sup>14</sup> Ward and Kurtz, *Ind. Eng. Chem., Anal. Ed.*, 1938, 10, 560.

The molal refractivity for  $n$ -paraffins  $R = M \cdot S$  becomes equal to 0.565  $M$ . Since  $M = 12.01n + (2n + 2) \cdot 1.008 = 2.016 + 14.026n$ , the molal refractivity will be :

$$R = 0.565 (2.016 + 14.026n) \\ = 1.14 + 7.924n. \quad (7)$$

A slightly different empirical formula is given by Huggins :<sup>15</sup>

$$R = 2.12 + 7.815n.$$

By plotting  $n_D$  vs.  $T/T_B$  for liquid  $n$ -paraffins from six to twelve C atoms a straight line (Fig. 1) is obtained. The equation of this line is

$$n_D = -0.181\tau + 1.530. \quad (8)$$

This means that (a)  $n$ -paraffins have the same refractive index for equal  $\tau$ , i.e. they are reduced, with regard to refraction, to one single liquid ; (b) the refraction index of  $n$ -paraffins varies linearly with  $\tau$ . (It should, however, be kept in mind that actual measurements for single  $n$ -paraffins were made in a restricted interval only, usually between 15-25°.) It is emphasized that if  $T/T_C$  were used instead of  $T/T_B$ , the representative points would not fall on one line.

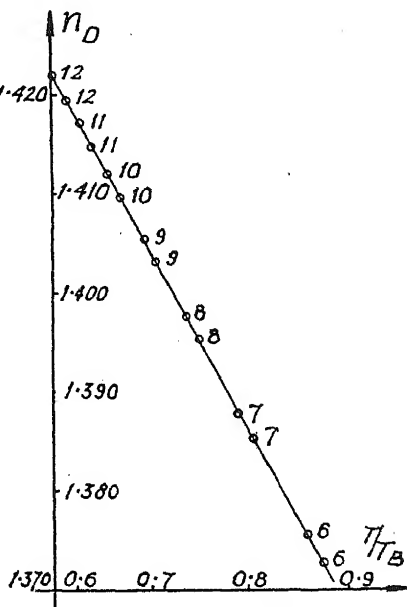


FIG. 1.—The figures next the circles represent the number of C atoms of the respective  $n$ -paraffin.

### The Relation between Density (Molal Volume) and $\tau$ .

From equations (5) and (8) it follows that

$$\rho = c\tau + d. \quad (9)$$

where  $c = -0.181/0.565$  and  $d = 0.530/0.565$ , i.e. the density of  $n$ -paraffins is a linear function of  $\tau$ . This equation perhaps does not hold exactly for the whole range of the liquid state, since it is not known if equation (8) is valid for this range. From diagram 2 it may be seen that 53 points of densities of  $n$ -paraffins fall fairly accurately on a straight line, in the temperature range between 0° and 100°. More points are not represented, falling too close to each other. Again, if the same densities are plotted vs.  $T/T_C$  a rather broad stripe is obtained, every single  $n$ -paraffin giving its own line, which does not coincide with that of the previous one.

From equation (9) we get the following expression for the molal volume of liquid  $n$ -paraffins :

$$V = M/(c\tau + d). \quad (10)$$

In Table III a comparison is made between observed data, those calculated by Egloff<sup>7</sup> and those given by equation (10).

It may be seen that the use of the boiling temperature fraction affords the formulation of a rather simple connection between molal volume and temperature.

**Cubical Expansion Coefficient.**—From the relation between density and  $\tau$  the cubical thermal expansion coefficient for liquid  $n$ -paraffins may be derived.

<sup>15</sup> Huggins, *J.A.C.S.*, 1941, 63, 116.

The coefficient of expansion is defined as :

$$\begin{aligned} \alpha &= dV/VdT & (11) \\ \text{or} & \alpha = -d\rho/\rho dT & (11') \\ \text{and putting} & \rho = cT/T_B + d & (9) \\ \text{we get} & \alpha = -c/(cT/T_B + d)T_B = -c/\rho T_B & (12) \end{aligned}$$

Thus, for a given  $\tau$  the expansion coefficient of  $n$ -paraffins is inversely proportional to their boiling temperature and the product of  $\alpha$ .  $T_B$  is constant (12'). This relation is formally analogous to Grüneisen's law,<sup>16</sup> which states that the product of the mean expansion coefficient (between absolute zero and the melting point) and  $T_M$  is constant for monatomic metals.

### Discussion of Results.

The relations obtained above, expressing certain properties of  $n$ -paraffins as functions of a "reduced temperature"  $T/T_B$  have so far been considered as empirical results, but it is interesting to note that similar relationships in terms of a "reduced temperature" can be obtained from the Lennard-Jones and Devonshire theory of the liquid state.<sup>17, 18</sup>

They assume that the work  $W$  which is required to convert the system from an ordered to a disordered state is proportional to the equilibrium energy  $\phi_0$ , since this energy is generated by the order-forces. This assumption can be considered to be generally true for all types of molecules. The method of calculation is statistical in nature and of general applicability.

For the case of simple molecules (inert gases,  $N_2$ ,

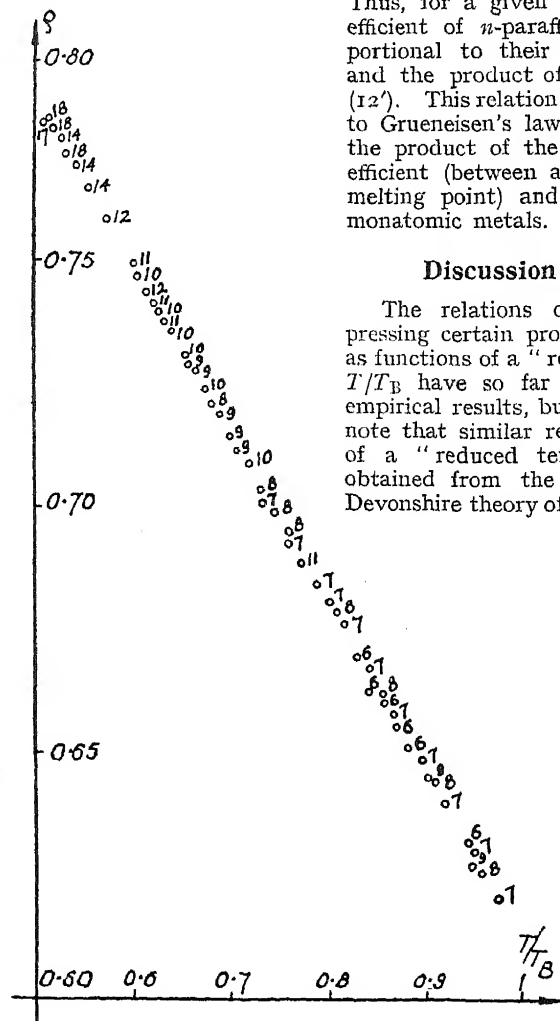


FIG. 2.—The figures next the circles represent the number of C atoms of the respective  $n$ -paraffin.

etc.) Lennard-Jones and Devonshire derived the following equation of state :

$$p = \phi_0/v_0 * F(v/v_0, kT/\phi_0) \quad (13)$$

where  $p$  is the pressure of the system,  $\phi_0$  is the energy required to separate two molecules from their position of minimum energy to infinity,  $v_0^*$  is

<sup>16</sup> Grüneisen, *Ann. Physik*, 1912, 39, 296.

<sup>17</sup> Lennard-Jones and Devonshire, *Proc. Roy. Soc., A*, 1939, 170, 464.

<sup>18</sup> Lennard-Jones and Devonshire, *ibid.*, 1938, 165, 1.

the specific volume of the system at absolute zero and  $v/v_0$  is the ratio of the volume of the system at temperature  $T$  to its volume at absolute zero,  $k$  is the usual gas constant,  $F$  is a function depending only on the crystal structure of the substance and the type of inter-molecular forces which are operative.

TABLE III

No. of C. Atoms.	$t_0$ .	$V$ obs.	$V$ Egloff.	$V^{10}$ .
6	— 19.2	124.04	124.3	123.0
7	— 3.08	142.49	142.61	142.20
8	11.5	160.97	160.90	160.90
9	25.0	179.66	—	180.0
10	36.4	198.27	—	198.57

We see that  $kT/\phi_0$  plays the role of a "reduced temperature" and  $v/v_0$  of a "reduced volume."

We shall consider what relations can be obtained by putting, according to Lennard-Jones and Devonshire

$$\phi_0 = kT_M/\beta. \quad (14)$$

This is equivalent to using a new "reduced temperature"  $\tau' = T/T_M$ .

We can write equation (13) in the form:

$$\phi v_0^*/\phi_0 = G(v/v_0, \tau'). \quad (13')$$

For zero pressure we have a functional relationship between  $v/v_0$  and  $\tau'$ :

$$G(v/v_0, \tau') = 0. \quad (13'')$$

Experimental data refer, however, to atmospheric pressure, but this does not affect essentially equation (13''); as pointed out by Lennard-Jones and Devonshire "the theory indicates that the effect of so small a pressure will be small." We can therefore write:

$$v/v_0 = Y(\tau'). \quad (15)$$

Where  $Y$  is the same function for all substances having the same function  $G$ .

In the derivation of the above equation (13) two assumptions have been made, namely, that the molecules have spherical symmetry and that they crystallize as a close-packed face-centred structure.

Similar assumptions can be made in the case of  $n$ -paraffins, since Müller<sup>19</sup> has shown that the molecules of  $n$ -paraffins behave as rigid cylindrical rods and<sup>20</sup> that in the solid state the molecules are arranged parallel to themselves in a close-packed structure, while Seyer, Patterson and Keays<sup>21</sup> have shown that the molecules of a  $n$ -paraffin remain orientated to a large degree in the liquid state, at any rate in the neighbourhood of the melting point.

There are, thus, good reasons for believing that an equation similar to (15) will apply to  $n$ -paraffins.

On the other hand Müller<sup>19</sup> has pointed out that there is a distinct structural difference between odd and even numbered hydrocarbon chains in the solid state. This difference is responsible for the alternations observed in some physical properties as lattice energy, melting point, molecular volume of the solid, etc.; when representing these properties as functions of  $n$ , two distinct curves are obtained for odd and even members.

<sup>19</sup> Müller, *Proc. Roy. Soc., A*, 1941, 178, 227.

<sup>20</sup> Müller, *ibid.*, 1932, 138, 514.

<sup>21</sup> Seyer, Patterson and Keays, *J.A.C.S.*, 1944, 66, 179.

$Y$  in equation (15) depends on the crystal structure, thus, if we apply an equation of this type to  $n$ -paraffins we shall expect two functions,  $Y_o$  ( $n$  odd) and  $Y_e$  ( $n$  even), to represent their properties.

We write, therefore :

$$(v/v_o)_{\text{odd}} = Y_o(\tau') \quad \text{and} \quad (v/v_o)_{\text{even}} = Y_e(\tau') \quad . \quad (16)$$

It is an experimental fact that  $T_B$  is a smooth function of  $n$ , whereas  $T_M$  varies smoothly only within each of the series, taken separately. We shall, therefore, try to use  $T/T_B$  as a new "reduced temperature." According to Lennard-Jones and Devonshire  $T_B/T_M$  is only approximately constant; since, however, their theory is not expected to hold exactly, the above step appears permissible. A certain measure for the applicability of the theory to our case is given by the dispersion of the ratio  $T_M/T_C$  (predicted constant for substances to which the theory holds good) as function of  $n$ . This ratio displays, indeed, a steady increase from 0.350 for  $n$ -hexane to 0.403 for  $n$ -octadecane and from 0.337 for  $n$ -heptane to 0.392 for  $n$ -heptadecane. Within these limits, we can consider  $T_B/T_M$  (eqn. (4)) as fairly constant for each series respectively.

From eqn. (4) :

$$(T_B/T_M)_{\text{odd}} = k_o' \quad \text{and} \quad (T_B/T_M)_{\text{even}} = k_e'$$

and equation (16) we get :

$$(v/v_o)_{\text{odd}} = Z_o(T/T_B) \quad \text{and} \quad (v/v_o)_{\text{even}} = Z_e(T/T_B) \quad . \quad (17)$$

If we now compare our equation (10) with eqn. (17) it is clear that (10) leads at once to a particular case of (17), *i.e.* with  $Z$  an inverse linear function of  $T/T_B$ . It is, furthermore, rather surprising to find that, over the range of applicability of equation (10), the functions  $Z_o$  and  $Z_e$  do not differ from each other. In other words, the use of the "reduced temperature"  $\tau = T/T_B$  enables certain properties of  $n$ -paraffins to be represented as a single function. (Whereas  $T/T_M$  or  $T/T_C$  do not.)

Lennard-Jones and Devonshire deduce that the coefficient of thermal expansion of the liquid just above the melting point is inversely proportional to  $T_M$ . In the case of  $n$ -paraffins, by logarithmic differentiation of eqn. (17) with respect to  $T$  we obtain our equation (12'), which states that the coefficient of thermal expansion of the liquid just above the melting point is inversely proportional to  $T_B$ .

These results are sufficient to indicate that, with due modifications, the equation of Lennard-Jones and Devonshire may apply to the case of  $n$ -paraffins and thus provide a theoretical explanation to the relations obtained above.

### Summary.

The existence of simple relationships between the refractive index, density, coefficient of thermal expansion and temperature in the  $n$ -paraffin series has been shown. These relationships seem to warrant an extension of the liquid state theory of Lennard-Jones and Devonshire to the case of  $n$ -paraffins.

The author wishes to express his gratitude to Prof. L. Farkas for his kind advice and constant interest and to Dr. M. Schiffer and Mr. H. J. G. Hayman for their valuable help throughout.

*Department of Physical Chemistry,  
The Hebrew University, Jerusalem.*

# THE ABSORPTION SPECTRA OF TRIPLE BOND MOLECULES IN THE VACUUM ULTRA VIOLET.

By W. C. PRICE AND A. D. WALSH.

Received 5th March, 1945.

## Part I. Unconjugated Molecules.

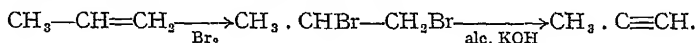
In a series of papers <sup>1, 2, 3, 4, 5</sup> we have dealt with the spectra of simple ethylenic molecules and of conjugated double bonds. The present work describes the spectra of triple bonds: Part I relates to the unconjugated molecules, acetylene, methyl acetylene, hydrogen cyanide and the cyanogen halides; Part II to the conjugated molecules diacetylene, dimethyl diacetylene and cyanogen.

### The Spectrum of Acetylene.

The strongest bands in the ultraviolet spectrum of acetylene occur below 1550 Å. and have already been studied by one of us: <sup>6</sup> they are Rydberg in type, being due to the excitation and ionization of one of the  $\pi$  electrons of the triple bond. A photograph of the acetylene spectrum is included here for comparison with that of methyl acetylene and also to show the weaker system of bands that extends from about 2000 to 1500 Å.\* This system consists of many diffuse bands, weak at first, increasing in intensity to a maximum around 1725 Å. and then becoming weak again. The bands have been reported by Herzberg <sup>8</sup> and by Rose.<sup>9</sup> Since both these authors used the hydrogen continuum as their source of light, neither was able to observe the complete system shown in the accompanying photograph and obtained by the use of the Lyman continuum. The bands are diffuse and their measurement difficult, the difficulty being further increased by interference from emission lines. The vibrational structure is complicated and many frequencies seem to be involved: a successful analysis has not yet been achieved.

### The Spectrum of Methyl Acetylene.

Methyl acetylene was prepared by the modification of the method of Johnson and McEwen <sup>10</sup> given by Pauling, Springall and Palmer.<sup>11</sup> Propylene was brominated to give dibromo propane, which was converted into methyl acetylene with alcoholic KOH.



The product was contaminated with traces of acetylene, but the use of comparison pictures enabled the bands of the latter to be eliminated.

The spectrum begins with two diffuse regions of absorption, the first

<sup>1</sup> Price and Tuttle, *Proc. Roy. Soc.*, 1940, 174, 207.

<sup>2</sup> Price and Walsh, *ibid.*, 1940, 174, 220.

<sup>3</sup> Price and Walsh, *ibid.*, 1941, 179, 201.

<sup>4</sup> Price and Walsh, *ibid.*, in course of publication.

<sup>5</sup> Walsh, *Trans. Faraday Soc.*, 1945, 41, 35.

<sup>6</sup> Price, *Physic Rev.*, 1935, 47, 444.

\* A still weaker absorption system occurs <sup>7</sup> in the region 2400-2000 Å.

<sup>7</sup> Kistiakowsky, *ibid.*, 1931, 37, 277.

<sup>8</sup> Herzberg, *Trans. Faraday Soc.*, 1931, 27, 378.

<sup>9</sup> Rose, *Z. Physik.*, 1933, 81, 751.

<sup>10</sup> Johnson and McEwen, *J. Amer. Chem. Soc.*, 1926, 48, 469.

<sup>11</sup> Pauling, Springhall and Palmer, *ibid.*, 1939, 61, 927.



## 382 ABSORPTION SPECTRA OF TRIPLE BOND MOLECULES

from about 1950 to 1880 Å. and the second from about 1750 to 1600 Å. These two regions take the place of the acetylene bands from 2000 to 1600 Å. and only appear at high pressures: though some bands are visible in them they are much less distinct than in acetylene. At about 1580 Å. a doublet occurs which has no analogue in the acetylene spectrum. It is stronger than the absorption regions to longer wavelengths, but rather weaker than the bands immediately following it on the short wavelength side. At 1540 Å. the strongest band of the whole spectrum occurs, corresponding to the acetylene band at 1510 Å. From 1540 Å. onwards the spectrum is very similar to that of acetylene, except that corresponding bands are moved through about 850 cm.<sup>-1</sup> towards the red.

In acetylene two Rydberg series were found, the bands of each series being easy to distinguish because of their differing structure: those of the first series had only *P* and *R* rotational branches and were single headed, those of the second series *P*, *Q* and *R* branches and were double-headed. In methyl acetylene the bands are too diffuse for this, but it is fairly easy to pick out two Rydberg series by analogy with the acetylene series. The acetylene bands suffer a fairly constant shift. The reality of the series found is supported by the large number of members observed for each. They can be represented by

$$\nu_0^n = 91240 - \frac{R}{(n + 0.48)^2} \quad . \quad . \quad . \quad (1)$$

$$\nu_0^n = 91100 - \frac{R}{(n + 0.04)^2} \quad . \quad . \quad . \quad (2)$$

Table I (1 and 2) respectively show the accuracy with which the two equations reproduce the observed frequencies. They also show the shifts of the bands relative to the corresponding bands of acetylene.

TABLE I.

<i>n</i>	$\nu_{\text{obs.}}$	$\nu_{\text{calc.}}$	$\nu_{\text{acet.}}$	$\nu_{\text{acet.}} - \nu_{\text{Me acet.}}$
----------	---------------------	----------------------	----------------------	--

## (1) The observed and calculated frequencies of the Rydberg bands of series (1).

			cm. <sup>-1</sup>	
2	73597	73369	74516	919
3	82237	82168	83140	903
4	85752	85753	86665	913
5	87592	87576	88431	871
6	88623	88617	89464	841
7	89273	89279	Obscured	—
8	89711	89714	90560	849
9	90020	90019	90860	840
10	90277	90241	—	—
11	90385	90387	—	—
12	90451	90536	—	—

## (2) The observed and calculated frequencies of the Rydberg bands of series (2).

2	64913	64727	65790	877
3	79225	79228	80116	891
4	84388	84376	85226	838
5	86793	86780	87636	843
6	88093	88092	88946	853
7	88890	88886	89743	853
8	89398	89403	90260	862
9	89711	89758	90610	899
10	90020	90012	—	—
11	90192	90200	—	—

Both series are very good. In the first, eleven members were observed and the extrapolation to the limit was only over about  $700\text{ cm}^{-1}$ . The limit may thus be given as  $11\cdot2590 \pm 0\cdot0005\text{ v}$ . In the second, ten members were observed and the extrapolation to the limit was over about  $800\text{ cm}^{-1}$ : the limit corresponds to  $11\cdot2417 \pm 0\cdot001\text{ v}$ . The separation of the two limits is only  $0\cdot017\text{ v}$ ., but it is to be noted that this separation is outside the limits of accuracy of the individual limits. It appears possible that the field produced by the methyl group splits the electronic levels by a kind of internal Stark effect.  $\text{H}_2\text{S}^{12}$  also gives two Rydberg series which go to closely the same, but not quite identical, limits.

The close parallel between the above series and the two series found for acetylene shows that a similar electron is being excited in the two molecules. By the study of heavy acetylene it was possible to make a vibrational analysis of the acetylene spectrum, indicating that this electron was one of the  $\pi$  valence electrons of the triple bond, a fact which was also evident from the rotational structure of the bands.

The reduction in first ionization potential from acetylene to methyl acetylene is to be ascribed to two effects—to a simple inductive effect (such as is present in the alkyl halides) transferring negative charge into the region of the triple bond; and possibly to the phenomenon known as hyperconjugation: by this, the three C—H bonds of the  $\text{CH}_3$  group behave rather like a triple bond and the  $\text{CH}_3 - \text{C}$  distance is abnormally shortened, while the first ionization potential is reduced just as that of diacetylene is reduced relative to acetylene.

The observed frequencies of the  $n = 2$  Rydberg bands of methyl acetylene and acetylene differ much less from their calculated values than do the early Rydberg bands of say the butadiene or aldehyde derivatives. This is because the ionization potential is considerably higher in the acetylene derivatives and so the low Rydberg orbitals do not lie so much within the dimensions of the molecule. Even in diacetylene (see later) the first ionization potential is still sufficiently high to give quite good agreement between the observed and calculated values of the early Rydberg bands. In butadiene and ethylene the first excited Rydberg orbital lies so much within the structure of the molecule that it partakes to some extent of  $V$  character. In acetylene and diacetylene, however, the first  $N \rightarrow V$  transition appears to be separated from the first Rydberg band.

### The Spectrum of Hydrogen Cyanide.

The strongest bands in the hydrogen cyanide spectrum occur from  $1120\text{ A.}$  onwards: they are all diffuse. From  $1550$  to  $1350\text{ A.}$  a somewhat weaker system occurs, the bands of which are sharp. They have already been reported by one of us<sup>13</sup> but are reproduced in Plate I for the sake of comparison with the other spectra here described. (On the accompanying photograph some diffuse absorption due to water vapour occurs between  $1350$  and  $1120\text{ A.}$ )

### The Spectra of the Cyanogen Halides.

The spectra of the cyanogen halides  $\text{ClCN}$ ,  $\text{BrCN}$  and  $\text{ICN}$  have been obtained and a full report will be published later. A few remarks are of interest here to fill in the general picture. The absorption is due to two main groups of electrons, *viz.*, the 4 non-bonding  $p\pi$  electrons of the halogen atom and the  $4\pi$  electrons of the triple bond. In the case of  $\text{ICN}$  the absorption is dominated by the non-bonding  $p\pi$  iodine electrons and the spectrum closely resembles that of  $\text{HI}$ , *i.e.*, an absorption continuum in the neighbourhood of  $2200\text{ A.}$  followed by sharp bands at  $1705$

<sup>12</sup> Price, *J. Chem. Physics*, 1936, 4, 147.

<sup>13</sup> Price, *Physic. Review*, 1934, 46, 529.

and 1580 Å. ("B" and "C" bands).<sup>14</sup> They are followed by others which converge on ionization potentials in the neighbourhood of 10.6 and 11.2 v. The positions of the bands relative to the alkyl halides and the halogen acids indicate that a small amount of negative charge is given up to the CN bond rather than extracted from it by the attached iodine. Dipole moment data support this since the cyanogen grouping is associated with a dipole moment of 3 Debye, the carbon atom being the positive end.

For the bromide and the chloride there are obviously very close similarities with the electronic states found for the halogen acids.<sup>14</sup> The band systems suffer slight displacements to long wavelengths relative to those of the corresponding acids due no doubt to the increasing electronegativity of Cl and Br relative to I. It is probable that some of the bands below about 1300 Å. are due to the excitation of CN electrons but they are too diffuse for sufficient information to be extracted from them to establish this point.

## Part II. Conjugated Molecules.

### The Spectrum of Diacetylene.

Diacetylene was prepared in two ways, first by the method of Strauss and Kollek<sup>15</sup> and second by the method due to Griner<sup>16</sup> and applied by Pauling, Springall and Palmer.<sup>11</sup> The first method was found to give very poor yields (*cf.* Pauling *et al.*). The second method consisted of refluxing the copper derivative of acetylene with potassium ferricyanide, but it was found that use of a large excess of ferricyanide (as recommended by Pauling *et al.*) resulted in the product containing HCN. A smaller quantity of ferricyanide gave a more satisfactory product.

The ultra-violet spectrum of diacetylene begins with a region of absorption around 2860 to 1900 Å. This has been studied by Woo and Chu.<sup>17, 18</sup> At shorter wavelengths much stronger bands occur. The appearance pressures of the strong bands of the far ultra-violet spectra of all acetylene derivatives seem to be very low and those of diacetylene particularly so. At low pressures the spectrum is transparent to 1630 Å. where the strongest band of the whole spectrum occurs. It is followed by other strong bands which become weaker in intensity and crowd more and more together as shorter wavelengths are reached. These are the characteristics of Rydberg bands and it was found possible to represent many of the bands by the two formulæ

$$\nu_0^n = 87060 - \frac{R}{(n + 0.05)^2} \quad (3)$$

$$\nu_0^n = 87024 - \frac{R}{(n + 0.48)^2} \quad (4)$$

Table II (3 and 4), respectively, show the accuracy of this representation. The limits of the two series are the same within the accuracy of extrapolation. Their mean corresponds to  $10.741 \pm 0.005$  v. The first member of each series occurs as a doublet.

A new system of strong bands begins around 1120 Å. These are referred to again in the discussion.

### The Spectrum of Dimethyl Diacetylene.

Dimethyl diacetylene was prepared by the method of Griner<sup>16</sup> used by Pauling, Springall and Palmer.<sup>11</sup> The copper derivative of methyl

<sup>14</sup> Price, *Proc. Roy. Soc. A*, 1938, 167, 216.

<sup>15</sup> Strauss and Kollek, *Ber.*, 1926, 59, 1664.

<sup>16</sup> Griner, *Ann. de Chimie Physique*, 1892, 26, 354.

<sup>17</sup> Woo and Chu, *J. Chem. Physics*, 1935, 3, 541.

<sup>18</sup> Woo and Chu, *ibid.*, 1937, 5, 786.

acetylene was refluxed with potassium ferricyanide and the resulting dimethyl diacetylene distilled in steam. The product had a melting-point of 64° C.

The near ultra-violet absorption has been studied by Macbeth and Stewart<sup>19</sup> who found no absorption maxima. Our plates show that at the pressures used the spectrum begins with an absorption region from 2000-1700 Å. A pair of bands separated by 2450 cm.<sup>-1</sup> comes first, followed by a stronger doublet at about 1880 Å., a strong band at 1800 Å. and a group of bands on the short wavelength side of this. A frequency of 2500 cm.<sup>-1</sup> is noticeable here. The bands from 2000 to 1700 Å. have no obvious analogue in the diacetylene spectrum.

At 1650 Å. the strongest bands of the whole spectrum occur in the form of two bands separated by 2500 cm.<sup>-1</sup>; these are obviously analogous to the strongest bands of the diacetylene spectrum. Several other strong bands occur in the region 1650-1400 Å. The separations of the strongest of these are given in Table III.

The strong bands from 1650 Å. onwards resemble the Rydberg bands of diacetylene, but unfortunately comparatively few could be observed

TABLE II.

"	$\nu_{\text{obs.}}$	$\nu_{\text{calc.}}$
(3) Observed and Calculated Frequencies of the Rydberg bands of series (3).		
	cm. <sup>-1</sup>	
2	60790	60948
3	75213	75263
4	80371	80370
5	82765	82757
6	84048	84062
7	Obscured	84852
8	85392	85366

(4) Observed and Calculated Frequencies of the Rydberg bands of series (4).

2	69126	69153
3	77954	77952
4	81545	81537
5	83355	83361
6	Obscured	84401
7	85065	85063

TABLE III.—FREQUENCIES OF BANDS IN THE 1650-1400 Å. REGION OF DIMETHYL DIACETYLENE.

cm. <sup>-1</sup> .	
59984	
2484	
62468	
2637	
65105	
2441	
67546	
2230	
69776	
2239	
72105	

TABLE IV.—OBSERVED AND CALCULATED FREQUENCIES OF THE RYDBERG BANDS OF SERIES (5).

"	$\nu_{\text{obs.}}$	$\nu_{\text{calc.}}$
cm. <sup>-1</sup>		
2	78727	78813
3	85265	85210
4	88010	88047
5	89550	89548
6	90478	90437

leading to the first ionization potential of dimethyl diacetylene. Since the bands are shifted to long wavelengths to diacetylene a lower ionization potential is indicated for the dimethyl derivative. The reduction in ionization potential relative to diacetylene is presumably due mainly to an inductive effect and perhaps partly to the effect of hyperconjugation.

The Rydberg bands leading to the second ionization potential can

<sup>19</sup> Macbeth and Stewart, *J. Chem. Soc.*, 1917, III, 831.

be better observed. They begin at about 1250 Å. and five of them can be measured. They fit the formula

$$\nu_0'' = 92810 - \frac{R}{(n + 0.80)^2} \quad (5)$$

Table IV shows the agreement between observed and calculated frequencies. The limit corresponds to  $11.45 \pm 0.02$  v. An earlier member of the series may lie in the region 1600-1400 Å.: there seem to be more strong bands here than there are diacetylene analogues.

### The Spectrum of Cyanogen.

The spectrum of cyanogen was obtained by heating mercuric cyanide and passing the evolved gas directly into the spectrograph.

The strongest bands begin at about 1320 Å. They are diffuse, but it can be seen that they crowd together to a limit around 900-850 Å. This corresponds to an ionization potential  $\sim 13.8$  v. (very roughly).

Cyanogen has a somewhat weaker absorption system from 1700 to 1450 Å.: it corresponds to the hydrogen cyanide region of 1550-1350 Å., the bands of which can actually be seen upon the high pressure cyanogen photograph, since a little hydrogen cyanide was present (probably formed in the discharge tube: the last traces of air are removed from the spectrograph by a hydrogen flow). There is much fine structure in the 1700-1450 Å. region and the vibrational analysis is difficult.

Cyanogen also has bands in the region 2300-1820 Å. They are weaker than the shorter wavelength absorption, but many of them can be seen upon the high pressure photograph. They have been reported by Woo and Badger,<sup>22</sup> who, however, found the structure too complex for complete analysis. Other weak bands have been reported by Woo and Liu<sup>23</sup> in the region 3020-2400 Å.

### Discussion.

In acetylene the 4  $\pi$  electrons normally occupy two orbitals,  $\chi_1$  and  $\chi_2$ , at right angles and both of axis perpendicular to that of the  $\sigma$  C—C orbital. These orbitals correspond to the same energy level. The electronic structure of diacetylene differs from that of acetylene in that the eight  $\pi$  electrons are now in two energy groups of four, *i.e.*, there are two energy levels both doubly degenerate. Two orbitals,  $\chi_1$  and  $\chi_2$ , of perpendicular symmetry axes correspond to the lowest occupied energy level; and two,  $\chi_3$  and  $\chi_4$ , correspond to the second occupied energy level. The  $\chi_1\chi_2$  energy level lies below and the  $\chi_3\chi_4$  level above the single level of acetylene. The values for the bonding energy levels are<sup>20</sup>

$$\frac{1}{2}[\pm \beta_s - \sqrt{\beta_s^2 + 4\beta_t^2}]$$

where  $\beta_s$  and  $\beta_t$  are the parameters called "resonance integrals" for the single and triple bonds respectively. The expression for the levels is precisely the same as for butadiene<sup>21</sup> except that  $\beta_t$  replaces  $\beta_d$ . For the purpose of rough comparison with other molecules, we may write

$$\beta = \beta_s = \beta_d = \beta_t$$

and so obtain Huckel's butadiene values for the energy levels ( $-0.62\beta$  and  $-1.62\beta$ ). Since consideration of the non-equality of the lengths of the links in butadiene changed the highest bonding energy level to  $-0.67\beta$ , we may estimate the highest bonding energy level in diacetylene as (very roughly)  $\sim -0.7\beta$ . Fig. 1 sets side by side the energy levels of acetylene and diacetylene.

<sup>20</sup> Penney, *Private communication*.

<sup>21</sup> Lennard-Jones, *Proc. Roy. Soc.*, 1937, 158, 280.

<sup>22</sup> Woo and Badger, *Physic Rev.*, 1932, 39, 932.

<sup>23</sup> Woo and Liu, *J. Chem. Physics*, 1937, 5, 161.

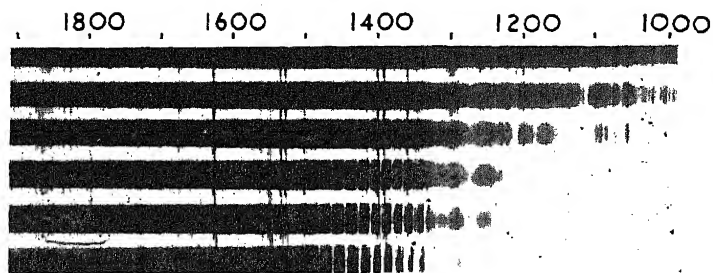
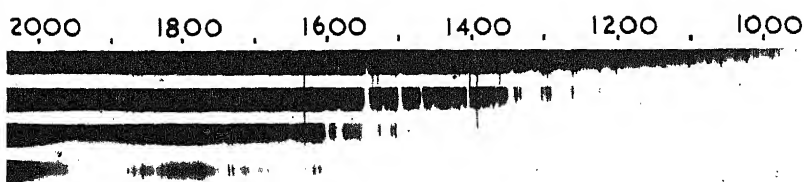
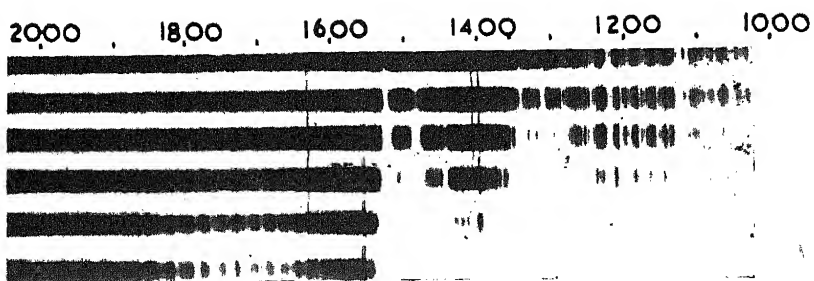


PLATE I.—The spectra of (a) acetylene, (b) methyl acetylene, and (c) hydrogen cyanide.

[To face page 386.]

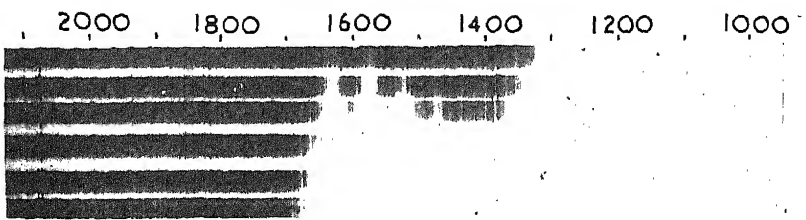
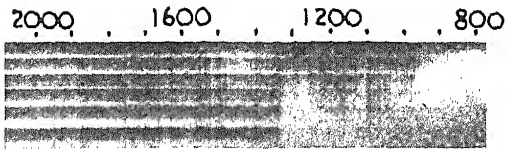
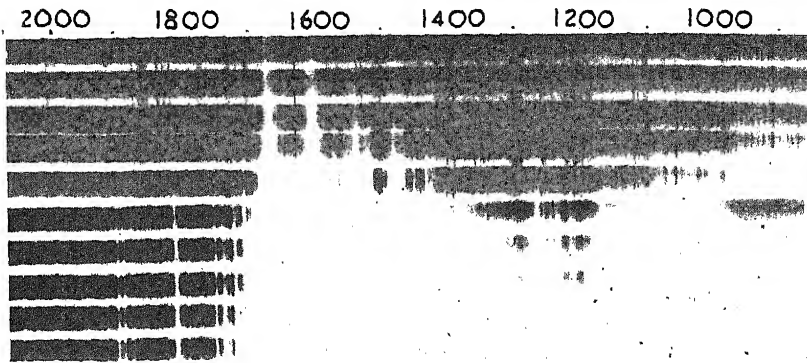
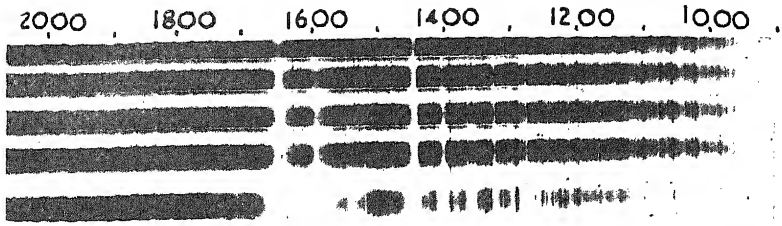
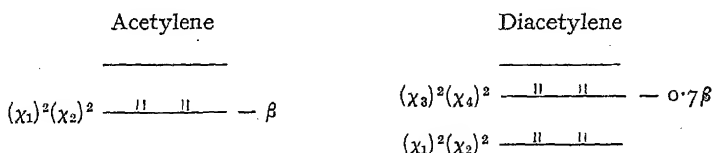


PLATE II.—The spectra of (a) diacetylene, (b) dimethyl diacetylene, (c) cyanogen low pressure, and (d) cyanogen, high pressure.

The ionization potentials found for acetylene and methyl acetylene are those of  $\pi$  electrons. We may assume that in diacetylene the first ionization potential is also due to the excitation of a  $\pi$  electron. This is supported by the facts that (a) the excitation must be that of an electron that has little bonding power because there is practically no vibrational structure in the spectrum; (b) the ionization potential found is lower than that of acetylene: the splitting of  $\pi$  energy levels described above means that such a lowered first ionization potential is expected. We may therefore identify the electron being removed at the first ionization potential as a  $\pi$  electron from the  $\chi_3\chi_4$  shell.

FIGURE I.



If we consider the normally occupied energy level of acetylene as  $-\beta$  (as in ethylene) and the highest normally occupied diacetylene energy level as  $-0.7\beta$ , we can get a value for  $\beta$  by assuming that the difference in first ionization potential of diacetylene and methyl acetylene is equal to the difference in binding energy of the highest occupied orbitals. Methyl acetylene, rather than acetylene, is chosen so as to make the environment of the  $\pi$  electrons as similar as possible. We get

$$0.3\beta = 11.25 - 10.74 = 0.51 \text{ V.}$$

$$\text{or } \beta = 1.7 \text{ V.}$$

The fact that this is of the right order of magnitude lends support to our value for the first ionization potential of diacetylene.

The strong bands starting around 1120 Å. in diacetylene are evidently the first strong resonance bands leading to the ionization of an electron from the  $\chi_1\chi_2$  shell; and the Rydberg series found for dimethyl diacetylene represents the excitation of a  $\chi_1\chi_2$  electron.

The dimethyl diacetylene spectrum indicates a lower ionization potential for both  $\chi_3\chi_4$  and  $\chi_1\chi_2$  electrons than in diacetylene and this is no doubt in part due to charge transfer. On the other hand, in dimethyl diacetylene, the presence of the bands between 2000 and 1700 Å. the complicated vibrational structure in the region 1600-1400 Å. region and the failure to appear of the higher members of the Rydberg series leading to the first ionization potential, all indicate a change in the structure of dimethyl diacetylene relative to diacetylene greater than a simple inductive effect would indicate.

The electronic structure of diacetylene and its relation to that of acetylene is of course very similar to the structure of butadiene and its relation to ethylene. The diacetylene structure may be said to have a two-dimensional  $\pi$  configuration, whereas butadiene has only a one-dimensional  $\pi$  configuration. The chief difference between the diacetylene and butadiene spectra is the absence of vibration in the former: the reasons for this are that (a) in diacetylene only one  $\pi$  electron out of eight is being excited, whereas in butadiene one out of four is affected—the change in force constant on excitation is therefore much greater for butadiene than for diacetylene, (b) the antibonding  $V$  state, which in butadiene perturbs the first Rydberg state, in diacetylene probably has a much lower energy than the first Rydberg state.

There should exist  $N \rightarrow V$  transitions for the diacetylene electrons as for those of butadiene. The diacetylene 2860-1900 Å. system probably



corresponds to the acetylene 2000-1550 Å. system and is perhaps to be identified as the  $N \rightarrow V_1$  transition: it is pushed to longer wavelengths relative to acetylene by virtue of the conjugation. If such an identification is correct, it is to be noted how much stronger in acetylene and diacetylene are the Rydberg bands than the  $N \rightarrow V_1$  transition. This is to be related to the high ionization potentials of these molecules (relative to butadiene), which cause the first excited orbital to be almost clear of the nuclear structure and therefore not to be modified by it.

Diacetylene bears the same relation to acetylene, as cyanogen does to hydrogen cyanide. The first ionization potential of hydrogen cyanide is given by Sponer<sup>24</sup> as 14.8 v. It probably corresponds to the removal of an electron from the C≡N bond. The shift of the cyanogen strong bands to long wavelengths relative to hydrogen cyanide and the consequent reduction in first ionization potential are the usual results of conjugation. The similarity of the structures of diacetylene and cyanogen has been pointed out by Timm and Mecke<sup>25</sup> and by Woo and Chu.<sup>17</sup> The two molecules are in fact isosteric. It is therefore probable that the 2300-1820 Å. cyanogen system is due to a transition analogous to that responsible for the diacetylene long wavelength bands.

This work was carried out in 1940, war-time conditions having delayed its publication. The authors desire to acknowledge financial assistance from the Department of Scientific and Industrial Research.

### Summary.

The spectra of acetylene, methyl acetylene, hydrogen cyanide, diacetylene, dimethyl diacetylene and cyanogen have been photographed in the vacuum ultra-violet. Two long Rydberg series have been found for methyl acetylene, leading to the limits  $11.2590 \pm 0.0005$  and  $11.2417 \pm 0.001$  v. Two well developed Rydberg series in diacetylene lead to the value 10.741 v. for the first  $\pi$  ionization potential of the molecule. In dimethyl diacetylene the second ionization potential of the  $\pi$  electrons is found to be 11.45 v. Discussions of all the spectra in terms of the electronic structures are given.

Laboratory of Physical Chemistry,  
Cambridge.

<sup>24</sup> Sponer, *Molekülspektren*, 1935, p. 133.

<sup>25</sup> Tim and Mecke, *Z. Physik.*, 1935, 94, 1.

## INORGANIC CHROMATOGRAPHY. PART I.— STATIC ADSORPTION MEASUREMENTS.

BY P. W. M. JACOBS AND F. C. TOMPKINS.

*Received 5th June, 1944, as amended 28th February, 1945.*

The application of chromatography to aqueous solutions of electrolytes has received comparatively little attention,<sup>1</sup> and the separations obtained are not generally clear cut.<sup>2</sup> Schwab and Jockers<sup>3</sup> have suggested that this is linked with the exchange capacity of the adsorbent, whereby an equivalent amount of Na<sup>+</sup> ions, present as impurities in the form of aluminates, is released. The conclusion was derived from a study of columns

<sup>1</sup> (a) Schwab, *Z. Electrochem.*, 1937, 43, 791. (b) Schwab and Dattler, *Angew. Chem.*, 1937, 50, 691. (c) Schwab and Dattler, *ibid.*, 1938, 51, 709. (d) Schwab and Jockers, *ibid.*, 1937, 50, 546. (e) Schwab and Jockers, *Naturwiss.*, 1937, 25, 44. (f) Schwab and Ghosh, *Angew. Chem.*, 1939, 52, 666. (g) Schwab and Ghosh, *ibid.*, 1940, 53, 39. (h) Taylor and Urey, *J. Chem. Physics*, 1938, 6, 429. (i) Flood, *Z. anal. Chem.*, 1940, 130, 327.

<sup>2</sup> Cf. figs. given in ref. 1 b, c, d, e.

<sup>3</sup> Ref. 1d.

and no quantitative measurements, which are best accomplished by static measurements, were made. Furthermore, chromatography has developed rapidly, and consequently many hypotheses are cited as if they were experimentally tested facts. It therefore seemed essential to examine in detail the form of the isotherm, the nature of the adsorption process, the effect of eluents on desorption, etc., before proceeding to a study of the various factors operative in columns.

### Experimental and Results.

Alumina was used as the adsorbent, and copper chloride, prepared from equimolar solutions of A.R.  $\text{CuCO}_3$  and A.R.  $\text{BaCl}_2$ , as the adsorbate. The Cu was analysed iodometrically, and the Cl potentiometrically, using the Volhard method. The alumina was activated by heating for various periods at different temperatures to obtain the conditions necessary for a reproducible surface. Certain general conclusions were noted—the

adsorption capacity decreased when the period of activation exceeded 1 hour; prewashing, immediately before activation, with distilled and tap-water and 1% and 5%  $\text{H}_2\text{SO}_4$  gave an increase in the order given, the reproducibility being best with the first; the adsorption increased with activation temperatures below  $480^\circ\text{C}$ ., and above this, it decreased (Fig. 1). Concordant results were obtained when

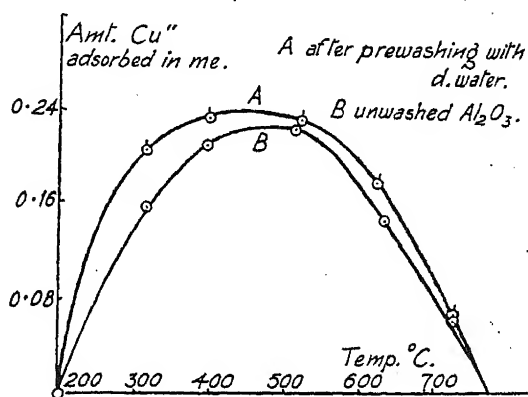


FIG. 1.

5 g.  $\text{Al}_2\text{O}_3$ , prewashed with 100 ml. d. water, were heated for 1 hour at  $480^\circ\text{C}$ ., cooled over saturated salt/sugar solution, and used immediately. On exposure to moist air, the adsorptive capacity decreased (25% in 3 days). In adsorption experiments, 1 g. activated  $\text{Al}_2\text{O}_3$  was swept into 50 ml. standard Cu solution, maintained at  $26.5^\circ\text{C}$ . (average room temperature) in a thermostat. The solution was agitated vigorously for 5 minutes, the adsorbent allowed to settle over the same period, decanted and analysed. Variations of 5% in the amount adsorbed were obtained and hence no correction was made for the simultaneous adsorption of water.

Typical isotherms are given in Fig. 2, the amount adsorbed being in me./1 g.  $\text{Al}_2\text{O}_3$ , and the equilibrium concentration in me./l. The adsorption was non-equivalent, that of the cation being in excess by 0.07–0.08 me. for all chlorides, except HCl (0.5 me.), in the higher concentrations. Isotherms for both cations and anions are reasonably well expressed by the Freundlich expression and by the equation,  $Q = k_1 + k_2 \log c$  (Fig. 2), as has been found in similar ionic adsorption systems.<sup>4</sup> Chromatograms of inorganic ions are normally eluted by acids; the effect of varying acidity on the  $\text{Cu}^{++}$  adsorption from solution (initially 80 me./l) is given in Fig. 3; the decrease is expressed by the equation,  $\log Q = k_a - k_b(\text{H}^+)$ . Similarly, Fig. 4 shows the decrease of  $\text{Cu}^{++}$  adsorption at constant acidity (i.e. corresponding to elution in columns); the  $\text{Cl}^-$  ion adsorption shows certain abnormalities.

<sup>4</sup> Kolthoff, *J.P.C.*, 1936, 40, 1027. Verwey, *Chem. Rev.*, 1935, 16, 363, where a bibliography is given.

For use in Part II, and to obtain further information about the nature of the adsorption process, the adsorption of other divalent cations in presence of the same anion ( $\text{SO}_4^{--}$ ) was measured. The amount adsorbed

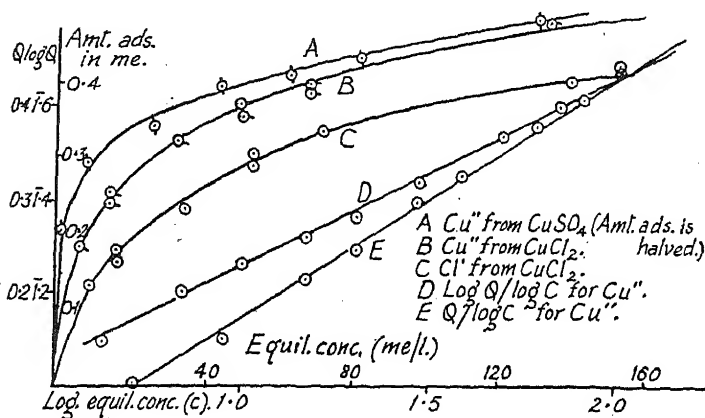


FIG. 2.

from approx. M/10 solutions was found to be a good criterion of the adsorption affinity, expressed here as  $100Q'/C'$ , where  $Q'$  is in me./5 g.  $\text{Al}_2\text{O}_3$  and  $C'$  is the initial concentration of adsorbate in me./50 ml. solution. Adsorptions were duplicated and the analyses triplicated; Table I gives the results and the method of analysis used.

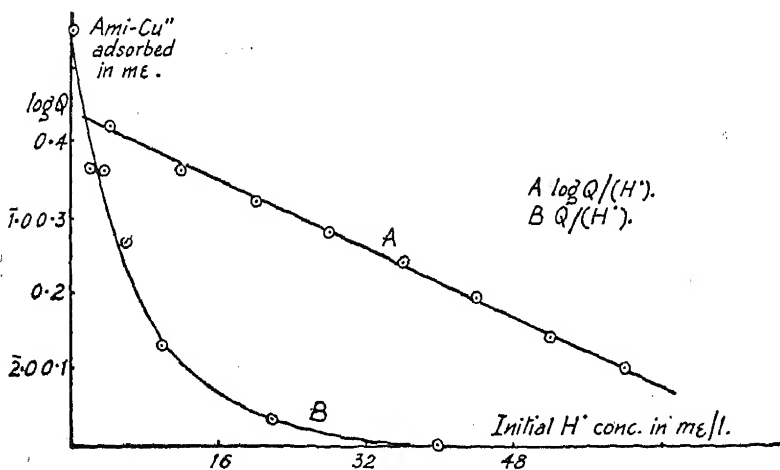


FIG. 3.

Schwab<sup>3</sup> concluded that separability was dependent on the Na content of the  $\text{Al}_2\text{O}_3$ ; "sodium poor" alumina was prepared by his method, the product being more compact, the particle size 2-3 times greater and the adsorptive capacity one-seventh that of the Merck's product. Prewashing with  $\text{NaOH}$  of various strengths, followed by activation, caused a linear increase of adsorption after a larger initial effect (discussed later) as shown in Fig. 5.

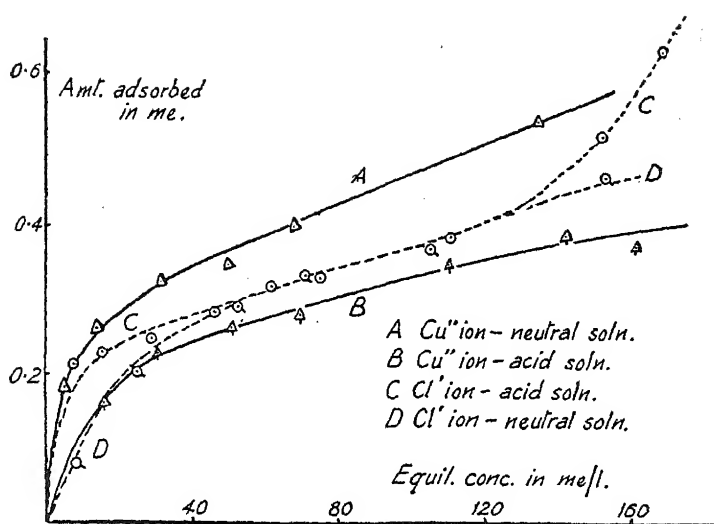


FIG. 4.

TABLE I

Adsorbate.	$C'$ .	$Q'$ .	$1000 Q'/C'$ .
Cu, volumetric KI and $\text{Na}_2\text{S}_2\text{O}_3$ .	10.00	5.08	5.08
Cd, potentiometric $\text{K}_4\text{Fe}(\text{CN})_6$ .	9.02	2.75	30.6
Zn, as Cd .	10.01	2.97	29.6
Ni, gravimetric, dimethylglyoxime .	9.41	2.77	28.0
Co, potentiometric, KCN .	11.02	2.72	24.7
Mn, volumetric, $\text{NaBiO}_3$ oxidation .	9.99	2.44	24.4
Mg, gravimetric, oxime .	10.30	2.27	22.0
$(\text{NH}_4)$ , volumetric, Kjeldahl .	9.62	1.07	11.1

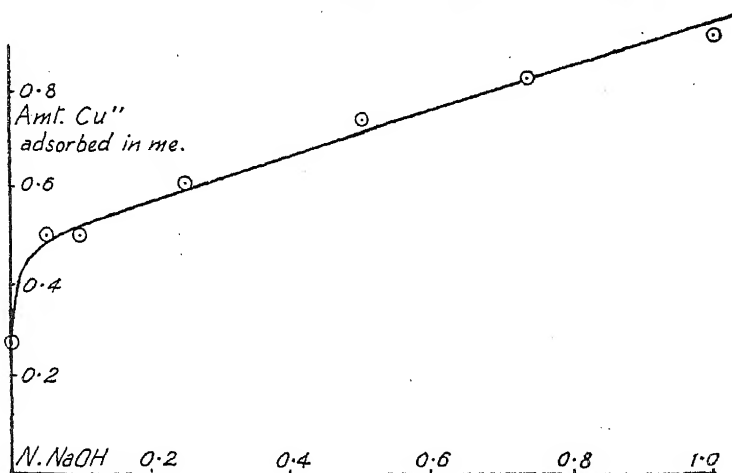
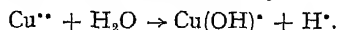


FIG. 5.

### Discussion.

The results are applied to columns in Part II, but are also of value since little work has been done on the adsorption of electrolytes by alumina.<sup>6</sup> Variation in the temperature and period of activation, prewashing, exposure to moist air after activation, etc., gives different adsorptive capacities and emphasises the need of strict control of conditions in chromatographic work. The effect of varying temperatures of activation (Fig. 1) is not specific to ionic adsorption since it has been found with  $N_2$ ,<sup>6</sup>  $H_2O$ ,<sup>7</sup> etc., as adsorbates. Deactivation on exposure to moist air (*cf.* <sup>8</sup>) suggests that below  $480^\circ C$ . activation is mainly effective in desorbing water. Similarly, the decrease above  $480^\circ C$ . runs parallel with the decreasing water content (*cf.* <sup>7</sup>). The latter can be due to (a) a transformation from a chain in which Al atoms are active, to a closed ring in which they are inactive;<sup>9</sup> (b) a desorption of water which was parasitic in a strange lattice, rendering it thermodynamically unstable and so more highly adsorbing; (c) the bonding of surface hydroxyl groups above  $480^\circ C$ . with elimination of water, the hydroxyl groups being responsible for adsorption. The adsorbing centres would be Al atoms in (a), lattice discontinuities in (b), and hydroxyl groups in (c). The latter is most probable and is consistent with the effect of prewashing and with the later discussion; thus prewashing effects increased adsorption because it promotes hydroxylation in the subsequent activation. The greater effect of tap-water (containing  $Ca(OH)_2$ ) and acids is due to an increase in exchange capacity (*cf.* later). Deactivation by moist air is caused by the adsorption of water followed by a slow surface crystallisation involving the elimination of centres active in adsorption—this is in accord with the effectiveness of water as a catalyst, as a result of polarisation, in many solid reactions. Similarly, activation exceeding 1 hour has the same effect, but here it is due to surface diffusion at the elevated temperatures.

The effect of prewashing with NaOH (Fig. 5) is due to the formation of aluminate, or ionic adsorption complex, during activation; these act by exchanging  $Na^+$  ions with cations of the adsorbate. Prewashing with tap-water and acids thus give less reproducible results than with distilled water since the increased exchange capacity depends fortuitously on the quantity of solution adhering to the  $Al_2O_3$  after filtration. If it is assumed that the aluminate formation depends directly on the NaOH concentration, the linear character of the plot at higher concentrations is brought about by the exchange between the sodium ion and a *univalent* ion, such as  $CuCl^+$  or  $Cu(OH)^+$ . At the lower concentrations, however, there is an abnormally large aluminate formation due to the greater reactivity of the centres of high free energy on the alumina, giving an initial large exchange. Sieverts and Jungnickel<sup>10</sup> found their alumina to contain  $Na_2CO_3$  and  $NaHCO_3$ , which are removable by washing, after which the  $Cu^{++}$  adsorption falls. This, however, is probably due to  $Cu^{++}$  being initially retained as the basic carbonate which, being insoluble, is highly adsorbed. Hydrolytic adsorption, or an exchange process involving  $H^+$  ions is eliminated, since both lead to an increase of acidity of the solution after adsorption, because  $Cu(OH)^+$  must be formed by a reaction of the type:



Thus with 5 g.  $Al_2O_3$ , using  $CaCl_2$  as adsorbate, the increase of acidity was never greater than corresponding to 0.75 ml.  $N/100$  NaOH, whereas the

<sup>6</sup> *Colloid and Capillary Chemistry*, Freundlich (trans. Hatfield), 1926; except for the adsorption of acids, or merely the cation, no later work has appeared.

<sup>7</sup> Krieger, *J.A.C.S.*, 1941, **63**, 2712.

<sup>8</sup> Milligan, *J.P.C.*, 1922, **26**, 247.

<sup>9</sup> Brockmann and Schodder, *Ber. B.*, 1941, **74**, 73.

<sup>10</sup> Alekseevskii, *J. Russ. Phys.-Chem. Soc.*, 1930, **62**, 817; *A.C.S. Abstr.*, 1931, **25**, 1138.

<sup>11</sup> Sieverts and Jungnickel, *Ber. B.*, 1943, **76**, 210.

non-equivalence of cation and anion adsorption required 40 ml. It thus suggests that the univalent complex ion,  $\text{CuCl}^+$  is liberated in exchange, as has been found in similar systems.<sup>11</sup> Schwab and Issidoridis<sup>12</sup> from absorption spectra data, however, find that the position of the bands and their absorption coefficients lie between those of the hydroxides and the ions in solution, and agree with the corresponding basic salts—no data is given regarding the possibility of univalent complex ions being present.

Analysis of the  $\text{CaCl}_2$  solution after adsorption by the method of Kolthoff and Lingane<sup>13</sup> for  $\text{Na}^+$  ions gave minute traces in accord with the preliminary spectroscopic analysis of the Na content of the alumina. It was possible that  $\text{Al}^{+++}$  ions were active in exchange due to the formation of an internal complex during activation. Analysis of the solution by the method of Yoe and Hill,<sup>14, 15</sup> however, gave only 5 % of that required to account for the non-equivalence; this was confirmed spectroscopically. At this stage only a few grams  $\text{Al}_2\text{O}_3$  remained; this was therefore subjected to a detailed spectroscopic examination. Using an improved technique which gave a spectrum rich in "impurity lines," 0.2 % Na, together with less than 0.01 % each of Mg, Ca, and Fe, was found. A re-examination of the micro-colorimetric method for Na revealed that the age of the uranyl acetate solution, no further supplies of which were available, prevented quantitative results from being obtained. The amount of Na (0.2 %) is sufficient to account for the non-equivalence of 0.7–0.8 me./1 g.  $\text{Al}_2\text{O}_3$  found. Since there is present no other impurity in sufficient quantity, it is highly probable that the  $\text{Na}^+$  ion/cation exchange accounts for the excess adsorption of cations. The difference found with HCl as adsorbate (0.5 me.) was proved to be due to the production of  $\text{Al}^{+++}$  ions by solution of the oxide in the acid. Furthermore, the approximately constant non-equivalence found with all chlorides at higher concentrations means that practically all the Na content must be engaged in exchange.

The adsorption process can be explained by the alumina functioning as an amphoteric ionic adsorbent which engages in both  $\text{H}^+$  ion/cation and  $\text{OH}^-$ /anion exchange, the non-equivalence being due to  $\text{Na}^+$  ion/cation exchange. It would be expected, however, that the  $\text{Cl}^-$  ion adsorption would be the same for all chlorides, and that the  $\text{Cu}^{++}$  ion adsorption should be independent of the anion present, since the alumina is highly polarised and any additional inductive effect by adsorption processes would be negligible, and consequently the two exchange processes would be sensibly independent. Alternatively, the surface of the adsorbent, assumed to be partly ionic, preferentially adsorbs one ion which then binds the ion of opposite charge by equivalent secondary adsorption,<sup>16</sup> the non-equivalence being due to  $\text{Na}^+$  ion/cation exchange; or, molecular adsorption of the adsorbate takes place together with additional exchange with the  $\text{Na}^+$  ion by the cation. In the latter case, where circumstances permit, two surface OH groups will be disposed such that regions of opposite charge are adjacent<sup>17</sup> and these attract the polar adsorbate molecule; this is in accord with the results of activation and deactivation where OH groups were assumed to be the adsorbing centres. There is little distinction between these two latter hypotheses, but in each there should be a connection between the amount adsorbed and the properties of the adsorbate molecule. Table II shows some typical properties and the adsorption affinities, based on the total adsorption, which is a good measure of the equivalent adsorption since the exchange capacity is

<sup>11</sup> Jenny and Elgabady, *J.P.C.*, 1943, **47**, 399.

<sup>12</sup> Schwab and Issidoridis, *Z. physik. Chem.*, B, 1942, **53**, 1.

<sup>13</sup> Kolthoff and Lingane, *J.A.C.S.*, 1933, **55**, 1871.

<sup>14</sup> Yoe and Hill, *ibid.*, 1927, **49**, 2395.

<sup>15</sup> Winter, Thrum and Bird, *ibid.*, 1929, **51**, 2721.

<sup>16</sup> Kolthoff, *J.P.C.*, 1936, **40**, 1027.

<sup>17</sup> Cf. Bernal and Megaw, *Proc. Roy. Soc., A*, 1935, **151**, 384.

practically independent of the nature of the cation. There is no connection between the solubilities of either the hydroxides, or of the sulphates, and the adsorption affinity, and that which apparently exists with the ease of precipitation of the basic salts may be disregarded since the parallelism also exists for the four corresponding hydroxides. This confirms the absence of hydrolytic adsorption; furthermore, secondary equivalent adsorption is unlikely since the adsorption in general increases with increasing solubility of the sulphates.<sup>18</sup> A parallelism does exist between the amount adsorbed and the ease of ionisation (except Ni, Co) and the M.Pt. of the salts, indicating that adsorbability is associated with the tendency to covalency, and that the adsorption is molecular. Thus  $\text{CuSO}_4$  (M.Pt.  $200^\circ\text{C}$ .) is more highly adsorbed than the chloride (M.Pt.  $498^\circ\text{C}$ .), as has been found (Fig. 2).

TABLE II

Cation.	Adsorption Affinity.	S.P. of Hydroxide.	Ease Pptn. Basic Salt.	Solubility $\text{SO}_4$ g.mol./l.	N.Pot. Volts.	B.Pt. —Cl.
Cu . .	50.8	$1.7 \times 10^{-13}$	—	0.31	0.34	decomp.
Cd . .	30.5	$2.3 \times 10^{-13}$	—	0.30	— 0.40	969
Zn . .	29.6	$5.0 \times 10^{-17}$	Zn	0.29	— 0.76	decomp.
Ni . .	28.0	$8.7 \times 10^{-19}$	—	0.18	— 0.22	973
Co . .	24.7	$1.6 \times 10^{-18}$	—	0.15	— 0.29	1049
Mn . .	24.4	$1.3 \times 10^{-14}$	Mn	0.33	— 1.00	1190
Mg . .	22.0	$2.3 \times 10^{-11}$	Mg	0.24	— 1.55	1421
Ca( $\text{Cl}_2$ ) .	15.0	$1.0 \times 10^{-4}$	Ca	0.001	— 1.90	1600

The "mixed" isotherms show that the adsorption can be controlled by the acidity and no greater efficiency of elution in columns will be found above 40 me./l HCl. Up to moderate concentrations there is a displacement effect whereby both adsorbates are less adsorbed when together than when alone in solution; at high concentrations the  $\text{Cl}^-$  ion adsorption is markedly increased, the shape of the isotherm suggesting interaction effects between oppositely charged ions. Nevertheless, the Freundlich equation is still applicable to the cation isotherms when both adsorbates are present.

### Summary.

The adsorption of cations and anions from aqueous solutions of electrolytes by alumina has been measured. The cation is more strongly adsorbed than the anion due to additional cation exchange adsorption. This is associated with the presence of sodium aluminate as an impurity, and is not due to hydrolytic adsorption, nor to an exchange involving either the  $\text{Al}^{+++}$  or  $\text{H}^+$  ion. The magnitude of the equivalent adsorption runs parallel with the covalent tendency of the adsorbate molecule.

The authors wish to express thanks to Dr. L. H. Ahrens of the Mineral Research Laboratories, Johannesburg, for many spectroscopic analyses, and one of us (P. W. M. J.) to the National Research Board of South Africa for a Research Scholarship held during the investigation.

Natal University College,  
University of South Africa,  
Pietermaritzburg,  
Natal, South Africa.

<sup>18</sup> Fajans and Erdey-Gruz; *Z. physik. Chem., A*, 1931, 158, 97.

# INORGANIC CHROMATOGRAPHY.

## PART II.—POSITION, RATE OF ADVANCE AND WIDTH OF ADSORBATE ZONES.

By P. W. M. JACOBS AND F. C. TOMPKINS.

*Received 5th June, 1944. As amended 28th February, 1945.*

The practical applications of chromatography are still largely empirical, because systematic quantitative data, from which the best conditions for a given process might be deduced, are lacking; similarly, its extension to quantitative determinations depends on a knowledge of various factors which are, as yet, understood in qualitative terms only. A few measurements by Cassidy,<sup>1</sup> and more complete studies by Weil-Malherbe<sup>2</sup> and Tiselius<sup>3</sup> represent the only work of this nature. Le Rosen<sup>4</sup> has noted a parallelism between rate of advance and position of band on the column, and Schwab *et. alia*<sup>5</sup> reported some semi-quantitative work chiefly on the relative position of cations and anions on alumina columns. The purpose here has been to provide quantitative measurements for use in inorganic chromatography, which can be incorporated with the results of Part I.<sup>6</sup>

### Experimental.

The sample of Merck's alumina and the conditions of activation were the same as previously described.<sup>6</sup> Columns were prepared in tubes, 11 mm. diameter, graduated in mm. Those obtained using dry alumina by various methods were rejected because of uneven band formation. Finally, 20 g. alumina were added to 50 ml. water at 90° C., vigorously agitated and the suspension poured into the tube under 10 cm. Hg. suction. The velocity of flow of solutions through the columns were obtained by a method similar to that used by Le Rosen. The rates of advance of the leading (front) and of the trailing (rear) edge of the band were recorded by noting the position, at definite times, at six different points round the tube, and taking the average.

### Results and Discussion.\*

The velocity,  $V_c^0$  was found to depend directly on  $P$ , inversely as  $s$ , and to be approximately independent of the diameter of the column (*cf.* Le Rosen). With columns, initially filled,  $V_c^0$  was constant within one minute of emergence of the solution. Values for four consecutively

<sup>1</sup> Cassidy, *J.A.C.S.*, 1940, **62**, 3076. Cassidy and Wood, *ibid.*, 1941, **63**, 2628.

<sup>2</sup> Weil-Malherbe, *J.C.S.*, 1943, 303.

<sup>3</sup> Tiselius, *Science*, 1941, **94**, 145; *Adv. in Coll. Science*, vol. 1, 1941.

<sup>4</sup> Le Rosen, *J.A.C.S.*, 1942, **64**, 1905.

<sup>5</sup> Schwab, *v.*, Part I, ref. 2.

<sup>6</sup> Jacobs and Tompkins, *preceding paper*.

\* The following symbols are employed (*cf.* 7, 8, 9).

$M$  = mass alumina per unit length in g.,

$s$  = length of column in cm.,

$\alpha$  = interstitial volume per unit length column,

$x$  = distance of any point from top of column ( $x = 0$ ),

$P$  = pressure difference at ends of column in cm. Hg.,

$V$  = volume in ml. solution poured through column initially full, after time  $t$  from  $t = 0$ ; *i.e.* volume passing any point in column after  $t = 0$ , and is thus a measure of time,

[Footnote continued overleaf.



prepared and apparently identical columns, for constant  $P$ , were 2.45, 2.66, 2.65 and 2.50, showing that constant packing was obtained; when  $V_c^0$  diverged largely from 2.50, the column was rejected. Standardisation

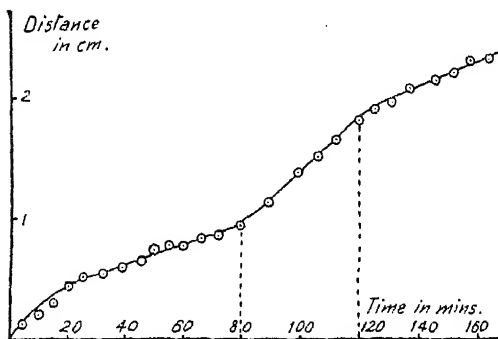


FIG. 1.

$V_c$  was doubled at 80 min. and reduced to the original value at 120 min. The high values of  $r_L$  are always obtained initially before the constant rate is attained; afterwards,  $r_L$  quickly responds to changes in  $V_c$ . With columns of the same value  $V_c^0$  value,  $V_c$  increases with HCl concentration ( $C$ ), according to:  $1/V_c = -kC^{\frac{1}{2}} + K$ ,  $\frac{1}{2}$  as shown in Table I. Since for strong electrolytes,<sup>10</sup>

$$(n_c/n_0 - 1) = AC^{\frac{1}{2}},$$

TABLE I.

$C_0(\text{H}^+)\text{me./l.}$	$AC^{\frac{1}{2}}$	$V_c$ mm./min.	$1/V_c$	$1/V_c$ calc. from $1/V_c = 0.04$ $- 4.354C^{\frac{1}{2}}$
5.0	0.0448	4.7	0.212	0.205
7.5	0.0548	6.0 <sub>8</sub>	0.165	0.162
10.0	0.0632	8.15	0.123	0.125
12.5	0.0708	10.0	0.100	0.092
15.0	0.0774	16.2	0.062	0.062

where  $A = 0.002$  for HCl, and  $n_c$  and  $n_0$  are the viscosities of HCl and water respectively,  $V_c$  is an inverse function of  $n_c$ . The rate of advance of bands, which depends on  $V_c$ , will thus be affected by merely by changes of viscosity. The relative rate  $R$  should thus replace  $r$ , as first suggested

$Q$  = amount of solute adsorbed per unit length column in milliequivalents (me), where  $Q = Q(V, x)$ , or  $Q(t, x)$ ,

$c_0$  = initial concentration in me./l. of solute in solution,

$c$  = concentration of solution at point,  $x$ , and time,  $t$ , where  $c = c(V, x)$ , or  $c(t, x)$ ,

$C$  = initial concentration of developing solution,

$f$  = adsorption isotherm of solute on alumina, where  $f = f(c)$ , and thus  $Q = Mf(c)$ ,

$V_c^0$  = constant rate of flow in mm./min. of water down packed column,

$V_c$  = rate of flow of developing solution down packed column, in mm./min.,

$r$  = rate of advance of edges of adsorbate zone in mm./min., where  $r_L$  refers to the leading, and  $r_t$  to the trailing edge,

$R$  = relative rate of advance of edges, or  $r/V_c$  ( $R_L, R_t$  as for  $r$ ).

by Le Rosen, but not experimentally justified. In practice,  $r$  varies directly as  $V_0$  over a narrow range only; it is thus better to adjust  $P$  to obtain approximate constancy of  $V_0$ , and then to use  $R$  to eliminate the smaller differences.

Experimental conditions corresponding to those demanded theoretically<sup>7, 8</sup> are obtained more precisely in formation of bands. Various initial concentration of  $\text{CuCl}_2$  ( $c_0$ ) were added

TABLE II.

$c_0(\text{CuCl}_2)$ me./l.	$R_1$ mm./min.	$Q$ me./1 g. $\text{Al}_2\text{O}_3$ .	$R_1 Q/c_0 \times 10^3$ .
10	0.014 <sub>8</sub>	0.66	0.96
25	0.035 <sub>8</sub>	0.72	1.02
50	0.060	0.87	0.97
100	0.109	0.90	0.98
150	0.150	0.99	0.99
200	0.190	1.05	1.00

continuously, and  $r_L$  measured. Table II gives the value of  $Q$  in equilibrium with  $c_0$ ,<sup>6</sup> and shows that  $c_0/Q(dx/dt)_{c_0}$  is a constant. The differential equation (cf. <sup>7</sup>) may be written,  $(dc/dx)_x = - (dQ/dV)_x$ , since experimentally  $(dc/dV)_x = 0$ . Since  $c$  is  $c(V, x)$ , this may be transformed to  $(dV/dx)_x = (dQ/dc)_x$ . For the  $\text{Cu}^{++}/\text{Al}_2\text{O}_3$  system,  $Q = kc^{1/n}$ , or  $1/Q(dQ/dc) = 1/nc$ , then  $c_0/Q(dx/dV)_{c_0}$ , or  $c_0Q(dx/dt)_{c_0}$  is a constant, as found experimentally. The rate of advance is thus directly proportional to  $n$ , and inversely as  $c^{1/n}$ .

The conclusion should be true of all cations studied in Part I, since the Freundlich equation was found applicable. The method of development of bands with appropriate reagents was rejected since the band was widened. Consequently, the volume of M/10 solution poured through columns of equal length before the solute was detectable with the reagent in the filtrate, was determined. Table III gives the method of detection,

TABLE III.

Cation.	Ads. Affinity.	Width for 10 ml. M/10(w).	$Wc_0/Q$ .	Method of Detection.
Cu . . .	50.8	2.30	117	Acid KI and starch
Cd . . .	30.6	3.88	119	Sodium sulphide
Zn . . .	29.6	3.60	101	$\text{K}_3\text{Fe}(\text{CN})_6$
Ni . . .	28.0	4.00	110	Dimethylglyoxime
Co . . .	24.7	3.85	95	$\alpha$ Nitroso $\beta$ naphthol
Mn . . .	24.4	4.86	118	Neutral $\text{KMnO}_4$
Mg . . .	22.0	5.83	128	Magneson

the adsorption affinity, and the width of band corresponding to 10 ml. M/10 solution; the conclusion is confirmed.

The acidity of solution largely effects the amounts adsorbed;  $R$  should therefore vary with HCl concentration of the developing solution. Bands formed from 3 ml.  $\text{CuCl}_2$  (75 me./l.) were first washed with water—this caused no movement, except that the leading edge was slightly advanced due to washing through  $\text{CuCl}_2$  solution lodged in the interstices. Schwab seems to have confused this with development, which here was effected with HCl (5-20 me./l.) and  $r_L$ ,  $r_i$  and  $V_0$  measured, and  $R_L$  and  $R_i$  calculated. These latter were initially high; the former falls slowly, but the latter quickly, to their constant values. In presence of acid, the amount adsorbed decreases and the band widens, thereby accounting for the high initial value of  $R_L$ . The acid emerging from the  $\text{Cu}^{++}$  band has

<sup>7</sup> Wilson, *J.A.C.S.*, 1940, **62**, 1583.

<sup>8</sup> De Vault, *ibid.*, 1943, **65**, 532.

a concentration less than  $C$  initially because it is highly adsorbed; with continual addition  $C$  is slowly attained. During this period, the adsorption of  $\text{Cu}^{++}$  is decreased, the band therefore widens thereby giving a high value of  $R_L$ . The greater the value of  $C$ , the higher is that initially of  $R_L$ , and the longer is the period before a constant rate is obtained.

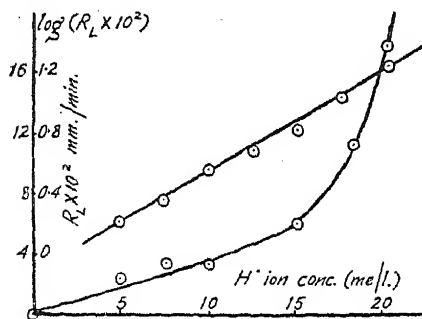


FIG. 2.

thus varies inversely as the amount adsorbed. It must be noted that the line of demarcation between the rear edge of the coloured band and the white adsorbent *appears* to be quite sharp on the column, although the concentration distribution of the solute in solution for a Freundlich isotherm extends asymptotically to the top of the column. Furthermore, the adsorptive capacity of the alumina at the *edge* is controlled largely by the initial  $\text{H}^+$  concentration of the  $\text{HCl}$ , and this determines to a large extent the average value of  $Q$  here. Writing the differential equation in the form,  $(dc/dx)_s/(dc/dV)_x + \alpha = -(dQ/dc)_x$ , and transforming by a similar treatment to that given above, then  $-K'/R_L + \alpha = -(dQ/dc)_x$ , where  $K'$  is a constant. But  $\log Q = k_a - k_b(\text{H}^+)$ , or  $dQ/dH = -k_b Q$ . Therefore, since we may write approximately,  $dQ/dH = (dQ/dc)_x$ , then  $K/R_L + \alpha = k_b Q$ , as found experimentally.

There is little verification, and none for cations, that the relative position of solutes depends on their adsorbability. The list of Schwab must be accepted with reserve because both the acidity and the anion were varied in the different groups, and these two factors largely influence cation adsorption.<sup>6</sup> Here  $\text{M}/10$  sulphates in neutral solution were employed, using his method; Table III summarises the results. The order may vary with concentration, the values of  $Q$  are therefore given for  $\text{M}/10$  solutions. The general agreement with his list suggests that the relative order is not affected by the acidity nor by the nature of the anion,

Quantitative relationships between  $Q$  and  $R$  will thus be more exactly observed at the trailing edge where such complications are for the most part absent. Fig. 2 shows that  $\log R_L$  varies directly with the  $\text{H}^+$  concentration, i.e.,

$$\log R_L = k' + k''(\text{H}^+).$$

Combining this with the relationship found previously,<sup>6</sup>

$$\log Q = k_a - k_b(\text{H}^+),$$

then,  $\log QR_L = K$ , where  $K$  is a constant. The rate of advance

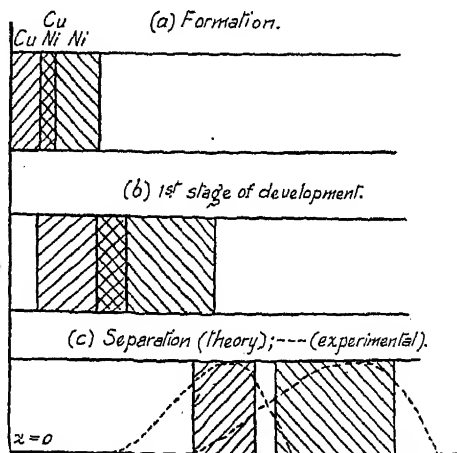


FIG. 3.

<sup>6</sup> Weiss, *J.C.S.*, 1943, 297.

providing that these are the same in the comparative experiments. No clear separation on formation and subsequent washing with water was obtained using mixed cation solutions. The results of Schwab, using this method in the quantitative analysis of ores, must therefore appear fortuitous.

The data obtained here on the width and rate of advance of Cu and Ni bands indicate that these should be separable on development with HCl. A Cu/Ni band, 1 cm. width, was developed with HCl. (5 me./l.)—the band widened to 2 cm. fairly quickly due to the reduction of the adsorptive capacity of the alumina by half in this acidity. Assuming separation to be visible when the bands have 0.2 cm. between them, the Ni band must move 0.6 cm. relative to the Cu band (*cf.* Fig. 3). In one

TABLE IV.

Relative order here	Cu	Cd	Zn	Ni	Co	Mn	Mg
Ads. affinity	50.8	30.6	29.6	28.0	24.7	24.4	22.0
Method of detection	—	Na <sub>2</sub> S	K <sub>3</sub> Fe(CN) <sub>6</sub>	—	KMnO <sub>4</sub>	—	Titan yellow
Schwab's order	Cu	Zn	Co	Ni	Cd	Mn	—

experiment,  $r(\text{Cu})$  was 0.15 mm./min. and  $r(\text{Ni})$  was 0.22. If the trailing Ni edge remains reasonably sharp, separation should be obtained in 90 min. The value of  $V_e$  here was 6 when transformed to ml./min.; thus about 500 ml. acid is required and the leading Ni edge would move through 2 cm. Actually, the edge was advanced 6 cm. without obtaining a white intermediate zone, due mainly to the spreading of the trailing edge. A more serious discordance is that the calculated value of  $R_L$  is about half that found experimentally. This is emphasised in Table II where it may be shown that the constant value of approximate unity corresponds to the exponent  $1/n$  in the Freundlich equation, whereas the experimental value is 0.39. The reason for this is at the moment obscure.

Nevertheless, the present results and those of Part I provide explanations of many of Schwab's observations. Using different absolute, but the same relative, concentrations of Cu and Co, he found the specific length ratio of bands to be approximately constant. Since both cations obey the Freundlich equation, then, as before,  $w_1/w_2 = n_1 c_1 Q_2 / n_2 c_2 Q_1$ , or  $w_1/w_2 = n_1 c_1^{(1-1/n)} / n_2 c_2^{(1-1/n)}$ , where  $w_1$  and  $w_2$  are the widths of the bands. Since  $n_1$  and  $n_2$  are about the same magnitude,  $w_1/w_2 = (c_1/c_2)^{(1-1/n)}$ . The ratio will thus be the same for different absolute but the same relative concentrations. If the latter is varied, this is no longer true, although a very approximate constancy is possible since  $1/n$  is fairly small; thus Schwab found the length per g. atom to vary between 1 and 1.48. It must be noted that the width of band is never proportional to  $c_0$ ; this fact, together with incomplete separability, absence of sharp edges, etc., considerably limits the application to quantitative estimations. Again a 'double Cu zone' obtained by him using a  $\text{CuSO}_4/\text{Cu}(\text{NO}_3)_2$  solution and the change in width of bands when a  $\text{CuSO}_4/\text{NiSO}_4$  was replaced by an equivalent  $\text{CuSO}_4/\text{Cu}(\text{NO}_3)_2$  solution, do not require a complicated theory involving double aluminate formation. The adsorption of  $\text{Cu}^{++}$  is greater from a sulphate solution than from an equivalent nitrate solution; a band of smaller width and deeper colour results. With both anions present, there will be a narrow, deeply coloured 'sulphate' zone at the top of the column, followed by a wider, less densely coloured 'nitrate' band. Similarly, the bands, particularly that of Ni, will be wider in the  $\text{CuSO}_4/\text{Ni}(\text{NO}_3)_2$  than in the  $\text{CuSO}_4/\text{NiSO}_4$  solution. This stresses the necessity of using the same anion both in the solution under analysis and in the developing solution, particularly in semi-quantitative estimations.

Schwab further reports that sharper zones are formed on sodium-rich

alumina; from his diagram, it is clear that the bands are narrower, more deeply coloured and their rate of advance is much slower. Now pre-treatment with NaOH effects increased adsorptive capacity, *e.g.* fourfold using  $N/10$  NaOH; thus the band on sodium poor alumina will be four times wider and move four times more quickly. Schwab reports a fivefold change. The effect is thus a consequence of an increased adsorptive capacity, and is anticipated even when the increase is not due to a larger exchange capacity.

White zones between coloured bands were never obtained here or by Schwab when mixed cation solutions were used. This may be due to the complicating influence of simultaneous anion adsorption; to the inability of any one cation (except  $H^+$ ) to replace to any large extent another cation already adsorbed; or to the adsorption being both exchange and molecular. Replacement of one cation by another would be expected to lead to clearer separations; an adsorbent functioning purely as a cation exchanger might therefore be more effective in inorganic chromatography. This is being investigated.

### Summary.

The relation of widths of bands of some cations on alumina columns, the rate of advanced when developed with HCl, and the relative positions have been studied and related to the results of Part I. The possible extension to quantitative estimations has been examined, and various observations of Schwab have been given alternative explanations.

One of the authors (P. J. M. J.) wishes to express thanks to the National Research Council and Board of South Africa for a Research Scholarship held during the investigation.

*Natal University College,  
University of South Africa,  
Natal, South Africa.*

---

## INORGANIC CHROMATOGRAPHY.

### PART III.—ELUTION CURVES.

By P. W. M. JACOBS AND F. C. TOMPKINS.

*Received 5th June, 1944. As amended 28th February, 1945.*

In Part II, the width and rate of advance of Cu bands were determined on an alumina column. The accuracy of the method was not high, but it showed that the differential equation describing the process was generally adequate. More precise information can be obtained from the concentration distribution of the adsorbate in the flowing solution. Since the isotherm for the system used is known,<sup>1</sup> the distribution of the adsorbed material on the adsorbent can be calculated. In addition, the volume of eluent used in advancing the band through a given distance provides a measure of its rate of movement. The method has been tentatively examined by Cassidy,<sup>2</sup> and developed by Weil-Malherbe<sup>3</sup> in a paper which appeared near the completion of this work. The purpose of this paper has been to extend and co-ordinate the data of Part II, and to test the validity of the differential equation when applied to a typical inorganic system.

<sup>1</sup> Jacobs and Tompkins, Part I.

<sup>2</sup> Cassidy, *J.A.C.S.*, 1940, **62**, 3076 and 1941, **63**, 2628.

<sup>3</sup> Weil-Malherbe, *J.C.S.*, 1943, 303.

**Experimental.**—The sample of Merck's alumina, the conditions of activation, and the preparation of the columns were the same as previously described.<sup>1, 4</sup> The diameter of the tube was increased to 2.45 cm. and the rate of filtration to 20 ml./min. Aliquots were titrated iodometrically with  $N/100$  thiosulphate.

### Results and Discussion.

The terminology used, additional to that of Part II, is the same as that of Weil-Malherbe, but his term, adsorptive, has been changed to the usual one, adsorbate.

The elution curves are classified as differential and integral, depending on whether they refer to the amount of adsorbate in successive aliquots, or to the amount in the total eluate volume.

**Formation.**—The formation of bands corresponds more precisely to the theoretical demands; particularly, the reversibility of adsorption is not involved. Copper bands were formed from neutral  $\text{CuSO}_4$  solution ( $c_0 = 100$  me/l.), and the threshold volume  $V_t$  determined. Subsequently, 3 ml. aliquots were collected successively for analysis until  $c_0$  was attained. The values of  $V_t$  so obtained were slightly uncertain because deviations from ideality in the column caused them to be low; those given in Table I

TABLE I.

Mass $\text{Al}_2\text{O}_3$ in g. (M).	$V_t$ (ml.).	$V_t/M$ .
2	7.7	3.85
4	14.8	3.70
7.5	28.0	3.70
12.5	48.0	3.84
15.0	56.7	3.78

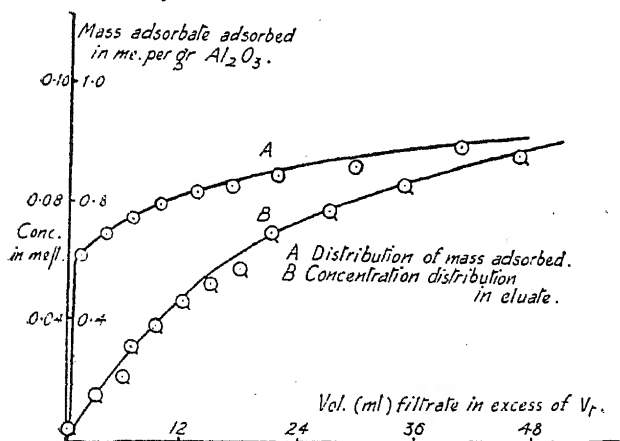


FIG. 1.

ing edge decreases with increasing advance of the band. In Fig. 1, the concentration distribution in solution at the front part of the band after being advanced 3 cm., together with the corresponding distribution of adsorbed matter on the alumina (calculated from the former and the isotherm) are plotted against the total volume of eluate. The edge of the adsorbed band is reasonably sharp and its position, judged visually as in Part II, must always be practically coincident with the  $V_t$  value—thus the two methods will yield the same conclusion.

<sup>4</sup> Jacobs and Tompkins, Part II.

<sup>5</sup> Weiss, *J.C.S.*, 1943, 297.

have been obtained therefore by extrapolation of the integral curves, which are initially linear, and show that  $V_t$  varies linearly with the weight of adsorbent, or length of column, in agreement with the conclusion of Part II. This is consistent with the Weiss solution for Freundlich isotherms,<sup>5</sup> despite the fact that the slope of the lead-

**Development.**—Sulphuric acid (20 me/l.) was used because in this acidity the isotherm is linear up to a Cu concentration of 60 me/l. when the saturated value was attained. The volume of aliquots collected was increased to 15 ml. since the rate of advance was about 1/10th that on formation.

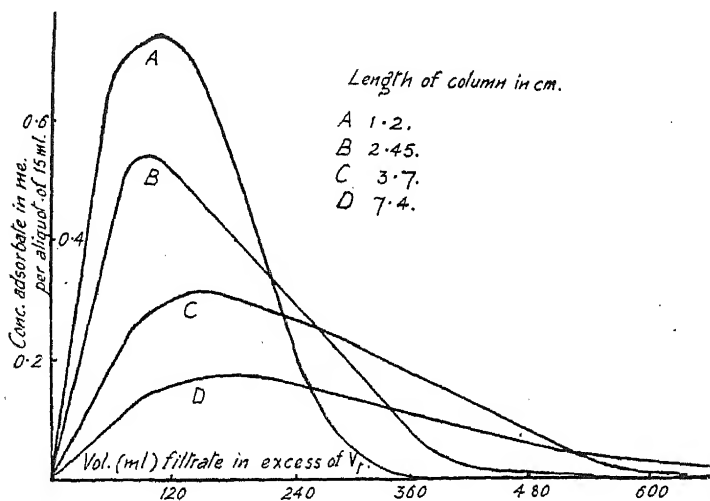


FIG. 2.

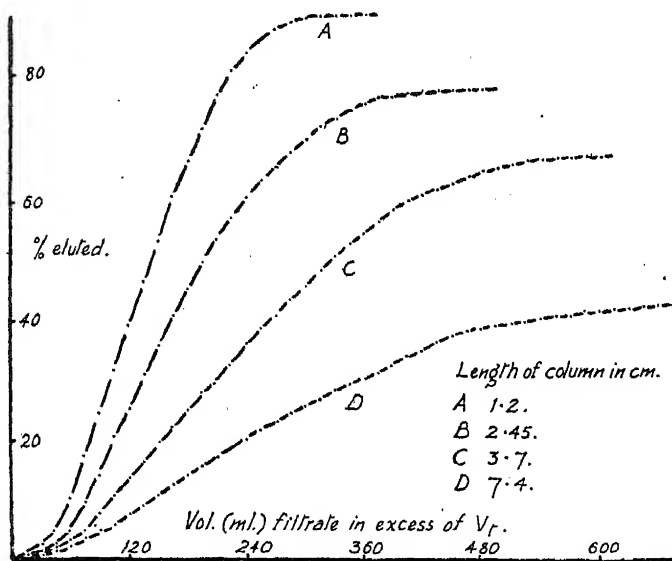


FIG. 3.

**Variation of Length of Column.**—The band was formed from 10 ml. neutral  $\text{CuSO}_4$  ( $c_0 = 100$  me/l.) and the weight of adsorbent varied; both  $V_f$  and the eluate concentrations were measured. Typical differential and integral plots are given in Figs. 2 and 3. The amount desorbed was always less than that used in formation, the amount remaining varied

directly as the weight of the adsorbent for the same strength of eluting acid. The lack of sharpness which becomes more marked on development is not solely occasioned by the retention of adsorbate by the column since the band widens considerably. The tail of the band has a concavity opposite to that of the head and becomes broad and diffuse in the longer columns. This is in accord with the predictions of a Freundlich isotherm but contrary to that expected when the isotherm is, as here, linear. The term, "width of band" used to describe the appearance on the adsorbent has little significance and can only be measured by the difference  $V_f - V_t$ , where  $V_f$  is the volume of filtrate collected after which no adsorbate is detected. The maximum concentration in the eluate decreases with length of column, the decrease being greater than can be accounted for by loss by retention on the column.

The integral plots are sigmoid with a short initial part of low gradient, a steep almost linear central portion and a flat tail, the length of which increases with increasing  $V_t$ . The values of  $V_t$  were obtained from these plots using the method of Weil-Malherbe; they vary directly as the weight of adsorbent (Fig. 4), in accord with theory for both Freundlich and linear isotherms.

#### Variation of $c_0$ .—

Using 10 g. alumina (length 2.45 cm.),  $v_0 = 10$  ml., and sulphuric acid of strength 20 me/l., the initial concentration of  $\text{CuSO}_4$  was varied in formation. The width of band increased with  $c_0$ , such that  $\log(\text{width})/\log c_0$  was a straight line of slope 0.95. Since

the exponent  $1/n$  in the Freundlich equation is here 0.19,<sup>1</sup> the theoretical value of the slope should be 0.81.<sup>4</sup> The higher value is due to the fact that the band width is measured after addition of water which clears Cu solution out of the interstices. Now the amount of Cu adsorbed in concentrations greater than 25 me. Cu/l. is almost constant, consequently the concentration of adsorbate in the pores is greater as  $c_0$  is increased. The solution which is driven out of the interstices is adsorbed at the leading edge and the band is widened by an amount approximately proportional to  $c_0$ . The log. plot above will thus be still linear but of higher slope than expected theoretically. The values of  $V_f$ ,  $V_t$  and thus of  $V_f - V_t$  are independent of  $c_0$  in agreement with the solution for a linear isotherm, which predicts a band of constant width moving with a constant velocity. There is, however, an anomaly here. The values of  $V_t$  do not measure the rate of advance since the leading edges after formation are at varying distances down the column. A band formed at high  $c_0$  has a smaller distance to travel before the leading edge reaches the bottom of the column, and thus apparently moves more slowly than that of a narrower band formed at low  $c_0$ . This result conflicts with the theoretical predictions. The value of  $V_f$  is, however, the same for all bands, but is considerably higher than that expected for a linear isotherm, i.e.  $2V_t$  or 470 ml. The maximum concentration eluted ( $C_m$ ) is not proportional to  $c_0$  as required for a linear isotherm, but obeys the equation,  $\log C_m = k \log c_0 + \text{constant}$  ( $Cp$ , Table II).

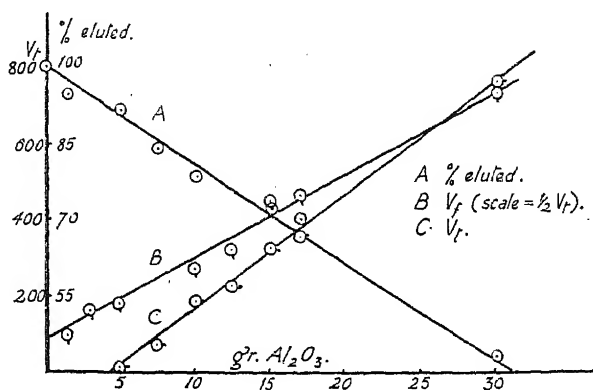


FIG. 4.



TABLE II.

$V_0$ (ml.).	$V_t$ (ml.).	$w$ (cm.).	$d$ (cm.).	$V_f$ (ml.).	$V_t/d$ .
5	235	0.45	2.00	695	118
7.5	201	0.80	1.65	701	122
15	124	1.40	1.05	724	118
20	59	1.93	0.52	689	112
25	0	2.45	0.00	705	—

In the above,  $w$  is the width of band on formation and  $d$  is the distance from its leading edge to the bottom of the column.

**Variation of  $v_0$ .**—Using  $c_0 = 100$  me/l.,  $v_0$  was varied, with all other conditions as in the previous series. Since  $R_L/Q c_0$  must be constant,\* the width of band increases with  $v_0$ ; this is found experimentally. The distance of advance of the leading edge increases therefore as  $v_0$  decreases; here  $V_t$  is linearly related to this distance and the rate of advance is thus a constant independent of  $v_0$ , as expected of a system with a linear isotherm. The anomaly reported in the  $c_0$  series is not apparent here although the only difference is the manner of varying the initial amount of adsorbate used in formation. Similarly,  $V_f$  is independent of  $v_0$  and the plot of  $\log C_m/\log v_0$  is linear (Cp. Table III).

TABLE III.

$c_0$ (me/l.).	$V_t$ (ml.).	$w$ (cm.).	$d$ (cm.).	$V_f$ (ml.).	$V_f - V_t$ .
25	230	0.25	2.20	584	354
40	230	0.40	2.05	609	379
50	220	0.50	1.95	582	362
60	240	0.65	1.80	592	352
75	220	0.85	1.60	592	370

**Variation of pH of Elution Solution.**—Using a column of 10 g. alumina,  $v_0 = 10$  ml. and  $c_0 = 100$  me/l., the band was developed with varying strengths of  $H_2SO_4$  solution. The percentage eluted increased with decreasing pH such that the logarithm of the amount retained was a linear function of the  $H^+$  ion concentration (Fig. 5), thereby confirming the static measurements of Part I. Similarly the rate of advance of the trailing edges, measured in terms of  $V_t$ , is proportional to this concentration (Cp. Part II). Combining these,  $\log Q/V_t$  is a constant, which may be approximately predicted theoretically (Cp. Part II). On the other hand,  $V_t$  varies inversely as the acidity; this, however, may be fortuitous since reasons have been given\* showing that little correlation of  $V_t$  and pH can be expected in short columns.

**General.**—The present system does not conform well to the ideal conditions required for the validity of the differential equation, and the correlation which does exist is for the most part with respect to the rate of advance of the leading edge as reflected in the  $V_t$  values. In particular, the concentration distribution in the "tail," which should possess a sharp edge for a linear isotherm, is largely different. This departure is linked with the irreversible nature of the adsorption processes, and probably with the simultaneous adsorption of anions. Work in progress using columns of zeolitic materials also suggests that the broadening of the tail is in part due to the slow rate of exchange between the Na ion present as impurities on the alumina and cations in solution. It is clear that alumina is un-

suitable as an adsorbent for inorganic chromatography, particularly for semi-quantitative work since the irreversibility and other factors emphasise the loss of sharpness at both edges during development and renders measurements of widths of bands of no great value. Similarly, the separability

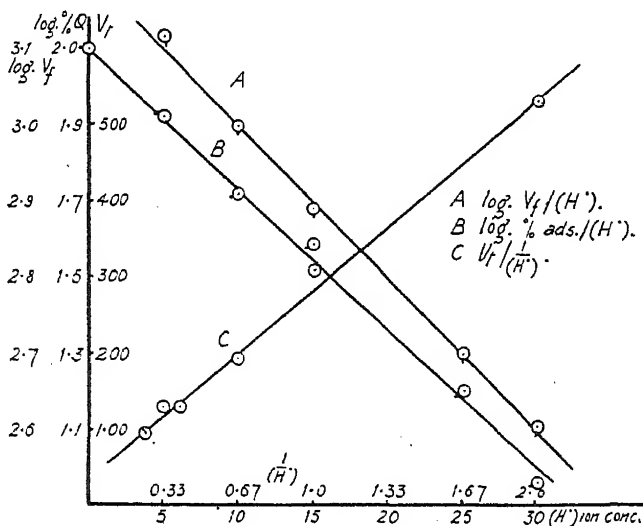


FIG. 5.

of cations becomes more difficult, if not impossible. The practical applications of the present results, *e.g.* to determine the eluant power the minimum length of column for full development, etc., need not be elaborated since they have been fully considered by Weil-Malherbe.

### Summary.

Differential and integral concentration distributions of Cu ions in solution have been obtained in a chromatographic study of the formation and development of bands on alumina columns. The variation of initial concentration and volume of  $\text{CuSO}_4$  solutions, of length of column and  $\text{pH}$  of eluting solutions have been investigated and the results confirm and extend the conclusions of Part I and II. Alumina is shown to be unsuitable as an adsorbent both from the view of separability of cations and of quantitative applications.

One of the authors (P. W. M. J.) wishes to express his thanks to the National Research Council and Board of South Africa for a Research Scholarship.

Natal University College,  
University of South Africa,  
Pietermaritzburg, Natal, S. Africa.

## THE FORM OF CATALYST POISONING CURVES.

BY E. B. MAXTED.

*Received 5th March, 1945.*

If the activity of a metallic catalyst, in for instance a hydrogenation system containing a poison, is plotted against the amount of poison present, a graph is obtained in which the activity of the catalyst usually first falls linearly or approximately linearly with increasing poison content. This relationship persists in many cases up to a stage of poisoning at which the greater part of the activity of the catalyst has been suppressed. It is then followed by an inflexion in the graph, after which the activity of the catalyst falls far less steeply with further increase in the poison content. Graphs of this form have been obtained experimentally by the author and his co-workers<sup>1</sup> for many cases of catalytic hydrogenation and for other reactions; and this linear variation in activity over at any rate the main part of the poisoning graph has been regarded as suggesting a uniform effective activity of all the catalysing or adsorbing points involved up to the advanced stage of poisoning corresponding with the region of inflexion; for it is otherwise difficult to see why the progressive suppression of the catalytic activity of point after point—by occupation by the poison—should lead to an equal diminution in the catalytic activity. There has, however, hitherto been a difficulty, in view of the occurrence of the bend in the graph, in extending this simple conception of surface uniformity to the adsorbing or catalysing elements involved in stages after the inflexion; and it was apparently necessary to assume the coming into action of secondary catalysing or adsorbing points of lesser activity, represented by less active surface elements or by lower (non-surface) layers in the catalyst lattice or even by adsorption or catalysis on or through an already adsorbed layer.

In a recent paper,<sup>2</sup> Herington and Rideal have made an important contribution to the theory of homogeneous catalysing surfaces, in that they have shown, by calculations based on random adsorption on a model lattice, that also the latter part (after the region of inflexion) of the poisoning graph for reactions such as catalytic hydrogenation can be accounted for without the necessity for assuming the coming into action of a second type of catalysing points. An essential basis in these calculations is the reasonable assumption that, if the poison or the substance hydrogenated is of a size greater than a single atom, each of these will require a set of adjacent surface elements, rather than a single surface element, for its accommodation. It is shown by Herington and Rideal that the factor introduced by the gradual disappearance, as the concentration of poison on the surface is increased, of unoccupied sites containing sufficiently large sets of adjacent surface elements to accommodate such molecules of poisons or reactants should, according to the conditions of the adsorption, either lead to a very nearly linear fall in the activity up to a certain degree of poisoning (this stage being followed by a rather sharp curvature) or, alternatively, the whole poisoning graph should be curved, the curvature being increased with an increase in the point-order of the adsorption, *i.e.* in the number of adjacent adsorbing points required for each molecule of poison or of reactant.

<sup>1</sup> Maxted, *J. Chem. Soc.*, 1921, 119, 225; 1922, 121, 1760; Maxted and Evans, *ibid.*, 1938, 2071, and other papers.

<sup>2</sup> Herington and Rideal, *Trans. Faraday Soc.*, 1944, 40, 505.

The first of these types of theoretical poisoning curve reproduces substantially the experimental poisoning graphs which have been observed by the author and his collaborators. In the experimental curves, the rather sudden deviation from the initial, approximately linear course has usually but not always, from its apparent sharpness, been drawn in graphs as a point rather than as a region of inflexion; but, as Herington and Rideal indicate in the 7-site curve in Fig. 3 of their paper, the exact course at the turn can only be followed if a large number of accurately determined points in the relatively short inflexion region are available; and, on the considered evidence of many measurements, it appears probable also to the author that the inflexion in the experimental graphs takes place over a region rather than at a point.

In view of the calculated possibility—especially with large poisons or large reactants—of the occurrence of poisoning graphs showing appreciable curvature from the start, it has been considered of interest to re-examine, in the first instance, the poisoning graphs given by large poisons. The present paper deals with the poisoning of platinum catalysts by thiophen and by  $\beta$ -thionaphthol for the hydrogenation of crotonic acid, these new measurements being carried out under conditions of the greatest possible precision. With both of these poisons, no appreciable curvature in the first part of the graph could be detected, substantially linear graphs up to the inflexion region being obtained in conformity with earlier experimental results and with the above-mentioned theoretical type of Herington and Rideal.

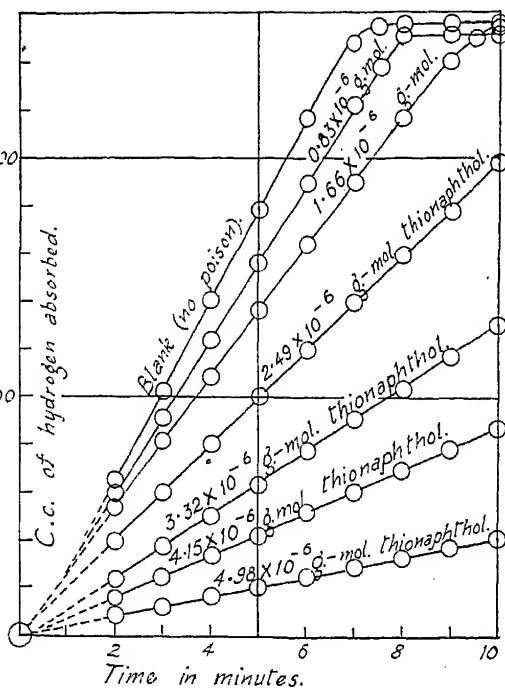


FIG. 1.

### Experimental.

The measurements of the activity of the catalyst at various stages of poisoning were made in a hydrogenation shaker at  $27^{\circ}$ . The charge consisted of 0.075 g. of stock platinum catalyst, 5 c.c. of 2N-crotonic acid in acetic acid solution and a further 5 c.c. of solvent, containing a known weight of the poison and made up of 3 c.c. of acetic acid and 2 c.c. of water. This inclusion of some water in the standard charge had been adopted in earlier work to permit the examination also of water-soluble poisons and was continued in the present measurements although the poisons were soluble in acetic acid.

In order to obtain accurate figures for the activity of the catalyst, it is necessary not only to adopt carefully controlled conditions of shaking but also to employ a catalyst which is affected as little as possible by

complications such as coagulation and which consequently maintains a constant activity throughout a run. Two stocks of platinum possessing these necessary properties were available. The first of these (Platinum I) consisted of an unsupported formate-reduced platinum which had previously been graded to a medium and approximately uniform grain size by the fractional sedimentation of its water suspension. This was considered to be the best available catalyst; and it was accordingly used for the poisoning work with thionaphthol, which is the larger of the two poisons examined and which would consequently be more likely to lead to a curved poisoning graph. This platinum gave almost pure zero-order hydrogenation runs. The second catalyst (Platinum II) was made by reducing, with hydrogen, kieselguhr-supported platinum chloride in glycerine suspension, followed by thorough washing with water. This supported catalyst contained about 20 per cent. of platinum.

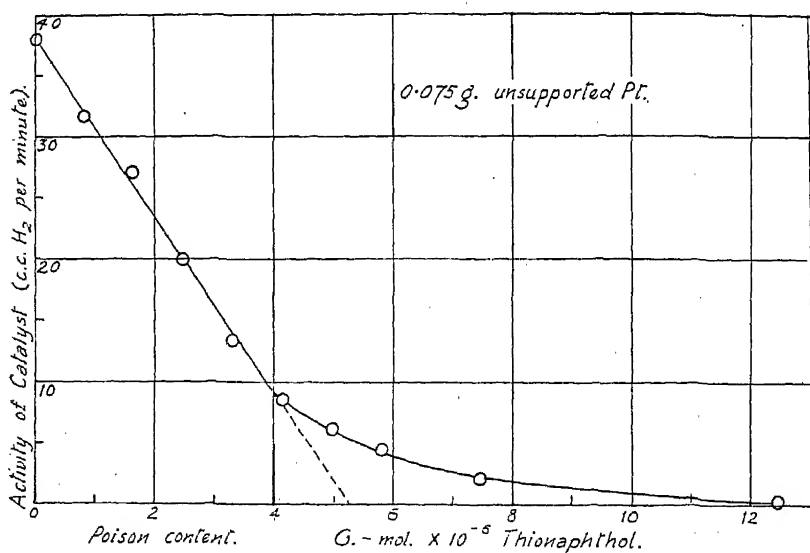


FIG. 2.

**Poisoning with  $\beta$ -Thionaphthol.**—Some hydrogenation runs with this poison, in the presence of 0.075 g. of Platinum I, are given in Fig. 1 in order to show the close conformity to a zero-order reaction course. Uniform shaking conditions, including the necessary preliminary dispersion of the finely divided catalyst, were usually established after about a minute from the time of switching on the shaking motor; and the hydrogenation rate then remained steady. From the slope of these lines for various concentrations of the poison, the corresponding activity of the catalyst can be obtained in the usual way. Fig. 2 is the graph derived by plotting these activities against the amount of poison present.

**Poisoning with Thiophen.**—The course of the hydrogenation runs with the catalyst (Platinum II) used for this poison was nearly of zero order but not so uniformly linear as in the runs with Platinum I (see Fig. 1); and, in order to obtain an accurate figure for the activity of the catalyst, it was necessary in the hydrogenation runs to correct for a small amount of curvature by differentiation for the rate of absorption of hydrogen at zero time, this rate being taken as representing the activity of the catalyst in the presence of the amount of poison contained in the charge. The

result of plotting these activities against the corresponding poison content is given in Fig. 3.

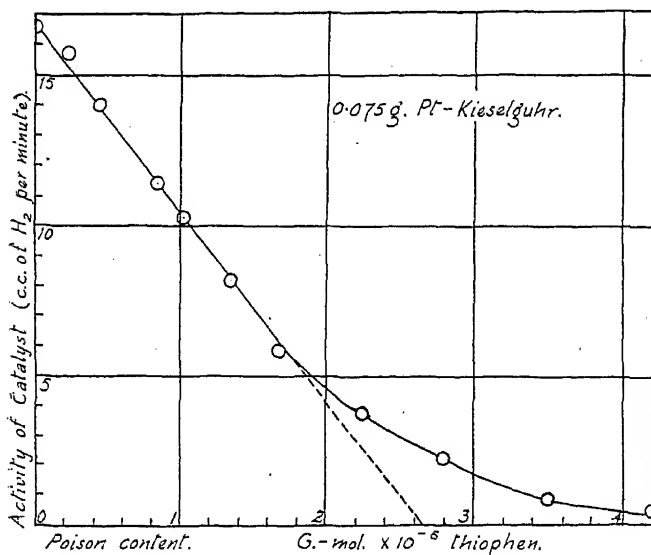


FIG. 3.

### Discussion.

The above work appears to confirm earlier results that, even with large poisons, the form of poisoning graphs in catalytic hydrogenation is sufficiently linear up to the region of inflexion to make practicable the comparison of the toxicities of different poisons by the use of a simple relationship of the type:  $k_c = k_0(1 - \alpha c)$ , in which  $k_0$  is the unpoisoned activity of the catalyst,  $k_c$  is its activity in the presence of a concentration,  $c$ , of the poison, and  $\alpha$  is the poisoning coefficient<sup>3</sup> (which is a measure of the toxicity).

This type of curve agrees well, as has already been mentioned, with one of the forms of poisoning graphs derived theoretically in Herington and Rideal's calculations for polypoint adsorption. In amplification of the treatment by these authors, it may perhaps be added that the adsorption of a large molecule, containing both an inherently toxic element, such as sulphur, and a non-toxic residue, must in all probability be treated as a special case of adsorption by virtue of the relatively long adsorbed life of the sulphur atom compared with that of the normally non-toxic remainder of the molecule. Thus, in the adsorption of, for instance, a long-chain sulphide or thiol, the molecule will be attached, as far as long-life adsorption is concerned, only by the sulphur head, the remainder of the molecule—save that it is maintained by its sulphur anchor within a close range of the surface—having a series of short adsorbed periods, separated by re-evaporation, during the relatively long adsorbed life of its anchor atom. This enforced propinquity of the molecule as a whole to the surface will cause its non-toxic portion to act obstructively to some extent<sup>4</sup> both during its periods of actual occupation of surface and, even during its non-adsorbed periods, by collision effects with impinging

<sup>3</sup> Maxted and Stone, *J. Chem. Soc.*, 1934, 26, 672.

<sup>4</sup> Maxted and Evans, *ibid.*, 1937, 603, 1004.

molecules of the reactants. Similar considerations will apply to thionaphthol and to thiophen.

Finally, as has also been mentioned by Herington and Rideal, a static survey of what sets of sites, containing sufficient adjacent adsorbing elements for the accommodation of large molecules, remain available, should contain a correction for the continuous change of occupation of individual sites, by evaporation and re-adsorption, even in the case of poisons.

### Summary.

The form of poisoning graphs, particularly for large poisons, in catalytic hydrogenation with platinum has been re-examined. No appreciable curvature in the first part of the graph, prior to the region of inflexion, could be detected with  $\beta$ -thionaphthol; and a similar poisoning graph was given by thiophen. The observed form corresponds with a type of poisoning graph recently deduced theoretically by Herington and Rideal.

*Department of Chemistry,  
University of Bristol.*

## THE DYEING OF CELLULOSE WITH DIRECT DYES. PART I. A REVIEW OF THE LITERATURE.

BY H. ALAN STANDING.

*(The British Cotton Industry Research Association.)*

### 1. Introduction.

The synthesis of Congo Red in 1884 led to the development of a class of dyestuffs directly substantive to cotton, which became known as the "Direct Cotton Dyestuffs"; these dyes were mainly the sodium salts of the sulphonic and carboxylic acids of disazo and polyazo compounds. Although the processes that occur in the dyeing of cotton and regenerated cellulose with these dyes have been extensively investigated since their discovery, it is only since 1933 that the investigations have been placed on a sound experimental basis. Prior to this time the investigations<sup>16, 22</sup> were almost exclusively concerned with the cause of the substantivity of these dyes on cotton, and led to a number of theories<sup>22, 23</sup> on which no general agreement was reached. The early investigations on the colloidal properties of dye solutions<sup>16, 118, 119</sup> proved more fruitful, and showed that the dye anions existed in solution as ionic micelles.

Although the necessity of working with pure dyes was appreciated by the early investigators, the methods of dye purification employed were by no means satisfactory, and it was not until 1931 that a relatively quick yet satisfactory method was developed by Robinson and Mills.<sup>20</sup> This had immediate repercussions on the progress of experimental work, and in 1933 Boulton, Delph, Fothergill and Morton<sup>8</sup> and independently Neale and Stringfellow<sup>59, 60</sup> published papers that may be regarded as the foundations of later work. Using pure dyes they investigated the kinetics of dye absorption by viscose sheet and yarn from dyebaths of known dye and salt concentrations. The use of viscose, especially in sheet form, instead of cotton, proved an experimental advance, since from the known dimensions of the sheet, the experimental results could be interpreted mathematically. Moreover these workers employed a length of liquor sufficiently great to ensure that the dye concentration remained practically constant during the absorption of the dye by the viscose. Such experimental conditions, although widely different from dyeing practice, gave experimental results capable of direct interpretation.

These results showed that the mass of dye absorbed per unit mass of cellulose increased with the time of dyeing and finally attained a limiting value although the dyebath was not exhausted. The limiting mass of dye absorbed per 100 grams of cellulose was termed the equilibrium absorption value. Photomicrographs<sup>5, 110</sup> of cross-sections of dyed yarns and the estimation of the absorbed dye in different portions of the dyed sheet<sup>60</sup> showed that when equilibrium was attained the dye was distributed uniformly throughout the material and not merely absorbed on its outer surface. For a fixed dye and salt concentration, the equilibrium absorption was found to be practically the same for different viscose yarns although the rate at which equilibrium was attained varied considerably from yarn to yarn. This clear distinction between equilibrium dyeing and the rate of attainment of equilibrium laid the foundations for future investigations which were directed along these two lines. Moreover it elucidated many of the earlier experimental results where the dye absorption corresponding to an arbitrary period of time had been measured with the result that equilibrium dyeing was not consistently attained. In this respect it is important to observe that in some of the work published since 1933 arbitrary periods of dyeing corresponding to technical practice have been purposely adopted, and the experimental data obtained from such experiments must therefore be interpreted in the light of dyeing kinetics rather than equilibrium dyeing.

## 2. The Purification of Direct Dyes.

Since the properties of aqueous dye solutions depend on the nature and concentration of any inorganic electrolyte present, it is essential to obtain the pure dye free from the inorganic electrolytes and coloured by-products that are present in the commercial dyestuff. Various methods of dye purification have been employed, but few prove to be both satisfactory and of general application. Thus it has been claimed that some dyes can be obtained pure by recrystallisation<sup>65, 70</sup> from the commercial sample with a water-alcohol mixture, but this method fails completely for many dyes.<sup>80</sup> The extraction of the dye from the commercial sample with organic solvents<sup>65, 101</sup> has been used, but again the method is of limited scope and may fail to separate the dye from any coloured by-products. Although dialysis methods<sup>65, 94</sup> are of general application, they are slow even when electrodialysis<sup>72</sup> or ultra-filtration<sup>69</sup> under pressure is used, and moreover suffer from the inherent disadvantage that the dye acid is formed by membrane hydrolysis.<sup>70</sup>

Precipitation methods depend upon obtaining the dye in an insoluble form which can then be washed free from inorganic electrolytes. The precipitation of the dye as the insoluble dye acid<sup>65</sup> has been used, but the dye acid is peptised by prolonged washing. Rose<sup>85</sup> has developed a successful method of precipitating the dye with an aryl guanidine hydrochloride; the insoluble organic salt so formed can be washed free from inorganic electrolytes and then dissolved in alcohol, whence the sodium salt of the dye can be precipitated by the addition of sodium methoxide. This method is claimed to free the dye from coloured by-products as well as from inorganic electrolytes.

Salting out methods depend on leaving the inorganic electrolytes in solution by the repeated salting out of the dye with a salt that can be subsequently extracted from the dye. Harrison<sup>27, 3</sup> repeatedly salted out the dye from aqueous solution with ammonium carbonate, which was subsequently removed from the dye by volatilisation; this method, however, gives a mixture<sup>80</sup> of the sodium and ammonium salts of the dye. Robinson and Mills<sup>80</sup> employed sodium acetate, and repeatedly salted out the dye from solution until the filtrate was free from chloride or sulphate. The sodium acetate remaining in the dye was then extracted with hot



alcohol, and some dyes could be finally crystallised out from a water-alcohol mixture. This method has proved not only successful but of wide application, and has consequently been extensively used. Ostwald <sup>62</sup> has criticised it on the grounds that the colloidal properties of the dye are altered by the alkalinity of the sodium acetate solution, but Robinson <sup>78</sup> has found no grounds for this criticism.

A criterion whereby the purity of the sample of purified dye can be established is highly desirable, but unfortunately, as Neale <sup>64</sup> has pointed out, the final decision whether a particular sample is sufficiently pure for a particular research problem is still a matter of subjective judgment based on the results of various tests. The direct estimation of the purified dye with titanous chloride has been used with varying degrees <sup>6, 64</sup> of success with different dyes. Estimation of the sodium content of the dye may reveal the presence of inorganic electrolytes, but like the previous method is useless for the detection of any coloured by-products that may be present in the purified sample. Such by-products can best be detected by means of the absorption spectra of the aqueous dye solutions although chromatographic analysis <sup>64</sup> by means of an alumina column has also been used. If these by-products differ considerably from the main dye in their substantivity on cotton, the absorption spectrum of an almost exhausted dye bath <sup>56</sup> will differ from that of a dye bath that has not been exhausted but is of the same dye and salt concentration as the exhausted dye bath. It is of interest to observe that within recent years the absorption spectra of the aqueous solutions of several purified direct dyes have been recorded in the literature.<sup>37, 39, 64</sup>

The hygroscopicity <sup>8</sup> of direct dyes necessitates careful and prolonged drying. Neale and Hanson <sup>57</sup> have observed that Benzopurpurin 4B when dried in an air oven at 110° C. for twenty-four hours still retains 1.6 per cent. of moisture, although Robinson <sup>81</sup> claims that air-oven drying is successful providing the dye is spread out in thin layers. Drying *in vacuo* over phosphorus pentoxide appears to be the safest procedure, however, and after drying phosphorus pentoxide and not calcium chloride <sup>82</sup> should be used in the desiccator.

### 3. The Properties of Aqueous Solutions of Direct Dyes.

Several workers have suggested that the properties of aqueous dye solutions are not reproducible. Thus Ostwald <sup>66</sup> and Hatschek <sup>30</sup> claimed that the viscosity of aqueous Benzopurpurin 4B solutions depended on their age and method of preparation, but Robinson and Mills,<sup>80</sup> having purified the dye by the sodium acetate method, found no evidence of such changes. They suggested that the results of previous workers were due either to the presence of inorganic electrolytes or to the dye solutions being supersaturated, and the extensive investigations made since 1931 have shown that, with few exceptions, the properties of aqueous dye solutions are reproducible providing the dyes are free from inorganic electrolytes.

Donnan and Harris <sup>15</sup> observed that whereas the electrical conductance of Congo Red solutions showed the dye to be a strong electrolyte, the osmotic pressure corresponded to an undissociated solute. This characteristic is shared by soaps, and McBain <sup>48</sup> has shown that the apparent anomaly can be qualitatively explained on the assumption that the anions are aggregated in solution, forming ionic micelles. The existence of such ionic micelles is now generally accepted, and such substances are known as colloidal electrolytes.<sup>98</sup>

Although the electrical conductance of dye solutions has been extensively investigated,<sup>108</sup> the work of Robinson and his collaborators <sup>51, 79, 80, 82</sup> has yielded most information about the constitution of these anionic micelles. They observed distinct maxima in the  $\Delta - \sqrt{C}$  curves for Congo Red and *meta*-Benzopurpurin 4B solutions at concentrations in the neighbourhood of  $2 \times 10^{-4}$  N., thus providing strong evidence of the

existence of ionic micelles whose degree of aggregation varies with the dye concentration. Transport number measurements<sup>51, 51</sup> showed that a small fraction of sodium ions, again varying with the dye concentration, was present in the anionic micelles, but the calculation of the average number of anions per micelle and the fraction of included sodium ions was necessarily only approximate owing to the unknown magnitude of the interionic forces. Robinson and Garrett conclude that in pure solution, the aggregation numbers of Congo Red and Benzopurpurin 4B are small, being about 2, while Bordeaux Extra exists in almost true solution. Osmotic pressure measurements made by Robinson and Selby<sup>52</sup> with these dyes lead to similar conclusions.

The determination of the degree of aggregation of the anionic micelles in dye solutions free from inorganic electrolytes is extremely difficult, and conductance and transport number measurements, although only approximate, are the most fruitful methods available. Kortüm<sup>57</sup> has shown that the deviations from Beer's Law of dye solutions about  $10^{-5}$  M. provide evidence of aggregation, but no values for the degree of aggregation can be deduced from the experimental data. Morton<sup>52</sup> has attempted to compare the degree of aggregation of several dyes in the absence and presence of sodium chloride by ultra filtration through viscose sheet, but the interpretation of the results is complicated both by electrokinetic effects<sup>107</sup> and by the absorption of the dyes on the membrane.

The size of the ionic micelles in solutions containing inorganic electrolytes is of special interest and early theories<sup>2, 24, 92</sup> attributed the efficacy of an addition of salt to the dyebath to the establishment of a particle size suitable for the dyeing process. Whereas the particle size<sup>20</sup> of the micelles in salt-free dye solutions cannot be determined from diffusion measurements, the Stokes-Einstein equation can be directly applied to the diffusion coefficient of the dye in the presence of a uniform and excess concentration of inorganic electrolyte. The application of the Stokes-Einstein equation assumes that the micelles are spherical, whereas the evidence of streaming double refraction<sup>117</sup> shows the micelles to be anisotropic; Herzog and Kudar<sup>32</sup> have shown, however, that the assumption of spherical particles involves appreciable errors only where the anisotropy is extreme.

Aqueous diffusion measurements<sup>40, 41, 43, 78, 107</sup> have shown that in the presence of inorganic electrolytes the degree of aggregation of the micelles varies from dye to dye and for most dyes increases with the electrolyte concentration. Increasing temperature<sup>107, 108</sup> invariably decreases the degree of aggregation, and at 90° to 100° C. most dyes are only slightly aggregated unless the concentration of the electrolyte is high. Thus, according to Valko,<sup>108</sup> the degree of aggregation of Sky Blue FF at 90° C. at a concentration of 0.2 g. per litre, can attain a value of 29 when the NaCl concentration is 2 N. although for NaCl concentrations less than 0.5 N. the aggregation is only of the order of 2. Lehner and Smith<sup>43</sup> claim that in the presence of inorganic electrolytes the degree of aggregation of Chlorazol Fast Red K (Colour Index 278) depends upon the age of the solution, but similar changes for other dyes have not been observed.

The effect of levelling agents on the degree of aggregation of aqueous dye solutions has been investigated by several workers. Many levelling agents are cationic or anionic active substances and they might therefore be expected to function as inorganic electrolytes and increase the particle size of the dye micelles. Valko<sup>108</sup> has observed that at 25° C. the aqueous diffusion coefficient of Sky Blue FF at a concentration of 0.2 g. per litre dye and 0.05 M. NaCl is reduced tenfold on the addition of 1 g. per litre Peregál OK, a cationic active substance. This corresponds to a thousand-fold increase in the aggregation of the dye micelles and Valko therefore concludes that Peregál OK possesses a strong affinity for the dye. Peregál O, which is non-ionic, gave at suitable concentrations a fourfold

reduction in the aqueous diffusion coefficient while the anionic active agents investigated, Igepon T, Nekals A and BX, only slightly reduced the aqueous diffusion of the dye. Valko concludes that levelling agents fall into two classes; those with affinity for the dye and those with affinity for the fibre. Weltzien and Froitzheim<sup>110</sup> have made similar observations with Sky Blue FF while Smith<sup>97</sup> working with Benzopurpurin 4B in the presence of lauryl sodium sulphate found only a small decrease in the aqueous diffusion coefficient of the dye on the addition of this levelling agent. Neale and Stringfellow<sup>64</sup> have observed that the absorption spectrum of Sky Blue FF is unaltered by the addition of  $\beta$ -naphthol, which is sometimes used as a levelling agent for direct dyes; this suggests that  $\beta$ -naphthol has no affinity for the dye.

Morton<sup>62</sup> has suggested that the dye micelles are not of uniform size but are polydisperse, existing in dynamical equilibrium, and has stressed the importance of such considerations when correlating the observed particle size with the rate of dye absorption by cellulosic materials. Unfortunately there is little direct evidence of the polydispersity of dye solutions, although it might be readily obtained by means of the ultra-centrifuge. Quesnel<sup>75</sup> has concluded by such measurements that Congo Red solutions of concentration 0.1 g. per litre dye and 0.1 M. in NaCl are monodisperse, the micelles being of uniform size corresponding to a molecular weight of 8000 to 9000. If dye solutions are polydisperse, the values of the micellar radius obtained from the Stokes-Einstein equation are mean values, but probably not number averages.

Little is known about the intermolecular forces responsible for micelle formation, but as Valko<sup>107</sup> has suggested, it is probable that the same intermolecular forces are responsible for both the aggregation of the dye anions and their adsorption on cellulose. Lehner and Smith<sup>42</sup> conclude from aqueous diffusion measurements that the extent to which a dye is aggregated by inorganic electrolytes is related to its chemical structure. Robinson and Mills<sup>80</sup> have observed that divalent cations are more effective than univalent cations in the flocculation of Benzopurpurin 4B, and trivalent cations are most effective. They suggest that although salting out plays a part in the flocculation of the dye, the flocculation is similar to that of lyophobic colloids. On the other hand, Ostwald claims that the solubility of Benzopurpurin 4B not only depends on the amount of solute present but that the first addition of inorganic electrolyte can increase the solubility of the dye. Thus for  $\text{Na}_2\text{SO}_4$  he observes a maximum solubility at a concentration of 0.001 M.  $\text{Na}_2\text{SO}_4$ . Robinson<sup>77</sup> however, finds no evidence of this, and questions<sup>78</sup> the purity of the dye used by Ostwald.

Many chemical methods<sup>101</sup> of estimating aqueous dye solutions have been used, but they are generally laborious and not entirely satisfactory, and colorimetric methods using either a visual colorimeter<sup>60, 107</sup> or for greater accuracy a photoelectric spectrophotometer<sup>37, 64</sup> have been generally adopted. For many dyes in aqueous solution Beer's Law is practically valid over a limited range of concentration. When inorganic electrolytes are present in the aqueous dye solutions it is necessary to compare the standards and unknown both containing the same electrolyte at the same concentration.

#### 4. The Equilibrium Absorption of Direct Dyes by Cellulose.

It has previously been mentioned that when a given mass of cellulose is immersed in a dyebath, the mass of dye absorbed by the cellulose increases with time and finally attains a limiting value known as the equilibrium absorption, and expressed as grams of dye absorbed per 100 g. of cellulose. Equilibrium dyeing is reversible<sup>8, 55</sup> and does not show the hysteresis effects found for the absorption and desorption of water vapour by cellulose. For a particular sample of cellulose the equilibrium absorp-

tion depends only on the following factors when equilibrium dyeing is attained, namely, the dye concentration, the salt concentration, and the temperature. The dependence of the equilibrium absorption on each of these factors individually when the other two are maintained constant has been fairly extensively investigated, although much of the work is confined to viscose sheet.

**The Estimation of Absorbed Dye.**—Although the mass of dye absorbed by cellulose has been estimated directly with titanous chloride,<sup>54, 115</sup> the method is laborious and requires a dye absorption of about 0.1 g. Since in much of the experimental work the mass of absorbed dye is of the order of milligrams, the methods of estimation that have been adopted all resort to colorimetric estimations either of the dye in solution or of the dyed fabric. They are :—

- (1) The determination of the decrease in the dyebath concentration.<sup>42, 111</sup>
- (2) The extraction of the adsorbed dye from the cellulose with a suitable solvent and the subsequent estimation of the dissolved dye.<sup>8, 60</sup>
- (3) The measurement of the reflection coefficient of the dyed fabric.<sup>42</sup>

Although the first method is the most straightforward, it is subject to large errors if the dyebath is only slightly exhausted. It is convenient in much of the experimental work to choose the liquor/yarn ratio so that the dyebath concentration at equilibrium dyeing differs by only 1 to 2 % from the initial dyebath concentration, and consequently the second method has been the most widely used. Water<sup>8</sup> and acetic acid<sup>104</sup> have been used as solvents for specific dyes, but aqueous pyridine<sup>8, 54, 76</sup> solutions (15 to 25 %) have proved to be of most general use providing the extraction is not carried out at high temperatures, when decomposition<sup>54, 55</sup> of the dye may occur. In both methods the dye in solution is estimated colorimetrically, and an accuracy of 1 to 2 % is claimed.<sup>55</sup> The third method<sup>42</sup> necessitates the use of a reflection spectrophotometer, and it is first necessary by means of either of the two previous methods to obtain a calibration curve relating the reflection coefficient of the dyed fabric at a definite wavelength to the concentration of absorbed dye. Lehner and Smith found that the plot of the logarithm of the reflection coefficient against the concentration of absorbed dye was approximately linear over a limited range of concentration. This method has not been widely used, and an accuracy of only 5 to 10 % is claimed.<sup>42</sup> Recently Neale and Stringfellow<sup>64</sup> have found that the absorption spectra of direct dyes in 25 % pyridine solutions are additive, and that it is therefore possible by means of the second method to estimate a mixture of two dyes absorbed on cotton.

**The Effect of Dye Concentration.**—When the salt concentration and the temperature are maintained constant, the equilibrium absorption increases with the dyebath concentration. Fig. 1 shows the isotherm obtained by Garvie and Neale<sup>20</sup> for the absorption of Sky Blue FF on viscose sheet at 90° C. in the presence of 5 g. per litre NaCl. At any one temperature, a series of absorption isotherms (relating the equilibrium absorption to the residual dyebath concentration) exists, each isotherm corresponding to a definite salt concentration. Very few such isotherms have been obtained since 1933, and these are mainly confined to Benzo-purpurin 4B<sup>8, 25</sup> and Sky Blue FF<sup>20</sup> on viscose sheet and cuprammonium yarn. Garvie and Neale<sup>20</sup> observed that the equilibrium absorption of Sky Blue FF on viscose sheet at 90° C. in the presence of 5 g. per litre sodium chloride was approximately proportional to the cube root of the residual dyebath concentration, thus showing that the isotherm can be represented by a Freundlich adsorption equation of the type

(Concentration of Absorbed Dye)

= constant (Residual Dyebath Concentration)<sup>n</sup>

where *n* is less than unity. This had been suggested by early investigators<sup>17</sup> but there are at present insufficient data to show whether this

type of equation is generally applicable to all such dye-absorption isotherms, and it is probable that deviations will be found for highly aggregated dyes.

In the absence of salt <sup>8, 25, 60, 94</sup> the equilibrium absorption of direct dyes on cotton and viscose sheet varies considerably from dye to dye, but for all dyes is considerably smaller than in the presence of salt. Neale and Stringfellow <sup>60</sup> have shown that in the absence of salt the equilibrium absorption of Sky Blue FF at 90° C. on viscose sheet can be accounted for by the dye present in the dye liquor imbibed by the sheet. This suggests that in the absence of salt this dye is not adsorbed by the cellulose at 90° C. Schramek and Götte <sup>94</sup> however, observed that other dyes (purified by dialysis) were fairly strongly adsorbed on cotton at room temperature in the absence of salt.

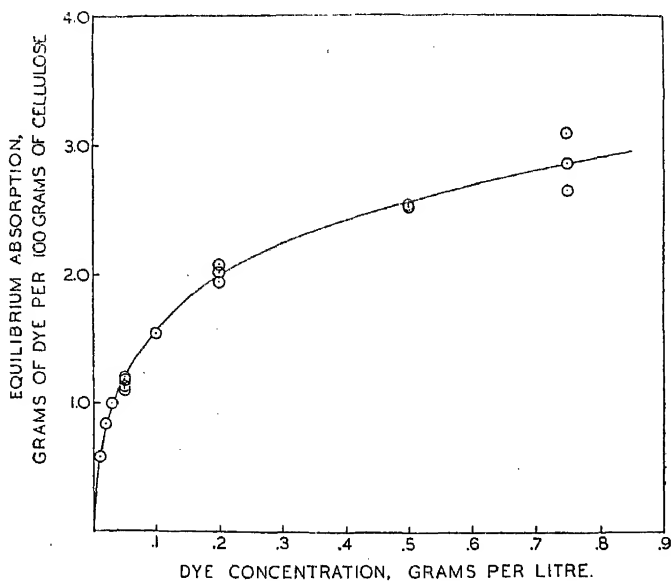


FIG. 1.—Variation of the equilibrium absorption of Sky Blue FF on viscose sheet at 90° C.

**The Effect of Temperature.**—Neale <sup>55</sup> has stressed the importance of ensuring that equilibrium dyeing is consistently attained in investigations of the temperature variation of the equilibrium absorption. This is important, since whereas equilibrium dyeing is generally attained within an hour at 90° C., it may take several days at 25° C. The observations <sup>111, 112</sup> of early workers that the amount of dye absorbed in a definite time passed through a maximum with increasing temperature simply arose from the fact that equilibrium dyeing was only attained at the higher temperatures. In general, when the salt and residual dye concentration are maintained constant, the equilibrium absorption of direct dyes on cellulose decreases with increasing temperature. <sup>8, 10</sup>

The temperature coefficient of the equilibrium absorption depends to a small extent on the dye, the cellulose, and the salt concentration. As a very rough generalisation, based on the observation of five dyes, Neale <sup>55</sup> estimates that the equilibrium absorption is halved for each 30° C. rise in temperature. Garvie, Griffiths and Neale <sup>10</sup> have found that the ratio of the equilibrium absorption of 0.05 g. per litre Fast Red K on viscose sheet at 25° C. to that at 90° C. is approximately independent of the

concentration of NaCl present providing it exceeds 2 g. per litre. On the other hand, the ratio of the equilibrium absorption of the dye on viscose sheet to that on cotton in the presence of 5 g. per litre NaCl decreases from 2.01 at 25° C. to 1.33 at 100° C. This may be related to the change in structure of cotton with increasing temperature suggested by Urquhart<sup>102</sup> to account for the absorption of water vapour by cotton over this temperature range. If this is so, care must be exercised in deducing the heat of dyeing from the temperature coefficient of the equilibrium absorption.

Although the general tendency is for the equilibrium absorption to decrease with increasing temperature Lehner and Smith<sup>41, 43</sup> have observed an exception for the sodium salt of *p*-sulpho-benzene-azobenzene-azo-6-benzoyl-*p*-aminobenzoylamino-1-naphthol-3-sulphonic acid, whose equilibrium absorption on cotton at 90° C. is higher than at 25° C. Aqueous diffusion measurements show that the average micellar radius in the dyebath at 25° C. is 18.8 Å. Lehner and Smith conclude from this and other evidence<sup>42, 43</sup> that the dyeing of cotton at 25° C. does not proceed readily if the radius of the dye micelles exceeds a limiting value, which they estimate as 18 Å. Similar suggestions have been made by Schäffer<sup>92</sup> and by Rose.<sup>84, 86</sup> Lehner and Smith stress, however, that if the average micellar radius exceeds this value, the determining factor is the polydispersity of the dye solution. If the dye solution is monodisperse, then the equilibrium absorption is relatively small, whereas if the solution is polydisperse with a dynamical equilibrium existing between the smaller and the larger micelles, the rate of dyeing may be retarded but it is still possible to obtain a high degree of exhaustion of the dyebath at equilibrium. As evidence of the latter case, Lehner and Smith state that a dyebath of Benzopurpurin, in which the average micellar radius is 36 Å. owing to the high concentration of NaCl present, is 95 per cent. exhausted by cotton at 50° C.

**The Effect of the Inorganic Electrolyte and its Concentration.**—The literature on the effect of the type and concentration of the inorganic electrolyte on the absorption of direct dyes by cotton and regenerated cellulose is extensive, but only the work of Boulton, Delph, Fothergill and Morton and that of Neale and his collaborators definitely applies to equilibrium dyeing. Other workers have generally investigated the problem from a more technical aspect by dyeing for an arbitrary period of time corresponding to that used in dyeing practice. Their results, although of direct technical importance, must therefore be interpreted in terms of the kinetics of dyeing.

In order to maintain both the temperature and the residual dyebath concentration constant throughout the investigations, it is necessary that the mass of dye absorbed by the cellulose shall be negligible compared with the total mass of dye present in the dyebath. By such means, Neale and his collaborators<sup>19, 25, 26, 60</sup> have determined the absorption isotherms (relating the equilibrium absorption to the concentration of sodium chloride present) for several dyes on cotton and regenerated cellulose. The equilibrium absorption increases with the concentration of NaCl present, but as is seen from Fig. 2, showing the absorption isotherms of 0.05 g. per litre Benzopurpurin 4B and Sky Blue FF at 90° C. on viscose sheet as obtained by Hanson and Neale,<sup>26</sup> the dependence of the equilibrium absorption on the NaCl concentration differs considerably from one dye to another. Such striking differences in the salt sensitivity of direct dyes are important in technical dyeing and Boulton and Reading<sup>4, 7</sup> and independently Neale<sup>65</sup> have tabulated equilibrium absorption data from which the relative salt sensitivities of many direct dyes may be judged. Since the relative absorption of direct dyes on cellulose dyed from a mixed dyebath differs considerably from the ratio of the equilibrium absorption of each dye on cellulose in the absence of a second dye, it does not follow, however, that such data can be directly applied to mixed dyebaths.

## 418 THE DYEING OF CELLULOSE WITH DIRECT DYES

The shape of the absorption isotherms relating the equilibrium absorption to the NaCl concentration when the dye concentration is maintained constant depends on the cellulose used. Thus the absorption isotherm<sup>26</sup> of 0.05 g. per litre Sky Blue FF on cotton at 90° C. can be represented by the Freundlich equation, whereas on viscose sheet and cuprammonium yarn the dye absorption isotherms are sigmoidal at the lower NaCl concentrations. Neale<sup>26, 61</sup> attributes the sigmoidal shape to the presence of carboxyl groups in the regenerated cellulose.

The early investigations of Wiktoroff<sup>115</sup> on the effect of equivalent concentrations of different electrolytes on the mass of dye absorbed by cotton in a definite time showed that the dye absorption increased with the valency of the cation of the inorganic electrolyte present. Although there is no evidence that equilibrium dyeing was attained in his experiments, later work has shown that this generalisation is true within certain

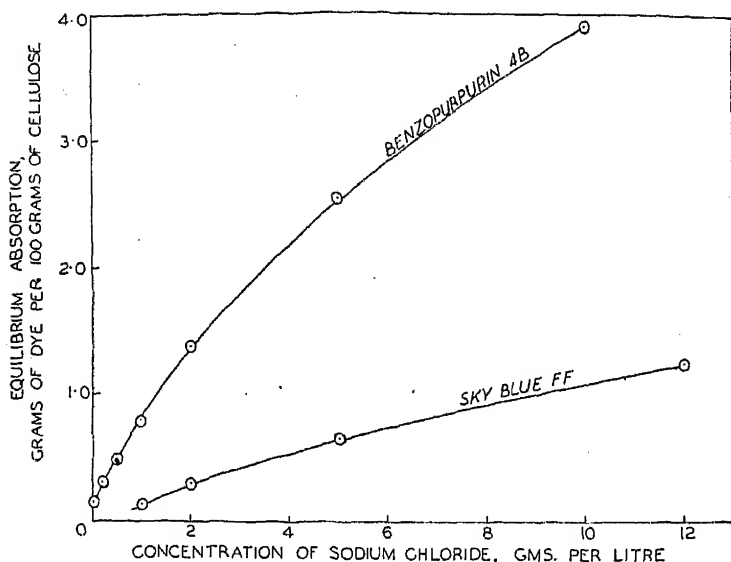
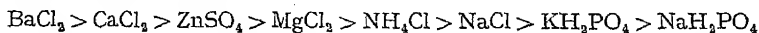


FIG. 2.—Variation of equilibrium absorption of Sky Blue FF and Benzopurpurin 4B on viscose sheet with the sodium chloride concentration. Dyebath concentration 0.05 gm. per litre dye. Temperature 101° C.

limits for equilibrium dyeing. Boulton, Delph, Fothergill and Morton<sup>8</sup> observed that for dyebaths of the same residual dye concentration and temperature the equilibrium absorption is approximately the same for equivalent concentrations of different inorganic electrolytes containing a univalent cation, while an equivalent concentration of an electrolyte with a divalent cation gave higher equilibrium absorption values. Neale and Patel<sup>68, 71</sup> have determined the absorption isotherms of Sky Blue FF and Benzopurpurin 4B on viscose sheet at 100° C. for a series of electrolytes. These absorption isotherms, relating the equilibrium absorption to the equivalent concentration of electrolyte present, intersect for concentrations higher than decinormal, showing that the relative effect of different electrolytes upon the equilibrium absorption depends on their concentration as well as the valency of their component ions. For electrolyte concentrations lower than decinormal, the equilibrium absorption of Sky Blue FF on viscose sheet decreases in the following order according to the electrolyte present :



Since the average micellar radius of many dyes increases with the concentration of inorganic electrolyte present, it might be expected that if a limiting micellar radius for direct dyeing exists, the equilibrium absorption would be found to pass through a maximum with increasing electrolyte concentration for a dye which is highly aggregated in solution and is monodisperse. Schramek and Götze,<sup>34</sup> Krotowa<sup>38</sup> and Lehner and Smith<sup>41</sup> have observed a maximum in the dye absorption by cotton at room temperature with increasing electrolyte concentration, but it is doubtful whether equilibrium dyeing was attained in their experiments. This fact is important since, as will be subsequently discussed, the rate of dyeing passes through a maximum with increasing concentration of inorganic electrolyte. Unfortunately apart from the absorption isotherm of Fast Red K<sup>19</sup> on viscose sheet at 25° C., which does not show a maximum, other work where equilibrium dyeing is definitely claimed is mainly confined to temperatures about 90° C. where the aggregation of the dye is considerably smaller than at room temperature. The work of Neale and Patel at 100° C. extends to decinormal electrolyte concentrations and shows no maximum although the dyes are most probably only slightly aggregated under such conditions. Later work by Neale and Stringfellow<sup>62</sup> at 90° C. shows that the equilibrium absorption of 1 g. per litre Sky Blue FF on cotton steadily increases as the sodium chloride concentration is increased from 50 to 100 g. and probably up to 200 g. per litre. Equilibrium is attained far more slowly when the salt concentration is 200 g. than when 100 g. per litre. Now Valko<sup>108</sup> has observed that the average micellar radius for 0.2 g. per litre Sky Blue FF at 90° C. increases with the concentration of sodium chloride present, being 18.9 Å. when the NaCl is 2 N. There can be little doubt, therefore, that the dye is considerably aggregated at the highest NaCl concentration, yet no evidence of a maximum is found although the rate of dyeing decreases considerably. These facts are not at variance with Lehner and Smith's contention of a maximum particle size above which dyeing does not readily occur, since it may be that Sky Blue FF solutions are polydisperse. It would appear, however, from the limited experimental evidence at present available that, for most dyes, the equilibrium absorption still increases steadily as the aggregation of the dye increases. For a complete elucidation of this problem, measurements of the polydispersity of dye solutions by means of the ultracentrifuge together with dye absorption measurements appear to be essential.

The absorption of direct dyes on cellulose from a mixed dyebath cannot be predicted from the equilibrium absorption of each of the dyes in the absence of the other. Boulton, Delph, Fothergill and Morton<sup>8</sup> have observed that from a mixed dyebath the absorption of each dye on the cellulose is less than it would be in the absence of the other dye. Neale and Stringfellow<sup>64</sup> have not only confirmed this observation, but have found that from a mixed dyebath the relative absorption of two dyes on cotton differs considerably from the ratio of the equilibrium absorptions of the two dyes. Thus for a mixture of Chlorazol Sky Blue FF and Chrysophenine G, the concentrations of absorbed dye on cotton at 90° C. are 0.062 and 0.288 g. per 100 g. of cotton, respectively, whereas the corresponding absorptions of the dyes when only one dye is present in the dyebath are 0.47 and 0.302. They also observed that the absorption spectra of direct dyes in aqueous solution are not additive, and that those pairs of dyes showing the greatest deviations in this respect also show the most anomalous absorptions in dyeing from mixed dyebaths. The effect of temperature on the relative absorptions of these two dyes from a mixed dyebath is also anomalous; whereas the amount of Chrysophenine absorbed by the cotton decreases with increasing temperature as would be expected, the amount of Sky Blue FF absorbed increases slightly with increasing temperature. From these facts Neale and Stringfellow conclude that the relative absorption of two dyes by cotton from a mixed



dyebath cannot be explained solely on the basis of the competition between the dyes for the cellulose, and they suggest that mutual interaction between the dyes in solution, as indicated by the absorption spectra, is responsible for the anomalous results. Neale and Stringfellow<sup>63</sup> have also investigated the absorption of Sky Blue FF on cotton previously dyed with a vat dye Cibacron Yellow R. They found that from a dye bath of 0.05 g. per litre Sky Blue and 5 g. per litre NaCl at 90° C., the absorption of the direct dye on the cotton increased with the percentage of Cibacron Yellow R present. When the cotton yarn contained 4 % of the vat dye, the absorption of the Sky Blue on the cotton corresponded to that obtained on the untreated yarn for a sodium chloride concentration of the order of 100 g. per litre. This greatly increased absorption was found to be due to the absorption of Sky Blue FF on the vat dye itself.

**The Equilibrium Absorption of Cotton and Regenerated Cellulose.**—The equilibrium absorption of direct dyes depends to a certain extent on the cellulose used. Weltzien and Schultze<sup>111</sup> observed that the absorption of Brilliant Benzo Blue 6B and Oxamine Red 3B in the presence of

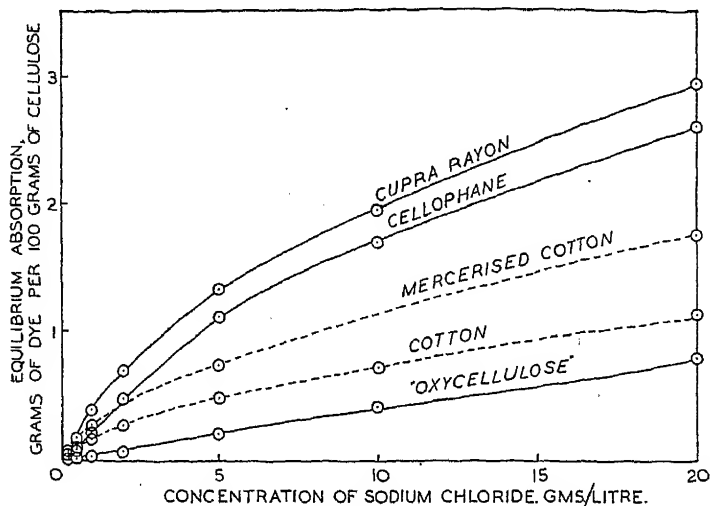


FIG. 3.—Variation of the equilibrium absorption with the sodium chloride concentration for Sky Blue FF on cotton and regenerated cellulose at 90° C.

sodium sulphate was greater on viscose and cuprammonium rayons than on cotton; in their experiments, however, equilibrium dyeing is not claimed. They also stress the importance of the ash content of the cellulose on the dye absorption, and Lehner and Smith<sup>41</sup> have found that the dye absorption on cotton increases slightly with the ash content. Photomicrographs<sup>95, 110</sup> of the cross sections of dyed regenerated cellulosic filaments indicate the presence of a skin that is dyed to a different extent from the interior of the filament.

Hanson, Neale and Stringfellow<sup>26</sup> have determined the absorption isotherms of Sky Blue FF on viscose rayon, cuprammonium rayon, cotton, and mercerised cotton as shown in Fig. 3. For NaCl concentrations greater than 2 g. per litre, the equilibrium absorption is greater on the regenerated cellulose than on the cotton. Mercerised cotton takes up more than does the unmercerised material, and the ratio of the equilibrium absorptions is approximately independent of the sodium chloride concentration, being of the same order as the ratio for water absorption. This suggests that the same groups in the cellulose are responsible for the absorption of both water and direct dyes.

Cotton which has undergone alkaline hypobromite oxidation shows a very much lower equilibrium absorption than does unoxidised cotton, and Neale and Stringfellow<sup>61, 62</sup> have shown that the equilibrium absorption steadily decreases as the carboxyl content of the cellulose is raised. For  $\text{Na}_2\text{SO}_4$  concentrations less than about 1.5 g. per litre the absorption isotherms for cotton and the regenerated celluloses shown in Fig. 3 intersect, the dye absorption on the cotton being then the greater. Hanson, Neale and Stringfellow<sup>26</sup> attribute this to the presence of carboxyl groups in the regenerated celluloses.

**Desorption of Direct Dyes.**—It is well known that direct dyes on cotton and regenerated cellulose are not fast to washing. Weltzien and Schultze<sup>111</sup> observed that when cotton and regenerated cellulose dyed with Oxamine Red 3B were washed in conductivity water at 70° C. for successive periods of twenty minutes, about 90 per cent. of the dye was removed after five washings. Similar measurements with Brilliant Benzo Blue 6B showed that this dye was washed out more slowly than Oxamine Red 3B. According to Leupin<sup>44</sup> when cotton dyed with a direct dye is repeatedly washed, the concentration of the dye in successive liquors decreases exponentially. The addition of salt to the wash liquor restrains "bleeding"; this is probably due to the dependence of equilibrium dyeing on the salt concentration. Lehner and Smith<sup>42</sup> conclude from measurements of the wash fastness of several dyes in the presence of sodium chloride that the wash fastness is related to the salt sensitivity of the dye. Smith<sup>97</sup> has found that aqueous solutions of anionic active agents, such as lauryl sodium sulphate have little more effect than water in removing dyes from cotton, while cationic agents such as cetyl pyridinium bromide greatly retard the bleeding of the dyed fabric.

## 5. Theories of Equilibrium Dyeing and Substantivity.

When equilibrium dyeing is attained, the concentration of dye is considerably greater in the water-swollen cellulose than in the external solution, showing that the intermolecular forces between the dye and the cellulose are greater than those between the dye and water. Although the exact nature of these intermolecular forces is not yet definitely established, there is no evidence for the formation of a covalent bond between the dye and the cellulose, and it is generally accepted that direct dyeing is an adsorption process<sup>10, 11</sup> occurring not only on the outer surface of the cellulosic yarn but also throughout the less ordered parts of the cellulose. The fact that the equilibrium absorption depends upon the salt concentration as well as the dye concentration clearly shows, however, that the adsorption process is more complex than those to which Langmuir's theory is applicable.

Early theories attributed the efficacy of additions of salt to the dye-bath to the establishment<sup>24</sup> of a particle size suitable for the dyeing process. As Valko<sup>107</sup> points out, however, it is more probable that the increase in the equilibrium absorption and in the aggregation of the dye micelles on the addition of salt are both due to a more fundamental physico-chemical process. Harrison<sup>21, 27</sup> observed that the negative zeta potential of cotton with respect to water is considerably reduced in the presence of inorganic electrolytes, and suggested that this negative zeta potential was responsible for the small absorption of direct dyes in the absence of inorganic electrolytes. Thus, according to Harrison, the efficacy of the addition of salt to the dye-bath lies in the elimination of the zeta potential, which he assumes would oppose the adsorption of the dye anions on the cotton. The theory is purely qualitative, and has received little attention until recently;<sup>87, 104</sup> it would appear necessary, however, to consider not only the zeta potential of the cellulose itself which is possibly due to carboxyl groups but also the zeta potential arising from the adsorption of the dye anions on the cellulose. Nevertheless, the theory was the

first attempt to explain the action of salt in terms of electrochemistry rather than in terms of the colloidal nature of the dye solutions, on which so much stress was laid in the early days.

Hanson, Neale and Stringfellow<sup>26</sup> have developed an electrochemical theory which correlates quantitatively the variation of the equilibrium absorption with the dye and salt concentrations. These workers postulate that the dye anions are first adsorbed by the cellulose and attract the sodium ions near them in order to preserve electroneutrality in the system. There is in consequence a greater concentration of sodium ions in the cellulose phase than in the dyebath, and the resulting concentration difference will tend to oppose the adsorption of the dye anions. The addition of NaCl tends to equalise the sodium ion concentration in the two phases, and thus facilitates the adsorption of the dye anions. Hanson, Neale and Stringfellow, by applying Donnan's theory of membrane equilibrium to the system, and by assuming that the concentration of dye anions adsorbed by the cellulose is directly proportional to the concentration of free dye anions in the cellulose phase, were able to correlate quantitatively the variation of the equilibrium absorption of Sky Blue FF on cotton at 90° C. with the concentration of dye and of sodium chloride in the dyebath. The theory also gave a qualitative explanation to the decrease in the equilibrium absorption as the carboxyl<sup>26, 62</sup> content of the cellulose increased.

On their assumption that the laws of membrane equilibria apply to the system, it follows that the concentrations of the ions of the inorganic electrolyte are different in the water and the cellulose phases and are governed by these laws. Usher and Wahbi<sup>104</sup> using viscose sheet investigated the distribution of ammonium and chloride ions between the water and the cellulose phases both in the absence and presence of direct dyes. These workers, however, differ from Hanson, Neale and Stringfellow in their definition of the cellulose phase, and calculate the ionic concentrations in the cellulose phase on the basis of the mass of water absorbed per 100 g. of viscose. On the other hand, Hanson, Neale and Stringfellow calculate the ionic concentrations in the cellulose phase on the basis of the mass of water adsorbed per 100 g. of cellulose from saturated water vapour, i.e. the bound water. This point is discussed at some length in later communications between Usher<sup>105</sup> and Neale.<sup>66</sup> Usher and Wahbi conclude that in the absence of dye, the distribution of the  $\text{NH}_4$  and Cl ions between the two phases obeys the Donnan membrane equilibrium when the concentration of the  $\text{NH}_4\text{Cl}$  in the water is 0.1 N., but not when 0.5 N. When dye was present, they found that in the cellulose phase the concentration of the  $\text{NH}_4$  ions was greater than that of the Cl ions, the difference increasing linearly with the concentration of absorbed dye. This observation confirms Neale's initial postulate that the dye anions are directly adsorbed by the cellulose. Usher and Wahbi conclude, however, that the effect of  $\text{NH}_4\text{Cl}$  on the dye absorption cannot be explained entirely on the basis of the Donnan membrane equilibrium and suggest that the  $\zeta$  potential of the cellulose also plays a part. There is little doubt from the results of both groups of workers that the dye anions are first adsorbed by the cellulose and that the function of salt does not lie in promoting the aggregation of the dye, but in establishing electrochemical conditions of the system such that adsorption of the dye anions is facilitated.

It is probable that these groups in the dye anion which are responsible for the adsorption of the dye on the cellulose are also responsible for the aggregation of the dye in solution and that substantivity is associated with, but not the result of, the colloidal properties of the dye. Lehner and Smith<sup>42</sup> have suggested that the tendency for direct dyes to aggregate in the presence of inorganic electrolytes provides a useful indication of the substantivity of the dyes on cellulose.

Although there is strong evidence that the dye anions are adsorbed by the cellulose, the nature of the bond between them is not yet definitely

established. The similarity in some respects between the absorption of water vapour and of direct dyes on cellulose and the fact that the absorption of direct dyes is considerably reduced when the cellulose is acetylated strongly suggests that the adsorption occurs on the hydroxyl groups of the cellulose. It is probable that the adsorption is due to a hydrogen bond formation<sup>10, 108</sup> between these hydroxyl groups and such groups as amino, hydroxy or ethoxy in the dye. From the temperature coefficient of the equilibrium absorption of Fast Red K on viscose sheet, Meyer<sup>50</sup> estimates the heat of dyeing to be 5 k.cal. per mole, a value of the same order as given by Pauling<sup>73</sup> for hydrogen bond formation. As Meyer points out, however, it is possible that a dye molecule is bound to the cellulose by more than one hydrogen bond. In this respect it is interesting to observe that Boulton and Morton<sup>5</sup> conclude from the dichroism<sup>74</sup> of cellulosic yarn and sheet when dyed with direct dyes that the adsorbed dye molecules are parallel to the cellulose chains. The observation of Krüger and Rudow<sup>30</sup> that the absorption spectra of dyed viscose sheet shows a displacement of the maxima compared with those of the aqueous dye solutions may be due to a bond formation between the dye and the cellulose. Since the absorption spectra of dye solutions depend, however, upon the degree of aggregation of the dye micelles, the change in the absorption spectra of the adsorbed dye cannot be taken as conclusive evidence of a cellulose dye complex.<sup>34, 35</sup>

Many attempts have been made<sup>88, 89, 91, 96</sup> to correlate the substantivity of direct dyes with their chemical structure. As a measure of substantivity Griffiths and Neale<sup>14</sup> have taken the equilibrium absorption of the dye on viscose sheet at 90° C. from a dyebath of 0.05 g. per litre dye and 5 g. per litre NaCl. On the other hand, Ruggli<sup>88</sup> considers the amount of absorbed dye remaining on cotton after immersing the skein in water to give a measure of the substantivity. These investigations have shown that the relation between chemical structure and substantivity is complex, depending both on the nature and position of the substituent groups. Ruggli and Lang<sup>90</sup> conclude from absorption measurements with cis and trans dyes that a straight molecule does not necessarily confer a greater substantivity. According to Schirm<sup>93</sup> the existence of a conjugated double bond is an essential criterion for substantivity. If dye adsorption is due to hydrogen bond formation, it is to be expected that the relation between the chemical structure and the substantivity of the dye will be complex and extremely sensitive to the position of the substituent groups.

The equilibrium absorption of a direct dye on cellulose will depend not only on the affinity of the dye for the cellulose but also on the number of active centres on the cellulose (probably the hydroxyl groups) accessible to the dye anions or micelles. The structure of cellulose<sup>14</sup> in relation to direct dyeing<sup>52, 6</sup> has been reviewed in some detail in the literature and consequently will be only briefly discussed here. In viscose rayon the cellulose chains tend to lie with their long axes in the spinning direction and, as is shown by X-ray analysis, in some regions attain a regular crystalline arrangement. It is generally accepted that the inter-crystalline regions,<sup>46</sup> which behave as amorphous matter to X-rays, consists of cellulose chains common to the crystalline regions, but considerably more randomly oriented than in those regions. Permeability measurements with viscose sheet indicate that in the dry state both the crystalline and intercrystalline regions are impervious to air,<sup>100</sup> but that in the water-swollen state the sheet is permeable to fairly large molecules such as those of direct dyes. X-ray analysis shows that in the swollen state the water molecules do not penetrate the crystalline regions, and the dye anions and micelles must therefore be confined to the intercrystalline regions. These regions consist of a relatively open three-dimensional network of cellulose chains more or less oriented along the spinning direction, and recent work<sup>18</sup> on the impregnation of cellulosic fibres with heavy metals suggests that fairly large

cavities (of the order of 100 Å.) are also present in these regions. The equilibrium absorption of direct dyes on cellulose will depend on the relative amount of the intercrystalline regions present, and to a less extent on the openness of these regions. From the equilibrium absorption of Sky Blue FF on viscose sheet, Neale and Stringfellow<sup>62</sup> estimate the area of the available adsorbing surface of the cellulose to be  $1.5 \times 10^6$  sq. cm. per g.

The openness of the intercrystalline regions has probably a far more pronounced effect on the rate of dyeing than on the equilibrium absorption. The spaces between the cellulose chains in these regions will be tortuous and irregular and will possess no well defined boundaries. Some workers have considered these spaces as approximating to capillaries, and from permeability measurements<sup>49, 52</sup> estimate the mean capillary radius for water-swollen viscose sheet to be 20 to 30 Å. Although this value cannot be taken too rigidly, it indicates that the spaces are small, and that the larger dye micelles will be considerably restricted if not prevented from entering parts of the intercrystalline region. Consequently, for a highly aggregated but polydisperse dye solution, only a small fraction of the dye micelles will probably be able to penetrate the intercrystalline regions where adsorption will occur, and at any instant the effective concentration of dye micelles which can be adsorbed by the cellulose will be less than that of the dyebath. It has previously been mentioned, however, that if a dynamical equilibrium exists between the smaller and the larger micelles, then the equilibrium absorption may still be relatively high even though many of the dye micelles are considerably aggregated, and the limited evidence at present available suggests that this is so for many direct dyes.

## 6. The Kinetics of the Dyeing Process.

Equilibrium is seldom attained in the technical dyeing of cellulosic materials with direct dyes, and consequently the mass of dye absorbed in a given time depends upon the rate of dyeing as well as the affinity of the dye for the cellulose. The early work on viscose dyeing<sup>116</sup> showed that a far more level dyeing was obtained with some dyes than with others, and subsequent investigation showed that, in general, the levelness and the rate of dyeing were related; <sup>7, 12</sup> those dyes that attain equilibrium on viscose most rapidly giving the most level dyeings.

It is therefore desirable from the technical standpoint to classify the direct cotton dyestuffs according to their dyeing speeds. Fig. 4 represents the dyeing of viscose yarn with Sky Blue FF at 90° C.; the absorption of the dye by the viscose, expressed as percentage exhaustion of the dyebath is plotted against the time of dyeing on a semi-logarithmic scale. The rate of dyeing if expressed as mass of dye absorbed per unit mass of cellulose per second clearly decreases with increasing time. In order to represent the dyeing speed by a single value, Boulton and Reading therefore introduced "the time of half dyeing" which is the time required for the absorption of the dye by the viscose to attain half its equilibrium value under the specified dyebath conditions. Thus the time of half dyeing represents how rapidly equilibrium dyeing is attained, and in general the smaller the time of half dyeing, the sooner is equilibrium dyeing attained.

It is obviously necessary to standardise the dyeing conditions for a comparison of one dye with another, and these workers chose an initial dyebath concentration of 0.5 per cent. (expressed on the weight of the fibre) and a liquor/yarn ratio of 40 to 1. The concentration of sodium chloride added was so chosen that at equilibrium the dyebath was 50 % exhausted, and the time of half dyeing therefore corresponded to 25 % exhaustion. By such means, the direct cotton dyestuffs have been classified <sup>7, 114</sup> according to their times of half dyeing of viscose at 90° C. and the values so obtained range from 0.07 minute for Icy Orange GS to 280 minutes

for Chlorazol Fast Pink BKS. Those dyes with the shortest times of half dyeing give the most level dyeings on viscose at 90° C. This classification is extremely useful particularly when choosing dyestuffs for compound shades when it is essential to choose those dyestuffs whose times of half dyeing are approximately equal.<sup>113, 114</sup>

**The Diffusion Theory.**—Although the measurements of the time of half dyeing provide a useful classification of the relative dyeing speeds of the direct cotton dyestuffs, it gives little information about the fundamental physico-chemical processes governing the rate of dyeing. It is difficult to interpret the kinetic curves theoretically since the dyebath concentration is steadily decreasing as exhaustion of the dyebath proceeds. Moreover, since the rate of dyeing depends on the surface area of the cellulosic material exposed to the dye liquor the use of yarn introduces further difficulties in the interpretation of the results. Consequently the experimental conditions that have been adopted in the experimental investigations of the kinetics of dyeing have been widely divorced from technical practice. Most of the work has been confined to viscose sheet, which may be considered as a rectangular sheet of known dimensions, and a length of liquor has been used such that the dyebath concentration remains practically constant during the dyeing.

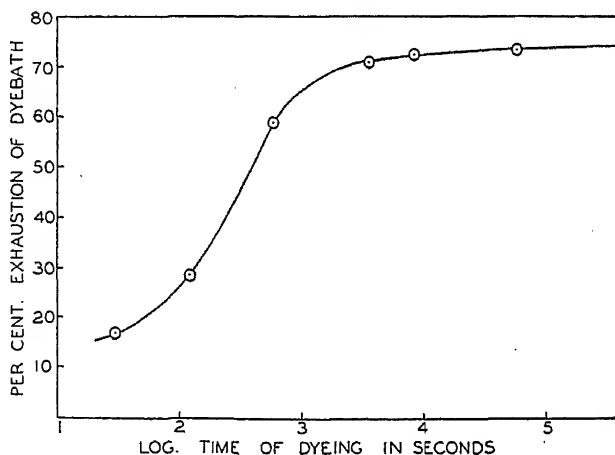


FIG. 4.—Absorption of Sky Blue FF by viscose yarn at 90° C. from a 40-volume bath containing 1.0 per cent. dye and 10.05 per cent sodium chloride.

The first accurate measurements of the kinetics of dye absorption were made by Boulton, Delph, Fothergill and Morton,<sup>8</sup> using viscose yarn, and by Neale and Stringfellow,<sup>10</sup> using viscose sheet. Both groups of workers purified their dyes by the method of Robinson and Mills, and determined the variation of the mass of dye absorbed with the time of dyeing. The results of Neale and Stringfellow for the absorption of Sky Blue FF on viscose sheet at 100° C. from a dyebath containing 0.05 g. per litre dye and 5 g. per litre sodium chloride are shown in Fig. 5. The line fitting the experimental points is derived from the equation

$$Q = Q_0 \left[ 1 - \frac{8}{\pi^2} \left\{ e^{-D \left( \frac{\pi}{l} \right)^2 t} + \frac{1}{9} e^{-D \left( \frac{3\pi}{l} \right)^2 t} + \frac{1}{25} e^{-D \left( \frac{5\pi}{l} \right)^2 t} + \dots \right\} \right]$$

where  $Q$  is the mass of dye absorbed per 100 g. of viscose in time  $t$ ,  $Q_0$  is the equilibrium absorption,  $l$  is the thickness of the viscose sheet and  $D$

is a constant. This expression, although referred to in the literature as Hill's equation,<sup>33</sup> has been derived by several workers for the diffusion<sup>1, 45, 47</sup> of a solute of constant concentration into a rectangular slab.  $D$  represents the diffusion coefficient of the solute into the slab, and although the series is infinite, in practice it is rapidly convergent and therefore represented with sufficient accuracy by the first few terms.<sup>33</sup> Boulton, Delph, Fothergill and Morton<sup>8</sup> observed that a similar expression appropriate to the diffusion of a solute into a cylinder fitted their experimental curves for viscose yarn. Both groups of workers therefore concluded that the kinetics of dyeing could be interpreted as a diffusion of the dye from the dyebath into the water-swollen cellulose. A similar suggestion was made by Schaffer<sup>32</sup> at the same time, but was not substantiated by experimental evidence.

Neale and Stringfellow<sup>60</sup> were able to correlate the absorption kinetics curves of Sky Blue FF on viscose sheets of different thicknesses by means

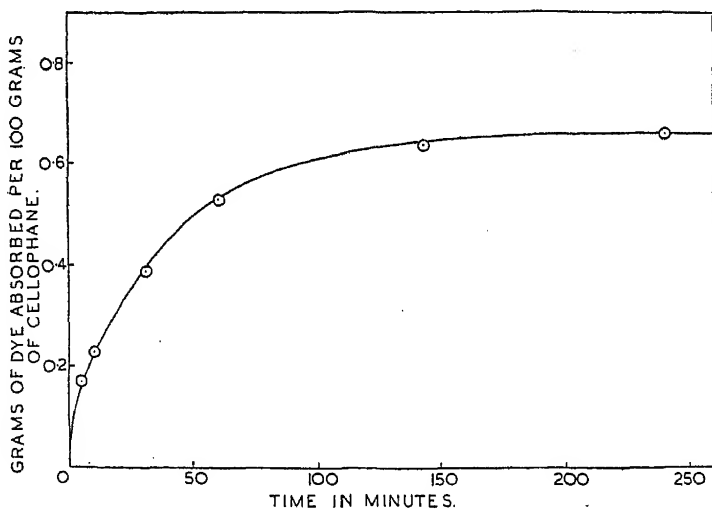


Fig. 5.—Absorption of Sky Blue FF by Cellophane at 100° C. Dyebath concentration, 0.05 gm. per litre dye, 5.0 gm. per litre-sodium chloride.

of the diffusion equation. Qualitative evidence of diffusion of the dye into the cellulose was given by photomicrographs<sup>5, 110</sup> of cross-sections of yarns dyed for different periods, where the slow penetration of the dye into the yarn was clearly visible. Boulton, Delph, Fothergill and Morton,<sup>8</sup> by clamping a viscose sheet between two plane surfaces so that the dye could only penetrate the sheet through its outer edges, observed that after dyeing, the dye had penetrated further along the direction of extrusion of the sheet than perpendicular to that direction, thus showing that the diffusion coefficient depended on the orientation of the cellulose chains in the sheet.

The diffusion equation that was found to fit the experimental kinetics curves applies only to a diffusion process for which Fick's Law<sup>36</sup> is valid, i.e. the diffusion coefficient is independent of the concentration of the diffusing solute. Consequently the good agreement found between the curves and this equation implied not only that the process was one of diffusion but that Fick's Law was also valid. Later work by Garvie and Neale<sup>20</sup> showed that the cellulosic diffusion coefficient\* of Sky Blue

\* A convenient shortening of "diffusion coefficient . . . into cellulose."

FF varied with the concentration of absorbed dye and consequently Fick's Law was not valid. The values of the cellulosic diffusion coefficients of direct dyes calculated on the basis of this equation are therefore only approximate, and probably represent the mean value of the cellulosic diffusion coefficients over the range of the absorbed dye concentration appropriate to each experiment. This fact is important since practically all the cellulosic diffusion coefficients of direct dyes recorded in the literature (with the exception of the work of Garvie and Neale<sup>20</sup>) are calculated from the kinetics curves on the basis of Fick's Law. Nevertheless these values, although approximate, can be taken as a measure of the dyeing speed, and in general the greater the cellulosic diffusion coefficient, the more rapidly is equilibrium dyeing attained.

When the dyebath concentration is maintained constant, the relationship between the cellulosic diffusion coefficient  $D$  and the time of half dyeing  $t_0$  required for the dye absorption  $Q$  to attain half the equilibrium value  $Q_0$  can be seen from the equation

$$Q = Q_0 \left[ 1 - \frac{8}{\pi^2} \left\{ e^{-D \left( \frac{\pi}{l} \right)^2 t} + \frac{1}{9} e^{-D \left( \frac{3\pi}{l} \right)^2 t} + \frac{1}{25} e^{-D \left( \frac{5\pi}{l} \right)^2 t} + \dots \right\} \right]$$

since on substituting for  $Q/Q_0$ , the expression becomes

$$\frac{\pi^2}{16} = \left\{ e^{-\left( \frac{\pi}{l} \right)^2 D t_0} + \frac{1}{9} e^{-\left( \frac{3\pi}{l} \right)^2 D t_0} + \frac{1}{25} e^{-\left( \frac{5\pi}{l} \right)^2 D t_0} + \dots \right\}$$

The only variables are the cellulosic diffusion coefficient  $D$  and the time of half dyeing  $t_0$ , and the higher the value of  $D$ , the smaller is the time of half dyeing. It should be noted that this expression is not applicable to Boulton and Reading's determination of the time of half dyeing since the dyebath concentration steadily decreases as dyeing proceeds. Nevertheless, in general, the higher the cellulosic diffusion coefficient the smaller is the time of half dyeing. Neale<sup>25</sup> has classified the direct cotton dyes according to their diffusion coefficients in viscose sheet at 90° C., the dyebath concentration being maintained constant at 0.05 g. per litre dye and 5 g. per litre sodium chloride. Thus his experimental conditions differ widely from those of Boulton and Reading in their measurements of the time of half dyeing where not only is the dyebath concentration steadily decreasing as dyeing proceeds but the concentration of sodium chloride, chosen to give 50 % exhaustion at equilibrium dyeing, varies considerably from dye to dye. Complete agreement between the relative dyeing speeds of direct dyes as determined by the two methods cannot therefore be expected; nevertheless, apart from certain exceptions, the agreement between the two classifications is reasonably good. As with the times of half dyeing, the cellulosic diffusion coefficients extend over a wide range from  $180 \times 10^{-8}$  cm.<sup>2</sup> per sec. for Icy Orange RS to  $0.71 \times 10^{-8}$  cm.<sup>2</sup> per sec. for Chlorazol Orange AG.

It is seen from the diffusion equation that  $Q$  the mass of dye absorbed in a time  $t$  depends not only on the diffusion coefficient  $D$  but also on the equilibrium absorption  $Q_0$ . Thus it does not follow that the mass of dye absorbed in a time  $t$  is greater for a dye with a high diffusion coefficient than for a dye with a low diffusion coefficient. Examples of the combined effect of the equilibrium absorption  $Q_0$  and the diffusion coefficient  $D$  on the mass of dye absorbed in an arbitrary time are given later when discussing the effect of temperature and of salt concentration on the dyeing kinetics.

**Effect of Dye Concentration.**—The cellulosic diffusion coefficients calculated from the kinetics curves depend upon the validity of Fick's Law. Neale<sup>25</sup> observed that the values so obtained for Sky Blue FF at 90° C. in viscose sheet increased as the dyebath concentration was increased, clearly showing that Fick's Law was not valid. It became



necessary therefore to devise an alternative method for the determination of the cellulosic diffusion coefficient of direct dyes which did not depend on the validity of Fick's Law for the calculation of the results. When Fick's Law is not valid it is highly desirable to employ a method whereby the distribution of the diffusing solute through the system can be determined. Garvie and Neale<sup>20</sup> achieved this by clamping a wad of viscose sheet between two halves of a diffusion cell each containing a dyebath of Sky Blue FF at 90° C. The dye could diffuse into the wad only through the outermost sheets, and by measuring the concentration of absorbed dye in each of the sheets after a definite period of dyeing, the distribution of the diffused dye in the wad could be determined. From the graphical analysis of the distribution curves so obtained for different periods of dyeing Garvie and Neale found that the cellulosic diffusion coefficient of the dye increased with the concentration of absorbed dye. Due to experimental difficulties and the unavoidable errors arising from the graphical analysis, the scatter of the experimental results rendered it difficult to determine the exact quantitative relationship between the cellulosic diffusion coefficient and the concentration of absorbed dye. They found, however, that the empirical equation

$$dS/dt = kC^{1/2}dC/dx$$

approximately fitted the experimental results where  $dS/dt$  is the flux of dye in the viscose sheet,  $dC/dx$  the concentration gradient of the dye in the sheet,  $C$  is the concentration of absorbed dye, and  $k$  is a constant.

The values of the cellulosic diffusion coefficient as determined graphically from the distribution curves do not depend on the diffusion equation based on Fick's Law, which was previously applied to the kinetics curves. Garvie and Neale<sup>20</sup> by applying this equation to their results, showed that the value of the cellulosic diffusion coefficient so obtained was within the range of values found by graphical analysis. It is probable, therefore, that the value given by the diffusion equation represents an approximate mean value over the range of absorbed dye concentration appropriate to each particular experiment. No other work on the deviations from Fick's Law for the cellulosic diffusion of direct dyes is recorded in the

literature, and the investigations subsequently described on the effect of temperature and of the salt concentration were made before such deviations were fully appreciated.

**Effect of Temperature.**—When the dye and the salt concentration are maintained constant, equilibrium is attained more rapidly at a higher than a lower temperature. This and the corresponding decrease in the equilibrium absorption are clearly seen in Fig. 6; the curves are those of Boulton, Delph, Fothergill and Morton<sup>8</sup> for the absorption of Chrysophenine by viscose rayon yarn. Garvie, Griffiths and Neale<sup>19</sup> have found a similar effect for the absorption of Fast Red K and Heliotrope 2B on viscose sheet, the calculated cellulosic diffusion coefficients of

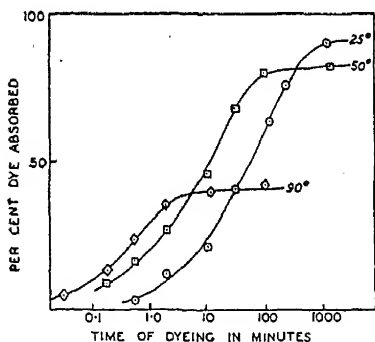


FIG. 6.—Absorption of Chrysophenine by a 300/36 Viscose yarn from a 40-volume bath containing 0.2 per cent. dye and 5.0 per cent. salt.

these dyes being roughly doubled for each 25° C. rise in temperature.

It is seen from Fig. 6 that the mass of dye absorbed by the cellulose can either increase, pass through a maximum, or decrease with increasing temperature according to the time of dyeing even though the diffusion

coefficient increases with increasing temperature. Dye absorption experiments, such as those of Weltzien and Schulze,<sup>11</sup> in which the dyeing is conducted for an arbitrary period of time, insufficient for the attainment of equilibrium at the lower temperatures, show either an increase or maximum in the dye absorption with increasing temperature. Whittaker's<sup>3, 13</sup> "temperature range test" for the classification of dyestuffs according to their levelling properties depends upon this principle. Level and therefore rapid dyeing dyestuffs give a maximum depth of shade on viscose, when dyed for a fixed time at a low temperature whereas unlevel and slow dyeing dyes give a maximum depth of shade at high temperatures. Since the levelness increases with the dyeing rate, viscose is normally dyed at 90° C.

**The Effect of Inorganic Electrolytes.**—Neale and his collaborators<sup>25, 58, 60</sup> have extensively investigated the effect of the nature and the concentration of inorganic electrolyte on the rate of dyeing of viscose sheet when the dyebath concentration and the temperature are maintained constant. The diffusion equation based on Fick's Law was found to fit

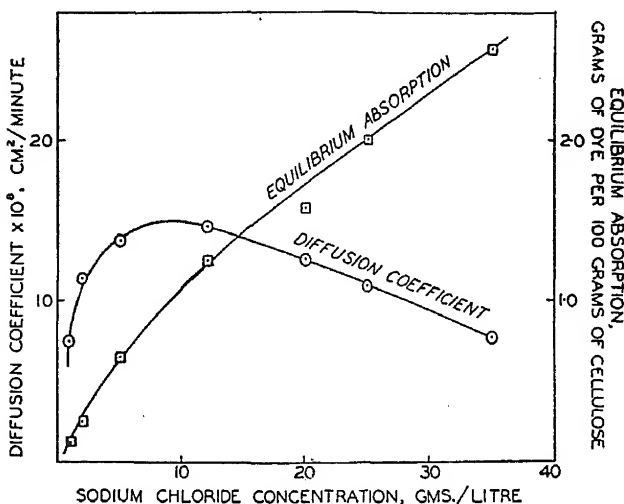


FIG. 7.—Variation of the cellulose diffusion coefficient and of the equilibrium absorption of Sky Blue FF with the sodium chloride concentration at 10° C.

the kinetics curves obtained reasonably well, and the appropriate values of the cellulosic diffusion coefficient corresponding to each salt concentration were calculated. They found that for several dyes at 90° C. the cellulosic diffusion coefficient passed through a maximum with increasing sodium chloride concentration. Fig. 7 shows the corresponding values of the equilibrium absorption and the cellulose diffusion coefficient of 0.05 g. per litre Sky Blue FF on viscose sheet at 101° C. as determined by Neale and Stringfellow.<sup>60</sup> Neale and Patel<sup>58</sup> have extended the work to other electrolytes and have found the effect to be general. The equivalent concentration of electrolyte corresponding to the maximum value of the cellulosic diffusion coefficient is generally lower for a multi-univalent electrolyte than for a uni-uni one. Photomicrographs of the cross-sections of dyed filaments of viscose and cuprammonium yarns by Weltzien and Froitzheim<sup>11</sup> clearly show the increased penetration of the dye on the addition of salt.

Since the cellulosic diffusion coefficient passes through a maximum with increasing salt concentration whereas the equilibrium absorption

steadily increases, the mass of dye absorbed in a fixed time will also either increase or pass through a maximum as the salt concentration increases. This has been observed by Lehner and Smith<sup>41</sup> for the absorption of Benzopurpurin 4B on cotton at 25° C. and 50° C. At 90° C., where equilibrium dyeing was probably attained, the dye absorption increased steadily with increasing sodium chloride concentration. Lehner and Smith attribute the decrease in dyeing speed with increasing salt concentration to the large particle size attained by the dye micelles in the presence of the salt. This may probably be the explanation for their experiments at 25° and 50° C., but it is unlikely that the maximum found by Neale and Stringfellow for Sky Blue FF at 101° C. (Fig. 7) for a concentration of about 10 g. per litre sodium chloride can be entirely attributed to this cause. According to Valko, the aggregation of 0.2 g. per litre Sky Blue FF at 90° C. in the presence of 0.5 N. NaCl is below 2.

Very little work has been done on the effect of levelling agents on the rate of dyeing. It is claimed that  $\beta$ -naphthol<sup>6</sup> increases the rate of dyeing. Many levelling agents are colloidal electrolytes and providing they have no affinity for the dye their effect on the rate of dyeing might therefore be expected to be similar to that of a uni-multi- or multi-uni-valent electrolyte according to whether they are anionic or cationic-active substances. Smith<sup>47</sup> has investigated the absorption of Benzopurpurin 4B on cotton at 25° C. in the presence of a cationic active levelling agent, and suggests that its chief function is in promoting the swelling of the fibre.

**The Rate of Dyeing of Yarns.**—The work of Neale and his collaborators on the kinetics of dyeing is mainly confined to viscose sheet, and apart from the work previously reviewed very few investigations of the kinetics of the dyeing of yarns have been made. Neale<sup>26</sup> has stressed the importance of agitation in such measurements on yarns, where it is essential that the entire surface of the yarn shall be accessible to the dye liquor. Boulton and Morton<sup>6</sup> have determined the rate of absorption of Sky Blue FF at 90° C. on cotton, viscose rayon and cuprammonium rayon by chopping the yarn into short lengths of about one millimetre and dyeing as a slurry. The curves showed that whereas in the initial stages the cotton was dyed more rapidly than the viscose, equilibrium was finally attained more slowly by the cotton. Cuprammonium rayon<sup>53</sup> dyed more rapidly than viscose, while the time of half dyeing of cotton<sup>6</sup> mercerised under tension was found to be approximately a quarter of that of the unmercerised material. Kinetic measurements with different cottons showed that there was a rough correlation between the fineness of the cotton hairs<sup>6</sup> and the rate of dyeing, the finer hairs dyeing more rapidly.

## 7. Present Position of the Diffusion Theory.

It is now generally realised that the kinetics of dyeing is a more complex process than one of simple diffusion of the dye into the water-swollen cellulose. Such a picture does not take into account the adsorption forces between the diffusing dye anions and the cellulose, and, as Valko<sup>107</sup> and Morton<sup>52</sup> have stressed, the observed cellulosic diffusion coefficient of a dye must depend upon the adsorption of the dye by the cellulose occurring simultaneously with the diffusion process. The kinetics of direct dyeing is essentially a process of diffusion into an adsorbing medium such as is reported in the literature<sup>81, 99, 109</sup> for other systems, and for which deviations from Fick's Law frequently occur. More experimental data on the deviations from Fick's Law occurring in the cellulosic diffusion of dyes should prove valuable for a fuller interpretation of the process.

The fact that the cellulosic diffusion coefficients reported in the literature are calculated on the basis of Fick's Law renders the interpretation of the results more difficult, for such values can only be approximate and probably represent the mean value of the cellulosic diffusion coefficient

over the range of absorbed dye concentration appropriate to each experiment. Morton<sup>52</sup> has drawn attention to the fact that whereas the aqueous diffusion coefficients of direct dyes at 90° C.,<sup>41, 48, 108</sup> are of the order of  $10^{-5}$  cm.<sup>2</sup> per sec., the calculated cellulosic diffusion coefficients are considerably smaller, ranging from  $10^{-8}$  to  $10^{-11}$  cm.<sup>2</sup> per sec. The aqueous diffusion coefficient of a dye anion in the presence of excess sodium chloride depends on the effective resistance of the solvent to the diffusing dye anion. When the dye anion diffuses in the water-swollen cellulose, the effective resistance to the diffusion of the dye anion is probably increased owing to the fine network of cellulose chains through which diffusion occurs, and on account of the adsorption forces tending to immobilise the dye anion. By assuming a linear absorption isotherm, Morton<sup>52</sup> has deduced approximate values of the cellulosic diffusion coefficients of several dyes when the effect of adsorption is allowed for. These values range from  $2 \times 10^{-6}$  to  $7 \times 10^{-7}$  cm.<sup>2</sup> per sec., and only approximate to the aqueous diffusion coefficients for the most rapid dyeing dyes, showing that the small values of the cellulosic diffusion coefficients cannot be entirely attributed to the effect of adsorption.

One factor that will give a smaller diffusion coefficient of direct dyes in cellulose than in water is the tortuous nature of the capillaries and the fact that the cross-sectional area of these capillaries is considerably less than the area of the viscose sheet. Thus in Garvie and Neale's<sup>20</sup> single sheet diffusion measurements, the viscose sheet between the dye solutions is in some respects similar to the sintered glass membrane used in aqueous diffusion measurements.<sup>36</sup> It is highly probable, however, that the fine network of cellulose chains also impedes the diffusion of the dye, since as previously mentioned, permeability measurements indicate a mean capillary radius of 20 to 30 Å. As Boulton and Morton<sup>6, 52</sup> suggest, the differences in dyeing speeds found for the regenerated celluloses is probably connected with the openness of the intercrystalline regions. Thus the swelling of cotton with caustic soda increases the dyeing speed, and the higher dyeing speed of cuprammonium rayon compared with viscose is in agreement with measurements of the permeability<sup>9</sup> of Cuprophane and Cellophane to sugars.

The effect of aggregation of the dye micelles on the cellulosic diffusion coefficient is not yet definitely established. At the higher salt concentration the cellulosic diffusion coefficient decreases as the salt concentration increases, but it has not yet been established whether this decrease is due to increasing aggregation of the dye or to the increase in the relative amount of adsorbed dye. Boulton and Morton<sup>6, 52</sup> suggest that a dynamical equilibrium, which can be restored in a few seconds at 90° C., exists between the single dye anions and the micelles, so that a continuous stream of dye molecules can pass from the dyebath into the fibre. On their hypothesis, the rate of dye absorption is governed by the relatively slow diffusion of the dye molecules in the cellulose. They suggest that rapidly dyeing dyes contain a relatively large fraction of single dye anions whereas slowly dyeing dyes contain only a small fraction. Neale has observed, however, that with certain exceptions the greater the equilibrium absorption of a dye on viscose, the smaller is the cellulosic diffusion coefficient. It is probable, therefore, that the wide range of cellulosic diffusion coefficients found for direct dyes is due not only to their relative degree of aggregation but also arises from the different affinities of the dyes for the cellulose.

It is seen that the simultaneous occurrence of the adsorption process and the diffusion of the dye in the cellulose, taken in conjunction with the structure of the cellulose itself, can explain qualitatively many of the experimental observations on the kinetics of dye absorption. Such considerations, however, do not explain the initial increase in the cellulosic diffusion coefficient as it passes through a maximum with increasing salt

concentration. It should be noted that these calculated values are taken over the range of absorbed dye concentration appropriate to each experiment, and that the upper limit of the absorbed dye concentration will therefore increase with increasing salt concentration. The steady decrease in the cellulosic diffusion coefficient once the maximum is passed may be due to the combined effects of increasing adsorption and aggregation of the dye. The existence of a maximum suggests that two opposing factors are operative in the diffusion process, and the initial increase of the cellulosic diffusion coefficient with increasing salt concentration may arise from the electrochemical nature of the system. Neale<sup>55</sup> has suggested that the salt reduces a repulsion of the diffusing dye anions by those already adsorbed on the cellulose, while Hartley<sup>28</sup> has suggested that the effect may arise from endosmosis. It is to be expected that in the relatively small intercrystalline regions of the cellulose, the electrical field arising from the adsorbed layer of the dye anions on the cellulose may play as important a part in the kinetics of dyeing as the particle size of the dye micelles.

In conclusion it is seen that both the experimental and the theoretical investigations of the kinetics of dyeing are far less developed than those of equilibrium dyeing. Although there is strong evidence that the dye diffuses into the swollen cellulose phase, little is yet definitely established concerning the relative effects of adsorption, the particle size of the dye micelles and of the interionic forces on the kinetics of dyeing.

#### REFERENCES.

- <sup>1</sup> Andrews and Johnson, *J. Amer. Chem. Soc.*, 1924, **46**, 640.
- <sup>2</sup> Auerbach, *Kolloid Z.*, 1921, **29**, 190; 1922, **30**, 165.
- <sup>3</sup> Azuma and Kameyama, *Phil. Mag.*, 1925, **50**, 1264.
- <sup>4</sup> Boulton, *J. Soc. Dyers and Col.*, 1938, **54**, 268.
- <sup>5</sup> Boulton and Morton, *ibid.*, 1939, **55**, 481.
- <sup>6</sup> Boulton and Morton, *ibid.*, 1940, **56**, 145.
- <sup>7</sup> Boulton and Reading, *ibid.*, 1934, **50**, 381.
- <sup>8</sup> Boulton, Delph, Fothergill and Morton, *J. Text. Inst.*, 1933, **24**, P. 113.
- <sup>9</sup> Brintzinger and Osswald, *Kolloid Z.*, 1935, **70**, 198.
- <sup>10</sup> Brode and Brooks, *J. Amer. Chem. Soc.*, 1941, **63**, 923.
- <sup>11</sup> Brode and Mark, *Papier Fabrikant*, 1937, **35**, 471.
- <sup>12</sup> Courtaulds Ltd., *Dyeing of Viscose with Direct Cotton Dyestuffs*, 1927.
- <sup>13</sup> Courtaulds Ltd., *Silk Journal*, 1928, April, **4**, 64.
- <sup>14</sup> Davidson, *Shirley Inst. Mem.*, 1936, **15**, 1; *J. Text. Inst.*, 1936, **27**, P. 144.
- <sup>15</sup> Donnan and Harris, *J. Chem. Soc.*, 1911, **99**, 1554.
- <sup>16</sup> Dreaper, *Chemistry and Physics of Dyeing*, Churchill, 1906.
- <sup>17</sup> Freundlich, *Colloid and Capillary Chemistry*, p. 754, Methuen & Co., 1926.
- <sup>18</sup> Frey Wyssling, *Protoplasma*, 1937, **27**, 372.
- <sup>19</sup> Garvie, Griffiths and Neale, *Trans. Faraday Soc.*, 1934, **30**, 271.
- <sup>20</sup> Garvie and Neale, *ibid.*, 1938, **34**, 335.
- <sup>21</sup> Gee and Harrison, *ibid.*, 1910, **6**, 42.
- <sup>22</sup> Georgievics, *Colloid Chemistry* (Alexander), Vol. IV, p. 197; Chemical Catalogue Co., 1932.
- <sup>23</sup> Griffiths and Neale, *Trans. Faraday Soc.*, 1934, **30**, 395.
- <sup>24</sup> Haller, *Kolloid Z.*, 1921, **29**, 95; 1922, **30**, 249.
- <sup>25</sup> Hanson and Neale, *Trans. Faraday Soc.*, 1934, **30**, 386.
- <sup>26</sup> Hanson, Neale and Stringfellow, *ibid.*, 1935, **31**, 1718.
- <sup>27</sup> Harrison, *J. Soc. Dyers and Col.*, 1911, **27**, 279.
- <sup>28</sup> Hartley, *Trans. Faraday Soc.*, 1935, **31**, 281.
- <sup>29</sup> Hartley and Robinson, *Proc. Roy. Soc. A*, 1931, **134**, 20.
- <sup>30</sup> Hatschek, *Kolloid Z.*, 1926, **39**, 300.
- <sup>31</sup> Henry, *Proc. Roy. Soc. A*, 1937, **171**, 215.
- <sup>32</sup> Herzog and Kudar, *Z. physikal. Chem. A*, 1934, **167**, 329, 343.
- <sup>33</sup> Hill, *Proc. Roy. Soc. B.*, 1928, **104**, 39.
- <sup>34</sup> Hodgson, *J. Soc. Dyers and Col.*, 1937, **53**, 175.
- <sup>35</sup> Hodgson and Holt, *ibid.*, 1937, **53**, 175.
- <sup>36</sup> Holmes, Shirley Institute Publication, *in press*.

- <sup>37</sup> Kortüm, *Z. physikal. Chem. B.*, 1936, **34**, 255.
- <sup>38</sup> Krotowa, *Kolloid Z.*, 1934, **69**, 94; 1935, **72**, 345.
- <sup>39</sup> Kruger and Rudow, *Ber. deut. chem. Ges.*, 1938, **71**, 707.
- <sup>40</sup> Lehner and Smith, *J. Amer. Chem. Soc.*, 1934, **56**, 999.
- <sup>41</sup> Lehner and Smith, *ibid.*, 1935, **57**, 497, 504.
- <sup>42</sup> Lehner and Smith, *J. Ind. Eng. Chem.*, 1935, **27**, 20.
- <sup>43</sup> Lehner and Smith, *J. Physic. Chem.*, 1936, **40**, 1005.
- <sup>44</sup> Leupin, *Textilberichte*, 1941, **22**, 635.
- <sup>45</sup> March and Weaver, *Physic. Rev.*, 1928, **31**, 1072.
- <sup>46</sup> Mark, *J. Physic. Chem.*, 1940, **44**, 764.
- <sup>47</sup> McBain, *Z. physikal. Chem.*, 1909, **68**, 477.
- <sup>48</sup> McBain, *Trans. Faraday Soc.*, 1913, **9**, 99.
- <sup>49</sup> McBain and Kistler, *ibid.*, 1930, **26**, 157.
- <sup>50</sup> Meyer, *Natural and Synthetic Polymers*, p. 274, Interscience Publishing Co., 1942.
- <sup>51</sup> Moilliet, Collie, Robinson and Hartley, *Trans. Faraday Soc.*, 1935, **31**, 120.
- <sup>52</sup> Morton, *ibid.*, 1935, **31**, 262, 283.
- <sup>53</sup> Morton, *ibid.*, 1935, **31**, 280.
- <sup>54</sup> Neale, *Amer. Dyes. Rept.*, 1934, **23**, 109.
- <sup>55</sup> Neale, *J. Soc. Dyers and Col.*, 1936, **52**, 252.
- <sup>56</sup> Neale, *ibid.*, 1943, **59**, 148.
- <sup>57</sup> Neale and Hanson, *Nature*, 1932, **129**, 761.
- <sup>58</sup> Neale and Patel, *Trans. Faraday Soc.*, 1934, **50**, 905.
- <sup>59</sup> Neale and Stringfellow, *J. Text. Inst.*, 1933, **24**, 145.
- <sup>60</sup> Neale and Stringfellow, *Trans. Faraday Soc.*, 1933, **29**, 1167.
- <sup>61</sup> Neale and Stringfellow, *J. Soc. Dyers and Col.*, 1940, **56**, 17.
- <sup>62</sup> Neale and Stringfellow, *ibid.*, 1940, **56**, 19.
- <sup>63</sup> Neale and Stringfellow, *ibid.*, 1940, **56**, 21.
- <sup>64</sup> Neale and Stringfellow, *ibid.*, 1943, **59**, 241.
- <sup>65</sup> Ostwald, *Kolloidchem. Beih.*, 1919, **10**, 176.
- <sup>66</sup> Ostwald, *Z. physikal. Chem.*, 1924, **111**, 62.
- <sup>67</sup> Ostwald, *Kolloid Z.*, 1934, **68**, 42.
- <sup>68</sup> Ostwald, *Trans. Faraday Soc.*, 1933, **29**, 347.
- <sup>69</sup> Overbeck, *Verbesserungen an Methoden zur Untersuchung von Kolloiden Farbstoffen*, Diss. Göttingen, 1926.
- <sup>70</sup> Parks and Keller, *Amer. Dyes. Rept.*, 1934, **23**, 445.
- <sup>71</sup> Patel, *ibid.*, 1934, **23**, 505.
- <sup>72</sup> Pauli and Weiss, *Biochem. Z.*, 1928, **203**, 104.
- <sup>73</sup> Pauling, *Nature of the Chemical Bond*, p. 313, Cornell Univ. Press.
- <sup>74</sup> Preston, *J. Soc. Dyers and Col.*, 1931, **47**, 313.
- <sup>75</sup> Quesnel, *Trans. Faraday Soc.*, 1935, **31**, 259.
- <sup>76</sup> Ratelade and Tschetvergov, *Rev. gén. Mat. Col.*, 1928, **32**, 302.
- <sup>77</sup> Robinson, *Trans. Faraday Soc.*, 1933, **29**, 352.
- <sup>78</sup> Robinson, *Proc. Roy. Soc. A.*, 1935, **148**, 681.
- <sup>79</sup> Robinson and Garrett, *Trans. Faraday Soc.*, 1939, **35**, 771.
- <sup>80</sup> Robinson and Mills, *Proc. Roy. Soc. A.*, 1931, **131**, 576.
- <sup>81</sup> Robinson and Moilliet, *ibid.*, 1934, **143**, 630.
- <sup>82</sup> Robinson and Selby, *Trans. Faraday Soc.*, 1939, **35**, 780.
- <sup>83</sup> Rose, *Amer. Dyes. Rept.*, 1927, **16**, 16.
- <sup>84</sup> Rose, *ibid.*, 1932, **21**, 52.
- <sup>85</sup> Rose, *Ind. Eng. Chem.*, 1933, **25**, 1028.
- <sup>86</sup> Rose, *ibid.*, 1933, **25**, 1265.
- <sup>87</sup> Rose, *Rayon Textile Monthly*, 1942, **23**, 161, 217, 287.
- <sup>88</sup> Ruggli, *Kolloid Z.*, 1933, **63**, 129.
- <sup>89</sup> Ruggli, *J. Soc. Dyers and Col.*, 1934, **50**, 77.
- <sup>90</sup> Ruggli and Lang, *Helv. Chim. Acta*, 1936, **19**, 996.
- <sup>91</sup> Ruggli and Leupin, *ibid.*, 1939, **22**, 1170.
- <sup>92</sup> Schäffer, *Z. angew. Chemie*, 1933, **46**, 618.
- <sup>93</sup> Schirm, *J. prakt. Chem.*, 1935, **144**, 69.
- <sup>94</sup> Schramek and Götte, *Kolloidchem. Beih.*, 1932, **34**, 218.
- <sup>95</sup> Schramek and Helm, *Kolloid Z.*, 1938, **85**, 291.
- <sup>96</sup> Schramek and Rümmler, *Kolloidchem. Beih.*, 1938, **47**, 133.
- <sup>97</sup> Smith, *Amer. Dyes. Rept.*, 1939, **28**, 146.
- <sup>98</sup> *Trans. Faraday Soc.*, 1935, **31**, 1421.
- <sup>99</sup> Tiselius, *J. Physic. Chem.*, 1936, **40**, 223.
- <sup>100</sup> Trillat and Matricon, *J. Chim. Physique*, 1935, **32**, 101.
- <sup>101</sup> Trotman and Fearson, *J. Soc. Dyers and Col.*, 1931, **47**, 344.

- <sup>102</sup> Urquhart, *Shirley Inst. Mem.*, 1924, 3, 367; *J. Text. Inst.*, 1924, 15, 559T.  
<sup>103</sup> Usher, *J. Soc. Dyers and Col.*, 1943, 59, 150.  
<sup>104</sup> Usher and Wahbi, *ibid.*, 1942, 58, 221.  
<sup>105</sup> Valko, *Kolloidchemische Grundlagen der Textilveredlung*, pp. 338-48, Berlin, 1937.  
<sup>106</sup> Valko, *Trans. Faraday Soc.*, 1935, 31, 278.  
<sup>107</sup> Valko, *ibid.*, 1935, 31, 230.  
<sup>108</sup> Valko, *J. Soc. Dyers and Col.*, 1939, 55, 174.  
<sup>109</sup> Ward, *Proc. Roy. Soc. A.*, 1931, 133, 506.  
<sup>110</sup> Weltzien and Froitzheim, *Monatshefte Seide u. Kunstseide*, 1939, 44, 185, 238, 269.  
<sup>111</sup> Weltzien and Schulze, *Kolloid Z.*, 1933, 62, 46.  
<sup>112</sup> Weltzien and Windeck-Schultze, *Z. angew. Chemie*, 1938, 51, 729.  
<sup>113</sup> Whittaker, *J. Soc. Dyers and Col.*, 1936, 52, 164.  
<sup>114</sup> Whittaker and Wilcock, *Dyeing with Coal Tar Dyestuffs*, pp. 248-62; Baillière, Tindall and Cox, 1942.  
<sup>115</sup> Wilkitoroff, *Kolloid Z.*, 1931, 55, 72.  
<sup>116</sup> Wilson and Imison, *J. Soc. Chem. Ind.*, 1920, 39, 322T.  
<sup>117</sup> Zocher, *Z. physikal. Chem.*, 1921, 90, 293.  
<sup>118</sup> Zsigmondy, *Chemistry of Colloids*, chap. xi; John Wiley & Sons, 1917.  
<sup>119</sup> Zsigmondy, *Z. physikal. Chem.*, 1924, 111, 211.

## TWO NEW MODIFICATIONS OF THE FOURIER METHOD OF X-RAY STRUCTURE ANALYSIS.

By A. D. BOOTH.

*Received 8th December, 1944.*

The course of approach normally adopted in crystal analysis is based on the concept of three-dimensional repetition originated by Bragg who showed<sup>1</sup> that the electron density at any point in a crystal could be represented by a three-dimensional Fourier series. It follows from this principle that the projection of the electron density on any principal plane has a two-dimensional repetition pattern and hence is capable of expression as a two-dimensional Fourier series.

In general the series are used after a set of approximate atomic parameters has been determined by one of the usual trial and error methods,<sup>2, 3</sup> and it is customary to start by refining two of these co-ordinates using Fourier projections. When, for the reasons to be discussed later, these cease to give useful information, all three co-ordinates are obtained with the greatest possible accuracy by means of Fourier sections and lines.

In preliminary work, Fourier projections have the advantages of requiring only a small number of terms of the type  $F(hko)$  and of giving information about all the atoms at the same time, but since in most structures overlapping occurs in projection the latter advantage is seldom realised and utilisation of only a small number of terms in itself reduces the accuracy of derived co-ordinates.

The methods of section and line syntheses remove the disadvantages of projections but introduce two additional drawbacks, that the co-ordinates have to be known with a fair degree of accuracy and also the rather serious fact that the time taken in computation with complex organic molecules is considerable; which probably accounts for the hitherto limited employment of three-dimensional syntheses in structure analysis. In order to obtain bond lengths of the accuracy now required in comparing various resonance theories of molecular structure, it is

<sup>1</sup> Bragg, *Phil. Trans. Roy. Soc.*, 1915, 215, 253.

<sup>2</sup> Bragg and Lipson, *Z. Kryst.*, 1936, 95, 323.

<sup>3</sup> Patterson, *ibid.*, 1935, 90, 517.

necessary to have atomic co-ordinates of the greatest precision available with a full use of the most advanced experimental technique. In view of the fact that in using projections only for structure analysis, the greater part of the available experimental data (*i.e.* general  $F(hkl)$  values) is either not observed or in any case not used, it is desirable that all structures investigated should have the concluding refinements effected by three-dimensional synthesis.

The present paper contains an account of two methods devised by the author having advantages intermediate between those of the standard methods just discussed. The first is a generalisation of the projection in which, instead of projecting the whole contents of a unit all upon a basal plane, only that part contained between specified planes is included. The second is a modification of the normal method of Fourier sections in which, instead of the usual single atom per synthesis, a number of atoms can, under suitable conditions, be obtained on the same section. In the description of both methods the treatment for the general case is given and then that for the particular monoclinic space group  $P_{21}/c$  in order to show the practical application; this space group was chosen since it is one which occurs in a high proportion of the organic compounds hitherto investigated and is thus likely to be useful for reference. While the general results given could easily be transformed to suit the symmetry of any particular space group it is in fact always quicker to obtain the particular results from the tables of Lonsdale.<sup>4</sup>

### (1) The Method of Section-projections.

The electron density at any point  $(x, y, z)$  in the unit cell of a crystal is given (Lonsdale<sup>4</sup>) by:

$$\rho(xyz) = \frac{1}{V} \sum_{-\infty}^{\infty} \sum_{-\infty}^{\infty} \sum_{-\infty}^{\infty} |F(hkl)| \cos \left[ 2\pi \left( h\frac{x}{a} + k\frac{y}{b} + l\frac{z}{c} \right) - \alpha(hkl) \right] \quad (1)$$

whence the projection of the electron density contained between the two panes  $z = z_1$  and  $z = z_2$  on the  $(c)$  face is, for orthogonal crystals:—

$$B_{z_1}^{z_2} = \int_{z_1}^{z_2} \rho(xyz) dz = \frac{1}{V} \sum_{-\infty}^{\infty} \sum_{-\infty}^{\infty} \sum_{-\infty}^{\infty} \frac{c}{2\pi l} |F(hkl)| \left\{ \sin \left[ 2\pi \left( h\frac{x}{a} + k\frac{y}{b} + l\frac{z_2}{c} \right) - \alpha(hkl) \right] - \sin \left[ 2\pi \left( h\frac{x}{a} + k\frac{y}{b} + l\frac{z_1}{c} \right) - \alpha(hkl) \right] \right\}.$$

Two special cases are of interest:—

(1) When  $z_2 = z_1 + c$  the above expression reduces to:

$$B_{z_1}^{z_1+c} = \frac{1}{A} \sum_{-\infty}^{\infty} \sum_{-\infty}^{\infty} |F(hko)| \cos \left[ 2\pi \left( h\frac{x}{a} + k\frac{y}{b} \right) - \alpha(hko) \right]$$

which is the ordinary formula for Fourier projections given by Bragg.<sup>5</sup>

(2) As  $z_2 \rightarrow z_1$ , the result becomes:—

$$\begin{aligned} B_{z_1}^{z_1+\delta z_1} &= \frac{1}{V} \sum_{-\infty}^{\infty} \sum_{-\infty}^{\infty} \sum_{-\infty}^{\infty} \frac{c}{\pi l} |F(hkl)| \cos \left[ 2\pi \left( h\frac{x}{a} + k\frac{y}{b} + l\frac{z_1}{c} \right) - \alpha(hkl) \right] \\ &\quad + \frac{l}{c} \delta z_1 \sin \left( \frac{l}{c} \delta z_1 \right) \\ &\simeq \frac{1}{V} \sum_{-\infty}^{\infty} \sum_{-\infty}^{\infty} |F(hkl)| \cos \left[ 2\pi \left( h\frac{x}{a} + k\frac{y}{b} + l\frac{z_1}{c} \right) - \alpha(hkl) \right] \delta z_1 \end{aligned}$$

<sup>4</sup> Lonsdale, *Simplified Structure Factor Tables*, 1936.

<sup>5</sup> Bragg, W. H. and W. L., *The Crystalline State*, 1933.



which is merely an expression of the fact that

$$\frac{1}{\delta z_1} B_{z_1}^{z_1 + \delta z_1} \rightarrow \rho(xy z_1), \quad (2)$$

i.e. an ordinary Fourier Section at height  $z_1$ .

For monoclinic crystals of space-group  $P_{21}/c$  (1) becomes (Lonsdale *loc cit.*)

$$\begin{aligned} \rho(xy z) = \frac{4}{V} \left\{ \sum_0^{\infty} \sum_0^{\infty} \sum_{k+l=2n} \left[ F(hkl) \cos 2\pi \left( h \frac{x}{a} + l \frac{z}{c} \right) \right. \right. \\ \left. \left. + F(\bar{h}kl) \cos 2\pi \left( -h \frac{x}{a} + l \frac{z}{c} \right) \right] \cos 2\pi k \frac{y}{b} \right. \\ \left. - \sum_0^{\infty} \sum_0^{\infty} \sum_{k+l=2n+1} \left[ F(hkl) \sin 2\pi \left( h \frac{x}{a} + l \frac{z}{c} \right) + F(\bar{h}kl) \sin 2\pi \left( -h \frac{x}{a} + l \frac{z}{c} \right) \right] \sin 2\pi k \frac{y}{b} \right\} \end{aligned}$$

From which the result is obtained :—

$$\begin{aligned} B_{y_1}^{y_2} = \frac{4}{A} \left\{ \sum_0^{\infty} \sum_0^{\infty} \sum_{k+l=2n} \left[ F(hkl) \cos 2\pi \left( h \frac{x}{a} + l \frac{z}{c} \right) + F(\bar{h}kl) \cos 2\pi \left( -h \frac{x}{a} + l \frac{z}{c} \right) \right] C_k \right. \\ \left. - \sum_0^{\infty} \sum_0^{\infty} \sum_{k+l=2n+1} \left[ F(hkl) \sin 2\pi \left( h \frac{x}{a} + l \frac{z}{c} \right) + F(\bar{h}kl) \sin 2\pi \left( -h \frac{x}{a} + l \frac{z}{c} \right) \right] S_k \right\} \end{aligned}$$

where

$$C_k = \frac{1}{2\pi k} \left[ \sin 2\pi k \frac{y_2}{b} - \sin 2\pi k \frac{y_1}{b} \right]$$

$$S_k = \frac{-1}{2\pi k} \left[ \cos 2\pi k \frac{y_2}{b} - \cos 2\pi k \frac{y_1}{b} \right].$$

It should be noted that proceeding to the limit  $k = 0$  in these results

$$\begin{aligned} C_0 &= \frac{1}{b} (y_2 - y_1) \\ S_0 &= 0 \end{aligned}$$

which is otherwise evident from the direct integration of the  $F(hkl)$  terms.

In order to compute the section-projections the ordinary method and tabulation used in Fourier sections is used with the exception that the preliminary table consists of values of  $C_k$  and  $S_k$  instead of the usual cos and sine.

## (2) The Method of Projected-Sections.

The expression for a Fourier section at height  $z_1$  is :—

$$\rho(xy z_1) = \frac{1}{V} \sum_{-\infty}^{\infty} \sum_{-\infty}^{\infty} |F(hkl)| \cos \left[ 2\pi \left( h \frac{x}{a} + k \frac{y}{b} + l \frac{z_1}{c} \right) - \alpha(hkl) \right].$$

Assuming that the atoms at  $z = z_1, z_2, z_3 \dots$  etc., have widely differing  $(xy)$  co-ordinates the sections through these atoms may be combined without interference to give :—

$$R(xy)(z_1 \dots z_r) = \sum_{m=1}^r \rho(xy z_m) \\ = \frac{1}{V} \sum_{m=1}^r \left\{ \sum_{k=1}^{\infty} \sum_{l=1}^{\infty} |F(hkl)| \cos \left[ 2\pi \left( h \frac{x}{a} + k \frac{y}{b} + l \frac{z_m}{c} \right) - \alpha(hkl) \right] \right\}.$$

Although this expression looks somewhat clumsy, in practice the computation is little more difficult than that for a single section. Considering the monoclinic space group previously mentioned

$$R(xyz)(y_1 \dots y_r) \\ = \frac{4}{V} \left\{ \sum_{k+l=2n}^{\infty} \sum_0 \left[ F(hkl) \cos 2\pi \left( h \frac{x}{a} + l \frac{z}{c} \right) + F(\bar{h}kl) \cos 2\pi \left( -h \frac{x}{a} + l \frac{z}{c} \right) \right] {}_sC_k \right. \\ \left. - \sum_{k+l=2n+1}^{\infty} \sum_0 \left[ F(hkl) \sin 2\pi \left( h \frac{x}{a} + l \frac{z}{c} \right) + F(\bar{h}kl) \sin 2\pi \left( -h \frac{x}{a} + l \frac{z}{c} \right) \right] {}_sS_k \right\},$$

where

$${}_sC_k = \sum_{m=1}^r \cos 2\pi k \frac{y_m}{b} \\ {}_sS_k = \sum_{m=1}^r \sin 2\pi k \frac{y_m}{b},$$

the tabulation being the same as that for an ordinary section with the exception of the preliminary table which consists of  ${}_sC_k$  and  ${}_sS_k$  instead of the normal cos and sine.

### Applications.

Both of the above methods have received extensive trials on several structures and the following general assessment of their advantages and disadvantages may be made.

**Section Projections.**—The method is most suitable for separating a molecule from its companions in the unit cell, especially when the atoms of the single molecule give a projection free from overlapping. It is found that if one of the boundary planes passes through an area of positive electron density of a molecule, distortion of the resultant projection is liable to occur in this region. For the special case in which the plane is normal to an interatomic bond there is no distortion and the method may be used. As the difference between the planes of section decreases the magnitude of the peaks obtained decreases; equation (2) makes it clear that to bring the results to the same scale as is usual in sections the values should be divided by  $(z_2 - z_1)$ . The particular advantage of the method lies in the simplicity of the preliminary table.

**Projected Sections.**—While this method gives no information not obtainable by means of ordinary sections, it greatly reduces the work involved, compared with that needed for a complete set of sectional syntheses, without in any way reducing the accuracy. The method is equally applicable to line syntheses in which case several atoms can be made to appear on the same line, although here the advantages are not so great, as the preliminary table forms the major operation of this type of synthesis and not many atoms can be obtained on a single line without mutual interference.

### Conclusion.

The following scheme is suggested as one which will materially shorten the time taken for structure analysis without in any way reducing the final accuracy of the results.

- (1) Determination of approximate parameters.
- (2) Refinement by means of projections.
- (3)       "       "       section projections.
- (4)       "       "       projected sections.
- (5) Final check by means of one set of standard section and line syntheses.

This work forms part of a programme of fundamental research on rubber undertaken by the Board of the British Rubber Producers' Research Association.

*British Rubber Producers' Research Association,  
48 Tewin Road,  
Welwyn Garden City, Herts.*

### REVIEWS OF BOOKS.

**Metallurgical Analysis by Means of the Spekker Photo-electric Absorptiometer.** By F. W. HAYWOOD and A. A. R. WOOD.  
(London, Adam Hilger, Ltd.) Pp. xii + 128. Price 18s.

Methods for the colorimetric estimation of metals have been known for 115 years, and their application has been widespread. The accuracy obtainable, however, has not been high, and rarely above suspicion, while considerable chemical manipulation has often been necessary. Until recently the ultimate judgment of equality of colour, whatever type of instrument was used, was the eye, and it was not uncommon for even highly skilled observers to disagree. The advent of photo-electric methods has done much to remove these disadvantages, but realisation of this change was slow. During the last four years, however, chiefly through the pioneer work of E. J. Vaughan, the potentialities of photo-electric instruments have been more widely exploited. This little book contains detailed instructions for twenty-six commonly required metallurgical analyses using the Spekker photo-electric absorptiometer suitable for routine use in control laboratories. They are designed, of course, for one particular instrument, but they must be suggestive to many other workers who do not possess it. The instructions, which are all well attested, are entirely practical—a little more explanation of why certain procedures have been adopted would have been an advantage—and will need to be read with some care if all are to be correctly understood and applied. Nevertheless, the book will be of considerable value in metallurgical laboratories—more so as the original papers are relatively few and widely distributed.

C. B. A.

# THE DIAMAGNETIC SUSCEPTIBILITY OF SOME ALKYL AND ARYL HALIDES.

BY C. M. FRENCH AND V. C. G. TREW.

*Received 22nd November, 1944. As revised 20th December, 1944.*

In a previous paper<sup>1</sup> a comparison was made between the diamagnetic susceptibilities of homopolar and heteropolar halogen atoms in chemical compounds, that is, between the atomic susceptibilities of halogen atoms obtained by Pascal from the molar magnetic mass susceptibilities of halogen-containing compounds, and the ionic susceptibility of the halogen ion in its typically polar compounds such as those with the alkali metals. During the course of that investigation, it was noted that there are considerable variations in the magnetic susceptibility values obtained by different investigators for the simpler halogen substituted derivatives of saturated aliphatic and aromatic hydrocarbons. In addition there were some gaps in the values for these compounds considered as a series. It was shown (*loc. cit.*) that a graphical method could be employed as a considerable guide to the reliability of experimental magnetic susceptibility values for related series of compounds in the same physical state. For the methyl and ethyl halides and the monosubstituted halogen derivatives of benzene, not only were there several differing values reported for experimental susceptibilities, but on plotting the observed molar susceptibility of the compound against the effective atomic number of the halogen atom, a wide divergence from the characteristic graphical relationship was found among members of a related series.

The importance of securing more accurate data for the diamagnetic susceptibility of organic compounds has recently, and since this work was initially undertaken, been stressed by Professor Sugden<sup>2</sup> and by W. R. Angus.<sup>3</sup> Professor Sugden draws attention to the lack of agreement between experimental values for the magnetic susceptibilities of various compounds obtained by different workers and different methods.

Benzene and acetone represent the only two liquids other than water for which any really satisfactory range of investigations has been made by a large number of workers, and even here the extreme values differ by some 1.5 %. Sugden points out that this uncertainty forms the principal difficulty in making any detached analysis of the relation between diamagnetism and chemical constitution, and obscures the causes of the divergences that exist between theoretical and experimental diamagnetic susceptibility values, a divergence that has also been pointed out in previous papers from this laboratory.

In view of the above, we have carried out measurements of the susceptibilities of those compounds which showed the widest discrepancies (see Table I for individual members), and which could be prepared or obtained readily.

In addition, some improvements in experimental technique for the determination of mass susceptibility by the modified Gouy method previously described<sup>4</sup> have been devised. The method described below is suitable for liquids only, but in this limited case, eliminates several sources of error inherent in the original method.

<sup>1</sup> Trew, *Trans. Faraday Soc.*, 1941, 37, 476.

<sup>2</sup> Sugden, 9th *Liversidge Lecture*, *J.C.S.*, 1943, 328.

<sup>3</sup> Angus and Hill, *Trans. Faraday Soc.*, 1943, 39, 185.

<sup>4</sup> Trew and Watkins, *ibid.*, 1933, 30, 1310.

TABLE I.\*

Compound.	Mass Susceptibility. $-\chi \times 10^6$ at 20° C.	Molar Mass Susceptibility. $-\chi_M \times 10^6$ .	Boiling Point (°C.)		Density ( $D_4^{20}$ ).		Refractive Index ( $n_D^{20}$ ).	
			Obs. val.	Lit. val.	Obs. val.	Lit. val.	Obs. val.	Lit. val.
$C_6H_5Cl$ <i>a</i>	0.6218 ± 0.0008	69.95	132	132 <i>d</i>	1.107	1.1066 <i>d</i>	1.5252	1.52479 <i>d</i>
$C_6H_5Br$ <i>a</i>	0.5030 ± 0.0011	78.92	156	155.6 <i>d</i>	1.497	1.497 <i>e</i>	1.5601	1.560 <i>e</i>
$C_6H_5I$ <i>a</i>	0.4476 ± 0.0011	91.30	188	188.45 <i>d</i>	1.832	1.832 <i>e</i>	1.6200	1.621 <i>e</i>
$CHBr_3$ <i>a</i>	0.3253 ± 0.0005	82.22	149.5	149.5 <i>d</i>	2.890	2.890 <i>e</i>	1.5980	1.598 <i>g</i>
$CHI_3$ <i>b</i>	0.2974 ± 0.0071	117.1	M.P. 119	119 <i>d</i>	—	—	—	—
$CCl_4$ <i>a</i>	0.4340 ± 0.0011	66.77	76.8	76.74 <i>d</i>	1.595	1.595 <i>e</i>	1.46110	1.4607 <i>e</i>
$CBr_4$ <i>c</i>	0.2826 ± 0.0014	93.73	M.P. 91	90.1 <i>d</i>	—	—	—	—
$C_6H_5Br$ <i>a</i>	0.5020 ± 0.0007	54.74	38	38.4 <i>d</i>	1.430	1.4307 } <i>d</i> 1.4555 }	1.4232	1.42386
$C_6H_5I$ <i>a</i>	0.4394 ± 0.0009	68.53	72	72.3 <i>d</i>	1.933	1.933 <i>e</i>	1.5141	1.513 <i>f</i>
$C_6H_6$ <i>a</i>	0.7020 ± 0.0007	54.79	80	80.08	0.87897	0.8788 <i>e</i>	1.5012	1.50165 <i>d</i>
$CH_3COCH_3$ <i>a</i>	0.5866 ± 0.0010	34.05	—	—	0.7915	0.7915 <i>e</i>	1.3589	1.3588 <i>e</i>

\* In column 1, (a) refers to susceptibility measurements made on the liquid, (b) to measurements on solutions containing from 11 % to 20 % of iodoform, and (c) to measurements on the solid.

In columns 5, 7 and 9, (d) refers to Heilbron's *Dictionary*, (e) to the International Critical Tables, (f) to Landolt-Börnstein, and (g) to the Chemical Catalog Co.

### Experimental.

Whenever possible, specimens of a single substance from different sources were examined. In all cases the specimens were subjected to rigorous purification by freezing, drying, redistillation in all-glass apparatus, or repeated recrystallisation, and the purity tested by reference to accepted standards of refractive index, density, and boiling or melting point. The specimens were also tested by means of thioglycollic acid for the presence of traces of iron, and shown to be free from this impurity. Determinations of the refractive index (sodium D line at 20° C.) were made using the Abbé refractometer, by Dr. D. M. Simpson, to whom the thanks of the authors are due. The results obtained, and a comparison with the values available in the literature are tabulated in Table I, columns 2-9.

The Gouy balance and method used for determining magnetic susceptibility have been described previously,<sup>4</sup> but a number of special points for ensuring greater precision have since been adopted. Using the D.C. mains current of 220 volts, with a sensitive ammeter and variable rheostat in series with the magnet coils, experiments were carried out to determine the best current strength at which to work, and it was found that at 2.8 amp. a maximum diamagnetic thrust was obtained on the specimen. Hence it was decided to work at a current strength of 3 amp. as being sufficiently low to prevent undue heating of the coils, but safely within the region at which the coils were saturated, thus ensuring a constant field at the lower end of the specimen. Experiments with fields below the saturation point showed that slight variations in the current caused small but measurable variations in pull, and hence it was considered most satisfactory to work just within the region of maximum field. When the pole pieces were 1.25 cm. apart and the current strength 3.0 amp. the field was 5290 gauss. Although a maximum field of 7000 gauss was obtainable using a smaller pole gap, it was found that this necessitated using a smaller volume of specimen, and the errors introduced by this more than neutralised the advantages of the higher field.

An average length of 7 cm. was used for most specimens since at 6 cm. above the centre of the pole pieces of the magnet the field was zero.

In the Gouy method of determining magnetic mass susceptibility

when the top of the specimen is in zero field and the bottom is in field  $H_1$ , the susceptibility is given by:—

$$10^6\chi = \frac{\alpha F}{W} + \frac{10^6 K_{\text{air}} V}{W}$$

where  $\chi$  = mass susceptibility of specimen,  $F$  = force on the specimen in mg.,  $W$  = weight of material in g.,  $K$  = the specific susceptibility of air =  $0.0294 \times 10^{-6}$ , and  $V$  = the volume in c.c.;  $\alpha = \frac{2l \times 10^6 \times 981}{H_1^2 \times 1000}$  and is a constant for the apparatus using a given field and constant length  $l$  of specimen.

It is usual to calibrate the apparatus with specimens of known susceptibility in order to determine  $\alpha$ , the balance constant. In order, however, to eliminate possible sources of error in filling susceptibility tubes to a constant mark, and from possible fluctuations in  $\alpha$ , a modification of the usual method was employed. Consecutive readings were made of the pull or thrust on the tube filled with air, with the standard liquid of known susceptibility, and with the liquid under investigation, using the same tube and suspension wire each time (platinum wire of diameter 0.004 in. was found most satisfactory).

$$\text{Since } 10^6\chi = \frac{\alpha F}{W} + \frac{0.0294 V}{W} \quad . \quad . \quad . \quad (1)$$

where  $F$  is the resultant pull on the liquid under investigation, and the other terms are as before,

$$10^6\chi = \alpha F/W + 0.0294/d \text{ where } d = \text{density of specimen} = W/V.$$

$$\text{Hence for liquid A: } 10^6\chi_A = \alpha F_A/W_A + 0.0294/d_A$$

or  $10^6\chi_A = \alpha F_A/Vd_A + 0.0294/d_A$  where  $V$  = volume of specimen to mark.

$$\text{Similarly for standard liquid B: } 10^6\chi_B = \alpha F_B/Vd_B + 0.0294/d_B$$

$$\text{whence } \frac{10^6\chi_A - 0.0294/d_A}{10^6\chi_B - 0.0294/d_B} = F_A d_B / F_B d_A \quad . \quad . \quad . \quad (2)$$

Substituting the measured values of  $F_A$  and  $F_B$ , the densities  $d_A$  and  $d_B$  of the specimens at the temperature of the experiment, and the known value of  $\chi_B$ , gives  $\chi_A$ , whence

$$10^6\chi_A = (10^6\chi_B - 0.0294/d_B) F_A d_B / F_B d_A + 0.0294/d_A \quad . \quad . \quad (3)$$

The above method eliminates the errors referred to, the only measured quantities being the forces  $F_A$  and  $F_B$  which can be measured to within 0.2 %. An accurate thermometer between the poles of the magnet was used to record the temperature at which experiments were carried out.

In considering the most suitable standards to use for diamagnetic susceptibility measurements, preliminary calibration of the balance and determination of the balance constant was carried out using pure paramagnetic substances as advocated by Sugden for general work with the Gouy balance. In later work with almost exclusively diamagnetic substances it was considered better to use as a standard, some pure diamagnetic substance whose susceptibility was accurately known, since the large paramagnetic pulls are of an entirely different order of magnitude from the diamagnetic measurements being carried out. For precision work it was decided not to use solid substances as the standard, as there may be small errors introduced in packing the material homogeneously in the tube.

Water, benzene, and acetone are the three substances whose susceptibility has been most reliably determined. Of these, water seems at first sight to be the best standard owing to its high susceptibility. Difficulties in obtaining and maintaining water in a high degree of purity make it less suitable as a standard than either benzene or acetone, provided that accepted standard values for these liquids can be obtained. In the case

of the latter two liquids, Sugden <sup>2</sup> has tabulated a large number of available susceptibility values. These figures show that though there is very fair average agreement, some of the values tend to be about a high mean value of  $-0.712 \times 10^{-6}$ , whereas some tend to come considerably lower about a mean of  $-0.702 \times 10^{-6}$ , for benzene. Acetone also shows a similar divergence of values. Angus and Hill,<sup>3</sup> using pure nickel chloride as standard, have recently published results for benzene in which agreement was obtained with the lower values. The discrepancy between individual values appears to be in part due to the use of different initial standards by different investigators. A careful redetermination of the susceptibility of benzene and of acetone was therefore carried out on the basis that the susceptibility of water  $= -0.720 \times 10^{-6}$ ; and using pure conductivity water as standard, results in agreement with the lower figure of  $-0.702 \times 10^{-6}$  for benzene were obtained. Similarly for acetone the lower figure is confirmed (see Table I). Hence the values are suggested as the most satisfactory standards for diamagnetic susceptibility work :—

$\chi$ acetone . . .	$-0.5866 \times 10^{-6}$
$\chi$ benzene . . .	$-0.7020 \times 10^{-6}$
$\chi$ water . . .	$-0.7200 \times 10^{-6}$

It may further be observed that much apparent difference in absolute values could be avoided if agreement could be reached by different workers on a suitable common standard. Both benzene and acetone are satisfactory as they can be obtained in a very high degree of purity. The benzene used in the present investigation was a Kahlbaum specimen whose boiling point and refractive index indicated it to be of a very high degree of purity (see Table I). The acetone used was of analytical purity and had been dried for a month over  $K_2CO_3$ . The susceptibility value for benzene being established in terms of water as standard, the benzene was used as the standard liquid for subsequent susceptibility measurements.

Of the substances measured in this investigation the only one which presented any difficulty was iodoform, and its susceptibility had not previously been recorded, probably because it is the only one of the series in the solid state. Attempts were made to measure the susceptibility of the tightly packed solid powder, but these had to be discontinued as the fine light flakes could not be packed into a homogeneous solid rod of material, and widely varying susceptibility results were obtained owing to unequal packing. Search was then made for a suitable solvent, but in many cases rapid darkening was observed due to the liberation of iodine. Ethyl iodide, one of the liquids being investigated, was found to be the most useful solvent, the solution not darkening appreciably in a time sufficient for susceptibility readings to be made. Even after some darkening had occurred, no appreciable alteration in the susceptibility was obtained.

### Results.

The results obtained for the molar mass susceptibilities of acetone, benzene, and the eleven other substances measured are shown in Table I, column 3. Each result is the mean of six closely agreeing values, and the maximum deviation is recorded in each case. All values are relative to conductivity water  $\chi = -0.720 \times 10^{-6}$ .

It will be noted that the result obtained for benzene, the substance for which the most recent comparative results are available, is in excellent agreement with that obtained by Angus and Hill<sup>3</sup> ( $0.702_3$ ). The value for bromobenzene is in good agreement with that of Bhatnagar, Nevgi and Khanna<sup>5</sup> ( $0.505$  at  $20^\circ C.$ ) but those for benzene and chlorobenzene are considerably lower than those obtained by these three authors ( $0.712$  for benzene, and  $0.644$  for chlorobenzene at  $20^\circ C.$ ). The value for carbon

<sup>5</sup> Bhatnagar, Nevgi and Khanna, *Z. Physik*, 1934, 89, 506.

tetrachloride is in fairly good agreement with that of Rao and Govindarajan<sup>6</sup> for this compound (0.438 at 20° C.).

In Fig. 1(a) the above experimental results for  $\chi$  are plotted, together with values due to Pascal<sup>7</sup> for those compounds which were not measured but are needed to complete the series. The relationships between the susceptibilities of the mono-, di-, tri-, and tetrahalides of the methane

series are shown against the effective atomic number of the halogen atom. Fig. 1(a) shows values for the di-, tri-, and tetrahalides of methane, the upper curve of each pair representing the Pascal theoretical susceptibilities without constitutive correcting constants; i.e. the sum of Pascal's atomic susceptibility values<sup>8</sup> for carbon and the four halogen atoms, corrected to bring to the modern standard for water. The lower curve of each pair represents the experimental values. Fig. 1(b) represents the similar curves for the monohalides of methane, ethane, and benzene, but since accurate values for ethyl chloride and methyl bromide are not available the shape of the curves including these two compounds can only

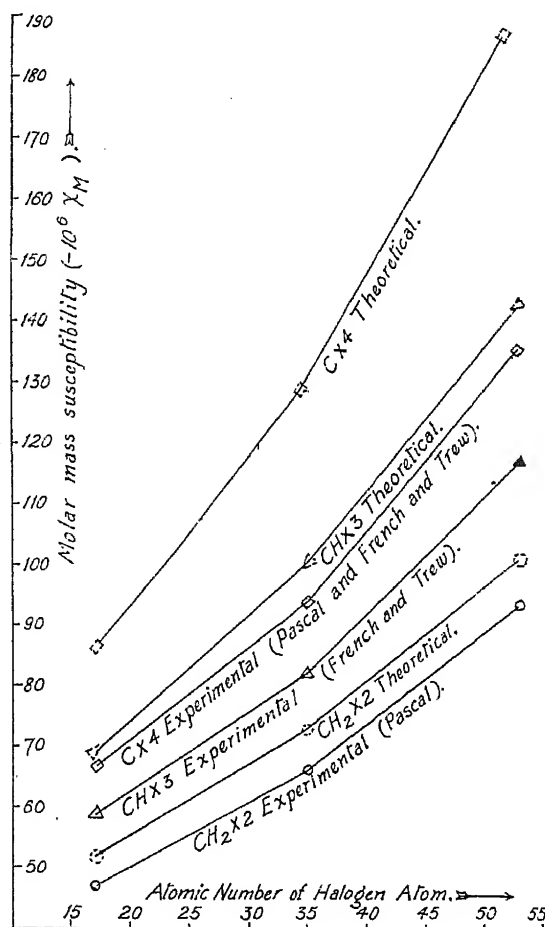


FIG. 1 (a).

be given tentatively and are represented on the graphs by broken lines. In each case the sum  $\Sigma \chi_A$  of the susceptibilities for the constituent atoms, but without constitutive correcting constants for linkings, is plotted close to the experimental curve. The constitutive constants for the linkings were omitted as it was considered that if individual experimental determinations by Pascal were slightly incorrect in certain cases, these would influence the values of his constitutive constants, and one of the objects

<sup>6</sup> Rao and Govindarajan, *Proc. Indian Acad. Sci. A*, 1942, **15**, 35.

<sup>7</sup> Pascal, *Ann. Chimie*, 1910, **19**, 5.

<sup>8</sup> Pascal, *Compt. rend.*, 1911, **152**, 862.



of this investigation was to resurvey the whole question of the causes of deviation between the theoretical susceptibilities and the experimental values.

At the bottom of Fig. 1(b) the characteristic curve for the homopolar halogen atoms using Pascal's atomic susceptibility values for these, is given. The Pascal theoretical curves are mainly included for the purpose of comparison with the slope of the experimental curves, for which they afford an excellent check.

### Discussion of Results.

The values obtained in the present investigation all fall on curves which have the characteristic inflexion point found for the homopolar halogen atoms. Pascal's value for the susceptibility of methyl bromide must obviously be considerably too high as it falls far from the characteristic curve and above the corresponding value for ethyl bromide obtained both by Pascal and by the authors. No value was available for ethyl chloride,

its susceptibility not yet having been measured. We were, under present conditions, unable to obtain a specimen of these two substances whose high volatility would, in any case, render susceptibility measurement difficult by the available apparatus. Hence a provisional value from the graph is suggested for methyl bromide of  $-10^6 \chi_M = 42.7$ , and for ethyl chloride of  $-10^6 \chi_M = 45.0$ .

The curves for the monohalides of methane and ethane run fairly parallel with the theoretical curves, whereas the

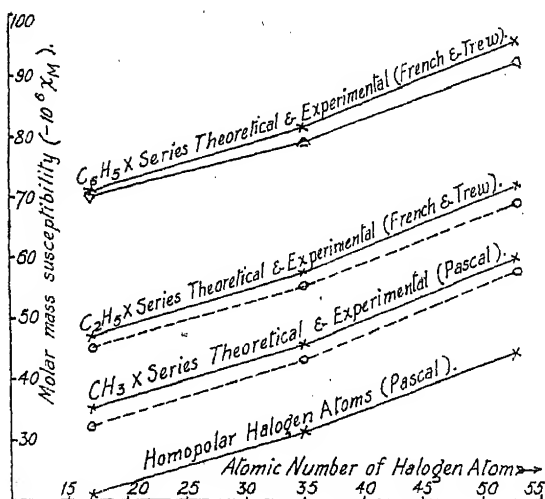


FIG. 1(b).

aryl halide series is more divergent. There is in fact a slight divergence in the case of the ethyl halides, but it is very small and hardly shows up graphically. These divergences are in agreement with Pascal's assignment of larger constitutive correcting constants to bromo-, and iodo-compounds than to chloro-compounds. The curves for the di-, tri- and tetrahalogen series show increasingly greater divergences from the Pascal atomic susceptibility curves—a fact already pointed out by Pascal himself.<sup>7</sup>

The present value for iodoform completes the trihalogen series curve—Fig. 1(a)—and it will be noted that the general shape fits in well with that of the other curves.

A study of Pascal's two papers<sup>7, 8</sup> dealing with the alkyl halides, shows that he fully recognised the anomalous nature of these compounds. He attributed the susceptibility deviations to constitutive effects within the molecule, ascribed in part to the interaction of hydrogen and halogen, producing an effect comparable to the formation of a double bond with consequent lowering of the molar susceptibility; and partly, in polyhalogen compounds, to an interhalogen interaction also serving to lower the dia-

magnetism. Pascal made no general comparative survey of his results for the alkyl halides as a whole, being more concerned to consider anomalous susceptibility values for various specific cases, and he derived constitutive correcting constants to allow for the above effects for various types of halogen-carbon linkings in the molecules. The results obtained in this present investigation bring out certain additional points. For methyl and ethyl halides the graph of the deviations of the experimental susceptibility values from the Pascal additive values plotted against the atomic numbers of the halogen atoms indicates that some correction may be needed in Pascal's constitutive constants. Figs. 2(a) and 2(b) represent the deviation curves obtained in this way. The deviations were calculated from the difference between the experimental susceptibility values given in Table II, column 7, and the sum of the individual atomic susceptibilities (Table II, column 2) as calculated by Pascal's method.\* The sum of Pascal's atomic

\* I.C.T., Vol. VI, p. 349, gives the Pascal atomic and atomic group susceptibilities.

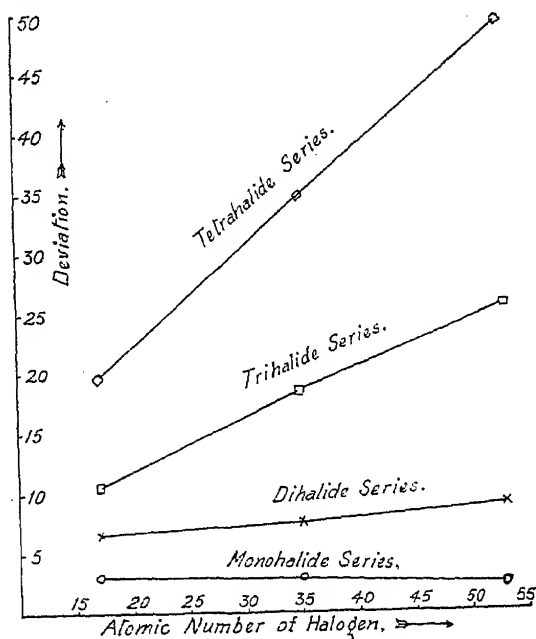


FIG. 2(a).

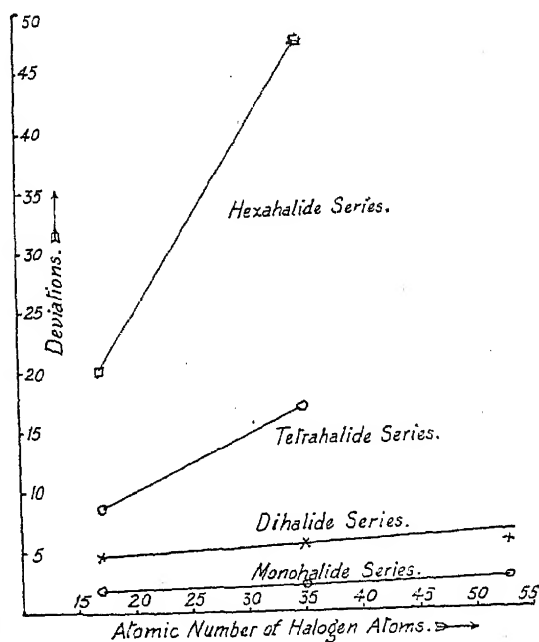


FIG. 2(b).

susceptibilities represents the molar susceptibility of the compound without allowance for constitutive effects within the molecule.

A number of interesting points may be noted from the deviation curves. For both methyl and ethyl monohalides the very slight deviation indicates that there is only a very small constitutive effect of between two and three units of atomic susceptibility, an effect that is appreciably the same for chloro-, bromo- and iodo-compounds. This constitutive effect was considered by Pascal to be due to the interaction of hydrogen and halogen within the molecule serving to lower the diamagnetism, but he derived his constitutive constants from investigations of the higher alkyl halides,<sup>3</sup>

TABLE II.\*  
COMPARISON OF EXPERIMENTAL AND THEORETICAL MAGNETIC SUSCEPTIBILITIES.

1 Compound.	— $10^6 \chi_M$ Theoretical.						
	2 Pascal $\Sigma \chi_A$ .	3a Pauling	3b Pauling.	4 Gray and Cruickshank.	5 Slater.	6 Angus.	7 Expt.
CH <sub>4</sub> . . .	17.7	19.4	19.8	17.7	18.7	17.2	16 <i>xc</i>
CH <sub>3</sub> Cl . .	34.9	39.5	40.0	—	36.2	32.5	32.0 <i>a</i>
CH <sub>2</sub> Cl <sub>2</sub> . .	52.1	59.4	60.7	46.6	53.8	47.9	46.6 <i>a</i>
CHCl <sub>3</sub> . .	69.2	79.3	81.1	61.4	71.4	63.3	58.8 <i>b</i> 58.3 <i>a</i>
CCl <sub>4</sub> . . .	86.4	99.6	101.5	75.9	88.9	78.6	66.8
CH <sub>3</sub> Br . .	45.4	61.1	62.1	—	49.0	45.0	42.8 <i>a</i>
CH <sub>2</sub> Br <sub>2</sub> . .	73.1	102.6	104.6	68.1	79.4	72.7	65.9 <i>a</i>
CHBr <sub>3</sub> . .	100.7	144.2	147.1	93.5	112.2	100.5	82.2 <i>c</i>
CBr <sub>4</sub> . . .	128.4	185.8	189.7	118.9	140.2	128.3	93.7 <i>c</i>
CH <sub>3</sub> I . . .	59.4	83.7	85.0	—	66.2	61.3	57.2 <i>a</i>
CH <sub>2</sub> I <sub>2</sub> . .	101.1	147.9	150.5	97.0	113.8	105.3	93.5 <i>a</i>
CHI <sub>3</sub> . . .	142.7	212.1	215.9	136.8	161.3	149.4	117.3 <i>c</i>
CI <sub>4</sub> . . . .	184.4	276.3	281.3	176.2	208.9	193.5	135.6 <i>a</i>
C <sub>2</sub> H <sub>5</sub> Cl . .	46.8	54.1	55.0	44.0	50.1	45.0	45.0 <i>xc</i>
C <sub>2</sub> H <sub>5</sub> Br . .	57.2	75.8	77.1	54.8	62.9	57.4	55.5 <i>c</i>
C <sub>2</sub> H <sub>5</sub> I . . .	71.2	99.4	100.0	69.2	80.1	73.7	68.5 <i>c</i>
C <sub>6</sub> H <sub>5</sub> Cl . .	70.7	93.9	$\begin{cases} 99.6 \text{ e} \\ 95.0 \text{ f} \end{cases}$	$\begin{cases} 87.9 \text{ e} \\ 51.5 \text{ f} \end{cases}$	86.7	75.7	69.9 <i>c</i>
C <sub>6</sub> H <sub>5</sub> Br . .	81.2	115.6	$\begin{cases} 121.6 \text{ e} \\ 117.0 \text{ f} \end{cases}$	$\begin{cases} 98.7 \text{ e} \\ 62.2 \text{ f} \end{cases}$	99.5	88.1	78.9 <i>c</i>
C <sub>6</sub> H <sub>5</sub> I . . .	95.2	138.2	$\begin{cases} 144.4 \text{ e} \\ 139.9 \text{ f} \end{cases}$	$\begin{cases} 113.0 \text{ e} \\ 76.6 \text{ f} \end{cases}$	116.7	104.4	91.3 <i>c</i>

\* In columns 3b and 4 two different values are given for the theoretical susceptibilities of the benzene derivatives; (e) refers to the internal ionic form, and (f) to the benzenoid form.

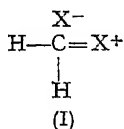
Of the experimental values (a) are those given by Pascal, (c) those of the present paper, and (b) a previously recorded value given by Trew. Values marked *x* are extrapolated ones.

which give a value of 3.07 for the linking  $\text{>C-Cl}$ , and 4.08 for the corresponding bromo-, and iodo-compounds. The above deviation curves indicate that for the first two members of the alkyl series the constitutive effect is rather lower (*i.e.* deviations of 2.9 for methyl chloride, 2.6 for methyl bromide, and 2.2 for methyl iodide, and 1.76, 1.75, and 2.72 for ethyl chloride, bromide, and iodide respectively). The deviations are very nearly constant for all three types of compounds.

In the case of the dihalide deviation curves it will be noted that the constitutive effect due to the halogen-hydrogen interaction is approximately double that in the monohalide series, and in addition the curves show a small but systematic rise in deviation on passing from chloro- to iodo-

compounds. Here, in addition to the small halogen-hydrogen interaction, there is the possibility of a halogen-halogen interaction; a deformation of the halogen atomic fields due to a polarisation effect with consequent lowering of diamagnetism. This effect, as the curves show, is greater for iodine than for bromine and chlorine, in agreement with the theoretical view of the greater polarisability of the iodine atom. The rapidly increasing slopes of the deviation curves for the tri- and tetrahalide series for the methyl compounds, and the incomplete tetrahalide and hexahalide curves for the ethyl compounds show that this polarisation effect increases with the introduction of more halogen atoms into the molecule. The straight line character of the deviation curves indicates the systematically additive nature of these deviations which are proportional to the atomic number of the halogen producing them. From the graphs, constitutive correcting constants could be derived for the various types of linkings with one or more halogen atoms present, but since these will obviously depend on the number of halogen atoms present and will be modified if hydrogen atoms are also present in the molecule, the attempt to deduce such constants is probably of no great value. The graphical representation of the general trend of these effects seems of more use and fully supports Pascal's suggestion made on a more restricted field of material, of two superposed effects within molecules of this type. The larger effect is, however, not the halogen-hydrogen interaction, but the polarisation effect due to the influence of halogen on halogen.

An interesting point in connection with this very much greater depression of magnetic susceptibility obtained when two or more halogen atoms are present is found in Pauling's views<sup>9</sup> on the possible resonance forms of the alkyl halide molecules. He points out that in a methyl halide with only one halogen atom the possibility of resonance to the double-bonded structure is prevented as there are only four orbitals available for bond formation. With two or more halogen atoms present, however, resonance to molecules of the type (I) may occur. Thus the halogen-hydrogen interaction in monohalogen compounds is not to be ascribed to double-bond formation, and the depression, in any case, small, is more likely to be due to a general limiting of the electron spread in the molecule with the introduction of the halogen. With the addition of more halogen atoms the possible resonance to the form indicated above would tend to produce the very considerable lowering of diamagnetism associated with the double bond (*i.e.* a maximum of 5.47 per complete double bond according to Pascal's determinations). Thus it is of interest that in the dihalide series the deviation for the most deformed molecule  $\text{CH}_2\text{I}_2$  (which would be expected to show the greatest double bond forming tendency) is 8.6 susceptibility units, which is greater than that of the monoiodo-compound  $\text{CH}_3\text{I}$  by 6.4 susceptibility units, a figure of the same order of magnitude as that given by Pascal for the double bond. The very much greater magnitude of the deviation for the tri- and tetrahalide series, however, indicates that polarisation of the halogen atoms themselves must also be a cause of lowering of diamagnetism.



When the curves for the susceptibility of the aryl halides are considered (Fig. 1 (b)) an additional effect not found with the alkyl halides is noted. These show a lowering of molar susceptibility of the same order of magnitude as the monohalogen compounds of methane and ethane, but unlike the alkyl compounds, there is a definite increase in the deviation in passing from aryl chloride to iodide. Thus it would appear that a larger benzene constitutive correcting constant should be employed for the aryl bromides and iodides than for the aryl chlorides. This result is in line with evidence from the dipole moments. While the monosubstituted methyl halides all have approximately the same dipole moment, 2.14,

<sup>9</sup> Pauling, *Nature of the Chemical Bond*, 1942, 217.

2.15 and 2.13, there is a fall in moment in the aryl halides from 1.56 to 1.38. Whether the fall in moment is due to a shortening in distance between the carbon and halogen or to a lessening of the charge  $\Delta e$ , the effect from both causes would produce a fall in the diamagnetic susceptibility. Shortening of the linking would cause decrease in the electron spread and lowering of susceptibility, while decrease in the effective charge  $\Delta e$  would cause a lowering of susceptibility since it has been pointed out<sup>1</sup> that homopolar atoms have a susceptibility some three units lower than heteropolar ones.

### Comparison with Theoretical Susceptibilities.

A number of methods for calculating theoretical molar mass susceptibilities are available, all based on the classical formula:—

$$\chi = \frac{-e^2}{6mc^2} \sum \bar{r}^2$$

but differing in the method of arriving at the value of  $\bar{r}^2$ . Thus van Vleck<sup>10</sup> and Pauling<sup>11</sup> have developed one method of obtaining the value of  $\bar{r}^2$  whence

$$\chi = -0.807 \times 10^{-6} \int_0^\infty r^2 (dz/dr) dr.$$

Using the most accurate values for the physical constants involved including the value  $0.5292 \times 10^{-8}$  cm. for  $a_0$ ,<sup>12</sup> we have calculated the theoretical susceptibilities by this method. The values are tabulated in Table II, column 3a, while in column 3b have been included values obtained by allowing for the unequal sharing of charges in the molecule as in the Gray and Cruickshank method which is discussed below. It will be noted that the unequal sharing of charge causes the susceptibility to be slightly higher, but the effect is small and does not mask the fundamental disagreement between theoretical and experimental values.

It is generally considered that the Pauling method gives susceptibilities which are too high, and a method due to Slater<sup>13</sup> using modified values for screening constants in calculating  $\bar{r}^2$  gives susceptibility values which are considerably lower. These are summarised in column 5 of Table II. These values, as in the other cases, are considerably too high for the heavier molecules. Angus<sup>14</sup> suggested that theoretical susceptibility values could be brought into closer agreement with experimental values by taking the *s* and *p* electrons separately in calculating the screening constants. Values calculated by this method using Angus's atomic susceptibility values are given in column 6 of Table II.

None of these methods can be strictly applied to a non-symmetrical molecule, neither is allowance made for bond effects in the molecule, and hence such effects may partially explain the high values obtained theoretically. The only system available so far, for calculation of bond effects is that of Gray and Cruickshank<sup>15</sup> who found it gives excellent agreement for a number of simple organic compounds. It was therefore considered useful to extend this method to this series of halogen compounds. In all cases their bond depressions, where available, have been used, but values for the halogen-carbon link were not available and have therefore been calculated in each case from the monomethyl halides where

<sup>10</sup> Van Vleck, *Physic. Rev.*, 1928, **31**, 587.

<sup>11</sup> Pauling, *Proc. Roy. Soc. A*, 1927, **114**, 181.

<sup>12</sup> R. T. Birge, August 1941. See Taylor and Glasstone, *Physical Chemistry*, Vol. I, p. 21, and Appendix.

<sup>13</sup> Slater, *Physic. Rev.*, 1930, **36**, 57.

<sup>14</sup> Angus, *Proc. Roy. Soc. A*, 1932, **136**, 569.

<sup>15</sup> Gray and Cruickshank, *Trans. Faraday Soc.*, 1935, **31**, 1491.

there is no possibility of interhalogen interaction. These theoretical values are given in Table II, column 4.

It will be noted in general, that of the methods which do not take into account the bond depressions, that of Angus gives results which are on the whole closest to the experimental susceptibilities of the present paper and of other recent work in this field. Even here, as with the other methods, theoretical values for compounds with more than one halogen atom present are higher than the experimental, an effect obviously due to the halogen-halogen interaction previously discussed. In the Gray and Cruickshank method, where bond depressions have been included, a similar result is obtained. Agreement is fair for the lower members of the series, but as before, an increasing divergence between theoretical and experimental values occurs as more halogen atoms are added. Attempts to evaluate bond depressions for the Slater and Angus methods also resulted in a divergence for the polyhalides though of a smaller magnitude.

It is therefore in question whether any standard set of bond depressions for such types of compounds can be evaluated, and it is probable that no general scheme can be evolved to bring the theoretical and experimental susceptibilities into alignment until exact theoretical calculations are available for the halogen-halogen polarisation.

### Summary.

1. Modifications are described in the Gouy method of measuring magnetic susceptibilities in precision work with liquids, details of the experimental conditions leading to the maximum degree of accuracy being given.

2. The suitability of various substances for use as standards is discussed, and the advantages of agreement among different workers on a common substance for this purpose, with an accepted susceptibility value is stressed.

3. Results for the determination of the susceptibilities of various alkyl and aryl halides are given, and where such measurements have not been possible in a given series, a value for the susceptibility is suggested from the graphical relationships.

4. A theoretical discussion on the significance of the results follows, and it has been shown that there is an increasing divergence between the experimental susceptibility values and the theoretical values calculated by any of the different methods available, with increasing number of halogen atoms in the molecule. The importance of this phenomenon which appears to be due to the polarisation effect of one halogen on another, and which was first noted by Pascal, has been confirmed.

*Laboratory for Physical Chemistry,  
Bedford College,  
Regent's Park, London, N.W. 1.*

# MULTIMOLECULAR ABSORPTION.

By A. B. D. CASSIE.

*Received 21st December, 1944.*

## 1. Introductory.

The absorption of gases at pressures of the order of the saturation pressure of the gas has proved less amenable to theoretical treatment than their absorption in monomolecular layers at low pressures. The general description of the phenomena is clear enough: some of the molecules are absorbed on to low energy sites, and as the gas pressure is increased molecules begin to condense on those already absorbed. The fundamental problem is to account for the condensation of molecules in excess of the monolayer. Brunauer, Emmett and Teller<sup>1</sup> have shown that the hypothesis of dipoles induced in the condensed molecules by those absorbed on low energy sites is inadequate to account for the condensation. They suggest that forces similar to those in the liquid state give the condensation, and assuming the multilayers to be identical with the liquid in bulk, they deduce an equation for the absorption isotherm by balancing evaporation and condensation for each layer. Their isotherm equation agrees very well with empirical isotherms; in particular, it has the sigmoid shape characteristic of empirical multimolecular isotherms.

The evaporation condensation mechanism appears plausible and gives agreement with experimental results, but the presence of liquid layers exerting a pressure less than the saturation pressure of the liquid requires considerable thermodynamic justification; for their existence in equilibrium with a vapour pressure less than the saturation pressure means that their free energy must be less than that for the liquid in bulk; and this immediately contradicts the assumption that they are identical with the liquid in bulk. The contradiction could be overcome if the entropy of the molecules in the liquid form was increased on absorption, because the increase in entropy would give the necessary decrease in free energy without requiring a change from the liquid form. The presence of identical molecules on low energy sites does, in fact, give the required increase of entropy: for the molecules in the liquid state can interchange with those on the low energy sites to give an entropy of mixing. It is this entropy of mixing that makes possible the condensation of molecules in the liquid form in the presence of molecules on low energy sites at pressures less than the saturation pressure of the liquid, and the corresponding free energy of mixing will be used in the present paper to deduce equations for multi-molecular absorption isotherms.

## 2. The General Method.

Multi-molecular absorption occurs when the pressure of the absorbed gas is comparable with the saturation pressure of its liquid: thus, if  $p_0$  is the saturation pressure of the liquid at the temperature at which a vapour pressure isotherm is obtained, the pressure,  $p$ , for the isotherm ranges from zero to  $p_0$ . The energy of a molecule in the bulk liquid is therefore a convenient zero of energy, and it is often useful to refer to the absorbed gas-solid system as the liquid-solid system.

The assumption made to deduce the theoretical isotherm is that if  $A$  mol. of the pure liquid are absorbed by unit mass of the solid,  $X$  are

Brunauer, Emmett and Teller, *J.A.C.S.*, 1938, **60**, 309.

absorbed on to low energy sites, and  $(A - X)$  are absorbed on to sites identical with those available to the molecules in the pure liquid. It is a generalised form of the assumption made by Brunauer, Emmett and Teller,<sup>1</sup> and implies that the forces giving the low energy sites are short range forces, or that the system is such that long range forces do not give a range of energies of absorption.

The first problem is to decide whether  $X$  is to be an independent or a dependent variable. The system, including the gas phase, has two degrees of freedom: if the temperature is fixed, the solid-liquid ratio may be varied, but for any value of the temperature and solid-liquid ratio, the pressure is determined, and the number of degrees of freedom is therefore two. According to the phase rule, the number of phases must equal the number of components for a system of two degrees of freedom, and if the solid and liquid are taken as the components, there can be only two phases; one is the gas phase, and the absorbate together with the absorbent can form only one phase. Thus, if the molecules in the liquid multilayers are to be identical with those in the low energy layer, the two, together with the absorbent, must be treated as one phase, and  $X$  becomes a dependent variable determined in terms of  $A$  by the condition that the distribution of the absorbed molecules between the low energy sites and the liquid sites must be such as to make the free energy of the phase a minimum.

The free energy,  $F$ , of this phase is the sum of three free energies:  $F_L$ , the free energy of the molecules in the liquid form,  $F_S$  that of the molecules in the low energy form, and  $F_M$ , the free energy of interchange or mixing of the molecules in the liquid with those in the low energy form.  $F$  is therefore given by:

$$F = F_L + F_S + F_M \quad (1)$$

The chemical potential,  $\mu_A$ , of the absorbed molecules is given by differentiating (1) with respect to  $A$ , or by:

$$\mu_A = \frac{\partial F}{\partial A}, \frac{\partial F}{\partial X} \cdot \frac{\partial X}{\partial A},$$

but the condition that  $X$  should be such as to make the free energy of the phase a minimum for any given value of  $A$  gives:

$$\frac{\partial F}{\partial X} = 0 \quad (2)$$

and

$$\mu_A = \partial F / \partial A \quad (3)$$

The free energy of mixing is readily derived because the mixture is perfect according to Fowler and Guggenheim's definition.<sup>2</sup> The interchange of a molecule on a low energy site with one on a liquid site involves no change in energy, and as the molecules are of the same size on either site they fulfil the conditions for a perfect mixture. The statistical problem is therefore to determine the number of ways of distributing  $X$  sites of one kind and  $(A - X)$  of the other amongst  $A$  molecules. It is:

$$g(X, (A - X)) = \frac{A!}{X!(A - X)!}$$

and the free energy of mixing is given by  $-RT \log(g)$ , or by:

$$\frac{F_M}{RT} = -A \log A + X \log X + (A - X) \log (A - X). \quad (4)$$

The free energy of the molecules in the liquid may be written:<sup>2</sup>

$$\frac{F_L}{RT} = -(A - X) \log j_L \quad (5)$$

<sup>2</sup> Fowler and Guggenheim, *Statistical Thermodynamics*, Cambridge, 1939, Ch. VIII.



where  $j_L$  is the partition function for molecules in the liquid, including the configurational partition function. The free energy of the molecules in the low energy state depends on the form assumed for this state: if the molecules are on localised sites, the free energy expression will be of one form, if they are mobile, it will be of another. If it is of the simple form assumed for the liquid in equation (5), no absorption isotherm is possible. Thus if  $F_g$  is written:

$$\frac{F_g}{RT} = -X \log j_L - \frac{wX}{RT} \quad (6)$$

Where  $w$  is the heat evolved per mol. of molecules adsorbed into the low energy state, and  $j_L$  is the partition function for these molecules which is assumed independent of  $X$ . Equation (2) now gives:

$$\frac{A - X}{X} = \frac{j_L}{j_A} e^{-w/RT}$$

or  $X = A/(1 + \beta') \quad (7)$

where  $\beta'$  is given by:

$$\beta' = \frac{j_L}{j_A} e^{-w/RT} \quad (8)$$

Equation (3) gives the chemical potential of the adsorbed molecules as:

$$\frac{\mu_A}{RT} = \log \frac{A - X}{A} - \log j_L \quad (9)$$

The chemical potential can be related to the pressure in the gas phase by the usual procedure. Thus,  $\mu_G$ , the potential of the molecules in the gas phase may be written: <sup>2</sup>

$$\mu_G = \alpha + RT \log p \quad (10)$$

where  $\alpha$  is a function of temperature but not of pressure. Equating  $\mu_G$  and  $\mu_A$  gives:

$$RT \log \frac{A - X}{A} - RT \log j_L = \alpha + RT \log p \quad (11)$$

For the pure liquid,  $X$  is zero and equation (11) becomes:

$$-RT \log j_L = \alpha + RT \log p_0 \quad (12)$$

and subtracting (12) from (11) gives:

$$\frac{p}{p_0} = \frac{A - X}{A} \quad (13)$$

Substituting for  $X$  from equation (7), gives for the isotherm:

$$\frac{p}{p_0} = \frac{\beta'}{1 + \beta'} \quad (14)$$

or there is only one pressure at which absorption can occur and the extent of the absorption is independent of the pressure.

One concludes, then, that the condition for an isotherm to exist is that the free energy of one of the two states must depend on the number of molecules per unit volume of the state, and not merely on the total number of molecules as has been assumed in equations (5) and (6). The low energy molecules are usually assumed to be those with a free energy depending on the number of molecules per unit volume, and this procedure will be followed here.

This result can, of course, be deduced directly from the phase rule. If the free energies for both states of the adsorbed molecules are independent of the number of molecules per unit volume, there can be no relation between the amount of adsorbate and adsorbent; the adsorbent

therefore becomes a separate phase and the number of degrees of freedom is reduced to one.

### 3. Multimolecular Absorption with Localised Sites.

If there are  $B$  localised sites per unit mass of the absorbing solid, the free energy for  $X$  molecules absorbed on to the sites is given by:<sup>3</sup>

$$\frac{F_s}{RT} = -B \log B + X \log X + (B - X) \log (B - X) - X \log j_s - \frac{wX}{RT} \quad (15)$$

where the zero of energy is that for molecules in the liquid state,  $w$  is the heat evolved when one mol. of molecules is absorbed from the liquid state on to the localised sites, and  $j_s$  is the partition function for a molecule absorbed on to the sites. Using this value for  $F_s$  in equation (1), and the expressions (4) and (5) for  $F_M$  and  $F_L$ , the condition (2) for the free energy of the phase to be a minimum becomes:

$$(A - X)(B - X) = \beta X^2 \quad (16)$$

where 
$$\beta = \frac{j_L}{j_s} e^{-w/RT} \quad (17)$$

As equation (15) does not contain  $A$  explicitly, the chemical potential of the absorbed molecules will again be given by equation (9), and the ratio of the vapour pressure to the saturation vapour pressure will be given by (13).  $X$  is, of course, determined by equation (16). Solving (16) for  $X$ , taking the lower root of the equation which corresponds to the minimum free energy, and substituting in (13) gives the isotherm equation as:

$$A = \frac{Bp}{(p_0 - p) \left\{ \beta + (1 - \beta) \frac{p}{p_0} \right\}} \quad (18)$$

Equation (18) is identical in form with that derived by Brunauer, Emmett and Teller<sup>1</sup> for multimolecular absorption using their evaporation-condensation mechanism.  $B$  has the same interpretation on both analyses, although the present analysis does not restrict the sites to a surface. They may be distributed throughout the solid as in a hygroscopic gel, and the theory may be used to analyse the absorption isotherms of gels; an example of this analysis is given in another paper.<sup>4</sup>

Brunauer, Emmett and Teller obtained the coefficient  $\beta$  in terms of uncertain evaporation and condensation coefficients whereas it is given here in terms of the heat of absorption on to the localised sites and the ratio of the liquid to the localised partition functions. A more direct physical interpretation may be obtained by writing it in terms of characteristic vapour pressures rather than in terms of partition functions. Thus, equation (15) gives the chemical potential,  $\mu_s$ , of the localised molecules when mixing is absent as:

$$\mu_s = RT \log \frac{X}{B - X} - RT \log j_s - w, \quad (19)$$

and the vapour pressure in equilibrium with the localised molecules is obtained by equating  $\mu_s$  to  $\mu_g$  as given by (10). A characteristic vapour pressure for localised sites is that,  $p_1$ , when one half of the sites is occupied;  $X$  is then  $\frac{1}{2}B$ , and equations (19) and (10) give:

$$-RT \log j_s - w = \alpha + RT \log p_1 \quad (20)$$

<sup>3</sup> Fowler and Guggenheim, *Statistical Thermodynamics*, Cambridge, 1939, Ch. X.

<sup>4</sup> Cassie, *following paper*.

Subtracting (12) from (20) gives :

$$\beta = \frac{j_L}{j_s} e^{-w/RT} = \frac{p_{\frac{1}{2}}}{p_0} \quad . \quad . \quad . \quad (21)$$

so that  $\beta$  is the ratio of the vapour pressure required to fill one half of the localised sites when mixing is absent, to the saturation vapour pressure of the pure liquid.

When  $p_0$  is large compared with  $p_{\frac{1}{2}}$  and  $p$ , equation (18) reduces to the Langmuir isotherm. When it is large compared with  $p_{\frac{1}{2}}$ , the isotherm is :

$$A = \frac{Bp}{p_{\frac{1}{2}} + p - p^2/p_0} \quad . \quad . \quad . \quad (22)$$

which is similar to Langmuir's isotherm until  $p$  approaches  $p_0$  when  $A$  increases rapidly. This extreme sigmoid isotherm is well illustrated by Katz's experiments<sup>5</sup> on the absorption of water by quartz and anorthite. His curves show that  $p_{\frac{1}{2}}$  is very small compared with the saturation pressure of water vapour, and as  $p$  is increased towards  $p_0$  the absorption rapidly increases. The results of Lehner and McHaffie<sup>6</sup> on the absorption of water by platinum, amalgamated platinum, and amalgamated silver also provide examples of the extreme sigmoid isotherm. They were unable to detect absorption on these surfaces until a high relative humidity was attained when absorption increased rapidly with increasing vapour pressure. The authors concluded that a critical vapour pressure was required before absorption occurred, but it is clear that they were dealing with a system in which  $p_{\frac{1}{2}}$  is very small compared with  $p_0$ , and that they were unable to detect the small amount absorbed on to localised sites; when, however,  $p$  was increased until it approached  $p_0$ , the absorption increased rapidly in accordance with equation (22).

Another special case of equation (18) arises when  $p_{\frac{1}{2}}$  is equal to  $p_0$ ;  $\beta$  is then unity, and the isotherm becomes :

$$A = \frac{Bp}{p_0 - p} \quad . \quad . \quad . \quad (23)$$

which is the isotherm for a perfect solution.

Intermediate values of  $\beta$  give curves of varying sigmoid shape, and a large amount of experimental data is available for these isotherms. Brunauer, Emmett and Teller<sup>1</sup> examined much of it for the absorption of argon, nitrogen, carbon dioxide, and other gases by catalytic and other surfaces at low temperatures. They found excellent agreement of the empirical isotherms with those predicted by equation (18). Their examination need not be repeated here although it may be taken as confirming the present theory. The coefficient  $B$  has the same interpretation on both analyses, but it may be pointed out that its value is most readily deduced from empirical isotherms by use of equation (13): this equation determines  $X$  for any point on the isotherm, and the limiting value of  $X$  as  $A$  is increased gives a good approximation to  $B$ . The values so deduced are not significantly different from those given by Brunauer, Emmett and Teller. When  $B$  is known,  $\beta$  may be determined from equation (16). Equation (16) can also be used to determine both  $B$  and  $\beta$  when the values of  $X$  for two points on the isotherm have been obtained from equation (13).

In their interpretation of the empirical data, Brunauer, Emmett and Teller assumed that the evaporation and condensation coefficients were such that  $\beta$  would be given by  $e^{-w/RT}$ . This assumption would be true if  $j_L$  were equal to  $j_s$ , but localisation of the molecules is likely to decrease the partition function considerably. A rough estimate of the

<sup>5</sup> Katz, *Proc. Acad. Sci. Amsterdam*, 1912, **15**, 449.

<sup>6</sup> Lehner and McHaffie, *J. Chem. Soc.*, 1925, **127**, 1568.

decrease and its effect on  $\beta$  can be obtained by use of the oscillator model for the liquid and for the localised molecules. If the internal degrees of freedom, including rotations of the molecules, are assumed the same in the gas, liquid and localised states, the partition function for the liquid may be written :<sup>2</sup>

$$j_L = \left(\frac{kT}{h\nu_L}\right)^3 \cdot e \cdot j_G \quad . \quad . \quad . \quad . \quad (24)$$

where  $j_G$  is the partition function for the molecules in the gas state, and  $\nu_L$  is an effective vibration frequency for the three harmonic oscillations replacing the three translational degrees of freedom. The term  $e$  appears because the molecules are not localised in the liquid. Similarly the partition function for the localised molecules may be written :

$$j_S = \left(\frac{kT}{h\nu_S}\right)^3 j_G \quad . \quad . \quad . \quad . \quad (25)$$

where  $\nu_S$  is the corresponding effective vibration frequency.  $\beta$  is now given by :

$$\beta = \left(\frac{\nu_S}{\nu_L}\right)^3 \cdot e \cdot e^{-w/RT} \quad . \quad . \quad . \quad . \quad (26)$$

The hypothesis of localised sites requires the minimum value for  $\nu_S$  to correspond to a characteristic temperature,  $h\nu_S/k$ , of twice the working temperature or more. Thus, absorption of argon at 100° K. would require a characteristic temperature of 200° K. or more, and the minimum value of  $\nu_S$  would be  $4 \times 10^{12}$  per sec.

The effective vibration frequency for the liquid state is more difficult to estimate. If the chemical potential,  $\mu_G$ , for the saturated vapour be written in the usual form :<sup>2</sup>

$$\mu_G = -RT \log \frac{kT(2\pi m kT)^{\frac{3}{2}}}{h^3} - RT \log j_G + \chi + RT \log p_0 \quad (27)$$

where the zero of energy is that of molecules in the pure liquid, and  $\chi$  is the heat of evaporation, equations (5), (24) and (27) give :

$$p_0 = \frac{(2\pi m)^{\frac{3}{2}}}{(kT)^{\frac{3}{2}}} \cdot \frac{\nu_L^3}{e} \cdot e^{-\chi/RT} \quad . \quad . \quad . \quad (28)$$

which may be compared with the relation corresponding to Tronton's rule :<sup>2</sup>

$$p_0 \sim 2.5 \times 10^{10} e^{-\chi/RT} \text{ dynes/cm.}^2 \quad . \quad . \quad . \quad (29)$$

to give  $\nu_L$ . Comparison of equations (28) and (29) give  $\nu_L$  for argon at 90° K. as around  $1.3 \times 10^{12}$  oscillations per sec.

These values of  $\nu_L$  and  $\nu_S$  when inserted in equation (26) give the factor  $(\nu_S/\nu_L)^3 \cdot e$  as of the order of 50 or more. Hence, even without any suppression of rotational degrees of freedom on localisation, the assumption that  $\beta$  is given by  $e^{-w/RT}$  is likely to err considerably, and Brunauer, Emmett and Teller's values for  $\omega$  are likely to be much too small. Comparison of their values for the absorption of argon, nitrogen and carbon dioxide on silica gel with the measured values of Magnus<sup>7</sup> shows that they are, in fact, too small: Magnus gives  $\omega$  as 1000 cal. per mol. for  $A$ , 1700 for  $N_2$ , and 3000 for  $CO_2$ , as compared with the values 600, 800 and 1300 cal. deduced by Brunauer, Emmett and Teller. Assuming Magnus' values to be correct, and using Brunauer, Emmett and Teller's values for  $\beta$  in equation (17), the ratio of  $j_L$  and  $j_S$  is found to be 10 for  $A$ , and 100 for  $N_2$  at 90° K., and 1000 for  $CO_2$  at 195° K. The value for  $A$  seems

<sup>7</sup> Magnus, *Z. physikal. Chem.*, **A**, 1929, **143**, 265.

rather small, whilst the large value for  $\text{CO}_2$  suggests that rotation of the molecules may be suppressed to some extent on localisation.

It is worth remarking that the heat of absorption of molecules on to localised sites is usually large and if the ratio of  $p_1$  to  $p_0$  were determined solely by the heat of absorption, it would usually be small, and the isotherms would usually be of the extreme sigmoid form obtained by Katz<sup>5</sup> for absorption of water vapour by quartz and anorthite. The decrease of the partition function on localisation compensates considerably for the large heat of absorption and increases  $p_1$  to such an extent that normal sigmoid curves become the general rather than the exceptional form for multimolecular isotherms.

#### 4. Multimolecular Absorption on a Mobile Monolayer.

The free energy function for a mobile monolayer depends on the form of the monolayer, and the form assumed here is that of a perfect gaseous film. It is doubtful if a condensed monolayer could lead to an absorption isotherm, as the free energy for such a film does not depend on the number of molecules per unit area, and a suitable free energy function would lead to a result similar to that of equation (14). This deduction will hold whether the film be monomolecular or multimolecular, and it is interesting to note that Adam<sup>8</sup> remarks that in every case yet worked out, the absorbed films of soluble substances are of the gaseous type. There is, of course, no essential difference between the absorption of a solute at the surface of a solution, and absorption from the gas phase, and Adam's remark confirms our general conclusion that an absorption isotherm, or a surface absorption that varies with concentration can only occur with a monolayer whose free energy varies significantly with the number of molecules per unit area, as is the case for gaseous films.

The free energy for a perfect gas film may be written :<sup>2</sup>

$$\frac{F_g}{RT} = -X \log j_s + X (\log X - 1) - wX \quad . \quad . \quad (29)$$

where  $j_s$  is the complete partition function of an absorbed molecule. Inserting this expression for  $F_g$  in equation (1) and minimising  $F$  with respect to  $X$  gives :

$$\frac{A - X}{X^2} = \frac{j_s}{j_g} e^{-w/RT} \quad . \quad . \quad . \quad (30)$$

Equation (13), relating  $A$  to the vapour pressure, is again unchanged as (29) does not contain  $A$  explicitly. Solving equation (30) for  $X$  and substituting in (13) gives the isotherm equation as :

$$A = \frac{p/p_0}{\beta(1 - p/p_0)^2} \quad . \quad . \quad . \quad (31)$$

The isotherm represented by (31) is totally different from that given by equation (18). It is everywhere convex to the pressure axis whereas that for the localised monolayer is strongly concave to the pressure axis for low pressures, and gradually changes with increasing pressure to the convex form. The literature does not contain many examples of isotherms of the form (31), and those that appear similar in form to (31) may not be due, in fact, to absorption on a mobile film ; for when  $B$  and  $\beta$  are both small for absorption on to localised sites, the isotherm may appear everywhere convex to the pressure axis merely because the measurements of pressure and of the amount of gas absorbed have not been sensitive enough to detect the low pressure region of the isotherm. If, however, the heat evolved when molecules from the liquid are absorbed is small or negative,

<sup>8</sup> Adam, *Physics and Chemistry of Surfaces*, Oxford, 3rd ed., 1941, p. 116.

the monolayer is almost certain to be mobile; for equation (21) shows that if  $\omega$  is negative and  $j_L$  is greater than  $j_s$ , as is required for localised sites,  $p_{\frac{1}{2}}$  will be much greater than  $p_0$ , and absorption would appear only at pressures greater than the saturation pressure. Hence absorption at pressures less than  $p_0$  when accompanied by small or negative values of  $\omega$  implies the presence of a mobile monolayer.

The one example that clearly fulfils these conditions is the absorption of water vapour by carbon. Coolidge<sup>9</sup> has made careful measurements of the absorption of water by carbon, and he finds that at a given relative humidity it increases with increasing temperature, indicating a negative value for  $\omega$ . He finds, too, that the isotherms are totally different from normal isotherms in that they are everywhere convex to the pressure axis. It is clear, then, that in this case the monolayer is gaseous. Bangham<sup>10</sup> has also concluded from his experiments on the swelling of charcoal on absorption of water vapour that the monolayer is of the gaseous type.

Quantitative agreement of equation (31) with Coolidge's empirical isotherms is surprisingly good in view of the difficulty of obtaining reproducible isotherms for the carbon-water vapour system. Thus, Coolidge's tabulated empirical observations can be inserted in equation (31) to give values for  $\beta$ . His observations at 100° C. give four values ranging from 0.09 to 0.10, and at 156° they range from 0.06 to 0.07. The lower temperature isotherms give less consistent values for  $\beta$ , the mean at 61° being around 0.15, and at 20°, 0.2. The poorer agreement at the lower temperatures is not surprising as the measurements are more difficult, and deviations of the monolayer from the perfect gas form will become more pronounced.

The temperature variation of  $\beta$  will be primarily due to the exponential term,  $e^{-\omega/RT}$ , and the graph of  $\log \beta$  plotted against the reciprocal of the absolute temperature should be linear. The values for the three highest temperatures do, in fact, lie accurately on a straight line whose slope gives  $\omega$  as -2200 cal. per mol. of water absorbed into the monolayer.

The value of  $\beta$  depends, of course, on the area available to the molecules in the carbon. Thus, the complete partition function for a molecule in the gas film may be written:<sup>3</sup>

$$j_s = a \cdot \frac{2\pi m kT}{h^2} \cdot \frac{kT}{h\nu_s} \cdot j_g \quad (32)$$

where  $a$  is the area available per g. of carbon, and the term  $(kT/h\nu_s)$  is the contribution of vibrations normal to the surface to the partition function. Equations (32) and (24) give:

$$\frac{1}{\beta} = \frac{j_s}{j_L} e^{\omega/RT} = a \frac{2\pi m \nu_L^3}{(kT) \cdot e \cdot \nu_s} e^{\omega/RT} \quad (33)$$

The area available to the molecules could be estimated from the value of  $\beta$ , if  $\nu_L$  and  $\nu_s$  were known. The value of  $\nu_L$  is probably around  $10^{12}$  oscillations per second, and  $\nu_s$  may be taken as around  $4 \times 10^{12}$ ; these values are probably no better than guesses for water, but they should indicate whether or not the observed values of  $\beta$  are of the right order of magnitude.  $\beta$  is 0.1 at 100° C., or  $1/\beta$  is 10 mg. per g. of carbon, or roughly  $3 \times 10^{20}$  molecules per g. of carbon. Inserting these values in equation (33) together with  $\omega$  as -2200 cal. per mol., gives  $a$  as 2000 sq. metres per g. of carbon. McBain<sup>11</sup> gives the surface of carbon as being as great as 10,000 sq. metres per g. and the rough calculated value of 2000 sq. metres is a very reasonable one.

<sup>9</sup> Coolidge, *J.A.C.S.*, 1927, 49, 712.

<sup>10</sup> Bangham, *Proc. Roy. Soc., A*, 1932, 138, 162.

<sup>11</sup> McBain, *Sorption of Gases by Solids*, Routledge, 1932, p. 13.

### Summary.

A general statistical method is given for dealing with the problem of a single species of molecule which may assume either of two forms in a single phase. The molecules may interchange between the two forms to give a free energy of interchange or mixing, and the distribution of the molecules between the two forms is determined by the condition that the total free energy of the phase should be a minimum.

The method is applied to multimolecular absorption which takes place (a) in the presence of localised sites, or (b) on to a mobile monolayer. The equation deduced for the absorption isotherm with localised sites is identical with that deduced by Brunauer, Emmett and Teller using an evaporation-condensation mechanism, although a more precise interpretation of the parameters in the equation is now possible. The equation represents a sigmoid curve which is concave to the pressure axis at low pressures.

It is shown that a mobile monolayer must be gaseous to give an absorption isotherm or to give surface absorption which varies with the concentration of the solute in the solution.

The isotherm for multimolecular absorption with a gaseous monolayer is everywhere convex to the pressure axis. The absorption of water vapour by carbon seems to be the one example of this type of absorption which has been fully established by experiment. The empirical isotherms agree excellently with the equation derived theoretically. Heat is absorbed when water molecules pass from water in bulk to the monolayer, the value per mol. being 2200 cal. The area covered by the gaseous film is also estimated.

### Acknowledgments.

I am much indebted to my colleagues, particularly Mr. R. C. Palmer and Mr. B. H. Wilsdon, Director of Research, for discussion of these problems, and my thanks are due to the Council of the Wool Industries Research Association for permission to publish this account.

---

## ABSORPTION OF WATER BY WOOL.

By A. B. D. CASSIE.

*Received 21st December, 1944.*

### 1. Introductory.

The theory of water absorption by textile fibres has varied from the solution hypothesis of Katz<sup>1</sup> to the capillary pore theory as applied by Hedges<sup>2</sup> to wool, and Peirce's theory<sup>3</sup> that part of the water is localised at certain units in the fibre with a large heat evolution, whilst the remainder fills the spaces available under attractive forces like those in a liquid without heat evolution. Peirce's theory is now the most commonly accepted one for textile fibres and Speakman<sup>4</sup> has recently applied it

<sup>1</sup> Katz, *Kolloidchem. Bei.*, 1917-18, 9, 1.

<sup>2</sup> Hedges, *Trans. Faraday Soc.*, 1926, 22, 178.

<sup>3</sup> Peirce, *J. Textile Inst.*, 1929, 20, T133.

<sup>4</sup> Speakman, *Trans. Faraday Soc.*, 1944, 40, 6.

to an analysis of the absorption isotherm of wool. Peirce established his theory by an evaporation-condensation mechanism, and although it is plausible from this point of view, it requires considerable explanation when examined thermodynamically. The most important feature of the absorption of water by textile fibres is that they absorb large quantities of water when exposed to water vapour pressures less than the saturation vapour pressure for pure water; they have, in fact, a water vapour pressure isotherm. This means that the free energy of the absorbed water must be less than that of liquid water at the same temperature. The free energy of the fraction absorbed with evolution of heat presents no difficulty, but it is difficult to account directly for the decrease in free energy of the fraction absorbed without evolution of heat. It could be assumed, of course, that this fraction is held in capillary pores, and Speakman<sup>4</sup> does refer to a fraction of the water as capillary water. His analysis postulates, however, a fraction of water absorbed on to localised sites with no evolution of heat, and as these sites are fully occupied at saturation pressure, the free energy for this part of the absorbed water must be much greater than that of liquid water.

Peirce's theory can be made consistent thermodynamically if the hypothesis of mixing<sup>5</sup> of the two fractions of water is used. This hypothesis has been applied successfully to a general analysis of multimolecular absorption and it leads to an equation for the absorption isotherm which is identical with that deduced by Brunauer, Emmett and Teller<sup>6</sup> for the particular case of multimolecular absorption on a surface using an evaporation-condensation mechanism. The present paper applies this hypothesis to an analysis of the wool absorption isotherm.

Analysis of the isotherm cannot be made directly with the observed curve because, as Barkas<sup>7</sup> has shown, the vapour pressure observed for water absorbed in a rigid gel is considerably influenced by the mechanical constraint exerted on the water by the swelling of the gel. The mechanical constraint exerts a hydrostatic pressure on the absorbed water, and as this pressure depends on the degree of swelling, the observed water vapour pressure also depends on the degree of swelling. An analysis of the wool-water isotherm is therefore possible only when the observed isotherm has been reduced to that for water absorbed under one hydrostatic pressure.

## 2. The Wool-water Isotherm at One Hydrostatic Pressure.

The change in hydrostatic pressure due to swelling can be calculated when the amount of swelling and the mechanical properties of the fibre are known. The swelling of wool fibres on absorption of water has been determined,<sup>8</sup> and Speakman<sup>9</sup> has given load-elongation curves for wool at various regains.\* Poisson's ratio is unknown, and to make possible an estimate of the change of hydrostatic pressure, it will be taken as 0.25, which is a usual value for solids. It is also necessary to make the rather drastic assumption that the fibres are isotropic in elastic properties.†

<sup>5</sup> Cassie (*preceding paper*).

<sup>6</sup> Brunauer, Emmett and Teller, *J.A.C.S.*, 1938, 60, 309.

<sup>7</sup> Barkas, *Trans. Faraday Soc.*, 1943, 28, 205.

<sup>8</sup> W.I.R.A., *private publication*, 1923, No. 19.

<sup>9</sup> Speakman, *J. Textile Inst.*, 1927, 18, T446.

\* Regain is the amount of water absorbed expressed as a percentage of the dry weight.

† *Note added 26th March, 1945.*—Since this paper was written, Mr. Warburton has been measuring the elastic constants of the closely allied keratin, horn, in these laboratories. He finds that  $\sigma$  is around 0.35, and taking into account the anisotropy of the wool fibre as revealed by its small longitudinal swelling, the coefficient of  $E\Delta r/r$  in equation (1) is found to be around 2, the value used for the calculations in this paper. The calculations are thus likely to be much



The values obtained for the change of hydrostatic pressure on swelling can thus be no better than estimates, but as any analysis of the isotherm must use an absorption curve that relates to one hydrostatic pressure, it is essential that the calculations be made.

If  $\Delta V$  is the swelling from zero moisture content, the change in hydrostatic pressure,  $\Delta P$ , is given by :

$$\Delta P = k \frac{\Delta V}{V}$$

where  $V$  is the volume of the fibres at zero regain, and  $k$  is their bulk modulus. Writing  $k$  in terms of Young's modulus,  $E$ , and Poisson's ratio,  $\sigma$ , gives :

$$\Delta P = \frac{E}{3(1 - 2\sigma)} \cdot \frac{\Delta V}{\Delta} = \frac{E}{(1 - 2\sigma)} \cdot \frac{\Delta r}{r} \quad (1)$$

where  $r$  is the radius of the fibre and  $\Delta r$  is the increase of radius on swelling;  $\Delta r/r$  is known,<sup>8</sup> and values for the product  $(E \cdot \Delta r/r)$  were obtained by reading the load in gm./cm.<sup>2</sup> at the known extension from Speakman's load-extension curves for wool at different relative humidities. Equation (1) then gives the change in hydrostatic pressure due to swelling.

When the change in hydrostatic pressure is known, reduction of the observed vapour pressures to a common hydrostatic pressure is made by the usual thermodynamic relation :<sup>10</sup>

$$\Delta P = \frac{RT}{M_v} \log \frac{h_0}{h} \quad (2)$$

where  $h_0$  is the observed vapour pressure,  $h$  is the vapour pressure for a common hydrostatic pressure, and  $M_v$  is the molar volume of the absorbed water. Inserting numerical values in (2), and taking  $M_v$  as 18 c.c. gives :

$$\Delta P = 3.2 \times 10^6 \log_{10} h_0/h \quad (3)$$

Table I gives the reduction of the 25° C. isotherm for wool to a common hydrostatic pressure using equations (1) and (3), and Fig. 1 shows the

TABLE I.—REDUCTION OF WATER VAPOUR PRESSURE ISOTHERM FOR WOOL.

Rel. Humidity %.	Regain. %.	Diam. Swelling %.	$\Delta P$ gm./cm. <sup>2</sup> $\times 10^6$ .	$\frac{h_0}{h}$	25° C.	
					$h_0$	$h$
					mm. of Mercury.	
0.0	0	0.0	0.0	1.00	0.0	0.0
2.5	2	0.64	4	1.33	0.6	0.45
12.0	5	2.0	16	3.15	2.9	0.92
21	7	2.9	22	4.85	5.0	1.03
35	10	4.4	22	4.85	8.4	1.74
60	15	7.0	21	4.5	14.4	3.2
78	20	10	16	3.15	18.6	5.9
88	25	13	14	2.75	21.0	7.7
95	30	16	12	2.35	22.7	9.6
100	33	18	10	2.05	23.8	11.6

more accurate than was originally realised. King's work<sup>11</sup> on the diffusion of water vapour through horn also confirms the analysis. I am indebted to Mr. Warburton and Mr. King for allowing me to quote their results before publication.

<sup>10</sup> Guggenheim, *Modern Thermodynamics*, Methuen, 1933, p. 63.

<sup>11</sup> King, *Trans. Faraday Soc.*, in the press.

observed and reduced isotherms. The outstanding feature of the reduced isotherm is that it is no longer a sigmoid curve. Much of the sigmoid shape of absorption isotherms of gels seems, in fact, to be due to the mechanical properties of the gel: the hydrostatic pressure increases as the swelling increases giving a rapid rise in the vapour pressure with regain; but when the swelling exceeds a value depending on the swelling material, 4 % in the case of wool, the elastic modulus decreases so rapidly that the hydrostatic pressure decreases with further increase in regain; the rate of increase of vapour pressure with regain then decreases to give the characteristic inflexion of the isotherm. Any reduction of the observed isotherm to one hydrostatic pressure must remove much of the sigmoid shape of the curve, and although the data of Table I may not be of much accuracy, the shape of the reduced curve is almost certainly correct. Thus the most uncertain factor in the calculations is the value chosen for  $\sigma$ , but a change in  $\sigma$  does not alter the shape of the reduced curve.

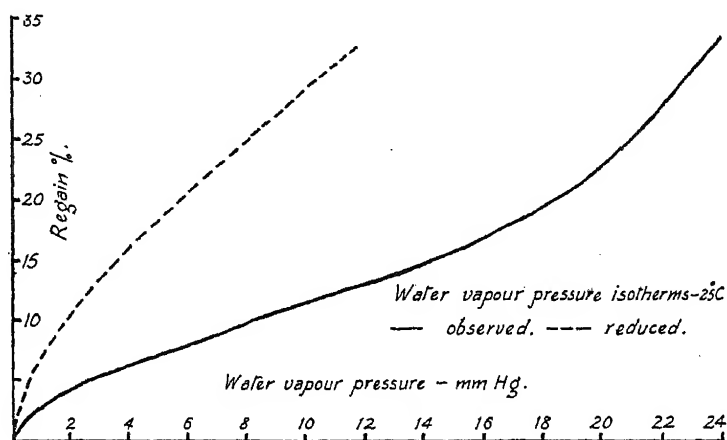


FIG. 1.

### 3. Hysteresis of the Wool Isotherm.

Barkas<sup>7</sup> has suggested that the hysteresis shown by vapour pressure isotherms of gels is largely a reflection of the mechanical hysteresis of the gel. A straight-forward application of equation (3) to the absorption-desorption isotherms indicates that this hypothesis is probably correct for wool. At a given regain, or at a given swelling, the hydrostatic pressure on the absorbed water will be greater during absorption than during desorption, and the observed vapour pressure at a given regain will be greater during absorption than during desorption. This qualitative description is in accord with experimental observations.<sup>12</sup> A semi-quantitative investigation may be made from Speakman's hysteresis curves.<sup>12</sup> If at a given regain, the relative humidity of the air in equilibrium with the absorption isotherm is  $H_1$ , and that in equilibrium with the desorption isotherm is  $H_2$ , equation (3) gives for the difference  $\delta P$ , in hydrostatic pressure on absorption and on desorption

$$\delta P = 3.2 \times 10^6 \log_{10} H_1/H_2. \quad (4)$$

Table II gives values of  $\delta P$  determined by equation (4) and Speakman's absorption and desorption isotherms.<sup>12</sup> They are seen to be of the same order of magnitude as the hydrostatic pressure changes,  $\Delta P$ , due to swelling

<sup>12</sup> Speakman, *J. Textile Inst.*, 1936, **27**, T185.

of the fibre on absorption of water. The values of  $\Delta P$  in Table I were calculated from the known elastic properties of the fibres, whilst the values of  $\delta P$  given in Table II have been obtained directly from the

TABLE II.—HYSTERESIS OF WOOL.

Regain %.	$H_1$ %.	$H_2$ %.	$\delta P$ (gm./cm <sup>2</sup> . $\times 10^5$ ).
5	13	9	5.4
7	25	18	4.6
10	40	34	2.2
15	68	61	1.4
20	87	82	0.8
25	95	93	0.5

hysteresis of the isotherms. The values of  $\delta P$  are smaller than those of  $\Delta P$ , and, in fact, fit in very well with the hypothesis that absorption hysteresis is a reflection of mechanical hysteresis.  $\delta P$  increases rapidly as the regain decreases, which is in

accord with the poor recovery of wool at low regains from deformations imposed at higher regains, a phenomenon known as "temporary set." No values are given below 5 % regain, as the isotherms are variable in this region, doubtless due to uncertain amounts of temporary set in the fibres.

#### 4. Heat of Wetting and Swelling of Wool.

Hedges<sup>2</sup> has measured the heat of wetting of wool, but part of the heat of sorption of water must be used to swell the fibres. Thus, if 1 g.

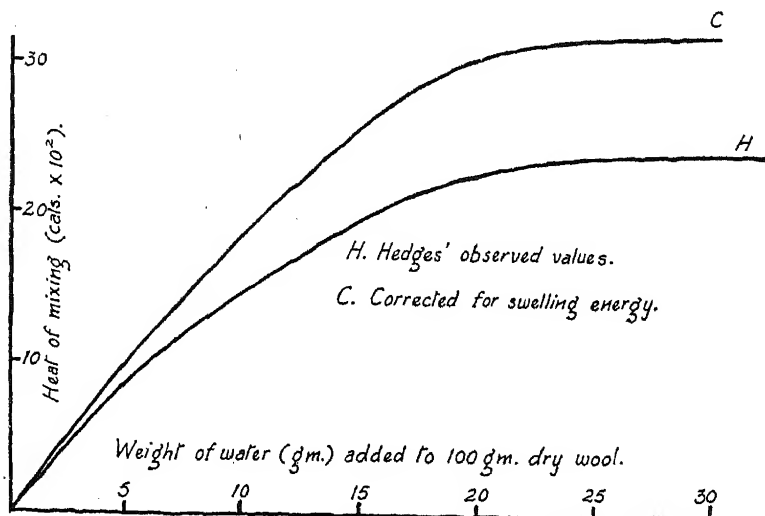


FIG. 2.

of liquid water is added to an infinite mass of wool at any given regain, the volume of the wool-water system is increased by approximately 1 c.c., and the amount of work done against the hydrostatic pressure is  $v\Delta P$ , where  $v$  is 1 c.c. Hedges gives values for  $Q$ , the heat evolved when 1 g. of water is added to an infinite mass of wool, and the total heat of mixing of liquid water and wool is given by integrating the curve of  $(Q + v\Delta P)$  plotted against regain. This has been carried through using the values

of  $\Delta P$  given in Table I. The results are shown in the upper curve of Fig. 2, the lower one giving Hedges' data.

### 5. Analysis of the Reduced Wool Absorption Isotherm.

The theory recently developed for multimolecular absorption<sup>5</sup> using the hypothesis of mixing of water molecules in the liquid state with those on low energy localised sites can be applied directly to the isotherm for wool reduced to one hydrostatic pressure. If  $A$  mol. of water are absorbed by 100 g. of wool which contains  $B$  mol. of localised sites,  $X$  mol. are absorbed on to the localised sites and  $(A - X)$  mol. are in the liquid state. Values of  $X$  may be determined from the isotherm and the equation<sup>5</sup>

$$\frac{p}{p_0} = \frac{A - X}{A} \quad (5)$$

where  $p$  is the water vapour pressure of the absorbed molecules and  $p_0$  is the saturation pressure of liquid water at the isotherm temperature.  $X$  must also fulfil the relation:<sup>5</sup>

$$(A - X)(B - X) = \beta X^2 \quad (6)$$

where  $\beta$  is  $p_1/p_0$ ,  $p_1$  being the vapour pressure required to fill one half of the localised site when water in the liquid state is absent. If  $X$  is obtained from equation (5) for two points on the isotherm,  $B$  and  $\beta$  can be determined from equation (6). This equation may then be used to calculate  $X$  for any given value of  $A$ .

Table III gives an analysis of the reduced wool absorption isotherm using the procedure outlined in the preceding paragraph. It is seen that there is excellent agreement of the values of  $X$  determined directly from

TABLE III.—ANALYSIS OF THE 25° C. ISOTHERM FOR 100 G. OF WOOL.

$A$ mol.	R.H. %	(1) $X$ mol.	(2) $X$ mol.	$\Delta H$ (cal. $\times 10^2$ ).	$w$ (cal. $\times 10^2$ ).
0.2	2.1	0.196	0.196	6.6	33.6
0.4	5.0	0.380 *	0.380	13	34.2
0.6	9.1	0.545	0.547	19	34.7
0.8	14.3	0.685	0.685	25	36.5
1.0	20.3	0.797 *	0.797	28.5	35.8
1.2	26.3	0.885	0.877	30.5	35.0
1.4	33.0	0.94	0.94	31.5	34.0
1.6	40.0	0.96	0.97	—	—
1.8	46	0.97	0.99	—	—

\* Used to determine  $B$  and  $\beta$ :  $B = 1.12$  mol.;  $\beta = 0.10$ .

(1) From column (2) and equation (5).

(2) From equation (6).

the isotherm by means of equation (5) and those calculated with equation (6). A further check on the values of  $X$  may be obtained from the heat of wetting curve, Fig. 2. If  $\Delta H$  is the heat evolved when  $A$  mol. of liquid water are mixed with 100 g. of wool,  $\Delta H$  is given by:

$$\Delta H = wX \quad (7)$$

where  $w$  is the heat evolved when 1 mol. of water is absorbed on to localised sites. If the analysis is correct,  $w$  should be a constant. The fifth column of Table III gives the values of  $\Delta H$  from Fig. 2, and the sixth column gives values of  $w$  obtained from equation (7) and the values of  $X$  calculated according to equation (6). It is seen that  $w$  is almost constant, again indicating the correctness of the theory.



# THE QUANTITATIVE RELATION BETWEEN THE ADAPTATIONS OF *BACT. LACTIS AEROGENES* TO TWO ANTIBACTERIAL AGENTS (methylene blue and proflavine).

BY J. M. G. PRYCE, D. S. DAVIES AND C. N. HINSHELWOOD.

Received 30th January, 1945.

Proflavine and methylene blue<sup>1</sup> both increase the lag of *Bact. lactis aerogenes*, and increase the mean generation time. Rapid adaptation to both drugs occurs and is reciprocal, adaptation to one conferring immunity to the other. This shows that the actions of the two drugs and the corresponding adaptive processes have important elements in common, and indeed might be identical.

There are, however, what appear at first sight to be important differences in the modes of action of the drugs in the following respects: first, the relation of lag to concentration for proflavine follows a curve which rises very slowly at first and then turns asymptotically towards infinite values of the lag, whereas for methylene blue the lag concentration-curves are, within the considerable errors of experiment, not appreciably different from linear over a fairly wide range. Secondly, training at successively higher proflavine concentrations causes a displacement of the lag-concentration curve by an amount equal to the value at which the cells were trained, whereas with methylene blue the degree of immunity attainable appears to reach a limit—which is approached at quite moderate training concentrations. The various quantitative relations are examined in this paper as closely as a somewhat erratic behaviour of the cells in methylene blue allows. A theoretical discussion on the lines already given for proflavine shows that in principle one should be able to predict the whole behaviour on training to methylene blue from the observations with proflavine, using only the data for the untrained cells in methylene blue. Comparison with experiment shows a qualitative agreement that is rather striking, and a degree of quantitative correspondence which, although inexact is significant. From this one may conclude either that the theory is correct and that the data are insufficiently controlled, or, more probably, that the theory of a common adaptive process represents the major part of, but not the whole truth.

## Experimental.

The general methods of experiment were as previously described.<sup>1</sup> The data in Figs. 1 and 3 were obtained by measuring the lags of various strains of *Bact. lactis aerogenes* in methylene blue or in proflavine over a range of concentrations. Except for the original untrained strain, the strains were obtained by 8-12 subcultures in presence of a given concentration of methylene blue followed by one or two subcultures in the standard medium (phosphate, glucose, ammonium sulphate, magnesium sulphate) to remove methylene blue from the culture, lest methylene blue carried over should affect growth in proflavine. In spite of frequent irregularities (in contrast with the regular behaviour of proflavine-trained cells) a pair of curves may be obtained for each trained strain, one representing the lags in methylene blue, the other the lags in proflavine. The former type of curve is characteristically almost linear, as may be seen in

<sup>1</sup> Davies, Hinshelwood and Pryce, *Trans. Faraday Soc.*, 1944, 49, 397.

Fig. 1, while each of the second type corresponds to a curve which might be obtained by training in a concentration  $P'$  of proflavine, as shown in Fig. 3. Thus a training concentration  $\bar{m}$  of methylene blue may be taken as equivalent to  $P'$  of proflavine as far as the adaptation provoked is concerned.

The untrained cells in methylene blue give moderately reproducible lags only. The best values correspond approximately to the linear relation

$$L - L_0 = 30m,$$

where  $L_0$  is the (minimal) lag in the absence of the dye,  $L$  that observed, and  $m$  the test concentration of methylene blue (in mg./litre).

Fig. 1 shows that as the training concentration  $\bar{m}$  is raised the lag concentration curves crowd together, i.e. there is a limit to the adaptation

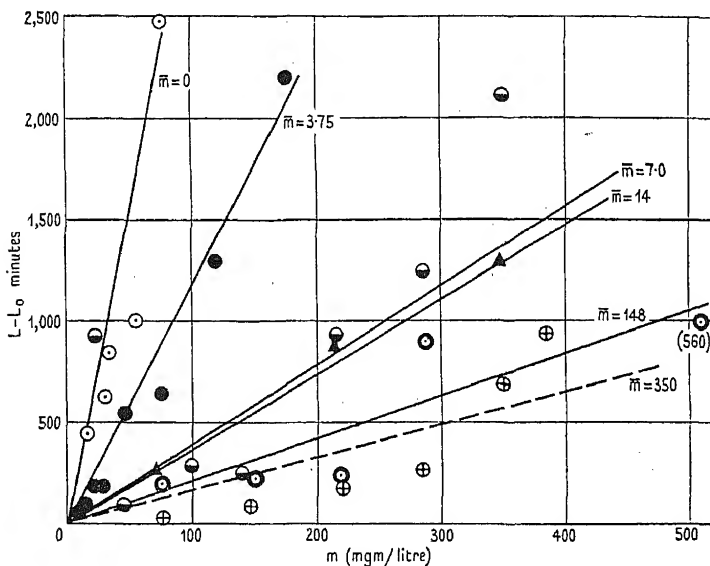


FIG. 1.—Lag-concentration curves for various trained strains in methylene blue.  $\bar{m}$  = training concentration:  $m$  = test concentration (expressed in mgm./litre).

Values of  $m$ : Open circles, 0; full circles, 3.75; half shaded circles, 7; triangles, 14; dark rimmed circles, 148; crossed circles, 350.

provoked. Fig. 3 shows that the equivalent proflavine training concentrations  $P'$  increase much less steeply than  $\bar{m}$ , and themselves also tend to a limit. The following discussion shows that the shape of the lag-concentration curves, their spacing for different values of  $\bar{m}$ , and the  $\bar{m}$ - $P'$  relation are interconnected.

### Discussion.

In previous papers <sup>1, 2</sup> we have assumed the cell to contain an adaptive system, consisting essentially of two interdependent enzymes (or a more complex system which may be idealised in this way). Enzyme 1 is responsible for the synthesis of a diffusible substance—which will be referred to in this discussion as M—itself utilised for the synthesis of enzyme 2. The rate of utilisation of M by enzyme 2 follows the equation:

$$R = kc/(1 + bc)$$

<sup>2</sup> Davies, Hinshelwood and Pryce, *Trans. Faraday Soc.*, 1945, 41, 163.

where  $c$  is the concentration of M built up by the balance of the processes of formation, utilisation and loss from the cell by diffusion or otherwise.

The action of the drug is supposed to be in reducing the synthesis rate of enzyme 2, without arresting the synthesis of enzyme 1: this it does by cutting down the supply of M and reducing  $c$ , *i.e.* it lowers the production of M by enzyme 1 without interfering with the actual growth of it. By assuming that division of the cell awaits the growth of enzyme 2 to some standard amount, and by setting down equations for the production, loss and utilisation of M—assumed to attain a steady concentration in the cell, it can be shown that this hypothetical enzyme model will have adaptive properties. During growth in presence of a drug an increased ratio of enzyme 1 to enzyme 2 would be established, and this change in enzyme balance would lead to an increased immunity to the drug.

These assumptions can be used to relate the concentration of a drug (fulfilling the above conditions) with its effect on the bacterial lag. The latter may not unreasonably be taken to be inversely proportional to the synthesis rate of enzyme 2—which in turn will be linked with the rate of formation of its products. The hypothesis is made because we have cause to believe that the lag ends when the concentration in the cells and medium of some active substance attains to a critical concentration. (The active substance is quite distinct from the substance M mentioned above.)

We write therefore

$$L = A/R \text{ where } A \text{ is constant} \quad (1)$$

whence

$$1/L = (k/A) \cdot c/(1 + bc).$$

Let  $c_1'$  be the stationary concentration of M characteristic of a given strain of cells, in the absence of drug and in the condition of minimal lag. In presence of the drug a new stationary concentration  $c$  is set up given by

$$c = c_1' - \phi(m), \quad (2)$$

where  $\phi(m)$  is a function of the drug concentration to be determined. We now have

$$\text{with no drug} \quad \frac{1}{L_0} = \frac{k}{A} \cdot \frac{c_1'}{1 + bc_1'}$$

$$\text{at conc. } m \text{ of drug} \quad \frac{1}{L} = \frac{k}{A} \left[ \frac{c_1' - \phi(m)}{1 + b\{c_1' - \phi(m)\}} \right]$$

$$\text{whence} \quad \frac{1}{L - L_0} = \frac{k}{A} \left[ \frac{c_1'^2}{\phi(m)} - c_1' \right] \quad (3)$$

This equation gives the increase of the minimal lag over normal when drug at concentration  $m$  is added to the medium;  $k/A$  is a constant, while  $c_1'$  is constant for a given trained strain, but varies from strain to strain.

For proflavine it has already been shown that  $\phi(m)$  may be taken simply as  $fm$  where  $f$  is a constant. This leads to results in agreement with experiment. It was also shown that  $c_1'$  was simply related to the training concentration,  $P$ , by the relation  $c_1' = f(54 + P)$ .  $k/A$  was given the value  $10^{-4}/f$  approximately. Moreover it appeared that the effect of training was to restore the value of  $c$  in presence of the drug from its reduced value to the original value it would have had for untrained cells in the normal medium.

The procedure for treating the results with methylene blue is as follows: we first determine the constants of equation (3) from the results of the experiments with proflavine, using  $\phi(m) = fm$  and the value for untrained cells,  $c_1' = 54f$ . We then use the result for untrained cells in methylene blue,  $L - L_0 = 30m$ , and by substitution in (3) obtain a series



of values of  $\phi(m)$  for different values of  $m$ . The relation of  $\phi(m)$  to  $m$  is shown in Fig. 2. It is calculated for more than one value of the constant  $k/A$ . The reason for this is simply that the best value of the constant for proflavine does not correspond with the best for methylene blue, and we wish to see what effects variation in the constants may have. What appears, independently of the precise value of  $k/A$ , is that  $\phi(m)$  increases much less than linearly with  $m$ . It is precisely this property of the methylene blue that governs its behaviour in the other respects to be considered.

The curve of  $\phi(m)/f$  against  $m$  can now be used to predict the effect of training in various concentrations of methylene blue.

If a concentration of methylene blue,  $m$ , reduces  $c$  to the same extent as a concentration  $P$  of proflavine, then we have  $\phi(m) = Pf$ . If, moreover, adaptation always restores  $c$  to its normal value, adaptation to  $\bar{m}$  of methylene blue will be equivalent to adaptation to  $P'$  of proflavine

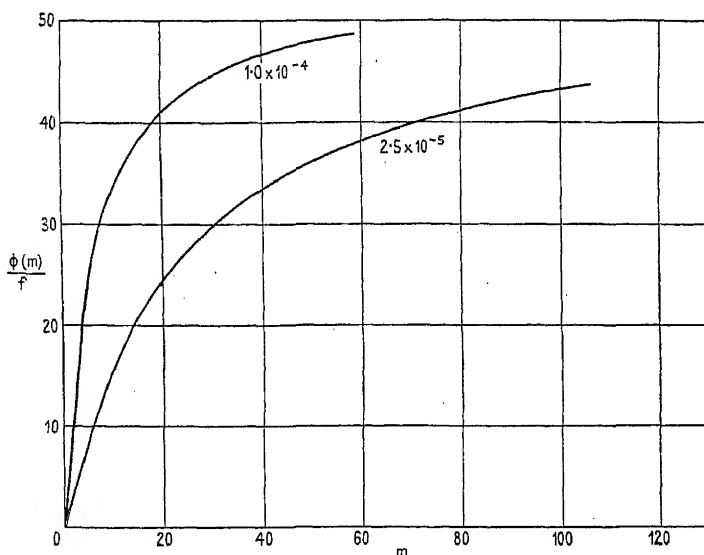


FIG. 2.—Relation of  $\phi(m)/f$  to  $m$ .

where  $\phi(\bar{m}) = fP'$ . From the  $\phi(m)/f$ ,  $m$  relation, we can therefore find the value of  $P'$  corresponding to any given  $\bar{m}$ .

In Fig. 3 the observed values of  $P'$  are plotted against  $\bar{m}$  and compared with the calculated values for two values of  $k/A$ . The general form of the experimental curve is accounted for. Using the value  $1.0 \times 10^{-4}$  for  $k/A$ , the value already given for the proflavine experiments the quantitative agreement is very much less satisfactory than that given by a considerably smaller value of the constant. The smaller value can, however, be used fairly satisfactorily—though it is far from the best value—for proflavine, since the results are insensitive to the precise value of this constant. This will be shown later. Anticipating this change, however, we will use the value  $2.5 \times 10^{-5}$  as a compromise between the best for proflavine and the best for methylene blue, and see how nearly the results for both can be expressed. Perhaps the most interesting point in Fig. 3 is the fact that theory indicates a limit to the degree of proflavine immunity producible by training in methylene blue.

The predicted limit occurs at a value of  $P' = 54$ , while the actual one is just under 30. This may well mean that the reciprocal training is only

partial, and that, superposed on their common action, the two inhibitors exert specific actions.

We now turn to consider the lags of methylene blue-trained strains in methylene blue. We will use the symbol  $m$  when referring to the test concentrations, and  $\bar{m}$  for training concentrations. If the value of  $c$  in normal medium for untrained cells is  $c_1$ , at concentration  $\bar{m}$  of the dye it will be given by

$$c = c_1 - \phi(\bar{m}).$$

If adaptation restores  $c$  to the normal value  $c_1$  (as indicated by the proflavine experiments), on removal of the drug  $c$  will increase still further to  $c_1'$ , expressed for a given trained strain by

$$c_1' = c_1 + \phi(\bar{m}).$$

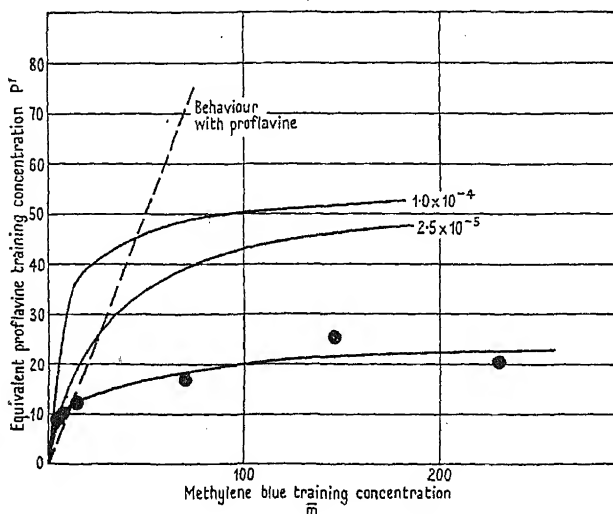


FIG. 3.—Relation of methylene blue and proflavine immunity.

This is the value for  $c$  for the strain trained at  $\bar{m}$  but tested in the normal medium without drug. If tested at a different methylene blue concentration,  $m$ , we shall have

$$\begin{aligned} c &= c_1' - \phi(m) \\ &= c_1 + \phi(\bar{m}) - \phi(m). \end{aligned}$$

From the proflavine results  $c_1 = 54f$ , whence

$$c = 54f + \phi(\bar{m}) - \phi(m).$$

Combining this with equation (3) we obtain

$$\frac{I}{(L - L_0)} = \frac{h}{A} \left[ \frac{\{54f + \phi(\bar{m})\}^2}{\phi(m)} - \{54f + \phi(m)\} \right].$$

The results calculated from this, taking  $h/A = 2.5 \times 10^{-5}/f$  are shown on comparison with experimental values in Fig. 4, the values of  $\phi(m)$  and  $\phi(\bar{m})$  being taken from Fig. 2. Once again there is a good qualitative representation of the main features, namely the absence of a sharp increase of lag as with proflavine, and the tendency to reach a limit as the value of  $\bar{m}$  is raised. Quantitatively the agreement is moderate only. The general spacing of the curves is more or less correctly given, but the shape

of the individual curves, especially at the higher values of  $m$ , is not so satisfactory. It must be borne in mind, however, that moderate changes in the form of  $\phi(m)$  will convert curves from the type convex to the  $m$ -axis to the concave type, with the linear type as an intermediate case. The form we have used for  $\phi(m)$  somewhat overemphasises the contrast between proflavine and methylene blue in respect of the form of the lag-concentration curves. The predicted effect of methylene blue at the highest concentrations is smaller than that observed: this may well be due to the fact—already envisaged as possible—that, superposed on the common action of the two drugs, are specific actions of each.

As stated above the value for  $k/A = 2.5 \times 10^{-5}$  taken as a compromise is not really the best representation of the proflavine results. It is, however, not a wholly inadmissible one. This is shown by Fig. 5 where the experimental values for proflavine are compared with those given by equation (3) with  $c_1' = 54$ , and  $k/A = 2.5 \times 10^{-5}$ . The former was the value

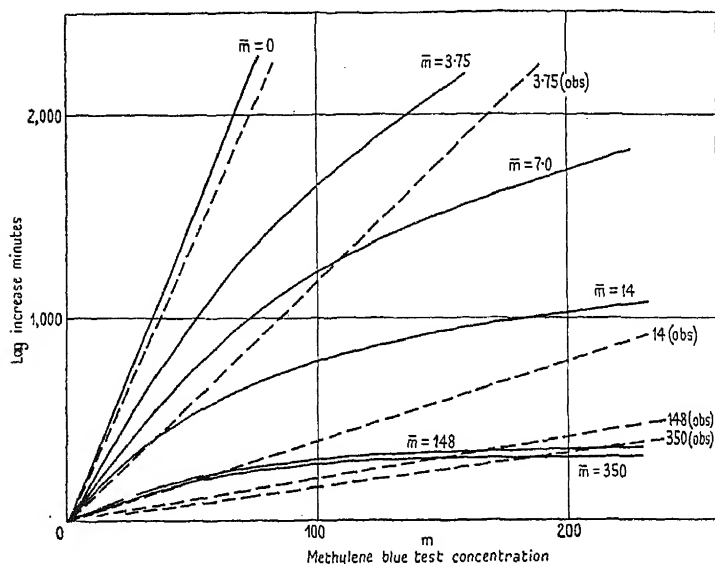


FIG. 4.—Calculated and observed families of lag-concentration curves for trained strains.

originally used, and is the really important constant: the latter of less determinative significance, and can be varied within limits.

Summarising the results of the calculations we may say that they reveal a significant correspondence between the behaviour of proflavine and that of methylene blue, and allow the semi-quantitative prediction of one type of behaviour from that of the other. Whether better numerical agreement would be obtained with more accurate results, or whether, superposed on the common actions of the two drugs, there are specific actions to which the theory is inapplicable is hard to say at present. But the above theoretical discussion would appear to cover a not inconsiderable part of the truth.

The variation of mean generation time with methylene blue concentration was recorded in a previous paper. It is of interest to note that it follows a course similar to that which would be calculated on the assumption that the growth rate itself runs parallel with the rate  $R$  (see above) which was assumed to determine the lag. The significance of this will not be further considered at present.

### Summary.

Proflavine and methylene blue both inhibit the growth of *Bact. lactis aerogenes*, and training to resist one of these substances confers on the cells a degree of immunity to the other.

The theory previously developed for training to proflavine (according to which a change of enzyme balance is provoked which restores the concentration in the cells of a certain intermediate to a standard level) is applied to results obtained on the adaptation of *Bact. lactis aerogenes* to methylene blue. From the lag-concentration curve of untrained cells in methylene blue, in conjunction with the earlier results for proflavine,

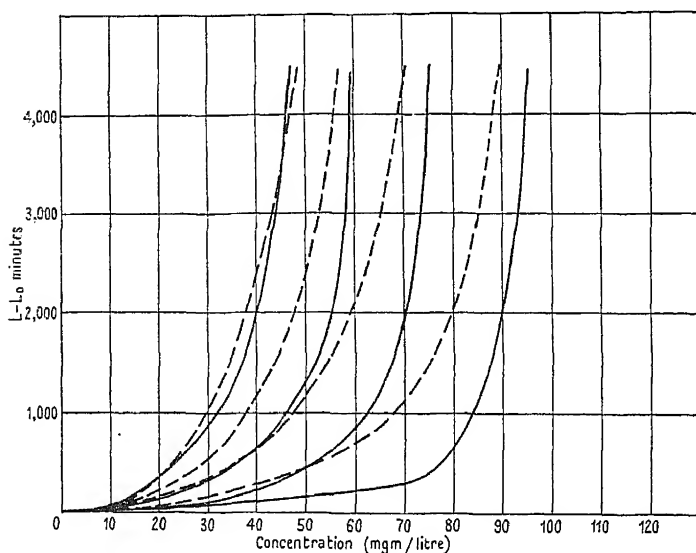


FIG. 5.—Proflavine lag-concentration curves: continuous lines—observed: broken lines—calculated with modified constant.

it is predicted: that there is a limit to the degree of adaptation to methylene blue which will occur: that the concentration of proflavine to which training in methylene blue gives cross immunity is also limited: that the lag-concentration curves for trained strains in methylene blue rise much less steeply than the corresponding curves for proflavine.

These anticipations are in qualitative agreement with the experimental observations: and there is some roughly quantitative correspondence, showing that the assumption of a common adaptive process is probably a major part of the truth. The discrepancies are such as to suggest that, superposed upon the common action of the two agents, there are specific actions.

*Physical Chemistry Laboratory,  
Oxford University.*

# THE MELTING-POINTS AND UNIT CELLS OF THE METHYLBENZENES.

By T. BEACALL.

Received 12th February, 1945.

The quantitative relations which exist between the melting-points of the members of the halogen-benzene series have already been described;<sup>1</sup> it has also been shown that in the case of the symmetrically substituted compounds (the only compounds for which data are available) the changes in melting-point are related to the changes in dimensions of the unit cell;<sup>2</sup> in the present paper similar considerations are applied to the methylbenzenes and to their halogen derivatives symmetrically substituted in the nucleus.

All of the twelve possible methylbenzenes are known; eight of them are liquid at ordinary temperature, and in some instances the melting-point has not been determined with any great degree of accuracy; thus, Beilstein's *Handbuch*<sup>3</sup> records for toluene values varying from  $-102^{\circ}\text{C}$ . to  $-92.4^{\circ}\text{C}$ ., while for  $\psi$ -cumene no melting-point is given either in Beilstein or in Heilbron's *Dictionary*,<sup>4</sup> and the only value available appears to be the m.p. of  $-61^{\circ}\text{C}$ . given in Stelzner's *Literatur-Register*.<sup>5</sup> In Table I are shown the melting-points of the series, the values stated being (except in the case of  $\psi$ -cumene) the selected data recorded in Heilbron's *Dictionary*.

TABLE I.—BENZENE, M.P.  $5.5^{\circ}\text{C}$ .

Methylbenzene.			M.P. ( $^{\circ}\text{C}$ .).
Monomethyl (toluene) . . . . .			$-95.0$ (f.p.)
Dimethyl (xylene) . . . . .	1 : 2		$-25.0$
	1 : 3		$-47.4$
	1 : 4		$-13.14$
Trimethyl . . . . .	Hemimellitene	1 : 2 : 3	$-15$
	$\psi$ -cumene	1 : 2 : 4	$-61$
	Mesitylene	1 : 3 : 5	$-53.5$ ( $-54.4$ )
Tetramethyl . . . . .	Prehnitene	1 : 2 : 3 : 4	$-6.4$
	Isodurene	1 : 2 : 3 : 5	$-24.1$ (f.p.)
	Durene	1 : 2 : 4 : 5	$80$
Pentamethyl			$53$ ( $51.5$ )
Hexamethyl			$164$

<sup>1</sup> *Recueil*, 1928, 47, 37.

<sup>2</sup> *Trans. Faraday Soc.*, 1943, 39, 214.

<sup>3</sup> Beilstein, *Handbuch der organischen Chemie*, 1922, Band 5.

<sup>4</sup> Heilbron and Bunbury, *Dictionary of Organic Compounds*, 2nd edn., 1943.

<sup>5</sup> Stelzner, *Literatur-Register der organischen Chemie*, 1926.

It is clear that there is a strong family likeness between this series of melting-points and those of the chloro- and bromo-benzenes; \* there are the familiar maxima at the 1:4-di, 1:2:4:5-tetra- and hexa-substituted compounds, and the marked lowering of melting-point caused by the introduction of a single substituent into the benzene molecule; in one respect there is a material difference; the symmetrical 1:3:5-tri-halogenbenzenes have high melting-points, intermediate between those of the symmetrical di- and tetra-compounds, whereas the melting-point of *s*-trimethyl-benzene is very low: a possible reason for this difference will be discussed later. The symmetrical and unsymmetrical series will now be considered in detail.

### The Symmetrical Di-, Tetra- and Hexa- Methylbenzenes.

As in the case of the chloro- and bromo-benzenes the melting-points of these three bodies (in degrees absolute) approximate closely to a geometrical series, the melting-point of durene ( $353^{\circ}$  K.) being very close to the mean ( $353.5-354^{\circ}$  K.) of those of *p*-xylene and hexamethylbenzene; *p*-xylene resembles *p*-dichlorobenzene in having an abnormally low m.p., the increment from benzene to *p*-xylene (1.03) being materially less than that from *p*-xylene to durene (1.23) or from durene to hexamethylbenzene (1.24).

**The Unit Cells of the Symmetrical Di-, Tetra- and Hexa-Methylbenzenes.**—The unit cell of hexamethylbenzene has been measured by Mrs. Lonsdale<sup>6</sup> and subsequently remeasured by Brockway and Robertson;<sup>7</sup> the unit cell is monomolecular and has the volume  $252 \text{ \AA}^3$  (Brockway and Robertson) or  $258.4 \text{ \AA}^3$  (Lonsdale); Robertson has also measured durene, the unit cell of which is bi-molecular and of volume  $430 \text{ \AA}^3$ ;<sup>8</sup> no X-ray measurements of crystalline *p*-xylene appear to have been recorded, but measurements of its density have been made by Rozenthal<sup>9</sup> and by Block;<sup>10</sup> calculation of the volume of a bi-molecular unit cell from the density values gives  $335.0 \text{ \AA}^3$  or  $335.7 \text{ \AA}^3$ . X-ray measurements of crystalline benzene have been recorded by Cox,<sup>11</sup> who found the unit cell to be tetra-molecular with volume  $489 \text{ \AA}^3$ .

If these unit cell values are expressed in terms of a constant number of molecules, it will be found that they approximate to an arithmetical series; Table II shows for two-molecule units the values of  $\delta V/n$ ,  $\delta V$  being the increase in volume over a similar benzene unit, and  $n$  being the number of pairs of substituents per molecule.

It is suggested that, as in the case of the symmetrically halogenated benzenes, the m.p. is determined by the linkage of the pairs of substituents in *p*-position to similar substituents in neighbouring molecules. The most complete analysis of a unit cell available is that of hexamethylbenzene by Brockway and Robertson;<sup>7</sup> these authors have shown that the methyl groups extend laterally from the plane of the benzene ring, the closest approach between

TABLE II.

Compound.	$\delta V/n$ .
<i>p</i> -Xylene . . . .	90.5 (91.2)
Durene . . . .	92.7
Hexamethylbenzene . .	86.5 (90.8)

\* See Table in paper.<sup>1</sup>

<sup>6</sup> Lonsdale, *Proc. Roy. Soc. A*, 1929, 123, 494.

<sup>7</sup> Brockway and Robertson, *J.C.S.*, 1939 (2), 1324.

<sup>8</sup> Robertson, *Proc. Roy. Soc. A*, 1933, 141, 594.

<sup>9</sup> Rozenthal, *Bull. Soc. Chim.*, 1936, 45, 585.

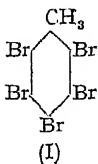
<sup>10</sup> Block, *Z. physik. Chem.*, 1911, 78, 410.

<sup>11</sup> Cox, *Nature*, 1928, 122, 401.

methyl groups of neighbouring molecules being from 3.90 to 3.99 Å., the corresponding distance in durene being 3.93 Å. The closest approach between methyl hydrogen atoms in adjacent molecules was found to be 2.00-2.25 Å., as compared with a distance of 1.97 Å. in solid methane; the authors remark "The packing of the molecules in the crystal is determined by the equilibrium distance between the hydrogen atoms in different molecules".†

So far as hexamethylbenzene and durene are concerned, the view put forward above that the m.p. is determined by the pairs of  $\text{CH}_3 \dots \text{CH}_3$  linkages between adjacent molecules appears in accordance with the results of X-ray analysis of the unit cell. It would be of interest to have measurements also for *p*-xylene; these might throw light on the apparent anomaly that while the computed volume of its unit cell has a normal value the m.p. is abnormally low.

**The Symmetrically Substituted Methylhalogenbenzenes.**—In paper (2) it was shown that in the *paradihalogennitrobenzene* series the quasi-independent effect upon the melting-point of a pair of halogen atoms in *para*-position persists. The series of symmetrically substituted methylhalogenbenzenes affords a wide field for testing the persistence of the effects of pairs of halogen atoms or methyl groups in *para*-position. A convenient way of making this test is to calculate the melting-points and compare the calculated values with the observed values; Table III shows the results of this for the thirty hexa-substituted compounds listed in Beilstein.<sup>3</sup> To calculate the melting-point (in degrees absolute) it is assumed that a pair of chlorine atoms in *para*-position has the same effect as in hexachlorbenzene (m.p. 500° K.), i.e.  $\sqrt[3]{500/278.5} = 1.213$ , that a pair of bromine atoms in *para*-position has the same effect as in hexabrombenzene (m.p. 579° K.), i.e.  $\sqrt[3]{579/278.5} = 1.276$ , and that a pair of methyl groups in *para*-position has the same effect as in hexamethylbenzene (m.p. 439° K.), i.e.  $\sqrt[3]{439/278.5} = 1.164$ ; where a chlorine and a bromine atom appear in *para*-position it is assumed that the effect is the geometric mean of the effects of the two pairs of halogens, and where a halogen atom and a methyl group appear in *para*-position, it is assumed that the effect is the geometric mean of the effects of a pair of halogen atoms and a pair of methyl groups; to obtain the m.p. of a given compound, the melting-point of benzene (278.5° K.) is multiplied by the appropriate factors for the three pairs of substituents in *para*-position; for example, pentabromtoluene (I) contains two pairs of bromine atoms in *para*-position and a "mixed" pair consisting of a bromine atom and the methyl group; the melting-point is thus given by



$$T = 278.5 \times 1.276^2 \times \sqrt{1.276 \times 1.164} = 553^\circ \text{ K.};$$

Beilstein gives values for the m.p. of this compound ranging from 552° to 558° K. while Heilbron gives the values 555° and 553°.

Of the 30 compounds tabulated, in 13 cases the difference between *T* obs. and *T* calc. is less than 1 %, in 11 cases the difference is between 1 and 3 %, and only in 6 cases does the difference exceed 3 %. In view of the uncertainty of some of the recorded data, this measure of agreement between the observed and calculated melting-points appears sufficient to justify the assumption that in this group of compounds the pairs of halogen atoms in *para*-position and of methyl groups in *para*-position retain their quasi-independent effects without material alterations save in a small minority of cases.

The physical meaning of this agreement between the observed melting-points and those calculated on the basis stated would seem to be that

† *Loc. cit.*<sup>7</sup>, p. 1331.

in this series of compounds the molecules are linked in the unit cells by the pairs of substituents in *p*-position as are the hexa-methyl and hexa-halogen-benzenes, and that in consequence the dimensions of the unit

TABLE III.

Compound.	<i>T</i> (obs.).	<i>T</i> (calc.).	% Diff.
Pentabromtoluene . . . . .	555 553	553	- 0.4 —
Pentachlortoluene . . . . .	491	488	- 0.6
6-Chlor-2 : 3 : 4 : 5-tetrabromtoluene . . .	531.2	539	+ 1.4
2 : 3 : 5 : 6-Tetrachlor-4-bromtoluene . . .	486	499	+ 2.7
Tetrabrom- <i>p</i> -xylene . . . . .	529-530 ; 526	528	- 0.3 + 0.4
Tetrabrom- <i>o</i> -xylene . . . . .	527.8 ; 535	528	— - 1.3
Tetrabrom- <i>m</i> -xylene . . . . .	520 ; 514	528	+ 1.5 + 2.7
Tetrachlor- <i>p</i> -xylene . . . . .	495 ; 491	477	- 3.7 - 2.9
Tetrachlor- <i>o</i> -xylene . . . . .	488	477	- 2.3
Tetrachlor- <i>m</i> -xylene . . . . .	492 485	477	- 3.1 - 1.6
6-Chlor-2 : 3 : 5-tribrom- <i>p</i> -xylene . . . .	507	515	+ 1.6
3 : 6-dichlor-2 : 5-dibrom- <i>p</i> -xylene . . . .	499	502	+ 0.6
3 : 5 : 6-trichlor-2-brom- <i>p</i> -xylene . . . .	492	489	- 0.6
4 : 6-dichlor-3 : 5-dibrom- <i>o</i> -xylene . . . .	506	502	- 0.8
4 : 6-dichlor-2 : 5-dibrom- <i>m</i> -xylene . . . .	503	502	- 0.2
2 : 6-dichlor-4 : 5-dibrom- <i>m</i> -xylene . . . .	488	502	+ 2.9
2 : 4 : 6-tribrom-1 : 3 : 5-trimethylbenzene .	497	504	+ 1.4
3 : 5 : 6-tribrom-1 : 2 : 4-trimethylbenzene .	498-9 ; 506	504	+ 1.0 - 0.4
4 : 5 : 6-tribrom-1 : 2 : 3-trimethylbenzene .	518	504	- 2.8
2 : 4 : 6-trichlor-1 : 3 : 5-trimethylbenzene .	477-8	467	- 2.3
3 : 5 : 6-trichlor-1 : 2 : 4-trimethylbenzene .	470	467	- 0.6
4 : 5 : 6-trichlor-1 : 2 : 3-trimethylbenzene .	490-1	467	- 5.1
4 : 6-dichlor-5-brom-1 : 2 : 3-trimethylbenzene	495-6	479	- 3.5
3 : 6-dibrom-1 : 2 : 4 : 5-tetramethylbenzene .	475-6 ; 472	481	+ 1.5 + 1.9
4 : 6-dibrom-1 : 2 : 3 : 5-tetramethylbenzene .	482 471.2	481	- 0.2 + 1.9
5 : 6-dibrom-1 : 2 : 3 : 4-tetramethylbenzene .	478	481	+ 0.6
3 : 6-dichlor-1 : 2 : 4 : 5-tetramethylbenzene .	462-3	458	+ 1.0
5 : 6-dichlor-1 : 2 : 3 : 4-tetramethylbenzene .	468	458	- 2.2
Brompentamethylbenzene . . . . .	433-5	460	+ 6.1
Chlorpentamethylbenzene . . . . .	428	448	+ 4.7

cells should be comparable, *mutatis mutandis*, with those of hexachlor-, hexabrom- or hexamethylbenzene. The only compound in which a check of this inference is at present possible is pentabromtoluene (No. 1 in Table III) of which the crystallographic data are given by Groth;<sup>12</sup>

<sup>12</sup> Groth, *Chemische Krystallographie*, 4, 362.



calculation of the volume of a two-molecule unit cell from the molecular weight (487) and the density (2.970) gives  $545 \text{ \AA}^3$ .

It has been pointed out above that in the symmetrical methylbenzenes the successive introduction into the benzene ring of one, two and three pairs of methyl groups in *p*-position produces a substantially constant increase in the volume of the two-molecule unit from benzene ( $244.5 \text{ \AA}^3$ ) to hexamethyl-benzene ( $504 \text{ \AA}^3$ , Brockway and Robertson); the overall increment in volume for a pair of methyl groups is thus  $86.5 \text{ \AA}^3$ ; a similar approximately additive rule applies to the symmetrical bromobenzenes; the hexabrombenzene two-molecule unit cell has the volume  $553.5 \text{ \AA}^3$ , so the overall increment in volume for a pair of bromine atoms is  $103 \text{ \AA}^3$ . If a similar additive relation holds for pentabromtoluene, which contains two pairs of bromine atoms and a "mixed" pair consisting of a bromine atom and a methyl group, the volume of a two-molecule unit cell should be given by  $244.5 + (2 \times 103) + (103 + 86.5)/2 = 545.2 \text{ \AA}^3$ .

In the case of this compound then, the calculated m.p. and calculated unit cell volume are practically identical with the observed m.p. and the unit cell volume deduced from the density.

In addition to the 30 hexa-substituted compounds dealt with above, Beilstein<sup>3</sup> records 12 symmetrical tetra-substituted compounds, namely, the halogen-trimethylbenzenes, the dihalogen-dimethylbenzenes and the trihalogentoluenes; we may take as examples the 2:5-dihalogen-*p*-xylenes. If it is assumed that in these bodies the two methyl groups have the same low effect as in *p*-xylene itself, the observed and calculated values of the m.p. of 2:5-dichlor-*p*-xylene agree within 1% ( $T_{\text{obs.}} = 344^\circ \text{K}$ ,  $T_{\text{calc.}} = 347.5^\circ \text{K}$ ); in the case of the 2:5-dibrom compound, however, the difference between the observed ( $348^\circ \text{K}$ ) and calculated ( $365.5^\circ \text{K}$ ) values amounts to 5%, and a similar difference appears in the case of 2-chlor-5-brom-*p*-xylene ( $T_{\text{obs.}} = 339^\circ \text{K}$ ,  $T_{\text{calc.}} = 356.5^\circ \text{K}$ ).

No X-ray data or even density values for these bodies appear to be available; the one tetra-substituted body for which a density value has been recorded is 2:4:5-tribrom-toluene (Groth, p. 360); a two-molecule unit cell computed from the molecular weight (329) and density (2.472) has the volume  $442.4 \text{ \AA}^3$ ; calculation of the cell volume from that of benzene by the addition of the increment values for one pair of bromine atoms and a "mixed" bromine-methyl pair gives  $244.5 + 103 + (103 + 86.5)/2 = 442.2 \text{ \AA}^3$ . Here again we find almost exact agreement between the unit cell volume deduced from the density and that obtained by extrapolation from the unit cell volume of benzene, although in this case the observed m.p. ( $385.6^\circ \text{K}$ ) is some 5% less than the calculated value ( $407.5^\circ \text{K}$ ). No explanation of the abnormally low m.p. of these bromo compounds can at present be given, but it is perhaps significant that a similar anomaly appears in the case of 2:5-dibromtoluene discussed below.

### The Mono-, as-Tri- and Penta-methylbenzenes.

The drop of  $100^\circ \text{C}$ . in melting-point, resulting from the introduction of a single methyl group into the benzene molecule, is very striking; as we proceed up the series the effect diminishes, as shown in the annexed Table IV.

The effect of the single methyl group in the symmetrically halogenated toluenes is shown in Table V.

The effect in the tetrabrom-, tetrachlor- and dichlor-toluenes approximates to that shown by pentamethyl-benzene, and it appears justifiable to assume that in these bodies, as in the symmetrical hexa-substituted bodies discussed above, the pairs of halogen atoms retain their quasi-independent effect. The abnormally low value shown by the dibromtoluene (and probably also by the chlor-bromtoluene) appears similar to those already mentioned in the cases of the 2:5 dibrom-*p*-xylene and 2:4:5-tribromtoluene.

**The Unit Cells of the Mono-, *as*-Tri- and Penta-Methylbenzenes.**—In paper (1) it was suggested that the striking contrast between the low melting-point of the asymmetrically substituted halogen-benzenes and the comparatively high melting-points of the symmetrical halogen-benzenes points to the presence in the asymmetrical bodies of a different type of linkage between the molecules in the unit cells, namely, a linkage of the asymmetric halogen atom in one molecule with a hydrogen atom in a neighbouring molecule, in other words, a head-to-tail linkage of the molecules. The similar contrast in melting-points between the symmetrical and asymmetrical methylbenzenes suggest that in the unit cells of toluene (and its symmetrical methyl and halogen derivatives) a similar head-to-tail linkage of adjacent molecules through methyl groups and hydrogen atoms exists. Until X-ray measurements of the unit cells of toluene (and its symmetrical methyl and halogen derivatives) are available, however, the suggested structure must remain tentative.

TABLE IV.

Compound.	M.P.	Ratio.
Toluene . . .	178	0.64
Benzene . . .	278.5	
<i>ψ</i> -Cumene . . .	212	0.74
<i>p</i> -Xylene . . .	286.5	
Pentamethylbenzene .	326	0.92
Durene . . .	353	

1 : 3 : 5-Trimethylbenzene.—In the halogenbenzene series the *s*-tri-substituted bodies have melting-points intermediate between those of the *para*-di- and *s*-tetra-substituted compounds. It would seem to follow, therefore, that if in the high melting-point di- and tetra-substituted compounds the pairs of halogen atoms in *p*-position are linked to halogen atoms of neighbouring molecules in the unit cells, the three single halogen atoms in the

TABLE V.

Compound.	M.P.	Ratio.
2 : 3 : 5 : 6-tetrabromtoluene	389-390	0.86
<i>s</i> -tetrabrombenzene . . .	453-454	
2 : 3 : 5 : 6-tetrachlortoluene .	366-367	0.89
<i>s</i> -tetrachlorbenzene . . .	412.5-413.5	
2 : 5-dibromtoluene . . .	(below 253)	<0.70
<i>p</i> -dibrombenzene . . .	360	
2-brom-5-chlortoluene . . .	liquid	?
<i>p</i> -chlorbrombenzene . . .	339	
2 : 5-dichlortoluene . . .	278	0.85
<i>p</i> -dichlorbenzene . . .	326	

*s*-tri-substituted bodies are similarly linked to halogen atoms in neighbouring molecules, the three hydrogen atoms in *para*-position to the halogens being linked to hydrogen atoms of adjacent molecules.

The effect of the pair of chlorine atoms in *p*-dichlorbenzene is to raise the melting-point by the factor 1.17; it seems reasonable to assume that the effect of a single chlorine atom similarly linked in the unit cell would be to increase the melting-point by  $\sqrt{1.17}$ ; the melting-point of *s*-trichlorbenzene would thus be  $278.5 \times 1.17^{\frac{1}{2}}$  and that of *s*-tribromobenzene  $278.5 \times 1.29^{\frac{1}{2}}$ ; the values so calculated (353° K. and 408° K.) are 5 % and 4 % respectively higher than the recorded values (336.5° and 393°). *s*-Trimethylbenzene however, instead of having a melting-point intermediate between that of *p*-xylene (13-14° C.) and that of durene (80° C.) has the very low melting-point of -53.5° (or -54.4°) C. This low melting-point seems to rule out the possibility of all the methyl groups being linked to methyl groups of adjoining molecules, and points rather

to one of the methyl groups having the  $\text{CH}_3 \dots \text{H}$  linkage as in toluene. On this view the arrangement of the mesitylene molecule in the unit cell would be: two methyl groups linked to methyl groups of adjacent molecules, with the hydrogen atoms in *p*-position to them linked to hydrogen atoms of neighbouring molecules, while the third methyl group is linked to a hydrogen atom of the next molecule, the hydrogen *para* to this methyl group being linked to a methyl group of an adjacent molecule.

If each methyl group which is linked to methyl increases the melting-point by the square root of the *p*-xylene effect, and if the methyl group which is linked to hydrogen has the same effect as the asymmetrical methyl group in 1:2:4-trimethylbenzene, then the melting-point of mesitylene should be numerically equal to that of 1:2:4-trimethylbenzene, *viz.*  $212^\circ \text{K.}$ ; the difference between this calculated value and the recorded value is about 3 %. In view of the scanty nature of the experimental evidence for the melting-points of 1:2:4- and 1:3:5-trimethylbenzene, the calculated and recorded values for 1:3:5-trimethylbenzene appear

TABLE VI.

Compound.	M.P. ( $^\circ\text{K.}$ ).	Effect of Methyl Group.
3:5-dichlortoluene . .	293	0.87
3-chlor-5-bromtoluene . .	298.9	0.88
3:5-dibromtoluene . .	312	0.86

in sufficient agreement to justify the provisional view of its unit cell structure described above.

It seems worth while in this connection to consider the related 1:3:5 bodies which contain both methyl groups and halogen atoms, *viz.* the 1:3-dimethyl-5-halogenbenzenes and 1:3-dihalogen-5-methylbenzenes. Both 5-chlor-1:3-xylene and 5-brom-1:3-xylene are liquid at ordinary temperature, whereas the 1:3-dihalogen-5-methylbenzenes (3:5-dihalogenoluenes) are solids. If it is assumed that in these dihalogenoluenes the two single halogen atoms have jointly the same effects as those of the pairs of halogen atoms assumed in Table III, the effect of the methyl group can be calculated; this is shown in Table VI.

The agreement of these values with those given in Table V seems a clear indication that in the 3:5-dihalogenoluenes the methyl group is linked in the same manner as is the methyl group in toluene and its symmetrically substituted derivatives, and this affords some confirmation for the structure of the mesitylene unit cell provisionally stated above.

### Summary and Conclusions.

The melting-points of the members of the methylbenzene series exhibit variations similar (with one exception) to those shown by the chlor- and brom-benzenes. The m.p.s. of *p*-xylene, durene and hexamethylbenzene approximate closely to a geometrical series; the volumes of the unit cells (expressed in terms of a constant number of molecules in each case) approximate to an arithmetical series. *p*-Xylene resembles *p*-dichlorbenzene in having an abnormally low m.p., but the volume of its unit cell (calculated from its molecular weight and density) has a normal value. It is suggested that in *p*-xylene, durene and hexamethylbenzene the pairs of methyl groups in *p*-position are linked to methyl groups of adjacent molecules; this view accords with the published X-ray data for durene and hexamethylbenzene.

The quasi-independent effects on the m.p. of the pairs of halogen atoms or methyl groups persist in the symmetrically substituted methylhalogen benzenes; particularly in the case of the hexa-substituted compounds the m.p. can be calculated with (in most cases) a close approximation to

the observed values; this is regarded as evidence that the unit cells of these bodies are constructed on the same pattern as the hexamethyl and hexa-halogenbenzenes; the volume of the unit cell of pentabromotoluene calculated from its molecular weight and density is in almost exact agreement with the value obtained by extrapolation from that of benzene by addition of the increments due to the three pairs of substituents; the volumes of the unit cell of 2 : 4 : 5-tribromotoluene computed by the two methods are also in almost exact agreement, although in this case the observed and calculated m.ps. differ by 5 %.

The lowering of m.p. caused by the introduction of a single methyl group into the benzene ring is repeated, though to a lesser extent, in the symmetrical homologues and halogen derivatives of toluene. It is suggested that this lowering of m.ps. points to a head-to-tail linkage of the toluene molecules in the unit cell. The low m.p. of mesitylene is contrasted with the comparatively high m.ps. of the symmetrical trihalogenbenzenes, and a tentative structure for the unit cell of mesitylene is suggested; confirmation of this suggested structure is given by the m.ps. of the 3 : 5-dihalogenotoluenes.

---

## PERMEABILITY OF KERATIN MEMBRANES TO WATER VAPOUR.

By G. KING.

*Received 2nd March, 1945.*

It is generally recognised that many cases of so-called diffusion in reality involve much more complicated processes than would be suggested by Fick's Law alone. The diffusion rate is not entirely controlled by the *concentration gradient*,<sup>1</sup> but depends to a great extent on the solubility of the absorbate. That is, deviations from Fick's Law are to be expected when intimate interaction occurs between the absorbate and absorbent.

Previous work in these laboratories<sup>1, 2</sup> has suggested that the transport of water and alcohol through keratin belong to this class of diffusion phenomena so that only the more general form of Fick's Law is applicable; *i.e.* the diffusion coefficient is a function of the concentration of the diffusing substance. In the present paper the variation of the diffusion coefficient of water in horn keratin is investigated quantitatively, and a theory of sorption formulated by Cassie,<sup>3</sup> is applied to the problem with considerable success.

### Experimental.

The general form of the apparatus is shown in Fig. 1. It was, of course, housed in an air thermostat which is not shown.

The membrane M, a film of horn approximately  $5 \times 10^{-3}$  cm. thick, covered a circular orifice about 1 inch in diameter. It was sealed with vacuum wax and clamped in position to prevent loosening due to repeated swelling. The whole membrane system was totally enclosed in a chamber A, formed by two short lengths of telescopic brass tubing to shield the membrane system from the full atmospheric pressure.

On opening taps  $T_1$  and  $T_2$  the whole system could be evacuated by means of a Hyvac Pump incorporating a  $P_2O_5$  drying tube. R is a water reservoir,  $G_1$  a mercury manometer, and B is a tube containing roughly

<sup>1</sup> King, *Trans. Faraday Soc. (in the press)*.

<sup>2</sup> King, *Nature*, 1944, 154, 575.

<sup>3</sup> Cassie, *Trans. Faraday Soc. (in the press)*.

1 g. of wool which acts as a source of constant water vapour pressure. On the other side of M is attached a Spoon Gauge  $G_2$  incorporating a tilting mirror system so that its sensitivity could be raised to about  $10^{-3}$  cm. of mercury per mm. deflection. It gave a reasonably linear response over a small range of pressure (Fig. 2).

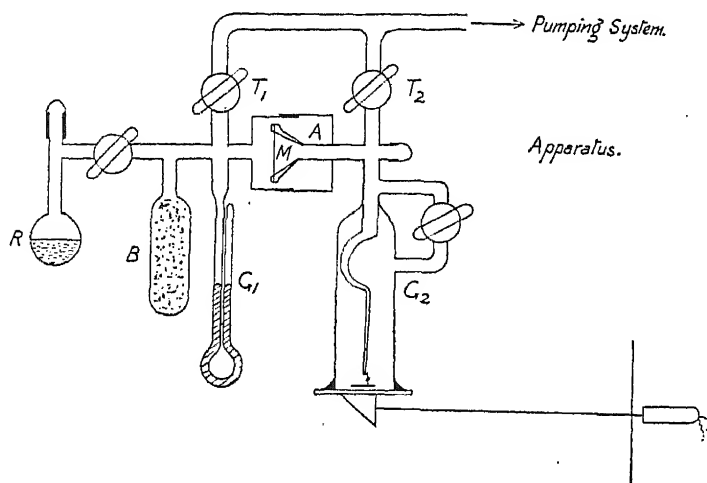


FIG. 1.

**Variation of Rate of Flow with Vapour Pressure difference across the Membrane.**—All observations were made after the steady state had been reached (about two hours), when there was no further accumulation of water at any point in the membrane, and the rate of flow,  $\eta$ , through any unit cross section of the membrane was constant.

Let  $C$  be the water concentration in the film at a distance  $x$  from the high pressure side.

If  $k$  represents the diffusion coefficient, a function of  $C$ , then

$$\eta = k \cdot \frac{dc}{dx} \text{ throughout the membrane.} \quad (1)$$

and if  $C_2$  and  $C_1$  are the water concentrations at the high and low vapour pressure faces respectively, and  $d$  is the membrane thickness,

$$\therefore \int_0^d \eta dx = \int_{C_2}^{C_1} k \cdot dc \quad (2)$$

or

$$\eta = \frac{1}{d} \int_{C_2}^{C_1} k \cdot dc \quad (3)$$

This is further simplified if we make  $C_1 = 0$ ; i.e. maintain the low pressure side at zero pressure by continuous pumping. If  $\eta$  is now measured for a series of values of  $C_2$  we obtain an expression which is the integral of the relation between the diffusion coefficient and concentration.

Different pressures were maintained on the high pressure side of M using the wool in B as a constant vapour pressure source, and  $\eta$  was determined by closing  $T_2$  and measuring the time taken by  $G_2$  to register

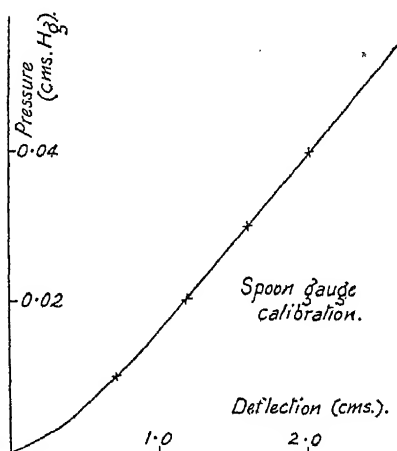


FIG. 2.

a small fixed increase in vapour pressure. Fig. 3, shows the relation obtained between the relative humidity on the high pressure side and  $\eta$ . It is seen that the rate of flow increases extremely rapidly above 70 % relative humidity, and it is further shown that the value of  $\eta$  obtained depends on whether any particular vapour pressure is approached from a higher or a lower value, that is, a marked hysteresis is obtained.

In order to correlate these results with the actual water concentration  $C$ , the vapour pressure isotherm for horn keratin was determined using a method previously described.<sup>1</sup> The curve is shown in Fig. 4. It was found to be very similar to that for the wool-water system, and exhibited a pronounced hysteresis effect. This effect was found to account to within experimental error for the hysteresis shown in Fig. 3, indicating that  $\eta$  is determined entirely by  $C$ , and not by the corresponding vapour pressure. Fig. 5 shows the resulting relation between  $\eta$  and the regain \* at the high pressure face at 25°C. From this curve the corresponding relation between  $k$  and regain was obtained by graphical differentiation, Fig. 6.

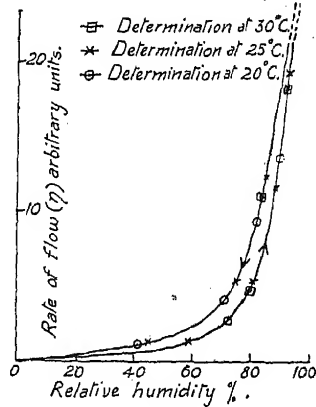


FIG. 3.

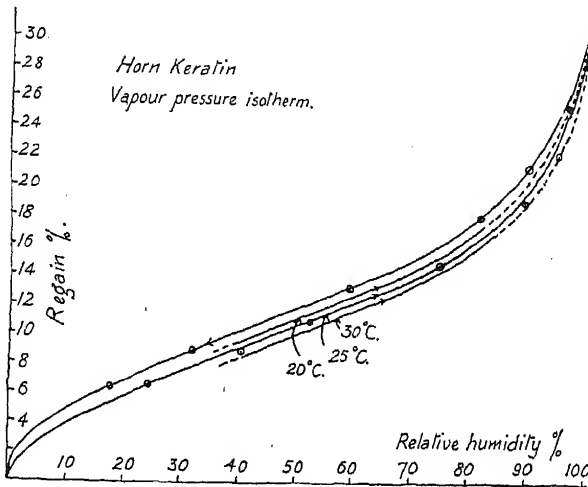


FIG. 4.

**Absolute Values of  $k$ .**—In determining absolute values of  $\eta$ , the perfect gas law is used and gives

$$\eta = \frac{V \cdot M}{RT} \cdot \frac{\Delta p}{\Delta t} \quad (4)$$

Where  $V$  is the volume of that part of the system collecting the water vapour on the low pressure side.  $\Delta t$  is the time required for a given increase in vapour pressure  $\Delta p$ .  $T$  is the absolute temperature.  $R$  the gas constant per g. mol.  $M$  the molecular weight of water.

\* Regain is the moisture content expressed as a percentage of the dry weight, and is proportional to  $C$ .

The absolute value of  $\eta$  can be determined when  $V$  is known. This was obtained by keeping  $\eta$  and  $\Delta p$  constant and increasing  $V$  by known amounts  $\Delta V$ . When  $\Delta V$  is plotted against  $\Delta t$  (Fig. 7), the unknown

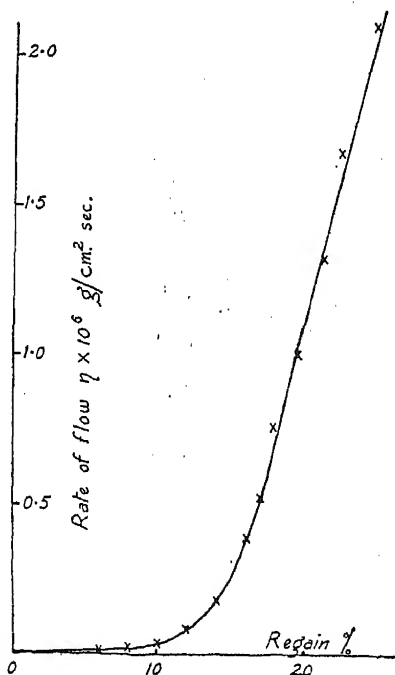


FIG. 5.

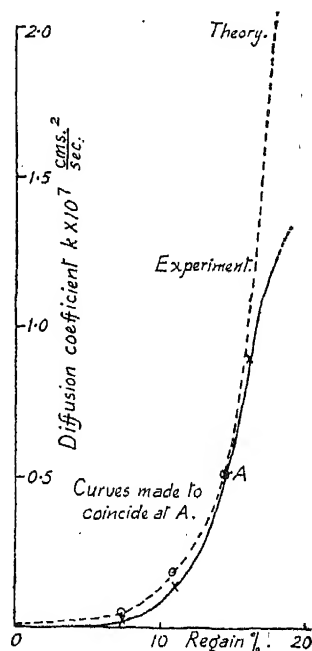


FIG. 6.

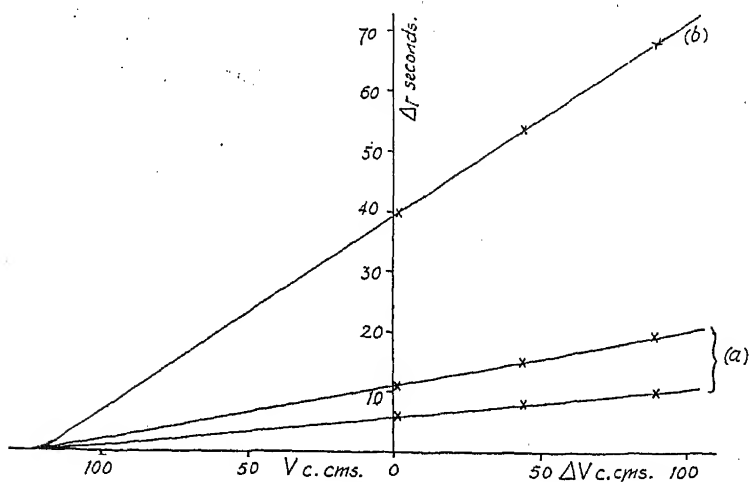


FIG. 7.

volume  $V$  is obtained by extrapolation. Thus it is found that  $k$  varies between the wide limits of  $10^{-7}$  cm.<sup>2</sup>/sec. at high regains, to less than  $10^{-9}$  cm.<sup>2</sup>/sec. as the keratin approaches dryness.

The lower value agrees reasonably well with that previously estimated from the rates of absorption of water by keratin films.<sup>1</sup>

The temperature effect in equation (4) may be neglected over the small range used (20° to 30° C.), but it was decided to investigate how far sorption on the walls of the 'collecting' volume affected the results. As this effect would be most pronounced for low values of  $\eta$  and  $T$ , two relations between  $\Delta V$  and  $\Delta t$  were determined, Fig. 7 (a) for high values of  $\eta$  and  $T$ , and (b) for low values, but in both cases the linear relationships showed that adsorption on to the walls of the apparatus was negligible.

**Effect on  $\eta$  of the Presence of air in the "High Pressure" side of the Membrane.**—During the initial stages of the experimental work it was found that  $\eta$  was extremely sensitive to very small quantities of air present in the high pressure side of the system, especially for high rates of flow. This effect was assumed to be similar to that found during vacuum distillation. The diffusion of the water vapour through the residual air in the system requires a vapour pressure drop between the water reservoir and the membrane surface, and a very slight decrease in vapour pressure at the surface will induce a large decrease in  $\eta$ , as may be seen from Fig. 3. No quantitative data appear to be available on the effect of residual gases on diffusion, and the ordinary relation for the interdiffusion of two gases does not apply to the above conditions where there is no transport of one of the components.

However, following Stefan's theory<sup>4</sup> of diffusion of water vapour through a stationary column of air, a quantitative description of the effect may be obtained, and using approximate data, the apparent decrease in permeability due to the presence of a small amount of air in the high pressure system is satisfactorily explained without assuming any effect of the air on the permeability of the membrane itself. The calculations are reproduced as an appendix.

**Temperature Coefficient.**—The relation between  $\eta$  and relative humidity was determined at three different temperatures (20°, 25° and 30° C.), and the results are shown in the combined graph in Fig. 3. It is noticeable that the values obtained at all three temperatures lie on the same curve both for adsorption and desorption. However, the rate of flow and  $k$  will still have an appreciable temperature coefficient because at any given relative humidity, the corresponding regain decreases with rise in temperature, cf. Fig. 4. Thus in effect  $k$  has a positive temperature coefficient, and if we determine the values of  $k$  corresponding to a regain of 16 % say, at 20° and 30° C., using Figs. 4 and 6, then the slope of the resulting relation between  $\log_e k$  and  $1/T$  gives an approximate value of 4,800 cal./mol. for the activation energy of the diffusion process at that particular regain value.

Owing to the extreme gradients assumed by the relation in Fig. 3, the temperature coefficients cannot be determined with a high order of accuracy at the upper and lower limits of the curve, particularly for values of relative humidity below about 30 %. The temperature coefficient at low regain values was therefore checked independently by a method previously described,<sup>1</sup> involving the determination of the rates of sorption of water vapour by horn films. In this case an activation energy of about 7,500 cal./mol. was obtained.

### The Diffusion Process.

It has been suggested by Barrer<sup>5</sup> that the activation energy for diffusion is determined entirely by the energy of hole formation in the lattice so that for diffusion through elastic media, low activation energies are generally obtained, independent to a large extent, of the size of the diffusing

<sup>4</sup> Stefan, *Sitz. Ber. Akad. Wiss. Wien, Math-naturw. Klasse.*, 1881, Abt. 2a, 83.

<sup>5</sup> Barrer, *Diffusion in and through Solids*, Cambridge University Press, 1941.



molecule. This suggests that a qualitative explanation of the dependence of  $k$  upon concentration is that the elasticity of keratin decreases with its water content.

However, Cassie<sup>2</sup> has shown that the hysteresis of the sorption isotherm for a wool-water system may be fully accounted for by the change of the elastic constraint experienced during swelling and shrinking. Thus it is possible to change the elastic constants of keratin at constant regain, by moving from the absorption to the desorption portions of the vapour pressure isotherm, *cf.* Fig. 4, but it is not possible to change  $\eta$  by performing this same operation. We must therefore conclude that the rigidity of the keratin lattice can exert but little control over  $k$ , at least, for values of  $C$  above about 6 %.

An alternative theory takes into account two states of the sorbed water, applying a theory of sorption developed by Cassie.<sup>3</sup> Cassie shows that if in 100 g. of absorbent there are  $B$  mol. of low energy sites, and if  $A$  mol. of absorbate are distributed amongst these sites so that  $X$  are occupied, then

$$(A - X)(B - X) = \beta X^2 \quad (5)$$

where  $\beta = a \cdot e^{-w/RT}$ ,  $a$  is a constant, slightly dependent on temperature, and  $w$  is the heat of sorption from liquid water for a low energy site.

It is reasonable to assume, that in order to diffuse, the water molecules must first attain the relatively mobile or liquid state of the  $(A - X)$  molecules, so that in these molecules we have the source from which we obtain activated diffusion.

Leonnard-Jones'<sup>6</sup> theory of surface diffusion can be applied to the diffusion of the "mobile" molecules through the unoccupied low energy sites, without restricting the sites to a two dimensional array situated on external or internal surfaces.

If  $\epsilon$  is the activation energy required for diffusion of these "mobile" molecules, then the rate of production of activated molecules per c.c. per second is:

$$\nu \cdot e^{-\epsilon/RT}$$

where  $\nu$  is a constant.

Applying Knudsen's Cosine Law, the rate of flow through unit area perpendicular to the  $x$  direction is given by:

$$T_x = \frac{1}{2} \nu \cdot e^{-\epsilon/RT} \lambda^2 \cdot \frac{d(A - X)}{dx} \quad (6)$$

where  $\lambda$  is the mean free path of the activated molecules before becoming deactivated, and immobile.

Then if we assume that mobility is lost only by encounters with the  $(B - X)$  mols. of unoccupied sites

$$\therefore \lambda \propto \frac{1}{(B - X)}$$

$$\text{and } T_x = \frac{1}{2} K \cdot e^{-\epsilon/RT} \frac{1}{(B - X)^2} \cdot \frac{d(A - X)}{dx} \quad (7)$$

But  $T_x = k \cdot dA/dx$ ,

$$\therefore k = \frac{1}{2} K \cdot e^{-\epsilon/RT} \frac{1}{(B - X)^2} \cdot \frac{d(A - X)}{dA} \quad (8)$$

where  $K$  is a constant.

Using Cassie's values of 1.12 and 0.1 for  $B$  and  $\beta$  respectively, obtained for the wool-water system,<sup>3</sup> values for  $(A - X)$  and  $(B - X)$  may be obtained from (5) for different values of  $A$  and therefore the expression for  $k$ , (8) may be compared directly with the experimental data of Fig. 6. The agreement is seen to be very good when we recall the very simple

<sup>6</sup> Leonnard-Jones, *Trans. Faraday Soc.*, 1932, 28, 349.

nature of the diffusing mechanism assumed. The abnormally rapid increase in  $k$  for large values of  $A$ , obtained for the theoretical curve is no doubt due to the fact that it has been assumed that the "mobile" molecules diffuse in an unrestricted manner except for encounters with vacant localised sites. This obviously cannot be so, and even if we neglect any retarding effect due to the presence of the keratin lattice, the maximum value of  $k$  should at most approach the value of  $2 \times 10^{-5}$  cm.<sup>2</sup>/sec.,<sup>7</sup> the coefficient for the self diffusion of water, as saturation is attained.

However, by introducing the term  $e^{-\epsilon/RT}$  we imply that the diffusing molecules may be deactivated otherwise than by encounters with the  $(B - X)$  vacant sites. It seems reasonable to assume that transport occurs by jumps between occupied sites of which there are  $X$  mols, suggesting that  $\lambda$  should be of the form

$$\frac{1}{\alpha \cdot X + (B - X)}$$

where  $\alpha$  determines the relative importance of the two types of encounters and has a value of about 0.05 for horn keratin. This expression rapidly approaches a constant value for  $\lambda$  as  $A$  increases and  $X$  approaches the value  $B$ , and thus  $k$  does not become infinite as saturation is approached. It is difficult, however, to interpret  $\alpha$  accurately, and this form does not increase our knowledge of the diffusion mechanism, although it improves the agreement of theory with experiment.

The simple relation obtained for  $k$ , will also account to some extent for the variation of the temperature coefficient of diffusion with concentration, owing to the fact that  $X$  is a function of  $\beta$  as well as of  $A$ . An increase in the energy of activation with decrease in water concentration is indicated as was found to be the case experimentally, but until more accurate experimental values are available we cannot place too much reliance on this agreement.

#### APPENDIX.

Stefan<sup>4</sup> has derived an expression for the diffusion of water vapour through a stationary column of air, but it includes an unknown constant which he calls the "coefficient of resistance," so that the relation remains somewhat empirical in character. A similar relation may be obtained, however, if we modify Meyer's Kinetic theory<sup>8</sup> for the interdiffusion of two gases, to obey the condition that one component does not undergo transport.

According to Meyer, the net transport  $\tau$ , per unit area perpendicular to the flow, of each of two interdiffusing gases  $A$  and  $W$  is given by:

$$\tau_A = n_A \cdot w - \frac{l_A \cdot v_A}{3} \cdot \frac{dn_A}{dx} \quad . \quad . \quad . \quad (1)$$

$$\tau_W = n_W \cdot w - \frac{l_W \cdot v_W}{3} \cdot \frac{dn_W}{dx} \quad . \quad . \quad . \quad (2)$$

Where  $n$  is the number of molecules per unit volume,  $v$  is the mean molecular velocity,  $l$  is the mean free path,  $w$  is some mean velocity about which the velocities of the component molecules are distributed in a Maxwellian manner.

Also  $(n_A + n_W) = \text{constant for all values of } x$ .

$$\therefore \frac{dn_A}{dx} = - \frac{dn_W}{dx} \quad . \quad . \quad . \quad (3)$$

<sup>7</sup> Glasstone, Laidler and Eyring, *The Theory of Rate Processes*, McGraw-Hill Book Co., 1941.

<sup>8</sup> Meyer, *Kinetic Theory of Gases* (English translation), 255.

If instead of making  $\tau_A = -\tau_W$ , we apply Stefan's condition of zero transport for one component, *i.e.*  $\tau_A = 0$  say, then

$$\tau_W = -\frac{1}{3} \cdot \frac{n_W \cdot l_A \cdot v_A + n_A \cdot l_W \cdot v_W}{n_A} \cdot \frac{dn_W}{dx} \quad (4)$$

and if  $n_A \rightarrow 0$

$$\therefore \tau_W = -\frac{1}{3} \cdot \frac{n_W l_A v_A}{n_A} \cdot \frac{dn_W}{dx} \quad (5)$$

So that the mass of the  $W$  component transported per unit area per second is :

$$-\frac{1}{3} \times 76 \times 981 \times 13.6 \times \frac{v_A \cdot L_A \cdot p_W \cdot M_W}{RT p_A^2} \cdot \frac{dp_W}{dx} \quad (6)$$

Where  $L_A$  is the mean free path of air molecules at normal temperature and pressure ( $\approx 9.5 \times 10^{-6}$  cm.),  $v_A$  is the mean molecular velocity of air at N.T.P. ( $\approx 5 \times 10^4$  cm./sec.),  $p_W$  is the water vapour pressure on the high pressure side of the membrane in cm., of Hg,  $p_A$  is the residual air pressure in cm. of Hg,  $M_W$  is the molecular weight of water,  $R$  is the universal gas constant per g. mol.,  $T$  is the absolute temperature.

Now let  $p_R$  be the water vapour pressure at the reservoir,  $p_M$  be the water vapour pressure at the membrane face,  $l$  be the length of tube connecting the reservoir and membrane ( $\approx 20$  cm.),  $b$  be the cross section area of this tube ( $\approx 0.5$  sq. cm.).

$\therefore$  The total flow of water vapour in g. per sec. when  $p_W \approx 2$  cm. Hg ( $25^\circ$  C.) from (6),

$$G_W = \frac{K}{p_A^2} (p_R - p_M) \quad (7)$$

Where  $K = 5 \times 10^{-6}$  g./sec.  $\times$  cm. Hg.

Now Fig. 3 shows that as we approach saturation  $\eta$  bears a linear relationship to  $p_M$  and so

$$G_W = \eta \times (\text{area of membrane}) = \alpha(p_M - D) \quad (8)$$

where  $D$  is a constant.

And assuming  $G_W \approx 10^{-5}$  g./sec., we obtain from Fig. 3

$$\alpha \approx 5 \times 10^{-5} \text{ g./sec.} \times \text{cm. Hg.}$$

Then from (7) and (8)

$$G_W = \frac{\alpha(p_R - D)}{\left(1 + \frac{\alpha}{K} p_A^2\right)} \quad (9)$$

But if  $p_A \approx 0.1$  cm. Hg,

$$\therefore \frac{\alpha}{K} \cdot p_A^2 \approx \frac{1}{10}$$

Therefore (9) may be further simplified by expanding the denominator in terms of  $\left[\frac{\alpha}{K} \cdot p_A^2\right]$  and neglecting terms of higher order than unity,

$$\therefore G_W \approx \alpha(p_R - D)(1 - 10p_A^2) \quad (10)$$

The term  $\alpha(p_R - D)$  gives the value for  $G_W$ , say  $G'_W$ , when there is no residual air in the system.

$$\begin{aligned} \therefore G_W &\approx G'_W(1 - 10p_A^2) \\ &\approx 0.9 G'_W \text{ when } p_A = 0.1 \text{ cm. Hg.} \end{aligned}$$

which is close to the order of the effect observed.

According to Chapman<sup>9</sup> the Kinetic Theory of gaseous diffusion as derived above is not strictly correct and may lead to erroneous results so the above solution cannot claim to be rigorous, but it should suffice to distinguish the origin of the effect.

### Summary.

The rate of diffusion of water vapour through a keratin membrane has been investigated over a range of vapour pressure gradients, and at different temperatures. The results show that the diffusion coefficient is a function of the water concentration, and the temperature, and that it is independent, to a large extent, of the elasticity of the keratin lattice. A theory of sorption previously developed by Cassie<sup>3</sup> is applied to the experimentally derived relation between diffusion coefficient and concentration, with some success.

An appendix to the paper explains quantitatively the apparent reduction in permeability of the membrane due to residual air in the "high pressure" side of the system.

I am grateful to Mr. B. H. Wilsdon, Director of Research, for his continued interest in the work, to Dr. A. B. D. Cassie for allowing me full access to his paper on the theory of sorption,<sup>3</sup> prior to publication, and to the Wool Industries Research Association for permission to publish these results.

<sup>9</sup> Chapman, *Phil. Mag. A*, 1928, 5, 630.

---

## THE MECHANISM OF SPARK IGNITION.

BY J. W. LINNETT, (MRS.) E. J. RAYNOR AND W. E. FROST.

*Received 20th March, 1945.*

There is still much difference of opinion regarding the mechanism of gaseous ignition and of the propagation of flame. The most extreme forms of these opinions on the ignition problem are, on the one hand, the thermal theory as formulated by Taylor-Jones, Morgan and Wheeler;<sup>1</sup> and, on the other, the chain theory as put forward by Mole.<sup>2</sup> The limiting form of the thermal theory is that, in order to cause ignition, it is necessary "to raise a sufficient volume of the gas to a sufficient temperature." No account is taken of the chemical processes that lead up to ignition. The limiting form of the chain theory, as presented by Mole, supposes that the local source of ignition introduces into a small portion of the gas a number of active atoms or radicals, and that if this number multiplies without limit then ignition results. Mole presumes that the active particles multiply by chain branching and are lost by diffusion, but he ignores completely any effect of changing temperature on the rate of multiplication or diffusion of the active particles.

In between these two extreme opinions is a treatment by Landau<sup>3</sup> of "Ignition by Local Sources." Landau, while supposing that the chemical processes in the small volume adjacent to the source were of the chain type, took as his criterion of ignition that the temperature should rise without limit at the centre of the small volume. He presumed that the local source introduced into a small volume a given concentration of active particles but he, like Mole, ignored completely the effect of changing temperature on the chemical processes.

<sup>1</sup> Taylor-Jones, Morgan and Wheeler, *Phil. Mag.*, 1922, 43, 359.

<sup>2</sup> Mole, *Proc. Physical Soc.*, 1936, 48, 857.

<sup>3</sup> Landau, *Chem. Rev.*, 1937, 21, 245.

The difficulty of testing these theories of ignition lies in the difficulty of measuring the quantities involved in the theories formulated. For instance, in the Landau theory, one of the important factors is the initial concentration of active particles produced by the local source. There is no means of measuring such a quantity. However attempts have been made to differentiate between the various theories of ignition. Coward and Meiter<sup>4</sup> determined the volumes of methane-air mixtures burnt by sparks which were just insufficient to cause general ignition. They concluded that the electric spark acted "mainly, perhaps entirely, as a source of thermal energy in igniting a gas mixture." On the other hand, Finch and Thompson<sup>5</sup> determined minimum igniting pressures for sparks of different energies and of different oscillation frequencies. They found that both the total energy dissipated and the rate of energy dissipation were unimportant but that the oscillation frequency was the vital factor. They concluded that "ignition is determined by the setting up of a sufficient concentration of suitably activated molecules." Results obtained by Silver<sup>6</sup> and by Paterson<sup>7</sup> on ignition by heated spheres have been interpreted by both a purely thermal treatment and by the chain-thermal treatment of Landau.

H. W. Thompson,<sup>8</sup> following a suggestion of Alyea and Haber,<sup>9</sup> carried out experiments on the minimum igniting pressures of mixtures of hydrogen and oxygen in the presence of various added gases (*cf.* also Coward, Cooper and Jacobs<sup>10</sup>). Thompson determined the minimum igniting pressure of electrolytic gas and found that this was lowered by the addition of inert gases. From this he concluded that the minimum igniting pressure was analogous to the low pressure limit of the low pressure explosion region at higher temperatures. He explained the lowering produced by inert gases by supposing that the latter prevented the diffusion of chain carriers to the walls of the ignition tube. He found that the results were quantitatively in agreement with this interpretation in that they obeyed the relation suggested by Melville and Ludlam<sup>11</sup> for the effect of inert gases on the "lower limit." Moreover, the relative diffusion coefficients that Thompson found for the different inert gases were entirely reasonable. So Thompson was able to explain the ignition of electrolytic gas at these low pressures (ca. 40 mm.) in terms of a purely chain theory, and his experiments showed no evidence of the thermal effect of the spark being the limiting factor under these conditions. However, the results he obtained are for rather low pressures (ca. a tenth or twentieth of an atmosphere) and the behaviour under these conditions may be quite different from that at higher pressures. This paper describes a repetition of Thompson's measurements with a less intense spark and their extension up to pressures of the order of half an atmosphere.

### Experimental Method.

The explosion was carried out in three different pyrex tubes, attachable through cone-socket joints to an apparatus for introducing the different gases which could be evacuated by a mercury pump backed by an oil pump. The tubes were all about 25 cm. long and two were of internal diameter 2.0 cm. and one of internal diameter 3.7 cm. The spark gap, which was situated centrally at a distance from the top of the tube about equal to half the diameter of the tube, consisted of two tungsten

<sup>4</sup> Coward and Meiter, *J.A.C.S.*, 1927, 49, 396.

<sup>5</sup> Finch and Thompson, *Proc. Roy. Soc., A*, 1931, 134, 343.

<sup>6</sup> Silver, *Phil. Mag.*, 1937, 23, 633.

<sup>7</sup> Paterson, *ibid.*, 1939, 28, 1; 1940, 30, 437.

<sup>8</sup> Thompson, *Trans. Faraday Soc.*, 1932, 28, 299.

<sup>9</sup> Alyea and Haber, *Z. physik. Chem., B*, 1930, 10, 193.

<sup>10</sup> Coward, Cooper and Jacobs, *J.C.S.*, 1914, 1069.

<sup>11</sup> Melville and Ludlam, *Proc. Roy. Soc., A*, 1931, 132, 108.

wires, sealed through the pyrex walls and having pyrex sheaths up to about 5 mm. from their ends so that they were held firmly in one position. The diameter of the tungsten wire was 0.37 mm. The distance between the tungsten points was measured photographically by throwing a shadow with parallel light on to a piece of photographic paper held immediately behind the wires. These distances in the three tubes were: Tube A of diameter 3.7 cm.: 1.7 mm.; Tube B of diameter 2.0 cm.: 1.4 mm.; Tube C of diameter 2.0 cm.: 0.42 mm. The spark was obtained from a small induction coil running off a battery of 4 v. All the gases used were obtained from cylinders and dried before entering the apparatus, except the hydrogen which was prepared from sulphuric acid and zinc and passed through tubes containing calcium chloride and soda lime before entering the apparatus. When different gases were put into the explosion tube they were mixed by withdrawing them several times into a mercury filled reservoir and then returning them to the explosion tube. The pressures of the gases were measured on a capillary mercury manometer. Explosion was observed either by seeing the flame or by noting the pressure change on passing the spark.

The minimum igniting pressures were determined by taking a fixed amount of "electrolytic gas" and mixing with it a measured amount, of the added gas. The mixture was then tested to see whether it could be ignited or not. Three successive failures to ignite were taken as showing that the mixture was non-ignitable. The same amount of electrolytic gas was then taken and a different amount of the added gas introduced, and the mixture tested after mixing. The process was repeated until the limit between ignitable and non-ignitable mixtures had been fixed. Mixtures close to the limit would sometimes ignite on the second or third sparking of a given mixture, having failed with the previous spark or sparks. However, this difficulty was small since it only led to an uncertainty of one or at the most two mm. in the limit.

**Experimental Results.** The effect of the addition of hydrogen, oxygen, nitrogen, argon and carbon dioxide on the minimum igniting pressure of "electrolytic gas" has been determined over a wide range for the tubes A and B, and for a narrower range, with nitrogen only, for tube C. The results are shown in Table I which lists the limiting pressures of electrolytic gas and of the added gas for different proportions of the latter.

### Discussion.

The effect of hydrogen, nitrogen and oxygen on the limiting ignition pressure of electrolytic gas for the wide tube A is shown in Fig. 1, the limiting pressure of electrolytic gas being plotted against the pressure of the added gas. These curves are typical, in general form, for all the cases studied. The most general observation of the present study is that the curves in Fig. 1 consist of two parts, one having a negative slope and the other a positive slope. It therefore appears that in small amounts the added gas exerts one type of effect, which is the same as that observed by H. W. Thompson, but that larger amounts exert a quite different effect. For instance, small amounts of nitrogen promote the ignition of electrolytic gas, but with larger amounts more electrolytic gas is necessary for ignition the greater is the pressure of the nitrogen. The results for these two regions will be examined in separate sections: Section A—The region in which the addition of more added gas aids ignition; Section B—The region in which the addition of more of the added gas hinders ignition.

#### Section A.

H. W. Thompson has interpreted the effect of inert gas in this region by supposing that the inert gas aids chain branching by preventing the diffusion of chain carriers to the walls where they are destroyed. The

TABLE I.—THE MEASURED LIMITING IGNITION PRESSURE.

The pressures are given in mm. of mercury;  $p_a$  is the pressure of electrolytic gas,  $p_a$  that of the added gas. The figures are listed for different added gases.

Tube A.			Tube B.		
$p_e$ .	$p_a$ .	$p_a/p_e$ .	$p_e$ .	$p_a$ .	$p_a/p_e$ .
Hydrogen.					
123	0	0.00	143½	0	0.00
100	130	1.30	137	22½	0.16
95	160	1.68	128	50½	0.39
93	228½	2.46	123½	72½	0.59
95	288	3.03	119½	99½	0.83
100	338½	3.39	114	139	1.22
			105½	179	1.70
			105	200½	1.91
			104	210½	2.02
			104½	230½	2.21
			108	250½	2.32
			114½	300½	2.62
			122	347	2.84
Oxygen.					
123	0	0.00	143½	0	0.00
100	11	0.11	111	14	0.13
69½	26½	0.38	81	30½	0.38
50½	37½	0.74	60½	40	0.66
40½	43	1.06	50½	47	0.93
30	50	1.67	41½	53	1.28
20	60	3.00	32½	61	1.88
17½	66½	3.80	22½	67½	3.00
17½	157½	9.00	20	70½	3.53
20	189	9.45	20	145½	7.28
30	295	9.83	22½	180	8.00
40	388½	9.71	30	268	8.93
			40	375	9.38
Argon.					
123	0	0.00	143½	0	0.00
112	9	0.08	130	12½	0.10
105	18	0.17	120	22	0.18
100	24	0.24	110	27	0.25
90	35	0.39	100	38½	0.39
80	44	0.55	90	47	0.52
70	57	0.81	80	59½	0.74
60	72	1.20	70	79	1.13
50	94½	1.89	60	93	1.55
45	118	2.62	50	119	2.38
45	181½	4.03	48	182	3.79
50	255½	5.11	50	231	4.62
55	317	5.76	55	299	5.44
60	370½	6.17	60	363	6.05
Carbon Dioxide.					
123	0	0.00	143½	0	0.00
105	9½	0.09	126	8	0.06
100	13	0.13	106	18½	0.17
90	21	0.23	91	30	0.33
80	26	0.33	81½	40	0.49
70	33	0.47	67	54	0.81
60	42½	0.71	57	65½	1.15
50	60½	1.21	51½	78	1.51
47	70½	1.50	51½	80	1.55
47	111	2.36	57	112½	1.97
50	127½	2.55	63	144	2.29
60	177	2.95	74	176	2.38
70	226	3.24	77½	195	2.52
80	260½	3.26	84	228½	2.72
			93½	268	2.87

TABLE I.—*Continued.*

Nitrogen.								
Tube A.			Tube B.			Tube C.		
123	0	0.00	143½	0	0.00	192	0	0.00
100	19	0.19	125	13	0.10	175	10	0.06
90	30½	0.34	109½	29	0.27	148½	34½	0.23
80	41	0.51	95	42½	0.45	119	71½	0.60
70	51½	0.74	79½	59	0.74	107½	93	0.87
60	61½	1.03	60	90	1.50	100	119	1.19
50	88½	1.77	50	118	2.36	100	325	3.25
45	113½	2.53	50	126	2.52			
45	125½	2.79	52½	194	4.08			
47	159½	3.39	55	237½	4.32			
50	214½	4.29	60	271	4.52			
55	273	4.96	70	355½	5.08			
60	319	5.32	75	380	5.07			
65	342½	5.27	80	409½	5.12			
70	362	5.17	90	464	5.16			
75	394	5.25						

promoting effect of the inert gas on ignition certainly suggests that the effect is one of reducing the rate of diffusion of chain carriers. However, the chain ignition theory of Mole, and the chain thermal theory of Landau, would certainly interpret this, not as preventing diffusion to the walls of the tube, but as preventing diffusion of these chain carriers out of the small volume round the source of ignition so that the concentration of chain carriers (or, according to Landau, the temperature) could rise without limit within the small volume. If the explanation of Thompson is correct,

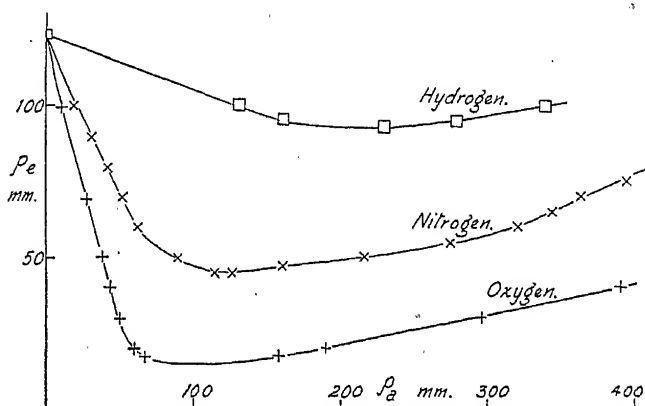


FIG. 1.

we should expect to find an effect of tube diameter on the behaviour; while if the latter explanation is the correct one, we should expect to find no effect of tube dimension but only one of spark dimension. Thompson, in his experiments, found that the tube diameter did affect the behaviour; but, on the other hand, Coward, Cooper and Warburton<sup>12</sup> could find no effect of tube size or shape in their experiments on the minimum igniting pressure of electrolytic gas. Our results also indicated that the tube diameter had no effect on the minimum igniting pressure but that the spark gap was the controlling factor (see later). Our results, like those of Coward, Cooper and Warburton, therefore suggest that the effect of inert gas is to be sought in their prevention of diffusion from a small volume

<sup>12</sup> Coward, Cooper and Warburton, *J.C.S.*, 1912, 2278.



round the spark. The reason for the difference between the results of H. W. Thompson and those of ourselves and of Coward, Cooper and Warburton may be that the former used a very much more intense spark and hence obtained ignition down to very much lower pressures. Our limiting pressures for electrolytic gas alone were of the order of a fifth of an atmosphere, those of Coward, Cooper and Warburton of the order of a tenth of an atmosphere, while those of H. W. Thompson were of the order of a twentieth of an atmosphere. The limiting factor for combustion of the gas in the tube may therefore have been, in Thompson's experiments, the limit of propagation of flame, whereas in our experiments and those of Coward and his co-workers the limiting factor was certainly ignition by the local source. We may therefore proceed to interpret our results on the assumption that in our experiments the inert gas prevents the loss of chain carriers by diffusion from a small region round the spark.

In the following calculations the treatment of Mole has been modified on the basis of more detailed knowledge of the mechanism of the hydrogen-oxygen reaction. Let us suppose that the spark introduces chain carriers into a small volume round it at a rate  $\alpha$ . Let the rate of increase of chain carriers by branching be proportional to the number of chain carriers and to some function of the pressures of hydrogen and oxygen:  $\beta \cdot n \cdot f(p_{H_2}, p_{O_2})$ , where  $n$  is the number of chain carriers in the small volume and  $\beta$  is a constant. Let the chain carriers be lost from the small volume at a rate proportional to  $n$ :  $\gamma \cdot n$ , where  $\gamma$  depends on the diffusion characteristics of the gas. Then the rate of growth of chain carriers is given by:

$$dn/dt = \alpha + \beta \cdot n \cdot f(p_{H_2}, p_{O_2}) - \gamma \cdot n.$$

The limiting value of  $n$  is reached when  $dn/dt$  becomes zero, and is given by:

$$n_1 = \frac{\alpha}{\gamma - \beta \cdot f(p_{H_2}, p_{O_2})} \quad (1)$$

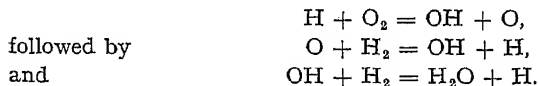
The limiting value will reach infinity if the second term in the denominator becomes equal to the first. The limiting condition for ignition will then be

$$\gamma = \beta \cdot f(p_{H_2}, p_{O_2}) \quad (2)$$

if we take, as Mole did, the increase of  $n$  without limit as the criterion of ignition. Now we must consider the way in which  $\gamma$  will vary with pressure and composition, and the nature of the function on the right-hand side of equation (2).

Since  $\gamma$  is the coefficient determining the rate of diffusion, it is equal to the reciprocal of  $\Sigma K_d \cdot p_g$ , the sum being taken for all gases present.  $K_d$  is the reciprocal of the diffusion coefficient.

It remains to decide a reasonable form for the function,  $f(p_{H_2}, p_{O_2})$  on the right hand side of equation (2). The probable succession of processes leading to chain branching is:



followed by  
and

The average lifetime of a hydrogen atom in the first stage will be proportional to the reciprocal of the oxygen pressure. Also the average duration of the two parts of the second stage will be proportional to the reciprocal of the hydrogen pressure. The average duration of the whole cycle of chemical reactions that leads to chain branching will therefore be

$$\begin{aligned} t_{av} &= k_1/p_{O_2} + k_2/p_{O_2} \\ &= \frac{k_1 \cdot p_{O_2} + k_2 \cdot p_{H_2}}{p_{O_2} \cdot p_{H_2}}. \end{aligned}$$

The rate of chain branching will be proportional to the reciprocal to  $t_{av}$ . so we have :

$$f(p_{H_2}, p_{O_2}) = \frac{p_{H_2} \cdot p_{O_2}}{k_1 \cdot p_{O_2} + k_2 \cdot p_{H_2}}$$

Thus equation (2) becomes :

$$\beta \cdot \frac{p_{H_2} \cdot p_{O_2}}{k_1 \cdot p_{O_2} + k_2 \cdot p_{H_2}} = \frac{I}{K_1 \cdot p_{H_2} + K_2 \cdot p_{O_2} + K_3 \cdot p_a} \quad (3)$$

where  $p_a$  is the pressure of the added gas.

The application of this formula to the present measurements will be considered in two parts: (i) The addition of hydrogen and oxygen to electrolytic gas; (ii) The addition of nitrogen, argon and carbon dioxide to electrolytic gas. It must be remembered that the above formula is intended to apply only to the experiments in the low pressure region. It will be assumed throughout that the build-up to  $n = \infty$  occurs before the hydrogen and oxygen have been used up appreciably.

(i) **Hydrogen-Oxygen Mixtures.**—If the graphs of  $p_{H_2}$  against  $p_{O_2}$  are plotted for the two tubes it is found that they are of the same form; and, moreover, that by making a scale adjustment of one of the curves relative to the other the two can be made virtually coincident. This shows that the behaviour of the two tubes is quite analogous as regards the effect of the gas pressures and differs only in the size and nature of the spark. The observed values of  $p_{H_2}$  and  $p_{O_2}$  at the limit of ignition are given in Table II, the figures being taken from Table I.

Formula (3) can be rearranged to a more convenient form :

$$\frac{k_1}{p_{H_2}} + \frac{k_2}{p_{O_2}} = \beta \cdot K_1 \cdot p_{H_2} + \beta \cdot K_2 \cdot p_{O_2} \quad (4)$$

The actual formulæ that have been used are :

$$\text{For Tube B: } \frac{1860}{p_{H_2}} + \frac{12,530}{p_{O_2}} = p_{H_2} + 3.68 p_{O_2} \quad (5a)$$

$$\text{For Tube A: } \frac{1860}{1.13 p_{H_2}} + \frac{12,530}{1.13 p_{O_2}} = 1.13 p_{H_2} + 3.68 (1.13 p_{O_2}) \quad (5b)$$

The third column of Table II lists the oxygen pressures calculated from equation (5) from the observed hydrogen pressures in the first column. The fourth and fifth columns of Table II give the difference and percentage difference between the calculated and observed oxygen pressures. The mean difference is 1.2 mm. and the mean percentage difference is  $2\frac{1}{2}\%$ . Considering the simplifying assumptions that were made in the derivation of equation (4) this agreement is surprisingly good.

Comparing equations (4) and (5) it will be seen that  $k_2/k_1 = 6.7$ , and  $K_2/K_1 = 3.68$ . The first ratio measures the relative rate constants of the reactions of chain propagators (O and OH) with hydrogen molecules and that of other chain propagators (H) with oxygen molecules. The above result indicates that the slow reaction in the chain branching process at equal oxygen and hydrogen pressures is  $H + O_2 = OH + O$ , and that this therefore is the controlling factor in the rate of chain branching.

$K_2/K_1$  measures the ratio of the diffusion coefficients of the chain carriers through hydrogen and oxygen. The chain carriers tending to diffuse out of the small local region round the spark are oxygen and hydrogen atoms and hydroxyl radicals. It is therefore a simplification to use only one diffusion term as was done in (3). The magnitude of  $K_2/K_1$  will be discussed in the next section.

(ii) **Inert Additions to Electrolytic Gas.**—In these experiments the ratio  $p_{H_2}/p_{O_2}$  was always two, so that equation (3) can be transformed to :

$$\beta' \cdot p_e = \frac{I}{K' \cdot p_e + K_3 \cdot p_a} \quad (6)$$

where  $p_e$  is the pressure of electrolytic gas ( $2\text{H}_2 + \text{O}_2$ ) and  $p_a$  is the pressure of the added gas. Equation (6) can be rearranged to give:

$$\frac{1}{K' \cdot p' \cdot p_e^2} - 1 = \frac{K_3}{K'} \cdot \frac{p_a}{p_e} \quad (7)$$

If for  $p_a = 0$ ,  $p_e = p_0$  equation (7) becomes:

$$\frac{p_0^2 - p_e^2}{p_e^2} = \frac{K_3}{K'} \cdot \frac{p_a}{p_e} \quad (8)$$

TABLE II.—LIMITING IGNITION CONDITIONS OF HYDROGEN-OXYGEN MIXTURES.

$p_{\text{H}_2}$ (obs.).	$p_{\text{O}_2}$ (obs.).	$p_{\text{O}_2}$ (calc.).	Difference	Percentage Difference.
<b>Tube B.</b>				
249.3	35.2	34.1	-1.1	-3
215.0	38.0	36.7	-1.3	-4
179.2	39.8	39.8	0.0	0
154.8	41.2	42.1	+0.9	+2
135.8	42.7	44.1	+1.4	+3
113.8	45.7	46.6	+0.9	+2
95.7	47.8	48.9	+1.1	+2
74.0	51.0	52.1	+1.1	+2
54.0	57.5	55.8	-1.7	-3
40.3	60.2	59.2	-1.0	-2
33.7	63.8	61.3	-2.5	-4
27.7	66.8	64.0	-2.8	-4
21.7	71.8	67.7	-4.1	-6
15.0	75.0	75.0	0.0	0
13.3	77.2	78.0	+0.8	+1
<b>Tube A.</b>				
223.3	31.7	29.9	-1.8	-6
196.7	33.3	33.1	-0.2	-1
168.0	35.0	34.4	-0.6	-2
82.0	41.0	43.6	+2.6	+6
66.7	44.3	45.8	+1.5	+3
46.3	49.7	49.6	-0.1	0
33.7	54.3	52.9	-1.4	-3
27.0	56.5	55.4	-1.1	-2
20.0	60.0	59.2	-0.8	-1
13.3	66.7	66.3	-0.4	-1
Mean			1.2	2½

Fig. 2 shows the term on the left-hand side of equation (8) plotted against  $p_a/p_e$  for the two gases, nitrogen and carbon dioxide. The results for all the tubes are included on the same graph. It will be seen that the points for a given gas fall on the same line, independently of the tube used, showing that  $K_3/K'$  is characteristic of the gas and independent of the tube, as would be expected. The values of  $K_3/K'$  for nitrogen, argon and carbon dioxide are 2.95, 2.75 and 4.5 respectively.

Now  $3K' = 2K_{\text{H}_2} + K_{\text{O}_2}$   
 and  $K_{\text{O}_2} = 3.68 K_{\text{H}_2}$   
 So  $K' = 1.89 K_{\text{H}_2}$ .

Therefore  $K_{\text{N}_2} = 5.6 K_{\text{H}_2}$ ;  $K_{\text{A}} = 5.2 K_{\text{H}_2}$ ; and  $K_{\text{CO}_2} = 8.5 K_{\text{H}_2}$ . These constants are the reciprocals of the diffusion coefficients, so that we have:  $D_{\text{O}_2} = 0.27 D_{\text{H}_2}$ ;  $D_{\text{N}_2} = 0.179 D_{\text{H}_2}$ ;  $D_{\text{A}} = 0.192 D_{\text{H}_2}$ ; and  $D_{\text{CO}_2} = 0.118 D_{\text{H}_2}$ . This also gives for the three inert gases:  $D_{\text{N}_2} = 1.52 D_{\text{CO}_2}$ ;  $D_{\text{A}} =$

$1.63 D_{CO_2}$ ; and  $D_A = 1.07 D_{N_2}$ . Now omitting, in the first place, the cases of hydrogen and oxygen, since these are not fully inert, we may calculate the approximate ratios of  $D_{N_2}/D_{CO_2}$ ,  $D_A/D_{CO_2}$ , and  $D_A/D_{N_2}$  for different diffusing particles. Let us take the cases of oxygen and hydrogen atoms (hydroxyl radicals are likely to diffuse in much the same manner as oxygen atoms). Using the following radii: H: 0.7 Å.; O: 1.3 Å.; N<sub>2</sub>: 1.89 Å.; A: 1.83 Å.; CO<sub>2</sub>: 2.33 Å., it is found that we calculate for hydrogen atoms diffusing:  $D_{N_2} = 1.38 D_{CO_2}$ ;  $D_A = 1.44 D_{CO_2}$ ;  $D_A = 1.04 D_{N_2}$ ; and for oxygen atoms diffusing:  $D_{N_2} = 1.39 D_{CO_2}$ ;  $D_A = 1.36 D_{CO_2}$ ;  $D_A = 0.98 D_{N_2}$ . It will be seen that the figures for hydrogen atoms' and

oxygen atoms are very similar, and that they are both in fair agreement, as regards order of magnitude, with the observed figures. The figures for hydrogen atoms are, if anything, slightly closer to the observed values, but the difference is small. For instance, the relative effectiveness of argon and nitrogen in preventing diffusion is that which would be expected for hydrogen atoms but not that to be expected for oxygen atoms diffusing. Carbon dioxide seems to be rather more effective in preventing diffusion relative to nitrogen and argon than would be expected theoretically. This might be due to the

fact that it interfered with the passage of hydrogen atoms by reacting with them in some way. However, it must be admitted that no decision can be made as to the nature of the important diffusing particles.

As regards hydrogen and oxygen, it is found that  $D_{H_2} = 5.6 D_{N_2}$  and  $D_{O_2} = 1.5 D_{N_2}$ . Theoretically we should expect: for hydrogen atoms diffusing:  $D_{H_2} = 1.9 D_{N_2}$  and  $D_{O_2} = 1.1 D_{N_2}$ ; and for oxygen atoms diffusing:  $D_{H_2} = 3.4 D_{N_2}$  and  $D_{O_2} = 1.0 D_{N_2}$ . For both the theoretical cases the observed values of  $D_{H_2}$  and  $D_{O_2}$  are too big relative to  $D_{N_2}$ , though the case of oxygen atoms gives the much closer agreement. The high observed values of  $D_{H_2}$  and  $D_{O_2}$  may be due to the fact that the inert gases exert a bigger cooling effect on the region round the spark than does either excess oxygen or excess hydrogen, since with these present the rate of reaction is greater, the rate of heat production is greater, and therefore the temperature of the local volume greater than if an inert gas is present. This higher temperature will render the outward diffusion of particles more rapid, and hence hydrogen and oxygen may

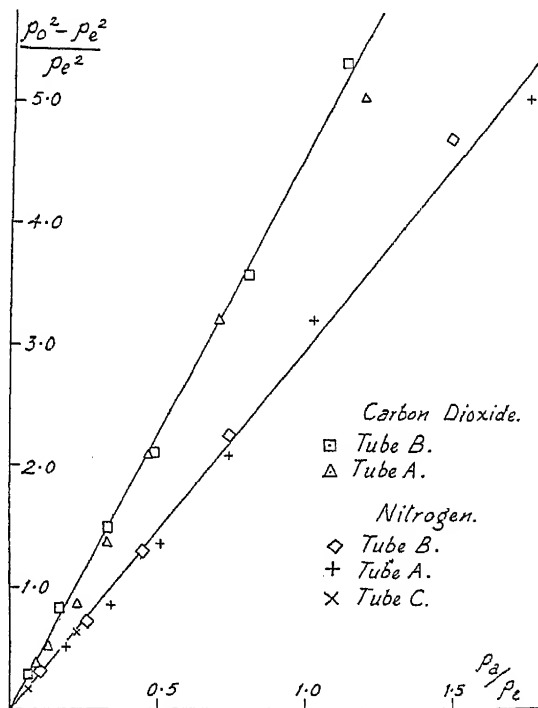


FIG. 2.

appear to have bigger diffusion coefficients than would be expected on a simple isothermal explanation.

The general conclusion therefore seems to be that the minimum igniting pressure of electrolytic gas in the presence of small amounts of nitrogen, argon, carbon dioxide, hydrogen and oxygen can be interpreted, to a satisfactory approximation, by the above modification of the theory of Mole, and therefore that this theory contains the essential features of the problem. However, in detail, there seem to be some anomalies which result from the simplifications introduced, such as, for example, the ignoring of the temperature in the zone of ignition. However the fact that the temperature can be ignored does suggest that the changes in temperature resulting from the introduction of small amounts of the inert gases are of secondary importance compared with the other factors concerned in this region.

**Effect of Tube Diameter and Spark Gap.**—The tube diameter, width of spark gap and limiting ignition pressure of electrolytic gas alone for the three tubes are given in Table III. It will be seen that the relation between the limiting pressure and the width of the spark gap is approx-

TABLE III.—EFFECT OF TUBE DIAMETER AND SPARK GAP ON THE LIMITING IGNITION PRESSURE.

Tube.	Tube Diameter (cm.).	Width of Spark Gap (mm.).	Limiting Ignition Pressure. (mm.).
A . . . .	3.7	1.7	123
B . . . .	2.0	1.4	143½
C . . . .	2.0	0.42	192

imately a linear one. The limiting ignition pressure varies regularly with the width of the spark gap, but not with the tube diameter. Further results with a different type of spark have confirmed this observation. So, in agreement with Coward, Cooper and Warburton, it is concluded that the diameter of the ignition tube, in experiments under the present conditions, has no effect on the incendiarity of the spark. As was stated previously, it seems possible that Thompson came to a different conclusion because he was working at considerably lower pressures than those of the present series.

## Section B.

The second region of limiting ignition pressures, namely that portion of the curve in Fig. 1 which has a positive slope, will now be considered. These results are plotted, for the wide tube A, in a different form in Fig. 3, the ratio  $p_a/p_e$  being plotted against the pressure of the added gas,  $p_a$ . It will be seen that in all cases the value of  $p_a/p_e$  seems to be approaching a limiting value at high pressures. In only one case has the limit certainly been reached and that is for nitrogen, for which the limiting ratio is 5.2. In the other cases it was not possible to reach the limit in the apparatus used for fear of bursting the ignition tube.

The obvious interpretation of this ratio reaching a limiting value seems to us to be a thermal one. If one considers a region immediately round the spark, for this volume to react explosively and initiate flame a sufficient degree and rate of chain branching must occur. Now the degree and rate of chain branching increase with rise of temperature and therefore a sufficient temperature must be maintained for a certain time in this region. Let us suppose that the spark is putting active particles into this region at a constant rate. Then the rate of production of heat by reaction will be proportional to  $p_e$ . The rate of rise in temperature caused

by this production of heat will be proportional to the rate of production and inversely proportional to the thermal capacity of the gas in the volume, which is of the form  $(C_e \cdot p_e + C_a \cdot p_a)$ . The constants,  $C$ , are proportional to the heat capacities of the gases. The rate of loss of heat by conduction outwards will be independent of the pressure if the composition is constant. Therefore the temperature maintained in the volume will depend on  $p_a/p_e$ , and also on the heat capacity of the added gas.

Therefore it seems that as we pass from low to high pressures in the present ignition system we pass from a region where the limiting factor is a chain, virtually non-thermal, condition to one that, at high pressures, is a largely thermal condition, namely the attaining of a temperature sufficient for adequate chain branching.

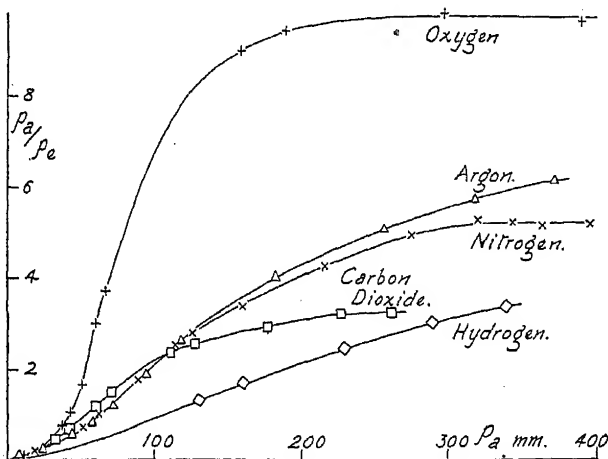


FIG. 3.

There are several results of the present investigation that support the interpretation presented above, though a full confirmation requires an extension of the results to higher pressures. For the three inert gases, carbon dioxide, nitrogen and argon, it appears that the limiting value of the  $p_a/p_e$  is ca.  $3\frac{1}{2}$ , 5.2 and something greater than  $6\frac{1}{2}$  respectively. This is the order that would be expected from the heat capacities of the gases. Carbon dioxide having the largest heat capacity per g. molecule has the greatest cooling effect; while argon, having the smallest heat capacity, has the smallest cooling effect. The electrolytic gas can "stand" only small additions of carbon dioxide, but quite large additions of argon. The limiting ratio for added oxygen is much higher (ca. 10). This is probably because the addition of oxygen accelerates the rate of reaction, and therefore the rate of heat production, in addition to the excess oxygen having a cooling effect. So the electrolytic gas can "stand" the addition of a much greater proportion of oxygen. For hydrogen the limiting value was not even approached. All that can be said is that the limiting ratio for hydrogen is certainly greater than that for carbon dioxide as would be expected from the relative heat capacities and from the participation of hydrogen in the reaction.

Another result that supports the present explanation is that the limiting ratio is independent of the tube used. Thus for nitrogen it is found to be 5.1 in one tube and 5.3 in the other. It appears that the same is likely to be true for argon and carbon dioxide though in neither case was the limit reached. It seems to be true for excess oxygen.

It is important to notice that the effect of the added gas in this region

is quite different from that in the low pressure region. Thus, in the low pressure region, nitrogen and argon are approximately equally effective, whereas in the high pressure region this is not the case. Also, in the low pressure region carbon dioxide is very much more effective in aiding ignition than hydrogen; but, at high pressures, it is more effective in hindering ignition. Therefore, there seems to be no doubt that the limiting factor in the high pressure region is quite different from the limiting factor in the low pressure region; and, at the present, the thermal explanation seems to account most satisfactorily for the results at high pressures.

### Summary.

The effect of added gas on the limiting ignition pressure of electrolytic gas has been studied. It is found that small amounts of the added gas aid ignition but that larger quantities hinder ignition. It is concluded that the first effect at low pressures results from the added gas preventing the diffusion of active chain propagators from the region of the spark, thus aiding the build up of explosive conditions in this region. The second effect at higher pressures seems to result from the cooling effect of the added gas and it is concluded that the limiting factor here is a thermal one. The limiting factor in ignition by the spark in the present experiments therefore changes from what may be called a chain factor to a thermal factor on passing from pressures of about a fifth of an atmosphere to pressures of about a half of an atmosphere. At atmospheric pressure and above it may therefore be concluded that the limiting factor would be a thermal one, though the reaction, of course, proceeds by a chain mechanism.

*Inorganic Chemistry Laboratory,  
Oxford.*

---

## THE ABSORPTION SPECTRA OF ACROLEIN, CROTONALDEHYDE AND MESITYL OXIDE IN THE VACUUM ULTRA-VIOLET.

BY A. D. WALSH.

*Received 29th March, 1945.*

Previous publications <sup>1, 2, 3, 4</sup> have described the spectra of ethylene and of the simplest examples of the conjugation of C=C groups. The spectra of formaldehyde <sup>5</sup> and acetaldehyde <sup>6</sup> have also been described. The present work was undertaken to study the conjugation of a C=C with a C=O group. The experimental details have been described in the previous papers.

### The Spectrum of Acrolein.

The acrolein used was a pure B.D.H. product.

The far ultra-violet spectrum (Plate I) begins with a strong, diffuse, region of absorption with a maximum at about 1935Å. No structure is visible in this region. It is probably analogous to the strong continua found in the alkylated ethylenes and butadienes, *i.e.* probably an N → V,

<sup>1</sup> Price and Tutte, *Proc. Roy. Soc., A*, 1940, **174**, 207.

<sup>2</sup> Price and Walsh, *ibid.*, 1940, **174**, 220.

<sup>3</sup> Price and Walsh, *ibid.*, 1941, **179**, 201.

<sup>4</sup> Price and Walsh, *in press*.

<sup>5</sup> Price, *J. Chem. Physics*, 1935, **3**, 256.

transition of the  $\pi$  electrons of the molecule. To shorter wavelengths the spectrum parallels in many respects that of acetaldehyde and reference should be made to the description already given<sup>6</sup> of the acetaldehyde spectrum. The first strong bands occur at shorter wavelengths in acrolein than in acetaldehyde. The 1800A. system of acetaldehyde has its acrolein analogue in a system whose strongest band is at 1750A., though its intensity is much greater in acrolein relative to the other bands in the spectrum than is the case for the 1800A. band of acetaldehyde. The 1650A. doublet of acetaldehyde is shifted in acrolein (1640A.) by a smaller amount to short wavelengths and is relatively much weaker. These differences probably arise from some mixing of the excited  $\pi$  electron orbitals with those of the non-bonding oxygen electrons. The dimensions to be expected for such low excited orbitals would make this appear very probable. In the range *c.* 1700-1550A. there is also a region of weak continuous absorption, rather like the subsidiary continuum in propylene lying a few hundred Angstroms to the short wavelength side of the first main continuum. Towards shorter wavelengths there is a more definite correlation of the bands with those of acetaldehyde. The band at 1470A. in acetaldehyde has an acrolein analogue at 1460A. As we go to shorter wavelengths we find that the acrolein bands are shifted not to short but to long wavelengths relative to the analogous bands of acetaldehyde. A new band seems to have appeared at 1480A.

Whereas in acetaldehyde the first few discrete bands observed were sharp and it was possible to see the sudden onset of predissociation, in acrolein, as in formaldehyde, the *first* discrete band—that at 1750A.—is predissociated and no fine structure (such as found in the 1800A. acetaldehyde system) is to be observed. This is probably connected with the short wavelength shift of the bands relative to acetaldehyde. (It is generally found that discrete bands due to carbonyl absorption occurring slightly to the long wavelength side of 1750A. are sharp while those at shorter wavelengths are diffuse.)

There are three strong bands in the 1750A. region and, as in acetaldehyde, the separations are not equal (1259 cm.<sup>-1</sup> and 1089 cm.<sup>-1</sup>). The third band appears much brighter than the second. The second Rydberg series described below has a missing first ( $n = 2$ ) member which may occur in this region and be responsible for some of the complications.

There is a conspicuous ionization potential at about 1220A. It is followed as usual by a region of continuous absorption due to the C—C and C—H bonds. The bands crowding together to the limit can be arranged into three series :

$$\nu_0^n = 81,500 - \frac{R}{(n + 0.85)^2} \quad . \quad . \quad . \quad (1)$$

$$\nu_0^n = 81,460 - \frac{R}{(n + 0.05)^2} \quad . \quad . \quad . \quad (2)$$

$$\nu_0^n = 81,516 - \frac{R}{(n + 0.32)^2} \quad . \quad . \quad . \quad (3)$$

These three series correspond to those found for acetaldehyde and are numbered similarly. As in acetaldehyde, the lower members of the first series again seem to consist of doublets, the doublet separation decreasing rapidly to zero. The table gives an idea of the accuracy of the equations (1), (2) and (3) respectively. The series are very good, though the agreement between observed and calculated frequencies is not quite so striking as in acetaldehyde. The smaller number of members observed is in part due to interference by emission lines and in part to the more rapid convergence of the bands. Series (2) in particular has fewer members, but its general appearance is good and it can be seen that several of its

<sup>6</sup> Walsh, *in press*.

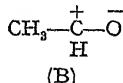
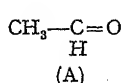


missing members should fall just where emission lines are observed. The three series have approximately the same limit:  $81,500 \text{ cm.}^{-1}$  probably accurate to at least  $\pm 50 \text{ cm.}^{-1}$ . This corresponds to  $10.057 \pm 0.06 \text{ v.}$  It is to be compared with the value  $10.2 \text{ v.}$  obtained by electron impact.<sup>7</sup>

The second member of series (3) in acetaldehyde is strongly predissociated: but it is interesting to notice that in acrolein, although the band occurs at only slightly shorter wavelengths, it is strong and shows no predissociation. The strong  $1400 \text{ \AA.}$  emission doublet probably partially obscures the band in acetaldehyde.

Though the first Rydberg members in acrolein are at shorter wavelengths than in acetaldehyde, the ionization potential is at a longer wavelength. This shows that qualitative inferences concerning the shifts of ionization potentials from shifts of long wavelength bands can only be relied upon where there is only one chromophore absorbing in the region concerned. In acrolein, absorption is due to the  $\pi$  electrons of the molecule and the non-bonding oxygen electrons; and the first Rydberg bands of the latter are affected by the orbitals of the neighbouring  $\pi$  electrons.

The great similarity of the acrolein spectrum below  $1700 \text{ \AA.}$  to that of acetaldehyde shows that it is dominated by the absorption due to the non-bonding  $2p_z$  lone pair electrons on the oxygen atom. The ionization limit observed again corresponds to the removal of one of these electrons. The lowered value, relative to acetaldehyde, must mean that there is an increased negative charge on the oxygen atom in acrolein. The acetaldehyde molecule has a structure intermediate to the two forms A and B,



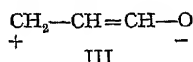
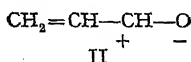
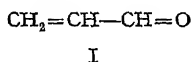
about 50 % of the character of each being thought to be normally present.<sup>8</sup> Evidence for the existence of ionic character comes from (a) a study of

TABLE I.

TABLE SHOWING THE OBSERVED AND CALCULATED FREQUENCIES OF THE RYDBERG BANDS OF SERIES (1), (2) AND (3).

Series I.			Series II.		Series III.	
2	67511	67990	2	55348	2	61128
3	73964	74097	3	69664	3	71558
4	76757	76835	4	74770	4	75623
5	78303	78293	5	obsured by 1300 $\text{\AA.}$ quintet	5	77639
6	79155	79161	6	78462	6	78768
7	79709	79719	7	79248	7	79467
8	80072	80099			8	79930
9	80357	80368			9	80235
10	80568	80568				
11	80731	80719				

the dipole moment of the  $\text{CH}_3\text{CHO}$  molecule, (b) the sensitivity of the  $\text{C}=\text{O}$  bond strength to substitution in the molecule and (c) the fact that in the similar molecule  $\text{HCHO}$  the observed first ionization potential<sup>5</sup> is  $\sim 2 \text{ v.}$  less than the ionization potential predicted by Mulliken<sup>9</sup> assuming no ionic character. Acrolein is a hybrid of the three forms, I, II and III.



<sup>7</sup> Sugden, unpublished work.

<sup>8</sup> Pauling, *The Nature of the Chemical Bond*, Cornell, 1940, pp. 75, 131.

<sup>9</sup> Mulliken, *I. Chem. Physics*, 1935, 3, 564.

The above spectroscopic facts show that the state of the oxygen atom in acrolein is not far different from that in acetaldehyde, though the total contribution of structures II and III to the hybrid must be slightly greater than that of structure (B) to the acetaldehyde molecule. In formaldehyde the ionic form must contribute considerably less to the hybrid than in acetaldehyde.

As already mentioned, there are important differences of intensity between the acrolein and acetaldehyde spectra. Whereas in acetaldehyde the 1800 Å. band is weaker than the 1650 Å. band, in acrolein the 1750 Å. band is much stronger than the 1650 Å. doublet. The components of this doublet are about equal in strength in acrolein, but in acetaldehyde the first member is the stronger. The third member of the 1750 Å. acrolein system has increased considerably in strength relative to the other members. Finally, the first member of the strong doublet at 1600 Å. in acetaldehyde has practically disappeared in acrolein—though the second member is still prominent.

The 1600 Å. doublet components in both acetaldehyde and acrolein have been left unassigned. The position of these bands seems to preclude their being a vibrational level of the 1650 Å. electronic transition. They must be assigned to an as yet unidentified electronic transition. It is possible that they inaugurate a fourth and weaker Rydberg series of the oxygen electrons. Some vibrational structure appears to follow them. As already stated, in acrolein only the second member (at 1585 Å.) is strong.

### The Spectrum of Crotonaldehyde.

The spectrum of crotonaldehyde starts with a strong continuous region of absorption (2100-1900 Å.), of maximum at about 2030 Å., similar to that of acrolein (2050-1850 Å.). The long wavelength shift is to be expected from the presence of the added  $\text{CH}_3$  group if the absorption is associated with the  $\pi$  electrons of the molecule. Discrete bands occur at 1800 Å. corresponding to the acetaldehyde bands at a closely similar wavelength. A separation  $\sim 1160 \text{ cm}^{-1}$  is here evident. This is rather less than the separation in acetaldehyde which fact would accord with the identification of the frequency as that of the  $\text{C}=\text{O}$  valence vibration, since it is known<sup>10</sup> that in the ground state this is reduced in crotonaldehyde ( $1689 \text{ cm}^{-1}$ ) and acrolein relative to acetaldehyde ( $1715 \text{ cm}^{-1}$ ).

While it is clear from relative intensities that the crotonaldehyde bands near 1800 Å. are not due to possible acetaldehyde impurity in spite of the fact that they lie at closely coincident wavelengths, the bands below 1700 Å. are so closely similar that it is felt that further work must be done to establish their association with crotonaldehyde.

### Electronic Structures of Acrolein and Crotonaldehyde.

The relevant electronic structure of the simple  $\text{C}=\text{O}$  group has been described in the paper on acetaldehyde. That of the simple  $\text{C}=\text{C}$  group is very similar, except that here we have no lone pair of non-bonding electrons. It may be represented

$$N : \dots (tt)^2 (\chi)^2$$

$(tt)^2$  represents a pair of electrons forming the first or  $\sigma$  bond of the group,  $(\chi)^2$  a pair forming the second or  $\pi$  bond. The  $(\chi)$  electrons are less firmly bound than the  $(tt)$  electrons and are therefore active in producing the longest wavelength absorption. Just as for the  $\text{C}=\text{O}$  group there was an excited orbital  $(\bar{\chi})$ , so for the  $\text{C}=\text{C}$  group there is an excited antibonding orbital  $(\bar{\chi})$ . The lowest excited state of the  $\text{C}=\text{C}$  group is thus.

$$V : \dots (tt)^2 (\chi)(\bar{\chi}).$$

<sup>10</sup> Hibben, *The Raman Effect*, Reinhold, 1939.

The effect of conjugating the two groups, C=O and C=C, is to alter the  $\sigma$  orbitals very little: but the effect upon the four  $\pi$  electrons (two from the C=O and two from the C=C) is to place them in two orbitals ( $\chi_1$ ) and ( $\chi_2$ ) (two electrons in each), of which the orbital ( $\chi_2$ ) lies *above* either of the normal ( $\chi$ ) orbitals of the  $\pi$  electrons of the separate C=C and C=O groups. Also the antibonding excited orbital ( $\bar{\chi}_2$ ) now lies at a *lower* energy level than either of the ( $\bar{\chi}$ ) antibonding orbitals associated with the separate C=C and C=O groups. Hence the normal state of the acrolein or crotonaldehyde molecule may be represented † (*cf.* McMurry<sup>11</sup>)

$$N: \dots (tt)^2(z\bar{t})^2(\chi_1)^2(\chi_2)^2y_0^2.$$

The three lowest energy excited states are

$$A_1: \dots (tt)^2(z\bar{t})^2(\chi_1)^2(\chi_2)^2(\bar{\chi}_2)y_0$$

$$B: \dots (tt)^2(z\bar{t})^2(\chi_1)^2(\chi_2)^2(z\bar{t})y_0$$

$$V_1: \dots (tt)^2(z\bar{t})^2(\chi_1)^2(\chi_2)(\bar{\chi}_2)y_0^2$$

and the three longest wavelength transitions are

$$N \rightarrow A_1 \quad N \rightarrow B \quad \text{and} \quad N \rightarrow V_1.$$

Of these, since the ( $z\bar{t}$ ) orbitals are practically unaltered by the conjugation,  $N \rightarrow B$  will lie at practically the same wavelength as in the case of simple aldehydes. Because of this and because of the general similarity to the acetaldehyde 1800 Å. ( $N \rightarrow B$ ) region, we may identify the 1800 Å. region in crotonaldehyde and the 1750 Å. system in acrolein as  $N \rightarrow B$  in type. Since the second member of the acrolein Rydberg series should occur in the 1750 Å. region, it is probably mixed Rydberg— $N \rightarrow B$  in character.

Since the ( $\bar{\chi}_2$ ) orbital is lower than the ( $\bar{\chi}$ ) level for either simple C=C or simple C=O, and since the ( $\chi_2$ ) level is higher than ( $\chi$ ), the transitions  $N \rightarrow A_1$  and  $N \rightarrow V_1$  will both be moved to long wavelengths as a result of the conjugation. In accord with this we find that the weak near ultra-violet absorption<sup>12, 13</sup> in crotonaldehyde and acrolein lies at *c.* 3300 Å. as compared with 2900 Å. in simple aldehydes. The shift of the weak absorption from 2900 Å. in acetaldehyde to longer wavelengths in crotonaldehyde and acrolein constitutes evidence that it is  $N \rightarrow A$  in type. Its position is to be compared with the position of the weak absorption in diacetyl and glyoxal<sup>14</sup> (two conjugated C=O groups) around 4000 Å. The latter two molecules, however, differ from acrolein and crotonaldehyde in that they have also a weak region of absorption around 2900 Å., as in simple aldehydes.

The  $N \rightarrow V_1$  transition in acrolein and crotonaldehyde must lie at longer wavelengths than the  $N \rightarrow V$  transition in ethylene (1745 Å.) or in acetaldehyde (1650 Å.). Hence it must be identified with the 1935 Å. region in acrolein and the 2030 Å. region in crotonaldehyde. In butene the C=C  $N \rightarrow V$  transition is only at 1800 Å. One sees how effective is the resonance or conjugation, compared with charge transfer, in pushing the first  $N \rightarrow V$  absorption to long wavelengths. In butadiene, with two conjugated C=C groups, the  $N \rightarrow V_1$  transition occurs at 2200 Å.: as might be expected, the crotonaldehyde or acrolein  $N \rightarrow V_1$  absorption lies between the butadiene transition and the transitions for the unconjugated molecules ethylene and acetaldehyde.

† This discussion assumes *complete* conjugation between the two groups C=C and C=O. Since the  $\pi$  ionization potentials in the separate C=C and C=O groups are not the same, this assumption is probably not fully justified.  $\chi_2$  is probably localised rather more in the C=C than the C=O group and  $\chi_1$  more in the C=O than the C=C. However, one *must* assume considerable conjugation occurs because of the big shift of  $N \rightarrow V_1$  from ethylene to acrolein on replacing an H by the strongly electronegative CHO group.

<sup>11</sup> McMurry, *J. Chem. Physics*, 1941, 9, 241.

<sup>12</sup> Eastwood and Snow, *Proc. Roy. Soc. A*, 1935, 149, 446.

<sup>13</sup> Lüthy, *Z. physik. Chem. B*, 1923, 107, 285.

<sup>14</sup> Thompson, *Trans. Faraday Soc.*, 1940, 36, 989.

The  $N \rightarrow V_1$  transition occurs at longer wavelengths in crotonaldehyde than in acrolein presumably because of a charge transfer effect similar to the shift of the butadiene  $N \rightarrow V_1$  absorption to long wavelengths in isoprene. It is noticeable that no strong bands occur in the spectra which can be attributed to Rydberg transitions of the  $\pi$  electrons: these transitions must be much weaker than those of the non-bonding oxygen electrons. Price and Tutte<sup>1</sup> have shown that in the alkyl ethylenes (*e.g.* butene, tetramethyl ethylene) relative to ethylene the intensity of the  $\pi$  Rydberg tends to pass into the  $N \rightarrow V$  transition. Toluene shows the same tendency, relative to benzene.<sup>15</sup> An analogous phenomenon is probably occurring here. It is interesting to note that the appearance pressure of the  $2p_y$  oxygen electronic bands is considerably lower even than that of the  $N \rightarrow V_1$  transition. However, the position of the  $N \rightarrow V_1$  continuum in acrolein and its probable linkage with the first Rydberg orbital of the  $\pi$  electrons (as in ethylene and butadiene) probably mean that the first  $\pi$  ionization potential is higher in acrolein than in crotonaldehyde (though both are less than the ethylene value (10.45 v.) and greater than the butadiene value (9.02 v.)\*)—just as the butadiene first ionization potential is higher than that of isoprene.

It is now possible to explain the intensity decrease of the 1650 Å. bands relative to the 1750 Å. bands in acrolein as compared with acetaldehyde. In acetaldehyde the 1650 Å. bands were mixed Rydberg— $N \rightarrow V$ . In acrolein the  $N \rightarrow V_1$  transition has moved to longer wavelengths as a result of the conjugation and left the 1650 Å. bands pure Rydberg in type. Hence the intensity of the 1650 Å. bands decreases. This is evidence that the assignment of transitions in acetaldehyde was correct.

In the above discussion we have neglected the four possible excited states

$$V_2: \dots (tt)^2(zt)^2(\chi_1)^2(\chi_2)(\bar{\chi}_1)\gamma_0^2$$

$$V_3: \dots (tt)^2(zt)^2(\chi_1)(\chi_2)^2(\bar{\chi}_2)\gamma_0^2$$

$$V_4: \dots (tt)^2(zt)^2(\chi_1)_1(\chi_2)^2(\bar{\chi}_1)\gamma_0^2$$

$$A_2: \dots (tt)^2(zt)^2(\chi_1)^2(\chi_2)^2(\bar{\chi}_1)\gamma_0$$

and the corresponding transitions  $N \rightarrow V_2$ ,  $N \rightarrow V_3$ ,  $N \rightarrow V_4$  and  $N \rightarrow A_2$ . By analogy with butadiene,<sup>16</sup> we may expect that acrolein and crotonaldehyde have (largely) a trans rather than a cis arrangement of the double bonds about the central single bond.† Similarly, glyoxal is probably largely *s-trans* at room temperature. Eastwood and Snow,<sup>12</sup> in order to explain the wide rotational structure and consequent low moment of inertia associated with the near ultra-violet bands of these molecules, also assign a trans nature to them. Mulliken<sup>17</sup> has shown that for trans conjugation the transitions  $N \rightarrow V_2$  and  $N \rightarrow V_3$  are forbidden. Because of this and strong masking by the Rydberg transitions,  $N \rightarrow V_{2,3}$  do not appear on our plates.  $N \rightarrow V_4$  will occur at shorter wavelengths.

<sup>15</sup> Walsh, *results in course of publication*.

\* It seems probable that the  $\chi_2$  ionization potential is less than that of the  $\gamma_0$  electrons. This means that the formulation of the normal state as given above departs from the customary convention of listing the occupied orbitals from left to right in the order of decreasing ionization potentials.

The reason why the non-bonding oxygen electrons are more easily photo-ionized or impact-ionized than the  $\pi$  electrons is probably because, being terminal electrons, they are more exposed to outside effects and are not partially protected by outlying atoms as in the case of the  $\pi$  electrons of the molecule. This would explain why electron impact experiments do not reveal the presence of a  $\chi_2$  ionization potential.<sup>7</sup> Possibly at high pressures this ionization potential would be observed. Alternatively, the electron impact value of 10.2 v. for acrolein may represent a composite value for  $\chi_2$  and  $\gamma_0$ .

<sup>16</sup> Sugden and Walsh, *ibid.*, 1945, 41, 76.

† In addition, crotonaldehyde apparently has a trans arrangement of the CO and CH<sub>3</sub> groups about the CC double bond.<sup>18</sup>

<sup>17</sup> Mulliken, *J. Chem. Physics*, 1939, 7, 121.

<sup>18</sup> Blacet, Young and Roof, *J. Am. Chem. Soc.*, 1937, 59, 608.

$N \rightarrow A_2$  might possibly be identified with the band at 1480 Å. which seems to have no analogue in the acetaldehyde spectrum. An excited state

$$D: \dots (it)^2(zt)^2(\chi_1)^2(\chi_2)^2(\tilde{t}\tilde{t})\gamma_0$$

will presumably not occur since the C=C group is so far separated from the oxygen atom.

Regions of absorption corresponding to the acrolein 1935 Å. continuum have been observed by Hausser<sup>19</sup> and by Hausser, Kuhn, Smakula

and Hoffer<sup>20</sup> for certain conjugated aldehydes in hexane solution. All these regions are to be interpreted as  $N \rightarrow V_1$ . Fig. 1 shows a plot of  $N \rightarrow V_1 \nu_{\max.}$  against the number of C=C groups for the five methyl compounds, acetaldehyde, crotonaldehyde, sorbic aldehyde, octatrienaldehyde, and decatetraenaldehyde.

TABLE II.

	$N \rightarrow V_1 \nu_{\max.}$ cm <sup>-1</sup> .	
	Hexane Solution.	Vapour Phase.
Acetaldehyde . . .	—	60,610
Crotonaldehyde . .	47,390	49,260
Sorbic aldehyde . .	38,460	—
Octatrienaldehyde .	32,360	—
Decatetraenaldehyde .	30,000	—

aldehyde and decatetraenaldehyde. In this figure the  $\nu_{\max.}$  values for sorbic aldehyde, octatrienaldehyde and decatetraenaldehyde are those of Hausser or Hausser *et al.* raised slightly, since the present vapour phase value for

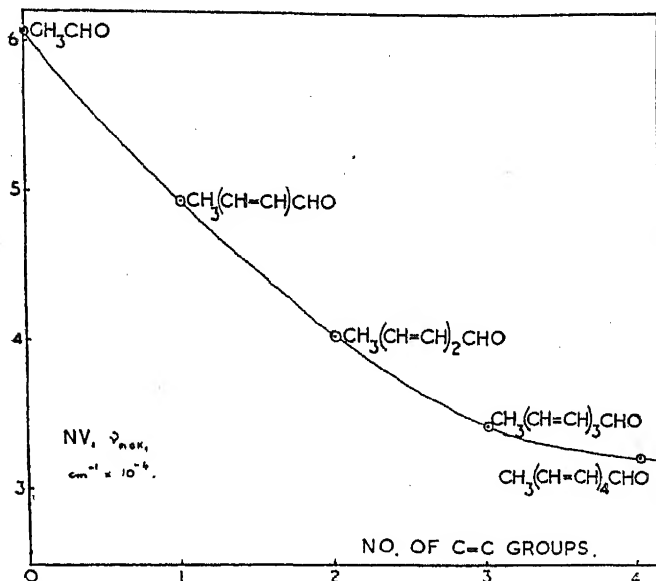


FIG. 1.

crotonaldehyde is slightly higher than the hexane solution value. As 0, 1, 2, 3 . . . C=C groups are inserted in the acetaldehyde molecule, the curve falls smoothly and enables the  $N \rightarrow V_1 \nu_{\max.}$  of higher methyl aldehydes to be predicted. Its regularity lends some support to the assignment of the  $N \rightarrow V_1$  transition in acetaldehyde to the 1650 Å. region. Table II gives the data from which the curve has been plotted.

A similar curve for formaldehyde, acrolein, etc., should also be smooth

<sup>19</sup> Hausser, *Z. tech. Physik.*, 1934, 15, 10.

<sup>20</sup> Hausser, Kuhn, Smakula and Hoffer, *Z. physik. Chem. B*, 1935, 29, 372.

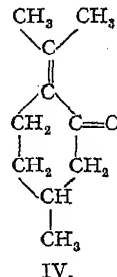
and should approach asymptotically the similar curve for ethylene, butadiene, hexatriene, octatetraene . . .,<sup>4</sup> but unfortunately values of  $\nu_{\max}$  are not available for the aldehydes above acrolein.

### The Spectrum of Mesityl Oxide.

The far ultra-violet spectrum of mesityl oxide is unfortunately diffuse. There are only four or five measurable bands to be seen. The first two of these occur as a doublet at about 1940 Å. superimposed upon a weaker region of absorption extending from about 2060 Å. to 1840 Å. and of maximum about 1920 Å. From 1840 Å. to 1700 Å. at low pressures the vapour is transparent. Thence continuous absorption begins, with a strong doublet at 1530 Å. and a weaker diffuse pair of bands at 1700 Å. At high pressures strong continuous absorption begins fairly sharply at about 2450 Å.

In the near ultra-violet mesityl oxide has two systems,<sup>21</sup> one in the region 3300-3100 Å. and a stronger one of maximum about 2400 Å. Our plates show that the latter only appears faintly at the pressures sufficient to bring out the bands described above.

With the exception of the 3300 Å. region (which is almost certainly  $N \rightarrow A$  in type) the assignment of the absorption regions observed can be little more than speculative. The 2400 Å. peak may represent the  $N \rightarrow V_1$  transition moved to long wavelengths relative to crotonaldehyde owing to the transference of negative charge from the  $\text{CH}_3$  groups. Pulegone (IV), which has much similarity to mesityl oxide has also a strong peak around 2400 Å.<sup>22</sup>



Just as the spectrum of acrolein has much similarity to that of acetaldehyde, so has the spectrum of mesityl oxide much resemblance to that of acetone. The 1940 Å. doublet corresponds closely in position and appearance to bands at 1950 Å. in acetone which are classified as  $N \rightarrow B$  in type.<sup>14</sup> Since the nuclear framework in the immediate vicinity of the C=O bond is the same in the two molecules and since the  $\pi$  orbital will be little altered by conjugation, we *expect* similarity in position and appearance of the  $N \rightarrow B$  bands in acetone and mesityl oxide if the charge borne by the oxygen atom is much the same in the two molecules. We may deduce that the non-bonding oxygen electrons in mesityl oxide probably have an ionization potential not far different from that of acetone. This is supported by the fact that the doublet at 1530 Å. in mesityl oxide occurs at almost identical wavelengths with a similar doublet in acetone and so is probably to be identified as a Rydberg transition of the oxygen  $2p_y$  electrons.

### Summary.

The spectra of acrolein and crotonaldehyde have been photographed in the vacuum ultra-violet. Three well-developed Rydberg series have been found for acrolein leading to a conspicuous ionization potential at  $10.57 \pm 0.06$  v. Below 1900 Å. the spectra are dominated by the bands due to absorption by the  $2p_y$  oxygen lone pair electrons. The electronic structures of the molecules are formulated and an assignment of the various possible transitions suggested. This supports an assignment previously suggested for the transitions in the acetaldehyde spectrum. The spectrum of mesityl oxide is briefly described.

This work was carried out in 1940-41, war-time conditions having delayed its publication. The author wishes to express his great indebtedness to Dr. W. C. Price for continuous encouragement and help.

Laboratory of Physical Chemistry,  
Cambridge.

<sup>21</sup> International Critical Tables, 5, 374.

<sup>22</sup> Lowry, Simpson and Allsopp, *Proc. Roy. Soc. A*, 1937, 163, 483.

# THE DYEING OF CELLULOSE WITH DIRECT DYES. PART II. THE ABSORPTION OF CHRYSOPHENINE BY CELLULOSE SHEET.

BY HECTOR F. WILLIS, JOHN O. WARWICKER, H. ALAN STANDING  
AND ALEXANDER R. URQUHART.

*Received 26th September, 1944.*

## 1. Introduction and Summary.

Previous work on the absorption of direct dyes by cellulose has been reviewed in the first paper of this series.<sup>1</sup> It should therefore be sufficient to point out here that much remains to be done before a real understanding of the dyeing process is obtained, and to indicate the ways in which the work now described may be regarded as contributing towards the attainment of that end. The paper describes experimental work on the absorption of Chrysophenine G by cellulose sheet, determined over a wide range of temperature and salt concentration. It presents a theory of the dyeing process that in most respects agrees well with the experimental data, and in particular offers a means of simplifying the presentation of the data corresponding to any one temperature. The energy released in the dyeing process is calculated, and found to be about 14 K.cal. per mole of dye adsorbed, a value that is not inconsistent with the assumption that each dye molecule is held to the cellulose by means of two hydrogen bonds.

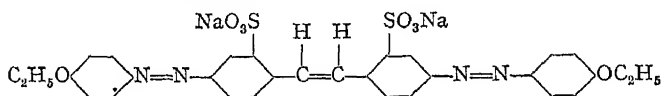
The theory presented is not applicable in its present form to dyes that aggregate in solution to form ionic micelles, and it is not improbable that much of its success when applied to Chrysophenine is due to the fact that this dye does not aggregate to any extent.<sup>2</sup> Nevertheless some of the theoretical conclusions are applicable with a fair degree of success to the experimental data of Neale and his collaborators for Benzopurpurine 4B, Chlorazol Sky Blue FF, and Chlorazol Fast Red K, though they also may only be slightly aggregated in solution at the temperatures considered—90° and 101° C. Work is proceeding on similar lines with a dye that is highly aggregated, and it is hoped that a comparison of observed and calculated results for such a dye may indicate the directions in which the theory has to be modified in order to make it more generally applicable.

## 2. Experimental Methods.

### (a) The Materials Used.

The cellulose used in the present work was "Cellophane" N600, sheet cellulose manufactured by the British Cellophane Co., Bridgwater. The glycerol present as plasticiser in this material was removed by leaving the sheets in running water for twenty-four hours; after this the sheets were steeped in *N*/10 hydrochloric acid at room temperature for two days, and then washed free from acid with distilled water. They were finally cut into 5 cm. squares and stored in distilled water until required for use, when they were air-dried and weighed, their moisture content being determined at the same time. The ash content of the material after purification in this way was 0.04 per cent.

The dyestuff Chrysophenine G (Colour Index No. 365) is a stilbene derivative with the constitution



It was supplied by the manufacturers, Messrs. I.C.I. (Dyestuffs) Ltd., in batch form, and was purified by the method of Robinson and Mills,<sup>3</sup> as follows: A hot concentrated solution of the dye is salted out by the addition of a saturated solution of sodium acetate, and the precipitated dye is filtered off, leaving much of the inorganic impurity in the filtrate. The dye is redissolved, and the process repeated several times until no trace of sulphate or chloride can be detected in the filtrate. It is then necessary to remove only the sodium acetate, and this is accomplished by repeated extraction with boiling alcohol until the presence of sodium acetate can no longer be detected. (The cacodyl test was used to detect the presence of acetate, and its absence from the final sample was confirmed by X-ray analysis of the latter.) The Chrysophenine purified by this process was finally crystallised from an alcohol-water mixture. The resulting material is a hygroscopic orange crystalline powder which retains appreciable amounts of water even on drying in an oven at 110° C. and consequently in this work it was always dried in a vacuum oven at 110° C. before it was weighed out for making up solutions.

It is necessary to ensure that the purified sample of the dye is free from coloured impurities as well as from inorganic electrolytes, and two methods have been used to test for the presence of such impurities. The first uses the technique of chromatographic analysis. A concentrated solution of the purified dye was gently poured on the top of a previously prepared column of Merck's alumina, and the dye was adsorbed as a well-defined coloured band at the top of the column. With water as solvent the band was then slowly developed through the column, and remained as a single band throughout the process. Although the absence of a second coloured band can be taken as a strong indication of the absence of coloured impurities, the test by itself is not a sufficient criterion of the purity of the dye, and consequently a second confirmatory test was used. This depends upon the fact that coloured impurities present with a dye are generally somewhat simpler substances that have a lower affinity for cellulose than the dye itself, with the result that the proportion of such substances is greater in an almost exhausted dyebath than in the initial dyebath, causing a change in the absorption spectrum. In order to compensate for the change in concentration of the dyebath it is of course necessary to compare the absorption spectrum of the almost exhausted dye solution with that of a solution of the same concentration prepared from the purified dye as a whole. The application of this test to Chrysophenine, purified by the method described above, showed no change in the absorption spectrum, and the tests taken together therefore provide strong evidence that the purified sample is free from coloured impurities as well as from inorganic electrolytes.

### (b) The Estimation of Aqueous Chrysophenine Solutions.

In this work the concentrations of aqueous solutions of Chrysophenine have been determined colorimetrically with the aid of a photoelectric spectrophotometer; the determination is, however, complicated by the fact that such solutions are phototropic,<sup>4</sup> their absorption spectra depending on whether the solutions have been illuminated or stored in the dark immediately before measurement. The absorption spectra shown in Fig. 1 for a solution of concentration 5 mg. per litre are characteristic; the upper spectrum D is that of a solution that had been stored in the dark



for about 18 hours before it was measured, while the lower spectrum I represents the same solution after illumination, which was accomplished by illuminating the solution in a parallel-sided glass cell of thickness 1 cm. for 10 minutes with a 100 watt lamp at a distance of about 1 inch. Illumination for periods longer than 10 minutes was found to produce no further change in the optical density of the solution at wave-lengths near the peak of the absorption spectrum. It is evident from the figure that

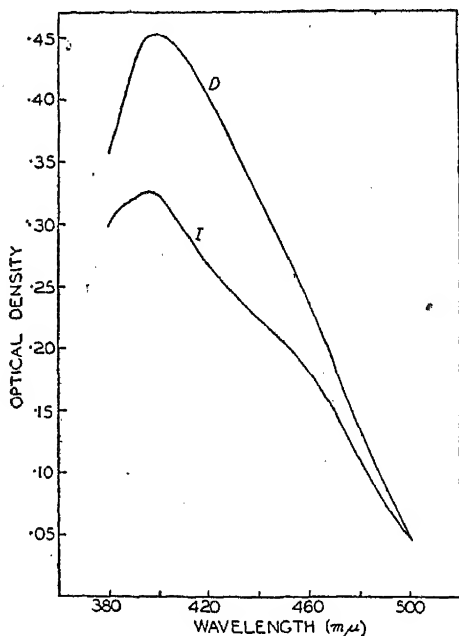


FIG. 1.—Absorption spectra of 5 mg. per litre Chrysophenine solution. D. Solution kept in dark. I. Solution illuminated.

not only is the peak of the absorption curve displaced to a slightly lower wavelength by the illumination but the extinction coefficient is also considerably reduced.

As for most phototropic phenomena, the change is reversible, the absorption spectrum of a previously illuminated solution returning to that of a "dark" solution in about 18 hours. Fig. 2 represents the variation with time of the optical density at a wavelength of 420  $m\mu$  of a 4 mg. per litre solution that had previously been illuminated and was then kept in the dark. Over the initial period of 7 hours, during which the optical densities were measured at frequent intervals, the rate of change is practically constant, and the change in density over a period of 5 minutes is small. On the other hand the optical density of a solution that had previously

been stored in the dark changes rapidly on illumination, and under the illuminating conditions described is complete in 10 minutes.

It is therefore more satisfactory to determine the concentrations of the solutions immediately after illumination; solutions of concentration 2.5, 5, and 10 mg. per litre were illuminated and their optical densities measured at a wavelength of 420  $m\mu$ . This wavelength is greater than that at the peak of the absorption spectrum (395  $m\mu$ ), but was chosen because both the intensity of the light and the sensitivity of the photocell are greater at this wavelength than at the peak. The plot of density against concentration shows that Beer's Law is valid up to 5 mg. per litre, but that there is a deviation of a few per cent. at a concentration of 10 mg. per litre. Solutions of unknown concentration were therefore diluted to about 5 mg. per litre and their optical densities determined at 420  $m\mu$ , their concentrations being then obtained by interpolation from the calibration curve.

When the solutions of unknown concentration contained known concentrations of inorganic electrolyte the standards were prepared with the same concentration of that electrolyte. Otherwise the technique of the determination was the same as for solutions of the pure dye.

### (c) The Determination of the Concentration of Chrysophenine in the Cellulose Sheet.

The main object of the present work was to obtain absorption isotherms relating the concentration of the dye absorbed in the cellulose to the concentration of the dye in the dyebath when equilibrium is attained. The concentration of the absorbed dye is expressed as grams of dye absorbed per 100 grams of cellulose, and is referred to as the equilibrium absorption.

If the initial dye concentration is known there are two main methods whereby the equilibrium absorption of the dye by the cellulose can be determined:—

- (1) By determining the decrease in the dyebath concentration, and
- (2) by determining directly the amount of absorbed dye in the sheet.

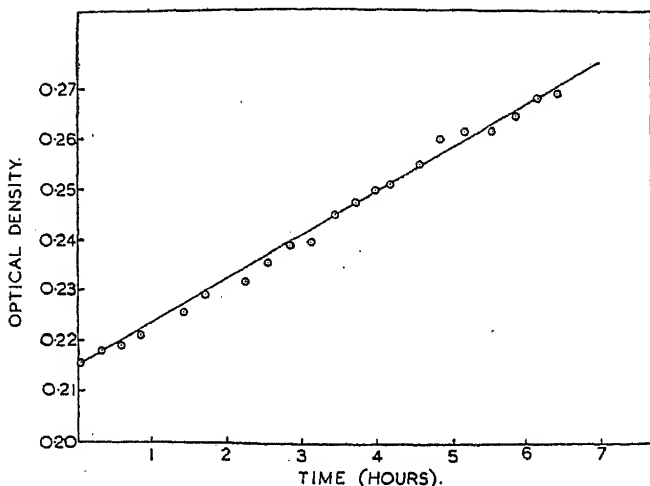


FIG. 2.—Change of optical density with time. Solution: Chrysophenine 4 mg. per litre; Sodium chloride 1 gm. per litre. Cell 1 cm. Wavelength 420  $m\mu$ .

The accuracy of the first method depends entirely on the degree of exhaustion of the dyebath. If the initial concentration of the dyebath of volume  $v$  is  $c_0$ , and the final dyebath concentration is  $c$ , then the mass of dye absorbed by the cellulose is  $v(c_0 - c)$ .\* Thus if the error of estimation of the final dyebath concentration is  $\Delta c$ , the relative error in the determination of the mass of dye absorbed is approximately  $\Delta c/(c_0 - c)$ . The denominator  $(c_0 - c)$  is small when the dyebath is only slightly exhausted, and the relative error is large. Thus in these circumstances the method is unsatisfactory; it can in fact be successfully applied only when the degree of exhaustion of the dyebath exceeds 50 per cent.

\* This expression is only approximate. The accurate expression would be  $\frac{m(c_0 - c)}{1 - c} + \frac{wc}{1 - c}$ , where  $m$  is the mass of dye liquor,  $c_0$  and  $c$  are the dye concentrations in g. per g. of dye liquor, and  $w$  is the amount of water absorbed by the sheet from the solution. In the calibration experiments, however, the liquor was always nearly exhausted, so that  $(1 - c)$  did not differ appreciably from 1. Since the ratio of the mass of dye liquor to that of cellulose was about 100 the necessary correction for the adsorbed water was of the order of 0.4 %, and was determined from the known dry weight of cellulose in the dyebath on the assumption that the amount of water adsorbed from these dilute solutions is the same as that adsorbed from saturated water vapour.

The second method is not dependent on the degree of exhaustion of the dyebath. The absorbed dye in the viscose sheet can be determined directly, either by stripping the dye from the sheet with a known volume of a hot aqueous solution of Cellosolve or pyridine, and then estimating the concentration of the extracted dye in the solution colorimetrically, or by direct colorimetric examination of the dyed sheet itself. The former method suffers from the disadvantage that it is sometimes difficult to extract the last traces of the dye from a heavily dyed sheet, and that decomposition of the dye may occur in hot extraction. The alternative method involves measuring the optical density of the dyed sheet at a given wavelength, and hence necessitates a preliminary calibration to relate the optical density to the concentration of absorbed dye. This calibration can be accomplished by the first method of determining the decrease in the dyebath concentration, the errors inherent in this method being avoided by so choosing the dye and salt concentrations in the calibration experiments that the dyebath is almost completely exhausted at the end of the dyeing.

The experimental technique used was as follows: A series of dye solutions of known dye and NaCl concentrations was prepared to give for the series of dyeings a sufficiently wide range of dye absorptions. Fifty c.c. of each dye solution was put into a resistance glass flask fitted with a ground glass stopper, and five squares of purified viscose sheet of known dry weight were threaded on a resistance glass hook and immersed in each flask, and the flasks were sealed with beeswax as a precaution against evaporation of the dye solution. Vigorous stirring of the thermostatted flasks was achieved by means of a reciprocating motor which rotated the flasks alternately in a clockwise and anticlockwise direction. The dyeing was continued until equilibrium was attained, when the viscose sheets were removed from the solution by means of the glass hook. They were rinsed in a cold concentrated solution of sodium chloride to remove adhering dye liquor and then hung on nickel hooks to dry.

The mass of dye absorbed by each set of five sheets was determined by diluting each of the residual dye solutions to a concentration in the neighbourhood of 5 mg. per litre and estimating the concentration of each of the diluted solutions colorimetrically as previously described. Since the volume of each solution was 50 c.c. the mass of dye absorbed by any particular set of sheets was  $50(c_0 - c)$  grams, where  $c_0$  and  $c$  are the initial and final dyebath concentrations respectively, expressed in grams per c.c. The dry weight of cellulose in each set of sheets was known, and the mass of absorbed dye was therefore expressed as grams of dye absorbed per 100 grams of cellulose.

As optical densities greater than unity cannot be accurately measured on the photoelectric spectrophotometer used, it was not possible to measure at a single wavelength the optical densities of all the sheets over the entire range of absorbed dye concentration. Four arbitrary wavelengths, 420, 500, 510, and 520  $m\mu$  were therefore chosen to cover the range of dye concentration, and four calibration curves were obtained, each appropriate to a certain range of concentration. Each sheet of a particular set was mounted between two glass plates, and its optical density measured at the appropriate wavelength. The necessary correction for the light reflected and absorbed by the glass plates and the viscose sheet was made by measuring the "optical density" of an undyed sheet mounted between the same glass plates. In practice several undyed sheets were so measured, and the mean "optical density" so obtained was subtracted from the optical density of the dyed sheet similarly measured. The optical densities of the five dyed sheets in any one set were found to be consistent to within about 5 %, indicating a fair uniformity in the thickness of the sheets.

The mean optical density of the five sheets in each set was plotted against the corresponding concentration of the absorbed dye. A straight

line was obtained at the wavelengths 420 and 500  $m\mu$ , showing that Beer's Law is applicable, but at the higher wavelengths there was a small deviation from Beer's Law. These calibration curves enable the concentration of the absorbed dye in any sheet of the same thickness to be determined from measurements of the optical density at the appropriate wavelength.

The dyed sheets are slightly phototropic; the optical density of a dyed sheet that has previously been kept in the dark is reduced by about 7 % when the sheet is illuminated for ten minutes by a 100 watt lamp at a distance of 1 inch. The existence of this effect was not realised when the calibration was done, and consequently standard illumination of the dyed film was not employed. A small random error is therefore present in the estimates of the density of the dyed films, according to the degree of illumination they received before measurement.

#### (d) The Determination of the Absorption Isotherms.

The equilibrium absorption of the dye by the cellulose at any definite temperature depends upon both the residual dyebath concentration and the concentration of inorganic electrolyte present; there are thus two independent variables, and the series of isotherms required at each temperature is necessarily extensive, each isotherm relating the concentration of absorbed dye to the dye concentration in the residual dyebath for a fixed concentration of inorganic electrolyte. In the present work a series of such isotherms was determined at each temperature, each isotherm corresponding to a definite concentration of NaCl. The temperature range studied extends from 20 to 97.5° C., and at the highest temperature a series of isotherms with  $\text{Na}_2\text{SO}_4$  as the inorganic electrolyte was also determined; finally isotherms were determined for dye solutions free from inorganic electrolyte.

The experimental technique used was very similar to that described above for the calibration experiments. For each experiment six solutions were prepared of varying dye concentration but constant salt concentration. At the beginning of an experiment these solutions were brought to the required experimental temperature in a thermostat, and a set of five purified viscose sheets of known dry weight was immersed in each solution; the flasks containing the solutions were then sealed with beeswax or picein according to the temperature. Dyeing was continued for a length of time that a preliminary experiment had shown to be ample for the attainment of equilibrium, whereupon the sheets were removed from the flasks, rinsed with concentrated sodium chloride solution, and dried. The mean optical density of each set was then determined as previously described for the calibration experiment, and the concentration of absorbed dye determined from the calibration curve.

Since both the concentration of absorbed dye on the cellulose and the weight of cellulose are known, the total mass of dye  $m$  absorbed by the cellulose is readily calculated. Then if the initial concentration of the dye solution of volume  $v$  is  $c_0$ , the concentration of the residual solution at equilibrium is  $(vc_0 - m)/v$ . The isotherms are of course obtained by plotting the concentration of absorbed dye against the residual dyebath concentration for each salt concentration studied.

### 3. Experimental Results.

The amounts of Chrysophenine absorbed by cellulose sheet from solutions of various dye and NaCl concentrations are given in Table I for a temperature of 97.5° C., and corresponding data for temperatures of 80, 60, 40, and 20° C. in Tables II-V; figures obtained at 97.5° C. with  $\text{Na}_2\text{SO}_4$  as electrolyte are presented in Table VI. If the dye uptake is plotted against the dye concentration for each salt concentration and temperature a series of isotherms is obtained; these are in many respects

## 512 ABSORPTION OF CHRYSOPHENINE BY CELLULOSE

similar to the isotherms generally found in adsorption work, as is evident from Fig. 3, where the data obtained in the presence of sodium sulphate are plotted. In particular the data conform to the Freundlich adsorption equation  $x = ac^n$ , where  $x$  is the amount adsorbed,  $c$  is the concentration

TABLE I.—ABSORPTION OF CHRYSOPHENINE G BY CELLULOSE AT 97.5° C., IN PRESENCE OF SODIUM CHLORIDE.

[(a) = Dyebath concentration, g. per l. (b) = Dye absorbed by cellulose, g. per 100 g.]

Concentration of sodium chloride, g. per litre.	40	a	0.00942	0.0163	0.0480	0.0777	0.114	0.225	0.365	0.476
		b	0.149	0.322	0.497	0.691	0.825	1.67	2.25	3.10
	20	a	0.0107	0.0270	0.0595	0.0940	0.127	0.282	0.448	0.590
		b	0.137	0.220	0.387	0.535	0.694	1.12	1.46	2.01
	10	a	0.0131	0.0321	0.0670	0.106	0.144	0.312	0.483	0.662
		b	0.113	0.171	0.315	0.422	0.538	0.839	1.12	1.32
	4	a	0.0156	0.0338	0.0758	0.119	0.162	0.338	0.520	0.710
		b	0.0896	0.155	0.231	0.297	0.360	0.588	0.760	0.861
	2	a	0.0178	0.0377	0.0805	0.125	0.169	0.355	0.539	0.732
		b	0.0685	0.117	0.186	0.241	0.296	0.426	0.580	0.652
	1	a	0.0855	0.1303	0.177	0.366	0.558			
		b	0.138	0.188	0.219	0.325	0.400			
	0.5	a	0.0436	0.0898	0.138	0.183	0.377	0.572		
		b	0.0613	0.0975	0.115	0.162	0.220	0.266		
	0.2	a	0.0459	0.0936	0.142	0.190	0.387	0.584		
		b	0.0389	0.0605	0.0721	0.0926	0.127	0.153		

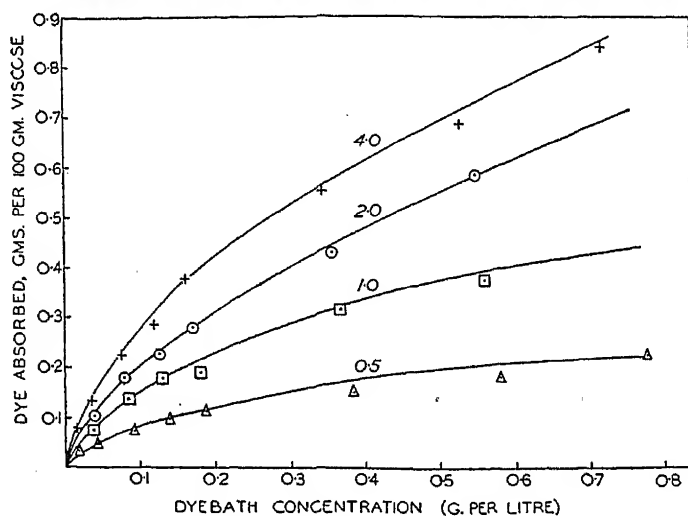


FIG. 3.—Absorption isotherms of Chrysophenine. Electrolyte, sodium sulphate. Temperature 97.5° C. Sodium sulphate concentration (g. per litre) indicated on each curve.

of the solution, and  $a$  and  $n$  are constants. This is illustrated by Figs. 4 and 5; in Fig. 4  $\log x$  is plotted against  $\log c$  for a series of NaCl concentrations at 97.5° C., while Fig. 5 shows similar relations for a fixed NaCl concentration and various temperatures. The lines are for the most part reasonably straight, although there is sometimes an indication of

TABLE II.—ABSORPTION OF CHRYSOPHENINE G BY CELLULOSE AT 80° C., IN PRESENCE OF SODIUM CHLORIDE.

[(a) = Dye bath concentration, g. per l. (b) = Dye absorbed by cellulose, g. per 100 g.]

Concentration of sodium chloride, g. per litre.	40	{ a	0.00773	0.0235	0.0490	0.121		
		{ b	0.404	0.732	1.44	2.67		
	20	{ a	0.0125	0.0343	0.0798	0.186	0.316	0.447
		{ b	0.359	0.629	1.15	2.05	2.72	3.38
	10	{ a	0.0219	0.0483	0.118	0.269	0.403	0.558
		{ b	0.269	0.495	0.783	1.26	1.89	2.32
	4	{ a	0.0240	0.0567	0.133	0.302	0.465	0.649
		{ b	0.249	0.415	0.639	0.936	1.29	1.44
	2	{ a	0.0287	0.0680	0.149	0.326	0.505	0.699
		{ b	0.204	0.306	0.484	0.710	0.906	0.962
	1	{ a	0.0388	0.0753	0.160	0.342	0.537	0.732
		{ b	0.155	0.236	0.383	0.552	0.610	0.649
	0.5	{ a	0.0371	0.0820	0.177	0.362	0.552	0.746
		{ b	0.123	0.172	0.224	0.361	0.459	0.520
	0.2	{ a	0.0435	0.0904	0.186	0.379	0.574	0.768
		{ b	0.0607	0.0916	0.137	0.200	0.252	0.306

TABLE III.—ABSORPTION OF CHRYSOPHENINE BY CELLULOSE AT 60° C., IN PRESENCE OF SODIUM CHLORIDE.

[(a) = Dye bath concentration, g. per l. (b) = Dye absorbed by cellulose, g. per 100 g.]

Concentration of sodium chloride, g. per litre.	20	{ a	0.00675	0.0193	0.0386	0.108		
		{ b	0.414	0.772	1.54	2.79		
	10	{ a	0.00915	0.0220	0.0565	0.145	0.275	0.357
		{ b	0.391	0.747	1.37	2.44	3.12	4.24
	4	{ a	0.0134	0.0355	0.0923	0.222	0.372	0.540
		{ b	0.350	0.617	1.03	1.70	2.18	2.48
	2	{ a	0.0196	0.488	0.120	0.284	0.452	0.629
		{ b	0.290	0.490	0.764	1.10	1.42	1.64
	1	{ a	0.0244	0.0607	0.140	0.316	0.504	0.691
		{ b	0.245	0.376	0.573	0.802	0.914	1.04
	0.5	{ a	0.0304	0.0726	0.160	0.344	0.535	0.727
		{ b	0.187	0.262	0.380	0.535	0.620	0.701
	0.2	{ a	0.0398	0.0845	0.178	0.372	0.563	0.757
		{ b	0.0978	0.148	0.206	0.269	0.350	0.410

TABLE IV.—ABSORPTION OF CHRYSOPHENINE BY CELLULOSE AT 40° C., IN PRESENCE OF SODIUM CHLORIDE.

[(a) = Dye bath concentration, g. per l. (b) = Dye absorbed by cellulose, g. per 100 g.]

Concentration of sodium chloride, g. per litre.	4	{ a	0.00565	0.0176	0.0490	0.148	0.283	0.422
		{ b	0.424	0.789	1.44	2.41	3.03	3.61
	2	{ a	0.00763	0.0236	0.0699	0.197	0.361	0.537
		{ b	0.405	0.731	1.24	1.95	2.28	2.51
	1	{ a	0.0148	0.0399	0.113	0.272	0.447	0.629
		{ b	0.336	0.575	0.830	1.22	1.47	1.63
	0.5	{ a	0.00217	0.0542	0.134	0.312	0.497	0.682
		{ b	0.271	0.438	0.632	0.840	0.985	1.13
	0.2	{ a	0.0328	0.0772	0.167	0.356	0.546	0.740
		{ b	0.165	0.218	0.316	0.424	0.514	0.576

## 514 ABSORPTION OF CHRYSOPHENINE BY CELLULOSE

slight curvature, and their slopes are not greatly different, indicating that the value of  $n$  does not vary to any large extent.

TABLE V.—ABSORPTION OF CHRYSOPHENINE BY CELLULOSE AT 20° C., IN PRESENCE OF SODIUM CHLORIDE.

[(a) = Dye bath concentration, g. per l. (b) = Dye absorbed by cellulose, g. per 100 g.]

Concentration of sodium chloride, g. per litre.	1	$\begin{cases} a \\ b \end{cases}$	0.00339 0.207	0.0111 0.372	0.0293 0.677	0.0872 1.08		
		$\begin{cases} a \\ b \end{cases}$	0.0183 0.303	0.0472 0.505	0.120 0.761	0.289 1.06		
	0.5	$\begin{cases} a \\ b \end{cases}$	0.0284 0.206	0.0670 0.316	0.155 0.427	0.339 0.580	0.526 0.703	0.716 0.802
		$\begin{cases} a \\ b \end{cases}$						
	0.2	$\begin{cases} a \\ b \end{cases}$						
		$\begin{cases} a \\ b \end{cases}$						

TABLE VI.—ABSORPTION OF CHRYSOPHENINE BY CELLULOSE AT 97.5° C., IN PRESENCE OF SODIUM SULPHATE.

[(a) = Dye bath concentration, g. per l. (b) = Dye absorbed by cellulose, g. per 100 g.]

Concentration of sodium sulphate, g. per litre.	4	$\begin{cases} a \\ b \end{cases}$	0.0166 0.0799	0.0358 0.135	0.0764 0.226	0.120 0.288	0.160 0.379	0.342 0.554	0.528 0.688	0.712 0.843
		$\begin{cases} a \\ b \end{cases}$	0.0390 0.105	0.0811 0.180	0.126 0.227	0.171 0.281	0.355 0.431	0.544 0.585		
	2	$\begin{cases} a \\ b \end{cases}$	0.0420 0.0762	0.0857 0.137	0.131 0.178	0.180 0.191	0.367 0.316	0.561 0.373		
		$\begin{cases} a \\ b \end{cases}$	0.0216 0.0321	0.0448 0.0492	0.0920 0.0765	0.139 0.100	0.188 0.115	0.384 0.152	0.581 0.181	0.777 0.223
	1	$\begin{cases} a \\ b \end{cases}$								
		$\begin{cases} a \\ b \end{cases}$								
	0.5	$\begin{cases} a \\ b \end{cases}$								
		$\begin{cases} a \\ b \end{cases}$								
	0.2	$\begin{cases} a \\ b \end{cases}$								
		$\begin{cases} a \\ b \end{cases}$								
	0.1	$\begin{cases} a \\ b \end{cases}$								
		$\begin{cases} a \\ b \end{cases}$								

Determinations of equilibrium absorption were made at 90° and 60° C. in the absence of any added electrolyte; the results are given in Table VII

TABLE VII.—ABSORPTION OF CHRYSOPHENINE BY CELLULOSE AT 90° AND 60° C. IN ABSENCE OF ADDED ELECTROLYTE.

90° C.					60° C.				
Dye bath concentration, g. per litre.	Dye absorbed by cellulose, g. per 100 g.				Dye bath concentration, g. per litre.	Dye absorbed by cellulose, g. per 100 g.			
0.096	0.0085	0.0085			0.19	0.036	0.021	0.041	0.033
0.190	0.023	0.021			0.24	0.061			
0.29	0.039	0.043			0.29	0.071			
0.38	0.057	0.055	0.048		0.38	0.102	0.099	0.089	0.110
0.47	0.076	0.076	0.079	0.083	0.48	0.146	0.112	0.116	0.108
0.57	0.093				0.57	0.153	0.159	0.153	0.149
0.66	0.132				0.67	0.178			
0.76	0.136	0.135	0.151	0.152	0.76	0.238	0.242	0.259	0.226
0.85	0.178				0.85	0.258			
0.94	0.208	0.196	0.221	0.204	0.95	0.352	0.324	0.327	0.323
1.12	0.292	0.298			1.13	0.377	0.417	0.380	
1.32	0.355	0.351			1.32	0.504	0.467		
1.50	0.401	0.432	0.422		1.51	0.549			
1.68	0.467	0.461			1.69	0.651	0.651		
1.87	0.518	0.583	0.506		1.88	0.749	0.750	0.709	0.728

and the absorption isotherms shown in Fig. 6. The values of the equilibrium absorption are less reproducible than those obtained in the presence of a foreign electrolyte, and the results of replicate experiments are given in the Table instead of a mean value for each concentration. In spite of

this greater variation in the experimental results the shape of the isotherms is fairly well defined (Fig. 6); showing a point of inflection, they

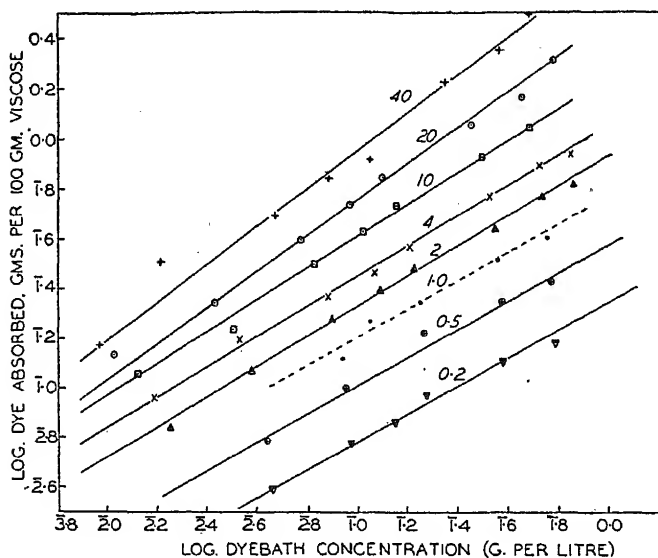


FIG. 4.—Absorption isotherms of Chrysophenine on viscose sheet at 97.5° C. Concentration of sodium chloride in gm. per litre is indicated on each line.

are essentially different from those obtained in the presence of sodium chloride or sulphate. They are, however, similar to the isotherms obtained

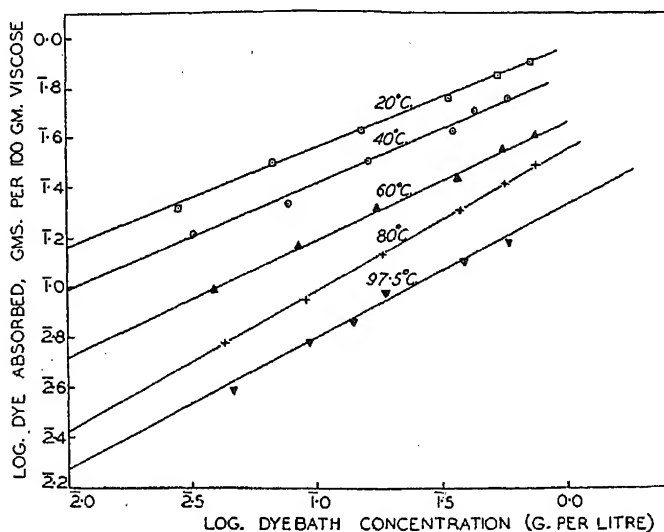


FIG. 5.—Absorption isotherms of Chrysophenine on viscose sheet at a fixed sodium chloride concentration of 0.2 g. per litre.

by Neale<sup>5</sup> for the absorption of Sky Blue FF by cellulose sheet over a range of relatively low sodium chloride concentrations; Neale attributes the sigmoid shape to the presence of oxycellulose in the sheet.



At 60° and 90° C. the values of the equilibrium absorption corresponding to a dyebath concentration of 1 g. per litre are 0.335 and 0.235 g. of dye per 100 g. cellulose. These values are appreciably higher than can be attributed to the absorption of the dye liquor by the sheet, and lead to the conclusion that, for Chrysophenine, adsorption of the dye by the cellulose occurs even in the absence of foreign electrolyte. This is at variance with the conclusion reached by other workers, using other dyes.<sup>6, 7</sup>

The results given above, in conjunction with many other sets of data recorded in the literature, have established the following facts about the uptake of dyes by cellulose:—

(1) The amount of dye absorbed by a sample of cellulose placed in a dyebath at a constant temperature increases with time to a definite limiting or equilibrium value dependent on the quality of the cellulose.

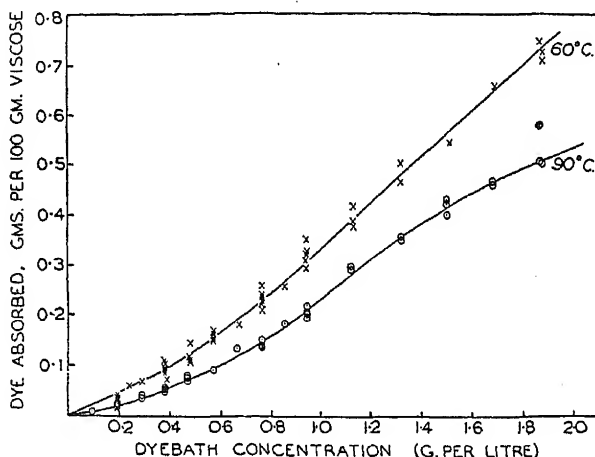


FIG. 6.—Absorption isotherms of Chrysophenine on viscose sheet in the absence of foreign electrolytes.

(2) The limiting amount of dye absorbed per unit mass of cellulose is a function only of (a) the dye concentration in the residual dyebath, (b) the concentration of electrolyte, and (c) the temperature. This statement implies that the absorption per unit mass of cellulose is independent of the manner in which the final equilibrium state is reached.

(3) At a given temperature and salt concentration the dye absorption at equilibrium increases with the dye concentration, rapidly at low concentrations, less rapidly at higher concentrations, but without the attainment of a saturation value.

(4) At a given temperature and dye concentration the dye absorption at equilibrium increases with the salt concentration, rapidly at low concentrations and less rapidly at higher concentrations.

(5) At given dye and salt concentrations the dye absorption at equilibrium decreases rapidly with increasing temperature.

In the succeeding sections of this paper an attempt will be made to develop a reasonable theory of the dyeing process that is consistent with these facts.

#### 4. A Theory of Direct Dyeing.

##### (a) Introduction.

The phenomenon of substantivity points to the existence of some sort of attractive force between the dye anions and the cellulose, and the

view taken here is that throughout the cellulose there exist numerous active centres, no doubt associated with the individual molecules, which are capable of attracting to them these ions. The nature or origin of this attraction will not initially be considered; whether it is due to a loose chemical binding force or to a pronounced Van der Waals' attraction does not make much difference to the theory except for one point: it is, strictly speaking, necessary to know whether the activity of a centre is affected by the fact that a dye ion has or has not been absorbed. If the attraction is of the chemical bond type it is probable that the attraction for other ions will cease when one ion has been absorbed, but if the attraction is of the Van der Waals' type it is probable that the activity does not vanish with the absorption of an ion. However, this is a point that need not be considered for the present, for the mathematical argument will be developed on the assumption that the activity does not vary with the number of ions already absorbed, and it will subsequently be shown that for comparatively small amounts of absorption little difference actually arises, and that in any case the necessary modification can be introduced, if required, for larger amounts of absorption.

The attraction between an active centre and the anionic dye micelle can be represented by a potential function  $\psi$ , which will vary with the distance from the active centre. The actual value of the potential at an active centre represents the energy per gram-molecule of dye adsorbed.

In order to keep the mechanism as simple as possible to begin with, it will be assumed for the time being that all ions of dye and electrolyte can be treated as points, and that they follow the laws for a perfect gas. Dissociation of all dye and electrolyte will be assumed to be complete, and it will be assumed that there is, in the first instance, no aggregation of the dye anions. The thermodynamic treatment is developed throughout in terms of concentrations instead of activities—an approximation that can be allowed for if the activities of aqueous dye solutions are known.

### (b) General Account of the Theory.

An account of the theory in general terms can now be given. The dyestuffs considered are of the type  $A^+R^-$ , where  $A^+$  is a simple cation and  $R^-$  a complex organic anion. The field of force must act upon the anions  $R^-$ , but there is no reason for supposing that a comparable attraction will be exerted upon any of the other types of ion present, because ordinary simple salts are not absorbed by cellulose in the way that dyes are.

Consider now a single centre of attraction, surrounded by a field of force described by a potential  $\psi$  whose value at any point will be a function of the position co-ordinates of the point, and will tend to zero at large distances from the centre. If  $\rho$  denotes the ionic concentration of the ions  $R^-$  at any point, the energy of attraction for any distribution of such ions will be  $\int \rho \psi dv$  (integrated over all space).

This quantity will tend to assume its lowest possible value, which means that, other factors being neglected, all the ions present would finally be concentrated at the centre. But the one important factor that will prevent this occurring in practice is the kinetic agitation common to all particles. From the opposite point of view, if there were no field of force this kinetic agitation would produce a uniform distribution of ions, but the field of force upsets this distribution, and a final state of equilibrium is reached when the two opposing tendencies are everywhere balanced. The resulting distribution is one that shows a maximum concentration at the centre of attraction, where  $\psi$  is lowest, and decreases to a steady value in the more remote parts of the field where  $\psi$  tends to a zero value.

It is obviously reasonable to assume that the total excess of dye concentrated in the neighbourhood of an active centre represents the dye preferentially absorbed by that centre, and that the total dye absorbed

by a finite portion of cellulose is simply the total contribution of all the active centres that it contains. The structure of the cellulose does not come into consideration at all (except in so far as it affects the value of  $\psi$ ), its function being merely to furnish over a localised portion of the dye-bath a distribution of active centres.

Consider now the effect of increasing the temperature. The mean kinetic agitation of the ions is increased, so that more opposition is offered to the absorption tendency of the field of force. The existing distribution is therefore upset, and a new equilibrium distribution is found in which there is a smaller concentration of ions in the neighbourhood of the active centres. An increase in temperature therefore produces a decrease in absorption, just as is observed in practice.

The influence of the presence of an electrolyte can be understood from similar considerations. Suppose, to begin with, that no electrolyte is present, and, for the sake of simplicity, only one dye molecule, AR. This molecule will be dissociated into  $A^+$  and  $R^-$ , and though these ions are nominally free, yet they cannot move far from one another because of the electrostatic force operating between them, which may be expressed by saying that a condition of electric neutrality must be maintained over any "physical element of volume." It follows then that the tendency of the dye cation  $A^+$  to move about at random communicates itself to the dye anion  $R^-$ , and so increases its effective kinetic agitation without making any contribution towards its energy of attraction. Hence the anions  $R^-$  will be less intensely concentrated round the active centre than if the cations  $A^+$  were absent. The mathematical development shows that the effect of adding electrolyte is to minimise this restraining action on the part of the cations  $A^+$ , and to allow the anions  $R^-$  to be absorbed more, as they would be if the cations  $A^+$  were absent. In the extreme case of infinite excess of electrolyte, the anions  $R^-$  operate as if they were completely free, and the absorption then has its maximum value for the particular temperature. It is thus seen that the effect of the presence of electrolyte is not to drive the dye on to the cellulose in a positive sense, but to neutralise an existing inhibitory effect.

The result of increasing the concentration of the dye solution is readily understood in a general way. For increased concentration means a greater number of available dye ions and therefore a greater density of anions in the neighbourhood of the active centres when equilibrium is attained. But when electrolyte is present the effect will not be proportional to the concentration of dye, because an increase in the concentration of dye reduces the ratio of the concentration of electrolyte to that of the dye, and so decreases the effect of the electrolyte. The result is that the absorption does not increase in proportion to the concentration of dye present, but increases at a smaller and smaller rate as the dye concentration is raised. This is as is found in practice.

### (c) Mathematical Development of the Theory.

(1) **The Symbols Used.**—The symbols used in the mathematical development of the theory are as follows:—

$A^+, R^-$	denote the ions constituting the molecule of the dye studied.
$B^+, S^-$	denote the ions of the electrolyte used to assist dyeing.
$a, b, r, s$	are the valencies of these ions.
$\alpha, \beta, \rho, \sigma$	the corresponding Greek letters, are the gram-ionic concentrations of the ions $A^+, B^+, R^-, S^-$ , respectively.
$\psi$	describes the potential field surrounding an active centre of attraction, so that $\rho\psi dv$ represents the energy of attraction
$-\psi_0$	of particles of type R located in an element of volume $dv$ , is the constant value that $\psi$ is assumed to possess for certain calculations.

$\alpha_0, \beta_0, \rho_0, \sigma_0$  are the values of  $\alpha, \beta, \rho, \sigma$  at infinity, which in practice will be the values possessed outside the cellulose phase.

$$X = e^{\frac{-\psi}{RT}}$$

$$p = \frac{s\sigma_0}{r\rho_0}$$

$w$  is defined by the equation  $w^{-a} + pw^{-b} = Xw^r + pw^s$ .

$v$  When the assumption  $\psi = -\psi_0$  is made,  $v$  is the volume associated with each active centre over which  $\psi_0$  extends.

$V$  is the total of such volumes in unit (dry) mass of cellulose.

$m$  is the amount of dye (in gram-molecules) preferentially absorbed by unit mass of cellulose.

$V_0$  is the specific volume of the (swollen) cellulose.

(2) **Dyeing in the Absence of an Inorganic Electrolyte.**—In the first instance the problem will be limited to the determination of the distribution of dye ions round a single centre of force, and the result will be applied subsequently to a system of many active centres on the assumption (later justified) that there is no mutual interaction between the various centres. Further, for the sake of simplicity, attention will first be directed to dyeing in the absence of inorganic electrolyte. The problem may therefore be stated in the following terms: given an infinite distribution of ions subject to the influence of a conservative field of force whose potential is  $\psi(x, y, z)$ , which decreases to zero at infinity, to determine the equilibrium distribution  $\rho(x, y, z)$  at any temperature  $T$ , the ions being assumed to obey the perfect gas laws.

When the system is in equilibrium, its total free energy must have a stationary value, so that variations of this energy must be zero for *all possible* small variations in the distribution  $\rho$  that are consistent with the condition that the total number of ions remains unaltered.

The free energy of the system is made up of two parts:—

(1) the potential energy of the ions in the field of force. This is simply  $\int_V \rho \psi dv$ , the integral being extended over all space.

(2) The energy of the system arising from the kinetic agitations of its separate ions. For one mole the free energy is  $RT \log \rho/\rho_1$  where  $\rho$  is the molar concentration and  $\rho_1$  is an arbitrary concentration taken as standard of reference. This is equivalent to a volume density of free energy of

$$(RT/v) \log \rho/\rho_1 = RT \rho \log \rho/\rho_1.$$

The total free energy is therefore

$$\int (RT \rho \log \rho/\rho_1 + \rho \psi) dv. \quad (1)$$

The variation of this integral is to be determined subject to the condition that the total amount of mass is conserved, a condition that is expressed by the equation

$$\int_V \rho dv = \text{constant}. \quad (2)$$

The method of the Lagrangian multipliers is used, the integral

$$I = \int_V (RT \rho \log \rho/\rho_1 + \rho \psi) dv + \lambda \int_V \rho dv \quad (3)$$

is formed where  $\lambda$  is a constant as yet undetermined, and the variation of this integral is determined for completely arbitrary but small variations of  $\rho$  giving

$$\delta I = \int_V (RT \log \rho/\rho_1 + RT + \psi + \lambda) \delta \rho \cdot dv.$$

The condition  $\delta I = 0$  is satisfied only if

$$RT \log \rho/\rho_1 + RT + \psi + \lambda = 0$$

which leads to

$$\log \frac{\rho}{\rho_1} = -\frac{\psi}{RT} - 1 - \frac{\lambda}{RT},$$

i.e.

$$\rho = \rho_1 e^{-1 - \frac{\lambda}{RT}} e^{-\frac{\psi}{RT}};$$

The constant  $\lambda$  may now be chosen so as to satisfy the particular conditions of the problem. Thus at infinity, where  $\psi = 0$ ,

$$\rho = \rho_1 e^{-1 - \frac{\lambda}{RT}}$$

and this may be equated to the density  $\rho_0$  at infinity, which may be regarded as known. This gives finally

$$\rho = \rho_0 e^{-\frac{\psi}{RT}} \quad . \quad . \quad . \quad . \quad . \quad (4)$$

which is a well-known result.

If now the field of force is due to an attractive centre,  $\psi$  will be negative, and  $\rho$  will evidently be greatest where  $\psi$  is numerically greatest;  $\rho$  will therefore rise as we approach the centre of attraction. The general effect is indicated in Fig. 7, where the dotted curve shows the way in which

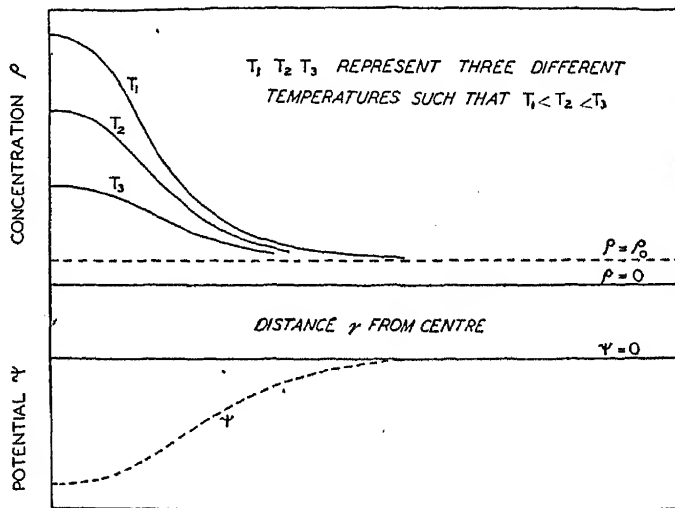


FIG. 7.—Variation of the potential  $\psi$  and the concentration  $\rho$  with the distance  $r$  from an active centre.

the potential may be expected to vary. The continuous curves show the consequent variation in particle density with the distance from the centre for different temperatures. An increase in the temperature is clearly seen to result in a decrease in the concentration of particles round the centre.

The quantity  $(\rho - \rho_0)$  integrated over all space can evidently be taken as a measure of the amount of matter absorbed by the active centre.

This simple example is given as an introduction to the more general problem which will now be considered, and which will be found to be of more direct application to the behaviour of dyes.

(3) **Dyeing in the Presence of a Multivalent Electrolyte.**—Let the dye dissociate into ions  $A^+$  and  $R^-$ , and the electrolyte into  $B^+$  and  $S^-$ . The charges carried by these ions are denoted by the corresponding small letters,  $a, r, b, s$  and the corresponding Greek letters  $\alpha, \rho, \beta, \sigma$ , are used to denote the molecular concentrations of these ions at any point of space.

As before there is assumed to exist a potential function  $\psi$  that operates only upon the dye anions  $R^-$ . The total energy due to the field is therefore  $\int_v \rho \psi dv$ . Each type of ion, however, makes a contribution towards the free energy of kinetic motion of the system, and the total free energy is

$$I = \int_v \left[ RT \left( \alpha \log \frac{\alpha}{c_0} + \beta \log \frac{\beta}{c_0} + \rho \log \frac{\rho}{c_0} + \sigma \log \frac{\sigma}{c_0} \right) + \psi \rho \right] dv \quad (5)$$

$c_0$  being the concentration taken as zero of reference.

To determine the actual equilibrium distributions for each type of ion present the complete variation of this integral for all possible small variations of each of the quantities  $\alpha, \beta, \rho, \sigma$ , must be equated to zero, the variations being subject to the following conditions:—

(i) The total amount of each kind of ion present remains unaltered in the variation, a condition that is expressed by the equations

$$\begin{aligned} \int_v \alpha dv &= \text{const.} & \int_v \rho dv &= \text{const.} \\ \int_v \beta dv &= \text{const.} & \int_v \sigma dv &= \text{const.} \end{aligned} \quad (6)$$

(ii) Throughout all space each physical element of volume  $dv$  remains electrically neutral. This is expressed by the relation

$$a\alpha + b\beta - r\rho - s\sigma = 0. \quad (7)$$

To calculate the variation of  $I$  subject to these conditions a new integral is formed:—

$$J = \int_v \left[ RT \left( \alpha \log \frac{\alpha}{c_0} + \beta \log \frac{\beta}{c_0} + \rho \log \frac{\rho}{c_0} + \sigma \log \frac{\sigma}{c_0} \right) + \psi \rho + \lambda \alpha + \mu \beta + \nu \rho + \omega \sigma + \phi(a\alpha + b\beta - r\rho - s\sigma) \right] dv \quad (8)$$

where, according to the theory of the Calculus of Variations, the coefficients,  $\lambda, \mu, \nu$  and  $\omega$  are to be treated as undetermined constants, and the coefficient  $\phi$  as an undetermined function of the spatial co-ordinates. The variation of this integral is

$$\begin{aligned} \delta J &= \int_v (RT \log \alpha/c_0 + RT + \lambda + a\phi) \delta \alpha \cdot dv \\ &+ \int_v (RT \log \beta/c_0 + RT + \mu + b\phi) \delta \beta \cdot dv \\ &+ \int_v (RT \log \rho/c_0 + RT + \psi + \nu - r\phi) \delta \rho \cdot dv \\ &+ \int_v (RT \log \sigma/c_0 + RT + \omega - s\phi) \delta \sigma \cdot dv. \end{aligned}$$

The relation  $\delta I = 0$ , subject to the conditions mentioned previously, is now equivalent to the relation  $\delta J = 0$  for certain particular values of the arbitrary quantities introduced, the variations  $\delta \alpha, \delta \beta, \delta \rho, \delta \sigma$  in the latter case being treated as completely independent. The relation  $\delta J = 0$  is evidently satisfied for arbitrary independent variations  $\delta \alpha, \delta \beta, \delta \rho, \delta \sigma$  only if the coefficients of these terms are separately zero. This leads to

$$\begin{aligned} \alpha &= c_0 e^{-1 - \frac{\lambda}{RT}} e^{-a\phi'} & \beta &= c_0 e^{-1 - \frac{\mu}{RT}} e^{-b\phi'} \\ \rho &= c_0 e^{-1 - \frac{\nu}{RT}} e^{r\phi'} e^{-\frac{\psi}{RT}} & \sigma &= c_0 e^{-1 - \frac{\omega}{RT}} e^{s\phi'} \end{aligned} \quad (9)$$

where

$$\phi' = \phi/RT.$$

Now it is the aim of this problem to express the amount of dye absorbed by cellulose in terms of the dye and electrolyte concentrations with which it is in equilibrium. It seems natural to interpret these concentrations in terms of the values of  $\alpha$ ,  $\beta$ ,  $\rho$ ,  $\sigma$  at infinity, where the influence of the field of force will be zero. If the values of  $\alpha$ ,  $\beta$ ,  $\rho$ ,  $\sigma$  at infinity are  $\alpha_0$ ,  $\beta_0$ ,  $\rho_0$ ,  $\sigma_0$  the results can be expressed in a simpler form. For put

$$\phi' = \phi'_0 + \chi$$

where  $\phi'_0$  is the value of the function  $\phi'$  at infinity. Then

$$\alpha = c_0 e^{-1 - \frac{\lambda}{RT} - a\phi'_0} e^{-a\chi}$$

and at infinity

$$\alpha_0 = c_0 e^{-1 - \frac{\lambda}{RT} - a\phi'_0}$$

The same process is applicable to  $\beta$ ,  $\rho$ , and  $\sigma$  giving equations

$$\begin{aligned} \alpha &= \alpha_0 e^{-a\chi}, & \beta &= \beta_0 e^{-b\chi}, \\ \rho &= \rho_0 e^{r\chi} e^{-\frac{\psi}{RT}}, & \sigma &= \sigma_0 e^{s\chi} \end{aligned} \quad (10)$$

The function  $\chi$  may now be determined by substituting the above expressions in the relation

$$a\alpha + b\beta - r\rho - s\sigma = 0,$$

giving

$$a\alpha_0 e^{-a\chi} + b\beta_0 e^{-b\chi} = r\rho_0 e^{-\frac{\psi}{RT}} e^{r\chi} + s\sigma_0 e^{s\chi}$$

which is an equation for the function  $\chi$  in terms of  $\psi$ . The equation simplifies somewhat by reason of the fact that since the molecules AR, BS are electrically neutral

$$a\alpha_0 = r\rho_0 \text{ and } b\beta_0 = s\sigma_0$$

so that, putting at the same time

$$e\chi = w, \quad e^{-\frac{\psi}{RT}} = X, \quad \text{and} \quad s\sigma_0/r\rho_0 = p,$$

the result is

$$w^{-a} + pw^{-b} = Xw^r + pw^s. \quad (11)$$

### (c) Solution of the Simplest Case.

The above equation (11) is an algebraic equation of general degree in  $w$ , for which it is impossible to lay down any general solution. An exact solution is possible, however, for certain particular values of  $a$ ,  $b$ ,  $r$  and  $s$ . The simplest possible case is  $a = b = r = s = 1$ , and as this should show the properties of the more general case, some attention will be devoted to it.

The solution is

$$w = \sqrt{\frac{p+1}{p+X}}$$

so that the complete formulæ for  $\alpha$ ,  $\beta$ ,  $\rho$ ,  $\sigma$  can now be written down. The expression for  $\rho$  is, however, the most interesting; it is

$$\rho = \rho_0 X \sqrt{\frac{p+1}{p+X}} \quad (12)$$

As indicated previously, it is reasonable to take the integral

$$\int_v (\rho - \rho_0) dv \quad (13)$$

(evaluated over all space) as our measure of the dye preferentially absorbed by an active centre, it being supposed that in practice almost the entire contribution of this integral is located in the immediate vicinity of the centre.

Now before the amount absorbed can be calculated, it is necessary to

know the form of the function  $\psi$ . Here there is no information to serve as guide; all that is known of the function  $\psi$  is that it must be such as to make the integral  $\int_v (\rho - \rho_0) dv$  convergent at infinity.

Nevertheless if the theory is to be developed further, some arbitrary form for  $\psi$  must be assumed. The most natural assumption is to suppose that  $\psi$  is an inverse power function of the distance from the attractive centre,  $\psi = k/d^{l-1}$  which corresponds to an attractive force varying as the inverse  $l$ th power of  $d$ . This leads to a very complicated integral, which, as can readily be shown, is not convergent unless  $l > 4$ . Hence if the law of force is of the inverse power type, the force must decrease more rapidly than with the inverse fourth power of the distance. The existence of such large inverse powers is by no means unlikely; measurements of the temperature variations of the viscosities of gases call for the existence of such forces ( $l \doteq 5$  to 12) for their interpretation.<sup>8</sup>

The difficulty of studying the consequences of such fields of force makes it desirable to confine initial investigation to a more simple type of field, and for the present it will be assumed that the potential  $\psi$  has a constant value  $-\psi_0$  inside a closed region surrounding the active centre, and that outside this region it is everywhere zero. This assumption can be regarded as furnishing a reasonable first approximation to the shape of the function, and so may be expected to lead to the general order of the results that would be derived from a more accurate calculation. In considering deviations from the resulting theory, the effect of modifying the calculation by using a modified form of potential function should always be borne in mind.

With the above simple form for the function  $\psi$  the integration required to determine the amount of dye absorbed,  $\int_v (\rho - \rho_0) dv$ , is simple; the result obtained is

$$\int_v (\rho - \rho_0) dv = v\rho_0 \left[ e^{\frac{\psi_0}{RT}} \sqrt{\frac{p + 1}{p + e^{\psi_0/RT}}} - 1 \right] \quad (14)$$

where  $v$  is the volume round the attractive centre over which the potential  $\psi_0$  extends. It is important to notice that this formula places no restriction on the shape of the volume  $v$ —it may have any shape whatsoever. This is fortunate, because in practice it is obvious that the bulky cellulose molecules will prevent the particles of dye having free access to all parts of space in the vicinity of an active centre associated with a cellulose molecule. It follows then that  $v$  denotes the volume covered by the potential  $\psi_0$  that is accessible to the dye anions.

With regard to the above formula, the quantity  $e^{\frac{\psi_0}{RT}} \sqrt{\frac{p + 1}{p + e^{\psi_0/RT}}}$  works out in practice to be extremely large, so that the effect of subtracting unity is negligible; the dye absorbed by a single centre therefore becomes

$$v\rho_0 e^{\frac{\psi_0}{RT}} \sqrt{\frac{p + 1}{p + e^{\psi_0/RT}}}$$

It has already been mentioned that cellulose is to be looked upon as furnishing innumerable centres of attraction, and it has to be considered whether the formula, derived for a single centre, can be applied directly to such a system. Two possible difficulties arise:—

(i) Difficulty would arise if there were any overlapping of the fields of force due to the various active centres. If there is no such overlapping, then the calculation is straightforward: the absorption of a system of centres is simply

$$V\rho_0 e^{\frac{\psi_0}{RT}} \sqrt{\frac{p + 1}{p + e^{\psi_0/RT}}}$$



where  $V$  refers to the total of all the contributory volumes associated with the individual centres. For the time being it will be assumed that there is no interference between the various potential fields; the above formula will therefore be accepted, and it will be shown, when actual numerical magnitudes are considered, that the assumption is probably justified.

(ii) The next point that requires consideration is that since a limited amount of dye is now absorbed by a very large number of centres instead of by one, the number of particles absorbed on the average per centre may work out to be small. This means that the quantities  $\alpha$ ,  $\beta$ ,  $\rho$ ,  $\sigma$  which have been treated as continuous functions, may turn out to be discontinuous. But this is not a real difficulty, for the above variables, which have hitherto been treated as densities, can be equally well understood in terms of the probabilities of locating a particular particle at any one spot, in which case the functions are again continuous, and the mathematical development is quite unaltered.

Now the formula for the dye absorption, as a result of these considerations is simply

$$m = V e^{\frac{\psi_0}{RT}} \sqrt{\frac{\frac{\sigma_0}{\rho_0} + 1}{\frac{\sigma_0}{\rho_0} + e^{\frac{\psi_0}{RT}}}} \quad (15)$$

the proper value for  $p$  being substituted. Examination of this formula shows that it accounts for the general way in which the dye absorption  $m$  varies with the temperature  $T$ , the dye concentration  $\rho_0$  and the electrolyte concentration  $\sigma_0$ . Consider first the variation with respect to  $\sigma_0$ , the electrolyte concentration.

$$\text{At } \sigma_0 = 0, \quad m = V \rho_0 e^{\frac{\psi_0}{2RT}},$$

$$\text{at } \sigma_0 = \infty, \quad m = V \rho_0 e^{\frac{\psi_0}{RT}},$$

and at intermediate concentrations  $m$  takes intermediate values, increasing steadily with  $\sigma_0$  at all values. Now the exponential  $e^{\psi_0/RT}$  works out to be extremely large in practice ( $\approx 10^8$  for Chrysophenine at  $80^\circ \text{C}$ .), so that there is an enormous ratio between  $e^{\psi_0/RT}$  and  $e^{\psi_0/2RT}$ ; the huge part that the presence of excess of electrolyte plays in the absorption of dye can therefore be understood. It may be noted in passing that the theory indicates the existence of a certain amount of preferential absorption even in the complete absence of electrolyte, though in actual value it will be very small. This circumstance is of interest because it has often been asserted that absorption does not take place in the absence of electrolyte.<sup>6, 7</sup> Examination of the absorption formula shows that increase of the temperature  $T$  should under all circumstances produce a decrease of the absorption  $m$ , for

$$\frac{\partial m}{\partial T} = -V \rho_0 \sqrt{1 + p} \cdot \frac{\psi_0}{RT^2} \frac{p e^{\frac{\psi_0}{RT}} + \frac{1}{2} e^{\frac{2\psi_0}{RT}}}{\left(p + e^{\frac{\psi_0}{RT}}\right)^{3/2}}$$

which is negative for all values of the variables. In the same way it is found that for given values of  $\sigma_0$  and  $T$ ,  $m$  increases continually with  $\rho_0$  at a rate that steadily decreases as  $\rho_0$  increases. This is just as is found in practice.

#### (d) Solution of the General Case.

The general case, when the quantities  $a$ ,  $b$ ,  $r$ ,  $s$ , have not the particular values assigned to them in the foregoing discussion, but have any values

whatsoever, may now be discussed. The equation requiring solution is

$$w^{-a} + pw^{-b} = Xw^r + pw^s. \quad (11)$$

This, as has already been stated, does not admit of ready solution in the general case, but because in practice the value of  $X$  is always extremely large a solution can be obtained by the method of successive approximations. Actually a solution to any required degree of accuracy could be secured by this method, but the successive approximations are so rapidly convergent that for most practical purposes it is only necessary to consider the first approximations.

The equation is written in the form

$$\frac{1}{p}w^{-a} + w^{-b} = \frac{X}{p}w^r + w^s.$$

In this equation each term is always positive, the term  $X$  is a large number of the order  $10^8$ , and  $p$  in practice varies from about 1 to  $10^4$ , so that  $X/p$  is never less than about  $10^4$ , and falls to that value only in extreme cases. Consideration of the equation then shows that it cannot be satisfied unless  $w$  is a very small quantity, and hence it is possible to develop a method of approximations by neglecting high powers of  $w$  in comparison with low powers.

Three cases need separate study:—

(i)  $b > a$ .

Multiply throughout by  $w^b$  in order to secure an equation in positive powers of  $w$ . Then

$$1 + \frac{1}{p}w^{b-a} = \frac{X}{p}w^{r+b} + w^{s+b}.$$

Now  $\frac{1}{p}w^{b-a}$  and  $w^{s+b}$  are certainly small quantities that can be neglected in comparison with the other terms present. Hence

$$\frac{X}{p}w^{r+b} = 1, \quad i.e. \quad w = \left(\frac{p}{X}\right)^{\frac{1}{r+b}}. \quad (16)$$

(ii)  $b = a$ .

Multiply throughout by  $w^b$ :

$$1 + \frac{1}{p} = \frac{X}{p}w^{r+b} + w^{s+b}$$

Here the term  $w^{s+b}$  can be neglected, so that

$$w = \left(\frac{1+p}{X}\right)^{\frac{1}{r+b}}. \quad (17)$$

(iii)  $b < a$ .

This case is difficult. Solution by the above perturbation method breaks down unless attention is confined to values of  $p$  that lie within a comparatively narrow range. Fortunately the solution for this case is not required in practice, because dyes are usually prepared as the salts of monovalent elements (e.g. sodium) where  $a = 1$ , so that the case  $b < a$  never arises.

The solutions in cases (i) and (ii) above represent first approximations. Second and more accurate approximations could be secured by the usual perturbation methods, but the modifications usually introduced are so small that it is unnecessary to consider them here. It need only be mentioned that the solutions given will be sufficiently accurate provided that:—

(i)  $p$  lies within certain limits (about 1 to  $10^4$ );

(ii) the value of  $r$  is not too large.

The greater the value of  $r$ , the lower is the upper limit of  $p$  that must be imposed in order that a given degree of precision may be ensured.

With Chrysophenine, where  $r = 2$ , the relative error in the dye absorption is only about 1 part in 500 at the most unfavourable point where  $p = 10^4$ . With dyes for which  $r$  is greater than 2 the first approximation may not be quite so good, and where  $r$  is rather large (say 5) it might be necessary to consider a second approximation if the absorption is to be studied for high values of  $p$ . But such cases would need to be considered individually, and there would still remain a wide range of values of  $p$  over which the above formulæ would be applicable with a degree of accuracy sufficient for practical purposes.

It should be noted in connection with these approximations that the formulæ cannot, of course, be used to study the effects of the presence of electrolytes at zero or infinite concentrations as was done for the exact solution studied previously.

Thus, on the assumption that the potential  $\psi$  can be considered constant over a certain range, the formulæ for the actual dye absorption can now be written

$$m = V\rho_0 X \left( \frac{p}{X} \right)^{\frac{r}{r+b}} \quad (b > a) \quad . \quad . \quad . \quad (18)$$

or

$$m = V\rho_0 X \left( \frac{p+1}{X} \right)^{\frac{r}{r+b}} \quad (b = a) \quad . \quad . \quad . \quad (19)$$

For the larger values of  $p$  these can be summed up by the single formula

$$m = V\rho_0 X \left( \frac{p}{X} \right)^{\frac{r}{r+b}} \quad (b \geq a) \quad . \quad . \quad . \quad (20)$$

Several useful deductions can be made from the theory presented above, but it is desirable to emphasise that in the course of its development it was necessary to introduce at a certain stage a simplifying assumption concerning the form of the potential function  $\psi$ . Conclusions that are drawn from any relation obtained subsequent to that stage must be treated with greater caution than conclusions that depend upon relations obtained before that stage, and the deductions made will therefore be discussed in relation to the assumptions made in deriving them.

## 5. General Deductions from the Theory.

It was found that the density of the dye distribution could be written as

$$\rho = \rho_0 e^{\frac{-\psi}{RT}} w^r \quad . \quad . \quad . \quad (10)$$

$w$  being determined by the relation

$$w^{-a} + pw^{-b} = Xw^r + pw^s \quad . \quad . \quad . \quad (11)$$

a statement that is independent of any assumption concerning  $\psi$ . The dye preferentially absorbed was seen to be

$$\int_v (\rho - \rho_0) dv = \rho_0 \int (e^{\frac{-\psi}{RT}} w^r - 1) dv \quad . \quad . \quad . \quad (13)$$

Although little progress can be made from this point without the introduction of simplifying assumptions, several general deductions of some interest can nevertheless be made.

### (i) The Absorption Isotherms for Constant Salt-Dye Ratios.

It is evident from the equation defining  $w$  (equation 11 above) that the solution for  $w$  will remain unaltered provided that  $p$  is kept fixed, *i.e.* provided that the ratio  $\sigma_0/\rho_0$  is maintained constant. Now an increase in the concentrations of salt and dye in the same ratio will evidently

leave  $\sigma_0/\rho_0$  unaltered, and so also  $w$ . The integral  $\int (e^{\frac{-v}{RT}} w^r - 1) dv$  is therefore kept constant, with the result that the dye absorption increases simply in proportion to the dye concentration. Thus the theory leads to the following conclusion:—

The amount of dye preferentially absorbed by a portion of cellulose should be proportional to the concentration of dye in the external solution at equilibrium, provided that the salt concentration is at the same time varied so as to maintain a constant ratio between the salt and dye concentrations.

This conclusion has been tested for Chrysophenine with the aid of the data given in Section III. The experimental isotherms there presented show the relations between the amount of dye absorbed by the cellulose and the concentration of the dye solution in which it is immersed, for a series of fixed concentrations of sodium chloride. Absorption isotherms

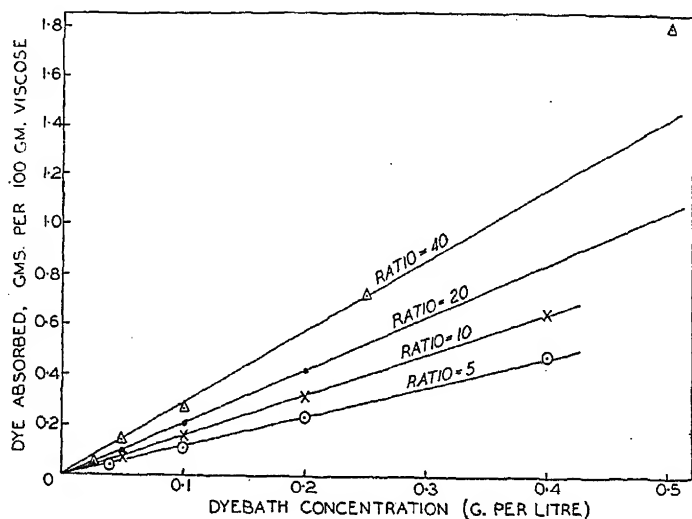


Fig. 8.—Absorption isotherms of Chrysophenine on viscose sheet at 97.5° C. for fixed salt/dye ratios.

corresponding to constant salt-dye ratios were obtained from the experimental isotherms by interpolation. An arbitrary salt-dye ratio was first chosen, and for any experimental isotherm representing a fixed NaCl concentration the appropriate residual dyebath concentration was calculated. The value of the amount of dye absorbed at this calculated dyebath concentration was then read from the experimental isotherm. This procedure was repeated for each of the experimental isotherms in turn to give corresponding values of absorbed dye and residual dyebath concentration for a series of fixed salt-dye ratios. The isotherms so obtained are shown in Figs. 8-11. The points lie very well on straight lines passing through the origin, the discrepancies that do occur being associated with the larger values of the dye absorption, where it is possible that the derived relation breaks down.

It is clear therefore that a simplification in the representation of dye absorption measurements is available for those data that conform to the rule. Normally the dye absorption (per unit mass) at any one temperature is regarded as a function of two parameters, the dye concentration and the salt concentration; hence for a complete description of the

dye absorption at any one temperature there is required a family of curves showing (say) the relation between the dye absorption and the dye concentration in solution for various constant values of the salt concentration. But the result now obtained shows that this is no longer necessary, for

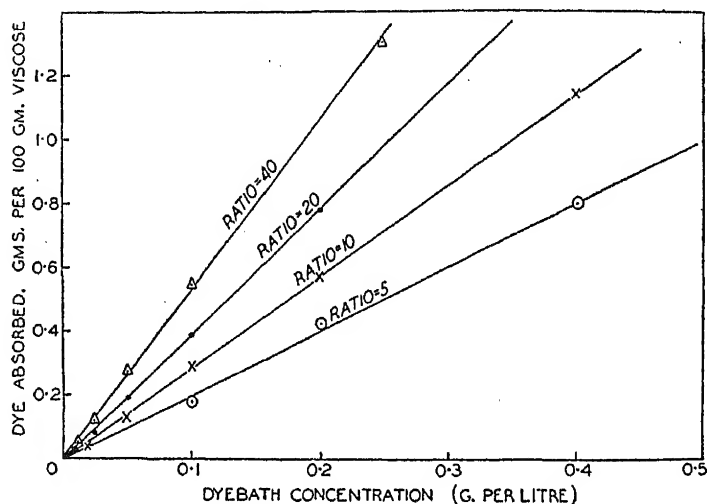


FIG. 9.—Absorption isotherms of Chrysophenine on viscose sheet at 80° C. for fixed salt/dye ratios.

the relation between the dye absorption and dye concentration at a constant value of the salt-dye ratio can be specified by a single quantity, namely the slope of the corresponding straight line. If this slope is plotted against the salt-dye ratio a single curve is obtained which provides all the information about the absorption at one temperature.

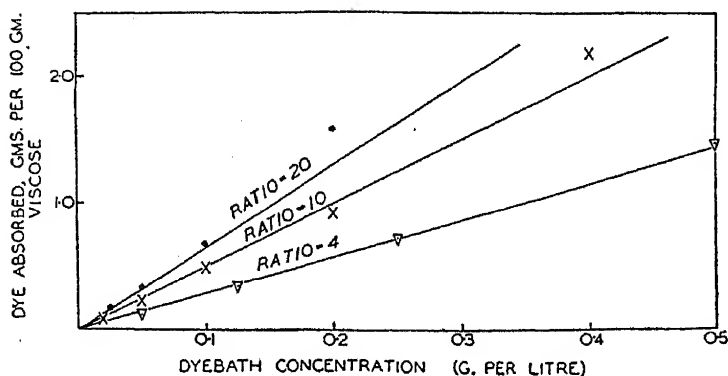


FIG. 10.—Absorption isotherms of Chrysophenine on viscose sheet at 60° C. for fixed salt/dye ratios.

## (ii) The Substantivity Ratio.

This result can be expressed in another way. The dye absorption for any particular mass of cellulose is

$$m = \rho_0 \int_0^{\infty} (e^{\frac{-\psi}{RT} w} - 1) dv \quad (13)$$

Since the integral has the dimensions of a volume, it may be written as  $\zeta V_0$  where  $V_0$  is the volume of the (swollen) cellulose and  $\zeta$  is a dimensionless quantity. If now  $m$  refers to the dye absorbed by 1 gm. (dry weight) of cellulose, then  $V_0$  will be the specific volume of the swollen cellulose. The number

$$\zeta = \frac{m}{\rho_0 V_0}$$

appears to be a most useful quantity in the discussion of the theoretical results, and will be referred to as the *Substantivity Ratio*. It measures the ratio between the concentration of preferentially absorbed dye in the cellulose phase and the concentration of dye in the external liquid phase. The dyeing formula can now be written as

$$\zeta = \frac{1}{v_0} \int_v^{\infty} (e^{\frac{-\psi}{RT} w} - 1) dv.$$

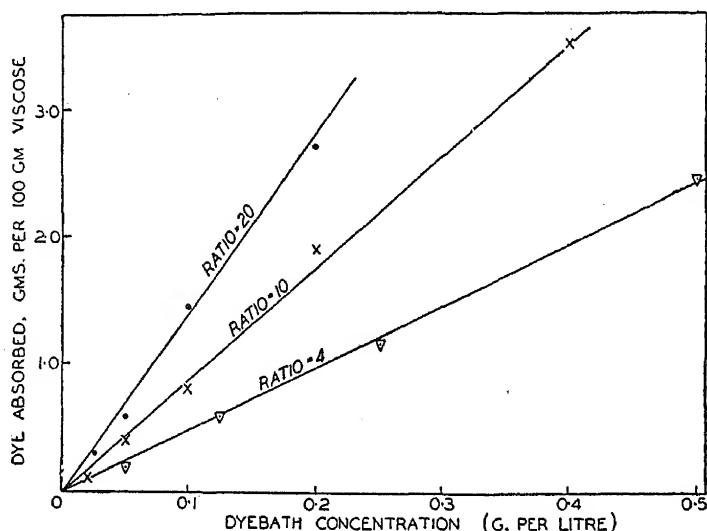


FIG. 11.—Absorption isotherms of Chrysophenine on viscose sheet at 40° C. for fixed salt/dye ratios.

Reference to equation (11) defining  $w$  shows that, for a given  $\psi$ ,  $w$  will be a function of  $p$  alone, so that  $\zeta$  will be a function of  $T$  and  $p$ , i.e. of  $T$  and the salt-dye ratio.

It is possible to check the foregoing conclusion by plotting the experimental values of  $\zeta$  against the salt-dye ratio. Sets of data from the various salt concentrations should now define one and the same curve. The relevant data for Chrysophenine are shown in Fig. 12 where, for convenience, logarithms of the quantities are plotted together. For each temperature the points generate a single line, which in most cases is practically straight, a point to be discussed later.

### (iii) The Effect of Different Electrolytes.

Without making any assumptions concerning the form of  $\psi$ , predictions can be made concerning the substantive effects of different electrolytes whose ions are similar in charge ( $b = s$ ). For each of such electrolytes the equation for  $w$  has the same form, and the actual value of  $w$  depends only upon  $p$ , which for a given dye concentration is proportional to the molecular concentration of the electrolyte. Hence for

a series of electrolytes the substantivity ratio  $\zeta$  should always have the same value for equal molar concentrations of the electrolytes. This has been tested for Chrysophenine at 60° C. Dye baths were prepared of exactly the same volume and dye concentration and with equal molar concentrations of NaCl, NaBr, KCl and KBr. Equal amounts of cellulose were added to each bath, so that the amounts of dye absorbed should have been identical. The results obtained are shown in Table VIII.

TABLE VIII.—ABSORPTION OF CHRYSOPHENINE BY CELLULOSE AT 60° C., IN THE PRESENCE OF VARIOUS ELECTROLYTES.

Electrolyte.	Concentration of electrolyte g. per litre.	Dye absorbed, g. per 100 g. cellulose.
Sodium chloride . . . .	2.00	0.123
Sodium bromide . . . .	3.52	0.123
Potassium chloride . . . .	2.55	0.133
Potassium bromide . . . .	4.07	0.133
Sodium sulphate . . . .	2.43	0.119

The agreement between the values obtained for the four salts is reasonably good, and is particularly good for the two sodium salts and the two potassium salts.

In order to compare the effects of salts with cations of the same valency ( $b$  the same) and anions of different valency ( $s$  different) it is necessary to use the approximate formula for  $\rho$  derived by the perturbation method

$$\rho = \rho_0 X (p/X)^{\frac{r}{r+b}}.$$

Since  $p = s\sigma_0/r\rho_0$ , equal substantive effects would be expected from concentrations of electrolyte for which  $s\sigma_0$  is the same. On this basis the concentration of  $\text{Na}_2\text{SO}_4$  required to produce the same effect as 2.00 g. per litre NaCl was calculated to be 2.43 g. per litre, and an experiment made at this concentration gave a dye absorption (Table VIII) of 0.119 g. per litre, in good agreement with the value 0.123 g. per litre obtained with NaCl.

A comparison of the effects of electrolytes with different values of  $b$  cannot be so readily made; it requires a knowledge of the value of  $X$ , and it has not been possible to determine anything more than the order of magnitude of this quantity. Difficulty is experienced in working with Chrysophenine in the presence of electrolytes for which  $b > 1$ , because "salting-out" is produced for such small concentrations of electrolyte that it is impossible to produce any appreciable substantivity. One conclusion can, however, be drawn. Since  $(p/X)$  is a small quantity

(say  $10^{-8}$  to  $10^{-4}$ ) it follows that  $(p/X)^{\frac{r}{r+b}}$  will increase considerably with  $b$ . Hence electrolytes for which  $b > 2$  should produce distinctly larger substantive effects than equivalent concentrations of electrolytes for which  $b = 1$ .

## 6. Special Deductions from the Theory.

It is now desirable to consider deductions that can be made from expressions that are derived on the assumption that the potential function  $\psi$  has a constant value  $\psi_0$  over a limited distance from the active centre.

### (i) The Relation between the Substantivity Ratio and the Salt-Dye Ratio.

A general expression for the dye absorption  $m$  at large values of  $p$  was obtained in the form

$$m = V\rho_0 X (p/X)^{\frac{r}{r+b}} \quad . \quad . \quad . \quad (20)$$

If  $m$  refers to the amount of dye absorbed by unit (dry) weight of cellulose,  $V$  will have a definite value which can be written as  $V = V_0/L$ , where  $V_0$  is the specific volume of the cellulose. The equation, in dimensionless form, then becomes

$$\zeta = \frac{m}{v_0 \rho_0} = \frac{1}{L} X \left( \frac{p}{X} \right)^{\frac{r}{r+b}}$$

and this will be the equation of the curves relating the substantivity ratio  $\zeta$  to the salt-dye ratio. The agreement between theory and observation can, however, be tested more easily by putting this equation in another form. By taking logarithms the equation becomes:

$$\log \zeta = \frac{b}{r+b} \log X - \log L + \frac{r}{r+b} \log p \quad (21)$$

Now  $X = e^{\frac{-v_0}{RT}}$ , an expression that depends on the temperature only. Hence at any one temperature the equation takes the form

$$\log \zeta = \frac{r}{r+b} \log p + \text{constant.}$$

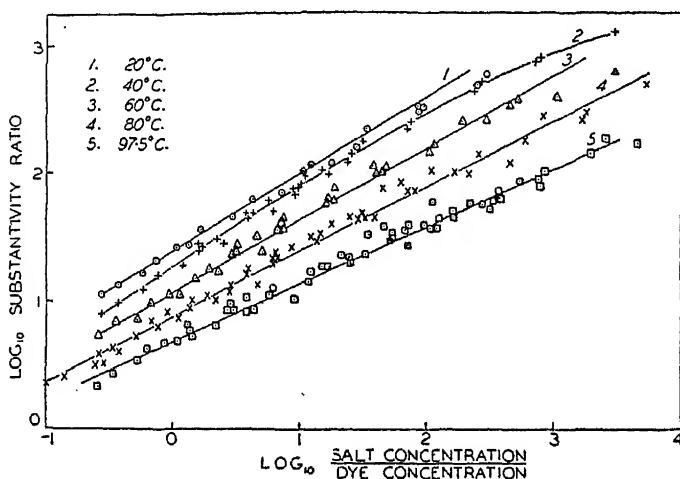


FIG. 12.—Absorption of Chrysophenine by viscose sheet at various temperatures. Electrolyte, sodium chloride.

Hence, if values of  $\log \zeta$  and  $\log p$  are plotted together a linear relationship should result, and the slope of the line should be  $r/(r+b)$ . At different temperatures different lines should result, but all with the same slope  $r/(r+b)$ .

The relevant data for Chrysophenine are plotted in Fig. 12; the quantities plotted are not identical with  $\log \zeta$  and  $\log p$  as defined above, but differ from them by constant amounts, for the concentrations have not been converted to molecular concentrations. The linear relationship appears to be quite strikingly obeyed at the higher temperatures, though at the lower temperatures there are definite indications of curvature. The precision of the results has been examined for the data for 80° C. The deviation of the points from the best straight line that can be drawn through them is such as to correspond to an average relative error of about 12 % in the quantity  $\zeta$ . This can hardly be considered large when it is



noted that the extreme limits in the values of  $p$  are in the ratio 40,000 : 1, whilst  $\zeta$  itself varies from about 2.0 to 500.

In the foregoing it has been assumed that the absorption is proportional to  $\log p$ . For Chrysophenine it should more strictly be taken to be proportional to  $\log (1 + p)$ , so that values of  $\log \zeta$  and  $\log (1 + p)$  should generate a straight line. Little difference arises when  $p$  is large (the more general case), but for the lower values of  $p$  the points  $\log (1 + p)$  diverge from a straight line, as is shown in Fig. 13. It appears then that the experimental data for the absorption are proportional to the factor  $p^{\frac{r}{r+b}}$  in practice rather than to the factor  $(p + 1)^{\frac{r}{r+b}}$  predicted by the theory.

The slopes of the straight lines are not all the same, as would be expected, but vary with the temperature. With the exception of the line for 40° C., which is too curved to attach any slope to it at all, there appears

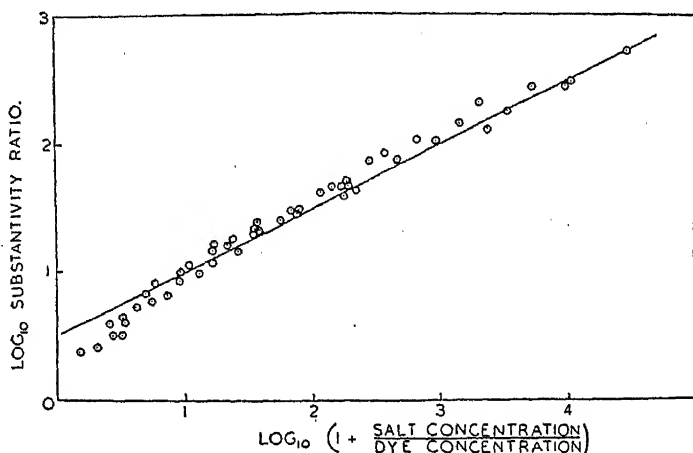


FIG. 13.—Absorption of Chrysophenine by viscose sheet at 80° C. Electrolyte, sodium chloride.

to be a progressive variation in the slope with temperature from 0.58 at 20° C. down to 0.45 at 97.5° C. Theory gives as the slope of these lines  $r/(r + b)$ ; for the system composed of Chrysophenine and NaCl  $r = 2$  and  $b = 1$ , giving a slope of 0.67, a value rather bigger than those found in practice, but of the same order of magnitude.

In Fig. 14 this method of plotting has been applied to some of the data obtained by Neale and his collaborators;<sup>7, 9, 10</sup> two of the lines obtained are straight, the other two show some tendency to be convex towards the log substantivity axis. The slopes of the lines,  $r/(r + b)$ , should be 0.67 for Benzopurpurine 4B and Fast Red K, and 0.80 for Sky Blue FF; the actual values observed (taken from the lines as a whole or from their straight line portions indicated on the Fig.) are 0.66 for Benzopurpurine 4B, 0.59 for Fast Red K at both 25° and 90° C., and 0.70 for Sky Blue FF. Again, therefore, the observed value tends to be rather lower than the calculated, but the discrepancy is not large.

It may be regarded as established, therefore, that the plot of  $\log \zeta$  against  $\log p$  is a straight line with a slope of the order of  $r/(r + b)$  but it has been noted that where there is any deviation from the straight line it is to make the curve convex towards the  $\log \zeta$  axis. The deduction that this plot should be a straight line was made from an expression derived as a first approximation following the assumption of the particular value

—  $\psi_0$  for  $\psi$ . It is now of interest to consider the more accurate formula that results from the calculation of second order terms. It is readily found that the more accurate formula is

$$\rho = \rho_0 X w^r = \rho_0 X \left( \frac{p}{X} \right)^{\frac{r}{r+b}} \left\{ 1 - \frac{r}{r+b} \left( \frac{p}{X} \right)^{\frac{s+b}{r+b}} \right\}.$$

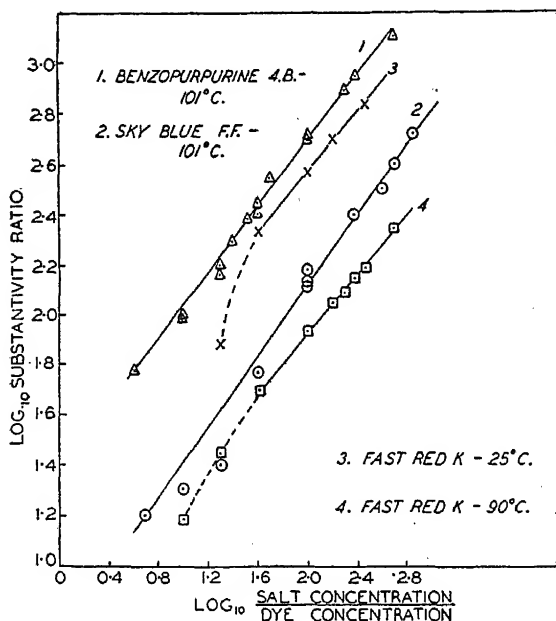


FIG. 14.—Absorption of various dyes by viscose sheet. Electrolyte, sodium chloride.

For small values of  $p$  this agrees with the previous formula, but for larger values of  $p$  the true value of  $\rho$  is always less than that given by the first approximation, and the same will therefore apply to the total absorption of dye. If therefore  $\log \zeta$  is plotted against  $\log p$  the approximate formula indicates a linear relationship at constant temperature, whereas the more

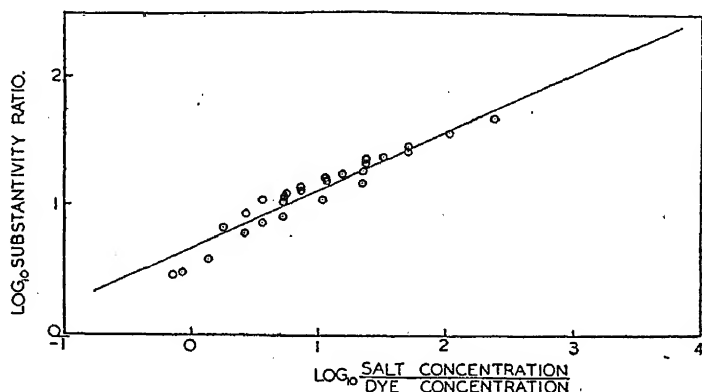


FIG. 15.—Absorption of Chrysophenine by viscose sheet. Temperature 97.5° C. Electrolyte, sodium sulphate. Straight line represents that for sodium chloride.

accurate forms shows that for larger values of  $p$  the curve should show a slight convexity towards the  $\log \zeta$  axis. This result should be true for all dyes, and the curves for Chrysophenine and the other dyes given in Figs. 12 to 15, show, when they are not completely straight, a curvature in just this direction.

Before leaving this question of the form of the  $\log \zeta - \log p$  plot it is of interest to show the result of making this plot for the data illustrating the comparative effects of NaCl and  $\text{Na}_2\text{SO}_4$ . On Fig. 15 the individual points represent data obtained with  $\text{Na}_2\text{SO}_4$ , while the straight line is that for NaCl at the same temperature. It is clear, therefore, that the two salts have identical effects when their concentrations are adjusted to correspond to the requirements of the present theory.

## (ii) The Shape of the Absorption Isotherms at Constant Salt Concentration.

For large values of  $p$ , the mass of dye absorbed per unit (dry) mass of cellulose is given by the general expression

$$m = V\rho_0 X \left( \frac{p}{X} \right)^{\frac{r}{r+b}} \quad . \quad . \quad . \quad (20)$$

Substituting for  $p$ ,

$$m = VX^{\frac{b}{r+b}} \left( \frac{s\sigma_0}{r} \right)^{\frac{r}{r+b}} \rho_0^{\frac{b}{r+b}}.$$

For isotherms at constant salt and varying dye concentration this takes the form

$$m = \text{constant } \rho_0^{\frac{b}{r+b}}$$

which is of the same form as the empirical relation

$$\text{dye absorbed} = \text{constant} \times (\text{dye concentration})^n$$

used by many workers and shown in Section III to be applicable to the data for Chrysophenine here presented. The theoretical equation to the isotherm as derived above is only valid for large values of  $p$ , otherwise equation (20) must be replaced by the expression

$$m = V\rho_0 X \left( \frac{p+1}{X} \right)^{\frac{r}{r+b}} \quad . \quad . \quad . \quad (19)$$

which on substituting for  $p$  does not lead to a simple relationship between  $m$  and  $\rho_0$ . The plot of  $\log m$  against  $\log \rho_0$  as shown in Figs. 4 and 5 gives a set of reasonably straight lines although there is sometimes an indication of curvature. It is noteworthy that when the NaCl concentration is 0.2 g. per litre and consequently  $p$  is small, the logarithmic relationship is still valid (Fig. 5) although the above theory is no longer applicable. This discrepancy between the experimental data and the theory is similar to that previously found for the plot of  $\log \zeta$  against  $\log p$ .

The value of  $n$  from the theory is  $b/(r+b)$  which for the system considered here is 0.33 and for the general case when  $b=1$  and  $r$  has any value,  $0 < n < \frac{1}{2}$ . Actually the experimental values of  $n$ , though limited in range, vary with the NaCl concentration, and are considerably higher than 0.33, only approaching this value when  $p$  is small; the expression for  $n$  cannot therefore be regarded as accurate. The values of the slopes of the log-log lines shown in Figs. 4 and 5 are given in Table IX.

TABLE IX.—VALUES OF  $n$  FOR THE EXPERIMENTAL ISOTHERMS.

<b>Isotherms at 97.5° C.</b>									
Salt Concentration (gm. per litre)	40	20	10	4	2	1	0.5	0.2	
$n$	0.76	0.71	0.63	0.61	0.60	0.57	0.57	0.56	
<b>Isotherms at salt concentration of 0.2 g. per litre.</b>									
Temperature, °C.	20	40	60	80	97.5				
$n$	0.40	0.43	0.47	0.56	0.56				

### (iii) The Shape of the Absorption Isotherms at Constant Dye Concentration.

If the dye concentration is maintained constant and the salt concentration varied the general equation

$$m = V\rho_0 X \left( \frac{p}{X} \right)^{\frac{r}{r+b}} \quad (p \gg 1)$$

becomes

$$m = \text{constant} \times \sigma^{\frac{r}{r+b}}$$

so that the plot of log (dye absorbed) against log (salt concentration) should be a straight line of slope  $r/(r+b)$ .

The data provided in this paper are not suitable for a test of this relation, but it can be tested by the data of Neale and his collaborators. Fig. 16 illustrates the application of this method of plotting to the data

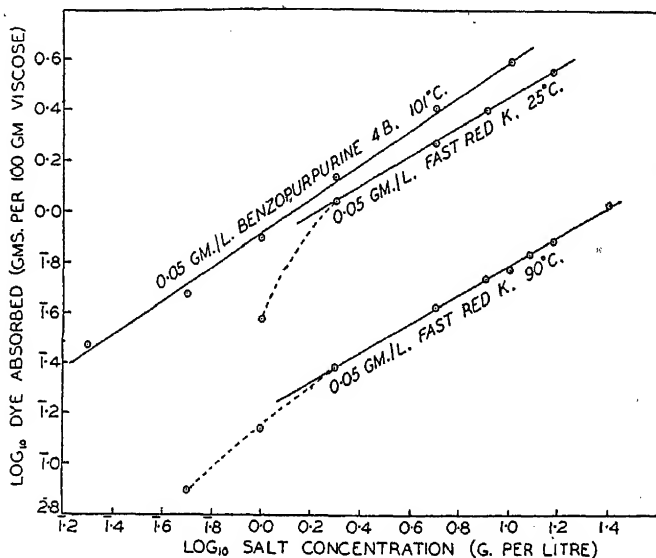


FIG. 16.—Absorption of Benzopurpurine 4B and Fast Red K on viscose sheet.

of Neale <sup>9, 10</sup> for the absorption by Cellophane sheet of Fast Red K at 25° and 90°, and of Benzopurpurine 4B at 101° C. from solutions of dye concentration 0.05 g. per litre. The graphs are reasonably good straight lines, except at the lowest salt concentrations with Fast Red K, where the corresponding values of  $p$  are 180 and 90 for the 25° and 90° C. plots respectively. The deviations cannot therefore be attributed to the value

## 536 ABSORPTION OF CHRYSOPHENINE BY CELLULOSE

of  $p$  being insufficiently large to justify the application of the theory. Moreover Benzopurpurine 4B gives a linear plot although the lowest value of  $p$  is 38. The slopes 0.57, 0.57 and 0.67 are not too divergent from the value of  $r/(r+b)$ , which is 0.67 for both dyes. Fig. 17 is a similar plot of Neale's data<sup>5</sup> for the absorption of Sky Blue FF by cotton and mercerised cotton. The line for mercerised cotton is straight, with a slope of 0.63 compared with 0.80 for  $r/(r+b)$  but the line for cotton is distinctly

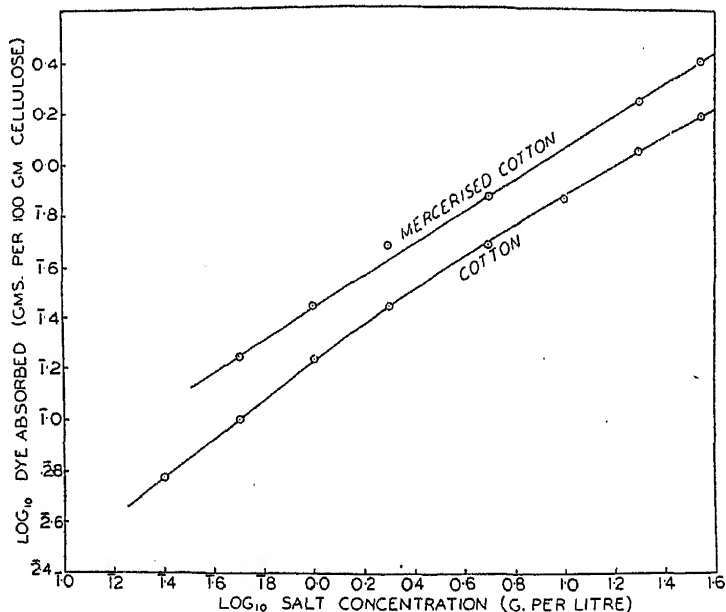


FIG. 17.—Absorption of Sky Blue FF on cotton and mercerised cotton at 90° C.

curved throughout. Even greater curvature is shown by the lines for the absorption of Sky Blue FF by cuprammonium rayon at 90° C. and by Cellophane at 90° and 101° C. This deviation from the straight line relationship at low salt concentrations is associated with a sigmoid shape of the isotherms themselves in the same region, which is attributed by Neale to the presence of ionised carboxyl groups in the viscose.

### 7. The Temperature Effect.

#### (i) The Variation of Substantivity with Temperature.

The formula derived previously

$$\log \zeta = \frac{r}{r+b} \log p - \log L + \frac{b}{r+b} \log X \quad (21)$$

indicates, for a fixed value of  $p$ , a simple temperature variation for  $\zeta$ , for since  $X = e^{w_0/RT}$

$$\log \zeta = \frac{b}{r+b} \cdot \frac{\psi}{RT} + \text{constant} \quad (22)$$

Hence, if values of  $\log \zeta$  are plotted against  $1/T$  for a fixed value of  $p$ , a straight line should result. The data presented in this paper provide no evidence that such a relationship is valid.

This cannot, however, be regarded as an argument against the general principles behind the theory, for it is not difficult to explain why the formula breaks down in this connection, whilst giving indications of being applicable in other directions. The simple relationship between  $\zeta$  and  $T$  deduced above is a consequence of the specially simple form for  $\psi$  chosen, and any other form would be unlikely to give this same result. Consider a different form for  $\psi$  defined by

$$\begin{array}{ll} \psi = -\psi_1 & a \leq d \leq a_1 \\ \psi = -\psi_2 & a_1 < d \leq a_2 \\ \psi = 0 & a_2 < d \end{array} \quad \left\{ \begin{array}{l} \text{where } d \text{ is the radial dis-} \\ \text{tance from the centre} \\ \text{of attraction.} \end{array} \right.$$

Solution is possible here just as before, the result being

$$\zeta = p^{\frac{r}{r+b}} \left( \frac{1}{L_1} e^{\frac{b}{r+b} \frac{\psi_1}{RT}} + \frac{1}{L_2} e^{\frac{b}{r+b} \frac{\psi_2}{RT}} \right)$$

where  $L_1$  and  $L_2$  are constants. This solution is sufficiently accurate provided that both the exponentials are large. Now this formula does not indicate any particularly simple relationship between  $\zeta$  and  $T$ , so it must be concluded that in the general case when  $\psi$  has any form whatsoever no simple relationship can be looked for between  $\zeta$  and  $T$ .

It will be remembered that the linear relation between  $\log \zeta$  and  $\log p$  was deduced on the basis of the simple assumption, and in view of the non-applicability of the temperature relation deduced on this assumption it is of interest to enquire to what extent the former result is dependent upon the form of  $\psi$ . It is evident from the result obtained above that  $\log \zeta$  is still linearly connected with  $\log p$  for the rather more complicated function there considered, and hence it is important to enquire whether this result is completely general and independent of the form of  $\psi$  chosen.

Consider now the formula for the density of dye

$$\rho = \rho_0 X w^r.$$

On the assumption that  $X \gg p$  this can be expressed in the form

$$\begin{aligned} \rho &= \rho_0 X \left( \frac{p}{X} \right)^{\frac{r}{r+b}} \\ &= \rho_0 e^{\frac{b}{r+b} \cdot \frac{\psi}{RT}} p^{\frac{r}{r+b}}. \end{aligned}$$

It may be assumed for the moment that this formula is applicable at all points of space, giving for the dye absorbed in a particular portion of space,

$$\rho_0 \int \left( e^{\frac{b}{r+b} \cdot \frac{\psi}{RT}} p^{\frac{r}{r+b}} \right) dv = \rho_0 p^{\frac{r}{r+b}} \int e^{\frac{b}{r+b} \cdot \frac{\psi}{RT}} dv$$

so that the dye absorption is proportional to  $p^{r/(r+b)}$  at a fixed temperature  $T$ . But actually the formula for  $\rho$  will not be valid at all points over which the integration is carried out. It will, however, be least accurate in those

regions where  $\rho$  is small, so that if the function  $e^{\frac{b}{r+b} \cdot \frac{\psi}{RT}}$  decreases sufficiently rapidly to zero the contribution to the integral from regions where  $\rho$  is small will itself be small, and the error introduced by using the approximate formula for  $\rho$  will also be small. Hence the result of carrying out the integration with the approximate formula for  $\rho$  may be regarded as giving a first approximation to the correct answer for quite a wide range of possible forms of the function  $\psi$ , so that the relation

$$\zeta = \text{constant} \cdot p^{\frac{r}{r+b}}$$

may be regarded as being to a large extent independent of the field of force operating.

This conclusion has been tested for the field of force created by the potential function

$$\psi = -P + Qr^3$$

a special case chosen because it admits of exact solution from beginning to end, when  $a = b = 1$ , and  $r = s = 2$ . Agreement between the exact formula so secured and the one obtained by the approximate method is in fact found to hold over a limited range of values of  $p$ , though this range is not nearly so large as when the function  $\psi$  has the form  $-\psi_0$ .

## (ii) The Energy of Dyeing.

It has been shown above that the extent to which the dye absorption varies with temperature is not consistent with the assumption  $\psi = -\psi_0$ . Nevertheless, for the sake of determining the order of magnitude of the effective value of  $e^{-\psi/RT}$  in practice it seems legitimate to make the assumption  $\psi = -\psi_0$  and to apply the resulting formula to a narrow range of temperatures. For a constant value of  $p$

$$\log \zeta = \frac{b}{r+b} \cdot \frac{\psi_0}{RT} + \text{constant} \quad . \quad . \quad . \quad (22)$$

Differentiating with respect to  $T$ ,

$$\frac{1}{\zeta} \cdot \frac{\partial \zeta}{\partial T} = -\frac{b}{r+b} \cdot \frac{\psi_0}{RT} \cdot \frac{1}{T}.$$

From actual data for Chrysophenine for a temperature of  $80^\circ \text{C}$ . ( $T = 353$ ), and  $p = 1$ , with  $b = 1$ , and  $r = 2$ ,

$$\psi_0/RT = 19.5.$$

The corresponding value of  $X = e^{\psi_0/RT}$  is of the order  $3.10^8$ . If, however, the value of  $b/(r+b)$  corresponding to the experimental value of  $r/(r+b)$  is used, the value of  $X$  is found to be about  $6.10^5$ . Whichever value is accepted the assumption made in the course of the development of the theory that  $X$  can be treated as a large quantity is justified.

The existence of a potential  $-\psi_0$  of negative value implies that the process of dyeing is an exothermic one. For each gram-molecule of dye absorbed a quantity of energy equal to  $\psi_0$  will be released, and this will be dissipated in the form of heat. From the figure just obtained for Chrysophenine at  $80^\circ \text{C}$ .

$$\begin{aligned} \psi_0/RT &= 19.5 \\ \psi_0 &= 19.5 \times 353 \times R \end{aligned}$$

and taking  $R = 2$  cal. the result is

$$\psi_0 \approx 14,000 \text{ calories.}$$

The liberation of this heat should produce a rise in the temperature of the dyebath, but calculation shows that the rise to be anticipated under favourable conditions is very small ( $0.01$  to  $0.1^\circ \text{C}$ ). But a serious difficulty in the way of detecting this rise in practice is that the dyeing process does not take place instantaneously, so that the liberation of heat will be spread over an awkwardly long interval of time.

From the formula

$$\log \zeta = \frac{b}{r+b} \log X - \log L + \frac{r}{r+b} \log p \quad . \quad . \quad . \quad (21)$$

and with the following values deduced from the experimental curves

$$\left. \begin{array}{l} \log_{10} X = 8.5 \\ \log_{10} \zeta = 0.5 \\ \frac{b}{r+b} = \frac{1}{3} \\ \log p = 0 \end{array} \right\} \text{ for } T = 353^\circ \text{ K.}$$

so that  $\log_{10} L$  is found to be 2.3,  
 $L$  is approximately 200.

The conclusion may therefore be drawn that the volume of the cellulose phase that is effectively under the influence of the various active centres is something like 1/200th of the total volume. This might appear to justify the earlier assumption that there is no mutual interaction between the fields of force of the various centres of activity, for if these centres are distributed randomly throughout the cellulose phase the amount of overlapping of the volumes associated with them will be negligible. Actually, however, it is fairly certain that the distribution of the centres of activity is far from random; this will be referred to again in the following section.

### (iii) The Heat of Dyeing.

In the previous section the theory has been used to calculate the heat change accompanying the absorption of one mole of dye, and it was found that such absorption should correspond to the liberation of about 14 K.cal. It is of interest to compare this value with that obtained directly from the experimental data by the use of the equation

$$\log_{10} \frac{c_1}{c_2} = \frac{Q}{4.58} \left( \frac{1}{T_2} - \frac{1}{T_1} \right)$$

where  $c_1$  and  $c_2$  are the concentrations in solution corresponding to the same amount of dye adsorbed at the temperatures  $T_1$  and  $T_2$ , and  $Q$  is the heat of dyeing.

This equation is, however, not readily applicable to the data, which include dye adsorbed with the entrained liquor as well as that adsorbed on the active centres. Where the substantivity is high, *i.e.* at high salt concentrations, practically all the dye is adsorbed, and the result obtained would be accurate, but unfortunately at high salt concentrations a plot of  $\log c_0$  against  $1/T$  does not yield a straight line, so that the above formula is inapplicable. At lower salt concentrations straight lines are obtained, but because the adsorbed dye forms a smaller proportion of the total the results will be less accurate. In spite of this the data for sodium chloride concentrations up to 4 g. per litre have been used, giving values of  $Q$  ranging from 9.3 to 15.9 K.cal., with probably greater weight to be attached to the higher values within this range. It is hoped later to obtain more accurate values by correcting for the absorbed dye, but meantime it may be noted that the range of values now obtained includes that derived in the previous section.

It is natural to enquire to what extent the magnitude of the heat of dyeing throws any light on the mechanism of the binding between dye and cellulose. Since esterification of cellulose inhibits its power of adsorbing direct dyes it may be assumed that the latter attach themselves to the hydroxyl groups. Examination of the constitutional formula of Chrysophenine shows that, apart from the ionic  $\text{SO}_3^-$  groups, about whose further combining power nothing is known, the combination is most likely to occur by the attachment of the etheric oxygen atoms of the dye to the hydroxyl groups of the cellulose, most probably by means of a hydrogen bond. The amount of energy released on the absorption of a mole of Chrysophenine—about 14 K.cal.—is much too large to be accounted for by the formation of a single hydrogen bond, but when atomic models of



cellulose and Chrysophenine are set up and one of the etheric oxygen atoms of the Chrysophenine model is laid alongside one of the hydroxyl groups of the cellulose model, then when the axes of the two models are parallel the other etheric oxygen is found to lie alongside another hydroxyl group. This suggests that two hydrogen bonds are formed per mole of Chrysophenine, and hence the energy released in the formation of one bond would be about 7 K.cal., which is a much more reasonable value for hydrogen bond formation.<sup>11</sup>

In the previous section by the application of the theory to the experimental data it was deduced that the volume of the cellulose phase that is effectively under the influence of the various active centres is only about 1/200th of the total volume. This cannot, however, be used to justify the assumption that there is no mutual interaction between the fields of force of the various centres, because according to modern views of the structure of cellulose there will be portions of the total volume—the ordered regions—that contain no active centres, the hydroxyl groups in these regions being mutually satisfied. On the other hand the use of the atomic models referred to above has shown quite plainly that once a dye molecule has been adsorbed to a hydroxyl group all the hydroxyl groups in the immediate neighbourhood are masked by the rest of the dye molecule, so that though there may be some interaction of centres there cannot be more than one dye molecule adsorbed to any such group of centres, and hence the general theory still applies in its essentials.

### 8. The Influence of Ionic Aggregation.

It is known that dyes of high affinity for cellulose generally show a pronounced tendency to form ionic aggregates, but whether the substantivity is in any way ascribable to the existence of such aggregates, or whether the two phenomena are to be regarded as due to a common cause, is hardly a settled question at present. In the theory advanced in this paper ionic aggregation has not been considered, nor is there sufficient known about the laws governing such aggregation to permit of quantitative deduction of its effects; qualitatively, the problem may be considered from two points of view.

It was shown earlier how an equilibrium distribution of dye results from the balancing of the opposing influences of field attraction and kinetic agitation. If  $n$  dye anions are grouped together sufficiently tightly to be treated as a single ionic micelle, then according to the theory of equipartition the average kinetic energy of translation of such a micelle will be exactly the same as that of a single dye anion, so that the large aggregate, in spite of its greater mass, offers no greater resistance to absorption, and no larger tendency to desorption, than a single anion. With regard to the binding between cellulose and dye there are two possible views.

If the attraction is due to general fields of force an aggregate of  $n$  anions should be attracted with a force  $n$  times as large as a single anion, and since this increased attraction is not offset by a similar increase of kinetic energy the result is an increase in the absorption of dye particles by the centres of attraction. In these circumstances the substantivity of a dye would depend on two factors—the existence of a potential  $\psi$ , and the tendency of the dye to form aggregates. For a series of dyes for which the values of  $\psi$  were similar, those dyes with the most pronounced tendency to form aggregates would show the strongest affinity to cellulose.

On the other hand this view may appear rather artificial; the treatment being based on energetics, aggregation of the dye anion is regarded as something to be accepted and allowed for, rather than something to be explained. If any explanation is sought, the most probable one would be that aggregation occurs through the medium of the residual valency

forces resident in certain groups in the dye anion, probably the same valency forces that are responsible for the attraction to cellulose. From this point of view aggregation in solution would be ascribed to the satisfaction of these residual valencies by other anions of the dye, and hence the attraction between the aggregate and cellulose would be much less than  $n$  times that of a single anion—it might, in fact, be no greater than that of single anion. There would, however, probably be an equilibrium between aggregated and single anions and dyeing might proceed through the medium of the latter. In these circumstances high substantivity would accompany aggregation rather than be a consequence of it, both being due to the existence of large residual valency forces.

In the foregoing account the question of the penetration of cellulose by large aggregates has not been considered, though it may exert an appreciable influence on the dyeing process. Even neglecting it, however, it is clear that there are serious difficulties in the way of putting any of these ideas on a quantitative basis. An aggregate of  $n$  dye anions cannot at one temperature be treated as a permanent structure with a constant internal energy, like an individual dye anion. The degree of aggregation will vary with the concentrations of dye and electrolyte, so that the energy of formation of such aggregates will have to be taken into consideration, but unfortunately no information is available about this quantity.

The theory put forward in this paper has been found to be fairly well applicable to Chrysophenine, which is not appreciably aggregated in solution.<sup>2</sup> Its applicability to a dye that is considerably aggregated in solution is at present being tested, and it is possible that the extent to which it is found applicable or inapplicable may indicate the directions in which modification is required. In the meantime it may be noted that the existence of ionic micelles must cause appreciable deviations from the laws of ideal electrolytes, and hence that the approximation, permissible with Chrysophenine, of using concentrations instead of activities, will probably prove inadmissible for a highly aggregated dye.

*British Cotton Industry Research Association,  
Shirley Institute, Didsbury, Manchester.*

#### REFERENCES.

- <sup>1</sup> Standing, Part I of this series.
- <sup>2</sup> Holmes and Standing, Parts III and IV of this series.
- <sup>3</sup> Robinson and Mills, *Proc. Roy. Soc. A*, 1931, **131**, 576.
- <sup>4</sup> Stearns, *J. Opt. Soc. Amer.*, 1943, **32**, 282.
- <sup>5</sup> Hanson, Neale and Stringfellow, *Trans. Faraday Soc.*, 1935, **31**, 1718.
- <sup>6</sup> Boulton, Delph, Fothergill and Morton, *J. Text. Inst.*, 1933, **24**, 113.
- <sup>7</sup> Neale and Stringfellow, *Trans. Faraday Soc.*, 1933, **29**, 1167.
- <sup>8</sup> Jeans, *The Dynamical Theory of Gases*, Cambridge University Press, 1921, p. 284.
- <sup>9</sup> Garvie, Griffiths and Neale, *Trans. Faraday Soc.*, 1934, **30**, 271.
- <sup>10</sup> Hanson and Neale, *ibid.*, 1934, **30**, 386.
- <sup>11</sup> Pauling, *The Nature of the Chemical Bond*, Cornell University Press, 1939, p. 313.

# THE DYEING OF CELLULOSE WITH DIRECT DYES. PART III.—THE AQUEOUS DIFFUSION OF DIRECT DYES.

BY FRANK H. HOLMES AND H. ALAN STANDING.

Received 26th September, 1944.

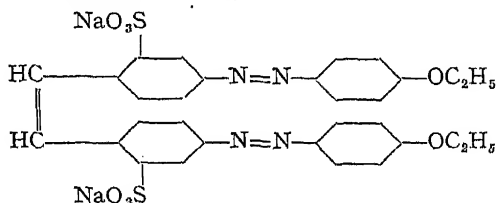
## 1. Introduction and Summary.

It is well known that most direct dyes are colloidal electrolytes, their aqueous solutions containing anionic micelles whose size is generally increased by the addition of inorganic electrolytes. In any study of the mechanism of the dyeing process a knowledge of the mean particle size of these micelles is therefore of some importance, and this question has been investigated by several workers. The measurement of the aqueous diffusion coefficient of a dye is at present probably the most fruitful method of determining the radius of such micelles in solution, and is moreover of direct interest in relation to the rate of diffusion of the dye in cellulose.

The whole question of diffusion in solution, with particular reference to the estimation of particle size, is discussed elsewhere<sup>1</sup> in some detail, and it may here be mentioned that Hartley and Robinson<sup>2</sup> have shown the importance of the influence of electrical forces on the diffusion of dyes and other colloidal electrolytes. On account of the electrical forces, data on the diffusion (into water) of commercial dyes containing unknown amounts of other electrolytes can yield no information about the radius of the ionic micelles. Measurements of the diffusion of pure dyes in water are of interest and have a significance to be discussed later; but when a dye diffuses in the presence of a uniform and sufficiently high concentration of another electrolyte the observed diffusion coefficient of the ionic micelle is directly proportional to its absolute mobility. Here the Stokes-Einstein equation may be applied<sup>3</sup> to give the radius of the diffusing micelle. Hartley and Robinson freed their dyes from other electrolytes by the method of Robinson and Mills<sup>4</sup> and recorded the first trustworthy diffusion results on dyes. Fuller data on the diffusion of pure dyes in water and in known uniform concentrations of other electrolytes are given, and particle sizes are calculated, in subsequent papers by Robinson,<sup>4, 5</sup> by Valkó,<sup>6, 7</sup> and by Lenher and Smith.<sup>8</sup> The dyes studied include Chlorazol Fast Red K, Congo Red, Bordeaux Extra, Benzopurpurine 4B, "meta"-Benzopurpurine, and Chlorazol Sky Blue FF. Little is known at present about whether the micelles are of uniform size in solution or are multidisperse<sup>9, 10</sup> in dynamic equilibrium; if the latter, then of course the calculated values of the micellar size will be mean values representing particles intermediate between the smallest and the largest present in the solution.

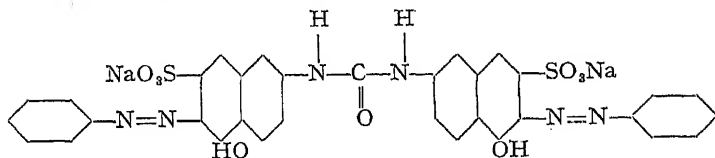
The object of the work described in the present paper was to investigate the aqueous diffusion of two dyes,

*Chrysophenine G* (Colour Index 365).



Molecular weight of dye anion, 634.

and *Direct Fast Orange SE* (Colour Index 326; and Schedler <sup>11</sup>).



Molecular weight of dye anion, 710.

The dyes were purified by the method of Robinson and Mills <sup>3</sup> as previously described for Chrysophenine in Part II of this series.<sup>12</sup> No record has been found in the literature of previous work on the aqueous diffusion of these dyes, but Whittaker and Wilcock <sup>13</sup> give their "times of half-dyeing" as 0.26 minute for Chrysophenine and 40.8 minutes for *Direct Fast Orange SE*; with respect to their rate of dyeing on viscose rayon they therefore exhibit markedly contrasting behaviour.

The diffusion coefficients of these dyes were determined at various temperatures and electrolyte concentrations, and were used to find the degree of aggregation of the dye anions. The results obtained indicate that in the presence of excess electrolyte Chrysophenine is only slightly aggregated, whilst *Direct Fast Orange* is appreciably aggregated. It is also shown that equivalent concentrations of different electrolytes with univalent cations have approximately the same effect on the diffusion, but that a salt with a bivalent cation has a more pronounced effect. The "mobilities" of the dye anions calculated from the diffusion coefficients obtained in the presence of another electrolyte are always greater than those obtained from conductivity measurements made on solutions of the pure dye. This discrepancy may be due to the inclusion of sodium ions in the anionic micelle, to an increased degree of aggregation in the presence of the electrolyte, or to both these causes. At least for *Direct Fast Orange SE* at 25° C. it would appear that the effect is due mainly to increased aggregation.

## 2. Experimental Methods.

### (a) The Diffusion Experiment.

The principle of all methods of determining the diffusion coefficient of a dissolved substance is that two uniform solutions of different known concentrations are brought into contact, usually with a plane horizontal interface, in a cell of known dimensions, diffusion is allowed to occur, and the resulting changes in concentration are observed at noted times. The porous plate method devised by Northrop and Anson <sup>14</sup> was used in this investigation; it has the characteristic feature that the two solutions are separated by a horizontal disc of sintered glass (the porous plate), which allows diffusion but prevents convection between the solutions. In each separate solution, however, convection occurs freely, and since the denser solution is uppermost gravitation is normally considered to promote mixing adequate to keep each solution homogeneous during the loss or gain of solute by diffusion. A concentration gradient therefore exists only in the liquid within the porous plate, and this simplifies the mathematical theory of the method. Conditions in the diffusing system approximate to a steady state, which greatly assists the interpretation of the results.<sup>15</sup>

The porous plate method has the additional virtues of experimental simplicity and great adaptability, being suitable over a wide range of diffusion coefficients; it is, moreover, the only convenient method for use at elevated temperatures.<sup>7</sup> Other advantages of some importance for work on dye solutions are:—

(i) The rate of diffusion of the dye anion in the presence of a uniform high concentration of a foreign electrolyte can be measured. In the well-known method of Fürth<sup>16</sup> such observations are sometimes vitiated by streaming.<sup>4, 8</sup>

(ii) The concentrations of the dye solutions can be determined at leisure, after the diffusion experiment has been completed.

The apparatus used is illustrated in Figs. 1 and 2. The plate A (Fig. 1) is made of sintered glass, and the tortuous channels through its thickness are generally of diameter between 5 and 15  $\mu$ , which manifoldly exceeds that of a dye micelle. The plate is about 3 cm. in diameter and about 0.2 cm. thick, and is fused into the end of a resistance-glass tube B, whose other end is sealed to a narrow tube C closed by a tap D, forming a cell of volume about 25 c.c. This cell normally contains the dye solution under investigation, and is held, by means of a tinfoil-covered rubber stopper, in an outer glass tube E so that the plate dips just below the surface of about 20 c.c. of solvent.

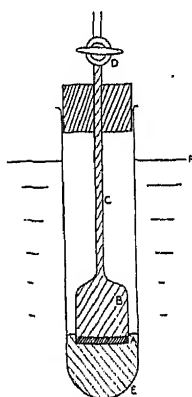


FIG. 1.

At the beginning of an experiment this assembly is immersed to the level F in a thermostat; thermal expansion forces some dye solution through the plate, and soon after thermal equilibrium is attained a continuous and almost steady distribution of concentration is established through the thickness of the plate. At this stage the cell is transferred to another similar tube that has been in the thermostat for some time, so that the plate is brought into contact with a fresh portion of solvent already at the experimental temperature. Transfer of dye through the plate now occurs by diffusion alone, and after a noted period of about 16 hours the solution below the plate is diluted to a suitable known volume and estimated spectrophotometrically in order to find how much dye has diffused. From these data and the constants of the apparatus the diffusion coefficient of the dye anion is calculated.

Owing to lack of knowledge of the *effective* dimensions of the porous plate the method is essentially one of comparison, not absolute determination, of diffusion coefficients; each plate is therefore calibrated by means of an experiment with a solute of known diffusion coefficient, yielding a calibration constant which embodies the unknown effective dimensions of the plate. Aqueous solutions of potassium chloride are probably the most reliable standards for calibration; the mean diffusion coefficient of potassium chloride over the concentration range from  $N/2$  to zero at 25° C. was taken, by interpolation from the data of Clack,<sup>17</sup> to be  $17.7 \times 10^{-6}$  cm.<sup>2</sup> per sec., and calibration experiments were made under these conditions. With potassium chloride the experimental results were reproducible to about 1%; with dye solutions the accuracy was variable but always lower. For the three diffusion cells used in the earlier part of this work, the calibration constants (in cm.<sup>-1</sup>) were:—

Cell 1 . 0.190; Cell 2 . 0.0702; Cell 3 . 0.0666.

The simple form of apparatus described above was used in much of the work at 25° and 40° C., but at 60° C. appreciable amounts of water evaporated from the external solution and condensed on the cooler upper parts of the vessel. (For convenience, the solutions above and below the plate are referred to as the internal and external solutions, respectively.) The resulting increase in the concentration of the dilute external solution does not, however, appreciably alter the concentration gradient of the dye, and hence does not affect its rate of diffusion; moreover, the evaporation does not affect the accuracy of the determination of the amount of dye diffusing in a given time, because the external solution is diluted to

a known volume before its concentration is determined. The evaporation has therefore no appreciable effect on the accuracy of a determination of the diffusion coefficient of a dye made in the absence of foreign electrolyte. If, however, such an electrolyte is present at an initially uniform concentration, the evaporation of water from the external solution alone creates a concentration gradient of the additional electrolyte which causes it to diffuse in the opposite direction to the dye, and it will be shown later that this may cause an appreciable alteration of the diffusion coefficient of the dye itself.

In order to minimise the evaporation that occurs at high temperatures the apparatus was rebuilt (Fig. 2) as a modification of that of Valkó;<sup>6</sup> a glass lid was fused to the cell and fitted by a ground-glass joint to the vessel containing about 45 c.c. of external solution. This closed apparatus could be submerged in the thermostat up to the tap, so improving the temperature control and preventing the condensation of water vapour in the upper parts of the vessel. The lid was also provided with a vertical outlet tube with glass stopper, enabling portions of the external solution to be withdrawn for estimation without stopping the experiment. After replacement of such a portion by an equal volume of solvent, diffusion was observed for another period, and in this way several determinations of the diffusion coefficient could be obtained from each experiment without any serious disturbance of the diffusing system.

For the attainment of thermal equilibrium and almost steady diffusion in this improved apparatus at least three hours were allowed to elapse between immersion in the thermostat and the beginning of the first period of diffusion. Each experiment then comprised three or four consecutive diffusion periods, usually of about 24 hours each. The essential requirement governing the duration of a diffusion period is that the increase in the external concentration should be sufficient for accurate estimation. Thus where the rate of diffusion proved low (at the lowest dye concentrations investigated) a diffusion period extended over several days. With high rates of diffusion, alternate 6-hour and 18-hour periods were convenient.

The relative change in the internal dye concentration during a diffusion period is not the same for experiments with different apparatus and diffusion coefficients. A typical example, however, is that in a cell of calibration constant  $0.07 \text{ cm.}^{-1}$  containing a dye of diffusion coefficient  $7 \times 10^{-6} \text{ cm.}^2 \text{ per sec.}$ , the internal concentration decreases by about 5 % during a 24-hour diffusion period when the external concentration is initially zero. If the external volume is about twice the internal volume, the external concentration increases correspondingly by about one-fortieth of the initial internal concentration.

It was observed in the series of experiments conducted at  $90^\circ \text{C.}$ , but not in those at  $60^\circ \text{C.}$  and lower temperatures, that the calibration constants of both diffusion cells used often showed an increase of about 4 % after an experiment lasting several days. Subsequent experiments at  $90^\circ \text{C.}$  caused a further increase. The practice was therefore adopted of recalibrating each diffusion cell after every experiment at  $90^\circ \text{C.}$ , and the calibration value corresponding to an experiment at  $90^\circ \text{C.}$  is taken as the value found immediately afterwards by recalibration at  $25^\circ \text{C.}$  As a result of six experiments at  $90^\circ \text{C.}$  the calibration constants of two diffusion cells increased through the following ranges of values (in  $\text{cm.}^{-1}$ ):—

Cell 2 (in rebuilt form) . . . . .	0.0732-0.0882
Cell 3 (in rebuilt form) . . . . .	0.0702-0.0941

The cause of this increase in the calibration constant (which is proportional to the ratio of the effective free cross-sectional area to the effective thickness of the porous plate) is not known with certainty, but is evidently connected with the use of elevated temperatures.

**(b) The Materials Used.**

The two dyes used in this work were obtained in batch form from their makers, and were purified by the method described by Robinson and Mills.<sup>3</sup> The application of this method to Chrysophenine has already been described,<sup>12</sup> and the method used for Direct Fast Orange SE was identical except that, for reasons given below, the temperature was not allowed to rise above 60° C. at any stage of the purification. The various tests for purity enumerated in a previous paper<sup>12</sup> indicated the absence of any other coloured material from the purified samples of the two dyes used in this work.

In working with Direct Fast Orange SE it soon became evident that the dye changes colour at high temperatures. The absorption spectrum

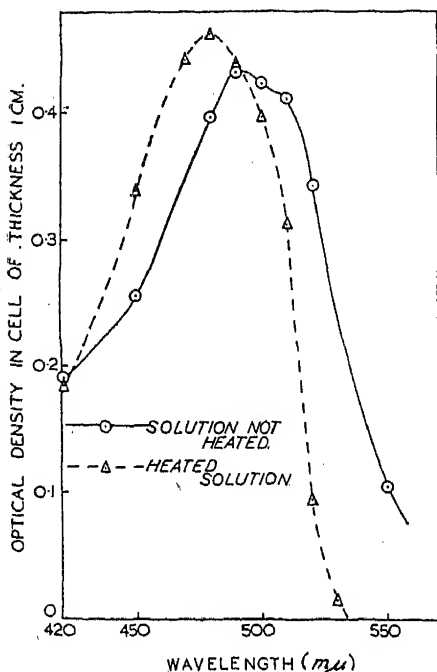


FIG. 3.—Effect of heat on Direct Fast Orange SE (C.A.C. sample).

of a solution of this dye (of concentration 0.005 g. per litre) containing no other electrolyte was measured before and after heating at 85° C. for four days. The spectra are shown in Fig. 3, from which it is evident that the heat-treatment has caused a shift of the absorption maximum towards lower wavelengths; after this treatment the dye was found to have only a slight substantivity for cellulose. A similar change in colour is also evident after heating for a short time at temperatures above 60° C., but here the change appears to be reversible, and no permanent effect has been noticed after prolonged heating at 60° C. Because of the instability of this sample of Direct Fast Orange SE no work has been done with it at temperatures above 60° C.

The other electrolytes used were of "A.R." quality.

**(c) Estimation of the Dye Solutions.**

The concentrations of all the dye solutions were determined by means of a photoelectric spectrophotometer; a detailed description of the method used for solutions of Chrysophenine has already been given.<sup>12</sup>

Aqueous solutions of Direct Fast Orange SE when free from inorganic electrolytes have an absorption spectrum similar to that shown by Curve A of Fig. 4. For such solutions Beer's Law is valid at most wavelengths near the peak of the absorption spectrum for a range of concentrations up to 10 mg. per litre. The estimation of such solutions is therefore straightforward—the solutions to be estimated are diluted to a concentration in the neighbourhood of 5 mg. per litre and the optical density of the diluted solution contained in a parallel-sided glass cell of thickness 1 cm. is measured by means of the photoelectric spectrophotometer previously referred to. Standard solutions of concentration 2.5, 5 and 10

mg. per litre are examined at the same wavelength, and the concentrations of the unknown solutions are calculated by interpolation.

It is, however, frequently necessary to estimate dye solutions containing known concentrations of an inorganic electrolyte, and the choice of the wavelength at which the optical densities are measured is then critical, for the absorption spectrum of an aqueous solution of the pure dye is different from that of the dye in the presence of inorganic electrolytes. The absorption spectra, shown in Fig. 4, of a solution of Direct Fast Orange SE, of concentration 5 mg. per litre, in the presence of different concentrations of sodium carbonate are characteristic. The effect of the sodium carbonate is to raise the peak of the spectrum, so that at most wavelengths the optical density of the solution depends on the concentration of sodium carbonate as well as on that of the dye. The three spectra, however, pass through a common point at a wavelength of  $527\text{m}\mu$ , and hence at this wavelength the optical density of the solution is directly proportional to the concentration of the dye present, and is independent of the concentration of sodium carbonate. At this wavelength the estimation is therefore again straightforward, and is identical with that for dye solutions containing no additional electrolyte. The phenomena described above were observed with all the electrolytes examined, but the appropriate wavelength for making the measurement varies slightly with the electrolyte present, being  $528\text{m}\mu$  for sodium sulphate and  $530\text{m}\mu$  for sodium chloride.

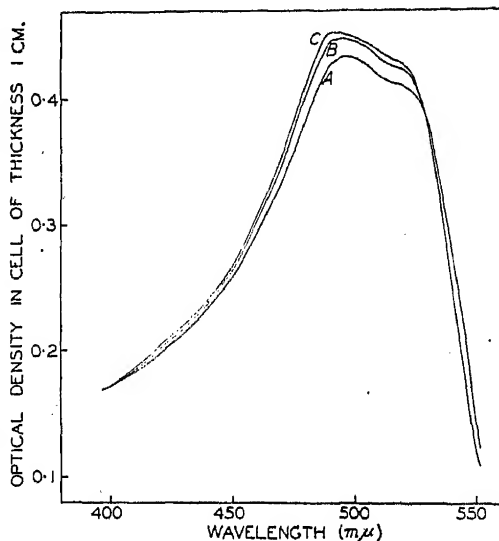


FIG. 4.—Absorption spectra of Direct Fast Orange.

A—5 mg./litre dye ; No  $\text{Na}_2\text{CO}_3$   
 B—5 mg./litre dye ;  $0.0453\text{ g./litre Na}_2\text{CO}_3$   
 C—5 mg./litre dye. ;  $0.906\text{ g./litre Na}_2\text{CO}_3$

#### (d) Calculation of the Diffusion Coefficient from the Experimental Observations.

When the simple technique was used the diffusion coefficient was calculated from the experimental observations by means of the logarithmic expression of Mehl and Schmidt,<sup>13</sup> which is equivalent to that derived by Northrop and Anson<sup>14</sup> in their paper introducing the method; it is

$$D\alpha = \frac{2\lambda}{(\lambda + 1)\tau} \log_{10} \frac{c''}{c'' - (\lambda + 1)c'} \quad (1)$$

where  $D$  is the diffusion coefficient,  $\alpha$  is the calibration constant of the diffusion cell,  $\lambda$  is the ratio  $\frac{\text{volume of external solution}}{\text{volume of internal solution}}$ ,  $\tau$  is the duration of the observed diffusion,  $c''$  is the dye concentration in the internal solution at the start of the observed diffusion (when the external concentration is zero), and  $c'$  is the external dye concentration after a length of



time  $\tau$ . This expression takes account of the gradual decrease in the concentration difference across the plate during the period of diffusion.

When the second form of apparatus was used, with the procedure of removing portions of the external solution and replacing them with solvent, allowance was made as follows for the resulting small abrupt increases in the concentration difference across the plate:—

Let  $L$  be the effective thickness of the porous plate, and  $A$  its effective free cross-sectional area for diffusion. On assembly of the apparatus, let the dye concentration in the internal solution be denoted by  $c$ , while that in the external solution is 0. At this stage the apparatus is placed in the thermostat to attain the experimental temperature and to allow the establishment of steady conditions. Let steady conditions obtain at time  $t_0$ , and let a fraction  $m_0$  of the dye in the external solution be withdrawn at  $t_0$ . (The decrease of volume is made good by the addition of an equal volume of solvent. From the point of view of the calculation it is immaterial whether the portion of solution is withdrawn before or after the addition of the solvent, but in order that the plate may be kept immersed throughout it is preferable to add the solvent first, mix thoroughly, and then withdraw the same volume of solution.)

Just before  $t_0$ , let the external concentration be  $C_0$ ; then the internal concentration  $= c - \lambda C_0$ . Just after  $t_0$ , the external concentration will be  $C_0(1 - m_0)$ , and hence the concentration difference across the plate will be  $c + m_0 C_0 - (\lambda + 1)C_0$ .

Diffusion now occurs without disturbance until time  $t_1$ , when a fraction  $m_1$  of the dye in the external solution is removed.

Just before  $t_1$ , let the external concentration be  $C_1$ .

At time  $t$  (between  $t_0$  and  $t_1$ ) let the external concentration be  $C$ .

Then the increase in the external concentration since just after  $t_0 = C - C_0(1 - m_0)$ .

$\therefore$  The concentration difference across the plate at time  $t$

$$= [c + m_0 C_0 - (\lambda + 1)C_0] - (\lambda + 1)[C - C_0(1 - m_0)]$$

$$= c - \lambda m_0 C_0 - (\lambda + 1)C.$$

Hence, from Fick's Law, at the time  $t$  the rate of transfer of dye

$$= DA \frac{[c - \lambda m_0 C_0 - (\lambda + 1)C]}{L}$$

where  $D$  is the effective mean diffusion coefficient over the range of concentration obtaining in the plate. But, since all the diffusing dye enters the external solution, the rate of transfer of dye  $= \lambda v \partial C / \partial t$ , where  $v$  is the volume of the internal solution.

$$\therefore \frac{dC}{c - \lambda m_0 C_0 - (\lambda + 1)C} = \frac{DA}{\lambda v L} dt.$$

Summing over the period of time between the observations of the external concentration,

$$\int_{c_0(1-m_0)}^{c_1} \frac{dC}{c - \lambda m_0 C_0 - (\lambda + 1)C} = \frac{A}{\lambda v L} \int_{t_0}^{t_1} D dt$$

$$\therefore \frac{1}{\lambda + 1} \ln \frac{c + m_0 C_0 - (\lambda + 1)C_0}{c - \lambda m_0 C_0 - (\lambda + 1)C_1} = \frac{\bar{D}A(t_1 - t_0)}{\lambda v L}$$

where  $\bar{D}$  is the effective mean diffusion coefficient (over the concentration range obtaining in the plate) during the period from  $t_0$  to  $t_1$ . Rearranged, and transformed so as to apply to logarithms to base 10, the equation becomes

$$\bar{D}\alpha = \frac{2\lambda}{(\lambda + 1)(t_1 - t_0)} \log_{10} \frac{c + m_0 C_0 - (\lambda + 1)C_0}{c - \lambda m_0 C_0 - (\lambda + 1)C_1} \quad (2)$$

where  $\alpha$ , the calibration constant,  $= \frac{2A}{vL} \log_{10} e$ .

By putting  $m_0 = 1$  and  $C_0 = 0$  (the conditions applying to the simple technique) the equation reduces to that already given (equation (1)) for the simpler method.

Reasoning similar to that given above shows that for the period from  $t_1$  to  $t_2$ ,

$$\overline{D}\alpha = \frac{2\lambda}{(\lambda + 1)(t_2 - t_1)} \log_{10} \frac{c - \lambda m_0 C_0 + m_1 C_1 - (\lambda + 1)C_2}{c - \lambda(m_0 C_0 + m_1 C_1) - (\lambda + 1)C_2} \quad (3)$$

and for the general case of the period from  $t_{n-1}$  to  $t_n$

$$\overline{D}\alpha = \frac{2\lambda}{(\lambda + 1)(t_n - t_{n-1})} \log_{10} \frac{c - \lambda \sum_{i=0}^{i=n-2} m_i C_i + m_{n-1} C_{n-1} - (\lambda + 1)C_{n-1}}{c - \lambda \sum_{i=0}^{i=n-1} m_i C_i - (\lambda + 1)C_n} \quad (4)$$

where  $m_i$  is the fraction of dye in the external solution removed at time  $t_i$ , and  $C_i$  is the external concentration just before  $t_i$ .

In each equation the numerator and denominator of the concentration ratio are respectively the concentration differences across the plate at the beginning and the end of the diffusion period. It is important to notice that the diffusion coefficient  $\overline{D}$  found from any of these equations is an integral value over a finite time for a concentration range changing slightly in that time. Although often referred to as the "diffusion coefficient," this quantity is more strictly termed the "mean diffusivity." It has been shown by Gordon<sup>19</sup> that the mean diffusivity over a fixed concentration range  $C_A$  to  $C_B$  is approximately equal to the true diffusion coefficient corresponding to the single concentration  $(C_A + C_B)/2$ .

### 3. Experimental Results and Discussion.

For each dye the mean diffusivity of the anion was measured in solutions free from and containing foreign electrolyte, and the influences of temperature and of concentration of dye and of electrolyte were studied. The three diffusion cells used in the work were originally of the simple type shown in Fig. 1, and as such are referred to as cells 1, 2 and 3, but for experiments at high temperatures cells 2 and 3, which had finer porous plates than cell 1, were built into the all-glass apparatus depicted in Fig. 2; these rebuilt cells are referred to as cells 2c and 3c. The identity of the cell used to obtain any given result is indicated in the tables that follow either by allocating a separate column to each cell or by giving the number of the cell in brackets immediately after the result. The dye concentrations given are the initial internal values; the external solutions consisted initially of dye-free solvent, so that the initial concentration gradient was of the dye ions alone.

When the simple cells were used each of the more important solutions was investigated by means of two or three experiments involving different porous plates, and the mean result was accepted as the mean diffusivity under the conditions obtaining. The agreement among the several values found for a given solution by the use of different cells and the degree of reproducibility of the results obtainable from any one cell varied considerably with the experimental conditions; no general figure for the mean deviation can be given, and the individual results are therefore given in addition to the mean values. With the all-glass cells used at high temperatures each experiment yielded several values, and with some solutions two or three experiments were performed. It was in general found that the agreement among the results was better when a foreign electrolyte was present than when the pure dye was studied.

$$D = RTB \quad . \quad . \quad . \quad . \quad . \quad (5)$$
$$D = \frac{RT}{6\pi N\eta\gamma} \quad (6)$$
$$D = \frac{RT}{F^2} 10^{-7} \left( \frac{1}{n_+} + \frac{1}{n_-} \right) \frac{uv}{u+v} \quad (7)$$

where  $F$  is the Faraday (in coulombs),  $u$  and  $v$  are the equivalent conductances and  $n_+$  and  $n_-$  the corresponding valencies of the cation and anion respectively. For most direct dyes the ratio of the equivalent conductance to the valency is greater for the cation than for the anion, and consequently the diffusion coefficient of the pure dye is greater than that of the dye anion, which depends only on the ratio  $v/n_-$ . Since the diffusion coefficient of the pure dye depends on the conductances of both the cation

and the anion the Stokes-Einstein equation is not applicable, and the diffusion coefficient alone can give no information about the size of the diffusing anion. If the appropriate values of the conductances  $u$  and  $v$  are known the charge  $n_-$  on the dye anion can be calculated, and hence

TABLES I AND II.—MEAN DIFFUSIVITIES IN SOLUTIONS FREE FROM FOREIGN ELECTROLYTE.

Temperature (°C.).	Dye concentration (g. per litre).	Mean diffusivity (cm. <sup>2</sup> /sec.) × 10 <sup>6</sup> .					
		Cell 1.	Cell 2.	Cell 3.	Cell 2c.	Cell 3c.	Mean.
1. Chrysophenine							
25	0.1	6.2	—	—	—	—	6.2
	0.2	6.3, 6.3	6.6	6.5	—	—	6.4
	0.5	6.6, 6.6	6.3, 7.0	6.9, 7.0	—	—	6.7
	1.0	6.6, 6.6	6.8	6.9	—	—	6.7
	2.0	6.8, 6.5, 6.4	—	—	—	—	6.6
40	0.2	9.8	9.6	9.7	—	—	9.7
	0.5	9.8	10.2, 10.3	10.1, 10.4	—	—	10.2
	0.8	9.4	10.2	10.9	—	—	10.2
	1.0	9.8	10.4, 10.7, 10.1	10.6	—	—	10.3
	2.0	9.2	9.5	9.8	—	—	9.5
60	0.5	—	—	—	—	15.1, 15.5, 14.8	15.1
	1.0	14.6, 14.5	14.9, 15.4	14.9	—	—	14.9
90	1.0	—	—	—	21.6, 22.8, 22.6	21.4, 22.6, 22.5, 21.8	22.2
2. Direct Fast Orange SE							
25	0.2	6.7, 6.7, 6.9	7.3	7.4	—	—	7.1
	0.25	7.6	—	—	—	—	—
	0.5	6.8, 7.1, 6.7	8.0	7.9	—	—	7.3
	1.0	6.6, 7.2	8.0	7.6	—	—	7.4
	2.0	6.5	6.7	7.5	—	—	6.9
	4.0	7.1	—	—	—	—	7.1
40	1.0	—	—	—	10.2, 9.6, 9.5	9.1, 9.3, 9.4, 9.8	9.6
60	0.2	13.7, 14.2, 14.5	13.7	14.0	—	—	14.0
	0.5	14.3, 14.0	13.9	13.7	—	14.1, 14.1, 13.4, 14.2	14.0
	1.0	14.1, 13.6	13.7	14.0	—	—	13.9

some information obtained about its degree of aggregation. Nevertheless the diffusion coefficient of the pure dye is relatively insensitive <sup>8</sup> to changes in the value of  $n_-$ , particularly when  $n_-$  is large. The form of the Nernst-Haskell equation is correspondingly such that small errors in the substituted values of the ionic conductances and the diffusion coefficient

introduce relatively large errors in the calculated value of  $\mu_{\infty}$  and hence this method is not very helpful either.

The data given in Tables I and II cannot therefore be used to assess the degree of aggregation of the dye anions. They are, however, useful in that they provide a check on the freedom from foreign electrolytes of the dyes used. By using the Nernst-Haskell equation Hartley and Robinson<sup>2</sup> have shown that in the absence of foreign electrolyte a dye that has a high conductivity must also have a high diffusion coefficient; the latter must in fact exceed a minimum theoretical value given (where sodium ion is the cation) by the equation

$$D = \frac{RT}{F^2} 10^{-7} \frac{\mu(A - \mu)}{A} \quad (8)$$

where  $\mu$  is the equivalent conductance of sodium ion,  $A$  is the equivalent conductance of the dye, and the other symbols have the same significance as before.

This minimum affords a valuable check of the purity of the dye. The presence of electrolytic impurity increases the value of  $A$  and hence increases the apparent minimum theoretical diffusion coefficient; on the other hand it can be shown by use of the general equations quoted by Vinograd and McBain<sup>21</sup> for the diffusion of ions in mixed electrolytes that the actual diffusion coefficient of the dye anion is decreased when any of the common electrolytes (sodium chloride, sulphate, or carbonate) diffuses with it into pure water. Since these effects are in opposite directions the presence of even a small amount of foreign electrolyte may lower the diffusion coefficient to a value below the calculated minimum, and the amount of electrolytic impurity that may remain undetected is in fact strictly limited.

In order to find the minimum theoretical diffusion coefficients for solutions of Chrysophenine G and Direct Fast Orange SE the equivalent conductances at infinite dilution were found by extrapolation from the conductivity data given in the succeeding paper of this series,<sup>22</sup> and were substituted in equation (8) together with corresponding values for the sodium ion. In Table III the calculated minima are compared with the observed mean values, and it will be seen that for all solutions examined the observed value exceeds the theoretical minimum.

TABLE III.—COMPARISON OF CALCULATED MINIMUM AND OBSERVED VALUES OF THE DIFFUSION COEFFICIENT.

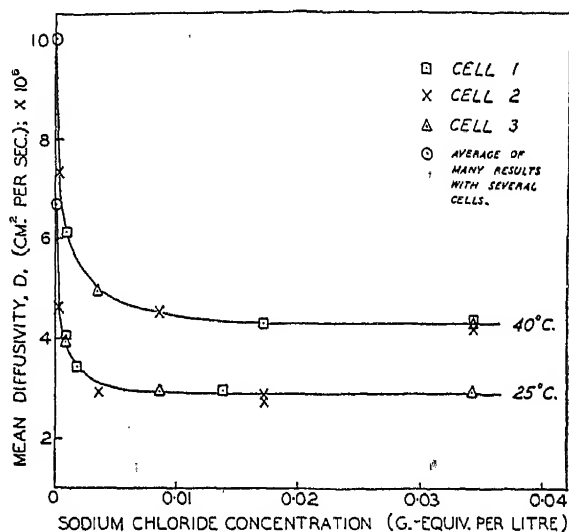
Dye.	Temperature (°C.)	$\mu$ .	$A$ .	Calculated minimum $D$ .	Mean observed $D$ .
Chrysophenine	25	50.1	87.4	$5.68 \times 10^{-6}$	$6.6 \times 10^{-6}$
	40	70	117	$7.85 \times 10^{-6}$	$10.0 \times 10^{-6}$
	60	95.5	157.5	$11.2 \times 10^{-6}$	$15.0 \times 10^{-6}$
	90	138.5	222	$16.9 \times 10^{-6}$	$22.2 \times 10^{-6}$
Direct Fast Orange SE	25	50.1	97.5	$6.45 \times 10^{-6}$	$7.2 \times 10^{-6}$
	40	70	130	$9.01 \times 10^{-6}$	$9.6 \times 10^{-6}$
	60	95.5	173	$12.7 \times 10^{-6}$	$14.0 \times 10^{-6}$

(b) The Diffusion of Chrysophenine in a Uniform Concentration of Sodium Chloride.

It has been noted above that the necessity of preserving electro-neutrality compels the ions of a diffusing electrolyte to move at the same rate, the ion with the lower absolute mobility being speeded up and that with the higher absolute mobility being slowed down by the potential

gradient between the ions of opposite charge. If, however, the ions are diffusing in a uniform concentration of another electrolyte this potential gradient is reduced and each ion tends to move at a rate depending on its own absolute mobility, *i.e.* at a rate controlled mainly by its size and shape. In an anionic dye of type  $\text{Na}_2\text{R}$ , the anion is much larger than the cation and hence has a lower absolute mobility; a decrease in the observed diffusion coefficient of the ion may therefore be expected to result from the uniform addition of a foreign electrolyte to the pure dye solution. This effect is evident from Table IV, and the very rapid decrease of the diffusion coefficient on the first small addition of electrolyte is shown by the curves of Fig. 5, where the data for a dye concentration of 0.5 g. per litre are plotted. This figure also shows that when the concentration of sodium chloride exceeds a certain value, the diffusion coefficient of the dye becomes independent of that concentration, suggesting that there is sufficient electrolyte present to eliminate the potential gradient normally established when an electrolyte diffuses. Similar results were obtained at the other

FIG. 5.  
Chrysophenine G,  
0.5 g. per litre.



two dye concentrations studied, and although there is some scatter of the experimental points the limiting diffusion coefficients obtained as means of the values at relatively high sodium chloride concentrations appear to be reliable.

At high sodium chloride concentrations the diffusion coefficient of Chrysophenine anion is practically independent of both dye and salt concentrations, and Fick's Law is applicable. It is clear from Table IV that in the intermediate domain where the potential gradient, though less than in the diffusion of the pure dye, still exists there are appreciable deviations from Fick's Law, the diffusion coefficient at a fixed sodium chloride concentration varying with the dye concentration.

The results presented in Table IV at 60° and 90° C., where the reproducibility of readings in an experiment is not always satisfactory, require further comment. The solutions containing salt concentrations 5.0, 10.0 and 20.0 g. per litre were examined in order to explore the domain where the salt concentration is very large compared with the dye concentration. These solutions flocculate at room temperature and were therefore prepared and constantly maintained near the experimental temperature, where they are stable. Although calculations indicate

TABLE IV.—MEAN DIFFUSIVITIES OF CHRYSOPHENINE G IN SOLUTIONS CONTAINING UNIFORM CONCENTRATIONS OF SODIUM CHLORIDE.

Temp. (°C.)	Sodium chloride concentration.		Mean diffusivity (cm. <sup>2</sup> per sec.) $\times 10^6$ at internal dye concentrations (g. per litre.)			
	(g. per litre.)	(g.-equiv. per litre.)	0.2.	0.5.	0.8.	1.0.
25	0.02	0.00034	4.19 (1)	4.63 (2)	—	5.18 (3)
	0.05	0.00086	3.48 (2), 3.45 (3)	3.96 (3), 4.05 (1)	—	4.51 (1, 2)
			Mean 3.47	Mean 4.00		Mean 4.51
	0.1	0.00171	3.20 (3)	3.46 (1)	—	3.62 (2)
	0.2	0.00342	3.15 (1)	2.94 (2)	—	3.32 (3)
	0.5	0.00855	2.78 (2)	2.94 (3)	—	3.11 (1)
	0.8	0.0137	2.94 (3)	2.96 (1)	—	2.66 (2)
	1.0	0.0171	3.05 (1), 3.00 (1)	2.87 (2), 2.74 (2)	—	2.98, 2.80 (3)
			Mean 3.03	Mean 2.81		Mean 2.89
	1.6	0.0274	—	—	—	2.90 (1)
40						2.60 (2)
						Mean 2.75
	2.0	0.0342	2.98 (2)	2.93 (3)	—	—
	0.02	0.00034	6.70, 6.67 (1)	7.34 (2)	7.91 (3)	—
			Mean 6.69			
	0.05	0.00086	5.42 (3)	6.15 (1)	6.45 (2)	—
	0.2	0.00342	4.70 (2)	4.98 (3)	5.18 (1)	—
	0.5	0.00855	4.62 (1)	4.51 (2)	4.58 (3)	—
	1.0	0.0171	4.55 (3)	4.32 (1)	4.36 (2)	—
	1.6	0.0274	—	—	4.35 (1)	—
60					4.19 (2)	
					4.29 (3)	
					Mean 4.28	
	2.0	0.0342	4.57 (1), 4.32 (2)	4.39 (1), 4.18 (2)	—	—
			4.41 (3)	4.29 (3)		
			Mean 4.43	Mean 4.29		
	1.0	0.0171	—	7.15, 6.95, 6.90 (3c);	—	—
				6.80, 6.01,		
				7.00, 6.60 (3c);		
				6.78, 7.11,		
90				7.67, 6.84 (2c)		
				Mean 6.89		
	2.0	0.0342	—	7.37, 7.16,	—	—
				7.72, 7.29 (3c);		
				6.92, 6.23,		
				6.80, 6.68 (2c)		
				Mean 7.02		
	5.0	0.0855	—	6.06, 6.28 (2c);	—	—
				6.53, 6.42, 6.14 (2c)		
				Mean 6.28		
90	10.0	0.171	6.49, 6.39 (3c);	—	—	—
			5.68, 6.09, 6.10,			
			6.56 (2c)			
			Mean 6.22			
	2.0	0.0342	—	12.1, 11.0, 12.5,	—	—
90				11.8 (2c); 11.6,		
				10.2, 13.9, 11.2,		
				10.8 (2c)		
				Mean 11.7		
	10.0	0.171	—	10.6, 11.3, 10.7 (3c)	—	—
90				10.3, 10.7, 11.3,		
				12.1 (2c)		
90				Mean 11.0		
	20.0	0.342	10.8, 8.9,	—	—	—
90			9.8 (2c); 8.8,			
			11.2, 9.6 (3c)			
90			Mean 9.85			

that in this domain the effect of the potential gradient is negligible, the observed diffusion coefficient at a fixed dye concentration decreases with increasing salt concentration at 60° and 90° C. Similarly at 90° C. the diffusion coefficient decreases with increase of the salt-dye ratio between the two highest salt concentrations studied. These results suggest that in this domain (which was not reached in the experiments at 25° and 40° C.) the degree of aggregation of the dye anion increases with increase of the salt-dye ratio. The lowest observed diffusion coefficients at 60° and 90° C. are substituted in subsequent calculations of the anionic radius and aggregation number.

When the dye diffuses in the presence of a uniform concentration of a second electrolyte the potential gradient between the diffusing cations and anions is diminished by an induced simultaneous diffusion of the ions of that electrolyte. Hartley and Robinson<sup>2</sup> have shown that under such conditions the observed diffusion coefficient of the dye anions is given by the equation

$$D = \frac{RT}{F^2} 10^{-7} \frac{v}{n_-} \left[ 1 + \frac{n_- \left( \frac{u}{n_+} - \frac{v}{n_-} \right)}{u + v + \frac{c'}{c} (u' + v')} \right] \quad (9)$$

where  $u'$  and  $v'$  are the equivalent conductances of the cation and anion of the second electrolyte,  $c'$  is the equivalent concentration of this electrolyte and  $c$  the equivalent concentration of the dye; in all the following values of  $c'/c$  for experiments conducted by the porous plate method,  $c$  is taken as the mean of the internal and external dye concentrations. The second term in the square brackets represents the contribution of the potential gradient to the diffusion coefficient. It has been mentioned above that at the lower salt concentrations the diffusion coefficient at a fixed salt concentration varies with the dye concentration, so that Fick's Law is not obeyed; this observation could be predicted from equation (9), because the second term inside the square brackets is constant not at a fixed salt concentration ( $c'$  constant) but at a fixed salt-dye ratio ( $c'/c$  constant). Actually, the data given provide some experimental confirmation of this. In Table V are given the diffusion coefficients (inter-

TABLE V.—MEAN DIFFUSIVITIES OF CHRYSOPHENINE IN SOLUTIONS CONTAINING UNIFORM CONCENTRATIONS OF SODIUM CHLORIDE.

Temperature (°C.)	Salt/Dye Ratio $c'/c$ .	Internal dye concentration (g. per litre).			
		0.2.	0.5.	0.8.	1.0.
25	0.58	—	4.5	—	4.5
	1.16	4.00	3.95	—	3.87
	2.33	3.60	3.40	—	3.32
	11.6	3.00	2.94	—	2.90
40	0.58	7.5	7.05	6.85	—
	1.16	6.6	6.00	5.90	—
	2.33	5.60	5.40	5.27	—
	11.6	4.75	4.50	4.40	—

polated where necessary) for three dye concentrations at varied concentrations of sodium chloride chosen so as to correspond to constant values of the dye-salt ratio, and although they are not quite independent of the dye concentration they are much more nearly so than the values for fixed low salt concentrations (Table IV).



However, the main point of interest arising from equation (9) is that as the salt-dye ratio  $c'/c$  increases the potential gradient diminishes, and with it the diffusion coefficient. When the salt-dye ratio is sufficiently high the effect of the potential gradient becomes negligible, and the diffusion coefficient is given by the equation

$$D = \frac{RT}{F^2} 10^{-7} \frac{\eta}{n_-} \quad (10)$$

In these circumstances the diffusion coefficient of the dye anion is directly proportional to the anionic mobility, which will in turn depend upon the shape and size of the anion and upon the interionic forces operating in the diffusion process. With regard to the latter Hartley<sup>23</sup> has pointed out that under these conditions only the relaxation term will be operating, and that even it will be considerably smaller in a diffusion process than in electrical conduction, where the anion and cation are moving in opposite directions. The interionic forces are therefore small, and as a first approximation can be neglected. Thus the observed diffusion coefficient of the dye anion in the presence of a theoretical excess of sodium chloride depends only on the shape and size of the diffusing anion, and the Stokes-Einstein equation can be applied to determine the anionic radius.

The value of the salt-dye ratio necessary to eliminate the effect of the potential gradient must vary considerably from dye to dye. The numerator of the term representing the contribution of the potential gradient to the diffusion coefficient can be shown to increase as the value of the anionic charge  $n_-$  increases. Since the anionic charge depends on the degree of aggregation it follows that a highly aggregated dye requires a higher salt-dye ratio to eliminate the effect of the potential gradient than a slightly aggregated dye. Moreover, if the degree of aggregation increases with increasing salt concentration when the dye concentration is maintained constant, the effect of the potential gradient will decrease only slowly with increasing salt concentration. It is therefore essential to consider the possible degree of aggregation of the dye when any doubt arises whether the salt-dye ratio is sufficiently high to eliminate the effect of the potential gradient.

In the interpretation of the data obtained at 25° and 40° C. for Chrysophenine there is no room for any such doubt. As the sodium chloride concentration is increased at a constant dye concentration the diffusion coefficient falls to a value that remains constant when the sodium chloride concentration is further increased. This must mean that the salt-dye ratio is sufficiently high to eliminate the potential gradient; the Stokes-Einstein equation can therefore be applied, yielding the results presented in Table VI. This table contains also the results from the highest salt-dye ratios examined at 60° and 90° C.

TABLE VI.—DIFFUSION COEFFICIENTS AND ANIONIC RADII FOR CHRYSOPHENINE IN SODIUM CHLORIDE.

Temperature (° C.)	25	40	60	90
$D$ (cm. <sup>2</sup> /sec.) $\times 10^6$	2.90	4.35	6.25	9.85
$r$ (Å.)	8.4	8.0	8.3	8.5
Aggregation number, $G$				
$\left\{ \begin{array}{l} \rho = 1.0 \\ \rho = 1.5 \end{array} \right.$	$\left\{ \begin{array}{l} 2.4 \\ 3.6 \end{array} \right.$	$\left\{ \begin{array}{l} 2.0 \\ 3.0 \end{array} \right.$	$\left\{ \begin{array}{l} 2.3 \\ 3.4 \end{array} \right.$	$\left\{ \begin{array}{l} 2.4 \\ 3.6 \end{array} \right.$

The validity of the Stokes-Einstein equation being assumed, the accuracy of the calculated values of the mean micellar radius  $r$  is of the same order as that of the experimental values of the diffusion coefficient.

It is, however, improbable that the dye micelles are spherical, and the values of their mean radius calculated on this assumption will therefore be approximate.

The calculated values of the aggregation number  $G$  represent the average number of single ions in an anionic micelle, and are based on the assumption that the micelles do not contain any cations. If these micelles are assumed to be spheres of radius  $r$  and density  $\rho$ , then  $G$  is given by the equation

$$G = \frac{N}{M} \cdot \frac{4}{3} \pi r^3 \rho \quad (11)$$

where  $N$  is Avogadro's number and  $M$  is the molecular weight of a single dye anion. Since  $G$  is proportional to the cube of the radius the error in the calculated values of  $G$  is considerably greater than in the values of the mean radius.

The value of the effective density of the diffusing micelle is not known exactly. Robinson<sup>4</sup> assumes it to lie between the density of the solution and that of the solid dye. Now for solute particles not affecting the structure of the water around them the density effective in diffusion is equal to the reciprocal of the partial specific volume as determined pyknometrically. The apparent partial specific volume of each pure dye in aqueous solution was therefore measured at concentrations 1.0, 2.0 and 4.0 g. per litre by the pyknometer method at 25° C. and was calculated by means of a convenient expression quoted by Kraemer.<sup>24</sup> For Chrysophenine and for Direct Fast Orange SE the apparent partial specific volume was found within experimental error to be independent of the dye concentration and to be unaltered by the addition of sodium chloride. The mean of the results for each dye was therefore taken as the true partial specific volume, from which the effective density of the dye as a whole was found.

If the value of the fraction of sodium included in the anion is known it is possible, by means of data for the apparent volume of the sodium ion in solution,<sup>25</sup> to deduce the partial specific volume of the dye anion from that of the whole dye. The fraction of included sodium is not, however, known for Chrysophenine or Direct Fast Orange SE. Since the intense electrostatic field due to the sodium ion breaks down the structure and thereby increases the density of the surrounding water, the apparent volume of the sodium ion in solution is negative.<sup>25</sup> The partial specific volume of the dye anion is therefore greater than that of the whole dye, and its effective density in solution is less. Thus the effective density of the whole dye may be taken as an upper limit to the possible values for the anion. Calculations show that, whatever the fraction of sodium included in the anion, the densities of the whole dye and of the anion differ by less than 10 %.

The densities of solid Chrysophenine and Direct Fast Orange SE were also measured, by the usual specific-gravity-bottle method, with cyclohexane as non-solvent liquid.

The density results are summarised as follows:—

	Density (g. per c.c.).	
	Chrysophenine.	Direct Fast Orange SE.
Whole dye in solution . . . .	1.50	1.66
Solid dye . . . . .	1.48	1.59

The change in volume on dissolving the dye is therefore small. This indicates that the anion (which constitutes more than 93 % by weight of either dye) does not materially affect the structure of the water around it. Hence it is permissible to equate the effective density of the dye anion to the reciprocal of its partial specific volume, and not seriously inaccurate to do so for the whole dye.

In the tables for Chrysophenine and Direct Fast Orange SE, lower

and upper limits for the aggregation number (as affected by the density assumed) are quoted. The lower limit assumes the dye anion to have a density 1.0 g. per c.c. (approximately that of the solution). The upper limit is based on the effective density of the whole dye in solution, and the true value is considered to lie within 10% of this upper limit.

The calculated values of  $G$  are, as pointed out above, more subject to error than those of the micellar radius; nevertheless it is evident from the values given that Chrysophenine is only slightly aggregated in the presence of sodium chloride.

(c) The Diffusion of Direct Fast Orange SE in a Uniform Concentration of Sodium Chloride.

Experiments similar to those described above were also made with Direct Fast Orange SE; the results obtained are presented in Table VII.

TABLE VII.—MEAN DIFFUSIVITIES OF DIRECT FAST ORANGE SE IN SOLUTIONS CONTAINING UNIFORM CONCENTRATIONS OF SODIUM CHLORIDE.

Temp. (°C.).	Sodium chloride concentration.		Mean diffusivity (cm. <sup>2</sup> per sec.) $\times 10^6$ , at internal dye concentrations (g. per litre).					
	(g. per litre).	(g. equiv. per litre).	0.02.	0.05.	0.1.	0.2.	0.5.	1.0.
25	0.025	0.00043	—	—	—	3.45 (1)	4.19 (1)	5.30 (1)
	0.05	0.00086	—	—	—	2.37 (2); 2.44 (3)	3.33 (1)	3.92 (1); 4.22 (2); 3.69 (2)
						Mean 2.41		Mean 3.94
	0.1	0.00171	—	—	—	2.21 (1)	2.65 (1)	2.78 (3)
	0.2	0.00342	—	—	—	1.90 (2)	1.91 (2)	2.24 (2)
	0.4	0.00684	—	—	—	1.77 (3)	1.72 (3)	1.95 (1)
	0.5	0.00855	—	—	—	—	—	—
	0.6	0.0103	—	—	—	1.59 (1)	1.59 (1)	1.58 (2)
	0.8	0.0137	—	—	—	—	—	1.40 (3)
	1.0	0.0171	—	—	—	1.44 (1)	1.46 (1); 1.42 (3)	1.50 (1); 1.43 (3)
						Mean 1.43	Mean 1.36	Mean 1.47
	2.0	0.0342	1.30 (1)	1.24, 1.29, 1.33 (1); 1.32 (3c)	1.26 (1); 1.27, 1.24 (2c)	1.23 (1); 1.11, 1.18 (3c)	1.26 (1); 1.07, 1.06 (3c)	—
				Mean 1.30	Mean 1.26	Mean 1.17	Mean 1.10	—
	4.0	0.0684	1.21 (1)	—	—	—	—	—
60	0.02	0.00034	—	—	—	8.11 (3)	9.67 (1)	11.0 (2)
	0.1	0.00171	—	—	—	5.58 (1)	6.20 (2)	7.03 (3)
	0.2	0.00342	—	—	—	5.20 (2)	5.34 (3)	5.62 (1)
	0.5	0.00855	—	—	—	4.56 (3)	4.42 (1)	4.35 (2)
	1.0	0.0171	—	—	—	4.27 (1)	3.93 (2)	3.85 (3)
	1.6	0.0274	—	—	—	—	—	3.31 (1); 3.40 (2); 3.51 (3)
								Mean 3.41
	2.0	0.0342	—	4.48 (1); 4.48 (2); 4.46 (3)	4.44 (1); 4.32 (2); 4.25 (3)	3.96 (1); 4.03 (2); 3.98 (3)	3.56 (1); 3.59 (2); 3.63 (3); 3.34, 3.76, 3.76 (3c)	—
				Mean 4.47	Mean 4.34	Mean 3.99	Mean 3.60	—
								—

Before the interpretation of these results is considered, it is desirable to refer briefly to their determination. Most of the data were obtained with

the original cells before they were built into the all-glass apparatus, and at 60° C. there was an appreciable amount of evaporation from the external solution. It has already been pointed out that this alters the diffusion coefficient when a second electrolyte is present because it induces diffusion of this electrolyte in the opposite direction to that of the dye, and it was therefore necessary to apply a correction to take account of this effect. By reasoning similar to that used by Hartley and Robinson<sup>2</sup> the diffusion coefficient of the dye anion diffusing simultaneously with a second electrolyte was found to be given by the equation

$$D = \frac{RT}{F^2} 10^{-7} \frac{v}{n_-} \left\{ \frac{n_- \left( \frac{v}{n_-} - \frac{u}{n_+} \right) \left[ 1 + \frac{\frac{\partial c'}{\partial h} \left( \frac{v'}{n_-'} - \frac{n'}{n_+'} \right)}{\frac{\partial c}{\partial h} \left( \frac{v}{n_-} - \frac{u}{n_+} \right)} \right]}{1 - \frac{(u+v) + (u'+v')c'/c}{1}} \right\} \quad (12)$$

where  $\partial c'/\partial h$  and  $\partial c/\partial h$  are the concentration gradients of the second electrolyte and the dye respectively; these are measured in the same direction, so that their ratio is negative where the second electrolyte diffuses in the opposite direction to the dye. The other symbols have the same significance as previously,  $u$ ,  $v$ ,  $n$ , and  $c$  referring to the dye and  $u'$ ,  $v'$ ,  $n'$ , and  $c'$  to the second electrolyte. In a uniform concentration of the second electrolyte the diffusion coefficient is given by equation (9):

$$D = \frac{RT}{F^2} 10^{-7} \frac{v}{n_-} \left\{ 1 - \frac{n_- \left( \frac{v}{n_-} - \frac{u}{n_+} \right)}{(u+v) + (u'+v')c'/c} \right\}$$

and hence the error due to the non-uniformity of concentration of the second electrolyte, which in its turn is due to the evaporation, is

$$- \frac{RT}{F^2} 10^{-7} \frac{v}{n_-} \left\{ \frac{n_- \frac{\partial c'/\partial h}{\partial c/\partial h} \left( \frac{v'}{n_-'} - \frac{u'}{n_+'} \right)}{(u+v) + (u'+v')c'/c} \right\}.$$

For calculation of the percentage error the desired diffusion coefficient may be taken as  $\frac{RT}{F^2} 10^{-7} \frac{v}{n_-}$ , the second term in the bracket (equation 9) being negligible in the presence of excess salt; hence

$$\% \text{ error} = - \frac{100 n_- \frac{\partial c'/\partial h}{\partial c/\partial h} \left( \frac{v'}{n_-'} - \frac{u'}{n_+'} \right)}{(u+v) + (u'+v')c'/c}.$$

The values of the diffusion coefficient given in Table VII for a temperature of 60° C. were, with the one exception of the diffusion coefficient determined in Cell 3c, where no evaporation occurred, corrected by the use of this equation; the correction was usually about 3 %.

The value of  $n_-$  to be substituted in the expression for the correction was found at each dye concentration by comparing the diffusion coefficient (interpolated from experimental results) at an almost uniform sodium chloride concentration of 1.5 g. per litre, with that found when the internal and external salt concentrations were intentionally made to be 1.0 and 2.0 g. per litre respectively. Allowance being made for the evaporation from the external solution in each of these experiments,  $n_-$  is the only unknown in the expression for the percentage difference between these results. As a working approximation, the resultant value of  $n_-$  for each dye concentration was taken to be valid for the whole investigated range of salt concentration, and on this basis the correction for evaporation was calculated for each experiment. On account of the small value of the correction, the approximations involved in its evaluation cause no significant error in the final result.

Equation (12), on which the correction is based, was checked by the experimental determination of the diffusion coefficient of Direct Fast Orange SE in the presence of non-uniform concentrations of sodium and potassium chloride. It will be seen from the equation that the correcting term becomes zero either when  $\partial c / \partial h$  is zero (*i.e.* when the second electrolyte is at a uniform concentration throughout) or when  $v'/n_- = u'/n_+$ . For sodium and potassium chlorides  $n$  has the value 1 throughout;  $u'$  for sodium ion is 95.5, and for potassium 132, whilst  $v'$  for chloride ion is 133 (all values correspond to 60° C.). Hence when the second electrolyte is sodium chloride ( $v'/n_- - u'/n_+$ ) is 37.5, whilst for potassium chloride it is 1; it would therefore be expected that the diffusion coefficient of the dye would be the same in a non-uniform as in a uniform concentration of potassium chloride, whereas for sodium chloride the values would be appreciably different. This was tested experimentally by measuring the diffusion coefficient of Direct Fast Orange SE (0.5 g. per litre) first in a uniform concentration of the salt (2 g. per litre), and then repeating the measurement with the concentration of salt in the external solution reduced to about half of its former value. The values obtained were:

	$D$ (cm. <sup>2</sup> /sec.) $\times 10^6$ .
Sodium chloride, uniform concentration . . . .	3.62
Sodium chloride, non-uniform concentration . . . .	3.11
Potassium chloride, uniform concentration . . . .	3.68
Potassium chloride, non-uniform concentration . . . .	3.68

The experimental results thus fully confirm the theoretical deduction.

The results given in Table VII are reproduced in Figs. 6 and 7, in which the diffusion coefficient is plotted against the sodium chloride concentration. From Fig. 6 (25° C.) it is evident that at any constant electrolyte

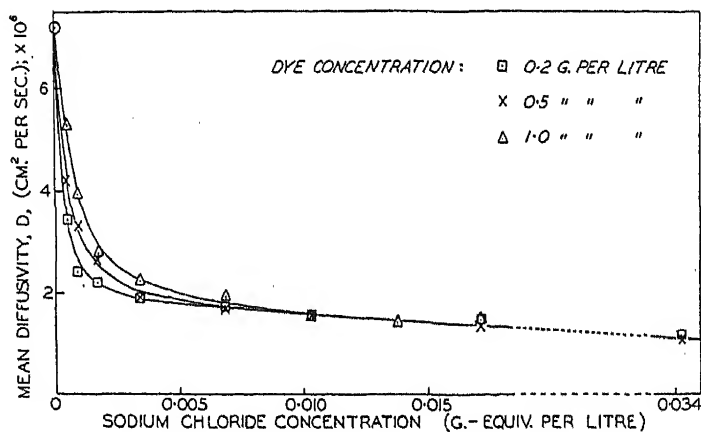
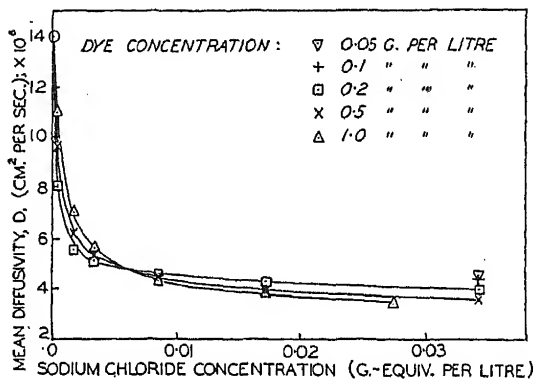


FIG. 6.—Direct Fast Orange SE in sodium chloride solution at 25° C.

concentration above 0.6 g. per litre the diffusion coefficient of Direct Fast Orange anion is, within the experimental error, independent of the dye concentration within the range 0.2 to 1.0 g. per litre. On the other hand at each constant dye concentration the diffusivity fails to attain a constant value in the observed range (which extends almost to the flocculation point) of sodium chloride concentration, continuing to decrease slightly on further addition of electrolyte even when the equivalent concentration of the electrolyte is 130 times the average of the internal and external equivalent concentrations of the dye.

The data for 60° C. are shown in Fig. 7. At low concentrations of sodium chloride the three curves lie in the same order as at 25° C., with the curve for the most concentrated dye solution uppermost, but when the sodium chloride concentration is increased the curves reverse their order instead of, as at 25° C., uniting to form one curve. They resemble those at 25° C., however, in indicating that the diffusion coefficient decreases steadily as the electrolyte concentration is increased.

FIG. 7.—Direct Fast Orange SE in sodium chloride solution at 60° C.



The steady decrease of the diffusion coefficient of Direct Fast Orange SE when the concentration of sodium chloride is increased to give a salt-dye ratio of over 100 is in striking contrast to the behaviour of Chrysophenine, whose diffusion coefficient becomes independent of the sodium chloride concentration at 25° and 40° C. when the salt-dye ratio is greater than about 20. The decrease may be due to any or all of the following causes:—

- (1) The retarding influences of the interionic forces increasing with the ionic strength of the solution;
- (2) A very gradual reduction of the potential gradient which is not eliminated at any observed salt-dye ratio;
- (3) An increasing aggregation of the dye anion as the sodium chloride concentration increases.

Now the effect of the interionic forces will be greater for a highly aggregated dye than for one only slightly aggregated, yet Robinson has found<sup>4</sup> that the diffusion coefficient of meta-Benzopurpurine, which is fairly highly aggregated in solution, becomes independent of the sodium chloride concentration as the latter is increased. There is therefore no evidence that the interionic forces operating on this dye, whose anion is highly charged, are sufficient to prevent the attainment of a constant diffusion coefficient, and it is therefore very improbable that the observed decrease in the diffusion coefficient of Direct Fast Orange SE can be attributed to such a cause.

The diffusion coefficient of Direct Fast Orange not only decreases with increasing sodium chloride concentration when the dye concentration is maintained constant, but it decreases with increasing dye concentration when the sodium chloride concentration is maintained constant at sufficiently large values, in particular at 60° C. This observation might, as Valkó<sup>6</sup> suggests, be taken as strong evidence that the sodium chloride is in excess, but such a criterion is not in itself sufficient. The diffusion coefficient of the dye anion in the presence of a second electrolyte not necessarily in excess is given by equation (9):

$$D = \frac{RT}{F^2} \cdot 10^{-7} \frac{v}{n_-} \left[ 1 + \frac{n_-(u/n_+ - v/n_-)}{u + v + (u' + v')c'/c} \right].$$

This equation may be written in the form

$$D = \frac{RT}{F^2} \cdot 10^{-7} \frac{v}{n_-} [1 + n_- E]$$

where  $E$  is proportional to the potential gradient between the diffusing cations and the anionic dye micelles. It has already been stressed that the contribution of the potential gradient to the observed diffusion coefficient  $D$  increases with the charge  $n_-$  of the anionic micelle. Thus a highly aggregated dye requires a higher salt-dye ratio  $c'/c$  to eliminate the effect of the potential gradient than a dye only slightly aggregated. This is obvious from physical considerations, for the force acting on the diffusing dye anion due to the potential gradient is the product of the potential gradient and the anionic charge  $n_-$ .

Now when the dye concentration is increased at constant sodium chloride concentration the salt-dye ratio  $c'/c$  diminishes, and hence the potential gradient will increase. Moreover, if the aggregation and hence the micellar charge  $n_-$  also increase with increasing dye concentration the effect of the potential gradient will be enhanced, *i.e.* the term  $n_- E$  will increase. The observed diffusion coefficient, however, is the product of  $(v/n_-)$  and  $(1 + n_- E)$ ; and  $(v/n_-)$ , the ratio of the mobility of the dye micelle to its charge, is inversely proportional to the micellar radius, and hence will decrease with increasing aggregation. Under such conditions the diffusion coefficient is the product of two factors, one of which increases and the other decreases, and the net result may therefore be either an increase or a decrease of the diffusion coefficient with increasing dye concentration. Hence it is theoretically possible to find a decrease in the diffusion coefficient (when the dye concentration is increased at constant sodium chloride concentration) even when the sodium chloride is not present in excess. Thus the decrease of the diffusion coefficient with increasing dye concentration that is observed when the sodium chloride concentration is maintained constant is not a sufficient criterion that the sodium chloride is so much in excess that the effect of the potential gradient can be neglected.

The application of the Stokes-Einstein equation to diffusion coefficients determined in the presence of a concentration of second electrolyte insufficient to eliminate the potential gradient between the ions of the diffusing electrolyte yields values of the degree of aggregation that are too small, and hence such data can at least be used to determine minimum values of the aggregation number. From the data of Table VII for the highest sodium chloride concentration of 2 g. per litre were obtained the minimum values of the aggregation number presented in Table VIII.

TABLE VIII.—MINIMUM AGGREGATION NUMBERS FOR DIRECT FAST ORANGE SE IN SODIUM CHLORIDE SOLUTION OF CONCENTRATION 2.0 G. PER LITRE.

Temp. (°C.).	Internal dye concentration (g. per litre).	Salt/Dye ratio.	$D(\text{cm.}^2/\text{sec.})$ $\times 10^6$ .	Radius $r$ (Å).	Aggregation Number. G.	
					$\rho = 1.0$ .	$\rho = 1.66$ .
25	0.05	520	1.30	18.7	23	39
	0.1	260	1.26	19.3	26	43
	0.2	130	1.17	20.8	32	53
	0.5	52	1.10	22.1	39	64
60	0.05	520	4.47	11.6	5.5	9.1
	0.1	260	4.34	11.9	6.1	10.1
	0.2	130	3.99	13.0	7.8	12.9
	0.5	52	3.60	14.4	10.3	17.1

These minimum values show that this dye is considerably more aggregated than Chrysophenine, both at 25° C. and at 60° C. By using the values of  $n_{-}$  and  $v$  (the charge and the calculated mobility of the Fast Orange anion in the presence of sodium chloride) quoted in Table X, the term  $n_{-}E$ , which shows the contribution of the potential gradient to the observed diffusion, has been tentatively evaluated by substitution in the appropriate expression in equation (9). The results, for a sodium chloride concentration of 2.0 g. per litre, are :—

Temp. (°C.) .	25				60			
Salt-dye ratio	520	260	130	52	520	260	130	52
$n_{-}E$ . . .	0.03	0.07	0.18	0.52	0.007	0.016	0.04	0.14

It is evident that except at the highest salt-dye ratios at 60° C., the electrolyte is not present in sufficient concentration to cause the effect of the potential gradient to be negligible.

At dye concentrations 0.2 to 1.0 g. per litre the highest sodium chloride concentrations used could not be appreciably exceeded without flocculation of the dye occurring, and therefore these results alone are not sufficient evidence that the degree of aggregation of the dye increases with the sodium chloride concentration at constant dye concentration. This possibility does, however, exist and receives strong support from a comparison<sup>22</sup> of these minimum aggregation numbers in sodium chloride solution with those deduced for pure dye solutions by a conductance method. Although the aggregation numbers given are minimum values the corrections that would have to be applied to obtain the true values increase as the salt-dye ratio decreases, and the results therefore show that the aggregation of the dye increases with increasing dye concentration when the salt concentration is maintained constant.

The results at both temperatures are more strictly comparable when the diffusion coefficients are plotted against the salt-dye ratio, as in Figs. 8 and 9. From these figures it is seen that at 25° C. and 60° C. the diffusion coefficient decreases with increasing dye concentration for all fixed dye-salt ratios. Although these ratios are not sufficiently high to eliminate the effect of the potential gradient, equation (9) shows that when the salt-dye ratio is constant the observed diffusion coefficient is independent of the dye concentration unless the mobility or the aggregation of the dye anion also changes. Now a change in the mobility of the dye anion can be due either to interionic effects or to a change in the degree of aggregation. It is extremely improbable that the relatively large decrease in the diffusion coefficient observed with increasing dye concentration can be attributed entirely to interionic effects, and hence the results lead to the conclusion that at 25° and 60° C. the aggregation of the dye increases with increasing dye concentration when the salt-dye ratio is maintained constant.

If the diffusion coefficient of Chrysophenine at 25° and 40° C. is plotted against the corresponding salt-dye ratio the curves for the different dye concentrations are almost identical, showing that the degree of aggregation is practically independent of the dye concentration.

#### (d) A Comparison of the Effects of Different Electrolytes.

According to the simple theory of diffusion exemplified by equation (9) the relative reduction in the diffusion coefficient of the dye anion on uniform addition of a foreign electrolyte depends on the concentrations of the electrolyte and the dye, on the charge of the dye anion, and to a slight



extent on the equivalent conductance of the electrolyte. Thus for fixed equivalent concentrations of electrolyte and dye the effect should be almost the same for different strong electrolytes, and in particular should not depend on the particular ions composing the electrolyte or on their valency unless they exert a specific influence on the aggregation of the dye anions. This was investigated experimentally with Direct Fast Orange SE at 60° C., sodium sulphate, sodium carbonate, potassium chloride, and magnesium

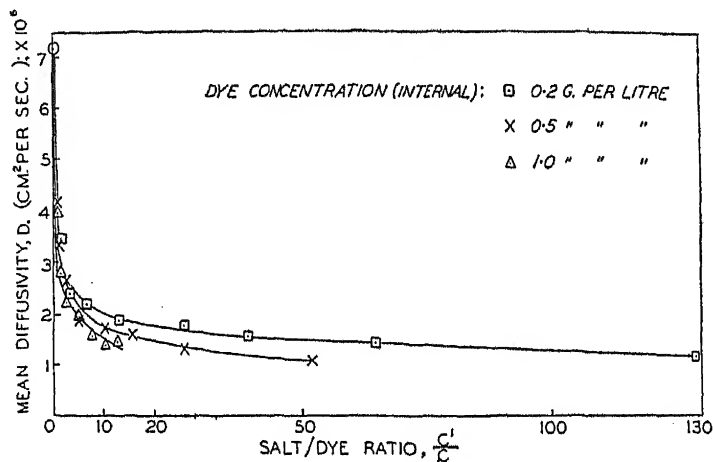


FIG. 8.—Direct Fast Orange SE in sodium chloride solution at 25° C.

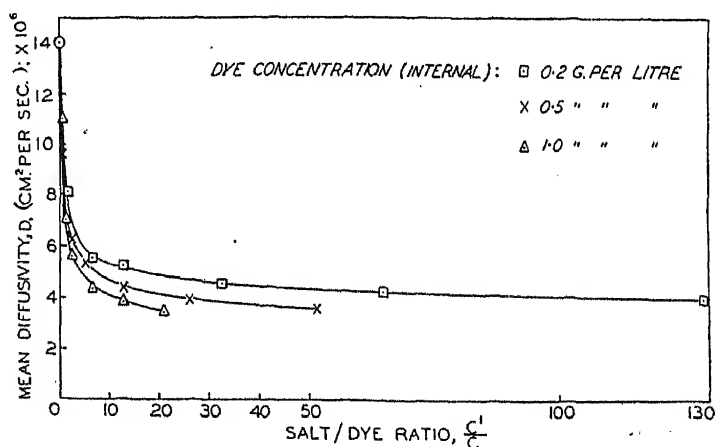


FIG. 9.—Direct Fast Orange SE in sodium chloride solution at 60° C.

chloride being used in turn in place of sodium chloride; the results are given in Table IX.

The diffusion coefficients measured in the presence of sodium chloride and sodium sulphate have been corrected, as already described, for the effect of evaporation from the external solution in the earlier type of apparatus.

These results show that sodium chloride, sodium sulphate, sodium carbonate, and potassium chloride have practically the same effect on the diffusion of the anion of Direct Fast Orange SE, while the effect of

magnesium chloride in decreasing the diffusion coefficient is greater. Only low concentrations of magnesium chloride can be used without flocculating the dye, and an additional comparison of the effects of this electrolyte and of sodium chloride was therefore made at a lower dye concentration in order to increase the salt-dye ratio. The experiments were again made at 60° C.; the electrolyte concentration was 0.00034 g. equivalent per litre and the dye concentration 0.2 g. per litre. The mean diffusivities of the dye anions were found to be: in the presence of sodium chloride,  $8.1 \times 10^{-6}$  cm.<sup>2</sup> per sec., and in the presence of magnesium chloride  $6.0 \times 10^{-6}$  cm.<sup>2</sup> per sec., so that even under these conditions magnesium chloride has a greater effect than sodium chloride.

TABLE IX.—MEAN DIFFUSIVITIES OF DIRECT FAST ORANGE SE (INTERNAL CONCENTRATION 0.5 G. PER LITRE) IN SOLUTIONS CONTAINING UNIFORM CONCENTRATIONS OF VARIOUS ELECTROLYTES.

Electrolyte concn. (g. equivalent per litre).	Mean diffusivity (cm. <sup>2</sup> per sec.) $\times 10^6$ .				
	NaCl.	Na <sub>2</sub> SO <sub>4</sub> .	Na <sub>2</sub> CO <sub>3</sub> .	KCl.	MgCl <sub>2</sub> .
0.00034	9.67 (1)	9.79 (2)	9.69, 9.49, 9.45, 9.30 (3c) Mean 9.48	—	7.24 (2c); 7.65, 7.48 7.00 (3c) Mean 7.34
0.00171	6.20 (2)	6.38 (1)	6.47, 6.09, 6.31, 6.37 (3c) Mean 6.31	6.36, 6.57, 6.43, 6.53 (3c) Mean 6.47	—
0.00855	4.42 (1)	4.58 (2)	4.60, 4.63 (3c) Mean 4.62	4.60, 4.60, 4.60, 4.58 (3c) Mean 4.60	—
0.0171	3.93 (2)	4.28 (1)	4.27, 4.37, 4.30 (3c) Mean 4.31	4.26, 4.28, 4.11 (3c) Mean 4.22	—
0.0342	3.56 (1); 3.59 (2); 3.63 (3); 3.34, 3.76 3.76 (3c) Mean 3.60	3.92 (2)	3.67, 3.72, 3.75, 3.66 (3c) Mean 3.70	3.61, 3.78, 3.63, 3.72, 3.68 (3c) Mean 3.68	—

Finally, an experiment was made with Chrysophenine, at a temperature of 60° C., a dye concentration of 0.2 g. per litre, and an electrolyte concentration of 0.000855 g. equivalent per litre. Again magnesium chloride had a greater depressive effect, the values of the mean diffusivity being: sodium chloride,  $11.3 \times 10^{-6}$  cm.<sup>2</sup> per sec., magnesium chloride,  $10.0 \times 10^{-6}$  cm.<sup>2</sup> per sec.

These results are obviously too scanty to permit any discussion of the cause of this difference, and the most that can be said is that there is a suggestion that a salt containing bivalent cations such as magnesium reduces the diffusion coefficient more than an equivalent concentration of a salt containing only univalent cations, such as the other four examined; this has also been observed by Garvie<sup>26</sup> with Chlorazol Fast Red K. It should be noted that in none of the comparisons made with magnesium chloride was the salt-dye ratio sufficiently high to allow the measured diffusion coefficient to approximate to the independent value for the dye anion, and hence the data cannot be used to compare the degree of aggregation of the dye in magnesium chloride with that in sodium chloride.

It is evident from Table IX that the other electrolytes used—sodium chloride, sodium sulphate, sodium carbonate, and potassium chloride—have approximately the same effect on the diffusion coefficient of Direct Fast Orange SE, and hence, since the observations extend to high electrolyte concentrations, on its degree of aggregation. This is of some technical importance in view of the "solubilising" influence often attributed to alkaline salts such as sodium carbonate, and it may be that any such influence is exerted more by effecting the removal of bivalent ions present in the water than by any specific effect of the salt itself.

(e) The Application of the Mobility Equation.

When the dye diffuses in the presence of excess sodium chloride the diffusion coefficient  $D$  of the dye anion is related to its mobility  $v$  by the equation

$$D = \frac{RT}{F^2} 10^{-7} \frac{v}{n_-} \quad . \quad . \quad . \quad . \quad (10)$$

This equation enables the mobility  $v$  to be calculated from the known values of the diffusion coefficient and the aggregation number provided that no sodium ions are included in the anionic micelle. Valkó<sup>8</sup> has found that the value so calculated for Benzopurpurine 4B is nearly twice the measured mobility of the dye anion in solutions free from any added electrolyte. Hartley<sup>23</sup> has suggested that this discrepancy can be attributed to a greater aggregation of the dye in the presence of sodium chloride than in its absence; this appears to be the most likely explanation, although the difference could be explained by the assumption that the anionic micelle contains an appreciable fraction of included sodium ions.

The application of equation (10) to the data for Chrysophenine and Direct Fast Orange SE leads to the results presented in Table X. In this

TABLE X.—MOBILITIES OF CHRYSOPHENINE AND DIRECT FAST ORANGE SE.

Dye.	Temp. (°C.)	Salt-Dye ratio.	$n_-$ (Stokes- Einstein).	$v$ (calculated).	$v$ (measured).
Chrysophenine	25	15-110	4.7	51	37
	40	30-110	4.1	64	47
	60	116-580	4.5	96	62
	90	1160	4.9	149	84
Direct Fast Orange SE	25	520	46.8	229	47
		260	51.2	243	47
		130	64.1	282	47
		520	11.0	166	78
	60	260	12.2	177	78
		130	15.6	210	78

table the values of the charge  $n_-$  are obtained, on the assumption that  $n_- = 2G$ , from the aggregation numbers  $G$  given in Tables VI and VIII. The minimum aggregation numbers, based on  $\rho = 1$ , are used so that the values of  $v$  for the dye anion in solutions containing sodium chloride (calculated from  $n_-$  by means of equation (10)) are in this respect minimum values. The measured values of  $v$  are from the conductance of pure dye solutions. For Direct Fast Orange at the lower salt-dye ratios the potential gradient is not completely eliminated, but it can be shown that under these conditions the calculated values of the mobility are *minimum* values. Here, also, therefore, there is a large discrepancy between the calculated and the measured values.

The experimental values<sup>22</sup> of the mobility  $v$  were obtained by subtracting the limiting equivalent conductance of sodium ion from that of the pure dye, and are therefore based on the assumption that no sodium ions are included in the anionic micelle. The values are the mobilities of anionic micelles of the same degree of aggregation as those present in solutions of the pure dye, and are lower than the calculated values, especially for Direct Fast Orange. The difference may be due either to a higher degree of aggregation in the presence of sodium chloride than in its absence, or to the fact that sodium ions are included in the micelle; no allowance is made for the latter possibility in obtaining the calculated values. The inclusion of sodium ions in the micelle would not only affect the value of the mobility determined from conductivity data but would also change the value of the micellar charge deduced from the aggregation number. Calculation shows that in order to reconcile the values obtained at 25° C. for Direct Fast Orange it would be necessary to assume that some 45 % of the sodium ions in the system are included in the anionic micelles; at 60° C. the difference is smaller, and it could be accounted for by the inclusion in the anionic micelles of 23 % of those present in the system. While the latter is perhaps a possible value for such inclusion, the former is very high—considerably higher than those found by Robinson and Moilliet<sup>27</sup> for Benzopurpurine 4B—and it is therefore probable that the difference between the two values of the mobility of the anion of Direct Fast Orange SE at 25° C. does in fact arise from an increased aggregation in the presence of sodium chloride.

*British Cotton Research Industry Assn.,  
Shirley Institute, Didsbury, Manchester.*

#### REFERENCES.

- <sup>1</sup> Holmes, *A Review of the Literature on Diffusion in Solution, and the Estimation of Particle Size from Diffusion Measurements*. In press; to be published by the B.C.I.R.A.
- <sup>2</sup> Hartley and Robinson, *Proc. Roy. Soc., A*, 1931, **134**, 20.
- <sup>3</sup> Robinson and Mills, *ibid.*, 1931, **131**, 576.
- <sup>4</sup> Robinson, *ibid.*, 1935, **148**, 680.
- <sup>5</sup> Robinson, *Trans. Faraday Soc.*, 1935, **31** (1), 245.
- <sup>6</sup> Valkó, *ibid.*, 1935, **31** (1), 230.
- <sup>7</sup> Valkó, *J. Soc. Dyers and Col.*, 1939, **55**, 173.
- <sup>8</sup> Lenher and Smith, *J. Physic. Chem.*, 1936, **40**, 1005.
- <sup>9</sup> Quensel, *Trans. Faraday Soc.*, 1935, **31** (1), 259.
- <sup>10</sup> Morton, *ibid.*, 1935, **31** (1), 262.
- <sup>11</sup> Schedler, *J. Soc. Chem. Ind.*, 1925, **44**, 397T.
- <sup>12</sup> Willis, Warwicker, Standing and Urquhart, *The Dyeing of Cellulose with Direct Dyes*, Part II. (*Shirley Institute Memoirs*, 1945, Vol. XIX, No. 17.)
- <sup>13</sup> Whittaker and Wilcock, *Dyeing with Coal-Tar Dyestuffs*, Baillière, Tyndall and Cox, 1942, p. 252.
- <sup>14</sup> Northrop and Anson, *J. Gen. Physiol.*, 1928, **12**, 543.
- <sup>15</sup> Clack, *A Research on Diffusion in Liquids*, Ph.D. Thesis, London, 1922.
- <sup>16</sup> Fürth, *Physikal. Z.*, 1925, **26**, 719.
- <sup>17</sup> Clack, *Proc. Physic. Soc. London*, 1924, **36**, 313.
- <sup>18</sup> Mehl and Schmidt, *Univ. Calif. Publ. Physiol.*, 1937, **8**, 165.
- <sup>19</sup> Gordon, *J. Chem. Physics*, 1937, **5**, 522.
- <sup>20</sup> Haskell, *Physic Rev.*, 1908, **27**, 145.
- <sup>21</sup> Vinograd and McBain, *J. Amer. Chem. Soc.*, 1941, **63**, 2008.
- <sup>22</sup> Holmes and Standing, *The Dyeing of Cellulose with Direct Dyes*, Part IV (*succeeding paper*).
- <sup>23</sup> Hartley, *Trans. Faraday Soc.*, 1935, **31** (1), 257.
- <sup>24</sup> Svedberg, Pedersen, *et al.*, *The Ultracentrifuge*, Clarendon Press, Oxford, 1940, pp. 59-60.
- <sup>25</sup> Rice, *Electronic Structure and Chemical Binding*, McGraw-Hill Book Co., 1940, pp. 409-11.
- <sup>26</sup> Garvie, *M.Sc. Thesis*, Manchester, 1933.
- <sup>27</sup> Robinson and Moilliet, *Proc. Roy. Soc. A*, 1933-4, **143**, 630.

# THE DYEING OF CELLULOSE WITH DIRECT DYES. PART IV. THE ELECTROLYTIC CONDUCTANCE OF AQUEOUS SOLUTIONS OF DIRECT DYES.

BY FRANK H. HOLMES AND H. ALAN STANDING

Received 26th September, 1944.

## 1. Introduction and Summary.

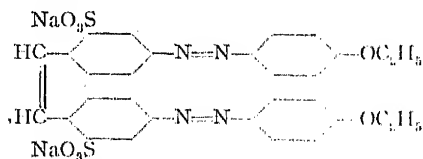
The degree of aggregation of direct dyes in the presence of an excess of an inorganic electrolyte can be readily determined from diffusion measurements by means of the Stokes-Einstein equation, but the diffusion coefficient of a pure dye depends upon the mobilities of the dye anion and cation, and this equation cannot therefore be used to determine the degree of aggregation of a dye in the absence of another electrolyte.<sup>1</sup> A second possibility is to use the Nernst-Haskell<sup>1</sup> equation:

$$D = \frac{RT}{F^2} 10^{-7} \left( \frac{1}{n_+} + \frac{1}{n_-} \right) \frac{uv}{u+v}$$

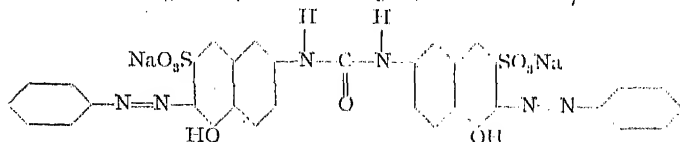
to determine the anionic charge  $n_-$  from the diffusion coefficient  $D$  and the ionic mobilities  $u$  and  $v$ ; the value of the charge of course gives the degree of aggregation provided that no cations are included in the micelle. Nevertheless the diffusion coefficient of a pure dye is relatively insensitive<sup>2</sup> to changes in the value of the anionic charge, particularly when the latter is large, and the form of this equation is correspondingly such that small errors in the values of the diffusion coefficient and of the mobilities can introduce relatively large errors in the calculated values of the charge of the anionic dye micelle. As a result measurements of electrolytic conductance provide the most satisfactory method of determining the aggregation number of a pure dye, in spite of the fact that the values so obtained are only approximate owing to the uncertainty of the interionic effects and the possibility that cations may be included in the anionic micelle.

The present paper deals with the conductance of three dyes:

*Chrysophenine G* (Colour Index 365)

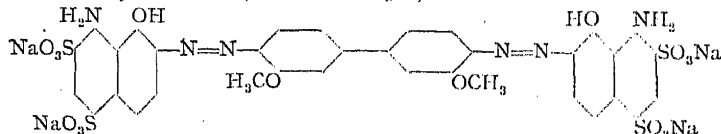


*Direct Fast Orange SE* (Colour Index 326; and Schueller<sup>3</sup>)



and

*Chlorazol Sky Blue FF* (Colour Index 518)



all of which were purified by the method of Robinson and Mills.<sup>4</sup>

The aggregation numbers were calculated from the conductance data by a method resembling that used by Robinson and Garrett,<sup>6</sup> but differing from it in some particulars; the results obtained show that none of these dyes can be considerably aggregated in aqueous solution free from any other electrolyte unless their micelles contain a large proportion of cations.

## 2. Experimental Method.

The conductances of the dye solutions were measured by means of a Wheatstone Bridge fitted with a modified form of the Wagner earth as described by Taylor and Acree;<sup>6</sup> Fig. 1 shows the wiring diagram of the circuit used. A valve oscillator O of frequency adjustable in the range 650 to 1900 cycles per second is the source of alternating current and  $R_1$  and  $R_2$  comprise the two arms of the metre bridge. The variable resistance  $R_3$  is non-inductively wound and  $R_4$  is the conductivity cell. The two variable resistances  $R_5$  and  $R_6$  are in parallel with the metre bridge and their junction E is earthed. A pair of 2,000 ohm ear-phones T are used as the current detector, and by means of the switch S can be connected across either CD or CE.

Three conductivity cells made of resistance glass and fitted with platinised electrodes were used. Their cell constants, determined at 20° C. with standard solutions of potassium chloride whose conductances were obtained from the data of Parker and Parker,<sup>7</sup> were 0.362, 0.1569 and 0.0421, and their use permitted the determination of conductances over a fairly wide concentration range. No attempt was made to prepare specially pure conductivity water for this work, ordinary distilled water being used. This water had a specific conductance of about  $2 \times 10^{-6}$  reciprocal ohms at 20° C., but the conductance of the water was measured at each temperature at which the dye solutions were examined, and the value for water was subtracted from that for the dye solution.

In making a determination the bridge is first balanced with the ear-phones across DC,  $R_4$  being adjusted so that the balance point is near the middle of the metre bridge. By means of the switch S the ear-phones are then connected across CE and  $R_5$  and  $R_6$  adjusted to reduce the sound in the ear-phones to a minimum. The ear-phones are then reconnected across CD, and  $R_1$  and  $R_2$  are readjusted to give a sharp balance point. By means of such successive adjustments a well-defined final null point is obtained.

## 3. Experimental Results and Discussion.

The conductances of solutions of the three dyes were measured at dye concentrations covering the range 0.05 to 4.0 g. per litre at temperatures of 20° to 98° C. for Chrysophenine, 20° to 60° C. for Direct Fast Orange SE, and 20° C. only for Chlorazol Sky Blue FF. The results are presented in Table I and plotted in Figs. 2-4.

The plot of the equivalent conductance against the square root of the equivalent concentration is practically linear for all three dyes except at

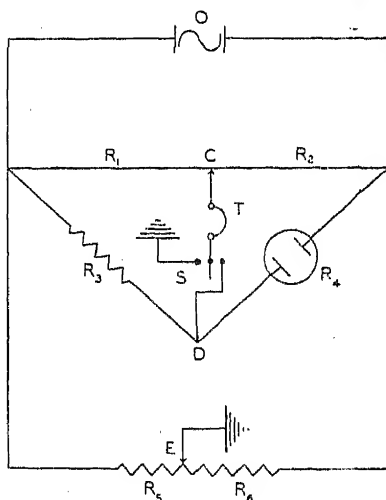


FIG. 1.

the lowest concentrations. In this region the results for Direct Fast Orange show a definite maximum at each temperature, those for Chrysophenine suggest the existence of such a maximum, while those for Chlorazol Sky

TABLE I.—CONDUCTANCE OF SOLUTIONS OF DIRECT DYES.\*

Dye.	Temp. °C.		* Dye concentration, g. per litre at 20° C.									
			0.05.	0.10.	0.15.	0.20.	0.30.	0.50.	1.0.	2.0.	3.0.	4.0.
Chrysophenine G (Equivalent weight 340)	20	$\sqrt{c}$	1.211	1.711		2.420		3.835	5.41	7.65	9.40	10.83
		$\Lambda$	72.8	72.8		75.5		72.5	70.4	67.0	64.3	62.4
	30	$\sqrt{c}$	1.210	1.710		2.420		3.830	5.40	7.65	9.37	10.82
		$\Lambda$	89.4	88.6		91.6		89.2	88.1	83.7	80.0	78.0
	40	$\sqrt{c}$	1.209	1.710		2.418		3.820	5.40	7.64	9.35	10.81
		$\Lambda$	106.2	106.5		110.3		108.1	106.0	101.5	97.3	94.7
	50	$\sqrt{c}$	1.204	1.708		2.415		3.810	5.39	7.63	9.34	10.80
		$\Lambda$	126	128.7		130.3		126.9	124.9	119.8	114.9	112.1
	60	$\sqrt{c}$	1.202	1.700		2.400		3.800	5.37	7.60	9.31	10.77
		$\Lambda$	148.7	147.2		151.9		146	144.4	138.8	133	131
	70	$\sqrt{c}$	1.200	1.697		2.400		3.795	5.355	7.59	9.30	10.71
		$\Lambda$	166.8	167.1		171.3		166	162.9	158.1	151.1	149.3
	80	$\sqrt{c}$	1.196	1.691		2.395		3.780	5.35	7.57	9.25	10.70
		$\Lambda$	193.9	193.1		194.2		187.1	184	177.2	171	168.8
	90	$\sqrt{c}$	1.191	1.683		2.380		3.770	5.325	7.53	9.24	10.66
		$\Lambda$	212.7	217.6		215.8		206.8	205	197.1	190.5	187.3
	98	$\sqrt{c}$	1.188	1.680		2.378		3.760	5.31	7.52	9.20	10.62
		$\Lambda$	237	234		236.3		224	221.8	212	206.5	202.4
Direct Fast Orange SE (Equivalent weight 378.2)	20	$\sqrt{c}$		1.626	1.992	2.299	2.816	3.636	5.141	7.274	8.906	10.29
		$\Lambda$		83.8	86.0	85.6	82.4	76.7	71.0	63.8	57.3	54.2
	25	$\sqrt{c}$		1.626	1.991	2.299	2.815	3.634	5.139	7.269	8.902	10.29
		$\Lambda$		96.6	98.0	95.5	92.0	85.6	80.1	71.9	65.1	62.0
	40	$\sqrt{c}$		1.621	1.986	2.292	2.808	3.624	5.128	7.250	8.879	10.25
		$\Lambda$		130	130.8	127.7	123.3	114.1	109	100	91.5	87.1
	60	$\sqrt{c}$		1.614	1.977	2.283	2.796	3.609	5.103	7.218	8.840	10.21
		$\Lambda$		171	177	170	166.8	160	149	140	131	126.1
Chlorazol Sky Blue FF (Equivalent weight 248.1)	20	$\sqrt{c}$	1.42	2.01		2.84		4.49	6.35	8.97	7.78†	
		$\Lambda$	93.9	95.0		91.6		86.9	80.9	74.4	77.5†	

\*  $\sqrt{c}$  is (square root of equivalent concentration)  $\times 10^2$ .  $\Lambda$  is equivalent conductance.

† Dye concentration, 1.50 g. per litre at 20° C.

Blue FF are too scanty to provide any evidence one way or the other. Robinson and Garrett \* have found such maxima for Congo Red and meta-Benzopurpurine, and have pointed out that the existence of a maximum

is definite evidence that at low concentrations the degree of aggregation of the dye increases with increasing concentration.

Robinson and Garrett have also shown that providing the fraction of cations included in the anionic micelle is known the aggregation number

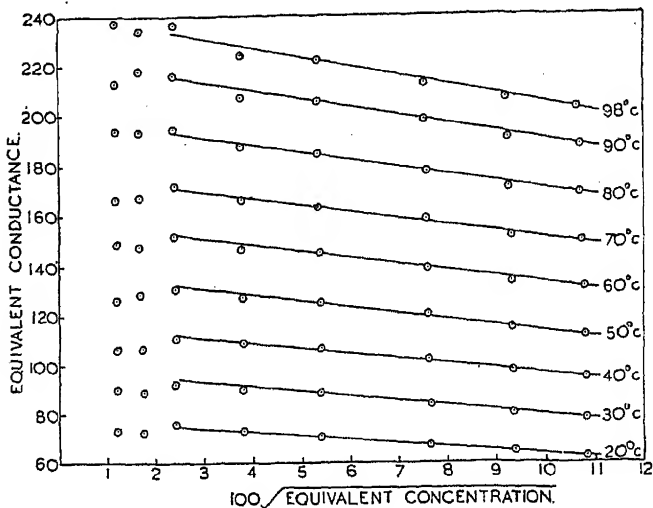


FIG. 2.—Chrysophenine G in water at various temperatures. Variation of equivalent conductance with concentration.

of the micelle can be calculated from the equivalent conductance of the micelle and that of a single dye anion. The latter they determined by extrapolating from the maximum of the  $\Lambda - \sqrt{c}$  curve downwards to infinite dilution, but at best this extrapolation can only be approximate, and more-

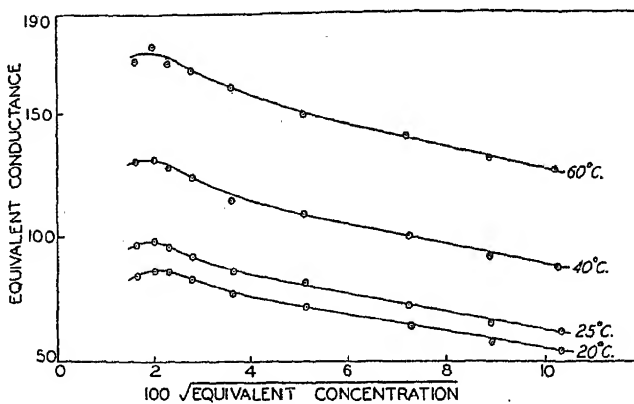


FIG. 3.—Fast Orange SE in water at various temperatures. Variation of equivalent conductance with concentration.

over demands accurate measurement of the conductances of extremely dilute solutions. In the present paper it has been preferred to calculate the equivalent conductance of a single anion by applying Stokes' Law. This also is only approximate, but since Stokes' Law has been used to calculate from the diffusion coefficient the degree of aggregation of the



dye anion in the presence of excess electrolyte<sup>8</sup> its use here should provide comparable values of the aggregation number of the dye in the absence of such electrolyte.

Since the anionic micelles may contain cations,<sup>5</sup> only a fraction  $f$  of the sodium ions present in the solution move towards the cathode in the conduction of electricity. Thus the equivalent conductance  $\Lambda$  of the dye is  $f(u_{\text{Na}} + v_g)$  where  $u_{\text{Na}}$  and  $v_g$  are the equivalent conductances of the sodium ion and of the anionic micelle respectively. Hence the equivalent conductance  $v_g$  of the anionic micelle is given by the equation

$$v_g = (\Lambda/f) - u_{\text{Na}} \quad (1)$$

Now let the dye anions, each of valency  $n$ , aggregate in solution to give micelles each containing  $G$  anions; a fraction  $(1 - f)$  of the sodium ions

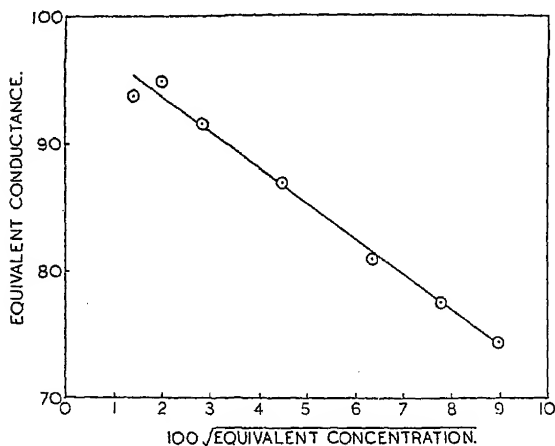


FIG. 4.—Chlorazol Sky Blue FF in water at 20° C. Variation of equivalent conductance with concentration.

will be included in these micelles. Thus the mean micellar charge is  $fFnG/N$  coulombs, where  $F$  is the Faraday (in coulombs) and  $N$  is Avogadro's number. Let the velocity of a micelle moving under a potential gradient of 1 volt per cm. be  $V$  cm. per sec. Then assuming the micelles to be spheres of radius  $r$ , we have on equating the frictional resistance given by Stokes' Law to the driving force in dynes:

$$6\pi\eta rV = f\frac{F}{N}nG \cdot 10^7 \quad (2)$$

where  $\eta$  is the viscosity of the solvent. But

$$V = \frac{v_g}{F} \quad (3)$$

Hence

$$6\pi\eta r v_g = f\frac{F^2}{N}nG \cdot 10^7 \quad (4)$$

If  $M$  is the molecular weight of the dye anion and  $\rho$  is the micellar density, then the aggregation number  $G$  is given by the equation

$$G = \frac{4}{3}\pi r^3 \rho \frac{N}{M} \quad (5)$$

Eliminating  $r$  from equations (4) and (5) and substituting for  $v_g$  from equation (1) we obtain

$$G = \left( \frac{3M}{4\pi N\rho} \right)^{\frac{1}{2}} \left( \frac{6\pi\eta N}{nfF^2 10^7} \right)^{\frac{2}{3}} \left( \frac{A}{f} - u_{Na} \right)^{\frac{2}{3}}$$

$$= 0.852 \left( \frac{M}{\rho} \right)^{\frac{1}{2}} \left( \frac{\eta}{fn} \right)^{\frac{2}{3}} \left( \frac{A}{f} - u_{Na} \right)^{\frac{2}{3}} \quad (6)$$

If no sodium ions are included in the anionic micelles this reduces to

$$G = 0.852 \left( \frac{M}{\rho} \right)^{\frac{1}{2}} \left( \frac{\eta}{n} \right)^{\frac{2}{3}} (A - u_{Na})^{\frac{2}{3}} \quad (7)$$

For Chrysophenine G and Direct Fast Orange SE the value taken for the micellar density  $\rho$  is the reciprocal of the partial specific volume of the whole dye in solution.<sup>8</sup> The true value, which cannot at present be determined, is considered to be less than 10 % below this value. The densities taken (in g. per c.c.) are

Chrysophenine G	1.50
Direct Fast Orange SE	1.66

It is assumed, after Valkó,<sup>2</sup> that  $\rho = 1.5$  for Chlorazol Sky Blue FF.

The equivalent conductance  $v_a$  of the anionic micelle varies with concentration, in part because of interionic effects. Robinson and Garrett<sup>5</sup> use values of  $v_a$  for finite concentrations, so obtaining values of the aggregation number that will be minimum values on account of the interionic effects. By a series of approximations they then correct for the interionic effects by applying Onsager's equation, so obtaining maximum values for the aggregation numbers. This method is also applicable to equations (6) and (7), but since these equations are only approximate a simpler method of determining  $v_a$  was preferred. The  $A - \sqrt{c}$  curve is almost linear over the higher range of concentration, and it was therefore assumed as a first approximation that over this range the aggregation number  $G$  and the fraction of free sodium  $f$  do not alter appreciably with concentration. Thus by extrapolating this linear part of the curve to infinite dilution a value  $A_0$  of the equivalent conductance is obtained which is approximately equal to that of dye of the same degree of aggregation as exists in the more concentrated solutions, but free from the interionic effects operating there. The values of  $A_0$  so obtained together with the corresponding limiting equivalent conductances of the sodium ion have been used in the application of equation (6) to the three dyes whose investigation is described in the present paper.

The calculated value of  $G$  depends fairly critically upon the fraction  $f$  of free sodium in the solution. The values of  $f$  for the three dyes under discussion are not known, and the calculation of such values from conductance and transport-number data is not exact.<sup>9</sup> Arbitrary values of 1.0, 0.95, 0.90 and 0.85 have therefore been taken, corresponding to the range of values found by Robinson and Moilliet<sup>9</sup> for meta-Benzopurpurine and Benzopurpurine 4B at concentrations up to centinormal. The values of  $G$  calculated from equation (6) with these arbitrary values of  $f$  are given in Table II, with, for comparison, the aggregation numbers of the dyes in the presence of sodium chloride as deduced from diffusion data. Since for Direct Fast Orange SE and Chlorazol Sky Blue FF the "diffusion" values of  $G$  vary with both dye and sodium chloride concentrations a representative range of values is given. Those for Chrysophenine and Direct Fast Orange SE are taken from the previous paper of this series;<sup>8</sup> those for Sky Blue have been taken from the data of Valkó.<sup>2</sup>

The calculated values of  $G$  for Chrysophenine are of the same order as those found for the dye in the presence of sodium chloride, but for Direct Fast Orange and Sky Blue the calculated values for the pure dyes are much lower than those determined in the presence of sodium chloride.

All the calculated values increase as  $f$  decreases (*i.e.* as the assumed proportion of sodium ion in the micelle increases), and the two sets of values obtained for Direct Fast Orange and Sky Blue could be reconciled by assuming a sufficiently high value for the fraction of sodium ion combined in the micelle. Calculation shows, however, that for Direct Fast Orange at 25° C. it is necessary to assume that  $f$  is 0.55 (taking  $\rho = 1$ ) or 0.44 (taking  $\rho = 1.66$ ) if the dye is taken to be as highly aggregated in pure solution as it is in the presence of sodium chloride at the highest salt-dye ratio studied. This means that at least 45 % of the sodium ions present are included in the anionic micelle, an assumption that seems highly improbable. Hence, although the calculated values of  $G$  may well be

TABLE II.—AGGREGATION NUMBERS OF CHRYSOPHENINE G, DIRECT FAST ORANGE SE, AND CHLORAZOL SKY BLUE FF.

Dye.	Temp. (°C.)	Aggregation Number $G$ of pure dye corresponding to various values of the fraction of free sodium $f$ .				Aggregation Number of dye in presence of another electro- lyte (from diffusion data).
		$f = 1.0$ .	$f = 0.95$ .	$f = 0.90$ .	$f = 0.85$ .	
Chrysophenine G . . . . .	25*	1.2	1.5	2.0	2.6	3.6
	40	1.1	1.4	1.8	2.3	3.0
	60	1.0	1.3	1.7	2.2	3.4
	90	0.8	1.1	1.5	1.9	3.6
Direct Fast Orange SE . . . . .	25	1.7	2.2	2.7	3.5	39.64
	40	1.5	2.0	2.5	3.2	
	60	1.4	1.7	2.2	2.9	9.17
Chlorazol Sky Blue FF . . . . .	20	1.0	1.3	1.6	2.0	7.23 (at 25° C.)

\* The limiting equivalent conductance of Chrysophenine at 25° C. is interpolated from those found from Table I.

inaccurate, they show when compared with the values obtained from diffusion measurements that the three dyes are only slightly aggregated in pure solution although two of them, Direct Fast Orange SE and Chlorazol Sky Blue FF, are appreciably aggregated in the presence of sodium chloride; the other, Chrysophenine, is only slightly aggregated even in the presence of salt. In this respect Direct Fast Orange and Chlorazol Sky Blue resemble Congo Red, Benzopurpurine 4B, and meta-Benzopurpurine, all of which Robinson and Garrett<sup>6</sup> found to be fairly highly aggregated in the presence of salt, and only slightly aggregated in pure solution.

#### REFERENCES.

- <sup>1</sup> Hartley and Robinson, *Proc. Roy. Soc. A*, 1931, 134, 20.
- <sup>2</sup> Valkó, *Trans. Faraday Soc.*, 1935, 31 (1), 230.
- <sup>3</sup> Schedler, *J. Soc. Chem. Ind.*, 1925, 44, 397T.
- <sup>4</sup> Robinson and Mills, *Proc. Roy. Soc. A*, 1931, 131, 576.
- <sup>5</sup> Robinson and Garrett, *Trans. Faraday Soc.*, 1939, 35 (1), 771.
- <sup>6</sup> Taylor and Acree, *J. Amer. Chem. Soc.*, 1916, 38, 2403.
- <sup>7</sup> Parker and Parker, *ibid.*, 1924, 46, 312.
- <sup>8</sup> Holmes and Standing, *The Dyeing of Cellulose with Direct Dyes*, Part III (*preceding paper*).
- <sup>9</sup> Robinson and Moilliet, *Proc. Roy. Soc. A*, 1933, 143, 630.

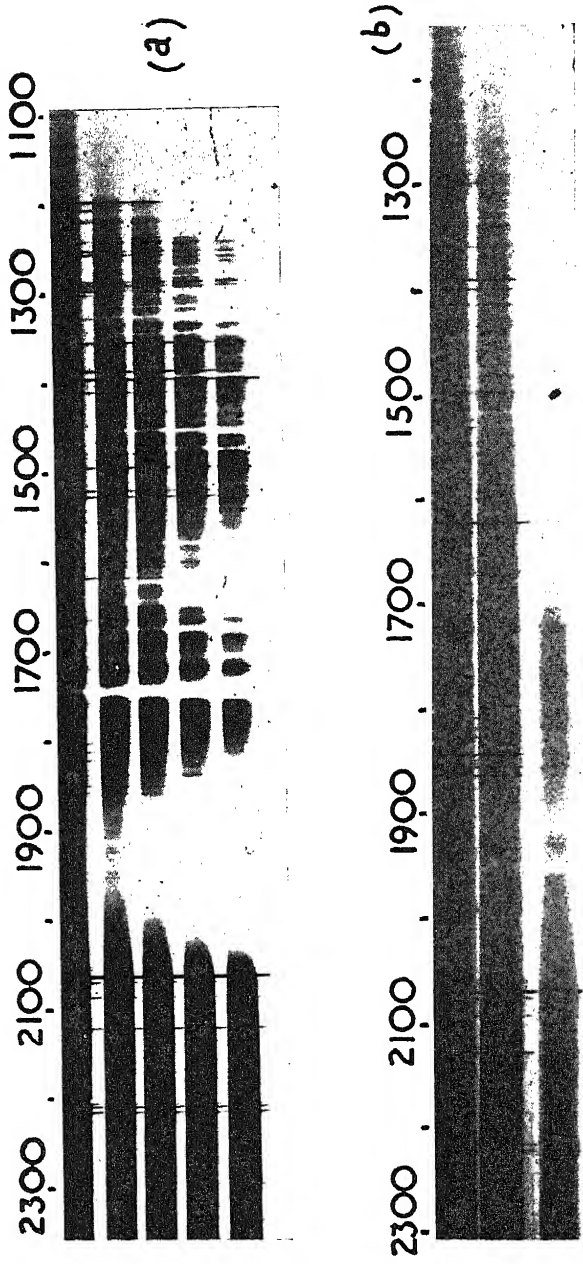


PLATE I.—The spectra of (a) acrolein, (b) mesityl oxide.

[See page 498.]

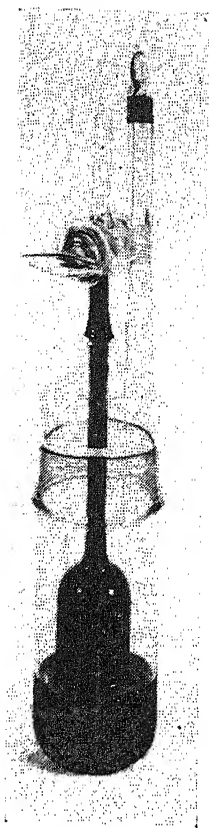


FIG. 2.

[See page 544.]

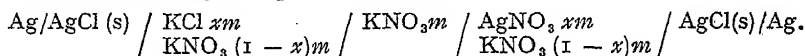
# THE ENERGY AND ENTROPY OF SOLUTION OF SILVER CHLORIDE IN METHANOL-WATER MIXTURES. PART I.

BY H. N. PARTON, D. J. DAVIS, F. HURST AND G. D. GEMMELL.

Received 6th July, 1944.

Latimer and Slansky<sup>1</sup> have obtained the standard entropy of solution of HCl and some alkali halides, in methanol-water mixtures by combining the heat of solution measurements of Slansky<sup>2</sup> with free energies of solution obtained from solubility and activity coefficient data. We have obtained similar information for AgCl in methanol-water mixtures containing 10, 20 and 50 % methanol by weight. The activity product and its temperature coefficient have been measured by means of the cell devised by Owen<sup>3</sup> for eliminating liquid junction potentials, and the thermodynamic properties of the solutions deduced by standard methods.

Owen's cell may be represented thus:—



The total ionic concentration (molal) in each of the three solutions making up the cell is  $2m$ , assuming complete dissociation, but of this a fraction  $x/2$  is made up of chloride ions in the left-hand compartment and silver ions in the right. The E.M.F. is given by

$$E = k \log \frac{a'_{\text{Ag}^+}}{a''_{\text{Ag}^+}} \pm E_j \quad (1)$$

where  $k = RT/F \log_e 10$ ,  $a'_{\text{Ag}^+}$ ,  $a''_{\text{Ag}^+}$  are the silver ion activities in the right- and left-hand compartments respectively, and  $E_j$  is the sum of the liquid junction potentials. Introducing the activity product of silver chloride for the left-hand compartment, and replacing activities by the product of ionic concentrations and activity coefficients, this expression becomes

$$E - 2k \log m = -k \log K + k \log f'_{\text{Ag}^+} f''_{\text{Cl}^-} \pm E_j \quad (2)$$

where  $K$  is the activity product of AgCl, and  $f$  is an activity coefficient.

If  $x$  is varied at constant  $m$ ,

$$\lim_{x \rightarrow 0} [E - 2k \log xm] = -k \log K + \lim_{x \rightarrow 0} [k \log f'_{\text{Ag}^+} f''_{\text{Cl}^-}] \quad (3)$$

since  $E_j$  vanishes when  $x = 0$ . For convenience in graphical treatment Owen adds the term  $2kA\sqrt{m}$  to each side of equation (3),  $A$  being the Debye-Huckel limiting slope for the particular solvent and temperature. Since this term is independent of  $x$ , equation (3) becomes

$$\lim_{x \rightarrow 0} [E - 2k \log xm + 2kA\sqrt{m}] = -k \log K + \lim_{x \rightarrow 0} [k \log f'_{\text{Ag}^+} f''_{\text{Cl}^-} + 2kA\sqrt{m}] \quad (4)$$

The function on the left of equation (4) is plotted against  $x$ , and the intercepts at  $x = 0$  are then plotted against  $m$ . Both plots are found to be

<sup>1</sup> Latimer and Slansky, *J.A.C.S.*, 1940, **102**, 2019.

<sup>2</sup> Slansky, *ibid.*, 1940, **62**, 2430.

<sup>3</sup> Owen, *ibid.*, 1938, **60**, 2229.

## 576 SILVER CHLORIDE IN METHANOL-WATER MIXTURES

linear, and extrapolation of the second to  $m = 0$ , where the activity coefficients are unity by definition, gives  $-k \log K$  and hence  $K$ , the activity product.

In this work sixteen cells have been measured in each solvent over a range of temperatures from 15° C. to 45° C., the values of  $m$  and  $x$  being shown in Table I.

TABLE I.

$$E_t = E_{30} - a(t - 30) + b(t - 30)^2.$$

		$x = 0.6.$	$x = 0.4.$	$x = 0.3.$	$x = 0.2.$
<b>m = 0.05</b>					
10%	$E_{30}$	0.3961	0.3744	0.3589	0.3380
	$a \times 10^3$	1.058	1.127	1.189	1.231
	$b \times 10^6$	1.6	0.7	4.7	3.0
20%	$E_{30}$	0.4081	0.3873	0.3718	0.3509
	$a \times 10^3$	1.004	1.046	1.117	1.181
	$b \times 10^6$	3.1	-0.6	0.3	1.1
50%	$E_{30}$	0.4503	0.4290	0.4139	0.3928
	$a \times 10^3$	0.870	0.883	0.941	1.015
	$b \times 10^6$	0.9	1.7	3.1	1.4
<b>m = 0.04</b>					
50%	$E_{30}$	0.4409	0.4196	0.4043	0.3828
	$a \times 10^3$	0.825	0.901	0.962	1.018
	$b \times 10^6$	1.9	1.9	4.0	3.1
<b>m = 0.03</b>					
10%	$E_{30}$	0.3717	0.3501	0.3350	0.3139
	$a \times 10^3$	1.094	1.161	1.222	1.282
	$b \times 10^6$	0.7	2.0	2.3	2.0
20%	$E_{30}$	0.3841	0.3626	0.3479	0.3264
	$a \times 10^3$	1.051	1.127	1.184	1.245
	$b \times 10^6$	0.9	3.3	1.0	0.9
50%	$E_{30}$	0.4280	0.4066	0.3911	0.3701
	$a \times 10^3$	0.888	0.936	1.029	1.081
	$b \times 10^6$	1.0	2.7	3.6	1.5
<b>m = 0.02</b>					
10%	$E_{30}$	0.3528	0.3313	0.3154	0.2946
	$a \times 10^3$	1.159	1.239	1.269	1.351
	$b \times 10^6$	1.1	0.86	2.9	2.4
20%	$E_{30}$	0.3643	0.3432	0.3283	0.3066
	$a \times 10^3$	1.131	1.226	1.254	1.326
	$b \times 10^6$	3.0	0.0	1.3	1.7
50%	$E_{30}$	0.4090	0.3874	0.3722	0.3511
	$a \times 10^3$	0.954	1.030	1.067	1.136
	$b \times 10^6$	2.1	4.0	4.7	4.6
<b>m = 0.01</b>					
10%	$E_{30}$	0.3183	0.2969	0.2819	0.2605
	$a \times 10^3$	1.280	1.349	1.377	1.449
	$b \times 10^6$	0.3	1.6	3.3	3.3
20%	$E_{30}$	0.3301	0.3091	0.2942	0.2727
	$a \times 10^3$	1.232	1.313	1.366	1.436
	$b \times 10^6$	1.9	0.4	-0.4	2.6

## Experimental.

All salts used were purified by two recrystallisations. Methanol was distilled, refluxed over fresh quicklime, and the last traces of water removed by refluxing over magnesium activated by iodine, followed by a final distillation with careful exclusion of moisture. For solutions containing

silver nitrate, methanol was treated as recommended by Pearce and Mortimer,<sup>4</sup> the distillate after refluxing with quicklime was treated with silver nitrate crystals, and finally refluxed for eight hours. The mixed solvents were made up by weight, vacuum corrections being applied. Stock solutions were prepared from the appropriate salts and others prepared from them by weight dilution except in the case of those containing silver nitrate in 50 % methanol. These showed signs of decomposition after two days, and were always prepared immediately before use.

Silver chloride electrodes were of the electrolytic type, treated as recommended by Smith and Taylor.<sup>5</sup> The cell was a modification of that used by Owen,<sup>6</sup> four electrodes being used for each set-up, and air being displaced by nitrogen. Each cell after assembly was allowed to stand overnight, and measurement begun at 15° C. next morning. When the E.M.F. had been steady at this temperature for an hour, the temperature was slowly raised to 20° C. by running hot water into the thermostat as cold water was run out, the change taking about ten minutes. Equilibrium at the higher temperature was thus established rapidly, and the process repeated till 45° C. was reached.

**Results.**—Table I records the results in compact form. The E.M.F.s for one cell, that is a given value of  $x$  and  $m$  in a given solvent, have been expressed in terms of the E.M.F. at 30° C. and the constants of the quadratic  $E_t = E_{30} - a(t - 30) + b(t - 30)^2$ ,  $a$  and  $b$  having been found by the method of least squares. From the measured  $E$  values, the function on the left of equation (4) was calculated for each cell, using  $k = 0.00019844T$ , and  $A = 0.506 \left( \frac{78.54 \times 298.1}{DT} \right)^{\frac{1}{2}}$  where  $A$  is the Debye-Huckel limiting

slope for water at 25° C. at which its dielectric constant is 78.54. The values of  $D$  for the various solvents were taken from the data of Akerlof,<sup>6</sup> those at intermediate temperatures being found by interpolation. The plots of this function against  $x$ , and those of the resulting intercepts at  $x = 0$  against  $m$ , were linear, as found by Owen<sup>3</sup> in the solvent water, and values of  $-k \log K$ , and hence  $-\log K$ , were found as described above. The values of  $-\log K$  in the three solvents were expressed as a function of the absolute temperature, the constants of the equation being obtained by the method of least squares. The equations are:

$$10\% \text{ methanol. } \log K = 6.1898 - 4163.3/T - 0.007559T \quad (5)$$

$$20\% \text{ methanol. } \log K = 5.2375 - 4080.8/T - 0.005997T \quad (6)$$

$$50\% \text{ methanol. } \log K = 13.500 - 5399/T - 0.02160T \quad (7)$$

The agreement between the experimental values of  $-\log K$  and those given by the equations is shown in Table II.

TABLE II.—ACTIVITY PRODUCTS OF SILVER CHLORIDE.

° C.	10 %.		20 %.		50 %.	
	$-\log K$ Obs.	$-\log K$ Equ. 5.	$-\log K$ Obs.	$-\log K$ Equ. 6.	$-\log K$ Obs.	$-\log K$ Equ. 7.
15	10.44	10.44	10.65	10.65	11.48	11.46
20	10.23	10.23	10.44	10.44	11.23	11.25
25	10.03	10.02	10.24	10.25	11.05	11.05
30	9.83	9.84	10.04	10.04	10.86	10.86
35	9.65	9.65	9.86	9.86	10.68	10.68
40	9.47	9.47	9.68	9.68	10.51	10.51
45	9.30	9.30	9.50	9.50	10.34	10.34

<sup>4</sup> Pearce and Mortimer, *J.A.C.S.*, 1918, 40, 509.

<sup>5</sup> Smith and Taylor, *J. Res. Nat. Bur. Std.*, 1938, 20, 837.

<sup>6</sup> Akerlof, *J.A.C.S.*, 1932, 54, 4125.



## 578 SILVER CHLORIDE IN METHANOL-WATER MIXTURES

The molal and molar solubilities of silver chloride were found as follows from the values of  $K$ .

Since

$$K = m_{\text{Ag}^+} m_{\text{Cl}^-} \cdot f_{\text{Ag}^+} f_{\text{Cl}^-},$$

and the molal solubility  $m_0 = (m_{\text{Ag}^+} m_{\text{Cl}^-})^{\frac{1}{2}}$ ,  $\log K = \log m_0^2 - 2A\sqrt{C_0}$ ,

assuming that the saturated solutions of silver chloride are sufficiently dilute for the activity coefficients to be given by the Debye-Huckel formula,  $-\log f = A\sqrt{C_0}$ , where  $C_0$  is the solubility on the molar scale. In these dilute solutions  $C_0 = m_0 \bar{d}_0$  where  $\bar{d}_0$  can be taken as the density of the solvent. The densities are given by Harned and Thomas<sup>7</sup> for 10 % and 20 % methanol-water mixtures, and for the 50 % solvent they were measured, being given by  $\bar{d}_t = 0.9055 + 0.000996(t - 30)$  over the temperature range studied. The equation  $\log m_0 = \frac{1}{2} \log K + A\sqrt{m_0 \bar{d}_0}$  was then solved by successive approximations, assuming first that  $\log m_0 = \frac{1}{2} \log K$ . The molar solubilities  $C_0$  were then found from  $C_0 = m_0 \bar{d}_0$ . The results are given in Table III.

TABLE III.—SOLUBILITY OF SILVER CHLORIDE.

t° C.	10 %.		20 %.		50 %.	
	$m_0 \times 10^6$ .	$C_0 \times 10^6$ .	$m_0 \times 10^6$ .	$C_0 \times 10^6$ .	$m_0 \times 10^5$ .	$C_0 \times 10^5$ .
15	0.604	0.593	0.475	0.460	0.182	0.167
20	0.770	0.756	0.599	0.579	0.243	0.223
25	0.970	0.951	0.752	0.725	0.279	0.273
30	1.217	1.191	0.953	0.917	0.373	0.338
35	1.502	1.467	1.180	1.133	0.459	0.413
40	1.849	1.801	1.452	1.390	0.558	0.500
45	2.250	2.187	1.778	1.716	0.680	0.605

From the values of  $\log K$  at a series of temperatures, thermodynamic data for the process  $\text{AgCl (s)} \rightarrow \text{Ag}^+(\text{soln.}) + \text{Cl}^-(\text{soln.})$  can be determined. Since  $-\Delta G^\circ = 2.3026 RT \log K$ , where  $\Delta G^\circ$  is the standard free energy

TABLE IV.

REACTION  $\text{AgCl (s)} \rightarrow \text{Ag}^+(\text{soln.}) + \text{Cl}^-(\text{soln.})$ .

Solvent.	15° C.	20° C.	25° C.	30° C.	35° C.	40° C.	45° C.
$\Delta G^\circ$ (calc.).							
10%	13,770	13,720	13,670	13,650	13,610	13,560	13,550
20%	14,040	14,000	13,960	13,920	13,880	13,850	13,820
50%	15,105	15,085	15,070	15,060	15,050	15,050	15,050
$\Delta H^\circ$ (cal. per mol.).							
10%	16,180	16,080	15,980	15,880	15,770	15,660	15,550
20%	16,390	16,310	16,230	16,130	16,040	15,950	15,860
50%	16,490	16,200	15,910	15,620	15,325	15,010	14,700
$\Delta S^\circ$ (cal. per degree per mol.).							
10%	8.36	8.05	7.74	7.36	7.01	6.71	6.29
20%	8.15	7.88	7.61	7.31	6.99	6.71	6.41
50%	4.81	3.82	2.85	1.86	0.87	-0.12	-1.10

<sup>7</sup> Harned and Thomas, *J.A.C.S.*, 1935, 57, 1666.

change for the reaction, equations for  $\Delta G^\circ$  as a function of  $T$  may be obtained from equations (5), (6) and (7). From  $\Delta S^\circ = d/dT(-\Delta G^\circ)$  and  $\Delta H^\circ = \Delta G^\circ + T\Delta S^\circ$ , the standard entropy and heat content changes may be obtained. Such data are listed in Table IV. These results will be discussed in a succeeding paper.

### Summary.

1. The activity product of silver chloride has been obtained from E.M.F. measurements in three mixtures of methanol and water, over a range of temperatures.
2. The solubility of silver chloride in each solvent has been obtained.
3. Thermodynamic quantities have been calculated for the process,  $\text{AgCl (s)} \rightarrow \text{Ag}^+(\text{soln.}) + \text{Cl}^-(\text{soln.})$

Canterbury University College,  
Christchurch, New Zealand.

---

## THE ENERGY AND ENTROPY OF SOLUTION OF SILVER CHLORIDE IN METHANOL-WATER MIXTURES. PART II.

BY H. N. PARTON AND D. D. PERRIN.

Received 6th July, 1944.

In continuation of the work described in the previous communication,<sup>1</sup> the activity product of silver chloride has been determined in a mixture of methanol and water containing 75 % by weight of methanol. The method was as previously described. Particular care was required in the purification of the methanol, which boiled at  $64.4^\circ \pm 0.05^\circ \text{C.}$ , and gave no reaction with Nessler's reagent and a very slight positive test for ketones by the method used by Hartley and Raikes.<sup>2</sup> Stock solutions were 0.05*m*, and dilutions were made by means of the equation  $x = (n-1)(1-y)$ , where  $x$  is the number of grams of solvent which must be added to 1 gram of solution to give a solution  $1/n$  times as strong, there being  $y$  grams of salt per gram of solvent. This equation is correct to 0.005 % for this work. A faint brown precipitate was observed in the stock solution containing silver nitrate after some weeks, but analysis showed it to weigh less than a milligram, and no further decomposition took place after filtering. The error will be less than that resulting from the preparation of smaller amounts of solution for each cell immediately before use. The cell and electrodes were as previously described, except that in the latter part of the work, the silver chloride electrodes were prepared as suggested by Hornibrook, Janz and Gordon,<sup>3</sup> reducing the time necessary for ageing. Dissolved air did not affect the potentials, as noted by Smith and Taylor<sup>4</sup> for aqueous solutions, and the use of nitrogen, adopted in the previous work, was eliminated.

The E.M.F.s of the cells are recorded in Table I. The functions used in the graphical determination of  $K$  were calculated as in the preceding paper, the dielectric constant of the solvent being obtained by interpolation from Akerlof's data,<sup>5</sup> and the density being determined by

<sup>1</sup> Previous paper.

<sup>2</sup> Hartley and Raikes, *J.C.S.*, 1925, 127, 524.

<sup>3</sup> Hornibrook, Janz and Gordon, *J.A.C.S.*, 1942, 64, 513.

<sup>4</sup> Smith and Taylor, *U.S. Bur. of Stds., J. Res.*, 1938, 20, 837.

<sup>5</sup> Akerlof, *J.A.C.S.*, 1932, 54, 4125.

TABLE I.

$t^{\circ}\text{C.}$	$15^{\circ}$	$20^{\circ}$	$25^{\circ}$	$30^{\circ}$	$35^{\circ}$	$40^{\circ}$	$45^{\circ}$
$m = 0.05.$							
$x = 0.6$	0.5047	0.5017	0.4990	0.4965	0.4940	0.4913	0.4881
$x = 0.4$	0.4884	0.4813	0.4782	0.4752	0.4718	0.4685	0.4647
$x = 0.3$	0.4702	0.4668	0.4634	0.4598	0.4558	0.4524	0.4487
$x = 0.2$	0.4496	0.4462	0.4425	0.4386	0.4343	0.4301	0.4254
$x = 0.1$	0.4151	0.4111	0.4068	0.4021	0.3972	0.3923	0.3869
$m = 0.04.$							
$x = 0.6$	0.4961	0.4928	0.4896	0.4871	0.4841	0.4816	0.4784
$x = 0.4$	0.4758	0.4723	0.4689	0.4657	0.4623	0.4590	0.4556
$x = 0.3$	0.4612	0.4574	0.4540	0.4505	0.4466	0.4427	0.4385
$x = 0.2$	0.4410	0.4371	0.4333	0.4293	0.4251	0.4207	0.4163
$x = 0.1$	0.4062	0.4017	0.3976	0.3930	0.3878	0.3829	0.3775
$m = 0.03.$							
$x = 0.6$	0.4840	0.4812	0.4779	0.4749	0.4718	0.4688	0.4656
$x = 0.4$	0.4641	0.4605	0.4571	0.4536	0.4499	0.4464	0.4423
$x = 0.3$	0.4491	0.4460	0.4421	0.4383	0.4345	0.4303	0.4260
$x = 0.2$	0.4293	0.4254	0.4213	0.4171	0.4127	0.4081	0.4038
$x = 0.1$	0.3946	0.3903	0.3858	0.3808	0.3756	0.3704	0.3651
$m = 0.02.$							
$x = 0.6$	0.4668	0.4638	0.4607	0.4573	0.4540	0.4504	0.4467
$x = 0.4$	0.4469	0.4432	0.4396	0.4358	0.4321	0.4283	0.4244
$x = 0.3$	0.4323	0.4283	0.4249	0.4208	0.4167	0.4124	0.4081
$x = 0.2$	0.4121	0.4080	0.4045	0.3997	0.3953	0.3905	0.3856
$x = 0.1$	0.3777	0.3731	0.3684	0.3632	0.3581	0.3527	0.3474

the pycnometer method. The density of 75 % methanol is given by  $d = 0.8507 - 0.000816(t - 30)$ . The solubility of AgCl was obtained as before. Table II gives the derived data, and shows the agreement

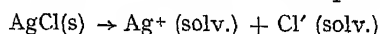
TABLE II.

$t^{\circ}\text{C.}$	$-\log K_{\text{obs.}}$	$-\log K_{\text{calc.}}$	$m_0 \times 10^6.$	$C_0 \times 10^6.$
$15^{\circ}$	12.30 <sub>9</sub>	12.30 <sub>9</sub>	0.702	0.606
$20^{\circ}$	12.12 <sub>3</sub>	12.12 <sub>4</sub>	0.870	0.747
$25^{\circ}$	11.94 <sub>2</sub>	11.94 <sub>3</sub>	1.072	0.916
$30^{\circ}$	11.76 <sub>5</sub>	11.76 <sub>5</sub>	1.315	1.119
$35^{\circ}$	11.59 <sub>0</sub>	11.59 <sub>0</sub>	1.611	1.365
$40^{\circ}$	11.41 <sub>8</sub>	11.41 <sub>8</sub>	1.963	1.654
$45^{\circ}$	11.24 <sub>8</sub>	11.24 <sub>9</sub>	2.388	2.000

between  $-\log K$  observed, and  $-\log K$  calculated by the equation

$$-\log K = 11.107 + 1720.6/T - 0.016558T.$$

From this equation the data of Table III for the process



have been calculated.

## Solvation of the Gaseous Ions.

The changes in energy and entropy for the process Ion (gaseous)  $\rightarrow$  Ion (solvated) can now be readily obtained. The heat of solvation of the gaseous ions is given by  $\Delta H^\circ_{\text{soln.}} = \Delta H^\circ - U$  where  $\Delta H^\circ$  is the standard heat of solution of the solid salt, and  $U$  is the lattice energy of the salt. Mayer's <sup>6</sup> value 205.7 for  $U_{\text{AgCl}}$  has been used.

The entropy of solvation is given by

$$S^\circ_{\text{soln.}} = (\bar{S}^\circ_{\text{Ag}^+} + \bar{S}^\circ_{\text{Cl}^-}) - (S^\circ_{\text{Ag}^+(\text{g})} + S^\circ_{\text{Cl}^-(\text{g})} - S_0),$$

that is by the difference between the sum of the partial molal ionic entropies, and the sum of the entropies of the gaseous ions. The former sum is given by

$$\bar{S}^\circ_{\text{Ag}^+} + \bar{S}^\circ_{\text{Cl}^-} = \Delta S^\circ + S^\circ_{\text{AgCl}}$$

where  $\Delta S^\circ$  is the standard entropy of solution, and  $S^\circ_{\text{AgCl}}$  is the molal entropy of the solid salt, taken as 22.97 E.U. from Latimer's <sup>7</sup> data. The standard entropies of the gaseous ions were found from the Sackur-Tetrode equation, being 39.34 E.U. for  $\text{Ag}^+$  and 36.64 E.U. for  $\text{Cl}^-$ .

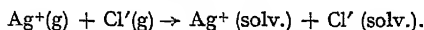
$S_0$  is a correction term, being the entropy change due to compression from the standard state for a gas, where 1 mol. occupies the gram molecular volume, to standard state in solution, of 1 mol per 1000 grams of solvent. This is given by  $S_0 = R \ln \frac{24.46}{\text{Sp. vol.}}$  at 25°C., and varies from 6.36 E.U. for water to 6.04 E.U. for 75 % methanol.

The free energy of solvation can be found from

$$\Delta G_{\text{soln.}} = \Delta H_{\text{soln.}} - T \Delta S_{\text{soln.}}$$

These thermodynamic quantities for AgCl in water (Owen <sup>8</sup>) 10 %, 20 % and 50 % methanol (previous communication), and 75 % methanol (this paper) are recorded in Table IV in the columns marked "expt."

TABLE IV.



VALUES IN KILOCALORIES, OR CALORIES PER DEGREE.

% CH <sub>3</sub> OH.	$-\Delta G_{\text{expt.}}$	$-\Delta G'$	$-\Delta G''$	$-\Delta H_{\text{expt.}}$	$-\Delta H''$	$-\Delta S_{\text{expt.}}$
0	180.2	218.7	162.1	190.1	164.4	33.1
10	179.7	218.5	162.0	189.7	164.4	33.3
20	179.5	218.3	161.8	189.5	164.4	33.5
50	178.2	217.5	161.3	189.8	164.3	38.5
75	177.0	216.3	160.3	191.1	164.3	47.1

<sup>6</sup> Mayer, *J. Chem. Physics*, 1933, 1, 327.

<sup>7</sup> Latimer, *Oxidation Potentials*, Prentice Hall, 1938.

<sup>8</sup> Owen, *J.A.C.S.*, 1938, 60, 2229.

### Discussion.

The free energy of solvation of gaseous ions can be evaluated approximately from Born's<sup>9</sup> equation for the reversible work necessary to take the ions, considered as charged spheres, out of the solvent regarded as a structureless dielectric medium,  $-\Delta G = \frac{Ne^2Z^2}{2r}(1 - 1/D)$  per mol. of ions of radius  $r$  and valence  $Z$ . The third column in Table IV gives the free energies  $\Delta G'$  for AgCl calculated from this formula, using the crystal radii 1.26 for Ag<sup>+</sup> and 1.81 for Cl<sup>-</sup>. Modifications of these radii for use in solution have been suggested by Latimer, Pitzer and Slansky,<sup>10</sup> and also by Voet.<sup>11</sup> The former add 0.85 Å. to the radii for cations, and 0.10 Å. for anions, to allow for the asymmetry of the water molecule. The fourth column of Table IV gives free energies  $\Delta G''$  calculated with this modification. Voet obtained a similar correction of 0.65 Å. for cations, which gives data 5 % larger than  $\Delta G''$ , and hence nearer the experimental figures.

The heats of solvation according to Born's formula will be given by

$$-\Delta H = \frac{Ne^2Z^2}{2r} \left( 1 - \frac{1}{D} + T \frac{\partial}{\partial T} \left( \frac{1}{D} \right) P \right).$$

The values given by this formula, using the corrected radius of Latimer, Pitzer and Slansky, are listed as  $\Delta H''$  in Table IV. Though considerably lower (less negative) than the experimental data, they agree in showing slight variation with solvent. This is also the case with the heats of solvation given for AgCl from the work of Eley and Evans<sup>12</sup> on water, and Eley and Pepper<sup>13</sup> on methanol. These calculations, involving definite assumptions about the structure of the solvents, lead to 155 K.cal. for  $-\Delta H$  in water, and 154 in methanol. The former figure differs from that given by Eley and Evan's table, which was obtained using a radius of 1.13 Å. (Goldschmidt) instead of 1.26 Å. (Pauling) for Ag<sup>+</sup>.

For salts of low solubility  $S$ , for which the activity coefficients of the saturated solutions are near unity, the Born equation requires that  $\log S$  should vary linearly with  $1/D$ . Ricci and Davis,<sup>14</sup> on the basis of the experimentally discovered constancy of the activity coefficients of saturated solutions in a series of solvents, give an equation

$$\log S_2 = \log S_1 + 3 (\log D_2 - \log D_1)$$

where  $S_2$  and  $S_1$  are the solubilities of a given salt in two solvents of dielectric constant  $D_2$  and  $D_1$  respectively. For AgCl the plot of  $\log S$  (on the molar scale, shown by Bell and Gatty<sup>15</sup> to be the correct one) against  $1/D$  deviates largely from linearity. On the other hand the plot of  $\log S$  and  $\log D$  is linear, with a slope of 4.4, instead of 3 as required by the equation of Ricci and Davis, which derives from the Debye-Huckel theory.

### Summary.

1. The activity product of AgCl in a 75 % methanol-water mixture has been measured over a temperature range, and the solubility derived.
2. Thermodynamic quantities for the solution processes of the solid salt, and of the gaseous ions have been derived and compared with data calculated by some theoretical formulæ.

Canterbury University College,  
Christchurch, N.Z.

<sup>9</sup> Born, *Z. Physik*, 1920, 1, 45.

<sup>10</sup> Latimer, Pitzer and Slansky, *J. Chem. Physics*, 1939, 7, 108.

<sup>11</sup> Voet, *Trans. Faraday Soc.*, 1936, 32, 1301.

<sup>12</sup> Eley and Evans, *ibid.*, 1938, 34, 1093.

<sup>13</sup> Eley and Pepper, *ibid.*, 1941, 37, 581.

<sup>14</sup> Ricci and Davis, *J.A.C.S.*, 1940, 62, 407.

<sup>15</sup> Bell and Gatty, *Phil. Mag.*, 1935, 19, 66.

# A METHOD FOR DETERMINING THE INSTANTANEOUS HARDNESS OF PLASTIC SUBSTANCES.

By A. CAMERON.

Received 1st January, 1945. Communicated by Professor E. K. RIDEAL.

In rheology the hardness, yield point or flow stress, are terms that are very often used, but are extremely difficult to measure in absolute units. This is because the material under investigation usually flows slightly during measurement, and so the resultant value is therefore a composite figure containing in addition a function of the plasticity of the material. This same problem is one that is common in metallurgy and therefore a search was made to see if any of the methods proposed by metallurgists could be applied to rheology. An approximate calculation also had to be made to find the speed at which any determination had to be carried out.

A concept was put forward by Maxwell in which he considered the rigidity and viscosity of a substance to be related by the "relaxation-time" of the material. Maxwell's relaxation time may be defined as the time taken by a stress applied to any system to fall to  $1/e$  of its original value. The equation relating these quantities is:—

$$\eta = G\lambda$$

where  $\eta$  = viscosity (poises),  $G$  = rigidity (dynes/sq. cm.),  $\lambda$  = relaxation time (seconds). Now it is clear that if any measurements are to be taken on a system they must be carried out at such a speed that the applied stress has had no time to relax, *i.e.* the measurements must be completed within the relaxation time of the material. The majority of methods usually employed on plastic substances, like greases, take an appreciable time to carry out. The result is that the material has flowed to a greater or lesser extent, and so viscosity effects complicate the interpretation of the results. A calculation of the Maxwell relaxation time of grease will be given later as an indication of the speed at which the determination must be done.

A high speed method for finding the hardness of a material was put forward by Martel<sup>1</sup> in 1895 and a rather similar method by Edwards.<sup>2</sup> He found that if a pyramid of known mass is allowed to fall freely, point downwards from a given height, the striking energy divided by the volume of the indentation is constant under certain conditions. He therefore proposed the Martel Hardness Number  $H$ , defined as the energy in kilogram-millimeters required to displace unit volume of the material under test. These hardness numbers have the units of a stress, energy is  $ML^2/T^2$  and volume is  $L^3$  so energy/volume is  $M/LT^2$ . It is interesting to know how this hardness is related to the flow pressure or yield stress of the material.

It is not entirely clear from Martel's paper what he considers as "unit volume"; apparently it is 1 cubic millimeter. Edwards took it to mean this and this would appear to give reasonable results. Now the values of the hardness as found by Martel are considerably larger than the yield stresses found in normal tensile testing measurements. This is not surprising as the speed at which the deformation was carried out was very

<sup>1</sup> Martel, *Comm. des Methodes d'Essai des Materiaux de Construction*, 1895, 3A, 261.

<sup>2</sup> Edwards, *J. Inst. Metals*, 1918, 20, 61.

large. A recent paper by Manjoine<sup>3</sup> shows that the yield stress of mild steel can increase tenfold at rates of strain of 1000 per second. The values of the hardness found by Martel are therefore of the same order as the values of the yield stress at high rates of strain.

It is not possible to obtain any definite data from his figures on the exact relation between the hardness and the high speed yield stress. It would not seem unreasonable to suppose that they are related.

In the case of greases these units are much too large and so the hardness will be expressed as gram-cm./c.c. displaced, *i.e.* g./cm.<sup>3</sup>.

It is possible to obtain a guide to the speeds necessary to carry out the penetrations from Maxwell's theory. The rigidity of any material can be obtained from  $E$ , the Young's Modulus by the relation

$$G = \frac{E}{2(1 + \sigma)} \text{ where } \sigma = \text{Poisson's ratio,}$$

which can be put equal to  $\frac{1}{2}$  in the case of greases, whence  $G = E/3$ . Young's Modulus for a grease is taken equal to  $10^5$  dynes/sq. cm. and the viscosity at very small rates of shear between  $10^3$  and  $10^5$  poises. The relaxation time is therefore between 3 and  $3 \times 10^{-2}$  seconds. Now let the cone be dropped from a height of 30 cm. and its mass so ordered that it penetrates about 1 cm. into the grease. If we assume, for the purpose of calculation, a constant retarding force on the cone, it takes  $0.8 \times 10^{-2}$  seconds to come to rest. This shows that the method should give results that are largely unaffected by plastic creep, as the applied stresses will not have time to relax.

There is one other point, which was raised in the discussion of Edward's paper, and that is, where all the material goes during the impact. Now it will be shown in the experimental part that there is a secondary effect starting when the cone penetrates deeply. It is thought that this effect is in some way related to the disposal of the displaced material.

The method was tried out on two greases to see if the hardness was constant when the mass of the cone, its angle, and the distance from which it was dropped were varied. A soda-grease of an Institute of Petroleum Technologists penetration number of 230 and a lime-grease of 85 penetration number were used.

### Experimental Method.

Cones of  $90^\circ$  and  $60^\circ$  apex were made by bending up circular blanks of sheet tin-plate, suitable segments having been cut from them to give the requisite cone angle. A stalk of  $1/8$  inch brass rod, 18 ins. long, was soldered inside the cone and was marked with file marks at 5 cm. intervals from the apex of the cone. A glass tube, in which the brass rod could slide easily, was clamped vertically above the grease, whose hardness was to be measured, and the tube was furnished with a mark a known height above the surface of the grease. By means of the marks on the rod and the mark on the glass tube, the cone could be dropped from various heights into the grease. Lead weights were made which could be put into the cone. The normal weight of the cone and rod was 40 grams.

The volume of penetration was found by measuring the distance  $x$  along the cone face that had been in contact with the grease. A pair of spring dividers were found very convenient for marking off the distance. It was sometimes seen that there was a thin band of grease on the cone a millimetre or two higher than the general level of grease in the container. This indicated that the striker had penetrated deeply and then had sprung out a little distance, due to the elasticity of the grease. The amount of penetration was calculated from the top of this band of grease and not from the general level, thus giving the "total indentation" and

<sup>3</sup> Manjoine, *J. Appl. Mech.*, A, 1944, II, 211.

not "recovered indentation."<sup>4</sup> The difference between the top of this band of grease and the general level was not much more than 1 or 2 mm. at the most.

A diagrammatic sketch of the experimental set-up is shown in Fig. 1.

A trial cone was made of 120° solid angle, but it was not used as very small irregularities in the surface of the grease made very large differences in the measured value of  $\alpha$ .

Indentations were carried out by dropping the cone from heights from 5 up to 35 cm. above the grease surface. The container was moved so that the cone struck a fresh, unworked part of the grease surface at each impact.

Extra weights were made from lead strip, giving striker masses of 85, 120 or 182 g. The 40 g. measurements were on the whole rather unreliable. The explanation is either that the striker penetrated such a small distance that any inhomogenities of the grease gave variable results, and with the larger masses the greater penetration averaged out any local variations in the composition, or else is due to some effect, not yet investigated, that occurs with small masses.

### Experimental Results.

The most significant result was that plotting total volume of grease displaced, against height of impact, gave straight lines, for each mass, within the experimental error. The heights varied between 5 and 35 cm. in 5 cm. steps. In one or two cases, the last point (corresponding to the greatest height), showed a slight falling off. This effect, which was not always observed, could probably be ascribed to the extra work required to remove a larger volume of grease, and it only occurs at deep penetrations.

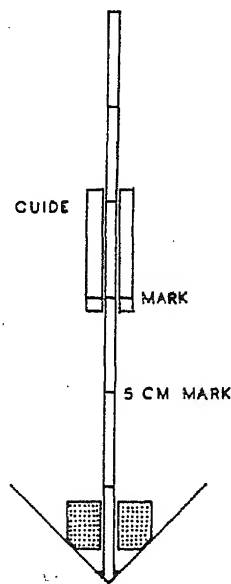


FIG. 1.

TABLE I.

Mass of Striker.	Hardness (g./sq. cm.).	
	60°.	90°.
<b>(A) Soda Grease.</b>		
40 g. . . .	323	274
85 g. . . .	303	294
120 g. . . .	296	282
182 g. . . .	288	292
<b>(B) Lime Soap Grease.</b>		
40 g. . . .	2460	1920
85 g. . . .	—	1780
120 g. . . .	—	1780
182 g. . . .	2400	1780

Results are listed for a soda grease (Table IA) of an I.P.T. Penetration Number of 230. Two cones were used, of 60° and 90° cone angle. The 40 g. results were somewhat variable (mean results being listed), and these are best neglected. It may be said then that the instantaneous hardness of the grease, from an average of the other figures, is  $292 \pm 10$  g./sq. cm.

Interesting results were obtained with the lime soap grease (Table IB). This was quite a hard grease

(I.P.T. Penetration 85). Considerable "piling-up" round the edge of the 60° cone was noticed and this piled-up material actually moved away from

<sup>4</sup> O'Neill, *The Hardness of Metals and its Measurement*, Chapman and Hall, London, 1934, pp. 17 ff.



the cone and thus leads to a smaller apparent volume displaced. This is illustrated in Fig. 2. Piling-up is a well-known trouble in all methods

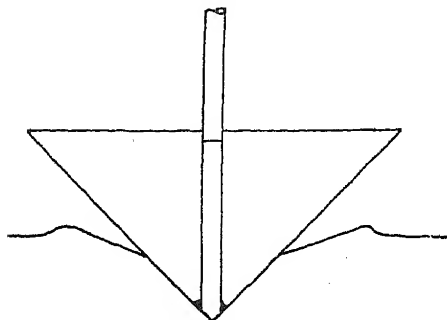


FIG. 2.

of indentation hardness testing,<sup>5</sup> and the cone angles must be chosen so that it does not occur. Edwards found a similar trouble with the metals he investigated. In the case of the lime grease we may take the hardness to be 1780 g./sq. cm. as no piling-up took place with the 90° cone. In general the 90° cone would seem to give the best results with extra weights added to give a mass of 85 g. or more.

### Conclusions.

It is seen that this method gives a convenient method of measuring the hardness of plastic substances, such as greases. It permits an "instantaneous" hardness value to be obtained, and thus obviates the disturbing influences of flow or creep which are encountered with conventional static methods.

### Summary.

A modification of a method due to Martel is described that enables the instantaneous hardness of plastic substances to be measured. A weighted cone is dropped from various heights on to the surface of the plastic. The hardness is given by the energy of impact divided by the volume displaced, which has the dimensions of a stress. This is shown to be substantially independent of the height of drop and weight of the cone. The chief advantage of the method is that the measurements are practically instantaneous, and so well within Maxwell's relaxation time. Errors due to the plastic flow of the system are therefore avoided.

The author would like to thank Professor E. K. Rideal, F.R.S., and Mr. G. D. S. MacLellan, for very useful discussions during the progress of this work.

*Department of Colloid Science,  
The University, Cambridge.*

<sup>5</sup> O'Neill, *op. cit.*, p. 22 ff.

---

## A NULL-POINT DETECTOR FOR DIRECT AND ALTERNATING CURRENT AND ITS USE IN CONDUCTANCE AND E.M.F. MEASUREMENTS.

BY KENNETH R. BUCK AND GILBERT F. SMITH.

*Received 3rd January, 1945.*

The type of instrument used to detect a balance point in an electrical circuit depends on whether direct or alternating current is used. In the one case the galvanometer and in the other case the telephone (or telephone and amplifier) is commonly used. It would obviously be an advantage to have a single instrument which, combining the functions

of both of these, will detect a balance point both with direct and alternating current. The present paper describes such an instrument, which employs as the detector the small cathode ray tube known as the "magic eye".\* It may be mentioned that, as used in this apparatus, the magic eye shows a brightly illuminated area on the fluorescent screen of the tube, this illuminated area being in the form of a cross. At the null-point the area of illumination is at a minimum and consequently the arms of the cross show a minimum width. The fluorescence is of sufficient intensity for the instrument to be used under all the conditions of illumination likely to be found in a laboratory.

The use of circuits involving the magic eye as a null-point detector for A.C. is well established,<sup>1</sup> and at least one commercial instrument makes use of it for this purpose; but as far as the authors are aware it has not been used hitherto in D.C. null-point detectors.

A full circuit diagram is given in the figure. This requires no detailed comment, but it may be noted that standard wireless components are used throughout and that consequently the detector can be easily constructed by anyone familiar with the conventions of the ordinary wireless

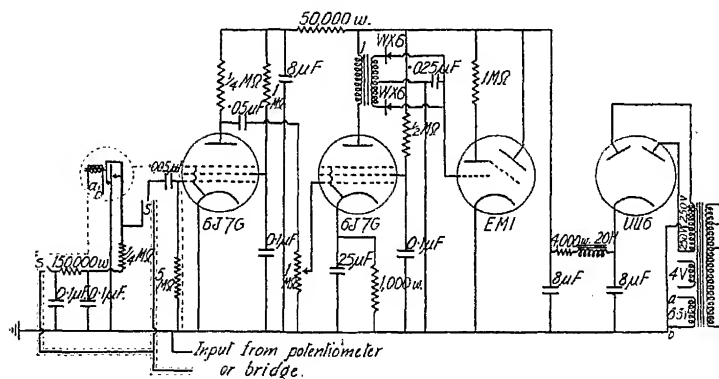


FIG. 1.

circuit diagram. The instrument is converted from an A.C. detector to a D.C. detector by means of the single switch S, which is of the double pole, double throw type. The success of the instrument as a null-point D.C. detector is largely determined by the choice of a suitable make and break. At present, few types are available for trial, but it was found that a Crossley make and break,<sup>†</sup> when modified by rewinding the coil for 6.3 v. is quite satisfactory. It makes 200 interruptions per second, which is the minimum for the sensitivity required. The output wave-form is very steep-fronted and roughly approximates to a square wave.

An important feature of the circuit is the use of a full wave rectifier ‡ followed by a smoothing circuit. This has obvious advantages in dealing with currents of unsymmetrical wave form, and in addition it ensures that the edges of the illuminated area are always perfectly sharp. This greatly facilitates accurate setting, thereby increasing the sensitivity.

If the maximum accuracy is to be obtained in using the detector, some attention should be paid to screening the apparatus from external electrical interference. We find it desirable to place an earthed metal sheet on the bench top underneath the potentiometer, cells, wheatstone bridge or other

\* As for example the Mullard E.M.I.

<sup>1</sup> See, for example, Hovorka and Mendenhall, *J. Chem. Edu.*, 1939, 16, 239.

<sup>†</sup> Made by the Crossley Corporation, Cincinnati, Ohio, U.S.A.

<sup>‡</sup> "Westector" made by the Westinghouse Co.

apparatus being used. In conductance measurements this simple screening suffices provided the conductivity cell is placed in an earthed thermostat. When the detector is used for D.C. measurements in conjunction with a potentiometer, as in the determination of the E.M.F. of a cell, the top of the potentiometer should be of metal, or should be metal covered, and the metal should be earthed. It is necessary to provide special screening for the experimental cell only when this has a very high internal resistance. A metal cover, enclosing the cell, and earthed by standing on the metal sheet on the bench, is entirely adequate for this purpose.

The detector is in use in these laboratories in a bridge circuit for the determination of the conductance of aqueous solutions, as well as in the ordinary potentiometric method for the measurement of the E.M.F. of cells. In the former case, with A.C. of a frequency 1000 cycles per second the sensitivity is of the order of 0.01 m.v. In the latter case, with cells of low internal resistance (less than 1000 ohms) the sensitivity is about 0.1 m.v. The sensitivity decreases only slightly with increase in the internal resistance of the cell. Thus, with a concentration cell of internal resistance as high as  $5 \times 10^5$  ohms, the sensitivity was still about 0.3 m.v. These figures show that the sensitivity of the detector for both D.C. and A.C. is at least as good as that which can be obtained with a galvanometer or with a telephone and amplifier when these are used under the conditions which ordinarily obtain in a laboratory. Moreover, it can be used easily and rapidly, since it is unaffected by noise and vibration and is practically instantaneous in response.

We anticipate that this detector will find a wide range of applicability, but we do not consider that in its present form it is suitable for use with a glass electrode. For the detector to be used for this purpose it would, however, only be necessary to make minor modifications. The existing wireless make and break would have to be replaced by one with an extremely well insulated and screened moving armature, which would allow of an input circuit similar to that described by Chun-Yu Lin.<sup>2</sup>

### Summary.

A null-point detector for D.C. and A.C. is described and its use in conductance and E.M.F. measurements is discussed. The detector is practically free from inertia and gives a visual indication.

*The University,  
Leeds.*

<sup>2</sup> *J. Sc. Inst.*, 1944, **21**, 48.

---

## ON THE DISTRIBUTION OF THE MOLECULAR WEIGHTS OF PROTEINS.

By J. P. JOHNSTON,\* H. C. LONGUET-HIGGINS AND A. G. OGSTON.

*Received 16th January, 1945.*

This is an attempt to find out whether any confidence can be placed in the hypothesis that the molecular weights of proteins fall together into certain groups. The hypothesis was originally due to Svedberg; in its latest form,<sup>1</sup> it states that the rule that the molecular weights are multiples of 17,600 by numbers  $2^m 3^n$  ( $m, n$  being zero or positive integers) is only

\* War Memorial student.

<sup>1</sup> Svedberg, *Proc. Roy. Soc. B*, 1939, **127**, 1.

approximate and that there is some obscuring factor, possibly a variation of the mean residue weight. Bull<sup>2</sup> has questioned the validity of the rule on the grounds of inspection of a logarithmic spectrum of molecular weights; our conclusions agree with his.

We have attempted a statistical examination of the data given by Svedberg;<sup>1</sup> these consist of 57 values determined by one or both of sedimentation velocity and sedimentation equilibrium. Two difficulties confront this attempt at once: first, the values quoted by Svedberg should not be regarded as final; his table could in certain cases be modified by the substitution or inclusion of more recent data; secondly, the hypothesis is not statistically explicit; it does not state what should be the breadth of scatter of the values about the round numbers nor the type of their distribution; nor does it indicate the number of values that are expected to be associated with any round number. With respect to the former difficulty, we have accepted the table of values exactly as given by Svedberg; we do not think that the inclusion of more recently obtained values would affect our conclusions. With respect to the latter, we have been compelled to set up alternative hypotheses of the distribution which, though necessarily arbitrary, may be regarded as being intrinsically as or more likely than that of Svedberg, and to examine whether the data fit one hypothesis better than they do another. We should state that we do not consider that any of the hypotheses of protein structure which claim to define molecular weight are sufficiently well established on their proper grounds to lend support to Svedberg's hypothesis.<sup>3, 4, 5</sup>

We have taken three main lines of approach. The first two of these are designed to show whether there is a significant grouping of any sort. The null hypothesis chosen is, that the logarithms of the molecular weights ( $M$ ) are distributed rectangularly in the range of  $\log M$  which they occupy; examination of the data shows that this is the best general and simple hypothesis over the lower two-thirds of the range of  $\log M$ , though the density of values is markedly lower in the upper third of the range; these methods are therefore applied only to the lower two-thirds. The first method consists of finding whether the distribution of the lengths of intervals between successive values of  $\log M$  differs significantly from that predicted by a rectangular distribution; if there is grouping, there should be an excessive proportion of long and short intervals. The second method tests whether, when the range is divided into a number of "cells" of equal length, the distribution of the numbers of cells that contain different numbers of values of  $\log M$  differs significantly from that predicted by a rectangular distribution; if there is grouping, there should be an excessive proportion of cells containing high and low numbers of values. For the third method, the null hypothesis is that the logarithms of the values of  $M$  occurring between two successive "round numbers" (multiples by powers of 2 and 3 of 17,600) are distributed rectangularly between those limits; a correlation function is used to test whether the observed values agree significantly better with the round numbers than is expected from the null hypothesis; this test is applied over the whole range of molecular weights.

Finally, we have set up an alternative hypothesis, which is not much less simple than that of Svedberg, and which agrees better with the data. We do not claim that this does more than to show that Svedberg's hypothesis is not in unique agreement with the data.

<sup>2</sup> Bull, *Advances in Enzymology*, 1941, 1, 1.

<sup>3</sup> Wrinch, *Proc. Roy. Soc. A*, 1937, 161, 505.

<sup>4</sup> Bergmann and Niemann, *J. Biol. Chem.*, 1938, 122, 577.

<sup>5</sup> Janssen, *Protoplasma*, 1939, 33, 410.

### The Numerical Values Used in Testing.

The values tabulated by Svedberg are derived from sedimentation velocity ( $M_s$ ) or sedimentation equilibrium ( $M_E$ ). In 20 cases values from both are given; for these the values of

$$\frac{1}{20} \sqrt{S \frac{(M_s - M_E)^2}{M_s^2}}$$

is 0.07 and the probability that this would be obtained from a normal distribution of errors is 0.4; accordingly the mean of  $M_s$  and  $M_E$  is used.

### The Interval Method.

The null hypothesis is that the values of  $\log M$  are distributed rectangularly, *i.e.* that

$$\phi(M)dM = k \cdot d(\log M).$$

The number of values of the interval between two successive values of  $\log M$  that would be expected to lie between chosen limits  $l_1$  and  $l_2$  is given by:

$$q_{\text{calc.}} = (N - 1) (e^{-kl_1} - e^{-kl_2})$$

where  $N$  is the number of values of  $\log M$  and  $k$ , their density, is given by:

$$k = (N - 1) / (\log M_{\text{max.}} - \log M_{\text{min.}}).$$

The results are shown in Table I. The most striking thing about these figures is the occurrence of two intervals greater than 0.15 in the first

TABLE I.

$l_1$	$l_2$	$q_{\text{calc.}}$	$q_{\text{obs.}}$
(1) For the first 20 values of $M$ —			
0.00	0.01	5.113	7
0.01	0.025	5.210	7
0.025	0.05	4.712	3
0.05	0.1	3.139	0
0.1	0.15	0.654	0
0.15 upward		0.172	2
		19.000	19
(2) For the next 29 values of $M$ (the rest of the lower $\frac{2}{3}$ of the range of $\log M$ )—			
0.00	0.005	3.170	4
0.005	0.01	2.800	2
0.01	0.025	6.678	4
0.025	0.05	6.936	9
0.05	0.075	3.802	3
0.075	0.10	2.083	4
0.10	0.15	1.770	2
0.15 upward		0.762	0

set; the probability of occurrence of a single interval of this length is 0.16 and of two such it is less than 0.025. The first set of 20 was chosen so as to include these two long intervals, which separate the first three Svedberg groups. The second set of 29 includes the divisions between the third to ninth Svedberg groups; the number of intervals found greater than 0.1 is in accordance with expectation.

Thus, the occurrence of the first two long intervals

is significant, while the occurrence of the others is not.

Apart from these two intervals, the agreement with expectation is good. Pooling the intervals from 0.05 upward in the first set and from 0.1 upward in the second set, the values of  $P$  obtained from  $\chi^2$  are 0.2 and 0.5 respectively, though the values of  $P$  are not accurate since the numbers in the groups are rather small.

### The Cell Method.

The Interval method would not reveal a grouping such that, though the distribution of intervals is in agreement with the null hypothesis, the intervals are arranged systematically according to size; for example, if the smaller and larger intervals are concentrated together or arranged periodically. The Cell method is designed to test for grouping of this type.

The logarithmic range is divided into a series of cells of equal length; for a rectangular distribution of  $\log M$ , the numbers of cells containing given numbers of values of  $\log M$  are given by the Poisson distribution. The number of cells,  $n_{\text{calc.}}$ , expected to contain  $p$  values of  $\log M$  is given by:

$$n_{\text{calc.}} = C \cdot e^{-m} (m^p / p!)$$

where  $C$  is the number of cells and  $m$  is the mean number of values of  $\log M$  per cell;  $n_{\text{obs.}}$  represents the observed value.

As before, this test is applied only to the first two-thirds of the range (48 values of  $\log M$ ). Apart from this, there are two arbitrary choices in applying the test. First, the length of the cell; no useful information can be obtained if the cells are too long or too short; a length of 0.1 (log units) was chosen as being most likely to yield a significant result and this has the advantage that it covers approximately the range of variation of molecular weight that might arise if the proteins of a group contain a constant number of amino acids per molecule of varying mean residue weight. Secondly, the point of origin of the set of cells; it would be expected that even a distribution in accordance with the null hypothesis might give an apparently significant deviation from it if the point of origin were suitably chosen. The observed distribution does in fact vary considerably with the point of origin chosen and so does the probability calculated for any one point of origin; the selection of an arbitrary origin is an arbitrary choice in sampling. The procedure used was therefore as follows: all the different distributions of  $n_{\text{obs.}}$  resulting from different positions of the origin within one cell length were obtained; these values of  $n_{\text{obs.}}$  were averaged, giving each value a weight proportional to the interval of  $\log M$  through which the origin could be moved without changing the distribution; the number of cells used (19) was sufficient to include all the values of  $\log M$  for all origins. This procedure should eliminate errors of sampling. It makes full use of the information available.

Table II shows that the values of  $\log M$  do not tend to fall into groups of this order of size.

TABLE II.— $C=19$ ,  $m=2.526$ .

$p$ .	$n_{\text{calc.}}$	$n_{\text{obs.}}$ (mean).	$\frac{(n_{\text{obs.}} - n_{\text{calc.}})^2}{n_{\text{calc.}}}$
0	1.520	1.695	0.020
1	3.840	5.947	1.156
2	4.850	2.820	0.850
3	4.083	2.731	0.448
4	2.578	3.265	0.183
5	2.130	2.542	0.080
and over			
			$\chi^2 = 2.737$
			degrees of freedom = 4 $P = 0.60$

distribution in accordance with the null hypothesis might give an apparently significant deviation from it if the point of origin were suitably chosen. The observed distribution does in fact vary considerably with the point of origin chosen and so does the probability calculated for any one point of origin; the selection of an arbitrary origin is an arbitrary choice in sampling. The procedure used was therefore as follows: all the different distributions of  $n_{\text{obs.}}$  resulting from different positions of the origin within one cell length were obtained; these values of  $n_{\text{obs.}}$  were averaged, giving each value a weight proportional to the interval of  $\log M$  through which the origin could be moved without changing the distribution; the number of cells used (19) was sufficient to include all the values of  $\log M$  for all origins. This procedure should eliminate errors of sampling. It makes full use of the information available.

Table II shows that the values of  $\log M$  do not tend to fall into groups of this order of size.

### The Correlation Function.

The null hypothesis is that, between consecutive round numbers (multiples by powers of 2 and 3 of 17,600), the values of  $\log M$  are distributed rectangulary; this contradicts Svedberg's hypothesis.

*Notation.*— $N$  = a number of molecular weights ( $M$ ).

$F(N)$  = the correlation function for  $N$  values.

*Definition.*—Let  $A, B$  be consecutive round numbers such that  $A \leq M < B$  for a particular protein.\* Let  $G = (AB)^{\frac{1}{2}}$ . Then

$$\frac{\log M - \log G}{\log B - \log A} \text{ lies between } 0 \text{ and } \frac{1}{2}.$$

Denote  $\left\{ 4 \cdot \frac{|\log M - \log G|}{\log B - \log A} - 1 \right\}$  by  $f(M)$ . Then  $f(M)$  has the following properties :

- (i) it lies between  $-1$  and  $+1$ ;
- (ii) if  $M$  is near a round number,  $f(M)$  lies near  $+1$ ;
- (iii) if  $M$  lies far from a round number,  $f(M)$  lies near  $-1$ ;
- (iv) for a rectangular distribution of  $\log M$  between  $\log A$  and  $\log B$ ,  $f(M)$  is equally likely to have any value between  $-1$  and  $+1$ .

$F(N)$  is the mean of  $N$  values of  $f(M)$ .

A value of  $F(N)$  between 0 and  $\pm 1$  indicates a certain degree of clustering of the values of  $M$  about round numbers; but such a clustering does not lend support to Svedberg's hypothesis unless the chance is small that the observed degree of clustering could arise from the more general distribution law given by the null hypothesis.

### Distribution of $F(N)$ .

Let  $\phi_N(x) \cdot dx$  be the chance that the value of  $F(N)$  for  $N$  values of  $M$ , distributed as in the null hypothesis, shall lie between  $x$  and  $x + dx$ . Then †

$$\phi_N(x) = \frac{N}{2\pi} \int_{-\infty}^{+\infty} e^{-iaxN} \cdot \frac{\sin N a}{a} \cdot da.$$

When  $N$  is  $> 10$ , this differs negligibly from :

$$\sqrt{\frac{3N}{2\pi}} \cdot e^{-\frac{3Nx^2}{2}};$$

that is,  $F(N)$  is normally distributed about 0 with a standard deviation  $s_N = \sqrt{1/3N}$ . The chance  $P$  that  $F(N)$  shall exceed a given value can thus be obtained from a table of normal deviates.

TABLE III.

Range.	$N$ .	$s_N$ .	Svedberg.		Alternative.	
			$F(N)$ .	$P$ .	$F(N)$ .	$P$ .
Complete . . . . .	56	0.077	0.137	0.076	0.223	0.004
First two Svedberg groups . . . . .	19	0.133	0.286	0.032	0.433	<0.001
Complete range less the first two Svedberg groups . . . . .	37	0.095	0.061	0.522	0.116	0.239
First two-thirds . . . . .	47	0.084	0.178	0.034	0.307	<0.001
First two-thirds less the first two Svedberg groups . . . . .	28	0.109	0.105	0.335	0.222	0.041

\* For the four values of  $M$  less than 17,600,  $A$  is undefined; for these we have arbitrarily put  $A = 17,600/2$ .

† We are indebted to Mr. F. J. Dyson for this solution. Before we had it, we had estimated the standard deviation from the distribution of the sum of  $N$  throws of a die, which gave results in good agreement with the true solution.

Table III shows the application of the correlation function to the Svedberg hypothesis over various ranges. It shows also the application to an alternative hypothesis, obtained by inspection of a logarithmic spectrum of molecular weights: namely, that the molecular weights tend to have values 1, 2,  $2^2$ ,  $3^2$ ,  $4^2$  . . . times 17,600.

Although in all cases  $F(N)$  is positive, showing a certain degree of clustering, this is significant for the Svedberg hypothesis only over the first two groups of values. The alternative hypothesis fits much better over the whole range.

### Conclusions.

These tests combine to show that there is some grouping of the lower molecular weights around the first two Svedberg numbers; but this grouping does not amount to more than the occurrence of two gaps in an otherwise rectangular distribution of  $\log M$ . Apart from this, Svedberg's hypothesis receives no support from the evidence.

There do not even appear to be groups of molecular weights such as could arise from sets of proteins containing the same numbers of amino acid residues per molecule, but having different mean residue weights.

However, that there is grosser grouping is indicated by the significant result of the correlation test applied to our alternative hypothesis, which is algebraically nearly as simple as Svedberg's. This grouping is not close and we do not think that it has any meaning in relation to protein structure.

We are grateful to Mr. Ivor Robinson for help and encouragement.

*Balliol College,  
Oxford.*

## A QUANTITATIVE STUDY OF THE CORROSION OF PURE ALUMINIUM.\*

BY F. A. CHAMPION.

*Received 8th February, 1945.*

The value of detailed investigation of the form of corrosion-time curves for providing a better understanding of corrosion processes and a sounder basis for the quantitative assessment of corrosion has been demonstrated by Bengough and his co-workers<sup>1-6</sup> in their work on the corrosion of iron and zinc. The present paper describes the first part of a similar investigation of the corrosion of aluminium. The investigation has been confined so far to aluminium of the highest purity and homogeneity which was obtainable in sufficient quantity: specimens of this metal were totally immersed in a horizontal position in normal potassium chloride solution, the corrosion being measured by the gasometric method developed by Bengough and his co-workers.<sup>1-4</sup>

\* This paper has been largely abstracted from a thesis approved by the University of London for the award of the Degree of Ph.D.

<sup>1</sup> Bengough, Stuart and Lee, *Proc. Roy. Soc., A*, 1927, **116**, 425.

<sup>2</sup> *Idem.*, *ibid.*, 1928, **121**, 88.

<sup>3</sup> *Idem.*, *ibid.*, 1930, **127**, 42.

<sup>4</sup> Bengough and Wormwell, *Rep. Corr. Comm. Iron Steel Inst.*, 1935, **3**, 128.

<sup>5</sup> Bengough, Lee and Wormwell, *Proc. Roy. Soc., A*, 1931, **131**, 494.

<sup>6</sup> *Idem.*, *ibid.*, 1931, **134**, 308.



### Details of Metal.

A billet of pure aluminium was cast and extruded to give a bar of 1.1/8 inch square section (marked C). After scrapping several feet from each end of the extruded bar, the remainder was cut into one foot lengths, which were marked with letters to show the position in the original bar, from CA at the front end (top end of ingot), through CZ, CAA, CAB, etc., to CBK at the back end. After trimming off 1/16 inch from each side of each length, specimens  $1 \times 1 \times \frac{1}{4}$  inches were parted off with as little distortion as possible in the milling machine, using B.P. liquid paraffin as lubricant, the specimens were numbered for identification, but the numbers bore no relation to the positions of the specimens in the one-foot lengths. Analysis<sup>7</sup> showed the metal to contain 0.002 % Si, 0.0002 % Fe and 0.0003 % Cu with no detectable difference between the back and front ends of the bar. A hand shaping machine fitted with a sharp tool made from high speed steel was used, as suggested by the work of R. May,<sup>8</sup> for the final mechanical preparation of the specimen, care being taken to avoid contamination of the specimen during this preparation: B.P. paraffin was again used as lubricant and possibly had another effect in restricting oxidation of the metal (which may occur more readily on metal which is being worked). The specimen, measuring approximately 2.5 cm.  $\times$  2.5 cm.  $\times$  0.5 cm., was then rinsed with A.R. benzene for half an hour in a modified form of Soxhlet apparatus, and annealed for 2 hours at 400° C. in a continuously evacuated Pyrex tube. It was then carefully dusted with filter paper and transferred to the corrosion apparatus.

Metallographic examination of the metal as extruded showed the grain size to be moderately uniform (60-400 grains per sq. mm.), except for an area of relatively large crystals at the back end of the extrusion. The back end as extruded also showed a ring of crystals which had very irregular boundaries and which appeared to be less worked than the metal inside or outside the ring, but this ring was scarcely visible after annealing. X-ray diffraction patterns showed the metal to be completely recrystallised after annealing and also showed the metal to be worked to a depth of 0.01 inch below the surface during the final mechanical preparation before annealing. Micro-examination showed very small gas blisters in annealed specimens especially towards the front end (corresponding to the top of the billet): there were no signs of inclusions.

### Experimental Method.

The essential features of the standard corrosion apparatus described by Bengough and Wormwell<sup>4</sup> were as follows:—

(a) A corrosion vessel of specified dimensions in which the specimen could be totally immersed in a pure saline solution saturated with a gas or mixture of gases.

(b) A platinum spiral in the gas space of the corrosion vessel which could be heated electrically to dull redness to burn the hydrogen evolved during corrosion.

(c) A gas burette and manometer connected to the corrosion vessel through a special stopcock, so that the changes in the quantity of gas in the corrosion vessel could be measured.

The design was modified in the following respects for this work on aluminium as shown in Figs. 1 and 2. In order to allow for the low rates of corrosion expected with pure aluminium, the apparatus was made more sensitive by (a) reducing the capacity of the apparatus, and especially

<sup>7</sup> Champion, *J. Inst. Metals*, 1943, 69, 58.

<sup>8</sup> The British Aluminium Co. Ltd., *Analysis of Aluminium and its Alloys*, Publication No. 399, 1941, 114-116.

<sup>9</sup> R. May, *private communication* through B.N.F.M.R.A.

of the gas space, while maintaining a large gas-liquid interface (the vessels had an internal diameter of 9.4 cm. and contained 250 c.c. of solution), and (b) by using (as in the early work of Bengough, Stuart and Lee<sup>1</sup>)

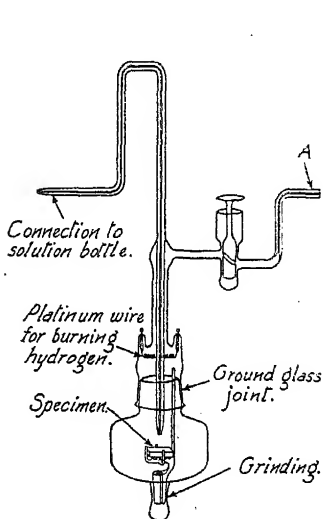


FIG. 1.—Corrosion vessel.

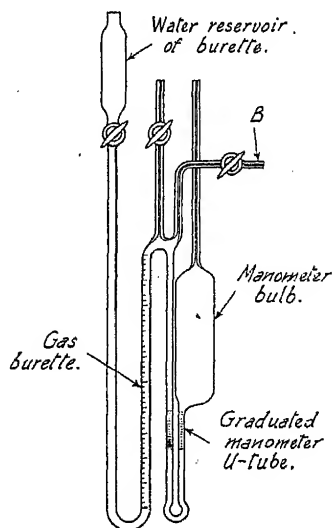


FIG. 2.—Gas burette and manometer.

a small gas burette which could be read with an accuracy of  $\pm 0.005$  c.c. No stopcocks were used on the corrosion vessel itself apart from the main stopcock on the tube connecting the corrosion vessel with the burette and manometer. The stand supporting the specimen was provided with four prongs instead of three in order to carry a square specimen. For the initial experiments a further modification was made by separating the apparatus into two distinct units, namely, (a) the corrosion vessel (Fig. 1), and (b) the burette and manometer (Fig. 2), so that a train of corrosion vessels could be connected (through the tube A) by rubber and glass tubing to one burette and manometer (by tube B): this modification was abandoned for the later experiments since it seemed possible that it might be a cause of abnormal results (although no definite evidence was obtained that the abnormal results observed resulted from this modification).

The solution bottle (Fig. 3) for the preparation of the corroding solution out of contact with air was similar to that described by Bengough, Stuart and Lee,<sup>3</sup> except that no provision was made for the determination of the conductivity of the water in the bottle. Since normal potassium chloride solution was used as the corroding medium, close control of the conductivity of the water used was considered to be unnecessary. The water used was obtained by redistillation of distilled water in a current

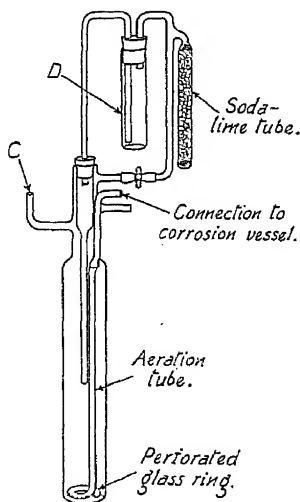


FIG. 3.—Solution bottle.

of pure air, after adding a little alkaline potassium permanganate: a fused silica condenser was used. The specific conductivity of the water obtained was usually about 1 and never exceeded 1.4 reciprocal megohms. The water was collected in the solution bottle by direct connection of tube C to the still: the requisite amount of potassium chloride was subsequently dissolved by forcing the water up into the salt tube D by means of oxygen pressure. The oxygen used in the corrosion tests was supplied in cylinders as hydrogen-free: no hydrogen could be detected in this gas by blank tests in the corrosion apparatus. This oxygen and the air used in the water distillation were each purified by a similar train consisting of: (a) a filter paper membrane, (b) soda lime granules, (c) dilute silver nitrate solution, (d) dilute sulphuric acid solution, and (e) redistilled water.

The apparatus was set up as described by Bengough, Stuart and Lee<sup>1</sup>: half an hour was allowed for the system to reach equilibrium, and the pressure in the corrosion vessel was finally balanced against the manometer of the apparatus:

subsequent changes in the gas phase were recorded as effects of corrosion. Immersion of the specimen normally occurred about 5 hours after completion of its mechanical preparation, while measurement of corrosion started about 45 minutes after immersion. The top surface of the specimen was 1.1-1.5 cm. below the surface of the solution and the oxygen pressure above the solution was maintained at  $760 \pm 2$  mm. Hg. The thermostat in which the experiments were made was insulated as well as possible from vibration and normally showed temperature variations of not more than  $\pm 0.05^\circ \text{C.}$ , the gradient across the bath being not more than  $0.02^\circ \text{C.}$  In the calculation of the results due allowance was made for the fact that absorption of oxygen by corrosion continued during the combustion of the hydrogen: the corrected volumes of hydrogen and oxygen so observed were converted to the equivalent weight of aluminium per unit area of specimen, and then added together to give the total corrosion per unit area.

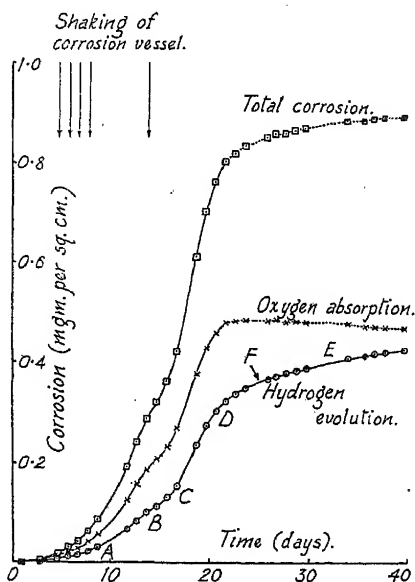


FIG. 4.—Corrosion-time curves for specimen CBD8 at  $25^\circ \text{C.}$

the majority of the corrosion-time curves obtained by this gasometric method were similar in shape for a considerable time after the commencement of corrosion: these are regarded as the normal curves for pure aluminium and are discussed first. Curves which showed major differences from these normal curves were regarded as abnormal. The most common abnormality consisted of apparent irregularities in oxygen absorption which fortunately had no effect on the hydrogen evolution measurements. These abnormal results are briefly discussed later under that heading.

## Results.

The majority of the corrosion-time curves obtained by this gasometric method were similar in shape for a considerable time after the commencement of corrosion: these are regarded as the normal curves for pure aluminium and are discussed first. Curves which showed major differences from these normal curves were regarded as abnormal. The most common abnormality consisted of apparent irregularities in oxygen absorption which fortunately had no effect on the hydrogen evolution measurements. These abnormal results are briefly discussed later under that heading.

**Normal Corrosion-Time Curves.**—Actual corrosion-time curves (of specimen CBD8) which are typical of these normal curves are reproduced

as full lines in Fig. 4 from which it will be seen that the three curves, for hydrogen evolution, oxygen absorption, and total corrosion respectively, are generally similar in shape. The corrosion rate is very low at the start of the experiment, increases to a maximum, declines to a minimum, and then rises to a second maximum before the final decline begins. These features of the curves are shown in Fig. 5, which was obtained from a large-scale version of Fig. 4: the slope ( $dy/dt$ ) of a smooth curve drawn through the experimental points was measured graphically at frequent intervals of time and was plotted (Fig. 5) against the corrosion ( $y$ ) which had occurred up to the corresponding times. It will be seen that the rise in the corrosion rate proceeds mainly according to the equation

$$dy/dt = \beta + \alpha y \quad (1)$$

where  $\alpha$  and  $\beta$  are constants, although their values depend upon whether the first or second maximum is being approached. The decline in the corrosion rate after the second maximum proceeds mainly according to the equation

$$dy/dt = \beta - \alpha y \quad (2)$$

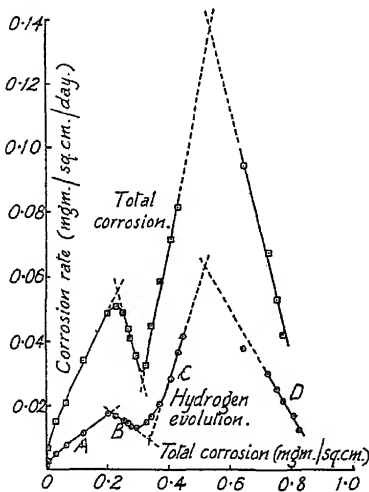


FIG. 5.—Analysis of total corrosion and hydrogen evolution curves of Fig. 4.

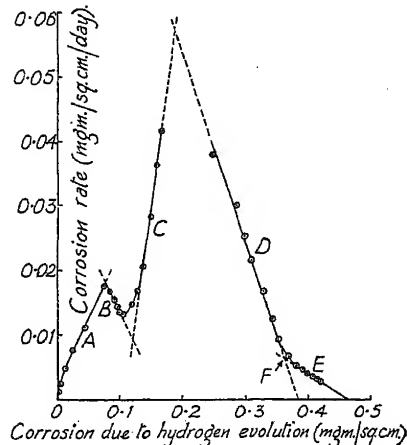


FIG. 6.—Analysis of hydrogen evolution curve of Fig. 4.

The decline in the rate as the minimum is approached probably also follows equation (2), although there is less experimental evidence for this conclusion owing to the shortness of this portion of the curve. The form of the oxygen absorption and total corrosion curves beyond this point is uncertain, owing to the frequent incidence of irregularities in the oxygen absorption measurements as shown by the broken lines in Fig. 4. In order to continue the exploration, the rate of corrosion due to hydrogen evolution is plotted in Fig. 6 against the corrosion due to hydrogen evolution. It will be seen that the equations (1) and (2) still apply over the range covered by Fig. 5, while equation (2) also applies to the continuation of the curve; but at the point F the values of  $\beta$  and  $\alpha$  decrease fairly abruptly (without change of sign) thus causing an inflexion in the curve. There have been suggestions that a similar inflexion occurs at the same time in the oxygen curve, but that this inflexion is less marked in the oxygen curve (and therefore also in the total corrosion curve) than in the hydrogen evolution curve. There are thus five different values to each

By integration of equation (1) we get

Although the temperature fluctuations had no appreciable effect on the corrosion process, close temperature control was evidently necessary for accurate gasometric measurements. The thermostat was therefore operated at 30° C. for the ensuing experiments in order to obtain better control of the temperature. The curves obtained at 30° C. were qual-

tatively similar to those obtained at 25.4° C. except that the minima in the curves were more pronounced at the higher temperature.

In Tables I-II are given characteristic values taken from the curves for various specimens which were not unduly affected by the abnormalities referred to above (p. 596): the parts of those curves which seemed unreliable because of such abnormalities, or because of insufficiently frequent measurements, were ignored in deriving these characteristic values. Since the hydrogen evolution curves were not affected by the abnormalities, most of the values of Tables I-II (namely those in columns M-X) were derived from these curves.

Consideration of the values given in Tables I-II for specimens exposed at 30° C. shows that while the curves were similar qualitatively (p. 596) they varied quantitatively, especially when expressed on a time basis as in columns H, K, M, O, Q, S. For the early stages of corrosion these variations in the time intervals showed marked correlation with the

TABLE I.—VALUES READ FROM NORMAL CORROSION CURVES.

Specimen.		Values from Total Corrosion Curves.					
Mark.	Surface Area (sq. cm.).	Period of Test, (days).	Incidence of Irregularities in Oxygen Absorption (days).	Position of 1st Max.		Position of Minimum.	
				Days.	Mg./sq. cm.	Days.	Mg./sq. cm.
A.	B.	E.	F.	H.	J.	K.	L.
CBE14*	19.9	74	28	13.0	0.2	17.0	0.35
CBD8*	18.9	40	28	12.5	0.24	14.8	0.32
CBD17	19.6	38	18	(4.7)	0.10	11.4	0.30
CBD18	18.9	95	22	6.3	0.17	9.4	0.32
CBD24	18.6	48	26	7.4	0.15	13.7	0.35
CBC4	19.3	51	13	4.3	0.12	8.9	0.30
CBC13	18.2	31	21	15.1	0.18	—	—
CBB2	19.2	75	28	7.0	0.18	9.0	0.26
CBA1	17.2	32	6	—	—	—	—
CBA2*	17.5	34	28	6	0.20	8.3	0.33

\* Corrosion conditions for these specimens non-standard (see text, pp. 598 and 604).

initial  $pH$  of the corroding solution. This correlation is shown in Table III by re-arrangement of the relevant values from Tables I-II. As corrosion proceeded, this correlation became less marked, as is shown, for example, by the time of occurrence of the inflexion F in the hydrogen evolution curve (column S).

The positions of the various inflexions of the curves when expressed in terms of the corrosion observed (columns J, L, N, P, R, T, U and V) showed less variation than the corresponding time intervals: the variation which did occur in the corrosion intervals was most marked in the early stages of corrosion, but showed no correlation with any known conditions at this early stage (e.g. columns J and N). As corrosion proceeded these "gravimetric" variations tended to decrease and also to show some correlation with the identity of the specimens. Thus the values given in columns T, U and V tended to decrease from the CBD specimens to the CBA specimens, i.e. as the position of the specimens in the original extruded bar moved from the back towards the front end of the bar. This is of particular interest with column V giving the values of  $\beta_s/\alpha_s$  since this parameter represents the total loss of metal to be

TABLE  
VALUES READ FROM HYDRO

Specimen Mark.	Values from Hydrogen					
	Position of 1st Max.		Position of Minimum.		Position of 2nd Max.	
	Days.	Mg./sq. cm.	Days.	Mg./sq. cm.	Days.	Mg./sq. cm.
A.	M.	N.	O.	P.	Q.	R.
CBE14* .	14	0.08	16	0.103	18.8	0.180
CBD8* .	12.2	0.076	15.1	0.120	17.5	0.187
CBD17 .	4.4	0.030	9.5	0.110	16.1	0.220
CBD18 .	6.4	0.063	10.6	0.138	14.4	0.210
CBD24 .	8.0	0.072	12.3	0.137	17.8	0.213
CBC4 .	4.2	0.045	8.9	0.131	—	—
CBC13 .	15.7	0.064	23.0	0.122	—	—
CBB2 .	6.7	0.06	9.0	0.096	17.6	0.187
CBA1 .	3.8	0.041	9.4	0.122	16.8	0.204
CBA2* .	6.2	0.08	8	0.11	16.4	0.26

\* Corrosion conditions for these specimens

† The values of Y were obtained by extra-

expected per unit area of the specimen if corrosion was allowed to proceed indefinitely, assuming that no further inflexions occurred in the curve. Moreover, since similar correlation was shown by the "imaginary ultimate corrosion"  $\beta_4/\alpha_4$  (column U), it seems feasible that the correlation would be maintained even if further inflexions did occur. Column W shows that the inflexion F occurs at an approximately constant position on the curve, namely when 79 % of the ultimate corrosion ( $\beta_5/\alpha_5$ )

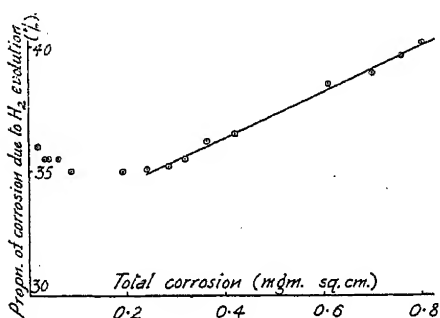


Fig. 7.—Hydrogen evolution from Specimen CBD8.

has occurred; the variations which occur in this percentage appear to be independent of the variations in corrosion conditions (such as the accidental variations in pH or the controlled variations in temperature from 25° to 30° C.) and the identity of the specimens: the variations are attributed to errors in the actual determinations and in the subsequent graphical analysis. The percentage difference between the imaginary ultimate corrosion ( $\beta_4/\alpha_4$ ) and the probable ultimate corrosion ( $\beta_5/\alpha_5$ )

was also found to be approximately constant at less than 20 %, as is shown by column X. Fig. 7 shows how the proportion of corrosion due to hydrogen evolution varied with specimen CBD8 as corrosion proceeded. The proportion for any given time was calculated (as a percentage) from the total hydrogen evolved up to that time and the corresponding value of the total corrosion. It will be seen that for a considerable period the percentage ( $x$ ) of cor-

## II.

## GEN EVOLUTION CURVES.

Evolution Curve.						Corrosion due to Hydrogen Evolution.	
Position of Inflection F.		$\beta_1/\alpha_1$ (mg./sq. cm.).	$\beta_2/\alpha_2$ (mg./sq. cm.).	$T/\bar{V}$ %.	$V-U/\bar{V}$ %.	% at $y=0$ .	Rate of Increase (%/mg./sq. cm.).
Days.	Mg./sq. cm.						
S.	T.	U.	V.	W.	X.	Y.†	Z.
29.1	0.370	0.391	0.452	82	13	30.5	9.0
25.0	0.361	0.384	0.466	78	18	32.7	9.2
21.4	0.304	0.349	0.400	76	13	26.5	57.9
21.9	0.352	0.385	0.440	80	13	32.6	20.4
31.5	0.349	0.389	0.412	84	6	32.2	40.6
< 24	< 0.35	—	0.422	—	—	39.6	15.4
—	—	—	—	—	—	28.0	26.6
30.2	0.297	0.320	0.395	75	19	32.2	13.8
22.7	0.270	0.304	0.340	80	11	39	50
20.3	0.320	0.350	0.397	81	12	30.3	16.8

non-standard (see text, pp. 598 and 604).

polation, see p. 600.

rosion due to hydrogen evolution is related to the corrosion ( $y$ ) which has occurred by the linear law,

$$x = Y + Zy \quad (6)$$

where  $Y$  would be the proportion at the beginning of corrosion if the law held from that time, while  $Z$  shows the relative rate of increase in hydrogen evolution. This relation was found to apply to all the other specimens given in Table II, and the appropriate values of  $Y$  and  $Z$  are given in columns  $Y$  and  $Z$  of Tables II and III. The initial proportion ( $Y$ ) showed a tendency to decrease as the initial  $pH$  of the solution increased (Table III), but this was evidently not the only factor affecting the proportion of hydrogen: the rate of increase in the proportion ( $Z$ ) showed no definite correlation with the  $pH$  values, but appeared to be less at the lower temperature of specimens CBE<sub>14</sub> and CBD<sub>8</sub>. Equation

TABLE III.—EFFECT OF ACIDITY OF SOLUTION ON THE CORROSION OF PURE ALUMINIUM. (EXTRACTED FROM TABLE I).

Specimen Mark.	Depth of Immersion (cm.).	Initial $pH$ of Solution.	Position of 1st Max. (days).		Position of Inflection F in $H_2$ Evolution Curve (days).	Corrosion due to $H_2$ Evolution.	
			By Total Corrosion.	By $H_2$ Evolution.		When $y=0$ (%).	Rate of Increase (%/mg./sq. cm.).
A.	C.	D.	H.	M.	S.	Y.	Z.
CBA <sub>1</sub>	1.5	5.0	—	3.8	23	(39)	50
CBC <sub>4</sub>	1.3	5.2	4.3	4.2	< 24	39.6	15.4
CBD <sub>18</sub>	1.4	5.2	6.3	6.4	22	32.6	20.4
CBD <sub>24</sub>	1.1	5.5	7.4	8.0	32	32.2	40.6
CBC <sub>13</sub>	1.5	5.8	15.1	15.7	—	28.0	26.6



(6) did not fit the experimental observations during the early stages of corrosion: for example it will be seen from Fig. 7 that the observed values of the proportion for CBD8 were higher than those given by equation (6) until almost 0.26 mg. of metal had been corroded per sq. cm., *i.e.* almost until the minimum in the curves of Fig. 4 had been reached. With other specimens this deviation from equation (6) usually ended before the first maximum and always ended before the minimum of the curve was reached: the extent and sign of the deviation also varied, but in most cases the initial observed values were less than those of equation (6). It seems probable that equation (6) holds up to the inflexion F, but no reliable information is available beyond that point owing to the incidence of abnormalities in the oxygen absorption readings (p. 596).

**Appearance of Specimens.**—The specimens were examined under the binocular microscope as soon as possible after removal from the corrosion vessel, and again after detaching the film with concentrated nitric acid. The films were white or slightly greyish in colour and consisted of at least two layers, namely,

- (a) a hard adherent layer next to the metal which could not be removed mechanically without damaging the metal beneath, and
- (b) a relatively loose fluffy type of film above, which could easily be rubbed off with the finger.

The upper layer was thicker on the top surface of the specimen than on the bottom, especially on specimens tested at the higher temperature (30° C.).

The relative difficulty experienced in removing the films with acid was taken as an indication of their protective value. This protection appeared

- (a) to be in general agreement with the mechanical adherence of the film,
- (b) to be due almost entirely to the lower layer of the film,
- (c) to be related to the corrosion which had occurred rather than to the time for which the specimen had been corroding,
- (d) to increase more rapidly on the top than on the bottom surface of the specimen.

Specimens which had passed the inflexion F in the hydrogen evolution curve required several hours' treatment with nitric acid at 30° C. whereas the films on specimens which had suffered very little corrosion were readily attacked with nitric acid at room temperature.

Examination of the specimen after removal of the film revealed general corrosion which was uniform except for selective attack at the grain boundaries. In the early stages the boundaries thus revealed by corrosion were in discontinuous lines, but as corrosion proceeded, continuous lines were formed to give a very clear etch. In several cases in which the corrosion process was well advanced (*e.g.* the curve had passed the inflexion F) this general corrosion was markedly more severe on the bottom than on the top surface: this observation is in agreement with the relative protection afforded by the films on the two surfaces as referred to above. Minute pits were evident on some of the specimens, notably CBD8, CBD17 and CBD24, and could usually be seen quite clearly under the microscope before removal of the film since they were not covered by visible film: with other specimens (still giving normal curves) microscopic examination revealed no pitting. The parts of the specimen which had been in contact with the glass supports of the corrosion vessel were usually free from visible film, but must have been covered by a transparent film since they rarely showed any more corrosion than the general surface of the specimen.

Apart from the variations referred to above, visual examination of the specimens during and after exposure showed no irregularity in thickness of the film on a given specimen.

**Abnormal Results.**—Nineteen tests were carried out under the conditions given on pages 594-96. Irregularities in the oxygen absorption occurred in all of these tests after four weeks (and in some cases before, as shown in Table I, column F). If the corrosion rate at the time was not high actual negative oxygen absorption readings of varying magnitude (up to 0.13 c.c. per day and 2 c.c. total) were obtained as shown by the broken line in Fig. 4. The hydrogen evolution curve usually remained undisturbed during these tests thus showing that unburnt hydrogen was not at any rate a major cause of this abnormality. Five experiments gave corrosion-time curves bearing little or no resemblance to the normal curves but approximating to a series of straight lines of varying slope with the hydrogen evolution abnormally low (sometimes accounting for less than 5 % of the total "corrosion" observed). Of the remaining 14 experiments, 10 are reported in Tables I and II while 4 more gave results similar to the early part of Fig. 4, but experimental difficulties resulted in termination of the experiments before useful quantitative results for quotation in Tables I and II had been obtained.

These abnormalities were investigated by means of (a) corrosion tests under conditions similar to those employed for the work on pages 596-602, (b) blank tests under similar conditions apart from the omission of the metal specimen and (c) examination of uncorroded specimens. In a few cases the measurements indicated slight evolution of hydrogen in the absence of a metal specimen. The following possible causes of the abnormalities were investigated: (a) leakage in the apparatus, (b) temperature disturbances, (c) gas in the metal, (d) formation of hydrogen peroxide, (e) other factors associated with the metal itself, and (f) bacterial infection of the system. The information so obtained was inconclusive as to the importance of bacterial infection, but indicated that the other factors were at least not major causes of the abnormalities. The investigation of this matter was still in progress when the research was interrupted by the war, and had not reached a stage suitable for detailed discussion.

### Discussion of Results.

The exponential equation (4) given on page 598 may be written

$$y = \beta/\alpha - \frac{1}{\alpha\gamma} e^{-\alpha(t-t_0)}$$

where  $t_0$  is the point at which this curve would cut the time axis. Thus when  $t = t_0$ ,  $y = 0$ , so that  $\beta/\alpha = \frac{1}{\alpha\gamma}$ . It is also clear that when  $t$  is infinite the value of  $y$  is

$$y_\infty = \beta/\alpha.$$

Hence equation (4) may be written more simply as

$$y = y_\infty[1 - e^{-\alpha(t-t_0)}]. \quad (7)$$

This form of the equation is more convenient when comparing the results of this investigation with those of other workers in the following discussion. The earlier part of the corrosion-time curve, up to the inflexion F, is first considered and then that inflexion and the later part of the curve are discussed.\*

**Earlier Part of Curves.**—Bengough, Stuart and Lee<sup>1,2</sup> obtained corrosion-time curves for zinc in potassium chloride solution with ample oxygen supply which appear to show close similarity to all the features of the curves given in Fig. 4 for aluminium except the minima in the latter curves. Thus Fig. 9 of their second paper,<sup>2</sup> showing the corrosion-time curves for specimen A69 in N./10 potassium chloride solution, may

\* The application of equation (7) to the loss of mechanical properties of aluminium alloys by corrosion has been considered elsewhere.<sup>18</sup>



underlying film, which is presumably formed by the interaction of ions at the surface of the metal, apparently provides increasing protection against the corrosion which is stimulated by the upper layer of the film: when the protection afforded has reached a high order, *i.e.* in the later part of the curve, this layer of the film will control the corrosion rate. Again the film formation may be expected to be proportional to the total corrosion, and so give an equation of the form

$$dy/dt = \beta - \alpha y. \quad (2)$$

Since the protection afforded by the lower layer of the film increases more rapidly on the top than on the bottom surface (*cf.* p. 602), the value of  $\alpha$  would be higher for the top than the bottom. The conditions for the edges of the specimen are presumably similar to those for the bottom surface.

The broken line curves of Fig. 8 have been drawn for (A) the bottom surface and the edges and (B) the top surface of the specimen from equations (1) and (2): the values for the parameters  $\alpha$  and  $\beta$  were chosen on the basis of the above argument and the experimental values so that equation (1) controlled the early part of each curve and equation (2) the later part of each curve. Since these curves record the corrosion occurring on the two portions of the specimen the corrosion of the whole specimen is represented by curve C which was obtained by the summation of curves A and B. It will be seen that

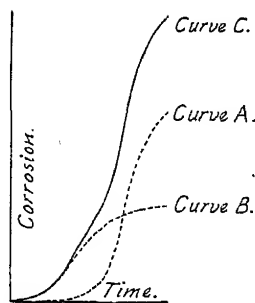


FIG. 8.—Theoretical corrosion-time curves.

- (1) the curve (C) contains all the features of the experimental curves of Fig. 4, up to the inflexion F;
- (2) the hypothesis correlates the differences in film formation on the top and bottom surfaces with the greater corrosion observed on the bottom surface in the more prolonged tests (p. 602);
- (3) the hypothesis correlates the greater differences between the top and bottom surfaces observed at 30° C. (p. 602) with the more prominent minima observed in the experimental curves at that temperature (p. 598).

Accurate quantitative observation of the corrosion process is not possible until the evolution of hydrogen and the absorption of oxygen has affected the gas phase of the system in the corrosion vessel: this evidently accounts for the deviation from equation (1) of the initial portion of the curve, *e.g.* up to total corrosion of about 0.02 mg. per sq. cm. in Fig. 5.

The proportion of the total corrosion accounted for by hydrogen evolution largely depends upon the overvoltage of the specimen. This overvoltage will be controlled at the commencement of corrosion by the configuration of the surface of the specimen, and the impurities exposed to the corroding solution; it is probably modified during the early stages of corrosion mainly by alterations in the former due to the corrosion proceeding. The variation in the proportion of hydrogen evolution with the different specimens during the early stages (p. 602) is attributed to these changes in the physical condition of the surface. The quantity of impurity produced would be expected to be proportional to the total corrosion which had occurred: the direct proportionality of hydrogen evolution to total corrosion which was observed after the minimum in the corrosion-time curves therefore suggests that these impurities control the hydrogen evolution during these later stages of the corrosion process.

Consideration of the corrosion-time curves observed by Steinheil and

Vernon on exposing aluminium to air and oxygen lends support to the above explanation (pp. 604-05) of the curves of Fig. 4.

Steinheil<sup>11</sup> condensed aluminium on to mica *in vacuo*, then admitted oxygen, and measured the increase in transparency due to oxidation of the metal. From these measurements he calculated the thickness of the alumina film formed. The experimental values for foil "XI" taken from Steinheil's graphs are given in Table IV, together with the corresponding values calculated from the equations

$$t = 6 \times 10^{-6} e^{500/y_2},$$

$$y_2 = 0.0440 [1 - e^{-0.0505(t+20)}].$$

It will be seen that the initial portion of the curve up to about 0.1 days closely follows the logarithmic equation, which is the type of equation given by Tammann<sup>12</sup> for the initial oxidation of metals. After about

TABLE IV.—OXIDATION OF ALUMINIUM AS OBSERVED BY STEINHEIL.

Time (days) ( <i>t</i> ).	Thickness of Oxide Film (microns).		
	Expt. Values.	Calculated Values.	
		<i>y</i> <sub>2</sub> .	<i>y</i> <sub>1</sub> .
0.0016	0.0104	0.0111	—
0.0018	0.0114	0.0114	—
0.0026	0.0117	0.0121	—
0.0033	0.0128	0.0126	—
0.0040	0.0132	0.0130	—
0.0044	0.0130	0.0132	—
0.0058	0.0135	0.0137	—
0.0067	0.0134	0.0140	—
0.0122	0.0149	0.0151	—
0.0130	0.0154	0.0153	—
0.0140	0.0152	0.0154	—
0.0144	0.0149	0.0155	—
0.0153	0.0149	0.0156	—
0.0241	0.0170	0.0166	—
0.0380	0.0175	0.0175	—
0.0749	0.0188	0.0188	—
0.84	0.0263	0.0234	0.0296
1.75	0.0290	0.0249	0.0303
3.71	0.0316	—	0.0316
4.72	0.0322	—	0.0322
5.80	0.0330	—	0.0329
7.81	0.0340	—	0.0341
8.79	0.0343	—	0.0347
11.95	0.0364	—	0.0361
12.95	0.0368	—	0.0366
15.15	0.0375	—	0.0374
19.0	0.0384	—	0.0386
20.0	0.0390	—	0.0389
30.0	0.0410	—	0.0410

2 days the curve closely follows the exponential equation (7). The values observed between 0.1 and 2 days lie between the values calculated from these two equations thus indicating a gradual transition. The other curve given by Steinheil (for foil X) covers only the first 0.07 days and was also found to be logarithmic. By differentiation of the logarithmic equation we have

$$dy/dt = k/t$$

so that initially the corrosion rate was a function of the time of exposure, but when the film reached a thickness of about 0.03  $\mu$  the corrosion rate was controlled by the film which had already been formed, as shown by equation (2) (p.597). Lustman<sup>13</sup>

has also examined Steinheil's results: he concluded that Tammann's logarithmic equation was applicable throughout, with an inflexion at about 1.75 day causing changes in the values of the parameters, but the agreement with the empirical values did not appear to be quite as good as in Table IV.

<sup>11</sup> Steinheil, *Ann. Physik*, 1934, 19, 465.

<sup>12</sup> Evans, *Metallic Corrosion Passivity and Protection*, 1937.

<sup>13</sup> Lustman, *Trans. Electrochem. Soc.*, 1942, 81, 363.

In Vernon's experiments<sup>14</sup> hard-rolled aluminium was cleaned by a steel wire brush and then exposed to London air, the resulting increase in weight being observed periodically. The values taken from Vernon's graph for 99.6 % metal (B) are given in Table V, together with the corresponding values calculated from the equations:—

$$y_2 = 0.245 [1 - e^{-0.40(t + 0.75)}],$$

$$y_2 = 0.305 [1 - e^{-0.069(t + 13)}].$$

It will be seen that all the observed values agree with those calculated by equation (7), although there are changes in the parameters of the equation (at 9.2 days): the latter changes constitute a further similarity between this curve and the curve of TABLE V.—ATMOSPHERIC CORROSION OF ALUMINIUM AS OBSERVED BY VERNON.

Fig. 4, but discussion of this point is deferred to page 608. The other two curves published by Vernon<sup>14</sup> for aluminium also conformed to equation (7). Evans<sup>15</sup> put forward the following equation to account for the "general shape" of Vernon's curves,

$$dy/dt = k(Y - y).$$

This is similar to equation (2) (p. 597) where  $k = \alpha$  and

$$Y = \beta/\alpha = y_{\infty}.$$

Evans suggested that this ultimate corrosion value represents the surface layer of metal disturbed during the preparation of the specimen, and that corrosion ceases when it reaches the "undisorganised" metal below: but since the metal was hard rolled it would be worked throughout its thickness. Moreover this explanation is not applicable to Steinheil's condensed aluminium "foil" or to the specimens used by the author: the ultimate corrosion of the latter specimens was equivalent to a depth of about 0.0001 in. (Fig. 4), whereas X-ray examination showed that the specimens were worked to a depth of about 0.01 in. (p. 594) and were then fully recrystallised on annealing. Evans has since suggested<sup>15</sup> mechanical cracking of the film to account for the shape of Vernon's curves but has not developed this argument mathematically.

It may be noted also that the equation given above for the first part of Vernon's curve involves an induction period of — 0.75 day, which shows that the curve would not follow this equation from the origin. Vernon's earliest observation was made after 0.4 day exposure, while Table IV indicates that the logarithmic equation is applicable only to the initial portion, probably less than 0.2 day, of Steinheil's curve. It seems quite possible therefore that there was an unobserved logarithmic initial portion to Vernon's curves, so that the form of these curves shows no divergence from that of Steinheil's curves.

Bryan and Morris<sup>16, 17</sup> have published corrosion-time curves for

<sup>14</sup> Vernon, *Trans. Faraday Soc.*, 1927, 23, 150.

<sup>15</sup> Evans, *Trans. Electrochem. Soc.*, 1943, 83, 340.

<sup>16</sup> Bryan, *Rep. Food Invest. Board, Dept. Sci. Indust. Res.*, 1938, 217.

<sup>17</sup> Bryan and Morris, *J. Soc. Chem. Ind.*, 1940, 59, 159.

aluminium of various purities (ranging from 99.2 to 99.992 %) in an alkaline, buffered solution of  $pH$  10.78 in the presence and absence of oxygen. Corrosion was assessed by determining the loss of weight of the specimens: the lower accuracy (as compared with the gasometric method) and the practical difficulty of obtaining frequent determinations by this method render the results unsuitable for detailed mathematical analysis. Their results are in qualitative agreement with those given in the present paper, however, despite the marked difference in corrosion conditions. The curves for the 99.992 % aluminium were similar to those of Fig. 4 except that the step in the curve (*i.e.* the minimum in the corrosion rate) and the inflexion F were not evident. With the less pure metal the initial increase in corrosion rate was much less and, in fact, was evident only in one case<sup>16</sup> where more frequent determinations had been made.

The similarity in the form of the corrosion-time curves observed for these different metals under various conditions suggested that the corrosion or oxidation is controlled in each case by the same type(s) of oxide film. The fact that no acceleration but only deceleration of corrosion was observed in the atmospheric corrosion tests is in accordance with the explanation put forward for the acceleration observed by the author (pp. 604-05), since the salts giving rise to corrosive corrosion products would not be likely to occur in sufficient quantities in those atmospheres. Steinheil's experiments apparently included (during the early stages) a type of alumina film not usually observed, since corrosion tests on aluminium almost invariably start on film-covered metal: on the other hand, the evidence for the exponential equation (2) is perhaps less convincing under the dry conditions employed by Steinheil.

**Later Part of Curves.**—Consideration of the later part of the corrosion-time curves shows further similarity between the results obtained by the author and other workers. Thus, the values for oxygen absorption observed for zinc (specimen A68) in N./5000 potassium chloride solution<sup>2</sup> are given in Table VI, together with the values ( $y_1$ ) calculated by Bengough, Stuart and Lee, assuming the parameters of equation (7) to remain constant throughout, and the values ( $y_2$  and  $y_3$ ) calculated by the present author, allowing for changes in the value of the parameters at the inflexion F (p. 597): the total corrosion curve for this specimen appeared to be similar to the oxygen absorption curve, but insufficient information was available to check this similarity mathematically. The close agreement between the observed and the calculated values when the inflexion F is recognised demonstrates the occurrence of that inflexion with zinc and the applicability of the exponential equation (7) beyond that inflexion: the values given in Table V show that the same is true for aluminium exposed to air. (Apparently Steinheil's curve detailed in Table IV had not reached the inflexion F). Further similarity between these results is shown in Table VI in which the relations between the parameters of the equations given in Tables V and VI are compared with the mean values of the author's observations (columns W and X of Table II). This agreement, especially in the position of the inflexion F relative to the ultimate corrosion, for these varied experimental conditions and between individual experiments made by the author (p. 600), supports the view that in each case the corrosion is controlled by the same type of film: it also indicates a fundamental change in the character of the film at this inflexion, the nature of which requires further investigation. The occurrence of the inflexion in the oxygen absorption curve for zinc, and the total corrosion curve for aluminium in air, indicates that the inflexion observed in the hydrogen evolution curve by the author was not due to any abrupt change in the proportion of corrosion accounted for by hydrogen evolution.

<sup>16</sup> Champion, A.S.T.M.-A.I.M.E., Symposium on Stress Corrosion Cracking, 1944, Preprint No. 17.

On continuing the exposure of his specimens beyond the period considered in Table V, Vernon<sup>14</sup> observed breaks in the curves which he attributed to cracking and subsequent repair of the film. It seems unlikely that such breaks would occur on immersed specimens in laboratory tests, especially since they occurred on the same date with different

TABLE VI.\*—CORROSION OF ZINC AS OBSERVED BY BENGOUGH, STUART AND LEE.

Time (days) (t).	True Oxygen Absorbed (c.c.).			
	Expt. Values.	Calculated Values.		
		$y_1$ .	$y_2$ .	$y_3$ .
2	2.8	2.9	3.0	—
4	7.9	7.9	7.8	—
6	12.5	12.3	12.2	—
8	16.4	16.2	16.3	—
10	19.75	19.7	19.8	—
12	22.65	22.65	22.8	—
14	25.3	25.38	25.5	—
16	27.7	27.7	27.8	—
18	29.8	29.8	29.7	—
20	31.5	31.7	31.4	—
24	34.6	34.8	34.7	—
28	37.1	37.6	37.1	—
34	39.9	40.0	39.8	—
40	41.6	41.7	41.5	—
46	42.6	42.9	42.7	42.7
50	43.1	43.4	—	43.0
60	44.0	44.3	—	43.9
70	44.75	44.8	—	44.8
80	45.6	45.1	—	45.6
100	47.0	45.3	—	47.0
150	49.6	45.4	—	49.6

\*  $y_1$  = values calculated by Bengough, Stuart and Lee.

$y_2 = 45.3[1 - e^{-0.063(t-8)}]$ .

$y_3 = 56.1[1 - e^{-0.0068(t+500)}]$ .

TABLE VII.—CONSTANCY IN RELATIONS OF PARAMETERS.

Metal.	Corrosive Agent.	Parameters.			Relations of Parameters.	
		Position of Inflection F (a).	$\beta_4/\alpha_4$ (b).	$\beta_5/\alpha_5$ (c).	$\frac{(a)}{(c)}\%$ .	$\frac{(c)-(b)}{(c)}\%$ .
Aluminium .	Chloride	—	—	—	79	13
Zinc . . .	Chloride	42.7	45.3	56.1	76	19
Aluminium .	Air	0.240	0.245	0.305	79	20

specimens irrespective of the time for which the specimen had been exposed, thus suggesting that they were due to variations in the exposure conditions. In this connection it is interesting to note that in Bryan's experiment<sup>16</sup> corrosion had ceased after 2 days' immersion and no further loss of weight was observed during the ensuing 5 days' immersion.



### Summary.

The corrosion of pure aluminium specimens totally immersed in a horizontal position in normal potassium chloride solution has been studied by periodical measurements of the hydrogen evolved and the oxygen absorbed. Irregularities in the corrosion-time curves and other abnormalities have occurred in many cases and require further investigation, but the typical corrosion-time curves appeared to be similar to those reproduced on a small scale in Fig. 4. The step in these curves is attributed to lack of synchronisation in the corrosion processes at the top and bottom surfaces respectively. The simple curve for a surface corroding under uniform conditions appears to be similar to curve (A) of Fig. 8. During the early stages the corrosion rate increases according to the following equation, probably owing to the effect of corrosion products on corrosion

$$dy/dt = \beta + \alpha y$$

where  $y$  is the corrosion,  $t$  the time of exposure and  $\beta$  and  $\alpha$  are constants: when a certain loss of metal has occurred the corrosion rate declines according to the following equation, probably owing to the formation of a protective film:—

$$dy/dt = \beta - \alpha y.$$

The integrated form of this equation may be expressed:—

$$y = \beta/\alpha [1 - e^{-\alpha(t-t_0)}]$$

where  $\beta/\alpha = y_{\infty}$  = ultimate corrosion  $t_0 = t$  when  $y = 0$ .

Slight changes in the values of the parameters  $\beta$  and  $\alpha$  caused a slight inflexion in the curve when 79 % of the ultimate corrosion had occurred: this inflexion may be associated with a critical stage in film formation. Over a considerable proportion of the curve, the proportion of corrosion due to hydrogen evolution bore a linear relation to the total corrosion which had occurred, which suggests that the hydrogen evolution was then controlled by the effect of impurities in the metal on the overvoltage.

The corrosion-time curves were more reproducible on the basis of the amount of metal corroded than on a time basis. The variations in the time intervals between the inflexions in the curves, which were more marked in the earlier stages of corrosion, appeared to be associated mainly with the corrosion conditions, but the corrosion rate was not controlled by the rate of supply of oxygen to the specimen. The smaller variations in the metal corroded at the later inflexions of the curve appeared to be associated with the characteristics of the metal.

Many of the features of these corrosion-time curves for aluminium show a marked resemblance to those obtained for zinc under similar conditions and for aluminium under different conditions by other workers, although the explanations put forward by those workers do not always apply.

The author is indebted to the British Aluminium Co. Ltd., for permission to publish this paper, and to Dr. A. G. C. Gwyer, Scientific Manager of the Company, under whose general direction the work proceeded. He also wishes to record his thanks to his colleagues in both the Laboratories and Works of the Company, and especially to Mr. N. D. Pullen, F.R.I.C., and Mr. E. E. Spillett, B.Sc., A.Inst.P. for their valued assistance and advice.

# THE MECHANISM OF THE HYDROLYSIS OF TRIMETHYL ORTHOPHOSPHATE.

BY E. BLUMENTHAL AND J. B. M. HERBERT

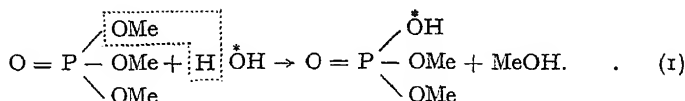
Received 20th February, 1945

In recent years the mechanisms of the acid and alkaline hydrolysis of carboxylic esters and of the acid catalysed esterification of carboxylic acids have been studied extensively by the use of the heavy oxygen isotope as indicator.<sup>1-3</sup> It seemed of interest to extend this work to the esters of non-carboxylic acids.

The experiments described below deal with the hydrolysis of the trimethyl ester of orthophosphoric acid. The mechanism of hydrolysis has been studied in presence of excess NaOH, in excess of dilute HCl and under conditions of "autohydrolysis",<sup>4</sup> i.e. in a solution which is initially neutral but which becomes progressively more acid as the products of hydrolysis accumulate.

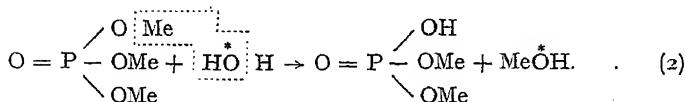
## Method.

The essential feature of the experiments is the hydrolysis of the trimethyl phosphate in presence of water containing excess of heavy oxygen isotope ( $O^{18}$ ), followed by the isolation of the methyl alcohol produced and determination of its heavy oxygen content. If the alcohol is found to contain the normal percentage of heavy oxygen this indicates that the overall change taking place during hydrolysis is:



the symbol  $\overset{*}{O}$  denoting oxygen which is enriched in the heavy isotope.

If, however, the heavy oxygen content of the alcohol is greater than normal the hydrolysis must have proceeded—wholly or partly—by the reaction:



The results will not, of course, indicate whether the actual hydrolytic agent is a water molecule as written above, a hydroxyl ion or a hydroxonium ion.

The above argument presupposes that there is no exchange of oxygen between water and methyl alcohol. According to Cohn and Urey<sup>5</sup> no such exchange is detectable in 7 hours at 100° C. According to Datta, Day and Ingold<sup>2</sup> the same holds true at 100° C. in presence of  $N_2/2$  HCl. Roberts and Urey<sup>6</sup> report no exchange in alkaline solutions at 70° C.

<sup>1</sup> Polanyi and Szabo, *Trans. Faraday Soc.*, 1934, **30**, 508.

<sup>2</sup> Datta, Day and Ingold, *J. Chem. Soc.*, 1939, 838.

<sup>3</sup> Roberts and Urey, *J. Amer. Chem. Soc.*, 1938, **60**, 2393.

<sup>4</sup> Hughes, Ingold and Masterman, *J. Chem. Soc.*, 1939, 840.

<sup>5</sup> Cohn and Urey, *J. Amer. Chem. Soc.*, 1938, **60**, 679.

<sup>6</sup> Roberts and Urey, *Ibid.*, 1938, **60**, 880.

## 612 HYDROLYSIS OF TRIMETHYL ORTHOPHOSPHATE

These results are incidentally confirmed by our own experiments reported below.

The interpretation of the results is complicated by the following considerations :

(a) The main reaction, *i.e.* hydrolysis, is complicated by side reactions as under, *viz.* :—

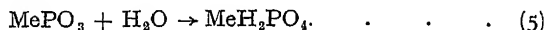
Dimethyl ether is formed either by the attack of methyl alcohol (produced by the hydrolysis) on the ester



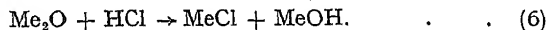
or by the reaction



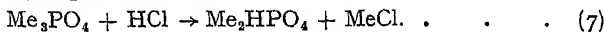
possibly followed by :



In the presence of hydrochloric acid demethylation of the ether takes place :



Methyl chloride is also formed both by esterification of the methyl alcohol and by the relatively rapid reaction :

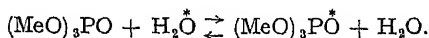


In alkaline solution and under conditions of autohydrolysis these considerations do not disturb the main reaction appreciably. They decrease the yield of methyl alcohol but all the alcohol found is produced by the hydrolysis and the isotopic composition of the water and of the alcohol both remain unaffected.

In presence of HCl however reactions 4 and 6 together provide a source of "normal" methyl alcohol independent of the hydrolyses, though the proportion of heavy oxygen in the water remains unaffected.

In our experiments the amount of HCl initially taken has been limited to 10 mole per cent. of the ester. This makes the initial mixture approximately molal in HCl but prevents excessive formation of methyl chloride. By the time that the amount of HCl has been appreciably diminished by the above side reactions sufficient hydrolysis has occurred to maintain the acidity of the mixture. In the autohydrolysis experiments the mixture, although initially neutral, has a final acidity not very different from that of the acid hydrolysis series.

(b) The heavy oxygen content of the water used may be reduced either by exchange of oxygen between the water and the glass walls of the reaction vessel or by exchange reaction between the water and the ester such as



It is therefore desirable to determine the concentration of heavy oxygen in the water at the beginning and end of each experiment.

(c) It is conceivable that the mechanism of hydrolysis may be different for the removal of the first and second methyl groups. It is therefore necessary to determine the extent to which hydrolysis has proceeded.

### Experimental.

**Materials used.**—The heavy oxygen water was prepared by Hertz's method of fractional diffusion through mercury vapour.<sup>7</sup> The water used had an excess density of about 200 p.p.m. The trimethyl phosphate was obtained by the fractionation of the commercial product *in vacuo*.

The caustic soda required for the alkaline hydrolysis was prepared *in*

<sup>7</sup> Hertz, *Z. Physik*, 1934, **91**, 810.

*situ* by the action of the heavy oxygen water on metallic sodium. The required amount of sodium was obtained by the decomposition of the calculated quantity of sodium azide.

### Preparation of the Reaction Mixtures.

The reaction vessel was made of German soda glass and had a capacity of about 10 ml.

In the alkaline hydrolysis series the desired weight of sodium azide was first introduced and decomposed by heating to  $350^{\circ}\text{C}$ . *in vacuo*. The nitrogen was pumped off and the required quantity of water distilled in and allowed to react with the sodium. After pumping off the hydrogen the ester was distilled into the mixture, the vessel was sealed off, and heated at  $100\text{--}110^{\circ}\text{C}$ . for 18–24 hours.

The neutral and acid mixtures were prepared in a similar way, the sodium azide being omitted.

The composition of the mixture was approximately: water 14 millimol., ester 2 millimol. together with either 3 millimol. NaOH or 0.18 HCl.

### Analysis of the Reaction Products.

The reaction vessel was connected to a vacuum line and the volatile constituents distilled into a small tap vessel cooled in liquid air.

The reaction vessel was then broken up in distilled water and the phosphoric acid residues estimated by titration with caustic soda using phenolphthalein and methyl orange as indicators according to the method of Cavalier.<sup>8</sup>

The mixture of volatile and gaseous components was warmed up to room temperature and the vapours allowed to escape into a vessel of known volume. The pressure developed gave an approximate measure of the methyl chloride plus ether formed during reaction. In the case of the acid hydrolyses the volatile components were distilled on to 2 mgm. of pure calcium oxide. (The consequent loss of heavy oxygen was allowed for.) No attack by HCl on the quicklime was observed indicating that practically all the HCl has been converted into methyl chloride. From these measurements the extents of hydrolysis and "decomposition" of the trimethyl phosphate can be estimated.

The remaining water-alcohol mixture was distilled into the fractionating column shown in Fig. 1 and the greater part of the methyl alcohol isolated. This fractionating column is an adaptation of the "rectification flask" developed by Benedetti-Pichler and his co-workers.<sup>9</sup> The boiler AB was filled with glass-wool and surrounded by a closely fitting glass tube wound with nichrome wire and heated to  $240^{\circ}\text{C}$ . The bulbous part BC of the column served to steady the ebullition, the fractionation taking place along the portion CD. The distillate was caught in the graduated capillary EF. After fractionation was completed the column was sealed off at C'.

The fractionation was carried out in an atmosphere of dry air. With

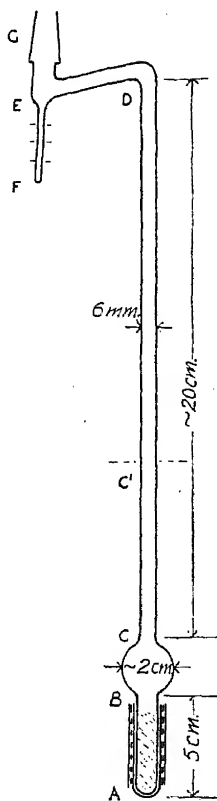


FIG. 1.

<sup>8</sup> Cavalier, *Comptes Rendues*, 1898, 127, 60.

<sup>9</sup> Gettler, Niederl and Benedetti-Pichler, *Microchemie*, 1932, 11, 173.

room temperatures of between 18° and 25° C. such columns were found to deliver distillates of pure methyl alcohol at pressures down to 14 cm. Hg, the optimum yields being obtained at the lowest pressures. The columns were tested with mixtures of 200 cu. mm. water and 90 cu. mm. methyl alcohol, corresponding in quantity and composition to those obtained from the hydrolysis products. From 70-90 % of the methyl alcohol was recovered in the pure state from these test solutions.

**Purity of the Methyl Alcohol.**—To detect small amounts of water in the methyl alcohol an adaptation of Emich's micro boiling-point method<sup>10</sup> was used. Three pairs of boiling-point capillaries were prepared, as shown in Fig. 2, one of each pair being filled with pure methyl alcohol

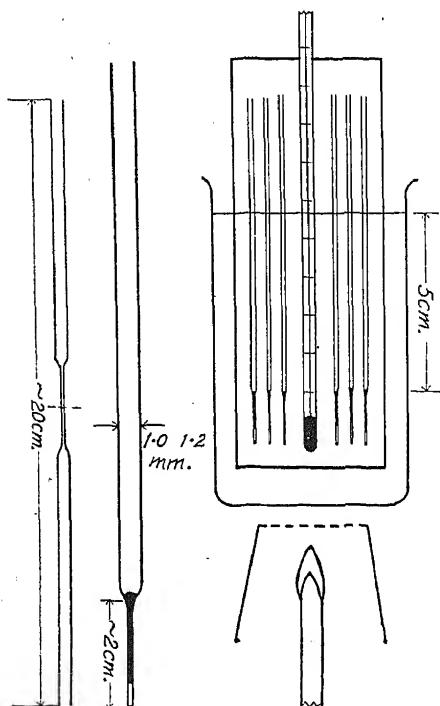


FIG. 2.

dried over metallic calcium; the other with the alcohol to be tested. The capillaries were heated in a well-stirred water bath, the rate of heating being reduced to 1° C. per minute on approaching the boiling range. On reaching the boiling range the droplets were observed during their period of steady ascent. Tests showed that with alcohol containing 1 mol. % water the droplets lagged behind those from pure methyl alcohol by about 3 cm. Three pairs of capillaries were used to obviate erratic results due to imperfectly filled capillaries.

### Determination of the Heavy Oxygen Content.

#### (a) In the Methyl Alcohol.

—The heavy oxygen content of the methyl alcohol was determined by converting the oxygen into water and measuring the excess density of the latter.

The alcohol was decomposed into carbon monoxide and hydrogen by circulation of the vapour over a white-hot platinum filament. Any undecomposed methyl alcohol was frozen out in a liquid air trap and the carbon monoxide reduced to water and methane by circulation with excess of hydrogen over a nickel catalyst. The details of this method, including the subsequent purification of the water produced, are described fully in a previous paper by Herbert and Lauder.<sup>11</sup> The excess density of the water was determined by the micropycnometer method of Gilfillan and Polanyi.<sup>12</sup> The probable error of the density determination is about 2 parts per million.

**(b) In the Water.**—The water residues from the fractionation described above were vaporised and the vapour circulated over a white-hot platinum filament to decompose methyl alcohol and other organic impurities. The

<sup>10</sup> Emich, *Monatsch. Chem.*, 1917, 38, 219.

<sup>11</sup> Herbert and Lauder, *Trans. Faraday Soc.*, 1938, 34, 432.

<sup>12</sup> Gilfillan and Polanyi, *Z. physik. Chem.*, 1933, 166, 254.

water was frozen out in a trap cooled to  $-80^{\circ}\text{C}$ . and the gaseous decomposition products pumped off. This process was repeated three times and the density of the water determined. A small correction has to be made for the exchange of oxygen between the water and the carbon monoxide produced by the cracking of the organic impurities. During the experiments on alkaline hydrolysis rather poorly reproducible results were obtained for the density of the water. Refinement of the technique, in the direction of more efficient "cracking", led to considerably better reproducibility in the work on autohydrolysis and hydrolysis in acid solutions (*cf.* Table I).

TABLE I

Expt.	$\Delta\rho\text{H}_2\text{O}$ init.	$\Delta\rho\text{H}_2\text{O}$ final.	$\Delta\rho$ alcohol.	Hydrolysis + Decomposition.	Decom- position
Alkaline hydrolysis.					
A7	181	159, 163, 172	0	1st stage 90:100 % 2nd stage 20-30 %	20 %
A8	181	155, 170, 172, 177	0.1		
A9	198	172, 174, 198, 203, 210, 242	0		
Autohydrolysis.					
B1	0	—	4	1st stage 90-100 % 2nd stage 90-100 %	20 %
B2	188	—	163		
B3	188	184, 185	134, 136		
B4	188	184, 190, 190	124, 129		
Acid hydrolysis.					
C1	0	—	0	1st stage 90-100 % 2nd stage 60 %	30 %
C2	188	175, 179, 180	114, 118		
C3	188	—	119		

### Results.

The results are summarised in Table I.  $\Delta\rho\text{H}_2\text{O}$  (initial) gives the excess density (in parts per million) of the heavy oxygen water used in the experiments.

$\Delta\rho\text{H}_2\text{O}$  (final) is the corresponding figure (where measured) for the residual water after the hydrolysis has been carried out.

$\Delta\rho_{\text{alcohol}}$  is the excess density of the water into which the alcohol produced in the hydrolysis is converted (for purposes of estimation). Each figure in these columns refers to a density determination on a separately purified sample of water. In column 5 under the heading "% hydrolysis + decomposition" is given the % of the methyl groups of the ester which have been removed whether as alcohol or, by side reactions, as dimethyl ether or methyl chloride.

"1st stage" refers to the conversion of trimethyl ester into dimethyl ester and "2nd stage" to conversion of the dimethyl ester into monomethyl ester. These figures are calculated from the titrations of the acid residues with caustic soda.

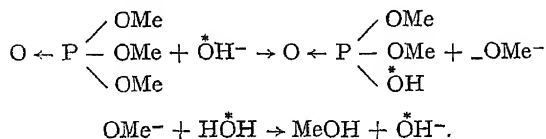
Column 6 "% decomposition" gives the amount of dimethyl ether plus methyl chloride formed, and is estimated from the pressure developed by the volatile products as described above.

The figures in column 5, calculated from the titration of the acid residues, show that the first methyl group has been completely removed in

## 616 HYDROLYSIS OF TRIMETHYL ORTHOPHOSPHATE

all cases and that considerable attack has taken place on the second methyl group, the removal of the latter being almost complete in the autohydrolysis series. Since it is unlikely that one stage proceeds to completion before the attack on the next alkyl group commences, it may be fairly concluded that the results involve the mechanism of hydrolysis of all three methyl groups of the ester.

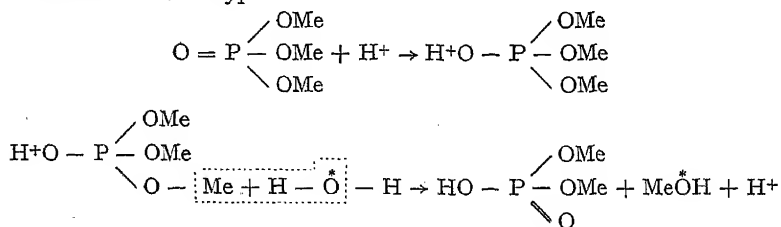
The figures in column 4 show that in the alkaline solution the hydrolysis has proceeded entirely by the breaking of the P—OMe bond, presumably by some mechanism as the following :—



The results incidentally confirm the absence of oxygen exchange between water and methyl alcohol under our experimental conditions. The figures for the density of the "heavy water" at the end of the experiment (column 3) do not show good agreement among themselves probably owing to insufficient purification in the earlier experiments.

In the autohydrolysis and acid hydrolysis series the density of the water decreases little, if at all, during the experiment. The figures here agree well among themselves and indicate that exchange of oxygen from the water has not taken place to any appreciable extent.

The figures for the heavy oxygen content of the alcohol produced are not quite unambiguous. They show definitely that 70 % of the hydrolysis has resulted in the splitting of the O—Me bond of the ester, *e.g.* by a mechanism of the type



Neither the precise point of attachment of the proton nor the degree of synchronisation of the removal of the methyl group and the attachment to it of the hydroxyl group are decided by the results of our experiments.

The fact that the excess density is only 120 instead of 188 p.p.m. may be due to the dilution with "normal" alcohol produced by the side reactions considered earlier in this paper, or to a different mechanism of hydrolysis of the third methyl group leading to normal instead of heavy alcohol. Another possibility is that two different hydrolysis mechanisms proceed simultaneously, the faster reaction yielding "heavy" alcohol, the slower one yielding "normal" alcohol.

The fact that the increased decomposition in the acid hydrolysis series is accompanied by the formation of a lighter alcohol rather favours the view that the deficiency in heavy oxygen content is due to dilution with normal methyl alcohol produced by the side reactions 4 and 6 above.

Further work on the isotopic composition of the ether formed is necessary to clear up this question.

In conclusion we wish to thank Professor Polanyi for helpful advice and criticism during the course of the work.

### Summary.

An investigation has been carried out on the hydrolysis of trimethyl orthophosphate using water enriched in heavy oxygen as "indicator".

The results show that during hydrolysis in alkaline solution the P—OMe bond of the ester is broken but that when the solution is acid or neutral the . O—Me bond breaks preferentially.

*Department of Chemistry,  
The University, Manchester 13.*

---

## EXTRAPOLATION OF THE EXPERIMENTAL CRITICAL TEMPERATURES OF THE NORMAL PARAFFINS.

BY J. CORNER.

*Received 6th March, 1945.*

*(Communicated by Prof. J. E. LENNARD-JONES.)*

### 1. Introduction.

The following attempt to extrapolate the observed critical temperatures of the normal paraffins was carried out to make possible a test of a theory of the critical temperatures of high members of the series. The results are presented separately because it is believed that they are of interest in themselves. The critical temperatures of the higher members are well over 600° K., so that appreciable decomposition takes place during experimental work in the critical region. This makes the extrapolated results of particular value; while critical temperatures as such are not of much importance in this region there is still considerable value in the scale of 'reduced temperatures' provided thereby.

Experimental results are known from methane to *n*-octane, and the extent of the available data is reduced by the fact that it is difficult to embody results for methane and ethane in formulæ fitting the higher members. This is a well-known feature of physical properties of a homologous series, and appears, for example, in the melting- and boiling-points of the paraffins. We exclude methane and ethane from our discussion.

Formulæ of various types have been fitted to the observations and it has been found that certain simple formulæ fit the experimental data with errors little greater than the uncertainties of the latter. These formulæ have been used for extrapolation to higher members of the series, and define a band within which one may expect the true critical temperatures to lie. This band is narrow at first but widens as one proceeds towards the higher members, and the uncertainty in the extrapolated critical temperature becomes of order 5% for  $C_{25}H_{52}$ . For many purposes this would mark the limit of use of the extrapolation. The uncertainty increases rapidly thereafter. The fact that the experimental results can be represented with errors of only 0.1° C. by formulæ with only three arbitrary constants, indicates that the observed results are not likely to be altered greatly in the near future. The uncertainty remaining in the extrapolation can be reduced only by determination of critical temperatures for higher paraffins than *n*-octane.

### 2. Data on Critical Temperatures and Boiling-points.

Relations between the critical temperature  $T_c$  and the boiling-point  $T_b$  have been found useful in extrapolation of  $T_c$ ; accurate values of  $T_b$  are known up to  $C_{18}$  while  $T_c$  is known only as far as  $C_8$ .



## 618 CRITICAL TEMPERATURES OF NORMAL PARAFFINS

Since the summaries of Cox,<sup>3,4</sup> there have been a number of experimental re-determinations and several critical compilations of data, such as those of Egloff, Sherman and Dull,<sup>7</sup> Deanesley and Carleton,<sup>5</sup> and Francis.<sup>8</sup> It is believed that the values listed in Table I are the best available at present. Their general accuracy is shown by the results of section 3, where it is shown that formulæ with only three arbitrary constants can be made to fit the observed values of  $T_c$  with errors of order 0.1° C. As some of these formulæ involve  $T_B$  as well as  $T_c$  this checks both  $T_B$  and  $T_c$  up to  $C_8$  to an accuracy of about 0.1° C.

Methane and ethane are omitted from Table I because it is usual to find that simple formulæ for the variation of the physical properties of normal  $C_nH_{2n+2}$  with change in  $n$ , break down for  $n = 1$  and rather less violently for  $n = 2$  (cf. Cox,<sup>4</sup> Egloff, Sherman and Dull,<sup>7</sup> and Francis<sup>8</sup> with reference to vapour pressures).

TABLE I.—EXPERIMENTAL BOILING-POINTS AND CRITICAL TEMPERATURES OF NORMAL  $C_nH_{2n+2}$ .

$n$	3	4	5	6	7	8
$T_B$ °K.	231.0 <sup>a</sup>	272.7 <sup>d, e</sup>	309.2 <sup>g, h, i</sup>	341.9 <sup>g, h</sup>	371.6 <sup>i, j</sup>	398.8 <sup>g, h, k</sup>
$T_c$ °K.	370.0 <sup>b, c</sup>	426.4 <sup>f</sup>	470.4 <sup>b</sup>	508.0 <sup>b</sup>	540.1 <sup>b</sup>	569.4 <sup>b</sup>
$n$	9	10	11	12	13	14
$T_B$ °K.	423.9 <sup>g, h, i, j</sup>	447.2 <sup>g, h</sup>	469.0 <sup>g</sup>	489.4 <sup>g, i</sup>	508.7 <sup>m</sup>	526.8 <sup>m</sup>
$n$	15	16	17	18		
$T_B$ °K.	543.8 <sup>m</sup>	559.7 <sup>m</sup>	574.6 <sup>m</sup>	588.5 <sup>m</sup>		

<sup>a</sup> Hicks-Bruun and Bruun, *J. Amer. Chem. Soc.*, 1936, **58**, 810, recommended by Burgoyne, *Proc. Roy. Soc. A*, 1940, **176**, 280.

<sup>b</sup> Young, *Sci. Proc. Roy. Soc. Dublin*, 1909, **12**, 389.

<sup>c</sup> Deschner and Brown, *Ind. Eng. Chem.*, 1940, **32**, 836.

<sup>d</sup> Dana, Jenkins, Burdick and Timm, *Refrig. Eng.*, 1926, **12**, 387.

<sup>e</sup> Aston and Messerley, *J. Amer. Chem. Soc.*, 1940, **62**, 1917.

<sup>f</sup> Seibert and Burrell, *ibid.*, 1915, **37**, 2683.

<sup>g</sup> Shephard, Henne and Midgley, *ibid.*, 1931, **53**, 1948.

<sup>h</sup> Mair, *Bur. Stand. J. Res.*, 1932, **9**, 457.

<sup>i</sup> Smittenberg, Hoog and Henkes, *J. Amer. Chem. Soc.*, 1938, **60**, 17.

<sup>j</sup> Smith and Matheson, *Bull. Bur. Stand.*, 1938, **20**, 641.

<sup>k</sup> Wojciechowski, *Proc. Amer. Acad. Arts Sci.*, 1940, **73**, 363.

<sup>l</sup> Mair and Streiff, *J. Res. Bur. Stand.*, 1940, **24**, 395.

<sup>m</sup> From compilation of Deanesley and Carleton, *J. Physic. Chem.*, 1941, **45**, 1104.

### 3. Formulæ for Extrapolation of the Critical Temperatures.

The following formulæ, each involving two arbitrary parameters, were fitted to the experimental results for  $n = 3$  to 8. In these and all other formulæ in this paper temperatures are given in degrees Kelvin and logarithms are to base 10. Three relations between  $T_c$  and  $n$  were tested:

$$T_c^{-1} = \alpha + \beta/n \quad . \quad . \quad . \quad . \quad . \quad (1)$$

$$T_c = \alpha + \beta/n \quad . \quad . \quad . \quad . \quad . \quad (2)$$

$$\log T_c = \alpha + \beta \log n. \quad . \quad . \quad . \quad . \quad . \quad (3)$$

The third is due to Aten.<sup>1</sup> The mean deviations are respectively 2.3°, 10.0° and 2.8° K. Four relations between  $T_c$ ,  $T_B$  and  $n$  were also tried:

$$T_c/T_B = \alpha + \beta \log (T_c/V_c) \quad . \quad . \quad . \quad . \quad . \quad (4)$$

$$T_c/T_B = \alpha + \beta n \quad . \quad . \quad . \quad . \quad . \quad (5)$$

$$T_B/T_c = \alpha + \beta n \quad . \quad . \quad . \quad . \quad . \quad (6)$$

$$T_c = \alpha + \beta T_B. \quad . \quad . \quad . \quad . \quad . \quad (7)$$

$V_c$  is the critical volume per mole. The first of these formulæ was derived<sup>2</sup> from a theory of liquids due to Lennard-Jones and Devonshire,<sup>10</sup> and though the theory assumes spherical symmetry of the molecules the relation (4) is the most successful of all these two-constant formulæ. With the constants taken as  $\alpha = 1.3696$ ,  $\beta = 0.8369$  the mean deviation in  $T_c$  is only  $0.4^\circ \text{K}$ . The mean deviations of (5), (6) and (7) are respectively  $1.5$ ,  $1.0$  and  $3.7^\circ \text{K}$ . The form (7) was proposed as an empirical relation by Livingston,<sup>11</sup> who also gave a more accurate formula with a term  $\gamma T_B^2$  on the right-hand side.

The following relations with three arbitrary parameters were tested in the same way:

$$\log T_c = \alpha + \beta \log (n + \gamma) \quad . \quad . \quad . \quad (8)$$

$$T_c = \alpha + \beta \log (n + \gamma) \quad . \quad . \quad . \quad (9)$$

$$\log T_c = \alpha + \beta \log n + \gamma n \quad . \quad . \quad . \quad (10)$$

$$\log (T_c/n) = (\alpha + \beta n)/(1 + \gamma n) \quad . \quad . \quad . \quad (11)$$

$$\log (T_c/n) = \alpha + \beta n + \gamma n^2 \quad . \quad . \quad . \quad (12)$$

$$T_c^{-1} = \alpha + \beta n^{-1} + \gamma n^{-2} \quad . \quad . \quad . \quad (13)$$

$$T_c = (\alpha + \beta n)/(1 + \gamma n) \quad . \quad . \quad . \quad (14)$$

Some of these are familiar. For example, type (9) with  $T_t$  in place of  $T_c$  has been applied to the melting-points of the paraffins by Moullin<sup>12</sup> and with  $T_B$  in place of  $T_c$  has been used to represent the boiling-points of aliphatic hydrocarbon series (Egloff, Sherman and Dull<sup>7</sup>). Best of (8) . . . (14) are (8) and (11), which have root-mean-square deviations between  $0.1$  and  $0.2^\circ \text{K}$ . Of the others, only (9) is better than (4) and that only by a trivial amount.

An attempt was now made to add a third term to (4), the best of the two-constant formulæ. It was found that

$$T_c/T_B = \alpha + \beta \log (T_c/V_c) + \gamma n \quad . \quad . \quad . \quad (15)$$

and

$$T_c/T_B = \alpha + \beta \log (T_c/V_c) + \gamma n^2 \quad . \quad . \quad . \quad (16)$$

were as good as (8) and (11). Finally modifications were made to the forms (8) and (11) in the hope of further improvement, but none of the alternatives tested showed a mean deviation less than double that of (8) and (11).

Inserting the numerical constants, we arrive at

$$T_c/T_B = 1.22616 + 1.19521 \log (T_c/V_c) + 1.5216 \times 10^{-2}n \quad (15a)$$

$$T_c/T_B = 1.33721 + 0.94631 \log (T_c/V_c) + 4.2545 \times 10^{-4}n^2 \quad (16a)$$

$$\log T_c = 2.47519 + 0.3340 \log (n - 1.1) \quad . \quad . \quad . \quad (8a)$$

$$\text{and } \log (T_c/n) = (2.37574 + 0.162956n)/(1 + 0.123296n) \quad . \quad . \quad . \quad (11a)$$

To use (15a) and (16a) for extrapolation we need  $T_B$ , which is known up to  $n = 18$ . The critical volume  $V_c$  is also required, but this can be estimated with sufficient accuracy from the critical density of  $0.234 \text{ g./c.c.}$  This is the value observed by Young<sup>14</sup> for  $n = 5, 6, 7$  and  $8$ .

In Fig. 1 we show the extrapolated critical temperatures up to  $n = 18$ , calculated from (15a), (16a), (8a) and (11a). The greatest deviation from the mean is  $18^\circ \text{K}$ , at  $n = 18$ ; this is a deviation of just over  $2\%$ . Also shown on Fig. 1 is an extrapolation of Young's critical temperatures for  $n = 5, 6, 7$  and  $8$ , carried out by Wilson and Bahlke.<sup>13</sup> This is not seriously out of line with our extrapolations.

The behaviour of (8a) and (11a) for  $n$  greater than  $18$  is shown in Fig. 2. The increasingly rapid divergence continues for all values of  $n$ , for it can be seen that for sufficiently large  $n$ , (8a) leads to  $T_c \propto n^{0.334}$  whereas (11a) gives  $T_c \propto n$ . The deviation of these curves from their mean reaches  $5\%$  at  $n = 25$ , so that the extrapolation beyond this point is of little use for either theory or practice. Further progress appears to require either the measurement of critical temperatures on paraffins above  $n$ -octane, or the correlation of physical properties with  $T_c$  followed

## 620 CRITICAL TEMPERATURES OF NORMAL PARAFFINS

by observation of such properties on high members of the series. The first alternative cannot be pushed far, because of decomposition during the experiments. The second alternative would not require such high

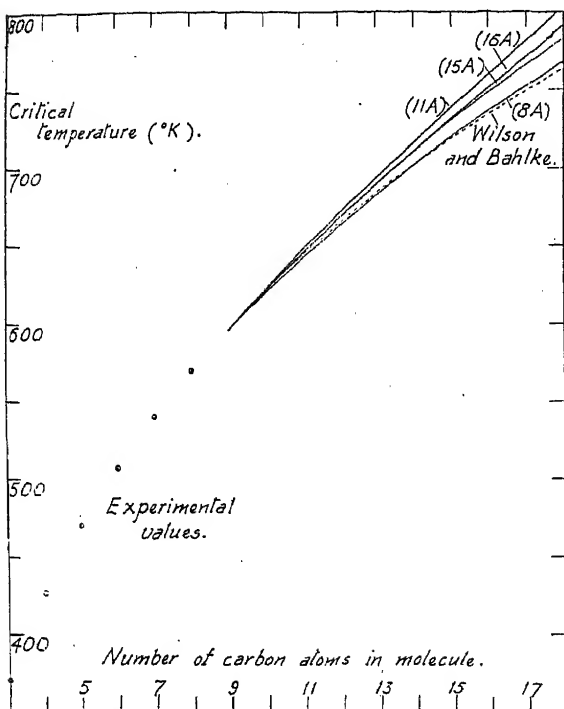


FIG. 1.

Critical temperatures of the normal paraffins up to  $C_{18}$ , extrapolated by the empirical formulae (8a), (11a), (15a) and (16a), together with an extrapolation by Wilson and Bahlke.

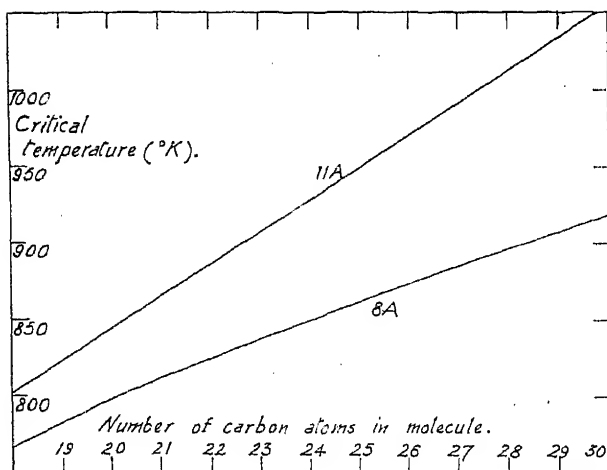


FIG. 2.

Critical temperatures of the normal paraffins above  $C_{18}$ , extrapolated by formulae (8a) and (11a) of the text.

temperatures but the lower accuracy of determination would make it worth while only at values of  $n$  of, say, 20. The possibilities of correlation with  $T_c$  are shown in the work of Egloff and Kuder<sup>6</sup> on molar

volumes of the liquid hydrocarbons, and Katz and Saltman<sup>9</sup> on surface tensions of the normal paraffins.

It might be expected that formulæ of types (8) and (11) would be superior to type (9) as a representation of the boiling-points of the normal paraffins. This is not the case. The form (9), used by Egloff, Sherman and Dull,<sup>7</sup> is much superior to the others. Our list of boiling-points is slightly different from those of Egloff, Sherman and Dull,<sup>7</sup> and by a least-squares fit to the data from  $C_3$  to  $C_{13}$  we find as best constants:

$$T_B = 726.98 \log (n + 4.1) - 388.03 \quad (17)$$

whose results differ very little from the formula

$$T_B = 745.42 \log (n + 4.4) - 416.31$$

recommended by Egloff, Sherman and Dull. The root-mean-square deviation from (17) is only  $0.3^\circ \text{K.}$ , compared with best values of  $1.5^\circ \text{K.}$  and  $2.2^\circ \text{K.}$  from the formulæ analogous to (8) and (11).

### Summary.

It is shown that the observed critical temperatures of the normal paraffins from propane to *n*-octane can be represented by four formulæ, each with three arbitrary parameters, with deviations of order  $0.1^\circ \text{K.}$  The use of these formulæ enables one to estimate critical temperatures of the higher paraffins, with an uncertainty which is small at first and increases rapidly later. The uncertainty is of order 5 % for  $n - C_{25}H_{52}$ .

I am indebted to Professor J. E. Lennard-Jones, F.R.S., for his interest in this work, and to the Director-General of Scientific Research and Development, Ministry of Supply, for permission to publish this note.

*Armament Research Department,  
Ministry of Supply.*

<sup>1</sup> Aten, *J. Chem. Physics*, 1937, 5, 264.

<sup>2</sup> Corner, *Trans. Faraday Soc.*, 1940, 36, 781.

<sup>3</sup> Cox, *Ind. Eng. Chem.*, 1935, 27, 1423.

<sup>4</sup> Cox, *ibid.*, 1936, 28, 613.

<sup>5</sup> Deanesley and Carleton, *J. Physic. Chem.*, 1941, 45, 1104.

<sup>6</sup> Egloff and Kuder, *Ind. Eng. Chem.*, 1942, 34, 372.

<sup>7</sup> Egloff, Sherman and Dull, *J. Physic. Chem.*, 1940, 44, 730.

<sup>8</sup> Francis, *Ind. Eng. Chem.*, 1941, 33, 554.

<sup>9</sup> Katz and Saltman, *ibid.*, 1939, 31, 91.

<sup>10</sup> Lennard-Jones and Devonshire, *Proc. Roy. Soc., A*, 1938, 165, 1.

<sup>11</sup> Livingston, *J. Physic. Chem.*, 1942, 46, 341.

<sup>12</sup> Moullin, *Proc. Camb. Phil. Soc.*, 1938, 34, 459.

<sup>13</sup> Wilson and Bahlke, *Ind. Eng. Chem.*, 1924, 16, 115.

<sup>14</sup> Young, *Sci. Proc. Roy. Soc. Dublin*, 1909, 12, 389.

## SOME NOTES ON THE THEORY OF UNIMOLECULAR GAS REACTIONS IN TRANSITION-STATE SYMBOLISM.

BY M. G. EVANS AND G. S. RUSHBROOKE.

*Received 29th March, 1945.*

### 1. Introduction.

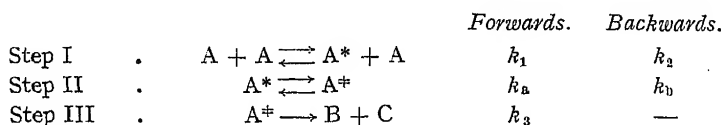
These notes on the theory of unimolecular gas reactions do not lay claim to any considerable originality. But recent contributions to the literature on unimolecular rate processes<sup>1</sup> would appear to confuse rather than clarify the essentials of a unimolecular mechanism: or, perhaps more precisely, the essentials of those mechanisms which apply in practice

<sup>1</sup> Eley, *Trans. Faraday Soc.*, 1943, 39, 168. Barrer, *ibid.*, 1942, 38, 322.

to known gas reactions. On the other hand those contributions have the advantage of dealing with unimolecular processes by means of the *transition-state method*: a valuable descriptive procedure which has come into use since the original papers by Fowler and Hinshelwood, Kassel and others were published.<sup>2</sup> We have therefore, *inter alia*, tried to show how Kassel's theory, which has not since been superseded, can be expressed in transition-state symbolism. For mathematical convenience we have employed classical rather than quantal statistics, but, of course, this is not essential to the argument. We have also tried to draw attention to those aspects of the problem of unimolecular processes which seem to us to stand in most need of further theoretical treatment.

## 2. The Model used.

The picture which we shall employ to describe a unimolecular process involves three familiar steps and may be expressed symbolically as follows:



Step I is bimolecular: it describes the effect of collisions in producing abnormal molecules,  $A^*$ , which we shall speak of as *energized*. Step II describes an internal change in an energized molecule to a more specific state in which we shall refer to it as *activated*. In step III an activated molecule spontaneously decomposes into two parts, B and C, *i.e.* the "reaction," as such, takes place. To each step, forwards or backwards, we assign a specific rate constant as shown above.

We shall, of course, have to specify the states of *energization* and *activation* (sometimes called "primary activation" and "secondary activation") much more definitely, but before doing so shall calculate the overall rate of the reaction on the assumption that equilibrium is set up in steps I and II.

The conditions for relative equilibrium between A,  $A^*$  and  $A^\ddagger$  molecules are

$$k_1 A^2 = k_2 A A^* + k_a A^* - k_b A^\ddagger \quad (1)$$

$$k_a A^* = k_b A^\ddagger + k_3 A^\ddagger \quad (2)$$

and, of course, 
$$\frac{dB}{dt} = k_3 A^\ddagger \quad (3)$$

These equations lead at once to the formula for the overall rate constant

$$k = \frac{1}{A} \frac{dB}{dt} = \frac{k_1 k_a k_3 A}{k_2 (k_b + k_3) A + k_a k_3} \quad (4)$$

## 3. Classification of Reactions on Basis Step II or Step III Rate-determining.

Equation (4) simplifies considerably if  $k_b \ll k_3$  or if  $k_3 \ll k_b$ . Considering these possibilities separately, we have:

Case (i):  $k_b \ll k_3$ ,

$$k = \frac{k_1 k_a A}{k_2 A + k_a}$$

and the reaction is unimolecular provided  $k_2 A \gg k_a$ , in which case

$$k_{un1} = k_a \cdot k_1 / k_2.$$

<sup>2</sup> See Kassel, *Kinetics of Homogeneous Gas Reactions*, Chemical Catalogue Co., 1932.

We see that we can refer also to this simple process as one in which step II is rate-determining.

Case (ii) :  $k_3 \ll k_b$ ,

$$k = \frac{k_1 k_a k_3 A}{k_2 k_b A + k_a k_3}$$

and the reaction is unimolecular provided  $k_2 A \gg k_3 \cdot k_a/k_b$ , in which case

$$k_{\text{uni}} = k_3 \cdot \frac{k_a}{k_b} \cdot \frac{k_1}{k_2},$$

so that we can then say that step III is rate-determining.

We shall give reasons below for suggesting that this does not, in practice, afford a sound classification of unimolecular processes. But before doing so we must specify the states of energization and activation more definitely. It is, however, instructive at this point to notice that in each of the above cases the basic cause of unimolecular behaviour is rapid de-energization (*i.e.* step I reverse), which in case (i) must be greater than the rate at which energized molecules become activated (step II) and in case (ii) must be greater than the rate at which the equilibrium concentration of energized molecules is destroyed by reaction of activated molecules (step III).

#### 4. Further Specification of the Model.

By *energization* we shall mean that a molecule has excess energy, of amount between  $\epsilon$  and  $\epsilon + d\epsilon$ , in not more than  $s$  harmonic-oscillations. This, as is well-known, gives \*

$$\frac{k_1}{k_2} = \frac{1}{(s-1)!} \left( \frac{\epsilon}{kT} \right)^{s-1} e^{-\epsilon/kT} \frac{d\epsilon}{kT} \quad (5)$$

By *activation* we shall mean that of this excess energy  $\epsilon$ , more than  $\epsilon_0$  is concentrated in one particular oscillator. Then

$$\frac{k_a}{k_b} = \left( \frac{\epsilon - \epsilon_0}{\epsilon} \right)^{s-1} \quad (6)$$

These equilibrium formulæ are standard statistical results (see, *e.g.* Kassel<sup>2</sup>). We shall return to a more detailed discussion of their applicability after deducing their immediate consequences (see §§ 9, 11).

#### 5. Case (i) : Step II Rate-Determining.

Provided  $k_2 A \gg k_a$  we have  $k_{\text{uni}} = k_a \cdot k_1/k_2$ . We can proceed on the basis of two alternative assumptions :

**Assumption (1) :**  $k_a = \text{constant}$ , independent of  $\epsilon$ , provided  $\epsilon \gg \epsilon_1$ , some critical energy, otherwise  $k_a = 0$ .

Then 
$$k_{\text{uni}} = k_a \cdot \frac{1}{(s-1)!} \left( \frac{\epsilon}{kT} \right)^{s-1} e^{-\epsilon/kT} \frac{d\epsilon}{kT}$$

and adding the contributions from all energized species (*i.e.*, integrating w.r. to  $\epsilon$  from  $\epsilon_1$  to  $\infty$ ) gives

$$k_{\text{uni}} = k_a \int_{\epsilon_1}^{\infty} \frac{1}{(s-1)!} \left( \frac{\epsilon}{kT} \right)^{s-1} e^{-\epsilon/kT} \frac{d\epsilon}{kT},$$

$$\text{i.e. } k_{\text{uni}} = k_a \left[ \frac{1}{(s-1)!} \left( \frac{\epsilon_1}{kT} \right)^{s-1} + \frac{1}{(s-2)!} \left( \frac{\epsilon_1}{kT} \right)^{s-2} + \dots \right] e^{-\epsilon_1/kT}, \quad (7)$$

which is the Polanyi-Hinshelwood<sup>3</sup> formula.

\* To avoid a rather clumsy modification of the notation we shall not introduce such symbols as  $d(k_1/k_2)$ ,  $dk_{\text{uni}}$ , etc., but leave it optional whether, *e.g.*  $k_{\text{uni}}$  denotes a total or differential quantity. The form of the r.h.s. will always remove any possibility of ambiguity.

<sup>3</sup> Polanyi, *Z. Physik*, 1920, 1, 337.

This formula, however, is intrinsically unlikely to be valid. For  $k_2$ , the rate of de-energization by collision, is almost certainly a constant, independent of  $\epsilon$ , since it can be shown that effectively every collision undergone by an energized molecule is de-energizing: and if  $k_2$  is constant we can further deduce (from (4)) that if energy is redistributed statistically on each collision \*

$$k = \frac{A}{A + k_a/k_2} \cdot k_a \left[ \frac{1}{(s-1)!} \left( \frac{\epsilon_1}{kT} \right)^{s-1} + \frac{1}{(s-2)!} \left( \frac{\epsilon_1}{kT} \right)^{s-2} + \dots \right] e^{-\epsilon_1/kT}$$

for all concentrations  $A$ : i.e. whether the reaction is unimolecular or not. This leads to

$$\frac{k_{un1}}{k} = 1 + \frac{k_a}{k_2 A} \quad (8)$$

( $k_{un1}$  = rate-constant at limitingly high pressures), implying that  $1/k$  and  $1/A$  (i.e. the reciprocal of the pressure) vary linearly: which is not found true experimentally.

**Assumption (ii).**— $k_b$  = constant, independent of  $\epsilon$  or  $\epsilon_0$ . This is an intrinsically much more reasonable assumption (and is, indeed, implied in the work of Polanyi and Wigner).<sup>4</sup> We should expect  $k_b \sim 10^{13}$ , the frequency of an internal vibration within the molecule. On the assumption (ii)

$$\begin{aligned} k_{un1} &= k_b \cdot \frac{k_a}{k_b} \cdot \frac{k_1}{k_2} \\ &= k_b \left( \frac{\epsilon - \epsilon_0}{\epsilon} \right)^{s-1} \frac{1}{(s-1)!} \left( \frac{\epsilon}{kT} \right)^{s-1} e^{-\epsilon/kT} \frac{d\epsilon}{kT}, \quad \epsilon \geq \epsilon_0 \end{aligned}$$

for each range,  $\epsilon - \epsilon + d\epsilon$ , of energization. Integrating over all possible energies of energization, we find

$$\begin{aligned} k_{un1} &= k_b \int_{\epsilon_0}^{\infty} \left( \frac{\epsilon - \epsilon_0}{\epsilon} \right)^{s-1} \frac{1}{(s-1)!} \left( \frac{\epsilon}{kT} \right)^{s-1} e^{-\epsilon/kT} \frac{d\epsilon}{kT}, \\ \text{i.e., } k_{un1} &= k_b e^{-\epsilon_0/kT} \quad (9) \end{aligned}$$

We shall not discuss the consequences of assumption (ii) for the reaction-rate at any pressure until § 7.

## 6. Case (ii): Step III Rate-Determining.

We now have  $k_{un1} = k_3 \cdot k_a/k_b \cdot k_1/k_2$  provided  $k_2 A \gg k_3 \cdot k_a/k_b$ , and so

$$k_{un1} = k_3 \left( \frac{\epsilon - \epsilon_0}{\epsilon} \right)^{s-1} \frac{1}{(s-1)!} \left( \frac{\epsilon}{kT} \right)^{s-1} e^{-\epsilon/kT} \frac{d\epsilon}{kT}, \quad \epsilon \geq \epsilon_0.$$

If we make the plausible assumption that  $k_3$ , the rate of reaction of an activated molecule, is independent of both  $\epsilon$  and  $\epsilon_0$  then we find, on integration,

$$k_{un1} = k_3 e^{-\epsilon_0/kT} \quad (10)$$

a formula of the same form as (9). But  $k_3$ , since we are now thinking of a single excited harmonic vibration leading to decomposition, must  $\sim 10^{13}$ . We have, therefore, in case (i) and in case (ii),

$$k_{un1} \sim 10^{13} e^{-\epsilon_0/kT}.$$

Since, however,  $k_b \sim k_3 (\sim 10^{13})$  our original distinction between the two cases has broken down.

To sum up at this stage, we may say that a classification of unimolecular reactions on the basis of whether step II or step III is rate-determining

\* Even if only certain collisions lead to a redistribution of energy, it is still possible for  $k_2$  to be independent of  $\epsilon$  for  $\epsilon \geq \epsilon_1$ .

<sup>4</sup> Polanyi and Wigner, *Z. physik. Chem., A*, 1928, 139, 439.

is not particularly helpful since it is probable that  $k_2$ ,  $k_b$  and  $k_3$  are constants and  $k_b \sim k_3 \sim 10^{13}$ . The possible alternative assumption that  $k_a$  is constant and not  $k_b$  can be ruled out since it leads to the unsubstantiated equation (8).

## 7. General Theory when $k_2^{\ddagger}$ , $k_b$ and $k_3^{\ddagger}$ are Constants.

Abandoning, therefore, the separation of our problem into cases (i) and (ii), we return to equation (4) which may be written

$$k = \frac{1}{A} \frac{dB}{dt} = \frac{k_b k_3}{k_b + k_3} \cdot \frac{\frac{k_a}{k_b} \cdot \frac{k_1}{k_2} A}{A + \frac{k_b k_3}{k_b + k_3} \cdot \frac{1}{k_2} \cdot \frac{k_a}{k_b}} \quad (4')$$

We now assume :

- (i)  $\frac{k_b k_3}{k_b + k_3} = \text{constant } (\sim 10^{13})$ ,
- (ii)  $k_a = \text{constant}$  (*i.e.* every collision de-energizing, and collision diameter constant).

Then, on the basis of (5) and (6), we have

$$k = \frac{k_b k_3}{k_b + k_3} \int_{\epsilon_0}^{\infty} \frac{A \left( \frac{\epsilon - \epsilon_0}{\epsilon} \right)^{s-1} \frac{1}{(s-1)!} \left( \frac{\epsilon}{kT} \right)^{s-1} e^{-\epsilon/kT} \frac{d\epsilon}{kT}}{A + \frac{k_b k_3}{k_b + k_3} \cdot \frac{1}{k_2} \left( \frac{\epsilon - \epsilon_0}{\epsilon} \right)^{s-1}}$$

$$\text{i.e. } k = \frac{k_b k_3}{k_b + k_3} e^{-\epsilon_0/kT} \frac{A}{(s-1)! (kT)^s} \int_0^{\infty} \frac{e^{-x/kT} dx}{x^{s-1} + \frac{k_b k_3}{k_b + k_3} \cdot \frac{1}{k_2} \cdot \frac{1}{(x + \epsilon_0)^{s-1}}} \quad (11)$$

in agreement with Kassel.\* We have, in fact, merely shown how Kassel's well-established formula can be derived on the basis of transition-state theory and in transition-state nomenclature.

## 8. Limiting Equations derived from Kassel's Formula.

(a) **High Pressures.**—If the first term in the denominator of (11) is always very much bigger than the second term therein, we have

$$k = k_{unl} = \frac{k_b k_3}{k_b + k_3} e^{-\epsilon_0/kT} \frac{1}{(s-1)! (kT)^s} \int_0^{\infty} x^{s-1} e^{-x/kT} dx$$

$$= \frac{k_b k_3}{k_b + k_3} e^{-\epsilon_0/kT} \quad \quad \quad (12)$$

$$\sim 10^{13} e^{-\epsilon_0/kT}$$

—of the same form as equations (9) and (10).

(b) **Low Pressures.**—On the other hand, the limiting *bimolecular* reaction-rate is given by

$$k_{bl} = \frac{k}{A} = \frac{k_2 e^{-\epsilon_0/kT}}{(s-1)! (kT)^s} \int_0^{\infty} (x + \epsilon_0)^{s-1} e^{-x/kT} dx$$

$$= k_2 e^{-\epsilon_0/kT} \left[ \frac{1}{(s-1)!} \left( \frac{\epsilon_0}{kT} \right)^{s-1} + \frac{1}{(s-2)!} \left( \frac{\epsilon_0}{kT} \right)^{s-2} + \dots \right] \quad (13)$$

—which is also the limiting bimolecular rate deduced on the basis of the Polanyi-Hinshelwood formula, equations (7) and (8).

\* *Loc. cit.*,<sup>2</sup> p. 103.



### 9. Further Comments on the Underlying Theory.

From our original equations, (1), (2) and (3), we can always deduce that

$$k_1 A^2 = k_2 A A^* + \frac{dB}{dt}$$

but, as it stands, this equation is useless for telling us anything about the rate-constant. To know the actual concentration,  $A^*$ , of energized molecules we have to elaborate the model further (as we have done above).

The additional equation  $dB/dt = k_a A^*$ , where  $k_a = \text{constant}$ , leads to equation (8) and so is ruled out on empirical grounds. We therefore involve the idea of *activation* following *energization*: and so obtain Kassel's formula, equation (11):

We see, too, that, since *energization* is a wider concept than *activation*, there is no point in introducing "differential activation," i.e. in writing

$$\frac{k_a}{k_b} = (s-1) \left( \frac{\epsilon - \epsilon^*}{\epsilon} \right)^{s-2} \frac{d\epsilon^*}{d\epsilon}, \quad \text{where } \epsilon_0 \leq \epsilon^* \leq \epsilon$$

unless we are also going to introduce a specific rate-constant,  $k_3$  dependent on  $\epsilon^*$ . We are hardly at liberty to do this while thinking of the activated states as simply excited states of a certain harmonic oscillator with constant frequency (classically). A much more necessary extension of the picture will be suggested below (§ 11).

### 10. Energies and Entropies of Activation.

If, in the usual transition-state nomenclature, we write

$$k = k_3 e^{-\Delta F^\ddagger/RT} \quad (14)$$

we find

$$\Delta F^\ddagger = -RT \ln \frac{k_b}{k_b + k_3} - RT \ln \int_{\epsilon_0}^{\infty} \frac{A \frac{1}{(s-1)!} \left( \frac{\epsilon - \epsilon_0}{kT} \right)^{s-1} e^{-\epsilon/kT} \frac{d\epsilon}{kT}}{A + \frac{1}{k_2} \cdot \left( \frac{k_b k_3}{k_b + k_3} \right) \left( \frac{\epsilon - \epsilon_0}{\epsilon} \right)^{s-1}}$$

and so

$$\begin{aligned} \Delta E^\ddagger &= RT^2 \frac{\partial}{\partial T} \ln k \\ &= -sRT + N \frac{\int_{\epsilon_0}^{\infty} \epsilon A \frac{1}{(s-1)!} \left( \frac{\epsilon - \epsilon_0}{kT} \right)^{s-1} e^{-\epsilon/kT} \frac{d\epsilon}{kT}}{\int_{\epsilon_0}^{\infty} \frac{A \frac{1}{(s-1)!} \left( \frac{\epsilon - \epsilon_0}{kT} \right)^{s-1} e^{-\epsilon/kT} \frac{d\epsilon}{kT}}{A + \frac{1}{k_2} \cdot \frac{k_b k_3}{k_b + k_3} \left( \frac{\epsilon - \epsilon_0}{\epsilon} \right)^{s-1}}} \\ &= -sRT + N \frac{\sum_{\epsilon=\epsilon_0}^{\infty} \epsilon A^\ddagger}{\sum_{\epsilon=\epsilon_0}^{\infty} A^\ddagger} \end{aligned}$$

where  $N$  is Avogadro's number; i.e.

$$\Delta E^\ddagger = N(\bar{\epsilon} - \bar{\epsilon}), \quad (\text{Tolman, ref. } ^5)$$

where

$\bar{\epsilon}$  = average energy of "reacting" species,  
 $\bar{\epsilon}$  = average energy of all species,

<sup>5</sup> Tolman, *J. Am. Chem. Soc.*, 1925, 47, 2652.

and, of course, from our definition  $\Delta E^\ddagger$  is the Arrhenius energy of activation (sometimes called  $\Delta E_A$ ).

It is important to observe, however, that the "reacting" species (*cf.* Tolman) are not the *energized* ones but the *activated* ones.

Moreover we find,

(a) At high pressures,

$$\Delta E^\ddagger = -sRT + N \frac{\int_0^\infty (x + \epsilon_0) x^{s-1} e^{-x/kT} dx}{\int_0^\infty x^{s-1} e^{-x/kT} dx}$$

$$= N\epsilon_0,$$

and

$$\Delta S^\ddagger = (\Delta E^\ddagger - \Delta F^\ddagger)/T$$

$$= \frac{N\epsilon_0}{T} + R \ln \int_{\epsilon_0}^\infty \frac{1}{(s-1)!} \left( \frac{\epsilon - \epsilon_0}{kT} \right)^{s-1} e^{-\epsilon/kT} \frac{d\epsilon}{kT} + R \ln \frac{k_b}{k_b + k_s}$$

$$= R \ln \frac{k_b}{k_b + k_s} < 0.$$

(b) At low pressures,

$$\Delta E^\ddagger = -sRT + sRT \frac{\left[ \frac{1}{s!} \left( \frac{\epsilon_0}{kT} \right)^s + \frac{1}{(s-1)!} \left( \frac{\epsilon_0}{kT} \right)^{s-1} + \dots \right]}{\left[ \frac{1}{(s-1)!} \left( \frac{\epsilon_0}{kT} \right)^{s-1} + \frac{1}{(s-2)!} \left( \frac{\epsilon_0}{kT} \right)^{s-2} + \dots \right]}$$

$$\rightarrow N\epsilon_0 - sRT \quad \text{if } \epsilon_0 \gg skT,$$

and (using above definition of  $\Delta F^\ddagger$ )

$$\Delta S^\ddagger = R \ln \int_{\epsilon_0}^\infty \frac{Ak_2}{k_3} \left( \frac{\epsilon}{kT} \right)^{s-1} e^{-\epsilon/kT} \frac{d\epsilon}{kT} + \frac{\Delta E^\ddagger}{T}$$

$$= R \ln \frac{Ak_2}{k_3} + \frac{\Delta E - N\epsilon_0}{T}$$

$$+ R \ln \left[ (s-1)! \left\{ \frac{1}{(s-1)!} \left( \frac{\epsilon_0}{kT} \right)^{s-1} + \frac{1}{(s-2)!} \left( \frac{\epsilon_0}{kT} \right)^{s-2} + \dots \right\} \right]$$

$$\rightarrow R \ln \frac{Ak_2}{k_3} - sR + R \ln \left( \frac{\epsilon_0}{kT} \right)^{s-1} \quad \text{if } \epsilon_0 \gg skT.$$

At low pressures, however, when the rate-process is bimolecular, it is more customary, in transition-state notation, to write, instead of (14)

$$k = Ak_2 e^{-\Delta F^\ddagger/RT} \quad (15)$$

and then the limiting form of  $\Delta S^\ddagger$ , when  $\epsilon_0 \gg skT$ , is simply

$$\Delta S^\ddagger = (s-1) \left[ R \ln \left( \frac{\epsilon_0}{kT} \right) - R \right] - R$$

as we should expect, since  $k \ln \frac{\epsilon_0}{kT} - k$  is the entropy of an harmonic oscillator of energy  $\epsilon_0$ .

## 11. Necessary Extension of the Model.

We have seen that in the strictly unimolecular region, *i.e.* at sufficiently high pressures

$$\Delta E^\ddagger \equiv RT^2 \frac{\partial}{\partial T} \ln k = N\epsilon_0$$

$$\Delta S^\ddagger = R \ln \frac{k_b}{k_b + k_s} < 0$$

and this at once reveals an important defect in the model which we have considered. For we have assumed that even in the activated state the particular bond (*i.e.* oscillator) to be broken is still undistorted (*i.e.* still performs harmonic oscillations), and that the specific reaction-rate,  $k_a$ , is merely the normal frequency of vibration of that oscillator. But studies of the potential-energy surfaces of reacting systems have shown that the potential-energy varies along the reaction path in the manner shown diagrammatically in Fig. 1. In our model we have artificially constrained our system, in configuration but not in energy, to the dotted curve in Fig. 1; which, therefore, has artificially decreased the entropy of the activated state.

The only way to correct for this is to replace our formula

$$\frac{k_a}{k_b} = \left( \frac{\epsilon - \epsilon_0}{\epsilon} \right)^{s-1}$$

by

$$\frac{k_a}{k_b} = \left( \frac{\epsilon - \epsilon_0}{\epsilon} \right)^{s-1} e^{\Delta S_\tau / R},$$

which implies that molecules with energy  $> \epsilon_0$  in a given bond can exist only if the energy and configuration of that bond correspond to  $\tau$  (Fig. 1). For high pressures we then obtain

$$k_{uni} = \left( \frac{k_b k_a}{k_b + k_s} e^{\Delta S_\tau / R} \right) e^{-\epsilon_0 / kT} \quad (16)$$

and so

$$\Delta S^* = \Delta S_\tau + R \ln \frac{k_b}{k_b + k_s} \quad (\Delta S_\tau > 0) \quad (17)$$

which differs from customary transition-state theory only in that we have allowed for the deviation of the actual number of activated complexes from the "equilibrium" number that there would be assuming no reaction to proceed (second term on r.h.s. of (17)).

The Arrhenius activation energy equals  $N\epsilon_0$  and is independent of  $T$ . This is to be expected since Classical energy distributions have been used throughout, and indeed the transition-state theory leads to the same conclusion when Classical rotational and vibrational partition-functions are employed.<sup>6</sup> Of course if  $k_s$  is written as  $kT/h$  or if quantal partition functions for rotations or vibrations have to be employed, there will be a small temperature variation of  $\Delta E_A$  in consequence. Moreover, any

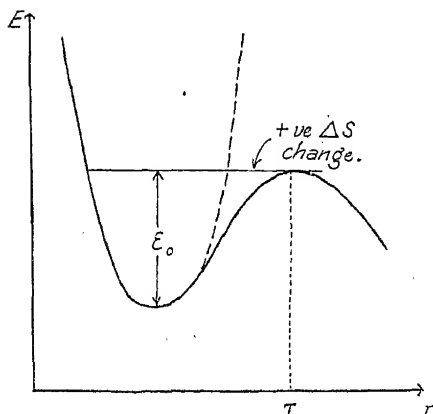


FIG. 1.

large increase of the bracketted factor above (equation 16) from a magnitude of the order  $10^{13}$  must be due to a large value of  $\Delta S_\tau$  and therefore to a large distortion of the molecular configuration in the transition-state. If the values reported in the literature\* really apply to the true unimolecular region, very considerable changes in structure and behaviour (in the transition-state) have to be invoked in order to account for  $\Delta S_\tau \sim 0$ .

<sup>6</sup> Glasstone, Laidler and Eyring, *The Theory of Rate Processes*, McGraw-Hill, 1941.

\* *Loc. cit.*, p. 296.

## 12. Summary and Conclusions.

Our conclusions may be summarized as follows :—

(1) A distinction between step II and step III as the rate-determining process is not helpful.

(2) The customary treatment (Kassel) can be described in terms of transition-state theory, but assumes that there is no deformation of the molecule in the activated complex.

(3) If this is taken care of, then the result obtained accords with that given by transition-state theory.

(4) In a purely Classical treatment the Arrhenius activation-energy  $= N\epsilon_0$ , is temperature independent (provided that the reaction is truly unimolecular and that rotations and vibrations of the molecule can be treated classically).

Finally,

(5) We should like to draw attention to the need for a direct theoretical computation of  $k_a$ . This has not been done by Polanyi and Wigner† nor by Slater‡—who circumvent the problem. Since  $k_a/k_b = \left(\frac{\epsilon - \epsilon_0}{\epsilon}\right)^{s-1}$  we can estimate the “effective” value of  $k_a$  from a comparison between our theoretical formula for  $k_{\text{unl}}$  and experimental data. In many cases (see Fowler and Guggenheim, ref.<sup>8</sup>) this appears to suggest that if  $k_b \sim 10^{13}$  then  $k_a \sim 10^9$  for the dominant energy-flow processes.

We can, in fact, take the matter further in this indirect way :

$$\text{for if } k_a = k_b \left( \frac{\epsilon - \epsilon_0}{\epsilon} \right)^{s-1}$$

where  $k_b = \text{constant}$ , then, since

$$\left( \frac{\epsilon - \epsilon_0}{\epsilon} \right)^{s-1} = \frac{\begin{array}{c} \text{number of arrangements of quanta for which energy} \geq \epsilon_0 \\ \text{in a particular oscillator} \end{array}}{\begin{array}{c} \text{number of arrangements of quanta with no restrictions} \\ \text{on the energy distribution} \end{array}}$$

and since all arrangements are *a priori* equally probable—in that the total energy is the same for all of them—our formula seems to imply that there is a complete rearrangement of the quanta every  $10^{-13}$  sec. and that, from any particular initial arrangement all possible “rearrangements” ( $10^{-13}$  sec. later) are equally probable. Though this seems to us a suggestive and physically plausible conclusion, the underlying picture remains rather indefinite in that we have still to ask what it is that produces a rearrangement of the quanta every  $10^{-13}$  sec. and whether the quanta should properly be thought of as localised in bonds or in normal modes of oscillation of the whole molecule.

We wish to thank Dr. H. Steiner for helpful points which he brought to our notice in discussion.

† *Loc. cit.*<sup>4</sup>

‡ Slater, *Proc. Camb. Phil. Soc.*, 1939, **35**, 56.

<sup>8</sup> Fowler and Guggenheim, *Statistical Thermodynamics*, Cambridge, 1939, § 1216.

# THE ADSORPTION OF PARAFFIN-CHAIN SALTS TO PROTEINS.

## PART II. THE INFLUENCE OF ELECTROLYTES AND $pH$ ON THE SEPARATION OF GELATIN-DODECYL SULPHATE COMPLEXES FROM AQUEOUS SOLUTIONS.

BY K. G. A. PANKHURST AND R. C. M. SMITH.

*Received 4th April, 1945.*

In studying the effect of ammonium nitrate on the separation of gelatin-dodecyl sulphate complexes in the iso-electric region, it was found that the concentration of dodecyl sodium sulphate (DSS) required to be added to a 0.5 % gelatin solution at 35° C. in order to obtain maximum separation was sensibly independent of electrolyte concentration between 0.45 N. and 2.00 N.<sup>1</sup> It was also shown (Fig. 1, Part I) that at lower concentrations of ammonium nitrate, although there are no well-defined inflexion points marking maximum separation, separation does occur at progressively lower concentrations of added DSS. Indeed at 0.35 N. ammonium nitrate complete peptisation has occurred at the concentration of DSS which corresponds to maximum separation at 0.45 N. electrolyte and above. This indicates that the rôle of the electrolyte is not simply that of a salting-out agent, but that it also plays a part in determining the constitution of the complex.

In this paper we have studied more completely the influence of various electrolytes over a wide range of  $pH$  values in an endeavour to separate the two possible effects of the electrolyte: (a) the salting out effect and (b) the effect on the composition of the complex.

**Experimental.**—The technique was the same as previously described<sup>1</sup> except that it was found convenient to work on a 15 c.c. scale instead of 100 c.c. without sacrificing accuracy. The electrolytes were of Analar grade or were standardised by volumetric methods. 0.5 % gelatin solutions were used throughout at 50° C. This temperature ensured the solution of the dodecyl sulphates, particularly potassium.

### Results.

**The Interdependence of Electrolyte and  $pH$ .**—In considering factors affecting the separation of complexes, *e.g.* electrolyte,  $pH$ , etc., two criteria appear to be important: (1) the concentration of added DSS corresponding to maximum separation (the inflexion point) and (2) the extent of separation, a measure of which is given by the deviation of the determined curve from the straight line corresponding to no separation. Criterion (1) we associate with a chemical effect determined by the constitution of the complex, whereas (2) corresponds with a salting-out effect, or the solubility of the complex in the particular environment in which it is prepared.

Mention has been made above of the evidence in Fig. 1, Part I, that the concentration of ammonium nitrate is important in determining the inflexion point in the isoelectric region. This is not very precisely determined since, at this  $pH$  value, with low ammonium nitrate concentration the inflexion point is not very well defined, and indeed at 0.25 N. electrolyte and below no separation occurs at all. Since, however, a similar and

<sup>1</sup> Pankhurst and Smith, *Trans. Faraday Soc.*, 1944, 40, 565.

better defined shift was obtained when  $pH$  was reduced at constant electrolyte concentration (Fig. 3, Part I), it was thought desirable to investigate the effect of ammonium nitrate at low  $pH$  values.

Fig. 1 shows the results obtained with such a series of ammonium nitrate concentrations at  $pH$  2.8 and demonstrates that as the ammonium nitrate concentration is reduced the inflexion point occurs at progressively lower added DSS concentrations, and that good separation occurs even in the absence of electrolyte. In the presence of 2.0 N. ammonium nitrate the separation range is so extended as completely to include that region in which separation occurs with this quantity of electrolyte at  $pH$  5.5 (see broken curve in Fig. 1). This provides further evidence that

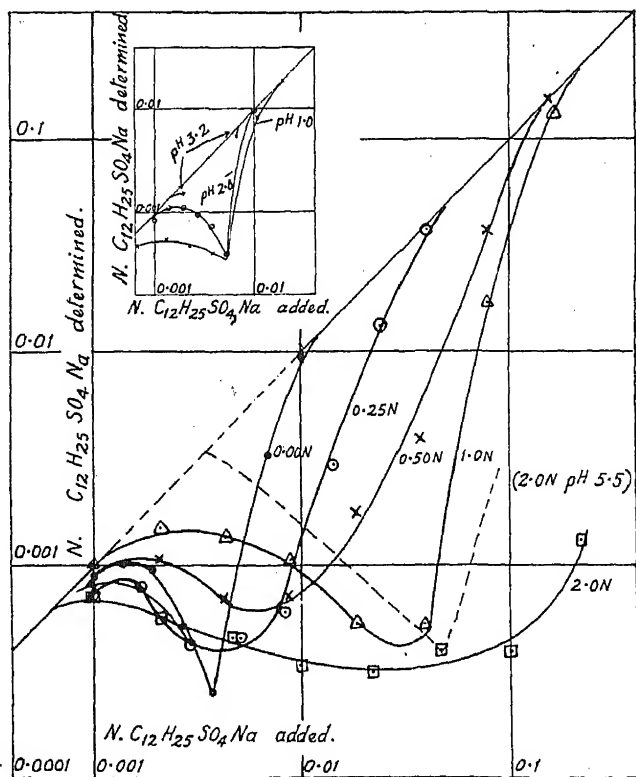


FIG. 1.

the ammonium nitrate is important in determining the nature of the complex, *e.g.* comparing the curves for 0.0 N. and 1.0 N. electrolyte in Fig. 1, each has a well-defined inflexion point, the latter at about eight times the concentration of added DSS of the former.

The effect of  $pH$  in the absence of electrolyte is shown in the inset to Fig. 1. At  $pH$  values above *ca.* 4.0 no separation is possible. At 3.2 there is slight precipitation but the segregation of the two phases is so slow that only the points where separation commences and peptisation is just complete are indicated. At  $pH$  2.8 and 1.0 well-defined inflexion points were obtained, both at 0.0045 N. added DSS, the lower  $pH$  giving a more complete separation. In the absence of electrolyte it appears that the position of the inflexion point, with respect to added DSS concentration, is independent of  $pH$ . Thus hydrogen ions are effective in salting out the complex when present in sufficient quantity, *i.e.* at  $pH$

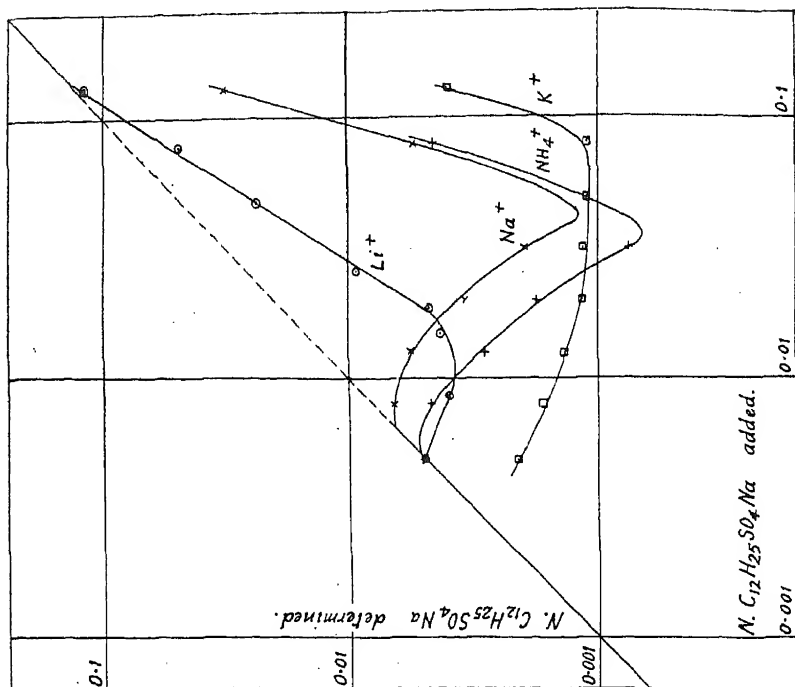


FIG. 3.

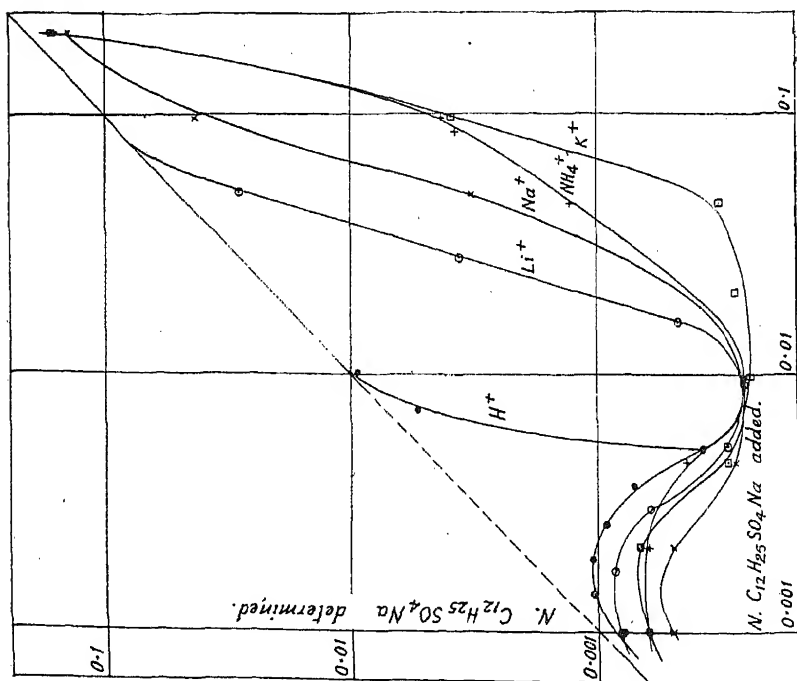


FIG. 2.

values of 3.5-4.0 and below. When other cations are present there is competition between these and the existing hydrogen ions for adsorption to the negatively charged parts of the complex, thus in the presence of 1.0 N. ammonium nitrate, as the  $pH$  is lowered the inflexion point moves to the left, indicating that increasing the concentration of hydrogen ions enables them to compete more effectively with the ammonium ions. The same effect is seen in Figs. 2 and 3 below for other cations.

**The Lyotropic Series of Cations and Anions.**—The effect of electrolyte cation and anion was studied using the following series of salts at  $pH$  values of 2.5-2.8, 5.3-5.5, and 10.2-10.6 (8.8-9.3 for the ammonium salts).

Cation series:  $LiCl$ ,  $NaCl$ ,  $KCl$ ,  $NH_4Cl$   
 Anion series:  $NH_4Cl$ ,  $NH_4Br$ ,  $NH_4I$ ,  $NH_4NO_3$

Figs. 2-7 show the results.

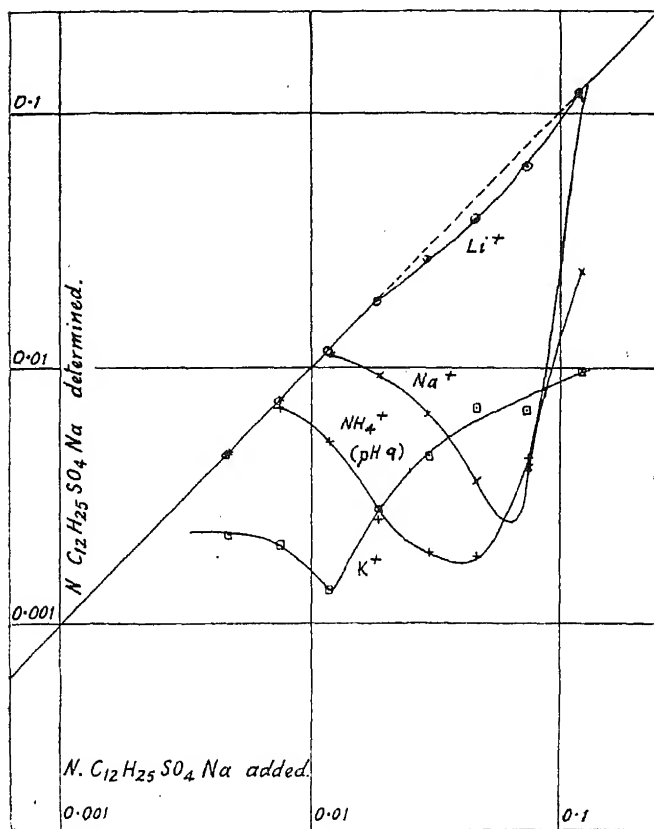


FIG. 4.

From Fig. 2 it is seen that for the cation series at a  $pH$  well below the isoelectric point, maximum separation, *i.e.* the point of lowest determined DSS, is substantially the same for each cation, but that the deviation from the theoretical straight line increases in the order:

$$Li^+ < Na^+ < NH_4^+ < K^+.$$

This is the reverse order of that which would be expected from consideration of the salting-out effect as governed by the degree of hydration of the ions, *i.e.* the most *strongly* hydrated ion has the *weakest* salting-out effect, whereas one would have expected the reverse to happen. The explanation



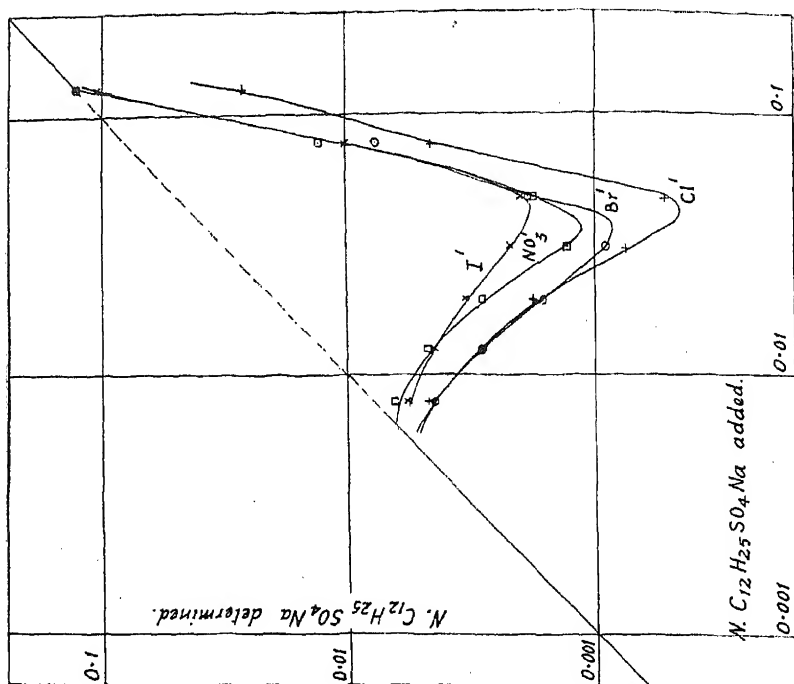


FIG. 6.

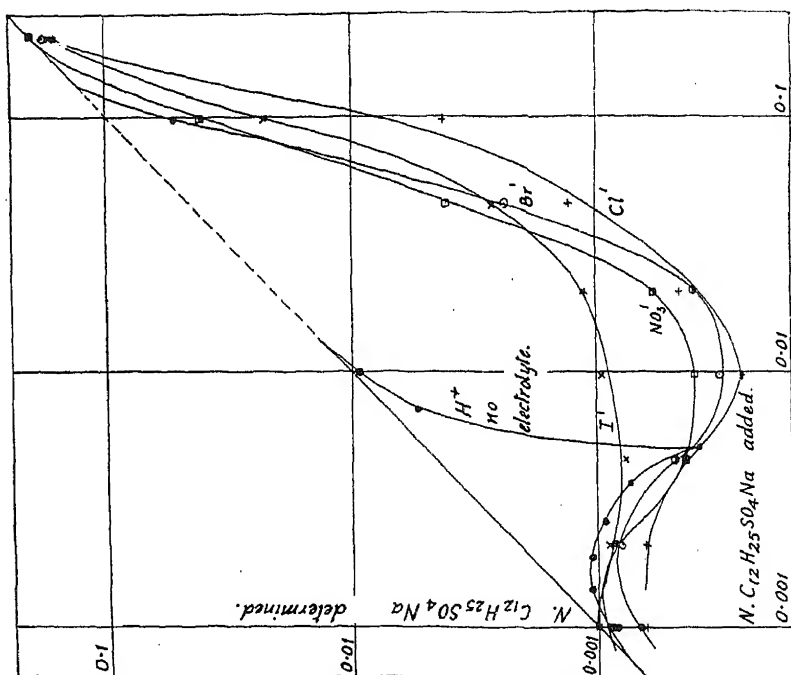


FIG. 5.

of this is probably that offered by Docking and Heymann,<sup>2</sup> when considering adsorption and salting-out effects of such ionic series on gelatin itself, based on the theory of Katz and Muschter,<sup>3</sup> *viz.* an ion which is strongly adsorbed to the protein confers on it solubility characteristics which it derives from its own hydration. Thus  $\text{Li}^+$  being both powerfully adsorbed and highly hydrated confers greatest water solubility on the complex. The increased efficiency as one progresses from  $\text{Li}^+$  to  $\text{K}^+$  is similar to that obtained by increasing the concentration of a single electrolyte at low  $\text{pH}$ , as shown in Fig. 1. With the cationic series at the isoelectric region and above a similar order is obtained, but the overall efficiency of the cations is less as the  $\text{pH}$  is raised (see Figs. 3 and 4).

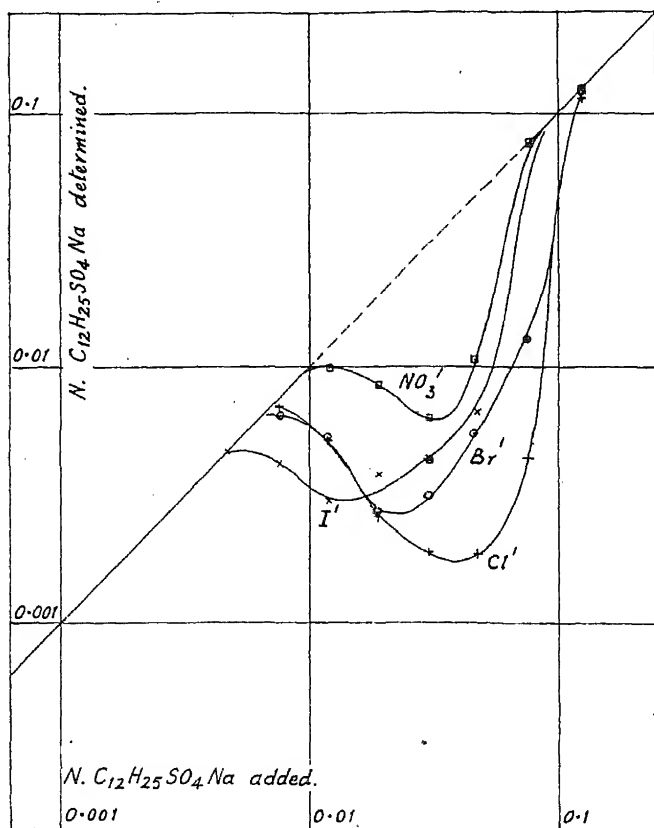


FIG. 7.

For the anion series at  $\text{pH}$  2.8 (Fig. 5) there is comparatively little difference in their efficiencies, but such differences that there are indicate the following series :

$$\text{I}' < \text{NO}_3' < \text{Br}' < \text{Cl}'.$$

According to Docking and Heymann,<sup>2</sup> iodide is the most strongly adsorbed ion of the series, but its degree of hydration is small. Chloride being least adsorbed and most hydrated exhibits the greatest salting-out effect. At the isoelectric point and above (Figs. 6 and 7) the above gradation is more marked. At  $\text{pH}$  9, however, it is interesting to note that there is a progressive shift of inflexion point to the left in the order  $\text{Cl}'$ ,  $\text{Br}'$ ,  $\text{I}'$ ,

<sup>2</sup> Docking and Heymann, *J. Physic. Chem.*, 1939, **43**, 513.

<sup>3</sup> Katz and Muschter, *Biochem. Z.*, 1932, **257**, 385.

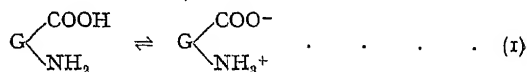
indicating that at high  $pH$  values the iodide is sufficiently adsorbed to the gelatin to compete with the DS anions, thereby causing the production of a complex less rich in DS ions. The same is true, *mutatis mutandis*, for the  $Br'$  ion.

### General Discussion.

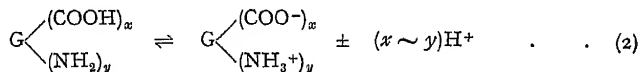
From the above it appears that complex formation and complex separation should be considered separately, even though such factors as electrolyte,  $pH$ , etc., influence both.

**Complex Formation.**—Evidence points to the electrostatic nature of the link between the DS anions and the basic groups in the protein. Putnam and Neurath<sup>4</sup> have come to the same conclusion in their work on the adsorption of DSS to other proteins.

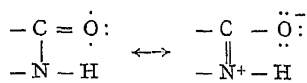
It has been customary for some workers to represent the protein molecule as a zwitterion in the same manner as is general for a simple amino acid:



This gives an inadequate representation of the polypeptide arrangement since it is most frequent that the carboxyl groups and amino groups are not equal in number, and others<sup>5</sup> have given the following as an alternative:



This, too, is not entirely adequate in explaining the zwitterion character of gelatin since it is only true if one ignores the basic imino nitrogens of the  $-\text{CO}-\text{NH}-$  groups in the polypeptide chain itself. It only truly represents the state of affairs after complete hydrolysis. The imide groups have some electropositive character and one can attribute a corresponding electronegative character to the carbonyls in the following manner.<sup>6</sup>



As Pauling points out, calculations based on this show that resonance is inhibited by the adsorption of a proton to the nitrogen and that in consequence salts formed by amides do not result from this cause, as happens with amines.

Since quantitative results on the adsorption of DS anions at  $pH$  values at and above the isoelectric region, in the presence of large amounts of ammonium nitrate, show that one DS anion is adsorbed for every nitrogen atom in the gelatin<sup>1</sup> it appears that practically every nitrogen is sufficiently electropositive under these conditions to adsorb, by an electrostatic link, one DS anion. From the evidence in the present paper it appears possible that the wetting agent anion can be replaced by simple electrolyte anions to varying extents depending on the availability of the nitrogens in the protein and the nature and concentration of the simple electrolyte anions.

Fig. 1 inset shows that increasing the hydrogen ion concentration below about  $pH$  3.0 results in no further shift of inflexion point to the left, *i.e.* there is no further reduction in the number of available nitrogens. This suggests that a limited number of nitrogens (rather less than 10 % of the

<sup>4</sup> Putnam and Neurath, *J. Amer. Chem. Soc.*, 1944, 66, 692.

<sup>5</sup> Cf. Sheppard, Houck and Dittmar, *J. Physic. Chem.*, 1942, 46, 165.

<sup>6</sup> Cf. Pauling, *The Nature of the Chemical Bond*, Cornell University Press, 1940, 207.

total)<sup>7</sup> are of such a nature that their power to combine with DS anions is not impaired by reduction of  $pH$ . Fig. 1 shows a shift of inflexion point to the right as electrolyte concentration is increased, at low  $pH$ , as if the electrolyte were increasing the availability of some of the nitrogen atoms for combination with DS anions. At this stage, we can see no explanation of this.

**Complex Separation.**—It has already been shown that the electrolyte ions can influence the solubility of a complex in two ways, *i.e.* a "salting-in" and a "salting-out" effect. Both of these depend on the extent to which the ions are adsorbed to the gelatin and their degree of hydration. The "salting-in" effect has maximum solubilising action when the strongly adsorbed ions are strongly hydrated, *e.g.*  $Li^+$ . The "salting-out" effect is maximum where a high degree of hydration is accompanied by low adsorption, *e.g.*  $Cl^-$ . The wetting agent anion is simply an example of a powerfully adsorbed ion with a very low degree of hydration.

### Summary.

The part played by electrolytes and the effect of  $pH$  on the formation and separation of complexes between gelatin and dodecyl sodium sulphate has been studied and the mechanism has been examined from the standpoint of the lyotropic series and the specific adsorption of the ions concerned.

We are pleased to record our thanks to Professor N. K. Adam, F.R.S., for helpful discussion, and to several of our colleagues on the staff of Messrs. Ilford Limited. Our thanks are also due to the Board of Directors of the above Company for permission to publish this work.

*The Research Laboratories,  
Ilford Limited, Selo Works,  
Warley, Essex.*

<sup>7</sup> The ratio of amino nitrogens in the side chains to the total nitrogens in the gelatin molecule is of the same order of magnitude (*vide* data compiled by Bowes, *Reports of the Progress of Applied Chemistry*, 1943, 28, 324).

## A THERMODYNAMIC STUDY OF BIVALENT METAL HALIDES IN AQUEOUS SOLUTION.

### PART XIII. PROPERTIES OF CALCIUM CHLORIDE SOLUTIONS UP TO HIGH CONCENTRATIONS AT 25°.

BY R. H. STOKES.

*Received 9th April, 1945.*

Although isopiestic data have usually been expressed relative to potassium<sup>1</sup> or sodium<sup>2</sup> chloride or sucrose<sup>3</sup> as reference substance, considerable use could be made of a 1 : 2 electrolyte as a subsidiary standard, provided that (a) its water activities and activity coefficients were well established over a wide range of concentration, and (b) the values at the lowest concentration used in isopiestic measurements, *viz.* 0.1 M., were known from accurate measurements at high dilutions. Such data are available for  $H_2SO_4$ , but this does not behave as a normal 1 : 2 electrolyte owing to the presence of the incompletely dissociated bisulphate ion.

<sup>1</sup> Robinson and Sinclair, *J. Amer. Chem. Soc.*, 1934, 56, 1830.

<sup>2</sup> Scatchard, Hamer and Wood, *ibid.*, 1938, 60, 3061.

<sup>3</sup> Smith and Smith, *J. Biol. Chem.*, 1937, 117, 209.

In the case of zinc chloride,<sup>4</sup> bromide,<sup>5</sup> and iodide,<sup>6</sup> measurements have been made which enable the activity coefficient at 0.1 M. to be fixed with confidence, but these salts are not well suited to isopiestic work, as the platinum vessels required for accurate results greatly reduce the rate of attainment of equilibrium in dilute solutions. Further, they all show abnormalities in concentrated solutions when compared with the alkaline earth halides. Of the remaining 1 : 2 salts,  $\text{CaCl}_2$  would seem to be the most satisfactory for our purpose. Shedlovsky and MacInnes<sup>7</sup> have made extremely careful measurements of the e.m.f.s at 25° of cells with transport containing  $\text{CaCl}_2$ , and, by combining their results with moving boundary transport numbers, have derived activity coefficients of very high accuracy in solutions from 0.0018 M. to 0.097 M. The present work deals with isopiestic measurements in more concentrated solutions, from 0.1 M. to 10 M., using  $\text{NaCl}$  and  $\text{H}_2\text{SO}_4$  as standards. As a result it is believed that the water activities and activity coefficients of calcium chloride at 25° are now known more accurately and over a wider concentration range than those of any other normal 1 : 2 salt.

### Experimental.

**Calcium Chloride.**—The best  $\text{CaCl}_2$  commercially available was "Baker's Analyzed" C.P. material, containing 0.37 % of alkali expressed as sulphate. It was found that recrystallization reduced the alkali content only slightly; consequently the Ca was precipitated as  $\text{CaCO}_3$ , and after prolonged washing this was dissolved in Analar  $\text{HCl}$ , with boiling to expel  $\text{CO}_2$ , to give a neutral solution about 3 M. in concentration. A second preparation was made in the same way from "Analar"  $\text{CaCO}_3$ , containing < 0.1 % of alkali expressed as sulphate, and "Baker's Analyzed" C.P.  $\text{HCl}$ . The solutions were then analysed gravimetrically in triplicate for chloride as  $\text{AgCl}$ . The isopiestic results for these two solutions were indistinguishable. Both solutions, however, gave results higher by about 0.4 % in the osmotic coefficient than those derivable from Robinson's<sup>8</sup> earlier measurements of the  $\text{CaCl}_2$ — $\text{KCl}$  ratio. In some preliminary measurements the "Baker's Analyzed"  $\text{CaCl}_2$ , even after recrystallization, was found to give isopiestic ratios lower by about the same amount. For this reason the values now obtained with the more highly purified material are to be preferred.

**Sodium chloride** was prepared by recrystallization and fusion of "Analar"  $\text{NaCl}$ .

**Sulphuric Acid.**—A stock solution of about 70 % by weight was prepared from "Baker's Analyzed" C.P.  $\text{H}_2\text{SO}_4$ , of A.C.S. specification, containing negligible impurities. This was stored in a special vessel under slight pressure so that it could be run out as required with minimum exposure to the air. Suitably diluted portions were analysed by weight-titration against A.R.  $\text{Na}_2\text{CO}_3$  dried at 270°. Other solutions were prepared as required by weight-dilution of the main stock. The apparatus was of the usual type, platinum dishes being used for the  $\text{H}_2\text{SO}_4$  solutions and silver for the  $\text{NaCl}$  and  $\text{CaCl}_2$ . Agreement between the duplicate dishes was in most cases better than 0.1 %. The experimental results are given in Table I.

**Standard Data.**—The values of  $\phi$  and  $a_w$  used for the reference solutions of  $\text{NaCl}$  and  $\text{H}_2\text{SO}_4$  were those given by Robinson.<sup>9</sup> Below 1.5 M.  $\text{NaCl}$  they are essentially the same as those given by Harned and Robinson,<sup>10</sup>

<sup>4</sup> Robinson and Stokes, *Trans. Faraday Soc.*, 1940, **36**, 740. Harris and Parton, *ibid.*, 1139.

<sup>5</sup> Stokes and Stokes, *in the press*.

<sup>6</sup> Bates, *J. Amer. Chem. Soc.*, 1938, **60**, 2983.

<sup>7</sup> Shedlovsky and MacInnes, *ibid.*, 1937, **59**, 503.

<sup>8</sup> Robinson, *Trans. Faraday Soc.*, 1940, **36**, 735.

<sup>9</sup> Robinson, *Trans. Roy. Soc. N.Z.*, 1945, **75**, 203.

<sup>10</sup> Robinson and Harned, *Chem. Rev.*, 1941, **28**, 452.

but at higher concentrations the later work of Olynyk and Gordon<sup>11</sup> on concentrated solutions of NaCl is given considerable weight. For H<sub>2</sub>SO<sub>4</sub>, reliance is placed mainly on the direct vapour pressure measurements of Shankman and Gordon,<sup>12</sup> although these differ considerably from the e.m.f. measurements of Harned and Hamer.<sup>13</sup> Some support for this choice is given below. Although the work of Shankman and Gordon on H<sub>2</sub>SO<sub>4</sub> probably represents the most accurate contribution hitherto made to our knowledge of water activities in very concentrated solutions,

TABLE I.

(a) Isopiestic molalities of CaCl<sub>2</sub> and NaCl; the CaCl<sub>2</sub> molality is the first of each pair of numbers.

0.0908	0.1255	0.1148	0.1586	0.2156	0.3034	0.2742	0.3901
0.3875	0.5617	0.4968	0.7366	0.6090	0.9232	0.6808	1.046
0.8382	1.325	0.8503	1.350	1.028	1.683	1.170	1.963
1.307	2.244	1.482	2.611	1.483	2.612	1.487	2.622
1.535	2.724	1.657	2.988	1.772	3.241	1.798	3.302
2.077	3.937	2.140	4.084	2.467	4.865	2.658	5.342
2.676	5.384	2.921	6.008	2.928	6.028	2.978	6.147
2.981	6.166						

(b) Isopiestic molalities of CaCl<sub>2</sub> and H<sub>2</sub>SO<sub>4</sub>; the CaCl<sub>2</sub> molality is the first of each pair.

2.951	4.329	3.072	4.520	3.362	4.985	3.715	5.561
3.929	5.899	4.126	6.237	4.422	6.742	4.525	6.916
4.635	7.116	4.928	7.611	4.967	7.687	5.366	8.381
5.473	8.557	5.511	8.622	5.611	8.801	6.064	9.547
6.394	10.091	6.425	10.136	6.640	10.456	6.861	10.786
6.862	10.780	6.874	10.813	7.092	11.115	7.233	11.315
7.286	11.383	7.326	11.434	7.341	11.456	7.354	11.483
7.430	11.582	7.431	11.575	7.525	11.715	7.775	12.041
7.914	12.199	8.023	12.331	8.193	12.552	8.749	13.209
8.963	13.458	9.785	14.371	10.071	14.701	10.159	14.800
10.750	15.429	10.771	15.442				

there is still room for further improvement, especially in certain regions of concentration not well covered by their measurements. Accordingly in presenting the data for CaCl<sub>2</sub> in Table II we have included the concentrations of the solutions isopiestic with round molalities of CaCl<sub>2</sub>, in order to facilitate recalculation in the event of more extensive standard data becoming available in the future.

Table II also gives the osmotic coefficients and water activities derived from the results in Table I. The activity coefficients relative to 0.1 M. were evaluated by tabular integration of the Randall and White<sup>14</sup> equation:

$$-\log \gamma = 0.4343h + \int h d \log m,$$

the integral being thrown into various equivalent forms at different parts of the concentration range. The value of  $\gamma$  at 0.1 M. was then fixed by means of the equation given by Shedlovsky and MacInnes.<sup>7</sup> For completeness, values of  $\gamma$  from 0.002 M. upwards, obtained from their equation, are included in Table II.

### Comparisons with other Work on CaCl<sub>2</sub>.

The most accurate vapour pressure measurements on CaCl<sub>2</sub> appear to be those of Bechtold and Newton<sup>15</sup> by a dynamic method. Although

<sup>11</sup> Olynyk and Gordon, *J. Amer. Chem. Soc.*, 1943, **65**, 224.

<sup>12</sup> Shankman and Gordon, *ibid.*, 1939, **61**, 2370.

<sup>13</sup> Harned and Hamer, *ibid.*, 1935, **57**, 27.

<sup>14</sup> Randall and White, *ibid.*, 1926, **48**, 2514.

<sup>15</sup> Bechtold and Newton, *J. Amer. Chem. Soc.*, 1940, **62**, 1390.

these workers report results at only three concentrations, each is the mean of several concordant values, and the soundness of their method seems to be established by the agreement between their results for  $\text{CaCl}_2$  and those of Tippetts and Newton.<sup>16</sup> In Table III their results are compared with those obtained from the isopiestic ratios; at the two higher concentrations it is clear that the use of the  $a_w$  values for  $\text{H}_2\text{SO}_4$  based on direct

TABLE II.\*

$m_{\text{CaCl}_2}$	$m_{\text{NaCl}}$	$m_{\text{H}_2\text{SO}_4}$	$a_w$	$\phi$	$\gamma$
0.002	—	—	—	—	0.853
0.005	—	—	—	—	0.790
0.01	—	—	—	—	0.732
0.02	—	—	—	—	0.669
0.03	—	—	—	—	0.631
0.05	—	—	—	—	0.583
0.1	0.1380	—	0.99540	0.854	0.524
0.2	0.2806	—	0.99073	0.862	0.478
0.3	0.4284	—	0.98590	0.876	0.460
0.4	0.5820	—	0.98086	0.894	0.453
0.5	0.7425	—	0.97552	0.917	0.454
0.6	0.9078	—	0.96993	0.940	0.458
0.7	1.079	—	0.96425	0.963	0.466
0.8	1.256	—	0.95819	0.988	0.476
0.9	1.440	—	0.95175	1.017	0.490
1.0	1.629	—	0.94505	1.046	0.506
1.2	2.024	—	0.93072	1.107	0.546
1.4	2.437	—	0.91522	1.171	0.595
1.6	2.864	—	0.8986	1.237	0.652
1.8	3.305	—	0.8808	1.305	0.721
2.0	3.758	—	0.8618	1.376	0.802
2.5	4.950	—	0.8091	1.568	1.076
3.0	—	4.404	0.7488	1.779	1.506
3.5	—	5.205	0.6870	1.983	2.118
4.0	—	6.026	0.6232	2.187	3.002
4.5	—	6.875	0.5587	2.394	4.29
5.0	—	7.740	0.4972	2.584	6.08
5.5	—	8.605	0.4405	2.756	8.46
6.0	—	9.449	0.3899	2.901	11.48
6.5	—	10.249	0.3467	3.009	14.94
7.0	—	10.990	0.3107	3.083	18.74
7.5	—	11.673	0.2812	3.127	22.63
8.0	—	12.306	0.2561	3.151	26.64
8.5	—	12.911	0.2334	3.166	30.8
9.0	—	13.496	0.2134	3.172	35.1
9.5	—	14.059	0.1954	3.172	39.5
10.0	—	14.610	0.1794	3.169	44.0
10.5	—	15.156	0.1649	3.107	48.8

\* Values of  $\gamma$  between 0.002 and 0.1 M. are taken from the data of Shedlovsky and MacInnes.

The data above 7 M. correspond to supersaturated solutions of  $\text{CaCl}_2$ .

Results at intermediate concentrations may be obtained by Besselian interpolation for  $a_w$ ,  $\phi$ , and  $\log \gamma$ .

V.P. measurements gives very fair agreement with the dynamic measurements, while the values derived from the e.m.f. measurements<sup>13</sup> on  $\text{H}_2\text{SO}_4$  are widely different. This gives us considerable confidence in the choice of the former as standards. The slightly higher water activities of Bechtold and Newton may well be due in part to their use of C.P.  $\text{CaCl}_2$

<sup>16</sup> Tippetts and Newton, *J. Amer. Chem. Soc.*, 1934, 56, 1675.

which still contained 0.12 % of alkali and Mg expressed as sulphates, since it was found that our unpurified material gave lower isopiestic ratios and higher water activities.

TABLE III.

$m_{\text{CaCl}_2}$	$a_w$ (Dynamic).	$a_w$ (Isopiestic).*
0.3043	0.9863 <sub>3</sub>	0.9856 <sub>5</sub>
3.0335	0.7458 <sub>3</sub>	(a) 0.7426 (b)
7.031	0.3096 <sub>4</sub>	(a) 0.3149 (b)

\*(a) Based on direct vapour pressure measurements on NaCl and H<sub>2</sub>SO<sub>4</sub>.

(b) Based on e.m.f. measurements on H<sub>2</sub>SO<sub>4</sub>.

The osmotic coefficient at 0.097 M. may be evaluated by integration of the activity coefficient data of Shedlovsky and MacInnes in the dilute solutions as 0.855, in excellent agreement with 0.854 from the isopiestic curve.

The dew-point measurements of Hepburn<sup>17</sup> on CaCl<sub>2</sub> gave  $a_w$  values with a mean deviation of 0.003 and a maximum deviation of 0.008 from our results; since his method gave in one case identical water activities in two solutions differing by 20 % in concentration (0.284 and 0.344 M.) it seems that these deviations are of the order of his experimental error. Results from cells involving the calcium amalgam electrode need not be considered here, since this electrode is now known to behave irreversibly.<sup>8</sup>

### Discussion.

The osmotic and activity coefficients attain very high values in the concentrated solutions, in marked contrast with zinc chloride.<sup>4</sup> It is of some interest to determine how far the validity of a Debye-Hückel equation, similar to that employed by Shedlovsky and MacInnes in the dilute solutions, will extend into higher concentrations. It is found that the equation

$$-\log \gamma = \frac{1.764\sqrt{c}}{1 + 2.826\sqrt{c}} - 0.1618c + \log(1 + 0.054m)$$

will reproduce  $\gamma$  with an accuracy of 1 in 500 from 0.002 up to 0.3 M., i.e. up to an ionic strength of unity, which is also the limit of validity of the corresponding equation for 1:1 salts.<sup>10</sup> Above 0.3 M. the calculated values of  $\gamma$  fall increasingly below the experimental values. The theoretical coefficient 1.764 in the above equation is based on the revised values of the physical constants.<sup>18</sup> The coefficient 2.826 corresponds to an "ionic diameter" of 4.96 Å.

### Summary.

Isopiestic measurements on CaCl<sub>2</sub> solutions at 25° have provided values of the water activity, osmotic coefficient, and activity coefficient, extending from 0.1 M. into supersaturated solutions (10 M.). These have been combined with the e.m.f. data of Shedlovsky and MacInnes on dilute solutions to provide a subsidiary standard for 1:2 salts at 25°, for which  $\gamma$  is known from 0.002 M. to 10 M.

Auckland University College,  
New Zealand.

<sup>17</sup> Hepburn, *J. Chem. Soc.*, 1932, 550.

<sup>18</sup> Manov, Bates, Hamer and Acree, *J. Amer. Chem. Soc.*, 1943, 65, 1765.



# A THERMODYNAMIC STUDY OF BIVALENT METAL HALIDES IN AQUEOUS SOLUTION. PART XIV. CONCENTRATED SOLUTIONS OF MAGNESIUM CHLORIDE AT 25°.

By R. H. STOKES.

Received 9th April, 1945.

Magnesium chloride in solutions up to 2 M. has been shown<sup>1</sup> to have the highest osmotic coefficient of the bivalent metal chlorides. It is of some interest to examine the behaviour of this salt up to saturation, and in this paper the earlier work is extended by isopiestic measurements against sulphuric acid.

## Experimental.

Stock solutions of  $\text{MgCl}_2$  and of  $\text{H}_2\text{SO}_4$ , of A.R. quality, were analysed respectively for chloride as  $\text{AgCl}$  and for sulphate as  $\text{BaSO}_4$ . The acid was also determined by weight titration against  $\text{Na}_2\text{CO}_3$ . A few preliminary determinations of the  $\text{MgCl}_2$ -KCl isopiestic ratio (Table Ia) gave

good agreement with the earlier measurements and served as a check on the concentration of the stock solution. The isopiestic molalities of  $\text{MgCl}_2$  and  $\text{H}_2\text{SO}_4$  are presented in Table Ib.

The saturated solution in equilibrium with  $\text{MgCl}_2 \cdot 6\text{H}_2\text{O}$  was found to be isopiestic with 10.61 M.  $\text{H}_2\text{SO}_4$ , of which the water activity, 0.3296, corresponds to 7.83 mm. Hg; Speranski<sup>2</sup> obtained 7.76 mm. by a manometric method. Although  $\text{MgCl}_2$  does not readily form supersaturated solutions, one measurement was obtained on a slightly supersaturated solution. This enabled a determination of

TABLE I.

(a) Isopiestic Molalities of  $\text{MgCl}_2$  and KCl at 25°.

$m_{\text{MgCl}_2}$	1.143	1.645	1.661	1.743	2.050
$m_{\text{KCl}}$	2.175	3.541	3.591	3.833	4.810

(b) Isopiestic Molalities of  $\text{MgCl}_2$  and  $\text{H}_2\text{SO}_4$  at 25°.

$m_{\text{MgCl}_2}$	2.168	2.480	2.782	2.829	3.111
$m_{\text{H}_2\text{SO}_4}$	3.327	3.860	4.379	4.463	4.959
$m_{\text{MgCl}_2}$	3.136	3.287	3.371	3.809	3.819
$m_{\text{H}_2\text{SO}_4}$	5.004	5.277	5.426	6.245	6.262
$m_{\text{MgCl}_2}$	3.843	4.026	4.373	4.502	4.893
$m_{\text{H}_2\text{SO}_4}$	6.307	6.658	7.345	7.608	8.427
$m_{\text{MgCl}_2}$	4.982	5.476	5.840*	5.925†	
$m_{\text{H}_2\text{SO}_4}$	8.615	9.740	10.61	10.84	

\* Saturated.

† Supersaturated.

the solubility to be made. A graph of  $m_{\text{MgCl}_2}/m_{\text{H}_2\text{SO}_4}$  against  $m_{\text{H}_2\text{SO}_4}$  was drawn for the region in the immediate vicinity of saturation, and by interpolating on it at 10.61 M.  $\text{H}_2\text{SO}_4$  the molality of the saturated solution was found to be 5.84<sub>0</sub>, or 55.6<sub>1</sub> g. per 100 g. of water. Seidell's compilation<sup>3</sup> includes three values for the solubility of  $\text{MgCl}_2$  at 25°, viz. 56.7, 55.26, 54.70. The mean, 55.55, agrees well with the present result, which is believed to be accurate to 0.2 %.

## Evaluation of the Activity Coefficient at 0.1 M.

In very few cases hitherto have we been able to fix the value of  $\gamma$  at 0.1 M. for 1 : 2 salts with certainty. In some cases reliable e.m.f. data in

<sup>1</sup> Robinson and Stokes, *Trans. Faraday Soc.*, 1940, 36, 733.

<sup>2</sup> Speranski, *Z. physik. Chem.*, 1910, 70, 521.

<sup>3</sup> Seidell, *Solubilities of Inorganic and Metal-Organic Compounds*, 3rd edition, Van Nostrand, New York, 1940.

dilute solutions have been available, but generally the value has been estimated from freezing-point data, or by a comparison of the osmotic coefficients at 0.1 M. with those of the few salts for which both  $\phi$  and  $\gamma$  are known at this concentration. In Part I of this series,<sup>1</sup>  $\gamma_{0.1}$  for  $\text{MgCl}_2$  was taken to be 0.565, from freezing-point data. The values for  $\text{MgBr}_2$  and  $\text{MgI}_2$  were then estimated as 0.582 and 0.599 respectively, by comparison with the chloride. It has since been shown, however,<sup>4</sup> that the osmotic coefficients of  $\text{MgI}_2$  and  $\text{ZnI}_2$  lie very close together up to 0.5 M.; consequently there is reason to believe that the value of  $\gamma_{0.1}$  for  $\text{MgI}_2$  should be close to 0.579,  $\text{ZnI}_2$  being known to have this value from e.m.f. measurements.<sup>6</sup> This suggests that all the values previously assigned to the magnesium halides were too high, and this is confirmed by an examination of the whole series of activity coefficient curves now available for 1:2 salts. The results for  $\text{CaCl}_2$  in the previous paper make possible a different method of obtaining  $\gamma_{0.1}$  which will now be described and tested.

In the case of isopiestic measurements on pairs of 1:1 salts, the equation of Robinson and Sinclair:<sup>5</sup>

$$\log \gamma = \log \gamma_{\text{ref.}} + \log R + \frac{2}{2.303} \int_0^m \frac{R-1}{\sqrt{(m\gamma)_{\text{ref.}}}} d\sqrt{(m\gamma)_{\text{ref.}}}$$

has been shown to fix the values of  $\gamma_{0.1}$  with good accuracy. The isopiestic ratio ( $R$ ) curve extrapolates smoothly to the theoretical limiting value of unity at zero concentration, and the integral

$$\int_0^{0.1} \frac{R-1}{\sqrt{(m\gamma)_{\text{ref.}}}} d\sqrt{(m\gamma)_{\text{ref.}}}$$

is readily evaluated. When the isopiestic ratio of a 1:1 salt to a 1:2 salt is plotted, however, the ratio at 0.1 M. shows no sign of approaching the value 1.5; it is usually in the vicinity of 1.4 and still apparently decreasing as  $m$  decreases. From the data of MacInnes *et al.*<sup>10</sup> for dilute solutions, osmotic coefficients for  $\text{CaCl}_2$  and  $\text{NaCl}$  have been evaluated. From these, the isopiestic ratio may be calculated in the region below 0.1 M., which is inaccessible to the isopiestic method. It is found that the ratio curve turns sharply upward just below 0.1 M., as in Fig. 1. It is therefore clearly impossible to extrapolate the ratio curve with any certainty. Nevertheless, the isopiestic ratio of any 1:2 salt to  $\text{KCl}$  or  $\text{NaCl}$  may be converted into its ratio to  $\text{CaCl}_2$  by means of the accurately known  $\text{CaCl}_2$ - $\text{NaCl}$  and  $\text{NaCl}$ - $\text{KCl}$  ratios. The ratio  $m_{\text{CaCl}_2}/m_{\text{MX}_2}$  may then be plotted against  $m_{\text{MX}_2}$  and in all cases so far examined this has given a smooth though not always linear

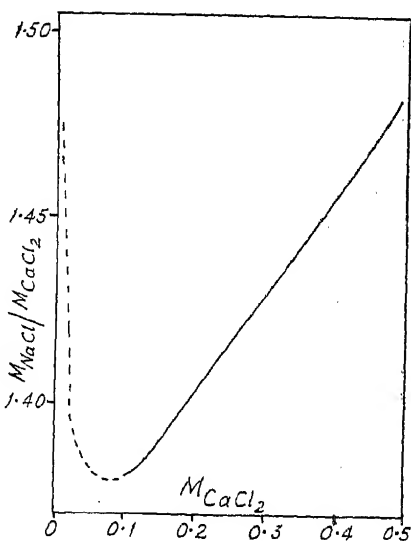


FIG. 1.—Isopiestic Ratio of Sodium Chloride to Calcium Chloride.

Full Curve—Experimental values.  
Broken Curve—Calculated from e.m.f. results.

<sup>4</sup> Stokes, *Trans. Faraday Soc.*, 1945, 41, 17.

<sup>5</sup> Robinson and Sinclair, *J. Amer. Chem. Soc.*, 1934, 56, 1830.

<sup>6</sup> Bates, *ibid.*, 1939, 60, 2983; see also ref. <sup>4</sup>.

extrapolation to unity at zero concentration. The curves for  $\text{MgCl}_2$  and the zinc halides are shown in Fig. 2.

Integration of the Robinson and Sinclair equation between 0 and 0.1 M. may now be carried out, using the  $\gamma$  values of Shedlovsky and MacInnes<sup>10</sup> for  $\text{CaCl}_2$ . For the zinc halides, the values obtained by this method for  $\gamma_{0.1}$  are:  $\text{ZnI}_2$ , 0.579;  $\text{ZnBr}_2$ , 0.541;  $\text{ZnCl}_2$ , 0.518.

The experimental values from e.m.f. measurements in dilute solutions are:  $\text{ZnI}_2$ ,<sup>8</sup> 0.581;  $\text{ZnBr}_2$ ,<sup>7</sup> 0.547;  $\text{ZnCl}_2$ ,<sup>8</sup> 0.515.

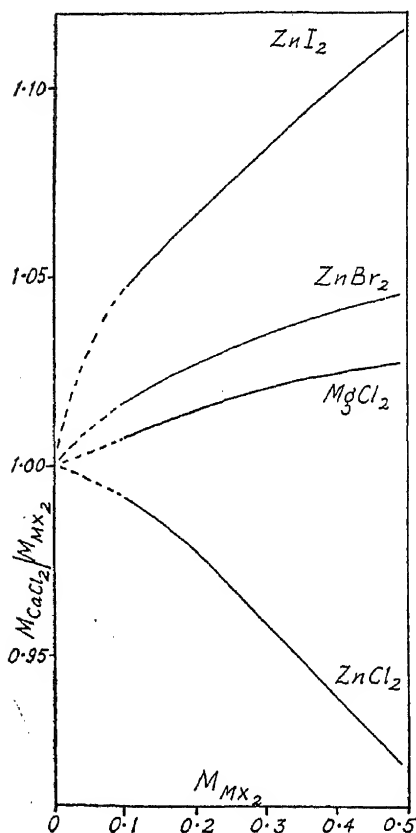


Fig. 2.—Isopiestic Ratio of Calcium Chloride to other 1 : 2 salts.

TABLE II.—WATER ACTIVITIES, OSMOTIC COEFFICIENTS, AND ACTIVITY COEFFICIENTS IN MAGNESIUM CHLORIDE SOLUTIONS AT 25°.

<i>m.</i>	<i>a<sub>w</sub>.</i>	<i>φ.</i>	<i>γ.</i>
0.1	0.99536	0.861	0.532
0.2	0.99057	0.877	0.492
0.3	0.98559	0.895	0.480
0.5	0.97475	0.947	0.484
0.7	0.9627	1.004	0.509
1.0	0.9419	1.108	0.574
1.2	0.9261	1.184	0.634
1.4	0.9088	1.264	0.713
1.6	0.8900	1.347	0.808
1.8	0.8698	1.434	0.922
2.0	0.8482	1.523	1.059
2.5	0.7885	1.759	1.54 <sub>9</sub>
3.0	0.7213	2.015	2.35 <sub>2</sub>
3.5	0.6514	2.266	3.60 <sub>8</sub>
4.0	0.5787	2.530	5.66
4.5	0.5068	2.795	8.94
5.0	0.4374	3.060	14.2 <sub>7</sub>
5.5	0.3711	3.335	23.2 <sub>8</sub>
5.84*	0.3296	3.516	32.2
6.0†	0.3102	3.610	38.0

\* Saturated.

† Obtained by extrapolation from the experimental point at 5.925 M. Results at intermediate concentrations may be obtained by Besselian interpolation for  $a_w$ ,  $\phi$ , and  $\log \gamma$ .

The agreement in the case of  $\text{ZnI}_2$  is excellent; for  $\text{ZnBr}_2$  and  $\text{ZnCl}_2$  it is still fair, being equivalent to 0.0004 volt and 0.0002 volt respectively in the determination of a standard potential in e.m.f. work. One may therefore use this method of extrapolating the isopiestic data with considerable confidence for other 1 : 2 salts. The value of  $\gamma_{0.1}$  so obtained for magnesium chloride is 0.532. This value has now been accepted in preference to the freezing-point value of 0.565 which was used in the earlier paper. The ratio  $m_{\text{CaCl}_2}/m_{\text{MgCl}_2}$  has also been worked out for the whole concentration range, from the data of this and the preceding paper. This has made possible the evaluation of  $\gamma$  at all concentrations by the Robinson

<sup>7</sup> R. H. Stokes and Jean M. Stokes, *Trans. Faraday Soc.*, in the press.

<sup>8</sup> Robinson and Stokes, *ibid.*, 1940, 36, 740.

and Sinclair equation, which is preferable to that of Randall and White,<sup>11</sup> since the term which is obtained by tabular integration contributes much less to  $\log \gamma$  than does the integral term of Randall and White. The integral can therefore be evaluated by larger steps without loss of accuracy. The  $\phi$  and  $a_w$  values were obtained similarly from the  $\text{CaCl}_2$  data, and checked by direct interpolation on the standard curves for  $\text{KCl}$  and  $\text{H}_2\text{SO}_4$ .

Values of  $a_w$ ,  $\phi$  and  $\gamma$  at round concentrations of  $\text{MgCl}_2$  are presented in Table II.

### Discussion.

The activity coefficient is seen to reach extraordinarily high values in the concentrated solutions. It seems probable, therefore, that complex ion formation and incomplete dissociation are of negligible importance in  $\text{MgCl}_2$ ; the heavy hydration of the free  $\text{Mg}^{++}$  ions then accounts qualitatively for the steep rise in the  $\gamma$  values. The contrast between these values and those for  $\text{ZnCl}_2$ <sup>9</sup> is very marked, although the  $\text{Zn}^{++}$  ion has practically the same crystallographic radius as the  $\text{Mg}^{++}$  ion. The negative transport numbers found in concentrated  $\text{ZnCl}_2$  solutions, however, prove the presence of complex anions in this salt, so that the zinc ions are not all free to form hydration sheaths.

### Summary.

Isopiestic measurements on  $\text{MgCl}_2$  solutions at  $25^\circ$  have given values of the water activity, osmotic coefficient, and activity coefficient up to saturation. The solubility and the vapour pressure of the saturated solution at  $25^\circ$  have also been determined. The equation of Robinson and Sinclair has been shown to give a fairly reliable extrapolation for  $\gamma_{0.1}$  when the isopiestic ratios of 1 : 2 salts are plotted in the form  $m_{\text{CaCl}_2}/m_{\text{MX}_2}$  and the  $\gamma$  values for  $\text{MgCl}_2$ , reported in an earlier paper, have been recalculated on a sounder basis by this equation.

Auckland University College,  
New Zealand.

<sup>9</sup> Harris and Parton, *Trans. Faraday Soc.*, 1940, 36, 1139.

<sup>10</sup> Brown and MacInnes, *J. Amer. Chem. Soc.*, 1935, 57, 1356; Shedlovsky and MacInnes, *ibid.*, 1937, 59, 503.

<sup>11</sup> Randall and White, *ibid.*, 1926, 48, 2514.

## A REVISION OF SOME BOND-ENERGY VALUES AND THE VARIATION OF BOND-ENERGY WITH BOND-LENGTH

By H. A. SKINNER.

Received 9th April 1945.

In his book "The Nature of the Chemical Bond", Pauling<sup>1</sup> has given a table of bond-energies for a large number of bonds. Pauling's values are derived, practically entirely, from thermochemical data compiled by Rossini and Bichowsky<sup>2</sup> and published in "The Thermochemistry of Chemical Substances," in 1936. Since that date, several new thermochemical and spectroscopic measurements have appeared, in consequence of which it now seems opportune to review the bond-energies as given by Pauling, in the light of more recent data.

<sup>1</sup> L. Pauling, *The Nature of the Chemical Bond*, 1939, chap. 2.

<sup>2</sup> Bichowsky and Rossini, *Thermochemistry of Chemical Substances*, 1936.

### 1. Single-bonded Diatomic Molecules.

Bond-energies in single-bonded diatomic molecules are directly obtainable from thermochemical or spectroscopic estimations of the heats of dissociation. Herzberg<sup>3</sup> has recently compiled an extensive and critical list of the molecular constants (including dissociation energy) of a large number of diatomic molecules: from Herzberg's quoted values the bond-energies (at room temp.) of  $H_2$ , the halogens, and the alkali-metals are as follows:—

H—H	104.1	Li—Li	27.2
F—F	63.5	Na—Na	18.5
Cl—Cl	58.1	K—K	12.8
Br—Br	46.3	Rb—Rb	12.2
I—I	36.4	Cs—Cs	11.3

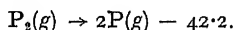
(all values in k.cal. mole<sup>-1</sup>).

These values are practically identical with the corresponding figures quoted by Pauling.

### 2. Bond-energies Derived from Polyatomic Molecules.

To derive the bond-energies of single covalent bonds linking multi-valent atoms (*e.g.* P—P, N—N, O—O) it is necessary to use data obtained on polyatomic molecules. If it can be assumed with reasonable certainty that the M—M bonds in a molecule  $M_x$  are all normal single bonds, then it follows that the M—M bond-energy is given by the heat of formation of  $M_x$  (gas) from the gaseous atoms ( $Q_a$ ) divided by the number of M—M bonds in the molecule  $M_x$ . The bond-energies P—P, As—As, S—S, Se—Se, and C—C may be computed by this method.

(a) **The P—P Bond-energy.**—Pauling quotes the value 18.9 k.cal. for the P—P bond energy. The derivation involves, at one stage, a knowledge of the dissociation energy of the  $P_2$  molecule, for which Bichowsky and Rossini quote:



A recent spectroscopic examination of the  $P_2$  molecule by Herzberg<sup>4</sup> shows the above value to be considerably in error, the recommended value now being 116.9 k.cal. Using Herzberg's value, the P—P bond-energy is derived as follows:

$$\begin{cases} (1) & P(c) \rightarrow P_4(g) - 13.2 & (\text{Ref. : B. and R.}) \\ (2) & P_4(g) \rightarrow 2P_2(g) - 30 & (\text{Ref. : B. and R.}) \\ (3) & P_2(g) \rightarrow 2P(g) - 116.9 & (\text{Ref. 4}) \end{cases}$$

whence:

$$\begin{aligned} P(c) &\rightarrow P(g) - 69.25 \\ P_4(g) &\rightarrow 4P(g) - 263.8 \end{aligned}$$

from which, since the  $P_4$  molecule contains 6 P—P bonds, the P—P bond-energy is 44 k.cal. mole<sup>-1</sup>.\*

<sup>3</sup> G. Herzberg, *Molecular Spectra and Molecular Structure*, 1939, p. 483.

<sup>4</sup> See ref 3, and Herzberg, Herzberg, Milne, *Can. J. Res.*, 1940, 18, 139.

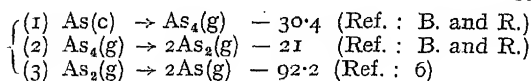
\* It should be noted that this value (44 k.cal.) refers to the P—P energy in the molecule  $P_4$ , in which the P—P—P angles are all equal to 60°.

In compounds in which the P—P bonds are directed at the normal angle of 90° (for  $\phi$  bonds), we might expect the P—P bond-energy to be greater than 44 k.cal. Using the method of Pauling<sup>5</sup> which relates bond-strength to the overlap of the radial parts of the wave-functions  $\psi p_x, \psi p_y, \psi p_z$  where

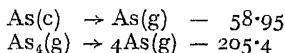
$$\begin{cases} \phi_x = \sqrt{3} \sin \theta \cos \phi \\ \phi_y = \sqrt{3} \sin \theta \sin \phi \\ \phi_z = \sqrt{3} \cos \theta \end{cases}$$

[Footnote continued on opposite page.]

(b) **The As—As Bond-energy.**—Pauling's value of 15.1 k.cal. for the As—As bond-energy uses the value of 35 k.cal. as quoted by Bichowsky and Rossini for the energy of dissociation of  $\text{As}_2(\text{g})$ . More recent spectroscopic measurements by Kinzer and Almy<sup>6</sup> yield 92.2 k.cal. for this quantity, from which we re-estimate the As—As bond-energy as follows :

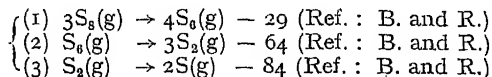


whence :

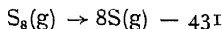


and the estimated As—As bond-energy =  $34.2 \text{ k.cal. mole}^{-1}$ .\*

(c) **The S—S Bond-Energy.**—The bond-energy of the S—S bond may be derived from thermal data involving the molecules  $\text{S}_8$ ,  $\text{S}_6$ , and  $\text{S}_2$ . The value estimated here differs from that of Pauling, in that we have chosen the recent value obtained by Olsson<sup>7</sup> for the heat of dissociation of the  $\text{S}_2$  molecule, i.e. 84 k.cal., in place of the value 102.6 k.cal. quoted by Rossini. The relevant thermochemical data are :

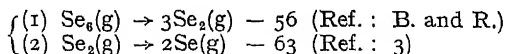


from which :

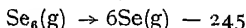


giving for the S—S bond-energy,  $\text{S—S} = 53.9 \text{ k.cal. mole}^{-1}$ .

(d) **The Se—Se Bond-energy.**—Herzberg<sup>3</sup> quotes the value 63 k.cal. for the heat of dissociation of the molecule  $\text{Se}_2(\text{g})$ ; combining this with thermal data quoted by Bichowsky and Rossini, we have :



from which



and the bond-energy  $\text{Se—Se} = 40.8 \text{ k.cal. mole}^{-1}$ .

(e) **The C—C Bond-energy.**—The C—C bond-energy has been derived from the heat of sublimation of diamond, to which it is simply related and given by  $\frac{1}{2}L$  (where  $L$  = sublimation heat). There has been much controversy concerning the value of  $L$ , and at the present time apparently good, but conflicting evidence points to each of the three values,  $L = 125$ ,

and  $\theta$ ,  $\phi$  are the angles used in spherical polar co-ordinates, the relative strength of two bonds with bond-angle  $90^\circ$ , and with bond-angle  $(90 - 2\alpha)^\circ$  is given by :

$$\frac{E_{90}}{E_{(90-2\alpha)}} = \frac{3}{3 \cos^2 \alpha}$$

$$\text{or } E_{(90-2\alpha)} = E_{90} \cdot \cos^2 \alpha.$$

In  $\text{P}_4$ , each P—P bond is strained through an angle  $\alpha = 15^\circ$  from the normal : since  $E_{(90-2\alpha)} = 44$ , we have  $E_{90} = 44/\cos^2 15^\circ$  or, the "normal" P—P bond-energy,  $E_{90} = 47.2 \text{ k.cal.}$

The transformation formula  $E_{(\theta-2\alpha)} = E_\theta \cos^2 \alpha$  must be regarded as an approximation : it is not certain that bond-strength is quantitatively related to the degree of overlap of the wave-functions, which assumption is made in deriving the formula.

<sup>5</sup> Pauling, *loc. cit.*<sup>1</sup>, p. 85.

<sup>6</sup> Kinzer, Almy, *Physic Rev.*, 1937, 52, 814.

\* The structure of  $\text{As}_4$  is exactly analogous to that of  $\text{P}_4$  with the angles As—As—As =  $60^\circ$ . The bond-energy  $34.2$  therefore refers to As—As bonds, strained through an angle of  $15^\circ$ . The "normal" bond-energy of As—As bonds at  $90^\circ$  angle is derived as  $36.7 \text{ k.cal.}$

<sup>7</sup> Olsson, *Z. Physik*, 1936, 100, 656 ; *Dissertation*, Stockholm, 1938.

$L = 136$ , and  $L = 170$  k.cal. Pauling chose the lowest of the above values as correct, and thus assumed the C—C bond-energy =  $\sim 62$  k.cal. mole<sup>-1</sup>.

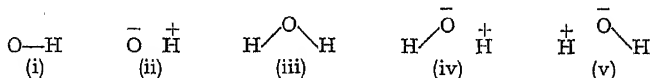
The principal evidence for the value  $L = 125$  derives from Herzberg's<sup>8</sup> interpretation of the spectrum of CO. This author concludes that the most probable value for the dissociation energy of CO is  $D(\text{CO}) = 210.8$  k.cal., which combined with the known heat of formation of CO yields the value 125 for  $L$ . On the other hand, Hagstrum and Tate<sup>9</sup> in a review of the evidence supplied by electron impact experiments on CO, conclude that the data is compatible only with the value  $D(\text{CO}) = 221.3$  k.cal., corresponding to  $L = 136$ . Evidence for the highest value ( $L = 170$ ) is provided by direct measurement of the sublimation heat by Marshall and Norton,<sup>10</sup> from measurement of the dissociation energy of cyanogen by White,<sup>11</sup> from theoretical calculations by Kynch and Penney,<sup>12</sup> whilst indirectly, Baughan<sup>13</sup> has argued that the high value of  $L$  provides a suitable explanation of the observed energy of rupture of the first C—H bond in methane, measured at  $\sim 102$  k.cal. by Kistiakowsky, Stevenson, and others.<sup>14</sup> Most of these arguments favouring  $L = 170$  have been criticised by Herzberg:<sup>15</sup> in addition, Mulliken and Rieke<sup>16</sup> deny that the theoretical calculations by Kynch and Penney provide evidence favouring  $L = 170$ .

This short (and incomplete) summary of the available evidence is sufficient to indicate the present uncertainty: we shall, therefore, not specify any particular choice for the C—C bond energy, but write it as  $\frac{1}{2}L$ , where  $L$  is given the values 125, 136, and 170 k.cal.

(f) **The O—O Bond-energy.**—The value 34.9 k.cal. derived by Pauling for the O—O bond-energy was obtained from the experimental value for the heat of formation of  $\text{H}_2\text{O}_2$ , coupled with the assumption that the —OH bond-energy in  $\text{H}_2\text{O}_2$  is identical with the —OH bond-energy in  $\text{H}_2\text{O}$ . In amending Pauling's value, it is in this latter assumption that we differ.

Dwyer and Oldenberg<sup>17</sup> have found that the bond energy in the free radical —OH is  $\sim 100$  k.cal., whereas the accurate thermal measurements of Rossini<sup>18</sup> lead to a mean bond-strength of OH in  $\text{H}_2\text{O}$  of 110.4 k.cal. This reduction in bond-strength in the free radical is reflected in the increase in bond-length compared with  $\text{H}_2\text{O}$  (0.971 Å. in —OH, compared with 0.955 Å. in  $\text{H}_2\text{O}$ ).

A tentative explanation of the weaker binding existing in the free radical, can be given in terms of the resonance structures participating in —OH



and  $\text{H}_2\text{O}$  molecules. In the radical, the two major contributing structures (i) and (ii) are matched in the water molecule by the corresponding

structures (iii), (iv), (v), but the completely ionic structure  $\text{H}^+ \text{O}^- \text{H}^+$

<sup>8</sup> Herzberg, *Chem. Rev.*, 1937, 20, 145.

<sup>9</sup> Hagstrum and Tate, *Physic. Rev.*, 1941, 59, 354.

<sup>10</sup> Marshall and Norton, *J.A.C.S.*, 1933, 53, 431.

<sup>11</sup> White, *J. Chem. Physics*, 1940, 8, 459.

<sup>12</sup> Kynch and Penney, *Proc. Roy. Soc., A*, 1941, 179, 214.

<sup>13</sup> Baughan, *Nature*, 1941, 147, 542.

<sup>14</sup> Anderson, Kistiakowsky, van Artsdalen, *J. Chem. Physics*, 1942, 10, 306. Stevenson, *ibid.*, 1942, 10, 291. Kistiakowsky and van Artsdalen, *ibid.*, 1944, 12, 469.

<sup>15</sup> Herzberg, *ibid.*, 1942, 10, 306.

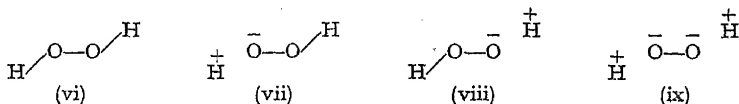
<sup>16</sup> Mulliken, Rieke, *Rev. Mod. Physics*, 1942, 14, 259.

<sup>17</sup> Dwyer, Oldenberg, *J. Chem. Physics*, 1944, 12, 351.

<sup>18</sup> Rossini, *Bur. Stand. J. Res.*, 1931, 6, 1.

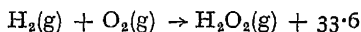
(which Pauling<sup>19</sup> has estimated to contribute some 8% to the total resonance in  $\text{H}_2\text{O}$ ) has no counterpart in the radical. It is possible that the resonance involving this structure is sufficient to explain the increased binding energy in  $\text{H}_2\text{O}$  over that in  $-\text{OH}$ .

If this explanation is correct, we may argue from it that the binding-energy of  $-\text{OH}$  in  $\text{H}_2\text{O}_2$  is likely to be less than the energy in  $\text{H}_2\text{O}$ . The major resonance structures in the molecule  $\text{H}_2\text{O}_2$  may be represented by (vi)-(ix)



and we may note that the purely ionic counterpart to the structure (x) is not possible. On the other hand, the resonance involving (ix) may be expected to increase the OH energy in  $\text{H}_2\text{O}_2$  over that in the radical. These considerations lead to the general conclusion that the  $-\text{OH}$  bond energy in hydrogen peroxide should lie within the limits 110.4–100 k.cal., probably slightly nearer the lower than the upper limit. We have chosen the value  $\text{OH} \sim 102$  k.cal., as the most likely.

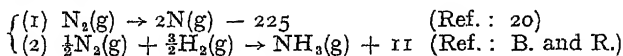
Bichowsky and Rossini quote :



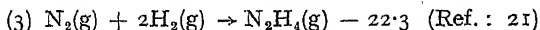
which yields for the heat of formation from gaseous atoms  $Q_{a(\text{H}_2\text{O}_2)} = 255.7$  k.cal. Using our chosen value 102 for the OH bond-energy, we obtain  $\sim 52$  k.cal. mole<sup>-1</sup> for the O—O bond-energy.\*

(g) **The N—N Bond-energy.**—The N—N bond-energy value of 20 k.cal. obtained by Pauling from the heat of formation of hydrazine, and the assumption that the NH bond-energy in hydrazine is the same as that in ammonia, is probably a low value : this is partially due to the assumption made concerning the NH bond-energy, and also because of the change recently proposed by Gaydon<sup>20</sup> in the value for the heat of dissociation of nitrogen.

The relevant thermochemical data are :



from which  $Q_{a(\text{NH}_3)} = 279.6$ , and the NH bond-energy in  $\text{NH}_3$  is 93.2 k.cal.



from which  $Q_{a(\text{N}_2\text{H}_4)} = 411.0$  k.cal.

The N—N bond-energy is thus given by  $411 - 4(\text{NH})$  where (NH) is the mean NH bond-strength in hydrazine.

An estimation of the NH bond-strength in  $\text{N}_2\text{H}_4$  can be made from a consideration of the resonance structures participating in the molecule, in similar manner to the estimation of OH in  $\text{H}_2\text{O}_2$ . The hydrazine molecule differs from  $\text{NH}_3$  in that resonance structures of the type

<sup>19</sup> Pauling, *loc. cit.*<sup>1</sup>, p. 71.

\* This value may be compared with a calculated value for the O—O bond-energy of  $\sim 55$  k.cal., derived from a semi-empirical quantum-mechanical method by Sokolov.<sup>22</sup> In a footnote in his paper, Sokolov refers to an estimation of the O—O energy in the ion  $\text{O}^--\text{O}^-$ , for which Kazarnovsky<sup>23</sup> obtained a bond-energy value of  $\sim 53$  k.cal.

<sup>20</sup> Gaydon, *Nature*, 1944, **153**, 407.

<sup>22</sup> Sokolov, *Acta Physicochim. U.R.S.S.*, 1944, **19**, 208.

<sup>23</sup> Kazarnovsky, *J. Phys. Chem. Russ.*, 1940, **14**, 320.



--- H<sup>+</sup>  
 N H<sup>+</sup> are not possible: this should render NH a weaker bond in N<sub>2</sub>H<sub>4</sub>  
 H<sup>+</sup>

than in NH<sub>3</sub>. The difference is probably very slight, since it is unlikely that the triply ionised structure contributes in a major way to the resonance in the NH<sub>3</sub> molecule. We have chosen to take NH ~ 92 k.cal. as the best value, which leads to a value of ~ 43 k.cal. for the N—H bond energy. The chosen value may be compared with the value ~ 48 k.cal. calculated by Sokolov<sup>21</sup> by a semi-empirical quantum-mechanical method.

(h) **The Si—Si Bond-energy.**—The value quoted by Pauling for the Si—Si bond-energy (42.5) derives from the heat of sublimation of silicon quoted at 85 k.cal. by Bichowsky and Rossini. There is, however, some uncertainty in this value; as Rossini writes:<sup>2</sup> "Ruff and Konshak measured what they believed to be the vapour pressure of silicon". Apart

TABLE I.—BOND-ENERGIES AND BOND-LENGTHS IN A—A BONDS.

H—H 104.1 0.74				
Li—Li 27.2 2.672	C—C $\frac{1}{2}L$ * 1.544	N—N (43) 1.47	O—O (52) 1.46	F—F 63.5 1.435
Na—Na 18.5 3.079	Si—Si (51.3) 2.32	P—P 47.2 2.20	S—S 53.9 2.07	Cl—Cl 58.1 1.989
K—K 12.8 3.923	Ge—Ge (34) 2.41	As—As 36.7 2.44	Se—Se 40.8 2.32	Br—Br 46.1 2.284
Rb—Rb 12.2 (4.23)				I—I 36.4 2.667
Cs—Cs 11.3 (4.47)				

\*  $L = 125, 136$  or  $170$ .

from this rather dubious measurement, there does not appear to be any direct thermochemical data available from which to make a reliable estimate of Si—Si energy. Probably the best estimate at present, derives from the kinetic measurements of Emeleus and Reid<sup>24</sup> on the thermal decomposition of disilane. These authors find that the first step in the decomposition is the rupture of the Si—Si bond, with which process an activation energy of 51.3 k.cal. is associated. We may identify this with the Si—Si bond-energy in disilane, and accept the value of ~ 51 k.cal. provisionally, until reliable thermal data is available.

(i) **The Ge—Ge Bond-energy.**—The sublimation heat of Ge is not known, and the value given by Rossini and Bichowsky (85 k.cal.) is an estimate only. As in the case of the Si—Si bond, no thermal data is yet available to enable an assessment to be made of the Ge—Ge bond-energy. The kinetic measurements by Emeleus and Jellinek<sup>25</sup> on the decomposition of digermane, which the authors state proceed by an initial rupture of the Ge—Ge bond, may be interpreted to imply that the Ge—Ge bond energy is approximately 34 k.cal./mole<sup>-1</sup>.

<sup>21</sup> Hughes, Corruccini, Gilbert, *J.A.C.S.*, 1939, 61, 2642. Hieber, Woerner, *Z. Elektro.*, 1934, 40, 252.

<sup>24</sup> Emeleus and Reid, *J.C.S.*, 1939, 1021.

<sup>25</sup> Emeleus and Jellinek, *Trans. Faraday Soc.*, 1944, 40, 93.

In Table I, the bond-energies of single normal bonds of type A—A derived above, are collected together, and listed with the bond-lengths with which these energies are associated.

### 3. Bond-energies of Bonds Type A—B.

The bond-energies of bonds of the general type A—B may be derived directly in case of single-bonded diatomic molecules (*e.g.* HCl) from the heats of dissociation: in case of polyatomic molecules, AB<sub>n</sub>, AB<sub>2</sub>, AB<sub>3</sub>, AB<sub>4</sub>, etc., the bond-energy *E* is given by  $Q_a/n$ , where  $Q_a$  = heat of formation of the gaseous molecule AB<sub>n</sub> from the gaseous atoms A and B. This equation assumes that all the bonds A—B in AB<sub>n</sub> are equivalent. It should be pointed out that the bond-energies calculated as above give the mean bond-energy of a bond within a molecule at the equilibrium internuclear distance: the *E* values so obtained are not necessarily the same as the energies that may be required to break an A—B bond in a molecule AB<sub>n</sub>: in general the energy required to break off a single atom from a polyatomic molecule will differ from the value *E* calculated as described.\*

In Tables II and III, bond-energies of a number of bonds to hydrogen and the halogens are tabulated, together with the relevant thermal data. In the columns headed  $E_{AM}$  calculated values of the bond-energies are given, derived from the arithmetic mean postulate of Pauling,<sup>26</sup> *i.e.*

$$E_{AM} = \frac{1}{2}(E_{A-A} + E_{B-B})$$

where the values A—A and B—B are taken from Table I. The columns headed  $\Delta E$  quote the values of  $E - E_{AB}$ .

\* TABLE II.—BOND-ENERGIES OF M—H BONDS.

Molecule.	Bond.	$Q_a$ .	<i>E</i> .	$E_{AM}$ *	$\Delta E$ .
CH <sub>4</sub>	C—H	(226.1 + <i>L</i> )	(56.5 + $\frac{1}{2}L$ )	(52 + $\frac{1}{2}L$ )	4.5
NH <sub>3</sub>	N—H	279.6	93.2	73.5	19.7
OH <sub>2</sub>	O—H	220.9	110.2	78.0	32.4
SH <sub>2</sub>	S—H	166	83	79.0	4.0
PH <sub>3</sub>	P—H	227.7	75.9	75.6	0.3
AsH <sub>3</sub>	As—H	171.5	57.2	70.4	-13.2
FH	F—H	148.8( <i>H</i> )	148.8	83.8	65.0
ClH	Cl—H	102.9( <i>H</i> )	102.9	81.1	21.8
BrH	Br—H	87.6( <i>H</i> )	87.6	75.1	12.5
IH	I—H	71.2( <i>a</i> )	71.2	70.2	1.0
SiH <sub>4</sub>	Si—H	319.5( <i>b</i> )	79.9	77.7	2.2
SeH <sub>2</sub>	Se—H	130.8	65.4	72.4	-7.0

\*  $Q_a$  values from Bichowsky and Rossini heats of formation, except those marked (*H*), taken from Herzberg.<sup>3</sup>

(*a*) Quoted by Hulbert and Hirshfelder.<sup>29</sup>

(*b*) Based on the assumption that the heat of sublimation of silicon = 102.6 k.cal. (*i.e.* twice the bond-energy). The  $E_{(Si-H)}$  value may be compared with the value 80.5 k.cal., obtained experimentally by Emeleus, Maddock, and Reid.<sup>30</sup>

If the *E* and  $\Delta E$  values given in Tables II and III are compared with the corresponding figures quoted by Pauling, it will be noted that although the *E* values differ in a number of the examples, the  $\Delta E$  values are closely similar. The bond-energy values recommended here do not, therefore, call for alteration in the electronegativity scale set up by Pauling on the basis of his original bond-energy values.

\* See papers by Butler and Polanyi,<sup>27</sup> and by Evans, Baughan and Polanyi.<sup>28</sup>

<sup>26</sup> Pauling, *loc. cit.*<sup>1</sup>, p. 48.

<sup>27</sup> Butler and Polanyi, *loc. cit.*, 1943, 39, 19.

<sup>28</sup> Evans, Baughan, Polanyi, *loc. cit.*, 1941, 37, 377.

<sup>29</sup> Hulbert, Hirshfelder, *J. Chem. Physics*, 1941, 9, 61.

<sup>30</sup> Emeleus, Maddock, Reid, *J.C.S.*, 1941, 357.

\* TABLE III.—BOND ENERGIES OF M-HALOGEN BONDS.

Molecule.	Bond.	$Q_a$ .	$E$ .	$E_{AM}$ .	$\Delta E$ .
ClF	Cl—F	86.5	86.5	60.8	25.7
ClBr	Cl—Br	53.0(H)	53.0	52.1	0.9
ClI	Cl—I	50.5(H)	50.5	47.2	3.3
BrI	Br—I	42.8(H)	42.8	41.2	1.6
OF <sub>2</sub>	O—F	117.0	58.5	57.7	0.8
OC1 <sub>2</sub>	O—Cl	98.9	49.5	55	—5.5
NF <sub>3</sub>	N—F	234.4(R)	78.1	53.2	24.9
NC1 <sub>3</sub>	N—Cl	138.6(R)	46.2	50.5	—4.3
CF <sub>4</sub>	C—F	(290 + L)	(72.5 + $\frac{1}{4}L$ )	(31.7 + $\frac{1}{4}L$ )	40.8
CCl <sub>4</sub>	C—Cl	(142 + L)	(35.5 + $\frac{1}{4}L$ )	(29.0 + $\frac{1}{4}L$ )	6.5
CBr <sub>4</sub>	C—Br	(96 + L)	(24.0 + $\frac{1}{4}L$ )	(23.0 + $\frac{1}{4}L$ )	1.0
SiF <sub>4</sub>	Si—F	589.7	147.4	57.4	90.0
SiCl <sub>4</sub>	Si—Cl	361.3	90.3	54.7	35.6
GeCl <sub>4</sub>	Ge—Cl	399.6	99.9	46.0	53.9
PCl <sub>3</sub>	P—Cl	226.4	75.5	52.6	22.9
PBr <sub>3</sub>	P—Br	185.2(R)	61.7	46.6	15.1
PI <sub>3</sub>	P—I	127.2(R)	42.4	41.8	0.6
AsCl <sub>3</sub>	As—Cl	210.1	70.0	47.4	22.6
AsBr <sub>3</sub>	As—Br	173.0	57.7	41.4	16.3
AsI <sub>3</sub>	As—I	128.2	42.7	36.6	6.1
SF <sub>6</sub>	S—F	509.1	84.8	58.7	26.1
SeF <sub>6</sub>	Se—F	481.7	80.3	52.1	28.2
SeCl <sub>2</sub>	Se—Cl	113.3	56.6	49.5	7.1

\* The  $Q_a$  values are derived from heats of formation by Bichowsky and Rossini, except those marked (H) from Herzberg, and those marked (R), taken from O. K. Rice.<sup>31</sup>

#### 4. Bond-energies of Multiple-bonded Linkages and the Variation of Bond-energy with Bond-length.

(a) C—C Bonds.—The energies of multiple-bonded C—C linkages can be estimated from thermochemical data on the unsaturated hydrocarbons,

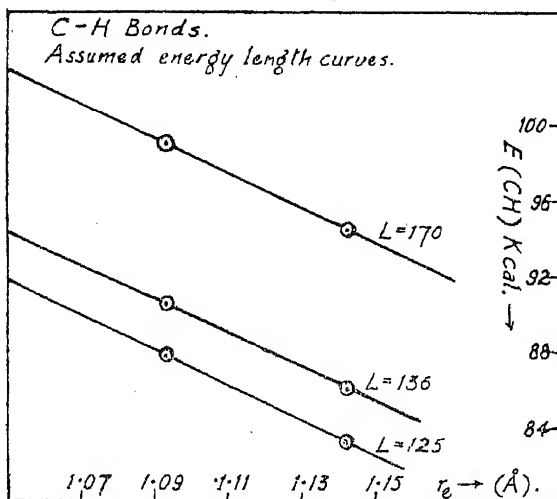


FIG. 1.

if reasonable values for the C—H bond-energies in these molecules can be assumed. The simple assumption that the C—H bond-energy can be put equal to  $E_{(CH)}$  in  $CH_4$  seems to us only justifiable in case where C—H has the same bond-length as it has in  $CH_4$ . Exact spectroscopic measurement has shown that in ethylene the C—H bond-length is 1.071 Å, and in acetylene, 1.057 Å — i.e. in both these molecules C—H is shorter than in  $CH_4$ . We shall postulate that *short bonds are strong bonds*, and apply this in an arbitrary manner to estimate the

<sup>31</sup> O. K. Rice, *Electronic Structure and Chemical Binding*, 1940, p. 192.

variation of bond-energy with length in C—H bonds. The assumption made is that there is a linear relationship between the energy and length of C—H links. The two points by which the curve is fixed are taken as

- (1) C—H in methane;
- (2) the "ideal" covalent C—H bond.

The length of (1) is accurately known,  $r_e = 1.093$  Å., and the energy is given by  $Q_a/4$ , where  $Q_a = (226.1 + L)$ . The length of (2) we assume

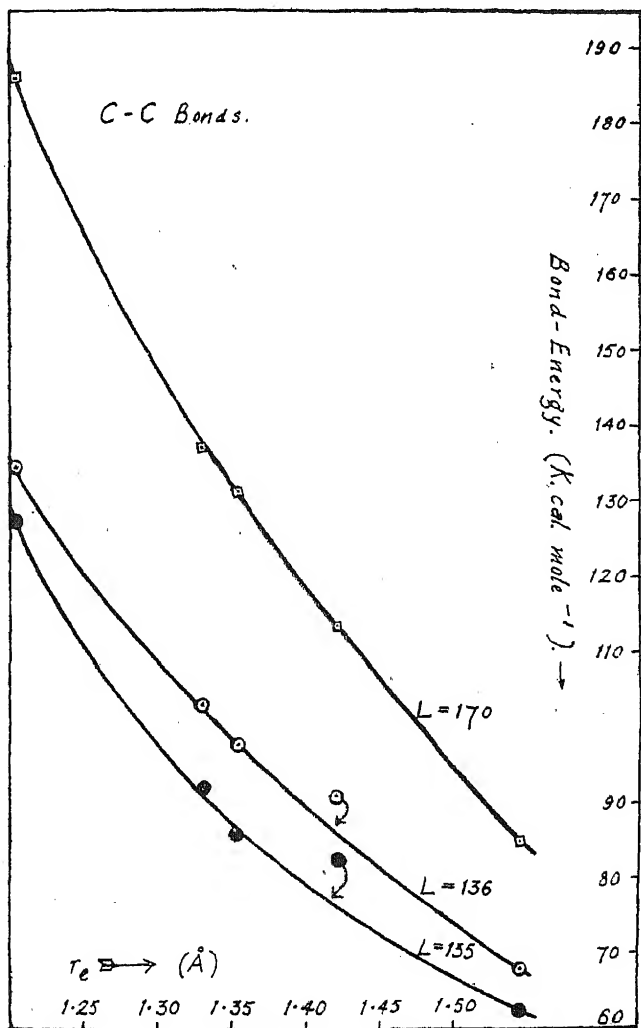


FIG. 2.

to be given by the sum of the covalent radii of C and H ( $r_e = \frac{1}{2}r_{CC} + \frac{1}{2}r_{HH}$ ) = 1.142 Å., and the energy we assume to be given by the additive mean postulate of Pauling, i.e.  $E(\text{CH}) = \frac{1}{2}(104.1 + \frac{1}{2}L)$ . The C—H energy-length curves derived from these assumptions are given for each of the three possible values of  $L$  in Fig. 1. From Fig. 1, we can obtain the C—H energies in ethylene, acetylene, and allene, in which compounds the C—H

lengths are known. These assumed energies, plus the accurate thermal data now available, enable the C—C energies to be obtained: the data are collected in Table IV, and the derived energy length curves for C—C bonds shown in Fig. 2. These may be compared with a similar curve drawn by Fox and Martin,<sup>32</sup> from which they differ slightly, in view of our assumption of the variability of the C—H bond-energies.

TABLE IV.—BOND-ENERGIES IN C—C LINKS.\*

Molecule.	$r_{C-C}$ .	$r_{C-H}$ .	$Q_f$ .	$Q_a$ .	$L = 125$ .		$L = 136$ .		$L = 170$ .	
					$E_{CH}$ .	$E_{CC}$ .	$E_{CH}$ .	$E_{CC}$ .	$E_{CH}$ .	$E_{CC}$ .
Diamond	1.5445 <sup>a</sup>	—	—	—	—	62.5	—	68	—	85
Graphite	1.4210 <sup>b</sup>	—	—	—	—	82.5	—	90.7	—	113.3
Ethylene	1.353 <sup>c</sup>	1.071 <sup>c</sup>	-12.56	(195.6 ± 2L)	89.9	86.0	92.5	97.6	101.1	131.2
Acetylene	1.204 <sup>d</sup>	1.057 <sup>d</sup>	-54.23	(49.9 ± 2L)	91.2	117.5	93.7	134.5	101.9	186.1
Allene	1.330 <sup>e</sup>	1.087 <sup>e</sup>	-46.05	(162.1 ± 3L)	88.3	92.0	91.0	103.0	99.5	137.0

\* (a) Riley.<sup>33</sup>

(b) Private communication from Dr. D. P. Riley.

(c) Galloway and Barker.<sup>34</sup>

(d) Herzberg, Patat and Spinks.<sup>35</sup>

(e) Eyster:<sup>36</sup> note that Eyster estimated C—H in allene, by use of Badger's rule, and that the allene distances are therefore less certain than the others quoted.

All  $Q_f$  values are taken from Rossini.<sup>37</sup>

It will be observed from Fig. 2 that whereas the points calculated for  $L = 170$  lie on a smooth curve, the points corresponding to the bond-energy in graphite lie slightly off the curves drawn for  $L = 125$  and  $L = 136$ . This may be interpreted to imply that  $L = 170$  is the correct value to assign to this quantity: but another explanation can be given, which would render the apparently good fit of the graphite point in the curve  $L = 170$  fortuitous. The energy of C—C in graphite was assumed equal to  $\frac{3}{2}L$ , since it is necessary to break the bonds attaching a given carbon atom to its three neighbours, when the given atom is volatilised from the graphite lattice. This assumption neglects the energy required to overcome the van der Waals attractive forces between the layers in the graphite lattice. Should the interlayer attractive forces correspond to an energy of 3.4 k.cal. per gram-atom (which would not seem unreasonable), the calculated C—C energy in graphite should be reduced by this amount, and the points for  $L = 125$  and  $L = 136$  would now lie on the smooth curves, whereas the point for  $L = 170$  would lie beneath the curve.

The C—H and C—C energy-length curves can be used as starting-points from which to derive similar curves for a number of different bonds. Before making this extension, however, we shall consider the C—C and C—H energies in the saturated hydrocarbons. Table V summarises the thermal data.

The assumption has been made (in Table V) that the C—C bond-distances remain the same in the higher hydrocarbons as in ethane: in so far as this is correct, there is a gradual decrease in the mean C—H bond-energy from  $CH_4$  to ethane, and the higher homologues.

Some special interest attaches to the compound cyclopropane: the electron diffraction investigation of  $C_3H_6$  gives  $1.53 \pm 0.03$  A. for the

<sup>32</sup> Fox, Martin, *J.C.S.*, 1938, 2106.

<sup>33</sup> Riley, *Nature*, 1944, 153, 587.

<sup>34</sup> Galloway, Barker, *J. Chem. Physics*, 1942, 10, 88.

<sup>35</sup> Herzberg, Patat, Spinks, *Z. Physik*, 1934, 92, 87.

<sup>36</sup> Eyster, *J. Chem. Physics*, 1938, 6, 580.

<sup>37</sup> Rossini, *The Chemical Background to Engine Research*, 1943, Chap. 2.

C—C distance, which seems to imply that whereas the C—C bond-energy is greater than in ethane, the C—H energy is markedly less. Since the C—C—C bonds are relatively under a greater strain than the H—C—H bonds, we should expect the contrary state of affairs. Even if the upper limit allowed by the diffraction study of 1.56 Å. is taken as the correct C—C distance, the C—H bond-energy still appears to be low. We are inclined to the view that in the case of cyclopropane, the C—C bond-energy is less than we should deduce from its observed length, and from Fig. 2.

TABLE V.—BOND-ENERGIES IN THE SATURATED HYDROCARBONS.\*

Molecule.	$Q_f$ .	$Q_a$ .	$r_{CC}$ .	$L = 125$ .		$L = 136$ .		$L = 170$ .	
				$E_{CC}$ .	$E_{CH}$ .	$E_{CC}$ .	$E_{CH}$ .	$E_{CC}$ .	$E_{CH}$ .
CH <sub>4</sub>			—	—	87.8	—	90.5	—	99.0
C <sub>2</sub> H <sub>6</sub>	20.19	(332.5 + 2L)	1.55 <sup>a</sup>	62	86.7	67.4	89.5	83.8	98.1
C <sub>3</sub> H <sub>8</sub>	24.75	(441.2 + 3L)	(1.55) <sup>b</sup>	62	86.5	67.4	89.3	83.8	97.9
n-C <sub>4</sub> H <sub>10</sub>	29.72	(550.2 + 4L)	(1.55) <sup>b</sup>	62	86.4	67.4	89.2	83.8	97.8
n-C <sub>5</sub> H <sub>12</sub>	34.72	(659.3 + 5L)	(1.55) <sup>b</sup>	62	86.3	67.4	89.1	83.8	97.8
cyclo-propane	— 12.81	(299.5 + 3L)	1.53 <sup>a</sup>	(63.7)	(80.6)	(69.8)	(83.0)	(87.8)	(91.0)

\*  $Q_f$  values from Rossini.<sup>27</sup>(a) Pauling and Brockway.<sup>28</sup>

(b) assumed.

The original statement made concerning the dependence of bond-energy and bond-length requires amendment, as follows: *the bond-energy of a bond within a molecule is a function of the bond-length, and the bond-angle: when the bonds are disposed at the "normal" bond angles, the energy is determined by the length, but should the bonds be strained through an appreciable angle, the bond-energy may be reduced without effecting a corresponding increase in bond-length.*

In cyclopropane, the C—C—C bond angle is 60°, corresponding to a strain in each C—C bond of 25°. Applying the transformation formula given in the footnote (p. 647), we may estimate (approximately) the "true" C—C bond-energy in C<sub>3</sub>H<sub>8</sub> by writing  $E_{60^\circ} = E_{109.5^\circ} \cos^2 25^\circ$ . The amended C—C energies yield values (Table VA) for  $E_{(CH)}$  which we consider more likely than those quoted in Table V. The reduction in bond-energy resulting from angular strain assists in explanation of the apparently negative resonance energies ( $\Delta E$ ) in OCl<sub>2</sub>, and perhaps in NCl<sub>3</sub> (see Table III). The bond-length in OCl<sub>2</sub> is roughly normal, and the O—Cl bond-energy should be equal to, or slightly greater than  $E_{AM}$ . But the bond-angle in OCl<sub>2</sub> has been measured at 115° corresponding to an angular strain in each O—Cl bond of 12½°, the effect of which will be to reduce the bond-energy by some 3 k.cal.

The ozone molecule is a further example in which the observed bond-energy (relative to its length) appears to be small: it is possible that in this case also the low energy results from angular strain.

(b) C—O Bonds.—The energies of the C—O bonds in a variety of molecules have been estimated, using Figs. 1 and 2 to derive the energies of the associated C—H and C—C bonds. The calculated energies and other data are given in Table VI.

<sup>28</sup> Pauling, Brockway, *J.A.C.S.*, 1937, 59, 1223.

TABLE VA.

$L = 125$ .		$L = 136$ .		$L = 170$ .	
$E_{CC}$	$E_{CH}$	$E_{CC}$	$E_{CH}$	$E_{CC}$	$E_{CH}$
52.3	86.3	57.2	89.3	72.1	98.9

\* TABLE VI.—BOND-ENERGIES AND LENGTHS OF C—O BONDS.

Molecule.	$r_{CO}$ .	$r_{C=O}$ .	$Q_f$ .	$Q_a$ .	$E_{(CO)}$ calc.		
					$L = 125$ .	$L = 136$ .	$L = 170$ .
CO	1.128	—	26.84	(85.8 + $L$ )	210.8	221.8	255.8
CO <sub>2</sub>	1.16	—	94.45	(212.5 + $L$ )	168.8	174.2	191.2
H <sub>2</sub> CO	1.21	—	28.7	(191.8 + $L$ )	145.0	150.6	165.8
CH <sub>3</sub> CHO	1.22	1.50	44	(311.2 + $2L$ )	145.2	149.3	162.9
glyoxal	1.20	1.47	75	(297.1 + $2L$ )	152.8	156.9	170.8
(CH <sub>3</sub> ) <sub>2</sub> O	1.42	—	46.4	(417.7 + $2L$ )	70.5	73.4	81.9
ethylene oxide	1.45	1.56	17	(284.2 + $2L$ )	62.5	64.7	71.5

\*  $Q_f$  values from Bichowsky and Rossini, bond-distances from Maxwell.<sup>39</sup>

Since the C—H distances are not accurately known in any of the compounds listed, certain assumptions have been made regarding the C—H energies. The assumptions follow from a recent paper by Linnett,<sup>40</sup> in which he has calculated the force-constants of the C—H bonds in several of the compounds here considered. Briefly, our assumptions are:

**Formaldehyde.**—The C—H distance is assumed = 1.114 Å. in accordance with the estimate of this distance made by Linnett from the calculated force-constant and Clark's rule.\*

**Glyoxal.**—We have assumed C—H in this compound to be equivalent to the C—H bond in CH<sub>4</sub>O.

**Acetaldehyde.**—Linnett finds that the force-constant for the aldehydic C—H is roughly the same as in CH<sub>3</sub>O, and the methyl C—H force-constant practically identical with that of C—H in CH<sub>4</sub>. Accordingly, we assume the aldehydic C—H to be equivalent to C—H in formaldehyde, and write the energy of the methyl C—H bonds equivalent to the C—H energy in methane.

**Dimethyl Ether.**—The C—H force-constant is calculated to be almost identical with that of C—H in methane, and we assume the energies of C—H to be the same as those in CH<sub>4</sub>.

\* TABLE VII.—BOND-ENERGIES AND LENGTHS OF C—N BONDS.

Molecule.	$r_{CN}$ .	$r_{OH}$ .	$r_{CO}$ .	$Q_a$ .	$E_{(CN)}$ calc.		
					$L = 125$ .	$L = 136$ .	$L = 170$ .
HCN	1.15 <sup>a</sup>	1.06	—	(133.8 + $L$ )	167.9	176.3	201.7
C <sub>2</sub> N <sub>2</sub>	1.16 <sup>b</sup>	—	1.37	(154.0 + $2L$ )	160.1	165.5	183.8
—CN	1.172 <sup>c</sup>	—	—	(13.4 + $L$ )	138.4	149.4	183.4
CH <sub>3</sub> N <sub>2</sub>	1.47 <sup>b</sup>	?	—	(380.0 + $L$ )	58.9	61.5	70.7

\* (a) Herzberg and Spinks.<sup>42</sup>(b) Quoted by Maxwell.<sup>39</sup>(c) Quoted by Herzberg.<sup>3</sup> $Q_a$  values (except —CN) derived from data given by Bichowsky and Rossini.<sup>39</sup> Maxwell, *J. Opt. Soc. Am.*, 1940, 30, 374.<sup>40</sup> Linnett, *Trans. Faraday Soc.*, 1945, 41, 223.

\* The value C—H = 1.111 Å. is obtained from the accurately known moments of inertia of the formaldehyde molecule (Dieke and Kistiakowsky<sup>41</sup>) if we assume the H—C—H angle to be the same (120°) as in ethylene, and write C—O = 1.21 Å.

<sup>41</sup> Dieke, Kistiakowsky, *Physic. Rev.*, 1934, 45, 4.<sup>42</sup> Herzberg, Spinks, *Proc. Roy. Soc., A*, 1934, 147, 434.

**Ethylene Oxide.**—We assume C—H in ethylene oxide to be equivalent to C—H in cyclopropane. In the calculations of the C—O energy, corrections have been made for the reduction in energy due to the angular strain.

The energy-length curve for C—O bonds is shown in Fig. 3. Although we have calculated the C—O bond-energies for all three values of  $L$  in Table VI, only the curve corresponding to  $L = 136$  is reproduced here, for reasons of economy of space. The curves for  $L = 124$  and  $L = 170$  are very similar in general form to the curve shown. It should not be concluded that we have any particular preference for the value  $L = 136$ , which is chosen solely because it approximates to a mean between the two extremes.

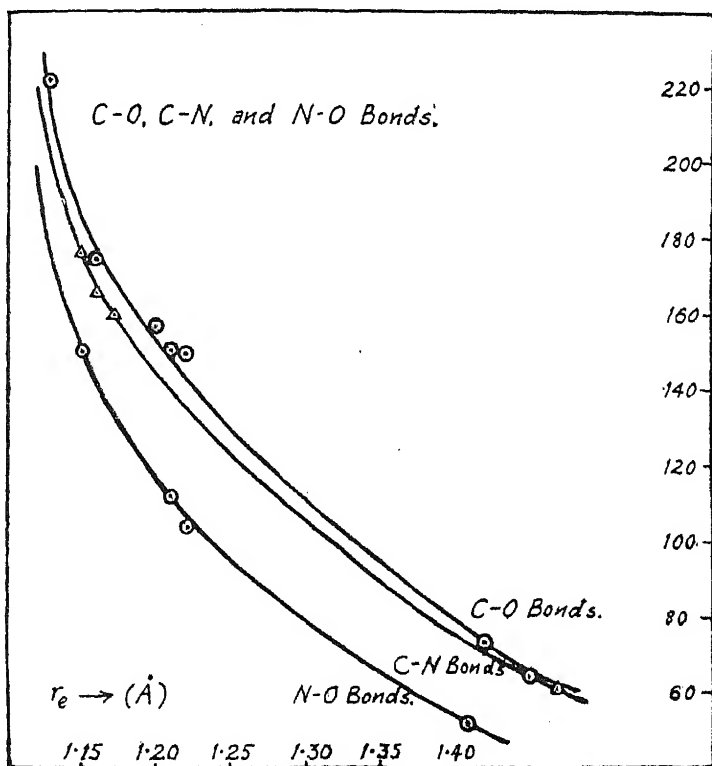


FIG. 3.

(c) **C—N Bonds.**—The energy-length curve for C—N bonds is given ( $L = 136$ ) in Fig. 3, and the thermal and other data summarised in Table VII.

In the estimation of the C—N energy in methylamine, we have assumed the N—H energy to be slightly less than in  $\text{NH}_3$  ( $E = 90$ ), and taken the C—H energy equal to the energy of C—H in ethane. These assumptions follow from the estimated force-constants in this molecule, as given by Linnett.<sup>40</sup>

(d) **N—O Bonds.**—The curve relating energy to length for N—O bonds is given in Fig. 3, and drawn from the data summarised below:—

(a) NO.	$Q_a = 149.9$	$r_{\text{NO}} = 1.150$	$E_{(\text{NO})} = 149.9$
(b) $\text{NO}_2$ .	$Q_a = 222.6$	$r_{\text{NO}} = 1.21$	$E_{(\text{NO})} = 111.3$
(c) $\text{HNO}_3$ .	$Q_a = 376.0$		



The structure of  $\text{HNO}_3$  has been shown to be (xi).<sup>43</sup> The two bonds,  $r_{\text{NO}} = 1.21$  have energy = 222.6 (as in  $\text{NO}_2$ ) and the  $-\text{OH}$  bond we assume to have an energy close to that of  $-\text{OH}$  in  $\text{H}_2\text{O}$ , which has been estimated previously at  $\sim 102$  k.cal. By difference, the energy of the  $\text{NO}$  bond,  $r_{\text{NO}} = 1.41$ , is calculated at 52 k.cal.

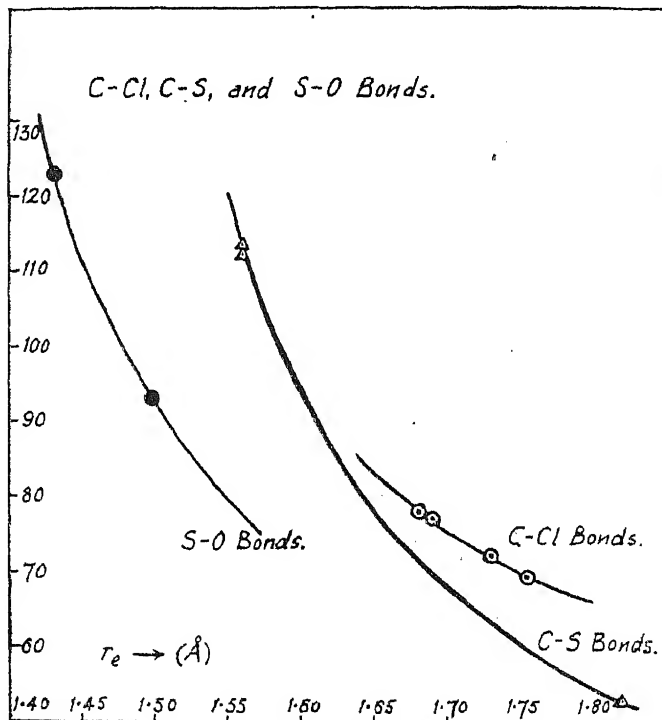
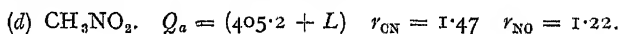


FIG 4.

The force-constant of the  $\text{C}-\text{H}$  bonds in nitromethane is slightly larger than that of  $\text{C}-\text{H}$  in methane, from which we assume  $r_{\text{OH}} = 1.09$  Å. The value  $E_{(\text{ON})}$  is taken from the  $\text{C}-\text{N}$  curve given in Fig. 3. The derived energy of the  $\text{N}-\text{O}$  bond is 103.5 k.cal. and is independent of the assumed value for  $L$ .

(e)  $\text{C}-\text{Cl}$  Bonds.—The  $\text{C}-\text{Cl}$  energy-length curve given in Fig. 4 ( $L = 136$ ), is based upon the data collected in Table VIII.

\* TABLE VIII.— $\text{C}-\text{Cl}$  BOND ENERGIES AND BOND-LENGTHS.

Molecule.	$r_{\text{C-Cl}}$	$r_{\text{O-O}}$	$r_{\text{C-O}}$	$Q_a$	$E_{(\text{C-Cl})}$ calc.		
					$L = 125$	$L = 136$	$L = 170$
$\text{CCl}_4$	1.755	—	—	$(142.1 + L)$	66.8	69.5	78.0
$\text{C}_2\text{Cl}_4$	1.73	1.38	—	$(110.2 + 2L)$	69.5	72.3	81.6
$\text{CH}_2=\text{CHCl}$	1.69	1.38	—	$(176.2 + 2L)$	73.9	77.3	88.6
$\text{COCl}_2$	1.68	—	1.21	$(170.6 + L)$	75.3	78.0	87.4

\* Bond-distances from Maxwell.<sup>49</sup>

$Q_a$  values derives from data given by Bichowsky and Rossini.

<sup>43</sup> Maxwell, Mosley, *J. Chem. Physics*, 1940, 8, 738.

The C—H bond-length in vinyl chloride has been assumed = 1.07 Å., to comply with the calculated force-constant, which is slightly larger than that of C—H in ethylene.

(f) C—S and S—O Bonds.—The curves for C—S and S—O bonds given in Fig. 4 are based upon very scanty data, and can only be taken as a rough indication of the energy-length variation in these bonds. The data used are given in Tables IX and X.

TABLE IX.—C—S BONDS.

Molecule.	$r_{0s}$ .	$r_{00}$ .	$Q_a$ .	$E_{(0-s)} \text{ calc.}$		
				$L = 125$	$L = 136$	$L = 170$ .
CS <sub>2</sub>	1.56	—	(91.2 + $L$ )	108.1	113.6	130.6
COS	1.56	1.16	(150.6 + $L$ )	106.8	112.4	129.4
(CH <sub>3</sub> ) <sub>2</sub> S	1.82	—	(376.9 + $2L$ )	50.1	52.9	61.5

In dimethyl sulphide, the C—H bonds are assumed equivalent to the C—H bonds in methane.

TABLE X.—S—O BONDS.

Molecule.	$r_{so}$ .	$Q_a$ .	$E_{(s-o)}$ .
SO	1.493	93.2	93.2
SO <sub>2</sub>	1.433	245.6	122.8

## 5. Discussion.

The curves shown in Figs. 1 to 4 bear a close similarity to one another in their general form. The deviation of the individual points from the smooth curves we have drawn is in no case large, and although the scarcity of molecules for which both reliable thermal and structural data is at present available, prevents a detailed examination of the postulate of a close relationship between bond-energy and length, the available data would suggest that these quantities are interdependent. This has been suspected, in a qualitative manner, for some time—as can be illustrated by quotation from a recent paper by Phillips, Hunter and Sutton<sup>44</sup>—“(there is) a general principle which is gaining recognition: viz.: that there is a connection between the length and strength of a bond, in as much as abnormally strong bonds tend to be abnormally short, and weak ones long”. The quantitative relation between the energy and bond-length can be expressed, approximately, by the equation  $Er^n = A$ , where  $E$  is the bond-energy,  $A$  is a bond-constant, and  $n$  a further bond-constant which appears to lie between the values 2.5 and 5.0 (that is, for the bonds here considered). This equation applies except for the shortest bonds (e.g. the molecules CO and NO do not fit in at all well). An equation of the type  $Er^n = \text{const.}$  might be expected by combining the empirical rule of C. H. D. Clark<sup>45</sup> ( $kr_e^6 = \text{const.}$ ), with the equation  $kr_e^2/E = \text{const.}$ , proposed by Sutherland.<sup>46</sup> The value of  $n$ , for C—C bonds, depends upon the chosen value for  $L$ , and is best represented by the values 2.5, 2.7 and 3.1 for the  $L$  values 125, 136 and 170. For C—O bonds, the best value

<sup>44</sup> Phillips, Hunter, Sutton, *J. Chem. Soc.*, 1945, 158.

<sup>45</sup> Clark, *Phil. Mag.*, 1935, 19, 476.

<sup>46</sup> Sutherland, *J. Chem. Physics*, 1940, 8, 161.

of  $n$  does not vary according to choice of  $L$ , and is 4.4 : for N—O bonds we find  $n = 4.9$ , and for C—N bonds  $n = 4.4$ .

The initial assumption made that in the case of C—H bonds the variation of the bond-energy with bond-length is a linear function is probably incorrect : none the less, we do not imagine that the replacement of the C—H curves in Fig. 1 by curves following the equation  $Er^4 = \text{const.}$ , would make an appreciable difference to the form of the curves derived from Fig. 1.

The bonds that have so far been considered have in all cases been either "normal" or "short" bonds. A few compounds in which the bonds are considerably longer than normal are known, and are of special interest, in so far as we should expect the long bonds to be weak.

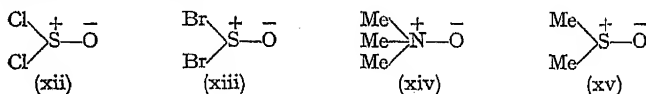
This expectation is borne out by examination of the bond-energies of the N—Cl and N—Br bonds in NOCl and NOBr, and of the SCl bond in thionyl chloride.

Electron diffraction measurements by Ketelaar and Palmer<sup>47</sup> on the molecules NOCl and NOBr have shown that in these compounds the N-halogen bonds are lengthened by some 0.2 Å. : the heats of formation of both compounds are quoted by Bichowsky and Rossini, from which the N-halogen bond-energies may be derived :

$$\begin{aligned}\text{NOCl: } Q_a &= 187.8 \\ \nu_{\text{NO}} &= 1.14, \text{ corresponding to } E_{(\text{NO})} = 160 \text{ k.cal.} \\ \nu_{\text{NOCl}} &= 1.95, \text{ and } E_{(\text{NOCl})} = 27.8 \text{ k.cal.} \\ \text{NOBr: } Q_a &= 180.8 \\ \nu_{\text{NO}} &= 1.15, \text{ corresponding to } E_{(\text{NO})} = 150 \text{ k.cal.} \\ \nu_{\text{NOBr}} &= 2.14, E_{(\text{NOBr})} = 30.8 \text{ k.cal.}\end{aligned}$$

Both the N—Cl and N—Br bonds appear to be weak compared with the normal bonds, for which  $\nu_{\text{NOCl}} = 1.73$ ,  $E_{(\text{NOCl})} = 50 \text{ k.cal.}$ , and  $\nu_{\text{NOBr}} = 1.88$ ,  $E_{(\text{NOBr})} = 45 \text{ k.cal.}$  Even by comparison with the N—Cl bond in  $\text{NCl}_3$  ( $E = 46.2$ ), which itself is a "weak" bond, the bond in NOCl is very much weakened.

The series of compounds  $\text{Cl}_2\text{SO}$ ,  $\text{Br}_2\text{SO}$ ,  $\text{Me}_3\text{NO}$  and  $\text{Me}_3\text{SO}$  are formally similar, in that resonance structures involving a co-ordinate linkage to the O atom probably contribute markedly to the total resonance in each of these molecules (xii-xv) :



In each of these compounds, electron diffraction measurements<sup>48</sup> have shown the co-ordinate linkages to be short, and the bonds other than the co-ordinate link to be long : accordingly, we might anticipate that the bond-energies of the S—Cl, S—Br, N—C and S—C bonds in these compounds are weaker than normal.

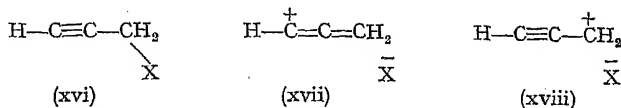
The thermal data required to test this expectation is available only in the case of thionyl chloride. From the heat of formation, we obtain  $Q_a = 216.4 \text{ k.cal.}$  : the observed S—O bond-length corresponds to  $E_{(\text{SO})} = 113 \text{ k.cal.}$ , from which  $E_{(\text{SOCl})} = 51.7 \text{ k.cal.}$  This is slightly less than the energy of a "normal" S—Cl bond ( $E = 56 \text{ k.cal.}$ ), agreeing with expectation since the extension of S—Cl in  $\text{SOCl}_2$  is also slight (observed S—Cl = 2.07 Å., normal S—Cl = 2.03 Å.). The bond is also weak by comparison with S—Cl in  $\text{S}_2\text{Cl}_2$ , for which  $\nu_{\text{SOCl}} = 1.99 \text{ Å.}$ , and  $E_{(\text{SOCl})} = 61 \text{ k.cal.}$

A further group of compounds in which "long" bonds have been measured are the propargyl halides. Electron diffraction studies by Pauling, Gordy, and Saylor<sup>48</sup> show the C—halogen bonds to be extended

<sup>47</sup> Ketelaar, Palmer, *J.A.C.S.*, 1937, 59, 2629.

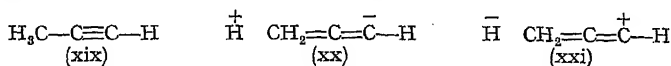
<sup>48</sup> Pauling, Gordy, Saylor, *J.A.C.S.*, 1942, 64, 1753.

above normal by 0.07, 0.04, and 0.03 Å. respectively, for the C—Cl, C—Br and C—I bonds. The authors assume resonance in the propargyl halides among the structures (xvi-xviii) :



and it seems probable that the extension in the C—X bonds is to be attributed mainly to the contribution of the ionic "no-bond" structure (xviii).

Similar resonance structures to those suggested in the propargyl halides have been postulated by Pauling, Springall, and Palmer<sup>49</sup> in the compound methyl acetylene, viz. (xix-xxi) :



By analogy with the propargyl halides, we might predict that the C—H bonds in the methyl group of methyl acetylene are longer than normal, and also "weak" bonds. The thermal data is compatible with this expectation : from the heat of formation of methyl acetylene ( $Q_f = -44.3$ ), we obtain  $Q_a = (163.9 + 3L)$  : using the C—C curve in Fig. 2, and the known C—C distances,  $E_{\text{CH}}$  methyl is estimated at 86.5, 88.1, and 94.1 k.cal., for  $L = 125$ , 136 and 170. These are all lower than the corresponding C—H energies in methane.

The examples are sufficient to show that the general postulate of a close relationship between bond-energy and bond-length is followed both in the weakest and the strongest bonds : this may be taken as good evidence for the general applicability of the postulate. A general criticism may be raised that is worth attention : namely, that no account has been taken of the effect of variation in the bonding orbitals used by a given bond in different molecules. In particular, criticism of the C—H curve given in Fig. 1 may arise for this reason.

According to Coulson,<sup>50</sup> the wave-function for a C—H bond may be written in the form :

$$\psi_a = a\psi_s + \sqrt{1 - a^2} \cdot \psi_p$$

where  $\psi_s$ ,  $\psi_p$  are the normalised 2s and 2p atomic wave-functions of the carbon atom, and  $a$  is a coefficient of "mixing", with the values  $a = 1$ ,  $\frac{1}{2}$ ,  $\sqrt{\frac{1}{3}}$  and  $\sqrt{\frac{1}{2}}$  for pure s, tetrahedral, trigonal, and diagonal bonds. Pauling has defined the strength of these bonds as  $= a + \sqrt{3(1 - a^2)}$ , so that the relative strengths of tetrahedral, trigonal and diagonal C—H bonds are expected to be in the ratio 2 : 1.991 : 1.932. This conclusion which implies that the C—H bonds decrease in energy passing from  $\text{CH}_4$  to  $\text{C}_2\text{H}_2$ , is directly opposite to the assumption we have made.

This argument is, however, contradicted in a recent paper by Mulliken, Rieke, and Brown.<sup>51</sup> These authors express the opinion that "hyperconjugation" occurs between an apparently saturated group such as  $-\text{CH}_3$ , and the bond adjacent to it. The  $-\text{CH}_3$  group is regarded as comparable with the  $-\text{C}\equiv\text{N}$  and  $-\text{C}\equiv\text{CH}$  groups, and may be written in the manner  $-\text{C}\equiv\text{H}_s$ . Mulliken labels the single and multiple bonds of a conjugated system as "acceptor" and "donor" bonds, the effect of the conjugation being that the acceptor bonds gain in energy, and the donor bonds lose, the net effect for the system is an energy increase corresponding to the resonance energy of hyperconjugation. Comparing

<sup>49</sup> Pauling, Springall, Palmer, *ibid.*, 1939, 61, 927.

<sup>50</sup> Coulson, *Trans. Faraday Soc.*, 1942, 38, 433.

<sup>51</sup> Mulliken, Rieke, Brown, *J.A.C.S.*, 1941, 63, 41.

ethane and acetylene from Mulliken's viewpoint, we may write the structures as  $\text{H}-\text{C}\equiv\text{C}-\text{H}$  and  $\text{H}_2\equiv\text{C}-\text{C}\equiv\text{H}_2$ . In acetylene the C—H bonds are "acceptor" bonds, whereas in ethane they are "donor" bonds, which difference in character implies that C—H is stronger in acetylene than in ethane.

Experimental investigation of the C—H energies in ethylene, and acetylene is needed to settle this point: in this respect, we may refer to two recent publications by Cherton<sup>52</sup> and Fonteyne<sup>53</sup> in which both authors claim to establish that the C—H energy is, in fact, larger in acetylene than in methane.

In conclusion, an attempt by Warhurst<sup>54</sup> to estimate theoretically the effect of resonance energy on bond-length is of interest, as it represents an approach to the problem considered here, by less empirical methods. Warhurst considers two types of resonance—single-bond multiple-bond resonance, and covalent-ionic resonance. For both these types, he concludes that the resonance energy is associated with bond-contraction. In case of the single-multiple bond resonance, Warhurst's conclusions are compatible, in general terms, with the empirical assumption of an energy-length relationship. The covalent-ionic type of resonance is more difficult to treat from a theoretical standpoint, and Warhurst's equations are not readily formulated in the manner of a simple energy-length relation. It may be that the chief exceptions to the simple rule are most likely to be found in bonds of the ionic-covalent type: and the method of approach to this problem, used by Warhurst, may reveal more exactly when exceptions should occur, if the method can be extended beyond its present level.

### Summary:

The bond-energies of the P—P, As—As, S—S, Se—Se and C—C bonds have been reconsidered in the light of recent spectroscopic and thermal data. Tentative alterations in the values of the O—O, N—N, Si—Si and Ge—Ge bond-energies are also proposed. The bond-energies of a number of bonds to hydrogen and the halogens are tabulated.

The assumption of a relationship between the energy and length of a bond is examined for C—C, C—O, C—N, N—O and C—Cl bonds, using the thermal and structural data at present available. The energy-length curves derived, are found to obey, approximately, an equation  $E\tau^n = A$ , where  $E$  is the bond-energy,  $\tau$  the bond-length, and  $n$  and  $A$  are specific bond-constants;  $n$  lies between the extreme values 2.5–5.0.

It is found that certain bonds which are longer than would normally be expected are correspondingly weaker than normal bonds.

The writer wishes to express his thanks to Professor M. Polanyi for helpful discussion and advice during the preparation of this paper.

*Chemistry Department,  
The University of Manchester,  
Manchester 13.*

<sup>52</sup> Cherton, *Bull. Soc. Chim. Belg.*, 1943, **52**, 26 (reported in *Chem. Abst.*, 1944, **38**, 5138).

<sup>53</sup> Fonteyne, *Naturwiss.*, 1943, **31**, 441 (reported in *Chem. Abst.*, 1944, **38**, 2863).

<sup>54</sup> Warhurst, *Trans. Faraday Soc.*, 1944, **40**, 26.

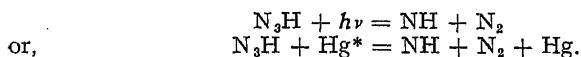
# THE IMINE RADICAL, NH.

By K. STEWART.

Received 8th October, 1940.\*

Of the large number of radicals postulated in reaction mechanisms only very few have received experimental verification. With the exception of hydroxyl, they are all carbon compounds.

The diatomic molecule NH has been fairly completely studied spectroscopically. It is recognised as a physically stable molecule; the six electronic states predicted by Mulliken have been verified experimentally.<sup>1</sup> However, its chemical stability will be essentially dependent on its environment. Lewis<sup>2</sup> and Steiner<sup>3</sup> postulated the intermediate formation of NH in the synthesis of ammonia from active nitrogen and atomic hydrogen. Beckman studied the photochemical<sup>4</sup> and the photosensitised<sup>5</sup> decompositions of azoimide and assumed that the first stage in the decomposition was the formation of NH and N<sub>2</sub>:



Lavin and Bates<sup>6</sup> streamed ammonia through an electric discharge and obtained an intense green afterglow, but were unable to detect NH spectroscopically (the NH band system 3370-3360 Å. was absent).

In attempting to verify the existence, and to study the properties, of a free radical it has been pointed out that the experimental conditions are the all important factor.<sup>7</sup> In general the radical will be most stable when diluted with a gas with which it does not react. The diluent serves to dissipate the energy liberated by the combination of, or reaction between, two radicals. Free radicals may, in general, be produced by three different methods, *viz.*, by thermal, photochemical, and electronic decompositions. It was found that azoimide was decomposed by the active material drawn from a glow discharge in nitrogen. As the reactive species in the active nitrogen are excited by electronic processes the reaction bears the same relation to an electronic decomposition as a photosensitised reaction bears to a photochemical one. The radical imine was identified by its reaction with hydrogen to form ammonia, and with benzene to form aniline and *m*-phenylene diamine.

## Experimental.

**Nitrogen.**—Owing to the large quantities of N<sub>2</sub> required the gas was drawn from a cylinder. It was purified in the following manner. The small amount of O<sub>2</sub> present (~1.5 %) was removed by passage over Cu gauze in the presence of ammonia.<sup>8,9</sup> The gas was washed with water to remove part of the NH<sub>3</sub>, and then dried and rendered NH<sub>3</sub>-free by

\* Publication delayed at request of Censor.

<sup>1</sup> Mulliken, *Rev. Mod. Physics*, 1930, 2, 60; 1932, 4, 7.

<sup>2</sup> Lewis, *J.A.C.S.*, 1928, 50, 27 and 2427.

<sup>3</sup> Steiner, *Z. Electrochem.*, 1930, 36, 807.

<sup>4</sup> Beckman and Dickinson, *J.A.C.S.*, 1928, 50, 1870; 1930, 52, 124.

<sup>5</sup> Myers and Beckman, *ibid.*, 1935, 57, 89.

<sup>6</sup> Lavin and Bates, *Proc. Nat. Acad. Sci.*, 1930, 16, 804.

<sup>7</sup> Pearson, *Ann. Reports*, 1937, 34, 264.

<sup>8</sup> van Brunt, *J.A.C.S.*, 1914, 36, 1448.

<sup>9</sup> Kraus and Parker, *ibid.*, 1922, 44, 2429.

phosphoric acid and  $P_2O_5$ . Finally the gas was passed through a charcoal trap cooled in liquid nitrogen into a 6.5 l. reservoir. During an experiment the pressure in the reservoir was maintained constant by a slow continual inflow of pure nitrogen.

**Hydrogen.**—Cylinder  $H_2$ , purified by passage through a tube packed with platinised asbestos catalyst at  $250^\circ C.$  followed by a U-tube cooled in liquid  $N_2$ , was used.

**Hydrazoic Acid.**—This was prepared in small quantities ( $\sim 1$  c.c. of liquid) and stored in a large globe at a pressure considerably below the vapour pressure at room temperature. Initially the method due to Gunther, Meyer and Müller-Skjold<sup>10</sup> was employed. In this, dry sodium azide reacts with stearic acid at  $70^\circ C.$ , pure hydrazoic acid is slowly evolved and may be condensed in liquid air. It was found to be both simpler and quicker to add the equivalent amount of  $1:1 H_2SO_4$  slowly to a saturated aqueous solution of sodium azide, *in vacuo*. The gas was distilled through a bath at  $-80^\circ C.$  into one cooled in liquid  $O_2$ . The vapour pressure of hydrazoic acid at  $-80^\circ C.$  is about 1 mm. This fractionation was repeated during the transference of the acid to the fractionation system. This system was built on the Stock principle, but with taps instead of mercury ventiles. The acid was fractionated through a bath at  $-78^\circ C.$ ; head and tail fractions were rejected. The vapour pressures at  $0^\circ C.$  of different samples were always the same, irrespective of the method of preparation. This value, 153 mm., was 10.7 mm. lower than the value reported by Gunther, Meyer and Müller-Skjold. The vapour pressure was measured over the range  $-78^\circ - 25^\circ C.$  Below  $0^\circ C.$  acetone-solid  $CO_2$  baths were used, above  $0^\circ C.$  a water bath. The temperatures were measured with  $NH_3$  and  $SO_2$  vapour tension thermometers, and in the higher temperature range with a mercury thermometer. The plot of  $\log_{10} p_{mm}$  against  $1/T$  gave a straight line the equation of which was found to be

$$\log_{10} p_{mm} = 8.198 - 1643/T.$$

The boiling-point, found by extrapolation, was  $35.8^\circ C.$  in good agreement with the value  $35.7^\circ C.$  reported by Gunther, Meyer and Müller-Skjold.

Both Schumacher<sup>11</sup> and Gunther, Meyer and Müller-Skjold report that azoimide decomposes rapidly in the presence of tap-grease and mercury. All their measurements were carried out in an all-glass apparatus, in which the use of both tap grease and mercury was avoided. It was found, however, that the gas could be stored without marked decomposition, in a carefully cleaned glass reservoir with a mercury manometer and an ordinary greased tap, at a pressure considerably below the vapour pressure at room temperature. In most cases the pressure was about 10 cm. Even with the special precautions taken, they experienced considerable difficulty in handling and storing the substance and reported fully on its treacherous nature. Their remarks are fully justified, although it does seem possible to keep small quantities of gaseous azoimide at low pressure without much risk. The solid and liquid materials are considerably more dangerous.

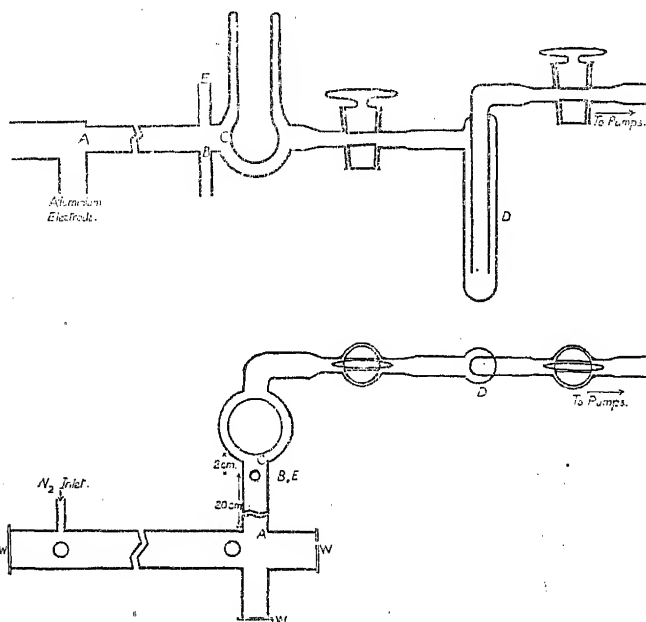
**Apparatus.**—The reaction system is shown schematically in Fig. 1a. The active species from the discharge enter the reaction zone at A; at B, 20 cm. further along the tube, the desired gas mixture enters the gas stream. The cooled surface, C, situated 2 cm. from B, can be cooled to any desired temperature. Provided the temperature is low enough, the majority of the product will be condensed on C and the remainder will be held by the trap D. Fig. 1b is a plan of the apparatus including the discharge tube. The quartz windows, *w*, enabled the discharge and the reaction zone to be examined spectroscopically. The dimensions of the

<sup>10</sup> Gunther, Meyer and Müller-Skjold, *Z. physik. Chem., A*, 1935, 175, 154.

<sup>11</sup> Meyer and Schumacher, *ibid.*, 1934, 170, 33.

major portions of the apparatus are given. The discharge tube electrodes were aluminium foil cylinders, 12 cm. long and 3 cm. diameter. An alternating current discharge was used. The high tension supply was obtained from a 10,000 v. oil-cooled transformer. The pumping system consisted of a Leybold three-stage mercury diffusion pump backed by a Gaede single-stage oil pump. Streaming rates up to 1500 l./sec. at 0.3 mm. were readily obtained with this pumping system.

**Procedure.**—In the absence of a method of measuring the concentration of any one of the species in active nitrogen the only way in which the experiments could be carried out so that the results would be comparable amongst themselves was to operate the discharge always under the same conditions. The discharge current was maintained constant at 280 ma. The discharge tube was air-cooled by means of an electric fan. The nitrogen pressure, measured by the Macleod gauge at E, was 0.22 mm.; this



FIGS. 1A, 1B.

pressure of nitrogen was used in all experiments. The quantity of nitrogen drawn through the discharge tube was 25.2 c.c. at N.T.P./min. The total quantity of gas drawn through the reaction system was somewhat greater than this. Nitrogen, purified by the method described, gave an active but non-luminous material in the reaction zone under these experimental conditions.

### Decomposition of Azoimide by Active Nitrogen.

Azoimide, diluted with an excess of nitrogen (7 : 1), was allowed to enter the active nitrogen stream in the reaction zone via the inlet tube B. The surface C was at room temperature. All condensable material was retained by the trap D cooled in liquid oxygen: non-condensable products were lost. The duration of each experiment was 3 hours. At the completion of an experiment the condensate in D was distilled via the tube E to a separate part of the apparatus, which was designed for



fractionation, analysis, etc. The product was examined by fractionation and by analysis and found to be azoimide. Tests were made for ammonia and for hydrazine; neither was detected. The amount of undecomposed azoimide was determined by measuring its pressure in a standard volume at a known temperature. The results for different partial pressures of azoimide are given in Table I. These results show that the amount of decomposition decreases with decreasing azoimide concentration. The results were not sufficiently reproducible for any relationship between the azoimide concentration and the extent of the decomposition to be found.

TABLE I.

Amount of $N_3H$ passing through reaction zone in 3 hours (g. mol. $\times 10^4$ ) . . .	15.9	11.0	11.0	5.4
Partial pressure of $N_3H$ in reaction zone (mm. $\times 10^3$ ) . . .	1.67	1.16	1.16	0.57
$N_3H$ collected unchanged (g. mol. $\times 10^4$ ) . . .	7.6	7.3	9.1	5.1
Fraction of $N_3H$ decomposed . . .	0.52	0.32	0.17	0.05

### Decomposition of Azoimide in the Presence of Hydrogen.

The experimental conditions were the same as for the decomposition of azoimide, except that the azoimide-nitrogen mixture was replaced by a mixture of  $N_3H$ ,  $H_2$ , and  $N_2$  or by one of  $N_3H$  and  $H_2$ . The reaction product was found to be a mixture of  $N_3H$  and ammonium azide. Hydrazine was not detected. Ammonium azide is readily volatile *in vacuo* so that the condensate could be distilled into the analysis apparatus.

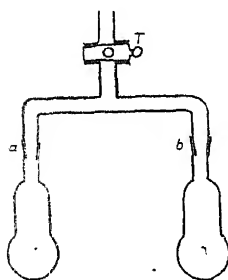


FIG. 2.

This apparatus is shown in Fig. 2. The two absorption bulbs A and B were attached to the apparatus by the ground joints *a* and *b* and connected to the vacuum line via the tap T. They were of equal volume, about 50 c.c. Accurately measured volumes of *N*./10 alkali and acid were run into A and B, respectively. The product was first condensed on to the alkali in A using liquid oxygen as the condensing agent. The alkali

was allowed to warm up and the bulk of the water distilled into the other bulb B. The distillation was repeated in the reverse direction and then the whole operation repeated again. This rather tedious procedure was found to be necessary owing to the small quantities of gas and the relatively large quantities of liquid used in A. The results are summarised in Table II. The amount of ammonia formed was always about 20 % of the azoimide destroyed. In the product from these experiments no trace of hydrazine was found.

TABLE II.

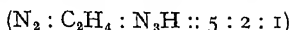
Constitution of the azoimide hydrogen, nitrogen mixture ( $N_3H:H_2:N_2$ ) . . .	1:5:0	1:5:0	1:1:5	1:1:5	1:1:5
Amount of azoimide passing into the reaction zone in 3 hr. (g. mol. $\times 10^4$ ) . . .	12.0	7.1	12.5	10.6	9.2
Partial pressure of $N_3H$ (mm. $\times 10^3$ ) . . .	1.26	0.75	1.32	1.12	0.97
$N_3H$ collected unchanged (g. mol. $\times 10^4$ ) . . .	nil.	nil.	8.3	8.5	6.0
Ammonia formed (g. mol. $\times 10^4$ ) . . .	2.00	1.50	0.92	0.54	0.62
Fraction of $N_3H$ converted to $NH_3$ . . .	0.17	0.18	0.21	0.26	0.19

### The Reaction Between Ammonia and Active Nitrogen.

Since ammonia is the product in the reaction between azoimide and active nitrogen in the presence of hydrogen it was necessary to determine whether ammonia itself was affected by active nitrogen. The experiments were carried out in an exactly similar manner to those with azoimide. It was found that ammonia was completely unaffected by the active material from the discharge.

### Decomposition of Azoimide in the Presence of Ethylene.

The azoimide-ethylene mixture, diluted with nitrogen



entered the gas stream containing active material from the discharge at B. C was at room temperature and D immersed in liquid oxygen. The product contained scarcely any ethylene, owing to the high streaming rate and the relatively high vapour pressure of ethylene at the temperature of liquid oxygen. It was thought that the compound ethylene imine might have been produced by the direct association of an ethylene molecule with an imine radical. An attempt to isolate ethylene imine as the picrate from the product failed. However, on warming the product with alkali a gas, which reacted alkaline to litmus, was evolved. This indicated the formation of a volatile base. It was not found possible to identify it.

### Decomposition of Azoimide in the Presence of Benzene.

The gas mixture was similar to that used in the experiments with ethylene. The mixture had the composition  $N_3H : C_6H_6 : N_2 :: 1 : 1 : 8$ . In these experiments the effect of cooling C to  $-78^\circ C$ . and  $-185^\circ C$ . was examined. At these lower temperatures it was found that a blue deposit collected on the surface of C. This condensate, which did not appear when C was warmer than  $-78^\circ C$ ., was readily volatile. On distillation, however, a change took place and the resulting condensate was white. This product was examined qualitatively for aromatic amines, more especially for aniline and the phenylene diamines. The product was treated as follows. To the condensate, which contained the unchanged benzene and azoimide in addition to the base, was added two drops of concentrated HCl and the whole allowed to warm up. The solution was then boiled to remove both the free benzene and the azoimide, the base hydrochloride remaining in solution. In a preliminary experiment the standard carbylamine test was employed and gave a weak positive reaction. The amounts were too small to allow diazotisation followed by coupling with a base to form a dyestuff to be characteristic. The microchemical test finally adopted was that due to Feigl,<sup>12</sup> which utilises the reaction of sodium aquopentacyanoferrate with primary aromatic amines to give characteristic colorations. The reagents are a 1 % aqueous solution of sodium aquopentacyanoferrate and a 10 % sodium hydroxide solution. The solution of sodium aquopentacyanoferrate is most readily prepared by allowing a solution of sodium nitroprusside to age or to irradiate it with ultra-violet light. After the removal of free azoimide and benzene by boiling the solution for a few minutes, it was transferred to a test-tube and diluted, if necessary, to 3 ml. To this solution was added two drops of the sodium aquopentacyanoferrate reagent (0.25 ml.) and 0.5 ml. of 10 % NaOH solution. On standing for several minutes, usually 5-15, a green colour developed. The three amines which give green or blue colorations are summarised below, together with the limiting concentrations at which the test is sensitive. The product

<sup>12</sup> Feigl and Chargaff, *Z. anal. Chem.*, 1928, 74, 376.

Amine . . . . .	Aniline	<i>p</i> -Phenylene diamine	Benzidine
Colour . . . . .	Green	Blue	Blue-green
Sensitivity limit . . . . .	0.5γ	0.1γ	1γ

gave a green coloration with bluish tinge, very different from that due to benzidine, but which could be reproduced by the addition of a trace of *p*-phenylene diamine to aniline. The reaction product was therefore aniline containing a little *p*-phenylene diamine. Neither the *o*- nor the *m*-phenylene diamine gave a coloration similar to the one observed. The colorations observed were compared in a semi-quantitative manner

TABLE III.

	Expt.	Aniline Formed, gm. mole $\times 10^4$ .
Surface cooled by liquid oxygen . . . . .	1	1.0
	2	0.7
	3	0.3
Surface cooled by solid carbon dioxide . . . . .	4	nil.
	5	0.3

with those given by known aniline solutions. The comparisons cannot be made quantitative as a little *p*-phenylene diamine is present. The results are summarised in Table III. It is noteworthy that the amount of product is of the same order as that of ammonia formed in the reaction between azoimide-hydrogen mixtures and active nitrogen. The

amount of aniline formed increases considerably when the temperature of the surface C is lowered from  $-78^\circ\text{C.}$  to  $-185^\circ\text{C.}$

### Discussion.

A free radical may be identified, either spectroscopically as in the case of hydroxyl,<sup>13</sup> or by examination of the products of a chemical reaction in which it takes part, as in the case of the alkyl radicals. Spectroscopically the imine radical has been extensively studied and the band systems associated with it are well known. Unfortunately, the radical concentration was too small to allow it to be detected either in absorption or emission. Experiments similar to those carried out by Steiner<sup>14</sup> on active nitrogen, in which an auxiliary discharge was employed in an attempt to excite the emission spectra of NH, failed.

The reactions employed in the detection of alkyl radicals are of the simple addition type. As imine is a bivalent radical the choice of reactants is both limited and difficult. Several metal imines have been reported: they are non-volatile compounds but little suitable as a means of identification. Organic imines are well known, but an attempt to isolate the simplest of these, ethylene imine, was inconclusive. Finally, two reactions from which the products would be readily identified, namely, the reactions between imine and hydrogen and imine and benzene were chosen as the means to proving the existence of the imine radical.

There is considerable evidence that the initial step in the breakdown of azoimide takes place according to the equation

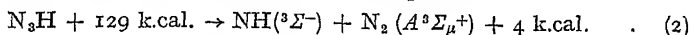


This initial step has been proposed by Beckman<sup>4, 5</sup> and his collaborators to explain the photochemical and the photosensitised decompositions of azoimide. Schumacher<sup>11</sup> arrived at the same conclusion as the result of experiments on the non-explosive thermal decomposition. If it is assumed that the NH bond strength is equal to 83 k.cal. (a third of the heat of formation of the three NH bonds in ammonia), then, since the heat

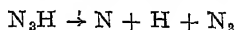
<sup>13</sup> Frost and Oldenburg, *J. Chem. Physics*, 1936, 4, 642.

<sup>14</sup> Bay and Steiner, *Z. physik. Chem.*, B, 1929, 3, 149.

of formation of azoimide from its elements is  $-71$  k.cal., reaction (1) is exothermic to the extent of  $18$  k.cal. Beckman and Dickinson showed that the light absorption of azoimide sets in at about  $2200$  Å. and attains a maximum at  $1990$  Å. The limit at  $2200$  Å. corresponds to an energy absorption of  $129$  k.cal. The combination of this energy with that available from the reaction itself provides sufficient energy for the reaction to take place with the production of a normal NH radical ( $A^3\Sigma^-$ ) and an excited  $N_2$  molecule ( $A^3\Sigma_u^+$ ) according to the equation



The small energy balance will probably appear as vibrational energy in the two molecules formed. It is unlikely that the alternative reaction



occurs consecutively with (2), as a mixture of nitrogen atoms and molecules would be expected to give rise to a nitrogen afterglow effect;<sup>15</sup> such an effect has not been reported. At the absorption maximum there is just about sufficient energy available for the reaction to take place with the production of an excited  $N_2$  molecule in the  $B^3\Pi_g$  state. Alternatively, the  $A^3\Sigma_u^+$  state could be excited to the seventh vibrational level. The transition from the  $B^3\Pi_g$  state to the  $A^3\Sigma_u^+$  state gives rise to the nitrogen first positive band system. Unfortunately experimental evidence about this point is lacking. However, Gleu<sup>16</sup> examined the chemiluminescence produced when a mixture of chlorazide and azoimide were passed through a heated tube. He observed a complicated band system which he was unable to characterise completely. The bands due to the NH transition  $B^3\Pi \rightarrow A^3\Sigma$  at  $3360$  Å. and at  $3370$  Å. were recognised. The remainder of the spectrum could not be analysed as the dispersion was insufficient to allow measurement of the bands. It seems possible that the first positive band system of nitrogen would be observed in this chemiluminescence.

When azoimide alone was decomposed by active nitrogen the reaction products were nitrogen and hydrogen. There was no indication that any polymer of NH was formed or that any of the hydrogen liberated reacted to form ammonia. The latter was due to the fact that the time available for reaction was never greater than  $0.1$  sec.; with the small concentration of hydrogen produced the reaction between NH and  $H_2$  could not take place to any appreciable extent. In the presence of hydrogen a considerable fraction of the azoimide decomposed reappeared as ammonia. In this case the hydrogen concentration was great enough to allow the reaction



to occur. This reaction is exothermic to the extent of  $62$  k.cal. It involves the rupture of an H—H bond and the formation of two N—H bonds, and will probably require a considerable energy of activation. At the low pressures employed the reaction must take place bimolecularly, on the walls of the reaction vessel, or on the cold surface of the condensing trap. If the instantaneous concentration of imine radicals is assumed to be equal to the number of azoimide molecules decomposed during the period the gas stream takes to cross the reaction zone, then it is possible to calculate a minimum value for the activation energy of reaction (3) provided that it is assumed to be homogeneous and bimolecular, and to show that a termolecular reaction is not possible. Under the experimental conditions ( $p_{H_2} \approx 10^{-3}$  mm.) each imine radical makes  $10^3$  collisions with  $H_2$  molecules in  $0.1$  sec. and this number of collisions is sufficient for the fraction  $0.2$  of the radicals produced to react to give ammonia. The number of collisions necessary for reaction is therefore  $5 \times 10^3$ , which corresponds to an energy of activation of  $5$  k.cal. The number

<sup>15</sup> Cario, *Z. Physik*, 1934, 99, 523.

<sup>16</sup> Gleu, *Z. Physik*, 1926, 38, 176.

of termolecular collisions would be  $c. 10^{-6}$  smaller, *i.e.* insufficient for the reaction  $\text{NH} + \text{H}_2 + \text{M}$  to take place.

The reaction between benzene and the imine radical occurs in two stages. The first stage, which takes place only on a surface cooled below  $-80^\circ \text{C}$ ., leads to the formation of a blue addition compound. This product, the composition of which is unknown, is stable only at temperatures below  $-80^\circ \text{C}$ . On being allowed to warm up the blue colour faded and a white volatile product containing aniline with excess benzene and azoimide was obtained on recondensation. The decomposition of the blue compound may lead to either aniline or aniline azide. There is no way of determining readily which of these is formed. Further, the amount of aniline detected may not be equal to the amount of blue compound formed, as it is uncertain that the blue material decomposes entirely into aniline.

The first step in the reaction may be the addition of the  $\text{NH}$  radical to the benzene molecule in a manner similar to the addition reaction postulated by Harteck and Geib<sup>17</sup> to account for the reaction between atomic hydrogen and molecular oxygen at low temperatures with the subsequent formation of hydrogen peroxide. When the temperature is allowed to rise a molecular rearrangement takes place with the formation of aniline. This reaction involves the rupture of a  $\text{C}-\text{H}$  bond and the subsequent formation of an  $\text{N}-\text{H}$  bond; this process is exothermic to the extent of  $\sim 25$  k.cal.

The experiments described suggest that the  $\text{NH}$  radical, already well known spectroscopically, is sufficiently stable to act as an intermediate in chemical processes, and may be classed as a free radical along with the alkyl radicals and hydroxyl.

### Summary.

1. It has been found that azoimide is decomposed by non-luminous active nitrogen.
2. The decomposition leads to the formation of the radical  $\text{NH}$  which was identified by its reaction with hydrogen to form ammonia and with benzene to form aniline.
3. The results are discussed.

The author wishes to thank the University of London, the Royal Society, and Messrs. Imperial Chemical Industries Ltd., for grants.

<sup>17</sup> Harteck and Geib, *Ber.*, 1932, **65**, 1551.

## ON THE NUMERICAL CONSEQUENCES OF CERTAIN HYPOTHESES OF PROTEIN STRUCTURE.

By A. G. OGSTON.

*Received 8th January, 1945.*

In a former paper,<sup>1</sup> the numerical consequences of the hypothesis of Bergmann and Niemann,<sup>2</sup> that amino acids recur at regular intervals in the polypeptide chains of proteins, was investigated. It was found that analytical intervals\* and ratios of the form  $2^m 3^n$  are not a necessary consequence of this type of arrangement.

<sup>1</sup> Ogston, *Trans. Faraday Soc.*, 1943, **39**, 151.

<sup>2</sup> Bergmann and Niemann, *J. Biol. Chem.*, 1937, **118**, 301; *ibid.*, 1938, **122**, 577.

\* The "analytical interval" of an amino acid is the reciprocal of the ratio of the number of residues of this acid to the total number of residues in an analytical unit of the protein. In the case of linear regularity, it is equal to the linear interval of recurrence.

Other types of regularity have been postulated in hypotheses of protein structure. In this paper, the consequences of three of these are examined, with particular reference to the analytical intervals that would be consistent with them. Hypotheses differ in their explicitness and therefore in the degree of latitude of their dependence on the occurrence of certain analytical intervals and ratios. It must be remembered that the occurrence of analytical intervals of the form  $2^m 3^n$  is by no means a confirmed or universal rule;<sup>3</sup> and that, even if a hypothesis is consistent with observed ratios, this is in general not a sufficient proof of its correctness.

### Astbury's Hypothesis.<sup>4</sup>

This suggests that soluble proteins have a laminated structure, each lamina consisting of parallel polypeptide chains; and that the chains are folded in a particular way, similar to that suggested by Astbury for fibrous proteins in the  $\alpha$ -configuration.

The model does not prescribe any regularity of recurrence of individual amino acids, though Astbury<sup>5</sup> takes the view that there may be some degree of regularity within the chain in relation to the recurrence of the pattern of the fold every 6 residues. There might also be a regularity of recurrence of chains in a lamina and of laminae as a whole. In fact, the model could be regarded as a three-dimensional grid in which each amino acid recurs at independent intervals in the three directions, in analogy with the linear recurrence of the Bergmann and Niemann hypothesis. It is of interest to examine the analytical consequences of this type of structure.

A protein may be represented by a rectangular three-dimensional structure whose planes are numbered in the three axes from a convenient point of origin. As in the linear case, the conditions of incongruence and of complete filling must be satisfied. The argument follows closely on that of the linear case.

An amino acid  $r$  occurs at  $x_1, y_1, z_1$  and recurs at intervals  $\xi_1, \eta_1, \zeta_1$ , in the three directions. The general condition for incongruence between any two amino acids is that, of the equations

$$x_1 + m\xi_1 = x_2 + n\xi_2 \quad . \quad . \quad . \quad (1)$$

$$y_1 + o\eta_1 = y_2 + p\eta_2 \quad . \quad . \quad . \quad (2)$$

$$z_1 + q\zeta_1 = z_2 + r\zeta_2 \quad . \quad . \quad . \quad (3)$$

at least one cannot be satisfied ( $m, n, o, p, q, r$  are any integers). If  $x_1 = x_2$  then equation (1) can always be satisfied, and similarly for (2) and (3); all three pairs of initial co-ordinates cannot be equal. If two of the pairs of initial co-ordinates are equal, then the third equation must not be satisfied.

This means that all amino acids which occur in a given row defined by two co-ordinates must have co-imprime intervals in the third direction; all amino acids occurring in a plane defined by one co-ordinate must have co-imprime intervals in at least one of the directions of the plane. These intervals obey all the laws of the linear case.

There are further limitations. Suppose that two amino acids occur in the row  $x, 1, 1$ , in the plane  $x, y, 1$ ; considering only recurrences in this plane, if the values of  $\eta$  are co-prime, then the values of  $\xi$  must be co-imprime. A third amino acid which does not occur in the row  $x, 1, 1$  must be co-imprime to each of the others with respect to either  $\xi$  or  $\eta$ ; if the former, then  $\xi_3$  need contain only the factor which is already common to  $\xi_1$  and  $\xi_2$ ; but if the latter, then  $\eta_3$  must contain both  $\eta_1$  and  $\eta_2$  as factors. If this instance is multiplied, it appears that a structure which is easy to

<sup>3</sup> Chibnall, *Proc. Roy. Soc., B*, 1942, 131, 136.

<sup>4</sup> Astbury, *Chem. Ind.*, 1941, 60, 491.

<sup>5</sup> Astbury, *Advances in Enzymology*, 1943, 3, 63.

satisfy is obtained only if the  $\xi$  values of all the amino acids in the plane  $x, y, 1$  are co-imprime; all the row-values of  $\eta$  may then be co-prime; otherwise, an amino acid which is co-prime to the rest with respect to  $\xi$  must contain all the other co-prime values of  $\eta$  as factors of its  $\eta$ .

Extension of the argument to the  $z$  direction is now easily performed by considering planes  $x'$  and  $y'$  and applying the same argument. All amino acids occurring in  $y'$  have co-imprime values of  $\xi$ , since this includes amino acids which occur in the row  $x, y', 1$ ; but since all values of  $\xi$  in the plane  $x, y, 1$  are co-imprime, it follows that all values of  $\xi$  throughout the structure are co-imprime. Similarly, all amino acids that occur in the plane  $x'$  have co-imprime values of  $\eta$ ; but the values of  $\eta$  between such planes are in general co-prime. Finally, all amino acids occurring in a row  $x', y'$  have co-imprime values of  $\zeta$ , but the values of  $\zeta$  between such rows may be in general co-prime.

The three axes of such a structure are thus distinguished from each other and it is tempting to identify them with the three distinct directions of the Astbury grid. The  $z$  axis is to be identified with the direction of the folded chain; each chain may have a basic  $\zeta$  interval independent of the rest, provided only that the whole length of the unit is the lowest common multiple of intervals in all the chains. The  $y$  axis corresponds with the direction at right angles to this within the laminae, the intervals being co-imprime within each lamina, but independent of those in other laminae; these intervals represent the repetition of whole chains within the lamina. The  $x$  axis is at right angles to the laminae, the  $\xi$  intervals representing the repetition of whole laminae.

The smallest unit of the structure is given by the product of smallest repeat lengths in the three axes; the smallest number of amino acids required is derived from the factors of the size of the smallest unit exactly as in the linear case. The analytical interval of an amino acid is the product of its intervals in the three axes; the occurrence of co-prime analytical intervals is forbidden.

As in the linear case, there is nothing to limit the primes that may occur as factors of intervals. Other considerations may, however, introduce limitations in particular cases:—

(1) It is reasonable to suppose, as Astbury<sup>5</sup> has suggested, that the repetition of the backbone fold each 6 residues will limit the recurrence of amino acids in such a way that they occur at corresponding situations relative to the fold. This condition is satisfied by intervals of 2, 3, 6 or higher multiples of these; 2 and 3 must occur as factors but there is no limitation of the primes that may enter into higher multiples.

(2) The dimensions of the molecule of a protein limit the repeat lengths; taking Astbury's<sup>5</sup> values of 10.3 Å. for the length of the fold (6 residues), 9.3 Å. for the backbone spacing and 9.8 Å. for the sidechain spacing in  $\alpha$ -keratin (these distances representing the contribution of a single chain to the dimensions of the molecule in the direction considered), a molecule of about 40 Å. in each direction would have repeat lengths of 24 (41.2 Å.), 4 (37.2 Å.) and 4 (39.2 Å.) in the  $z, y$  and  $x$  axes respectively. None of the intervals in a molecule of these dimensions can contain a prime greater than 3; for, if 5 is admitted as a factor, the smallest repeat lengths in the three axes are 30, 5 and 5, in each case 25 per cent. too great.

It would thus be expected that a unit of less than 400 residues, having this type of regularity and of approximately cubic shape would not exhibit primes greater than 3.

The treatment outlined could be extended to cover simple regularities other than rectangular; for example, a 2-dimensional hexagonal pattern is described with 2 axes at 60° and unoccupied places represented by the series

$$1, 1 \qquad 2, 2 \qquad 3, 3$$

with  $\xi = \eta = 3$  in each case.

### Janssen's Hypothesis.<sup>6</sup>

This hypothesis is unsupported by other than analytical evidence and is of little interest except for the fact that, while predicting analytical intervals of the Bergmann and Niemann form, it does permit the co-existence in the structure of amino acids having co-prime analytical intervals.

It describes the molecule as a ribbon of  $3^2$  parallel chains, each of length  $2^3 \times 2^n$  residues; 8 of these (A chains) are identical while the ninth (B chain) is different; in each chain amino acids occur with linear regularity. An amino acid may occur in either or both of the A and B chains; if in both, it has the same interval in each.

The following integral analytical intervals can therefore occur:

Amino acid in A chains only:  $3^2 \cdot 2^{n-3}, \dots, 3^2 \cdot 2, 3^2$

Amino acid in B chains only:  $3^2 \cdot 2^n, \dots, 3^2 \cdot 2, 3^2$

Amino acid in both chains:  $2^n, \dots, 2^2, 2, 1$ .

If the interval of occurrence in the chain of an amino acid occurring A chains only is less than  $2^3$ , the analytical interval is not integral.

### Wrinch's Hypothesis.<sup>7</sup>

The chemical, steric and crystallographic evidence for or against this hypothesis need not be discussed here; it is of interest in the present context because, although it does not postulate any regularity of occurrence of particular amino acids, it is definitive with respect to the number of residues in a structural unit and their arrangement in space. The cyclol link is not essential to the structure, serving only (in thought) to lock it into shape; the amino acids can have the positions postulated and be linked in open or closed peptide chains in a variety of ways without its help.

It has been claimed<sup>8</sup> that this model will account for the Bergmann and Niemann ratios, though the question does not seem to have been considered closely. At the outset it is clear that, since the number of residues is  $72 \times n'^2$ , for values of  $n'$  less than 5, any integral analytical interval must be of the form  $2^m 3^n$ . We shall deal here only with the case  $n' = 1$ .

Two types of regularity can occur: regularity relative to the geometry of the model and linear regularity within the chains that compose it.

(1) **Geometrical Regularity.**—The model permits a given amino acid to occur with 2-, 3-, 4- or 6-fold symmetry with respect to the 4 triangular or 4 hexagonal faces or to the 6 "slots" of the model. In addition to this, its symmetry of occurrence in a face or relative to a "slot" may be taken into consideration. Thus, if the highest symmetry of occurrence in a face or round a "slot" is demanded, that is 3, 6 or 9 residues in a face or 2 or 4 residues round a "slot," the following numbers of residues can occur in the model

3, 6 or 9 times 1, 2, 3 or 4  
and  
2 or 4 times 2 or 6.

All these numbers give integral analytical intervals. But if lower symmetry in a face or round a "slot" is allowed, there may be 1, 2, 4, 5, etc., residues in a face or 1 or 3 round a "slot" as well as the numbers given above; some of these numbers do not lead to integral analytical intervals.

(2) **Linear Regularity.**—Considering only the case of closed chains, two questions arise: first, what closed chains are possible; secondly, how far linear regularity in them is consistent with the Bergmann and Niemann ratios and with geometrical regularity.

<sup>6</sup> Janssen, *Protoplasma*, 1939, **33**, 410.

<sup>7</sup> Wrinch, *Proc. Roy. Soc., A*, 1937, **161**, 505.

<sup>8</sup> Wrinch, *ibid.*, *B*, 1939, **127**, 24.





(b) Linear regularity is possible within any of these chains, but only in the cases of the (6)-, (18)- and (54)-chains are linear intervals of the form  $2^m 3^n$  consistent with integral analytical intervals; in all other cases the linear intervals must contain higher primes in order to be consistent with integral analytical intervals: conversely, analytical intervals of the form  $2^m 3^n$  do not necessitate linear intervals of this form.

There are 6 kinds of places in the  $n' = 1$  model relative to its geometry, 3 on each hexagonal and 3 on each triangular face (Fig. 2). The occurrence of each kind of place in a closed chain is regular only in the cases of the (2)- and (6)-chains where the intervals of recurrence are 2 and 6 respectively. In all larger chains the recurrence is only semi-regular, in the sense that, although only certain intervals of recurrence are found, these succeed one another in a way which is not simply related to the type of linear recurrence that has so far been considered. Examples are given in Table II.

There is one special case of very high symmetry. In this there are 14 rings: a (6)-chain centrally placed on each hexagonal face, occupying *a* and *b* places only; a similar (6)-chain on each triangular face occupying

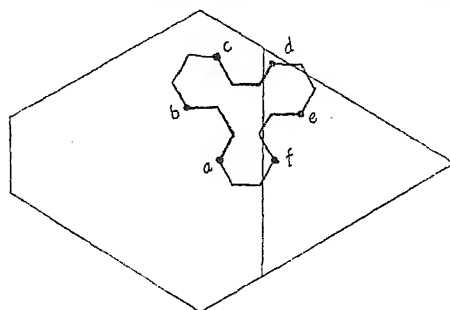


FIG. 2.

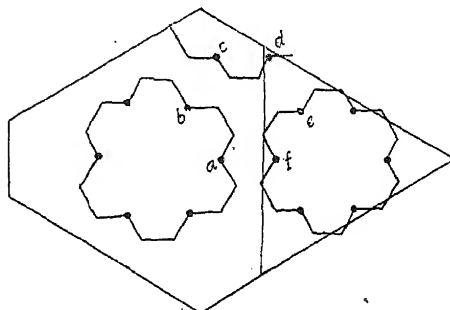


FIG. 3.

TABLE II.

Place.	Intervals of Recurrence.		
	(14)-chain.	(42)-chain.	(66)-chain.
<i>a</i>	2, 12	8, 2, 8, 2, 2, 8, 12	12, 8, 2, 8, 2, 2, 8, 2, 2, 8, 12
<i>b</i>	2, 12	8, 2, 8, 2, 2, 8, 12	12, 8, 2, 8, 2, 2, 8, 2, 2, 8, 12
<i>c</i>	6, 8	2, 8, 2, 10, 8, 2, 10	2, 10, 2, 8, 2, 10, 2, 10, 8, 2, 10
<i>d</i>	4, 2, 8	2, 8, 2, 10, 8, 2, 10	2, 10, 2, 8, 2, 10, 2, 10, 8, 2, 10
<i>e</i>	2, 4, 8	10, 10, 2, 8, 2, 2, 8	2, 2, 8, 10, 12, 10, 2, 8, 2, 2, 8
<i>f</i>	6, 8	10, 10, 2, 8, 2, 2, 8	2, 2, 8, 10, 12, 10, 2, 8, 2, 2, 8

only *e* and *f* places; and a (4)-chain around each "slot" formed of *c* and *d* places. In this case also simple linear regularity within the chains is consistent with geometrical regularity. In Fig. 3 this structure is illustrated, showing two (6)-chains and half of a (4)-chain.

### Conclusions.

The only positive conclusion arising from this work is that of the possibility of a three-dimensionally regular pattern in the Astbury model

consistent with analytical intervals of the form  $2^{m/3}$ . For the rest, it is shown what types of intervals may be expected. Analytical evidence cannot in itself be conclusive; on the one hand, in the Wrinch model, analytical intervals of a given type do not necessarily imply either the same type of interval in its component chains or geometrical regularity; on the other hand, it is quite possible, as Chibnall<sup>3</sup> and Astbury<sup>5</sup> have suggested, that the separate component units of a protein molecule may have linear regularities which do not combine to give simple analytical ratios in the whole molecule.

*Balliol College,  
Oxford.*

---

## THE MAGNETIC SUSCEPTIBILITY OF POSITION ISOMERS IN THE DISUBSTITUTED BENZENE SERIES.

BY C. M. FRENCH.

*Received 16th January, 1945.*

A study of the magnetic susceptibility of various groups of isomeric disubstituted benzene derivatives led Bhatnagar<sup>1</sup> to the conclusion that "in the case of aromatic isomerides the value of  $\chi_M$  for *ortho*- is maximum, and the values for *meta*- and *para*-isomerides, like their other physical properties, are near together." The compounds on which these conclusions were based were, however, relatively few in number, and with one exception (the nitro-group in the two nitrotoluenes measured) the substituent groups were all *o-p* directing, *i.e.* their tendency is to repel electrons to the benzene ring. Cabrera and Fahlenbrach<sup>2</sup> later observed that whereas values obtained by them for *o*- and *m*-cresol agreed with those given by Bhatnagar, there was a marked difference in the values obtained by the different investigators, for the nitrotoluenes. Thus Bhatnagar found the susceptibility of *o*-nitrotoluene greater than that of the *m*-compound, but measurements by Cabrera and Fahlenbrach indicated that of the three isomers of nitrotoluene, the *m*-compound shows the largest, and the *p*-compound the smallest susceptibility.

The results of an investigation by Kido<sup>3</sup> of the magnetic susceptibility of 25 disubstituted benzene derivatives, showed that in many cases the conclusions of Bhatnagar were supported. In the case of the nitrobenzoic acids however, the *m*-compound had a larger diamagnetic susceptibility value than the *o*-compound, and in the case of the xylenes the *m*-compound showed the largest susceptibility of the three isomers. A comparison of the experimental results was made with values calculated by the additive law of ionic susceptibilities, and where "the sign, either of positive or negative polarity, of the substituent group is based on an electronic interpretation of Brown and Gibson's rule of substitution," the calculated and observed susceptibilities are closest together. In view, therefore, both of the relative paucity and conflicting nature of the data, and the unsuccessful attempts noted recently by Angus,<sup>4</sup> to correlate the differences in the susceptibility of the isomers with other physical data, it was decided to redetermine the susceptibility of certain compounds, and to

<sup>1</sup> Bhatnagar, Mathur and Mal, *Phil. Mag.*, 1930, 10, 101. Bhatnagar and Mathur, *ibid.*, 1931, 11, 914.

<sup>2</sup> Cabrera and Fahlenbrach, *Z. Physik*, 1934, 89, 682.

<sup>3</sup> Kido, *Sci. Rep. Tohoku Imp. Univ.*, 1936, 24, 701.

<sup>4</sup> Angus, *Ann. Repts. Chem. Soc.*, 1941, 38, 32.

extend the range of compounds investigated, examining in the first instance, only compounds containing purely *o-p*, or purely *m*-directing groups. Accordingly measurements were made of the magnetic susceptibility of a series of disubstituted benzene derivatives in which the substituent groups showed a definite gradation in electron repelling powers, from the strongly *o-p* orienting hydroxyl group, to the electron attracting and consequently *m*-orienting carboxyl group.

### Experimental.

The compounds examined were first of all purified very carefully by repeated recrystallisation, redistillation in all-glass apparatus, or by freezing, until a high degree of purity was attained as evidenced by reference to such accepted standards as melting-point, boiling-point, refractive index and density. The refractive indices were determined at 20° C. by means of an Abbé refractometer. Finally, before measurements of susceptibility were made, all compounds were tested for the presence of iron, and shown to be free from this impurity.

The Gouy balance and method described previously<sup>5</sup> was used for the measurement of the magnetic susceptibility of the solid compounds. In the case of the liquids, however, the modification recently described<sup>6</sup> was employed.

A D.C. current of 220 volts and 3.0 amperes was used, and this, with a pole gap of 1.25 cm., gave a field of 5300 gauss.

The susceptibility tubes were compactly filled to a length of 7 cm.

### Method of Calculation.

The susceptibility of the solids was calculated by the equation :<sup>5</sup>—

$$10^6 \chi_A = \frac{F_A \alpha + 10^6 K_{air} V}{W_A}$$

where  $\chi_A$  is the susceptibility of the substance under investigation,  $F$  is the thrust on the specimen in mg.,  $V$  the volume of the specimen in c.c.,

and  $\alpha$  the balance constant =  $\frac{2l \times 10^6 \times 981}{H^2 \times 1000}$ , where  $H$  is the field strength.

For liquids, however, the modified formula<sup>6</sup> was used :—

$$10^6 \chi_A = \left( 10^6 \chi_B - \frac{0.0294}{d_B} \right) \frac{F_A d_B}{F_B d_A} + \frac{0.0294}{d_A}$$

where the subscript "B" refers to the standard liquid, in this case benzene ( $\chi_B = -0.702 \times 10^{-6}$ ), and  $d_A$  and  $d_B$  are the densities of the liquid under investigation and benzene respectively.

### Results.

The results for the magnetic susceptibility measurements of the compounds investigated are given in Table I. Column 4 gives the specific susceptibility, while column 5 gives the molar mass susceptibility. All the magnetic susceptibility results are a mean of six closely agreeing values. The probable error in the experimental values for the specific susceptibility of the liquids is 0.0010, and of the solids 0.0030.

The literature values for the melting-points and boiling-points shown in Table I are those given in Weissberger and Proskauer's *Organic Solvents*. The densities of *o*- and *m*-dimethoxybenzene were found experimentally

<sup>5</sup> Trew and Watkins, *Trans. Faraday Soc.*, 1933, 29, 1310.

<sup>6</sup> French and Trew (*in the Press*).

TABLE I.

1 Substance.	2 Observed.		3 Lit. Val. of M.Pt. or B.Pt.	4 Specific Suscept. $-\chi_s \times 10^6$ .	5 Molar Suscept. $-\chi_M \times 10^6$ .	6 Other Recorded Values.	
	M.Pt.	B.Pt.				Molar Suscept.	Reference.
Catechol . . . . .	103	—	105	0.6248	68.76	64.5, 66.0	Allen <sup>7</sup>
Resorcinol . . . . .	110	—	110	0.6112	67.26	67.9	Pascal
Hydroquinone . . . . .	170.5	—	170.3	0.6040	66.47	70.0	Kido <sup>3</sup>
						60.9, 63.1	Allen <sup>7</sup>
						64.5	Palacios and Poz <sup>8</sup>
<i>o</i> -Dimethoxybenzene . . . . .	—	206	206	0.6329	87.39	—	
<i>m</i> -Dimethoxybenzene . . . . .	—	216	216.5-217.5	0.6316	87.21	—	
<i>p</i> -Dimethoxybenzene . . . . .	56	—	56	0.6275	86.65	—	
<i>o</i> -Phenylenediamine . . . . .	103	—	102-103	0.6662	71.98	—	
<i>m</i> -Phenylenediamine . . . . .	63	—	63-64	0.6529	70.53	—	
<i>p</i> -Phenylenediamine . . . . .	140	—	140, 147	0.6503	70.28	—	
<i>o</i> -Dichlorobenzene . . . . .	—	179	179-179.5	0.5734	84.26	86.3	Kido ; <sup>3</sup> Cabrera and Fahlenbrach <sup>2</sup>
<i>m</i> -Dichlorobenzene . . . . .	—	172	172	0.5661	83.19	84.5	Kido <sup>3</sup>
<i>p</i> -Dichlorobenzene . . . . .	53	—	53	0.5644	82.93	90.9	Pascal
<i>o</i> -Dinitrobenzene . . . . .	118	—	118	0.3921	65.98	74.3	Kido <sup>3</sup>
<i>m</i> -Dinitrobenzene . . . . .	90	—	89.57	0.4197	70.53	72.8	Kido <sup>3</sup>
<i>p</i> -Dinitrobenzene . . . . .	173	—	173-174	0.4064	68.30	66.9	Pascal
Phthalic acid . . . . .	205	—	231, 191	0.5035	83.61	70.6	Kido <sup>3</sup>
<i>iso</i> -Phthalic acid . . . . .	307	—	345-347	0.5097	84.64	74.1	Hadfield, Cheneveau and Geneau <sup>9</sup>
Terephthalic acid . . . . .	300	—	ca. 300	0.5029	83.51	80.9	Gray and Birse <sup>10</sup>
<i>m</i> -Nitrobenzoic acid . . . . .	147	—	147-148	0.4556	76.11	77.03	Kido <sup>3</sup>
<i>m</i> -Nitrobenzoic acid . . . . .	141	—	140-141	0.4802	80.22	77.19	Kido <sup>3</sup>
<i>p</i> -Nitrobenzoic acid . . . . .	238	—	238	0.4718	78.81	77.86	Kido <sup>3</sup>
<i>o</i> -Nitrobenzaldehyde . . . . .	46	—	43-44	0.4517	68.23	—	
<i>m</i> -Nitrobenzaldehyde . . . . .	58	—	58	0.4538	68.55	—	
<i>p</i> -Nitrobenzaldehyde . . . . .	106	—	106	0.4407	66.57	—	

<sup>2</sup> Allen, Ph. D. Thesis, London, 1942. <sup>3</sup> Allen, Ph. D. Thesis, London, 1942. <sup>4</sup> Proc. Roy. Soc., 1917, 94, 65.

<sup>5</sup> Hadfield, Chem. Ind., 1914, 108, 2707.

<sup>6</sup> Palacios and Poz, *Anal. Fis. Quim.*, 1935, 33, 627.

<sup>7</sup> Allen, Ph. D. Thesis, London, 1942.

<sup>8</sup> Allen, Ph. D. Thesis, London, 1942.

<sup>9</sup> Hadfield, Chem. Ind., 1914, 108, 2707.

<sup>10</sup> Gray and Birse, *J. C.S.*, 1914, 108, 2707.

to be 1.086 and 1.0705 respectively (values given in Weissberger and Proskauer's *Organic Solvents* are 1.086 and 1.0705). The densities of *o*- and *m*-dichlorobenzene were found to be 1.304 and 1.288 respectively (corresponding literature values are 1.3048, *International Critical Tables*; and 1.2881, Heilbron's *Dictionary of Organic Compounds*).

The refractive indices of *o*- and *m*-dimethoxybenzene were found experimentally to be 1.534 and 1.525 respectively (no previously recorded values available); and the refractive indices of *o*- and *m*-dichlorobenzene were found to be 1.5501 and 1.5467 respectively (corresponding values given in the *International Critical Tables* are 1.549 and 1.546).

Table II, column 2, gives the molar susceptibility values for the mono-substituted derivatives corresponding to the disubstituted compounds shown in Table I. In the two cases where the two substituents are different—the nitrobenzaldehydes and the nitrobenzoic acids—a value for the monosubstituted derivative cannot exist.

TABLE II.

1 Substance.	2 Molar Suscept. — $\chi_M \times 10^6$ .	3 Author.	4 Angus Theor. Value for — $\chi_M \times 10^6$ .	5 Difference between Exptl. and Theor. Values.
Phenol . .	60.9 60.6	Pascal Kido <sup>8</sup>	66.38	5.48 5.78
Anisole . .	72.64 74.05	Pascal Bhatnagar <sup>11</sup>	76.44	3.80 2.39
Aniline . .	63.56 63.84 64.40 65.14	Kido <sup>8</sup> Bhatnagar <sup>11</sup> Oxley <sup>12</sup> Azim <sup>13</sup>	70.42	6.86 6.58 6.02 5.38
Chlorobenzene	68.85 69.5 71.0 71.9 72.45 74.70	Kido <sup>8</sup> Rao <sup>14</sup> French <sup>6</sup> Mathur <sup>15</sup> Bhatnagar <sup>11</sup> Oxley <sup>12</sup>	75.73	6.88 6.23 4.73 3.83 3.28 1.03
Benzoic acid .	67.9 70.2	Gray <sup>10</sup> Kido <sup>8</sup>	80.09	12.01 9.89
Nitrobenzene .	61.0 61.40 61.43 61.53 61.53 61.94 62.14 62.63 62.63 62.76	Azim <sup>13</sup> Oxley <sup>12</sup> Rao <sup>16</sup> Bhatnagar <sup>11</sup> Kido <sup>8</sup> Seely <sup>17</sup> Rao <sup>17</sup> Cabrera <sup>2</sup> Cabrera <sup>18</sup> Rao <sup>14</sup>	77.72	16.72 16.32 16.29 16.19 16.19 15.78 15.58 15.09 15.09 14.98

<sup>11</sup> Bhatnagar, Nevgi and Khanna, *Z. Physik*, 1934, 89, 506.

<sup>12</sup> Oxley, *Phil. Trans.*, 1914, 214, 109.

<sup>13</sup> Azim, Bhatnagar and Mathur, *Phil. Mag.*, 1933, 16, 580.

<sup>14</sup> Rao and Sivaramakrishnan, *Ind. J. Physics*, 1931, 6, 509.

<sup>15</sup> Mathur, *ibid.*, 1934, 8, 207.

<sup>16</sup> Rao and Varadachari, *Proc. Ind. Acad. Sci. A*, 1934, 1, 77.

<sup>17</sup> Rao, *Ind. J. Physics*, 1934, 8, 483.

<sup>18</sup> Cabrera and Fahlenbrach, *Anal. Fis. Quim.*, 1934, 32, 543.

<sup>19</sup> Seely, *Physic. Rev.*, 1936, 49, 812.

at all positions in the ring, but a maximum increase in the *o*-position, it is to be expected that the compound with the two electron repelling substituents in the *o*-position to each other will have the maximum diamagnetic susceptibility, since on the Langevin treatment,<sup>21</sup> a decrease in effective positive charge will result in an increase in diamagnetism. It is, however, to be remarked, that on this basis the increase in negative charge on the *p*-position is, although slightly less than that on the *o*-position, considerably greater than that on the *m*-position, and accordingly it might be expected that the *p*-compound would have an appreciably greater diamagnetic susceptibility than the *m*-compound, and only slightly less than that of the *o*-compound. An examination of the results of the present investigation indicate, however, the reverse effect, the *p*-isomer having in each case a lower susceptibility than the *m*-compound. This observation is supported by a great number of the susceptibility determinations of Kido<sup>3</sup> and of Cabrera and Fahlenbrach,<sup>2</sup> but there appear to be certain exceptions to it in the data presented by Cabrera and Fahlenbrach, and by Bhatnagar.<sup>1</sup>

Similarly, in the case of a group that attracts electrons from the benzene ring, there is a decrease in electron density at all positions in the ring, but

TABLE III.

Substance.	Difference in $-\chi_M \times 10^6$ .	
	<i>o</i> - <i>m</i> .	<i>o</i> - <i>p</i> .
Dihydroxybenzene .	+ 1.50	+ 2.29
Dimethoxybenzene .	+ 0.21	+ 1.68
Phenylenediamine .	+ 1.45	+ 1.70
Dichlorobenzene .	+ 1.07	+ 1.33
Dinitrobenzene .	- 4.64	- 2.41
Benzene Dicarboxylic acid .	- 1.03	+ 0.10
Nitrobenzoic acid .	- 4.11	- 2.70
Nitrobenzaldehyde .	- 0.32	+ 2.34

lowest susceptibility, but that the values for the *o*- and *p*-compounds would be close together, a regularity which again seems not to be confirmed by the present work. It may be, however, that these polarisation effects of the substituent groups are sometimes sufficiently weakened on relaying through the benzene ring to the *p*-position to be masked by other possible disturbing influences, such as the effect of the substituent groups on each other.

It may be remarked that with the exception of the hydroxybenzenes, the graphs for the susceptibility of compounds with *o-p* directing groups show values for all three isomers which are lower than might be expected from the additivity rule, while the graph for *m*- and *p*-dinitrobenzene shows values higher than would be expected. This would indicate that effects other than those due to pure electron repulsion or attraction are involved, since the latter would result in curves with a divergence in the opposite direction. Such observed divergences are, however, small, and obviously depend on the correctness of the values adopted for both the mono- and disubstituted compounds. It is apparent, therefore, that as observed by Sugden in a general statement,<sup>20</sup> further measurements of the susceptibility of a number of organic compounds by different methods are desirable.

A correlation has been attempted by Bhatnagar<sup>1</sup> between the size of the substituent groups, and the difference in susceptibility between the *o*- and *p*-compounds, and the *o*- and *m*-compounds. An examination of

<sup>21</sup> Langevin, *Ann. Chim. Physique*, 1905, 5, 70; *J. Physique*, 1905, 4, 678.

Table III, which shows these differences in the series of compounds measured in the present investigation, fails, however, to establish any close relationship between these quantities. For example, the differences between the susceptibility values of the dimethoxybenzenes is smaller than between the corresponding values of the dihydroxybenzenes, the substituent group being smaller in the latter case. For the dichlor- and dinitrobenzenes, however, the variation is in the opposite direction, the latter compound having both the larger substituent group, and the greater differences between the susceptibilities of its isomers. Indeed, apart from the change of sign in the difference *o* — *m*-, on passing from compounds with *o*-*p* directing groups to those with *m*-directing groups, perhaps the most striking feature is the generally appreciably higher numerical difference between the susceptibilities of the isomers when a nitro-group is one of the substituents, than when the nitro-group is absent. The exact significance of this observation is not immediately apparent, but it is perhaps noteworthy that other investigators, including Pascal, have observed anomalous effects in compounds containing the nitro-group.

### Comparison with Theoretical Values.

It will at once be apparent that calculations of theoretical molar susceptibility values on the methods of Pauling,<sup>22</sup> Slater,<sup>23</sup> or Angus<sup>24</sup> cannot give different values for different isomeric compounds since they are based purely on the additive values of the constituent atoms, and no account is taken of bond depressions; although of these methods, that of Angus gives the closest approximation to the experimentally determined values. These methods of calculation are based on the classical formula:—

$$\chi = \frac{-e^2}{6mc^2} \bar{r}^2.$$

Van Vleck<sup>25</sup> and Pauling<sup>22</sup> have calculated the value of  $\bar{r}^2$  as

$$\bar{r}^2 = a_0^2 \frac{n^4}{(Z-S)^2} \left[ 1 + 3/2 \left\{ 1 - \frac{l(l+1) - 1/3}{n^2} \right\} \right]$$

where  $a_0$  is the radius of the one-quantum orbit of hydrogen.

Substituting the value so obtained for  $\bar{r}^2$ , and introducing numerical values for physical constants, the value of the susceptibility per gram atom is given by:—

$$\chi = -2.010 \times 10^{-6} \sum \frac{n^4}{(Z-S)^2} \left\{ 1 - \frac{3l(l+1) - 1}{5n^2} \right\}$$

and the ionic susceptibility is given by:—

$$\chi = -0.807 \times 10^{-6} \int_0^\infty r^2 (dz/dr) dr.$$

The method due to Slater<sup>23</sup> involves the use of modified values for screening constants in calculating  $\bar{r}^2$ , and Angus<sup>24</sup> further suggested that theoretical susceptibility values could be brought into closer agreement with experimental values by taking the *s* and *p* electrons separately in calculating the screening constants. According to the Angus method of calculation,<sup>24</sup> and using the more accurate values for the physical constants, including the value  $0.5292 \times 10^{-8}$  cm. for  $a_0$ ,<sup>26</sup> now available, the values of the atomic susceptibility ( $-\chi_A \times 10^6$ ) of C<sup>0</sup>, H<sup>0</sup> and O<sup>0</sup> are 7.69, 2.37, and 6.02 respectively. The molar mass susceptibility of phenol for

<sup>22</sup> Pauling, *Proc. Roy. Soc. A*, 1927, 114, 181.

<sup>23</sup> Slater, *Physic. Rev.*, 1930, 36, 57.

<sup>24</sup> Angus, *Proc. Roy. Soc. A*, 1932, 136, 569.

<sup>25</sup> Van Vleck, *Physic. Rev.*, 1928, 31, 587.

<sup>26</sup> Birge, Taylor and Glasstone's *Physical Chemistry*, Vol. I, p. 21.



example, will, if no regard is paid to charge distribution, therefore be given by :—

$$-\chi_M \times 10^6 = (6 \times 7.69) + (6 \times 2.37) + 6.02 = 66.38.$$

Similarly the molar mass susceptibility of dihydroxybenzene will be given by :—

$$-\chi_M 10^6 = (6 \times 7.69) + (6 \times 2.37) + (2 \times 6.02) = 72.40$$

Pascal's method <sup>27</sup> also, whilst allowing for constitutive effects in addition to the purely additive effects due to the different atoms in the molecule, is unable to distinguish between various isomers.

The method due to Gray and Cruickshank <sup>28</sup> allowing for bond depressions is potentially the method that would give closest agreement with the experimental data, but owing to the difficulty in formulating adequately, the various canonical structures for the different isomeric disubstituted benzenes, this method again fails to afford the different susceptibility values for these isomers.

TABLE IV.

Substance.	Angus Value of $-\chi_M \times 10^6$ .	Differences between Exptl. and Theorl. Values.		
		<i>ortho</i> -	<i>meta</i> -	<i>para</i> -
1	2	3	4	5
Dihydroxybenzene . . .	72.40	3.64	5.14	5.93
Dimethoxybenzene . . .	97.26	9.99	10.20	11.67
Phenylenediamine . . .	80.48	8.50	9.95	10.20
Dichlorobenzene . . .	91.10	6.84	7.91	8.17
Dinitrobenzene . . .	95.08	29.81	24.55	26.78
Benzene Dicarboxylic acid .	99.82	16.21	15.18	16.31
Nitrobenzoic acid . . .	97.45	21.34	17.23	18.64
Nitrobenzaldehyde . . .	91.43	23.20	22.88	24.86

Table IV, in which, in columns 3, 4 and 5, are given the differences between the experimentally determined values for the isomeric disubstituted benzenes and the theoretical susceptibilities calculated on the Angus method <sup>24</sup> (column 2), shows some interesting points. Thus in compounds with *o-p* directing groups, the differences are generally of the order of 10 or less; whilst for compounds with *m*-directing groups the differences are greater than 15 and generally greater than 20. An examination of similar differences for the monosubstituted benzenes reveals a similar effect. Thus in column 5 of Table II, are given the differences between the susceptibility values of monosubstituted compounds and the theoretically determined values for those compounds on the Angus method.<sup>24</sup> Again, compounds with a *m*-directing group show an appreciably greater difference than those with *o-p* directing groups. It appears again also, that in compounds containing a nitro- group, the experimentally determined susceptibility shows a deviation from the theoretical value, greater than in compounds which have no nitro- group.

### Summary.

1. The diamagnetic susceptibility values for various isomeric disubstituted benzenes have been determined using the Gouy method.

<sup>27</sup> Pascal, *Ann. Chim. Physique*, 1910, 19, 5.

<sup>28</sup> Gray and Cruickshank, *Trans. Faraday Soc.*, 1935, 31, 1491.

2. It is shown that the *o*-compound has the highest susceptibility of the three isomers when the substituent is *o-p* directing, and the *m*-compound has the highest susceptibility when the substituent is *m*-directing. A tentative explanation of this phenomenon is put forward.

3. Certain other quantitative differences are noted between compounds containing *o-p* directing groups and those containing *m*-directing groups, and further, the apparently anomalous effect due to the presence of a nitro-group is noted.

Laboratory for Physical Chemistry,  
Bedford College,  
Regent's Park, N.W.1.

---

## THE OSMOTIC AND ACTIVITY COEFFICIENTS OF SODIUM AND POTASSIUM DIHYDROGEN PHOSPHATE AT 25°.\*

By JEAN M. STOKES.

Received 24th January, 1945.

The activity coefficient of a potassium salt is usually lower than that of the corresponding sodium salt at the same concentration; indeed, there is generally a uniform decrease of activity coefficient with increasing atomic number of the alkali metal cation in order of  $\text{Li} > \text{Na} > \text{K} > \text{Rb} > \text{Cs}$ . This is true for the alkali metal chlorides, bromides, and iodides and, also holds for the nitrates. The order is not confined to salts containing an anion of the noble gas type because the same order has been found to occur with sodium and potassium thiocyanate.<sup>1</sup> On the other hand, there are a few significant cases known in which the order is exactly reversed; lithium, sodium and potassium hydroxide<sup>2</sup> may be quoted as one example; another is the series of alkali metal formates<sup>3</sup> and acetates.<sup>4</sup> It has been pointed out<sup>5</sup> that this reversal of order of the activity coefficients seems to occur whenever the anion is that of a weak acid, such as acetic acid or water, and a mechanism of "localised hydrolysis" has been postulated to account for this behaviour.

It is therefore desirable to make further measurements on the sodium and potassium salts of a series of weak acids of widely different dissociation constant. As a part of this investigation the primary salts of phosphoric acid have now been studied. Unfortunately, this choice was not a good one because it is now found that the phosphates give a series of very low activity coefficients, similar to those of the nitrates, corresponding to ion association of the Bjerrum type. Moreover, the sodium salt proved unexpectedly difficult to measure, the reproducibility of the results being of a considerably lower order than is experienced when working with other salts. The cause of this difficulty has not been discovered. Nevertheless, as an addition to our knowledge of this class of salts with very low activity coefficients, the data for  $\text{NaH}_2\text{PO}_4$  and  $\text{KH}_2\text{PO}_4$  are of interest. Experimental results are given in Table I.

The osmotic and activity coefficients of these two salts, calculated from the isopiestic data of Table I, are given in Table II. As reference

\* Communicated by Dr. R. A. Robinson.

<sup>1</sup> Robinson, *J. Amer. Chem. Soc.*, 1940, 62, 3131.

<sup>2</sup> Harned and Swindells, *ibid.*, 1926, 48, 126; Harned and Hecker, *ibid.*, 1934, 56, 650; Harned and Cook, *ibid.*, 1937, 59, 496.

<sup>3</sup> Scatchard and Prentiss, *ibid.*, 1934, 56, 807.

<sup>4</sup> Ref. 3. See also Robinson, *ibid.*, 1935, 57, 1165; 1937, 59, 84.

<sup>5</sup> Robinson and Harned, *Chem. Rev.*, 1941, 28, 419.

values the data quoted by Robinson and Harned <sup>5</sup> for KCl were used but the requisite adjustment was made in the reference values at high concentrations, using the more recent data of Olynnyk and Gordon.<sup>6</sup>

TABLE I.—MOLALITIES OF ISOPIESTIC SOLUTIONS OF POTASSIUM CHLORIDE AND SODIUM OR POTASSIUM DIHYDROGEN PHOSPHATE AT 25°.

NaH <sub>2</sub> PO <sub>4</sub> .	KCl.	NaH <sub>2</sub> PO <sub>4</sub> .	KCl.	NaH <sub>2</sub> PO <sub>4</sub> .	KCl.	NaH <sub>2</sub> PO <sub>4</sub> .	KCl.
0.1262	0.1240	1.052	0.9092	2.469	1.919	3.945	2.924
0.1479	0.1442	1.209	1.022	2.630	2.004	4.232	3.120
0.2020	0.1955	1.590	1.305	2.956	2.246	4.547	3.345
0.3285	0.3116	1.673	1.367	3.182	2.403	4.868	3.577
0.3526	0.3332	1.843	1.485	3.184	2.405	5.136	3.770
0.4782	0.4429	1.992	1.590	3.290	2.472	5.414	3.962
0.5570	0.5105	2.312	1.811	3.528	2.630	5.561	4.057
0.5897	0.5366	2.348	1.832	3.741	2.779	5.624	4.119
0.8520	0.7545	2.405	1.870	3.858	2.859	6.585	4.810
1.032	0.8944						

KH <sub>2</sub> PO <sub>4</sub> .	KCl.	KH <sub>2</sub> PO <sub>4</sub> .	KCl.	KH <sub>2</sub> PO <sub>4</sub> .	KCl.	KH <sub>2</sub> PO <sub>4</sub> .	KCl.
0.0993	0.0972	0.4029	0.3669	0.7450	0.6351	1.395	1.081
0.1148	0.1115	0.4123	0.3736	0.8503	0.7126	1.452	1.122
0.1412	0.1355	0.4425	0.3972	0.8940	0.7437	1.555	1.186
0.1578	0.1512	0.5636	0.4994	0.9523	0.7850	1.570	1.196
0.1708	0.1632	0.5942	0.5240	1.159	0.9268	1.752	1.309
0.2764	0.2580	0.7130	0.6134	1.206	0.9600	1.820	1.347
0.3814	0.3481	0.7157	0.6134	1.230	0.9772		

TABLE II.—OSMOTIC AND ACTIVITY COEFFICIENTS OF SODIUM AND POTASSIUM DIHYDROGEN PHOSPHATE AT 25°.\*

m.	NaH <sub>2</sub> PO <sub>4</sub> .		KH <sub>2</sub> PO <sub>4</sub> .	
	φ.	γ.	φ.	γ.
0.1	0.911	0.744 (−3)	0.901	0.731 (−3)
0.2	0.884	0.675 (−3)	0.868	0.653 (−2)
0.3	0.864	0.629 (−3)	0.843	0.602 (−2)
0.4	0.847	0.593 (−1)	0.823	0.561 (−1)
0.5	0.832	0.563 (+1)	0.805	0.529 (−1)
0.6	0.819	0.539 (+1)	0.789	0.501 (0)
0.7	0.808	0.517 (+2)	0.773	0.477 (+1)
0.8	0.798	0.499 (+2)	0.760	0.456 (+1)
0.9	0.789	0.483 (+1)	0.747	0.438 (0)
1.0	0.780	0.468 (0)	0.736	0.421 (0)
1.2	0.765	0.442 (−1)	0.716	0.393 (−4)
1.4	0.751	0.420	0.698	0.369
1.6	0.739	0.401	0.683	0.348
1.8	0.729	0.385	0.669	0.332
2.0	0.721	0.371	—	—

NaH<sub>2</sub>PO<sub>4</sub>.

m 2.5	3.0	3.5	4.0	4.5	5.0	5.5	6.0	6.5
φ 0.705	0.696	0.691	0.691	0.694	0.699	0.706	0.713	0.721
γ 0.343	0.320	0.305	0.293	0.283	0.276	0.270	0.265	0.261

[For footnotes <sup>5</sup> and <sup>6</sup> see opposite page.

## Discussion.

The activity coefficients of  $\text{KH}_2\text{PO}_4$  are close to those of  $\text{AgNO}_3$ ,<sup>7</sup> and  $\text{RbNO}_3$ ;<sup>8</sup> up to a concentration of 1.8 M. the activity coefficients of  $\text{AgNO}_3$  and  $\text{KH}_2\text{PO}_4$  do not differ by more than 0.006. The data may be represented by an extended Debye-Hückel equation:

$$\log \gamma = - \frac{0.5091 \sqrt{c}}{1 + 0.3286a \sqrt{c}} + Bc - \log (1 + 0.036 m).$$

This equation is valid up to 1.2 M., the highest concentration at which the necessary density data are available for converting molalities to volume concentrations, if  $a = 2.5 \text{ \AA}$  and  $B = -0.088$ .

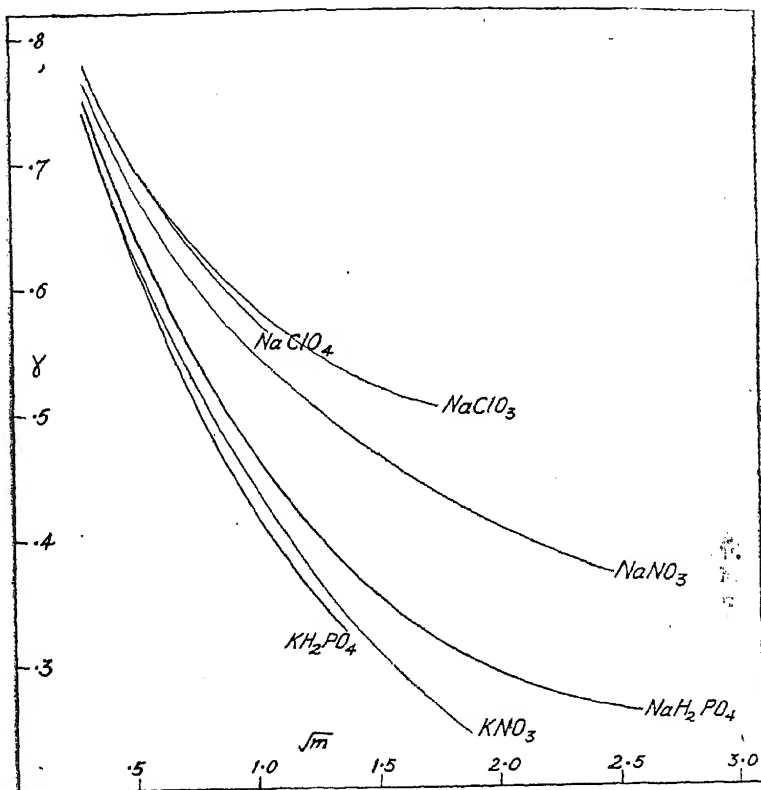


FIG. 1.

The activity coefficients of  $\text{NaH}_2\text{PO}_4$  lie between those of  $\text{KNO}_3$  and  $\text{NaNO}_3$ . Up to 1.2 M., the Debye-Hückel equation holds with  $a = 3 \text{ \AA}$  and  $B = -0.0606$ .

The negative values of the terms linear in the concentration are noteworthy; on Bjerrum's theory of ion pair formation, each salt should be

<sup>6</sup> Olmynk and Gordon, *J. Amer. Chem. Soc.*, 1943, **65**, 224.

\* The figures in parentheses give the deviations, in the third place of  $\gamma$ , between the observed activity coefficients and those calculated by an extended Debye-Hückel equation. A positive sign indicates that the calculated values are higher than the observed.

<sup>7</sup> Robinson and Tait, *Trans. Faraday Soc.*, 1941, **37**, 569.

<sup>8</sup> Robinson, *J. Amer. Chem. Soc.*, 1937, **59**, 84.

<sup>3</sup> *J. Chem. Soc.*, 1943, 157.

throughout and vacuum corrections of weighings were made whenever significant. As a check on the stock solution, a part of it was equilibrated against KCl in the isopiestic vapour pressure apparatus and was found to give results in excellent agreement with the "solution A" of Part X of this series.

The Zn electrodes were of 5 % Zn amalgam, prepared by heating A.R. Zn with redistilled mercury, washing with dilute acid, and filtering while hot. The Ag—AgBr electrodes were of the type described by Keston.<sup>4</sup> Since the measurements were made entirely by artificial light no blackening of the cells was considered necessary. The cell vessels were of two types, an H cell (Fig. 1a) for the concentration range 0.05 M. to 1 M., and the form shown in Fig. 1b, of lower internal resistance, for the more dilute solutions. The potentiometer was a Leeds and Northrup type K2 and three new standard cells (from the Eppley Laboratories), kept in an oil bath, were used for standardisation. The thermostat was controlled to  $\pm 0.02^\circ$ , the thermometer being checked against one with a N.P.L. certificate.

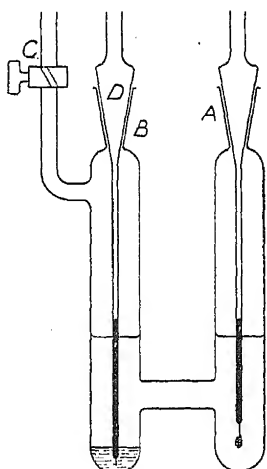


FIG. 1a.

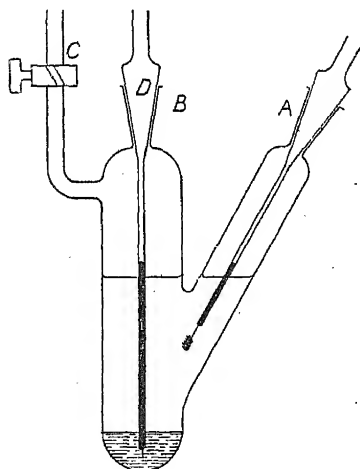


FIG. 1b.

The cells were set up in an atmosphere of hydrogen as follows: A solution of the required concentration was prepared by weight dilution of the stock. The solution, contained in a separating funnel with a capillary outlet, was saturated with hydrogen by successive evacuations and admissions of the gas, and its concentration calculated from the final weight. With the AgBr electrode in position at A and the opening B closed with a temporary stopper, the inlet C was connected alternately to the vacuum and hydrogen lines until all air was "rinsed" out. The stopper at B was then removed and the cell solution run in against a vigorous stream of hydrogen. A 2-3 c.c. portion of the clean amalgam, warmed until entirely liquid, was then added (without stopping the hydrogen flow) and finally the opening B closed by the ground-in contact rod D. After closing tap C the cell was left at  $25^\circ$  in the thermostat overnight, or at least for several hours, to attain equilibrium. E.m.f. readings were then taken at  $5^\circ$  intervals in the following order:  $25$  to  $40^\circ$ ,  $40$  to  $20^\circ$ ,  $20$  to  $25^\circ$ . In a few cases where the  $25^\circ$  value changed by more than 0.1 mv. the run was discarded. Usually the three  $25^\circ$  results, taken over a period of eight to twelve hours, agreed to better than 0.05 mv. A few

<sup>4</sup> *J. Amer. Chem. Soc.*, 1935, 57, 1671.

of the cells were held at 25° for some days and it was found that in most cases two to three days elapsed before any significant drop in e.m.f. occurred.

The experimental results are given in Table I. The electromotive forces at each concentration may be expressed as a quadratic in the temperature:

$$E_t = E_{30} (\text{calc.}) + a(t - 30) + b(t - 30)^2.$$

The values of  $E_{30}$  (calc.),  $a$  and  $b$ , obtained by the method of least squares are also given in Table I; with these values the quadratic reproduces

TABLE I.—E.M.F.s OF THE CELL  $\text{Zn-Hg} \mid \text{ZnBr}_2 \mid \text{AgBr-Ag}$  FROM 20° TO 40°.

<i>m.</i>	$E_{20}$	$E_{25}$	$E_{30}$	$E_{35}$	$E_{40}$	$E_{30}$ (calc.)	$a \times 10^6$	$b \times 10^6$
0.002026	1.06016	1.06108	1.06189	1.06249	1.06302	1.06187	+14.3	-2.8
0.003250	1.04350	1.04420	1.04475	1.04519	1.04547	1.04476	+9.9	-2.7
0.004250	1.03415	1.03473	1.03512	1.03540	1.03550	1.03514	+6.7	-3.1
0.007622	1.01420	1.01436	1.01440	1.01428	1.01403	1.01439	-0.8	-2.8
0.008216	1.01155	1.01172	1.01172	1.01163	1.01147	1.01173	-0.5	-2.1
0.01281	0.99640	0.99640	0.99612	0.99581	0.99533	0.99615	-5.5	-2.8
0.01887	0.98367	0.98344	0.98308	0.98251	0.98176	0.98307	-9.5	-3.6
0.03210	0.96639	0.96586	0.96517	0.96436	0.96338	0.96518	-15.0	-2.9
0.05705	0.94746	0.94670	0.94575	0.94467	0.94345	0.94576	-20.1	-3.0
0.07289	0.93944	0.93859	0.93758	0.93636	0.93500	0.93757	-22.2	-3.5
0.1000	0.92896	0.92801	0.92684	0.92550	0.92401	0.92684	-24.8	-3.6
0.2028	0.88477	0.90347	0.90201	0.90032	0.89837	0.90201	-31.9	-4.4
0.3810	0.88102	0.87940	0.87774	0.87594	0.87408	0.87773	-34.7	-1.8
0.4554	—	0.87231	—	—	—	—	—	—
0.6986	0.85544	0.85385	0.85233	0.85073	0.84908	0.85232	-31.7	-0.6
0.7082	0.85475	0.85327	0.85167	0.85011	0.84855	0.85168	-31.1	-0.3
0.9900	0.84030	0.83895	0.83766	0.83629	0.83508	0.83763	-26.2	+0.6

the experimental results to better than 0.03 mv. For graphical representation of the 25° results the arbitrary deviation function,

$$\kappa = E_{25} + 0.07918 \log m,$$

is very convenient since  $\kappa$  covers a range of only a few millivolts. In Fig. 2 the present results and those of previous workers<sup>2, 3</sup> are shown in this

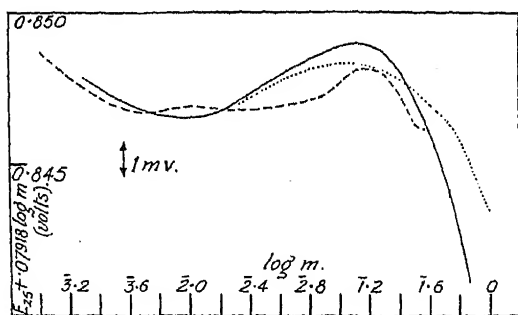


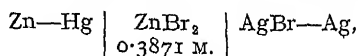
FIG. 2.—Comparison of e.m.f. measurements of cells containing zinc bromide at 25°. The experimental points are not shown as in each of the three sets of data they lie very close to the smooth curves.

Present work.

— — — Egan and Partington.

..... Parton and Mitchell.

form. The e.m.f.s observed by Egan and Partington would be expected to differ from ours by a constant amount, viz., the e.m.f. of the cell,



in which the molality is that of the fixed side of their double cell. By interpolation in our results this e.m.f. is 0.87880 volt. This amount has therefore been added to their e.m.f.s to simplify the comparison.

It will be seen that the discrepancies among the three sets of results are considerable. Therefore in order to check our own data we have computed the water activities

in solutions above 0.1 M. by the method described in Part XI of this series, using the  $\alpha$  function defined above to facilitate the integration. The results in Table II are in good agreement with our isopiestic data for another preparation of  $\text{ZnBr}_2$ .

TABLE II.—WATER ACTIVITIES IN  $\text{ZnBr}_2$  SOLUTIONS AT 25°.

$m$ .	$\alpha_w$ (e.m.f.).	$\alpha_w$ (isopiestic).
0.1	0.9953	0.9953
0.2	0.9904	0.9905
0.3	0.9852	0.9853
0.5	0.9742	0.9743
0.7	0.9625	0.9627
1.0	0.9453	0.9454

#### Standard Potentials of the Cell.

The Debye-Hückel theory gives a close correlation between the osmotic behaviour of a salt and the effective diameter of its ions. Agreement with experimental data is obtained, however, only with the use of diameters much larger than those derived from crystallographic measurements and the difference may be attributed to the presence of a hydration sheath, the extent of which is probably controlled by electrostatic forces.

Since the electrostatic field at the surface of an ion of given valency depends only on the diameter, the degree of hydration, and hence the Debye-Hückel parameter should be dependent only on the crystallographic radius. The radii of Mg and Zn ions are 0.65 and 0.74 Å. respectively so that we should expect the osmotic coefficient of a Zn salt to be very close to that of the corresponding Mg salt unless "chemical" differences, such as complex ion formation, occur. This parallelism is shown very clearly by the nitrates

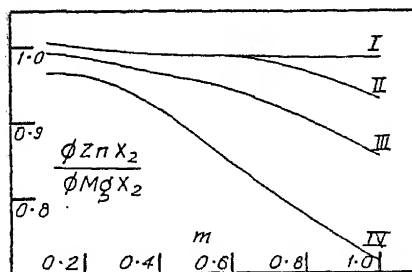


FIG. 3.—Ratio of osmotic coefficients of zinc and magnesium salts.

I = Nitrates, II = Iodides,  
III = Bromides, IV = Chlorides.

and perchlorates of Mg and Zn<sup>5, 6</sup> where complex ion formation is difficult to visualise. In Fig. 3 we have plotted the ratio  $\phi_{\text{ZnX}_2} / \phi_{\text{MgX}_2}$  for the nitrates and halides. From this graph it is apparent that the similarity between Zn and Mg salts holds for the iodides up to about 0.5M.; at higher concentrations the ratio departs rapidly from unity, and that it is the Zn salt rather than the Mg salt which is anomalous is readily appreciated from a plot of  $\phi$  against  $\sqrt{m}$  (Fig. 4). With  $\text{ZnBr}_2$  and even more with  $\text{ZnCl}_2$  abnormality is found at lower concentrations and Fig. 3 suggests that it is not permissible to regard  $\text{ZnBr}_2$  as fully dissociated even at 0.1 M.

<sup>5</sup> Robinson, Wilson and Ayling, *ibid.*, 1942, 64, 1469.

<sup>6</sup> Barbara J. Levien, *Thesis*, University of New Zealand, 1944.



Accordingly we have thought it advisable for the purpose of making the extrapolation of the standard potential of the cell to limit ourselves to the region below an ionic strength of 0.05. It is true that the Hückel equation:

$$-\log \gamma = \frac{A \sqrt{\mu}}{1 + B \sqrt{\mu}} - C \mu + \log (1 + 0.054 m)$$

will represent the activity coefficient of  $\text{ZnBr}_2$  up to considerably higher concentrations, provided a proper choice is made of the values of the  $B$  and  $C$  coefficients, but in view of the abnormality of the osmotic coefficient at high concentrations this agreement can only be considered fortuitous. If this restriction is made on the concentration range used, then the Bates<sup>7</sup> extrapolation function:

$$E^0 = E + k \log 4 + 3 k \log m - 3kA \sqrt{\mu} / (1 + B \sqrt{\mu}) - 3k \log (1 + 0.054 m)$$

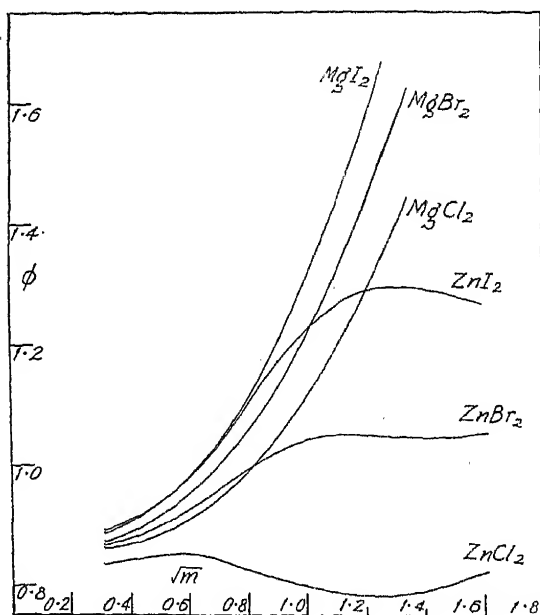
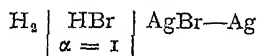


FIG. 4.  
Osmotic coefficients  
of magnesium and  
zinc halides.

gives a plot which is linear in  $m$  for any value of the effective ionic diameter from zero to  $6\text{\AA}$ ., although the choice of diameter does have a small effect on the value of the extrapolated standard potential. Thus at  $25^\circ$  the result for zero diameter is  $0.83370 V$  and for  $6\text{\AA}$ . it is  $0.83392 V$ . We have thought it best to use a value of  $5.5\text{\AA}$ . at all temperatures, *i.e.* a value slightly below that of  $6\text{\AA}$ ., used by Bates for  $\text{ZnI}_2$ . It is to be noted that as  $\text{ZnI}_2$  behaves normally up to higher molalities than  $\text{ZnBr}_2$ , Bates was able to use a wider concentration range for extrapolation and thus to determine a probable value of the ionic diameter.

The standard potentials of the cell at the five temperatures are given in Table III where we have also tabulated the standard potentials of the zinc electrode, obtained by subtracting those of the cell:



<sup>7</sup> *J. Amer. Chem. Soc.*, 1938, 60, 2983.

TABLE III.—STANDARD POTENTIALS OF THE CELL: Zn—Hg/ZnBr<sub>2</sub>/AgBr—Ag AND OF THE ZINC ELECTRODE (ON THE MOLALITY SCALE).

Temp.	$E^0(\text{ZnBr}_2)$ .	$E^0(\text{Zn})$ this work.	$E^0(\text{Zn})$ Bates.	Difference, mv.
20°	0.83684	0.76312	0.76322	-0.10
25°	0.83388	0.76260	0.76275	-0.15
30°	0.83084	0.76213	0.76226	-0.13
35°	0.82766	0.76166	0.76176	-0.10
40°	0.82430	0.76123	0.76117	+0.06

The standard potentials may be represented by :

$$E_t^0 = E_{30}^0 + a^0(t - 30) + b^0(t - 30)^2$$

where

$$E_{30}^0 = 0.83084, a^0 = -62.6 \times 10^{-6}, b^0 = -2.7 \times 10^{-8} \text{ for } E^0(\text{ZnBr}_2),$$

and

$$E_{30}^0 = 0.76212, a^0 = -9.4 \times 10^{-5}, b^0 = 0.5 \times 10^{-8} \text{ for } E^0(\text{Zn})$$

given by Owen and Foering.<sup>8</sup> These  $E^0(\text{Zn})$  values agree very satisfactorily with those of Bates,<sup>7</sup> especially in view of the fact that in comparing the two sets of  $E^0(\text{Zn})$  values four different electrolytes and four extrapolations are involved.

If a comparison be made with the corresponding results of Robinson and Stokes<sup>9</sup> for ZnCl<sub>2</sub>, it will be seen that the standard potentials of Zn derived from the chloride cells are approximately 0.2 mv. lower than those from the bromide cells. It has been shown in this paper that ZnCl<sub>2</sub> can certainly not be regarded as normally dissociated at the concentrations used by Robinson and Stokes for their extrapolation; consequently, although a discrepancy of 0.2 mv. is not large, less weight should be given to the  $E^0$  values derived from the chloride cells than to the values now obtained from the bromide cells, in the extrapolation of which results in only the most dilute solutions were used.

#### Activity Coefficients.

The stoichiometric activity coefficients at round concentrations are given in Table IV. For this calculation the e.m.f.s were interpolated

TABLE IV.—ACTIVITY COEFFICIENTS AND HEAT CONTENTS OF ZINC BROMIDE.

<i>m.</i>	$\gamma$ 20°.	$\gamma$ 25°.	$\gamma$ 25°.*	$\gamma$ 30°.	$\gamma$ 35°.	$\gamma$ 40°.	$\bar{L}_2(25^\circ)$ Cal.	$\bar{L}_2(30^\circ)$ Cal.
0.002	0.856	0.855	—	0.854	0.854	0.853	—	—
0.003	0.834	0.830	—	0.829	0.828	0.826	—	—
0.005	0.798	0.795	—	0.794	0.792	0.791	—	—
0.007	0.774	0.771	—	0.769	0.767	0.766	—	—
0.01	0.747	0.743	—	0.742	0.741	0.738	310	290
0.02	0.686	0.682	—	0.679	0.677	0.676	440	410
0.03	0.648	0.645	—	0.642	0.640	0.637	480	440
0.05	0.605	0.601	—	0.598	0.595	0.592	640	590
0.07	0.579	0.574	—	0.571	0.568	0.564	750	690
0.1	0.554	0.547	(0.547)	0.543	0.540	0.536	980	860
0.2	0.518	0.511	0.512	0.506	0.502	0.499	1190	960
0.3	0.515	0.506	0.503	0.502	0.496	0.491	1430	1380
0.5	0.525	0.515	0.513	0.504	0.493	0.481	2110	2260
0.7	0.552	0.537	0.531	0.521	0.505	0.489	3040	3350
1.0	0.582	0.559	0.558	0.535	0.513	0.488	4370	4800

\* From isopiestic data.

to these round concentrations with the aid of deviation functions similar to the one illustrated in Fig. 2 and the activity coefficients then calculated by the usual equation. It will be noted that the activity coefficient in 0.1 M. solution at 25° is found to be 0.547. The isopiestic measurements, reported previously,<sup>1</sup> were based on  $\gamma = 0.555$  from the data of Parton and Mitchell,<sup>2</sup> so that it will be necessary to reduce all the activity coefficients given in the earlier paper in the ratio 0.547/0.555 in order to conform with this new value at 0.1 M. When this is done the agreement between the e.m.f. and isopiestic values is reasonably good, as is apparent from a comparison of the two columns in Table IV for 25°. It was not thought worthwhile to carry the e.m.f. determinations into solutions more concentrated than 1 M., as an uncertainty of unpredictable magnitude and sign might be introduced by the solubility of AgBr in the electrolyte. In this region the isopiestic method should be more reliable.

#### Relative Partial Molal Heat Contents.

Values of  $\bar{L}_2$  for  $\text{ZnBr}_2$  were obtained by combining the Gibbs-Helmholtz equation with the quadratics relating e.m.f. and temperature to give:

$$\bar{L}_2 = -2F[(E_{30} - E^0_{30}) - 303.15(a - a^0) - (T^2 - 303.15^2)(b - b^0)].$$

It must be realised that a variation of 0.01 mv. per degree in the temperature coefficient of the e.m.f. involves a change of 140 cal. per mol. in  $\bar{L}_2$ ;

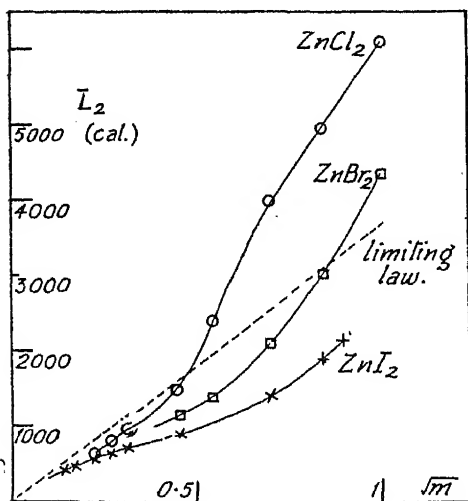


FIG. 5.—Partial molal heat contents of zinc halide solutions.

If the partial molal heat contents of  $\text{ZnCl}_2$ ,<sup>3</sup>  $\text{ZnBr}_2$  and  $\text{ZnI}_2$ <sup>7</sup> are plotted against  $\sqrt{m}$ , as in Fig. 5, an interesting contrast is obtained. At all concentrations  $\bar{L}_2$  for  $\text{ZnI}_2$  is less than the value calculated by the limiting Debye equation, although it approaches the limiting slope at concentrations less than 0.01 M. Zinc chloride follows the limiting slope more closely even up to 0.2 M. at which concentration a normal electrolyte shows wide deviation from the limiting law. At high concentrations  $\bar{L}_2$  for  $\text{ZnCl}_2$  increases rapidly and exceeds the value calculated by the limiting equation.  $\text{ZnBr}_2$  exhibits an intermediate behaviour but its abnormality at high

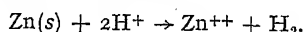
consequently the  $\bar{L}_2$  values below 0.01 M. are of the magnitude of the experimental error. In Table IV we have recorded values of  $\bar{L}_2$  to a degree of approximation consistent with the accuracy of the e.m.f. data. This has been done for two temperatures, 30° and 25°, the latter set being convenient for comparison with other data whilst the former corresponds to the temperature at which  $\bar{L}_2$  is most accurately evaluated, *i.e.* the temperature in the middle of the range over which the e.m.f.s were measured.

We do not believe that the accuracy of the second differential with respect to temperature over this short range justifies the tabulation of heat capacity data.

concentrations is evident; thus the  $\bar{L}_2$  curves are consistent with the osmotic coefficient curves in that they indicate an unusual behaviour, most prominent in the chloride and least in the iodide.

### The Entropy of the Zinc Ion.

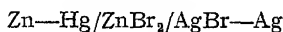
From the equation given in Table III for the standard potential of the zinc electrode we may find, by differentiation with respect to the temperature, the entropy change of the reaction:



The value obtained is  $\Delta S^\circ = -4.57$  cal./degree/mol. at  $25^\circ$  compared with  $-4.7_8$  derivable in the same way from the data of Robinson and Stokes<sup>9</sup> for  $\text{ZnCl}_2$  and  $-4.6_1$  obtained by Bates<sup>10</sup> from his work on  $\text{ZnI}_2$ . Latimer, Pitzer and Smith<sup>11</sup> used  $-4.5$  entropy units. Using the entropy values of 31.23 and 9.95 for hydrogen and zinc metal respectively,<sup>12</sup> the entropy of the zinc ion would be  $-25.9$  entropy units, in agreement with the value given by Bates and only 0.2 units lower than that given by Latimer, Pitzer and Smith. This difference is scarcely significant in view of the probable error of the final result but the value of  $-25.9$  may be preferred.

### Summary.

E.m.f. measurements have been made of the cell:



at  $5^\circ$  intervals between  $20^\circ$  and  $40^\circ$  and at 16 concentrations between 0.002 and 1 M. The standard potentials of the cell have been derived and also those of the zinc electrode, the latter being in good agreement with other values obtained from measurements on  $\text{ZnI}_2$ . Considerations are advanced to show that  $\text{ZnCl}_2$  cells are not the most suitable for the extrapolation of the standard potentials but that  $\text{ZnBr}_2$  cells are satisfactory at low concentrations.

Activity coefficients of  $\text{ZnBr}_2$  have been computed and found to be in reasonable agreement with those deduced from isopiestic vapour pressure measurements.

The partial molal heat contents at  $25^\circ$  and  $30^\circ$  have been computed and the e.m.f. data have been used to substantiate one stage in the calculation of the entropy of the zinc ion.

Auckland University College,  
New Zealand.

<sup>9</sup> Robinson and Stokes, *Trans. Faraday Soc.*, 1940, **36**, 740.

<sup>10</sup> *J. Amer. Chem. Soc.*, 1939, **61**, 522.

<sup>11</sup> *Ibid.*, 1938, **60**, 1829.

<sup>12</sup> Kelley, *Bureau of Mines, Bull.* 394, U.S. Government Printing Office, Washington, D.C., 1936.

# A REVIEW OF SOME OF THE RECORDED OBSERVATIONS INVOLVING ASYMMETRIC TRANSFORMATIONS.

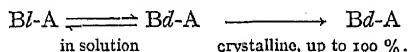
BY MARGARET M. JAMISON.

Received 26th January, 1945.

Most of the experimental work to be described here is familiar to all chemists as furnishing answers to the question "Is the compound X optically active or not?". The object of the present discussion is to correlate the answers to the question "What happens to X as part of a diastereoisomeric pair when it is present in solution or crystallises out from it?", X being optically labile. It must constantly be borne in mind that the authors quoted were usually concerned primarily with the first question, and that the evidence available for answering the second may very well be slight without in any way invalidating the first or affording any ground for criticism.

## (1) Second-Order Asymmetric Transformations.

If a pair of diastereoisomers having one optically unstable component is present in saturated solution and one form begins to crystallise, the whole of the product may then appear as the single crystalline diastereoisomer, as long as the rate of interconversion of the two forms is greater than the rate of crystallisation. For example, a salt in which the basic component B is optically stable and the acid A optically unstable, and B*z*-A less soluble than B*l*-A, behaves thus



In order to recognise this effect unequivocally it is necessary to remove the stably asymmetric agent B and demonstrate the activity which has been induced in A: factors such as the optical instability of A in absence of B or the chemical character of the entity BA may preclude this incontrovertible proof, and less conclusive though often persuasive stereochemical arguments may have to be called in, *e.g.* the mutarotation of the deposited material in another solvent and consideration of its specific rotation compared with that of salts of B with inactive acids, coupled with effectively complete precipitation of BA as a uniform substance.

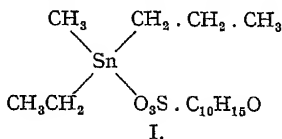
It will be seen from the following examples that this process can take place with diastereoisomers which are ionised in solution and therefore have no reality until the point of crystallisation is reached, as well as with those which because of suppression of dissociation for one reason or another are always entities containing two centres of asymmetry, one labile and the other not.

## Examples of Proved Asymmetric Transformation of the Second Order.

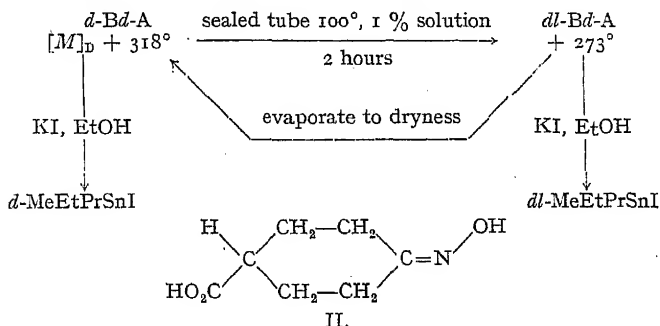
Pope and Peachey<sup>1</sup> crystallised methyl-ethyl-*n*-propyltin *d*-camphorsulphonate (I) from water, obtaining only one salt,  $[M]_D + 95^\circ$  in water (subtracting the value for the camphorsulphonate ion,  $[M]_D$  for the basic radical is about  $+45^\circ$ ); treatment of this salt with potassium iodide gave *d*-methylethyl-*n*-propyltin iodide. The inversion presumably in-

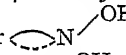
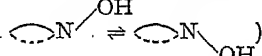
<sup>1</sup> *Proc. Chem. Soc.*, 1900, 16, 42.

volves a flat tin cation. In their second case of asymmetric transformation, that of methylethyl-*n*-propyltin *d*- $\alpha$ -bromocamphorsulphonate, which crystallised from acetone in fractions of constant specific rotation ( $[M]_D + 318^\circ$  in water at ordinary temperature), the same authors carried out an interesting demonstration of the nature of the process.<sup>2</sup> Allowing  $+270^\circ$  for the molecular rotation of the acid radicle they assumed that they had the salt *d*-base *d*-acid,  $[M]_D + 48^\circ$  being attributed to the *d*-base part.



On heating a 1 % aqueous solution of the salt for 2 hours at  $100^\circ$  in a sealed tube the  $[M]_D$  fell to  $+273^\circ$  and the solution presumably then contained the *d*-bromocamphorsulphonate of the *dl*-base. On evaporating to dryness, the product had  $[M]_D + 315^\circ$  and had obviously undergone reconversion into *d*-base *d*-acid. Decomposition of this salt with potassium iodide gave a dextro-rotatory iodide, while decomposition of the supposed partial racemate gave inactive iodide.



A solution of quinine and oximinocyclohexane-4-carboxylic acid (II) (owing its potential optical activity to the non-planar  group and its optical instability to the ease of the conversion )

in 30 parts of water gave an 80 % yield of the quinine *l*-acid salt ( $+2\frac{1}{2}H_2O$ );<sup>3</sup> the authors, Mills and Bain, observed that the salt crystallised from an inactive mother liquor and appended the classic explanation: "of the two diastereoisomeric quinine salts, that of the *l*-acid must be the less soluble in water, and thus crystallises first from an aqueous solution containing equal quantities of the two salts. The excess of quinine *d*-acid salt thereby left in solution, however, racemises very rapidly, so that in spite of the removal of the quinine *l*-acid salt, an approximate equality is maintained between the quantities of the two salts in the solution." Decomposition of the quinine *l*-salt with sodium hydroxide gave a sodium salt  $[M]_D - 91^\circ$ . A similar transformation was effected using morphine in hot ethyl alcohol and gave the salt morphine *d*-acid, which yielded dextro-rotatory ammonium salts on treatment with ammonium hydroxide.

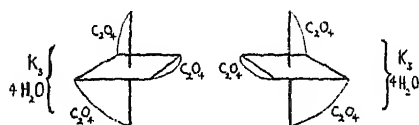
From a hot alcoholic solution of potassium dihydrogen trioxalochromate and two molecular proportions of strychnine Werner<sup>4</sup> obtained a salt potassium distrychnine trioxalochromate ( $+4H_2O$ ) (III) having a specific rotation  $[\alpha]_D + 430^\circ$  in water; further crops of crystals from the mother liquor were also dextro-rotatory. The rotation with respect to

<sup>2</sup> *Proc. Chem. Soc.*, 1900, 16, 116.

<sup>3</sup> *J. Chem. Soc.*, 1910, 97, 1866.

<sup>4</sup> *Berichte*, 1912, 45, 3061.

the trioxalochromiate ion mutarotated almost to zero in  $1\frac{1}{4}$  hours, and Werner proved that he was handling the *d*-base *d*-acid by converting it

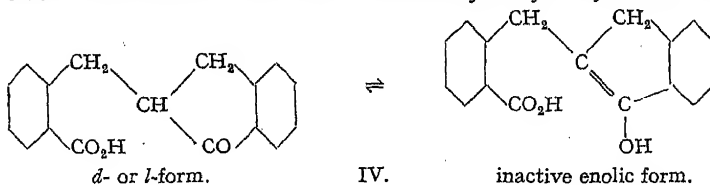


III.

into *d*-tripotassium trioxalochromiate. Furthermore, when potassium distrychnine trioxalochromiate was dissolved in hot water in dilute solution, crystals of tristrychnine *l*-trioxalochromiate ( $+4\text{H}_2\text{O}$ ) separated  $[\alpha]_D^{20} - 300^\circ$  in water, additional fractions being *l*-rotatory also:

Werner noted that the mother liquor from which crystallisation was taking place was "practically inactive." This would not be expected if *resolution* was taking place. Decomposition of the *l*-tristrychnine salt with potassium iodide gave the *l*-rotatory tripotassium trioxalochromiate.

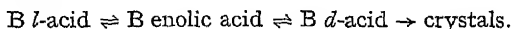
Leuchs and Wutke<sup>5</sup> found that 2-*o*-carboxybenzyl-*r*-hydrindone (IV)

*d*- or *l*-form.

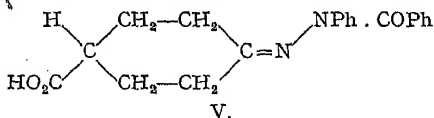
IV.

inactive enolic form.

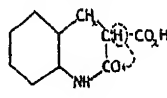
and one molecule of brucine crystallise from acetone to give a 94 % yield of a salt which on decomposition with sulphuric acid leaves a dextro-rotatory acid ( $[\alpha]_D^{20} + 64^\circ$ , mutarotating in chloroform). They assume that the optically inactive enolic form is the intermediate between the two active ketonic forms and that the asymmetric transformation is accomplished thus:—



Following up their demonstration of optical activity in the oxime, Mills and Bain<sup>6</sup> found that the quinine salt of the *N*-benzoylphenylhydrazone of cyclohexanone-4-carboxylic acid (V) crystallises from a mixture of methyl alcohol and water to give the *l*-quinine *d*-salt (decomposition with the appropriate alkali gives the sodium, ammonium or potassium salt of the *d*-acid). Unfortunately, the percentage yield on crystallisation is not recorded, and it is therefore not possible to state



V.



VI.

categorically that the separation is not, on this evidence, a *resolution*; however, the authors record that concentration of the mother liquor yielded nothing but the *d*-acid salt, which makes it appear likely that transformation has taken place. The semicarbazone of cyclohexanone-4-carboxylic acid was "activated" in the same way by crystallisation of its morphine salt from aqueous methyl alcohol, the salt obtained giving a dextro-rotatory ammonium salt on treatment with ammonium hydroxide.

A neat piece of work by Leuchs<sup>7</sup> demonstrates second-order transformation with formal simplicity. 2.4 g. of hydrocarbostyryl-3-carboxylic acid (VI) and 4.07 g. of anhydrous quinidine were dissolved in 40 c.c. of methyl alcohol: three crystalline fractions were collected (amounting in all to 6.2 g. of a salt containing two molecules of water of crystallisation). Each fraction was decomposed by hydrochloric acid at  $-10^\circ$

<sup>5</sup> *Berichte*, 1913, 46, 2420.

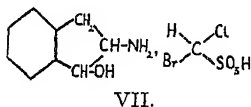
<sup>6</sup> *J. Chem. Soc.*, 1914, 105, 64.

<sup>7</sup> *Berichte*, 1921, 54, 830.

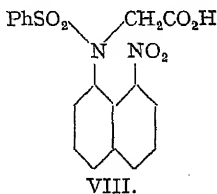
and the acid obtained dissolved in 5.5 % solution in glacial acetic acid and its racemisation watched at 18°. The specific rotations of the samples are given in the accompanying table. Leuchs referred the optical instability to the existence of the inactive enolic form as an intermediate.

Fraction.	Weight.	$\alpha_D$ .	$[\alpha]_D^{18^\circ}$ .
1	4 g.	+ 1.08°	+ 56.4°
2	1.5 g.	+ 1.09°	—
3	0.7 g.	+ 1.04°	—

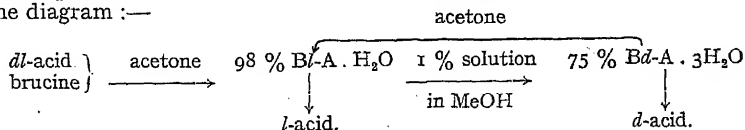
When the *l*-hydroxyhydrindamine salt of *dl*-chlorobromomethane sulphonic acid (VII),  $M[\alpha]_D$  in methyl alcohol  $-72^\circ$ , was dissolved in acetone which contained a little methyl alcohol a salt was deposited having  $M[\alpha]_D$  in methyl alcohol  $-173^\circ$  initially but exhibiting mutarotation to  $-72^\circ$  on keeping.<sup>8</sup> Read and McMath concluded that the crystallisation had resulted in asymmetric transformation to the *l*-base *l*-acid salt. They also carried out the preparation of the mirror-image salt *d*-base *d*-acid, using *d*-hydroxyhydrindamine under similar conditions. Attempts to remove the optically active base or to replace it with benzidine or  $\beta$ -naphthylamine gave optically inactive products: but by mixing equal quantities of the salts *d*-base *d*-acid and *l*-base *dl*-acid, in which the rotation of the basic parts cancel each other, they obtained a residual  $[M]_D$  of  $+49^\circ$  which they attributed to the positive acid. In a later



paper<sup>9</sup> these same authors describe interesting behaviour of chlorobromo-acetic acid and *l*-hydroxyhydrindamine in their crystallisation as salts from chloroform containing a little methyl alcohol. Slow deposition from a cold solution gave *l*-base *dl*-acid,  $[M]_D$  in chloroform containing a little methyl alcohol  $-50^\circ$ , while rapid cooling of a hot solution to supersaturation gave *l*-base *d*-acid in 75 % yield,  $[M]_D$  approximately  $0^\circ$ , changing to  $-50^\circ$  on warming and keeping. The mother liquor from this crystallisation deposits *l*-base *dl*-acid. Use of *d*-hydroxyhydrindamine enabled the *d*-base *l*-acid and *d*-base *dl*-acid to be prepared: an attempt to remove the optical activity to be due to the acid and to find its rotation by taking equal weights of *d*-base *l*-acid and *l*-base *dl*-acid in chloroform containing methyl alcohol resulted in a fleeting observation of  $\alpha_D = 0.1^\circ$ , 1.5 mins. after wetting with solvent. It is therefore uncertain whether this is a true asymmetric transformation or not.



Mills and Elliott<sup>10</sup> extended the scope of the phenomenon when they found one substance, the brucine salt of N-benzenesulphonyl-8-nitro-1-naphthylglycine (VIII), which underwent asymmetric transformation of the labile acid part in opposite directions in two different solvents: each of the diastereoisomeric salts was decomposed to give an active acid, so that the result was in effect as if a resolution had been performed. The first asymmetric transformation, to base *l*-acid,  $H_2O$  from acetone, took place almost quantitatively, while that from methyl alcohol gave 75 % of the possible base *d*-acid,  $3H_2O$ . The sequence of changes is clear from the diagram:—



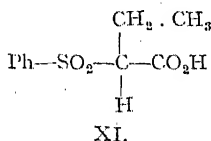
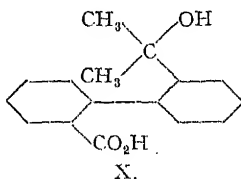
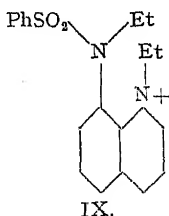
<sup>8</sup> Read and McMath, *J. Chem. Soc.*, 1925, 127, 1572    <sup>9</sup> *Ibid.*, 1926, 2183.

<sup>10</sup> *Ibid.*, 1928, 1291.



The cause of activity in this molecule is the restriction of the rotation of the substituted amino group by the nitro group, resulting in asymmetry.

Using another compound owing its potential activity to restriction of rotation, in this case a base, Mills and Breckenridge<sup>11</sup> record similar optical behaviour. 8-Benzenesulphonethylamino-1-ethylquinolinium *d*- $\alpha$ -bromo-camphor- $\pi$ -sulphonate (IX) crystallised slowly from a mixture of ethyl acetate and acetone giving the salt *d*-base *d*-acid, 2H<sub>2</sub>O which showed mutarotation in the *l*ævo direction in water, chloroform and ethyl alcohol; on shaking a chloroform solution of the salt *before* mutarotation with aqueous potassium iodide the *d*-quinolinium iodide was obtained. Unfortunately, the percentage weight of salt crystallising is not recorded, so that there is nothing formally to differentiate the crystallisation from a resolution; however, it is unlikely that a substance showing optical instability in three such diverse solvents as chloroform, water and alcohol

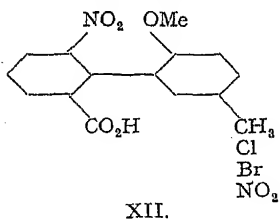


would be stable enough for resolution in ethyl acetate solution. Using the *d*- $\alpha$ -bromocamphorsulphonate in a mixture of methyl alcohol and ethyl acetate the *l*-base *d*-acid was obtained and gave a *l*ævo rotatory iodide on decomposition.

Corbellini and Angeletti<sup>12</sup> reported that 2'-( $\alpha$ -hydroxyisopropyl) diphenyl-2-carboxylic acid (X) and brucine formed a salt which crystallised from ethyl alcohol as brucine *l*-acid in 83 % yield, a figure which was raised to 97.6 % on repetition by Jamison and Turner<sup>13</sup> who also describe an analogous transformation from chloroform solution by evaporating to dryness on a boiling water bath with continuous stirring to accelerate crystallisation. Decomposition with mineral acids gave the *l*-rotatory acid.

A similarly complete conversion has been observed of the brucine salt of  $\alpha$ -phenylsulphonebutyric acid (XI), which crystallises from acetone as the salt brucine *l*-acid; this salt is decomposed by hydrochloric acid to give the *l*-rotatory acid. A tautomeric mechanism is postulated for the optical inversion.<sup>14</sup>

Work on relative optical stability within various series has led to the discovery of several examples of second-order asymmetric transformation among substituted diphenyl derivatives. Yuan and Adams<sup>15</sup> have a good case, for example, in the behaviour of brucine *dl*-2 : 5-dimethoxy-2'-nitro-6'-carboxydiphenyl which crystallises from water in three fractions amounting in all to 90 % of the theory, and all having the same specific rotation: decomposition with ice-cold hydrochloric acid gave the *l*-acid. The cinchonidine salt behaved similarly. In a later paper<sup>16</sup> the same authors describe equally conclusive evidence for the asymmetric second-order transformation of 2-nitro-6-carboxy-2'-methoxy-5'-methyldiphenyl (XII) and the series with



<sup>11</sup> J. Chem. Soc., 1932, 2209.

<sup>12</sup> Atti. R. Accad. Lincei, 1932, 15, 968.

<sup>13</sup> Jamison and Turner, J. Chem. Soc., 1942, 437.

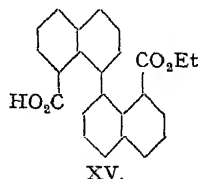
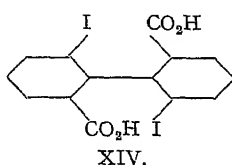
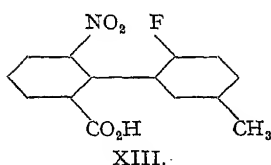
<sup>14</sup> J. Amer. Chem. Soc., 1932, 54, 4410.

<sup>15</sup> Ibid., 1932, 54, 2966.

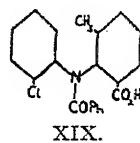
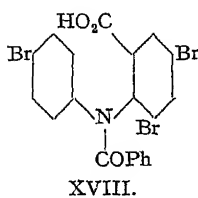
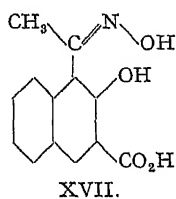
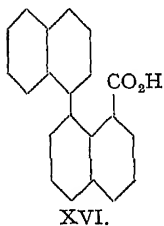
<sup>16</sup> Ibid., 1932, 54, 4434.

Cl, Br and  $\text{NO}_2$  in the 5' position by brucine in alcohol containing varying amounts of water. Yuan and Adams among others, use the word "resolution" to describe this process: this would appear to be a misuse of the term, which has hitherto referred to the separation of a racemic mixture into its stereoisomeric constituents, not conversion of it all into one form.

Stoughton and Adams<sup>17</sup> record the dextro asymmetric transformation of 2-nitro-6-carboxy-2'-fluoro-5'-methyldiphenyl (XIII) with brucine from ethyl alcoholic solution: quinine effected the same conversion. Searle and Adams<sup>18</sup> found that the dibrucine salt of 2:2'-diiodo-6:6'-dicarboxydiphenyl (XIV) crystallised from 95 % ethyl alcohol in three identical



fractions totalling 83 % of the possible quantity, which could be shown by decomposition with 6 N. hydrochloric acid and separation of the *l*-acid to be the single diastereoisomer. It is noteworthy that crystallisation from methyl alcohol did not favour second-order transformation but gave a mixture of crystals of diastereoisomers which could be separated by hand picking. Working in the dinaphthyl series Meisenheimer and Beisswenger<sup>19</sup> found that ethyl hydrogen 1:1'-dinaphthyl-8:8'-dicarboxylate (XV) underwent theoretical conversion into the brucine *l*-acid,  $3\text{H}_2\text{O}$  salt from ethyl acetate containing a little methyl alcohol: decomposition with dilute mineral acid led to the separation of the *l*-acid. A second acid, 1:1'-dinaphthyl-8-carboxylic acid (XVI), and brucine dissolved in ethyl acetate gave a solution which could be made to deposit base *l*-acid.  $\text{H}_2\text{O}$  or base *d*-acid.  $\text{H}_2\text{O}$  according to which of these was used to inoculate it. The same authors, with Theilacker,<sup>20</sup> describe similar activation by alkaloids of  $\beta$ -(2-hydroxy-3-carboxy-1-naphthyl) methyl ketoxime (XVII).



N-benzoyl-2:4:4'-tribromo-6-carboxydiphenylamine (XVIII) when dissolved in acetone containing 1 m. of cinchonidine deposited 1 m. of cinchonidine *d*-salt in 94 % yield: deposition of crystals could be accelerated by boiling the solution without loss of optical purity in the product. Treatment with pyridine followed by dilute HCl gave the *d*-acid.<sup>21</sup> An almost quantitative yield of brucine *l*-N-benzoyl-2'-chloro-2-methyl-6-carboxydiphenylamine (XIX) is deposited from a salt of the racemic acid and brucine by slow crystallisation from a mixture of ethyl alcohol and ether. Decomposition with formic acid and ice-cold hydrochloric acid gave the *l*-acid.<sup>22</sup>

<sup>17</sup> *J. Amer. Chem. Soc.*, 1932, **54**, 4426.

<sup>18</sup> *Ibid.*, 1933, **55**, 1649.

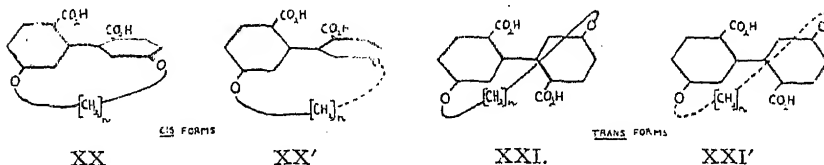
<sup>19</sup> *Berichte*, 1932, **65**, 32.

<sup>20</sup> *Annalen*, 1932, **495**, 249.

<sup>21</sup> Jamison and Turner, *J. Chem. Soc.*, 1938, 1646.

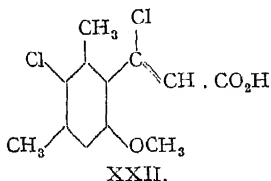
<sup>22</sup> *Idem.*, *J. Chem. Soc.*, 1940, 264.

Adams and Kornblum<sup>23</sup> investigated the effect of chain length in the bridge of the compounds (XX, XXI) on their optical stability, and in the course of the work describe two cases of what now appears to be second-order asymmetric transformation.



When  $n$  is large enough, the four forms above, all optically active, should be present together at equilibrium in solution, and a suitable alkaloid and solvent should be capable of bringing out one of the forms as a crystalline salt. The authors found that when  $n = 10$ , brucine in methyl alcohol gave a 77 % yield of a dibrucine salt in the first fraction, and a further quantity of the same salt from the mother liquor; decomposition with

hydrochloric acid gave a dextro rotatory acid. In the case where  $n = 8$  cinchonine acts as a transforming agent in ethyl alcohol to give three fractions (representing 91 % of the theoretical quantity) all with the same specific rotation and each giving a *l*-acid on decomposition with hydrochloric acid.



Adams and Gross<sup>24</sup> demonstrating optical activity in a substituted benzene derivative found that the quinine salt of  $\beta$ -chloro- $\beta$ -(2-methoxy-4, 6-dimethyl-5-chlorophenyl) acrylic acid (XXII) was deposited from ethyl acetate in a series of fractions all of which had the same specific rotation and yielded the dextro acid on treatment with hydrochloric acid.

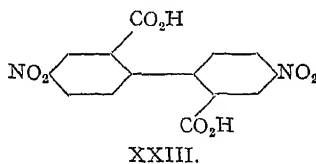
### Examples of Inferred Second-Order Asymmetric Transformation in Absence of Direct Observation of Optical Activity in the Separate Activated Substance.

From the study of cases of proved asymmetric transformation listed above it appears that the secondary characteristics (*i.e.* other than the removal of the transforming agent to leave a detectably asymmetrically activated body) are:—

1. Crystallisation produces *one* salt (*i.e.* all fractions identical) from a solution which originally contained the two types, for example, *d*-base *l*-acid and *d*-base *d*-acid.

2. This salt when dissolved in another solvent may

(a) mutarotate, or  
(b) deposit another form, or  
(c) show a rotation which is strikingly different from that of the resolving agent: this latter kind of evidence can only be accepted with great reserve.



4 : 4'-Dinitrodiphenic acid (XXIII) (1 g., 1 m.) and quinine hydrate (2.3 g., 2 m.) dissolved in 96 % ethyl alcohol deposited the following fractions: (1) 1.75 g. salt, m.p. 207-208°,  $[\alpha]_D^{20} + 108.4^\circ$  in  $\text{CHCl}_3$ ; (2) 0.8 g. salt, m.p. 207-208°,  $[\alpha]_D^{22}$  in  $\text{CHCl}_3 + 110.3^\circ$ . Removal of the base from these fractions gave an optically inactive acid; nevertheless,

<sup>23</sup> J. Amer. Chem. Soc., 1941, 63, 188.

<sup>24</sup> *Ibid.*, 1942, 64, 1786.

Kuhn and Albrecht<sup>25</sup> assert that this is an asymmetric transformation for the following reasons:—

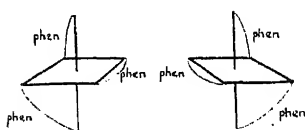
(a) the product, all the same substance, represents 80 % of the possible yield,

(b) quinine *m*-nitrobenzoate and quinine phthalate have the specific rotations  $-163.5^\circ$  and  $-168.2^\circ$  in the same circumstances, pointing to the above being the salt of a dextro acid (but see Kharasch, Senior, Stanger and Chenicek,<sup>25, 26</sup> on the anomalous rotation of quinine salts; this piece of evidence would appear from their work to be anything but conclusive), and

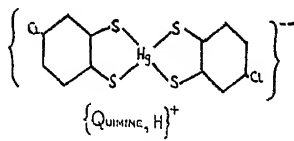
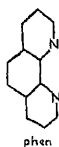
(c) the acid falls into a series with two, one and no nitro-groups in the *o*-position in diphenic acid:—

6 : 6'-dinitrodiphenic acid	resolvable with brucine	acid optically stable.
4 : 6'-dinitrodiphenic acid	resolvable with quinine	acid racemises.
4 : 4'-dinitrodiphenic acid	asymmetric transformation with quinine	acid too unstable to see active.

Pfeiffer and Quehl<sup>27</sup> claim to have observed optical activation in the field of octahedral asymmetry. Zinc  $\beta$ -camphorsulphonate with 3.5 M. of phenanthroline (XXIV) crystallised from water to give an 80 % yield:



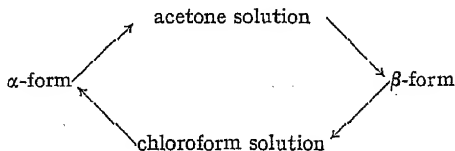
XXIV.



XXV.

of a salt  $[\text{Zn}(\text{phen})_3]\text{O} \cdot \text{SO}_2\text{C}_{10}\text{H}_{16}\text{O} \cdot 7\text{H}_2\text{O}$ . After purification by fractionation from acetone and water a 1/1000 M. in 25 c.c. of water had a rotation  $\alpha_D$  of  $0.0^\circ$  while for the zinc camphorsulphonate alone it was  $+0.93^\circ$ . Working in the reverse order, a solution of 1/1000 M. zinc  $\beta$ -camphorsulphonate in 25 c.c. of water,  $\alpha +0.92^\circ$ , was treated with 3 M. of phenanthroline, when  $\alpha$  fell immediately to  $+0.09^\circ$ , ammonia, pyridine or ethylenediamine showing no such effect. Pfeiffer and Quehl attribute this change in rotation to the preferential formation of the *l*- $[\text{Zn}(\text{phen})_3]^{++}$  complex in presence of the camphorsulphonate ion, although conversion into the corresponding dibromide or dinitrate resulted in optically inactive products.

Mills and Clark<sup>28</sup> prepared the diquinine salt of a complex anion of mercury with 4-chlorobenzene-1:2-dithiol (XXV). If the mercury valencies are tetrahedrally disposed the complex can exist in two mirror image forms. Crystallisation produced two distinct forms, styled  $\alpha$  and  $\beta$ . The  $\alpha$ -form dissolved in acetone began to deposit the  $\beta$ -form within a few minutes: the  $\beta$ -form dissolved in chloroform deposited the  $\alpha$ . Both forms come out with solvent of crystallisation. Mutarotation of the freshly dissolved substances was looked for as low as  $-35^\circ$  but was not detected. It would appear that there are three possible explanations of this behaviour:



<sup>25</sup> *Annalen*, 1927, 455, 272.

<sup>27</sup> *Berichte*, 1931, 64, 2667.

<sup>26</sup> *J. Amer. Chem. Soc.*, 1934, 56, 1646.

<sup>28</sup> *J. Chem. Soc.*, 1936, 175.

(a) dimorphism of a stable mercury complex salt, involving crystallisation with the solvent, an insufficient explanation since the two forms after loss of solvent retain their difference in solubility;

(b) *cis* and *trans* forms of a flat mercury cation, also inadequate, as dimorphism could then be shown by metallic salts;

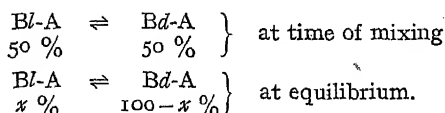
(c) second-order asymmetric transformation between diastereoisomers with a tetrahedral mercury cation.

Dismissing (a) and (b), and proving that internal dissociation does not occur, the authors favour the last explanation.

## (2) First-Order Asymmetric Transformations.

Kuhn<sup>28, 29</sup> called the effect which he and Albrecht observed in the case of the quinine salt of 4:4'-dinitrodiphenic acid an *asymmetrische Umlagerung erster Art*—referring to an optical activation which ceases to exist when the transforming agent is removed. This definition seemed satisfactory at first but further consideration reveals that it is difficult to apply, for "ceases to exist" is a criterion which may depend on the standard of laboratory technique which is used for the detection of the unstable optical activity. The use of an altered definition was therefore suggested,<sup>21, 22</sup> and clearly set out in 1942.<sup>13</sup>

Suppose, to take a representative example, a configuratively unstable optically active acid exists in solution: it consists of equal quantities of *l*-acid and *d*-acid. On the addition of one form of an optically active, optically stable base there is immediate formation of the diastereoisomers *Bl*-A and *Bd*-A in equal quantities; these have different optical stabilities in solution and a change begins to take place until the equilibrium is reached.



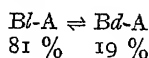
The setting up of this equilibrium is the first-order transformation.

The primary essential for the operation of the process is the *reality of diastereoisomers in solution*, and therefore it would not be expected to take place in the case of salts in ionising solvents such as water nor, for example, in the diastereoisomeric *d*- and *l*-8-benzenesulphonylethylamino-1-ethylquinolinium-*d*-bromo-camphor- $\pi$ -sulphonates in  $\text{CHCl}_3$  prepared by Mills and Breckenridge.<sup>11</sup> This is the salt of a quaternary ammonium base and therefore must be ionised in solution even in chloroform: it did not show first-order transformation, and evidence for its absence is afforded by calculating from the figures given by the authors the extent of mutarotation of the *l*-base *d*-acid and *d*-base *d*-acid in chloroform. These values are  $[\alpha]_{\text{D}}^{25} 108.4^\circ$  and  $106.7^\circ$  respectively: they represent equality within the limits of experimental error on substances that show mutarotation, and demonstrate that there is no differentiation detectable between the diastereoisomers in solution: in fact they do not exist until crystallisation takes place.

The first milestone in the study of optical activation (first-order transformation) in solution is generally considered to be the work of Read and McMath<sup>8</sup> on *l*-hydroxyhydrindamine chlorobromomethanesulphonate. The salt *l*-base *l*-acid in anhydrous acetone (purified through the bisulphite compound) had  $[M]_{\text{D}} - 256^\circ$  three minutes after wetting with solvent, mutarotating to  $-187^\circ$  in less than an hour. The salt *l*-base *d*-acid under the same conditions had an initial  $[M]_{\text{D}} - 71^\circ$  changing to  $-187^\circ$  in the same time (see Fig. 1). Assuming proportionality between rotation

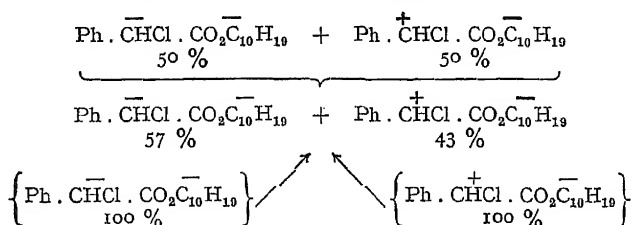
<sup>29</sup> *Berichte*, 1932, 65, 49.

and concentration and no dissociation of the salts, the authors calculated the equilibrium composition to be



They were not able to carry out the highly desirable experiment of removing the optically active base and demonstrating directly the excess of *d*-acid at equilibrium.

Shortly before this work was done, McKenzie and Smith<sup>30</sup> had made experiments on the rotation of *l*-menthyl esters of phenylbromoacetic and phenylchloroacetic acids in ethyl alcohol in presence of a very small concentration of alcoholic potash. The results, in those cases which are free from complicating factors, demonstrate first-order transformation from all three possible starting points, the *d*-acid *l*-ester, the *l*-acid *l*-ester and the *dl*-acid *l*-ester.<sup>31</sup> For example, changes in rotation make it clear that the following scheme is operable in *l*-menthyl phenylchloroacetate :—



The most striking effect, mutarotation of a *dl*-mixture of esters in alcohol on adding one drop of alcoholic potash has been shown to take place with the related substances *l*-menthyl *dl*-phenylbromoacetate, *l*-menthyl *dl*-phenylchloroacetate, *l*-menthyl *dl*-mandelate and amygdalin<sup>32</sup> where the transforming agent is the gentio-biose residue. The properties of the diastereoisomeric pairs of esters, their unequal rates of saponification in particular, and the optical instability of the acids means that removal of the activating *l*-menthyl residue to leave the acid in a state which would be reliably indicative of its equilibrated optical composition in solution in the form of the ester is not possible.

McKenzie and Smith say that "the velocity of the catalysis is greater with the *l*-menthyl *d*-phenylchloroacetate than with its diastereoisomeride." They arrived at this conclusion by calculating the percentages of original ester left after certain lengths of time in each case, a calculation which neglects the fact that the system is moving towards an equilibrium composition which is not that of the racemate. However, they publish their actual readings for change of rotation with time in the *d*-*l*- and *l*-*l*-esters, and from these data<sup>30</sup> rate constants for approach to equilibrium can be

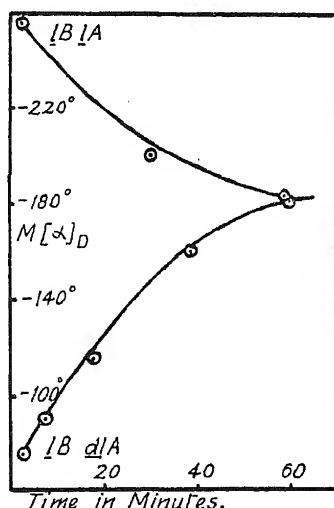


FIG. 1.

<sup>30</sup> *J. Chem. Soc.*, 1924, 125, 1582; see also Ritchie, *Asymmetric Synthesis and Asymmetric Induction*, 1933, p. 83.

<sup>31</sup> *Berichte*, 1925, 58, 894.

<sup>32</sup> Smith, *ibid.*, 1931, 64, 1115.

calculated which are in as good agreement as might be expected from velocity measurements made without temperature control, and with regard to the possible side reactions; in any event, the evidence is not such as to justify calling the rates different. The authors were prepared to find that there is a difference in the rates of the catalysed reactions of the diastereoisomers, but they failed to see, as did many other workers about this time in the same field, that the relevant "reaction" is *partial inversion* and not partial racemisation. The nature of their material and the fact that the activated group could not be isolated without isomeric change made this work of McKenzie and Smith unsuitable for the inception of a general theory: with the theory established, their experimental work falls into place and lends it convincing support.

Kuhn and Albrecht<sup>25</sup> went so far as to presume an optical activation in solution without seeing any mutarotation in the case of 4:4'-dinitrodiphenic acid and quinine in alcoholic solution, entirely on account of a large difference of rotation, carrying it over to the opposite sign, between the quinine and the salt. Lesslie and Turner,<sup>26</sup> observed similar effects in diphenic acid itself with no less than six alkaloids. Since the work of Kharasch, Senior, Stanger and Chenicek,<sup>20</sup> these authors, together with Winton,<sup>24</sup> have reconsidered the results which led them to believe that quinine diphenate mutarotated at ordinary temperatures as a consequence of optical activation, and shown that the optical stability is not of this order but a much lower one and is only just perceptible at  $-30^{\circ}$ .

Mills and Elliott were the first to prove by isolation of the activated substance in its optically active form that the mutarotation observed in an optical activation was due to the production of one diastereoisomer in excess over the other.<sup>10</sup> Such proof is very desirable, for mutarotation might in any one case be due to several possible things—slowness of salt formation, solvation with change of rotation, change of temperature on solution, etc. They took 0.183 g. of their N-benzenesulphonyl-8-nitro-1-naphthylglycine in 25 c.c. of chloroform, and 0.221 g. (1.18 m.) of brucine in the same volume of chloroform and mixed the solutions.  $\alpha_{5461}$  changed from  $-0.78^{\circ}$  to  $-0.22^{\circ}$  ( $l = 4$ ) at a temperature which rose from  $0.7^{\circ}$  to  $1.5^{\circ}$  during the experiment. That this change was due to the establishment of excess of the *l*-base *d*-acid over the diastereoisomeric form was proved by taking a solution of 50 c.c. of chloroform containing the same weight of *dl*-acid and 0.211 g. of brucine, leaving it to stand for three hours and then extracting it with ice-cold dilute sulphuric acid adding a little acetone to keep the acid in solution. The chloroform-acetone solution was dextro-rotatory, mutarotating almost to zero at  $1.2^{\circ}$ .

Several of the observations of Pfeiffer and Quehl<sup>27, 28</sup> have been claimed as first-order transformations, although in no case is there any proof of the reality of the activation. Solutions of zinc  $\beta$ -camphorsulphonate, zinc  $\alpha$ -bromo- $\pi$ -camphorsulphonate and zinc quinate change their rotations by very considerable amounts when (optically inactive)  $\alpha$ -phenanthroline or  $\alpha$ : $\alpha'$ -dipyridyl is added; the authors attribute this to the preferential formation of one of the two possible mirror-image zinc octahedral complexes. When it is considered that the salt  $[\text{Zn}(\text{phen})_2] \text{X}_2$  must be completely ionised in solution, *i.e.*, the complex to be activated is entirely separated from the transforming agent, this seems to be a most striking result. But if their explanation is correct, a more remarkable example is the following: to an aqueous solution of cinchonine hydrochloride and zinc sulphate having a rotation of  $+5.29^{\circ}$ , 3 m. of  $\alpha$ -phenanthroline was added. The rotation immediately became  $-1.89^{\circ}$  and changed on standing to  $-2.46^{\circ}$ . A similar observation was made using strychnine sulphate in place of the cinchonine hydrochloride, including the final mutarotation. If this really is a case of asymmetric transforma-

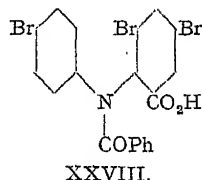
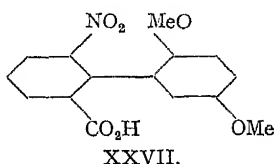
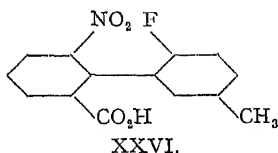
<sup>23</sup> *J. Chem. Soc.*, 1934, 347.

<sup>25</sup> *Berichte*, 1932, 65, 560; 1933, 66, 415.

<sup>26</sup> *Ibid.*, 1941, 257.

tion, it is unique that the labile asymmetric *cation* is being influenced by another *cation* which is presumably in no way attached to it. Removal of the cinchonine by precipitation with alkali left an optically inactive zinc salt. An alternative explanation in these cases is that the zinc in solution is originally combined with the alkaloid which is progressively displaced by the phenanthroline, accompanied by mutarotation. There are several other examples of this kind in the papers of Pfeiffer and his co-workers.

It is possible that a description of a case of first-order transformation lies in an observation in a paper by Stoughton and Adams<sup>17</sup> on the stability of diphenyl compounds. Crystallisation of 2.75 g. of 2-fluoro-5-methyl-2'-nitro-6'-carboxydiphenyl (XXVI) and 3.94 g. of brucine from 150 c.c. of ethyl alcohol resulted in a first crop of salt *l*-Bd-A.  $\frac{1}{4}$ H<sub>2</sub>O weighing 5.1 g.: when dissolved in chloroform this substance had  $[\alpha]_D^{20} - 3.2^\circ$ , but the authors record that if the solution was made up at 0° the value of  $[\alpha]_D^{20}$  was  $+13^\circ$  and mutarotated to the value  $-3.4^\circ$ . Unless the temperature coefficient of rotation is very large it would appear therefore that  $+13^\circ$  is nearer to that of the base *d*-acid salt and that  $-3.4^\circ$  represents an equilibrium value which might of course be that of the partial racemate, but if it is not, stands for an asymmetric transformation. The authors were concerned with producing series of differently restricted diphenyl compounds and did not pursue this line of investigation.



Although Yuan and Adams<sup>18</sup> consider that the following evidence does not justify the diagnosis of first-order transformation, it merits a careful survey and inclusion here. Brucine in wet alcohol causes 2:5-dimethoxy-2'-nitrodiphenyl-6'-carboxylic acid (XXVII) to undergo second-order asymmetric transformation to the *l*-base *l*-acid salt; the earliest observed  $[\alpha]_D$  in chloroform was  $-167^\circ$ ; mutarotation occurred to  $+3.2^\circ$  in 100 minutes and the extrapolated value for the initial reading was  $-180^\circ$ . A solution of brucine and the *racemic* acid in equimolecular quantities in chloroform had an initial  $[\alpha]_D^{25}$  of  $-8.6^\circ$  changing to  $+3.3^\circ$  in 80 minutes. Yuan and Adams say "this may have been due to slowness of salt formation in the organic solvent. It was not due to the fact that the mixture consisted of unequal quantities of *l*-*l*- and *l*-*d*-salts . . ." because precipitation from the solution with petroleum ether gave a salt which produced an inactive acid on decomposition with hydrochloric acid. Examining these results: if we assume that  $-180^\circ$  and  $-8.6^\circ$  are the specific rotations of the *l*-base *l*-acid and *l*-base *dl*-acid respectively, the specific rotation due to combined *l*-acid is  $-(180 - 8.6)^\circ = -171.4^\circ$ . Mutarotation from *l*-base *dl*-acid to equilibrium takes place over  $-8.6 - 3.3^\circ = -11.9^\circ$ , this representing  $11.9/171.4 \times 100$ , *i.e.* about 7% disproportionation. In other words the equilibrated solution may be assumed to contain 53.5% of the *l*-base *d*-acid and 46.5% of the *l*-base *l*-acid. It is little wonder that precipitation of this solution with petroleum ether, which would hardly be quantitative, produced either the partial racemate or a mixture of salts indistinguishable from it.

Among other acids in a series which provided much good material for the study of the subject in general, N-benzoyl-4:6:4'-tribromodiphenylamine-2-carboxylic acid (XXVIII) was the first to be investigated thoroughly.<sup>21</sup> With many other labile compounds it owes its optical



activity to restricted rotation within the molecule and its optical instability to the fact that given sufficient energy the molecule can pass through an intermediate flat stage to give the mirror image form. This acid underwent first-order asymmetric transformation in chloroform in the dextro direction with *nor-d-ψ*-ephedrine and in the laevo direction with cinchonidine. The latter change was investigated more fully: the cinchonidine *d*-acid salt was prepared by a second-order transformation in acetone, and a mixture of 64 % base *l*-acid and 36 % base *d*-acid salts by a crystallisation amounting to the first stage of resolution in the same solvent at  $-15^{\circ}$ . Their ranges of mutarotation in chloroform and rates of approach to equilibrium are tabulated:—

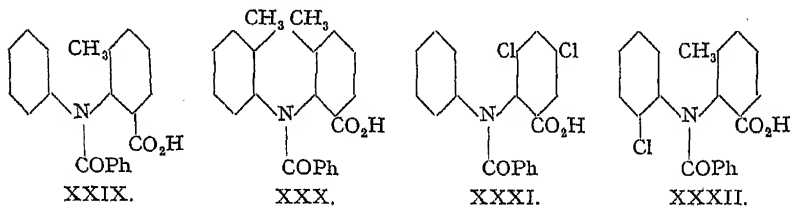
	$[\alpha]_{5461}^{18.0^{\circ}}$ initial.	$[\alpha]_{5461}^{18.0^{\circ}}$ final.	$k^{17.7^{\circ}}$ $\log_{10}$ min. <sup>-1</sup>
base <i>l</i> -acid . . .	$-105^{\circ}$	$-44.5^{\circ}$	0.0200
base <i>d</i> -acid . . .	$+194^{\circ}$ (extrap.)	$-44.5^{\circ}$	0.0206
base <i>dl</i> -acid . . .	$-40.4^{\circ}$	$-44.5^{\circ}$	(range too small for measurement)

The measured velocity constant  $k$  of course represents the sum of the velocity constants of inversion,  $k_d$  and  $k_l$ , of the two diastereoisomers: their difference is responsible for first-order asymmetric transformation. Assuming that dissociation in solution is negligible,

$$\frac{k_d}{k_l} = \frac{\text{concentration } l\text{-base } l\text{-acid at equilibrium}}{\text{concentration } l\text{-base } d\text{-acid at equilibrium}}$$

and in this case, concentration being proportional to rotation,  $k_d = 0.0105$  and  $k_l = 0.0101$ : the difference is very small, but it is, of course, real.

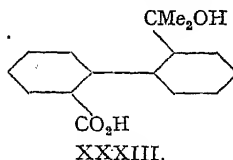
The preparation of a diversity of acids in this series<sup>22</sup> provided material for many more examples of first order transformation. N-benzoyl-2-methyl-diphenylamine-6-carboxylic acid (XXIX) showed mutarotation in presence of *nor-d-ψ*-ephedrine in chloroform containing 1/40 of ethyl alcohol by volume. N-benzoyl-2:2'-dimethyldiphenylamine-6-carboxylic acid (XXX) also mutarotated in presence of cinchonidine in the same



solvent. The originally *l*-rotatory cinchonidine solution became immediately more *l*-rotatory on addition of the *dl*-acid and then mutarotated in the dextro direction. This observation disposes of any possibility of observed mutarotations being due to slowness of salt formation, which would cause mutarotation in the opposite direction. N-benzoyl-2:4-dichloro-diphenylamine-6-carboxylic acid (XXXI) showed mutarotation with *nor-d-ψ*-ephedrine in chloroform and with cinchonidine in chloroform containing 1/40 of ethyl alcohol by volume. This solution after equilibration was extracted with mineral acid and gave a specimen of dextro-rotatory acid, establishing with certainty the assumed activation. N-benzoyl-2-methyl-2'-chlorodiphenylamine-6-carboxylic acid (XXXII) showed mutarotation with quinidine and with brucine in the same chloroform-alcohol solution. The behaviour of Mills and Elliott's<sup>10</sup> N-benzene-sulphonyl-8-nitro-1-naphthylglycine with cinchonidine in chloroform was

examined: the cinchonidine *l*-salt mutarotated from  $[\alpha]_{5461}^{25} - 255.5^\circ$  to  $-87.3^\circ$ , while the rotation of the cinchonidine *dl*-salt went from  $-35.5^\circ$  to  $-87.3^\circ$ . This represents an equilibrium composition of 38 % *l*-base *d*-acid and 62 % of *l*-base *l*-acid.

The kinetic experiments on simple optical activation were completed<sup>13</sup> by showing that the rate of approach to equilibrium was the same starting from base *l*-acid and from base *dl*-acid, a result which was, of course, predictable, but which depended for demonstration on finding a large enough range of mutarotation starting with the *dl*-acid. The brucine salt of *l*-2'-( $\alpha$ -hydroxyisopropyl)-diphenyl-2-carboxylic acid (XXXIII), obtained by second-order asymmetric transformation from ethyl alcohol, mutarotates from  $[\alpha]_{5461}^{25.15} - 47.04^\circ$  to  $+1.46^\circ$  with a first-order velocity constant  $k^{25.15} (\log_{10} \text{ hours}^{-1}) = 0.0277$  in chloroform ( $c = 6.835$ ;  $l = 2$ ) the first reading made 20 minutes after wetting. A mixture of the *dl*-acid and brucine in equimolecular proportions in chloroform shows a change of rotation from  $[\alpha]_{5461}^{25.15} - 5.08^\circ$  to  $+1.90^\circ$ , the change following the first-order law with a velocity constant of  $k^{25.15} = 0.0280 (\log_{10} \text{ hours}^{-1})$ , sufficiently good agreement with that of the salt to show that the same process is under observation. The equilibrium composition in chloroform calculated from these figures is 58 % of the *d*-acid salt and 42 % of the *l*-acid salt, assuming no dissociation.



### First-Order Transformation, Second-Order Transformation and Resolution.

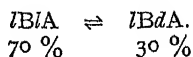
It now becomes interesting to investigate the relation between the two kinds of asymmetric transformation of an optically labile substance and the boundary between the second and optical resolution. An immediate difficulty is presented in the rarity of known substances which will undergo the three or even two of the three processes in or from the same solvent.

The first two effects have been demonstrated with 2'-( $\alpha$ -hydroxyisopropyl)-diphenyl-2-carboxylic acid and brucine in chloroform but not both at the same temperature.<sup>13</sup> The relevant observations were as follows: the equilibrium composition of the brucine salt in chloroform is 58 % of the base *d*-acid and 42 % of the base *l*-acid; when such a solution is evaporated on a boiling water bath with constant stirring to induce crystallisation as soon as it is possible, base *l*-acid crystallises. If we make the assumption that the equilibrium composition is not sensibly altered between room temperature and  $100^\circ$  (compare the case of  $\alpha$ - and  $\beta$ -glucose, ratio of concentrations in solution unaltered between  $0^\circ$  and  $40^\circ$ <sup>30</sup>) it follows that the base *d*-acid is more stable in solution while the base *l*-acid has the greater tendency to come out of it, *i.e.* is less soluble.

In the class of second-order transformations involving crystallisation of diastereoisomers which are ionised in solution so that the labile centre is not in combination with the activating agent until crystallisation takes place, the diastereoisomers have no joint reality in solution and, as has already been pointed out, there can be no first-order transformation. That is to say, if one diastereoisomeric salt is dissolved in a solvent in which the acid part is labile, mutarotation takes place towards an equilibrium composition which is that of the partial racemate: the rate constant  $k$  for the approach to equilibrium from base *d*-acid or base *l*-acid is made up of  $k_d$  and  $k_l$ , the rates of partial inversion of base *d*-acid and base *l*-acid, where these are equal and their sum is what has long been referred to as the rate of partial racemisation.

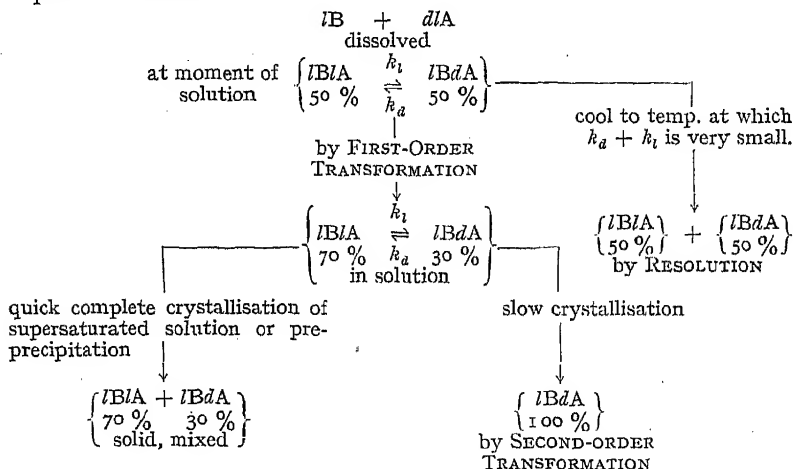
<sup>30</sup> Moelwyn Hughes, *Kinetics of Reactions in Solution*, 1933 edn., p. 45.

Let us consider a hypothetical case in which a *dl*-acid (optically unstable) and a *l*-base (optically stable) are dissolved in a *non*-dissociating solvent: the diastereoisomers have different free energies and mutarotation therefore begins immediately towards an equilibrium, say to



Neglecting all the complicating possibilities of supersaturation, accidental inoculation, crystallisation of a different entity from those existing in solution (*e.g.* with solvent, if the solvent is not similarly attached in solution) or the separation of a crystalline partial racemate, if, then, the solution becomes saturated by evaporation of the solvent it will begin to deposit crystals: and if the rate of crystallisation is less than the rate of mutarotation, then all of the salt which comes out will be in the one *IBdA* form, and the solution from which it is crystallising will show the equilibrium specific rotation. But suppose on the other hand, that the equilibrated solution is taken and cooled quickly to a temperature which brings it well below the saturation point of both salts and at which rate of crystallisation is faster than rate of mutarotation, then the material crystallising might well be mainly base *l*-acid with some base *d*-acid. The third possibility in crystallisation phenomena is that a solution of the base *dl*-acid is cooled immediately after dissolving to a temperature below which mutarotation can occur at an effective speed, when of course, given the usual necessary solubility conditions a straightforward resolution can be carried out and base *d*-acid and base *l*-acid separated by fractional crystallisation.

This is a simplified picture, but it has proved interesting to examine the scant and scattered literature on the subject with it in mind in an attempt to correlate the several valuable but unrelated observations on "optical activation."



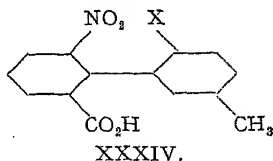
Sometimes the difference in free energy is so slight that one form or the other may crystallise haphazard without apparent difference in experimental procedure: thus Mills and Bain<sup>2</sup> found that in crystallising the quinine salt of their oximinocyclohexane-4-carboxylic acid from ethyl acetate sometimes there was a preponderance of the *d*-acid and sometimes of the *l*-acid in the salt produced. They obtained their purest (optically) specimen of quinine *l*-acid salt by deliberately choosing a solvent, dilute acetic acid, which would secure that the rate of racemisation should be as high as possible compared with that of crystallisation.

Although Read and McMath<sup>8,9</sup> in their two papers describe several experiments which bear an apparent relation to this argument, closer scrutiny shows that interpretation is far from simple because of the large number of solvents, both pure and mixed, which they used. For example, their classic first-order transformation to an equilibrium of *l*BdA 81%  $\rightleftharpoons$  *l*BdA 19% was carried out in specially purified and dried acetone, while the second-order transformation took place from acetone-methyl alcohol; also, the second crystalline form which can be obtained is not the diastereoisomer but the partial racemate *l*BdA. Another somewhat complicating factor in the use of the results for an argument other than that for which they were employed by the authors, is the fact that *l*-hydroxyhydrindamine as the benzenesulphonate itself shows a certain amount of mutarotation in methyl alcohol— $[M]_D$  in methyl alcohol changes from  $-100^\circ$  to  $-76^\circ$  in eight hours—and that the salt *l*BdA is so little soluble in "ordinary" acetone that by the time it can be got into solution by heating its mutarotation is lost. This makes it impossible to bring into line with any certainty the interesting observation that evaporation of an acetone solution deposits crystals having  $[M]_D - 93^\circ$  mutarotating in acetone to  $-154^\circ$ : evaporation to crystallisation and redissolving giving a repetition of the optical cycle. In their second paper<sup>9</sup> the crystallisation of *l*-hydroxyhydrindamine chlorobromoacetate was carried out in two ways from chloroform solution containing a little methyl alcohol. Slow deposition in the cold gave the *l*BdA, while rapid cooling of a supersaturated solution gave crystals of *l*BdA, but after about an hour, *i.e.* when the solution was cool, *l*BdA began to separate on top of the original crystals.

McKenzie and Smith,<sup>30</sup> during the resolution of *l*-menthyl *dl*-phenylchloroacetate by crystallisation from rectified spirit found, as a result of experience of many crystallisations, that the *l*-menthyl *d*-acid salt was the less soluble of the pair of diastereoisomers: this can now be linked with the fact that the equilibrium state in ethyl alcohol consists of an excess of the *l*-menthyl *l*-acid salt, if it be assumed that the small concentration of potassium hydroxide added has no appreciable effect on the system other than to confer the necessary mobility for the attainment of equilibrium. There is evidence for parallel behaviour in *l*-menthyl *dl*-phenylbromoacetate.

The behaviour of N-benzoyl-2:4:4'-tribromodiphenylamine-6-carboxylic acid with cinchonidine in acetone provides examples of both second-order transformation and resolution and illustrates the distinction between them.<sup>21</sup> The *dl*-acid dissolved with an equivalent of cinchonidine in acetone at room temperature or at the boiling point deposits *l*BdA in almost quantitative yield. Having found values of the velocity constant of mutarotation of this salt at different temperatures and thereby the values of B and E in the Arrhenius equation  $k = Be^{-E/RT}$  calculation shows that resolution might be possible at  $-15^\circ$  owing to the smallness of  $k$  there. Accordingly 1 M. of *dl*-acid and 1 M. of cinchonidine were dissolved in warm acetone and, as soon as crystallisation began, cooled to  $-15^\circ$ . The *l*BdA crystallised out, almost exactly 50% of the total weight, and evaporation of the filtrate *in vacuo* while still cold gave a mixture of 64% of *l*BdA and 36% of *l*BdA.

Another general view of the relation of second-order transformation and resolution can be made by considering a series of compounds in which the relative optical stability can be predicted to vary progressively: for example, Kuhn and Albrecht's<sup>25</sup> series of dinitrodiphenic acids, or the set of 2'-substituted (XXXIV) 2-nitro-5'-methylidiphenyl-6-carboxylic acids of Stoughton and Adams,<sup>17</sup> where the 2' position carries Br, Cl



or F, with brucine in ethyl alcohol. When X is Br or Cl the crystallisation process at room temperature is one of resolution, early crops having negative rotations and later crops positive; when X is the smaller F atom crystallisation takes place with second-order transformation, all crops having the same rotation; and an apparent first-order transformation has been observed, but not in the same solvent.

### The Effect on First-Order Transformation Equilibria of Adding an Excess of the Labile Acid.

The equilibrium rotation of a 1:1 acid:base solution (equivalent quantities) in a non-ionising solvent (optically unstable acid, optically stable base) has been found to be extremely sensitive to an excess of the *dl*-acid in several cases, an effect which is not due to suppression of dissociation in the diastereoisometric salts.<sup>21, 22</sup> *N*-benzoyl-2-methyl-2'-chlorodiphenylamine-6-carboxylic acid and quinidine in chloroform containing 1/40 ethyl alcohol by volume affords a good example.

0.1620 g. of quinidine in 20 c.c. of the solvent,  $l = 2$ , had a rotation  $\alpha_{5461}^{20}$  of  $+4.8^\circ$ . When 1 m. of the *dl*-acid was added the rotation changed immediately to  $+4.35^\circ$ , and on standing mutarotated to  $+2.99^\circ$ ; with

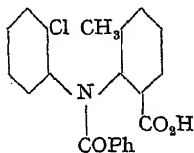
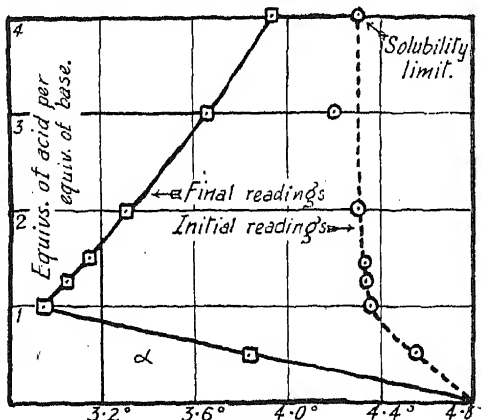


FIG. 2.



2 m. of acid the original  $\alpha_{5461}^{20}$  of  $+4.30^\circ$  changed to  $+3.32^\circ$ ; with 3 m.  $+4.32^\circ$  changed to  $+3.67^\circ$ . The total result is clearly seen on the

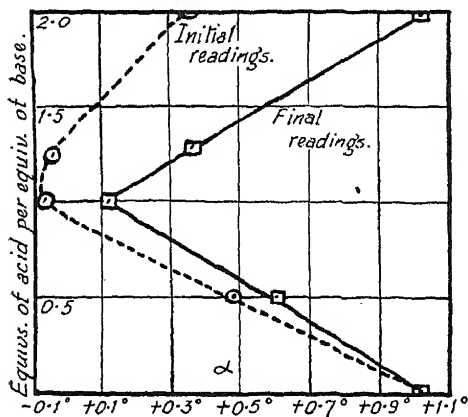


FIG. 3.

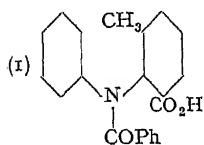
graph (Fig. 2). The rate of approach to equilibrium increased with increase in concentration of acid. Decomposition with mineral acid of equilibrated solutions always gave the *l*-acid.

Many other examples of this type of behaviour were found: in some cases the curve for mutarotated solutions lay to the other side of the original curve, e.g. *N*-benzoyl-2 : 4-dichlorodiphenylamine-6-carboxylic acid with *nor-d*- $\psi$ -ephedrine in chloroform, the final rotation was nearer to that of the base than the original value (Fig. 3). Also it can be seen that the

"initial" curve is not always of the ideal type shown in the first example:

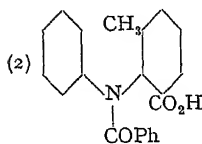
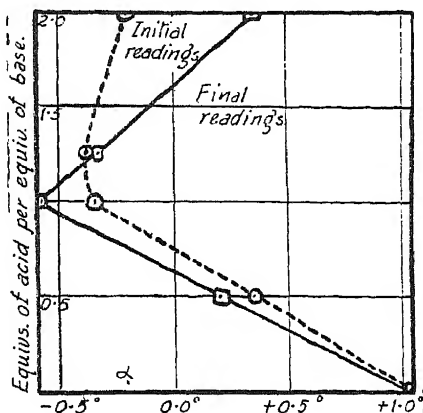
in a case such as this one it is considered to contain all the extraneous effects contributing to change of rotation (such as concentration) while the difference between the initial and final curves can only be due to an optical activation effect.

The cases which were most fascinating were those in which the initial and final curves crossed over. This happened with



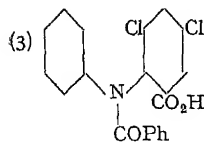
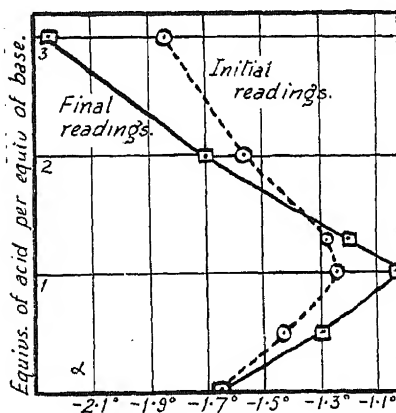
and *nor-d-ψ*-ephedrine  
in chloroform

FIG. 4.



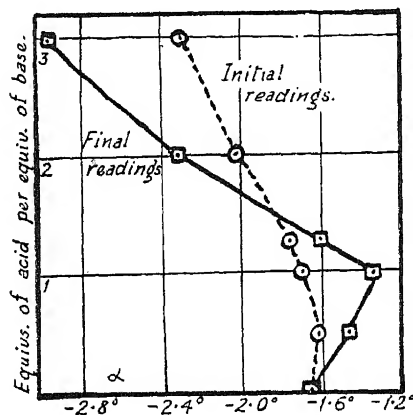
and cinchonidine in  
chloroform/EtOH

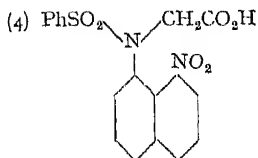
FIG. 5.



and cinchonidine in  
chloroform/EtOH

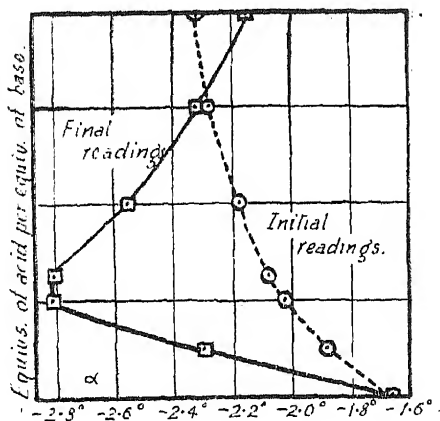
FIG. 6.





and cinchonidine in  
chloroform/EtOH

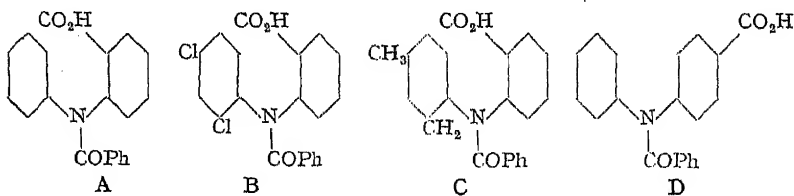
FIG. 7.



Decomposition of equilibrated solutions demonstrated the reality of the transformations underlying these mutarotations: in example (3), for instance (Fig. 6), extraction with mineral acid of the solutions after mutarotation showed that at the 1 : 1 ratio *d*- and at the 3 : 1 ratio *l*-acid was present (either free or combined as salt) in excess. In the fourth example similar decomposition gave acids which, from the 1 : 1 and 2 : 1 mixtures, were *l*-rotatory, from the 3 : 1 inactive and from the 4 : 1 *d*-rotatory. In effect, both forms of an active acid (not, of course, optically pure) were obtained *without ever separating* a salt—extracted directly from solutions in the same solvent in which optical activations had taken place in opposite directions.

### The Addition Curve Technique and Extremely Labile Optically Active Compounds.

This "addition curve" method has been used to predict potential optical activity where there was no other indication of it at room temperature.<sup>21</sup> The series of related acids in which rotation blocking with



consequent asymmetry might be expected to operate, show none of the hitherto established phenomena relating to optical isomerism at ordinary temperatures. However, the curves in the diagram (Fig. 8) were obtained on adding the acids progressively to *nor-d-ψ*-ephedrine in chloroform: no mutarotation was observed during the experiments—there are no "initial" curves—the "final" curve is obtained immediately. Thus it appeared that it was worth while to look further for activity in acids A, B and C, and not in acid D: that is an interesting first differentiation for a start, for it is what might have been predicted from their structures. Working at  $-31^\circ$  it was possible to detect a mutarotation with acid C and *nor-d-ψ*-ephedrine, acid : base ratio roughly 4 : 1,  $\alpha_{540}$  changed from  $-4.03^\circ$  to  $+2.15^\circ$ , half-life period 2.4 minutes. Acid B mutarotated more quickly in the same circumstances: each process followed the first

order law. Acid A, on the contrary, showed no such mutarotation, but it would hardly be stretching a point to say, as within the series, that its optical activity is demonstrated by the addition curve.

This brief description shows that with discreet handling the "addition curve" technique, far from "obscuring its interpretation and lessening its value as a means of demonstrating optical activity in labile systems" (Mills<sup>37</sup>) extends the field of optical observation covered by the activation process into realms which were hitherto unattainable. The only occasions on which it could "affect the diagnostic value of the activation process"<sup>37</sup> as already outlined previous to this time would be those on which non-equivalent quantities of base and acid were taken and happened by chance to lie on the point where the initial and final curves crossed over: risk of this mistake can easily be eliminated by always looking for mutarotation at more than one acid : base ratio.

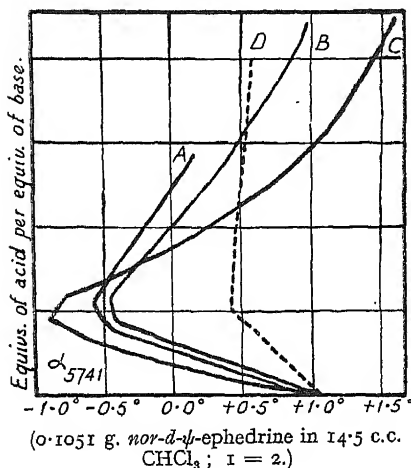


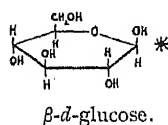
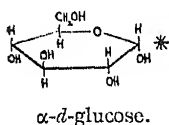
FIG. 8.

### Asymmetric Transformation and the Sugar Series.

In the light of this collected information on first- and second-order asymmetric transformations it is of the utmost interest to re-examine some well-established data in the sugar series which might be relevant to the subject.

#### 1. *d*-Glucose.

*d*-Glucose exists in solution in two forms,  $\alpha$ - and  $\beta$ -*d*-glucose. Any other forms must be present in negligible quantity.<sup>38</sup> These forms are



interconvertible by inversion of the carbon atom marked with an asterisk and this is the only carbon atom whose configuration is not rigidly fixed. Therefore the whole molecule can be considered as if it were one of a pair of diastereoisomers with one labile and one stable component, the  $\alpha$ -carbon atom being the unstable and the rest of the molecule the stable part: the diastereoisomers are, of course, "real" as long as the sugar is in the ring form. The optically stable part will exert an asymmetric influence on the unstable part, but it will be impossible to remove the influential group and see the results of first- or second-order transformation in the remainder.

(a) *d*-Glucose in Water. The composition of a mixture of the two forms of *d*-glucose in water at equilibrium has long been calculated from the rotations of the two forms and of their equilibrium solution: some of the latest published figures are those of Kendrew and Moelwyn Hughes,

<sup>37</sup> Mills, "The Stereochemistry of Labile Compounds," Presidential Address, *J. Chem. Soc.*, 1943, 194.

<sup>38</sup> Andrews and Worley, *J. Phys. Chem.*, 1927, 1880; Kendrew and Moelwyn Hughes, *Proc. Roy. Soc., A*, 1940, 176, 353.



who incorporate some values from Hudson and Yanovsky<sup>39</sup>; these are for water solutions:—

$\alpha$ - <i>d</i> -glucose [ $\alpha$ ] <sub>5893</sub> <sup>22.2°</sup> + 110.0°	equilibrium + 52.56°	$\beta$ - <i>d</i> -glucose + 19.7° at 20°.
--	-------------------------	--

The equilibrium composition, assuming dissociation from the ring form to be negligible, is 64 %  $\beta$ - and 36 %  $\alpha$ -form. This equilibrium appears to be unaffected by temperature between 0° and 40°.<sup>36</sup> When *d*-glucose is crystallised from cold water  $\alpha$ -*d*-glucose. H<sub>2</sub>O is *always* obtained,<sup>40</sup> while crystallising from water between 35° and 40° gives the anhydrous form, again of  $\alpha$ -glucose.<sup>41</sup> It therefore crystallises out from a solution containing excess of the  $\beta$ -form. Crystals of the  $\beta$ -form cannot be obtained by such gentle methods; Tanret obtained it by long standing of the  $\alpha$ -form at 105°, and Whistler and Buchanan<sup>42</sup> obtained it by taking an 85 % glucose solution and evaporating it during two hours (in 50 g. quantities) *in vacuo* at 100° to a solid mass of crystals consisting of  $\beta$ -glucose. (There are various other methods of affecting "second-order transformation" to  $\alpha$ - or to  $\beta$ -*d*-glucose: thus Hudson and Dale,<sup>43</sup> recommend a cold crystallisation from aqueous acetic acid resulting in 75 % to 80 % pure anhydrous  $\alpha$ -glucose and a hot quick crystallisation giving 93 % of  $\beta$ -glucose: these workers also recognised that the velocity constant for approach to equilibrium  $k$  was the sum  $k_\alpha$  and  $k_\beta$  and therefore the same from whichever side the measurement started.<sup>44</sup> *d*-Glucose is too soluble in water for the relative solubilities of the  $\alpha$ - and  $\beta$ -forms to be measured directly, but general practice would certainly lead one to the view that the  $\alpha$ -form is the less soluble.

(b) *D*-Glucose in 80 % Ethyl Alcohol. Hudson and Yanovsky give the following values:—<sup>39</sup>

$$[\alpha]_D^{20^\circ} \left. \begin{array}{l} \alpha\text{-glucose} + 115.5^\circ \\ \beta\text{-glucose} + 20.3^\circ \end{array} \right\} \text{equilibrium} + 59.3^\circ$$

there is therefore an excess of the  $\beta$ -form in solution at equilibrium. The solubilities found directly were 2.0 g.  $\alpha$ -form in 100 c.c., 4.9 g.  $\beta$ -form in 100 c.c.; the  $\alpha$ -form is the one crystallising, but as the hydrate.

(c) *D*-Glucose in Absolute Methyl Alcohol. Andrews and Worley<sup>38</sup> give the following values:—

$$[\alpha]_{5461}^{25^\circ} \left. \begin{array}{l} \alpha\text{-glucose} + 138.4^\circ \\ \beta\text{-glucose} + 26^\circ \end{array} \right\} \text{equilibrium} + 75.8^\circ$$

there is therefore excess of the  $\beta$ -compound at equilibrium. Lowry<sup>45</sup> obtained crystals of the  $\alpha$ -form from methyl alcohol. He also showed that the solubilities in this solvent were small and did not interfere with each other, and in this and a paper by Hudson and Dale it is shown to be justifiable to use the relationship

$$K = \text{equilibrium const.} = \frac{k_\alpha}{k_\beta} = \frac{S - S_\alpha}{S_\alpha},$$

where  $S_\alpha$  is the initial solubility of the  $\alpha$ -form and  $S$  the solubility at equilibrium, to calculate the rotation of the as then unknown  $\beta$ -compounds.

## 2. *d*-Mannose.

(a) *d*-Mannose in Water. Hudson and Yanovsky<sup>39</sup> using the solubility-rotation relationship calculated that the specific rotation of the

<sup>39</sup> J. Amer. Chem. Soc., 1917, 39, 1013.

<sup>40</sup> Tanret, *Compt. rend.*, 1895, 120, 1061.

<sup>41</sup> Behr, *Berichte*, 1882, 15, 1104; see also Newkirk, *Ind. Eng. Chem.*, 1938, 28, 760.

<sup>42</sup> J. Biol. Chem., 1938, 125, 557.

<sup>43</sup> J. Amer. Chem. Soc., 1917, 39, 320.

<sup>44</sup> See also Lowry, *J. Chem. Soc.*, 1904, 85, 1551.

then unknown  $\alpha$ -mannose was  $+30^\circ$ , knowing that the specific rotation  $[\alpha]_D^{20}$  of  $\beta$ -*d*-mannose was  $-17^\circ$ , and that that of the equilibrated solution in water was  $+14.6^\circ$ . Six years later Levene<sup>45</sup> prepared  $\alpha$ -mannose and confirmed their prediction. There is thus excess of the  $\alpha$ -form at equilibrium, the *opposite* from the *d*-glucose equilibrium. While *d*-mannose has not been crystallised from water, it is worthy of note that Levene says: "under conditions when glucose and galactose appear in the  $\beta$ -form, mannose crystallises in the  $\alpha$ -form and *vice versa*," quoting three cases to support this statement.

(b) *d*-Mannose in 80 % Ethyl Alcohol. In this solvent also the  $\alpha$ -form is present at equilibrium in excess;  $[\alpha]_D^{20}$   $\beta$ -form  $-14.9^\circ$ , equilibrium  $+25.7^\circ$ ,  $\alpha$ -form  $+35^\circ$  (predicted by Hudson and Yanovsky and observed by Levene). The  $\beta$ -form is stable under this solvent.

### 3. Lactose and Galactose.

A similar relationship holds for these sugars in water, in which the  $\beta$ -form is in excess at equilibrium and the  $\alpha$ -form crystallises out, but as the hydrate.<sup>39, 46</sup>

This short discussion is sufficient to show that the study of asymmetric transformation is in its infancy; no doubt there are many more examples as yet uncollected and a wealth yet to be discovered as the technique for exploring the phenomena of unstable optical activity becomes finer. Compounds which owe their asymmetry to restricted rotation are highly suitable for the study of optical kinetics, their lability being free from disturbing influences which may complicate other forms of instability; they are not known to occur in nature, but what is predicted from the simple system may be applied with proper discretion to the more complicated. It seems likely that instances of disturbed optical equilibria as well as the second-order transformations may play an important part in the building up of the asymmetric molecules which are characteristic of living matter.

The author wishes to record her indebtedness to Professor E. E. Turner, F.R.S., in whose laboratory the foregoing discussion has largely developed.

Bedford College,  
London.

<sup>45</sup> *J. Biol. Chem.*, 1932, 329.

<sup>46</sup> Tanret, *Bull. Soc. Chim.* 1871 (iii), 15, 195.

# A NEW GENERAL EQUATION FOR THE LIQUID-VAPOUR RELATIONS OF BINARY SYSTEMS.\*

## PART I. THEORETICAL AND EXPERIMENTAL BASIS.

BY A. M. CLARK.

Received 23rd February, 1945.

The equilibrium between liquid and vapour in systems containing two or more volatile components is of particular interest in the theory and practice of fractional distillation. The most convenient and simple relation between liquid and vapour compositions is that expressed by Raoult's Law :

$$p_1 = P_1 c_1$$

in which  $p_1$  is the partial pressure of a component in the vapour phase in equilibrium with its solution at a molar concentration  $c_1$  and  $P_1$  is the

### LIST OF SYMBOLS.\*

In the choice of symbols every effort has been made to be consistent, to avoid duplication, and where possible, to follow precedent, but these separate ideals are not fully compatible. In order to assist the reader, each symbol has been defined on its introduction into the text, and it is not therefore necessary to consult the following list in order to follow the argument.

- $A$  Constant term in Van Laar Equation.
- $B$  Constant term in Van Laar Equation.
- $H$  The amount of heat transferred between the liquid and vapour phases in accomplishing a given enrichment.
- $K$  (with no subscript) Ratio of molar latent heats of two components, with that of less volatile as numerator, *i.e.*  $K = Q_2/Q_1$ .
- $K$  (with subscript)  $K_G$  = overall mass transfer coefficient on a gas composition basis.
- $L$  The height of a packed column required to perform a given enrichment.
- $N$  With no subscript, indicates the number of theoretical plates required to perform a given separation. With a subscript,  $N$  indicates a number of transfer units.
- $P$  Vapour pressure of a pure component.
- $Q$  Molar latent heat of a pure component.
- $R$  The gas constant.
- $S$  Entropy.
- $T$  Temperature on the absolute scale.
- $X, Y$  Ratio of molar concentrations of the components of a binary mixture in the liquid and vapour phases respectively. Subscript "L" attached to these symbols indicates that the ratios are measured in terms of units of equal latent heat.
- $a$  Defined by  $a = dY/dX$  when the equilibrium of a binary system is expressed by the equation  $Y = aX + b$ .
- $b$  The constant term in the equilibrium equation  $Y = aX + b$ .
- $c$  Molar concentration of a component in the liquid phase.
- $d$  The intercept on the  $Y$  axis of the asymptote to the  $X$   $Y$  curve derived from the Van Laar relation.
- $h$  (with no subscript) The constant term in the equation  $y = mx + h$  defining the operating line of a distillation system under finite reflux.
- $h$  (with subscript G or L) Indicates mass transfer coefficients for gas and liquid films respectively.
- $m$  The slope of the operating line for a given distillation, when represented by the equation  $y = mx + h$ . Also defined by  $m = \frac{p}{p + 1}$ .
- $n$  The number of mols. of liquid passing through a system in unit time.

vapour pressure of the pure component at the same temperature. When the system contains two volatile components Raoult's Law gives the relation :

$$\frac{y}{1-y} = \frac{P_1}{P_2} \frac{x}{1-x} \quad . \quad . \quad . \quad . \quad . \quad (1)$$

- $p$  (with subscript) Partial pressure of a component in the vapour phase (Ats.).  
 $p$  (without subscript) Value of  $y$  at point of intersection of equilibrium and operating lines on  $x-y$  diagram.  
 $q$  Value of  $x$  at point of intersection of equilibrium and operating lines on  $x-y$  diagram.  
 $r$  The common ratio in a geometrical series.  
 $s$  A term in a geometrical series.  
 $x$  Molar concentration of more volatile component in the liquid phase.  
 $y$  Molar concentration of more volatile component in the vapour phase.  
 $\alpha$  Ratio of the vapour pressures of the pure components of a binary system, i.e.  $\alpha = P_1/P_2$ .  
 $\gamma$  The activity coefficient of a component.  
 $\delta$  Constant term when equilibrium equation is expressed in the "derived" form  $\phi = \delta\chi + \tau$ .  
 $\lambda$  Constant term when operating equation is expressed in the form  $\phi = \lambda\chi + \sigma$ .  
 $\mu$  Gibbs' chemical potential.  
 $\rho$  "Reflux ratio" in a distillation system.  
 $\sigma$  Constant term when operating equation is expressed in the form  $\phi = \lambda\chi + \sigma$ .  
 $\tau$  Constant term when equilibrium equation is expressed in the "derived" form  $\phi = \delta\chi + \tau$ .  
 $\phi\phi'$  Functions of composition of vapour phase defined by :

$$\phi = \frac{1-y-p}{p-y} \quad \text{and} \quad \phi' = \frac{1-y+p}{y-p}.$$

- $\chi \chi'$  Functions of composition of liquid phase defined by :

$$\chi = \frac{1-x-q}{q-x} \quad \text{and} \quad \chi' = \frac{1-x+q}{x-q}.$$

- $\Pi$  Total vapour pressure of a system.  
 $\Sigma$  The sum of a series.

### Subscripts.

- 1, 2 Attached to  $P$ ,  $Q$ ,  $p$  and  $c$  (and to  $x$  and  $y$  in Part I. only) denote properties of the separate components of a binary system.  
 $s$  Attached to  $s$ , indicate consecutive steps in a geometrical series.  
 $X$ ,  $Y$  Attached to  $x$ ,  $y$ ,  $X$  and  $Y$ , indicate limiting values of these functions under given conditions (Part II. only).  
 (These separate uses are made clear in the context.)  
 $e$  The base of Napierian Logarithms.  
 $OG$  Attached to  $N$ , indicates the number of overall transfer units based on changes in gas composition required to perform a given enrichment.  
 $G$  Refers to the gas phase.  
 $H$  Indicates that composition is expressed in "molar" units.  
 $L$  Refers to the liquid phase. Also used to indicate units of equal latent heat.  
 $M$  Attached to  $N$ , indicates the number of mass transfer units required to perform a given enrichment.  
 $MT$  Attached to  $N$ , indicates the number of mass transfer units required to perform a given enrichment at total reflux.

### Superscripts.

- ' Indicates that the quantity under discussion refers to that part of the system in which the less volatile component is dominant, e.g. the region of the  $x-y$  diagram below the conjugate point.  
 $*$  Signifies that the quantity thus marked refers to the equilibrium line as distinct from the operating line, e.g.  $y^*$  indicates the composition of the vapour phase in *equilibrium* with a liquid of composition  $x$ , when  $y$  is the composition of the vapour phase in *contact* with liquid of composition  $x$ .

### Abbreviation.

(H.T.U.) = "Height of a transfer unit."

in which  $y$  and  $x$  are the molar concentrations of the more volatile component in the vapour and liquid phases respectively. If the vapour pressures of the pure components ( $P_1$  and  $P_2$ ) are known, this equation enables the relative liquid and vapour compositions of the system to be determined, either at constant temperature or at constant pressure. In the former case  $(P_1/P_2)_T$  is constant, but in the latter case, which is the more important in distillation, as that process is usually carried out at constant pressure, it becomes a variable, since by the Clausius-Clapeyron approximation,

$$d \log_e \left( \frac{P_1}{P_2} \right)_T = \Delta Q \frac{dT}{RT^2}$$

in which  $\Delta Q$  is the difference between the molar heats of vaporisation of the components.

When the molar heats of vaporisation of the components are approximately equal, it is possible to assume a constant value for the "relative volatility"  $P_1/P_2$ , even at constant pressure. When this is permissible, fairly simple mathematical relations can be developed, which enable the behaviour of the system on fractional distillation to be expressed in terms of "theoretical plates," "transfer units," or other theoretical devices. In default of any simple relation between the compositions of the two phases, the behaviour of the system under any imposed conditions of distillation must be evaluated by graphical methods, which are frequently more tedious, and are not readily adaptable to the theoretical study of distillation.

Unfortunately very few systems rigidly obey Raoult's Law, and still fewer fulfil the condition of constant relative volatility, and the mathematical analysis of distillation behaviour is therefore severely restricted. The law itself implies that the behaviour of a molecule of either component is independent of its environment, and this condition can only be realised in practice if the components of the system obey the same equation of state. If the Theory of Corresponding States is also to be satisfied, it is to be expected that Raoult's Law will be obeyed, even approximately, only by systems in which the components are adjacent members of the same homologous series, or have closely similar critical constants. In general, this is found to be the case.

A number of attempts have been made to describe the behaviour of systems which deviate from Raoult's Law in terms of general equations based on thermodynamic relations and depending upon a general equation of state.

The exact thermodynamic relation describing a phase in equilibrium within itself was formulated by Gibbs :

$$-SdT + Vd\pi - \sum_1 n_i d\mu_i = 0$$

in which  $n_i$  is the number of molecules of component ( $i$ ) in the phase and  $\mu_i$  is the chemical potential of that component. The condition for equilibrium between two phases is that both shall be at the same temperature and pressure and that  $\mu$  for each component shall be the same in each phase.

For a vapour phase which is a perfect gas, at fixed temperature,

$$d\mu_1 = RT d \log_e p_1.$$

The equation for 1 mol. of a liquid phase of two components at constant temperature may be written :

$$V_{11q}.d\pi = x_1 d\mu_1 + x_2 d\mu_2.$$

If this phase is in equilibrium with a vapour phase  $d\mu_1$  and  $d\mu_2$  are same in each, and by substitution we obtain :

$$V_{11q}.d\pi = RT(x_1 d \log_e p_1 + x_2 d \log_e p_2).$$

For  $RT$  we may write  $\pi V_{\text{vap}}$ , in which  $V_{\text{vap}}$  is the molar volume of the vapour phase. By re-arrangement:

$$\frac{V_{\text{liq.}}}{V_{\text{vap.}}} \cdot \frac{d\pi}{\pi} = x_1 d \log_e p_1 + x_2 d \log_e p_2.$$

At ordinary pressures,  $\frac{V_{\text{liq.}}}{V_{\text{vap.}}}$ , the ratio of the molar volumes of the two phases is very small, and the left-hand side of this equation may be equated to zero without serious error. We then obtain as the condition of equilibrium at constant temperature:

$$x_1 d \log_e p_1 + x_2 d \log_e p_2 = 0.$$

This is a derivative of the Gibbs equation attributed to Duhem and Margules. Alternatively the relation between liquid and vapour compositions may be expressed in terms of activity coefficients,  $\gamma$ , using the definition

$$p = \pi \gamma x$$

in which  $\gamma$  appears as a "correction factor" in the statement of Raoult's Law. By differentiation and substitution for  $d \log_e p$  the Gibbs-Duhem equation is readily obtained in the form:

$$\frac{d \log_e \gamma^1}{d \log_e \gamma_2} = - \frac{x_2}{x_1} \quad (2)$$

A number of attempts have been made to integrate this equation on the basis of a general equation of state. Among the useful results obtained may be mentioned those of Van Laar,<sup>1</sup> Margules,<sup>2</sup> and Scatchard and Hamer.<sup>3</sup> These have been reviewed and compared by Carlson and Colburn.<sup>4</sup> In all these attempts the object has been to derive separate equations for the activity coefficients of the two components, which can then be used, in conjunction with their vapour pressures in the pure state, to determine the relations between the two phases. In using these equations at constant pressure, and consequently with varying temperature, it must be assumed that the activity coefficient varies to a negligible extent with temperature over the range extending between the boiling points of the two components. If the behaviour of the system is to be completely defined by these methods with respect to temperature, pressure and composition, it is necessary to make use of further approximating assumptions, and the equations which are finally obtained give only an indirect relation between the compositions of the two phases, which is the most important property of the system in the study of fractional distillation.

If we define the behaviour of the system by the modified expression of Raoult's Law, the two partial equations may be combined to give:

$$y_1/y_2 = P_1/P_2 \cdot \gamma_1/\gamma_2 \cdot x_1/x_2. \quad (3)$$

This expression relates the composition of the two phases in terms only of the ratios of the activity coefficients of the two components and of their vapour pressures in the pure state. It is sufficient, therefore, to know only the relative rather than the absolute values of the activity coefficients in order to express composition relations. It is to be anticipated that simpler relations will exist between the ratio of the activity coefficients, and composition of the phases, than those required to define their absolute values.

<sup>1</sup> Van Laar, *Physicalisch-Chemische Probleme*. Also *Z. physik. Chem.*, 1910, 72, 723.

<sup>2</sup> Margules, *Sitzber. Akad. Wiss. Wien. Math. natur. Klasse II*, 1895, 104, 1243.

<sup>3</sup> Scatchard and Hamer, *J. Am. Chem. Soc.*, 1935, 57, 1805.

<sup>4</sup> Carlson and Colburn, *Ind. Eng. Chem.*, 1942, 34, 581.

The compositions of the two phases of a binary system may be expressed in terms of molar ratios equally as well as by molar concentrations. The weight-ratio of high-boiling to low-boiling component has been extensively used by Hausbrand<sup>12</sup> as the most convenient means of expressing composition in calculations concerning the distillation of binary systems, and his book contains a number of tables in which liquid and vapour compositions are related in these terms.

If we define composition in terms of molar ratios  $X$  and  $Y$ , such that

$$X = x_1/x_2 \text{ and } Y = y_1/y_2$$

in which  $(x_1 + x_2)$  and  $(y_1 + y_2)$  both equal unity, we obtain the expression:

$$Y = P_1/P_2 \cdot \gamma_1/\gamma_2 \cdot X \quad (4)$$

When the system obeys Raoult's Law,  $\gamma_1 = \gamma_2 = 1$ , and when the "relative volatility,"  $P_1/P_2$ , can be given a constant value denoted by  $\alpha$ , the compositions of the two phases are related by the very simple linear expression:

$$Y = \alpha X.$$

In this relation it is immaterial which component provides the denominator in defining molar ratio. It is equally possible to express the behaviour of the system by the reciprocal ratios:

$$Y' = \frac{1}{\alpha} X'$$

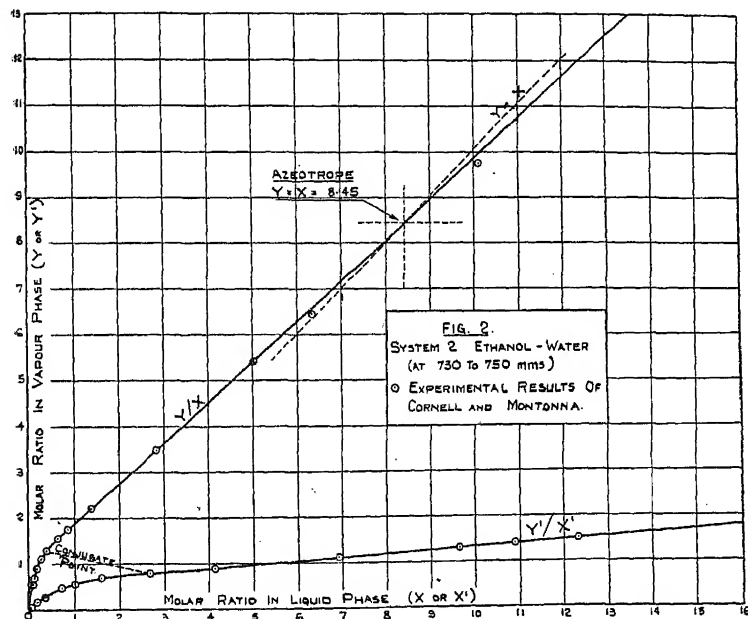
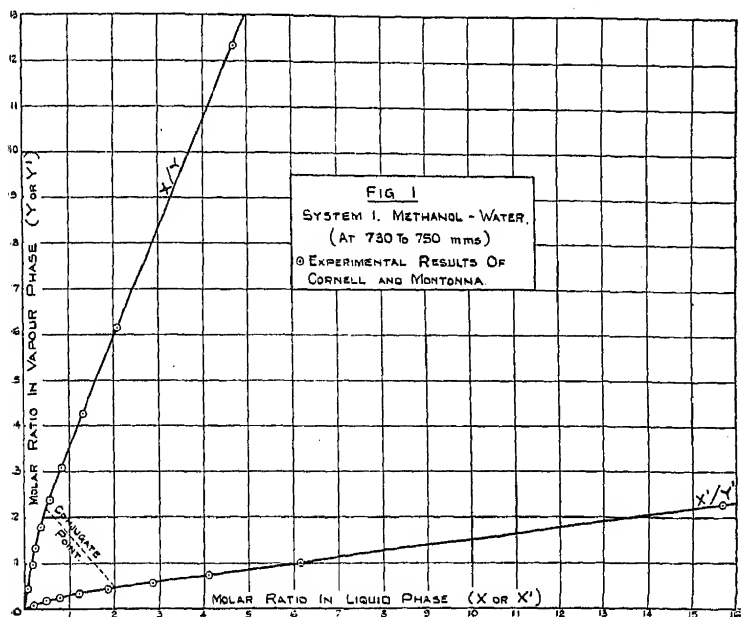
in which  $X' = x_2/x_1 = 1/X$  and  $Y' = y_2/y_1 = 1/Y$ .

(For convenience, in this paper an apostrophe is used to signify relative values in which the more volatile component provides the denominator.)

If the principle of using relative rather than absolute variants to express the behaviour of a binary system is extended to "non-ideal" systems, defined as those which deviate from Raoult's Law, it soon becomes evident that the relations in composition between the phases have been greatly simplified. (See Figs. 1 and 2 in which the liquid-vapour compositions of the systems Methanol-Water and Ethanol-Water at atmospheric pressure are plotted in this manner.) It is found that the curve relating molar ratios shows no point of inflexion, such as frequently occurs in a plot based on the more conventional units of molar concentration. On the other hand, the curves for all systems appear to conform quite closely to a single general type. Near the origin they are concave towards one axis, but the curvature rapidly diminishes, and above certain values of the molar ratios the curves are to all intents and purposes rectilinear.

Curves with similar characteristics are obtained, whichever form of the molar ratio is used. The occurrence of an azeotropic mixture is indicated by the intersection of either of the curves with the line  $Y = X$ , but no change in direction occurs at this point. In this way the compositions of the two phases can be related by either of two curves, depending upon whether the compositions are expressed in terms of  $X$  and  $Y$ , or  $X'$  and  $Y'$ . As these are reciprocal properties it follows that high values on the  $(X, Y)$  curve correspond with low values on the  $(X', Y')$  curve, and vice versa. The extreme rectilinear portion of either curve, thus corresponds with the initial concave portion of the other. If the rectilinear portion were sufficiently extensive in each case to correspond with the whole of the concave portion of the reciprocal curve, it would then be possible to use only the straight portion of each curve to relate liquid and vapour compositions over the whole system. Examination of the experimental results obtained by various investigators for a large number of different systems, has shown that this condition is satisfied with surprisingly high accuracy in the majority of cases, both at constant pressure and at constant temperature, and it therefore affords a simple

and convenient relation which is of considerable service in the application of mathematical methods to a study of fractional distillation.



The principle which governs this procedure may be formally stated as an empirical rule: "In a system of two volatile components containing one liquid and one vapour phase, either at constant pressure or at constant



temperature, the ratios of the quantities of the two components in either phase bear a simple linear relationship with one another when the ratios are expressed so that the dominant component in the system provides the numerator." The dominant component is not necessarily that which is present in the greater concentration, although at extreme concentrations this is invariably the case. At intermediate concentrations the dominant component is determined by the behaviour of the system. The units of quantity are not defined, as it will be shown later that the relation is true not only for molar ratios but for the ratios in any units of mass.

In algebraic notation the rule states that the composition of the vapour in equilibrium with a given liquid in a binary system may be represented by one or other of the two equations:

$$Y = aX + b \quad . \quad . \quad . \quad . \quad (5a)$$

$$\text{and} \quad Y' = a'X' + b' \quad . \quad . \quad . \quad . \quad (5b)$$

in which  $aba'b'$  are constants, using whichever equation is appropriate to the region of the system under consideration. These equations may be translated back into the more conventional terms of concentration by substituting:

$$Y = \frac{y}{1-y}, \quad X = \frac{x}{1-x}$$

$$Y' = \frac{1-y}{y}, \quad X' = \frac{1-x}{x}.$$

The two following equations in  $x$  and  $y$  are then obtained:

(a) For high values of  $x$

$$\frac{y}{1-y} = \frac{ax}{1-x} + b \quad . \quad . \quad . \quad . \quad (6a)$$

(b) For low values of  $x$

$$\frac{1-y}{y} = \frac{a'(1-x)}{x} + b' \quad . \quad . \quad . \quad . \quad (6b)$$

In order that the entire system may be continuously covered by these two equations, it is necessary that equations (6a) and (6b) should have a point of contact at some value of  $x$  between 0 and 1.0. It is readily shown that this condition is satisfied when

$$\pm \sqrt{aa'} \pm \sqrt{bb'} = 1 \quad . \quad . \quad . \quad . \quad (7)$$

and at the point of coincidence, which may be termed the "conjugate point"

$$X = \frac{x}{1-x} = \sqrt{\frac{a'b}{ab'}} \quad . \quad . \quad . \quad . \quad (8)$$

This relationship limits to three the number of parameters required to describe the behaviour of a system which falls completely within the rule, and with this knowledge it should be possible to predict the relative compositions of liquid and vapour phases at any point in the system on the basis of three accurately determined experimental values, or four if the correlation of equation (7) be not employed.

### Experimental Basis.

In the accompanying Table I calculated values for the composition of the vapour in equilibrium with a given liquid under stated conditions are compared with actual experimental values for ten different systems. The figures are tabulated as in most cases the plotted results do not show how small is the deviation between calculated and experimental values.

The systems have been selected with a view to testing the linear rule

as stringently as possible. With two exceptions which are named in the notes on individual systems, actual experimental values from a single, apparently reliable, source have been used in preference to data from collections, such as those in Perry<sup>5</sup> and Kirschbaum,<sup>6</sup> which have sometimes been compiled by selection of results from a variety of sources. It has been found in a number of cases, that the use of "smoothed" experimental results can introduce apparent anomalies which do not, in fact, exist.

In calculating values of vapour composition by means of the linear equations, the experimental results for a particular system were first plotted with molar ratios in the two phases as co-ordinates, and the best straight line was drawn through each set of results, neglecting deviations at low numerical values. The procedure was repeated with molar ratios in the reciprocal form. From the two straight lines thus obtained values of the constants  $a$ ,  $a'$  (the slopes of the straight lines), and  $b$ ,  $b'$  (their intercepts on the  $Y$  or  $Y'$  axes) were determined. By substituting these values in equations (6a) and (6b) equations were obtained for the equilibrium curves in terms of molar concentration. Values for the vapour composition calculated from these equations for the given values of liquid composition are compared with the direct experimental results. In each case the value of the function  $\sqrt{aa'} \pm \sqrt{bb'}$  is given as an indication of the continuity between the two equations. In the accompanying graphs (Graphs 1-10)\* the calculated and experimental results are compared with molar concentrations as co-ordinates. Actual experimental points are indicated by circles. The broken lines indicate the course of the calculated curves when they are projected beyond the congruent point in the direction in which they become invalid. Calculations have been made with a 10-inch slide rule. Further explanatory notes on the individual systems are given below:

*System 1.—Methanol-Water at 730-750 mm.* Experimental results by Cornell and Montonna.<sup>7</sup>

*System 2. Ethanol-Water at 730-750 mm.*—Experimental results by Cornell and Montonna.<sup>7</sup>

*System 3. Ethanol-Water at 25° C.*—Experimental results by Dobson.<sup>8</sup>

There is a slight discrepancy between the experimental and calculated results at the lowest ethanol concentrations. The very steep slope of the  $x$ - $y$  curve in this region would emphasise any slight experimental error, and accurate sampling of the vapour phase without disturbance of the liquid composition would be difficult for the same reason. The discrepancy may therefore be due to experimental error.

*System 4. n-Propanol-Water at 1 At.*—The experimental results are by Gadwa, as recorded in Perry,<sup>5</sup> but they appear to have been smoothed as they are not coincident with those plotted by Carlson and Colburn<sup>4</sup> from the same source.

Apart from a slight discrepancy at the lowest propanol concentration for which the same explanation may be offered as in the case of System 3, there is very close agreement between the experimental and the calculated figures. Nevertheless, there is slight lack of continuity between the two parts of the equilibrium curve on either side of the conjugate point, shown by the deviation of the function  $\sqrt{aa'} + \sqrt{bb'}$  from unity. As a result, the two parts of the curve have a point of intersection rather than a common tangent at the conjugate point. A possible explanation of this anomaly, provided it is real, is that the formation of a second liquid phase

<sup>5</sup> Perry, *Chemical Engineer's Handbook* (2nd edn.), 1941, p. 1360, McGraw-Hill Book Co., U.S.A.

<sup>6</sup> Kirschbaum, *Destillier- und Rektifiziertchnik*, Berlin, 1940 (Photo-Litho. Reproduction by Edwards Bros. Inc. Ann. Arbor, Michigan, 1943).

<sup>7</sup> Cornell and Montonna, *Ind. Eng. Chem.*, 1933, **25**, 1331.

<sup>8</sup> Dobson, *J. Chem. Soc.*, 1925, 127, 2866.

\* See pp. 731, 732.

TABLE I.

1. SYSTEM : METHANOL-WATER (at 730 to 750 mm. of mercury).

Mol. fraction of methanol in liquid phase ( $x$ )	0.007	0.017	0.060	0.140	0.196	0.296	0.354	0.452	0.566	0.677	0.825	0.913	0.916
Mol. fraction of methanol in vapour ( $y$ )—													
(a) experimental	0.056	0.113	0.307	0.498	0.573	0.644	0.705	0.755	0.810	0.860	0.925	0.966	0.966
(b) calculated	0.050	0.113	0.307	0.498	0.575	0.642	0.704	0.752	0.808	0.860	0.926	0.964	0.965
Linear Equations	$Y' = 0.131 X' + 0.20$						$Y = 2.45 X + 1.0$						

At Conjugate Point :  $x = 0.34$ .

$$\sqrt{aa'} + \sqrt{bb'} = 1.012.$$

2. SYSTEM : ETHANOL-WATER (at 730 to 750 mm. of mercury).

Mol. fraction of ethanol in liquid phase ( $x$ )	0.003	0.005	0.008	0.012	0.025	0.042	0.058	0.075	0.084	0.094	0.126	0.194	0.272	0.382	0.460	0.488	0.581	0.741	0.864	0.952
Mol. fraction of ethanol in vapour ( $y$ )—																				
(a) experimental	0.025	0.046	0.089	0.122	0.223	0.307	0.359	0.400	0.417	0.435	0.473	0.527	0.564	0.608	0.636	0.650	0.690	0.778	0.866	0.948
(b) calculated	0.030	0.059	0.090	0.126	0.219	0.301	0.355	0.397	0.412	0.434	0.476	0.525	0.564	0.603	0.633	0.645	0.689	0.778	0.868	0.949
Linear Equations	$Y' = 0.077 X' + 0.565$										$Y = 0.885 X + 0.97$									

At Conjugate Point :  $x = 0.27$ .Azeotrope :  $x$  (experimental) = 0.894,  $x$  (calculated) = 0.894.

$$\sqrt{aa'} + \sqrt{bb'} = 1.000.$$

TABLE I. (Continued).

## 3. SYSTEM: ETHANOL-WATER (at 25° C.).

Mol. fraction of ethanol in liquid phase ( $x$ ) . . .	0.025	0.053	0.092	0.134	0.167	0.202	0.285	0.336	0.490	0.582	0.785
Mol. fraction of ethanol in vapour ( $y$ )—											
(a) experimental . . .	0.179	0.317	0.434	0.513	0.544	0.569	0.610	0.629	0.678	0.710	0.815
(b) calculated . . .	0.213	0.338	0.442	0.508	0.542	0.570	0.612	0.629	0.677	0.710	0.815
Linear Equations . . .	$Y' = 0.085 X' + 0.42$								$Y = 0.86 X + 1.26$		

At Conjugate Point:  $x = 0.37$ 

$$\sqrt{aa'} + \sqrt{bb'} = 0.997.$$

4. SYSTEM: *n*-PROPANOL-WATER (at 1 At.).

Mol. fraction of propanol in liquid phase ( $x$ ) . . . . .	0.02	0.04	0.06	0.10	0.20	0.30	0.40	0.432	0.50	0.60	0.70	0.80	0.85	0.90	0.96
Mol. fraction of propanol in vapour ( $y$ )—															
(a) experimental . . . . .	0.216	0.320	0.351	0.372	0.392	0.404	0.424	0.432	0.452	0.492	0.551	0.641	0.704	0.778	0.900
(b) calculated . . . . .	0.265	0.323	0.348	0.372	0.391	0.398	0.419	0.429	0.454	0.498	0.559	0.645	0.703	0.776	0.894
Linear Equations . . . . .	$Y' = 0.027 X' + 1.45$ $Y = 0.33 X + 0.50$														

At Conjugate Point:  $x = 0.4$ 

$$\sqrt{aa'} + \sqrt{bb'} = 0.944.$$

TABLE I (continued).

5. SYSTEM : WATER-*n*-BUTANOL (at 1 At.).

Mol. fraction of water in liquid phase ( $x$ )	0.039	0.065	0.070	0.257	0.275	0.305	0.496	0.552	0.577	0.982	0.986	0.992	0.998
Mol. fraction of water in vapour phase ( $y$ )—													
(a) experimental	0.267	0.323	0.352	0.629	0.641	0.662	0.736	0.750	0.750	0.758	0.754	0.843	0.951
(b) calculated	0.238	0.303	0.353	0.630	0.643	0.660	0.735	0.748	0.753	0.755	0.756	0.839	0.950
Linear Equations . . . .	$Y' = 0.12 X' + 0.24$										$Y' = 0.036X + 1.10$		

$$\sqrt{aa'} + \sqrt{bb'} = 0.579.$$

6. SYSTEM : *n*-BUTANOL-*n*-BUTYL ACETATE (at 1 At.).

Mol. fraction of <i>n</i> -butanol in liquid phase ( $x$ )	0.109	0.208	0.295	0.361	0.433	0.447	0.510	0.544	0.555	0.575	0.608	0.646
Mol. fraction of <i>n</i> -butanol in vapour phase ( $y$ )—												
(a) experimental	0.207	0.332	0.413	0.465	0.517	0.529	0.569	0.601	0.607	0.619	0.642	0.669
(b) calculated	0.203	0.330	0.416	0.469	0.519	0.527	0.564	0.598	0.606	0.619	0.640	0.667
Linear Equations . . . .	$Y' = 0.44 X' + 0.35$										$Y' = 0.80 X + 0.54$	
Mol. fraction of <i>n</i> -butanol in liquid phase ( $x$ )	0.679	0.710	0.726	0.729	0.731	0.756	0.828	0.865	0.913	0.960	0.980	0.995
Mol. fraction of <i>n</i> -butanol in vapour phase ( $y$ )—												
(a) experimental	0.692	0.715	0.734	0.729	0.733	0.750	0.813	0.850	0.895	0.942	0.964	0.989
(b) calculated	0.691	0.715	0.727	0.729	0.736	0.752	0.815	0.850	0.899	0.951	0.975	0.994
Linear Equation . . . .	$Y = 0.80 X + 0.54$											

At Conjugate Point  $x = 0.5$ .

$$\sqrt{aa'} + \sqrt{bb'} = 1.028.$$

Azeotrope :  $x$  (experimental) = ca. 0.73,  $x$  (calculated) = 0.729.

TABLE I (continued).

7. SYSTEM: WATER-FORMIC ACID (at 1 At.).

Mol. fraction of water in liquid phase ( $x$ ) . . . . .	0.221	0.389	0.441	0.522	0.630	0.720	0.793	0.858	0.911	0.959
Mol. fraction of water in vapour phase ( $y$ )—										
(a) experimental . . . . .	0.141	0.361	0.441	0.576	0.721	0.823	0.888	0.929	0.962	0.983
(b) calculated . . . . .	0.171	0.360	0.435	0.571	0.721	0.826	0.888	0.930	0.960	0.983
Linear Equations . . . . .	$Y' = 1.57X' - 0.69$				$Y = 2.48X - 1.64$					

$$aa' - bb' = 0.91$$

8. SYSTEM: WATER-ACETIC ACID (at 730 to 750 mm. of Mercury).

Mol. fraction of water in phase ( $x$ ) . . . . .	0.268	0.278	0.370	0.449	0.515	0.592	0.635	0.686	0.724	0.765	0.799	0.826	0.831	0.858	0.883	0.909	0.911	0.930	0.949	0.967	0.969
Mol. fraction of water in vapour phase ( $y$ )																					
(a) experimental . . . . .	0.388	0.404	0.500	0.578	0.640	0.708	0.745	0.785	0.813	0.842	0.864	0.881	0.884	0.902	0.919	0.935	0.936	0.930	0.962	0.976	0.977
(b) calculated . . . . .	0.385	0.396	0.500	0.580	0.641	0.708	0.743	0.783	0.810	0.840	0.864	0.880	0.884	0.902	0.919	0.936	0.937	0.950	0.963	0.976	0.977
Linear Equations . . . . .	$Y' = 0.58 X' + 0.013$										$Y = 1.345 X + 1.10$										

$$aa' + bb' = 1.000.$$

TABLE I (continued).

9. SYSTEM: BENZENE-TOLUENE (at 1 At.).

Mol. fraction of benzene in liquid phase ( <i>x</i> )	0.014	0.10	0.20	0.30	0.40	0.50	0.60	0.70	0.80	0.962
Temperature (°C.)	110.0	106.3	102.3	98.8	95.5	92.4	89.5	86.9	84.5	81.0
Mol. fraction of benzene in vapour phase ( <i>y</i> )										
(a) calculated from Raoult's Law	0.032	0.207	0.374	0.509	0.620	0.713	0.790	0.855	0.911	0.985
(b) calculated from linear equations.	0.032	0.208	0.373	0.510	0.618	0.712	0.790	0.855	0.911	0.985
Linear Equations	$Y' = 0.425 X' - 0.019$					$Y = 2.38 X - 0.115$				

$$\sqrt{aa'} - \sqrt{bb'} = 1.000.$$

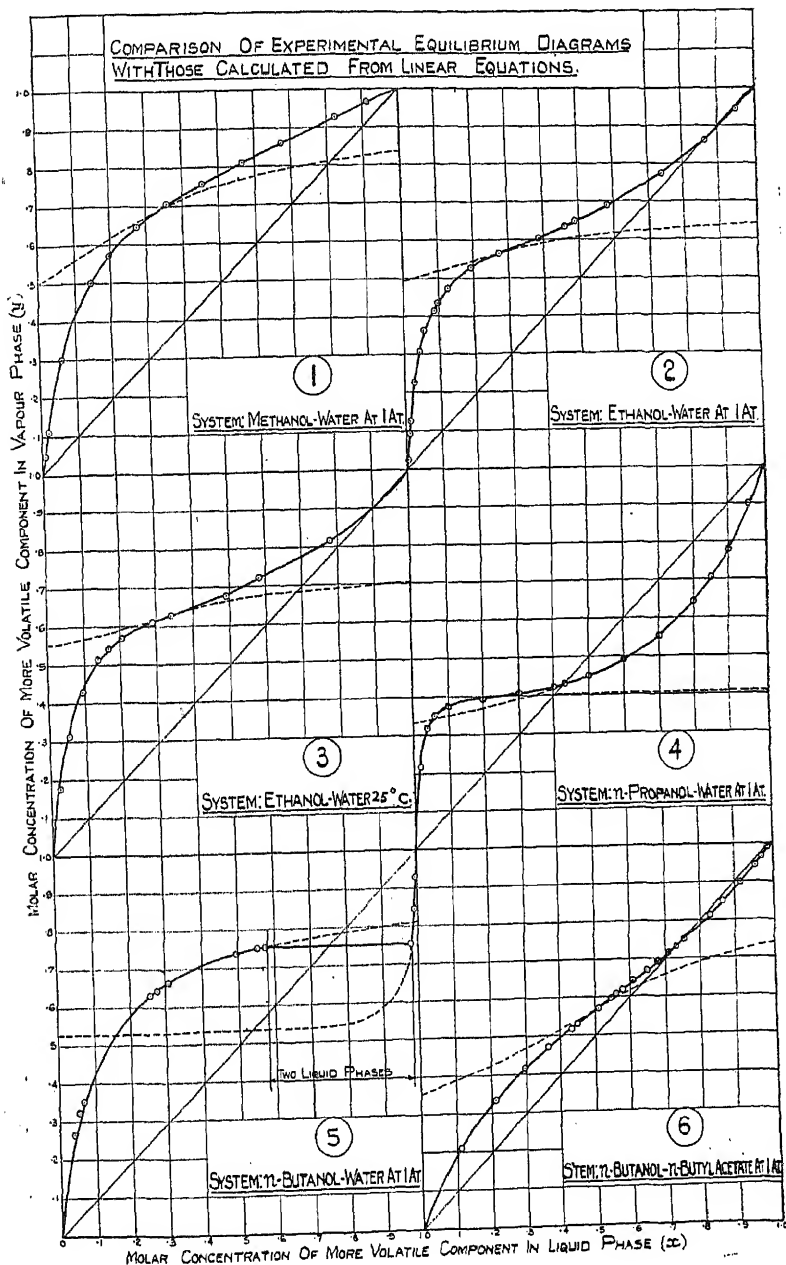
10. SYSTEM: BENZENE-*n*-HEPTANE (at 1 At.).

Temperature (°C.)	95.8	94.8	93.5	92.1	90.7	86.8	84.7	84.4	83.1	82.15	81.8	81.2	80.45	80.15
Mol. fraction of benzene in liquid phase ( <i>x</i> )	0.052	0.116	0.162	0.210	0.264	0.424	0.538	0.554	0.638	0.716	0.750	0.819	0.903	0.955
Mol. fraction of benzene in vapour phase ( <i>y</i> )														
(a) experimental	0.116	0.224	0.297	0.357	0.426	0.594	0.692	0.691	0.738	0.789	0.813	0.862	0.921	0.960
(b) calculated	0.108	0.223	0.297	0.300	0.427	0.586	0.677	0.693	0.740	0.790	0.814	0.861	0.924	0.964
Linear Equations	$Y' = 0.445 X' + 0.10$					$Y = 1.23 X + 0.66$								

$$\sqrt{aa'} + \sqrt{bb'} = 0.996.$$

is imminent at this point. This suggestion is emphasised by the behaviour of System 5.

System 5. *Water-n-Butanol at 1 At.*—Experimental results by Stockhardt and Hull.<sup>9</sup>



<sup>9</sup> Stockhardt and Hull, *Ind. Eng. Chem.*, 1931, 23, 1438.



TABLE I (continued).

## 9. SYSTEM: BENZENE-TOLUENE (at 1 At.).

Mol. fraction of benzene in liquid phase ( $x$ )	0.014	0.10	0.20	0.30	0.40	0.50	0.60	0.70	0.80	0.962
Temperature ( $^{\circ}$ C.)	110.0	106.3	102.3	98.8	95.5	92.4	89.5	86.9	84.5	81.0
Mol. fraction of benzene in vapour phase ( $y$ )										
(a) calculated from Raoult's Law	0.032	0.207	0.374	0.509	0.620	0.713	0.790	0.855	0.911	0.985
(b) calculated from linear equations.	0.032	0.208	0.373	0.510	0.618	0.712	0.790	0.855	0.911	0.985
Linear Equations	$Y' = 0.425 X' - 0.019$					$Y = 2.58 X - 0.115$				

$$\sqrt{aa'} - \sqrt{bb'} = 1.000.$$

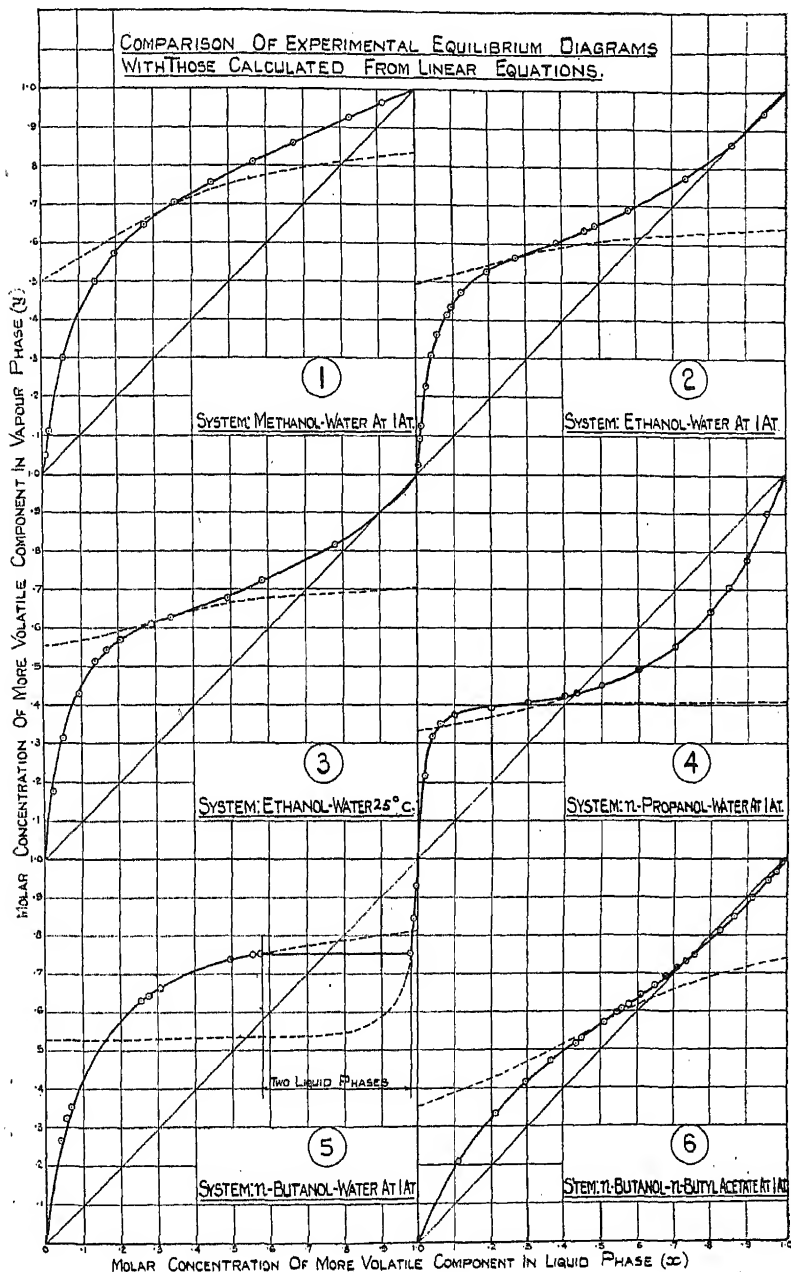
10. SYSTEM: BENZENE-*n*-HEPTANE (at 1 At.).

Temperature ( $^{\circ}$ C.)	96.8	94.8	93.5	92.1	90.7	86.8	84.7	84.4	83.1	82.15	81.8	81.2	80.45	80.15
Mol. fraction of benzene in liquid phase ( $x$ )	0.052	0.116	0.162	0.210	0.264	0.424	0.538	0.554	0.638	0.716	0.750	0.819	0.903	0.955
Mol. fraction of benzene in vapour phase ( $y$ )														
(a) experimental	0.116	0.224	0.297	0.357	0.426	0.594	0.692	0.691	0.738	0.789	0.813	0.862	0.921	0.960
(b) calculated	0.108	0.223	0.297	0.360	0.427	0.586	0.677	0.693	0.740	0.790	0.814	0.861	0.924	0.964
Linear Equations	$Y' = 0.445 X' + 0.10$					$Y = 1.23 X + 0.66$								

$$\sqrt{aa'} + \sqrt{bb'} = 0.996.$$

is imminent at this point. This suggestion is emphasised by the behaviour of System 5.

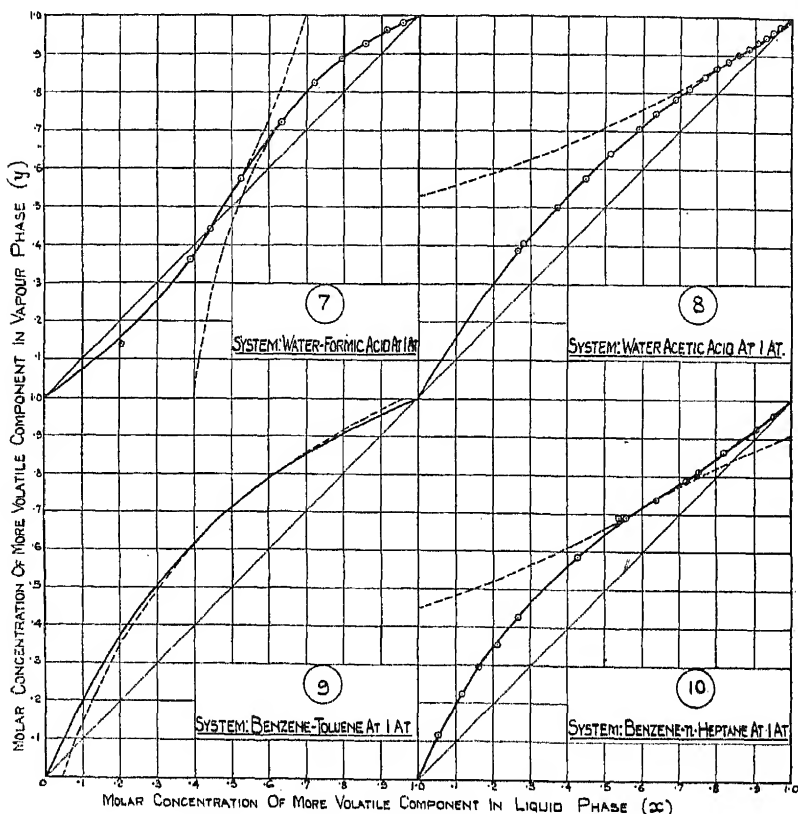
*System 5. Water-n-Butanol at 1 At.*—Experimental results by Stockhardt and Hull.<sup>9</sup>



<sup>9</sup> Stockhardt and Hull, *Ind. Eng. Chem.*, 1931, 23, 1438.

This system forms two liquid phases over the range of liquid composition between  $x = 0.58$  and  $x = 0.98$ . The two parts of the equilibrium curve can be accurately expressed by linear equations, but the calculated curves have no common tangent ( $\sqrt{aa'} + \sqrt{bb'} = 0.579$ ). The equations do not define precisely the three-phase area, but it must obviously occur within the range in which the two calculated curves overlap. According to Carlson and Colburn<sup>4</sup> this system cannot be reconciled with any of the integrated forms of the Gibbs-Duhem equation.

*System 6. n-Butanol-n-Butyl Acetate at 1 At.*—Experimental results by Brunjes and Furnas.<sup>10</sup>



*System 7. Water-Formic Acid at 1 At.*—Experimental results by Othmer.<sup>11</sup> There is good agreement between experimental and calculated values above the conjugate point, but there is a discrepancy at the lowest water concentration and some lack of continuity between the two curves ( $\sqrt{aa'} + \sqrt{bb'} = 0.91$ ). As pointed out by Carlson and Colburn, formic acid is associated in the vapour phase, which therefore cannot behave as a perfect gas. The Van Laar equations, or other integrations of the Gibbs-Duhem equation which depend on this assumption cannot therefore be expected to apply to this system. The experimental data below the conjugate point are too scanty to decide whether the linear rule is

<sup>10</sup> Brunjes and Furnas, *ibid.*, 1935, 27, 396.

<sup>11</sup> Othmer, *ibid.* (Anal), 1932, Ed. 4, 232.

also invalid, or whether the experimental results themselves are at fault. This system deserves further experimental study.

*System 8. Water-Acetic Acid.*—Experimental results by Cornell and Montonna.<sup>7</sup>

This system is of particular interest, as acetic acid is also associated in the vapour phase, and it would therefore be expected to show anomalous behaviour if the linear rule were restricted to systems with a perfect vapour phase. In fact, the calculated values are almost perfectly coincident with the experimental results. If the equilibrium data given in Perry<sup>6</sup> are used there is an apparent anomaly. This evidently arises from an attempt to reconcile the results of Cornell and Montonna with those of Bergstrom, as quoted by Hausbrand.<sup>12</sup> There is a slight discrepancy between the two which is clearly brought out by applying the linear rule. The system is further interesting on account of the high concentration of the more volatile component at the conjugate point ( $x = 0.86$ ), and the low value of the constant  $b'$  (0.013). The result is that the system over most of the range of concentration appears to behave almost as if the two components had constant relative volatility, and the slight inflexion at the conjugate point which is strongly emphasised when the linear rule is applied to the results of Cornell and Montonna is otherwise apt to be overlooked. The conformity of this system with the linear rule emphasises the necessity for further work on the formic acid-water system.

*System 9. Benzene-Toluene at 1 At.*—This system is commonly regarded as "ideal" in its conformity with Raoult's Law, and this view is supported by experiment.<sup>13, 14</sup> There is, however, sufficient difference between the molar latent heats of the components to make the use of a constant value for the relative volatility unreliable. The composition of the phases has therefore been calculated by the use of Raoult's Law and the vapour pressures of the pure components at temperatures between their respective boiling-points. The calculated temperatures agree almost exactly with those given in the International Critical Tables for the boiling-points of corresponding mixtures of the pure components. The values of vapour composition thus calculated are used in the case of this system instead of actual experimental values to test the application of the linear rule. The two sets of values coincide within the accuracy of calculation.

*System 10. Benzene-n-Heptane at 1 At.*—The experimental results for this system were obtained by the author, and have not previously been published. The experimentally-determined equilibrium temperatures are also given. Conformity with the linear equations appears to be within experimental error.

**General Comments.**—From the cases which have been examined in detail, it is clear that the linear rule provides a simple and highly accurate relation between the compositions of liquid and vapour at equilibrium for a large number of binary systems, either at constant pressure or at constant temperature. Although this relation is mainly empirical, its accuracy appears to be within experimental error, with one or two doubtful exceptions. It is concluded that the rule is sufficiently accurate and widely valid for it to be used with confidence in the mathematical development of distillation theory.

The linear equations do not, of course, present a complete expression of the equilibrium relations, as they give no information concerning the variation of temperature or pressure with composition. In this respect they do not compete with the equations of Van Laar, Margules and Scatchard, by which the activities of the components are separately

<sup>12</sup> Hausbrand, *Principles and Practice of Industrial Distillation*, 1926. Translated by Tripp, Wiley, New York.

<sup>13</sup> Bell and Wright, *J. Physic. Chem.*, 1927, **31**, 1884.

<sup>14</sup> Zmaczynski, *J. Chim. Physique*, 1930, **27**, 503.

defined, but within this limitation they appear to have a wider validity than any equations which have been proposed hitherto.

### Relation Between Linear Rule and Van Laar Equations.

According to Carlson and Colburn <sup>4</sup> the equations of Van Laar present the most useful and generally valid integration of the Gibbs-Duhem relation. As re-arranged by these authors, but with reference to the exponential base, these equations are :

$$\log_e \gamma_1 = \frac{A}{\left[1 + \frac{Ax_1}{Bx_2}\right]^2} \quad \dots \quad (9a)$$

$$\log_e \gamma_2 = \frac{B}{\left[1 + \frac{Bx_2}{Ax_1}\right]^2} \quad \dots \quad (9b)$$

in which  $A$  and  $B$  are constants representing the terminal values of  $\log \gamma_1$  and  $\log \gamma_2$  respectively at zero concentration of the corresponding component. This relation is obtained by putting  $x_1 = 0$  in eq. (9a) and  $x_2 = 0$  in eq. (9b). These equations, when used in conjunction with the vapour pressures of the pure components, express completely the equilibrium of a binary system with the use of only two adjustable constants,  $A$  and  $B$ . The linear equations use four adjustable constants,  $a$ ,  $b$ ,  $a'$  and  $b'$ , although these are usually restricted by the continuity condition ( $\pm \sqrt{aa'} \pm \sqrt{bb'} = 1$ ). It is of interest to examine how far the linear rule is compatible with the Van Laar equations, since the use of only two constants in the latter suggests that a systematic relation should exist between the  $a$  and  $b$  constants of the linear equations, at least in the case of systems to which the Van Laar equations apply.

There is a simple relation between the Van Laar constants and the " $a$ " values in the linear equations. By making  $x_1$  and  $x_2$  zero in eqns. (9a) and (9b) respectively, it is seen that

$$A = \log_e (\gamma_1)_0 \quad \text{and} \quad B = \log_e (\gamma_2)_0,$$

i.e.  $A$  and  $B$  are the limiting values of the logarithms of the activity coefficients of the two components at zero concentration. Also, for the pure components the activity coefficients are unity.

According to the linear rule, for high values of  $x_1$  (or  $X$ ) :

$$\frac{\gamma_1}{\gamma_2} = \frac{P_1 \gamma_1 x_1}{P_2 \gamma_2 x_2} \equiv a \frac{x_1}{x_2} + b,$$

$$\text{or} \quad Y = \frac{P_1 \gamma_1 X}{P_2 \gamma_2} \equiv aX + b.$$

$$\text{Differentiating :} \quad \frac{dY}{dX} = \frac{P_1 \gamma_1}{P_2 \gamma_2} = a,$$

$$\text{as} \quad x_1 \rightarrow 1.0, \quad X \rightarrow \infty \quad \text{and} \quad \gamma_1 \rightarrow 1 \quad \text{while} \quad \gamma_2 \rightarrow (\gamma_2)_0.$$

$$\text{Therefore :} \quad \text{Lt} \quad \frac{dY}{(X \rightarrow \infty) dX} = \left(\frac{P_1}{P_2}\right)_{T_1} \frac{1}{(\gamma_2)_0} = a.$$

Hence  $a$  is the limiting value of the relative activity of the two components when component 2 is at zero concentration.

Substituting for  $(\gamma_2)_0$

$$B = \log_e \left(\frac{P_1}{P_2}\right)_{T_1} - \log_e a \quad \dots \quad (10b)$$

$$\text{Similarly :} \quad A = \log_e \left(\frac{P_2}{P_1}\right)_{T_2} - \log_e a' \quad \dots \quad (10a)$$

$P_1$  and  $P_2$  are the vapour pressures of the pure components at the same temperature, fixed by the conditions at either end of the system. The Van Laar constants can thus be obtained readily from the "a" constants of the linear equations:

By combining equations (3), (9a) and (9b), and substituting  $Y = y_1/y_2$  and  $X = x_1/x_2$  the Van Laar equations yield the following relation between  $Y$  and  $X$  over the whole system.

$$Y = \frac{P_1}{P_2} X e^{\frac{AB(B-AX^2)}{(B+AX)^2}} \quad (11)$$

By differentiation :

$$\frac{dY}{dX} = \frac{P_1}{P_2} e^{\frac{AB(B-AX^2)}{(B+AX)^2}} \left[ 1 - \frac{2A^2B^2X(X+1)}{(B+AX)^3} \right] \quad (12)$$

If the Van Laar equations are to give a linear relation between  $X$  and  $Y$  at high values of  $X$  and  $Y$  the value of this differential must approach a constant value as  $X$  increases, and the differential may then be described by the linear equation :

$$Y = X \frac{dY}{dX} + d \quad (13)$$

Substituting for  $dY/dX$  from eq. (12), and for  $Y$  from eq. (11), we obtain the following expression for  $d$  :

$$d = \frac{P_1}{P_2} e^{\frac{AB(B-AX^2)}{(B+AX)^2}} \left[ \frac{2A^2B^2X^2(X+1)}{(B+AX)^3} \right] \quad (14)$$

In the limit ( $X \rightarrow \infty$ ) this expression reduces to :

$$\left( \text{Lt. } X \rightarrow \infty \right) d = \left( \frac{P_1}{P_2} \right)_{T_1} e^{-B} \frac{2B^2}{A} \quad (15)$$

Similarly, as  $X$  increases,  $dY/dX$  approaches its limiting value

$$\left( \text{Lt. } X \rightarrow \infty \right) \frac{dY}{dX} = \left( \frac{P_1}{P_2} \right)_{T_1} e^{-B} \quad (16)$$

At the limit of concentration at which the concentration of the more volatile component approaches unity, the Van Laar equations thus give a linear relation between  $X$  and  $Y$ , expressed by the equation :

$$Y = \left( \frac{P_1}{P_2} \right)_{T_1} e^{-B} X + \left( \frac{P_1}{P_2} \right)_{T_1} e^{-B} \frac{2B^2}{A}$$

This is the equation of the asymptote to the curve represented by eq. (11). The corresponding equation at the opposite limit of concentration is :

$$Y' = \left( \frac{P_2}{P_1} \right)_{T_2} e^{-A} X' + \left( \frac{P_2}{P_1} \right)_{T_2} e^{-A} \frac{2A^2}{B}$$

If these equations are to be identified with the corresponding linear equations at the extremes of concentration, the following relations must be satisfied :

$$\begin{aligned} \text{(i)} \quad a &= \left( \frac{P_1}{P_2} \right)_{T_1} e^{-B} & \text{(ii)} \quad b &= \left( \frac{P_1}{P_2} \right)_{T_1} e^{-B} \frac{2B^2}{A} \\ \text{(iii)} \quad a' &= \left( \frac{P_2}{P_1} \right)_{T_2} e^{-A} & \text{(iv)} \quad b' &= \left( \frac{P_2}{P_1} \right)_{T_2} e^{-A} \frac{2A^2}{B} \end{aligned} \quad (17)$$

The Van Laar equations may be reconciled with the linear rule over the whole system if these relations hold, and if the values of the constants  $A$  and  $B$  are of an order which makes the differential coefficient (eq. 12)

practically constant for all values of  $X$  above a certain small value, while the differential coefficient  $dY'/dX'$  is also practically constant for all values of  $X'$  above the reciprocal of the same small value.

If this reconciliation can be effected for a given system, the linear rule becomes a corollary of the Van Laar equations, and relations may be obtained between the constants of the linear equations which limit the number of constants necessary to define the system to the two ( $A$  and  $B$ ) which are used by Van Laar (at constant temperature).

Elimination of  $A$  and  $B$  from the set of equations (17) readily gives the following relations between the  $a$  and  $b$  constants of the linear equations:

$$b = \frac{2aB^2}{A} = \frac{-2a \left[ \log_e \frac{1}{a} \left( \frac{P_1}{P_2} \right)_{T_1} \right]^2}{\log_e \left[ a' \left( \frac{P_1}{P_2} \right)_{T_2} \right]} \quad (18a)$$

$$b' = \frac{2a'A^2}{B} = \frac{2a' \left[ \log_e a' \left( \frac{P_1}{P_2} \right)_{T_2} \right]^2}{\log_e \left[ \frac{1}{a} \left( \frac{P_1}{P_2} \right)_{T_1} \right]} \quad (18b)$$

The correlation between the linear rule and the Van Laar equations may be tested by comparing the values of  $b$  and  $b'$  calculated from equations (18a) and (18b) with those obtained directly from the empirical equations fitted to the experimental results. This is done in the following table:

TABLE II.

No.	System.	$a$ .	$a'$ .	$b$ .		$b'$ .		$\left(\frac{P_1}{P_2}\right)_{T_1}$	$\left(\frac{P_1}{P_2}\right)_{T_2}$	$T_1$ °C.	$T_2$ °C.
				Found.	Calcd.	Found.	Calcd.				
1	2	3	4	5	6	7	8	9	10	11	12
1	Methanol-Water (1 at.)	2.43	0.131	1.0	1.68	0.20	0.31	4.11	3.45	64.46	100
2	Ethanol - Water (1 at.)	0.885	0.077	0.97	0.92	0.565	0.50	2.300	2.228	78.3	100
3	Ethanol - Water (25° C.)	0.86	0.085	1.26	1.24	0.42	0.39	2.48	2.48	(25)	(25)
4	<i>n</i> -Propanol-Water (1 at.)	0.33	0.027	0.50	0.272	1.45	0.55	1.10	1.10	97.19	100
5	Water- <i>n</i> -Butanol (1 at.)	0.036	0.12	1.10	0.76	0.24	0.14	2.0	1.8	100	117.7
6	<i>n</i> -Butanol- <i>n</i> -Butyl Acetate (1 at.)	0.80	0.44	0.54	0.67	0.35	0.57	1.3	1.3	117.7	126.5
7	Water - Formic Acid (1 at.)	2.48	1.57	-1.64	-8.7	-0.69	-0.74	1.01	1.01	100	100.7
8	Water - Acetic Acid (1 at.)	1.345	0.58	1.10	-3.23	0.013	0.022	1.82	1.86	100	118.2
9	Benzene-Toluene (1 at.)	—	—	—	—	—	—	—	—	80.12	110.6
10	Benzene- <i>n</i> -Hep- tane (1 at.)	1.23	0.445	0.66	1.18	0.10	0.19	1.77	1.69	80.1	98.4

Strictly speaking, the Van Laar equations should be applied only to systems at constant temperature. The activity coefficients vary only slowly with temperature, however, and it may usually be assumed that they remain constant over the temperature range covered by the system at constant pressure. When the relative volatility of the components

also remains fairly constant over the same temperature range, as in the case of most of the systems studied (col. 9 and 10) the calculated constants (col. 6 and 8) might be expected to show good qualitative agreement with those of the linear equations (col. 5 and 7) if the Van Laar equations are to express the equilibrium accurately. The only example in which the comparison is strictly valid is No. 3—ethanol-water at the constant temperature of 25° C. This case shows very close agreement between the values of the  $b$  constants obtained by the two methods, from which it may be deduced that both the Van Laar and the linear equations express this equilibrium accurately.

For the same system under constant pressure (No. 2) the agreement is reasonably close, although there is a temperature variation of about 22° C. One might therefore expect other systems to show a like measure of agreement over a similar temperature range.

For most of the other systems, however, the agreement is by no means so good, although with some outstanding exceptions there appears to be a rough correlation between the values of corresponding constants. Excluding the doubtful case of water and formic acid, the most notable discrepancy is between the two values of the " $b$ " constant for the system water-acetic acid. The linear rule accurately expresses the behaviour of this system, while the Van Laar equations are invalid both on practical and theoretical grounds. On the whole it would appear that the linear equations express the relation between liquid and vapour composition more accurately at constant pressure than the Van Laar equations, and have a wider application. The empirically determined form of the " $b$ " constants appears more reliable than that calculated from the Van Laar relations, even at constant temperature, while at constant pressure it provides an additional parameter which covers changes in relative vapour pressures of the pure components with temperature. It is suggested that the linear equations rest on the same thermodynamic basis as the equations of Van Laar and others, but that they contain a hidden cancellation of some of the errors which arise from the approximating assumptions which are made in deriving expressions for the separate activity coefficients.

### Summary.

It is demonstrated that the compositions of liquid and vapour phases of a binary system of two volatile components can be accurately represented, in the majority of cases, by a combination of two linear equations of the type  $Y = aX + b$  in which  $Y$  and  $X$  are the molar ratios of the components, with the dominant component providing the numerator, and  $a$  and  $b$  are empirical constants. The constant  $a$  can be identified with the activity ratio of the components when the dominant component is at a concentration of unity. It is shown that, under certain circumstances, these empirical linear equations can be reconciled with integrated forms of the Gibbs-Duhem equation, particularly the Van Laar integration, and in such cases a systematic relation exists between the  $a$  and  $b$  constants of the linear equations. On the whole, however, the linear equations appear to be more accurate and more widely valid than the Van Laar equations, which should, in theory, be restricted to constant temperature and pressure.

The linear equations do not give a complete statement of equilibrium conditions, as they do not define the temperature of the system, but on account of their simplicity and wide application they are aptly suited to the mathematical treatment of the theory of fractional distillation. Their use for this purpose is developed in Part II of this communication.



## PART II.

### APPLICATION TO THE THEORY OF PRACTICAL DISTILLATION.

(A table of nomenclature is given at the beginning of Part I.)

In Part I of this communication it has been shown that the liquid and vapour compositions of a system of two volatile components may be related by means of simple equations. This section demonstrates the use of these equations in the mathematical treatment of the theory of fractional distillation, and develops a number of general relations between the change in composition of the phases and the other variants of a distillation system.

#### Theoretical Basis.

According to the theorem of McCabe and Thiele,<sup>15</sup> the behaviour of a system undergoing fractional distillation may be defined by means of two curves within the same axes, and described as the equilibrium line and operating line respectively. The graph thus formed is known as the operating diagram. The equilibrium line relates the compositions of the two phases at equilibrium, while the operating line relates the actual compositions of the two phases in contact at different parts of the fractionating system, under conditions of dynamic equilibrium within the apparatus. The operating line is fixed solely by the necessity for satisfying the laws of conservation of mass and energy within the system. The components of the system are transferred in either direction between the phases in a manner which is obviously determined by the deviation from equilibrium of the phases at any interface. This deviation is defined by the relative positions of the equilibrium and operating lines, but it cannot give a quantitative measure of the rate of approach to equilibrium, or the velocity of transfer between the phases, except in conjunction with other relations depending upon the mechanism of transfer and the factors controlling it. A number of different methods have been proposed for relating the change in composition which occurs in a fractionating column with the other variables of the system, which include reflux ratio, height of column, and properties of packing. These methods depend upon the theory which is adopted concerning the mechanism of transfer. At least three separate theories are at present in use for this purpose. They cannot readily be correlated because in the absence of simple relations between the compositions of the phases they must be applied very largely by graphical methods, which do not lend themselves to systematic comparison. For a complete statement of the theories the reader is referred to the original sources, but they may conveniently be alluded to under the following titles :

(i) *The Method of Theoretical Plates*.—This uses as a unit of transfer the change in composition which would be effected in one stage if the two phases moving countercurrently through the fractionating column were arrested at intervals and allowed to reach equilibrium before resuming their travel.

(ii) *The Method of Mass Transfer Units* (Chilton and Colburn <sup>16</sup>).—This method is based on the theory that fractional distillation follows a diffusional mechanism, the rate of diffusion of a given component across the interfacial boundary being governed by the difference between the actual partial pressure of that component in the vapour phase and its partial pressure in equilibrium with the liquid phase.

<sup>15</sup> McCabe and Thiele, *Ind. Eng. Chem.*, 1925, 17, 605.

<sup>16</sup> Chilton and Colburn, *ibid.*, 1935, 27, 255.

(iii) *The Heat Transfer Theory* (Kirschbaum<sup>17</sup>).—This theory depends upon the fact that the vapour in a distillation column is always at a higher temperature than the liquid in contact with it, but that heat can flow between the phases only by means which involve evaporation of the liquid and condensation of the vapour. The approach to thermal equilibrium is used as a measure of the approach to material equilibrium.

The mathematical relations between these several theories under certain conditions are developed in the following sections on the basis of the general equilibrium equations which have been described.

### (1) Calculation of Number of Theoretical Plates at Total Reflux.\*

The number of theoretical plates required to effect a given enrichment may be found by the erection of steps on the operating diagram alternating between the equilibrium and operating lines between the given limits of composition. If both lines are rectilinear, the areas enclosed by the steps and either line form a series of similar triangles, and there is a constant ratio between corresponding sides of consecutive triangles which is the same as the ratio of the slopes of the lines. The steps between the lines thus form a series in geometrical progression, and the number of theoretical plates required to effect a given change in concentration may be found by summation of this series.

Thus :

$$\Sigma = s_1 \frac{r^N - 1}{r - 1} \quad (1)$$

where  $\Sigma$  is the change in composition of a given phase between the two ends of the system,  $s_1$  is the change in composition produced by the first theoretical stage,  $r$  is the ratio of the slopes of the equilibrium and operating lines and  $N$  is the total number of theoretical plates required to effect the given enrichment.

When composition is expressed in terms of mol. ratios, the upper part of the equilibrium diagram is represented by the linear equation :

$$Y = aX + b$$

and the operating line at total reflux by the equation :

$$Y = X.$$

The given enrichment in terms of mol. ratio is  $X_2 - X_1 = \Sigma$ .

The enrichment performed by the first theoretical stage ( $s_1$ ) is :

$$s_1 = aX_1 + b - X_1.$$

The ratio of the slopes of the equilibrium and operating lines is :

$$r = a.$$

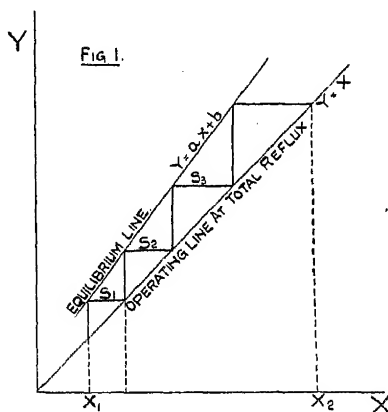
Substituting in the general equation (1) we get :

$$(X_2 - X_1) = [(a - 1)X_1 + b] \left[ \frac{a^N - 1}{a - 1} \right]$$

whence 
$$N \log a = \log \left[ \frac{X_2(a - 1) + b}{X_1(a - 1) + b} \right] \quad (2a)$$

<sup>17</sup> Kirschbaum, *Forschung Z.V.D.I.*, 1933, 77, 401. (See also ref. 6.)

\* This example is illustrated by Fig. 1.



This simple formula gives the number of theoretical plates at total reflux for any given enrichment in terms of the constants ( $a$  and  $b$ ) of the linear equation :

$$Y = aX + b.$$

In practice, care must be taken to use the linear equation which is valid for the part of the equilibrium diagram in which the enrichment takes place. If the range of enrichment includes the conjugate point the number of theoretical plates must be calculated in two steps, covering the ranges above and below the conjugate point respectively.

If the symbols  $X$  and  $Y$  are used to represent mol. ratios in the liquid and vapour phase respectively with the mol. quantity of the more volatile component as denominator, and  $X'$  and  $Y'$  are used to represent their reciprocals,

$$\text{i.e.} \quad X = \frac{1}{X'} = \frac{x}{1-x}$$

and

$$Y = \frac{1}{Y'} = \frac{y}{1-y}$$

where  $x$  and  $y$  have their usual significance as molar concentrations of the more volatile component in the two phases, then eq. (2a) may be used to obtain the number of theoretical plates above the conjugate point, while the corresponding equation for the part of the system below that point is :

$$N' \log a' = \log \left[ \frac{X'_2(a' - 1) + b'}{X'_1(a' - 1) + b'} \right] \quad (2b)$$

Substitution of mol. ratios by the more usual units of molar concentration gives the following pair of equations valid above and below the conjugate point respectively :

$$N \log a = \log \left[ \frac{(1 - x_1) \left( x_2 + \frac{b}{a - b - 1} \right)}{(1 - x_2) \left( x_1 + \frac{b}{a - b - 1} \right)} \right] \quad (3a)$$

$$N' \log a' = \log \left[ \frac{x_1 \left( \frac{a' - 1}{a' - b' - 1} - x_2 \right)}{x_2 \left( \frac{a' - 1}{a' - b' - 1} - x_1 \right)} \right] \quad (3b)$$

(In these equations the base of the logarithms is immaterial.)

These equations are less formidable than they appear at first sight, since they consist largely of easily evaluated constants.

In the case of the "ideal" system, the constants  $b$  and  $b'$  are zero, while  $a = 1/a' = \alpha$ , the "relative volatility" of the two components.

Equations (3a) and (3b) then both reduce to the form :

$$N \log \alpha = \log \left[ \frac{x_2(1 - x_1)}{x_1(1 - x_2)} \right] \quad (4)$$

which is the well-known Fenske<sup>18</sup>-Underwood<sup>19</sup> expression for the number of plates at total reflux in the case of the ideal system. In terms of mol. ratios, this equation becomes even more simple, *viz.*,

$$N \log \alpha = \log X_2/X_1 \quad (4a)$$

## (2) Application to Systems of which the Components have Different Molar Heats of Vaporisation.

When the components of a binary system have different molar heats of vaporisation, the operating line on the McCabe-Thiele diagram under

<sup>18</sup> Fenske, *Ind. Eng. Chem.*, 1932, **24**, 482.

<sup>19</sup> Underwood, *Tr. Inst. Chem. Eng.*, 1932, **10**, 112 (Eq. 9).

conditions of partial reflux ceases to be rectilinear when the compositions of the phases are expressed in terms of molar concentration. This complication is sometimes avoided by using arbitrary units of mass for each component, so chosen that a unit of each component has the same heat of vaporisation. This object may be achieved by attributing to one component—usually the less volatile—a fictitious molecular weight which effects the required adjustment. The units of mass thus obtained may be nominated "lols."

The use of "lolar" units of concentration requires an adjustment in the position of the equilibrium curve, except in the case of the "ideal" system, expressed by the equation:

$$\frac{y}{1-y} = \frac{P_1}{P_2} \cdot \frac{x}{1-x},$$

in which  $P_1/P_2$  remains constant. This equation gives the same relative values of concentration either in molar or lolar units. This case presents an impossibility, however, because thermodynamic considerations insist that  $P_1/P_2$  cannot remain constant if the molar heats of vaporisation are different. For this reason, although the use of "lolar" units may simplify graphical procedure, it has hitherto been of little assistance in the mathematical treatment of distillation, as such methods have been restricted to "ideal" systems.

When the linear equations are used to express the equilibrium of a system, the use of "lolar" units is much more generally useful, as the rectilinear relationship between the compositions of the phases is not impaired by the units of mass employed, and the procedure of mathematical analysis may consequently be extended to non-ideal systems. This is made clear in the following discussion.

By definition:

$$\begin{array}{lcl} 1 \text{ mol. of component 1} & = & 1 \text{ lol.} \\ 1 & \text{,,} & \text{,,} & 2 = K \text{ lols.} \end{array}$$

when  $K = Q_2/Q_1$  in which  $Q_1$  and  $Q_2$  are the molar heats of vaporisation of the respective components.

In terms of molar ratios the equilibrium curve for the system above the conjugate point is expressed by:

$$\begin{aligned} Y &= aX + b \\ \text{or} \quad y_1/y_2 &= ax_1/x_2 + b \end{aligned}$$

in which  $y_1/y_2$  and  $x_1/x_2$  represent the relative numbers of molecules of either component in each phase.

In terms of "lolar" ratios:

$$Y_L = y_1/Ky_2 = Y/K \quad \text{and} \quad X_L = x_1/Kx_2 = X/K$$

which give, on substituting in the linear equation:

$$Y_L = aX_L + b/K \quad . \quad . \quad . \quad . \quad (5a)$$

Similarly, below the conjugate point:

$$Y'_L = a'X'_L + b'K \quad . \quad . \quad . \quad . \quad (5b)$$

In terms of mass ratio, therefore, the equilibrium curve remains a straight line of which the slope is independent of the units of mass employed. A change in the units of mass involves an adjustment only of the constant term in the linear equation.

Equations (2a) and (2b), or (3a) and (3b), thus provide an accurate expression for the number of theoretical plates at total reflux, irrespective of the units of mass employed, provided the appropriate values of the  $b$  constants are used in the equations.

**(3) Calculation of Number of Theoretical Plates at Finite Reflux.**

It has been pointed out that the number of theoretical stages required to effect any given change in concentration in a system can readily be computed by means of a simple geometrical progression when both operating and equilibrium lines for the system can be expressed by linear equations in the same units. It has also been shown that, for a large number of binary systems, the equilibrium curve can be expressed by a pair of linear equations when composition is expressed in terms of molar or lolar ratios. When these units are adopted the operating curve at total reflux is also a straight line. Unfortunately, however, the operating line at partial reflux ceases to be rectilinear when expressed in molar (or lolar) ratios, although it remains straight when expressed in terms of molar concentration.

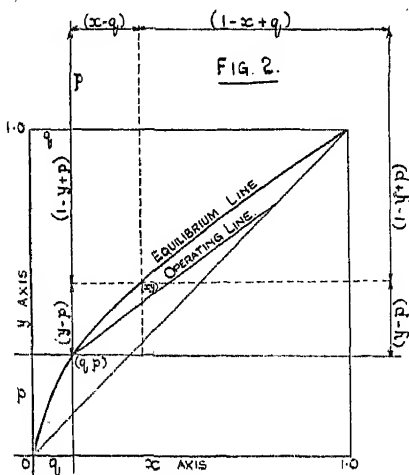
This is shown algebraically as follows :

The equation for the operating line at partial reflux in terms of molar concentrations may be written :

$$y = mx + \frac{1}{2}k.$$

To transpose to units of molar ratio, substitute  $y = \frac{Y}{Y+1}$  and  $x = \frac{X}{X+1}$ .

Then 
$$\frac{Y}{Y+1} = \frac{mX}{X+1} + k.$$



This equation is linear in  $X$  and  $Y$  only when  $m + k = 1$ , i.e. at total reflux ( $Y = X$ ), or when one of the components is separated in the pure state ( $x_a = 1.0$ ). The problem to be solved if the number of theoretical plates at finite reflux is to be calculated analytically is to find a unit of composition which gives both equilibrium and operating lines as linear equations. This is the problem which has, in effect, been solved by Smoker<sup>20</sup> in the case of the "ideal" system. It can be solved for systems which obey the straight line rule by similar methods. The basis of the procedure is given below, and is illustrated by Fig. 2.

**Case 1: At Low Concentrations of more Volatile Component.**—In terms of molar concentrations we have the following equations :

Equilibrium line : 
$$\frac{1-y}{y} = \frac{a'(1-x)}{x} + b' \quad \dots \quad B(1)$$

Operating line : 
$$y = mx + k \quad \dots \quad B(2)$$

Let  $(q, p)$  be the co-ordinates on the  $xy$  diagram (Fig. 2) of the point of intersection of the equilibrium and operating lines.

The values of  $q$  and  $p$  may be obtained by substituting them for  $x$  and  $y$  respectively in equations B(1) and B(2) and solving simultaneously.

Now, arbitrarily, let  $\phi' = \frac{1-y+p}{y-p}$  and  $\chi' = \frac{1-x+q}{(x-q)}$ .

<sup>20</sup> Smoker, *Tr. Am. Inst. Chem. Eng.*, 1938, 34, 165.

Then, in terms of  $\phi'$  and  $\chi'$ ,

$$y = \frac{p\phi' + p + 1}{\phi' + 1} \quad \text{and} \quad x = \frac{q\chi' + q + 1}{\chi' + 1}.$$

Substitute these values for  $x$  and  $y$  in equations B(1) and B(2).

This gives :

For the equilibrium line :

$$\frac{\phi'(1 - p) - p}{1 + p + \phi'p} = \frac{a'[\chi'(1 - q) - q]}{1 + q + \chi'q} + b' \quad \text{B(1a)}$$

and for the operating line :

$$\frac{1 + p + \phi'p}{\phi' + 1} = \frac{m(1 + q + \chi'q)}{\chi' + 1} + k \quad \text{B(2a)}$$

This substitution has the result of expressing the  $X', Y'$  relation in terms of co-ordinates  $\chi'$  and  $\phi'$  originating at the point of intersection of the equilibrium and operating lines.  $\chi'$  and  $\phi'$  are arbitrary units of composition which are of value only if their use gives linear equations for the operating and equilibrium lines. It remains, therefore, to show that equations B(1a) and B(2a) are both linear in  $\phi'$  and  $\chi'$ . The test of linearity is that terms in  $\phi' \chi'$  should cancel one another (after fractions have been eliminated).

The collected terms in  $\phi' \chi'$  from eq. B(1a) are :

$$\phi' \chi' [q(1 - p) - a'p(1 - q) - b'pq].$$

But, since values of  $p$  and  $q$  satisfy both equations B(1) and B(2), we get, from eq. B(1) :

$$\frac{1 - p}{p} = \frac{a'(1 - q)}{q} + b'$$

$$\therefore q(1 - p) - a'p(1 - q) - b'pq = 0.$$

The collected terms in  $\phi' \chi'$  from eq. B(1a) thus cancel one another, and eq. B(1a) is therefore linear in  $\phi'$  and  $\chi'$ .

Similarly, collected terms in  $\phi' \chi'$  from eq. B(2a) are :

$$\phi' \chi' (p - mq - k).$$

But from eq. B(2),

$$p = mq + k.$$

Terms in  $\phi' \chi'$  therefore cancel one another, and eq. B(2) is also linear in  $\phi'$  and  $\chi'$ .

We have thus fulfilled the required condition that both operating and equilibrium lines should be expressed by linear equations, and from this point the number of theoretical plates may be simply calculated by means of the geometrical progression rule (see p. 739).

The validity of this procedure has been proved for the lower part of the  $xy$  diagram, *i.e.* when the equilibrium may be expressed by eq. B(1). It remains to extend the procedure to the upper part of the diagram, above the conjugate point.

**Case 2: At High Concentrations of more Volatile Component.**—The equilibrium equation is :

$$\frac{y}{1 - y} = \frac{ax}{1 - x} + b \quad \text{T(1)}$$

The operating equation is :

$$y = mx + k \quad \text{T(2)}$$

This time, substitute for  $x$  and  $y$  in terms of  $\chi$  and  $\phi$ , defined by the relations :

$$\phi = \frac{1 - p - y}{p - y} \quad \text{and} \quad \chi = \frac{1 - q - x}{q - x}$$

where  $p$  and  $q$  are obtained by substituting for  $y$  and  $x$  respectively in equations T(1) and T(2) and solving simultaneously.

Now the equilibrium equation in terms of  $x$  and  $\phi$  becomes :

$$\frac{1 - p - p\phi}{p + p\phi - \phi} = \frac{a(1 - q - qx)}{(q + qx - x)} + b \quad . \quad . \quad T(1a)$$

and the operating equation becomes :

$$\frac{1 - p - p\phi}{1 - \phi} = \frac{m(1 - q - qx)}{(1 - x)} + k \quad . \quad . \quad T(2a)$$

By the same procedure as in Case 1, it may be shown that both these equations are linear in  $\phi$  and  $x$ , and the proof of the method is therefore complete.

### General Procedure for Analytical Estimation of Number of Theoretical Plates.

A general procedure may now be formulated for the estimation, entirely by analytical methods, of the number of theoretical plates required to effect a given separation at any given reflux ratio, for any system which obeys the straight-line rule.\* The method is accurate even for systems of which the components have different molar latent heats, provided that equations based on "lolar" units are used. The perfect system provides a special case which falls within the general procedure.

The procedure to be followed is laid down as a number of consecutive steps :

(1) Obtain the equilibrium curve for the system in the form of the two alternative linear equations :

$$Y' = a'X' + b' \quad . \quad . \quad . \quad (B)$$

$$\text{and} \quad Y = aX + b \quad . \quad . \quad . \quad (T)$$

and determine their conjugate point. The terms in  $Y$  and  $X$  may be either in molar or latent heat units, whichever are appropriate.

(2) Decide which linear equation to use, according to whether that part of the system in which the enrichment takes place lies above or below the conjugate point on the  $xy$  diagram. If the range of enrichment includes the conjugate point, a separate calculation must be made for each portion of the range on either side of that point.

(3) Obtain the operating equation in the form :

$$y = mx + k$$

and the equilibrium equation in the appropriate form in units of molar concentration, *i.e.*

$$\frac{1 - y}{y} = \frac{a'(1 - x)}{x} + b' \quad . \quad . \quad . \quad (B)$$

$$\text{or} \quad \frac{y}{1 - y} = \frac{ax}{1 - x} + b \quad . \quad . \quad . \quad (T)$$

(4) Substitute the values  $y = p$  and  $x = q$  in both the operating and equilibrium equations and solve simultaneously to obtain numerical values of  $p$  and  $q$ .

(5) Substitute numerical values for  $a$  (or  $a'$ ),  $b$  (or  $b'$ ),  $k$ ,  $m$ ,  $p$ , and  $q$  in the equations :

\* An exceptional case which cannot be solved by means of this procedure must, however, be noted. In certain systems, *e.g.* ethanol-water, when the equilibrium curve above the conjugate point is convex towards the  $x$ -axis, the operating line may fail to intersect the appropriate portion of the equilibrium line, and the co-ordinates ( $q$ ,  $p$ ) become imaginary. No simple solution to the problem has been found for such cases.

*Operating*

$$\frac{1 + p + p\phi'}{1 + \phi'} = \frac{m(1 + q + q\chi')}{1 + \chi'} + k \quad . \quad . \quad . \quad (B)$$

or

$$\frac{1 - p - p\phi}{1 - \phi} = \frac{m(1 - q - q\chi)}{1 - \chi} + k \quad . \quad . \quad . \quad (T)$$

*Equilibrium*

$$\frac{\phi' - p\phi' - p}{1 + p + p\phi'} = \frac{a'[\chi' - q\chi' - q]}{1 + q + q\chi'} + b' \quad . \quad . \quad . \quad (B)$$

or

$$\frac{1 - p - p\phi}{p + p\phi - \phi} = \frac{a[1 - q - q\chi]}{q + q\chi - \chi} + b \quad . \quad . \quad . \quad (T)$$

These equations are linear in  $\phi$  (or  $\phi'$ ) and  $\chi$  (or  $\chi'$ ). They may therefore be readjusted (neglecting terms in  $\phi\chi$  or  $\phi'\chi'$ ) to simple linear equations of the form :

*Operating*

$$\phi' = \lambda'\chi' + \sigma' \quad . \quad . \quad . \quad . \quad (B)$$

or

$$\phi = \lambda\chi + \sigma \quad . \quad . \quad . \quad . \quad (T)$$

*Equilibrium*

$$\phi' = \delta'\chi' + \tau' \quad . \quad . \quad . \quad . \quad (B)$$

or

$$\phi = \delta\chi + \tau \quad . \quad . \quad . \quad . \quad (T)$$

in which  $\delta$ ,  $\lambda$ ,  $\sigma$  and  $\tau$  have numerical values.

(6) Express  $x_1$  and  $x_2$  (the compositions at either end of the enrichment range) in terms of  $\chi_1$  (or  $\chi'_1$ ) and  $\chi_2$  (or  $\chi'_2$ ) by substituting in the equations :

$$\chi' = \frac{1 - (x - q)}{x - q} \quad . \quad . \quad . \quad . \quad (B)$$

or

$$\chi = \frac{1 - (x + q)}{q - x} \quad . \quad . \quad . \quad . \quad (T)$$

(7) The number of theoretical plates required to perform the enrichment between  $x_1$  and  $x_2$  is finally obtained by substituting the derived values in the following equation, and solving it for  $N$  (the number of theoretical plates).

$$N' \log \frac{(\delta')}{(\lambda')} = \log \left[ \frac{\chi'_2(\delta' - \lambda') + \tau' - \sigma'}{\chi'_1(\delta' - \lambda') + \tau' - \sigma'} \right] \quad . \quad . \quad . \quad (B)$$

or

$$N \log \frac{(\delta)}{(\lambda)} = \log \left[ \frac{\chi_2(\delta - \lambda) + \tau - \sigma}{\chi_1(\delta - \lambda) + \tau - \sigma} \right] \quad . \quad . \quad . \quad (T)$$

In detailing this procedure, where alternative equations are given, they have been labelled either (B) or (T). For compositions below the conjugate point on the  $(x, y)$  diagram the (B) series must be followed. Above the conjugate point the (T) series is valid. The most complicated case is that of a continuous still operating at finite reflux, when the range of enrichment includes the conjugate point. This system has two operating lines, one of which extends on either side of the conjugate point. If the number of theoretical plates required for this system is to be determined entirely by analytical methods the systems must be divided, for purposes of calculation, into three sections, the intervening boundaries of which are at the  $x$  values occurring at the conjugate point and at the point of intersection of the two operating lines. The analytical procedure is then carried out for each section in turn.

Although this procedure is no more complicated than that involved in the application of the Smoker method to the perfect system at finite reflux, it is not the author's intention to suggest that it should, in general, be substituted for the more usual graphical method. In most cases its use would be more in the nature of a *tour de force* in analytical procedure



than a convenient means of computation. Even in those cases which do not readily lend themselves to graphical methods it is usually possible to devise, by the use of approximations, more simple analytical methods than that involved by the full procedure, without appreciable loss in accuracy.

#### (4) Application of the Linear Rule to the Calculation of Mass Transfer Units.

When fractional distillation is performed in packed towers as distinct from bubble-plate columns, it has been proposed by Chilton and Colburn<sup>16</sup> to use, as a basis for still design, a unit which avoids the suggestion of discontinuity implied by the theoretical plate concept, and which regards fractional distillation as a process of material diffusion. The unit proposed is the "mass transfer unit" and it is defined by the equation:

$$N_M = \int_{y_1}^{y_2} \frac{dy}{y^* - y} \quad \dots \quad C(1)$$

in which  $N_M$  is the number of mass transfer units required to perform an enrichment between the limits of vapour phase composition denoted by  $y_1$  and  $y_2$ ;  $y^*$  is the composition of the vapour in equilibrium with a liquid of composition  $x$ , and  $y$  is the composition of the vapour in contact with a liquid of composition  $x$ .

In other words  $(x, y^*)$  and  $(x, y)$  are the co-ordinates of points on the equilibrium and operating lines on the  $(x, y)$  diagram for a given value of  $x$ .

Alternatively, since the operating line may be given the equation:

$$y = mx + k, \text{ whence } dy = m dx,$$

we may write:

$$N_M = \int_{x_1}^{x_2} \frac{m dx}{y^* - y} \quad \dots \quad C(1a)$$

and, at total reflux, when  $m = 1$ , and  $y = x$ :

$$N_{MT} = \int_{x_1}^{x_2} \frac{dx}{y^* - x} \quad \dots \quad C(2)$$

Equation C(2) can readily be integrated mathematically in the case of the "ideal" system, when:

$$\frac{y^*}{1 - y^*} = \frac{\alpha x}{1 - x}$$

giving:

$$N_{MT} = \int_{x_1}^{x_2} \frac{dx}{y^* - x} = \log_e \left[ \frac{1 - x_1}{1 - x_2} \right] + \frac{1}{\alpha - 1} \log_e \left[ \frac{x_2(1 - x_1)}{x_1(1 - x_2)} \right].$$

The integration of the equation for the perfect system under finite reflux has been performed by Underwood<sup>21</sup> by means of a procedure similar to that used by Smoker in calculating the number of theoretical plates under the same conditions.

In the absence of simple equations for the equilibrium curve of an imperfect system, however, the integration of any of these equations in the general case has had to be performed graphically, a tedious necessity which has considerably hampered the use of the method.

The linear rule removes this restriction since it provides a simple relation between  $x$  and  $y^*$ .

The integration of equation C(2) in the general case at total reflux may be performed either in terms of  $x$  or  $X$  (or  $X'$ ).

<sup>21</sup> Underwood, *J. Inst. Petroleum*, 1943, 29, 147.

Considering first the case when  $x_1$  is above the conjugate point, and the equilibrium equation is :

$$Y = aX + b$$

we have :  $x = \frac{X}{X+1}$  and  $dx = \frac{dX}{(X+1)^2}$

Also :  $\frac{y^*}{1-y^*} = aX + b$ , whence  $y^* = \frac{aX + b}{aX + b + 1}$ .

By substitution in eq. C(2) :

$$\begin{aligned} N_{MT} &= \int_{x_1}^{x_2} \frac{dx}{y^* - x} = \int_{x_1}^{x_2} \frac{(aX + b + 1)dX}{(X+1)(aX - X + b)} \\ &= \int_{x_1}^{x_2} \left[ \frac{1}{(X+1)} + \frac{1}{(aX - X + b)} \right] dX \\ &= \int_{x_1}^{x_2} \left[ \log_e (X+1) + \frac{1}{(a-1)} \log_e (aX - X + b) \right] \\ &= \int_{x_1}^{x_2} \left[ \log_e \frac{1}{(1-x)} + \frac{1}{(a-1)} \log_e \frac{x(a-b-1) + b}{1-x} \right] \end{aligned}$$

Finally :

$$N_{MT} = \log_e \left[ \frac{1-x_1}{1-x_2} \right] + \frac{1}{a-1} \log_e \left[ \frac{[x_2(a-b-1) + b](1-x_1)}{[x_1(a-b-1) + b](1-x_2)} \right] \quad C(3T)$$

It will be noted that the large second term in this equation is also found in the expression for the number of theoretical plates at total reflux (eq. (3a)).

Substituting for this expression we get the very simple relation between number of theoretical plates and number of mass transfer units at total reflux :

$$N_{MT} = \frac{N \log_e a}{a-1} - \log_e \left[ \frac{1-x_2}{1-x_1} \right] \quad C(4T)$$

The corresponding equations for the part of the  $x, y$  diagram below the conjugate point are readily obtained by substituting  $(1-x_1)$  for  $x_1$  and  $(1-x_2)$  for  $x_2$ , adding the indicating suffix to the constant terms.

These equations are :

$$N'_{MT} = \frac{1}{(a'-1)} \log_e \frac{x_1[x_2(a'-b'-1) - (a'-1)]}{x_2[x_1(a'-b'-1) - (a'-1)]} - \log_e \frac{x_2}{x_1} \quad C(3B)$$

and  $N'_{MT} = \frac{N' \log_e a'}{a'-1} - \log_e \frac{x_2}{x_1} \quad C(4B)$

These equations, relating the number of transfer units with the equivalent number of theoretical plates provide a convenient and interesting means of comparing these two forms of calculus for still design. This matter will again be mentioned later.

The integration of the general case involving finite reflux can be accomplished in a similar manner if composition is first expressed in terms of the  $\phi$  and  $\chi$  functions used in estimating the number of theoretical plates at finite reflux.

Above the conjugate point (by definition)

$$y = \phi - \frac{1}{\phi+1} \text{ and } x = q - \frac{1}{\chi+1}$$

Then  $y^* - y = \frac{1}{\phi+1} - \frac{1}{\phi^*+1} = \frac{\phi^* - \phi}{(\phi^*+1)(\phi+1)}$

in which  $\phi$  and  $\phi^*$  are ordinates on the operating and equilibrium lines respectively for a given value of  $\chi$

$\phi^*$  and  $\phi$  are both linearly related to  $x$  by the equations (p. 745) :

$$\begin{aligned}\phi^* &= \delta x + \tau \\ \phi &= \lambda x + \sigma.\end{aligned}$$

Then, in terms of  $x$

$$y^* - y = \frac{x(\delta - \lambda) + \tau - \sigma}{(\delta x + \tau + 1)(\lambda x + \sigma + 1)}.$$

Also, by differentiation  $dy = m dx = \frac{m \lambda x}{(x + 1)^2}.$

Substituting :

$$N_M = \int_{y_1}^{y_2} \frac{dy}{y^* - y} = \int_{x_1}^{x_2} \frac{m(\delta x + \tau + 1)(\lambda x + \sigma + 1)}{(x + 1)^2 [\lambda x(\delta - \lambda) + \tau - \sigma]} dx \quad \text{C(5)}$$

Equation C(5) can be re-arranged in the form

$$N_M = m \int_{x_1}^{x_2} \left[ \frac{A}{x + 1} + \frac{B}{(x + 1)^2} + \frac{C}{[\lambda x(\delta - \lambda) + \tau - \sigma]} \right] dx$$

in which  $A$ ,  $B$  and  $C$  are constants, and integrated by the method of partial fractions. The values of  $A$ ,  $B$  and  $C$  in terms of  $\delta$ ,  $\lambda$ ,  $\tau$  and  $\sigma$  are, however, rather cumbersome, and the method is laborious.

### (5) Application of the Linear Rule to the Heat Transfer Theory of Distillation.

An alternative means of measuring the amount of transfer involved under given conditions of distillation has been proposed by Kirschbaum.<sup>17</sup> It is based on the theory that enrichment in a distillation column is accomplished by a process of condensation and evaporation, the liquid or vapour produced in either case being in equilibrium with the phase from which it comes, and therefore different from it in composition.

If the two components have the same molar latent heats, and specific heats are negligible in comparison, it may be shown that the amount of heat which must be transferred between the two phases in accomplishing a given enrichment is :

$$H = Qn \int_1^{x_2} \frac{dx}{(y^* - x^*)} \quad \text{H(1)}$$

in which  $Q$  is the molar latent heat of either component,  $n$  is the number of mols. of liquid passing through the system in unit time,  $x^*$  is the composition of the liquid phase in equilibrium with a vapour of composition  $y$ , and  $y^*$  is the composition of the vapour in equilibrium with a liquid of composition  $x$ , when  $(x, y)$  are the co-ordinates of a point on the operating line.

If the composition is expressed in latent heat units, or "lols,"  $Q$  remains constant and the equation becomes almost exact. (For complete precision units of constant enthalpy should be used.)

Equation H(1) can be integrated mathematically for the case of total reflux in the same manner as eq. C(2).

Substituting for  $y^*$  and  $x^*$  we get (above the conjugate point) :

$$\int_{x_1}^{x_2} \frac{dx}{y^* - x^*} = \frac{1}{a + 1} \int_{x_1}^{x_2} \frac{(aX + b + 1)(X - b + a)}{(X + 1)^2(aX - X + b)} dX$$

which readily gives :

$$\int_{x_1}^{x_2} \frac{dx}{y^* - x^*} = \frac{1}{a + 1} \left[ \frac{(a - b - 1)(X_2 - X_1)}{(1 + X_2)(1 + X_1)} + \frac{a}{a - 1} \log_0 \frac{(a - 1)X_2 + b}{(a - 1)X_1 + b} \right].$$

This expression is again related to that for the number of theoretical plates at total reflux, since from eq. (2a) :

$$N \log_0 a = \log_0 \frac{(a - 1)X_2 + b}{(a - 1)X_1 + b}.$$

Making this substitution, we get :

$$\int_{x_1}^{x_2} \frac{dx}{y^* - x^*} = \frac{1}{a+1} \left[ \frac{(a-b-1)(X_2 - X_1)}{(1+X_2)(1+X_1)} + \frac{aN \log_e a}{a-1} \right] \quad H(2T)$$

or, in terms of  $x$  :

$$\int_{x_1}^{x_2} \frac{dx}{y^* - x^*} = \frac{Na \log_e a}{a^2 - 1} + \frac{(a-b-1)(x_2 - x_1)}{(a+1)} \quad H(2aT)$$

The corresponding expressions for the part of the system below the conjugate point are :

$$\int_{x_1}^{x_2} \frac{dx}{y^* - x^*} = \frac{1}{a'+1} \left[ \frac{a' N \log_e a'}{a' - 1} - \frac{(a-b-1)(X_2 - X_1)}{(1+X_2)(1+X_1)} \right] \quad H(2S)$$

and,

$$\int_{x_1}^{x_2} \frac{dx}{y^* - x^*} = \frac{Na' \log_e a'}{a'^2 - 1} - \frac{(a'-b'-1)(x_2 - x_1)}{(a'+1)} \quad H(2aS)$$

It will be noted that, apart from the values of the constants, the only difference between corresponding expressions is a change in the sign of the second term.

### Relations between Transfer Units and Theoretical Plates.

For convenience in discussion, the mathematical relations which have been evaluated for a system operating *under total reflux* are repeated here :

	Below the Conjugate Point.	Above the Conjugate Point.
	<i>Number of Theoretical Plates :</i>	
1.	$N = \frac{1}{\log a'} \log \left[ \frac{x_1[a' - 1 - x_2(a' - b' - 1)]}{x_2[a' - 1 - x_1(a' - b' - 1)]} \right]$	$N = \frac{1}{\log a} \log \left[ \frac{(1-x_1)[b + x_2(a-b-1)]}{(1-x_2)[b + x_1(a-b-1)]} \right]$
	<i>Number of overall mass transfer units based on changes in gas composition at total reflux (<math>N_{MT} = N_{OG}</math>) :</i>	
2.	$\int_{x_1}^{x_2} \frac{dy}{y^* - y} = \frac{N' \log_e a'}{a' - 1} - \log_e \frac{x_2}{x_1}$	$\int_{x_1}^{x_2} \frac{dy}{y^* - y} = \frac{N \log_e a}{a - 1} - \log_e \frac{(1-x_2)}{(1-x_1)}$
	<i>Heat Transfer Units (<math>\frac{H}{Q_H}</math>) :</i>	
3.	$\int_{x_1}^{x_2} \frac{dx}{y^* - x^*} = \frac{Na' \log_e a'}{a'^2 - 1} - \frac{(a'-b'-1)(x_2 - x_1)}{a' + 1}$	$\int_{x_1}^{x_2} \frac{dx}{y^* - x^*} = \frac{Na \log_e a}{a^2 - 1} + \frac{(a-b-1)(x_2 - x_1)}{a + 1}$

It will be seen that the integrated expression for the amount of transfer accomplished consists in all cases of two parts, of which the first is directly related to the number of theoretical plates required for the transfer, and is otherwise independent of composition changes, while the second part is related to the limits of composition.

For values of  $a'$  approaching unity  $\frac{\log_e a'}{a' - 1} \rightarrow 1.0$ , and as, for such cases, the number of theoretical plates required for a substantial enrichment is large,  $\log_e x_2/x_1$  becomes vanishingly small compared with  $N$ . In the limiting case, therefore, the number of overall mass transfer units becomes the same as the number of theoretical plates. This relation is, of course, well known.

Similarly, as  $a'$  approaches unity the value of  $\frac{a' \log_e a'}{a'^2 - 1}$  approaches 0.5 and  $\int_{x_1}^{x_2} \frac{dx}{y^* - x^*}$  approaches 0.5  $N$ . A few test cases will show that

these limiting relations are true, to a close approximation, over a wide range of practical conditions. In other words a given amount of transfer may be represented by a number of mass transfer units or by approximately the same number of theoretical plates, and the amount of heat transferred, calculated according to the heat transfer theory, is approximately the same for each theoretical plate.

Although these conditions hold broadly over fairly wide ranges of enrichment, a different state of affairs emerges when only a small change in composition is considered. If we take as a unit the amount of enrichment represented by a single theoretical plate, then the relation between  $x_2$  and  $x_1$  is obtained by substituting  $x_1 = x$  and  $x_2 = y$  in eqs. B(1) and T(1).

We then have :

$$\lim_{(x_1 \rightarrow 0)} \frac{x_2}{x} = \frac{1}{a}$$

and

$$\lim_{(x_1 \rightarrow 1.0)} \frac{1 - x_2}{1 - x_1} = \frac{1}{a}$$

As  $x_1$  approaches zero, we obtain, as the limiting value for the number of mass transfer units per theoretical plate (*i.e.* when  $N'$  is unity) :

$$\frac{N'_{0g}}{N'} \longrightarrow \frac{\log_e a'}{a' - 1} - \log_e \frac{1}{a'}$$

*i.e.*

$$\frac{N'_{0g}}{N'} \longrightarrow \frac{a' \log_e a'}{a' - 1},$$

and similarly, as  $x_1$  approaches unity :

$$\frac{N_{0g}}{N} \longrightarrow \frac{a \log_e a}{a - 1}$$

As a practical example, in the case of the methanol-water system,  $a' = 0.132$  and  $a = 2.42$ . The limiting values of  $N_{0g}/N$  at either end of the system are then 0.305 and 1.506 as  $x_1$  approaches zero and unity respectively. Although on the average over a wide range of the system, therefore, the number of mass transfer units at total reflux is approximately the same as the number of theoretical plates, the number of transfer units per theoretical plate may vary approximately five-fold. The unit used for design in the application of the transfer unit method is the "height of a transfer unit"  $(H.T.U.)_{0g}$  which is inversely proportional to the mass transfer coefficient  $K_g$  and is defined by :

$$dL/d(N_{0g}) = (H.T.U.)_{0g},$$

in which  $L$  is a measure of column height. For a small amount of transfer such as that represented by a single theoretical plate we may assume that  $K_g$  remains approximately constant, and write :

$$N_{0g}/L \propto K_g.$$

Towards the ends of the system the number of transfer units per theoretical plate varies rapidly. If, therefore, the H.E.T.P. is reasonably constant the transfer coefficient  $K_g$  must also vary rapidly in those regions. There is experimental evidence to show that this is indeed the case and that the H.E.T.P. is much more constant than the H.T.U.

Colburn<sup>22</sup> has shown that, according to the two-film diffusional theory :

$$\frac{1}{K_g} = \frac{1}{h_g} + \frac{1}{h_L} \frac{dy^*}{dx},$$

in which  $h_g$  and  $h_L$  are the individual gas and liquid film coefficients. If the liquid film is controlling, therefore, the overall coefficient varies

<sup>22</sup> Colburn, *Tr. Am. Inst. Chem. Eng.*, 1939, 35, 211.

inversely with the slope of the equilibrium line (at total reflux) and  $(H.T.U.)_{0g}$  varies directly with the same quantity.

Although experimental examination of distillation behaviour over small intervals of concentration near the ends of a system of suitable type is difficult, Duncan *et al.*,<sup>23</sup> have produced evidence that, in distillation, H.T.U. does vary directly with the slope of the equilibrium line, which points to the conclusion that the process of fractional distillation is controlled by the liquid film. Consequently, as Furnas has pointed out,<sup>24</sup> the H.T.U. may, and does, vary fifteen or twenty-fold between different parts of the same system.

On the other hand, examination of the integrated form of the heat transfer equation shows that the amount of heat transferred (at fixed mass rates) is very nearly the same per theoretical plate at all parts of a given system and, in molal latent heat units, is very nearly the same for all systems. The quantity  $\frac{a \log_e a}{a^2 - 1}$  deviates only slowly from 0.5 as  $a$  recedes from unity while the second term vanishes as the limits of the system are approached.

Taking the system methanol-water as a rather searching example, the following relative molar quantities have been calculated for the amount of heat transferred for a single theoretical plate at different parts of the system under total reflux. (The constants  $b$  and  $b'$  in the linear equations have been corrected to a "lolal" basis.)

Corresponding values of  $\int_{x_1}^{x_2} \frac{dy}{y^* - y}$  are given for comparison :

Lolal	$\{x_1 = 0$	0.01	0.07	0.36	0.50	1.00
Concentrations	$\{x_2 = 0$	0.070	0.335	0.696	0.770	1.00
$\int_{x_1}^{x_2} \frac{dx}{y^* - x^*}$		0.27	0.34	0.53	0.45	0.40
$\int_{x_1}^{x_2} \frac{dy}{y^* - y}$		0.31	0.39	0.77	1.38	1.40
					1.40	1.51

There is a two-fold variation in the amount of heat transferred per theoretical plate over the whole system, but most of this occurs very close to the water end. Over the greater part of the system the quantity is almost constant, and theoretical plates may thus be regarded approximately as units of equal heat transfer.

This discussion is not intended as a comparison of the relative merits of different methods of still design. It has been introduced only for the purpose of illustrating the use of the analytical methods which have been developed and of indicating their possibilities in the interpretation of experimental data. It suggests, for instance, that in the experimental investigation of various theories of distillation mechanism, particular attention should be paid to the behaviour of the system over small ranges of composition at either end.

### Summary.

The linear rule proposed in Part I to relate the compositions of liquid and vapour in systems of two volatile components, is used to develop the mathematical treatment of the theory of fractional distillation. It is shown that the linear relationship is independent of the units of mass which are used to define the quantity ratio of the two components. Exact expressions are obtained for the number of theoretical plates required to obtain a given difference in composition in a fractionating system at

<sup>23</sup> Duncan, Koffolt and Withrow, *Tr. Am. Inst. Chem. Eng.*, 1942, 38, 259.

<sup>24</sup> Furnas, *ibid.*, 1939, 35, 587.

either total or partial reflux. These expressions remain valid when the molar heats of vaporisation of the components are unequal, provided that the compositions of the phases are defined in units of mass of equal latent heat.

An integrated expression is obtained for the equation of Chilton and Colburn describing the performance of a fractionating column on the basis of the diffusional theory of fractional distillation under the condition of total reflux, and also for Kirschbaum's equation relating the performance of a column with the amount of heat transferred between the phases under the same condition.

The linear rule makes it possible to demonstrate that there is a simple relation between each of these integrals and the number of theoretical plates required for the same performance.

The use of these relations in deciding the mechanism of fractional distillation by experimental study is suggested and illustrated.

*Research Department,  
Imperial Chemical Industries, Ltd.,  
Billingham.*

## A THERMODYNAMIC STUDY OF BIVALENT METAL HALIDES IN AQUEOUS SOLUTION. PART XV. DOUBLE CHLORIDES OF UNI- AND BIVALENT METALS.

BY R. A. ROBINSON AND R. H. STOKES.

*Received 30th May, 1945.*

In Part II of this series<sup>1</sup> measurements were reported of the vapour pressures of solutions corresponding to the double salt,  $K_2BaCl_4$  or  $(2KCl \cdot BaCl_2)$ . An analysis of the experimental results led to the conclusion that this pair of salts exhibited little or no complex ion formation, the data being capable of reasonable interpretation on the assumption that the component salts retained their identity in solution with comparatively small specific interaction.

Further measurements have now been made on solutions corresponding to  $K_2MCl_4$  where  $M = Mg, Mn, Co, Ni$  or  $Cu$ . The  $Mg$  salt was selected because it was thought that, as in the case of  $BaCl_2$ , complex ion formation was not likely to occur and an opportunity would be provided to ascertain the extent of interaction to be expected between component salts of this type in solution in the absence of complex ion formation. In addition, some measurements have been made on  $K_2Ca(NO_3)_4$  solutions with the same objective, as it was thought that metal nitrates would be even less likely to exhibit complex ion formation than the chlorides. Measurements have also been made on solutions of  $Li_2CaCl_4$  where high concentrations can be reached. In a further communication it is intended to report on solutions of  $KCl$  containing various ratios of zinc and cadmium halides.

In this paper it should be understood that formulæ of the type  $K_2MCl_4$  will be used as a convenient designation of the stoichiometric composition of the solution, without any commitment to an hypothesis of complex ion formation such as  $[MCl_4]^{--}$ .

It will not be necessary to record all the measurements made, but in Table I there are given the isopiestic ratios  $R = m_{KCl}/m_{K_2MCl_4}$ , at round

<sup>1</sup> Robinson, *Trans. Faraday Soc.*, 1940, 36, 735.

concentrations of the double salt and at a temperature of 25°, read from a plot of the experimental results.

TABLE I.—ISOSPIESTIC RATIOS,  $m_{\text{KCl}}/m_{\text{K}_2\text{MX}_4}$ .

$m$ .	$\text{K}_2\text{MgCl}_4$ .	$\text{K}_2\text{BaCl}_4$ .	$\text{K}_2\text{MnCl}_4$ .	$\text{K}_2\text{CoCl}_4$ .	$\text{K}_2\text{NiCl}_4$ .	$\text{K}_2\text{CuCl}_4$ .	$\text{K}_2\text{Ca}(\text{NO}_3)_4$ .
0.05	3.42	3.44	3.39	3.39	3.42	3.36	3.27
0.1	3.46	3.44	3.42	3.43	3.45	3.38	3.21
0.2	3.55	3.44	3.48	3.49	3.52	3.42	3.10
0.3	3.63	3.46	3.54	3.56	3.58	3.45	3.00
0.5	3.80	3.52	3.64	3.69	3.71	3.48	2.83
0.7	3.96	3.57	3.70	3.81	3.84	3.48	2.68
1.0	4.18	3.62	3.74	3.95	4.00	3.39	2.50
1.2	—	3.63	3.75	4.01	4.06	3.32	2.41
1.4	—	—	—	—	—	3.24	2.34
1.6	—	—	—	—	—	—	2.27
1.8	—	—	—	—	—	—	2.20

The values for  $\text{K}_2\text{BaCl}_4$  were taken from a previous paper<sup>1</sup>.

The first significant feature to be noted in Table I is the fact that the group of salts,  $\text{K}_2\text{MCl}_4$ , where  $M = \text{Mg}, \text{Ba}, \text{Mn}, \text{Co}$  and  $\text{Ni}$ , have isopiestic ratios lying between  $R = 3.39$  and  $R = 4.18$ . Considering the five salts,  $\text{MgCl}_2$ ,  $\text{BaCl}_2$ ,  $\text{MnCl}_2$ ,  $\text{CaCl}_2$  and  $\text{NiCl}_2$ , previous investigations in this series have shown that their isopiestic ratios to potassium chloride cover the range 1.37 to 2.33 between 0.1 M. and 2 M. Now, if the ratio  $R = m_{\text{KCl}}/m_{\text{K}_2\text{MCl}_4}$  lies between 1.37 and 2.33 for a series of salts, we should predict approximate range of 3.37 to 4.33 for  $R = m_{\text{KCl}}/m_{\text{K}_2\text{MCl}_4}$  corresponding to a similar series of double salts, *provided no complex ion formation occurs*. This predicted range is almost exactly what is found and consequently our preliminary examination of the data suggests that in the case of these five salts little or no complex ion formation occurs.

A more detailed examination of the data is hampered by our lack of knowledge of the vapour pressures of mixed solutions. However, we shall examine the consequences of two reasonable approximations and test their validity by applying them to the data for potassium magnesium chloride, the salt which might be supposed to be the least likely to exhibit complex ion formation.

**First Approximation.**—It will be assumed that the vapour pressure lowering of an  $x$  M. solution of  $\text{K}_2\text{MgCl}_4$  (*i.e.* a solution  $2x$  M. to  $\text{KCl}$  and  $x$  M. to  $\text{MgCl}_2$ ) can be put equal to the sum of the vapour pressure lowerings of a  $2x$  M.  $\text{KCl}$  solution and an  $x$  M.  $\text{MgCl}_2$  solution. This assumes that the vapour pressure lowering due to one salt is not affected by the presence of the other salt, an assumption which cannot be exactly true but the consequences of which it will nevertheless be interesting to investigate.

For example an 0.5 M. solution of  $\text{K}_2\text{MgCl}_4$  is found to be isopiestic with 1.900 M.  $\text{KCl}$  whose molal vapour pressure lowering  $(p^0 - p)/m$  is 0.7552. The vapour pressure lowering of the  $\text{K}_2\text{MgCl}_4$  solution is therefore  $0.7552 \times 1.900 = 1.435$  mm. This is the experimental value. The calculated value is obtained as follows: the concentration of  $\text{KCl}$  is 1 M., the molal vapour pressure lowering of  $\text{KCl}$  at this concentration is 0.7559 and the  $\text{KCl}$  makes a predicted contribution of 0.756 mm. Previous work has shown that 0.5 M.  $\text{MgCl}_2$  is isopiestic with 0.793 M.  $\text{KCl}$  whose vapour pressure lowering is 0.601 mm. The constituent salts of  $\text{K}_2\text{MgCl}_4$  are therefore predicted to make a contribution of  $0.756 + 0.601 = 1.357$  mm., a result which differs by 5.4 % from the observed value.

**Second Approximation.**—It will next be assumed that the vapour pressure lowering of an  $x$  M. solution of  $\text{K}_2\text{MgCl}_4$  is equal to that due to



2*x* M. KCl and *x* M. MgCl<sub>2</sub> separately, the molal vapour pressure lowering of each salt being taken at the same total ionic strength as *x* M. K<sub>2</sub>MgCl<sub>4</sub>. In this way some attempt is made to allow for the influence of one salt on the other.

Thus, for an 0.5 M. K<sub>2</sub>MgCl<sub>4</sub> solution (ionic strength = 2.5) it is found experimentally that the vapour pressure lowering is 1.435 mm. The calculated value is obtained as follows: the molal vapour pressure lowering of KCl at an ionic strength of 2.5 (2.5 M.) is 0.7590. Since the double salt is 1 M. to KCl we predict a contribution of 0.759 mm. due to the KCl. An MgCl<sub>2</sub> solution of ionic strength 2.5 would be 0.833 M. and previous work has shown that such a solution would be isopiestic with 1.453 M. KCl whose vapour pressure lowering is 1.095 mm. The predicted contribution of the MgCl<sub>2</sub> is therefore  $(0.5/0.833) \times 1.095 = 0.657$  mm. The calculated vapour pressure lowering is therefore  $0.759 + 0.657 = 1.416$  mm., which agrees within 1.3 % with the observed value.

Extending these two methods over a concentration range of K<sub>2</sub>MgCl<sub>4</sub> we get the data in Table II.

TABLE II.—COMPARISON OF OBSERVED AND PREDICTED VAPOUR PRESSURE LOWERINGS OF K<sub>2</sub>MgCl<sub>4</sub> SOLUTIONS.

<i>m.</i>	Obs. <i>Δp.</i>	First method.		Second method.	
		Calc. <i>Δp.</i>	Per cent. Diff.	Calc. <i>Δp.</i>	Per cent. Diff.
0.1	0.266	0.267	0.4	0.264	0.8
0.2	0.539	0.538	0.2	0.532	1.3
0.3	0.825	0.800	3.0	0.812	1.5
0.5	1.435	1.357	5.4	1.416	1.3
0.7	2.109	1.944	8.0	3.090	0.9
1.0	3.227	2.895	10.3	3.225	0.1

It is clear that the second and more reasonable approximation gives good agreement with the observed values. Unfortunately the method has one limitation; since potassium chloride is saturated at 4.8 M., the highest concentration of K<sub>2</sub>MgCl<sub>4</sub> to which the method can be applied is 0.96 M. For calculations at 1 M. K<sub>2</sub>MgCl<sub>4</sub> a slight extrapolation of the KCl data from 4.8 to 5 M. must be made.

Table III gives the percentage difference between the observed vapour pressure lowerings and those calculated by the second method for each of seven double salts.

TABLE III.—PERCENTAGE DEVIATIONS BETWEEN CALCULATED AND OBSERVED VAPOUR PRESSURE LOWERINGS OF DOUBLE SALT SOLUTIONS.

<i>m.</i>	K <sub>2</sub> MgCl <sub>4</sub>	K <sub>2</sub> BaCl <sub>4</sub>	K <sub>2</sub> MnCl <sub>4</sub>	K <sub>2</sub> NiCl <sub>4</sub>	K <sub>2</sub> CoCl <sub>4</sub>	K <sub>2</sub> CuCl <sub>4</sub>	K <sub>2</sub> Ca(NO <sub>3</sub> ) <sub>2</sub>
0.1	-0.8	-0.1	-0.8	-1.5	-0.8	0.0	-1.5
0.2	-1.3	-1.0	-0.6	-0.7	-0.2	+0.1	-2.0
0.3	-1.5	-0.6	-0.9	-0.4	-0.2	+0.5	-2.0
0.5	-0.9	+0.4	-0.1	+0.3	+0.3	+2.3	-2.2
0.7	-0.9	+1.0	+1.7	+0.9	+0.9	+4.0	+1.4
1.0	-0.1	+2.4	+4.6	+2.6	+3.1	+8.8	—

A positive sign indicates that the calculated value is higher than the observed.

Finally some measurements were made on solutions of the double salt, Li<sub>2</sub>CaCl<sub>4</sub> up to high concentrations (4 M.), using lithium chloride as refer-

ence salt. The vapour pressure lowerings for this salt have already been evaluated.<sup>2</sup> The results are given in Table IV.

TABLE IV.—OBSERVED AND CALCULATED VAPOUR PRESSURE LOWERINGS OF SOLUTIONS OF  $\text{Li}_2\text{CaCl}_4$ .

$m\text{Li}_2\text{CaCl}_4$	$m\text{LiCl}$	$\Delta p$ (obs.)	$\Delta p$ (calc.)	Per cent. Diff.
0.1652	0.5590	0.459	0.467	+0.2
0.5292	1.853	1.716	1.725	+0.5
0.8861	3.191	3.336	3.348	+0.4
1.287	4.705	5.544	5.530	-0.3
1.461	5.391	6.66	6.55	-1.6
1.813	6.721	8.83	8.69	-1.6
2.071	7.735	10.54	10.17	-3.5
2.499	9.363	13.11	12.46	-5.0
2.898	10.85	15.12	14.33	-5.2
3.113	11.61	16.03	15.22	-5.0
3.173	11.76	16.20	15.45	-4.6
3.307	12.29	16.76	15.94	-4.9
3.833	13.99	18.29	17.53	-4.2

We must now estimate the vapour pressure lowering to be expected in the event of complex ion formation. If this process were complete in the case of 1 M.  $\text{K}_2\text{MgCl}_4$  it should simulate closely the behaviour of 1 M.  $\text{CaCl}_2$  whose water activity has been shown<sup>3</sup> to be 0.9451 corresponding to a vapour pressure lowering of 1.304 mm. The observed value is 3.227 and that calculated on the assumption of no complex ion formation is 3.225. The question arises whether this small difference of 0.002 mm. (which is somewhat larger with other salts) is due to slight formation of complex ions. We believe that this is not so, for two reasons. In the first place, if the difference is attributed to complex ion formation, it would be expected to become more marked with increasing concentration; the experiments with  $\text{Li}_2\text{CaCl}_4$  have been carried to high concentrations without any such enhancement of the difference. Secondly, it can be shown that the observed differences, of the order of 3 %, also occur with salt pairs where complex ion formation is most unlikely. Thus Owen and Cooke<sup>4</sup> have made vapour pressure measurements of mixtures of KCl and LiCl in various ratios at total ionic strengths of 1, 2 and 3. The mixtures in equimolecular amounts may be treated as solutions of  $\text{KLiCl}_2$  and vapour pressure lowerings calculated by the second method described above can be compared with the observed. At total ionic strength of 1, 2 and 3, the percentage deviations of calculated from observed values are 0.2, 2.0 and 3.5 % respectively, the calculated value being higher than the observed in each case. Of the seven double salts in Table III, only one,  $\text{K}_2\text{CuCl}_4$ , exhibits a deviation substantially different from that observed with the simple salt pair  $\text{KCl} + \text{LiCl}$ .

It may be concluded, therefore, that (a) the simple additivity rule of vapour pressure lowerings may be used to detect complex ion formation if such occurs to any marked extent, and (b) with the possible exception of  $\text{K}_2\text{CuCl}_4$ , there is no sound basis for postulating the existence of complex ions of the type  $\text{MgCl}_4^{--}$ ,  $\text{BaCl}_4^{--}$ ,  $\text{MnCl}_4^{--}$ ,  $\text{NiCl}_4^{--}$ ,  $\text{CoCl}_4^{--}$  or  $\text{Ca}(\text{NO}_3)_4^{--}$  in solutions not greater than 1 M. in concentration. Absence of  $\text{CaCl}_4^{--}$  ions in  $\text{Li}_2\text{CaCl}_4$  is indicated up to much higher concentrations. It is, of course, possible that complex ion formation might be detected in some of these cases if experiments were made at sufficiently high concentrations.

<sup>2</sup> Robinson, *Trans., Faraday Soc.*, next paper.

<sup>3</sup> Stokes, *ibid.*, 1945, 41, 637.

<sup>4</sup> Owen and Cooke, *J. Amer. Chem. Soc.*, 1937, 59, 2273.

### Summary.

Isopiestic measurements have been made on solutions of mixed salts of the type  $2\text{KCl} + \text{MCl}_2$ , where  $\text{M} = \text{Mg}, \text{Ba}, \text{Mn}, \text{Ni}, \text{Co}$  or  $\text{Cu}$ , on  $2\text{KNO}_3 + \text{Ca}(\text{NO}_3)_2$ , and on  $2\text{LiCl} + \text{CaCl}_2$ , the latter to high concentrations. A simple additivity rule for vapour pressure lowerings has been discussed. No sound evidence has been discovered in favour of the existence of complex ions, except possibly of  $\text{CuCl}_4^{--}$ , in the concentration regions studied.

Auckland University College,  
New Zealand.

---

## THE WATER ACTIVITIES OF LITHIUM CHLORIDE SOLUTIONS UP TO HIGH CONCENTRATIONS AT 25°.

By R. A. ROBINSON.

Received 30th May, 1945.

The water activities in solutions of sulphuric acid at high concentrations have been measured by Shankman and Gordon.<sup>1</sup> Determinations on calcium<sup>2</sup> and magnesium chloride<sup>3</sup> and sodium hydroxide<sup>4</sup> have recently been extended to high concentrations and interest therefore attaches to solutions of a 1—1 electrolyte of the noble gas type. To fill this gap, measurements are now reported on lithium chloride by the isopiestic method.

### Experimental.

Lithium chloride was made by neutralisation of Eimer and Amend's lithium hydrate followed by four recrystallisations. It was used in the form of a concentrated stock solution whose strength was determined by chloride analysis, and more dilute stock solutions were prepared as required. The solutions were equilibrated in silver dishes as preliminary experiments showed that platinum dishes gave the same results, indicating the absence of corrosion of silver by lithium chloride solutions. Measurements were made against sulphuric acid and sodium chloride as standards and are reported in Table I. A few determinations were made at low concentrations as a check on those previously reported.<sup>5</sup>

### Discussion.

From the isopiestic results, water activities, osmotic coefficients and activity coefficients have been evaluated. A set of reference values has been adopted which up to 1.5 M. NaCl are essentially those given by Robinson and Harned<sup>6</sup> but at higher concentrations considerable weight is given to the more recent work of Olynky and Gordon.<sup>7</sup> For sulphuric

<sup>1</sup> Shankman and Gordon, *J. Amer. Chem. Soc.*, 1939, **61**, 2370.

<sup>2</sup> Stokes, *Trans. Faraday Soc.*, 1945, **41**, 637.

<sup>3</sup> Stokes, *ibid.*, 1945, **41**, 642.

<sup>4</sup> Åkerlöf and Kegeles, *J. Amer. Chem. Soc.*, 1940, **62**, 620.

<sup>5</sup> Robinson and Sinclair, *ibid.*, 1934, **56**, 1830.

<sup>6</sup> Robinson and Harned, *Chem. Rev.*, 1941, **28**, 419.

<sup>7</sup> Olynky and Gordon, *J. Amer. Chem. Soc.*, 1943, **65**, 204.

acid reliance has been placed mainly on the direct vapour pressure measurements of Shankman and Gordon,<sup>1</sup> although these differ considerably from the e.m.f. measurements of Harned and Hamer.<sup>8</sup>

TABLE I.—ISOPLESTIC RESULTS AT 25°.

<i>m</i> LiCl.	<i>m</i> NaCl.	<i>m</i> LiCl.	<i>m</i> NaCl.	<i>m</i> LiCl.	<i>m</i> NaCl.	<i>m</i> LiCl.	<i>m</i> NaCl.
0.2080	0.2117	0.9729	1.056	2.132	2.442	2.205	2.538
2.470	2.878	2.971	3.526	2.994	3.552	3.408	4.102
3.562	4.305	3.828	4.659	3.982	4.870	4.067	4.986
4.395	5.432	4.509	5.590	4.695	5.841	4.705	5.865
4.883	6.106						

<i>m</i> LiCl.	<i>m</i> H <sub>2</sub> SO <sub>4</sub> .	<i>m</i> LiCl.	<i>m</i> H <sub>2</sub> SO <sub>4</sub> .	<i>m</i> LiCl.	<i>m</i> H <sub>2</sub> SO <sub>4</sub> .	<i>m</i> LiCl.	<i>m</i> H <sub>2</sub> SO <sub>4</sub> .
3.228	2.913	3.801	3.401	3.865	3.464	5.380	4.764
5.760	5.099	6.715	5.958	6.869	6.104	8.329	7.478
8.586	7.734	9.450	8.570	10.302	9.396	10.845	9.952
12.523	11.592	12.605	11.681	13.006	12.073	13.407	12.441
13.480	12.512	14.112	13.116	14.628	13.594	15.052	13.992
15.512	14.371	16.116	14.896	16.798	15.424	16.875	15.487
16.974	15.501	18.206	16.553	18.926	17.096	19.074	17.189
19.569	17.559	20.019*	17.873				

\* Supersaturated solution.

TABLE II.—WATER ACTIVITIES, OSMOTIC COEFFICIENTS AND ACTIVITY COEFFICIENTS OF LITHIUM CHLORIDE SOLUTIONS AT 25°.

<i>m</i> .	<i>a<sub>w</sub></i> .	<i>φ</i> .	<i>γ</i> .	<i>m</i> .	<i>a<sub>w</sub></i> .	<i>φ</i> .	<i>γ</i> .
0.1	0.99662	0.939	0.790	8.0	0.5381	2.150	5.05
0.2	0.99325	0.939	0.757	8.5	0.5038	2.239	5.94
0.3	0.98983	0.945	0.744	9.0	0.4710	2.322	6.94
0.4	0.98635	0.954	0.740	9.5	0.4396	2.401	8.08
0.5	0.98281	0.963	0.739	10.0	0.4101	2.474	9.36
0.6	0.97919	0.973	0.743	10.5	0.3817	2.546	10.83
0.7	0.97549	0.984	0.748	11.0	0.3550	2.613	12.46
0.8	0.97172	0.995	0.755	11.5	0.3303	2.674	14.25
0.9	0.96791	1.006	0.764	12.0	0.3070	2.731	16.23
1.0	0.9640	1.018	0.774	12.5	0.2857	2.782	18.35
1.2	0.9560	1.041	0.796	13.0	0.2657	2.830	20.6
1.4	0.9477	1.066	0.823	13.5	0.2471	2.874	23.1
1.6	0.9391	1.091	0.853	14.0	0.2298	2.915	25.8
1.8	0.9302	1.116	0.885	14.5	0.2142	2.949	28.6
2.0	0.9210	1.142	0.921	15.0	0.2000	2.978	31.5
2.5	0.8966	1.212	1.026	15.5	0.1867	3.002	34.4
3.0	0.8702	1.286	1.156	16.0	0.1751	3.023	37.5
3.5	0.8417	1.366	1.294	16.5	0.1647	3.034	40.3
4.0	0.8116	1.449	1.483	17.0	0.1551	3.042	43.2
4.5	0.7799	1.533	1.710	17.5	0.1459	3.053	46.3
5.0	0.7471	1.619	1.979	18.0	0.1377	3.057	49.3
5.5	0.7123	1.712	2.32	18.5	0.1299	3.062	52.4
6.0	0.6784	1.795	2.67	19.0	0.1226	3.066	55.6
6.5	0.6438	1.880	3.13	19.5	0.1163	3.065	58.7
7.0	0.6083	1.971	3.67	20.0	0.1100	3.063	61.7
7.5	0.5729	2.061	4.30				

<sup>8</sup> Harned and Hamer, *J. Amer. Chem. Soc.*, 1935, 57, 27.

Attention should be drawn to the extraordinarily high values of the activity coefficient, 61.7, at a concentration of 20 M. A value of 48.8 is reported<sup>2</sup> for 10.5 M.  $\text{CaCl}_2$  and of 38.0 for<sup>3</sup> 6 M.  $\text{MgCl}_2$ . For 16 M.  $\text{HCl}$  Åkerlöf and Tearle<sup>9</sup> give  $\gamma = 41.5$  whilst Stokes has made some measurements in this laboratory which indicate that  $\text{NaOH}$  attains a value of 33.9 at 29 M.

The equation :

$$-\log \gamma = 0.5092 \sqrt{c}/(1 + 0.3286 \sqrt{c}) - 0.111c - 0.007c^2 + \log(1 + 0.036m),$$

corresponding to a mean distance of approach of the ions of 4.25 Å., represents the activity coefficients to within 0.002 up to 1 M. and holds within 2 % up to 10 M. At higher concentrations, however, it predicts activity coefficients much higher than the observed, e.g. 47.7 against 31.5 at 15 M. and 249 against 61.7 at 20 M.

The saturated solution was found to be in equilibrium with 17.822 M.  $\text{H}_2\text{SO}_4$  and from a plot of the isopiestic ratio against  $m_{\text{H}_2\text{SO}_4}$  the concentration of the saturated solution of  $\text{LiCl}$  at 25° was found to be 19.947 M. or 45.83 g. of  $\text{LiCl}$  per 100 g. of saturated solution, in very good agreement with the value given by Seidell.<sup>10</sup>

### Summary.

Isopiestic measurements have been made on lithium chloride solutions up to 20 M. at 25°. Water activities, osmotic coefficients and activity coefficients have been calculated. The solubility at 25° is 45.83 g. per 100 g. of saturated solution.

Auckland University College,  
New Zealand.

<sup>9</sup> Åkerlöf and Tearle, *J. Amer. Chem. Soc.*, 1937, **59**, 1854.

<sup>10</sup> Seidell, *Solubilities of Inorganic and Metal Organic Compounds*, 3rd edn., Van Nostrand, New York, 1940, p. 912.

## RESEARCHES ON ELECTRO-ENDOSMOSIS

BY A. J. RUTGERS AND M. DE SMET.

Received 7th December, 1944.

1. In this paper we intend to give a brief account of our researches on electro-endosmosis, which were carried out in the years 1940-1942.

As is well known, two methods present themselves for the determination of the electrokinetic potential ( $\zeta$ -potential) at the liquid-solid interface in glass capillaries.

(1) Measurement of the streaming potential.

(2) Measurement of the electro-endosmosis-velocity.

Previous experiments<sup>1</sup> had shown that, in contradiction to the Helmholtz-Smoluchowski-equation, the radius of the capillary had a big influence upon the value of the streaming potential. Assuming that this influence must be ascribed to surface-conductance, a "true"  $\zeta$ -c curve could be calculated, but it was obvious that a more direct measurement of  $\zeta$  was highly desirable. We therefore decided to develop a method for the determination of the electro-endosmosis velocity, from which the electrokinetic potential can be calculated; in the relation between these quantities conductance does not play a part.<sup>2</sup>

<sup>1</sup> Verlende, *Proc. Kon. Akad. Wetensch. Amsterdam*, 1939, 42, 764. Rutgers, *Trans. Faraday Soc.*, 1940, 36, 69.

<sup>2</sup> De Smet, *Bull. Acad. Roy. Belg.*, III, No. 12, 14, 1941; No. 4, 8, 1942.

We start from Poisson's equation in cylindrical co-ordinates

$$\Delta\psi = \frac{1}{r} \frac{\partial}{\partial r} \left( r \frac{\partial\psi}{\partial r} \right) + \frac{1}{r^2} \frac{\partial^2\psi}{\partial\phi^2} + \frac{\partial^2\psi}{\partial z^2} = - \frac{4\pi\rho}{D}$$

which for axial symmetry ( $\partial/\partial\phi = 0$ ) and linear decay of potential along the  $z$ -axis ( $\partial/\partial z^2 = 0$ ) changes into

$$\frac{1}{r} \frac{d}{dr} \left( r \frac{d\psi}{dr} \right) = - \frac{4\pi\rho}{D}$$

or

$$\rho = - \frac{D}{4\pi r} \frac{d}{dr} \left( r \frac{d\psi}{dr} \right). \quad (1)$$

Our second fundamental equation describes the frictional force  $dF_{fr}$  upon a layer of liquid between two co-axial cylinder surfaces:

$$dF_{fr.} = d \left[ \eta S \frac{dv}{dr} \right] = d \left[ \eta 2\pi r l \frac{dv}{dr} \right] \quad (2)$$

where  $r$  is the radius,  $l$  the length of the cylindrical shell,  $\eta$  the viscosity,  $dv/dr$  the velocity gradient in the liquid.

If a potential difference  $E$  is applied to the ends of a capillary of length  $l$ , the intensity of the field is  $E/l$ , the force per cm.<sup>2</sup>  $\rho^E/l$ , and the electric force  $dF_{el}$  on the liquid in the cylindrical shell

$$dF_{el.} = 2\pi r l \frac{\rho E}{l} dr = - \frac{DE}{2} d \left( r \frac{d\psi}{dr} \right) \quad (3)$$

where equation (1) has been used.

In the stationary state we have

$$dF_{fr.} + dF_{el.} = 0$$

giving:

$$d \left[ \eta 2\pi r l \frac{dv}{dr} \right] - \frac{DE}{2} d \left( r \frac{d\psi}{dr} \right) = 0$$

or

$$\eta 2\pi r l \frac{dv}{dr} - \frac{DE}{2} r \frac{d\psi}{dr} = \text{Const.}$$

In the axis of the capillary  $r = 0$  and  $d\psi/dr = 0$ ; hence  $\text{Const.} = 0$ , and therefore

$$\frac{dv}{dr} = \frac{DE}{4\pi\eta l} \frac{d\psi}{dr} \quad (4)$$

$$v(r) = \frac{DE}{4\pi\eta l} \psi + \text{Const.}$$

For  $r = R$ ,  $v = 0$  and  $\psi = \xi$ ; hence

$$\text{Const.} = - \frac{DE\xi}{4\pi\eta l}$$

and

$$v(r) = \frac{DE}{4\pi\eta l} (\psi - \xi). \quad (5)$$

The volume of liquid passing per second through a cross-section of the capillary is given by

$$\begin{aligned} V &= \int_0^R v(r) 2\pi r dr = \frac{DE}{2\eta l} \int_0^R (\psi - \xi) r dr = \\ &= - \frac{DE}{2\eta l} \int_0^R (\xi - \psi) r dr = - \frac{DE}{4\eta l} \left[ \xi R^2 - 2 \int_0^R \psi r dr \right]. \end{aligned} \quad (6)$$

This is the final formula for the electrosmotic velocity in a cylindric capillary. It differs from the Helmholtz-Smoluchowski formula by the second term in the right hand side.

If we take into account that this term is small in proportion to the first one as long as the thickness of the layer where  $\psi$  differs appreciably from zero is small with respect to the radius of the capillary, and if we neglect this correction term, we obtain Helmholtz-Smoluchowski's well-known equation

$$v = \frac{V}{\pi R^2} = - \frac{DE\zeta}{4\pi\eta l} \quad (7)$$

The negative sign in (7), which we will omit hereafter, means that for a positive value of  $\zeta$  the velocity of the liquid and the electric field are of opposite sense.

2. A diagram of the apparatus used is given in Fig. 1. We see a principal vessel, in the shape of a horizontal cylinder (accommodated in a brass case) with ground joints; and a pear-shaped auxiliary vessel, also with its axis horizontal, but perpendicular to the axis of the principal vessel; this last vessel has a capacity of 800 c.c., the auxiliary vessel of some 400 c.c. The concentration of the solution in the large vessel can be changed by means of the concentrated solution in the small spherical vessel, one drop of which can be pressed through a capillary tube into the large one.

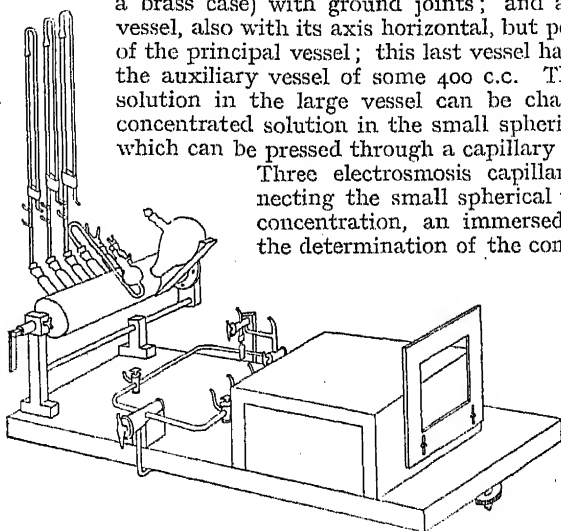


FIG. 1. Diagram of apparatus.

Three electrosmosis capillaries, the capillary connecting the small spherical vessel for changing the concentration, an immersed pair of electrodes for the determination of the conductivity, and a supply tube for purified nitrogen pass by means of ground joints through the six vertical tubes. A system of conduit tubes (not shown) and taps allow the application of nitrogen pressure to all parts of the apparatus where needed, so that all manipulations can be effected in perfect separation

from the atmosphere. Special care was given to the preparation of the pure water ( $\sigma \approx 2 \times 10^{-7}$  ohm $^{-1}$  cm. $^{-1}$ ). The capillaries are made of Jena 16111 glass; the length of the capillary between the electrodes (A and B; Fig. 2a) is some 5 cm.; tensions of 600, 500, 400, 300, and 600 v. are applied in succession, corresponding to a field strength of 120-60 v./cm. (Coehn and Raydt; 880 v./cm.). A wider capillary is sealed on either side of the capillary AB, in one of which a window has been made by grinding off; the other capillary is bent through an angle of 135°.

To describe the manipulations we introduce the terms "measuring position" (m.p.) and "filling position" (f.p.) (Fig. 2a and b). In the f.p. the free end of the capillary is vertical, the auxiliary vessel is empty, the principal vessel is filled with 400 c.c. of liquid, the other end of the capillary is immersed; the liquid is forced into the capillaries under pressure (many times to and fro); the free end of the capillary is open to the atmosphere, but is protected against CO $_2$ .

The principal vessel is accommodated in a brass case, which can rotate about a horizontal axis, suspended in a support; this support is mounted upon a big board which rests on the table with two fixed legs and one

adjusting screw. By a rotation of  $90^\circ$  about the axis of the principal vessel the free ends of the capillaries are brought into a horizontal position; the auxiliary vessel then points slantingly downward and is filled with liquid from the principal vessel; the immersed ends of the capillaries are now free, and in the capillaries there is a thread of liquid, bounded on either side by the gaseous phase. By suitable application of pressure each thread is moved into the horizontal part of the capillaries, so that one of its ends can be observed with the microscope.

In the m.p. the thread of liquid is almost, but never perfectly horizontal; it usually moves slowly under gravity in the capillary; the position is improved by means of the adjusting screw, until the thread no longer moves. Then the potential of 600 v. is applied, and the time required for traversing 20, 30, 40, 60, or 80 divisions of the micrometer is measured; 100 divisions correspond to 0.9012 cm.; then the potential is reversed; this is repeated five times; this procedure is repeated with potentials of 500, 400, 300 and again 600 v. We had made sure previously, by measuring simultaneously at the upper and lower faces, that these two layers move always with the same velocity.

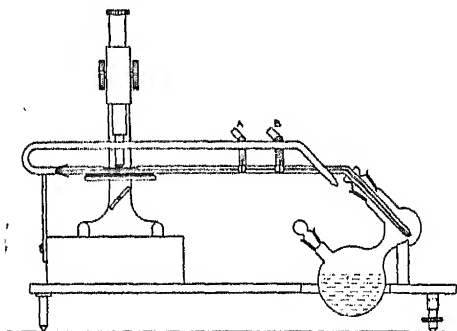


FIG. 2a.—"Measuring Position."

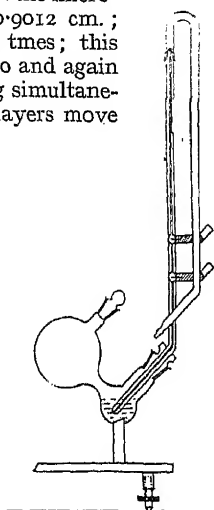


FIG. 2b.—"Filling Position."

After the velocity has been measured in the first capillary, it is turned  $90^\circ$  in its ground joint, which brings it into a vertical position; now the velocity in the second or third capillaries can be measured. Then the capillaries are rotated back through  $90^\circ$ , so that the apparatus is completely back in the m.p.; it is then rotated into the f.p.; the pear-shaped auxiliary vessel empties itself into the principal vessel, the liquid in the capillaries is also forced into this vessel, and by measuring the conductivity we make sure that no accident has happened; then the concentration in the principal vessel is changed by forcing one or more drops of the concentrated solution from the small spherical vessel into the principal vessel and the next measurement can start.

A consequence of this construction was that the observation window in the sealed-on capillary was at a distance of some 15 cm. from the nearest end of the capillary proper, which itself measures only some 5 cm. If the sealed-on capillaries had the same width as the capillary proper, they would offer resistance to the electrosmotic flow three times as large as the resistance of the capillary proper, so that corrections of more than 100 % would have to be applied to the result of the measurement. In order to avoid this, the sealed-on capillaries were taken 2 or 3 times as wide as the capillary proper; if the radius of the capillary proper is  $r$ , those of the sealed-on capillaries  $r_1$  and  $r_2$ , and the lengths of the liquid thread in these capillaries  $l$ ,  $l_1$ , and  $l_2$  respectively, it can be easily proved that equation (7) must be replaced by



$$v = \frac{DE\zeta}{4\pi\eta l} \frac{r_2^2}{r^2} \left\{ 1 + \frac{l_2 l}{r_2^4/r^4} + \frac{l_1/l}{r_1^4/r^4} \right\} \quad (8)$$

or

$$\zeta = \frac{4\pi\eta}{D} \frac{r_2^2}{r^2} \left\{ 1 + \frac{l_2/l}{r_2^4/r^4} + \frac{l_1/l}{r_1^4/r^4} \right\} \frac{v}{E/l} \quad (9)$$

With  $l_2/l \sim 3$ ,  $r_2/r \sim 3$ , the value of the correction terms are  $3/81 \sim 4$  per cent., a permissible amount. The values of  $l_2$  and  $l_1$  must be determined in each experiment. They were measured with regard to two fixed marks determining two constant lengths  $l_{10}$  and  $l_{20}$ .

3. The reliability of the method was tested by measurements on two sets of 3 capillaries, all from identical glass; the capillaries I, II and III were all of the same diameter; two were cut from the same capillary, one next to the other; the third from another capillary. In the set I, IV, V the ratio  $r_1/r$  was varied, and the value of  $r$  too (by a factor 2.5); the data are given in Table I.

TABLE I.

	$r$ .	$r_1$ .	$r_2$ .	$l$ .	$l_{10}$ .	$l_{20}$ .
	cm					
I . .	0.01095	0.03485	0.03392	4.80	7.20	15.30
II . .	0.01122	0.03596	0.03667	4.75	5.40	15.20
III . .	0.01099	0.03716	0.03716	4.65	7.75	14.50
I . .	0.01095	0.03485	0.03392	4.80	7.20	15.30
IV . .	0.01099	0.02450	0.02560	4.95	4.95	15.20
V . .	0.02485	0.05159	0.05209	4.65	7.30	14.80

The times were read off by means of a Hartmann and Braun stop clock, giving tenths of a second; they varied from 3 to 10 seconds.

The apparatus was cleaned by means of a mixture of warm  $\text{HNO}_3$  and  $\text{H}_2\text{SO}_4$ ; the former (1) solution, consisting of  $\text{K}_2\text{Cr}_2\text{O}_7$  and  $\text{H}_2\text{SO}_4$  was rejected, in order to exclude the possibility of charging the glass wall with  $\text{Cr}^{+++}$ -ions.

The results of the experiments with the two sets of capillaries are given in Table II; the electrolyte used was KCl.

TABLE II. [KCl;  $(-\zeta)$  in mv.]

$c$ .	$-\zeta_I$ .	$-\zeta_{II}$ .	$-\zeta_{III}$ .	$-\zeta_I$ .	$-\zeta_{IV}$ .	$-\zeta_V$ .
0	154.4	155.6	157.4	153.2	144.2	153.2
1	151.3	149.4	153.2	145.9	139.9	145.9
2	148.8	148.9	149.3	142.3	136.9	142.3
5	145.0	142.9	147.2	137.1	131.7	137.1
10	140.6	139.3	142.1	132.9	127.7	132.9
20	134.5	133.0	137.3	129.1	123.5	129.1
50	125.5	123.6	128.2	120.1	109.8	120.1
100	117.3	114.7	118.6	114.5	106.9	114.5
200	109.6	106.3	112.8	105.9	98.6	105.9
500	94.9	91.4	97.0	88.6	83.2	88.6
1000	79.4	76.3		76.3	69.3	76.3

From Table II we see that, although individual influences (of the solution or of the capillary) are undeniable, the variations in the  $\zeta$ -potential, derived from these widely different measurements remain generally smaller than 10 mv.

We therefore conclude that the new method can give reliable  $\zeta$ -values; by means of this method  $\zeta$ - $c$  curves have been determined for solutions of 1-1, 2-1, 3-1 and 4-1-valent electrolytes, the results of which are given in section 4. We shall note that the curve obtained for KCl has the same shape (absence of a maximum) as the "true  $\zeta$ - $c$  curves" found by means of streaming potentials (surface conduction taken into account), but that an important discrepancy exists between the numerical values of  $\zeta$  (Fig. 3); this discrepancy is the subject of a further investigation.

4. The electrosmotic velocity at 22.5° C. of solutions of  $\text{KNO}_3$ ,  $\text{NH}_4\text{NO}_3$ ,  $\text{LiNO}_3$ ,  $\text{CsNO}_3$ ,  $\text{AgNO}_3$ , and  $\text{HNO}_3$ ; of  $\text{KCl}$ ,  $\text{KI}$ ,  $\text{KOH}$ ,  $\text{K}_2\text{SO}_4$  and  $\text{K}_4\text{FeCy}_6$  at a concentration of 0, 1, 2, 5, 10, 20, 50, 100, 200, 500, 1000, 2000, 5000, and 10,000  $\mu$  equiv./l. was measured. Each measurement was performed in duplicate with capillaries I and IV; the  $\zeta$ -values, obtained from these different capillaries agreed very well indeed; the mean was taken, and  $\zeta$ - $\log c$  curves are given in Figs. 4 and 5. The  $\zeta$ - $c$  curves, given in Fig. 6, of  $\text{HNO}_3$  and  $\text{KOH}$  (and of  $\text{KNO}_3$ ) have a special character.

Similar measurements were performed on solutions of 2-1-valent electrolytes:  $\text{Zn}(\text{NO}_3)_2$ ,  $\text{Mg}(\text{NO}_3)_2$ ,  $\text{Ca}(\text{NO}_3)_2$ ,  $\text{Ba}(\text{NO}_3)_2$ . The results are given in Fig. 7.

Similar measurements were carried out on solutions of  $\text{Al}(\text{NO}_3)_3$ ,  $\text{La}(\text{NO}_3)_3$ ,  $\text{Ce}(\text{NO}_3)_3$  and  $\text{Th}(\text{NO}_3)_4$ ; further, on solutions of electrolytes with a capillary active cation or anion, *viz.* of crystal violet and of sodium isobutyl-naphthalene sulphonate. The results are given in Fig. 8.

In Fig. 9 we give a survey of the various types of results obtained.

### Discussion of Results.

It is seen from Figs. 4, 5 and 6 that all  $\zeta$ - $\log c$  curves for electrolytes with univalent cation have the same character, those for  $\text{HNO}_3$  and  $\text{KOH}$  excepted. For solutions of  $\text{HNO}_3$  the relation between  $\zeta$  and  $\log c$  is linear; for solutions of  $\text{KOH}$  the value of  $(-\zeta)$  rises strongly if we pass from pure water to a concentration of 1  $\mu$  equiv./l. This behaviour is exactly what one would expect for the total difference of potential  $\epsilon$ , measured with a hydrogen-ion electrode; for in this case  $\epsilon$  is given by

$$\epsilon = \frac{RT}{nF} \ln \frac{c}{c_0} = \epsilon_0 + 0.058 \log c.$$

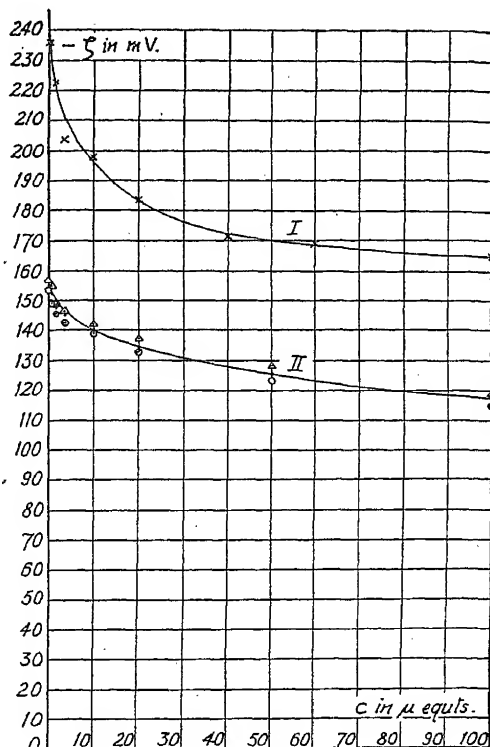


FIG. 3.

Curve I:  $(-\zeta)$ - $c$ -curve from streaming potentials.

Curve II:  $(-\zeta)$ - $c$ -curve from electro-endosmosis.

For  $\text{HNO}_3$  the slope of the  $\epsilon$ -log  $c$  curve, however, is not 58 mv., but only 32 mv.; this discrepancy can be explained in various ways; it can

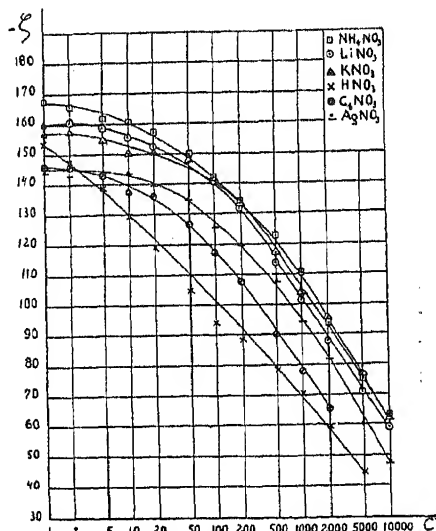


FIG. 4.—( $\epsilon$ —)log  $c$ -curves.

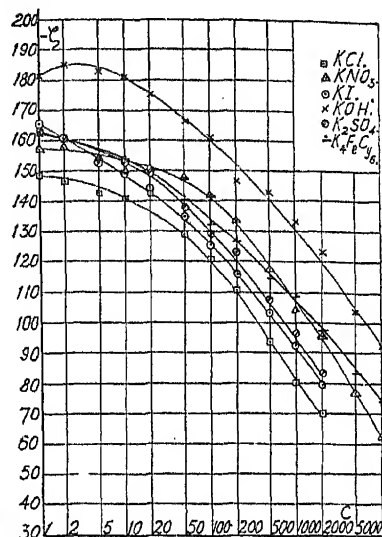


FIG. 5.—( $\epsilon$ —)log  $c$ -curves.

be assumed, *e.g.* that  $c_0$ , the H-ion concentration in the glass wall, is not a constant, but depends on the H-ion concentration in the liquid according to

$$c_0 = \alpha c^{0.45}.$$

For then 
$$\epsilon = 0.058 \log \frac{c}{\alpha c^{0.45}} = \epsilon'_0 + 0.032 \log c.$$

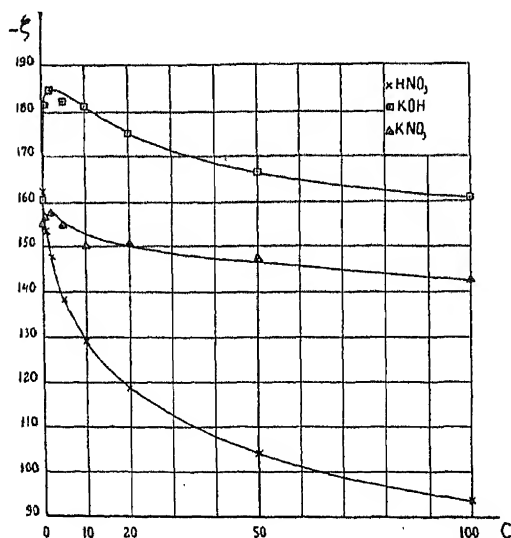


FIG. 6.  
( $\epsilon$ —) $c$ -curves.

The way in which the glass wall absorbs H-ions from the solution can therefore be represented by Freundlich's well-known adsorption-isotherm.

The  $\zeta$ -log  $c$  curves for the 1-1-valent salts (Figs. 4 and 5) are all of the same character: In the region of 1-100  $\mu$  equiv./l they have a feeble slope, a strong curvature at some 100  $\mu$  equiv./l, and from 200-10,000  $\mu$  equiv./l are almost linear with a slope of 42 mv.

In the region from 1-100  $\mu$  equiv./l the wall behaves principally as a H-ion electrode: since the concentration of H-ions does not change on addition of salt, neither does the  $\zeta$ -potential change; in the region of strong curvature, between 100 and 200  $\mu$  equiv./l, the wall changes from a H-ion electrode to a K, Li, Cs,  $\text{NH}_4$  or Ag-ion electrode.

For the solutions with bivalent cations very nearly linear  $\zeta$ -log  $c$  curves have been obtained (Fig. 7); the slope is 25 to 26 mv., very near to the value of 29 mv. for a true Mg, Ca, Ba or Zn electrode. The horizontal

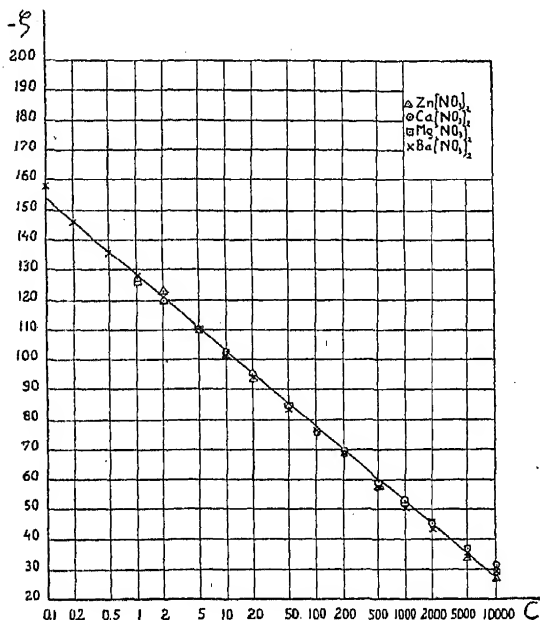


FIG. 7.  
( $\zeta$ —)-log  $c$ -curves.

part in the curve, which seems to be missing in Fig. 7, was easily brought to light by measurements on  $\text{Ca}(\text{NO}_3)_2$  at 0.01, 0.02, 0.05 and 0.1  $\mu$  equiv./l (Fig. 9).

It would be of interest to compare these results for  $\zeta$  with direct measurements of  $\epsilon$  by means of a glass-electrode, blown from the glass of the capillary, with which these  $\zeta$ -values have been obtained; as we did not have the opportunity to carry out these measurements, let us compare our  $\zeta$ - $c$  curves with the  $\epsilon$ - $c$  curves of other scientists (Horowitz,<sup>3</sup> Freundlich and Ettisch,<sup>4</sup> Lengyel and Blum,<sup>5</sup> Tendeloo and Zwart Voorspuyl<sup>6</sup>). Now Horowitz, working with Jena glass 16<sup>m</sup> has already come to the conclusion, that in certain concentration intervals this glass behaves as a Na-ion electrode, as a Ag-ion electrode, hence this result for  $\epsilon$  agrees perfectly well with our results for  $\zeta$  for 1-1 and 2-1-valent electrolytes.

In the case of the 3-1 and 4-1 types of electrolytes, and of the capillary

<sup>3</sup> Horowitz, *Sitzb. Akad. Wiss. Wien*, 1925, 134, 11A, 335, 355.

<sup>4</sup> Freundlich and Ettisch, *Z. physik. Ch.*, 1925, 116, 401.

<sup>5</sup> Lengyel and Blum, *Trans. Faraday Soc.*, 1934, 30, 461.

<sup>6</sup> Tendeloo and Zwart Voorspuyl, *Rec. Trav. Chim.*, 1942, 61, 531.

active electrolytes, the linearity of the  $\zeta$ -log  $c$  curves has completely disappeared. We think therefore that the influence on the  $\zeta$ -potential in these cases must be ascribed to some other mechanism as in the foregoing cases. This agrees with the result of Freundlich and Ettisch,<sup>4</sup> that a small quantity of  $\text{Th}(\text{NO}_3)_4$ , which was sufficient for a reversal of sign of the  $\zeta$ -potential, was of practically no influence upon the  $\epsilon$ -potential.

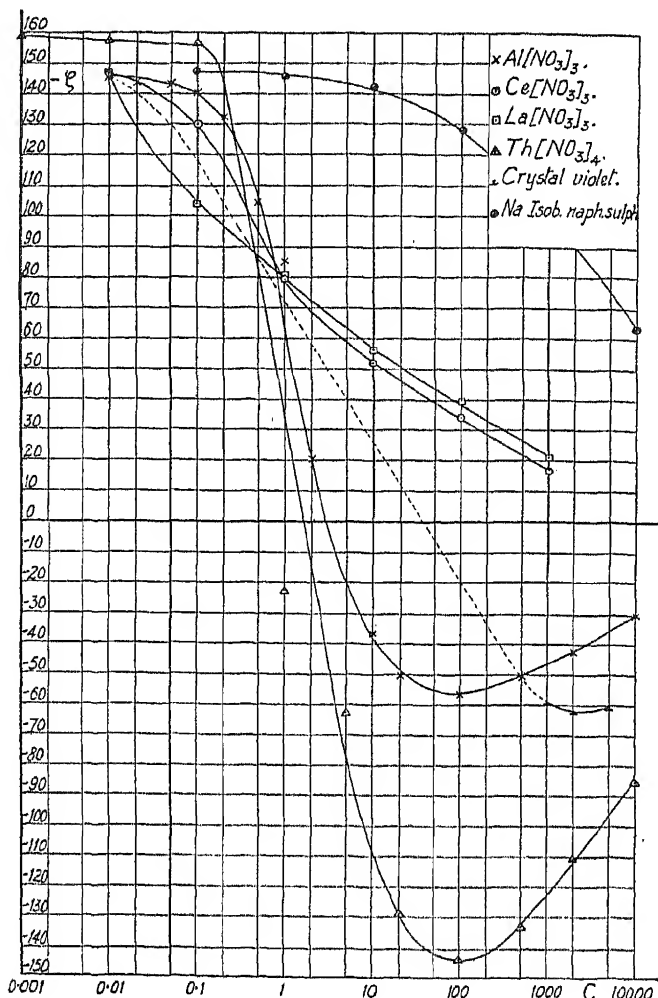


FIG. 8.—( $\zeta$ )-log  $c$ -curves.

This leads us to Fig. 10, for the potential, from which by application of Poisson's equation the density of electric charge may be deduced; we see that a triple layer results.

The same explanation might hold for crystal violet: the capillary-active cations tend to leave the water, and concentrate at the glass wall, charging it positively; the  $\text{Cl}$  ions remain in the diffuse outer layer, charging it negatively; the original negative charge inside the glass remains unchanged.

We sought support for this interpretation of the behaviour of crystal violet by experiments with an anion-capillary-active electrolyte, sodium isobutylnaphthalene sulphonate, as we hoped that addition of this electrolyte would charge the wall more strongly negative. But the "symmetry" of the two experiments was too incomplete. We had, it is true, reversed the charge of the ion to be expelled from the water, but in the second

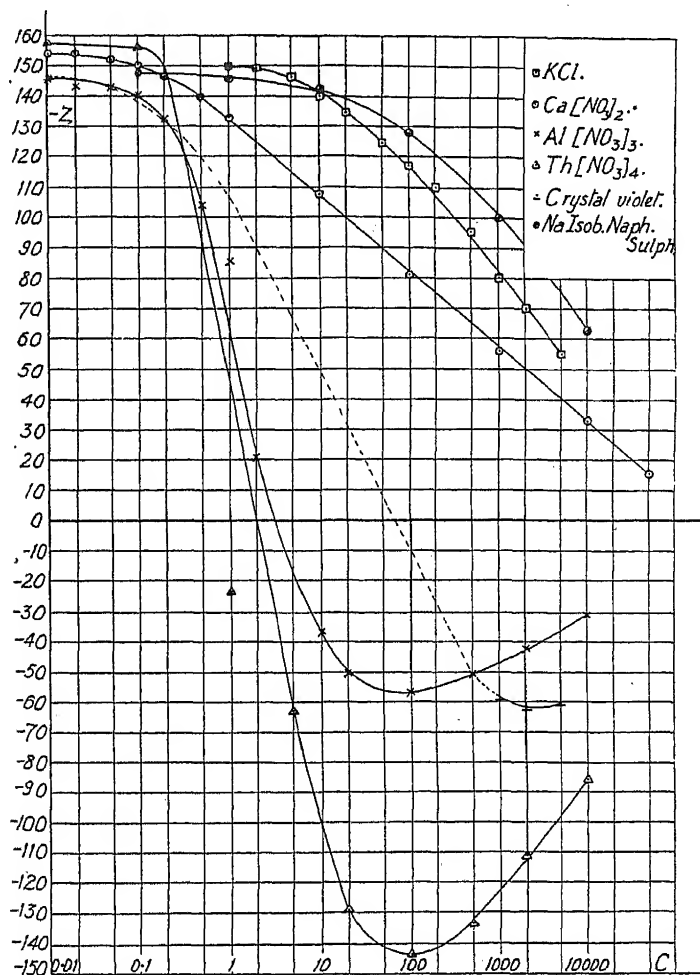


FIG. 9.— $(-\xi)$ - $\log c$ -curves.

experiment we could not prevent the wall from acting as a Na-ion exchange electrode, with as a consequence the production of a  $\xi$ - $\log c$  curve of the well known type for univalent electrolytes.

Finally, together with Mr. Delfosse<sup>7</sup> a series of experiments was performed on organic solvents. The dimensions of the apparatus were adapted for working with small amounts of liquid (30 c.c.; Fig. 11).

<sup>7</sup> De Smet and Delfosse, *Bull. Acad. Roy. Belg.*, IV, No. 10, 1942.

NL plays the part of the principal vessel, M that of the auxiliary one. The capillaries are mounted at  $C_1$  and  $C_2$ , the change of concentration is effected through D, the conductivity measured at E. The apparatus can rotate along the axis  $xy$ ; in order to avoid loss of liquid by evaporation, capillaries were used as connecting tubes between the apparatus and the system of taps. KI was used as an electrolyte. The solvents were the purest products of Schering-Kahlbaum; the alcohols were dried on sodium, distilled in an all Jena 161<sup>III</sup> glass apparatus with a long fractionating column; acetone subjected to one single distillation had a specific conductivity reduced to less than  $10^{-7}$  ohm<sup>-1</sup> cm.<sup>-1</sup>. The results are given in Fig. 12 (on a logarithmic scale) and Fig. 13; the values of the conductivity  $\sigma_0$  of the pure substances are also given in the table.

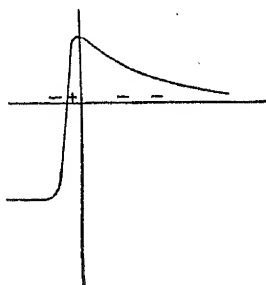


FIG. 10.—Charge distribution (triple layer), following from  $\psi$ -curve for  $\text{Th}(\text{NO}_3)_4$ .

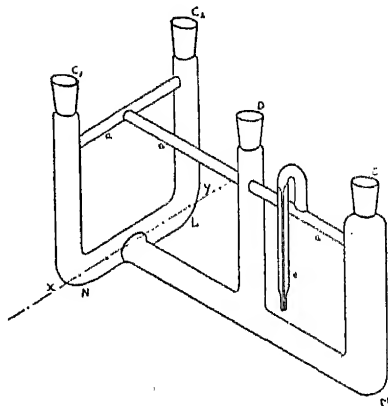


FIG. 11.—Schematic drawing of apparatus for measurements with organic liquids.

We draw attention to the fact that with a 1-1-valent non-capillary-active electrolyte (KI) reversal of charge could be obtained in a number of cases. It is further interesting that the horizontal part of the  $\zeta$ -log  $c$  curves is most pronounced in the case of water, then methyl-, ethyl-,  $n$ - and *iso*-propylalcohol follow, finally acetone.

We now compare our results for the pure substances with those of earlier workers <sup>8, 9, 10</sup> (Table III ( $-\zeta$ ) in mv.). The relative data of Coehn

TABLE III.—VALUES OF ( $-\zeta$ ) FOR PURE SUBSTANCES.

	Quincke and Tereschin.	Coehn and Raydt (acetone).	Coehn and Raydt (water).	Fairbrother and Balkin.	Our results.	D.
Water . . . . .	60	264	148	55	148	80
Methylalcohol . . . . .	40	238	133	—	123	35
Ethylalcohol . . . . .	80	233	130	—	170	24
Acetone . . . . .	—	230	129	62	230	21
<i>n</i> -Propylalcohol . . . . .	—	184	104	55	139	19.5
<i>iso</i> -Propylalcohol . . . . .	—	—	—	—	150	18.3

<sup>8</sup> Quincke and Tereschin, *Wied. Ann.*, 1887, 32, 333.

<sup>9</sup> Coehn and Raydt, *Ann. Physique*, 1909, 30, 777.

<sup>10</sup> Fairbrother and Balkin, *J. Chem. Soc.*, 1931, 389, 1564.

and Raydt have been converted into absolute ones, just by equating their value for water, and then by equating their value for acetone to ours; the last column contains the values of the dielectric constant  $D$  of the various liquids. As will be seen from the last two columns, our results do not agree with Coehn and Raydt's rule.

### Summary.

A new method for the measurement of the electro-endosmotic velocity has been developed. The velocity with which a thread of liquid in a capil-

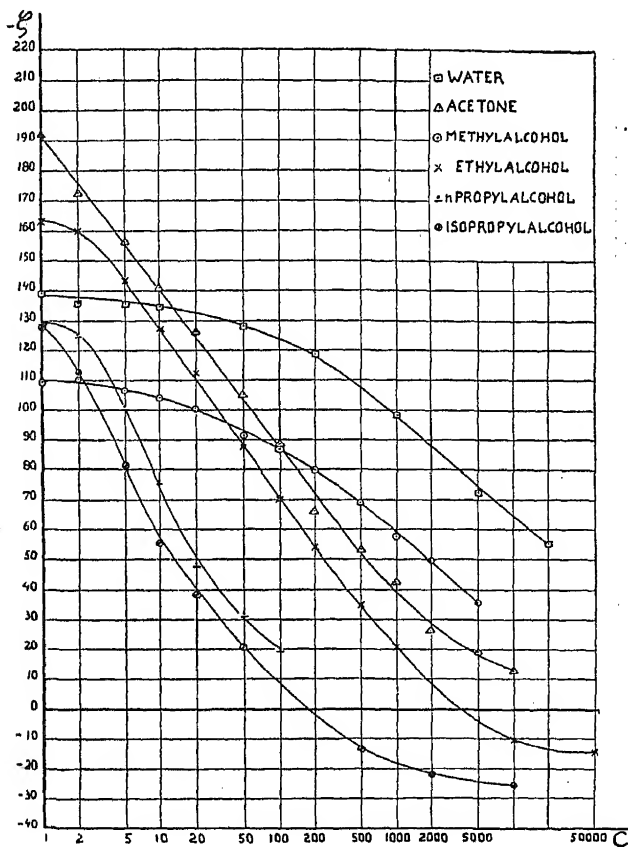


FIG. 12.— $(-\zeta)$ -log  $c$ -curves.

lary moves under the influence of an electric field of 120-60 v./cm. is measured by means of a microscope with ocular micrometer; the values of the  $\zeta$ -potentials calculated from these measurements proved to be independent of the radius of the capillary over a 2.5-fold range.  $\zeta$ -potentials have been determined for aqueous solutions of  $\text{KNO}_3$ ,  $\text{NH}_4\text{NO}_3$ ,  $\text{LiNO}_3$ ,  $\text{CsNO}_3$ ,  $\text{AgNO}_3$ ,  $\text{HNO}_3$ ,  $\text{KCl}$ ,  $\text{KI}$ ,  $\text{KOH}$ ,  $\text{K}_2\text{SO}_4$ , and  $\text{K}_4\text{FeCy}_6$ , at concentrations of 0, 1, 2, 5, 10, 20, 50, 100, 200, 500, 1000, 2000, 5000 and 10,000  $\mu$  equiv./l. for solutions of  $\text{Zn}(\text{NO}_3)_2$ ,  $\text{Ca}(\text{NO}_3)_2$ ,  $\text{Mg}(\text{NO}_3)_2$  and  $\text{Ba}(\text{NO}_3)_2$  at the same concentrations; for solutions of  $\text{Al}(\text{NO}_3)_3$ ,  $\text{La}(\text{NO}_3)_3$  and  $\text{Ce}(\text{NO}_3)_3$  at concentrations of 0, 0.01, 0.1, 1, 10, 100, 1000



and  $10,000\mu$  equiv./l. and of  $\text{Th}(\text{NO}_3)_4$  at concentrations of 0, 0.001, 0.01, 0.1, 1, 5, 20, 100, 500, 2000 and  $10,000\mu$  equiv./l.; on solutions of crystal violet and of sodium *isobutylnaphthalene* sulphonate (substances with a capillary-active cation or anion) between 0.01 and 5000 or  $10,000\mu$  equiv./l.

The results obtained can be interpreted in the following way:—

For the electrolytes with univalent cations, the  $\zeta$ -log  $c$  curves are all of the same character, except those for  $\text{HNO}_3$  and  $\text{KOH}$ ; for solutions of  $\text{HNO}_3$  the glass wall behaves in a certain sense as a H-ion electrode; the same holds for very dilute solutions of  $\text{KOH}$ ; for all the other electrolytes of this group ( $\text{KNO}_3$ ,  $\text{NH}_4\text{NO}_3$ ,  $\text{LiNO}_3$ ,  $\text{CsNO}_3$ ,  $\text{AgNO}_3$  . . .) the

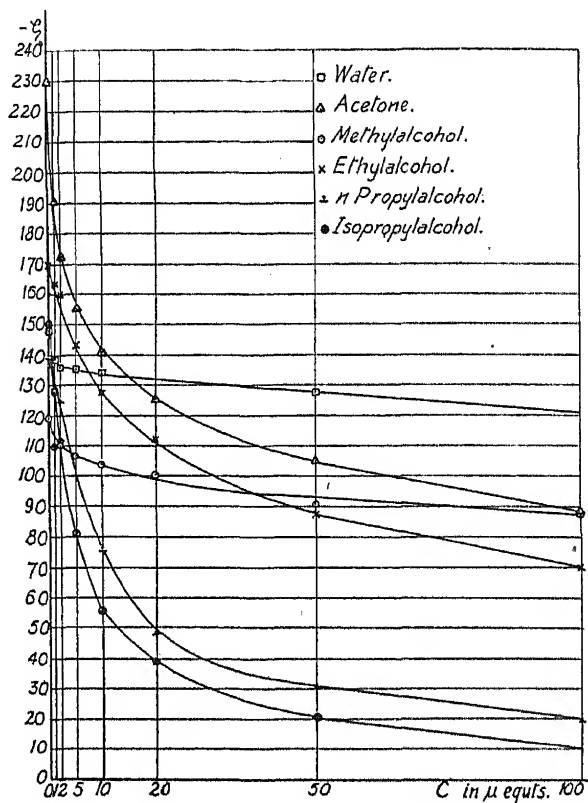


FIG. 13.—( $-\zeta$ )- $c$ ' curves.

wall behaves as a H-ion electrode between 0 and  $100\mu$  equiv./l. and as a K,  $\text{NH}_4$ , Li, Cs or Ag-, . . . electrode between 200 and  $10,000\mu$  equiv./l. (fairly linear  $\zeta$ -log  $c$  curves in this region, however, with a slope of 42 mv.).

For the electrolytes with divalent cations, the glass wall behaves as a perfect Mg, Ca, Ba, or Zn electrode (linear  $\zeta$ -log  $c$  curves with a slope of 25 to 26 mv.).

For the 3-1 and 4-1 types of electrolytes, as well as for crystal violet and sodium *isobutylnaphthalene* sulphonate the linearity of the  $\zeta$ -log  $c$  curves disappears completely. This behaviour must therefore be explained in a different way.

Finally the apparatus was adapted to measurements with organic solvents, and  $\zeta$ -potentials determined for solutions of KI in water, acetone,

methyl-, ethyl-, *n*-propyl- and isopropyl-alcohol at concentrations of 0, 1, 2, 5, 10, 20, 50, 100, 200, 500, 1000, 2000, 5000, 10,000 and sometimes 50,000  $\mu$  equiv./l; the  $\zeta$ -log  $c$  curves do not differ in principle from those obtained for water; the extension in concentration at which the glass wall behaves as a H-ion electrode decreases in the order: water, methyl alcohol, ethyl alcohol, *n*-propyl alcohol, isopropyl alcohol, acetone. In the cases of ethyl, *n*-propyl and isopropyl alcohols the sign of the  $\zeta$ -potential could be reversed by means of KI.

*Laboratory of Physical Chemistry,  
University of Ghent, Belgium.*

## ON A DIRECT CALCULATION OF THE VISCOSITY OF A LIQUID, BOTH UNDER ORDINARY PRESSURES AND HIGH PRESSURES, FROM THE VISCOSITY OF ITS VAPOUR, ON THE BASIS OF A NEW EQUATION OF STATE.

By D. B. MACLEOD.

*Received 26th March, 1945.*

### Introduction.

The author has developed a revised equation of state on the assumption that the volume of the molecules, in a fluid, is a function of the total pressure within the fluid. Van der Waals' equation of state was written <sup>1</sup>

$$(p + a/v^2)[v - b_0(1 - BP + CP^2)] = RT$$

where

$$P = p + a/v^2.$$

This idea of a compressible molecule was used, in a later paper,<sup>2</sup> to explain the failure of Bakker's equation for the latent heat of vaporisation. By introducing an extra term  $\int_{b_1}^{b_2} P db$ , into Bakker's equation, calculations of the latent heat of vaporisation, agreeing with the experimental values, were made. The term  $\int_{b_1}^{b_2} P db$  represents the actual work done on the molecules themselves. In this paper, this work term is used as a basis of a new theory of viscosity and, in fact, for a new theory of the fluid state.

Attempts to explain the viscosity of liquids have been made by two different methods of approach. On the one hand, Andrade<sup>3</sup> has developed a theory based upon the idea of a transference of momentum. On the other hand, various authors have developed equations of the form  $\eta = Ae^{Q/RT}$  in which attempts have been made to relate  $Q$  to the latent heat of vaporisation, the latent heat of fusion or to forces residual from the solid state. The values of  $Q$ , however, although appearing to bear some relation to these quantities, was in no sense identical with them.

### The Viscosity Equation.

The author<sup>4</sup> has shown that the frequency of vibration of a molecule could be expected to be proportional to  $\sqrt{T}/(v - v_0)$  where  $(v - v_0)$  stands for the free space within the liquid. If, now,  $Q$  stands for the actual work,

<sup>1</sup> *Trans. Faraday Soc.*, 1944, **40**, 439.

<sup>3</sup> *Phil. Mag.*, 1934, **17**, 497, 698.

<sup>2</sup> *Ibid.*, 1945, **41**, 122.

<sup>4</sup> *Proc. Physic. Soc.*, 1938, **50**, 788.

per gram molecule, done on the molecules themselves, due to their compressibility, it might be expected that the viscosity of a liquid could be

written  $\eta_e = \frac{A\sqrt{T} \cdot v}{v - v_0} e^{Q/RT}$  where  $A$  is a constant;  $\frac{v - v_0}{v}$  represents

the ratio of the free space, to the total volume, at any given volume. On applying this equation to an actual liquid, namely carbon tetrachloride, for which the quantity  $Q$  had already been worked out and published,<sup>2</sup> it was observed that the product  $A\sqrt{T}$  came to a quantity of the same order as the viscosity of a vapour. The equation was, therefore, amended and the viscosity of the liquid written directly in terms of the viscosity of the vapour, by the equation

$$\eta_e = \eta_{vap} \cdot \frac{v_e}{v_e - b_e} \cdot \frac{v_{vap} - b_{vap}}{v_{vap}} \cdot e^{Q/RT}.$$

As  $\frac{v_{vap} - b_{vap}}{v_{vap}}$  is practically unity, the equation could be written

$$\eta_e = \eta_{vap} \cdot \frac{v_e}{v_e - b_e} \cdot e^{Q/RT}.$$

All the quantities in this equation had been previously determined and published<sup>1, 2</sup> for three substances, namely, pentane, carbon tetrachloride and benzene. It remained, therefore, a simple matter to test its adequacy.

It must be understood that neither  $b_0$  nor  $Q$  are constants but both can be obtained, at any temperature, from the revised equation of state, that is, without reference to actual viscosity measurements. It will be observed that the equation presents no difficulties, from the point of view of dimensions, because both  $v_e/(v_e - b_e)$  and  $Q/RT$  are pure ratios. In the vaporous conditions, where  $(v_e - b_e)/v_e$  becomes unity and  $Q$  becomes negligibly small, the viscosity of the liquid merges into that of the vapour. It is, also, noticeable that if the molecule be considered incompressible, so that  $Q$  is 0, the equation develops into a form, which attributes the viscosity merely to a transference of momentum. In this form it has already been discussed by the author<sup>4</sup> and successfully applied to mono-atomic substances. In view, however, of the results of this paper some revision may be necessary in the treatment, even of these substances.

It is proposed now to apply this equation to the three mentioned substances. It will be admitted that the number of substances chosen is small, but as these substances are typical and taken at random, there seems no reason why a similar agreement should not be obtained with other substances. Further, all the constants required have already been published. It is necessary, however, to draw attention to the fact that the original equation of state was developed on the, admittedly, approximate assumption that at the critical temperature  $b_c$  is equal to  $v_c/2$ . The nature of the argument in the original paper<sup>1</sup> indicated clearly that a variation from this value should be expected in individual substances. This variation, if sufficient to be important, could only be determined, however, by trial and error methods.

An unfortunate handicap proved to be the lack of some of the desired experimental data. The viscosity of benzene vapour from 0° C. to 200° C. is obtainable from the values given in the International Critical Tables. The viscosity of the liquid up to the boiling point can also be obtained from the same tables. Fortunately the viscosity of liquid benzene, for a further hundred degrees above the boiling point, is given in the L.B.M. Tables. This enables a study for benzene to be carried over a range of 200° C. The author was unable, however, to find a value for the viscosity of carbon tetrachloride vapour. Values, to be compared with experiment, have, however, been computed. The viscosity of isopentane vapour was obtainable, but not that of pentane. It is not likely that they will

differ much. A complete study is given for benzene and the other substances carried forward as far as possible at present.

Table I for benzene is explained as follows: column I gives the absolute

TABLE I.—BENZENE.

$$a = 2.075 \times 10^7.$$

Temp. ° K.	$\eta_{\text{liq.}}$ obs.	$\eta_{\text{vap.}}$ obs.	Mol. vol.	$p + \frac{a}{v^2}$	$v - b$ .	$b$ .	$Q_1$ .	$Q_2$ .	$Q_3$ .
273	0.039025	0.04686	86.75	2755	8.29	78.46	1392	1372	1372
283	0.03759	0.04723	87.79	2690	8.80	78.99	1364	1322	1344
293	0.03649	0.04750	88.84	2627	9.34	79.50	1322	1284	1302
303	0.03562	0.04775	89.90	2565	9.89	80.01	1290	1250	1270
313	0.03492	0.04798	91.06	2494	10.50	80.56	1257	1220	1237
323	0.03437	0.04820	92.20	2439	11.09	81.11	1225	1190	1205
333	0.033905	0.04844	93.46	2374	11.74	81.72	1190	1170	1170
343	0.03351	0.04863	94.67	2313	12.41	82.26	1160	1140	1140
353	0.03317	0.04882	95.96	2251	13.12	82.84	1130	1115	1110
373	0.03263	0.04918	98.40	2143	14.60	83.8	1050	1072	1050
404	0.03197	0.04995	103.2	1953	17.2	86.0	930	956	930
434	0.03154	0.03168	108.7	1760	20.5	88.2	830	850	830
459	0.03125	0.03115	114.4	1597	24.8	89.6	760	780	760

temperature, column II the experimental viscosity of the liquid, and column III the experimental viscosity of the vapour. Column IV gives the molecular volumes from the best available figures. Column V gives the total pressures,  $p + a/v^2$ , using for  $a$  the value  $2.073 \times 10^7$ , already published.<sup>1</sup> Column VI gives the free space  $v - b = RT/(p + a/v^2)$ . Subtracting  $(v - b)$  from the molecular volume, column VII, representing  $b$ , the volume of the molecules, is obtained. In the earlier paper  $Q_1 = \int_{b_1}^{b_2} P db$  was given as 1090 calories per gram molecule at  $363^\circ \text{K}$ . The values in this column, above this temperature, are those previously determined. The values below this temperature were obtained by multiplying the change in  $b$  by the mean pressure between each  $10^\circ \text{C}$ . and converting into calories. All the quantities required to calculate the viscosity of the liquid from the vapour or of the vapour from the liquid are now available.

Assuming, for example, the value of the viscosity of the liquid at  $0^\circ$ , the corresponding value for the viscosity of the vapour will be given, from the above figures, using the equation

$$\begin{aligned} \eta_{\text{vap}} &= \eta_{\text{liq.}} \cdot \frac{v - b}{v} e^{-Q/RT} \\ &= 0.009025 \times \frac{8.29}{86.75} \times e^{-\frac{1392}{546}} = 0.04668. \end{aligned}$$

The experimental value at  $0^\circ \text{C}$ . is 0.04686.

The nature of the subsequent agreement can be seen by comparing  $Q_2$ , which has been calculated, using the observed values of the viscosity of the liquid and vapour, assuming  $Q$  as the unknown. The agreement is actually more satisfactory than that indicated by these two columns. As already indicated, the values of  $Q_1$  below  $363^\circ \text{K}$ . were obtained from the value of 1090 for  $363^\circ$  quoted from the earlier paper. This value was obtained by the method of estimating squares and as the total heat involved was of the order of 7000 calories, no attempt was made to secure great accuracy in a figure involving an error of one in seven hundred. If the basis value at  $363^\circ$  be taken as 1070 instead of 1090, as in the last

column,  $Q_3$ , the similarity of the two columns is more marked. The equation connecting the viscosity of the liquid and the vapour has, therefore, been followed over a range of nearly  $200^\circ \text{C.}$  and the divergence is not more than 2 to 3 %. Further, the equation enables the viscosity of the fluid to be traced continuously right through the critical condition. Unfortunately no experimental data are available for the viscosity of a fluid in the neighbourhood of the critical condition, due no doubt to the technical difficulty of devising a method for measuring viscosity under these conditions.

It must be admitted that the success of the above analysis gives strong support to the physical reality of the quantities used. It also indicates that the quantity, missing hitherto, to give a satisfactory explanation of viscosity, is the actual work done on the molecules themselves.

The next substance to be discussed is carbon tetrachloride, set out in Table II. As already mentioned, the experimental values for the viscosity

TABLE II.—CARBON TETRACHLORIDE.

$$a = 2.216 \times 10^7.$$

Temp. °K.	$\eta_{\text{liq. obs.}}$	Mol. vol.	$p + \frac{a}{v^2}$	$v - b$	$b$	$Q_1$	$Q_2$	$\eta_{\text{vap.}}$ (calc.).
273	0.01346	94.20	2497	9.15	85.05	1321	1294	0.04116
283	0.01133	95.35	2438	9.71	85.64	1286	1260	0.04118
293	0.00969	96.52	2379	10.31	86.21	1253	1231	0.04122
303	0.00842	97.68	2322	10.92	86.76	1220	1207	0.04125
313	0.00738	98.95	2263	11.57	87.38	1187	1181	0.04128
323	0.00654	100.22	2207	12.25	87.97	1156	1159	0.04131
333	0.005825	101.55	2150	12.96	88.59	1124	1136	0.04137
343	0.00524	103.00	2090	13.74	89.26	1090	1115	0.04143

of the vapour were not available. The last column gives values computed from the liquid. The column  $Q_1$  has been obtained, as in the case of benzene, from the value of 1060 cal., quoted from the earlier paper, at  $353^\circ \text{K.}$  While unable to check the absolute values of the viscosity, their rate of increase, with temperature, bears a close resemblance to that of benzene. It might well be, however, that the absolute value may be in error 10 % or more. The column headed  $Q_2$  has been calculated from the equation

$$\frac{\eta}{\sqrt{T}} \cdot \frac{v - b}{v} = A e^{Q/RT}.$$

In this equation the experimental value of the vapour viscosity has been replaced by the quantity  $A\sqrt{T}$ . The simple Maxwell theory of the viscosity of gases leads to such an expression but it is well known that actual gases and vapours show a much greater increase of viscosity, with rise of temperature, than indicated by the simple theory.

While the analysis for this substance is less complete than in the case of benzene, it indicates that the quantity  $Q_1$  is of the right order to connect the viscosity of the vapour with that of the liquid, by the equation proposed.

The remaining liquid to be discussed is pentane. Here a comparison has been made with the viscosity of *isopentane* vapour, that of pentane not being available. The column  $Q_1$  has been obtained from the published value of  $Q_1$  for  $313^\circ \text{K.}$ , namely, 920 cal. It will be observed that the absolute values in this case are considerably lower than the quoted experimental values. The change with temperature follows, however, the experimental figures closely. In view of the processes involved in the

computation of  $Q$ , an agreement for the absolute value, within a few per cent., could hardly be expected. Further, as  $Q$  comes in as an exponential term, a small error in its original estimation has a marked effect on the calculation of the viscosity.

TABLE III.—PENTANE.

$$a = 2.114 \times 10^7.$$

Temp. ° K.	$\eta_{\text{liq. obs.}}$	Mol. vol.	$\phi + \frac{a}{v^2}$	$v - b$	$b$	$Q$	$\eta_{\text{vap. calc.}}$	$\eta_{\text{vap. obs.}}$
273	0.02283	111.1	1712	13.3	97.8	1053	0.0450	0.0463
283	0.02255	112.8	1662	14.3	98.5	1025	0.0453	0.0466
293	0.02232	114.5	1613	15.2	99.3	993	0.0456	0.0469
303	0.02212	116.5	1561	16.3	100.2	960	0.0461	0.0473
313	(0.02193)	118.8	1498	17.5	101.3	920	0.0465	0.0476

### Viscosity Under Pressure.

It is now proposed to apply the methods used above to analyse the data for the viscosity of pentane under pressure. The standard experimental work, in this field, has been done by Bridgman and the experimental quantities used have been taken from his book, *The Physics of High Pressure*. It has been the fate of other equations proposed for liquids under ordinary conditions, that they have been unable to predict the very high viscosities revealed by Bridgman's measurements. Bridgman himself suggested a possible interlocking of the molecules to account for these very high values. He expressed doubt that a mathematical expression could be obtained to analyse the results. It will be shown that, without any other than energy considerations, the experimental values can be explained with precision. As both benzene and carbon tetrachloride solidify under a pressure a little above 2000 atmospheres, the discussion in this section will be confined to pentane. For this substance, data are available up to 10,000 atmospheres. At that pressure the viscosity of the liquid is some forty times that of the liquid under ordinary pressures and consequently several thousand times that of the vapour.

Bridgman gives the relative volumes for pentane at temperatures of 0° C., 50° C. and 95° C., for pressures up to 10,000 kg. per sq. cm. Unfortunately his viscosity measurements were made at 30° C. and 75° C. It was necessary, therefore, to obtain the relative volumes at 30° C. by interpolation between 0° C. and 50° C. The final calculations showed that the small uncertainty in this interpolation could be important. It has been remarked that other equations have failed to explain the very high values reached by the viscosity of the liquid under pressure. It was soon apparent, however, that the author's equation, applied directly, gave calculated values several times as great as the observed values. It was also obvious why this was so. The equation of state, proposed by the author, assumed that in a liquid, under ordinary conditions, the internal forces are of the nature of attraction. Bridgman (pp. 140 and 141) points out that this actually is so. It is proved from the thermodynamic relation

$$\left(\frac{\partial E}{\partial p}\right)_T = -T \cdot \left(\frac{\partial v}{\partial T}\right)_p - p \cdot \left(\frac{\partial v}{\partial p}\right)_T.$$

At low pressures the second term is negligibly small and as the first term is positive, the internal energy decreases with increasing pressure. At higher pressures, the second term increases so that, when these two quantities become equal, the repulsive force neutralises the attractive force,

and the effective pressure on the liquid is then exactly the applied pressure. The pressure at this point is given by

$$p = -T \left( \frac{\partial v}{\partial T} \right)_p / \left( \frac{\partial v}{\partial p} \right)_T = T \left( \frac{\partial p}{\partial T} \right)_v.$$

Further, the relative magnitude of the repulsive force to the attractive force at other pressures is given by the ratio of  $p \left( \frac{\partial v}{\partial p} \right)_T / T \cdot \left( \frac{\partial v}{\partial T} \right)_p$ ,

that is  $\frac{p}{T \cdot (\partial p / \partial T)_v}$ . As the attractive force is computed throughout by the quantity  $a/v^2$ , the repulsive force can be obtained directly from this quantity by multiplying by the above ratio, computed directly from the observed values of  $p$ ,  $v$  and  $T$ . For pentane the reversal occurs at 30° C. between 6000 and 7000 kg. per cm.<sup>2</sup> pressure. It is, therefore, necessary to write the equation of state for liquids under pressure as

$$\left( p + a/v^2 - \frac{p}{T(\partial p / \partial T)_v} \cdot a/v^2 \right) (v - b) = RT.$$

The quantity  $a$  being the original value of  $a$  obtained for the substance, the whole quantity within the first bracket can be determined directly from the experimental figures. Dividing  $RT$  by this quantity enables  $(v - b)$  to be obtained as before and  $b$  computed.

One further step remains to be taken. Writing the repulsive force, for brevity, as  $f(P)$ , the equation of state can be written

$$(p + a/v^2)(v - b) = RT + f(P)(v - b).$$

The two terms on the left-hand side of the equation represent the work being done on the liquid causing it to contract, and the two terms on the right the work being done by the liquid in opposing the contraction. The first term on the right represents the resistance due to the average kinetic energy of the molecules, while the second represents a static repulsive force. It would, in fact, be possible to reproduce the same resistance to contraction by dispensing with the repulsive force and replacing it by an increase in the average kinetic energy of the molecules. In that case a hypothetical temperature  $T'$  might be added to  $T$  such that  $f(P)(v - b) = RT'$ . It would then be the obvious thing to replace  $RT$  in the expression  $e^{Q/RT}$  by  $R(T + T')$ . From these considerations, the viscosity of a liquid at pressure  $p$  would be expressed in terms of the viscosity at a pressure  $o$  by the equation

$$\eta_p = \eta_o \cdot \frac{v_o - b_o}{v_p - b_p} \cdot \frac{v_p}{v_o} \cdot e^{Q/R(T + T')}$$

where  $Q$  is the work done on the molecules themselves in passing from a pressure  $o$  to  $p$ . All the quantities here involved can be obtained directly from the experimental measurements of  $p$ ,  $v$  and  $T$  and in no way involve the viscosity measurements themselves.

The next table sets out these quantities computed directly from the experimental figures, for pentane, supplied by Bridgman. The logarithms of the observed and calculated viscosities are compared in the last columns.

Column I gives the applied pressures in kilograms per sq. cm. Column II gives the molecular volumes and column III  $a/v^2$ , using the previous

value of  $a$  namely  $2.114 \times 10^7$ . The quantities  $\frac{p}{T \cdot (\partial p / \partial T)_v}$  which, multiplied by column III, give the repulsive force in column IV, were carefully computed by my assistant, Mr. Roth, and myself. The sum of columns I and III less IV, gives  $P_o$ , the effective pressures. The successive values of  $Q$  were obtained by multiplying the change in volume of  $b$  by the mean pressure and converting into calories. The method of obtaining

$RT'$  has been explained. The observed and calculated viscosities are then compared.

TABLE IV.—PENTANE AT 303° K.

$$a = 2.114 \times 10^7.$$

Pr. in kg. cm <sup>2</sup> .	Mol. vol.	$\frac{a}{v^2}$	$f(P)$ .	$P_e$ .	$v - b$ .	$b$ .	$Q$ .	$RT'$ .	Log $\eta$ calc.	Log $\eta$ obs.
0	116.4	1556	0	1556	16.30	100.1	—	—	—	—
1,000	102.7	2005	671	2334	10.87	91.83	384	175	0.334	0.315
2,000	98.64	2253	1110	3143	8.07	88.77	200	—	—	—
3,000	93.00	2444	1570	3874	6.54	86.46	193	—	—	—
4,000	90.22	2597	1940	4657	5.45	84.77	172	253	0.845	0.847
5,000	88.02	2728	2364	5304	4.73	83.29	177	—	—	—
6,000	86.11	2851	2752	6099	4.16	81.95	183	—	—	—
7,000	84.45	2964	3162	6802	3.73	80.72	189	—	—	—
8,000	82.96	3073	3373	7700	3.29	79.67	182	265	1.385	1.360
9,000	81.80	3160	3576	8584	2.95	78.85	169	—	—	—
10,000	80.80	3240	—	—	—	—	—	—	—	—

It must be agreed that the result is a complete vindication of the method. It means, in fact, that with a moderate uncertainty in the absolute value of the viscosity of the vapour, the viscosity of pentane has been followed continuously from the vaporous condition to that of a liquid at 8000 atmospheres, through a range of several thousand times, without the introduction of a single arbitrary constant. Further, it is based upon an entirely new view of the nature of fluids, replacing the conventional incompressible molecule by one for which the compressibility has been determined and for which the work done on it has been computed.

### Summary.

(1) The viscosity of a liquid has been calculated from the viscosity of its vapour, by using the vibration frequency and the work done on the actual molecules, during the condensation from the vapour to the liquid.

(2) This work had been computed in an earlier paper and depends on the postulate of a compressible molecule.

(3) The viscosity of pentane up to 8000 atmospheres has been calculated directly from the liquid under no pressure without the introduction of any arbitrary constants.

In conclusion I wish to express my thanks to Mr. Roth and Major Straker for their assistance with the computations involved in this paper.

*Physics Department,  
Canterbury University College,  
Christchurch, New Zealand.*



# THE ADAPTATION OF *BACT. LACTIS AEROGENES* TO HIGH CONCENTRATIONS OF PROFLAVINE.

BY D. S. DAVIES, C. N. HINSHELWOOD AND J. M. G. PRYCE.

Received 5th June, 1945.

## Adaptation to High Proflavine Concentrations.

**Spontaneous Reversion.**—Previous work has shown that *Bact. lactis aerogenes*, when grown in media containing proflavine at a given concentration,  $P$ , acquires immunity to the action of the drug at all concentrations up to a value which just exceeds  $P$  itself. A series of strains differing quantitatively in tolerance to proflavine may be obtained by training at various drug concentrations. The mechanism of this adaptation has been discussed in terms of a simple model, in which the expansion of particular enzymes is assumed to compensate their lowered activity.<sup>1</sup>

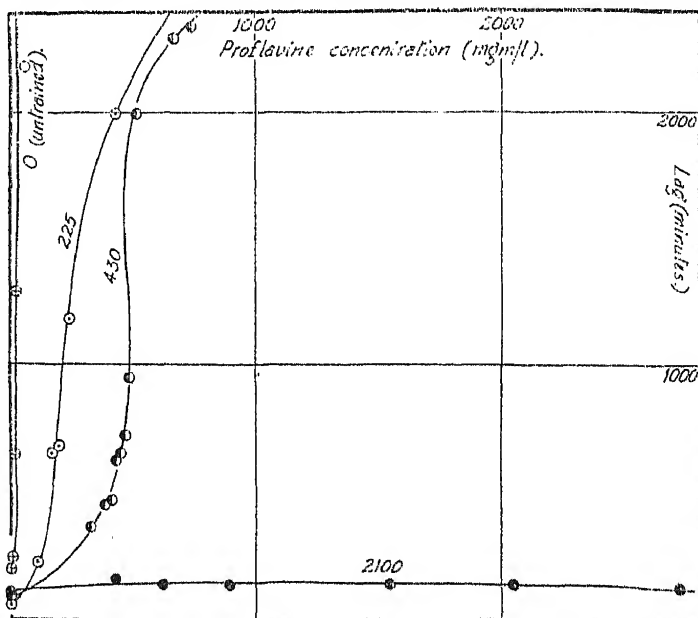


FIG. 1.—Adaptation to high concentrations of proflavine. Numbers on curves indicate training concentration.

The drug affects lag and growth rate, qualitatively, in a similar way. The influence on the lag is, however, more marked, and has been chosen in the present work as the criterion of adaptation.

The question arises whether there is any limit to the degree of adaptation attainable. In the earlier work concentrations up to 430 mg./l. were studied. The range has now been extended to 2300 mg./l. Adaptation still occurs, but at the higher concentrations the response is in certain respects rather different. A strain trained at a low value of  $P$  will not

<sup>1</sup> Davies, Hinshelwood and Pryce, *Trans. Faraday Soc.*, 1945, 41, 163.

grow at all at ( $P + 50$ ), whereas for  $P = 430$  the strain will grow up to 1540 mg./l. (though with increased lag). Further training at  $P = 1540$  confers practically complete immunity to 3000 mg./l., the highest concentration which it was practicable to use (Fig. 1).

For the higher values of  $P$  the attainment of maximum immunity requires ten to twenty subcultures in contrast to the rapidity of the adaptation at the lower values of  $P$ .

A somewhat complex picture is presented by the behaviour of trained cells when returned to the normal medium. Those trained at  $P = 43$  retain their immunity during many subsequent passages through the drug-free medium, but those trained at  $P = 1540$  show a marked reversion after a few passages. Under normal circumstances this reversion is far from complete, but stops at a definite equilibrium state. The residual immunity, which is still considerable, persists during many subcultures in the normal medium. These facts are illustrated in Fig. 2 which shows

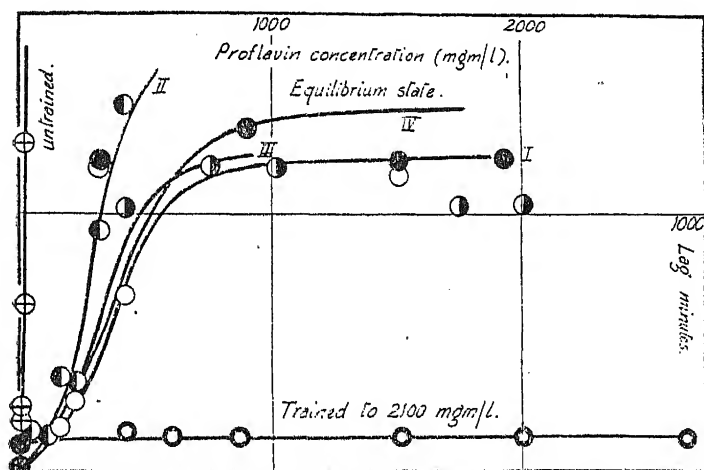


FIG. 2.—Reversion of trained cells to equilibrium state.

- I. Series 1.—1 subculture in normal medium.
- II. Series 1.—18 subcultures in normal medium.
- III. Series 2.—4 subcultures in normal medium.
- IV. Series 2.—24 subcultures in normal medium.

some characteristic lag-concentration (lag minimal with respect to age of cells) curves for strains, initially trained to the maximum possible extent, and then grown in absence of the drug. The rapid but limited reversion is evident.

The attainment of the state just described represents a fairly well marked stage in the development of the adaptation. The reversion was found to be the same for cells which had just attained complete immunity (as measured by the absence of lag in presence of proflavine) as for those which had been subcultured a further 20 times at the high proflavine concentration. On the other hand, a total of 80 passages gave rise to a strain which retained its full immunity for at least several passages through the normal medium. Thus it appears that ultimately the immunity attained may be not only complete but stable, though the stable state is reached only after very thorough training indeed. The extent of the reversion from the state of complete but unstable immunity does not appear to depend upon small variations in the history of the cells during the training process. In one experiment two strains were trained in different ways to grow ultimately in 1540 mg./l. First, both were grown

until immune to 225 mg./l.: one was then transferred to 430 and then to 1540, while the other was trained in gradual stages up to 430 mg./l. and then grown 6 times alternately in 430 mg./l. and normal medium, before a final transfer to 1540 mg./l. The reversion of both strains was similar.

As regards the properties of the highly trained cells, both in proflavine and in the normal medium, the growth rate and the lag-age relationships are, within the limits of measurement, identical with those of the untrained cells in the normal medium. Certain enzymatic differences between the strains can be detected and will be discussed elsewhere, but essentially the cells stably immune to 2000 mg./l. proflavine showed the reactions of a typical strain of *Bact. lactis aerogenes*. (We are indebted to Dr. Vollum for an independent examination of the strain.)

**Artificially Induced Reversion.**—Preliminary work<sup>2</sup> had indicated that cells immune to one antibacterial substance might regain their

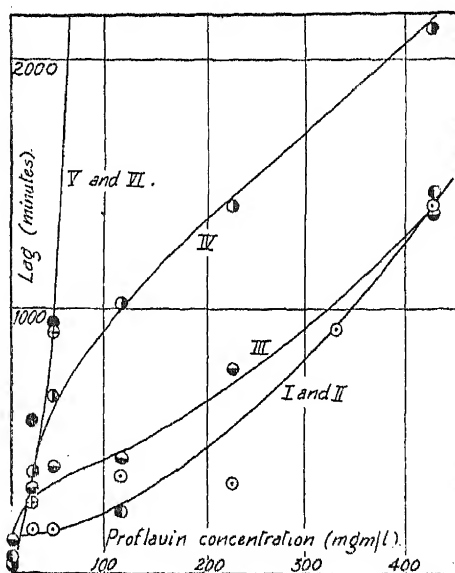


FIG. 3.—Reversion induced by phenols.

- I. Immune parent strain.
- II. 0.023 % cresol.
- III. 0.038 % cresol.
- IV. 0.052 % cresol.
- V. 0.07 % cresol.
- VI. 0.14 % phenol.

sensitivity when grown in presence of another. In particular, it was found that proflavine-resistant organisms lost their immunity when grown under suitable conditions in presence of tertiary butyl alcohol or *m*-cresol.

Further work has shown that the reversion induced in this way by *t*-butyl alcohol is erratic and rarely complete. On the other hand, cells grown under the appropriate conditions in *m*-cresol lose their adaptation in a systematic and reproducible manner.

The parent strain for most of these experiments was one which had been trained initially to 2000 mg./l. and then grown several times in the normal medium. As stated in the preceding section, this results in a partial lapse of immunity, but yields cells stably immune to proflavine concentrations up to about 200 mg./l.

These cells were inoculated into a series of media containing various amounts of cresol and at three different ages—during the logarithmic phase, at the end of it, and twenty-four hours later. From each of the cresol-cultures that grew, cells were inoculated into the normal medium once or twice, and thence (at the stage of minimum lag) into a series of

<sup>2</sup> Davies, Hinshelwood and Pryce, *Trans. Faraday Soc.*, 1944, 40, 397.

media containing proflavine, to measure the extent of the residual immunity, if any.

Maximum reversion was found with the cresol cultures inoculated from a young, actively growing, parent. For these the various lag-proflavine concentration curves are shown in Fig. 3. For comparison, the lag-concentration curve for the untreated cells is also given. It can be seen that a graded reversion occurs, which increases regularly with rising cresol concentration. The shape of the curves will be commented on later. Complete loss of immunity only occurs when there is enough cresol to delay growth for one to two days.

It was thought that this behaviour might be connected with the tendency of *Bact. lactis aerogenes* to grow into long filamentous forms in presence of *m*-cresol.<sup>3</sup> Reversion was, however, observed without filament formation in cresol. Indeed, proflavine-trained organisms very rarely grew into the thread-like forms under conditions where normal untrained cells quite regularly did. Moreover, growth in presence of phenol—which has not been observed to give rise to the filament forms—also causes some lapse of immunity. In general, it may be said that adaptation to proflavine is reversed with considerable difficulty. Cells adapted to the lower proflavine concentrations are stable even to the cresol-induced reversion. A strain trained to 68 mg./l. showed little or no loss of immunity when subcultured in cresol under conditions which would have caused complete reversion of a more highly trained strain.

### Discussion.

The hypothesis already advanced supposes that the drug exerts its principal action in inhibiting the operation of a particular enzyme, and thus, indirectly, others dependent on it: that there is in consequence an increase per cell in the amount of enzymes whose synthesis is not affected, and that these (or one of them) produce in consequence greater supplies of an intermediate, which compensates for the action of the drug. In the first part of the following discussion this hypothesis will be assumed.

#### (a) Adaptation to Very High Concentrations.

There is, according to the hypothesis referred to, no reason why immunisation should not be carried to the highest drug concentrations. The fact, however, that beyond a certain point training at a given concentration immunises to far higher concentrations calls for an explanation. A simple hypothesis is that the amount of drug which the cell can take up is limited. Above a certain concentration,  $c_{\text{max}}$ , further additions of drug to the medium are irrelevant to what happens in the cell. The following course of events would then be expected. As the cells are progressively trained, a state is reached where they will just grow, though with a long lag, at  $c_{\text{max}}$ .—and, by hypothesis, with the same lag at much higher concentrations. At this stage the lag-concentration curve for the strain, instead of rising steeply to infinity at a certain point, would turn over horizontally. Completion of the training merely lowers this horizontal line until the strain grows with no lag at any concentration. This is what is observed.

#### (b) Reversion to an "Equilibrium" State.

As described above, certain strains of highly trained cells may revert in drug-free medium, not to the original state of unadapted cells, but to a sort of equilibrium state, corresponding not to the highest, but still to a considerable degree of training. According to the hypothesis referred to at the beginning of this discussion, when cells are returned to the

<sup>3</sup> Spray and Lodge, *Trans. Faraday Soc.*, 1943, 39, 425.

normal medium two cases arise. In the first, there is a restoration of the normal enzyme balance and in the second, a retention of the changed balance. The removal of the drug action allows the expanded part of the enzyme system to produce metabolites in excess of the normal. If this excess stimulates the increase of the inhibited part of the enzyme system relatively to the expanded part reversion occurs. If the excess metabolite fails to stimulate this readjustment, then there is no reversion. Since rates of enzyme synthesis must be related to substrate concentration by equations resembling adsorption isotherms, the growth of enzymes involved in reversion may easily be independent of excessive metabolite concentrations, in which case there will be no response to the removal of the drug, and no reversion will occur.

As far as this argument goes, there is no reason why an indefinitely high degree of training should not be retained. But new factors must enter into the situation. We have two states of affairs: in one the highly trained strain reverts rapidly to an equilibrium state of lower training; in the other, much more difficult to attain, it is stable.

The explanation must be sought in the relation of the expanded enzyme systems to the rest of the cell. In response to the drug action the expansion can occur readily, and adaptation is complete (from the point of view of lag and growth rate) as soon as the changed balance is established. But an excessive degree of expansion can hardly occur without setting up some kind of strain in the rest of the cell. The easing out of this is necessary before the adaptation is stable. The equilibrium state described above would represent the maximum enzyme modification which the cell will tolerate without strain. The course of training is thus envisaged in the following way: first, enzyme expansion without strain (stable) up to a maximum: then, further enzyme expansion accompanied by strains in the cell: finally, a more complex adaptation of the cell as a whole whereby the strain is relieved and the highest degrees of adaptation become stable.

The strain referred to might quite well be of a purely structural or crystallographic nature—and in some ways this is the simplest hypothesis to make: this type of interpretation has been developed in order to explain adaptation to utilise alternative carbon sources.<sup>4</sup>

Alternatively, the strain might represent certain excessive demands upon the metabolic processes of the cell enzymes generally. Since training to the high concentration does in fact occur, the demands for the synthesis of the expanded enzymes are being met in presence of the drug. Reversion might mean that they are not met in the normal medium. The reason may well be that some part of the enzyme system has not only been produced in abnormally large amount by the adaptation but, when the drug is removed, operates per unit amount at an increased rate. This involves extra demands on certain substrates. Such demands may compete with others, including those which supply materials for the synthesis of the expanded part of the enzyme system itself. Thus its own excessive expansion is indirectly responsible for the cutting off of its own supplies. Hence its growth rate, relatively to that of the cell as a whole, may be adversely affected, and it will shrink until other enzymes are again able to supply it. The equilibrium state will then be reached.

According to this view the equilibrium state is a function of the enzyme balance in the cell as a whole, and can therefore, in principle, depend upon the adaptive history of the cell. In this way we might explain the great stability to reversion of the cells which had been given 80 further training passages through proflavine. In the course of this long history all kinds of auxiliary adjustments could have occurred, making other enzymes assume a more harmonious balance with the expanded ones. These changes could be qualitative ones as well as simply quantitative

<sup>4</sup> Postgate and Hihshelwood, *Trans. Faraday Soc.*, 1945, in the press.

ones, the original sequence of processes involved in growth being gradually superseded by others.

### (c) Reversion in Relation to Selection.

It would be imprudent not to consider how far the facts about reversion of training can be explained by the superposition of adaptive changes within the cells and selective shifts in the balance of an inhomogeneous population. We will begin by assuming an inhomogeneously trained population of cells. The degree of training of a given cell can be specified in terms of the drug concentration  $\bar{P}$  to which it is fully adapted, and the whole population will be characterised by the frequency distribution of  $\bar{P}$  values. If this distribution has a sharp maximum in the region of  $\bar{P}_1$ , then the culture as a whole will appear to show this degree of adaptation. There will be some cells with values of  $\bar{P}$  less than  $\bar{P}_1$ , down to a limit of  $\bar{P}_2$ . As training proceeds the limit  $\bar{P}_2$  gradually moves up from zero towards  $\bar{P}_1$ . Now if we further assume that the less highly trained cells have a certain advantage in the normal medium over the more highly trained ones, then, in the absence of the drug, the population balance will shift so that  $\bar{P}_{\max}$ , (determining the behaviour of the culture as a whole) shifts from the region of  $\bar{P}_1$  to that of  $\bar{P}_2$ . We shall then, for the three stages of proflavine training, have the following relations. For low degrees of training, the distribution has a sharp maximum near the training concentration. For the highly trained cells there is a maximum near the training concentration, and definite numbers of cells with values of  $\bar{P}$  down to  $\bar{P}_2$  which is considerably lower. The reversion is limited by this value, below which there were supposed to be no cells in the trained culture. Very elaborate training may eliminate all the cells with values of  $\bar{P}$  much below  $\bar{P}_1$ , in which case the culture would be stably trained. But this final elimination would be difficult and lengthy.

This view of the matter has at first sight great advantages in explaining the facts about reversion and might seem to supersede the discussion given in the earlier paragraphs. But the advantage is more apparent than real. In the first place, there is no evidence that the less highly trained strains are in any way more favourably placed for growth in the normal medium. In the second place, a statistical distribution of  $\bar{P}$  values is very unlikely to arise except from causes which will continue to operate in the partially de-trained strain. Therefore, to explain the limited reversion we have to invoke some hypothesis to explain why, when  $\bar{P}$  falls below a certain value, no cells of lower resistance appear, or why, if they do appear, they do not outgrow the others. We are thus faced with the original problem once more. That selection must operate to some extent is clear, and is discussed in a later paragraph, but it can hardly interpret the facts without auxiliary hypotheses which might as well be applied directly to the cell material in general.

The situation would, of course, be different if the population were always an inhomogeneous mixture of *non-interconvertible* strains of different drug sensitivity, the relative proportions of which are modified by training. The reasons for rejecting this extreme form of the selection view are as follows: (1) the degree of adaptation is quantitatively related to the drug concentration, to explain which an infinite number of substrains would have to be postulated—an unlikely assumption unless the strains may be formed one from another. (2) Stable trained strains, from which by hypothesis all sensitive members have been eliminated, can suffer induced reversion. (3) The alternative hypothesis of changes in the cell material as a whole interprets the facts sufficiently well.

### (d) The Superposition of Adaptation and Selection.

In spite of what has just been said, selection must automatically be *superimposed* on any other adaptive mechanism.

On the one hand, in training, it will accentuate and accelerate the operation of other mechanisms, since the first cells to become adapted, even if they owe their priority only to chance, will have an opportunity to outgrow the rest. Although on this basis it is only necessary theoretically for one cell to become adapted initially, this adaptation will have been conditioned by the drug concentration in the medium and the degree of immunity will correspond. Thus the rate only, and not the final extent of the adaptation will be modified by selection.

On the other hand, selection may seriously retard the loss of adaptation. If by some treatment (such as growth in presence of cresol) the population is almost entirely de-trained, so that only a small fraction of immune cells remain, these survivors will tend to outgrow their more sensitive competitors. The quantitative aspect of this is interesting. Suppose 1 % of immune cells were left in the population. As an approximation, consider *separately* the behaviour of the two parts of the inhomogeneous culture when inoculated into media containing the original antibacterial at various concentrations, *i.e.* we imagine that we inoculate with 100 cells, and that in one case the 99 sensitive ones grow, while in the other

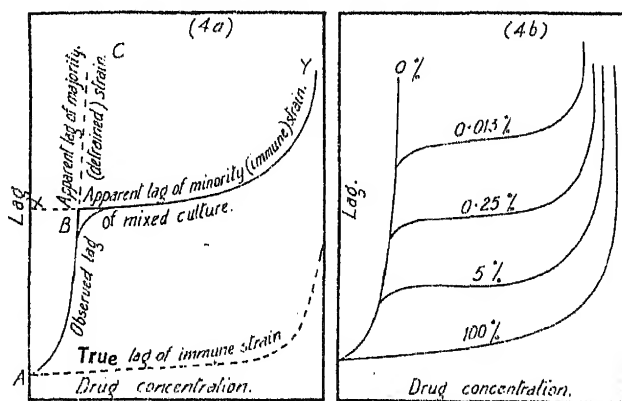


FIG. 4.

- (a) Apparent lag-concentration curves of mixed strain.  
 (b) Lag-concentration curves for cultures containing varying proportions of immune cells.

case only the 1 immune one grows. We plot two curves showing the relation between drug concentration and the *apparent* lag of each strain (*i.e.* the value found by extrapolating observed logarithmic growth curves back to the same *total* initial count of 100). ABC (Fig. 4a) represents the curve for the more sensitive majority. XBY is that for the immune minority. XBY lies well above the true lag-concentration curve for the immune cells because it is calculated on the assumption that the inoculum is 100 whereas in fact only one grows in the way shown. X lies in fact above the real value by the time taken for the count to increase from 1 to 100. (A on the other hand only differs from the true lag by the time taken to grow from 99 to 100.) Now consider the apparent lag determined experimentally for the mixed strain when both sensitive and immune strains are imagined to grow in competition. The lag observed is the *lower* of the two values given by curves ABC and XBY. The measured value therefore follows the curve ABY. At the point B the immune strain, in spite of its handicap from paucity of numbers, now reaches the threshold of visible growth before the sensitive strain. As the proportion of immune cell progressively drops the point X rises so

that the successive lag concentration-curves for the mixed strain constitute the family shown in Fig. 4b.

For a complete lapse of immunity every cell in the culture must be individually modified. Thus loss of immunity may well be much more difficult than its original acquisition. As long as a few cells remain immune the inhomogeneous culture will behave qualitatively as described. Quantitatively, of course, the simplifying assumption of independent growth will not be satisfied.

#### (e) Induced Loss of Proflavine Immunity during Growth in Presence of Phenols.

The curves in Fig. 3, showing the residual immunity of proflavine-trained cells after growth in graded cresol concentrations, can be reasonably interpreted as practical examples of the family of curves shown schematically in Fig. 4b. This would imply that growth in cresol deprives most but not all proflavine-adapted cells of their immunity, and that the residual proportion of trained cells is smaller the higher the cresol concentration.

In view of the simplifying assumptions made in the discussion in the last section, the correspondence between Fig. 3 and Fig. 4b would not be expected to be more than general and qualitative. But with this reservation the ideas there expressed would seem to account for the experimental facts.

#### Summary.

When trained by successive subculture in presence of proflavine at concentration,  $P$ , up to 200 mg./l., *Bact. lactis aerogenes* acquires the ability to grow without lag at concentrations up to, but very little exceeding,  $P$ . After adaptation to higher concentrations, however, complete immunity may be attained, cells trained at 1500 mg./l., for example, growing immediately (provided they are of suitable age) at any concentration up to 3000 mg./l.

The complete adaptation is not initially stable. Cells trained to grow at 2000 mg./l. pass through the following stages: adaptation incomplete: adaptation complete (*i.e.* cells grow without lag) but unstable—*i.e.* some of the immunity is lost on subculture in the absence of the proflavine: adaptation both complete and stable.

In the unstable phase reversion occurs, not to the unadapted state, but to an equilibrium state corresponding to a lower, though still considerable degree of adaptation. The stable state is only reached after very prolonged training.

An induced loss of adaptation occurs when the cells are grown under appropriate conditions in presence of phenols.

Selection of resistant types is considered an inadequate explanation of these facts: a theory of enzyme expansion and modification is preferred, though the superposed operation of selection on the other changes provides an explanation of certain quantitative facts about the phenol-induced reversion.

*Physical Chemistry Laboratory,  
Oxford University.*



## REVIEWS OF BOOKS.

### **Handbook of Mineral Dressing, Ores and Industrial Minerals.**

By ARTHUR F. TAGGART. (Chapman & Hall, 1945.) Pp. 1915.  
Price £2 10s.

The earlier edition of this book, which appeared in 1927 under the title *Handbook of Ore Dressing*, suffered, to quote the author, "the usual fate of technical handbooks." Indeed in these days of revolutionary change in engineering and scientific practice generally, it is doubtful whether any book written is not out of date, in many respects at least, almost as soon as it is published. However, the many users of the earlier edition, who have come to regard it as the standard work in this field, will find the present volume no less comprehensive than its predecessor.

This is volume 1 of the handbook, dealing with the occurrence and treatment of metallic ores and non-metallic minerals. A second volume is planned to cover the preparation of fuels, and the processes by which the mineral concentrates are converted into useful products.

Many sections have been completely rewritten, for example, those on the metallic minerals, grinding, flotation, and sampling and testing. Recent developments have necessitated the expansion or revision of much of the earlier edition, particularly the sections on crushing, screening, washing, gravity concentration and electrical concentration. The general scope of the book has been greatly extended by the inclusion of entirely new chapters on industrial minerals, cement, dust collection and air-sizing, and dry grinding.

In his preface the author records his opinion that practice is still the best index of expectable performance, but despite this conviction the greatly improved resumé of recent experimental and theoretical research which introduces each section, indicates that the value of scientific investigation is not underestimated. The handbook is therefore no less useful to research workers in this field, than to those engaged in the practice of ore dressing.

R. C. S.

**Polymer Bulletin** (Vol. 1, No. 1). Edited by PAUL M. DORV (Interscience Publishers, Inc., New York, 1945. Pp. 1-23.) Subscription price, \$2.40 a year.

This Polymer Bulletin is a new and unusual venture for an academic establishment to use as a medium for giving news of its activities. Since Professor Mark went to the Polytechnic Institute of Brooklyn, New York, he has built up a very large and vigorous school of high polymer chemistry. This school is not necessarily confined to doing research but in it there are post-graduate courses of instruction and there are held at intervals discussions on specialised topics. There is, therefore, a special excuse for publishing this Bulletin which records the activities of the Bureau and gives in rather different form a description of the equipment

of the laboratory and the progress of some of the main topics of research. In this way intending visitors may thereby get a very much more complete idea of the kind of laboratory to which they may go for some period of time. The Bulletin is published bi-monthly and is well illustrated.

H. W. M.

**Structural Inorganic Chemistry.** By A. F. WELLS. (Humphrey Milford, The Clarendon Press, Oxford, 1945.) Pp. vii + 590. Price 25s. net.

Mr. Wells has earned our gratitude by writing this comprehensive yet detailed treatise on modern structural inorganic chemistry. The book is in two parts. The first is a general account of the theories of atomic and molecular structure and of the modern methods of investigating structure, with special emphasis on those matters relevant to the solid state: the second is a systematic exposition of present knowledge about the structures of inorganic compounds. It is an ambitious undertaking; and Mr. Wells can be congratulated on the high degree of success which he has achieved. He has provided us with a most valuable collection of information in a stimulating, balanced, and very readable form. The printers are also to be congratulated on their work.

One hopes that the book will run into at least a second edition; so some constructive criticisms may be offered. The separation into two parts seems rather too rigid, with the result that the illumination of the facts in Part II by the principles in Part I is not as complete as it could be. There is some trace of the tendency, common among crystallographers, to regard chemistry as merely a branch of solid geometry. Finally, the annotation should be improved. Secondary sources of information about particular substances are used too freely; and the method of reference, while only inconvenient if detailed information about a structure is sought, is of very little use at all for giving sources relating to general statements.

Notwithstanding these last remarks, the book is a notable achievement and is strongly to be recommended.

L. E. S.

**"Synthetic Rubber from Alcohol: A Survey based on the Russian Literature."** By A. TALALAY and M. MAGAT. (Interscience Publishers, 1945.) \$5.00.

This book falls into two sections, of which the first comprises two chapters, dealing with the chemistry and technology of the Russian processes for the production of synthetic polybutadiene rubber. This section contains a most interesting and valuable survey of the Russian literature, in the form of a connected account of the process and discussion of the principles involved. It is naturally impossible for the reviewer to estimate how far the account given represents current Russian practice.

The second and larger section is divided into two chapters, entitled "Polymerisation" and "Physico-chemical Properties of the Polymer." The object is to discuss the theoretical basis of the production of synthetic rubber, and to consider how the reported properties of the material can be correlated with its structure. This rather ambitious programme

has led to the inclusion of very useful brief summaries of some modern theoretical developments in the physics and chemistry of polymers. In these sections the treatment is, of course, general, and references are mainly to American and British work. As far as possible, however, examples of the application of these ideas are drawn from the literature on Russian synthetic rubber. Indeed, it would almost seem that where no suitable illustration could be found in the Russian work, a subject is omitted altogether. It is difficult otherwise to understand why no reference at all is made to the very important advances which have been made in elucidating the elasticity of rubber like polymers.

The technology of the rubber—its compounding, vulcanisation and practical use—is not discussed at all. The section on physico chemical properties is confined to the raw polymer, and deals with such topics as structure, molecular weight, plasticity, solubility and chemical reactivity (especially oxidisability).

The main value of this book to English readers will be in providing a guide to the very extensive Russian literature. All who have worked on rubber or polymers will be aware of the long standing need for such a service. Abstracts are seldom full enough to be of much service and the language bars most workers from the original papers; such a survey as this is the more welcome. This thorough and critical review sets the Russian work against a background of contemporary work in other countries, and will enable the extent of its very real contribution to be more widely realised.

G. G.

## MINUTES OF THE 39TH ANNUAL GENERAL MEETING

Held on THURSDAY, 28th September, 1945, at 10.30 a.m., at University College, London, W.C. 1.

The President, Professor E. K. RIDEAL, M.B.E., D.Sc., F.R.S., was in the Chair.

1. The Minutes of the 38th Annual General Meeting were taken as read and confirmed.
2. The Annual Report and Statement of Accounts, together with the report of the Auditors for the year 1944, were presented by the Honorary Treasurer, who emphasized the continuing financial soundness of the Society. The Report was unanimously adopted, and on the motion of Professor E. G. Evans, seconded by Dr. O. J. Walker, the thanks of the Society were accorded to Dr. Slade for his successful trusteeship of the Society's affairs.
3. The Officers and Ordinary Members of Council were elected to take office on the 1st October as follows :—

### *President.*

PROF. W. E. GARNER, D.Sc., F.R.S.

### *Vice-Presidents who have held the Office of President.*

PROF. F. G. DONNAN, C.B.E., Ph.D., F.R.S.

PROF. C. H. DESCH, D.Sc., F.R.S.

PROF. N. V. SIDGWICK, Sc.D., D.Sc., F.R.S.

PROF. M. W. TRAVERS, D.Sc., F.R.S.

PROF. E. K. RIDEAL, M.B.E., D.Sc., F.R.S.

### *Vice-Presidents.*

PROF. A. FINDLAY, PRES., R.I.C., D.Sc.

R. LESSING, Ph.D.

C. H. GOODEVE, D.Sc., F.R.S.

PROF. M. POLANYI, F.R.S.

R. O. GRIFFITH, M.Sc.

PROF. S. SUGDEN, D.Sc., F.R.S.

### *Honorary Treasurer.*

R. E. SLADE, D.Sc.

### *Chairman of the Publications Committee.*

PROF. A. J. ALLMAND, D.Sc., F.R.S.

### *Ordinary Members of Council.*

T. BEACALL, O.B.E.

PROF. H. W. MELVILLE, Ph.D., F.R.S.

G. M. BENNETT, M.A., Sc.D.

F. I. G. RAWLINS, M.Sc., F.R.S.E.,  
F.INST.P.

A. CARESS, B.A., Ph.D.

PROF. C. W. DAVIES, M.Sc.

H. W. THOMPSON, M.A., B.Sc., D.Phil.

PROF. M. G. EVANS, D.Sc.

O. H. WANSBOROUGH-JONES, Ph.D.

R. W. LUNT, Ph.D.

The President then, on behalf of the members, welcomed the President-Elect to his forthcoming office and amid acclamation, Professor Garner expressed his appreciation of the honour accorded to him and his resolve to do his utmost to serve the Society.

Thereupon Professor Ingold, on behalf of British members, and Professor Kruyt, for overseas members, expressed to Professor Rideal the Society's thanks for his untiring and eminently successful work for the Society during a critical seven years in its history. Professor Rideal, in thanking the members, expressed his personal thanks to his colleagues upon the Council, to the Secretary and to Miss Kornitzer in the Society's offices. He had hoped that the 1000th member of the Society would be elected during his Presidency ;

it was therefore a special pleasure to him, when about to relinquish office, to announce that, despite the removal from the Register of all enemy members, there were that day 1054 members of the Society.

The President referred with grief to the loss the Society had suffered by the gallant death of Professor Leif Trønstad in Norway after the successful accomplishment of his important mission in April. Professor Donnan told the Society of the murder by the enemy of the Society's distinguished member, Professor Ernst Cohen.

4. The thanks of the Society were accorded with acclamation to the other retiring Officers and Members of Council.

This concluded the business of the Meeting.

### MINUTES OF A SPECIAL GENERAL MEETING

Held at University College, London, at 11 a.m. on 27th September, 1945.

The notice convening the meeting having been read by the Secretary, the Rules of the Society were unanimously amended in manner following:

In rules 3, 5, 7, 13, 14, 15, wherever the words "Student Member" or "Student Members" appear, substitute "Junior Member" or "Junior Members," as the case may be.

# Transactions of the Faraday Society.

## AUTHOR INDEX—VOLUME XLI, 1945.

	PAGE
Alcock, T. C. See <i>Bunn, C. W.</i> , and	
Beacall, T. The Melting-Points and Unit Cells of the Methylbenzenes . . .	472
Beament, J. W. L. An Apparatus to Measure Contact Angles . . .	45
Bell, R. P. Bond Torsion in the Vibrations of the Benzene Molecule . . .	293
— See <i>Coulson, C. A.</i> , and	
Belton, J. W., and Evans, M. G. Studies in the Molecular Forces involved in Surface Formation. II: The Surface Free Energies of Simple Liquid Mixtures . . .	1
Bilmes, L. A Theory of the Calender Effect in Rubber-like Materials . . .	81
Blumenthal, E., and Herbert, J. B. M. The Mechanism of the Hydrolysis of Trimethyl Orthophosphate . . .	611
Booth, A. D. Two New Modifications of the Fourier Method of X-ray Structure Analysis . . .	434
Buck, Kenneth R., and Smith, G. F. A Null-Point Detector for Direct and Alternating Current and its use in Conductance and E.M.F. Measurements . . .	586
Bunn, C. W., and Alcock, T. C. The Texture of Polythene . . .	317
Butler, E. T., Mandel, Erna, and Polanyi, M. The Rates of Pyrolysis and Bond Energies of Substituted Organic Iodides. Part II . . .	298
Cameron, A. A Method for Determining the Instantaneous Hardness of Plastic Substances . . .	583
Cannon, C. G., and Sutherland, G. B. B. M. The Infra-Red Absorption Spectra of Coals and Coal Extracts . . .	279
Cassie, A. B. D. Multimolecular Adsorption . . .	450
— Absorption of Water by Wool . . .	458
Champion, F. A. A Quantitative Study of the Corrosion of Pure Aluminium . . .	593
Chang, Sze-Tseng. See <i>Woo, Sho-Chow</i> , and	
Clark, A. M. A New General Equation for the Liquid-Vapour Relations of Binary Systems. Part I: Theoretical and Experimental Basis . . .	718
Part II: Application to the Theory of Practical Distillation . . .	738
Conn, G. K. T. A Thermocouple Bolometer Detector . . .	192
Corner, J. Extrapolation of the Experimental Critical Temperatures of the Normal Paraffins . . .	617
Coulson, C. A., and Bell, R. P. Kinetic Energy, Potential Energy and Force in Molecule Formation . . .	141
Davies, D. S. See <i>Pryce, J. M. G.</i> , <i>Davies, D. S.</i> and <i>Hinshelwood, C. N.</i>	
— Hinshelwood, C. N., and Pryce, J. M. The Adaptation of <i>Bact. Lactis Aerogenes</i> to Varying Concentrations of an Antibacterial Drug (Proflavine) . . .	163
— The Adaptation of <i>Bact. Lactis Aerogenes</i> to High Concentrations of Proflavine . . .	778
Davis, D. J. See <i>Parton, H.</i> , <i>Davis, D. J.</i> , <i>Hurst, F.</i> , and <i>Gemmell, G. D.</i>	
Evans, M. G. See <i>Belton, J. W.</i> , and	
— and Rushbrooke, G. S. Some Notes on the Theory of Unimolecular Gas Reactions in Transition State Symbolism . . .	621
Evans, U. R. The Laws of Expanding Circles and Spheres in Relation to the Lateral Growth of Surface Films and the Grain-Size of Metals . . .	365
Ferry, Miss J., Gee, Geoffrey, and Treloar, L. R. G. The Interaction between Rubber and Liquids. VII: The Heats and Entropies of Dilution of Natural Rubber by Various Liquids . . .	340
Fogg, A. H., and Lodge, R. M. The Mode of Antibacterial Action of Phenols in Relation to Drug-Fastness . . .	359
French, C. M. The Magnetic Susceptibility of Position Isomers in the Disubstituted Benzene Series . . .	676
— and Trew, V. C. G. The Diamagnetic Susceptibility of some Alkyl and Aryl Halides . . .	439
Frith, Elizabeth M. The Effect of Solvent Type on the Viscosity of Very Dilute Solutions of Long Chain Polymers . . .	17
— The Interaction of Plasticizers and Polymers . . .	90
Frost, W. E. See <i>Linnett, J. W.</i> , <i>Raynor, Mrs. E. J.</i> , and	
Gee, G. See <i>Ferry, J.</i> , <i>Gee, G.</i> , and <i>Treloar, L. R. G.</i>	
Gemmell, G. D. See <i>Parton, H. N.</i> , <i>Davis, D. J.</i> , <i>Hurst, F.</i> , and	
Guggenheim, E. A. The Number of Arrangements on a Lattice of Molecules each occupying several sites . . .	107
— Statistical Thermodynamics of the Surface of a Regular Solution . . .	150

	PAGE
Hall, M. N. A., Martin, S. L. H., and Rees, A. L. G. The Solubility of Hydrogen in Zirconium and Zirconium-Oxygen Solid Solutions . . .	306
Hathway, D. E. See <i>Hodgson, H. E.</i> , and	
Herbert, J. B. M. See <i>Blumenthal, E.</i> , and	
Hickling, A. The Anodic Behaviour of Metals. Part I: Platinum . . .	333
Hinschelwood, C. N. See <i>Davies, D. S.</i> , <i>Hinschelwood, C. N.</i> , and <i>Pryce, J. M. G.</i>	
— See <i>Pryce, J. M. G.</i> , <i>Davies, D. S.</i> , and	
Hodgson, H. E., and Hathway, D. E. The Absorption Spectra of some Mononitronaphylamines, with Observations on their Structures . . .	115
Holmes, F. H., and Standing, H. A. The Dyeing of Cellulose with Direct Dyes. Part III: The Aqueous Diffusion of Direct Dyes . . .	542
— Part IV: The Electrolytic Conductance of Aqueous Solutions of Direct Dyes . . .	568
Hunter, E., and Oakes, W. G. The Effect of Temperature on the Density of Polythene . . .	49
Hurst, F. See <i>Parton, H. N.</i> , <i>Davis, D. J.</i> , <i>Hurst, F.</i> , and <i>Gemmell, G. D.</i>	
Hutchinson, E. On the Measurement of the Thermal Conductivity of Liquids . . .	87
Ingold, C. K. The Application of Infra-red Spectra to Chemical Problems. General Introduction . . .	172
Jacobs, P. W. M., and Tompkins, F. C. Inorganic Chromatography. Part I: Static Adsorption Measurements . . .	388
— Part II: The Position, rate of advance and width of adsorbate zones . . .	395
— Part III: Elution Curves . . .	400
Jamison, Margaret M. A Review of Some of the Recorded Observations involving Asymmetric Transformations . . .	696
Jenkins, H. O. The Temperature Dependence of Ionic Dissociations . . .	138
Johnston, J. P., Longuet-Higgins, H. C., and Ogston, A. G. On the Distribution of the Molecular Weights of Proteins . . .	588
Kellner, L. The C-C Valency Vibrations of Organic Molecules . . .	217
King, G. Sorption of Vapours by Keratin and Wool . . .	325
— Permeability of Keratin Membranes to Water Vapour . . .	479
Linnett, J. W. The Force Constants of Some CH, NH and Related Bonds . . .	223
— Raynor, Mrs. E. J., and Frost, W. E. The Mechanism of Spark Ignition . . .	487
Lodge, R. M. See <i>Fogg, A. H.</i> , and	
Longuet-Higgins, H. C. See <i>Johnston, J. P.</i> , <i>Longuet-Higgins, H. C.</i> , and <i>Ogston, A. G.</i>	
Macleod, D. B. A Calculation of the Latent Heat of Vaporisation Based on a Revised Equation of State . . .	122
— On a Direct Calculation of the Viscosity of a Liquid, Both under Ordinary Pressures and High Pressures, from the Viscosity of its Vapour, on the basis of a New Equation of State . . .	771
Mandel, E. See <i>Butler, E. T.</i> , <i>Mandel, E.</i> , and <i>Polanyi, M.</i>	
Martin, S. L. H. See <i>Hall, M. N. A.</i> , <i>Martin, S. L. H.</i> , and <i>Rees, A. L. G.</i>	
Maxted, E. B. The form of Catalyst Poisoning Curves . . .	406
Mibashan, A. On Some Physical Properties of Normal Paraffins . . .	374
Oakes, W. G. See <i>Hunter, E.</i> , and	
Ogston, A. G. On the Numerical Consequences of Certain Hypotheses of Protein Structure . . .	670
— See <i>Johnston, J. P.</i> , <i>Longuet-Higgins, H. C.</i> , and	
Pankhurst, K. G. A. A Simple Single-Wire Surface Pressure Balance . . .	156
— and Smith, R. C. M. The adsorption of Paraffin-Chain Salts to Proteins. Part II: The Influence of Electrolytes and pH on the separation of gelatindodecyl sulphate complexes from aqueous solutions . . .	630
Parton, H. N., Davis, D. J., Hurst, F., and Gemmell, G. D. The Energy and Entropy of Solution of Silver Chloride in Methanol-Water Mixtures. Part I . . .	575
— and Perrin, D. D. The Energy and Entropy of Solution of Silver Chloride in Methanol-Water Mixtures. Part II . . .	579
Perrin, D. D. See <i>Parton, H. N.</i> , and	
Philpotts, A. R. See <i>Willis, H. A.</i> , and	
Polanyi, M. See <i>Butler, E. T.</i> , <i>Mandel, E.</i> , and	
Price, W. C., and Walsh, A. D. The Absorption Spectra of Triple Bond Molecules in the Vacuum Ultra Violet . . .	381
Pryce, J. M. G. See <i>Davies, D. S.</i> , <i>Hinschelwood, C. N.</i> , and	
— Davies, D. S., and Hinschelwood, C. N. The Quantitative Relation between the Adaptations of <i>Bact. Lactis Aerogenes</i> to Two Antibacterial Agents (methylene blue and proflavine) . . .	465

	PAGE
Raine, H. C., Richards, R. B., and Ryder, H. The Heat Capacity, Heat of Solution and Crystallinity of Polythene . . . . .	56
Raynor, Mrs. E. J. See <i>Linnett, J. W. Raynor, Mrs. E. J., and Frost, W. E.</i>	
Rees, A. L. G. See <i>Hall, M. N. A., Martin, S. L. H., and</i>	
Richards, R. B. The Melting of Polythene . . . . .	127
— See <i>Raine, H. C., Richards, R. B., and Ryder, H.</i>	
Richards, R. E., and Thompson, H. W. An Absorption Cell for Molten Solids and Heated Liquids . . . . .	183
Rideal, E. K. The Application of Infra-red Spectra to Chemical Problems. Introduction . . . . .	171
Robinson, R. A. The Water Activities of Lithium Chloride Solutions up to High Concentrations at 25° . . . . .	756
— and Stokes, R. H. A Thermodynamic Study of Bivalent Metal Halides in Aqueous Solution. Part XV: Double Chlorides of Uni- and Bivalent Metals . . . . .	752
Rushbrooke, G. S. See <i>Evans, M. G., and</i>	
Rutgers, A. J., and De Smet, M. Researches on Electro-Endosmosis . . . . .	758
Ryder, H. See <i>Raine, H. C., Richards, R. B., and</i>	
Sheppard, N., and Sutherland, G. B. B. M. Some Infra-Red Studies on the Vulcanisation of Rubber . . . . .	261
Simpson, Miss D. M. The Assignment of the Vibrational Frequencies and the Force Field of the Ozone Molecule . . . . .	209
Skinner, H. A. A Revision of Some Bond Energy Values and the Variation of Bond Energy with Bond Length . . . . .	645
Smet, M. De. See <i>Rutgers, A. J., and</i>	
Smith, Gilbert F. See <i>Buck, Kenneth, R., and</i>	
Smith, R. C. M. See <i>Pankhurst, K. G. A., and</i>	
Standing, H. A. The Dyeing of Cellulose with Direct Dyes. Part I: A Review of the Literature . . . . .	410
— See <i>Holmes, F. H., and</i>	
— See <i>Willis, H. F., Warwicker, J. O., Standing, H. A., and Urquhart, A. R.</i>	
Stewart, K. The Imine Radical, N. H. . . . .	663
Stokes, Jean M. The Osmotic and Activity Co-efficients of Sodium and Potassium Dihydrogen Phosphate at 25° . . . . .	685
— See <i>Stokes, R. H., and</i>	
Stokes, R. H. A Thermodynamic Study of Bivalent Metal Halides in Aqueous Solution. Part XI: The Osmotic and Activity Coefficients of Zinc Iodide at 25° . . . . .	12
— Part XIII: Properties of Calcium Chloride Solutions up to High Concentrations at 25° . . . . .	637
— Part XIV: Concentrated Solutions of Magnesium Chloride at 25° . . . . .	642
— See <i>Robinson, R. A., and</i>	
— and Stokes, J. M. Part XII: Electromotive Force Measurements on Zinc Bromide Solutions . . . . .	688
Stout, H. P. The Kinetics of the Electrodeposition of the Azide Ion . . . . .	64
Sugden, T. M., and Walsh, A. D. The Ionization Potentials of Butadiene . . . . .	76
Sutherland, G. B. B. M. See <i>Cannon, C. G., and</i>	
— See <i>Sheppard, N., and</i>	
— and Thompson, H. W. Developments in the Technique of Infra-red Spectroscopy . . . . .	174
— See <i>Thompson, H. W., and</i>	
— and Willis, H. A. Measurement of Cell Thickness . . . . .	181
— Some new Peculiarities in the Infra-red spectrum of Diamond . . . . .	289
Temple, R. B. See <i>Thompson, H. W., and</i>	
Thompson, H. W. See <i>Richards, R. E., and</i>	
— and Sutherland, G. B. B. M. The Use of Infra-red Absorption in Analysis . . . . .	197
— See <i>Sutherland, G. B. B. M., and</i>	
— and Temple, R. B. The Infra-red Spectra of Furan and Thiophen . . . . .	27
— and Torkington, P. The Infra-red Spectra of Compounds of High Molecular Weight . . . . .	246
— See <i>Torkington, P., and</i>	
— and Whiffen, D. H. Sources of Radiation and Absorption Cells . . . . .	180
— See <i>Whiffen, D. H., Torkington, P., and</i>	
Tompkins, F. C. See <i>Jacobs, P. W. M., and</i>	
Torkington, P. See <i>Thompson, H. W., and</i>	
— See <i>Whiffen, D. H., Torkington, P., and Thompson, H. W.</i>	
— and Thompson, H. W. Solvents for Use in the Infra-red . . . . .	184
— The Infra-red Spectra of Fluorinated Hydrocarbons. I . . . . .	236



	PAGE
Treloar, L. R. G. See <i>Ferry, J., Gee, G., and</i>	
Trew, V. C. G. See <i>French, C. M., and</i>	
Tuckett, R. F. The Degradation of High Polymers	351
Urquhart, A. R. See <i>Willis, H. F., Warwicker, J. O., Standing, H. A., and</i>	
Walsh, A. D. The Absorption Spectra of the Chloro-Ethylenes in the Vacuum Ultra-Violet	35
— The Absorption Spectra of Acrolein, Crotonaldehyde and Mesityl Oxide in the Vacuum Ultra-Violet	498
— See <i>Price, W. C., and</i>	
— See <i>Sugden, T. M., and</i>	
Warwicker, J. O. See <i>Willis, H. F., Warwicker, J. O., Standing, H. A., and Urquhart, A. R.</i>	
Whiffen, D. H., Torkington, P., and Thompson, H. W. The Use of Infra-red Absorption in Analysis. B. Examples of Analyses	200
— See <i>Thompson, H. W., and</i>	
Willis, H. A. See <i>Sutherland, G. B. B. M., and</i>	
— and Philpotts, A. R. Two Time-Saving Devices in the Conversion of Energy Records into Percentage Absorption Curves	187
Willis, H. F., Warwicker, J. O., Standing, H. A., and Urquhart, A. R. The Dyeing of Cellulose with Direct Dyes. Part II: The Absorption of Chrysophenine by Cellulose Sheet	506
Woo, Sho-Chow, and Chang, Sze-Tseng. The Absorption Spectrum of Methylgloxal	157

## INDEX TO REVIEWS—VOLUME XLI, 1945.

Boas-Traube, S. See <i>British Colliery Owners Research Association and British Coal Utilisation Research Association</i>	
British Coal Utilisation Research Association. Proceedings of a Conference on the Ultra-fine Structure of Coals and Cokes, held at the Royal Institution, London, 1943	101
— See <i>British Colliery Owners Research Association and</i>	
British Colliery Owners Research Association and British Coal Utilisation Research Association. Report of Discussions: Determination of Particle Size in Sub-Sieve Range. D. G. Skinner, S. Boas-Traube, R. L. Brown and P. G. W. Hawksley	102
Brown, R. L. See <i>British Colliery Owners Research Association and British Coal Utilisation Research Association</i>	
Deitz, Victor, R. Bibliography of Solid Adsorbents	169
Harris, Milton, and Mark, H. Fibers. 1944. Issue No. 1.	47
Hawksley, P. G. W. See <i>British Colliery Owners Research Association and British Coal Utilisation Research Association</i>	
Haywood, F. W., and Wood, A. A. R. Metallurgical Analysis by Means of the Spekker Photo-electric Absorptionmeter	438
Lewis, H. K., and Co. Ltd. Catalogue of Lewis's Medical, Scientific and Technical Lending Library	170
Magat M. See <i>Talalay, A., and</i>	
Mark, H. See <i>Harris, Milton and</i>	
Polymer Bulletin. Vol. 1, No. 1	786
Russell, H., Jr. See <i>Yost, D. M., and</i>	
Sandell, E. B. Colorimetric Determination of Traces of Metals. Chemical Analysis, Vol. III	48
Skinner, D. G. See <i>British Colliery Owners Research Association, and British Coal Utilisation Research Association</i>	
Taggart, A. F. Handbook of Mineral Dressing, Ores and Industrial Minerals	786
Talalay, A., and Magat, M. Synthetic Rubber from Alcohol	787
Wells, A. F. Structural Inorganic Chemistry	787
Wood, A. A. R. See <i>Haywood, F. W., and</i>	
Yost, D. M., and Russell, H., Jr. Systematic Inorganic Chemistry	103

## PROCEEDINGS OF THE FARADAY SOCIETY.

Minutes of the 38th Annual General Meeting	105
Minutes of the 39th Annual General Meeting	789
Minutes of a Special General Meeting	790





**Indian Agricultural Research Institute (Pusa)**  
**LIBRARY, NEW DELHI-110012**

This book can be issued on or before.....

Return Date	Return Date